

**PERFORMANCE ASSESSMENT
for the
H-AREA TANK FARM
at the
SAVANNAH RIVER SITE**



November 2012

Prepared by: Savannah River Remediation LLC
Closure & Waste Disposal Authority
Aiken, SC 29808



Prepared for U.S. Department of Energy Under Contract No. DE-AC09-09SR22505

REVISION SUMMARY

REV. #	DESCRIPTION	DATE OF ISSUE
0a	Initial issue to DOE-SR	09/17/2010
0b	Issue for LFRG Review	11/18/2010
0	Initial Issue	03/14/2011
1A	Incorporation of revision 0 comments and lessons learned from FTF activities. Issue to DOE-SR for review	08/31/2012
1	Incorporated DOE comments and issued to support HTF NDAA Section 3116 Draft Basis Document Consultation	11/14/2012

TABLE OF CONTENTS

REVISION SUMMARY	ii
TABLE OF CONTENTS.....	iii
APPENDICES	viii
LIST OF FIGURES	xii
LIST OF TABLES.....	xxvi
ACRONYMS.....	xxxiv
1.0 EXECUTIVE SUMMARY	38
2.0 INTRODUCTION	45
2.1 General Approach.....	45
2.1.1 Performance Assessment Scoping Meeting.....	46
2.1.2 Modeling Process.....	47
2.2 General Facility Description	48
2.2.1 Savannah River Site.....	48
2.2.2 H-Area Tank Farm.....	49
2.3 Facility Life Cycle.....	49
2.4 Related Documents	50
2.4.1 Groundwater Protection Management Program	50
2.4.2 Savannah River Site End State Vision.....	51
2.4.3 Savannah River Site Long Range Comprehensive Plan.....	51
2.4.4 High-Level Waste Environmental Impact Statement	52
2.4.5 Federal Facility Agreement for the Savannah River Site	52
2.5 Performance Criteria.....	53
2.5.1 DOE M 435.1-1 Performance Objectives and Requirements.....	53
2.5.2 10 CFR 61 Performance Objectives	54
2.6 Summary of Key Assessment Assumptions.....	55
2.6.1 General Facility Description Assumptions	55
2.6.2 Site Characteristics Assumptions.....	55
2.6.3 Facility Design Assumptions	56
2.6.4 Stabilized Contaminant Characteristics Assumptions	56
2.6.5 Integrated Conceptual Model Assumptions.....	57
3.0 DISPOSAL FACILITY CHARACTERISTICS.....	60
3.1 Site Characteristics.....	61
3.1.1 Geography and Demography	61

3.1.2	Meteorology and Climatology	67
3.1.3	Ecology	70
3.1.4	Geology, Seismology, and Volcanology	73
3.1.5	Hydrogeology	86
3.1.6	Geochemistry	100
3.1.7	Natural Resources	100
3.1.8	Natural and Background Radiation.....	103
3.2	<i>Principal Facility Design Features</i>	104
3.2.1	Waste Tanks.....	105
3.2.2	Ancillary Equipment.....	152
3.2.3	Waste Tank Grouting.....	188
3.2.4	Closure Cap.....	195
3.3	<i>Evaluation of Inventory Constituents</i>	215
3.3.1	Evaluation of Radionuclides in Principal Decay Chains	215
3.3.2	Evaluation of Remaining Radionuclides	215
3.3.3	Evaluation of Chemicals.....	216
3.4	<i>Inventory Methodology</i>	216
3.4.1	Initial Waste Tank Inventory Estimates.....	217
3.4.2	Annulus and Type II Tank Sand Pad Inventory Estimates.....	218
3.4.3	Waste Tank Inventory Adjustments.....	226
3.4.4	Final Waste Tank Inventory Estimates	227
3.4.5	Ancillary Equipment Inventory Estimates.....	234
4.0	ANALYSIS OF PERFORMANCE	239
4.1	<i>Overview of Analyses</i>	240
4.2	<i>Integrated Conceptual Model of Facility Performance</i>	242
4.2.1	Source Term Release	244
4.2.2	Radionuclide Transport.....	270
4.2.3	Exposure Pathways and Scenarios.....	323
4.2.4	Summary of Key Transport Assumptions.....	350
4.3	<i>Modeling Codes</i>	354
4.3.1	Modeling Codes Used.....	355
4.3.2	Software QA	362
4.3.3	Model Checking.....	363
4.4	<i>Closure System Modeling</i>	364
4.4.1	Individual Waste Tank Modeling	364

4.4.2	Systems and Potential Degradation	373
4.4.3	Evaluation of Integrated System Behavior	382
4.4.4	Modeling Process.....	394
4.5	<i>Airborne and Radon Analyses</i>	456
4.5.1	Air and Radon Pathway Conceptual Model.....	457
4.5.2	Air and Radon Pathway Diffusive Transport Model	458
4.5.3	Summary of Key Air and Radon Pathway Assumptions.....	463
4.5.4	Air Pathway Analysis	464
4.5.5	Air Pathway Model Factors for a Unit Curie.....	469
4.5.6	Radon Analysis	474
4.5.7	Radon Pathway Model Results	477
4.6	<i>Biotic Pathways</i>	479
4.6.1	Bioaccumulation Factors	479
4.6.2	Human Health Exposure Parameters (Consumption Rates)	486
4.7	<i>Dose Analysis</i>	489
4.7.1	Dose Conversion Factors	490
4.7.2	MOP Dose Analysis.....	493
4.7.3	Intruder Dose Analysis	493
4.7.4	Analysis Approach.....	493
4.8	<i>RCRA/CERCLA Risk Evaluation</i>	493
4.8.1	Integrated Conceptual Model.....	494
4.8.2	Risk Assessment	497
5.0	RESULTS OF ANALYSIS	499
5.1	<i>Source Term Analysis and Release Results Process</i>	499
5.2	<i>Environmental Transport of Radionuclides</i>	500
5.2.1	Groundwater Concentrations at 100 Meters	501
5.2.2	Sensitivity Run Radionuclide Determination	520
5.2.3	Groundwater Concentrations at the Seepines	523
5.3	<i>Air Pathway and Radon Analyses</i>	526
5.4	<i>Biotic Pathways</i>	532
5.4.1	MOP at the 100-Meter Well Dose Pathways	532
5.4.2	MOP at the Stream Dose Pathways	542
5.5	<i>Dose Analysis</i>	550
5.5.1	MOP at 100-Meter Groundwater Pathway Dose Results	550
5.5.2	MOP at Stream Groundwater Pathway Dose Results.....	575

5.5.3	MOP All-Pathway Dose Results.....	579
5.6	<i>Uncertainty and Sensitivity Analyses</i>	580
5.6.1	Uncertainty and Sensitivity Analyses using Probabilistic Modeling.....	580
5.6.2	GoldSim Benchmarking.....	582
5.6.3	Parameters Evaluated in the HTF Probabilistic Model.....	607
5.6.4	HTF Probabilistic UA/SA Model	649
5.6.5	Sensitivity Analysis using HTF Probabilistic Model.....	671
5.6.6	Barrier Analysis using the PORFLOW Deterministic Model	681
5.6.7	Sensitivity Analysis using the HTF Deterministic Model	685
5.6.8	Sensitivity Analysis Using the HTF Probabilistic Model.....	723
5.6.9	Sensitivity Analysis Using the HTF Probabilistic Model in Deterministic Mode..	731
5.7	<i>RCRA/CERCLA Risk Analysis</i>	732
5.7.1	Principal Threat Source Material	732
5.7.2	Contaminant Migration Constituents of Concern	733
5.7.3	Evaluation of Results	736
5.8	<i>ALARA Analysis</i>	736
6.0	INADVERTENT INTRUDER ANALYSIS	739
6.1	<i>Groundwater Concentrations at 1 Meter</i>	739
6.2	<i>Acute Exposure Scenarios</i>	753
6.2.1	Acute Intruder Ingestion Dose Pathway - Ingestion of Re-Suspended Drill Cuttings	753
6.2.2	Acute Intruder Inhalation Dose Pathway - Inhalation of Drill Cuttings	754
6.2.3	Acute Intruder Direct Exposure Dose Pathways - Direct Exposure to Drill Cuttings	754
6.3	<i>Chronic Exposure Scenarios</i>	755
6.3.1	Chronic Intruder Ingestion Dose Pathways	755
6.3.2	Chronic Intruder Direct Exposure Dose Pathways	762
6.3.3	Chronic Intruder Inhalation Dose Pathways	763
6.4	<i>Inadvertent Intruder Analysis Results</i>	765
6.5	<i>Inadvertent Intruder Uncertainty/Sensitivity Analyses</i>	770
6.5.1	Intruder Single Parameter Deterministic Sensitivity Analysis	771
6.5.2	Intruder Probabilistic Uncertainty Analysis.....	777
7.0	INTERPRETATION OF RESULTS	780
7.1	<i>Performance Assessment Results</i>	780
7.1.1	Integrated System Behavior	780

7.1.2	Groundwater Pathway Results	784
7.1.3	Airborne Dose	789
7.1.4	All-Pathways Dose	789
7.1.5	Inadvertent Intruder Dose	791
7.1.6	Radon Flux	794
7.1.7	Summary of Performance Assessment Results	794
7.2	<i>Conservatism Included in the HTF PA</i>	797
7.2.1	General	797
7.2.2	Closure Cap	798
7.2.3	Waste Tanks	799
7.2.4	Contaminant Zone and Contaminant Release Model	799
7.2.5	Inventory	800
7.2.6	Grout	800
7.2.7	Steel Liner	800
7.2.8	Stainless Steel Transfer Lines and Ancillary Equipment	801
7.2.9	Volatile Radionuclide and Radon Analyses	802
8.0	PERFORMANCE EVALUATION	803
8.1	<i>Use of Performance Assessment Results</i>	803
8.2	<i>Further Work</i>	804
9.0	PREPARERS	806
10.0	REFERENCES	817
11.0	GLOSSARY	839

APPENDICES

APPENDIX A: WASTE FLUX FROM HTF SOURCES.....A-1

- A.1: Flux Leaving the Liner of HTF Waste Tanks and Contamination Zone (CZ) of Ancillary Equipment.....A.1-1*
- A.2: Waste Flux Entering the Water Table from HTF Waste Tanks and Ancillary Equipment.....A.2-1*

APPENDIX B: 100-METER RADIOLOGICAL AND CHEMICAL CONCENTRATIONS.....B-1

- B.1: 100-Meter Radiological and Chemical Concentrations at the Upper Three Runs Aquifer - Upper Zone.....B.1-1*
- B.2: 100-Meter Radiological and Chemical Concentrations at the Upper Three Runs Aquifer - Lower Zone.....B.2-1*
- B.3: 100-Meter Radiological and Chemical Concentrations at the Gordon Aquifer.....B.3-1*

APPENDIX C: SEEPLINE SENSITIVITY RUN RADIONUCLIDE CONCENTRATIONS.....C-1

APPENDIX D: 100-METER SENSITIVITY RUN RADIONUCLIDE CONCENTRATIONS (100,000 YEARS).....D-1

APPENDIX E: 100-METER SENSITIVITY RUN RADIONUCLIDE CONCENTRATIONS FOR SELECTED SOURCES.....E-1

APPENDIX F: COMPARISON OF SENSITIVITY RUN RADIONUCLIDE CONCENTRATIONS AT THE SEEPLINE AND VARIOUS AQUIFER DEPTHS.....F-1

- F.1: Comparison of Seepage Peak Concentrations.....F.1-1*
- F.2: Ratios of Peak Concentrations Across Aquifers of the 100-Meter Boundary.....F.2-1*

APPENDIX G: 1-METER RADIOLOGICAL AND CHEMICAL CONCENTRATIONS.....G-1

- G.1: 1-Meter Radiological and Chemical Concentrations at the Upper Three Runs Aquifer - Upper Zone.....G.1-1*
- G.2: 1-Meter Radiological and Chemical Concentrations at the Upper Three Runs Aquifer - Lower Zone.....G.2-1*
- G.3: 1-Meter Radiological and Chemical Concentrations at the Gordon Aquifer.....G.3-1*

APPENDIX H: 100-METER RESULTS FOR NO CLOSURE CAP.....H-1

- H.1: Waste Flux Entering the Water Table from HTF Waste Tanks and Ancillary Equipment for No Closure Cap.....H.1-1*
- H.2: 100-Meter Radiological Concentrations for No Closure Cap.....H.2-1*

APPENDIX I: 100-METER SENSITIVITY RUN RADIONUCLIDE CONCENTRATIONS FOR CASE B.....	I-1
APPENDIX J: 100-METER SENSITIVITY RUN RADIONUCLIDE CONCENTRATIONS FOR CASE C.....	J-1
APPENDIX K: 100-METER SENSITIVITY RUN RADIONUCLIDE CONCENTRATIONS FOR CASE D.....	K-1
APPENDIX L: 100-METER SENSITIVITY RUN RADIONUCLIDE CONCENTRATIONS FOR CASE E.....	L-1
APPENDIX M: 100-METER SENSITIVITY RUN RADIONUCLIDE CONCENTRATIONS FOR SYNERGISTIC CASE.....	M-1
APPENDIX N: 100-METER SENSITIVITY RUN RADIONUCLIDE CONCENTRATIONS FOR GROUT TRANSITION CASES.....	N-1
<i>N.1: Fast Transition, Case A.....</i>	<i>N.1-1</i>
<i>N.2: Slow Transition, Case A.....</i>	<i>N.2-1</i>
<i>N.3: Fast Transition, Case C.....</i>	<i>N.3-1</i>
<i>N.4: Slow Transition, Case C.....</i>	<i>N.4-1</i>
APPENDIX O: 100-METER SENSITIVITY RUN RADIONUCLIDE CONCENTRATIONS FOR SOLUBILITY SENSITIVITY CASES.....	O-1
<i>O.1: Worst Case Solubilities.....</i>	<i>O.1-1</i>
<i>O.2: Worst Case Solubilities with Realistic E_h (Oxidized Region III).....</i>	<i>O.2-1</i>
<i>O.3: Worst Case Solubilities with Iron Co-precipitation.....</i>	<i>O.3-1</i>
APPENDIX P: 100-METER SENSITIVITY RUN RADIONUCLIDE CONCENTRATIONS FOR CALCAREOUS ZONE PRESENCE.....	P-1
APPENDIX Q: 100-METER SENSITIVITY RUN RADIONUCLIDE CONCENTRATIONS FOR K_d VARIABILITY.....	Q-1
<i>Q.1: Half K_d Values.....</i>	<i>Q.1-1</i>
<i>Q.2: Quarter K_d Values.....</i>	<i>Q.2-1</i>
APPENDIX R: 100-METER SENSITIVITY RUN RADIONUCLIDE CONCENTRATIONS FOR BASE CASE (CASE A) LINER FAILURE VARIABILITY.....	R-1
<i>R.1: Type I, Zero Liner Failure Time, Case A.....</i>	<i>R.1-1</i>
<i>R.2: Type I, Early Liner Failure Time, Case A.....</i>	<i>R.2-1</i>
<i>R.3: Type I, Nominal Liner Failure Time, Case A.....</i>	<i>R.3-1</i>
<i>R.4: Type I, Late Liner Failure Time, Case A.....</i>	<i>R.4-1</i>
<i>R.5: Type II, Zero Liner Failure Time, Case A.....</i>	<i>R.5-1</i>

R.6: Type II, Early Liner Failure Time, Case A.....R.6-1
R.7: Type II, Nominal Liner Failure Time, Case A.....R.7-1
R.8: Type II, Late Liner Failure Time, Case A.....R.8-1
R.9: Type III, Zero Liner Failure Time, Case A.....R.9-1
R.10: Type III, Early Liner Failure Time, Case A.....R.10-1
R.11: Type III, Nominal Liner Failure Time, Case A.....R.11-1
R.12: Type III, Late Liner Failure Time, Case A.....R.12-1
R.13: Type IV, Zero Liner Failure Time, Case A.....R.13-1
R.14: Type IV, Early Liner Failure Time, Case A.....R.14-1
R.15: Type IV, Nominal Liner Failure Time, Case A.....R.15-1
R.16: Type IV, Late Liner Failure Time, Case A.....R.16-1

**APPENDIX S: 100-METER SENSITIVITY RUN RADIONUCLIDE
CONCENTRATIONS FOR CASE C LINER FAILURE VARIABLILITY.....S-1**

S.1: Type I, Zero Liner Failure Time, Case C.....S.1-1
S.2: Type I, Early Liner Failure Time, Case C.....S.2-1
S.3: Type I, Nominal Liner Failure Time, Case C.....S.3-1
S.4: Type I, Late Liner Failure Time, Case C.....S.4-1
S.5: Type II, Zero Liner Failure Time, Case C.....S.5-1
S.6: Type II, Early Liner Failure Time, Case C.....S.6-1
S.7: Type II, Nominal Liner Failure Time, Case C.....S.7-1
S.8: Type II, Late Liner Failure Time, Case C.....S.8-1
S.9: Type III, Zero Liner Failure Time, Case C.....S.9-1
S.10: Type III, Early Liner Failure Time, Case C.....S.10-1
S.11: Type III, Nominal Liner Failure Time, Case C.....S.11-1
S.12: Type III, Late Liner Failure Time, Case C.....S.12-1
S.13: Type IV, Zero Liner Failure Time, Case C.....S.13-1
S.14: Type IV, Early Liner Failure Time, Case C.....S.14-1
S.15: Type IV, Nominal Liner Failure Time, Case C.....S.15-1
S.16: Type IV, Late Liner Failure Time, Case C.....S.16-1

**APPENDIX T: 100-METER SENSITIVITY RUN RADIONUCLIDE
CONCENTRATIONS FOR CASE E LINER FAILURE VARIABLILITY.....T-1**

T.1: Type I, Zero Liner Failure Time, Case E.....T.1-1

T.2: Type I, Early Liner Failure Time, Case E.....T.2-1
T.3: Type I, Nominal Liner Failure Time, Case E.....T.3-1
T.4: Type I, Late Liner Failure Time, Case E.....T.4-1
T.5: Type II, Zero Liner Failure Time, Case E.....T.5-1
T.6: Type II, Early Liner Failure Time, Case E.....T.6-1
T.7: Type II, Nominal Liner Failure Time, Case E.....T.7-1
T.8: Type II, Late Liner Failure Time, Case E.....T.8-1
T.9: Type III, Zero Liner Failure Time, Case E.....T.9-1
T.10: Type III, Early Liner Failure Time, Case E.....T.10-1
T.11: Type III, Nominal Liner Failure Time, Case E.....T.11-1
T.12: Type III, Late Liner Failure Time, Case E.....T.12-1
T.13: Type IV, Zero Liner Failure Time, Case E.....T.13-1
T.14: Type IV, Early Liner Failure Time, Case E.....T.14-1
T.15: Type IV, Nominal Liner Failure Time, Case E.....T.15-1
T.16: Type IV, Late Liner Failure Time, Case E.....T.16-1

**APPENDIX U: 100-METER SENSITIVITY RUN RADIONUCLIDE
CONCENTRATIONS FOR CEMENTITIOUS DEGRADATION
VARIABILITY.....U-1**

U.1: Type I, Slow Degradation.....U.1-1
U.2: Type I, Fast Degradation.....U.2-1
U.3: Type II, Slow Degradation.....U.3-1
U.4: Type II, Fast Degradation.....U.4-1
U.5: Type III, Slow Degradation.....U.5-1
U.6: Type III, Fast Degradation.....U.6-1
U.7: Type IV, Slow Degradation.....U.7-1
U.8: Type IV, Fast Degradation.....U.8-1

LIST OF FIGURES

Figure 1.0-1: HTF Centerline Flows and Sector Designations..... 40

Figure 1.0-2: Peak All-Pathways MOP Dose for HTF 42

Figure 1.0-3: Statistical Time History of MOP Doses for All Cases (0 to 10,000 Years) 44

Figure 2.1-1: HTF PA Modeling Relationships..... 47

Figure 3.1-1: Physical Location of SRS 62

Figure 3.1-2: Location of SRS and Adjacent Areas 63

Figure 3.1-3: Predominant SRS Operational Area Location Map..... 64

Figure 3.1-4: Layout of the GSA 65

Figure 3.1-5: General Layout of HTF..... 66

Figure 3.1-6: SRS Meteorological Monitoring Network..... 69

Figure 3.1-7: Regional Geological Provinces of Eastern United States 74

Figure 3.1-8: Regional Physiographic Provinces of South Carolina 75

Figure 3.1-9: Topography of the GSA..... 76

Figure 3.1-10: General Soil Associations for SRS 77

Figure 3.1-11: Historical Seismic Events in the Southeast..... 81

Figure 3.1-12: Seismic Events within a 50-Mile Radius of SRS..... 82

Figure 3.1-13: Regional Scale Faults for SRS and Vicinity 83

Figure 3.1-14: Regional NW to SE Cross Section..... 87

Figure 3.1-15: Comparison of Chronostratigraphic, Lithostratigraphic, and Hydrostratigraphic Units in the SRS Region 88

Figure 3.1-16: Potentiometric Surface of the UTRA..... 89

Figure 3.1-17: Potentiometric Surface of the Gordon Aquifer 90

Figure 3.1-18: Hydrostratigraphic Picks in GSAD..... 92

Figure 3.1-19: Laboratory Determined Permeability Data in GSAD 92

Figure 3.1-20: Multiple Well Pump Test Data in GSAD 93

Figure 3.1-21: Single Well Pump Test Data in GSAD..... 93

Figure 3.1-22: Slug Test Data in GSAD..... 94

Figure 3.1-23: Conceptual Diagram of Groundwater Flow beneath the GSA 96

Figure 3.1-24: Savannah River Basin Dams..... 97

Figure 3.1-25: Savannah River Site Watershed Boundaries and Major Tributaries..... 98

Figure 3.1-26: GSA Gauging Stations..... 99

Figure 3.1-27: Major Sources of Radiation Exposure near SRS 104

Figure 3.2-1: Layout of HTF Including Ancillary Equipment	105
Figure 3.2-2: Typical Type I Tank.....	108
Figure 3.2-3: Typical Type I Tank Floor Configuration.....	109
Figure 3.2-4: Typical Working Slab Construction for Type I Tanks	110
Figure 3.2-5: Typical Basemat Construction for Type I Tanks	110
Figure 3.2-6: Typical Steel Liner Construction for Type I Tanks	111
Figure 3.2-7: Typical Steel Liners Construction for Type I Tanks (Late Construction Phase). 112	
Figure 3.2-8: Close-Up of Figure 3.2-7 Showing the Annulus.....	112
Figure 3.2-9: Typical Construction of a Type I Tank Concrete Vault.....	113
Figure 3.2-10: Typical Riser Construction for Type I Tanks	114
Figure 3.2-11: Support Column - Construction Phase.....	115
Figure 3.2-12: Sketch of Typical Support Column Top/Bottom Detail	116
Figure 3.2-13: Column Layout Detail.....	116
Figure 3.2-14: Type I Tank Cooling Coils - Construction Phase	117
Figure 3.2-15: Type I Tank Backfill	118
Figure 3.2-16: Typical Type II Tank	119
Figure 3.2-17: Type II Tank Working Slab and Basemat.....	120
Figure 3.2-18: Soil Hydration System below Type II Tanks.....	121
Figure 3.2-19: Lower Sand Pad Installation over the Basemat	122
Figure 3.2-20: Type II Tank Early Construction of Primary and Secondary Liner.....	123
Figure 3.2-21: Type II Tank - Early Stage of Vault Construction.....	124
Figure 3.2-22: Type II Tank - Late Stage of Vault Construction	125
Figure 3.2-23: Type II Tank Annulus Corner Detail	125
Figure 3.2-24: Support Column Dimension Details	126
Figure 3.2-25: Type II Tank Cooling Coils	127
Figure 3.2-26: Type II Tank Backfill Detail.....	128
Figure 3.2-27: Typical HTF Type III Tank	129
Figure 3.2-28: Typical HTF Type IIIA Tank.....	130
Figure 3.2-29: Early Construction of a Type III and IIIA Tanks Basemat.....	131
Figure 3.2-30: Drilled Working Slab of a Type IIIA Tank.....	132
Figure 3.2-31: Typical Leak-Detection Channel Grid in Type IIIA Tank Basemat.....	133
Figure 3.2-32: Radial Air Grooves for a Typical Type IIIA Tank	135
Figure 3.2-33: Typical Type IIIA Tank Primary and Secondary Liner - Early Construction ...	135

Figure 3.2-34: Typical Type IIIA Tank Primary and Secondary Liner - Partial Construction .	136
Figure 3.2-35: Typical Center Column Roof Support in a Type III and IIIA Tanks.....	137
Figure 3.2-36: Type III and IIIA Tanks Vent Duct Work	138
Figure 3.2-37: Typical Type III and IIIA Tanks Side Wall Rebar	139
Figure 3.2-38: Typical Type III and IIIA Tanks Top Preparation for Concrete Pour	140
Figure 3.2-39: Final Construction of a Typical Type III and IIIA Tanks.....	140
Figure 3.2-40: Insertable Coolers Used in Type III Tanks	141
Figure 3.2-41: Insertable Cooling Coil Installed in a Type III Tank.....	142
Figure 3.2-42: Typical Conical (Umbrella) Type of Deployable Cooling Coil	142
Figure 3.2-43: Cooling Coils in a Type IIIA Tank	143
Figure 3.2-44: Typical Type III and IIIA Tank - Backfill Complete.....	144
Figure 3.2-45: Typical HTF Type IV Tank	145
Figure 3.2-46: Type IV Tank Basemat Placement.....	146
Figure 3.2-47: Type IV Tank Basemat Showing Geometry of Drainage Channels	146
Figure 3.2-48: Type IV Tank Primary Liner Construction.....	147
Figure 3.2-49: Type IV Tank Dome Construction.....	148
Figure 3.2-50: Type IV Tank Concrete Vault Construction	149
Figure 3.2-51: Type IV Tank Vault Wall Shotcrete Application	149
Figure 3.2-52: Type IV Tanks with Backfill - Vermiculite Bags Showing.....	150
Figure 3.2-53: Type IV Tanks Backfill Complete	151
Figure 3.2-54: HTF Ancillary Equipment Locations.....	153
Figure 3.2-55: HTF Transfer Line Construction at Tank 30H.....	167
Figure 3.2-56: Type I Line Encasement (Sealed Concrete Trench)	168
Figure 3.2-57: Type II Line Carbon Steel Jacket.....	168
Figure 3.2-58: Type III Line Concrete Asbestos Jacket	169
Figure 3.2-59: Typical Diversion Box and Pump Pit Layout	170
Figure 3.2-60: Construction of Typical HTF PP	171
Figure 3.2-61: Interior View of HPP-3	172
Figure 3.2-62: Construction of HTF CTS PP Building 242-3H (Old)	173
Figure 3.2-63: Concentrate Transfer System PP and Pump Tank	173
Figure 3.2-64: 242-H Evaporator System Schematic	175
Figure 3.2-65: 242-H Evaporator Vessel Top View	176
Figure 3.2-66: 242-16H Evaporator System Schematic	177

Figure 3.2-67: 242-16H Evaporator Vessel Top View	178
Figure 3.2-68: 242-25H Evaporator System Schematic	179
Figure 3.2-69: 242-25H Evaporator Vessel and Cell Top View	180
Figure 3.2-70: View of the Bottom of the 242-25H Evaporator Vessel.....	181
Figure 3.2-71: 242-25H Evaporator Overheads System Condenser.....	182
Figure 3.2-72: Interior of HDB-1.....	183
Figure 3.2-73: HDB-3 during Construction Phase	184
Figure 3.2-74: Typical Leak Detection Box	186
Figure 3.2-75: Typical Modified Leak Detection Box	187
Figure 3.2-76: Typical Type I Tank Grouting Configuration.....	190
Figure 3.2-77: Typical Type II Tank Grouting Configuration	190
Figure 3.2-78: Typical Type III Tank Grouting Configuration	191
Figure 3.2-79: Typical Type IIIA Tank Grouting Configuration	191
Figure 3.2-80: Typical Type IV Tank Grouting Configuration.....	192
Figure 3.2-81: Aerial View of HTF	197
Figure 3.2-82: West Hill Area Aerial View.....	197
Figure 3.2-83: East Hill Area and HPP-5 and HPP-6 Aerial View	198
Figure 3.2-84: The HTF Closure Cap General Concept	202
Figure 3.2-85: The H-Area Tank Farm Closure Cap Conceptual Design Footprint	203
Figure 3.2-86: Closure Cap Conceptual Design, Sections A-A and B-B	204
Figure 3.2-87: Closure Cap Conceptual Design, Sections C-C and D-D	205
Figure 3.2-88: Closure Cap Conceptual Design, Section E-E.....	206
Figure 3.2-89: Closure Cap Conceptual Design, Section F-F	206
Figure 3.2-90: Closure Cap Toe and Side Slope Configuration Concept.....	209
Figure 3.2-91: The HELP Model Scenario and Results for Closure Cap Design Initial Conditions	211
Figure 4.1-1: H-Area Tank Farm Modeling Input Relationships	241
Figure 4.2-1: Conceptual Model of Pore Fluid Evolution and Plutonium Dissolution from the Residual Waste Layer	245
Figure 4.2-2: E_h Evolution during Simulated Grout Aging	250
Figure 4.2-3: Simulated Evolution of pH in Grout Pore Fluids Entering Residual Waste Layer	250
Figure 4.2-4: Simulated Evolution of Mineralogy in Tank Grout.....	251

Figure 4.2-5: Basis for Four Conditions Controlling Pore Fluid Chemistry in Residual Waste Layer of Partially Submerged Waste Tanks 253

Figure 4.2-6: pH and E_h Curves Resulting from Mixing End-member Pore Fluid Compositions for Conditions B, C, and D 254

Figure 4.2-7: pH and E_h Transitions in Grout Pore Fluid as Grout Degrades in Submerged Waste Tanks 256

Figure 4.2-8: General Flow for Selection of Solubility Controlling Phases 259

Figure 4.2-9: E_h -pH Diagram Showing Typical Regimes for Various Natural Waters 261

Figure 4.2-10: E_h -pH Diagram Showing E_h of SRS Background Water Table Wells in Relation to Iron Speciation 261

Figure 4.2-11: Uncertainty in Solubility Estimations for Neptunium, Plutonium, Uranium, and Technetium under the Six CZ Pore Fluid Conditions 269

Figure 4.2-12: Conceptual Closure Model for HTF 273

Figure 4.2-13: Closure Cap Concept for HTF 274

Figure 4.2-14: HTF PORFLOW Model Stream Traces and 100-Meter Boundary 276

Figure 4.2-15: GSA Boundary Conditions 279

Figure 4.2-16: North-South Cross-Section of GSA/PORFLOW Computational Mesh 280

Figure 4.2-17: Perspective View of GSA/PORFLOW Computational Mesh 281

Figure 4.2-18: North-South Cross Sections of GSA/PORFLOW Model - Horizontal and Vertical Hydraulic Conductivity Variations Views 282

Figure 4.2-19: The GSAD Database Relationship 283

Figure 4.2-20: Water Table Contour Maps for GSA 284

Figure 4.2-21: Comparison of (a) GSA/PORFLOW Model Predicted and (b) 2003 Water Table Maps 286

Figure 4.2-22: The GSA Geologic Cross-Section Location Map 291

Figure 4.2-23: Comparison of E-Area, F-Area, and H-Area Vadose Zone Using Core Descriptions and Gamma Ray Logs 292

Figure 4.2-24: Comparison of H-Area Vadose Zone Using CPT Logs 293

Figure 4.2-25: Working Slab for Tanks 13 through 16 294

Figure 4.2-26: Working Slab (Low Quality Concrete) Characteristic Curves 295

Figure 4.2-27: Upper and Lower Vadose Zone Characteristic Curves 296

Figure 4.2-28: Backfill Characteristic Curves 297

Figure 4.2-29: Procured Sand Characteristic Curves 302

Figure 4.2-30: Recommended Characteristic Curves for Waste Tank Grout and Concrete 305

Figure 4.2-31: Scenario with Well Water as Primary Water Source 337

Figure 4.2-32: Scenario with Stream Water as Primary Water Source	339
Figure 4.2-33: Acute Intruder Drilling Scenario.....	344
Figure 4.2-34: Chronic Intruder Agricultural (Post-Drilling) Scenario.....	347
Figure 4.3-1: Modeling Code Integration for HTF PA.....	356
Figure 4.3-2: Modeling Code Integration for HTF PA (Details of Water Flow and Transport)	357
Figure 4.4-1: Typical Type I Tank Modeling Dimensions	366
Figure 4.4-2: Typical Type II Tank Modeling Dimensions.....	368
Figure 4.4-3: Typical Type III Tank Modeling Dimensions	370
Figure 4.4-4: Typical Type IIIA Tank Modeling Dimensions	371
Figure 4.4-5: Typical Tank IV Tank Modeling Dimensions	373
Figure 4.4-6: Base Case Modeling Conditions	375
Figure 4.4-7: Case B Modeling Conditions	376
Figure 4.4-8: Case C Modeling Conditions	378
Figure 4.4-9: Case D Modeling Conditions.....	379
Figure 4.4-10: Case E Modeling Conditions	380
Figure 4.4-11: Ancillary Equipment Case Modeling Conditions	381
Figure 4.4-12: Model Process Flow	395
Figure 4.4-13: PORFLOW GSA Modeling.....	397
Figure 4.4-14: HTF PORFLOW Model Stream Traces and 100-Meter Boundary	398
Figure 4.4-15: PORFLOW Type I Tank Model	400
Figure 4.4-16: PORFLOW Type I Tank Model, Lower Corner Detail.....	401
Figure 4.4-17: PORFLOW Type II Tank Model.....	401
Figure 4.4-18: PORFLOW Type II Tank Model, Lower Corner Detail.....	402
Figure 4.4-19: PORFLOW Type III Tank Model Detail.....	402
Figure 4.4-20: PORFLOW Type III Tank Model, Lower Corner Detail	403
Figure 4.4-21: PORFLOW Type IV Tank Model, Domed Roof Explicitly Modeled.....	403
Figure 4.4-22: PORFLOW Type IV Tank Model, Lower Corner Detail	404
Figure 4.4-23: PORFLOW Type IV Tank Model, Tank Top Corner Detail.....	404
Figure 4.4-24: Type I Tank Flow Field - Year 100	405
Figure 4.4-25: Type I Tank Flow Field - Year 10,000	405
Figure 4.4-26: Type I Tank Flow Field (Immediately Prior to Liner Failure) - Year 11,397 ...	406
Figure 4.4-27: Type I Tank Flow Field - Year 20,000	406

Figure 4.4-28: Type II Tank Flow Field - Year 100	407
Figure 4.4-29: Type II Tank Flow Field - Year 10,000	407
Figure 4.4-30: Type II Tank Flow Field (Immediately Prior to Liner Failure) - Year 12,687 ..	408
Figure 4.4-31: Type II Tank Flow Field - Year 20,000	408
Figure 4.4-32: Type III Tank Flow Field - Year 100.....	409
Figure 4.4-33: Type III Tank Flow Field - Year 10,000.....	409
Figure 4.4-34: Type III Tank Flow Field (Immediately Prior to Liner Failure) - Year 12,751 ..	410
Figure 4.4-35: Type III Tank Flow Field - Year 20,000.....	410
Figure 4.4-36: Type IV Tank Flow Field - Year 100	411
Figure 4.4-37: Type IV Tank Flow Field (Immediately Prior to Liner Failure) - Year 3,638 ..	411
Figure 4.4-38: Type IV Tank Flow Field - Year 10,000	412
Figure 4.4-39: Type IV Tank Flow Field - Year 20,000	412
Figure 4.4-40: PORFLOW Type IV Tank Fast Flow Path Model	417
Figure 4.4-41: Layout and Instrumentation for VZMS at Slit Trenches	419
Figure 4.4-42: Basis for HTF PORFLOW Model and VZMS Data Comparison	420
Figure 4.4-43: HTF PORFLOW Model and VZMS Tritium Data Comparison	421
Figure 4.4-44: Surveyed SeepLines Compared to GSA/PORFLOW Model Simulation	421
Figure 4.4-45: Comparison of GSA/PORFLOW Groundwater Pathlines to Tritium Plume Emanating from E-Area Mixed Waste Management Facility	422
Figure 4.4-46: Comparison of GSA/PORFLOW Groundwater Pathlines to Contaminant Plumes Emanating from F Area	423
Figure 4.4-47: Comparison of GSA/PORFLOW Groundwater Pathlines to Tritium Contaminant Plume Emanating from H Area.....	424
Figure 4.4-48: Top Level of the HTF Stochastic Model	433
Figure 4.4-49: Contents of the Container <i>HTFTanks_Transport_Model</i>	435
Figure 4.4-50: Schematic of Modeled Components for Type I and II Tanks.....	437
Figure 4.4-51: Schematic of Modeled Components for Type III, IIIA, and IV Tanks.....	438
Figure 4.4-52: Sample Control File for <i>ReadFlowFields.DLL</i>	446
Figure 4.4-53: Contents of the Container <i>HTFAncillary_Equipment_Model</i>	447
Figure 4.4-54: HTF Waste Tank Sources with Hypothetical 100-Meter Well Location.....	451
Figure 4.4-55: PORFLOW Generated Stream Traces from Waste Tanks with Hypothetical 1- Meter and 100-Meter Boundaries	455
Figure 4.5-1: Schematic of HTF PORFLOW Model Grid for Air and Radon Pathway Analyses for Type I Tanks.....	460

Figure 4.5-2: Schematic of HTF PORFLOW Model Grid for the Air and Radon Pathway Analyses for Type II Tanks..... 461

Figure 4.5-3: Flux at Land Surface per Curie of Radionuclide Remaining Type I Tanks 469

Figure 4.5-4: Flux at Land Surface per Curie of Radionuclide Remaining in Type II Tanks ... 470

Figure 4.5-5: Radioactive Decay Chains Leading to Rn-222 475

Figure 4.5-6: Rn-222 Flux at Land Surface Resulting from Unit Source Term for Type I Tanks 477

Figure 4.5-7: Rn-222 Flux at Land Surface Resulting from Unit Source Term for Type II Tanks 478

Figure 4.8-1: Integrated Conceptual Site Model for HTF 495

Figure 5.2-1: 100 Meter Distance from HTF 502

Figure 5.2-2: Stream Traces from HTF 503

Figure 5.2-3: Contaminant Plume Leaving HTF (Aerial View)..... 504

Figure 5.2-4: Contaminant Plume Leaving HTF (Cross Section View)..... 505

Figure 5.2-5: HTF PORFLOW 1-Meter and 100-Meter Model Evaluation Sectors 506

Figure 5.2-6: HTF PORFLOW Seepage Evaluation Sectors 524

Figure 5.5-1: 100-Meter Sector MOP Peak Groundwater Pathway Dose Results within 1,000 Years 553

Figure 5.5-2: 100-Meter Sector MOP Peak Groundwater Pathway Dose Results within 10,000 Years 554

Figure 5.5-3: 100-Meter Sector MOP Peak Groundwater Pathway Dose Results within 100,000 Years 555

Figure 5.5-4: Individual Radionuclide Contributors to the Sector A 100-Meter Peak Groundwater Pathway Dose - 1,000 Years..... 558

Figure 5.5-5: Individual Radionuclide Contributors to the Sector A 100-Meter Peak Groundwater Pathway Dose - 10,000 Years..... 559

Figure 5.5-6: Individual Radionuclide Contributors to the Sector A 100-Meter Peak Groundwater Pathway Dose - 100,000 Years..... 560

Figure 5.5-7: Individual Radionuclide Contributors to the Sector B 100-Meter Peak Groundwater Pathway Dose - 1,000 Years..... 561

Figure 5.5-8: Individual Radionuclide Contributors to the Sector B 100-Meter Peak Groundwater Pathway Dose - 10,000 Years..... 562

Figure 5.5-9: Individual Radionuclide Contributors to the Sector B 100-Meter Peak Groundwater Pathway Dose - 100,000 Years..... 563

Figure 5.5-10: Individual Radionuclide Contributors to the Sector C 100-Meter Peak Groundwater Pathway Dose - 1,000 Years..... 564

Figure 5.5-11: Individual Radionuclide Contributors to the Sector C 100-Meter Peak
Groundwater Pathway Dose - 10,000 Years..... 565

Figure 5.5-12: Individual Radionuclide Contributors to the Sector C 100-Meter Peak
Groundwater Pathway Dose - 100,000 Years..... 566

Figure 5.5-13: Individual Radionuclide Contributors to the Sector C 100-Meter Peak
Groundwater Pathway Dose - 1,000 Years..... 567

Figure 5.5-14: Individual Source Contributors to the Sector A 100-Meter Peak Groundwater
Pathway Dose - 10,000 Years..... 568

Figure 5.5-15: Individual Source Contributors to the Sector B 100-Meter Peak Groundwater
Pathway Dose - 10,000 Years..... 569

Figure 5.5-16: Individual Source Contributors to the Sector C 100-Meter Peak Groundwater
Pathway Dose - 10,000 Years..... 569

Figure 5.5-17: MOP at 100-Meter Peak Water Ingestion Dose within 1,000 Years for the 100-
Meter Sectors 572

Figure 5.5-18: MOP at 100-Meter Peak Water Ingestion Dose within 10,000 Years for the 100-
Meter Sectors 573

Figure 5.5-19: MOP at 100-Meter Peak Water Ingestion Dose within 100,000 Years for the 100-
Meter Sectors 573

Figure 5.5-20: MOP at 100-Meter Peak Vegetable Ingestion Dose within 1,000 Years for the
100-Meter Sectors..... 574

Figure 5.5-21: MOP at 100-Meter Peak Vegetable Ingestion Dose within 10,000 Years for the
100-Meter Sectors..... 574

Figure 5.5-22: MOP at 100-Meter Peak Vegetable Ingestion Dose within 100,000 Years for the
100-Meter Sectors..... 575

Figure 5.5-23: MOP at Stream Peak Groundwater Pathway Dose within 10,000 Years 576

Figure 5.5-24: MOP at Stream Peak Groundwater Pathway Dose within 20,000 Years 577

Figure 5.5-25: Individual Radionuclide Contributors to the Fourmile Branch Groundwater
Pathway Dose - 20,000 Years..... 577

Figure 5.5-26: Individual Radionuclide Contributors to the UTR Groundwater Pathway Dose -
20,000 Years 578

Figure 5.5-27: MOP Peak 100-Meter Sector All-Pathway Dose within 10,000 Years 579

Figure 5.6-1: Mass Release from Type I Tank 9 - Ra-226 (Base Case)..... 586

Figure 5.6-2: Mass Release from Type I Tank 9 - Tc-99 (Base Case) 586

Figure 5.6-3: Mass Release from Type I Tank 9 - I-129 (Base Case)..... 587

Figure 5.6-4: Mass Release from Type I Tank 9 - Np-237 (Base Case) 587

Figure 5.6-5: Mass Release from Type I Tank 9 - Cs-135 (Base Case) 588

Figure 5.6-6: Mass Release from Type II Tank 13 - Ra-226 (Base Case)..... 590

Figure 5.6-7: Mass Release from Type II Tank 13 - Tc-99 (Base Case)..... 590

Figure 5.6-8: Mass Release from Type II Tank 13 - I-129 (Base Case)..... 591

Figure 5.6-9: Mass Release from Type II Tank 13 - Np-237 (Base Case) 591

Figure 5.6-10: Mass Release from Type II Tank 13 - Cs-135 (Base Case)..... 592

Figure 5.6-11: Mass Release from Type II Tank 15 - Ra-226 (Base Case)..... 593

Figure 5.6-12: Mass Release from Type II Tank 15 - Tc-99 (Base Case)..... 594

Figure 5.6-13: Mass Release from Type II Tank 15 - I-129 (Base Case)..... 594

Figure 5.6-14: Mass Release from Type II Tank 15 - Np-237 (Base Case) 595

Figure 5.6-15: Mass Release from Type II Tank 15 - Cs-135 (Base Case)..... 595

Figure 5.6-16: Mass Release from Type IV Tank 24 - Ra-226 (Base Case)..... 597

Figure 5.6-17: Mass Release from Type IV Tank 24 - Tc-99 (Base Case) 597

Figure 5.6-18: Mass Release from Type IV Tank 24 - I-129 (Base Case) 598

Figure 5.6-19: Mass Release from Type IV Tank 24 - Np-237 (Base Case)..... 598

Figure 5.6-20: Mass Release from Type IV Tank 24 - Cs-135 (Base Case) 599

Figure 5.6-21: PORFLOW Model Species-Specific Dose Contributions for Sector A 601

Figure 5.6-22: GoldSim Model Species-Specific Dose Contributions for Sector A 601

Figure 5.6-23: Plume Formed by a Steady Release of a Conservative Constituent from Tank 13
..... 602

Figure 5.6-24: Comparison between PORFLOW and GoldSim Total Dose Results for Base
Case, Sector A..... 603

Figure 5.6-25: Comparison between PORFLOW and GoldSim Total Dose Results for Base
Case, Sector B..... 603

Figure 5.6-26: Comparison between PORFLOW and GoldSim Total Dose Results for Base
Case, Sector C..... 604

Figure 5.6-27: Comparison between PORFLOW and GoldSim Total Dose Results for Base
Case, Sector E..... 604

Figure 5.6-28: Comparison between PORFLOW and GoldSim Total Dose Results for Base
Case, Sector F 605

Figure 5.6-29: Comparison between PORFLOW and GoldSim IHI Results 606

Figure 5.6-30: Difference between the Mean of Peaks and the Peak of Means 652

Figure 5.6-31: Statistical Time History of MOP Doses for Base Case (0 to 10,000 Years) 654

Figure 5.6-32: Statistical Time History of MOP Doses for Case D (0 to 10,000 Years) 654

Figure 5.6-33: Statistical Time History of MOP Doses for All Cases (0 to 10,000 Years) 655

Figure 5.6-34: Statistical Time History of MOP Doses for All Cases (0 to 100,000 Years) 655

Figure 5.6-35: Illustration of the Effects of Modified Solubility Controls on Technetium in Tank 12, Base Case, Realization R 12 670

Figure 5.6-36: Example of a GBM Model Fit Plot..... 674

Figure 5.6-37: Radionuclide-Specific MOP Dose from any Sector within 20,000 Years, Base Case..... 676

Figure 5.6-38: Radionuclide-Specific MOP Dose from any Sector within 20,000 Years, Case D 678

Figure 5.6-39: Radionuclide-Specific MOP Dose from any Sector within 20,000 Years, All Cases 680

Figure 5.6-40: Case B MOP Groundwater Pathway Dose 689

Figure 5.6-41: Case B Individual Radionuclide Contributors to MOP Groundwater Pathway Dose 689

Figure 5.6-42: Case C MOP Groundwater Pathway Dose 690

Figure 5.6-43: Case C Individual Radionuclide Contributors to MOP Groundwater Pathway Dose 690

Figure 5.6-44: Case D MOP Groundwater Pathway Dose 691

Figure 5.6-45: Case D Individual Radionuclide Contributors to MOP Groundwater Pathway Dose 691

Figure 5.6-46: Case E MOP Groundwater Pathway Dose..... 692

Figure 5.6-47: Case E Individual Radionuclide Contributors to MOP Groundwater Pathway Dose 692

Figure 5.6-48: No Closure Cap Case MOP Groundwater Pathway Dose – 10,000 Year..... 693

Figure 5.6-49: No Closure Cap Case MOP Groundwater Pathway Dose – 20,000 Year..... 694

Figure 5.6-50: No Closure Cap Case Individual Radionuclide Contributors to MOP Dose – 20,000 Years 694

Figure 5.6-51: Synergistic Case MOP Groundwater Pathway Dose by Sector - 10,000 Years 695

Figure 5.6-52: Synergistic Case MOP Groundwater Pathway Dose by Sector - 20,000 Years 696

Figure 5.6-53: Synergistic Case Individual Radionuclide Contributors to MOP Dose – 20,000 Years 696

Figure 5.6-54: Base Case MOP Groundwater Pathway Dose 697

Figure 5.6-55: Base Case Individual Radionuclide Contributors to MOP Groundwater Pathway Dose 698

Figure 5.6-56: Case B MOP Groundwater Pathway Dose 698

Figure 5.6-57: Case B Individual Radionuclide Contributors to MOP Groundwater Pathway Dose 699

Figure 5.6-58: Case C MOP Groundwater Pathway Dose 699

Figure 5.6-59: Case C Individual Radionuclide Contributors to MOP Groundwater Pathway Dose	700
Figure 5.6-60: Case D MOP Groundwater Pathway Dose	700
Figure 5.6-61: Case D Individual Radionuclide Contributors to MOP Groundwater Pathway Dose	701
Figure 5.6-62: Case E MOP Groundwater Pathway Dose.....	701
Figure 5.6-63: Case E Individual Radionuclide Contributors to MOP Groundwater Pathway Dose	702
Figure 5.6-64: Base Case Grout Transition Time Study.....	703
Figure 5.6-65: Case C Grout Transition Time Study.....	703
Figure 5.6-66: Individual Radionuclide Contributors to MOP Dose for Base Case Fast Grout Transition Time.....	704
Figure 5.6-67: Individual Radionuclide Contributors to MOP Dose for Base Case Slow Grout Transition Time.....	704
Figure 5.6-68: Individual Radionuclide Contributors to MOP Dose for Case C Fast Grout Transition Time.....	705
Figure 5.6-69: Individual Radionuclide Contributors to MOP Dose for Case C Slow Grout Transition Time.....	705
Figure 5.6-70: Comparison of Solubility Studies with the Base Case.....	707
Figure 5.6-71: Individual Radionuclide Contributors to MOP Dose for the Pessimistic Solubility with no Iron Co-precipitation.....	707
Figure 5.6-72: Individual Radionuclide Contributors to MOP Dose for the Typical Solubility with no Iron Co-precipitation.....	708
Figure 5.6-73: Individual Radionuclide Contributors to MOP Dose for the Pessimistic Solubility with Iron Co-precipitation.....	708
Figure 5.6-74: Comparison of the Calcareous Zone Sensitivity MOP Dose to the Base Case MOP Dose.....	709
Figure 5.6-75: Individual Radionuclide Contributors to MOP Dose for the Calcareous Zone Sensitivity Case.....	710
Figure 5.6-76: Soil K_d Variability MOP Groundwater Pathway Dose	711
Figure 5.6-77: Individual Radionuclide Contributors to MOP Dose, Normal K_d (Base Case)	711
Figure 5.6-78: Individual Radionuclide Contributors to MOP Dose for Half the Soil K_d	712
Figure 5.6-79: Individual Radionuclide Contributors to MOP Dose for Quarter the Soil K_d ...	712
Figure 5.6-80: No Fast Flow Path Type I Tank MOP Dose (Base Case).....	714
Figure 5.6-81: No Fast Flow Path Type II Tank MOP Dose (Base Case).....	714
Figure 5.6-82: No Fast Flow Path Type IV Tank MOP Dose (Base Case).....	715

Figure 5.6-83: No Fast Flow Path Type III and IIIA Tank MOP Dose (Base Case)..... 715

Figure 5.6-84: Partial Fast Flow Path Type I Tank MOP Dose (Cases B and C) 716

Figure 5.6-85: Partial Fast Flow Path Type II Tank MOP Dose (Cases B and C) 716

Figure 5.6-86: Partial Fast Flow Path Type IV Tank MOP Dose (Cases B and C)..... 717

Figure 5.6-87: Partial Fast Flow Path Type III and IIIA Tanks MOP Dose (Cases B and C)... 717

Figure 5.6-88: Full Fast Flow Path Type I Tank MOP Dose (Cases D and E) 718

Figure 5.6-89: Full Fast Flow Path Type II Tank MOP Dose (Cases D and E) 718

Figure 5.6-90: Full Fast Flow Path Type IV Tanks MOP Dose (Cases D and E)..... 719

Figure 5.6-91: Full Fast Flow Path Type III and IIIA Tank MOP Dose (Cases D and E) 719

Figure 5.6-92: Cementitious Degradation Timing Type I Tank MOP Dose 720

Figure 5.6-93: Cementitious Degradation Timing Type II Tank MOP Dose..... 721

Figure 5.6-94: Cementitious Degradation Timing Type IV Tank MOP Dose 721

Figure 5.6-95: Cementitious Degradation Timing Type III and IIIA Tanks MOP Dose 722

Figure 5.6-96: Water Ingestion Rate Variability on MOP Groundwater Pathway Dose..... 723

Figure 5.6-97: PORFLOW Stream Traces with Hypothetical 100-Meter Boundary and
Associated GoldSim Well Locations 724

Figure 5.6-98: Comparison of Base Case Results with Sum of Max Dose, All Sectors, Base Case
..... 726

Figure 5.6-99: Comparison of Base Case Results with Sum of Max Dose, All Sectors, Max
Velocity Analysis..... 729

Figure 5.6-100: Comparison of Base Case Results with Sum of Max Dose, All Sectors, Min
Velocity Analysis..... 730

Figure 5.6-101: Comparison of Base Case Results with Sum of Max Doses, All Sectors, Mean
Velocity Analysis..... 731

Figure 5.6-102: 100-Meter Sector MOP Peak Groundwater Pathway Dose Results within
1,000,000 Years Using the GoldSim Model in Deterministic Mode..... 732

Figure 6.4-1: Acute Intruder Dose Results within 10,000 Years - Drilling into a 3-Inch Transfer
Line 766

Figure 6.4-2: Concentration of Contributing Radionuclides in the Soil from Drill Cuttings 767

Figure 6.4-3: Annual Dose to Chronic Intruder - 10,000 Years after HTF Facility Closure..... 768

Figure 6.4-4: Annual Dose to Chronic Intruder - 20,000 Years after HTF Facility Closure..... 770

Figure 6.5-1: Acute Intruder Dose Impact from Drilling into a 4-inch Transfer Line vs. a 3-inch
Transfer Line..... 772

Figure 6.5-2: Chronic Intruder Dose Impact from Drilling into a 4-inch Transfer Line vs. a 3-
inch Transfer Line..... 772

Figure 6.5-3: Acute Intruder Dose Impact from Drilling into Tank 13 vs. a 3-inch Transfer Line 774

Figure 6.5-4: Chronic Intruder Dose Impact from Drilling into Tank 13 vs. a 3-inch Transfer Line 774

Figure 6.5-5: Hypothetical Drilling Locations within the 1-Meter Facility Boundary..... 775

Figure 6.5-6: Chronic Intruder Dose Results - Drilling into Select Locations within 1-Meter Facility Boundary..... 776

Figure 6.5-7: Chronic Intruder Dose Contributors for a Well Drilled within the 1-Meter Boundary, Near Tank 12..... 776

Figure 6.5-8: Probabilistic IHI Dose Results from a Well near Tank 12, within 1-Meter Boundary..... 778

Figure 6.5-9: Comparison of Probabilistic Doses to Deterministic Doses from a Well near Tank 12, within 1-Meter Boundary..... 779

Figure 7.1-1: Individual Radionuclide Contributors to Sector-A 100-Meter Peak Groundwater Pathway Dose, 10,000 Years, Base Case..... 781

Figure 7.1-2: Individual Source Contributors to Sector-A 100-Meter Peak Groundwater Pathway Dose, 20,000 Years, Base Case 781

Figure 7.1-3: Model Input Timeline for Various HTF Model Segments 782

Figure 7.1-4: Statistical Time History of MOP Doses for All Cases (0 to 10,000 Years) 787

Figure 7.1-5: Statistical Time History of MOP Doses for All Cases (0 to 100,000 Years) 788

Figure 7.1-6: Peak All-Pathways MOP Dose within 10,000 Years..... 790

Figure 7.1-7: Peak All-Pathways MOP Dose within 100,000 Years..... 791

Figure 7.1-8: Peak Acute Dose to the IHI within 10,000 Years 792

Figure 7.1-9: Peak Dose to the IHI within 10,000 Years..... 792

Figure 7.1-10: Peak Dose to the IHI within 20,000 Years..... 793

LIST OF TABLES

Table 1.0-1: Key Values from Regulatory Documents 39

Table 1.0-2: Summary Radiological Results for HTF 41

Table 3.1-1: Population Distribution and Percent of ROI for Counties and Selected Communities
..... 67

Table 3.1-2: Characterization and Monitoring Data in the GSAD 94

Table 3.1-3: Water Quality in the Savannah River Upstream and Downstream from SRS
(Calendar Year 2010)..... 102

Table 3.1-4: Water Quality in Selected SRS Streams (Calendar Year 2010)..... 102

Table 3.1-5: Well Monitoring Results for Major Areas within SRS, 2007-2008..... 103

Table 3.2-1: Waste Tank Locations and Elevations for HTF 106

Table 3.2-2: Type II Tank Primary Liner Thicknesses 122

Table 3.2-3: Minimum Primary Liner Plate Thicknesses for Type III and IIIA Tanks..... 134

Table 3.2-4: Type IV Tank Side Penetrations in Primary Liner 147

Table 3.2-5: HTF Transfer Line Segment Listing 154

Table 3.2-6: HTF Pump Pit Sizes and Elevations..... 170

Table 3.2-7: Evaporator System Locations and Elevations 174

Table 3.2-8: Diversion Boxes and Associated Service 183

Table 3.2-9: Mechanical and Chemical Requirements for Grout Material 193

Table 3.2-10: Physical and Chemical Factors Related to Grout Stability 194

Table 3.2-11: Closure Cap Initial Configurations Evaluated and Condition Results 199

Table 3.2-12: Function of the Conceptual Closure Cap Layers..... 207

Table 3.2-13: Closure Cap Potential Degradation Mechanisms and Course of Action..... 212

Table 3.2-14: Conceptual Closure Cap Estimated Infiltration over Time 214

Table 3.3-1: Radionuclides of Concern 216

Table 3.3-2: Chemical Inventory of Concern 216

Table 3.4-1: Waste Removal Process Residual Volumes 218

Table 3.4-2: Tank Annulus Material Volume Estimates 219

Table 3.4-3: Estimated Annulus Radiological Inventories (2032) 220

Table 3.4-4: Estimated Annulus Chemical Inventories 221

Table 3.4-5: Type II Sand Pad Radiological Inventory (2032) 223

Table 3.4-6: Type II Sand Pad Chemical Inventory 225

Table 3.4-7: Waste Tank Groupings 227

Table 3.4-8: Waste Tank Groupings for Pu-238.....	227
Table 3.4-9: Estimated Radiological Inventory (Ci) at Closure	228
Table 3.4-10: Estimated Chemical Inventory (kg) at Closure	232
Table 3.4-11: Estimated Radiological Inventory (Ci) in Transfer Lines at Closure.....	234
Table 3.4-12: Estimated Chemical Inventory (kg) in Transfer Lines at Closure.....	235
Table 3.4-13: Estimated Radiological Inventory in Pump Tanks and CTS Tank at Closure	236
Table 3.4-14: Estimated Chemical Inventory in Pump Tanks and CTS Tank at Closure	236
Table 3.4-15: Estimated Radiological Inventory (Ci) in Evaporator Vessels at Closure	237
Table 3.4-16: Estimated Chemical Inventory (kg) in Evaporator Vessels at Closure.....	237
Table 4.2-1: Summary of Chemical Phases.....	243
Table 4.2-2: Proposed Tank 18 Grout Formulation.....	246
Table 4.2-3: Chemical Compositions of Major Grout Constituents and Bulk Composition of Proposed Grout	246
Table 4.2-4: Calculated Normative Mineralogy of Proposed Grout and Equilibrium Mineralogy as Recalculated by GWB	247
Table 4.2-5: Infiltrating Water Composition Used in Grout Evolution Simulations.....	248
Table 4.2-6: Minerals Allowed in Simulations of Tank Grout Chemical Evolution.....	249
Table 4.2-7: E _h , pH, and Dissolved Inorganic Carbon at Different Chemical Conditions during Simulated Evolution of Tank Grout.....	251
Table 4.2-8: Groundwater Composition Used to Mix with Grout Pore Fluids to Produce Conditions B, C, and D.....	252
Table 4.2-9: Chemical Compositions of Contaminated Zone Pore Fluids for Conditions A, B, C, and D.....	255
Table 4.2-10: Pore Fluid Compositions Used for Solubility Estimates for Each Chemical Condition.....	260
Table 4.2-11: Calculated Solubility and Controlling Phases of Radionuclides of Interest	263
Table 4.2-12: Estimated Solubilities of Neptunium, Plutonium, and Uranium in Oxidized Regions II and III at E _h Values in Equilibrium with Dissolved Oxygen	265
Table 4.2-13: Solubility of Host Iron Phases the Pore Fluids of the Different Chemical Conditions.....	267
Table 4.2-14: Apparent Solubilities (mol/L) of Potentially Coprecipitated Elements	267
Table 4.2-15: Vadose Zone Thickness beneath HTF Waste Tanks.....	275
Table 4.2-16: Upper Vadose Zone and Effective Saturated Zone Soil Properties	277
Table 4.2-17: Hydraulic Head Residuals - GSA/PORFLOW Model and Field Data through 2006	287

Table 4.2-18: Conceptual Closure Cap Layers Top to Bottom	289
Table 4.2-19: Conceptual Closure Cap Infiltration over Time	289
Table 4.2-20: Waste Tank Working Slab Information by Type	294
Table 4.2-21: Estimated Working Slab Material Properties of Interest.....	295
Table 4.2-22: Estimated Vadose Zone Material Properties of Interest.....	296
Table 4.2-23: Estimated Backfill Material Properties of Interest	297
Table 4.2-24: Waste Tank Backfill Information by Type.....	298
Table 4.2-25: Recommended K_d Values for the Vadose Zone	300
Table 4.2-26: Estimated Sand Material Properties of Interest	302
Table 4.2-27: Vadose Zone Thickness for HTF	303
Table 4.2-28: Cementitious Material Initial Properties	304
Table 4.2-29: Recommended K_d Values for Cementitious Materials.....	307
Table 4.2-30: Cementitious Material Degradation Transition Times (Yrs) by Waste Tank Type	313
Table 4.2-31: Comprehensive Sensitivity Analysis of Carbon Steel Liner	317
Table 4.2-32: Carbon Steel Liner Life Estimates by Waste Tank Type.....	319
Table 4.2-33: Corrosion Induced Failure Times for Stainless Steel Transfer Lines	320
Table 4.2-34: Analysis of Stainless Steel Transfer Lines Submerged in Groundwater.....	322
Table 4.2-35: Upper Vadose Zone and Effective Saturated Zone Soil Properties	323
Table 4.2-36: Potential MOP Stabilized Contaminant Exposure Pathways	324
Table 4.2-37: Potential Intruder Waste Exposure Pathways	329
Table 4.4-1: Waste Tank Case Summary	374
Table 4.4-2: Type I Tank Process Change Timeline	383
Table 4.4-3: Type I Tank (No Liner) Process Change Timeline	384
Table 4.4-4: Type II Tank Process Change Timeline	385
Table 4.4-5: Type II Tank (No Liner) Process Change Timeline.....	386
Table 4.4-6: Type III Tank Process Change Timeline.....	387
Table 4.4-7: Type IIIA Tank Process Change Timeline.....	388
Table 4.4-8: Type IIIA Tank West Process Change Timeline.....	389
Table 4.4-9: Type IV Tank Process Change Timeline	390
Table 4.4-10: PORFLOW Materials Palette	416
Table 4.4-11: Liner Failure Times	426
Table 4.4-12: Parametric Cases (No Fast Flow Zones)	427

Table 4.4-13: Parametric Cases (Partial Fast Flow Zones).....	428
Table 4.4-14: Parametric Cases (Full Fast Flow Zones).....	429
Table 4.4-15: Vertical Discretization of the Basemat by Waste Tank Type	444
Table 4.4-16: Instruction Data Passed to <i>ReadFlowFields.DLL</i>	445
Table 4.4-17: Data Extracted from the Flow Field Files	445
Table 4.4-18: Vertical Discretization of the Unsaturated Zone by Ancillary Equipment Source	448
Table 4.4-19: Summary of Biotic Pathways by Receptor.....	449
Table 4.4-20: Contaminant-Specific 100-Meter Concentration to Seepline Concentration Ratio	453
Table 4.4-21: Inadvertent Intruder Analysis Wells.....	455
Table 4.5-1: Layers and Thicknesses for Type I and II Tanks and Cover Material	458
Table 4.5-2: Particle Density, Total Porosity, Average Saturation, and Air-Filled Porosity by Layer for Type I and II Tanks Baseline Scenario	463
Table 4.5-3: Radionuclides and Compounds of Interest for Air and Radon Pathway Analyses	465
Table 4.5-4: Apparent Inverse Henry’s Law Coefficients for Various Pore Solutions for Waste Tanks.....	466
Table 4.5-5: Apparent Inverse Henry’s Law Coefficients and K_d by Radionuclide (Type I and II Tanks)	467
Table 4.5-6: Effective Air-Diffusion Coefficients by Radionuclide/Compound and Material for Type I and II Tanks and Closure Cap	468
Table 4.5-7: Peak Fluxes for Each Radionuclide for Type I Tanks.....	470
Table 4.5-8: Peak Fluxes for Each Radionuclide for Type II Tanks	471
Table 4.5-9: 100-Meter DRFs and Type I Tank Exposure Levels within 10,000 Years.....	472
Table 4.5-10: 100-Meter DRFs and Type II Tank Exposure Levels within 10,000 Years.....	472
Table 4.5-11: UTR Seepline (2,360 Meter) DRFs and Type I Tank Exposure Levels within 10,000 Years	472
Table 4.5-12: UTR Seepline (2,360 Meter) DRF and Type II Tank Exposure Levels within 10,000 Years	473
Table 4.5-13: Fourmile Branch Seepline (1,170 Meter) DRFs and Type I Tank Exposure Levels within 10,000 Years	473
Table 4.5-14: Fourmile Branch Seepline (1,170 Meter) DRFs and Type II Tank Exposure Levels within 10,000 Years	473
Table 4.5-15: Simulated Peak Instantaneous Rn-222 Flux over 10,000 Years at the Land Surface for Type I Tanks.....	478

Table 4.5-16: Simulated Peak Instantaneous Rn-222 Flux over 10,000 Years at the Land Surface for Type II Tanks	478
Table 4.6-1: Soil-to-Vegetable Transfer Factors (Unitless)	481
Table 4.6-2: Feed-to-Milk Transfer Factors (d/L)	482
Table 4.6-3: Feed-to-Beef Transfer Factors (d/kg).....	483
Table 4.6-4: Water-to-Fish Bioaccumulation Factors (L/kg)	484
Table 4.6-5: Feed-to-Poultry Transfer Factors (d/kg).....	485
Table 4.6-6: Feed-to-Egg Transfer Factors (d/kg).....	485
Table 4.6-7: Crop Exposure Times and Productivity	486
Table 4.6-8: Physical Parameters.....	487
Table 4.6-9: Individual Exposure Times and Consumption Rates	488
Table 4.7-1: Internal and External DCFs.....	490
Table 5.2-1: Baseline Case	501
Table 5.2-2: Approximate Aquifer Travel Distance to HTF 100-Meter Boundary.....	503
Table 5.2-3: Radiological 100-Meter Concentrations for UTRA-UZ	507
Table 5.2-4: Radiological 100-Meter Concentrations for UTRA-LZ.....	510
Table 5.2-5: Radiological 100-Meter Concentrations for the Gordon Aquifer	513
Table 5.2-6: Chemical 100-Meter Concentrations for UTRA-UZ	517
Table 5.2-7: Chemical 100-Meter Concentrations for UTRA-LZ.....	518
Table 5.2-8: Chemical 100-Meter Concentrations for Gordon Aquifer	519
Table 5.2-9: Determination of Sensitivity Run Radionuclides for the 100-Meter Boundary....	521
Table 5.2-10: Seepline Sensitivity Run Radionuclide Concentrations for UTR	525
Table 5.2-11: Seepline Sensitivity Run Radionuclide Concentrations for Fourmile Branch	525
Table 5.3-1: Projected Total HTF Inventory of Gaseous Radionuclides.....	526
Table 5.3-2: 100-Meter Boundary DRFs and Type I Tank Dose within 10,000 Years.....	527
Table 5.3-3: 100-Meter Boundary DRFs and Type II Tank Dose within 10,000 Years	527
Table 5.3-4: Fourmile Branch Seepline DRFs and Type I Tank Dose within 10,000 Years	528
Table 5.3-5: Fourmile Branch Seepline DRFs and Type II Tank Dose within 10,000 Years ...	528
Table 5.3-6: UTR Seepline DRFs and Type I Tank Dose within 10,000 Years	529
Table 5.3-7: UTR Seepline DRFs and Type II Tank Dose within 10,000 Years	529
Table 5.3-8: Projected Type I or II Tanks Inventory of Isotopes Producing Rn-222.....	530
Table 5.3-9: Peak Instantaneous Rn-222 Flux at Land Surface from Type I Tanks	530
Table 5.3-10: Peak Instantaneous Rn-222 Flux at Land Surface from Type II Tanks	531

Table 5.5-1: MOP at 100-Meter Peak Groundwater Pathways Dose by Sector	551
Table 5.5-2: MOP at 100-Meter Peak Groundwater Pathway Dose Individual Radionuclide Contributions at Peak Years – Sectors C (1,000 years) and A (10,000 years)	566
Table 5.5-3: MOP at 100-Meter Peak Groundwater Pathway Dose Individual Source Contributions at Peak Years - Sectors A and C Peak	570
Table 5.5-4: MOP at 100-Meter Peak Groundwater Pathway Dose Individual Contributions at Peak Years - Sector C	571
Table 5.5-5: MOP at 100-Meter Peak Groundwater Pathway Dose Individual Contributions at Peak Years - Sector A	571
Table 5.5-6: MOP at 100-Meter Peak Water Ingestion Doses by Sector	572
Table 5.5-7: MOP at Stream Peak Groundwater Pathways Dose.....	576
Table 5.5-8: MOP at Stream Peak Groundwater Pathway Dose Individual Contributions for Fourmile Branch	578
Table 5.5-9: MOP at Stream Peak Groundwater Pathway Dose Individual Contributions for UTR.....	579
Table 5.6-1: Summary of Selected Waste Tanks.....	584
Table 5.6-2: Summary of Selected Ancillary Equipment.....	584
Table 5.6-3: Radiological Inventory Multipliers	610
Table 5.6-4: Chemical Inventory Multipliers for All Waste Tank Types.....	614
Table 5.6-5: Case Probability for All Waste Tank Types.....	615
Table 5.6-6: Liner Failure Times	616
Table 5.6-7: Parametric Cases (No Fast Flow Zones).....	617
Table 5.6-8: Parametric Cases (Partial Fast Flow Zones).....	618
Table 5.6-9: Parametric Cases (Full Fast Flow Zones).....	619
Table 5.6-10: Probability Distributions for Various Phases Controlling Reduced Region II Solubility.....	620
Table 5.6-11: Probability Distributions for Various Phases Controlling Oxidized Region II Solubility.....	620
Table 5.6-12: Probability Distributions for Various Phases Controlling Oxidized Region III Solubility.....	621
Table 5.6-13: K_d Variability in the HTF GoldSim Model	622
Table 5.6-14: Basemat Thickness Variability in the HTF GoldSim Model	623
Table 5.6-15: Probability Distribution of Liner Failure Times by Waste Tank Types and Case	627
Table 5.6-16: Pore Volume Distribution for Chemical Condition Step Change	629

Table 5.6-17: Mean Darcy Velocity from Waste Tanks.....	631
Table 5.6-18: Mean Darcy Velocity from Ancillary Equipment.....	632
Table 5.6-19: Distribution for Saturated Zone Thickness	633
Table 5.6-20: Saturated Zone Width for Waste Tanks	633
Table 5.6-21: Saturated Zone Width for Ancillary Equipment	634
Table 5.6-22: Probability of Drilling into the Aquifers	634
Table 5.6-23: Stochastic Crop Exposure Times and Productivity.....	635
Table 5.6-24: Stochastic Physical Parameters	636
Table 5.6-25: Stochastic Individual Exposure Times and Consumption Rates.....	637
Table 5.6-26: Stochastic Human Consumption Rates for Poultry and Eggs	638
Table 5.6-27: Stochastic Transfer Factors for Milk.....	639
Table 5.6-28: Stochastic Transfer Factors for Beef.....	642
Table 5.6-29: Stochastic Transfer Factors for Fish.....	645
Table 5.6-30: Time Stepping for Probabilistic (Uncertainty and Sensitivity) Modeling	650
Table 5.6-31: GoldSim Model Files Used in the Probabilistic UA/SA.....	651
Table 5.6-32: Statistics of the Peak Doses within Any Time Step	652
Table 5.6-33: Peak Doses of the Statistics.....	653
Table 5.6-34: Five Highest MOP Dose Results from 1,000 Base Case Realizations within 10,000 Years	657
Table 5.6-35: Five Highest MOP Dose Results from 1,000 Case D Realizations within 10,000 Years	662
Table 5.6-36: Five Highest MOP Dose Results from 1,000 All Cases Realizations within 10,000 Years	666
Table 5.6-37: Most Sensitive Parameters for the Endpoints of Interest for Base Case	675
Table 5.6-38: Most Sensitive Parameters for the Endpoints of Interest for Case D	677
Table 5.6-39: Most Sensitive Parameters for the Endpoints of Interest for All Cases	679
Table 5.6-40: Summary of Waste Tanks Selected for Barrier Analysis.....	682
Table 5.6-41: Summary of Radionuclides Selected for Barrier Analysis.....	682
Table 5.6-42: Barrier Analysis Variability	683
Table 5.6-43: Barrier Analyses Configuration Case Summary by Material Zone	684
Table 5.6-44: Base Case and Alternative Cases Peak Doses.....	686
Table 5.6-45: Synergistic Sensitivity Case Solubility Controlling Phases	688
Table 5.6-46: Values for Solubility Study	706
Table 5.6-47: Liner Failure Times.....	713

Table 5.6-48: Peak Dose Results for Various Periods of Time	726
Table 5.6-49: Average Saturated Zone Darcy Velocities for Waste Tanks.....	728
Table 5.7-1: Groundwater Radionuclide Concentrations at 1 Meter from HTF.....	733
Table 5.7-2: Groundwater Chemical Concentrations at 1 Meter from HTF.....	735
Table 6.1-1: Radiological 1-Meter Concentrations for UTRA-UZ	741
Table 6.1-2: Radiological 1-Meter Concentrations for UTRA-LZ.....	744
Table 6.1-3: Radiological 1-Meter Concentrations for Gordon Aquifer	747
Table 6.1-4: Chemical 1-Meter Concentrations for UTRA-UZ	750
Table 6.1-5: Chemical 1-Meter Concentrations for UTRA-LZ.....	751
Table 6.1-6: Chemical 1-Meter Concentrations for Gordon Aquifer	752
Table 6.4-1: Acute Intruder Dose Contributors	767
Table 6.4-2: Chronic Intruder Peak Dose Contributors - 10,000 Years after HTF Facility Closure	769
Table 7.1-1: Summary Statistics from Uncertainty Analyses.....	786
Table 7.1-2: Summary of the Performance Assessment Results	795

ACRONYMS

ACP	Area Completion Projects
ALARA	As Low As Reasonably Achievable
ARF	Airborne Release Factor
ARP	Actinide Removal Process
CAB	Citizens Advisory Board
CAP-88	Clean Air Act Assessment Package - 1988
CERCLA	Comprehensive Environmental Response, Compensation, and Liability Act
CFD	Computational Fluid Dynamics
CFR	Code of Federal Regulation
CLM	Central Climatology
CMCOC	Contaminant Migration Constituents of Concern
COPC	Constituent of Potential Concern
CPT	Cone Penetration Test
CRC	Cesium Removal Column
CSH	Calcium Silicate Hydrate
CSRA	Central Savannah River Area
CTS	Concentrate Transfer System
CWA	Clean Water Act
CZ	Contamination Zone
DB	Diversion Box
DCF	Dose Conversion Factor
DOE	U.S. Department of Energy
DOE-HQ	U.S. Department of Energy - Headquarters
DOE-SR	U.S. Department of Energy - Savannah River Operations Office
DRF	Dose Release Factor
DSA	Documented Safety Analysis
DWPF	Defense Waste Processing Facility
EIS	Environmental Impact Statement
EPA	U.S. Environmental Protection Agency
ERDMS	Environmental Restoration Data Management System
ETF	Effluent Treatment Facility
FEPs	Features, Events, and Processes
FFA	Federal Facility Agreement

FORTRAN	Formula Translating System
FTF	F-Area Tank Farm
GBM	Gradient Boosting Model
GCL	Geosynthetic Clay Liner
GCP	General Closure Plan
GM	Geometric Mean
GS	General Service
GSA	General Separations Area
GSAD	General Separations Area Database
GSD	Geometric Standard Deviation
GTG	GoldSim Technology Group LLC
GWB	The Geochemist's Workbench
HDPE	High Density Polyethylene
HELP	Hydrologic Evaluation of Landfill Performance
HTF	H-Area Tank Farm
IBM	International Business Machine
ICM	Integrated Conceptual Model
ICP-MS	Inductively Coupled Plasma - Mass Spectrometry
ICRP	International Commission on Radiological Protection
IHI	Inadvertent Human Intruder
ISMS	Integrated Safety Management System
LDB	Leak Detection Box
LLW	Low-Level Waste
MCL	Maximum Contaminant Level
MCU	Modular Caustic Side Solvent Extraction Unit
MEI	Maximally Exposed Individual
MLDB	Modified Leak Detection Box
MOP	Member of the Public
MP	Management Policy
MSL	Mean Sea Level
MWCO	Molecular Weight Cut-Off
NCRP	National Council on Radiation Protection and Measurements
NDAA	Ronald W. Reagan National Defense Authorization Act for Fiscal Year 2005
NERP	National Environmental Research Park

NESHAP	National Emissions Standards for Hazardous Air Pollutants
NPDES	National Pollutant Discharge Elimination System
NRC	U.S. Nuclear Regulatory Commission
NRMP	Natural Resources Management Plan for the Savannah River Site
ORNL	Oak Ridge National Laboratory
OS/VS2	Operating System/Virtual Storage 2
OU	Operable Unit
PA	Performance Assessment
PC	Performance Category
PCA	Pollution Control Act
PMP	Probable Maximum Precipitation
PP	Pump Pit
PRG	Preliminary Remediation Goal
PS	Production Support
PTSM	Principal Threat Source Material
PUREX	Plutonium-Uranium Extraction Process
QA	Quality Assurance
QAMP	Quality Assurance Management Plan
QC	Quality Control
R ²	Coefficient of Determination
RCRA	Resource Conservation and Recovery Act
RESRAD	RESidual RADioactivity Computer Software
RI	Remedial Investigation
ROD	Record of Decision
ROI	Region of Influence
RSL	Regional Screening Level
SA	Sensitivity Analysis
SC	Safety Class
SCDHEC	South Carolina Department of Health and Environmental Control
SCS	Soil Conservation Service
SDF	Saltstone Disposal Facility
SDWA	Federal Safe Drinking Water Act
SI	Sensitivity Indices
SMA	Strong Motion Accelerometer

SP	Service Pack
SQAP	Software Quality Assurance Plan
SREL	Savannah River Ecology Laboratory
SRNL	Savannah River National Laboratory
SRS	Savannah River Site
SS	Safety Significant
TCCZ	Tan Clay Confining Zone
TEDE	Total Effective Dose Equivalent
UA	Uncertainty Analysis
USACE	U.S. Army Corps of Engineers
USCS	Unified Soil Classification System
USDA	U.S. Department of Agriculture
USGS	U.S. Geological Survey
UTR	Upper Three Runs
UTRA	UTR Aquifer
UTRA-LZ	UTRA-Lower Zone
UTRA-UZ	UTRA-Upper Zone
VZMS	Vadose Zone Monitoring System
WAC	Waste Acceptance Criteria
WCS	Waste Characterization System
WES	Waterways Experiment Station

Note: Some units of measure have been included in this list however; most units of measure are common to the technical discipline of this PA's target audience and have not been defined.

1.0 EXECUTIVE SUMMARY

The H-Area Tank Farm (HTF) at the Department of Energy's (DOE) Savannah River Site (SRS) is an active facility consisting of 29 waste tanks and associated ancillary equipment (e.g., transfer lines, evaporators, and pump tanks). The HTF waste tanks are in varying degrees of service or waste removal operations with waste that was generated primarily from the H-Canyon chemical separations processes. The HTF, which began radioactive waste operations in 1955, continues today to receive routine transfers of waste from the H-Canyon operations.

This HTF Performance Assessment (PA) was prepared to support the operational closure of the HTF underground waste tanks and ancillary equipment. This PA provides the technical basis and results to be used in the development of performance-based, risk-informed decisions related to the closure of HTF including the development of subsequent documents that will assess and demonstrate compliance with the pertinent requirements identified in the regulatory documents listed below for waste tank operational closure and eventual final facility closure of the HTF.

- U.S. Department of Energy Manual 435.1-1 (DOE M 435.1-1)
- *Ronald W. Reagan National Defense Authorization Act (NDAA) for Fiscal Year 2005*, Section 3116 (NDAA Section 3116)
- South Carolina Department of Health and Environmental Control Regulations Chapter 61, Articles 67 and 82 (SCDHEC R.61-67, SCDHEC R.61-82)
- *Federal Facility Agreement for the Savannah River Site (FFA)*

The regulatory process includes a HTF 3116 Basis Document, which will be used to demonstrate compliance with the criteria set forth in NDAA Section 3116. A Draft HTF 3116 Basis Document will be developed and approved by the DOE in consultation with the U.S. Nuclear Regulatory Commission (NRC). Approval of a separate document, the HTF 3116 Determination, by the Secretary of Energy is then required to determine that the residual waste remaining in the waste tanks and ancillary structures following cleaning activities (as described in the Draft HTF 3116 Basis Document) can be managed as non-high-level waste (HLW) for purposes of closure decisions. The Secretary of Energy determination under NDAA Section 3116 incorporates by reference Title 10 Code of Federal Regulations, Part 61 (10 CFR 61), Subpart C performance objectives. This HTF PA provides the technical basis that will be used to demonstrate compliance with 10 CFR 61.41 (Protection of the General Population from Releases of Radioactivity), and 61.42 (Protection of Individuals from Inadvertent Intrusion) performance objectives in the HTF 3116 Basis Document.

The 10 CFR 61, Subpart C performance objectives are comparable to the performance objectives from DOE M 435.1-1 in that specific objectives are defined for a future member of the public (MOP) and a future inadvertent intruder. The HTF PA has also been prepared to support implementation of applicable DOE M 435.1-1 requirements including an HTF Tier 1 closure plan, waste tank-specific special analyses, and Tier 2 closure plans.

Compliance with the SCDHEC regulations will be demonstrated using two primary documents that are supported by this HTF PA. The first is to be an HTF General Closure Plan (GCP), which will establish the general protocols, requirements, and processes for final facility closure of the HTF. The second document(s) are waste tank-specific closure modules that authorize the operational closure of a specific waste tank, group of waste tanks, or ancillary equipment. Both the HTF GCP and the waste tank-specific closure modules are reviewed and approved by the DOE and SCDHEC.

The key requirements from these documents necessitate development and calculation of the following for the HTF:

- Projected radiological doses to a hypothetical MOP
- Projected radiological doses to a hypothetical inadvertent intruder
- Projected radiological doses to a human receptor via the air pathway
- Projected radon flux
- Projected water concentrations (Table 1.0-1)

All of these calculations were performed to provide results over significant periods of time (i.e., hundreds to thousands of years) into the distant future to inform closure activities within HTF today or in the near future. The water concentrations were calculated for both radioactive and chemical contaminants at multiple locations outside the HTF.

Table 1.0-1: Key Values from Regulatory Documents

Document	MOP Dose	Inadvertent Intruder Dose	Air Pathway Dose	Radon Flux	Groundwater Protection
DOE M 435.1-1	25 mrem/yr	500 mrem/yr – acute 100 mrem/yr – chronic	10 mrem/yr	20 pCi/m ² /s at ground surface	< MCL
NDA Section 3116: 10 CFR 61.41 and 61.42	25 mrem/yr	500 mrem/yr	N/A	N/A	N/A
SCDHEC Primary Drinking Water Regulations	N/A	N/A	N/A	N/A	< MCL

N/A = Not applicable

MCL = Maximum Contaminant Level

The HTF PA modeling consisted of a hybrid approach of both deterministic modeling for performance results and probabilistic plus targeted deterministic modeling for uncertainty and sensitivity analyses (UA/SA). Deterministic evaluations were used to assess the Base Case and to perform single parameter SA, all utilizing the 3-D PORFLOW computer code. The Base Case evaluation utilized what can be characterized as “most probable yet defensible” discrete input parameter values and yielded a single set of annual doses over time. The PORFLOW deterministic evaluation modeled flow and transport in both the near field and far field. A series of 72 discrete flow profiles were also developed using the PORFLOW model to establish a set of flow parameters that were utilized in a GoldSim analytical model that was developed for

probabilistic evaluations. The probabilistic model results were benchmarked against the deterministic model to ensure consistency in model results. The probabilistic evaluation ensured that collective impacts were evaluated in the UA and sensitive parameters were identified in the SA.

The deterministic and probabilistic models both used a general HTF Integrated Conceptual Model (ICM) that simulates radiological and chemical contaminant release from the 29 waste tanks and associated ancillary structures in the HTF. An independent conceptual waste release model was used to simulate stabilized contaminant release from the grouted waste tanks based on various chemical phases in the waste tanks, controlling solubility and thereby affecting the timing and rate of release from the contamination zone (CZ), (i.e., the lower region of the waste tank that is modeled to contain the residual material). This ICM approach considers the integrity of the waste tank steel liners and cementitious barriers during waste tank modeling. Case A is the Base Case modeling configuration for the waste tanks, while Cases B through E are sensitivity cases that utilize alternate, less probable waste tank configurations with different sets of underlying assumptions regarding liner integrity, cementitious material degradation, and fast flow path potential as described in detail in Section 4.4.2, and summarized in Table 4.4-1.

To assess dose impacts from the HTF, and to account for the unique groundwater flow below and adjacent to the HTF, the 100-meter boundary was determined and broken down into a series of sectors designated as “A” through “F.” Figure 1.0-1 shows the centerline flow patterns for each HTF waste tank and the sector designations.

Figure 1.0-1: HTF Centerline Flows and Sector Designations



The modeling results in the HTF PA provide the technical information at different points of assessment that can be utilized in the subsequent regulatory decision documents. The MOP doses are provided at 100 meters, consistent with the requirements of DOE M 435.1-1, in addition to the Upper Three Runs (UTR) and Fourmile Branch seeplines, and were calculated using the parameters presented in Sections 4.6 and 4.7. This HTF PA provides groundwater radionuclide concentrations at 1 meter, 100 meters, and exposure points at the two seeplines impacted by the HTF. The groundwater concentrations are provided for each of the three potentially impacted aquifers as applicable, as a part of the HTF groundwater modeling. The HTF PA also provides groundwater concentrations for chemical contaminants at 1 meter and 100 meters. In addition, this HTF PA provides inadvertent intruder doses consistent with the requirements of DOE M 435.1-1 and 10 CFR 61.42, as well as analyses for the air pathways and radon ground-surface flux consistent with the requirements of DOE M 435.1-1. The key radiological results from the HTF PA Base Case modeling and dose calculations are summarized in Table 1.0-2.

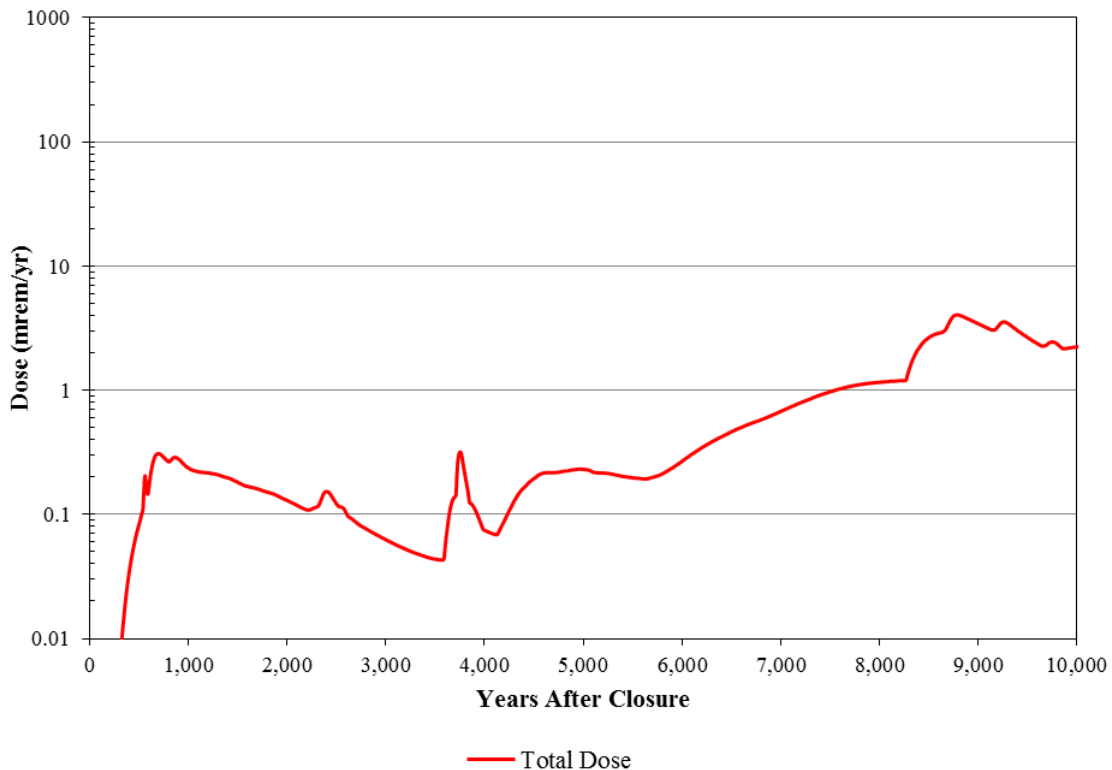
Table 1.0-2: Summary Radiological Results for HTF

Location	Peak Dose		
	All-Pathways Dose (mrem/yr)	Groundwater Pathway Dose (mrem/yr)	Air Pathway Dose (mrem/yr)
100 meters from HTF	0.3 (Within 1,000 Years) 4 (Within 10,000 Years)	0.3 (Within 1,000 Years) 4 (Within 10,000 Years)	< 0.0001
At Seeplines (UTR and Fourmile Branch)	< 0.1 (Within 10,000 Years)	< 0.1 (Within 10,000 Years)	< 0.0001
	Acute Dose (mrem)	Chronic Dose (mrem/yr)	
1 meter from HTF (Inadvertent Intruder)	1 (Within 1,000 Years)	40 (Within 1,000 Years)	
	Peak Radon Flux (pCi/m²/s)		
Ground Surface	~ 2E-15		

To put the HTF radiological doses into perspective, it should be noted that an individual flying on a roundtrip transcontinental trip in the United States will receive approximately 5 millirem during the course of these flights. The average United States citizen receives 620 millirem in a year (NCRP-160) and individuals living in Denver, Colorado will receive greater than 1,000 millirem each year due to the higher “natural” terrestrial and cosmic radiation levels in this area.

The peak all-pathways annual dose for the MOP at 100 meters is calculated using the highest 100-meter, groundwater pathway dose results in combination with the air pathway results. As described in Section 5.3, the air pathway dose is negligible; therefore, the all-pathway dose is the same as the groundwater pathway dose. The peak all-pathways annual dose regardless of sector is shown in Figure 1.0-2 for a period of 10,000 years following final HTF closure activities.

Figure 1.0-2: Peak All-Pathways MOP Dose for HTF



For HTF, the peak 100-meter groundwater pathway dose within 10,000 years following closure is from Sector A (4 mrem/yr), with the next highest peak doses originating in Sectors B (2 mrem/yr) and C (2 mrem/yr). The majority of contaminants migrating from Type I and II tanks follow a path to the 100-meter boundary at Sector A. Sectors B and C receive the majority of contaminant concentrations from plumes emanating from Type II and IV tanks. The maximum doses within 10,000 years for the Base Case are recorded in Sectors A, B, and C because 1) certain Type I and II tanks (e.g., Tanks 12, 14, 15, and 16) initially have degraded liners at closure (i.e., liners are conservatively not considered in the model for these tanks) thus releases from these waste tanks can start much earlier, 2) residuals in the annulus and sand pads in Type I and II tanks (where applicable) release prior to liner failure, and 3) Type IV tanks have liners that fail during the 10,000-year period. Type III and IIIA tanks do not contribute to the peak dose within a 10,000-year period because the steel liner is assumed to remain an impediment to flow during this time-period. This is also true for the Type I tanks that have initially intact liners at facility closure and do not have residuals present in their respective tank annuli.

It is important to recognize that the peak doses are associated with specific locations and times. Because there are over 40 unique and independent inventory sources modeled in the HTF model, there is significant temporal and spatial complexity inherent in the modeling system. Removal of any one inventory source may reduce the doses (including the peak dose where applicable) associated with that source, but the overall HTF PA peak dose will not necessarily be reduced by a corresponding amount; the overall HTF PA peak dose may merely move to a different location

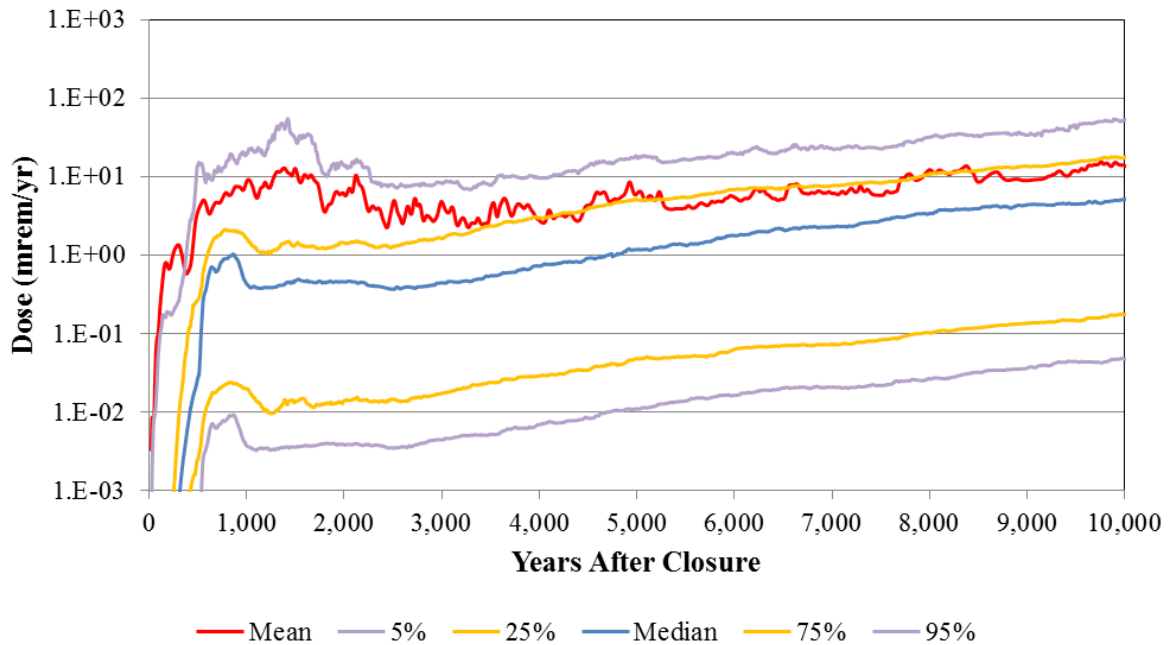
and time. The peak groundwater pathway doses vary over time and location (e.g., the six HTF sectors) and, while not fully independent (due to plume overlap), there is variability across the six sectors.

In addition to the Base Case deterministic analysis, various deterministic sensitivity analyses were performed. Section 5.6.7 presents dose results for the alternate cases, designated Cases B through E, as well as the impact to dose from not modeling a closure cap. These alternative cases were developed to provide insight into the impacts if less probable degradation mechanisms occurred in the waste tank systems over time compared to the most probable conditions modeled within the Base Case. Section 4.4.2 describes the different cases, Cases B through E, in detail. Section 5.6.7.3 describes the conditions of the no closure cap analysis. Results of these improbable sensitivity cases show that the complete hydraulic degradation of the waste tank grout (and annulus grout) at 500 years, and the inclusion of fast flow paths through the grout, as modeled for Cases B and D, has the most impact on peak dose within 10,000 years. These conditions result in an earlier peak dose and a peak dose magnitude increase (e.g., from 4 mrem/yr in Base Case to over 14 mrem/yr in Cases B through D). The “No Closure Cap” Case peak dose (approximately 5 mrem/yr) is not significantly greater than the Base Case peak.

Section 5.6.7 also presents dose results for various sensitivity studies of significant parameters (e.g., grout transition time, key solubility values, liner failure time). These sensitivity studies show that there are multiple barriers to release and variability surrounding a single barrier does not appear to be so great as to have an unacceptable impact on peak dose within 10,000 years. In addition, the sensitivity studies show that dose impact of an individual parameter can be highly dependent on other parameters with the impact of the sensitivity varying to different degrees depending on the parameters involved, with the sensitivity often varying non-linear and/or counter-intuitively in some cases.

A series of probabilistic analyses were developed for further understanding of the model and its associated input parameters, and to support risk-inform closure decisions for the HTF. UA/SA can be used to place the deterministic analyses results into context (i.e., to risk inform the deterministic results). The peak of the mean all-pathways doses within 10,000 years using the probabilistic model (e.g., for Base Case) was 13 mrem/yr from the UA. The median (50th percentile) and 95th percentile values for Base Case were 2.3 mrem/yr and 24 mrem/yr, respectively. In addition to the Base Case analyses, a set of realizations was performed as part of the probabilistic analyses to collectively evaluate the effects of all postulated waste tank cases. In this “All Cases” analysis, every waste tank model independently sampled the possible waste tank cases during each realization, allowing the probabilistic analysis to consider waste tank case variability. Figure 1.0-3 provides the statistical time history of MOP doses for the All Cases analysis.

Figure 1.0-3: Statistical Time History of MOP Doses for All Cases (0 to 10,000 Years)



The peak-groundwater radionuclide concentrations were calculated, and on an individual radionuclide basis, all of the radionuclides were less than the MCL or Preliminary Remediation Goal (PRG) at a distance of 1 meter from the HTF within 1,000 years with the MCL values for beta and photon emitters calculated per EPA 815-R-02-001. The total beta-gamma radionuclides, when calculated on a per-year basis, are less than the total beta-gamma limit. The peak concentrations for 26 chemicals were calculated, and all were less than the MCL or Regional Screening Level (RSL) at a distance of 1 meter from the HTF within 1,000 years.

2.0 INTRODUCTION

The potential radiological dose to receptors typically is evaluated with a PA model that simulates the release of radionuclides from the closure site, transport of radionuclides through the environment, and exposure to potential receptors from residual material. The PA process provides the technical basis for subsequent decision documents to demonstrate compliance with the performance objectives of the 10 CFR 61, DOE O 435.1, Chg. 1, FFA, and SCDHEC R.61-82 and R.61-67. The HTF PA utilized an enhanced inter-agency scoping meeting process during the development/planning phases of the HTF PA, which resulted in an increased understanding of the HTF PA modeling approaches and assumptions.

2.1 General Approach

The PAs are used to assess the long-term fate and transport of residual contamination in the environment and provide the DOE with reasonable assurance that the operational closure of the SRS tank farm underground radioactive waste tanks and ancillary equipment will meet defined performance objectives for the protection of human health and the environment into the future.

The HTF PA was completed to support multiple decision documents, including the HTF GCP and tank-specific closure modules. These documents support the closure of waste tanks to meet the FFA commitments. [WSRC-OS-94-42] The HTF PA development process included a public scoping meeting with the interface agencies in the input development stage. The purpose of the scoping meeting held during the development/planning phase of HTF PA inputs was to identify potential issues early, assess the reasonableness of key modeling assumptions, and reduce the risk of significant rework and remodeling after the HTF PA is finalized.

In accordance with the FFA, DOE obtained wastewater construction and operating permits from SCDHEC for the waste tanks. The DOE is now operationally closing the SRS waste tanks that do not meet the standards established in Appendix B of the FFA. [WSRC-OS-94-42]

After waste removal operations, any residual contaminants will be stabilized and the waste tanks shall be removed from service (operationally closed) in accordance with the PCA S.C. Code Ann., Section 48-1-10, et seq. (1985) and all applicable regulations promulgated pursuant to the PCA. [WSRC-OS-94-42, Section IX.E.(4)] Applicable regulations include SCDHEC Regulation 61-67, *Standards for Wastewater Facility Construction* and SCDHEC Regulation 61-82, *Proper Closeout of Wastewater Treatment Facilities*. Removal from service includes operational closure of the waste tank systems and then removal from Construction Permit #17,424-IW and the FFA, which will control the subsequent remediation of the HTF. [WSRC-OS-94-42] The DOE followed this process in closure of Tanks 17 and 20, located in the F-Area Tank Farm (FTF).

The general protocols that the DOE is following in closing the underground waste tank systems appear in the HTF GCP. Each waste tank system will have a detailed waste tank-specific closure module, and after each waste tank system operational closure activities have been satisfactorily completed, the waste tank system will be removed from the conditions of Construction Permit

#17,424-IW. The contents of the HTF GCP and the waste tank-specific closure modules will be consistent with applicable regulations implementing the PCA S.C. Code Ann., Section 48-1-10, et seq. (1985). [Title 48_Chapter 1_SC Laws]

Because of previous releases to the environment, the HTF will be closed under provisions of the FFA after all the individual waste tank and ancillary equipment, as applicable, are operationally closed. In the FFA, each tank farm has been designated as an “operable unit” (OU). The OUs will undergo closure in accordance with the FFA (Sections XI through XVI) and any RCRA/CERCLA response action relating to the waste tank systems. [WSRC-OS-94-42 Appendix C]

Relative to the performance objectives for the tank farms, this closure process facilitates consideration for both single waste tank and collective waste-tank system impacts from the closed waste tanks and related ancillary equipment. In the area, in determining the final closure status of the General Separations Area (GSA), the impacts from both the waste tank systems and previous release sites will be considered.

The HTF PA is prepared to support implementation of applicable DOE O 435.1, Chg. 1 requirements, including the Tier 1 closure plan. The HTF PA is also prepared in support of the waste determination process to ensure the NDAA Section 3116 criteria are met before the waste tanks are operationally closed. The NDAA was passed by congress on October 9, 2004, and signed by the President on October 28, 2004. Section 3116 of the NDAA contains the criteria for DOE to use to classify waste as non-HLW for on-site disposition purposes and is applicable only to South Carolina and Idaho. The DOE intends to coordinate the waste determination and state-closure plan approval efforts to support the waste-tank closure schedule provided in the FFA. [NDAA_3116, WSRC-OS-94-42]

2.1.1 Performance Assessment Scoping Meeting

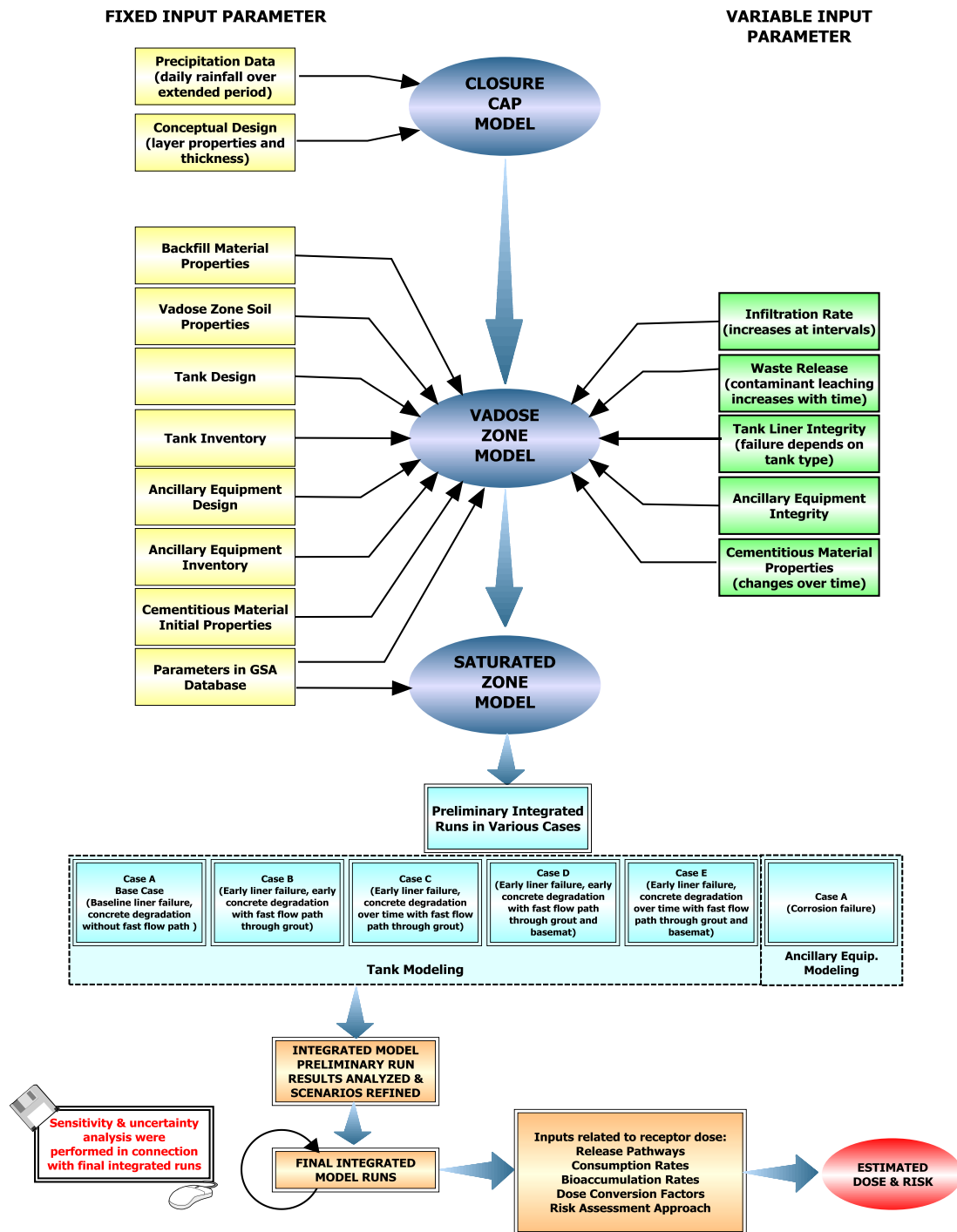
Completion of closure activities such that they meet FFA commitments created the desire to reduce the comment resolution schedule durations and any potential remodeling resulting from the reviews of the HTF PA after completion. It was therefore prudent to have a scoping meeting during HTF PA input data development to obtain up-front understanding, and discuss assumptions to minimize downstream rework and remodeling. While it is recognized that concerns may surface on input parameters utilized after modeling and additional reviews are completed, the up-front review and comments will minimize the risk and severity of concerns after completion of modeling.

The purpose of the scoping meeting was to facilitate candid technical discussion on input parameters related to the HTF PA modeling. To accomplish this goal, on April 20 through 22, 2010, a public meeting with representatives from SCDHEC, EPA, and the NRC was held to discuss and review individual input packages. [ML100970781] This scoping meeting (and the HTF PA process in general) also incorporated improvements from previous PA developments, in particular lessons learned from the FTF PA.

2.1.2 Modeling Process

Figure 2.1-1 illustrates the general process followed in implementing the ICM for the HTF PA. This figure shows the three component models and their key inputs.

Figure 2.1-1: HTF PA Modeling Relationships



Some key inputs involve fixed parameters that do not change over time, these are shown on the left side of Figure 2.1-1 where as the key inputs on the right side, do change over time. The manner in which an input changes is described in later sections of this PA. Input packages were prepared as review materials for the scoping meeting. The input package contents and any action items from the scoping meetings are incorporated into the respective HTF PA sections. The enhanced consultation process advantages are further discussed in *Enhanced Consultation Process for Waste Determination Activities Conducted Under the Ronald W. Reagan National Defense Authorization Act for Fiscal Year 2005*, a memo issued by the NRC in June of 2007 concerning the FTF PA scoping meetings process. [ML071550458]

As shown in Figure 2.1-1, five waste tank cases and one ancillary equipment case were identified for the model runs, which were accomplished using the applicable computer codes identified in Section 4.3. These cases were analyzed by running the models using different combinations.

The results of the preliminary model runs were analyzed. Based on this analysis, the model was refined. After these refinements were made, the final model runs were performed. The UA/SAs were performed in connection with the final model runs, with the results being incorporated into the final model runs. The SA included a series of model runs to evaluate the importance of specific barriers to radionuclide release.

The result of this process produced potential contaminant concentrations in groundwater that could affect a MOP or an intruder. The data for radiological contaminants were used in combination with the inputs related to receptors (Figure 2.1-1) to estimate the potential dose to a hypothetical MOP or an intruder. The data for non-radiological contaminants were used as specified in Section 4.8 to determine the resulting risk to the hypothetical MOP. This risk assessment approach followed the SRS Area Completion Projects (ACP) protocols for human health and ecological risk assessments. [ERD-AG-003_F.17, ERD-AG-003_P.1.4, ERD-AG-003_P.1.5, ERD-AG-003_P.5.2, ERD-AG-003_P.10.1]

2.2 General Facility Description

2.2.1 Savannah River Site

The SRS is located in south-central South Carolina, approximately 100 miles from the Atlantic Coast. The major physical feature at SRS is the Savannah River, approximately 20 miles of which serves as the southwestern boundary of the site and the South Carolina-Georgia border. The SRS encompasses portions of Aiken, Barnwell, and Allendale counties in South Carolina. The SRS occupies approximately 310 square miles, or 198,000 acres, and contains operations, service, and research and development areas. The developed areas occupy less than 10 % of the SRS footprint while the remainder of the site is undeveloped forest or wetlands. [SRS-REG-2007-00002]

2.2.2 H-Area Tank Farm

H Area is in the north-central portion of the SRS and occupies 395 acres. Section 3.1.1 provides detailed location information for H Area and the location of HTF within H Area. The HTF is an active facility consisting of 29 carbon steel waste tanks in varying degrees of service or waste removal operations. The waste was generated primarily from the H-Canyon chemical separations processes.

The proposed sequence of events for closure of the HTF is as follows:

- Operational closure of the Type I, II, and IV waste tanks, and finally the Type III and IIIA waste tanks. The ancillary equipment, such as transfer lines, pump tanks, pump pits (PPs), diversion boxes (DBs) and valve boxes, will be retired from service as appropriate with a goal of closing geographic sections of the HTF in stages.
- Following closure of a geographic section, that section will be left in an interim state in preparation for final facility closure of the HTF OU. For example, the section may be filled in with backfill after operational closure of the individual waste tanks and ancillary equipment to establish an even-grade elevation with the remainder of the HTF.
- Following operational closure of all the HTF waste tanks and ancillary equipment, the HTF will undergo final facility closure of the HTF OU in accordance with the FFA. [WSRC-OS-94-42]

2.3 Facility Life Cycle

The HTF waste tanks were built during five separate construction periods, with a different waste tank design for each period, leading to the designation of the following five different waste tank groups:

- Tanks 9 through 12 are Type I waste tanks and were constructed in the early 1950's
- Tanks 13 through 16 are Type II waste tanks and were constructed between 1955 and 1956
- Tanks 21 through 24 are Type IV waste tanks and were constructed between 1958 and 1962
- Tanks 29 through 32 are Type III waste tanks and were constructed between 1966 and 1970
- The fifth group of 13 waste tanks, which consists of Tanks 35 through 43 and 48 through 51 are Type IIIA waste tanks and they were constructed between 1974 and 1981.

The listed waste tank types and numbers identified above are located in the HTF and are not sequential because waste tank numbers 1 through 8, 17 through 20, 25 through 28, 33 and 34, and 44 through 47 are all located in the FTF and they are addressed in the FTF PA issued previously. [SRS-REG-2007-00002] The history of the construction periods for the waste tanks is documented in the *Annual Radioactive Waste Tank Inspection Program – 2011*, SRR-STI-2012-00346. Waste tank liner and ancillary equipment integrity is discussed in Section 4.2.2.2.6.

The HTF is currently in the operational period during which waste transfers into the HTF are still permitted. Waste removal from the waste tanks is also in progress during the operational period.

Once the HTF waste tanks and ancillary equipment have been closed, it is anticipated that a closure cap will be installed (for the purpose of this PA, a 100-year period of institutional control is assumed to begin after the closure cap is installed). Receipt operations will end several years prior to final closure (i.e., the beginning of 100-year period of institutional control), which is currently anticipated in 2032.

The closure cap will be monitored, maintained, and repaired as necessary during the institutional control period.

2.4 Related Documents

The HTF PA was prepared within the regulatory context of low-level waste (LLW) management per DOE O 435.1, Chg. 1 and the associated implementation manual (DOE M 435.1-1). Additional context has been added to address NDAA Section 3116, SCDHEC wastewater construction and operations permit regulations, and the SRS FFA pursuant to Section 120 of CERCLA and Sections 3008(h) and 6001 of RCRA. [SCDHEC R.61-67, SCDHEC R.61-82, DHEC_01-25-1993, WSRC-OS-94-42] The *Radioactive Waste Management Manual* and the *Format and Content Guide for U.S. Department of Energy Low-Level Waste Disposal Facility Performance Assessments and Composite Analyses - DRAFT* were also relied on for guidance. [DOE M 435.1-1, DOE Format Guide] This PA was influenced by, and has an influence on, other documents that are discussed in this section.

2.4.1 Groundwater Protection Management Program

In accordance with the FFA, DOE obtained the Permit #17,424-IW from SCDHEC for the underground liquid waste tanks. The HTF GCP and tank-specific closure modules will document requirements for protection of water resources. These documents support the operational closure of waste tanks to meet FFA commitments. [WSRC-OS-94-42] The FFA requires SRS to comply with all applicable federal, state, and local regulations for the operation, closure, and any RCRA/CERCLA remediation of the HTF OU. The appropriate measures for protection of water resources have been determined to be the State Primary Drinking Water Regulations (SCDHEC R.61-58) MCLs. The MCLs for the radionuclides is based on 4 mrem/yr for beta-gamma emitting nuclides, 15 pCi/L for alpha-emitting nuclides, and 5 pCi/L for radium. The MCLs are listed with the 100-meter results in Section 5.2 and the 1-meter results in Section 6.1.

The plan for protection of groundwater at SRS is documented in the Savannah River Site Groundwater Protection Program (SRNS-TR-2009-00076). The hydrogeologic information utilized in this HTF PA is consistent with that in the groundwater protection program. The Savannah River Site Groundwater Protection Program is focused on those activities regulated by external agencies (i.e., SCDHEC and EPA). Consistent with guidance for preparing the HTF PA, the requirement of DOE O 435.1, Chg.1 to identify impacts to water resources has been addressed by assessing the concentrations of radioactive or chemical contaminants against standards for public drinking water supplies established by SCDHEC. [SRNS-TR-2009-00076, DOE O 435.1, Chg. 1]

2.4.2 Savannah River Site End State Vision

The *Savannah River Site End State Vision* focuses on site facilities and areas that are the responsibility of the DOE Office of Environmental Management, which includes the HTF. [PIT-MISC-0089] This document describes planned end states for these facilities and areas. It indicates that each of the 29 underground waste tanks in the HTF will be cleaned, filled with grout to stabilize residual material, and operationally closed. Like the *Savannah River Site Long Range Comprehensive Plan*, which is addressed below, the *Savannah River Site End State Vision* is founded on the following basic assumptions about land ownership and use. [PIT-MISC-0041, PIT-MISC-0089]

- The entire site will be owned and controlled by the federal government in perpetuity
- The property will be used only for industrial purposes
- Site boundaries will remain unchanged
- Residential use will not be allowed on-site

The DOE solicited public input into the *Savannah River Site End State Vision*. The document contains an appendix that addresses public comments received, including recommendations/endorsement from the SRS Citizens Advisory Board (CAB). [PIT-MISC-0089]

2.4.3 Savannah River Site Long Range Comprehensive Plan

The *Savannah River Site Long Range Comprehensive Plan* provides the framework for integrating the SRS mission and vision with ecological, economic, cultural, and social factors in a regional context to support decision-making for near-term and long-term use of the site. This plan reflects a cooperative working relationship between the DOE and the State of South Carolina. [PIT-MISC-0041]

The *Savannah River Site Long Range Comprehensive Plan* describes the current site conditions, defines a vision for the evolution of the site over the next 50 years, outlines actions to achieve the vision, and guides the allocation of resources toward attainment of that vision. This plan provides guidance and direction for the future physical development of the site and provides a framework within which detailed analyses will be conducted to determine the courses of action required to reach optimum site configuration. The plan is based on specific assumptions. If these assumptions were to change, the plan would be updated to reflect the changed conditions. Chapter 3 of the *Savannah River Site Long Range Comprehensive Plan* contains the Future Land Use Plan. [PIT-MISC-0041] Guidelines on which the SRS land use is based include:

- Giving priority to protection of workers and the public
- Maintaining site security
- Maintaining other appropriate institutional controls
- Considering worker, public, and environmental risks, benefits, and costs
- Restricted use programs for units regulated under CERCLA or under RCRA
- Maintaining existing SRS boundaries
- Continuing federal ownership of the land
- Prohibiting residential use of any SRS land

The DOE considered stakeholder input on future use of the site property, as was solicited in development of the *Savannah River Site End State Vision*. Chapter 3 of the *Savannah River Site Long Range Comprehensive Plan* describes future use of the site that was developed with input from public meetings, workshops, and consultation with state and federal agencies. [PIT-MISC-0041, PIT-MISC-0089]

2.4.4 High-Level Waste Environmental Impact Statement

In May 2002, the DOE issued the *High-Level Waste Tank Closure Final Environmental Impact Statement* (EIS) on waste tank cleaning and stabilization alternatives. [DOE-EIS-0303] The DOE studied five alternatives:

- Empty, clean and fill waste tank with grout
- Empty, clean and fill waste tank with sand
- Empty, clean and fill waste tank with saltstone
- Clean and remove waste tanks
- No action

The EIS concluded the “empty, clean, and fill with grout” option was preferred. The DOE also issued an EIS Record of Decision (ROD) selecting the “empty, clean, and fill with grout” alternative for SRS waste tank closure. [DOE-EIS-0303 ROD]

Evaluations described in the EIS showed the “empty, clean and fill with grout” alternative to be the best approach to minimize human health and safety risks associated with closure of the waste tanks. [DOE-EIS-0303 ROD] This alternative offers several advantages over the other alternatives evaluated such as:

- Provides greater long-term stability of the waste tanks and their residual waste than the “empty, clean, and fill waste tank with sand” approach
- Provides for retaining radionuclides within the waste tanks by use of reducing agents in a fashion that the “empty, clean, and fill waste tank with sand” would not
- Avoids the technical complexities and additional worker radiation exposure of the “empty, clean, and fill with waste tank with saltstone” approach
- Produces smaller impacts due to radiological contaminant transport than the “empty, clean, and fill with waste tank with sand/saltstone” alternatives
- Avoids the excessive personnel radiation exposure and greater occupational safety impact that would be associated with the “clean and remove waste tanks” alternative

2.4.5 Federal Facility Agreement for the Savannah River Site

The FFA entered into agreement by SCDHEC, the DOE, and the EPA “governs the corrective/remedial action process from site investigation through site remediation and describes procedures... for that process.” [WSRC-OS-94-42] The FFA results in enforceable timetables for the closure of waste tanks as well as provisions for prevention and mitigation of releases or potential releases from the waste tank systems. Pursuant to the FFA, Section IX, SRS received construction and operating approval from SCDHEC on March 3, 1993 (Permit #17,424) for the HTF with the exception of Tank 50. [DHEC_01-25-1993] The primary vessel for Tank 16 has been cleaned and is not available for service.

Tank 50 received operating approval from SCDHEC on September 12, 1988 (Permit #14520). [DHEC_09-12-1988] The FFA, Section IX.E, addresses the eventual elimination of waste tanks and ancillary equipment from service and the operational closure of the waste tanks. For waste tanks and systems that are governed under a wastewater construction permit, the closure must be performed in accordance with the South Carolina PCA, and applicable regulations implementing that Act. [WSRC-OS-94-42, Title 48_Chapter 1_SC Laws]

The SRS waste tanks that do not meet secondary containment standards, as established in the FFA, must be operationally closed per the FFA schedule. There are 24 waste tanks at SRS that do not meet the secondary containment standards. Twelve of these waste tanks are located in HTF. Within the FTF, Tanks 17 and 20 have been previously operationally closed, and Tanks 18 and 19 in FTF are the next two waste tanks that have been operationally closed.

The DOE has determined that there are previous release sites in the waste tank systems that may require response actions under the FFA. These release sites were previously included in the FFA by DOE at the time of approval for evaluation and possible remediation under a separate schedule. [WSRC-OS-94-42]

2.5 Performance Criteria

The PA objectives are identified in DOE M 435.1-1 and 10 CFR 61 referenced by the NDAA. Section 3116 of the NDAA specifies the criteria for DOE to classify residual waste as non-HLW for purposes of onsite disposition. The NDAA is applicable only to South Carolina and Idaho. The DOE intends to coordinate the waste determination and state closure-plan approval efforts to support the waste-tank closure schedule provided in the FFA. [NDAA_3116, WSRC-OS-94-42]

2.5.1 DOE M 435.1-1 Performance Objectives and Requirements

The DOE LLW disposal performance objectives are defined in DOE M 435.1-1 IV.P (1). DOE Headquarters (DOE-HQ) issued a letter from Mr. Rispoli to Mr. Allison, *Compliance with DOE M 435.1-1 Waste Incidental to Reprocessing Requirements and Implementation of Section 3116(a) of the National Defense Authorization Act for Fiscal Year 2005 (NDAA)*, which offers guidance and clarification concerning the requirements in DOE O 435.1, Chg.1 when the requirements of NDAA Section 3116 are also applicable to avoid duplication of efforts. [DOE_02-09-2006]

The DOE LLW disposal performance objectives (DOE M 435.1-1 IV.P (1)) are:

“Low-level waste disposal facilities shall be sited, designed, operated, maintained, and closed so that a reasonable expectation exists that the following performance objectives will be met for waste disposed of after September 26, 1988:

(a) Dose to representative members of the public shall not exceed 25 mrem (0.25 mSv) in a year Total Effective Dose Equivalent (TEDE) from all exposure pathways, excluding the dose from radon and its progeny in air.

(b) Dose to representative members of the public via the air pathway shall not exceed 10 mrem (0.10 mSv) in a year TEDE, excluding the dose from radon and its progeny.

(c) *Release of radon shall be less than an average flux of 20 pCi/m²/s (0.74 Bq/m²/s) at the surface of the disposal facility. Alternatively, a limit of 0.5 pCi/l (0.0185 Bq/l) of air may be applied at the boundary of the facility.”*

Item (a) is similar to 10 CFR 61.41 and this PA provides the information relative to items (b) and (c) for completeness.

In addition to the DOE LLW disposal performance objectives cited above, the following information from DOE M 435.1-1 IV.P (2) is considered.

(g) *For purposes of establishing limits on radionuclides that may be disposed of near-surface, the performance assessment shall include an assessment of impacts to water resources.*

(h) *For purposes of establishing limits on the concentration of radionuclides that may be disposed of near-surface, the performance assessment shall include an assessment of impacts calculated for a hypothetical person assumed to inadvertently intrude for a temporary period into the low-level waste disposal facility. For intruder analyses, institutional controls shall be assumed to be effective in deterring intrusion for at least 100 years following closure. The intruder analyses shall use performance measures for chronic and acute exposure scenarios, respectively, of 100 mrem in a year and 500 mrem total effective dose equivalent excluding radon in air.*

Item (g) is similar to the SCDHEC groundwater protection requirement and the acute exposure performance measure from item (h) is similar to 10 CFR 61.42. Information on the chronic exposure performance measure from item (h) is included for completeness.

2.5.2 10 CFR 61 Performance Objectives

Subpart C of 10 CFR 61 lists the five performance objectives, which are reproduced below:

“Section 61.40 General requirement.

Land disposal facilities must be sited, designed, operated, closed, and controlled after closure so that reasonable assurance exists that exposures to humans are within the limits established in the performance objectives in Sections 61.41 through 61.44.”

“Section 61.41 Protection of the general population from releases of radioactivity.

Concentrations of radioactive material which may be released to the general environment in ground water, surface water, air, soil, plants, or animals must not result in an annual dose exceeding an equivalent of 25 millirems to the whole body, 75 millirems to the thyroid, and 25 millirems to any other organ of any member of the public. Reasonable effort should be made to maintain releases of radioactivity in effluents to the general environment as low as is reasonably achievable.”

The NRC acknowledged that using a performance objective of 25 mrem/yr effective dose is acceptable versus considering individual organ doses. [NUREG-1854]

“Section 61.42 Protection of individuals from inadvertent intrusion.

Design, operation, and closure of the land disposal facility must ensure protection of any individual inadvertently intruding into the disposal site and occupying the site or contacting the waste at any time after active institutional controls over the disposal site are removed.”

The NRC acknowledged that using a whole body dose-equivalent limit of 500 mrem/yr effective dose is appropriate to assess intruder scenarios. [NUREG-1854]

“Section 61.43 Protection of individuals during operations.

Operations at the land disposal facility must be conducted in compliance with the standards for radiation protection set out in part 20 of this chapter, except for releases of radioactivity in effluents from the land disposal facility, which shall be governed by Section 61.41 of this part. Every reasonable effort shall be made to maintain radiation exposures as low as is reasonably achievable.”

“Section 61.44 Stability of the disposal site after closure.

The disposal facility must be sited, designed, used, operated, and closed to achieve long-term stability of the disposal site and to eliminate to the extent practicable the need for ongoing active maintenance of the disposal site following closure so that only surveillance, monitoring, or minor custodial care are required.”

2.6 Summary of Key Assessment Assumptions

Numerous assumptions were made in assessing the performance of HTF and are noted and discussed in subsequent sections. A summary of the key assumptions in the analyses prepared in support of the HTF PA are listed below. Assumptions pertaining to models used in support of the HTF PA refer to the deterministic Base Case model. Assumptions pertaining to alternative model cases are discussed in Section 4.2.2.

2.6.1 General Facility Description Assumptions

The *Long Range Comprehensive Plan* assumes that the entire site will be owned and controlled by the federal government in perpetuity. [PIT-MISC-0041] However, for the purpose of this PA, no federal protection is assumed beyond the 100-year period of institutional control. The 100-year period of institutional control is assumed to begin in year 2032. A list of specific key model assumptions can be found in Table 5.2-1.

2.6.2 Site Characteristics Assumptions

Infiltration rates and aquifer depths can vary naturally over long periods. Short-term changes in these parameters (e.g., seasonal, annual fluctuations, etc.) are not simulated in the conceptual model due to extended time ranges involved in the model. A steady-state model

was used to approximate the flow field and the groundwater divide between the two streams, for example, UTR and Fourmile Branch, remained constant over the course of the modeling.

The HTF flow model uses available data to simulate a future precipitation rate and the resulting infiltration rate is expected to change over time as the closure cap degrades. The characterization and monitoring data for the SRS GSA is extensive, and provides a clear understanding of hydrogeology of the HTF and is a reasonable data set to represent long-term conditions.

2.6.3 Facility Design Assumptions

The PA assumes no significant structural changes to the waste tanks or ancillary equipment during the closure process. Significant additions or changes to these features could alter the performance assessment results.

Erosion control is maintained via the closure cap as detailed in Section 3.2.4.4. The erosion barrier maintains a minimum 10 feet of clean material above the HTF to act as an intruder deterrent (Table 3.2-12). Infiltration control of the HTF is expected to operate as estimated in Section 3.2.4. Tables 3.2-11 and 3.2-14 and Figure 3.2-91 provide specific design and performance values.

2.6.4 Stabilized Contaminant Characteristics Assumptions

2.6.4.1 Inventory

The estimate of residual activity in the waste tanks and ancillary equipment is expected to be a reasonably conservative estimate of the actual residual inventory and is described in Section 3.4. An initial radionuclide screening process was developed and performed to support characterization efforts and is applicable to the HTF PA modeling as described in Section 3.3. *H-Area Tank Farm Closure Inventory for use in Performance Assessment Modeling* (SRR-CWDA-2010-00023, Rev. 3) Appendix A describes the detailed screening from CBU-PIT-2005-00228 (*High-Level Waste Tank Farm Closure, Radionuclide Screening Process (First-Level), Development and Application*) to reduce an initial list of 849 radionuclides to 159. SRR-CWDA-2010-00023, Rev. 3 Appendix B further screens the 159 radionuclides down to the radionuclides of concern listed in Table 3.3-1.

The list of chemical constituents was derived from a screening process consisting of several steps to arrive at an appropriate list of constituents to be included in the waste tank closure inventory estimates. The approach was developed for use in screening the chemicals of interest in Tanks 18 and 19; since the chemical constituents for FTF and HTF are assumed the same, using the developed list was appropriate. Table 3.3-2 lists the chemical constituents of concern.

2.6.4.2 Grout Fill

Prior to waste tank final closure, each waste tank will be emptied, cleaned, and filled with a stabilizing grout. [DOE-EIS-0303, DOE-EIS-0303 ROD] Ancillary equipment such as DBs, PPs, and pump tanks will also be grouted to prevent subsidence (Section 3.2.3.1). The purpose of this stabilization is to maintain waste tank structure and minimize water

infiltration over an extended period, thereby impeding release of stabilized contaminants into the environment.

The grout will have a specific formulation, designed to meet certain mechanical and chemical performance requirements. The mechanical requirements of the grout consist of adequate hydraulic conductivity to slow/minimize infiltration and radionuclide movement, adequate compressive strength to withstand the overburden load and provide a physical barrier to discourage intruders. The chemical requirements of grout include high pH and a low E_h . The chemical requirements ensure the reducing capability of the grout recipe, which is an assumption used in the waste release model (e.g., Table 4.2-4). Section 3.2.3 discusses and Table 3.2-9 outlines the key requirements for the grout.

2.6.4.3 Contamination Zone

The residual waste tank inventory is modeled in distinct segments. Any residual material remaining within the waste tank primary liner (e.g., on the tank floor, on cooling coils, on the waste tank walls) is modeled as a discrete layer at the bottom of the waste tanks, below the grout fill (this discrete layer is referred to as the CZ). For Type I and II tanks, residual material remaining within the waste tank secondary liner (either on the liner floor or within the sand pad in the liner) is modeled as a discrete layer at the bottom of the waste tank annulus. For Tank 16, residual material remaining within the sand pad below the waste tank secondary liner is modeled as a discrete layer beneath the bottom of the waste tank secondary liner.

2.6.5 Integrated Conceptual Model Assumptions

2.6.5.1 Liner Failure

The time of potential initial waste release from the closed waste tanks is upon failure of the carbon steel waste tank liners. The waste tank and ancillary equipment failure times are therefore important assumptions used in the ICM. The failure times vary with waste tank design, owing to differences in liner properties and current liner conditions. The bases for the liner failure times used in the ICM are discussed in Section 4.2.2, which summarizes the conclusions from the liner degradation analyses reported in WSRC-STI-2007-00061 and SRNL-STI-2010-00047. The Base Case model assumptions use these conclusions and include:

- As documented in C-ESR-G-00003, Tanks 9 through 16 all currently have documented leak sites, while all other waste tanks in HTF do not have any documented leak sites. While Tanks 9 through 16 have documented leak sites, based upon present leak site numbers and physical locations, it is assumed that at the time of HTF final closure, liners are not a barrier to flow for Type I Tank 12, and Type II Tanks 14, 15, and 16. The leak sites on the other waste tanks are small in number and/or located near the top of the waste tank liner away from the CZ. [C-ESR-G-00003]
- All Type IV tanks are assumed to have liner failure within the compliance period.

- The remaining Type I and Type II tanks (excluding those identified above), and all Type III and IIIA tanks have intact steel liners at HTF final closure and do not fail within a 10,000-year period.

The probabilistic model, described in Section 4.4.4.2 and 5.6.3, applies waste tank liner failure times according to distributions determined from the steel liner degradation analyses reports, WSRC-STI-2007-00061 and SRNL-STI-2010-00047.

2.6.5.2 Contaminant Release and Movement

The rates of contaminant release and movement from the waste tanks and ancillary equipment (where applicable) are principally controlled by these factors:

- Moisture infiltration to the HTF from the overlying soil (Table 3.2-14)
- Physical properties (e.g., hydraulic conductivity), state (e.g., integrity) of the waste form (including grout, CZ, cementitious materials), and soil (Section 4.2 tables and figures)
- Chemical properties and state (e.g., E_h and pH) of the grout and CZ (Figures 4.2-9, 4.2-10 and Table 4.2-7)

The waste release conceptual model assumes water infiltrates from the ground surface, through the closure cap, and into the waste tank grout providing the pore fluids necessary to leach contaminants from the CZ. The release of contaminants from the CZ is based on solubility controls described in Section 4.2.1. Solubility controls applied to submerged waste tanks are handled differently than those applied to non-submerged waste tanks (Table 4.2-10 and 4.2-11).

The cementitious materials (e.g., waste tank grout, roof, walls, grouted annulus, and basemat) are assumed to degrade over time as described in Section 4.2.2.2, and will influence the HTF contaminant transport processes in cementitious materials and soils including advection, diffusion, dispersion, and sorption. Colloidal transport is not modeled since it is not expected to have a significant effect based on several colloidal studies described in Section 4.2.2. Contaminant transport through the cementitious materials and soils is impeded by sorption, as represented through the K_d of the soils (Section 4.2.2.2.2 and Table 4.2-25) and cementitious materials (Section 4.2.2.2.4 and Table 4.2-29).

The concrete material properties are based on concrete surrogate samples obtained from a P-Area Reactor wastewater tank basemat. The assumption is the surrogate is representative of the waste tanks basemats/concrete. The results of basemat testing are in WSRC-STI-2007-00369 and presented in Section 4.2.2.2.4. The P-Area Reactor basemat was selected based on similar function (foundation support to a waste tank) and strength properties (3,000 psi) to basemats used under HTF waste tanks.

Based on the contaminant plume evidence in Figures 5.2-3 through 5.2-5 and the discussion in Section 5.2.1, the groundwater concentrations are the highest concentration at 100 meters or further from the HTF.

2.6.5.3 Multiple Cases

Five waste tank cases and one ancillary equipment case are assumed to cover conditions in the groundwater model that represent what may occur within a 10,000-year period. While only one case (Base Case) was presented as the Base Case (Section 5.5), the various alternative cases were considered in the probabilistic analyses (Section 5.6.4 and 5.6.5) and in the deterministic sensitivity analyses (Section 5.6.7).

3.0 DISPOSAL FACILITY CHARACTERISTICS

Section 3.1 provides information regarding site characteristics including detailed information furnished for those characteristics that influence the contaminant transport modeling assumptions provided in Chapter 4.

- Section 3.1.1 provides a general description and layout of the site and the HTF to orient the reader and includes the population distribution of the surrounding area as well as future land use planning for information purposes.
- Section 3.1.2 describes meteorological and climatological data collection at SRS. This data collection determines appropriate modeling assumptions related to rainfall and temperature to assess the performance of the HTF closure cap presented in SRNL-ESB-2008-00023 and WSRC-STI-2007-00184. Dose Release Factors (DRFs) are developed from atmospheric dispersion conditions based on the meteorological data collected and are used to model the dispersion of gaseous contaminants emanating to the surface from the closed HTF site described in Section 4.5.
- Section 3.1.3 provides a general description of the ecology of the site for information purposes.
- Section 3.1.4 provides information regarding the geology and seismology of the site that is used to determine appropriate modeling parameters for the PA.
- Section 3.1.5 provides information regarding the hydrogeology of the site that determines the modeling assumptions related to the flow of surface water and groundwater.
- Section 3.1.6 identifies the sources of information available regarding the geochemistry of the soils and cementitious material that determines the modeling assumptions related to the depletion of radionuclides during their migration to potential sites of release to the environment.
- Sections 3.1.7 and 3.1.8 address natural resource management of the site and sources of natural and background radiation exposure, respectively, for information purposes.

Section 3.2 describes in detail the design and construction features of existing HTF waste tanks and ancillary equipment and the proposed design and construction features of HTF waste tank and ancillary equipment grouting system and the HTF closure cap concept.

- Sections 3.2.1 and 3.2.2 provide the details of design and construction of the HTF waste tanks and ancillary equipment, respectively.
- Section 3.2.3 provides the functional performance and design requirements of the grouting system to provide for stabilized contaminant immobilization, intruder deterrence, structural stability, and a chemical environment to retard the mobility of certain radionuclides by increasing their insolubility.
- Section 3.2.4 provides the design performance requirements and constructability

requirements for the proposed HTF closure cap concept and the results of the infiltration analysis of the closure cap presented in SRNL-ESB-2008-00023 and WSRC-STI-2007-00184.

Section 3.3 identifies the stabilized contaminants at the time of the HTF closure.

- Section 3.3.1 provides an initial radionuclide screening process.
- Section 3.3.2 lists the radionuclides that are used in the assessment modeling that have passed through the screening process.
- Section 3.3.3 lists the non-radionuclides that are used in the assessment modeling.
- Section 3.4 presents the inventory methodology used to characterize the radiological and a non-radiological inventories used in the PA analyses.
- Section 3.4.1 provides the estimated radioactive and non-radioactive inventory in the HTF waste tanks based on sample analysis, process history data collected within the Waste Characterization System (WCS), special analyses, and assumed remaining stabilized contaminants volume for waste tanks not yet cleaned.
- Section 3.4.2 provides waste tank inventory adjustments based on operations, inventory developments, and modeling efforts.
- Section 3.4.3 provides the estimated inventory remaining inside ancillary equipment including waste transfer lines (considering diffusion, oxide film layer, and residual material following flushing), pump tanks, and evaporator systems.

3.1 Site Characteristics

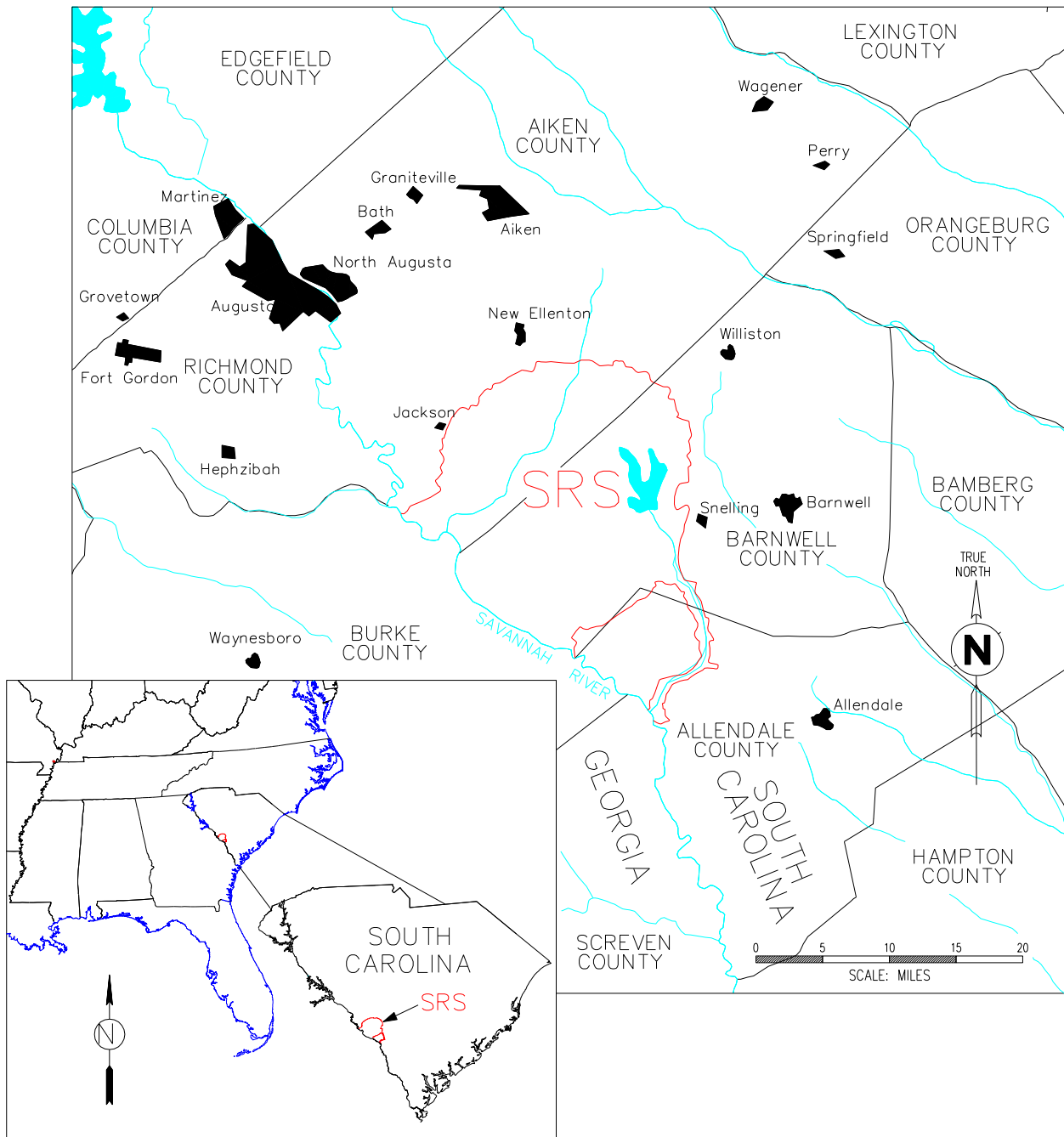
Evaluation of radionuclide transport from the HTF, and of human exposure resulting from release of radionuclides to the environment, requires careful consideration of factors affecting transport processes and exposure potential. Topographic features and hydrogeologic characteristics strongly affect the direction and flow of radionuclides potentially released from the closure site. Projected land use and population distributions affect the estimation of human exposure. In this section, the relevant natural and demographic characteristics of H Area and the surrounding area are discussed.

3.1.1 Geography and Demography

3.1.1.1 SRS Site Description

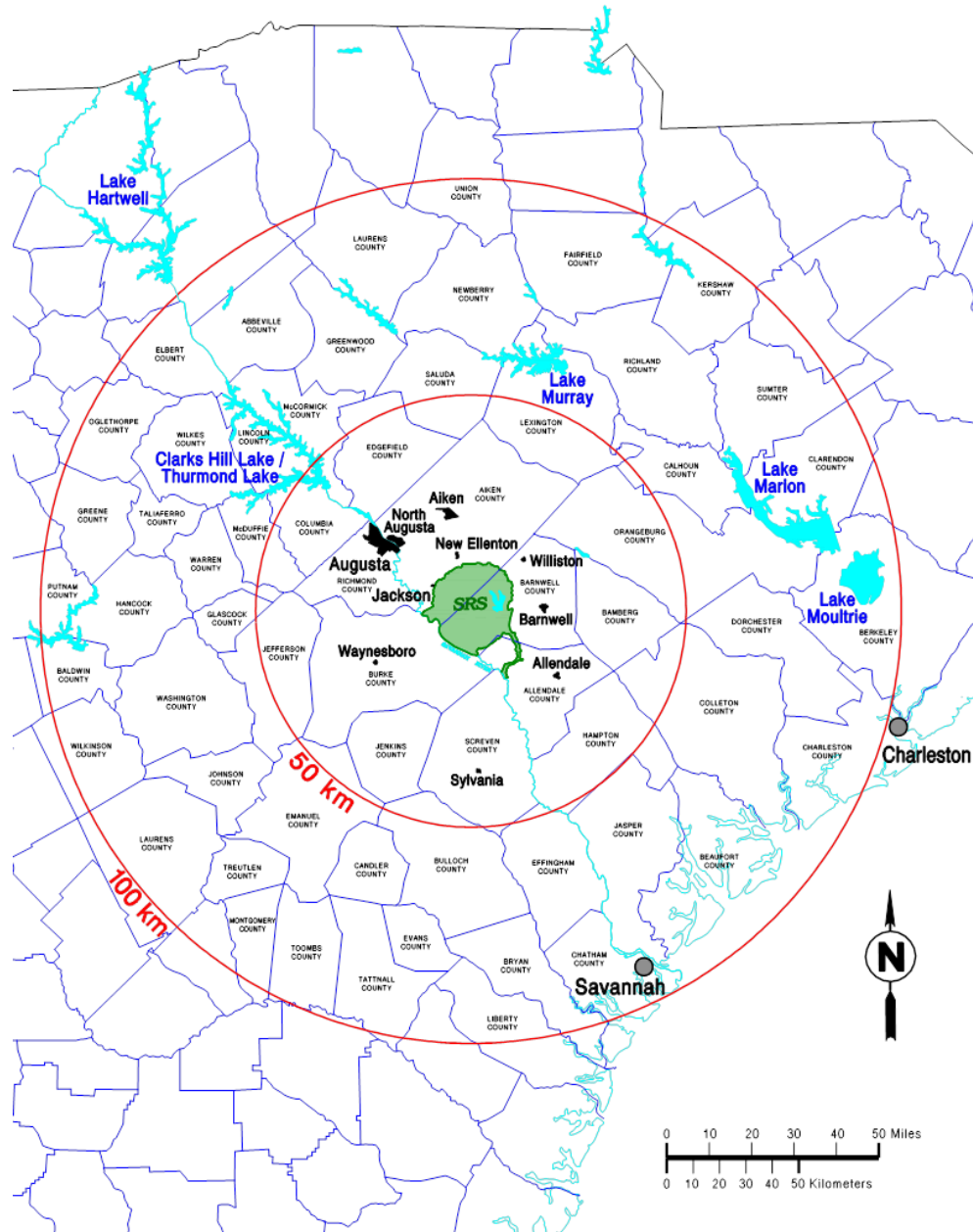
Construction of the SRS (one of the facilities in the DOE complex) started in the early 1950s to produce nuclear materials (such as Pu-239 and tritium). The site covers approximately 310 square miles in South Carolina and borders the Savannah River. The SRS encompasses approximately 198,000 acres in Aiken, Allendale, and Barnwell counties of South Carolina. The site is approximately 12 miles south of Aiken, South Carolina, and 15 miles southeast of Augusta, Georgia, as shown in Figure 3.1-1. [SRNS-STI-2011-00059]

Figure 3.1-1: Physical Location of SRS



Prominent geographic features within 30 miles of the SRS include the Savannah River and Clarks Hill Lake (also known as Thurmond Lake), shown in Figure 3.1-2. The Savannah River forms the southwest boundary of the SRS. Clarks Hill Lake is the largest nearby public recreational area. This reservoir lies on the Savannah River approximately 40 miles upstream of the center of SRS.

Figure 3.1-2: Location of SRS and Adjacent Areas

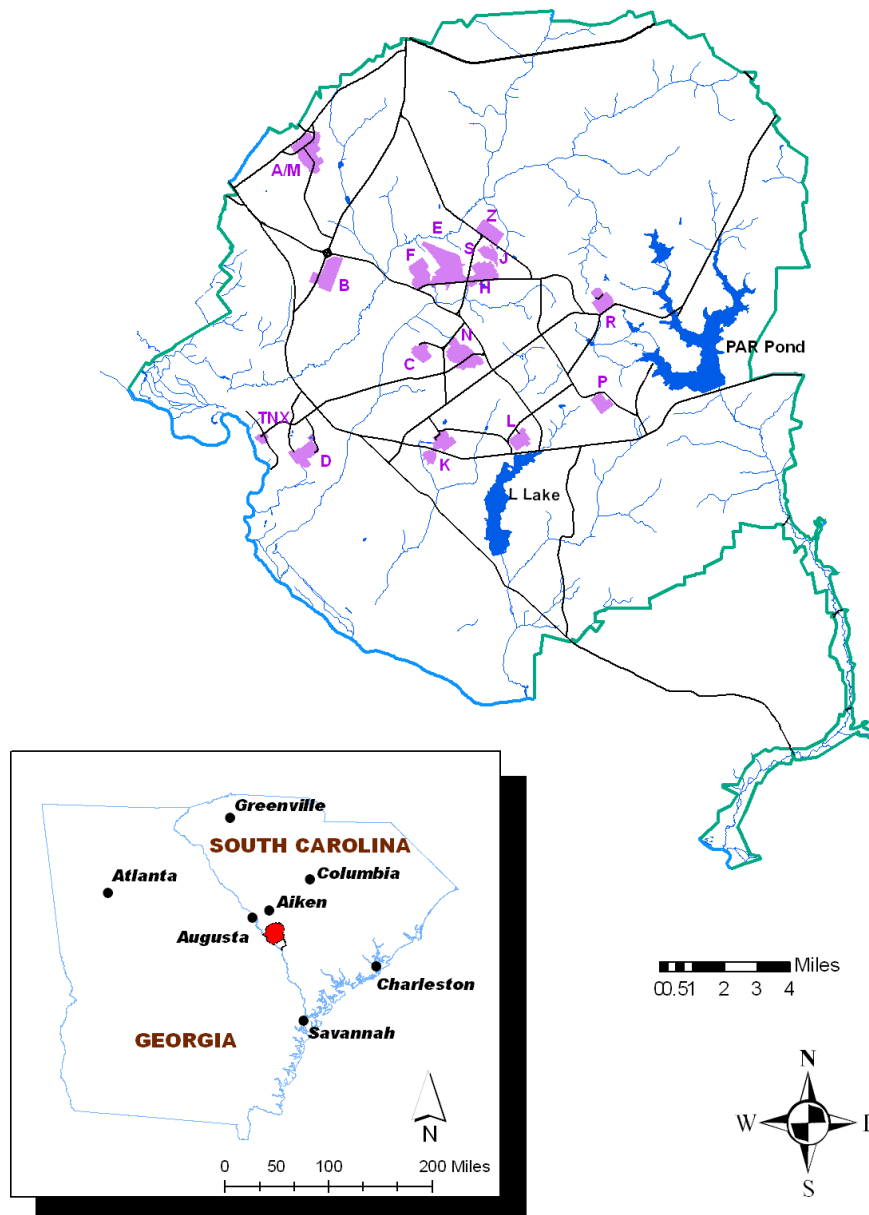


Within the SRS boundary, prominent water features include PAR Pond and L Lake, shown in Figure 3.1-3. The PAR Pond, a former reactor (P and R) cooling water impoundment, covers approximately 2,700 acres and lies in the eastern sector of the SRS. L Lake, another former reactor cooling water impoundment, covers approximately 1,000 acres and lies in the southern sector of the SRS. [WSRC-IM-2004-00008]

Figure 3.1-3 also shows the major operational areas at the SRS. Prominent operational areas, both past and present, include, Separations (F and H Areas), Waste Management Operations (E Area), Liquid Waste Disposition (F, H, J, S, and Z Areas), and the Reactor Areas (C, K, L,

P, and R). The Savannah River National Laboratory (SRNL) and Savannah River Ecology Laboratory (SREL) are located in A Area. Administrative and support services are located in B Area and construction administration activities are located in N Area. D Area, a heavy water facility, M Area, a fuel and target fabrication area, and TNX (purely code letter designation), the first semi-works-scale facility for separations equipment development and testing, have undergone deactivation and decommissioning.

Figure 3.1-3: Predominant SRS Operational Area Location Map



3.1.1.2 Closure Site Description

The HTF is in H Area, which is located in the central region of the SRS. Figure 3.1-4 presents the area known as the GSA. The GSA is located atop a ridge that runs southwest to northeast forming the drainage divide between UTR to the north and Fourmile Branch to the south. The GSA contains the F-Area and H-Area Separations Facilities, the S-Area Defense Waste Processing Facility (DWPF), the Z-Area Saltstone Facility, and the E-Area LLW disposal facilities. The HTF is an active facility consisting of 29 carbon steel waste tanks (Figure 3.1-5) in varying degrees of service or waste removal processes. The waste was generated primarily from the H-Canyon chemical separations processes. The HTF design features (e.g., waste tanks, transfer lines, evaporator systems) are discussed in more detail in Sections 3.2.1 and 3.2.2.

Figure 3.1-4: Layout of the GSA

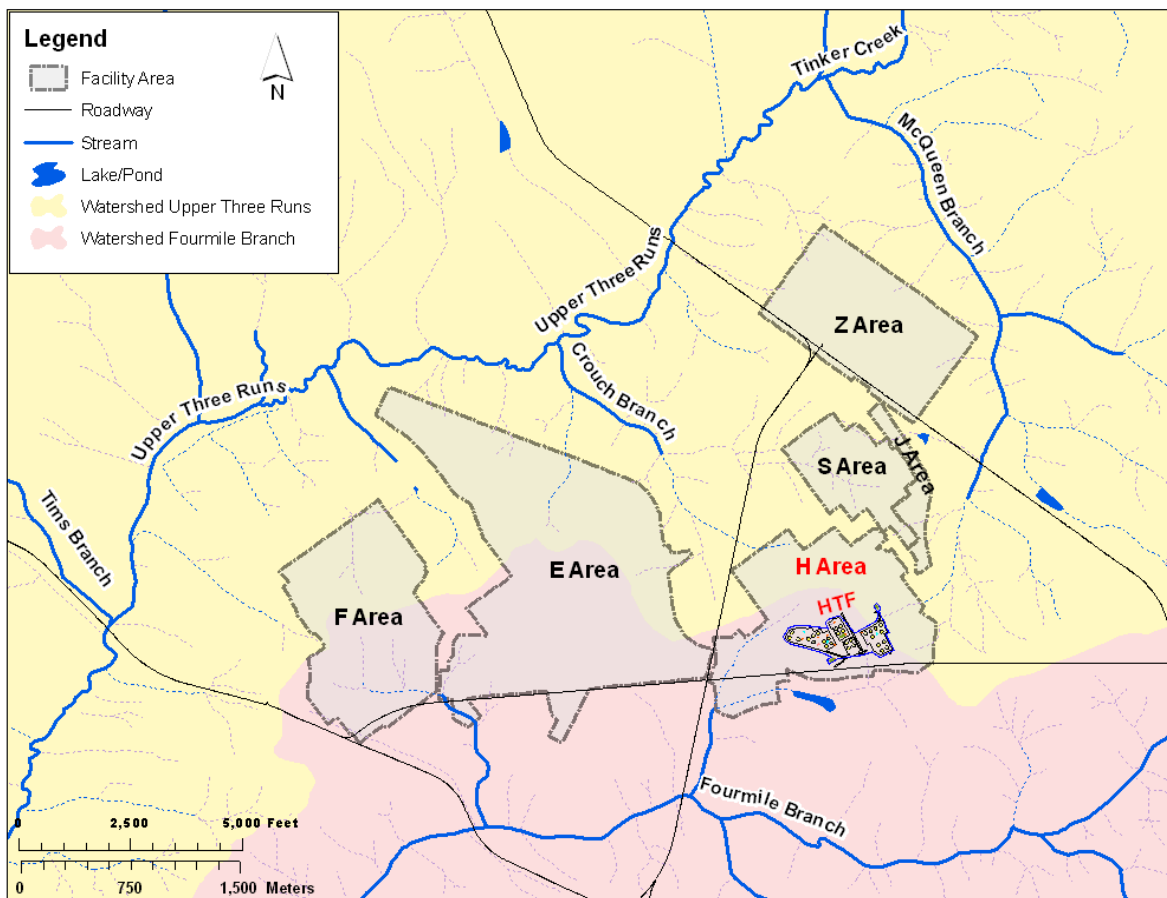


Figure 3.1-5: General Layout of HTF



3.1.1.3 Population Distribution

According to U.S. Census Bureau data, the estimated 2010 population in the eight-county region of influence (ROI) was 571,637. Four of the counties lie in South Carolina and include Aiken, Allendale, Bamberg, and Barnwell. The other four counties lie in Georgia and include Burke, Columbia, Richmond, and Screven (see Figure 3.1-2). The ROI includes the counties immediately adjacent to SRS and the counties where the majority of SRS workers reside. Approximately 85 % of the population in the ROI lives in the following three counties, Aiken (28.0 %), Richmond (35.1 %), and Columbia (21.7 %). Only approximately 15 % of the population in the ROI lives in the remaining counties as shown in Table 3.1-1. [SRR-LWDL-2012-00001]

Table 3.1-1: Population Distribution and Percent of ROI for Counties and Selected Communities

Jurisdiction	2000 Population	2010 Population	% Change	2010 % of Region
SOUTH CAROLINA				
Aiken County	142,552	160,099	12.3 %	28.0 %
Allendale County	11,211	10,419	-7.1 %	1.8 %
Bamberg County	16,658	15,987	-4.0 %	2.8 %
Barnwell County	23,478	22,621	-3.7 %	4.0 %
GEORGIA				
Burke County	22,243	23,316	4.8 %	4.1 %
Columbia County	89,288	124,053	38.9 %	21.7 %
Richmond County	199,775	200,549	0.4 %	35.1 %
Screven County	15,374	14,593	-5.1 %	2.6 %
Eight-County Total	520,579	571,637	9.8 %	

[SRR-LWDL-2012-00001]

From 2000 to 2010, the population in the eight-county region grew an estimated 9.8 %. Columbia County had the highest growth at 38.9 % followed by Aiken County with a growth of 12.3 % and Burke County with a growth of 4.8 %. Allendale, Bamberg, Barnwell, and Screven Counties experienced a net population loss. [SRR-LWDL-2012-00001]

The *High-Level Waste Tank Closure Final Environmental Impact Statement* contains population projections and further information regarding the region around SRS. [DOE-EIS-0303]

3.1.1.4 Land Use Present and Planned

Land within a 5-mile radius of the HTF is entirely within the SRS boundaries and its current use is for industrial purposes or as forested land. The classification of the current land use within the entire GSA is heavy nuclear industrial. Two key planning documents contain the plans for the future of the SRS and are identified below and described in Sections 2.4.2 and 2.4.3.

- The Savannah River Site End State Vision, PIT-MISC-0089
- The Savannah River Site Long Range Comprehensive Plan, PIT-MISC-0041

3.1.2 Meteorology and Climatology

3.1.2.1 General SRS Climate

The SRS region has a humid subtropical climate characterized by relatively short, mild winters and extended, hot, and humid summers. Summer-like conditions (including mid to late summer heat waves) typically last from May through September when the area is frequently under the influence of a western extension of the semi-permanent subtropical high-pressure system, most commonly known in North America as the Bermuda High. Winds in summer are light and cold fronts generally remain well north of the area. On average, greater than one-half of the days register temperatures in excess of 90°F during the summer months. As this maritime tropical mass comes inland, it rises and forms localized scattered afternoon and evening thunderstorms that are often intense. The influence of the

Bermuda High begins to diminish during the fall as continental air masses become more prevalent, resulting in lower humidity and more moderate temperatures.

Average rainfall during the fall is usually the least of the four seasons. In the winter months, mid-latitude low-pressure systems and associated fronts often migrate through the region. As a result, conditions frequently alternate between warm, moist, subtropical air from the Gulf of Mexico region and cool, dry, polar air. The Appalachian Mountains to the north and northwest of the SRS help to moderate the extremely cold temperatures that are associated with occasional outbreaks of Arctic air. Consequently, less than one-third of winter days have minimum temperatures below freezing on average, and days with temperatures below 20°F are infrequent. Measurable snowfall occurs on an average of once every two years. Tornadoes occur more frequently in spring than the other seasons of the year. Although spring weather is somewhat windy, temperatures are usually mild and humidity is relatively low. [WSRC-TR-2007-00118]

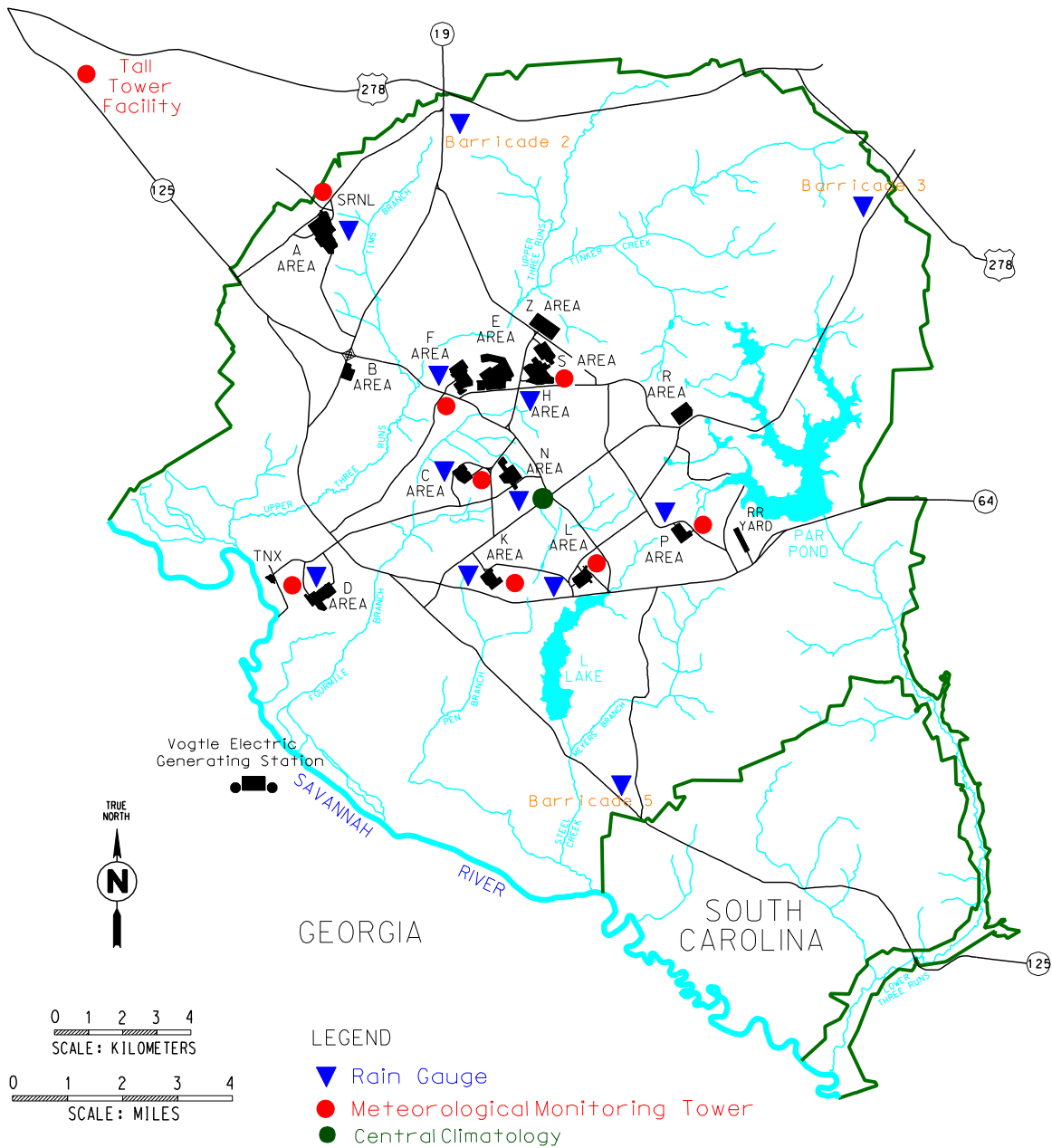
3.1.2.2 Meteorological Data Collection

The collection of SRS meteorological data is from a network of nine primary monitoring stations (Figure 3.1-6). Towers located adjacent to each of eight areas (A, C, D, F, H, K, L, and P Areas) are equipped to measure wind direction and wind speed at 201.3 feet above ground and to measure temperature and dew point at both 6.6 feet and 201.3 feet above ground. A ninth tower near N Area, known as the Central Climatology (CLM) site, is instrumented with wind, temperature, and dew point sensors at four levels: 6.6 feet (13.2 feet for wind), 59.4 feet, 118.8 feet, and 201.3 feet. The CLM site is also equipped with an automated tipping bucket rain gauge, a barometric pressure sensor, and a solar radiometer near the tower at ground level. Data acquisition units at each station record a measurement from each instrument at one-second intervals. Every 15 minutes, 900 data points are processed to generate statistical summaries for each variable, including averages and instantaneous maxima. The results are uploaded to a relational database for permanent archival. [WSRC-TR-2007-00118]

In addition, the Tall Tower facility near Beech Island, South Carolina, provides a set of high quality meteorological measurements that is unique to the Southeastern United States. This facility utilizes fast-response sonic anemometers, water vapor sensors, barometric pressure sensors, slow-response temperature sensors, and relative humidity sensors. The data are collected at 100 feet, 200 feet, and 1,000 feet above ground level. Spread-spectrum modems at each measurement level transmit raw data to a redundant set of personal computers at the SRNL. Data processing software on the personal computers determine mean values and other statistical quantities every 15 minutes and uploads the results to the relational database.

Collection of precipitation measurements are from a network of rain gauges across the SRS (Figure 3.1-6). Twelve of these gauges are read manually by site personnel once daily, usually around 6:00 a.m. The daily data are reported to the SRNL Atmospheric Technologies Center, where it is technically reviewed and manually entered into a permanent electronic database. The other is an automated rain gauge at the CLM site previously addressed above.

Figure 3.1-6: SRS Meteorological Monitoring Network



[WSRC-TR-2007-00118]

3.1.2.3 Data Pertinent To PA Modeling

Weather data pertinent to the PA modeling are atmospheric dispersion, precipitation, and air temperature. Each is discussed below.

3.1.2.3.1 Atmospheric Dispersion

Since the mid-1970s, a 5-year database of meteorological conditions at the SRS has been updated in order to support dose calculations for accident or routine release scenarios for on-site and off-site populations. The meteorological database includes wind speed, wind direction, temperature, dew point, and horizontal and vertical turbulence intensities. The most recent database is for the time period January 1, 2002 through December 31, 2006, and consists of 1-hour time averages of temperature and dew point; wind speed, direction, and turbulence. [WSRC-STI-2007-00613] These data are for determining DRFs in the evaluation for air pathways dose modeling described in Section 4.5, and was reported in SRNL-STI-2010-00018.

3.1.2.3.2 Precipitation

Compilations of rainfall data obtained from meteorological data collection described above for years 1952 through 2006 for the site and for years 1961 through 2006 from the 200-F weather station are in WSRC-STI-2007-00184. An average precipitation level result of 48.5 in/yr was gathered from the 55-year monitoring period for the site and 49 in/yr from the 200-F weather station. These data are for determining appropriate rainfall assumptions for the performance evaluation of infiltration through the closure cap described in Section 3.2.4 and evaluated in WSRC-STI-2007-00184.

3.1.2.3.3 Air Temperature

A compilation of air temperature data obtained from meteorological data collection (described above) for years 1968 through 2005 is in WSRC-STI-2007-00184. For this 37-year period, the annual average air temperature was approximately 64°F with an average monthly air temperature from a low of approximately 46°F, to a high of approximately 81°F. These data are for determining appropriate assumptions for the performance evaluation of infiltration through the closure cap described in Section 3.2.4 and evaluated in WSRC-STI-2007-00184.

3.1.3 Ecology

Comprehensive descriptions of the SRS ecological resources and wildlife are in *SRS Ecology: Environmental Information Document* and briefly discussed in this section. [WSRC-TR-2005-00201]

The SRS supports abundant terrestrial and semi-aquatic wildlife, as well as a number of species considered threatened or endangered. Since the early 1950s, the site has changed from 67 % forest and 33 % agriculture to 94 % forest, with the remainder in aquatic habitats and developed areas. Wildlife populations correspondingly shifted from forest-farm edge utilizing species to a predominance of forest-dwelling species. The SRS now supports 44

species of amphibians, 60 species of reptiles, 255 species of birds, and 55 species of mammals. These populations include urban wildlife, several commercially and recreationally important species, and a few threatened or endangered species. Protection and restoration of all flora and fauna to a point where their existence is not jeopardized are principal goals of federal and state environmental programs. Those species of plants and animals afforded governmental protection are referred to collectively as “species of concern.” [WSRC-TR-2005-00201]

The SRS has extensive, widely distributed wetlands, most of which are associated with floodplains, creeks, or impoundments. In addition, approximately 200 Carolina bays occur on SRS. Carolina bays are unique wetland features of the Southeastern United States. They are isolated wetland habitats dispersed throughout the uplands of SRS. The approximately 200 Carolina bays on SRS exhibit extremely variable hydrogeology and a range of plant communities from herbaceous marsh to forested wetland. [DOE-EIS-0303]

The Savannah River bounds SRS to the southwest for approximately 20 miles. The river floodplain supports an extensive swamp, covering approximately 15 square miles of SRS with a natural levee separating the swamp from the river. Timber was cut in the swamp from the turn of the century until 1951, when the Atomic Energy Commission assumed control of the area. At present, the swamp forest is comprised of two kinds of forested wetland communities. Areas that are slightly elevated and well drained are characterized by a mixture of oak species, as well as red maple, sweet gum, and other hardwood species. Low-lying areas that are continuously flooded are dominated by second-growth bald cypress and water tupelo. [DOE-EIS-0303]

The SRS supports abundant herpetofauna because of its temperate climate and diverse habitats. The species of herpetofauna include 17 salamanders, 27 frogs and toads, 1 crocodylian, 13 turtles, 9 lizards, and 36 snakes. The class Amphibia is represented on-site by 2 orders, 11 families, 16 genera, and 44 species. The Reptilia are represented by 3 orders, 12 families, 41 genera, and 59 species. [WSRC-TR-2005-00201]

More than 255 species of birds can be found at the SRS. Waterfowl and wading birds, as well as many upland species use the SRS aquatic habitats year round. The site’s Carolina bays and emergent marshes are used by 67 % of these birds. This type of habitat is used by 68 % of the upland species. Edge or shoreline areas account for high numbers of upland birds at the Carolina bays and emergent marshes, stream, and small drainage corridors, and river swamp habitats. The aquatic birds are most common in open water habitats. [WSRC-TR-2005-00201]

Large mammals inhabiting the site include white-tailed deer and feral hogs. Raccoon, beaver, and otter are relatively common throughout the wetlands of the SRS. In addition, the gray fox, opossum, bobcat, gray squirrel, fox squirrel, eastern cottontail, mourning dove, northern bobwhite, and eastern wild turkey are common at SRS. Threatened or endangered plant and animal species known to exist or that might be found on the overall site include the smooth purple coneflower, wood stork, red-cockaded woodpecker, and short-nose sturgeon. [WSRC-TR-2005-00201]

The HTF is located within a densely developed, industrialized area of SRS. The immediate area provides habitat for only those animal species typically classified as urban wildlife. Species commonly encountered in this type of urban landscape include the Southern toad, green anole, rat snake, rock dove, European starling, house mouse, opossum, and feral cats and dogs. Grasses and landscaped areas within the GSA in proximity to the HTF also provide some marginal terrestrial wildlife habitat. A number of ground-foraging bird species (e.g., American robin, killdeer, and mourning dove) and small mammals (e.g., cotton mouse, cotton rat, and Eastern cottontail) that use lawns and landscaped areas around buildings may be present at certain times of the year, depending on the level of human activity (e.g., frequency of mowing). Pine plantations managed for timber production by the U.S. Forest Service (under an interagency agreement with DOE) occupy surrounding areas.

The Fourmile Branch seepline area is located in a bottomland, hardwood forest community. The canopy layer of this bottomland forest is dominated by sweet gum, red maple, and red bay with an occasional sweet bay throughout. The understory consists largely of saplings of these same species, as well as an herbaceous layer of smilax, dog hobble, giant cane, poison ivy, chain fern, and hepatica. At the seepline upland edge, scattered American holly and white oak occur. Dominant along Fourmile Branch in this area are tag alder, willow, sweet gum, and wax myrtle. The seepline is located in a similar bottomland, hardwood forest community. [DOE-EIS-0303]

No endangered or threatened fish or wildlife species have been recorded near the UTR and Fourmile Branch seeplines. The seeplines and associated bottomland community do not provide habitat favored by endangered or threatened fish and wildlife species known to occur at SRS. The American alligator is the only federally protected species that could potentially occur in the area of the seeplines. Fourmile Branch does support a small population of American alligator in its lower reaches, where the stream enters the Savannah River swamp. [DOE-EIS-0303]

According to studies on UTR, documented in the *SRS Ecology: Environmental Information Document*, the macroinvertebrate communities of UTR drainage are unusual. [WSRC-TR-2005-00201] They include many rare species and species not often found living together in the same freshwater system. Since UTR is a spring-fed stream and is colder and generally clearer than most surface water at its low elevation, species typical of unpolluted streams in northern North America or the southern Appalachian Mountains are found here along with lowland (Atlantic Coastal Plain) species.

The fish community of UTR is typical of third and higher order streams on the SRS that have not been greatly affected by industrial operations, with shiners and sunfish dominating collections. The smaller tributaries of UTR are dominated by shiners and other small-bodied species (i.e., pirate perch, madtoms, and darters) indicative of un-impacted streams in the Atlantic Coastal Plain. In the 1970s, the U.S. Geological Survey (USGS) designated UTR as a National Hydrological Benchmark Stream due to its high water quality and rich fauna. However, this designation was rescinded in 1992 due to increased development of the UTR watershed north of the SRS site boundaries. [DOE-EIS-0303]

3.1.4 Geology, Seismology, and Volcanology

Regional and local information on the geologic and seismic characteristics of the HTF are presented in this section. Because the SRS is not located within a region of active-plate tectonics characterized by volcanism, volcanology is not an issue of concern in this PA, and thus further discussion of this topic is omitted from the following discussion. [WSRC-IM-2004-00008]

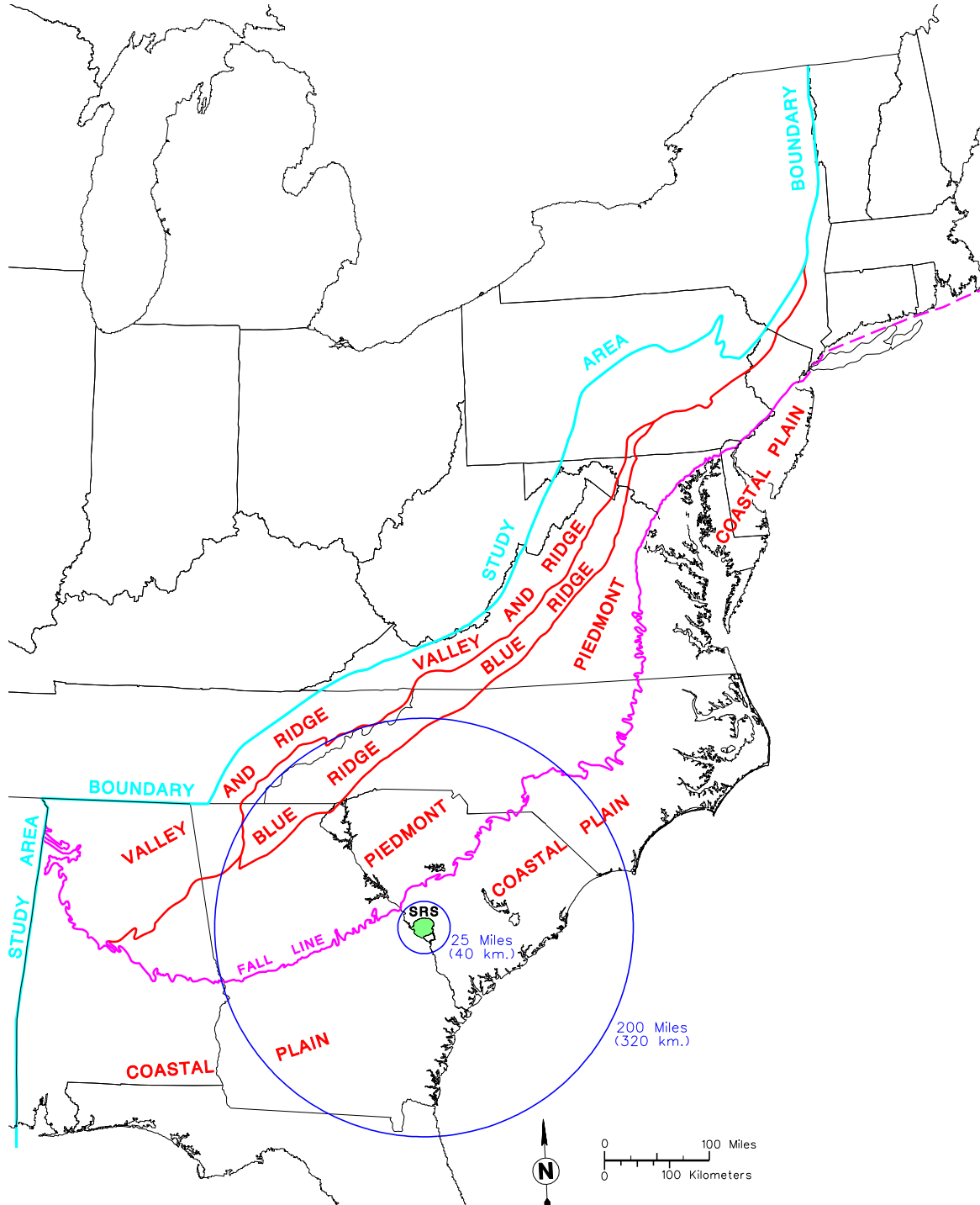
3.1.4.1 Regional and Site-Specific Topography

The SRS is on the Atlantic Coastal Plain Physiographic Province approximately 25 miles southeast of the Fall Line that separates the relatively unconsolidated Coastal Plain sediments from the underlying Piedmont Physiographic Province. Beneath the Coastal Plain, sedimentary sequences reveal two geologic terrains. One is the Dunbarton basin, a Triassic-Jurassic Rift basin filled with lithified terrigenous and lacustrine sediments. The other is a crystalline terrain of metamorphosed sedimentary and igneous rock that may range in age from Precambrian to late Paleozoic derived from the crystalline igneous and metamorphic rocks of possibly late Precambrian to late Paleozoic age in the Piedmont Province. Early to middle Mesozoic (Triassic to Jurassic) rocks occur in isolated fault-bounded valleys either exposed within the crystalline belts or buried beneath the Coastal Plain sediments. The Coastal Plain sediments were derived from erosion of the crystalline rocks during late Mesozoic (Cretaceous) in stream and river valleys, and are represented locally by gravel deposits adjacent to present-day streams and by sediments filling upland depressions (sinks and Carolina Bays). The Cretaceous and younger sediments are not significantly indurated. The total thickness of the sediment package at SRS varies between approximately 700 feet at the northwest boundary and 1,200 feet at the southeast boundary. [WSRC-TR-95-0046]

Figure 3.1-7 shows the relationship of SRS to overall regional geological provinces, and Figure 3.1-8 details the regional physiographic provinces in South Carolina. As can be seen on Figure 3.1-8, much of SRS lies within the Aiken Plateau, and this Plateau has an approximate 5 % slope to the southeast. Savannah and Congaree Rivers bound the plateau, which extends from the Fall Line to the Orangeburg escarpment. The highly dissected surface of the Aiken Plateau is characterized by broad interfluvial areas with narrow, steep-sided valleys. Local relief can be as much as 300 feet. Figure 3.1-9 shows the topography and 20-foot contour lines of the GSA. [WSRC-TR-95-0046]

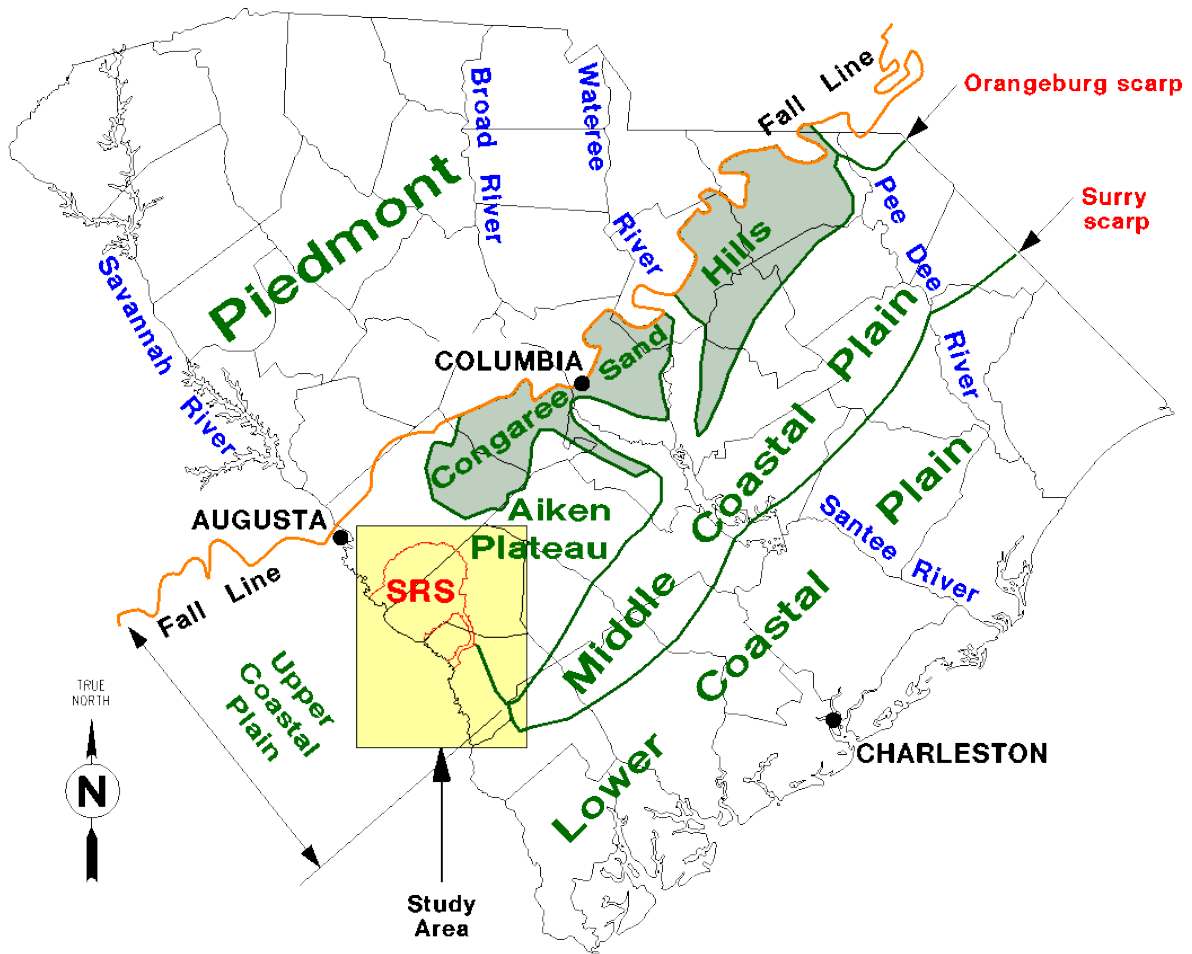
Currently, HTF storm water drainage is directed to an outfall, which will be unaffected by HTF operations and waste tank closure activities. The installation of the HTF closure cap (Section 3.2.4) will necessitate changes to the HTF drainage system, which will be designed later as part of the overall closure of HTF.

Figure 3.1-7: Regional Geological Provinces of Eastern United States



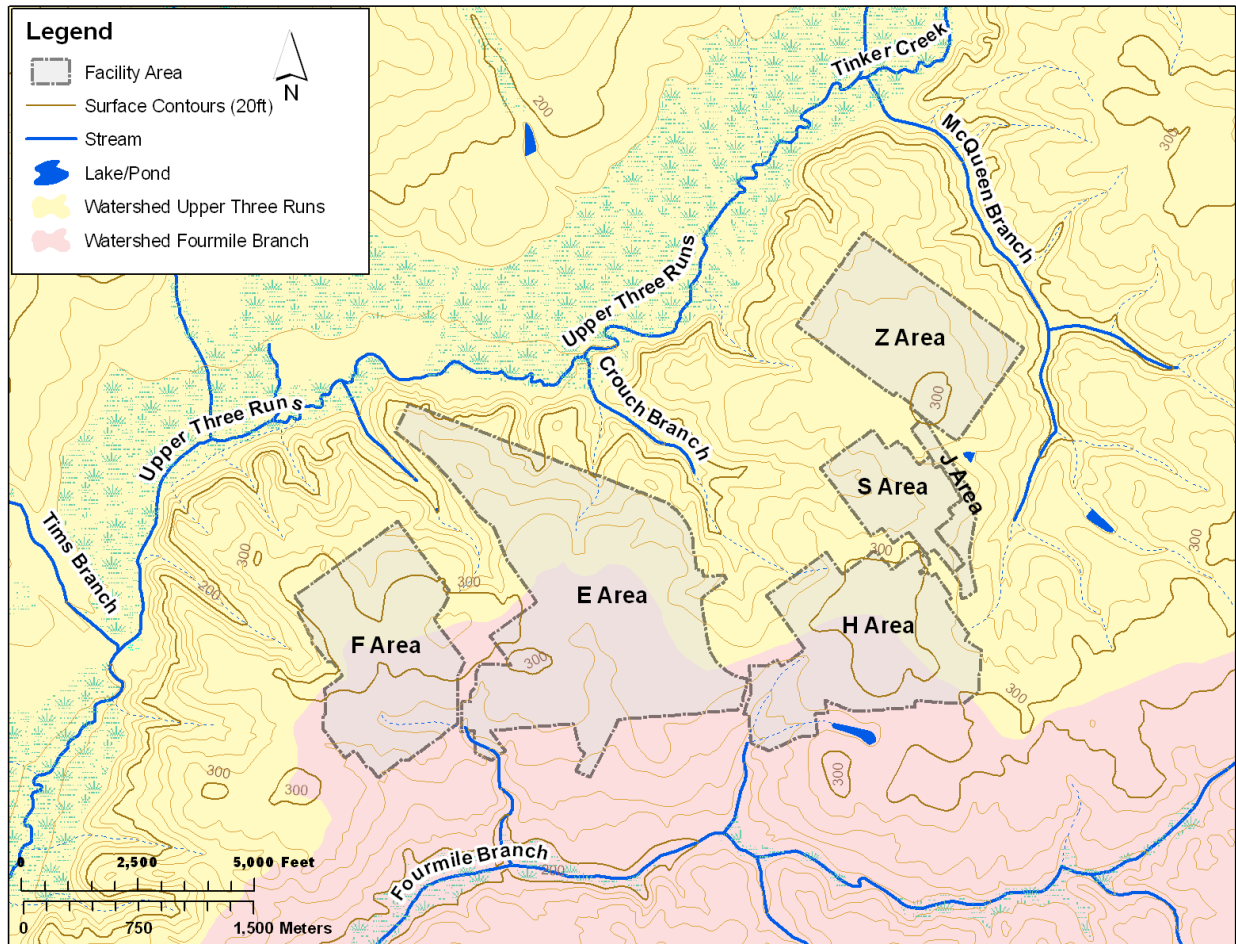
[WSRC-TR-2000-00310, Figure 1]

Figure 3.1-8: Regional Physiographic Provinces of South Carolina



[WSRC-TR-95-0046, Figure 2-3]

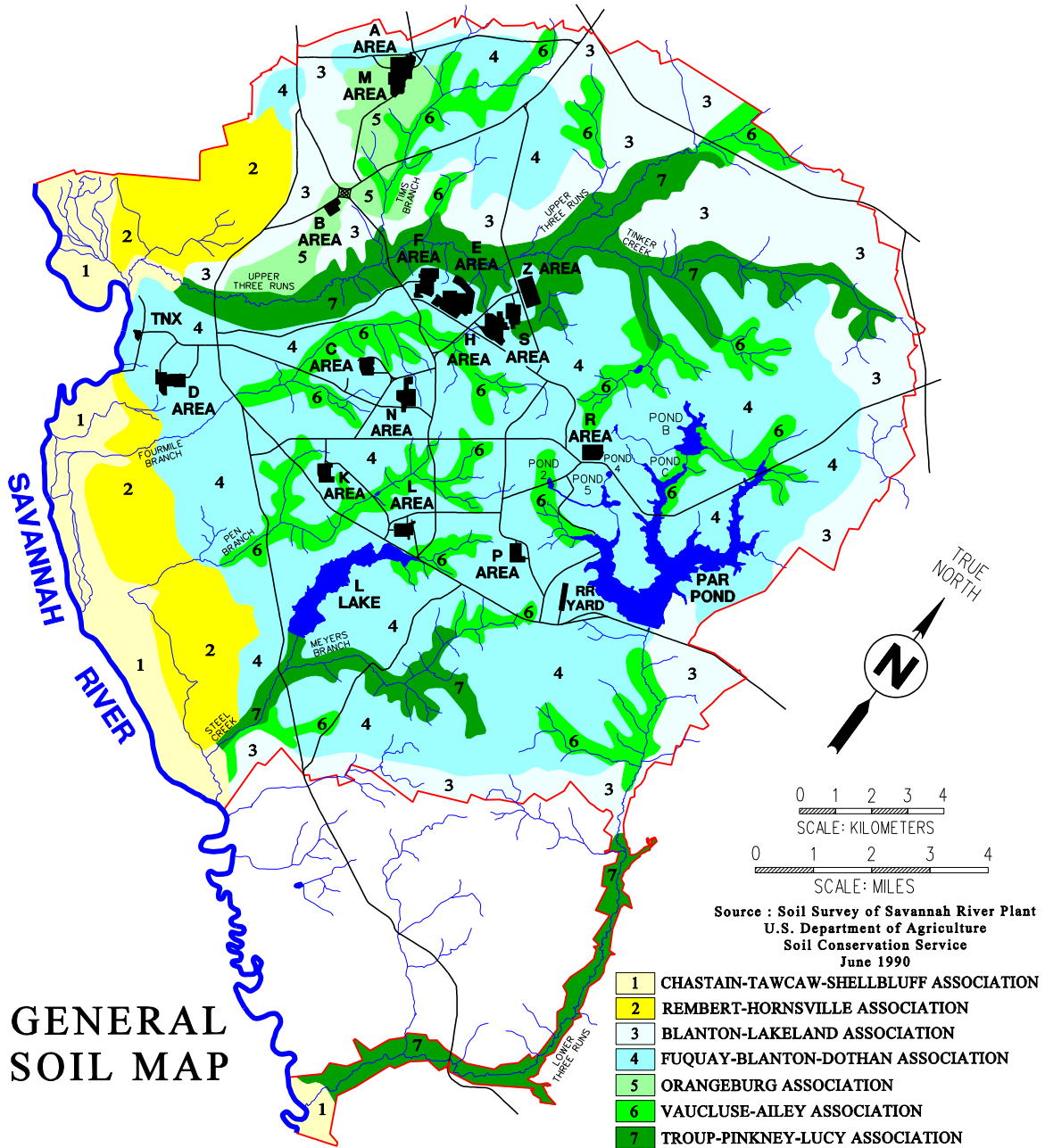
Figure 3.1-9: Topography of the GSA



3.1.4.2 Local Geology and Soils

SRS is comprised of seven major soil associations. They are Chastain-Tawcaw-Shellbluff, Rembert-Hornsville, Blanton-Lakeland, Fuquay-Blanton-Dothan, Orangeburg, Vacluse-Ailey, and Troup-Pinkney-Lucy. Figure 3.1-10 delineates the general soil associations for SRS. Details regarding these associations may be found in the *Soil Survey of the Savannah River Plant Area, Parts of Aiken, Barnwell, and Allendale Counties, South Carolina*. [PIT-MISC-0104]

Figure 3.1-10: General Soil Associations for SRS



The overall general soil association for H Area is the Fuquay-Blanton-Dothan. The most predominant soil types within H Area are classified as Udorthents. Udorthents consist of well-drained soils that formed in heterogeneous materials, which are the spoil or refuse from excavations and major construction operations. Udorthents range from sandy to clayey, depending upon the source of material or geologic parent material. Udorthents are most commonly associated with well drained to excessively drained upland soils. A few small, poorly drained areas that have spoil are also included. Typical profiles for Udorthents are not shown due to the lack of consolidation within short distances. Clayey soil has demonstrated good retention for most radionuclides. There are also areas that consist of cross-bedded, poorly sorted sand with lenses and layers of silt and clay.

The uppermost geologic unit in the HTF is comprised of the middle to late Miocene-age Upland Unit, which extends over much of SRS (see Figure 3.1-15). The term "Upland Unit" is an informal name used to describe sediments at higher elevations located in the Upper Coastal Plain in southwestern South Carolina. This area has also been referred to as the Aiken Plateau. The Upland Unit includes the vadose zone and a portion of the UTR Aquifer - Upper Zone (UTRA-UZ). The occurrence of cross-bedded, poorly sorted sands with clay lenses in the Aiken Plateau indicates fluvial deposition (high-energy channel deposits to channel-fill deposits) with occasional transitional marine influence. This depositional environment results in wide differences in lithology and presents a very complex system of transmissive and confining beds or zones. The lower surface of the Upland Unit is very irregular due to erosion of the underlying formations. [DOE-EIS-0303]

A notable feature of the Upland Unit is its compositional variability. This formation predominantly consists of red-brown to yellow-orange, gray, and tan colored, coarse to fine grained sand, pebbly sand with lenses and beds of sandy clay and clay. Generally vertically upward through the unit, sorting of grains becomes poorer, clay beds become more abundant and thicker, and sands become more argillaceous and indurated. In some areas, small-scale joints and fractures, both of which are commonly filled with sand or silt, traverse the unit. The mineralogy of the sands and pebbles primarily consists of quartz, with some feldspar. In areas to the east-southeast, sediments may become more phosphatic and dolomitic. The soils in the Upland Unit may contain as much as 20 % to 40 % clay. [DOE-EIS-0303]

Below the Upland Unit lies the Tobacco Road Formation, consisting of red, brown, tan, purple, and orange quartz sands, and clayey quartz sands. These sands are fine to coarse moderately to poorly sorted, with minor clay laminae. In general, the sands of the Tobacco Road Formation are muddier, more micaceous, and more highly colored than the sands of the underlying Dry Branch Formation. The base of the Tobacco Road Formation is marked in places by a coarse layer that contains flat quartz pebbles. Clay laminae in the upper part of the formation suggest that some of the unit was deposited in a transitional, low-energy environment, such as a tidal flat. The Tobacco Road Formation is approximately 20-foot thick and is part of the UTRA-UZ. [SRNL-STI-2010-00148]

Underlying the Tobacco Road Formation is the Dry Branch Formation, consisting of variably colored, poorly sorted to well-sorted sand with the interbedded tan to gray clay. The upper portion of the Dry Branch Formation is within the UTRA-UZ. The middle to lower portion of the Dry Branch Formation includes the Twiggs Clay; a semi-confining clay layer also

designated as the Tan Clay Confining Zone (TCCZ), which separates the UTRA-UZ from the UTRA – Lower Zone (UTRA-LZ).

Below the Twiggs Clay are the Clinchfield and Santee Formations. In H Area, the Santee Formation is composed of mixed clastic and carbonate materials, with clastic material being dominant; the interpreted depositional scenario is a moderate energy, middle shelf environment, with input of both clastic and carbonate sediments. Lithologic and petrographic studies have divided the Santee Formation in the GSA into eight microfacies, quartz sand (stone), terrigenous mud (stone), skeletal lime mudstone, skeletal wackestone, skeletal packstone, skeletal grainstone, microsparite, and siliceous mudstone. [WSRC-RP-94-54] None of these depositional environments contains significant amounts of limestone that would be conducive to the formation of large subsurface voids, karst, or caves within the vicinity of HTF.

The calcareous zones, located within the Santee Formation, contain “soft zones.” Characterization activities reported in various early documents describe potential voids, drilling fluid losses, and grout takes associated with the Santee Formation at SRS. Soft zones have been encountered beneath most of SRS, but are less common in the northwest (updip) and more common in the southeastern (downdip near K Area) regions. This distribution appears to correlate with the well-documented pattern of increasing carbonate content in the Santee Formation to the southeast. This lateral variation in carbonate content reflects the original range of depositional environments, from nearshore and inner shelf environments with primarily terrigenous input in the northwest, to quiet water, outer shelf conditions of carbonate accumulation in the southeast (in the vicinity of K Area). [WSRC-RP-94-54, WSRC-TR-99-4083]

A recent evaluation of more than 60 years of investigation and research into the occurrence, origin, and behavior of soft zones confirms that soft zones beneath SRS are not cavernous voids, but are small, isolated, poorly connected 3-D features filled with loose, fine-grained, water saturated sediment. [SRNL-TR-2012-00160]

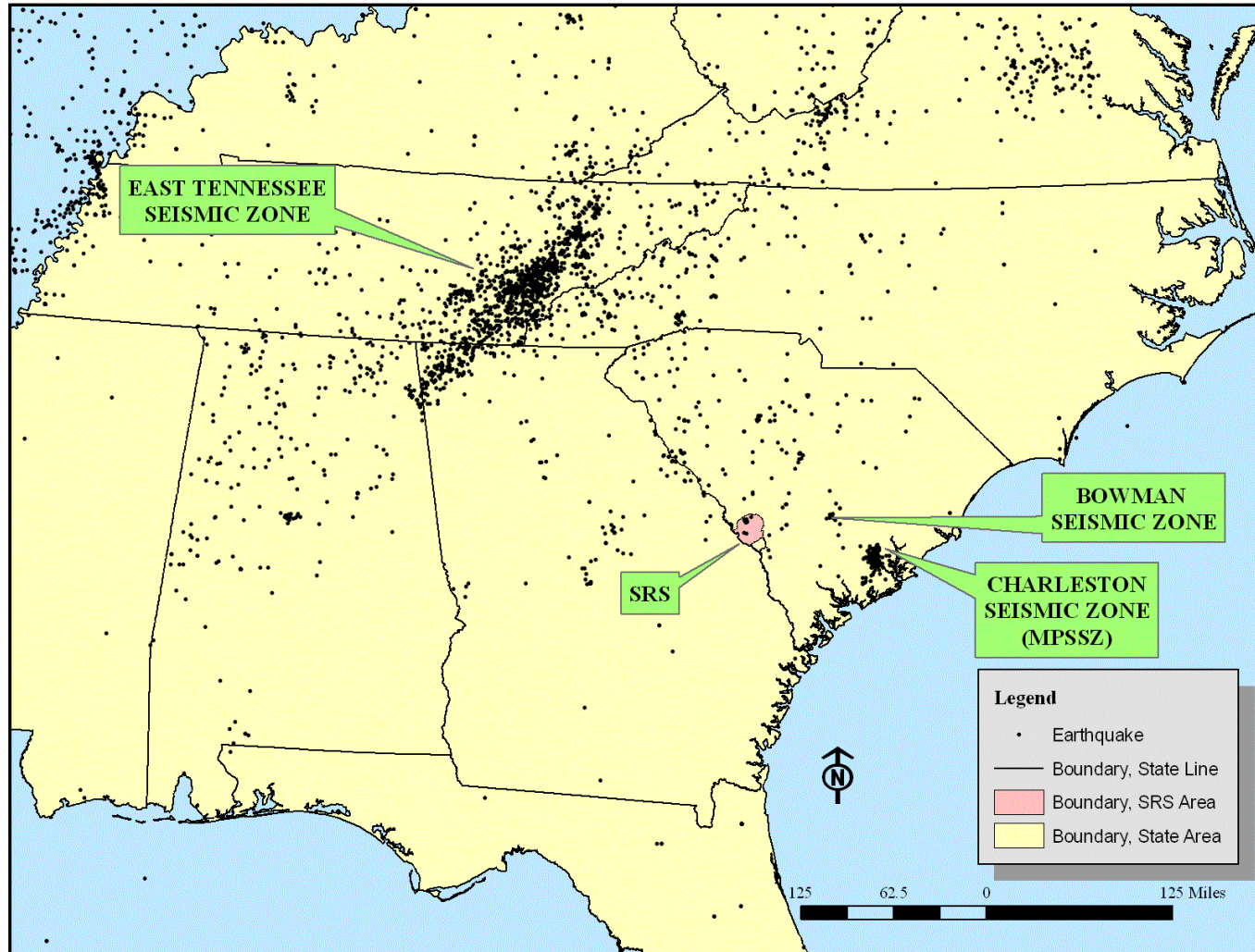
In the GSA, which includes HTF, there is no evidence of actual subsurface voids, karst, or caves that would act as open flow conduits. In historical and recent literature, no documentation was found of void spaces or other phenomena that would influence contaminant migration in a manner not already captured in the GSA Database (GSAD). As described in Section 3.1.5.2, the GSAD was developed using field data and interpretations for the GSA and vicinity and is a subset of site-wide data sets of soil lithology and groundwater information. The GSAD is used as the basis of hydrogeologic input values into the computational model for groundwater flow and contaminant transport as described in Section 4.2.3.1.3. Underlying the Santee Formation is the Warley Hill Formation, often referred to as “Green Clay,” which forms the hydrologic barrier separating the UTRA-LZ from the underlying Gordon Aquifer of the Congaree Formation.

A more detailed description of the geology and soils of the H Area can be found in a report titled *Hydrogeologic Framework of West-Central South Carolina*. [PIT-MISC-0112]

3.1.4.3 Seismology

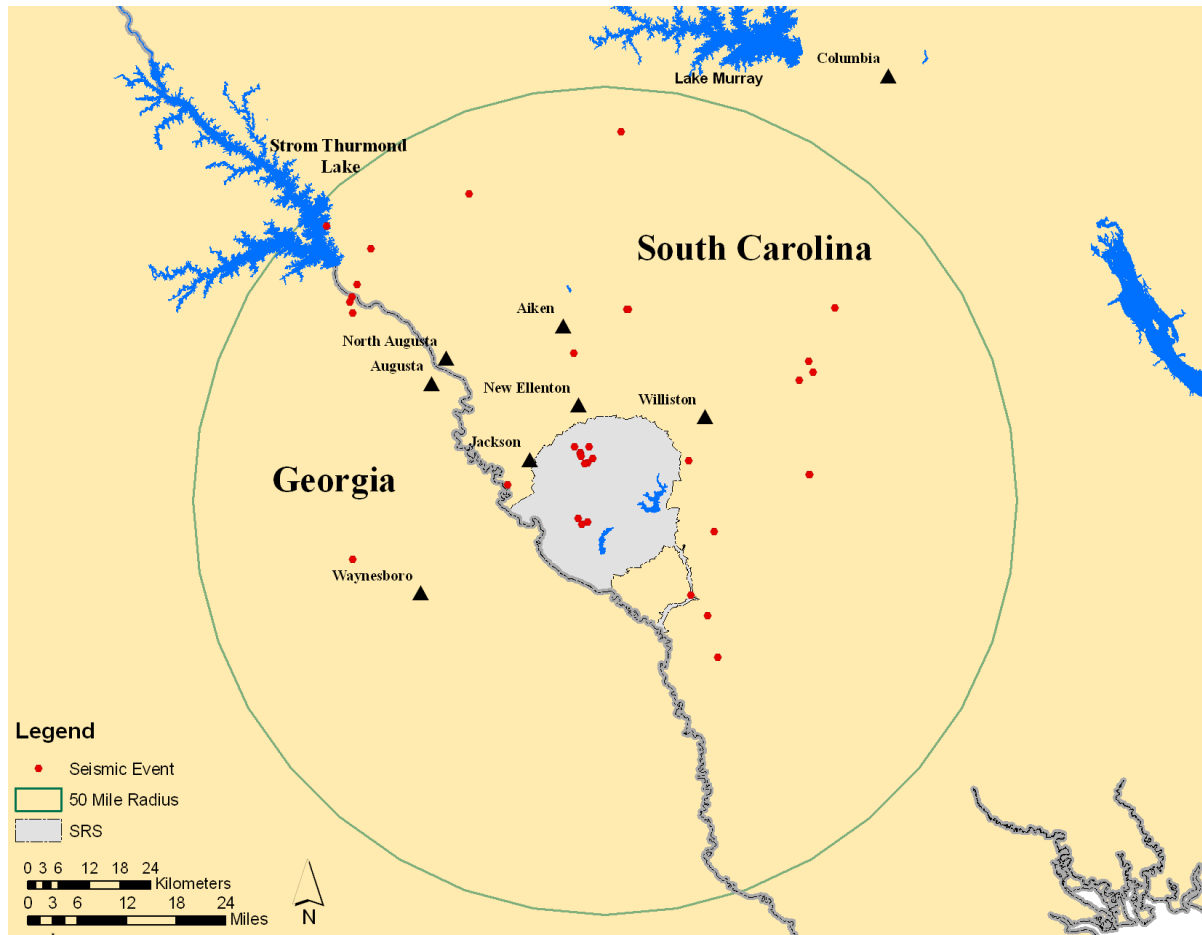
The seismic history of the Southeastern United States (of which SRS is a part) spans a period of nearly three centuries, and is dominated by the Charleston earthquake of August 31, 1886 (estimated magnitude of 7.0). The historical database for the region is essentially composed of two data sets extending back to as early as 1698. The first set is comprised of pre-network, mostly qualitative data (1698 to 1974), and the second set covers the relatively recent period of instrumentally recorded or post-network seismicity, 1974 through April 2009. Figure 3.1-11 shows the locations of historical seismic events in the Southeast. Figure 3.1-12 denotes the epicenter locations of seismic events within a 50-mile radius of SRS. [WSRC-MS-2003-00617, USGS OFR 2010-1059]

Figure 3.1-11: Historical Seismic Events in the Southeast



[USGS OFR 2010-1059]

Figure 3.1-12: Seismic Events within a 50-Mile Radius of SRS



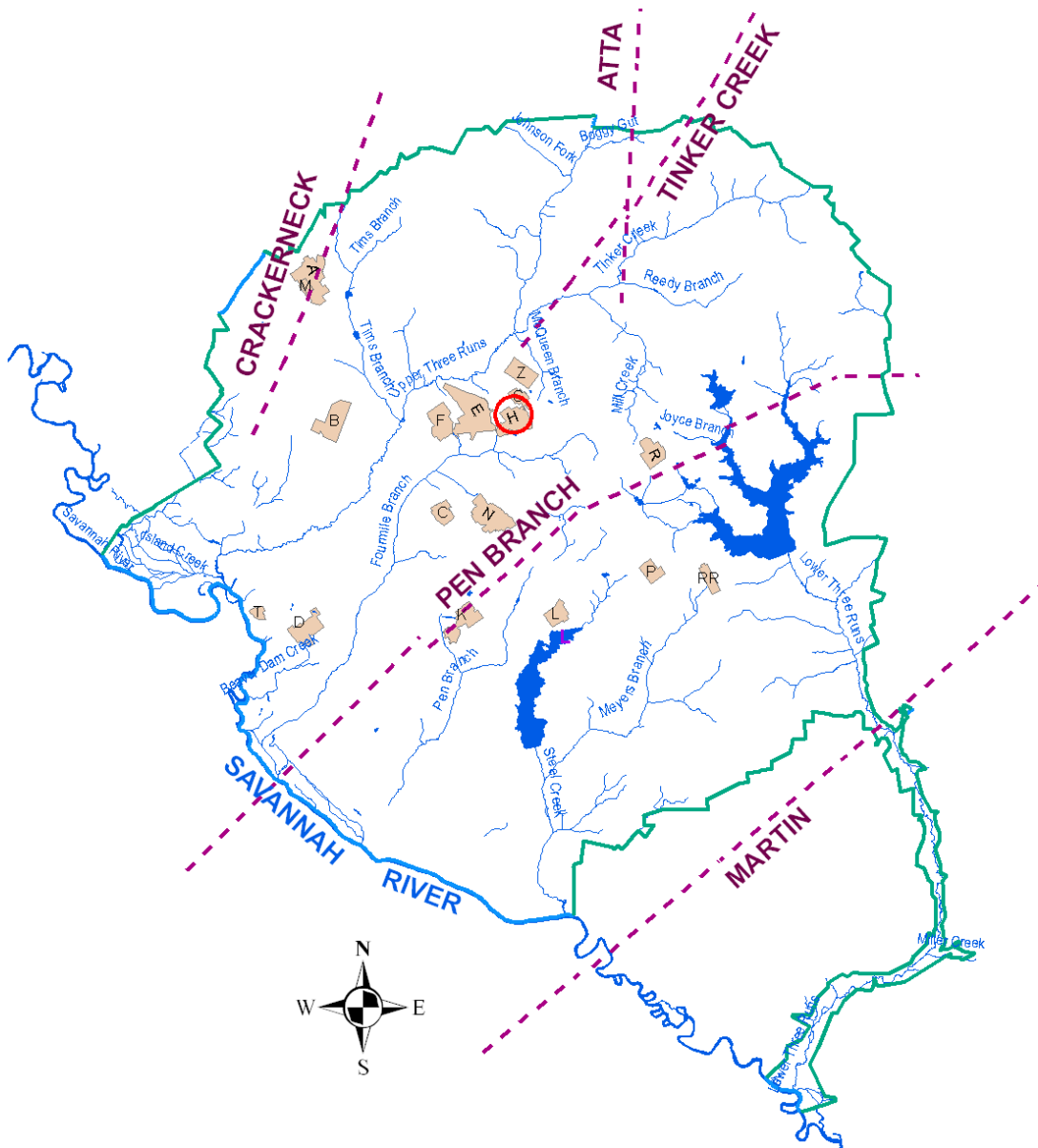
[Modified from WSRC-MS-2003-00617]

The most recent seismic event occurring within a 50-mile radius of SRS was on March 27, 2009, with a magnitude of 2.6. No damage to SRS was recorded. However, there have been four earthquakes with epicenter locations within SRS. They occurred June 9, 1985 (magnitude of 2.6), August 5, 1988 (magnitude of 2.0), May 17, 1997 (magnitude of 2.5), and October 8, 2001 (magnitude of 2.6). No strong motion accelerometers were triggered because of these earthquakes. Note that additional seismic events with epicenter locations within SRS occurred shortly after the October 2001 earthquake however, these seismic events were attributed to aftershocks and not actual earthquakes. [WSRC-MS-2003-00617]

The regional faults within the SRS and vicinity are shown in Figure 3.1-13. A study entitled *Comparison of Cenozoic Faulting at the Savannah River Site to Fault Characteristics of the Atlantic Coast Fault Province: Implications for Fault Capability* (WSRC-TR-2000-00310) provides additional data. This study concludes that these regional faults exhibit the same general characteristics, are closely associated with the faults of the Atlantic Coastal Fault Province, and thus are part of the Atlantic Coastal Fault Province. Several faults of the Atlantic Coastal Fault Province have been the subject of detailed investigations. In all cases,

the conclusion has been reached that these faults have not had a movement within the past 35,000 years and no movement of a recurring nature within the past 500,000 years. Inclusion in the Atlantic Coastal Fault Province means that the historical precedent established by decades of previous studies on the seismic hazard potential for the Atlantic Coastal Fault Province is relevant to faulting at the SRS. [WSRC-TR-2000-00310]

Figure 3.1-13: Regional Scale Faults for SRS and Vicinity



[WSRC-TR-2000-00310, Figure 10]

In 1976, a short-period seismic network was established. In 1999, a 10-station strong motion accelerometers network was installed throughout the complex. Detailed information regarding seismic characteristics at SRS can be found in the Documented Safety Analysis (DSA), WSRC-IM-2004-00008.

As noted in Section 3.1.4.2, soft zones have been reported in various early documents. The soft zones described in these documents are described as voids, drilling fluid losses, and grout takes associated with the Santee Formation beneath SRS that may be susceptible to seismic activity. However, in spite of their under consolidated nature, soft zones have survived for a very long time and remain structurally competent in the presence of significant overburden stresses. [SRNL-TR-2012-00160]

The predicted behavior of soft zones under both static and dynamic conditions has been modeled for numerous SRS facilities. These calculations show soft zones to be stable under static conditions; dynamic analyses predict that soft zones will not collapse in response to a design basis earthquake. [WSRC-TR-99-4083] The design basis earthquake and associated ground motion, measured in peak ground acceleration for construction of facilities at the SRS (ground motion 0.2 force of gravity) is based on historic seismic events in the region, the geologic literature, and attenuation relations. [WSRC-TR-90-0284]

As a conservative approach, the design for some SRS facilities assumes that soft zones will collapse (compress) in response to applied stress. An analysis for a proposed facility (Actinide Packaging and Storage Facility) within the GSA calculated that collapse of a relatively thick (approximately 8 inches) two-layer soft zone would only cause a ground surface settlement of about 4 inches. [K-CLC-F-00034]

Although such conservative calculations are an important aspect of nuclear safety evaluations, it is noteworthy that soft zones in the Eocene age Santee Formation have survived without collapsing for tens of millions of years and have presumably persisted in spite of many earthquakes, including design basis earthquakes and less frequent events of even greater magnitude. [SRR-CWDA-2011-00054 RAI-SS-3]

A structural assessment was prepared for operationally closed waste tanks. Waste tank settlement can occur due to two loads, static load and seismic loads. Static settlement is likely to occur due to the large overburden load from the closure cap. This settlement is expected to be relatively uniform. Any static differential settlement would be small in magnitude and cause a grout-filled waste tank to rotate as a rigid body. Small magnitudes of rigid body rotation will induce only small lateral forces that can be considered negligible. Therefore, static differential settlement is not considered further. [T-CLC-F-00421]

Seismic differential settlement can occur due to liquefaction and soft zone settlement. Soft zones are often areas of under-consolidated material in a stronger matrix material that essentially forms a soil arch, allowing the soft zones to remain under-consolidated. A large seismic event could cause the soil arch to fail resulting in settlement as consolidation occurs in the under consolidated material until it is normally consolidated. The maximum tensile stresses resulting from this consolidation on the grout-filled waste tanks is an overstress of 4 %, occurring for a small depth. Since this stress occurs only for an extreme settlement case

and due to the many bounding assumptions made in the structural assessment, it was concluded that there is very high confidence the grout-filled waste tank will not crack. [T-CLC-F-00421]

In addition, for the E-Area vaults in the GSA a structural degradation study was prepared. This study included an evaluation of ground motion effects on the vaults. Ground motion magnitudes were extrapolated from SRS performance categories (PCs) PC-1 to PC-4 site-specific seismic criteria. For horizontal acceleration, a 0.45 force of gravity value was obtained by extrapolating the zero period accelerations (i.e., peak ground acceleration) of the SRS design response for PC-1 to PC-4. [T-CLC-E-00018]

For vertical acceleration (2.0 force of gravity), a bounding approach was taken by extrapolating the peak of the SRS horizontal design response spectra for PC-1 to PC-4. This approach results in the large discrepancy between horizontal and vertical acceleration. This bounding approach for vertical acceleration was used in the structural degradation study because the item of concern was a buried roof slab with voids below. Therefore, the E-Area vault roof could respond differently than the ground (i.e., not peak ground acceleration). As the stabilized waste tanks will have no significant voids after grouting, this issue is not a concern. [T-CLC-E-00018]

Due to the lack of vertical/horizontal studies for low probability of exceedance events at SRS the same bounding criteria used in the E Area study were used for the structural assessment for closed waste tanks. [T-CLC-F-00421] However, it is recognized that 2.0 force of gravity is a bounding number. It is not a realistic number for ground acceleration at SRS. At the nearby Vogtle Electric Generating Plant, the vertical/horizontal ratio for the maximum considered event was 1.0, so a similar ratio should be considered acceptable for the SRS tank farms. [NUREG-1923] Based on a vertical/horizontal ratio of 1.0, the maximum vertical acceleration would be 0.45 force of gravity, much less than 2.0 assumed.

The PC-3 return period is 2,500 years (probability of exceedance $4.0E-04$), and the PC-4 return period is 10,000 years (probability of exceedance $1.0E-04$). In the E Area analysis 1-D soil analyses indicated the differential lateral displacement between the top and bottom elevations of the E-Area vault (approximately 28 feet in height) were 0.05 inches for a PC-3 event and 0.09 inches for a PC-4 event. The height differential in the E-Area vaults is similar to the height differential of the waste tanks. Extrapolating to probability of exceedance $1.0E-06$ (a very low probability event) gives a maximum lateral differential displacement of 0.22 inches. For this small amount of deformation, the soil would deform locally at the boundaries of the grout-filled waste tank and stresses induced in the waste tank structure will be minimal. [T-CLC-E-00018]

The impacts from seismic events are considered in the conceptual model. To simulate potential conditions in the HTF closure system, multiple waste tank cases were identified for analysis. While the cases and the potential seismic events are not explicitly linked, the types of cracks caused by the credible seismic events at the HTF are assumed bounded by the cases and the occurrence probability associated with the cases in the stochastic modeling.

Seismic considerations are also included in the design of the conceptual closure cap to ensure seismic induced degradation mechanisms are addressed. Section 3.2.4 discusses the

conceptual closure cap design, which will further consider and handle static loading induced settlement, seismic induced liquefaction and subsequent settlement, and seismic induced slope instability.

3.1.5 Hydrogeology

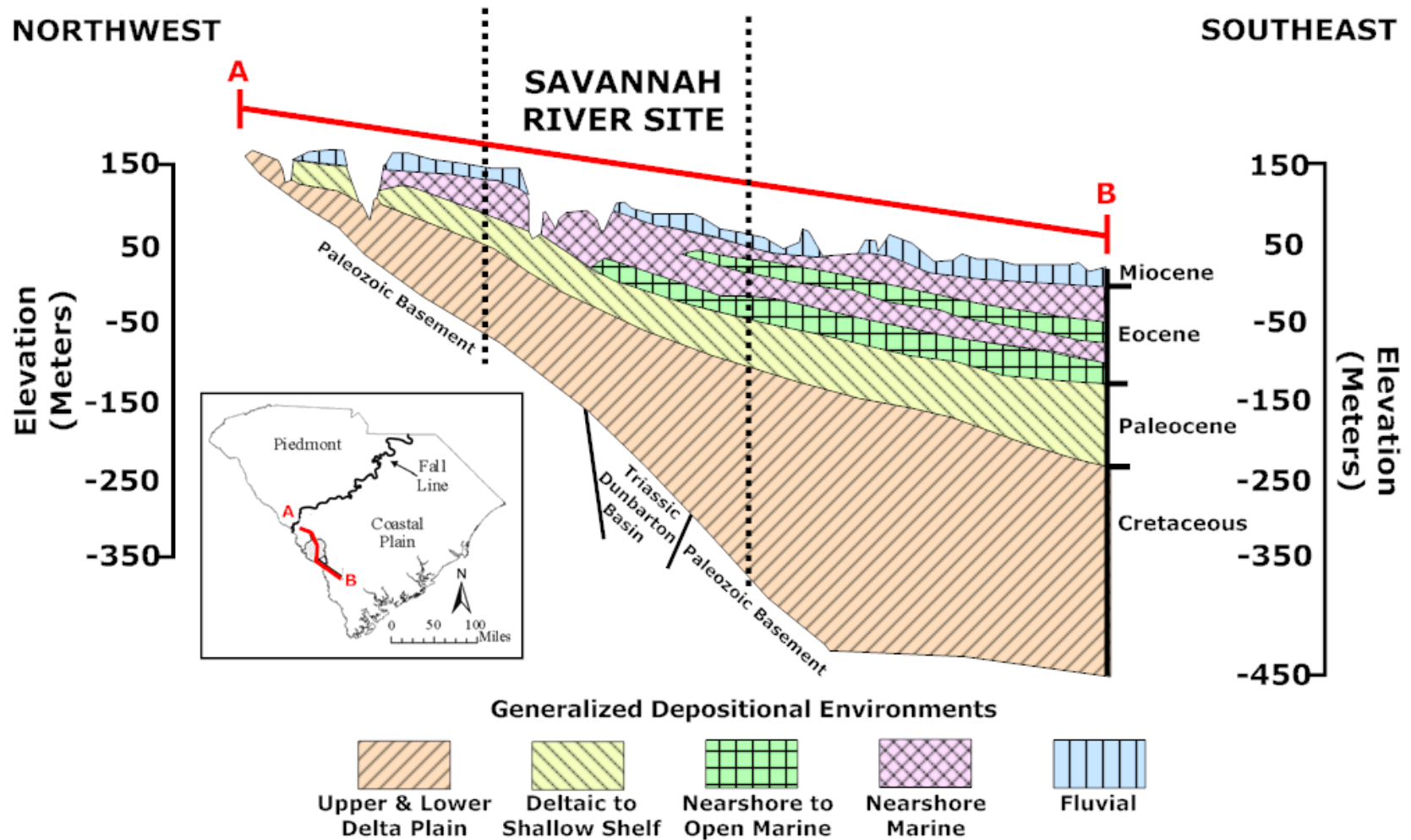
An understanding of the hydrogeology of the HTF is required in order for an estimate of the fate and transport of the residual HTF contaminants to be modeled. Characterization and monitoring data in the SRS GSA is extensive and provides a clear understanding of the hydrogeology containing the HTF, and permitted generation of the GSAD. Additional background information supporting this conclusion is presented in Section 3.1.5.2.

3.1.5.1 Regional Hydrogeology

The SRS lies in the Atlantic Coastal Plain, a southeast-dipping wedge of unconsolidated and semi-consolidated sediment, which extends from its contact with the Piedmont Province at the Fall Line to the continental shelf edge. Sediments range in geologic age from late Cretaceous to recent and include sands, clays, limestones, and gravels. This sedimentary sequence ranges in thickness from essentially zero at the Fall Line to more than 4,000 feet at the Atlantic Coast. At SRS, coastal plain sediments thicken from approximately 700 feet at the northwestern boundary to approximately 1,400 feet at the southeastern boundary of the site and form a series of aquifers and confining or semi-confining units. [WSRC-STI-2006-00198]

Figure 3.1-14 shows a generalized cross-section of the sedimentary strata and their corresponding depositional environments for the Upper Coastal Plain down-dip through the SRS into the Lower Coastal Plain. Figure 3.1-15 shows the regional lithologic units discussed in Section 3.1.4.2 and their corresponding hydrostratigraphic units at the SRS. This classification system is consistent with the established system and is now widely used as the SRS standard. [SRNL-STI-2010-00148]

Figure 3.1-14: Regional NW to SE Cross Section



[WSRC-STI-2006-00198]

Figure 3.1-15: Comparison of Chronostratigraphic, Lithostratigraphic, and Hydrostratigraphic Units in the SRS Region

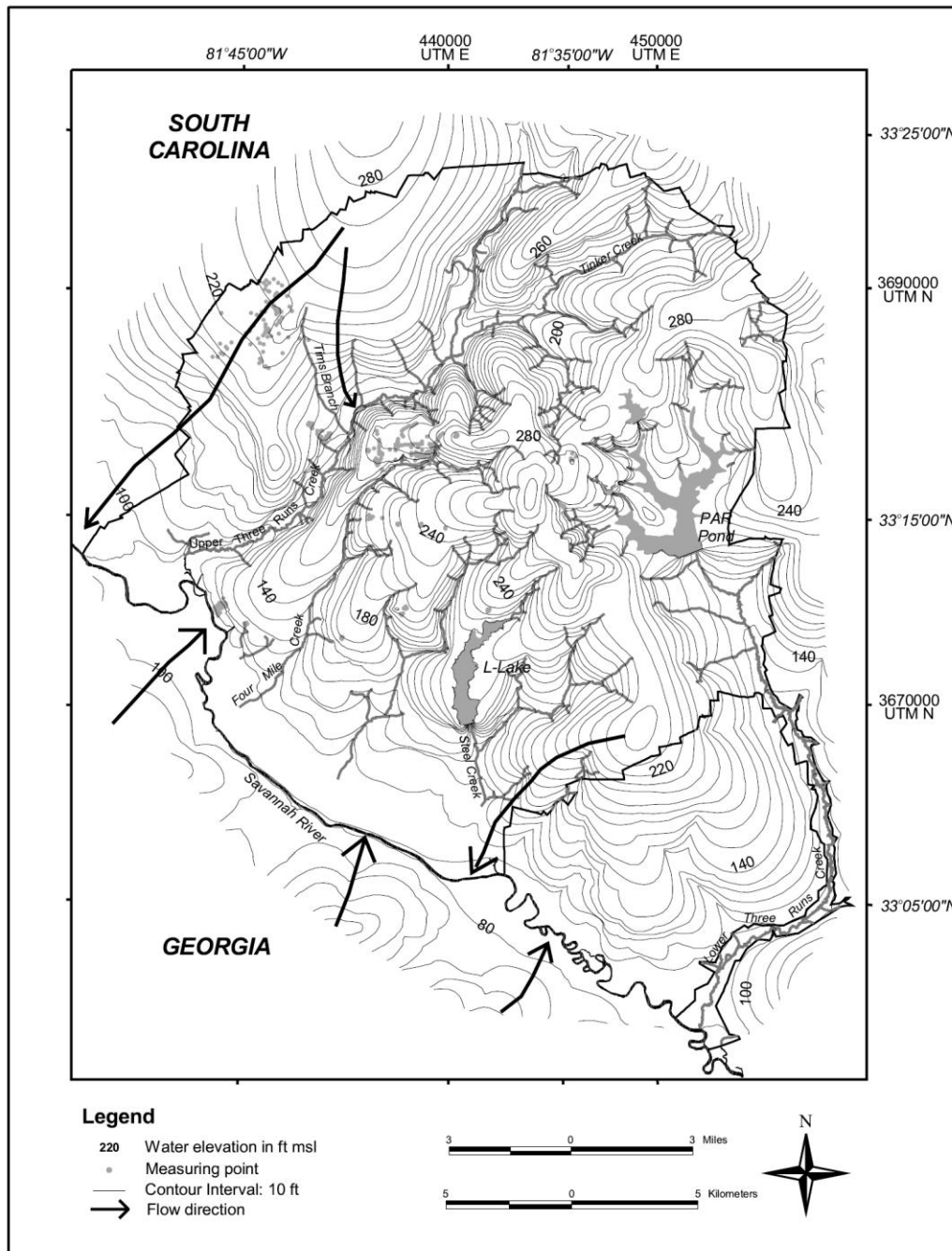
CHRONOSTRATIGRAPHIC UNITS			LITHOSTRATIGRAPHIC UNITS		HYDROSTRATIGRAPHIC UNITS				
ERA	System	Series	Group	Formation					
CENOZOIC	Tertiary	Miocene(?)		"Upland" unit	Aquifer Upper Zone		Floridan Aquifer System		
		Eocene	Upper	Barnwell Group	Tobacco Road Sand	Upper Three Runs Aquifer		Tan Clay Confining Zone	
					Dry Branch Formation				Irwinton Sand Mbr.
									Twiggs Clay Mbr.
									Griffins Landing Mbr.
		Clinchfield Formation	Aquifer Lower Zone						
		Middle		Orangoburg Group	Santee Formation	Gordon Confining Unit		Gordon Aquifer Unit	
					Warley Hill Formation				
					Congaree Formation				
		Lower		Black Mingo Group	Fourmile Branch Formation	Crouch Branch Confining Unit		Crouch Branch Aquifer	
Upper	Snapp Formation								
	Lang Syne Formation								
	Sawdust Landing Formation								
Lower		Lumbee Group	Steel Creek Formation	McQueen Branch Confining Unit	McQueen Branch Aquifer				
Upper Cretaceous			Black Creek Group						
			Middendorf Formation						
			Cape Fear Formation	undifferentiated					
MESOZOIC	Triassic		Newark Supergroup	Sedimentary Rock (Dunbarton Basin)	Meyers Branch Confining System		Southeastern Coastal Plain Hydrogeologic Province		
LATE(?) PROTEROZOIC	Pre-Cambrian(?)			Crystalline Basement Rock	Dublin-Midville Aquifer System				
					Piedmont Hydrogeologic Province				

[SRNL-STI-2010-00148]

Figures 3.1-16 and 3.1-17 illustrate potentiometric maps of the UTRA and Gordon Aquifer. Groundwater within the Floridan Aquifer system flows toward streams and swamps and into the Savannah River at rates ranging from inches to several hundred feet per year. The depth to which nearby streams cut into sediments, the lithology of the sediments, and the orientation of the sediment formations control the horizontal and vertical movement of the groundwater. The valleys of smaller perennial streams in the GSA, such as Fourmile Branch, McQueen Branch, and Crouch Branch, allow discharge from the shallow saturated geologic formations. The valleys of major tributaries of the Savannah River (e.g., UTR) drain formations of greater depth. With the release of water to the streams, the hydraulic head of

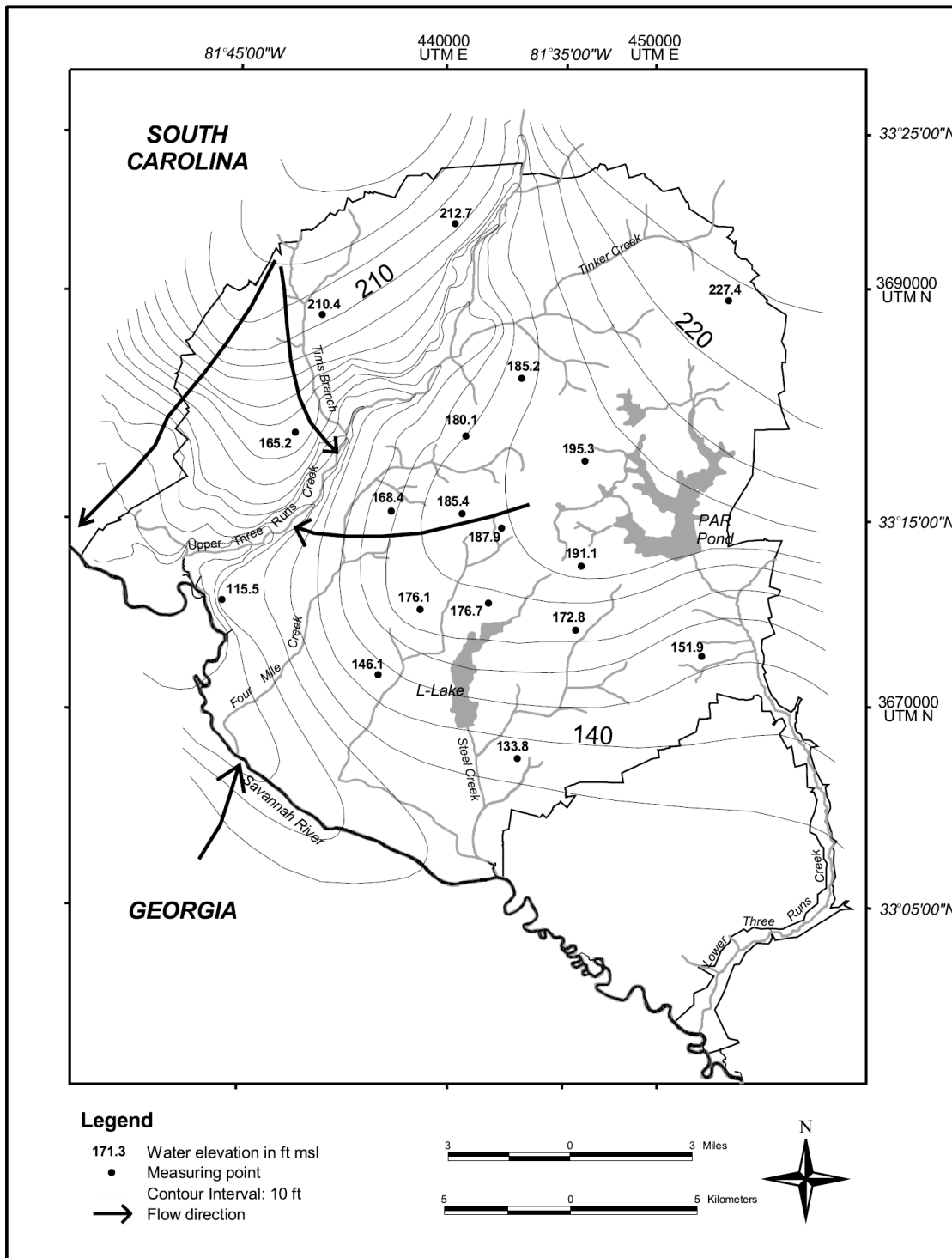
the aquifer unit releasing the water can become less than that of the underlying unit. If this occurs, groundwater has the potential to migrate upward from the lower unit to the overlying unit. [DOE-EIS-0303]

Figure 3.1-16: Potentiometric Surface of the UTRA



[SRNS-STI-2011-00059]

Figure 3.1-17: Potentiometric Surface of the Gordon Aquifer



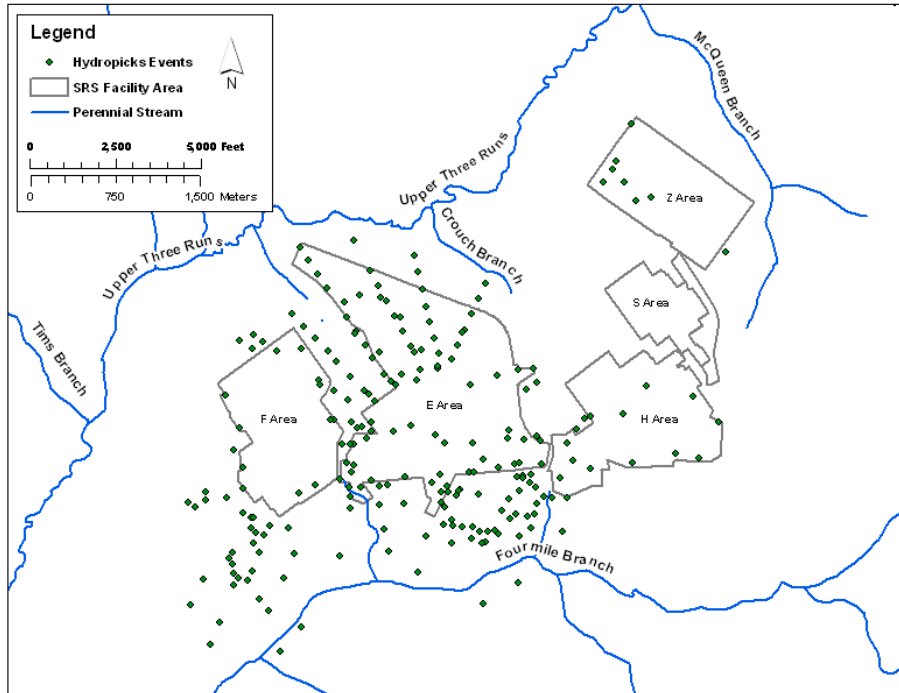
[SRNS-STI-2011-00059]

3.1.5.2 Characterization of Local Hydrogeology

The GSA has been the focus of numerous geological and hydrogeological investigations. Early work included installation of monitoring wells in the 1950's and 1960's. Further characterization and monitoring were conducted in the area during the 1970's through present time, largely to support groundwater monitoring and decommissioning activities. The GSAD was developed using field data and interpretations for the GSA and vicinity through 1996. Although characterization and monitoring have been ongoing, the additional data has not altered fundamental understanding of groundwater flow patterns and gradients in the GSA. The GSAD is a subset of site-wide data sets of soil lithology and groundwater information. Figure 3.1-18 shows the location of all hydrostratigraphic picks used in the GSAD. Picks were made based on a combination of geophysical logs, Cone Penetration Test (CPT) logs, and core descriptions. Figures 3.1-19 through 3.1-22 show the locations of laboratory permeability data, multiple well pump tests, single well pump tests, and slug test data used in the GSAD. Table 3.1-2 presents a summary of the characterization and monitoring data in the GSAD. These data provide detailed understanding of local hydrogeology beneath the HTF. See WSRC-TR-96-0399, Volumes 1 and 2, for a more comprehensive discussion of the data set. The GSAD, comprising the SRS characterization and monitoring data and interpretations, is used as the basis of hydrogeologic input values into the computational model for groundwater flow and contaminant transport as described in Section 4.2.2.1.3.

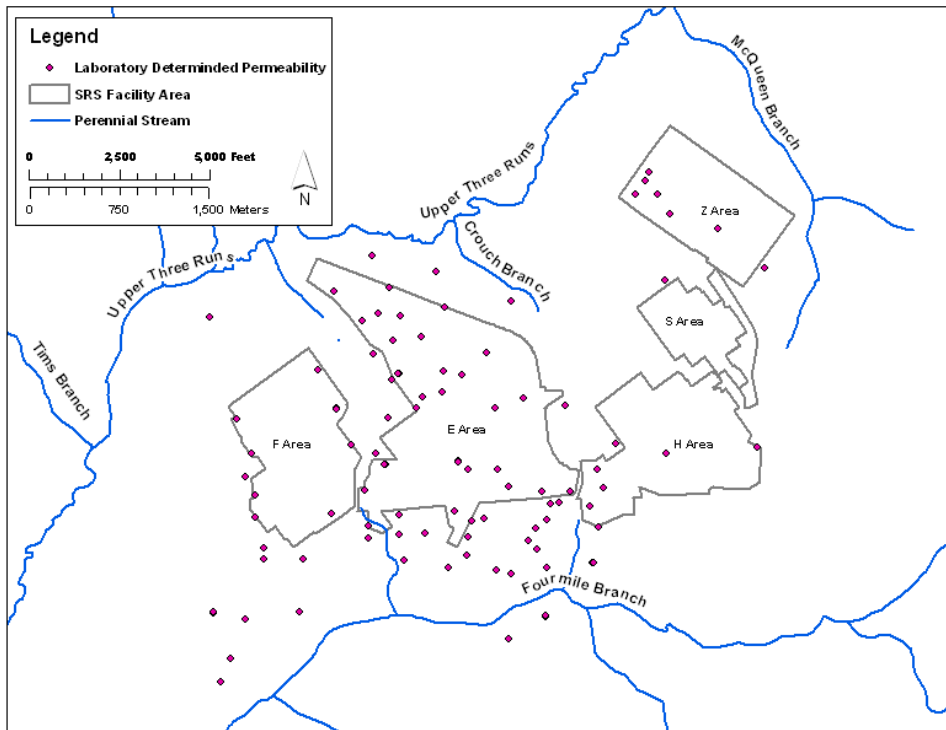
As described in Section 3.1.4.2, calcareous zones within the UTRA-LZ have been documented to contain soft zones, often related to dissolution of carbonate material. Soft zones at the SRS have not been studied using tracer tests; however, no unusual hydraulic gradients or unexpected flow conditions have been documented in the HTF or the GSA. Soft zones have however, been the subject of many general and facility-specific investigations. These studies have shown that the soft zones are isolated, discrete, poorly connected, non-uniformly distributed features within the UTRA-LZ. Although their size and shape vary greatly, their average thickness is generally only a few feet with a postulated maximum lateral dimension approximately 10 to 20 feet or less. [K-ESR-G-00013]

Figure 3.1-18: Hydrostratigraphic Picks in GSAD



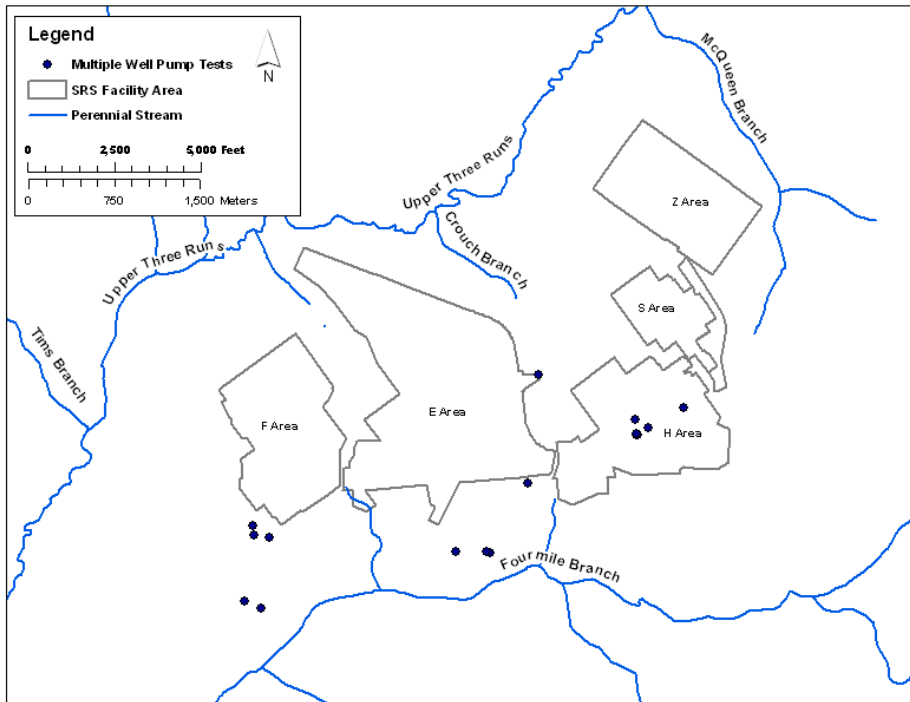
[WSRC-TR-96-0399, Vol. 1]

Figure 3.1-19: Laboratory Determined Permeability Data in GSAD



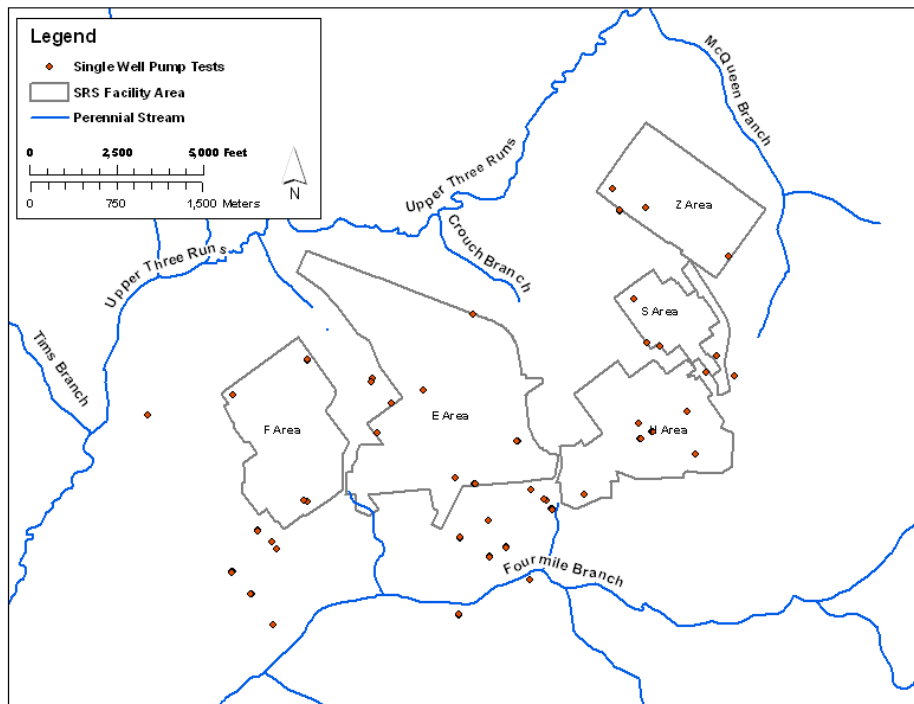
[SRNL-ESB-2007-00035]

Figure 3.1-20: Multiple Well Pump Test Data in GSAD



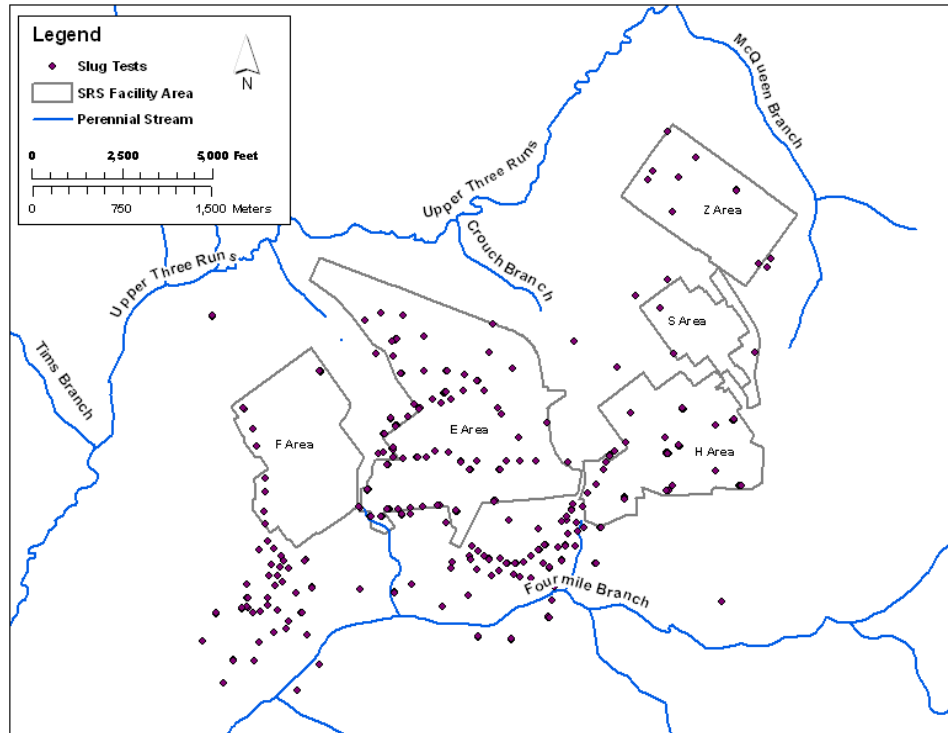
[WSRC-TR-96-0399, Vol. 2]

Figure 3.1-21: Single Well Pump Test Data in GSAD



[WSRC-TR-96-0399, Vol. 2]

Figure 3.1-22: Slug Test Data in GSAD



[WSRC-TR-96-0399, Vol. 2]

Table 3.1-2: Characterization and Monitoring Data in the GSAD

Data Type	Quantity	Reference
Sediment Core Descriptions	204 Locations approximately 37,500 ft	WSRC-TR-96-0399, Vol. 1, App. B
Tops of Hydrostratigraphic Units/Zones		
Crouch Branch Confining Unit	52 Locations	WSRC-TR-96-0399, Vol. 1, App. A-3
Gordon Aquifer Unit	146 Locations	
Gordon Confining Unit	161 Locations	
UTRA-LZ	222 Locations	
TCCZ	225 Locations	
Permeability Measurements		
Pump Tests	85 Values	WSRC-TR-96-0399, Vol. 2, App. B
Slug Tests	481 Values	
Laboratory Permeability	258 Values	
Water Levels		
Gordon Aquifer Unit	79 Locations	WSRC-TR-96-0399, Vol. 2, App. C
UTRA-LZ	173 Locations	
UTRA-UZ	387 Locations	

3.1.5.3 Groundwater Flow in the GSA

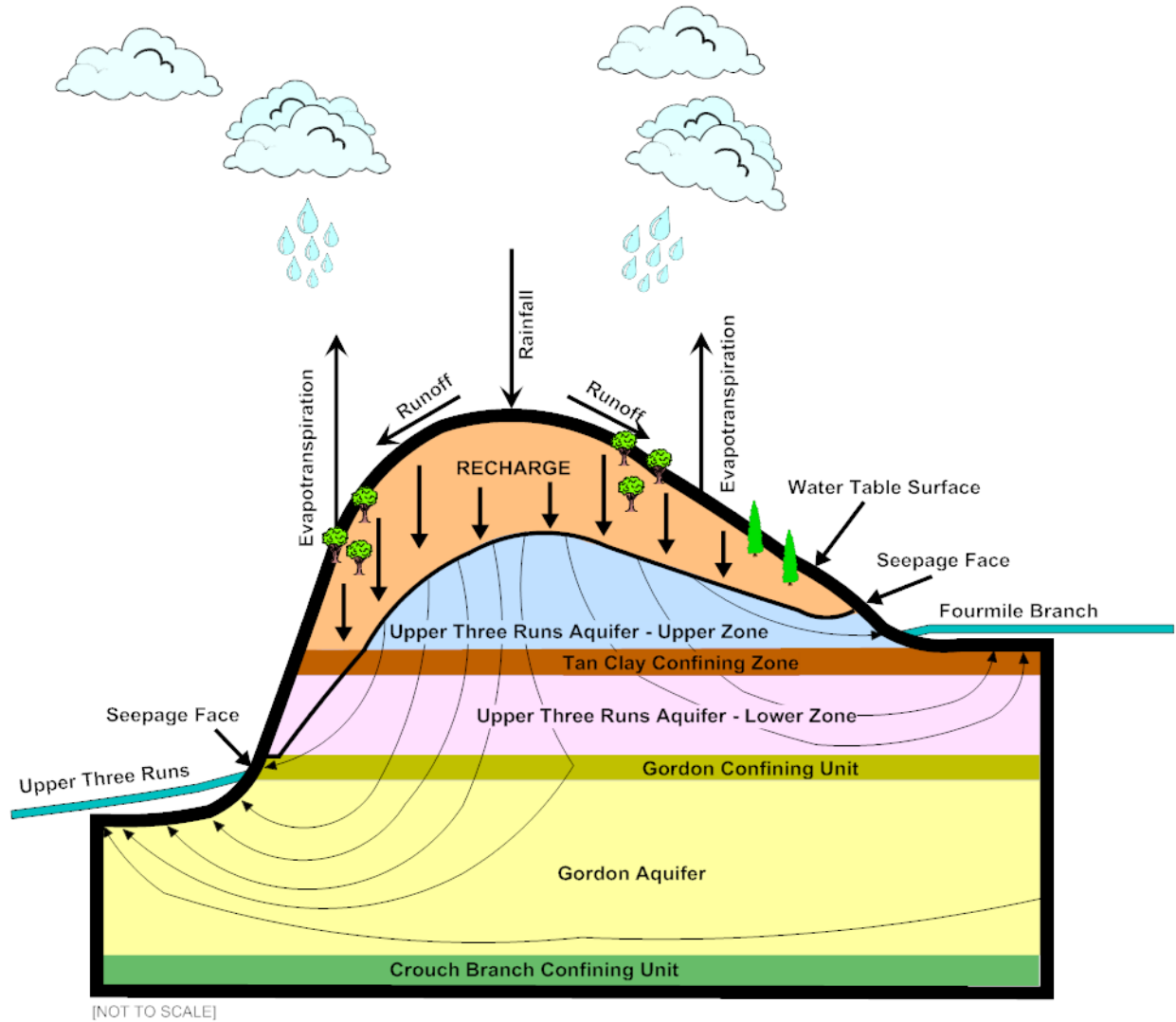
The aquifers of primary interest for HTF modeling are the UTRA-UZ, UTRA-LZ, and Gordon Aquifer. Plate 17 of the *Hydrogeological Framework of West-Central South Carolina* (PIT-MISC-0112) gives the leakance coefficient of the Crouch Branch Confining Unit (of the Meyers Branch Confining System) as roughly 3E-06 per day, which corresponds to 0.13 in/yr for every 10 feet of head difference. The measurement of head difference across the Crouch Branch Confining Unit is zero to 20 feet causing an upward flow averaging 0.13 in/yr. [PIT-MISC-0112] Flow across the unit is therefore a small fraction of total recharge, and is negligible in the HTF modeling. Potential contamination from the HTF is not expected to enter the deeper Crouch Branch Aquifer because an upward gradient exists between the Crouch Branch and Gordon Aquifers near UTRA. Figure 3.1-23 is a cross-sectional schematic representation of groundwater flow patterns in the UTRA and Gordon Aquifer along a north-south cross-section running through the center of HTF, shown with significant vertical exaggeration. Section 4.2.2.1.3 provides the modeling inputs associated with groundwater flow characteristics obtained from the GSAD.

Although calcareous zones containing soft zones have been identified in the UTRA-LZ (Section 3.1.4.2) during the 20-year period spanned by investigations used to populate the GSAD at more than 15 locations near HTF, no open flow conduits or other factors have been identified that would critically influence contaminant transport.

In addition, a further evaluation of more than 60 years of onsite investigation and research into soft zone occurrence, origin, and behavior concludes that soft zones at the SRS appear not to be a critical influence on either groundwater flow or contaminant transport. [SRNL-TR-2012-00160]

Calcareous zones and associated soft zones are not treated separately in the flow model because they are isolated and discontinuous in the GSA, representing only a small fraction of the UTRA-LZ. These features occur near the base of the UTRA-LZ in the GSA and do not extend through the entire thickness of the aquifer. [WSRC-TR-99-4083]

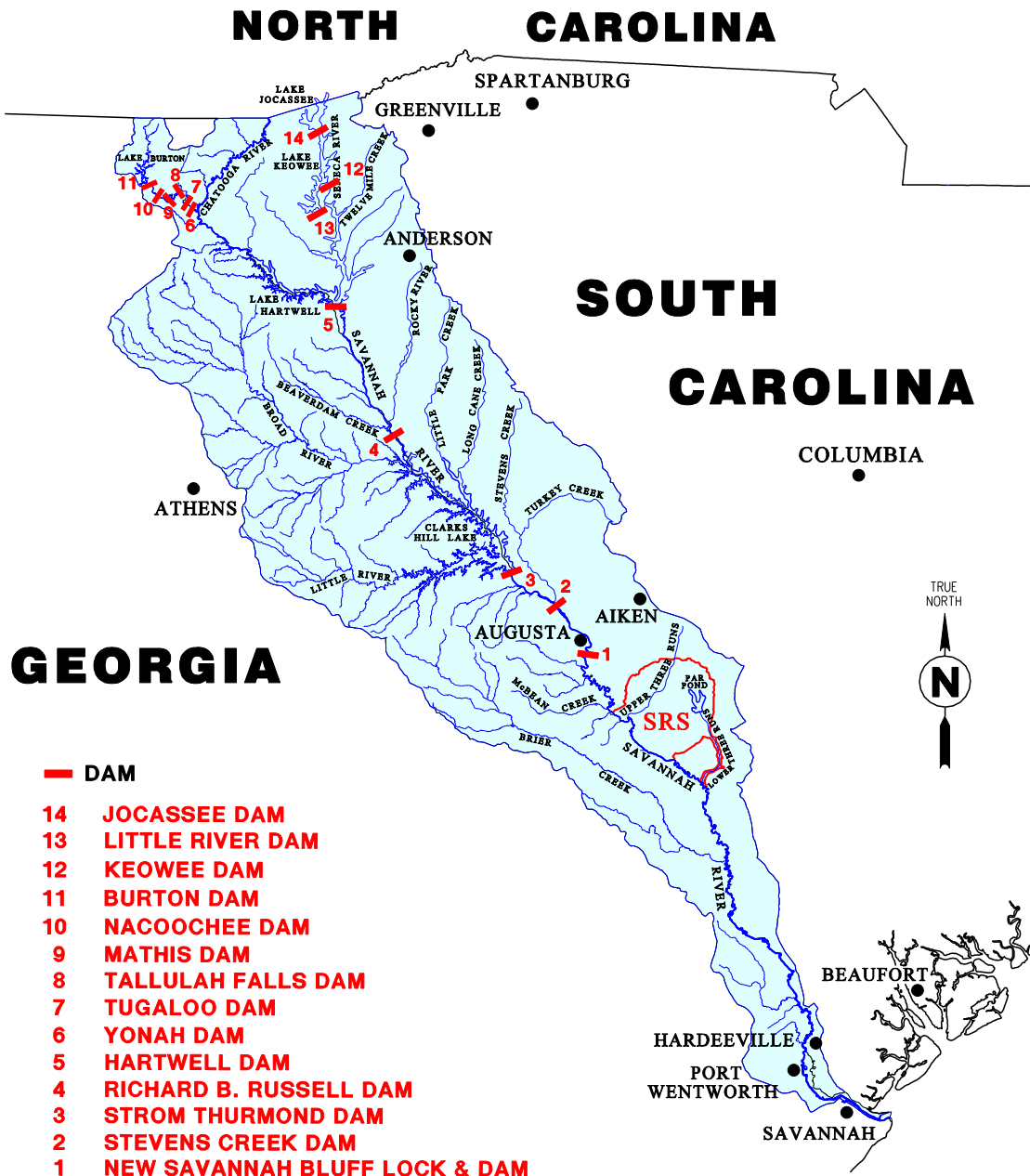
Figure 3.1-23: Conceptual Diagram of Groundwater Flow beneath the GSA



3.1.5.4 Surface-Water Flow in the GSA

The Savannah River, which forms the boundary between Georgia and South Carolina, is the principal surface-water system near the SRS. The river adjoins the site along its southwestern boundary for a distance of approximately 20 miles and the site is 160 river-miles from the Atlantic Ocean. Five upstream reservoirs Jocassee, Keowee, Hartwell, Richard B. Russell, and Clarks Hill Lake (also known as Thurmond Lake), minimize the effects from droughts and the impacts of low flow on downstream water quality and fish and wildlife resources in the river. Figure 3.1-24 shows the Savannah River Basin dams. The long-term yearly Savannah River flow at the SRS averages 10,400 ft³/s. [WSRC-TR-2005-00201, Table 4-24] For 2010, the measured average annual flow rate was 6,603 ft³/s. [SRNS-STI-2011-00059]

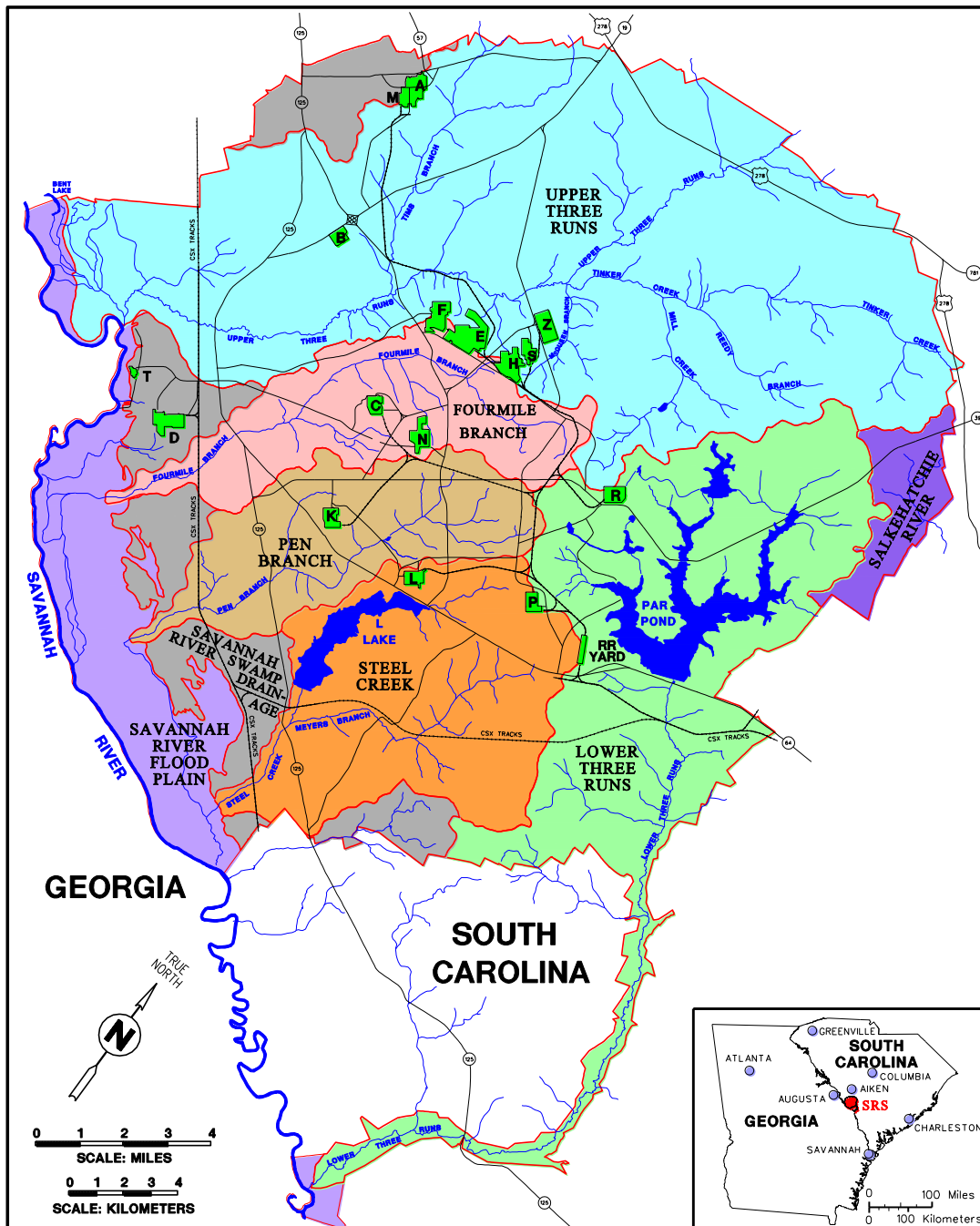
Figure 3.1-24: Savannah River Basin Dams



The major tributaries that occur on the SRS are UTR, Fourmile Branch, Pen Branch, Steel Creek, and Lower Three Runs (Figure 3.1-25). These tributaries drain all of SRS with the exception of a small area on the northeast side, which drains to a tributary of the Salkehatchie River. Each of these streams originates on the Aiken Plateau in the Coastal Plain and descends 50 to 200 feet before discharging into the river. The source of most of the surface water on SRS is either natural rainfall (Section 3.1.2), water pumped from the Savannah

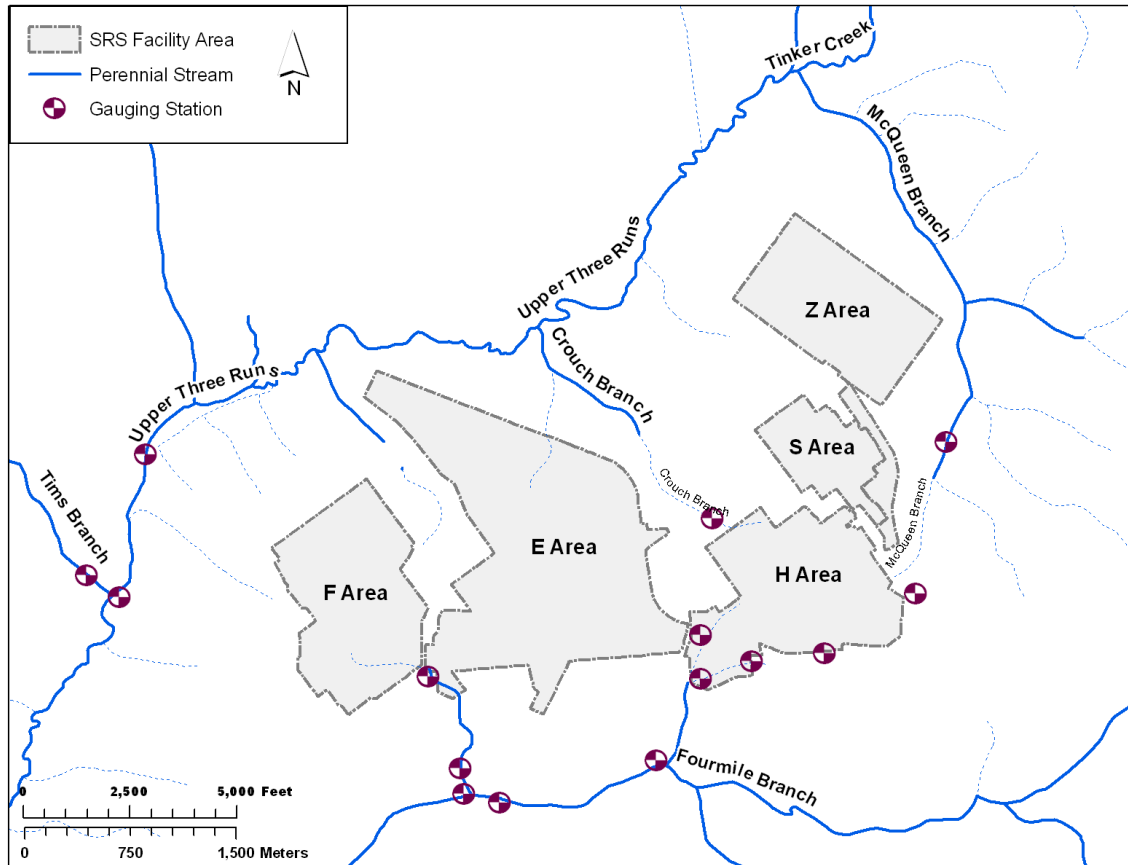
River and used for cooling site facilities, or groundwater discharging to surface streams. The streams, which historically have received varying amounts of effluent from SRS operations, are not commercial sources of water. Downstream of the SRS, the river supplies domestic water and is used for commercial and sport fishing, boating, and other recreational activities. [DOE-EIS-0303]

Figure 3.1-25: Savannah River Site Watershed Boundaries and Major Tributaries



The natural flow of the SRS streams range from 8 ft³/s in smaller streams to 245 ft³/s in UTR. [WSRC-IM-2004-00008] Gauging stations located in the GSA (Figure 3.1-26) monitor flows for UTR and Fourmile Branch. Both Fourmile Branch and UTR are measured monthly for water flow, temperature, and quality. The annual *Savannah River Site Environmental Report for 2010* contains detailed information on flow rates and water quality of the Savannah River and the SRS streams. [SRNS-STI-2011-00059]

Figure 3.1-26: GSA Gauging Stations



The SCDHEC regulates the physical properties and concentrations of chemicals and metals in the SRS effluents under the National Pollutant Discharge Elimination System (NPDES) program. Also regulated by SCDHEC, biological water quality standards for the SRS waters have classified the Savannah River and SRS streams as “Freshwaters.” [DOE-EIS-0303] Freshwaters are described as suitable for primary and secondary contact recreation and as a source for drinking water supply after treatment in accordance with SCDHEC requirements. Freshwaters are suitable for fishing, for the survival and propagation of a balanced indigenous aquatic community of fauna and flora, and for industrial and agricultural uses. [SCDHEC R.61-68]

The longest of SRS streams, UTR, is a large blackwater stream in the northern part of the SRS that discharges to the Savannah River. It drains an area of over 195 square miles and is approximately 25 miles long, with its lower 17 miles within the SRS boundaries. This stream receives more water from underground sources than other SRS streams and is the only stream with headwaters arising outside the site. The UTR is the only major tributary on the SRS that has not received thermal discharges. The UTR valley has meandering channels, especially in the lower reaches, and its floodplain ranges in width from 0.25 to 1 mile. It has a steep southeastern side and gently sloping northwestern sides. [DOE-EIS-0303]

Fourmile Branch is a blackwater stream that originates near the center of the SRS and flows southwest for 15 miles before emptying into the Savannah River. It drains an area of approximately 22 square miles inside the SRS including much of F, H, and C Areas. Fourmile Branch flow is generally perpendicular to the Savannah River behind natural levees and enters the river through a breach downstream from Beaver Dam Creek. In its lower reaches, Fourmile Branch broadens and flows via braided channels through a delta formed by the deposition of sediments eroded from upstream during high flows. Downstream from the delta, the channels rejoin into one main channel. Most of the flow discharges into the Savannah River while a small portion flows west and enters Beaver Dam Creek. The valley is V-shaped, with sides varying from steep to gently sloping. The floodplain is up to 1,000 feet wide. [DOE-EIS-0303]

Flood hazard recurrence frequencies have been calculated for the various SRS site areas. The calculated flood water levels for Fourmile Branch near H Area, for the probability of 100-year, 1,000-year, and 10,000-year returns are about 234.3, 235.2, and 235.8 feet above mean sea level (MSL), respectively. As shown in Section 3.2, the lowest elevation of any waste tank basemat in HTF is 239.9 feet above MSL; thus, the highest flood water level of approximately 236 feet above MSL is below the lowest elevation of residual radioactive material. In addition, the lowest elevation of the lower foundation layer of the proposed closure cap is 280 feet above MSL, which is about 44 feet above the highest flood water level of 236 feet. Therefore, flooding will not affect the HTF and is therefore not considered in this PA. [WSRC-TR-99-00369, SRNL-ESB-2008-00023]

3.1.6 Geochemistry

The migration of radionuclides in the subsurface environment is dependent on physical and chemical parameters or properties of cementitious materials, soils, and groundwater. Studies and analyses have been conducted to determine appropriate K_d values. The data used in the radionuclide transport model is presented in Sections 4.2.2 and 4.2.3.2 specific to the GSA and is not reproduced in this section.

3.1.7 Natural Resources

Natural resources at SRS are managed under the *Natural Resources Management Plan for the Savannah River Site* (NRMP) prepared for the DOE by the U.S. Department of Agriculture (USDA) Forest Service - Savannah River. [NRMP-2005] The NRMP, which governs the SRS natural resource management was updated in May 2005 and fosters the following principles:

- All work will be done in accordance with integrated safety management components found in DOE Policy 450.4A, *Integrated Safety Management Policy*
- Environmental stewardship activities will be compatible with future SRS missions
- The SRS will continue to protect and manage SRS natural resources
- Sustainable resource management will be applied to SRS natural resources
- Close cooperation will be maintained among organizations when managing and protecting the SRS natural resources
- The results of research, monitoring, and operational findings will be used in the management of SRS natural resources
- Restoration of native communities and species will continue
- Employees, customers, stakeholders, state natural resource officials, and regulators will be invited to participate in the natural resource planning process
- The SRS will maintain the area as a National Environmental Research Park (NERP)

3.1.7.1 Water Resources

The SRS monitors non-radioactive liquid discharges to surface waters through the NPDES, as mandated by the Clean Water Act (CWA). As required by EPA and SCDHEC, SRS has NPDES permits in place for discharges to the waters of the United States and South Carolina. These permits establish the specific sites to be monitored, parameters to be tested, and monitoring frequency, as well as analytical, reporting, and collection methods. [SRNS-STI-2011-00059] Continuous surveillance monitoring of site streams occurs downstream of several process areas to detect and quantify levels of radioactivity in effluents transported to the Savannah River. [SRNS-STI-2011-00059]

Table 3.1-3 characterizes Savannah River water quality both upstream and downstream of the SRS. Table 3.1-4 characterizes water quality in UTR and Fourmile Branch downstream of the GSA.

**Table 3.1-3: Water Quality in the Savannah River Upstream and Downstream from SRS
(Calendar Year 2010)**

Parameter	Unit of Measure	Upstream ^b		Downstream ^c	
		Minimum	Maximum ^a	Minimum	Maximum ^a
Aluminum	mg/L	0.105	0.487	0.11	0.57
Cadmium	mg/L	ND	ND	ND	ND
Chromium	mg/L	ND	ND	ND	ND
Copper	mg/L	ND	0.517	ND	0.0083
Dissolved Oxygen	mg/L	4.6	19.9	4.28	11.31
Gross Alpha Radioactivity	pCi/L	ND	1.59	ND	1.31
Lead	mg/L	ND	ND	ND	0.0023
Mercury	mg/L	ND	0.000023	ND	0.000024
Nickel	mg/L	ND	ND	ND	0.0066
Nitrate (as N)	mg/L	0.18	0.38	0.12	0.58
pH	pH units	6.25	7.32	6.42	7.41
Phosphate	mg/L	0.095	0.17	0.079	0.17
Suspended solids	mg/L	2	10	5	20
Temperature	°F	44.2	75.9	43.3	79.2
Tritium	pCi/L	ND	265	98.6	957
Zinc	mg/L	0.0022	0.0087	0.0013	0.0352

Notes: Information extracted from SRNS-STI-2011-00059 accompanying data files. Parameters are those the DOE routinely measures as a regulatory requirement or as part of ongoing monitoring programs.
a The maximum listed concentration is the highest single result found during one sampling event
b Data from sampling location RM-160
c Data from sampling location RM-118.8
ND Non-detectable

Table 3.1-4: Water Quality in Selected SRS Streams (Calendar Year 2010)

	Temperature (°F)	pH	Dissolved Oxygen (mg/L)	Total Suspended Solids (mg/L)
Sampling Location: Fourmile Branch (Downstream from GSA)^a				
Mean	60.2	6.8	7.0	2.9
Range	39.0 – 77.2	6.4 – 7.2	3.3 – 11.5	0 – 6
Sampling Location: UTR (Downstream from GSA)^b				
Mean	58.2	6.2	7.8	6.1
Range	42.5 – 75.0	5.7 – 7.2	4.9 – 16.1	1 – 12

Notes: All data extracted from SRNS-STI-2011-00059 accompanying data files
a Stream sample location FM-6
b Stream sample location U3R-4

3.1.7.1.1 Groundwater

The Federal Safe Drinking Water Act (SDWA) was enacted in 1974 to protect public drinking water supplies. The SRS domestic water is supplied by 17 separate systems, all of which utilize groundwater sources. The A Area and D-Area drinking water facilities are actively regulated by SCDHEC, while the remaining smaller water systems receive a reduced level of regulatory oversight. The K-Area drinking water system was

incorporated into the A Area system in 2010, and removed from SCDHEC's water system inventory. [SRNS-STI-2011-00059]

Table 3.1-5 provides the summary of maximum groundwater monitoring results for those areas that most likely discharge to UTR or Fourmile Branch obtained from the *Savannah River Site Environmental Report for 2008*, which represents the latest annual summary of well monitoring results summarized by area. [SRNS-STI-2009-00190] The groundwater in these areas is not being consumed and active remediation projects are in progress to address the groundwater conditions.

Table 3.1-5: Well Monitoring Results for Major Areas within SRS, 2007-2008

Location	Major Contaminants	Units	2007 Max	MCL	2008 Max	Likely Outcrop Point
E Area	Tritium TCE ^b	pCi/L ppb	30,800,000 370	20,000 0.5	29,200,000 460	UTR/Crouch Branch in North; Fourmile Branch in South
F Area	TCE ^b Tritium Gross alpha Beta	ppb pCi/L pCi/L pCi/L	52.2 73,000 2,120 380	5.0 20,000 15 4 mrem/yr ^a	60 130,000 1,470 628	UTR/Crouch Branch in North; Fourmile Branch in South
F-Area Seepage Basin	Tritium Gross alpha Beta	pCi/L pCi/L pCi/L	5,710,000 523 1,870	20,000 15 4 mrem/yr ^a	4,810,000 777 2,100	Fourmile Branch
H Area	Tritium Gross alpha Beta	pCi/L pCi/L pCi/L	67,200 25.5 55.6	20,000 15 4 mrem/yr ^a	74,800 14.9 81.9	UTR/Crouch Branch in North; Fourmile Branch in South
H-Area Seepage Basins	Tritium Gross alpha Beta	pCi/L pCi/L pCi/L	3,020,000 88.4 2,970	20,000 15 4 mrem/yr ^a	3,120,000 85 2,050	Fourmile Branch

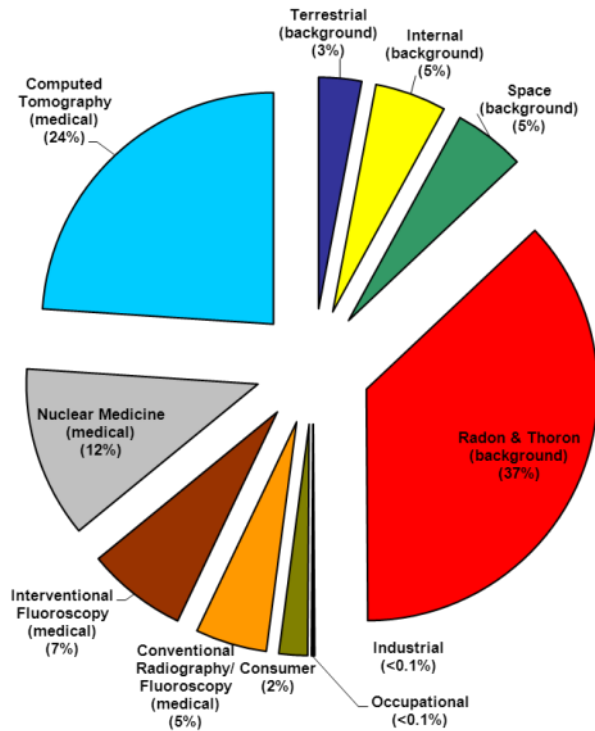
a The activity (pCi/L) equivalent to 4 mrem/yr varies according to which specific beta emitters are present in the sample. [SRNS-STI-2009-00190]

b Trichloroethylene

3.1.8 Natural and Background Radiation

All human beings are exposed to sources of ionizing radiation that include naturally occurring and man-made sources. Individual's average dose contribution estimates from various sources were obtained from the review information presented in National Council on Radiation Protection and Measurements (NCRP) Report 160 and are shown in Figure 3.1-27. On average, a person living in either the United States or the Central Savannah River Area (CSRA) receives approximately the same annual radiation dose of 620 mrem/yr. [NCRP-160] The dose from SRS operations to the maximally exposed offsite individual during calendar year 2010 was estimated to be 0.11 millirem. [SRNS-STI-2011-00059]

Figure 3.1-27: Major Sources of Radiation Exposure near SRS

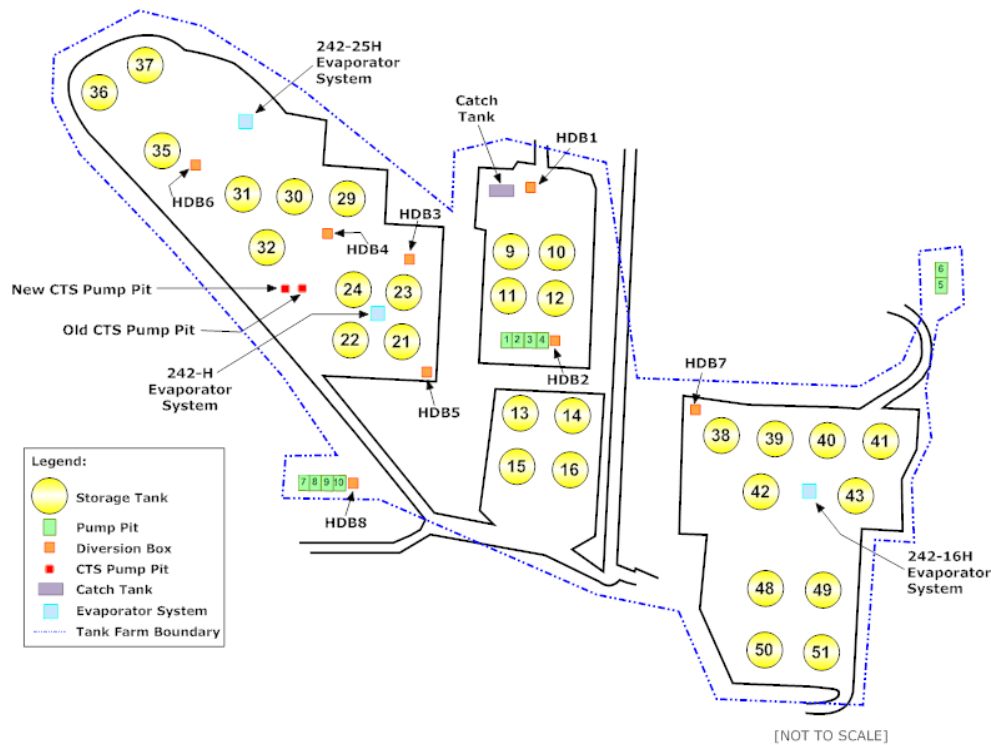


The major source of radiation exposure to an average MOP in the CSRA is attributed to naturally occurring radiation (311 mrem/yr) and medical exposure (300 mrem/yr). This naturally occurring radiation is often referred to as natural background radiation and includes dose from background radon and its decay products (228 mrem/yr), cosmic radiation (33 mrem/yr), internal radionuclides occurring naturally in the body (29 mrem/yr), and natural radioactive material in the ground (21 mrem/yr). The dominant medical sources include dose from computed tomography (147 mrem/yr), nuclear medicine (77 mrem/yr), and radiography/fluoroscopy (77 mrem/yr). The remainder of the dose is from consumer products (13 mrem/yr), industrial/educational/research activities (< 1 mrem/yr), and occupational exposure (< 1 mrem/yr). [NCRP-160]

3.2 Principal Facility Design Features

The HTF occupies a 45-acre site within an area of the SRS commonly referred to as the GSA, which encompasses E, F, H, J, S, and Z Areas (Figure 3.1-9). The HTF consists principally of three control rooms, approximately 74,800 feet of transfer lines, 10 PPs (each has one pump tank except HPP-1 which has none), two concentrate transfer system (CTS) PPs, one catch tank, three evaporators, and 29 waste tanks (Figure 3.2-1).

Figure 3.2-1: Layout of HTF Including Ancillary Equipment



In order to model the potential risk associated with the HTF stabilized contaminant inventory expected to remain after the closure of the HTF, locations with the potential for stabilized contaminant retention and the design features affecting those locations were identified. There are two primary categories of facility design with the potential for stabilized contaminant retention in the HTF 1) waste tanks and 2) ancillary equipment.

Waste tanks refer to the 29 subsurface carbon steel tanks in the HTF designed for storing aqueous liquid wastes. Ancillary equipment refers to the other equipment used in the HTF to transfer waste (e.g., transfer lines, pump tanks) and reduce waste volume through evaporation (e.g., the evaporator systems).

3.2.1 Waste Tanks

There are 29 waste tanks in HTF. The waste tanks are all built of carbon steel and reinforced concrete, but the designs vary. There are four principal types of waste tanks in the HTF, designated as Type I, II, III, IIIA, and IV tanks. The waste tanks were constructed at different times during which design features were improved on. Waste tank design types are covered in Sections 3.2.1.1 through 3.2.1.4

The HTF waste tank numbering along with their design type is as follows:

- Type I: Tanks 9 through 12
- Type II: Tanks 13 through 16
- Type IV: Tanks 21 through 24
- Type III: Tanks 29 through 32
- Type IIIA: Tanks 35 through 43 and 48 through 51

The HTF waste tank locations (North and East coordinates) and working slab top elevations are summarized in Table 3.2-1.

Table 3.2-1: Waste Tank Locations and Elevations for HTF

Tank	North Location	East Location	Working Slab Top (MSL)	References
9	71680.0	62005.0	241.4	W715395
10	71680.0	62109.0	241.4	W715395
11	71580.0	62005.0	239.9	W715395
12	71580.0	62109.0	239.9	W715395
13	71318.0	62043.0	270.33	W163048
14	71318.0	62160.0	270.33	W163048
15	71200.0	62043.0	270.33	W163048
16	71200.0	62160.0	270.33	W163048
21	71463.0	61772.0	281.42 ^a	W230826 W230945
22	71463.0	61660.0	281.42 ^a	W230826 W230945
23	71577.0	61772.0	281.42 ^a	W230826 W230945
24	71577.0	61660.0	281.42 ^a	W230826 W230945
29	71778.5	61636.0	283.5	W236439
30	71778.5	61520.0	282.5	W236439
31	71778.5	61404.0	281.5	W236439
32	71662.5	61462.0	280	W236439
35	71865.0	61220.0	282.7	W449843
36	71990.0	61075.0	283.7	W449843
37	72052.0	61175.0	283.7	W449843
38	71290.0	62490.0	291.09	W449843
39	71290.0	62610.0	292.09	W700834
40	71290.0	62730.0	292.09	W700834
41	71290.0	62850.0	291.09	W700834
42	71170.0	62590.0	293.09	W700834
43	71170.0	62800.0	293.09	W700834
48	70956.0	62610.0	288.14	W706301
49	70956.0	62735.0	288.14	W706301
50	70820.0	62610.0	285.64	W706301
51	70820.0	62735.0	285.64	W706301

^a The elevation shown for the Type IV tanks is at the bottom of the floor slab, there is no working slab under the Type IV tanks.

The main component of a waste tank is the primary liner where the liquid waste is contained. The primary liner is cylindrical in shape and made of carbon steel. Each primary liner type differs in size and capacity.

Type I, II, III, and IIIA tanks are enclosed by a secondary liner, which is larger in diameter than the primary liner. The secondary liner, like the primary liner, is constructed of carbon steel. Since the secondary liner is larger in diameter than the primary liner, an area is formed between them called the annulus. The annulus differs in size and capacity for each waste tank type. The annulus serves several purposes for the waste tanks. It provides a collection point for any leakage from the primary liner and provides a method for heating or cooling the primary liner wall in conjunction with the annulus ventilation system. The Type IV tanks do not have a secondary liner.

A reinforced concrete vault surrounds the secondary liner. The vault concrete provides both structural support and radiation shielding. The bottom part of the concrete vault is called the basemat. Underneath the basemat of the Type I, II, III, and IIIA tanks is a working slab.

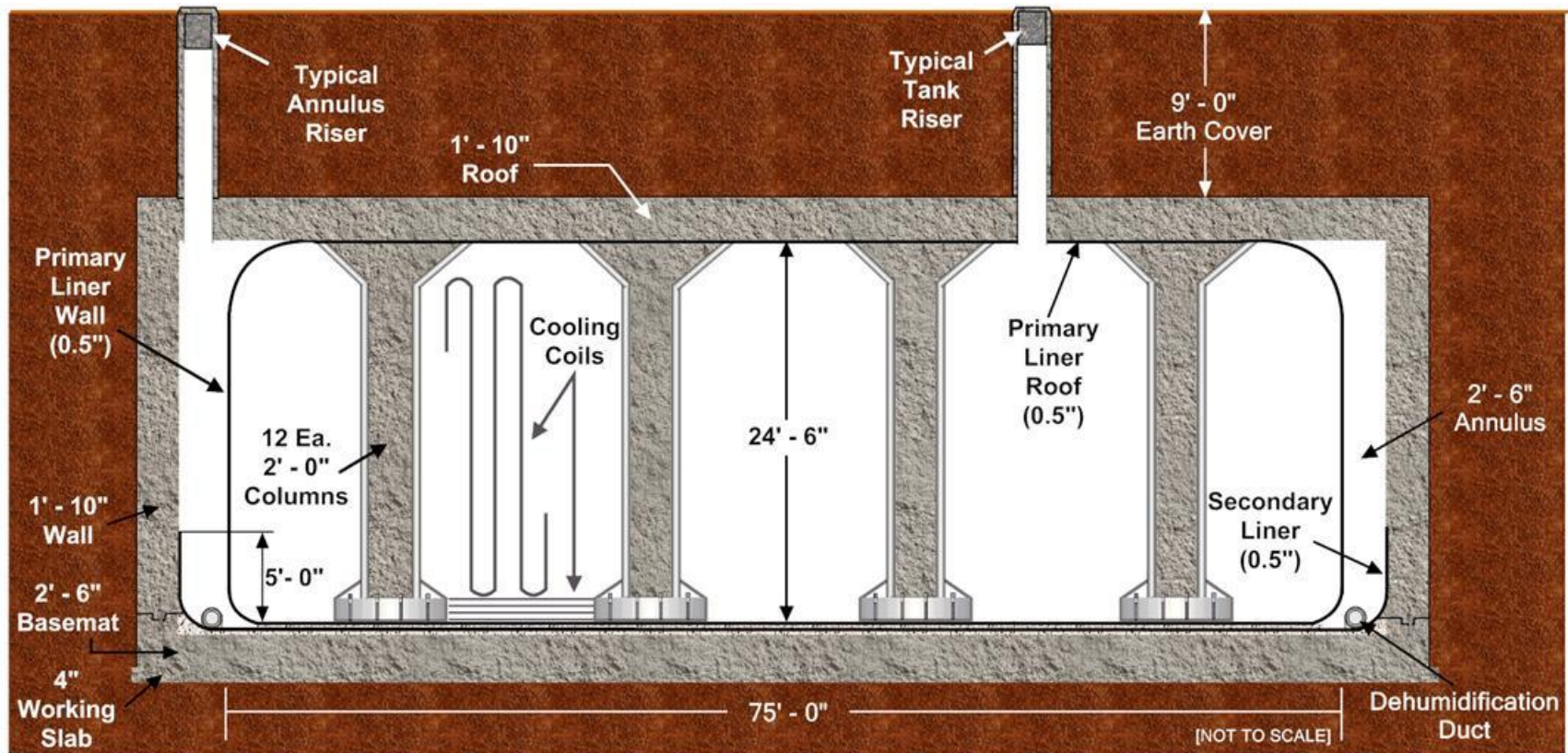
The primary cooling method for the liquid waste is provided by cooling water (containing chromate for corrosion control) that runs through cooling coils located inside the primary liner. These cooling coils are installed in Type I, II, III, and IIIA tanks and the cooling coil design for each waste tank type varies. Type IV tanks do not have cooling coils.

Risers provide access to the waste tank and annulus interiors. Risers are used primarily for inspections, level detection, dip samples, and the installation of equipment such as annulus jets, dip tubes, thermocouples, conductivity probes, ventilation inlet and outlets, reel tapes, hydrogen monitors, and waste removal equipment. Lead or concrete plugs are inserted in the riser opening if no equipment is installed. The riser structures are made of concrete and lined with carbon steel. Riser layout is dependent on the specific waste tank being discussed. However, waste tanks of a given type have similar equipment installed in the risers. Riser plugs can weigh anywhere from a few pounds to several thousand pounds.

3.2.1.1 Type I Tanks

There are four Type I tanks in the HTF. The HTF Type I tanks were constructed in the early 1950s. These waste tank primary liners are 75 feet in diameter and 24.5 feet high, with a nominal operating capacity of 750,000 gallons. A typical Type I tank is shown in Figure 3.2-2.

Figure 3.2-2: Typical Type I Tank



3.2.1.1.1 Working Slab and Basemat

The working slab for a Type I tank is 4-inches thick, with a radius of 42 feet 5 inches, and has a 2-inch wire mesh layered in the middle. [W145293] The concrete for the working slab was installed with 2,500-psi strength at a 28-day cure time. [W145225] A 1.5-inch thick layer of plaster/waterproofing membrane sits above the working slab. [W145573] A 30-inch reinforced concrete base (basemat) sits on top of the plaster. [W145293] The basemat was also installed with 2,500-psi strength at a 28-day cure time. [W145225] A 3-inch layer of construction grout fill sits on top of the basemat and the secondary liner sits above the grout. In addition, a 3-inch thick layer of grout is placed between the base of the primary liner and the secondary liner. [W145293] Figure 3.2-3 portrays the details of a typical Type I tank floor formation. Figure 3.2-4 shows the soil preparation and working slab construction for a typical Type I tank. Figure 3.2-5 shows Type I tank basemat construction.

Figure 3.2-3: Typical Type I Tank Floor Configuration

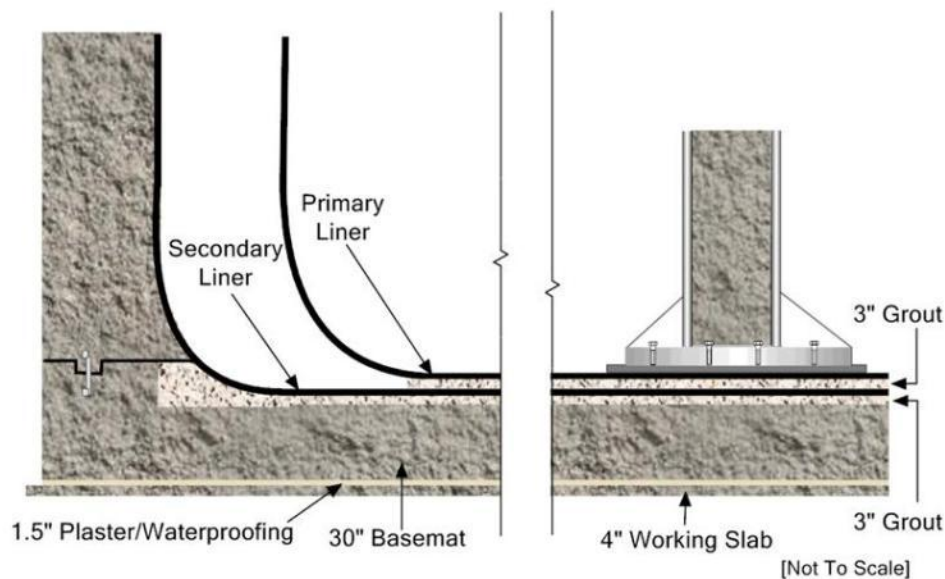


Figure 3.2-4: Typical Working Slab Construction for Type I Tanks



Figure 3.2-5: Typical Basemat Construction for Type I Tanks



3.2.1.1.2 Primary and Secondary Liner

The primary liner for Type I tanks is a cylinder of 0.5-inch thick carbon steel. The inner radius of the primary liner is 37 feet 6 inches and the inner height is 24 feet 6 inches. The walls of the primary liner are welded to the top and bottom of the waste tank by a 0.5-inch thick, curved knuckle plate. The steel specifications, including material and welding information, are provided in W145379. Figure 3.2-6 shows the typical construction of the primary and secondary steel liners for a Type I tank.

Figure 3.2-6: Typical Steel Liner Construction for Type I Tanks



Type I tanks have an annular space with a width of 2.5 feet. The base of the annular space is formed between the 5-foot high secondary liner and primary liner. The upper annular space is formed between the concrete vault and the primary liner. Carbon steel stiffener angles are located at the top of the secondary liner. All the seams in the bottom plates of the secondary liner are full penetration butt-welded using a backup strip on the underside. The steel specifications, including material and welding information, are provided in W145367. The primary liner sits on a 3-inch layer of grout (above the secondary liner). The secondary liner sits on a 3-inch layer of grout on top of the concrete basemat. [W145573] Figure 3.2-7 shows the typical construction of both the primary and secondary liners in the later construction phase; and Figure 3.2-8 presents a close-up, showing the 5-foot high carbon steel secondary liner.

**Figure 3.2-7: Typical Steel Liners Construction for Type I Tanks
(Late Construction Phase)**

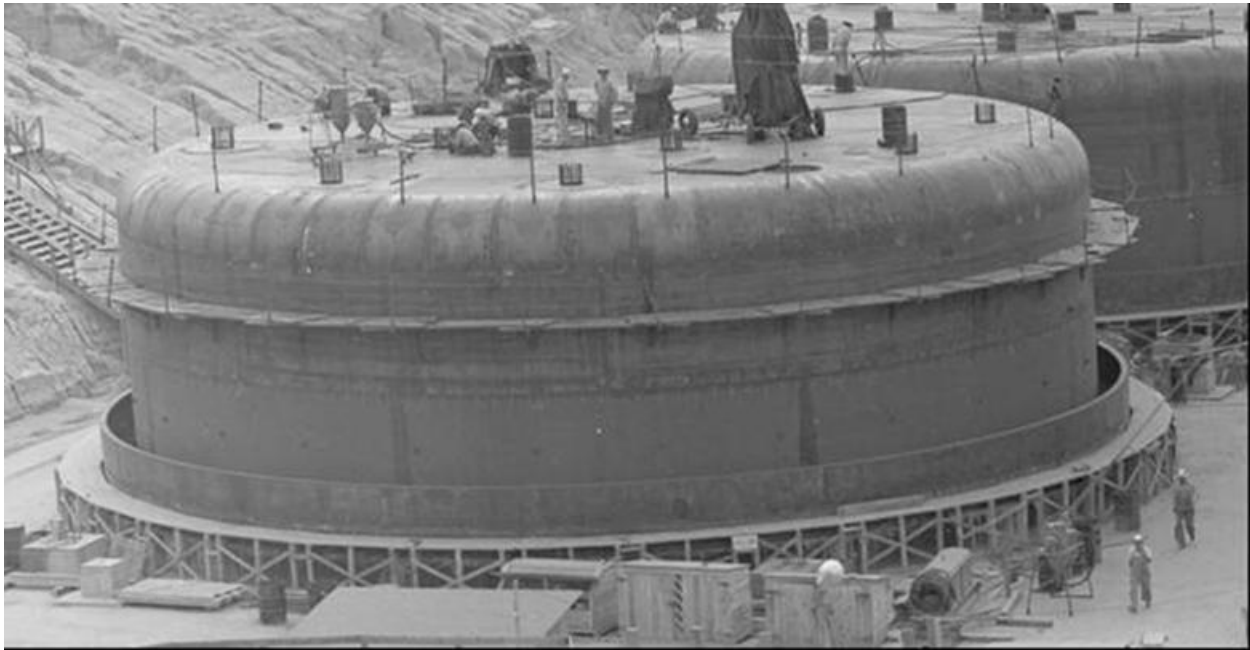


Figure 3.2-8: Close-Up of Figure 3.2-7 Showing the Annulus



The primary liner has transfer line penetrations near the top of the tank. There are 3-inch stainless steel inlet waste-transfer lines that enter the primary liner through the top knuckle and terminate inside the waste tank. The transfer lines are each enclosed in a 4-inch carbon steel jacket pipe where they bridge across the waste tank annulus. Each jacket pipe is welded to the primary liner; the internal pipe is free to move to accommodate thermal expansion and contraction. [W145573, W148413]

3.2.1.1.3 Waste Tank Concrete Vault

A concrete vault, 80-foot inner diameter, surrounds the Type I tank primary liner. The space between the vault and the primary liner creates a 2 foot 6-inch wide annulus. The vault is formed by 22-inch thick reinforced concrete roof and walls that surround the primary container and connect to the basemat. The vault concrete was installed per construction drawing specifications, with 2,500-psi strength. The walls have horizontal construction joints however; no vertical construction joints were used. [W145225] Figures 3.2-9 and 3.2-10 show the typical construction of the concrete vault and risers (see Section 3.2.1 for description of the waste tank risers) for the Type I tanks.

Figure 3.2-9: Typical Construction of a Type I Tank Concrete Vault



Figure 3.2-10: Typical Riser Construction for Type I Tanks



Because of the presence of the water table around the HTF Type I tanks, the concrete vaults included waterproofing. At the bottom of the concrete vault, a 5-ply layer of bituminous impregnated cotton fabric (waterproofing membrane) was placed between the 4-inch thick concrete working slab and the concrete basemat. An additional 5-ply layer of waterproofing membrane was placed above the 5-ply layer from the bottom of the concrete vault up to the basemat/vault wall construction joint. Between these two layers of waterproofing membrane exists a 0.25-inch thick flashing of metal reinforced fabric. A 5-ply layer of waterproofing membrane was placed on the top of the concrete vault and covered with a 0.25-inch layer of cement plaster or fiberboard, which was covered with 2 inches of shotcrete. An additional 3-ply layer of waterproofing membrane was placed below the 5-ply layer from the top of the concrete vault down to the roof/vault wall construction joint. A 0.25-inch thick flashing separates the two layers of waterproofing membrane. A 5-ply layer of waterproofing membrane was also installed on the concrete vault walls and a 4-inch thick brick wall was constructed 4 inches from the waterproofing membrane on the concrete vault wall. The 4-inch annular space between the brick wall and the waterproofing membrane on the concrete vault wall was filled with bituminous grout (hot sand asphalt mastic). [W158908]

3.2.1.1.4 Support Columns

Twelve concrete and steel columns support the roof of a Type I tank (Figures 3.2-11 and 3.2-12). These columns were made from steel pipes welded to a steel bottom plate. The pipes are 0.5-inch thick carbon steel with a 2-foot outside diameter and are filled with concrete. The columns have flared capitals at the top also filled with concrete. The bottoms of the columns are cylindrical and have eight, 1-inch thick stiffeners on each column. The columns are welded to the top and bottom of the primary liner. The steel specifications, including material and welding information, are provided in W145225 and W145379. Figure 3.2-13 portrays the column layout detail per W145573.

Figure 3.2-11: Support Column - Construction Phase

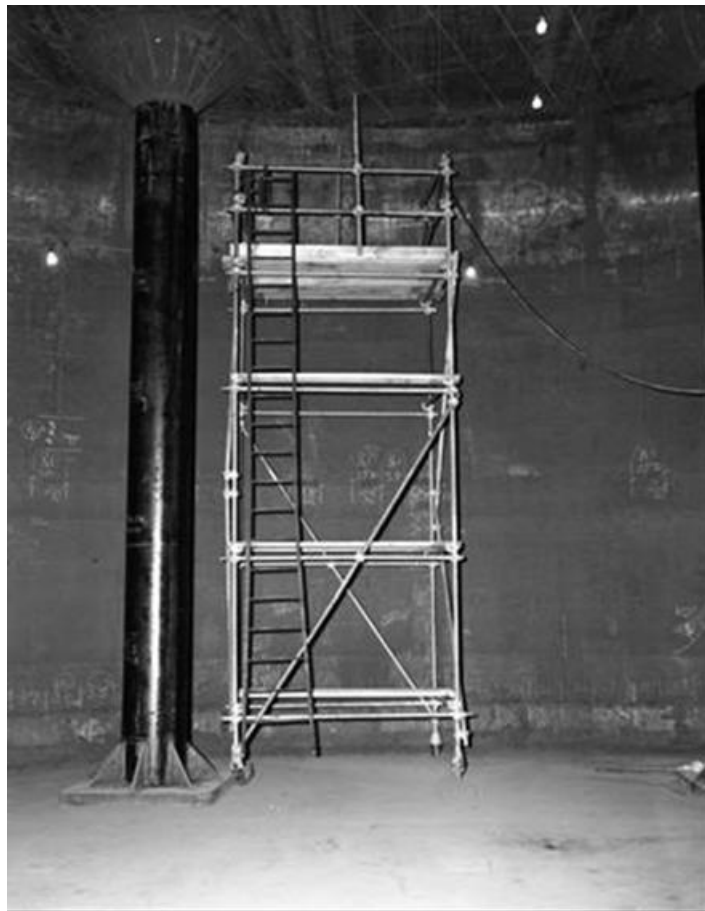


Figure 3.2-12: Sketch of Typical Support Column Top/Bottom Detail

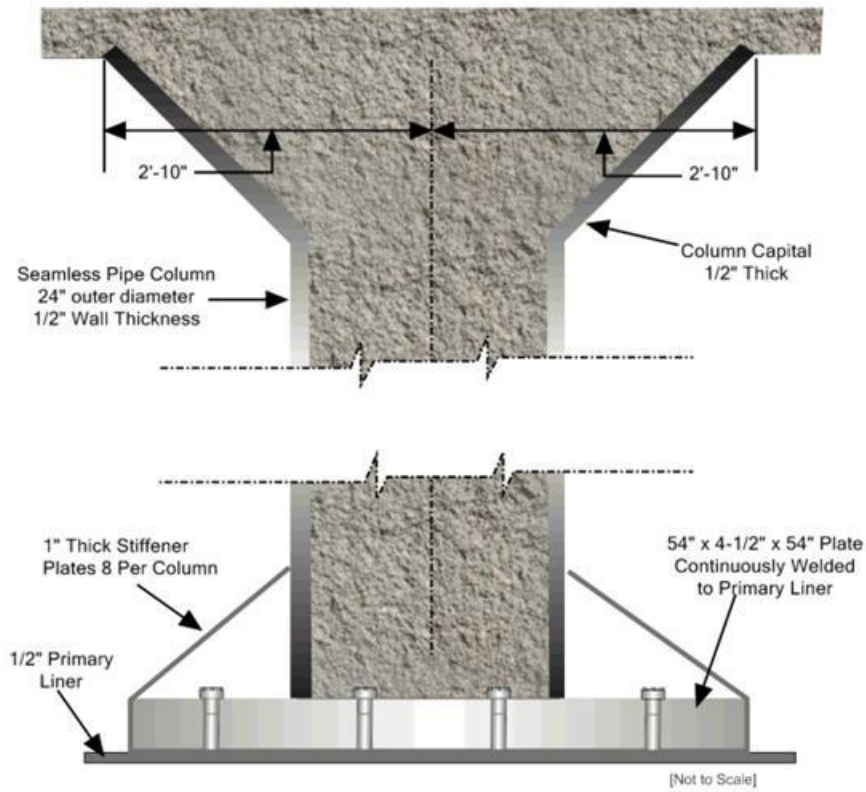
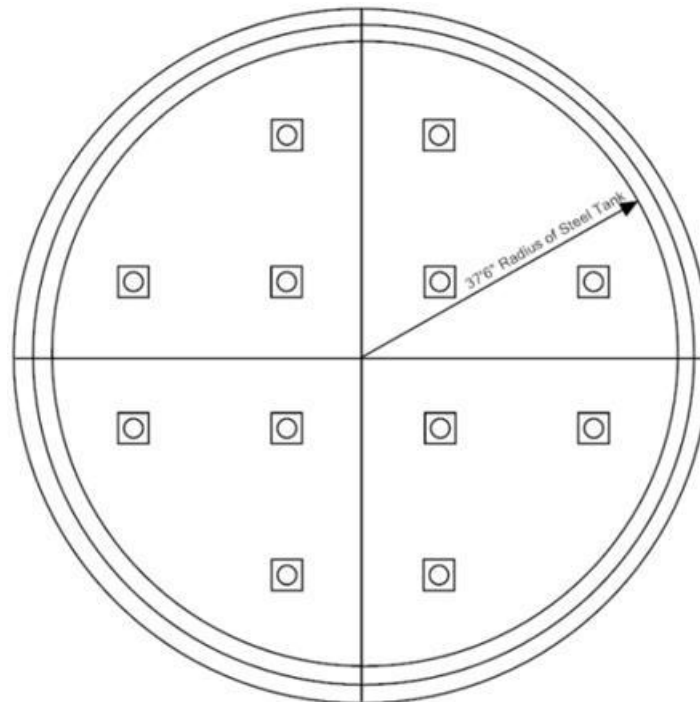


Figure 3.2-13: Column Layout Detail



3.2.1.1.5 Cooling Coils

The Type I tanks are equipped with a cooling system. The waste tanks have 34 vertical cooling coils that are supported by hanger and guide rods that are welded to the primary liner. [D116048] Two horizontal cooling coils, which are supported by guide rods that are welded to the primary liner, extend across the bottom of the waste tanks. [D116001] The cooling coils are 2-inch diameter schedule 40 carbon steel seamless pipe. Figure 3.2-14 shows typical Type I tank cooling coils during construction. [D116048, D116001]

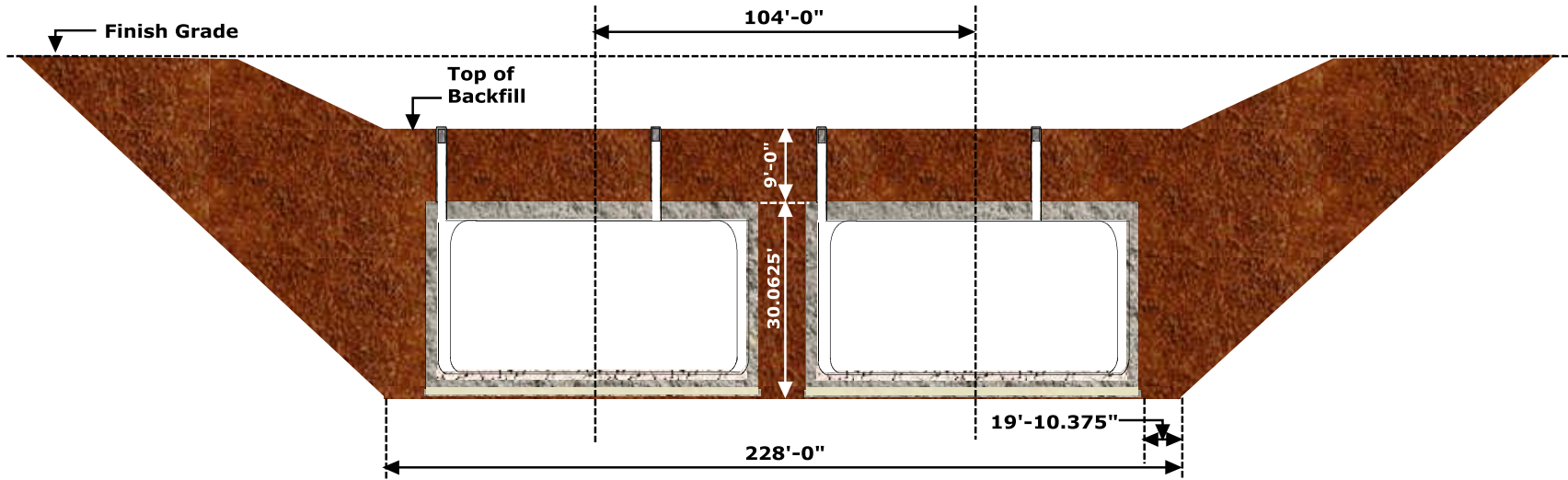
Figure 3.2-14: Type I Tank Cooling Coils - Construction Phase



3.2.1.1.6 Soil and Backfill Description

The Type I tank backfill was installed per W145225. The waste tank tops were covered with a minimum of 9 feet of backfill. Figure 3.2-15 shows the typical structure of the waste tanks and emplacement of backfill material. [W146377]

Figure 3.2-15: Type I Tank Backfill



[Not to Scale]

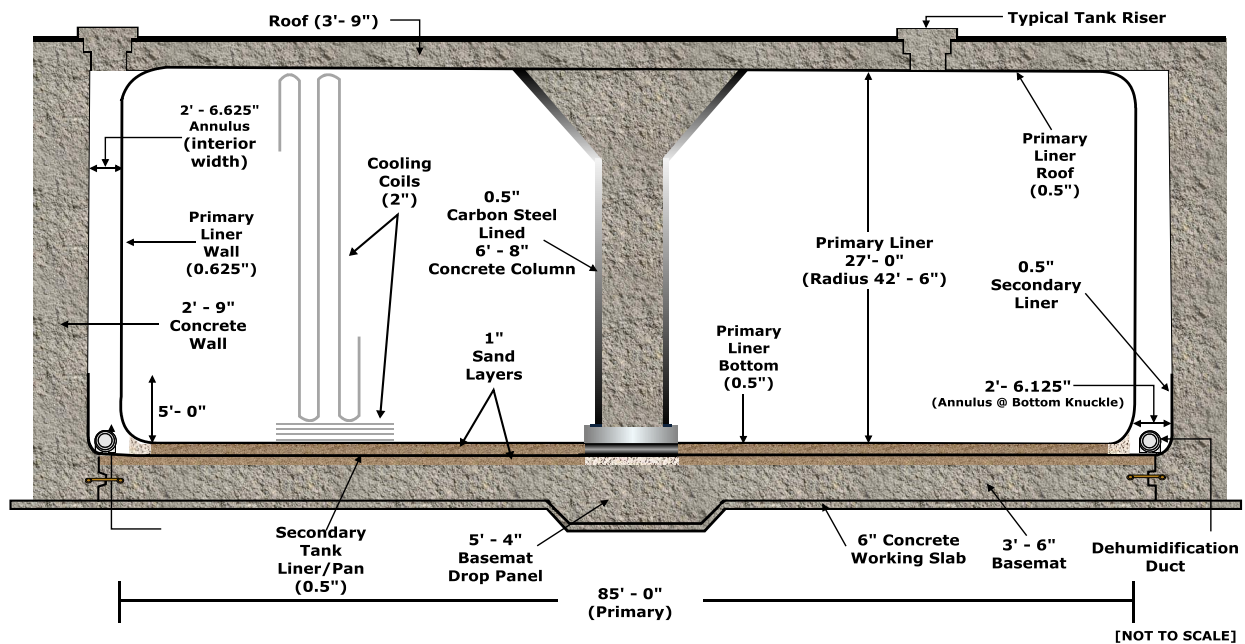
3.2.1.2 Type II Tanks

There are only four Type II tanks at SRS. They are located in the HTF and are Tanks 13 through 16. The HTF Type II tanks were constructed between 1955 and 1956. A typical Type II tank is presented in Figure 3.2-16.

The HTF Type II tank dimensions are as follows:

- Type II primary liner inner radius is 42 feet 6 inches (excluding 0.625-inch liner width). [W162672]
- Type II secondary liner inner radius is 45 feet 1.5 inches (excluding 0.5-inch liner width). [W162688]
- Type II primary liner inner height is 27 feet. [W162672]
- Type II tanks have a nominal operating capacity of 1,030,000 gallons.

Figure 3.2-16: Typical Type II Tank



3.2.1.2.1 Working Slab and Basemat

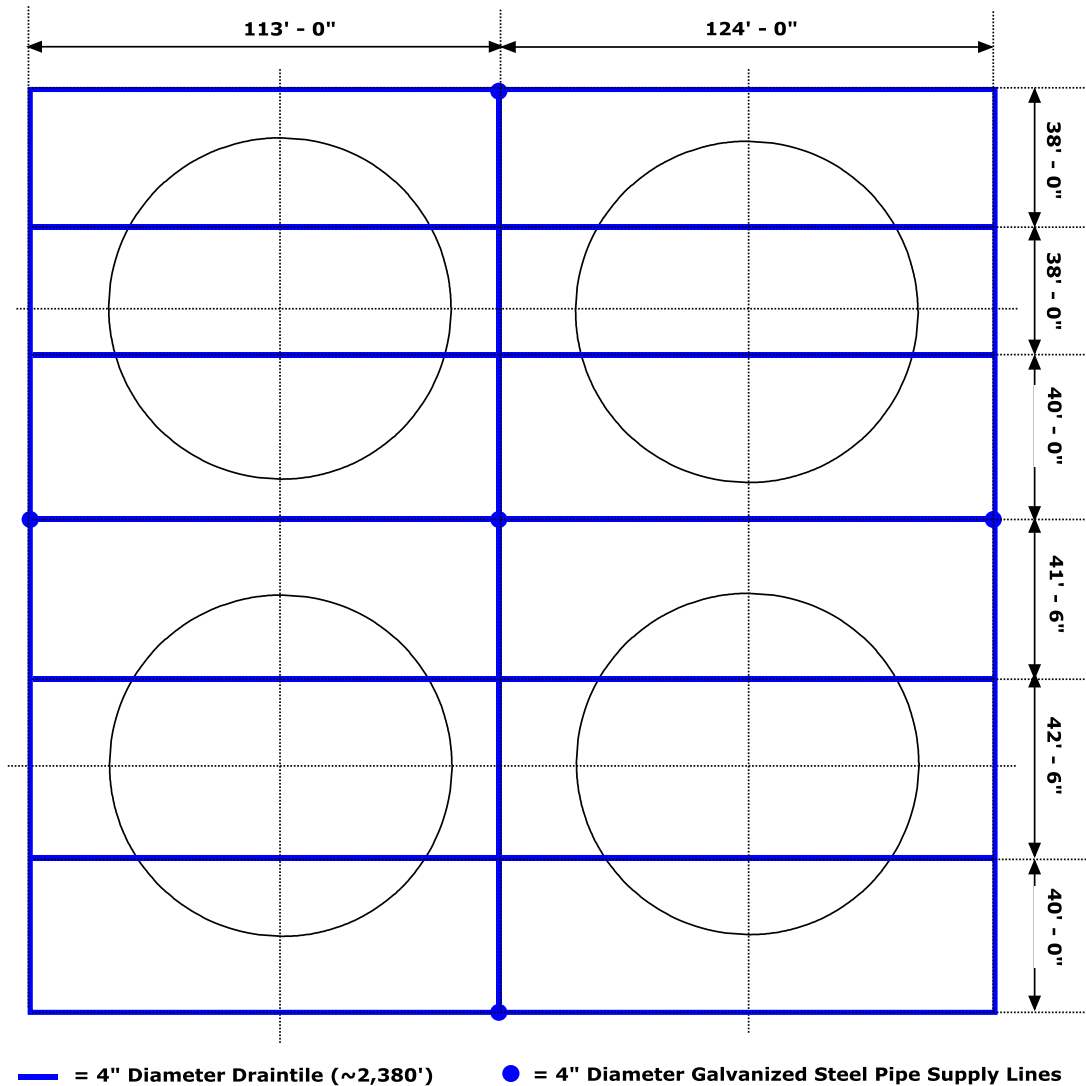
The working slab for the Type II tanks is 6 inches thick with the four waste tanks placed within a 255 foot x 274-foot rectangle. [W163048] Figure 3.2-17 presents the working slab for the four waste tanks. The concrete for the working slab was installed with 3,000-psi strength at a 28-day cure time. A 3 foot 6-inch thick reinforced concrete basemat is located on top of the working slab. The basemat was also installed with 3,000-psi strength at a 28-day cure time. [W162675] There is a 1-inch layer of sand between the top of the basemat and the secondary liner. There is also a 1-inch layer of sand between the secondary liner and primary liner. [W163018] The basemat has reinforcing bars placed throughout. The depth, length, and type of rebar vary depending upon the location within the basemat. [W162675]

Figure 3.2-17: Type II Tank Working Slab and Basemat



A soil hydration system and five feed wells were installed beneath the Type II tanks to address potential issues with soil shrinkage and settlement. The hydration system consists of an interconnecting grid comprised of 4 inch diameter drain tile (perforated piping) located 18 inches below the working slab (Figure 3.2-18). Five supply lines (feed wells) made of 4-inch galvanized steel piping were connected to the grid to allow water to be injected below the working slab. The drain tile was installed inside a 24-inch deep by 18-inch wide trench filled with sand and aggregate. The bottom 6 inches of the trench was filled with sand that half buried the drain tile while the remaining 18 inches of the trench was filled with aggregate. [W163048, W163278] The soil hydration system was never used for soil hydration since the water table under the Type II tanks is higher than anticipated and soil dehydration is not a problem. However, although no longer in use, in the past, this soil hydration system was used to monitor groundwater levels. The soil-hydration system wells were used in the 1960s and 1970s to pump water from beneath Tank 16 as part of the Tank 16 groundwater monitoring effort. [DP-1358]

Figure 3.2-18: Soil Hydration System below Type II Tanks



(Not To Scale)

[W163278]

3.2.1.2.2 Primary and Secondary Liner

The primary liner for Type II tanks is a cylinder made of carbon steel per W162672. The primary liner walls and bottom are connected via a curved knuckle plate that is welded to both the liner walls and bottom. The steel specifications, including material and welding information are provided in W162672. The primary liner thicknesses within the waste tank are identified in Table 3.2-2. [W162672]

Table 3.2-2: Type II Tank Primary Liner Thicknesses

Location	Thickness
Top and bottom	0.5 inch
Upper knuckle	0.562 inch
Wall	0.625 inch
Lower knuckle	0.875 inch

The Type II tank primary liner was constructed above a 1-inch sand pad placed on top of the secondary liner. An additional 1-inch sand pad is located beneath the secondary liner (Figure 3.2-19). [W163018] In accordance with the requirements of W163018, both sand pad layers consists of clean, hard, durable, siliceous particles free from foreign material (i.e., procured and washed sand free of silt or clay), and uniformly graded from standard sieves #16 and #100. The size of the sand grain ranges from 0.15 millimeter (#100 sieve) to 1 millimeter (#16 sieve), and is classified as fine to medium sand per the Unified Soil Classification System and fine to coarse per USDA classification.

Figure 3.2-19: Lower Sand Pad Installation over the Basemat



The secondary liner for the Type II tank forms an annulus space 30.625 inches wide between the primary liner and concrete wall. The upper portion is formed by the concrete wall while the bottom is formed by the 5-foot high carbon steel annulus pan (secondary liner). Type II tank primary and secondary liners are shown in Figure 3.2-20.

Figure 3.2-20: Type II Tank Early Construction of Primary and Secondary Liner



The secondary liner material is 0.5-inch carbon steel. [W162688] A carbon steel stiffener angle is located at the top of the secondary liner. All the seams in the bottom plates of the secondary liner are full penetration butt-welded using a backup strip on the underside. Drawings W163018 and W162672 provide the steel specifications, including material and welding information.

Type II tank tops are equipped with risers which provide access into the primary and secondary liner interiors. A 3-inch stainless steel waste transfer line penetrates the primary liner through the upper knuckle by way of a 4-inch schedule 40 pipe that is welded to the primary liner. The annular space between the 3-inch pipe and the 4-inch pipe is packed with asbestos wicking. [W162672]

3.2.1.2.3 Concrete Vault

The Type II tanks are completely enclosed in a concrete vault. A 95 foot 8.5-inch outer diameter concrete vault surrounds the Type II tank primary liner creating a 2 foot 6.625-inch wide annulus.

The vault is formed by 2 foot 9-inch thick reinforced concrete walls and a 3 foot 9-inch thick reinforced concrete roof that surrounds the primary liner and connects to the basemat. [W163018] The concrete vault height is approximately 34 feet 6 inches. The vault concrete was installed with 2,500-psi strength at a 28-day cure time. The sidewalls have horizontal construction joints however; no vertical construction joints were used except at basemat. There are copper water stops at the bottom of the concrete vault wall. [W163018]

Figures 3.2-21 and 3.2-22 show both early and late stage Type II tank concrete vault construction. Figure 3.2-23 portrays the details of a typical Type II tank floor/annulus space arrangement.

Figure 3.2-21: Type II Tank - Early Stage of Vault Construction



Figure 3.2-22: Type II Tank - Late Stage of Vault Construction

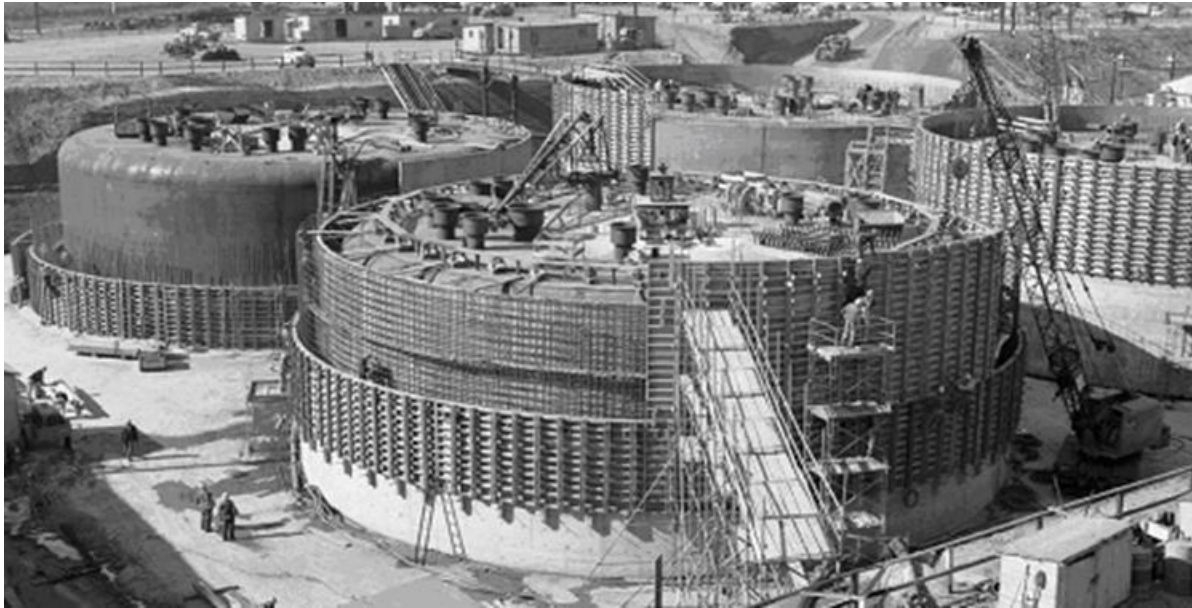
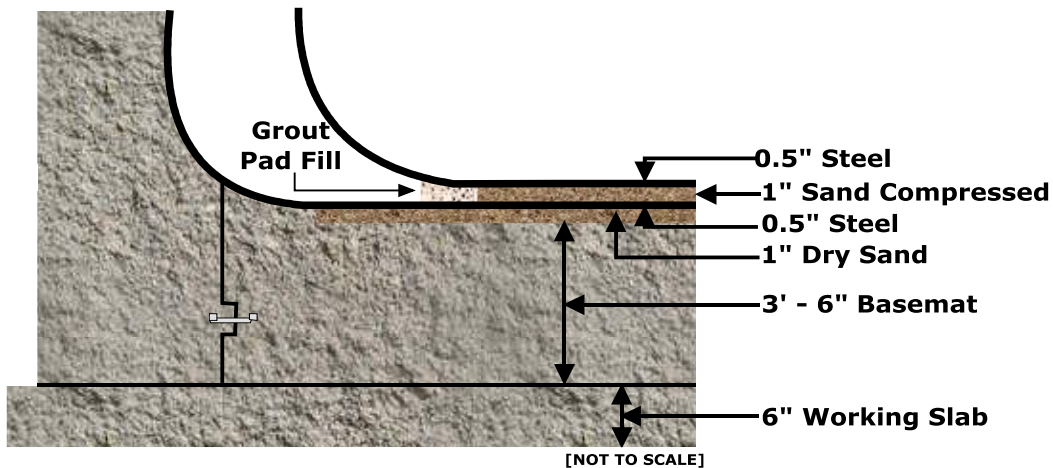


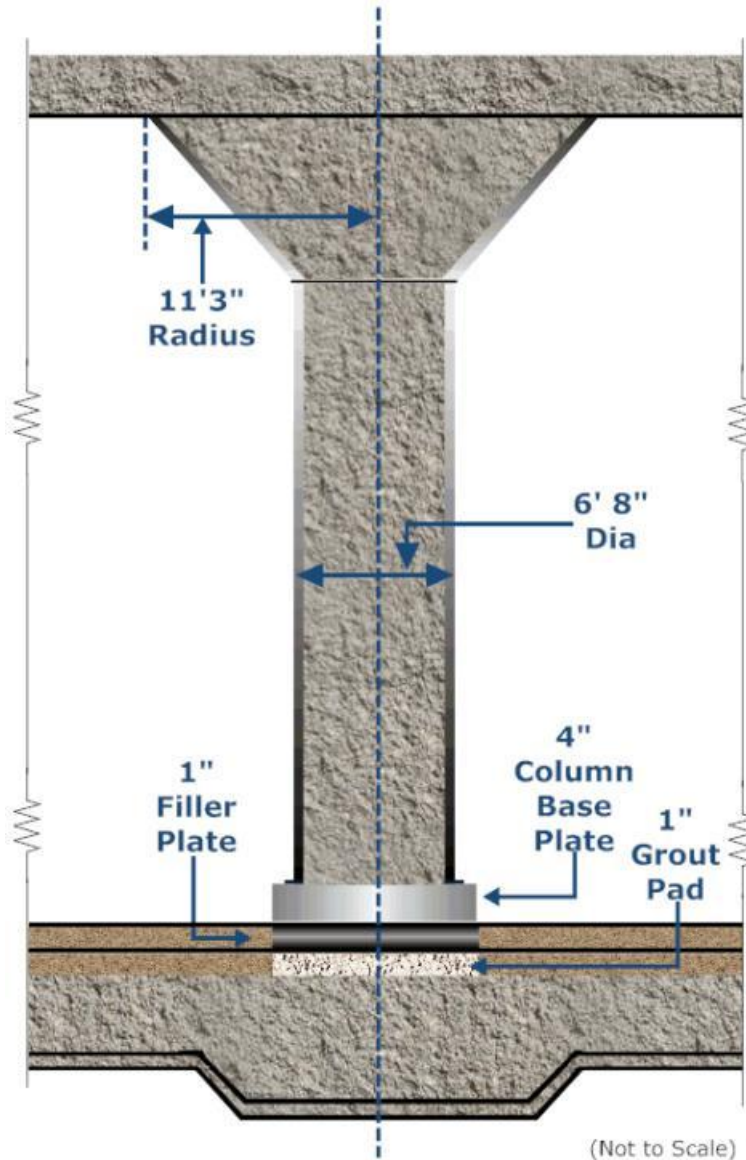
Figure 3.2-23: Type II Tank Annulus Corner Detail



3.2.1.2.4 Support Columns

One central reinforced concrete and steel column supports the roof of a Type II tank (Figure 3.2-24). The carbon steel column has a thickness of 0.5 inch and an inside diameter of 6 feet 8 inches. The steel column was welded to a steel bottom plate and filled with concrete. The column has a reinforced, concrete filled, flared capital at the top. The concrete for the steel column was installed with 3,000-psi minimum compressive strength at a 28-day cure time. [W163018] The steel specifications, including material and welding information, are provided in W162672. The support column concrete is reinforced with varying length and types of rebar. [W162676]

Figure 3.2-24: Support Column Dimension Details



3.2.1.2.5 Cooling Coils

The Type II tanks are equipped with 44 cooling coils (Figure 3.2-25). The waste tanks have 40 vertical cooling coils (20 operating and 20 auxiliary) that are supported by hanger and guide rods that are welded to the top and bottom of the primary liner. [W163593] The four bottom cooling coils (two operating and two auxiliary coils) extend across the bottom of the waste tanks, and are supported by guide rods and steel angles welded to the bottom of the primary liner. [W163658] The cooling coils are 2-inch diameter schedule 40 carbon steel seamless pipes. The total coil length is 14,700 feet for operating coils and 14,700 feet for auxiliary coils. [W163593]

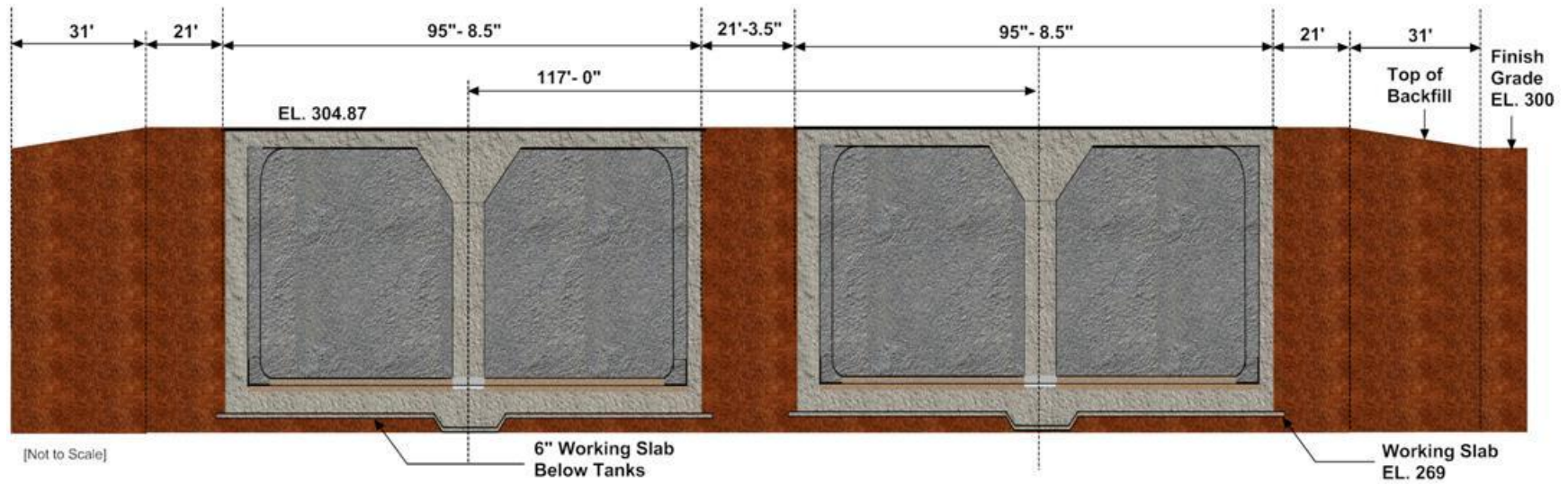
Figure 3.2-25: Type II Tank Cooling Coils



3.2.1.2.6 Soil and Backfill

The Type II tank backfill was installed per drawing W163048 specifications. The backfill below the working slab is test controlled compacted backfill not to contain more than 7 % material passing through a #200 sieve. Excavated backfill soil around the waste tanks consisted of suitable approved soil to allow satisfactory consolidation. The backfill around the waste tanks was placed in successive, uniform layers with a compacted thickness no more than 12 inches. The backfill layers around the tanks were rolled with earthwork equipment until uniformly compacted to specification. In areas inaccessible to such equipment, the backfill was compacted with approved hand or mechanical tampers. The backfill around the waste tanks was brought to an elevation level with the top of the waste tanks and extended laterally for a minimum of 21 feet. The backfill was then sloped down at an angle less than 1:1 for a lateral distance of 31 feet, reaching final grade at an elevation of 300 feet above MSL. Figure 3.2-26 shows the backfill structure. [W163048]

Figure 3.2-26: Type II Tank Backfill Detail



3.2.1.3 Type III and IIIA Tanks

There are four, Type III tanks (Tanks 29-32) and 13 Type IIIA tanks (Tanks 35 through 37, 38 through 43, and 48 through 51) in the HTF. The Type III tanks were constructed between 1966 and 1970. The Type IIIA tanks were constructed between 1974 and 1981. The primary liners are 85 feet in diameter and 33 feet high with a nominal operating capacity of 1,300,000 gallons. [W236519] Typical HTF Type III and Type IIIA tanks are shown in Figures 3.2-27 and 3.2-28, respectively. Note that Tanks 35, 36, and 37 have been designated as Type IIIA tanks but they differ from Figure 3.2-28 in that these waste tanks have a flat roof with a uniform 4-foot concrete thickness, similar to the Type III tanks. Additionally, Tank 35 has insertable cooling coils rather than permanently installed cooling coils.

Figure 3.2-27: Typical HTF Type III Tank

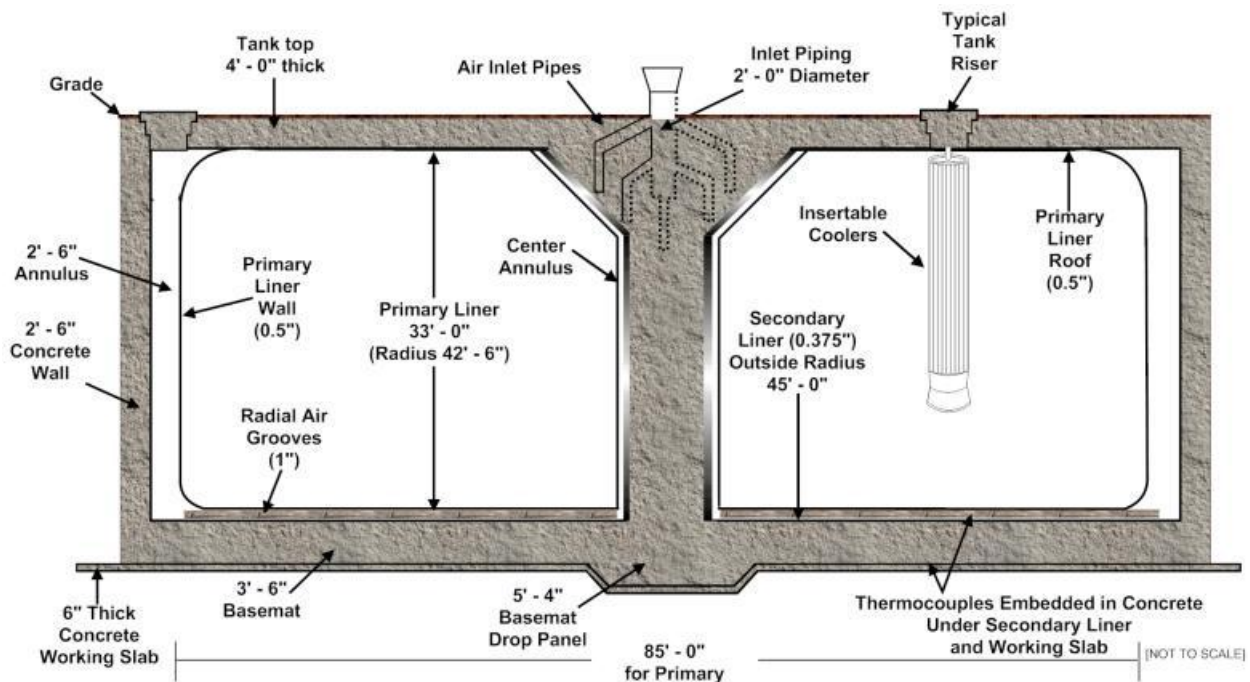
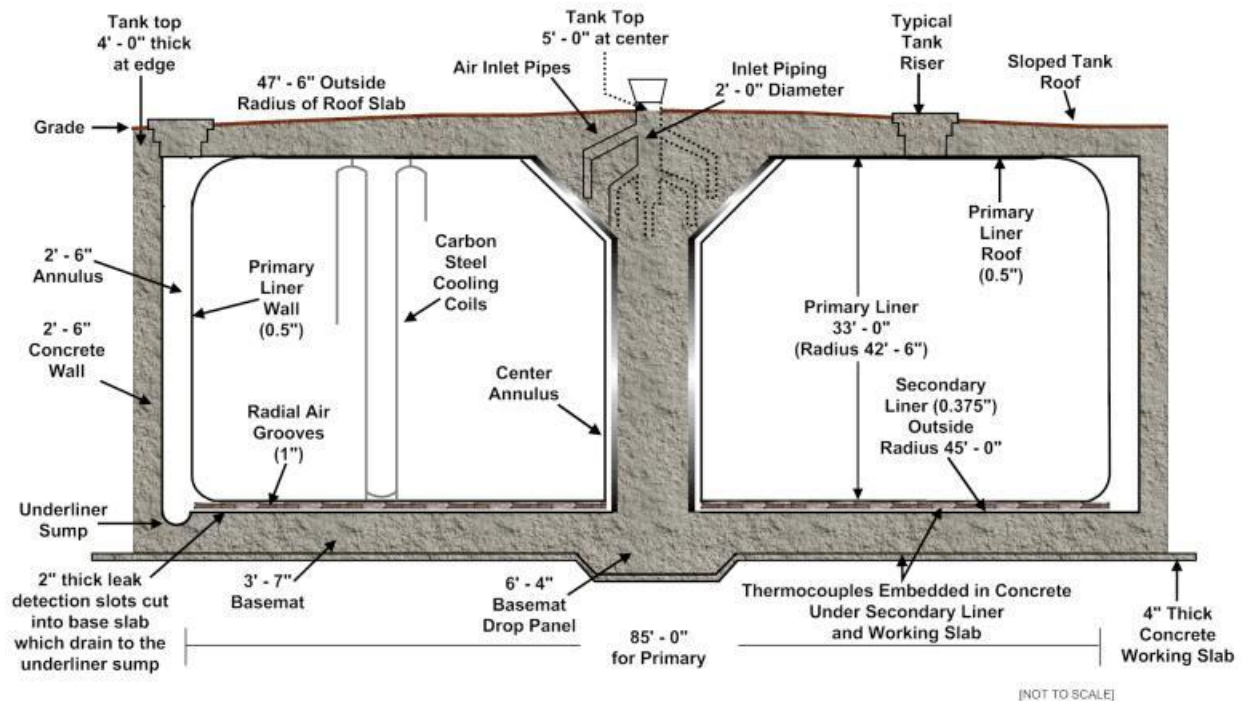


Figure 3.2-28: Typical HTF Type IIIA Tank



3.2.1.3.1 Type III Working Slab and Basemat

The concrete basemat rests on a 6-inch thick (minimum) construction-working slab that slopes away as it extends 30 feet beyond the edge of the waste tank. The working slab is under all four Type III tanks (Tanks 29 through 32). [W236495] The basemat is 3-foot 6-inches thick (5 feet 4 inches at the drop panel in the waste tank center) with a radius of 45 feet (not including the wall radius of 2 foot 6 inches). [W236562] Figure 3.2-29 shows the early construction of a typical Type III and IIIA basemat.

Figure 3.2-29: Early Construction of a Type III and IIIA Tanks Basemat



The basemat concrete was installed with reinforcing bars placed throughout, with the length and type of bar varying depending upon the location. The basemat also includes a water stop embedded in the circumference. [W236495, W236562]

3.2.1.3.2 Type IIIA Working Slab and Basemat

The working slab rests on undisturbed soil. [W448847, W700855, W707138] Tanks 35 through 37, 38 through 43, and 48 through 51 were built on a single working slab that extends out at least 25 feet beyond the edge of the waste tanks. [W449843, W700834, W706301] Prior to the placement of backfill, the working slab was broken up or perforated with 4-inch diameter holes spaced 18 inches apart, center-to-center between the waste tanks to prevent perched water (Figure 3.2-30).

The basemat rests on the 4-inch (minimum) thick working slab. The basemat thickness is 3 feet 7 inches (6 feet 4 inches at the drop panel in the waste tank center) and a radius of 45 feet (not including the wall radius of 2 foot 6 inches). The basemat has reinforcing bars placed throughout, with the length and type of bar varying depending upon the location. A water stop is provided at the basemat-to-vault wall joint. [W448847, W700505, W707138]

Figure 3.2-30: Drilled Working Slab of a Type IIIA Tank



Tanks 38 through 43 and 48 through 51 have an underliner sump located between the secondary liner and basemat. A grid of interconnected radial channels that are 2 inches deep by 4 inches wide is grooved into the basemat. The secondary liner rests on top of the concrete basemat. Figure 3.2-31 shows the leak-detection channel grid in a typical Type IIIA basemat. The channels are sloped to drain through a center collection pipe to a sump located inside the concrete vault wall. A 1.5-inch stainless steel access pipe rises to grade from the sump to allow for liquid measurement, sampling, and the pumping out of collected liquid. [W701336, W707253]

Figure 3.2-31: Typical Leak-Detection Channel Grid in Type IIIA Tank Basemat



If both the primary liner and the secondary liner develop a leak, liquid will collect in the channels of the leak detection grid and then drain to the sump. The sump can be monitored by conductivity probes that alarm when liquid contacts the probes.

Tanks 35 through 37 each had 56 thermocouples installed on the outside of the primary liner. [W449815] Tank 38 has 34 thermocouples that were installed on the outside of the primary liner. [W700715] Each of the remaining Type IIIA tanks (39 through 43 and 48 through 51) have 22 thermocouples that were installed on the outside of the primary liner. [W707031] All Type IIIA tanks have a thermocouple located on the top of the basemat and another thermocouple located just below the working slab. [W702019] Tanks 35 through 37 have an additional thermocouple that was installed approximately 10 feet below the working slab. [W449931]

3.2.1.3.3 Primary and Secondary Liners

The Type III and IIIA tank primary liners have a radius of 42 feet 6 inches (inside) and a height of 33 feet. The Type III and IIIA tank liners are made of two concentric cylinders joined by curved knuckle plates to washer shaped top and bottom plates. The minimum thickness of each plate is provided in Table 3.2-3. Drawing W236562 identifies the primary liner steel plate specifications including material and welding information for Tanks 29 through 32, drawing W448849 for Tanks 35 through 37, drawing W700856 for Tanks 38 through 43, and drawing W707114 for Tanks 48 through 51.

Table 3.2-3: Minimum Primary Liner Plate Thicknesses for Type III and IIIA Tanks

Location	Tanks 29-32 Thickness (in) [W236519]	Tanks 35-37 Thickness (in) [W448842]	Tanks 38-43 Thickness (in) [W700856]	Tanks 48-51 Thickness (in) [W707114]
Top and floor	0.5	0.5	0.5	0.5
Upper knuckle	0.5	0.5	0.5	0.5
Outer liner				
Upper band	0.5	0.5	0.5	0.5
Middle band	0.5	0.625	0.625	0.625
Lower band	0.5	0.5	0.875	0.875
Column liner				
Upper band	0.5	0.625	0.5	0.5
Lower band	0.5	0.875	0.625	0.625
Lower Knuckle				
Outer	1.0	0.875	0.875	0.875
Inner (at column)	0.625	0.625	0.625	0.625

The primary liner sits on a bed of insulating material grooved to channel airflow to the secondary annulus liner. [W236993, W702700] The insulating bed has radial grooves so that ventilating air can flow through the slots, and any leakage from the primary liner bottom or center annulus flows to the outer annulus. The Type III tanks have a 6-inch thick layer of insulating material with 1-inch deep x 2-inch wide slots. [W236993] The Type IIIA tanks have an 8-inch thick layer of insulating material with 2-inch deep x 5-inch wide slots. [W702700] Figure 3.2-32 shows the grooved radial air slots for a typical Type IIIA tank and Figure 3.2-33 shows the grooved radial air slots emerging from below the primary liner.

Figure 3.2-32: Radial Air Grooves for a Typical Type IIIA Tank



Figure 3.2-33: Typical Type IIIA Tank Primary and Secondary Liner - Early Construction



The secondary liner for the Type III and IIIA tanks is 0.375-inch thick carbon steel. [W236562] The secondary liner is the full height of the primary liner and has a 90-foot outside diameter forming a 2-foot 6-inch annular space between the primary and secondary liners. Figures 3.2-33 and 3.2-34, show the primary and secondary liners for a typical Type IIIA tank during construction.

Figure 3.2-34: Typical Type IIIA Tank Primary and Secondary Liner - Partial Construction



Type III tanks (Tanks 29 through 32) have a number of penetrations through the primary and/or secondary liner at the waste tank top ranging in size from approximately 9 inches to 36 inches in diameter. Two pairs of stainless steel lines penetrate the primary liner at the upper knuckle. One pair is the main waste inlet lines that are 3 inches in diameter and enter the waste tank through a 10-inch diameter carbon steel sleeve that is welded to the primary liner. The 10-inch sleeve traverses the annular space and mates into a 12-inch carbon steel sleeve that is welded to the secondary liner and penetrating through the concrete vault wall. The second pair is the spare waste inlet lines that are 2 inches in diameter and enter the waste tank through a 6-inch diameter steel sleeve that is welded to the primary liner. The 6-inch sleeve traverses the annular space and mates into an 8-inch carbon steel sleeve that is welded to the secondary liner and penetrating through the concrete vault wall. Both pairs of inlet lines have asbestos wicking packed within the annular space between the larger and smaller sleeves. [W236519]

Similar to the Type III tanks, the Type IIIA tanks have a number of penetrations through the primary and/or secondary liner at the waste tank top ranging in size from approximately 9 inches to 52 inches in diameter. In addition, the Type IIIA tanks (except Tank 35) have multiple penetrations to accommodate the valve house on the waste tank top for the permanently installed cooling coils. Penetrations exist on the side of the Type

IIIA tanks at various locations along the upper knuckle, similar in design to the side penetrations described above for the Type III tanks. [W449795, W449796, W449797]

3.2.1.3.4 Type III Tank Center Column

The Type III primary liner roof is supported by a steel-lined concrete center support column that was made as an integral part of the basemat. This design does not require the waste tank bottom to support the weight of the roof support column, as it does in the Type I and II tanks, thereby reducing stress on the primary waste tank bottom (Figure 3.2-35). At the center column, the secondary liner diameter is 6 feet 6 inches and the primary liner diameter is 6 feet 9 inches. [W236562]

Type III Tanks have air ventilation/cooling system supply ducts to the radial air grooves embedded in the center support column (Figure 3.2-36). [W236499]

The column concrete in each waste tank was installed with a 3,000-psi compressive strength at 28-day cure time. [W236562] Reinforcing bars are placed throughout the center support column with variation in length and type depending upon the location. [W236499]

Figure 3.2-35: Typical Center Column Roof Support in a Type III and IIIA Tanks



Figure 3.2-36: Type III and IIIA Tanks Vent Duct Work



3.2.1.3.5 Type IIIA Tank Center Column

The Type IIIA tank roof support for the primary liner is provided by a steel-lined concrete center support column with a diameter of 6 feet 2 inches. The center support column is made as an integral part of the concrete basemat; therefore, the waste tank bottom does not support the weight of the roof support column, as does the Type I and II tanks, thus reducing stress on the primary liner bottom (Figure 3.2-35). At the center column, the secondary liner is 6 foot 2-inches in diameter (6-foot 1-inch for Tanks 48 through 51) and the primary liner is 6 foot 9-inches in diameter. [W448842, W700856, W707114]

Type IIIA tanks have air ventilation/cooling system supply ducts to the radial air grooves embedded in the center support column (Figure 3.2-36). [W448844, W704339, W707111]

The column concrete was installed with a 3,000-psi compressive strength at 28 days. [W448847, W700855, W707138] Reinforcing bars were placed throughout the center support column with the length and type varying depending upon the location. [W448844, W704340, W707138]

3.2.1.3.6 Type III and IIIA Tanks Concrete Vaults

The Type III and IIIA tanks are completely enclosed in a concrete vault. The concrete vault roof is 48 inches thick and the walls are 30 inches thick. The thick vault concrete enclosure eliminates the need for an earthen cover for shielding on the top of the Type III and IIIA tanks. All Type III tanks and the Type IIIA Tanks 35 through 37 have a flat roof. The roof on each of the Type IIIA Tanks 38 through 43 and 48 through 51 is sloped with the roof being 5-foot thick at the waste tank center and 4-foot thick at the waste tank edge. The concrete vault wall and the roof have reinforcing bars placed throughout, with the length and type varying depending upon the location (Figure 3.2-37). All Type III and IIIA tanks have a 24-ounce water stop at the basemat-wall joint with all seams brazed watertight. [W236562, W448847, W704339, W707138] The concrete and reinforcing bar, walls, basemat, and top roof slab were installed per construction drawing specifications. [W236577, W706690, W236499, W448844]

Figure 3.2-37: Typical Type III and IIIA Tanks Side Wall Rebar



The Type III and IIIA tanks have both a center and outer annulus. The center annulus is formed between the primary liner and the roof support column. The center annulus allows for ventilation airflow to the waste tank bottom, then out to the outer annulus through the radial air grooves. Figure 3.2-38 shows placement of the waste tank top reinforcing bars and center annulus supply-ventilation ductwork in preparation for concrete pouring. The Type IIIA tanks have conductivity probes that cross through the waste tank top concrete into the center annulus. [W448849, W700856, W707114]

Multiple conductivity probes are also installed in the outer annulus to provide redundant leak detection capability. No primary waste tank leakage has been detected in the Type III and IIIA tanks. A completed Type IIIA tank (prior to receiving backfill) is shown in Figure 3.2-39.

Figure 3.2-38: Typical Type III and IIIA Tanks Top Preparation for Concrete Pour

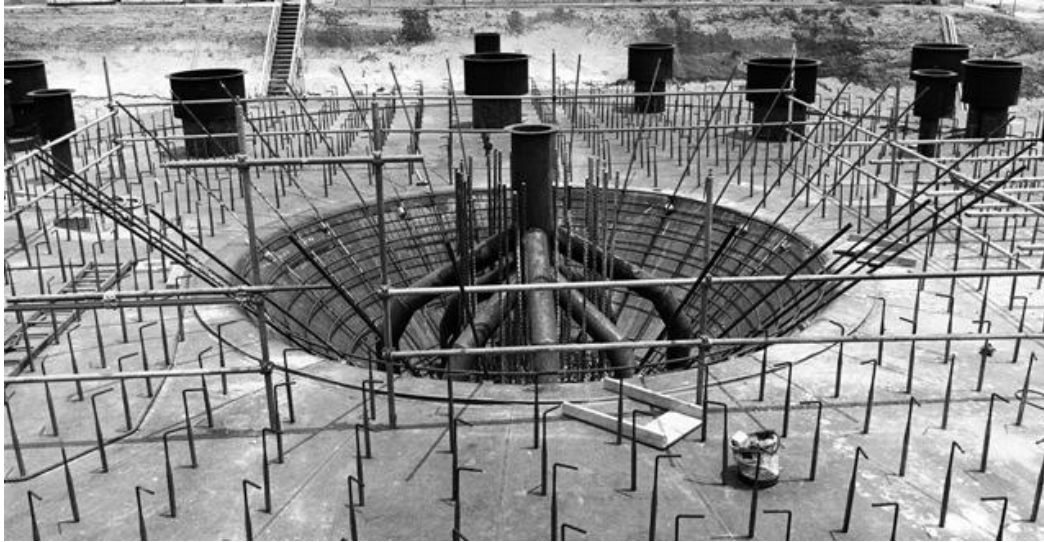


Figure 3.2-39: Final Construction of a Typical Type III and IIIA Tanks



3.2.1.3.7 Type III Cooling Coils

Type III Tanks 29 through 32 each have deployable cooling coils that were installed after the waste tank was completed. The deployable coils are installed through the waste tank risers and supported by the waste tank roof. Figures 3.2-40 through 3.2-42 depict the various designs used for the deployable coolers in Tanks 29 through 32. Tank 29 has nine deployable coils, Tank 31 has seven deployable coils, and Tanks 30, 32, and 35 each have five deployable coils. Type III tanks do not have horizontal cooling coils along the waste tank bottom. Type III tank bottoms are cooled by forced air that passes through grooved channels in the concrete insulating slab between the primary liner and secondary liner. [W236993]

Figure 3.2-40: Insertable Coolers Used in Type III Tanks

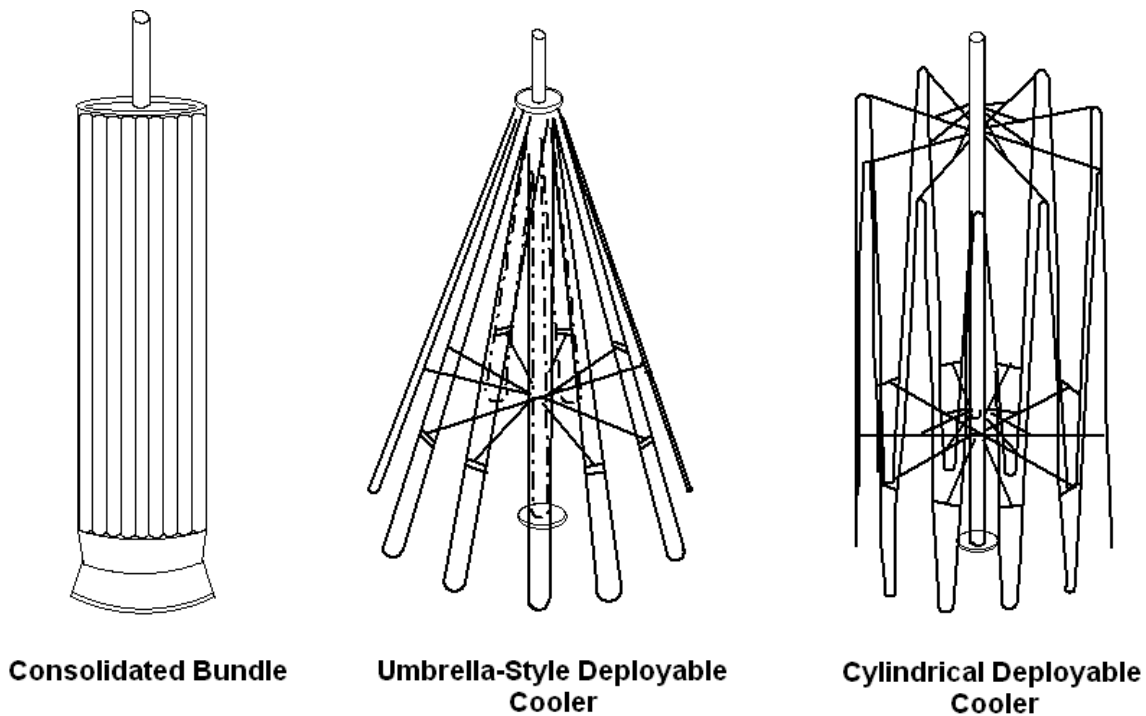


Figure 3.2-41: Insertable Cooling Coil Installed in a Type III Tank

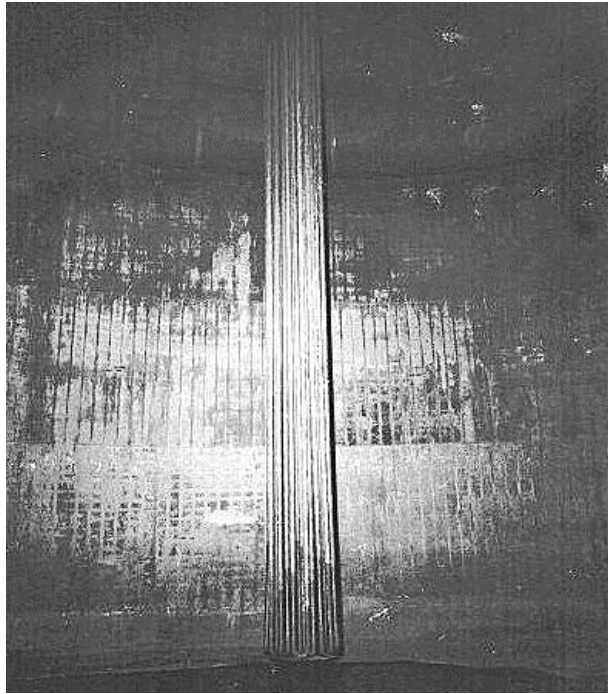


Figure 3.2-42: Typical Conical (Umbrella) Type of Deployable Cooling Coil



3.2.1.3.8 Type IIIA Cooling Coils

All Type IIIA tanks, except Tank 35, have permanently installed cooling coils similar to those in the Type I and II tanks. Like the Type III tanks, Tank 35 had deployable cooling coils installed after construction. With the exception of Tank 35, Type IIIA tanks have top and bottom supported vertical coils on 3-foot triangular centers. The cooling coils supports are welded to the bottom of the primary liner. There are 246 vertical coils mounted 9 inches off the bottom of the waste tank and spaced on 3-foot centers. The coils are made of 2-inch carbon steel pipe. [W449710, W700286, W701130, W708852]

All Type IIIA tank bottoms are cooled by forced air that passes through grooved channels in the concrete insulating slab between the primary liner and secondary liner to supplement the vertical cooling coils. [W448840, W449824, W702700, W707288] Figure 3.2-43 shows a typical cooling coil arrangement.

Figure 3.2-43: Cooling Coils in a Type IIIA Tank



3.2.1.3.9 Type III and IIIA Tanks Soil and Backfill

All areas receiving backfill (including sloped areas) were prepared per W700834. Prior to placing backfill, either the working slab was broken up or 4-inch diameter holes, 18 inches on center were punched in the slab. In other areas receiving backfill, the soil cover (e.g., vegetation, top soil, soil-erosion protection layer) was removed and the ground scarified to a depth of 4 inches. Backfill with the amount (percent) of water most favorable to achieve not less than 95 % of the maximum dry density was used. [W701036]. Backfill was placed to within 1 foot of the elevation of the top of the Type III and IIIA tanks. [W231220, W700242, W701036, W704700] Figure 3.2-44 shows a typical Type III and IIIA tanks after completion of backfill placement.

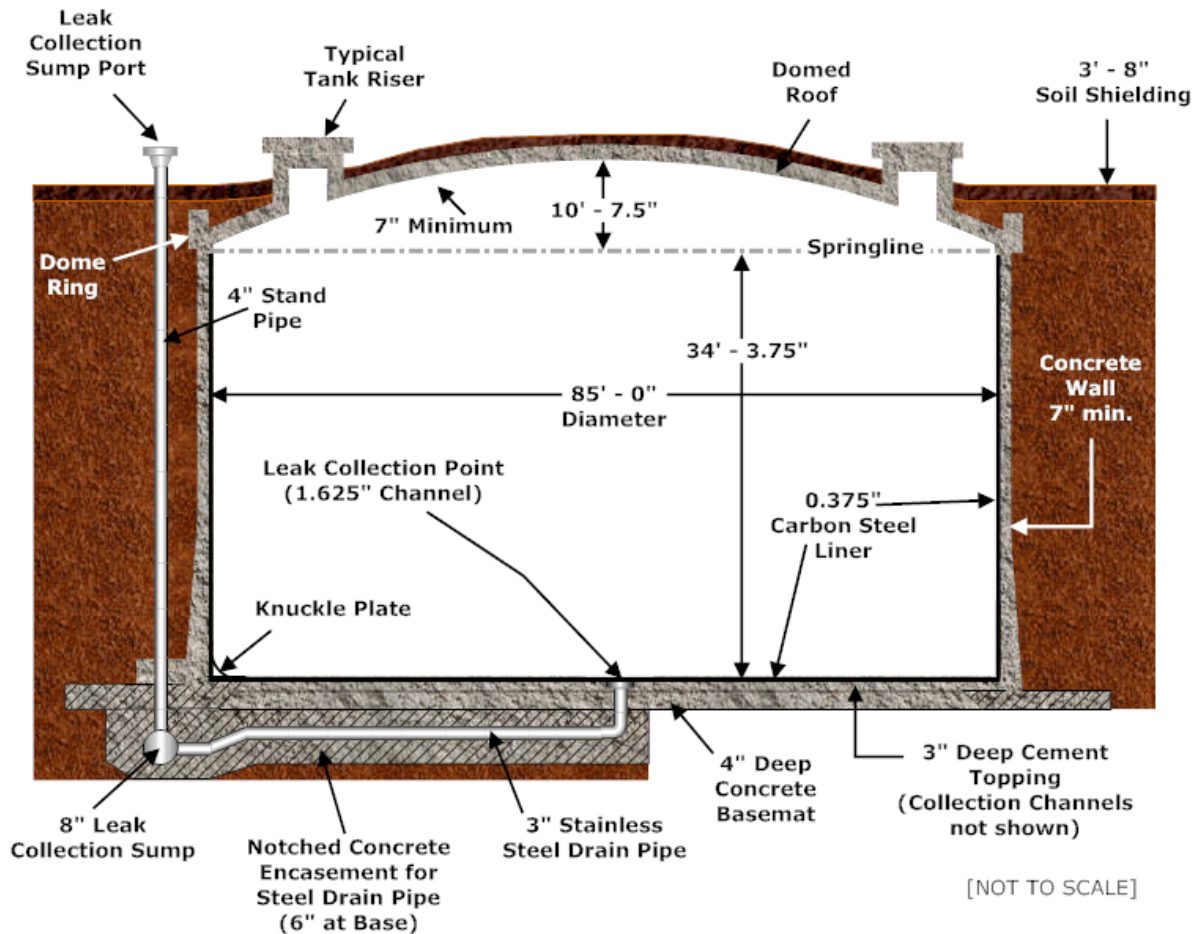
Figure 3.2-44: Typical Type III and IIIA Tank - Backfill Complete



3.2.1.4 Type IV Tanks

There are four Type IV tanks in HTF (Tanks 21 through 24). The Type IV tanks were constructed between 1958 and 1962. A typical HTF Type IV tank structure is shown in Figure 3.2-45. These waste tanks have a single liner with a spherical, reinforced concrete, domed roof that supports itself. Type IV tanks are 85 feet in diameter and approximately 34 feet high at the side wall, with a nominal operating capacity of 1,300,000 gallons. [DP-478]

Figure 3.2-45: Typical HTF Type IV Tank



3.2.1.4.1 Basemat and Cement Topping

A Type IV tank bottom layer is a reinforced basemat that is 4 inches thick. The basemat was installed with a thickness tolerance of plus 0.5 inch and minus 0.25 inch. [W230945] The testing of concrete and concrete materials was in accordance with W230945.

The basemat is covered with a wire mesh covered by a 3-inch cement topping with a float and trowel finish giving a maximum tolerance of ± 0.125 inch from true level. Figure 3.2-46 shows the placement of the basemat. Drainage channels (1.625 inch deep and approximately 3.5 inches wide) used for leak detection were formed in the cement topping (Figure 3.2-47). The channels coincide with the locations of welds and backup strips. [W230945]

Figure 3.2-46: Type IV Tank Basemat Placement



Figure 3.2-47: Type IV Tank Basemat Showing Geometry of Drainage Channels

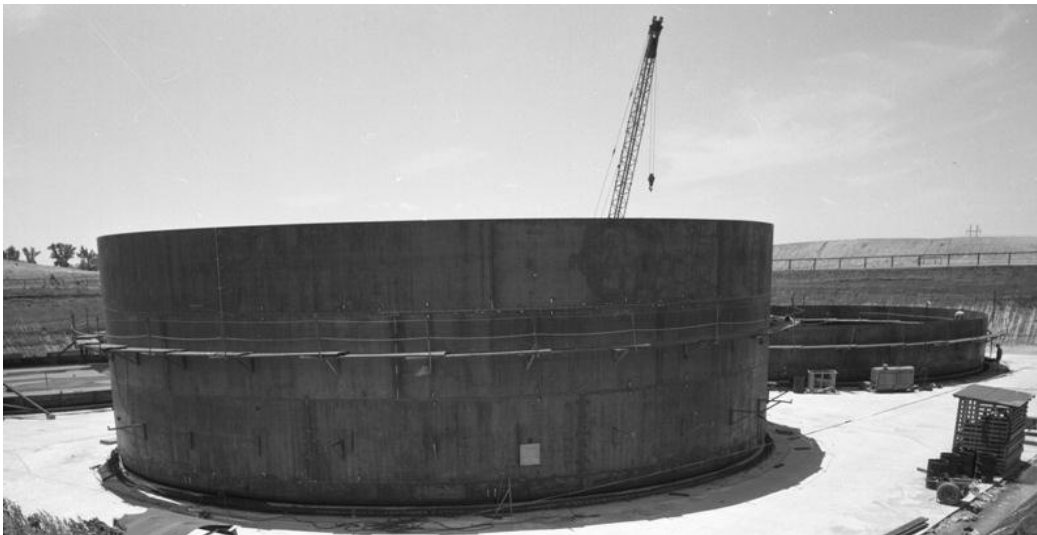


A 3-inch stainless steel drainpipe to collect any leakage is located at the center of the basemat. The drainpipe was placed below the 4-inch basemat and runs to an 8-inch long collection chamber (8 inches in diameter) below the footing at the edge of the waste tank wall. A 4-inch diameter pipe connects the leak collection chamber to the surface so that a leak collection probe might be placed in the chamber. [W230945]

3.2.1.4.2 Primary Liner

The Type IV tank primary liner is a cylinder (open at the top) made of 0.375-inch carbon steel plates and 0.4375-inch knuckle plates. [W230907] The primary waste tank liner is reinforced internally with three circumferential 4-inch carbon steel stiffener angles and is anchored externally to the concrete wall. The primary carbon steel liner material is identified and installed per specifications listed in W230907. Figure 3.2-48 shows the primary liner during Type IV tank construction.

Figure 3.2-48: Type IV Tank Primary Liner Construction



Penetrations through the primary liner and the side concrete (vault) wall exist to accommodate processing needs. The process lines penetrate the waste tank liner and concrete (vault) wall through sleeved penetrations. The size and material type for the process lines and the penetration sleeves are identified in Table 3.2-4.

Table 3.2-4: Type IV Tank Side Penetrations in Primary Liner

Tank No.	Process Line	Sleeve Welded to Primary Liner	Reference Drawings
21 - 24	3-inch schedule 40 stainless steel core pipe with 6-inch schedule 20 stainless steel jacket	10-inch schedule 40 carbon steel	W231244 W234134
21 - 24	3-inch schedule 40 stainless steel (two per waste tank)	10-inch schedule 40 carbon steel	W231244
21	4-inch stainless steel	6-inch schedule 40 carbon steel	W231210 W231244

3.2.1.4.3 Waste Tank Concrete Vault

The Type IV tank is completely enclosed in a concrete vault. After the wall foundation and basemat had been set and cured, the annular space between them was filled with metallic non-shrink grout with a compressive strength at least equal to that of the basemat. [W230976] The wall footing total width is 4 feet 10 inches, with 2 feet of the wall footing extending underneath the primary liner. The wall and wall footing contain vertical and horizontal reinforcing steel bars as detailed in drawings W230945 and W230976.

The waste tank roof consists of a spherical reinforced concrete dome made of concrete 7 to 10 inches thick (the dome concrete is thicker near the risers). The concrete dome is reinforced throughout with steel bars. Figure 3.2-49 shows the reinforced steel bars prior to the placement of the concrete. The dome has an internal curvature radius of 90 feet 4 inches and a rise of 10 feet 7.5 inches above the springline. The dome shape of the roof provides its own structural support; therefore, the concrete roof is not lined with carbon steel on the inside. The dome was constructed of Class A concrete that developed 5,000-psi at a 28-day cure time. [W231023] Each waste tank has six peripheral risers, each providing a 2-foot diameter opening into the waste tank interior. The riser locations are detailed in drawing W231206. Figure 3.2-50 shows the concrete vault for a Type IV tanks and the peripheral risers on the waste tank dome.

Figure 3.2-49: Type IV Tank Dome Construction



Figure 3.2-50: Type IV Tank Concrete Vault Construction



There is no secondary steel liner for the Type IV tanks. The concrete vault for a Type IV tank was built around the primary steel liner with the wall and the dome ring formed by shotcrete and reinforcing bars. [W230976] The walls were shot in vertical strips to avoid any horizontal joints around the waste tank and vertical joints were staggered in subsequent layers. The shotcrete was applied in successive layers from 0.75 inches to a maximum of 2 inches to provide the buildup thickness required per specification in W230976. Figure 3.2-51 shows the application of shotcrete on the wall of a Type IV tank.

Figure 3.2-51: Type IV Tank Vault Wall Shotcrete Application



The walls (concrete and liner) form a cylinder with an inner diameter of 85 feet and a height of 34 feet 3.75 inches at the springline surmounted by the dome ring. The core wall is 7 inches thick at the top and 11 inches at the bottom. The dome ring and wall were made monolithic by shooting the layers continually from the bottom to the top of the wall. The vertical reinforcing in the wall was also carried up into the dome ring. The dome ring and wall act as a unit with a joint between dome ring and dome slab and a joint between the wall and floor. [W230976]

The dome ring and the wall were prestressed by round bands to provide compression of the wall during operating conditions. [W230976]

3.2.1.4.4 Soil and Backfill

Earth was excavated from the area surrounding Tanks 21 through 24 to a depth of 17 feet below existing grade. [W230826] Since no annulus exists for these waste tanks, a three-layer backfilling system is used to surround the sidewalls of the concrete vault. [W231221] The backfill consists of a vermiculite fill layer, a special manually compacted fill of soil, and a test controlled compacted fill of soil. The vermiculite fill, (minimum 8 inches thick) added in bags, provides a cushion layer for expansion of the primary liner with temperature variations of the waste tank and waste tank contents from the foundation to the underside of the dome ring. As each bag layer was placed, voids behind and between bags were filled with earth backfill. When the fill came up to the top of a course of vermiculite bags, additional bags were placed against the waste tank. [DP-478, Section 8] Standard compaction of excavated soil (sandy clay) was performed around and over waste tanks. [W230976, W231023, W231221] The final test-controlled compacted fill was packed and rolled with heavy equipment. Figure 3.2-52 shows the placement of the vermiculite bags along the waste tank wall with backfilling operations approximately 50 % complete. The waste tanks were finally covered with a minimum of 3 feet 8 inches of compacted soil (Figure 3.2-53). [W231023]

Figure 3.2-52: Type IV Tanks with Backfill - Vermiculite Bags Showing

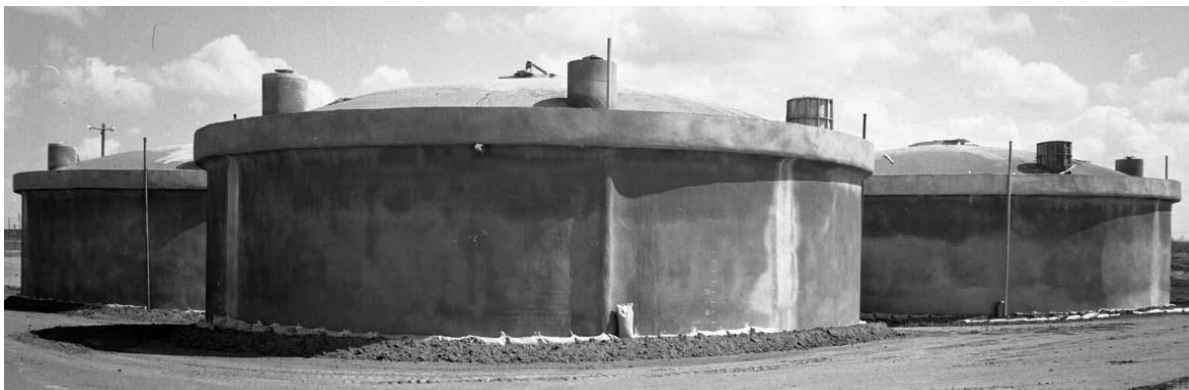


Figure 3.2-53: Type IV Tanks Backfill Complete



3.2.1.5 Water Infiltration through Waste Tank Design Features

Multiple waste-tank design elements serve to minimize water infiltration. The concrete vaults and steel liners serve to retard water flow through the waste tanks. The design features assumed in the HTF modeling are described in detail in Section 4. In addition, the waste tank tops are covered by the HTF closure cap (Section 3.2.4), and the waste tank liners are filled with cementitious material (Section 3.2.3), which will further limit the amount of water infiltration into the waste tank CZ.

3.2.1.6 Waste Tank Design Features Structural Stability/Degradation

Waste tank carbon steel primary liner and concrete vault structural stability is provided by the closure concept of grouting voids. The EIS considered several alternatives for the HTF waste tanks, including filling them with low-level contaminated grout or leaving a remaining void above the first grout lift with grout fill being the preferred alternative. [DOE-EIS-0303 ROD] In this PA, it is assumed that the entire waste tank is filled with grout therefore structural failure (i.e., collapse) is not considered. The HTF modeling included the impact of waste tank degradation (e.g., cracking or corrosion leading to increased hydraulic conductivity), and is described in detail in Section 4.2.2.2.

A structural evaluation was performed on Type IV Tanks 18 and 19 in the FTF to demonstrate that the waste tanks would maintain structural integrity during grouting activities. [T-CLC-F-00373] An additional analysis was performed to show that there would be minimal settlement (approximately 2 inches maximum) of the waste tanks even after they are grouted and a closure cap installed. [K-CLC-F-00073]

The long-term structural behavior/integrity of a grout filled waste tanks was evaluated. Mechanisms that could lead to cracking, such as material degradation, seismic loads, and settlement were analyzed. The analyses concluded that these mechanisms would not cause the grout filled waste tank to crack. [T-CLC-F-00421]

3.2.1.7 Waste Tank Design Features as Inadvertent Intruder Barrier

Multiple elements of the waste tank design serve as inadvertent intruder barriers. The HTF closure cap, waste tank concrete roof, and waste tank grout fill are considered sufficient to prevent drilling into the waste form given well drilling practices in the region and the presence of nearby land without underground concrete obstructions. The presence of the

earthen cover and the intruder barrier will prevent the worker from coming in contact with the waste form during construction of a basement for a residence as an inadvertent intruder. Section 4.2.3 contains a detailed discussion of the inadvertent intruder and exposure scenarios that are considered credible based on the waste tank design.

3.2.2 Ancillary Equipment

The HTF contains ancillary equipment with a residual radiological inventory that must be accounted for as a part of facility closure. This ancillary equipment includes buried pipe (transfer lines), pump tanks, and evaporators, all of which have been in contact with liquid waste over the operating life of the facility. The ancillary equipment was used in the HTF to transfer waste (e.g., transfer lines, pump tanks) and reduce waste volume through evaporation (e.g., the evaporator systems), or treat wastes (e.g., Actinide Removal Process (ARP), Modular Caustic Side Solvent Extraction Unit (MCU)). The amount of contamination on these components depends on such factors as the service life of the component, its materials of construction, and the contaminating medium in contact with the component.

Figure 3.2-54 identifies locations of specific ancillary equipment relative to the HTF waste tanks and relative to other components. The following HTF locations were considered in the PA waste modeling (discussed further in Section 4.4.2).

- The HTF transfer line system (74,800 linear feet), including transfer line jackets, leak detection boxes (LDBs), cleanout ports, and other transfer line secondary containment systems (e.g., the Type I tank transfer line encasements)
- The HTF pump tanks (i.e., HPT 2-10, CTS PT-242-3H, and CTS PT 242-18H)
- The HTF PPs (i.e., HPP 1-10, CTS PP-242-3H, and CTS PP-242-18H)
- The 242-H evaporator system, including the evaporator cell and system support tanks (e.g., mercury collection tank, cesium removal column (CRC) pump tank, and overheads tanks)
- The 242-16H evaporator system, including the evaporator cell and system support tanks (e.g., mercury collection tank, CRC pump tank, and overheads tanks)
- The 242-25H evaporator system, including the evaporator cell and system support tanks (e.g., condenser, mercury collection tank, and overheads pumps and tanks)

Figure 3.2-54: HTF Ancillary Equipment Locations



The initial conceptual design and approach used in the HTF PA modeling is an aphysical simplification of the actual infrastructure of HTF ancillary equipment design. This approach is required for analytical modeling. Certain equipment features and design elements have been omitted in the conceptual model.

Transfer line inventory is modeled by distributing the assumed inventory uniformly throughout the HTF modeling cells. The pump tanks, evaporator pots, and CTS tanks are modeled as uniform inventories spread throughout a single modeling cell at the location of the applicable ancillary source. Other HTF ancillary equipment (i.e., DBs, valve boxes, catch tank, evaporator cells, and overheads tanks) are not modeled. This approach is because these locations did not serve as primary waste containment, and therefore will not contain significant radiological inventory at closure. Additionally, ancillary equipment in the ARP/MCU facilities is not modeled, as these facilities will be extensively cleaned or decontaminated, and/or removed to support closure activities.

3.2.2.1 Transfer Line System

The HTF transfer line details are provided in Table 3.2-5 and based on reference drawings and data obtained from the Structural Integrity Database (M-ML-G-0005), an engineering database developed to help control and maintain the technical baseline of the SRS facilities including the HTF.

Table 3.2-5: HTF Transfer Line Segment Listing

Line No.	From (a)	To	Core Material (b)	Core Diameter (inches)	Jacket Diameter (inches)	Line Length (ft)	Cross-Sectional Area (ft ²)
1	HDB-1(24)	HPP-1(2)	SS	3	Encasement	342	100
2	HDB-1(15)	HPP-1(3)	SS	3	Encasement	339	99
3	HDB-1(27)	HPP-2(2)	SS	3	Encasement	325	95
4	HDB-1(18)	HPP-2(3)	SS	3	Encasement	322	94
5	HDB-1(22)	HPP-3(2)	SS	3	Encasement	308	90
6	HDB-1(13)	HPP-3(3)	SS	3	Encasement	305	89
7	HDB-1(25)	HPP-4(2)	SS	3	Encasement	304	89
8	HDB-4(3)	HPP-1(16)	SS	3	Encasement	304	89
9	HDB-2(6)	HPP-3(23)	SS	3	Encasement	70	20
10	HPP-1(5)	HDB-2(5)	SS	3	Encasement	60	18
11	HPP-2(4)	HDB-2(4)	SS	3	Encasement	50	15
12	HPP-2(5)	HDB-2(3)	SS	3	Encasement	63	18
13	HPP-3(4)	HDB-2(8)	SS	3	Encasement	56	16
14	HPP-3(5)	HDB-2(7)	SS	3	Encasement	60	18
15	HPP-4(4)	HDB-2(2)	SS	3	Encasement	30	9
17	HDB-2(16)	Tank 13	SS	3	Encasement	173	50
18	HDB-2(15)	cut & capped	SS	3	Encasement	0	0
19	HDB-2(14)	Tank 15	SS	3	Encasement	293	85
20	HDB-2(13)	Tank 15	SS	3	Encasement	293	85
21	Tank 15 & Tank 16 Valve Box	HDB-2(12)	SS	3	Encasement	289	84
22	HDB-2(11)	Tank 16	SS	3	Encasement	293	85
23	HDB-2(10)	Tank 14	SS	3	Encasement	173	50
24	HDB-2(9)	Tank 14	SS	3	Encasement	173	50
27	Tank 13(7)	HDB-2(22)	SS	3	4	256	50

Table 3.2-5: HTF Transfer Line Segment Listing (Continued)

Line No.	From (a)	To	Core Material (b)	Core Diameter (inches)	Jacket Diameter (inches)	Line Length (ft)	Cross-Sectional Area (ft ²)
29	HDB-5(11)	HDB-2(20)	SS	3	4	282	82
30	HDB-5(10)	HDB-2(19)	SS	3	4	290	85
31/107	HDB-2(18)	HDB-4(13)	SS	3	10	700	204
32/106	HDB-2(17)	HDB-4(15)	SS	3	10	700	204
33E	HDB-1(11)	Tank 9	SS	3	Encasement	81	24
34E	HDB-1(12)	Tank 10	SS	3	Encasement	81	24
36E	HDB-1(14)	Tank 12	SS	3	Encasement	181	53
39E	HDB-1(17)	Tank 11	SS	3	Encasement	181	53
41E	#91	HDB-1(19)	SS	3	Encasement	50	15
42E	HDB-1(20)	Tank 9	SS	3	Encasement	81	24
43E	HDB-1(21)	Tank 10	SS	3	Encasement	81	24
45E	HDB-1(23)	Tank 12	SS	3	Encasement	181	53
48E	HDB-1(26)	Tank 11	SS	3	Encasement	181	53
100	HDB-3(3)	Tank 23 (NW)	SS	3	6	25	7
100(EVAP)	Tank 32(TP)	242-25H Evaporator (P8)	SS	2	8	423	84
101(DB3)	HDB-3(2)	Tank 21(NE)	SS	3	6	160	47
101(DB4)	HDB-4(11)	Tank 29	SS	2	3	81	16
101E	Tank 23(N)	HDB-5(7)	SS	3	10	280	82
102(DB4)	Tank 29(TJ)	HDB-4(9)	SS	3	8	103	30
102(DB6)	HDB-6(8)	Tank 35(C1)	SS	3	10	83	24
102/RCZ74	HDB-6(2)	HDB-8(21)	SS	3	6	1,176	343
103	Tank 14(2)	Tank 13(7)	SS	3	4	370	108
103(DB4)	HDB-4(6)	Tank 31(C1)	SS	3	10	190	55
103(DB6)	HDB-6(9)	Tank 36(C1)	SS	3	10	463	135

Table 3.2-5: HTF Transfer Line Segment Listing (Continued)

Line No.	From (a)	To	Core Material (b)	Core Diameter (inches)	Jacket Diameter (inches)	Line Length (ft)	Cross-Sectional Area (ft ²)
104(DB4)	HDB-4(4)	Tank 32(TJ)	SS	3	8	110	32
104 (DB6)	HDB-6(10)	Tank 37(C1)	SS	3	10	575	168
105(DB4)	HDB-4(8)	Tank 30(C1)	SS	3	10	84	25
105/HHP14	HDB-8(20)	HDB-6(1)	SS	3	6	1,176	343
108	HDB-4(12)	HDB-5(9)	SS	3	10	460	134
109	HDB-4(10)	Tank 29(C1)	SS	3	8	103	30
110	Tank 31(TJ)	HDB-4(5)	SS	3	8	190	55
111	Tank 32(C1)	HDB-4(3)	SS	3	8	110	32
112	Tank 30(TJ)	HDB-4(7)	SS	3	8	84	25
140	244-H (RBOF)	HDB-3 (1)	SS	3	6	852	249
151	Tank 35(TJ)	HDB-6(5)	SS	3	10	81	24
201	Tank 36(TJ)	HDB-6(6)	SS	3	10	463	135
251	Tank 37(TJ)	HDB-6(7)	SS	3	10	575	168
451	Tank 13(TP)	242-H Evaporator	SS	3	6	427	125
452	242-H Evaporator vent	Tank 13	SS	3	6	427	125
475	242-25H Evaporator (P4)	Tank 29(C2)	SS	3	8	239	70
476	242-25H Evaporator (P5)	Tank 30(C2)	SS	3	8	188	55
477	242-25H Evaporator (P6)	capped/not installed	SS	3	8	116	34
479	242-25H Evaporator (P18)	Tank 37(C2)	SS	3	8	251	73
501	242-H Evaporator	HCTS(2)	SS	3	8	282	82
504	HCTS (27)	Tank 29	SS	3	4	90	26
505	HCTS (21)	Tank 32 cut & capped	SS	2	3	90	18
506	Tank 31(C2)	Tank 32 cut & capped	SS	2	3	289	57
507	Tank 31(C2)	Tank 30 cut & capped	SS	2	3	165	33

Table 3.2-5: HTF Transfer Line Segment Listing (Continued)

Line No.	From (a)	To	Core Material (b)	Core Diameter (inches)	Jacket Diameter (inches)	Line Length (ft)	Cross-Sectional Area (ft ²)
508	Tank 30 cut & capped	Tank 29(C2)	SS	2	3	73	14
509	Tank 29 cut & capped	HCTS (24)	SS	2	8	253	50
535	242-25H Cell(P12)	Tank 32(C2)	SS	2	8	456	90
552	242-25H Hg Tank overheads	Tank 32	SS	2	8	463	92
665	Tank 12(7) TJ	Line 930 at HDB-2	CS	3	4	80	23
671	Tank 11(6)	Tank 11(7)	SS	3	4	16	5
703A	ITP filter cell #1	#1554A	SS	3	6	34	10
705A	ITP filter cell #1	Tank 48(E2)	SS	6	10	57	31
910	#2225	#911	SS	3	4	130	38
911	Tank 10(2) TJ	#41E to HDB-1(19)	CS	3	8	212	62
930	Tank 11(7)	HDB-2(29)	CS	3	4	140	41
1051	HDB-4(2)	HDB-6(13)	SS	3	6	641	187
1052	HDB-6(11) sump	Tank 35(C2)	SS	2	4	58	11
1100	221H HHW HDR#1	HPP-6(1)	SS	3	10	750	219
1101	221H LHW HDR#4	HPP-5(1)	SS	3	10	771	225
1102	221H LHW HDR#3	HPP-5(2)	SS	3	10	760	222
1103	221H HHW HDR#2	HPP-6(2)	SS	3	10	760	222
1103A	ITP filter cell #2	#703A	SS	3	6	31	9
1104	221H LDB#4	#1000 at HPP-6	CS	1.5	N/A	752	119
1105A	ITP filter cell #2	Tank 48(E2)	SS	6	10	72	40
1151A	Tank 48(G)	ITP filter cell #2	SS	6	10	135	75
1152A	Tank 48(H)	ITP filter cell #1	SS	6	10	165	91
1251A	Tank 49 transfer valve box drain	#8318 to #8415 to drain cell	CS	3	Encasement	108	32

Table 3.2-5: HTF Transfer Line Segment Listing (Continued)

Line No.	From (a)	To	Core Material (b)	Core Diameter (inches)	Jacket Diameter (inches)	Line Length (ft)	Cross-Sectional Area (ft ²)
1252A	Tank 49 transfer valve box	#1660	SS	3	6	10	3
1253A	Tank 49 transfer valve box	Late Wash facility	SS	3	6	893	260
1451A	#1661	Tank 49	SS	3	6	13	4
1501	Tank 39(TJ)	Tank 43(C1)	SS	3	6	350	102
1501A	Tank 22 valve box	Tank 22 side port	SS	3	4	53	15
1502A	Tank 22 valve box	#5811	SS	3	4	17	5
1503A	HDB-5(3)	Tank 22 valve box	SS	3	4	205	60
1528	Tank 38(TJ)	Tank 43(R)	SS	3	6	586	171
1552A	ITP building	cut & capped	SS	3	6	22	6
1554A	ITP hold tanks	Tank 48	SS	3	6	78	23
1555A	#1552A	#1566A	SS	3	6	16	5
1555A (cut)	ITP building	cut & capped	SS	3	6	19	6
1566A	ITP wash valve	Tank 48(B3)	SS	3	6	65	19
1576	Tank 41(TJ)	Tank 43	SS	3	6	314	92
1596	#16102	Tank 43	SS	3	6	338	99
1626	Tank 43(TJ)	HDB-7(10)	SS	3	10	815	238
1628	Tank 43 (R) pump	242-16H Evaporator (N12)	SS	1	6	104	11
1651	242-16H Evaporator (N10)	Tank 43(C3)	SS	2	6	79	16
1653	242-16H Evaporator (N9)	Tank 41(C3)	SS	2	6	164	32
1654	242-16H Evaporator (N8)	Tank 40(C3)	SS	2	6	92	18
1660	#1252A	#3056	SS	3	10	404	118
1661	#1701A	#1451A	SS	3	6	292	85
1662	#16053 at Tank 51	Tank 43	SS	3	10	451	132
1663	Tank 50(TJ)	Tank 43 cut & capped	SS	3	10	620	181

Table 3.2-5: HTF Transfer Line Segment Listing (Continued)

Line No.	From (a)	To	Core Material (b)	Core Diameter (inches)	Jacket Diameter (inches)	Line Length (ft)	Cross-Sectional Area (ft ²)
1701A	Tank 48(B5) TTP	#1661	SS	3	6	58	17
1825	Tank 24(TJ)	HDB-5(8)	SS	3	10	396	116
1905A/SSP2	Tank 50 (B5) TTP	Low point drain tank	SS	4	6	3,371	1264
2225	Tank 9(3) TJ	#910	SS	3	4	5	1
2701	242-16H Evaporator (N4)	Tank 39(C3)	SS	2	6	114	23
2702	242-16H Evaporator (N3)	Tank 38(C3)	SS	2	6	206	41
2703	242-16H Evaporator bottom line clean out drain	Tank 38	SS	1.5	3	93	15
2708	242-16H Evaporator (N2)	Tank 42(C3)	SS	2	6	77	15
2722	Tank 42(C1) valve box	Tank 43	SS	3	8	381	111
3051	HDB-7(11)	Tank 43(C1)	SS	3	10	815	238
3052	HDB-7(12)	Tank 41(C1)	SS	3	10	515	150
3053	HDB-7(13)	Tank 40 valve box	SS	3	10	377	110
3054	HDB-7(14)	Tank 39(C1)	SS	3	6	238	69
3055	HDB-7(15) drain	Tank 38	SS	1.5	4	51	8
3056	#1660	HDB-7(20)	SS	3	12	394	115
3057	HDB-7(19)	Tank 48(C1)	SS	3	12	404	118
3059	Tank 50(C1) TJ	HDB-7(21)	SS	3	12	855	249
3060	#16052	HDB-7(22)	SS	3	12	975	284
3062	HDB-8(3)	HDB-7(23)	SS	3	6	1,152	336
3063	HDB-8(2)	HDB-7(24)	SS	3	6	1,154	337
3068	HDB-2(31)	HDB-7(5)	SS	3	10	472	138
3069	HDB-2(30)	HDB-7(6)	SS	3	10	472	138
3070	HDB-7(3)	HDB-8(1)	SS	3	10	1,173	342

Table 3.2-5: HTF Transfer Line Segment Listing (Continued)

Line No.	From (a)	To	Core Material (b)	Core Diameter (inches)	Jacket Diameter (inches)	Line Length (ft)	Cross-Sectional Area (ft ²)
3071	HDB-8(4)	HDB-7(4)	SS	3	10	1,173	342
3083	HDB-7(17)	Tank 38(C1)	SS	3	6	64	19
3084	Tank 42(C1) valve box	HDB-7(18)	SS	3	8	285	83
3094	HPP-6(6)	HDB-7(1)	SS	3	10	857	250
3095	HPP-6(7)	HDB-7(2)	SS	3	10	857	250
3096/RCZ73	HDB-8(15)	HDB-7(9)	SS	3	8	1,206	352
3097	HPP-5(6)	HDB-7(7)	SS	3	10	816	238
3098	HPP-5(7)	HDB-7(8)	SS	3	10	816	238
3102	HDB-7(25)	HDB-8(16)	SS	3	8	1,180	344
3378	242-16H Evaporator overheads drain	Tank 43	SS	2	4	100	20
3934	242-16H (N6)	Tank 50	SS	2	6	342	68
3958	242-16H CRC feed pumps	Tank 42(M)	SS	1.5	6	86	14
3964	Tank 42(M)	242-16H OH receiver	SS	1.5	6	86	14
5811	#1502A	Tank 22(S)	SS	3	4	5	1
6386	ETF WC Tk2	Tank 50 VB	SS	2	6	1,286	255
8352	LDB drain cell (2)	Tank 48	SS	2	4	46	9
12261	Tank 15(7) TJ	916 valve box at Tank 16	SS	3	4	119	35
13568	916 valve box Tank 16	#21 to HDB-2(12)	SS	3	4	296	86
14101	#3084 at Tank 42 valve box	#2722 at Tank 42 valve box	SS	3	4	5	1
15912	#16053	Tank 51 drain valve box	SS	3	4	27	8
15913	#3060	Tank 51 drain valve box	SS	3	4	4	1
15914	Tank 51 drain valve box	#16055	SS	3	4	2	1
15961	Tank 51(B5) TTP	Tank 51 transfer valve box	SS	3	4	25	7

Table 3.2-5: HTF Transfer Line Segment Listing (Continued)

Line No.	From (a)	To	Core Material (b)	Core Diameter (inches)	Jacket Diameter (inches)	Line Length (ft)	Cross-Sectional Area (ft ²)
16051	Tank 51 transfer valve box	Tank 51(C1) jet	SS	3	4	45	13
16052	Tank 51 transfer valve box	#3060	SS	3	4	43	13
16054	Tank 51 transfer valve box	DWPF LPPP sludge tank	SS	3	10	1,131	330
16055	Tank 51 transfer valve box	Tank 51(C1) jet	SS	3	6	35	10
16101	Tank 40 transfer valve box	Tank 40(C1)	SS	3	4	28	8
16102	Tank 40 transfer valve box	#1596	SS	3	6	54	16
16103	Tank 40 transfer valve box	Tank 40(C1)	SS	3	6	62	18
16104	Tank 40 transfer valve box	DWPF LPPP sludge tank	SS	3	10	1,360	397
16262	Tank 40(V2)	Tank 40 transfer valve box	SS	3	4	41	12
16312	Tank 40(B5)	Tank 40 transfer valve box	SS	3	4	22	6
16460	Tank 40(C1)	Tank 40 transfer valve box	SS	3	4	36	11
16462	#16102	Tank 40 drain valve box	SS	3	4	11	3
16463	Tank 40 drain valve box	#16101	SS	3	4	25	7
210001	Tank 21(S)	Tank 21 valve box	SS	3	4	22	6
210002	Tank 21 valve box	Tank 21(SW) spare inlet	SS	3	4	71	21
210003	Tank 21 valve box	HDB-5(6)	SS	3	4	89	26
HHP16	HPP-9(5)	HDB-8(13)	SS	3	Encasement	30	9
HHP17	HDB-8(4)	HPP-9(3)	SS	3	Encasement	30	9
PSP11	HPP-7(5)	HDB-8(3)	SS	3	Encasement	50	15
PSP12	HDB-8(16)	HPP-7(4)	SS	3	Encasement	50	15
RCZ20	Auxiliary pump pit	HDB-8(8)	SS	3	6	2,350	685
RCZ36	LW hold tank	HDB-8(7)	SS	3	6	2,350	685
RCZ75	HDB-5(1)	HDB-8(17)	SS	3	6	311	91
RCZ76	HDB-8(18)	HDB-5(2)	SS	3	6	311	91

Table 3.2-5: HTF Transfer Line Segment Listing (Continued)

Line No.	From (a)	To	Core Material (b)	Core Diameter (inches)	Jacket Diameter (inches)	Line Length (ft)	Cross-Sectional Area (ft ²)
RCZ92	ETF valve pit	HDB-8(6)	SS	3	8	1,260	386
RCZ94	ETF conc DB	HDB-8(5)	SS	4	10	150	56
RCZ117	HDB-8(1)	HPP-7(3)	SS	3	Encasement	50	15
RCZ120	HPP-8(5)	HDB-8(14)	SS	3	Encasement	50	15
RCZ121	HDB-8(6)	HPP-8(2)	SS	3	Encasement	40	12
RCZ122	HDB-8(2)	HPP-8(3)	SS	3	Encasement	40	12
RCZ123	HDB-8(11)	HPP-8(4)	SS	3	Encasement	40	12
RCZ125	HPP-9(2)	HDB-8(7)	SS	3	Encasement	30	9
RCZ126	HPP-9(4)	HDB-8(10)	SS	3	Encasement	30	9
RCZ128	HDB-8(8)	HPP-10(3)	SS	3	Encasement	20	6
RCZ129	HPP-10(5)	HDB-8(9)	SS	3	Encasement	20	6
RCZ130	HDB-8(5)	HPP-10(4)	SS	3	Encasement	20	6
RCZ131	HDB-8(12)	HPP-10(2)	SS	3	Encasement	20	6
RCZ135	HPP-7(2)	HDB-8(15)	SS	3	Encasement	50	15
HB-241942-WTS-L-13052	Tank 42 riser B3 WTS-P-5	Tank 42 transfer valve box	SS	3	4	41	12
HB-241951-WTS-L-15910	Tank 51 riser C1	Transfer valve box WTS-V-78	SS	3	4	26	8
HB-241951-WTS-L-16011	Tank 51 riser V1	Valve box WTS-V-8 line used for flushing	SS	3	4	35	10
HB-241951-WTS-L-16053	Tank 51 valve box WTS-V-76 tie-in	#15912	SS	3	4	23	7
HI-241278-WTS-L-1459	ARP Filtrate line at tie-in to S-512000-RCZ37	Line WTE-L-1459 (at MCU wall/seal plate)	SS	3	4	42	12
HI-241278-WTS-L-1657	Line from seal plate at line WTE-L-1657	tie-in at RCZ38 alias 1253A	SS	3	4	42	12

Table 3.2-5: HTF Transfer Line Segment Listing (Continued)

Line No.	From (a)	To	Core Material (b)	Core Diameter (inches)	Jacket Diameter (inches)	Line Length (ft)	Cross-Sectional Area (ft ²)
HI-241278-WTS-L-1755	Line from seal plate at line WTE-L-1755	Tie-in at SDP1	SS	3	4	40	12
HI-241949-WTS-L-651A	Tank 49 riser B5 WTS-P-3	Tank 49 VBX (above ground)	SS	3	6	56	16
HI-241949-WTS-L-656A	Tank 49 riser B3 WTS-P-4	Tank 49 VBX (above ground)	SS	3	6	47	14
HI-241950-LD-L-8424	Drain line from Tank 50 valve box	Tank 50	CS	3	N/A	21	6
HL-241000-WTS-L-3	Tie-in line HL-241000-WTS-L-49E	HPP-2(2) via encasement	SS	3	N/A	43	13
HL-241000-WTS-L-33E	HDB-1(11)	Tank 9	SS	3	N/A	142	41
HL-241000-WTS-L-34E	HDB-1(12)	Tank 10	SS	3	N/A	132	39
HL-241000-WTS-L-35E	HDB-1(13)	HPP-3(3)	SS	3	N/A	356	104
HL-241000-WTS-L-36E	HDB-1(14)	Tank 12	SS	3	N/A	230	67
HL-241000-WTS-L-41E	#911	HDB-1(19)	SS	3	N/A	69	20
HL-241000-WTS-L-42E	HDB-1(20)	Tank 9	SS	3	N/A	124	36
HL-241000-WTS-L-43E	HDB-1(21)	Tank 10	SS	3	N/A	116	34
HL-241000-WTS-L-44E	HDB-1(22)	Tie-in with HL-241035-WTS-L-5	SS	3	N/A	318	93

Table 3.2-5: HTF Transfer Line Segment Listing (Continued)

Line No.	From (a)	To	Core Material (b)	Core Diameter (inches)	Jacket Diameter (inches)	Line Length (ft)	Cross-Sectional Area (ft ²)
HL-241000-WTS-L-45E	HDB-1(23)	Tank 12	SS	3	N/A	215	63
HL-241000-WTS-L-48E	HDB-1(26)	Tank 11	SS	3	N/A	215	63
HL-241000-WTS-L-49E	HDB-1(27)	Tie-in with HL-241000-WTS-L-3	SS	3	N/A	319	93
HL-241-035-WTS-L-16	HDB-2(1)	HPP-4(5)	SS	3	N/A	18	5
HL-241-035-WTS-L-17	HDB-2(16)	Tank 13	SS	3	N/A	177	52
HL-241-035-WTS-L-18-102	HDB-2(15)	Line #102 at Tank 13 cut & capped at HDB-5	SS	3	N/A	171	50
HL-241-035-WTS-L-19	HDB-2(14)	Tank 15	SS	3	N/A	351	102
HL-241-035-WTS-L-2	HDB-1(15)	HPP-1(3)	SS	3	N/A	388	113
HL-241-035-WTS-L-20	HDB-2(13)	Tank 15	SS	3	N/A	355	104
HL-241-035-WTS-L-22	HDB-2(11)	Tank16	SS	3	N/A	359	105
HL-241-035-WTS-L-23	HDB-2(10)	Tank 14	SS	3	N/A	185	54
HL-241-035-WTS-L-24	HDB-2(9)	Tank 14	SS	3	N/A	187	55
HL-241035-WTS-L-3071	HDB-2(28)	cut & capped at HDB-2	SS	3	10	8	2

Table 3.2-5: HTF Transfer Line Segment Listing (Continued)

Line No.	From (a)	To	Core Material (b)	Core Diameter (inches)	Jacket Diameter (inches)	Line Length (ft)	Cross-Sectional Area (ft ²)
HL-241035-WTS-L-33	HDB-2 overflow to encasement	Tie-in with #68E	SS	3	N/A	140	41
HL-241035-WTS-L-4	HDB-1(18)	HPP-2(3)	SS	3	N/A	367	107
HL-241035-WTS-L-5	Tie-in line HL-241000-WTS-L-44E	HPP-3(2) via encasement	SS	3	N/A	29	8
HL-241035-WTS-L-6	HDB-1(13)	HPP-3(3)	SS	3	N/A	358	104
HL-241035-WTS-L-7	HDB-1(25)	HPP-4(2)	SS	3	N/A	329	96
HL-241035-WTS-L-8	HDB-1(16)	HPP-4(3)	SS	3	N/A	340	99
HL-241035-WTS-L-8E	HDB-1 Encasement drain	Catch tank	SS	3	N/A	399	116
HL-241035-WTS-L-9-HPP1	HPP-1(4)	HDB-2(6) cut & capped	SS	3	N/A	87	25
HL-241035-WTS-L-HP68E	Encasement line #33	Line #8E tie-in	SS	3	N/A	60	18
HL-241035-WTS-L-IAL-25	HDB-2(24)	cut & capped near HDB-8	SS	3	4	660	193
HL-241035-WTS-L-IAL-26	HDB-2(23)	cut & capped near HDB-8	SS	3	4	660	193
HL-241052-WTS-L-21	HDB-5(4)	Tank 21 south riser	SS	1.5	3	94	15
HL-241911-WTS-PSP-5362	Tank 11 annulus transfer line south riser, including new spool piece	Tank 11 Riser 6	SS	3	4	25	7

Table 3.2-5: HTF Transfer Line Segment Listing (Continued)

Line No.	From (a)	To	Core Material (b)	Core Diameter (inches)	Jacket Diameter (inches)	Line Length (ft)	Cross-Sectional Area (ft ²)
HL-241916-WTS-L-20E	Tank 16(TJ)	Tank 13(5)	SS	3	4	200	58
HM-242016-WEE-L-3932	Evaporator (N5)	Tank 48	SS	2	4	200	40
HM-242016-WEE-L-3933	Evaporator (N11)	Tank 49	SS	2	4	185	37
HM-242016-WEE-L-3935	Evaporator (N7)	Tank 51	SS	2	3	359	71
Total (Carbon Steel)						1,313	283
Total (Stainless Steel)						73,487	21,240
Grand Total (Carbon Steel and Stainless Steel)						74,800	21,523

- a. Number in “()” is riser or nozzle identifier
b. SS = Stainless Steel, CS = Carbon Steel.

The HTF has 74,800 linear feet of transfer line with line segments ranging from a few feet in length to almost 3,400 feet. The HTF waste transfer lines are typically constructed of a stainless steel primary core pipe and are normally located below ground. Those lines that are above or near the surface are shielded to minimize radiation exposure to personnel. Figure 3.2-55 shows typical construction for transfer lines. All of the primary transfer lines have secondary containments of some type. The majority of primary transfer lines are surrounded by another pipe (jacket) constructed of carbon steel, stainless steel, or cement-asbestos. These jackets typically drain to LDBs, Modified LDBs (MLDBs), or to another primary or secondary containment (e.g., a waste tank). The balance of the primary transfer lines are located inside covered, concrete encasements, which perform the same secondary containment functions as the jacketed type previously described. Multiple (core) waste transfer lines may be contained in a single secondary containment jacket or concrete encasement. [W236508, W148228]

Figure 3.2-55: HTF Transfer Line Construction at Tank 30H

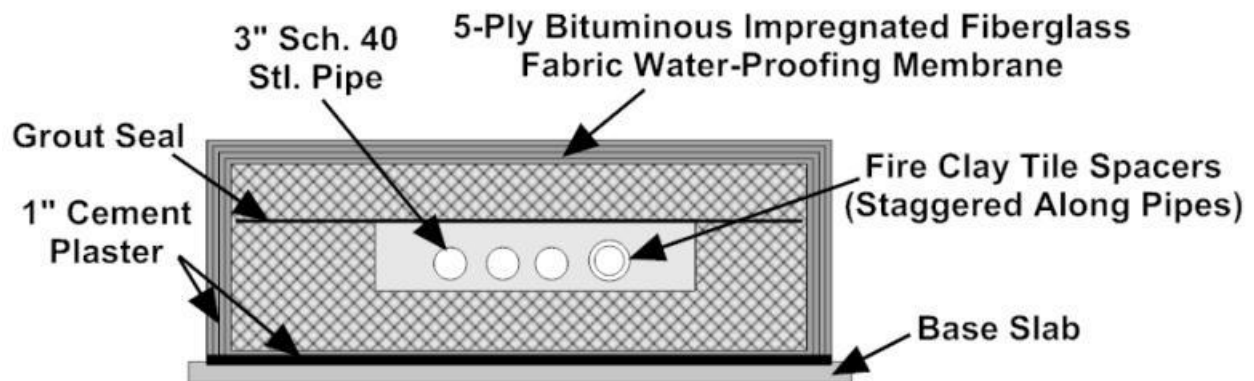


Waste transfer lines are typically sloped to be self-draining and where a pipe transitions from one size to another, the bottom of the pipe is generally aligned to prevent a situation that would prevent waste from draining to the intended tank. The line segments are supported using rod or disk-type core pipe spacers, core pipe supports, jacket supports, jacket guides, or other approved methods. Typically, core pipe spacers and supports are of stainless steel welded to the core pipe and jacket, while jacket supports and guides are of stainless steel with a concrete support. [C-CH-H-8096]

The following types of transfer lines exist in the HTF (it should be noted that designation of transfer line type and waste tank type are not related):

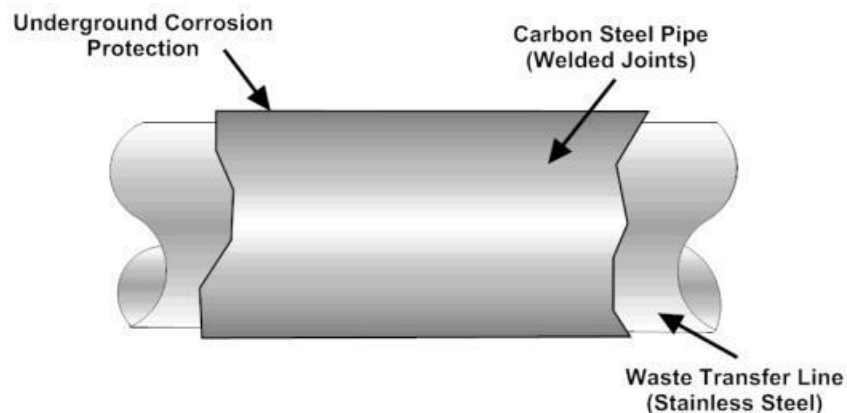
Type I transfer line - The core pipe is enclosed in a covered reinforced concrete encasement below ground and constructed of stainless steel (e.g., transfer lines from HDB-1 to Tanks 9 through 12) as shown in Figure 3.2-56. Core pipe leakage into the encasement and in-leakage of groundwater into the encasement will gravity drain to the catch tank. The catch tank is described later.

Figure 3.2-56: Type I Line Encasement (Sealed Concrete Trench)



Type II Transfer Line - The core pipe is stainless steel inside a carbon steel jacket (Figure 3.2-57). Pipe joints are typically welded and leak tested. Most jackets are encased in insulation. The portion of the carbon steel pipe in contact with the soil is protected against corrosion with polyethylene film wrap or bituminous coating. Type II transfer lines are the most common type of transfer lines in use.

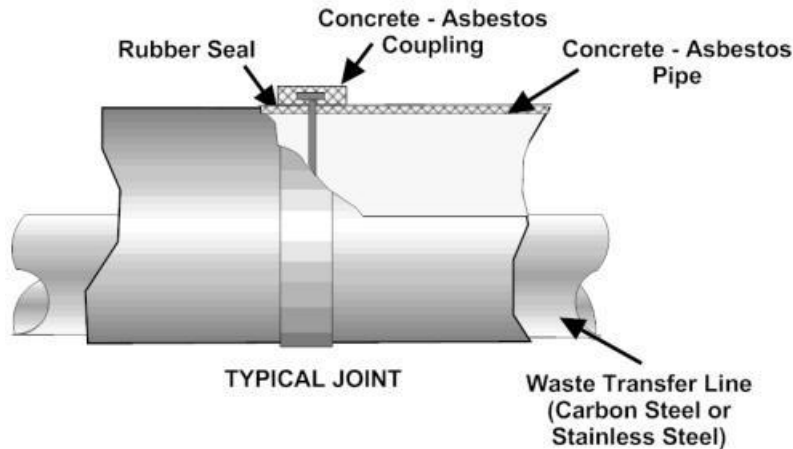
Figure 3.2-57: Type II Line Carbon Steel Jacket



Type IIA Transfer Line - Type IIA lines are similar to Type II except that both core pipe and jacket are of carbon steel. In HTF, there are very few lines of this type, and they are all associated with Tanks 10 through 12 only.

Type III Transfer Line - The core pipe is stainless steel within a cement-asbestos secondary containment that has rubber seals in the joints between the sections of cement-asbestos (Figure 3.2-58). Very few of these lines exist in the HTF and the few that do are associated with HDB-3.

Figure 3.2-58: Type III Line Concrete Asbestos Jacket



Type IV Transfer Line - Type IV lines are similar to Type II except that both the core pipe and jacket are stainless steel. This type of line in HTF is commonly found in use in conjunction with the evaporator systems, especially within the confines of the evaporator cells.

Type VI Transfer Line - Type VI transfer lines are designed to transfer evaporator overheads to and from the CRC. These lines do not have secondary containment. There are a few of these lines in HTF associated with the CRCs in the evaporator systems.

3.2.2.2 Pump Pits and Pump Tanks

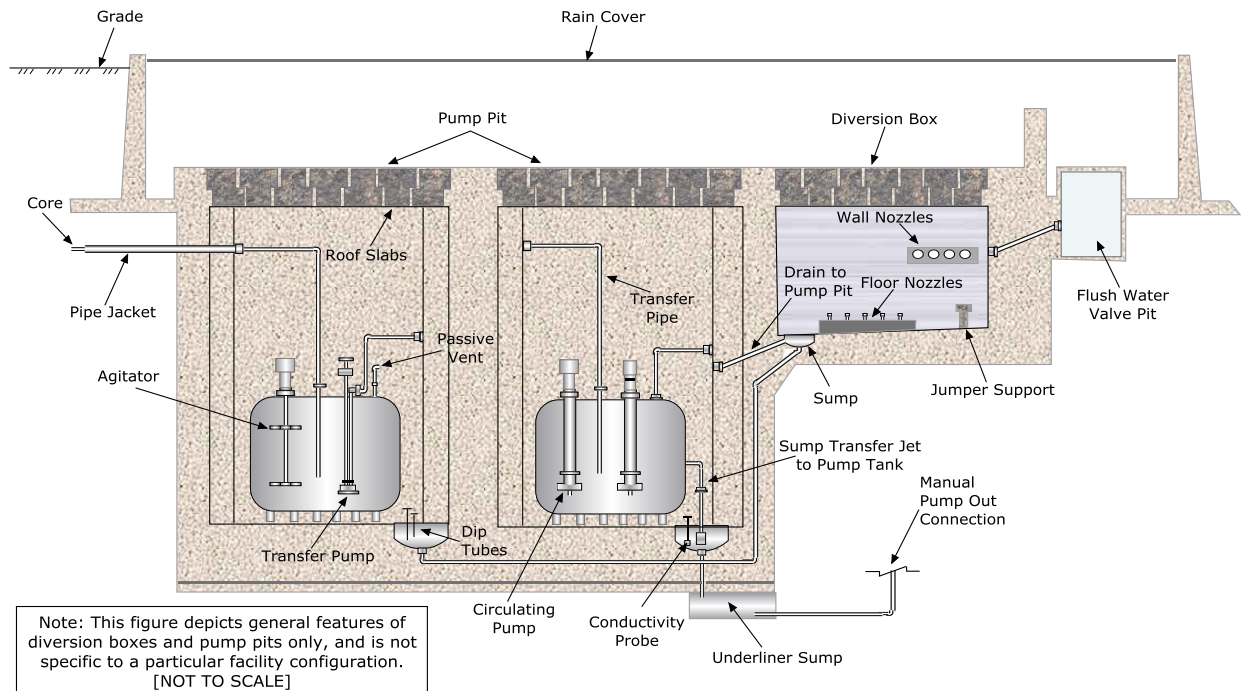
The HTF has 12 PPs (HPP-1 through HPP-10) and the CTSs, old and new. Table 3.2-6 provides a summary of the size and location of the PPs. The PPs are reinforced concrete structures (usually lined with stainless steel) and located below grade at the low points of the transfer lines. The PPs typically have walls that are 2 to 3 feet thick with sloped floors that are approximately 3 feet thick and concrete cell covers that are 2 to 4 feet thick. All PPs house a pump tank (with the exception of HPP-1) and provide secondary containment for the pump tanks. The CTS was used to facilitate transfers of the concentrate from the 1H Evaporator to selected waste tanks. A second CTS pit was needed to replace the original CTS pit to accommodate additional waste tanks. See Figure 3.2-54 for locations of PPs and CTS pits relative to other tank farm components. HPP-1 through HPP-4 and HPP-7 through HPP-10 are co-located with a DB. See Figure 3.2-59 for a typical DB and PP layout. [W163386, W163527]

Table 3.2-6: HTF Pump Pit Sizes and Elevations

Pump Pit	Interior Dimension of Floor Area (ft)	Northern Location ^a	Eastern Location ^a	Minimum Elevation of PP Bottom (ft above MSL)	Minimum Elevation of PP Top (ft above MSL)	References
HPP-1	15 X 15	71477	62007.5	246.9 ^b	282.33	W163386 W163527
HPP-2	15 X 15	71477	62025.5			
HPP-3	15 X 15	71477	62043.5			
HPP-4	15 X 15	71477	62061.5			
HPP-5	18 X 15	71659.5	62950	272.88 ^b	306.5	W714951 W714352
HPP-6	18 X 15	71680.5	62950			
HPP-7	18 X 18	71141.5	61579.5	250 ^c	294	W778702 W778815
HPP-8	18 X 18	71141.5	61601.0			
HPP-9	18 X 18	71141.5	61622.5			
HPP-10	18 X 18	71141.5	61644.0			
CTS (OLD) (242-3H)	14 X 14	71585.8	61549.5	297.18	323	W238758 W238746
CTS (NEW) (242-18H)	14 X 14	71585.83	61506.5	295.625	325	W702909 W702913

- a Approximate to centerline of PP
- b Bottom of structural slab
- c Bottom of concrete below sump

Figure 3.2-59: Typical Diversion Box and Pump Pit Layout



HPP-1 through HPP-4/HPT-2 through HPT-4 - The walls of HPP-1 through HPP-4 are 2 feet 6 inches to 3 feet 9 inches thick with sloped floors that are approximately 3 feet thick (2 feet 9 inches minimum). The cells are 15 feet square. [W163386] The cell covers consist of 12 concrete slabs that are approximately 1 foot 4 inches thick (four across and three high for each PP). [W163613]. Sheets of 16-gage stainless steel cover the walls and 11-gage stainless steel sheets cover the floor and sump of the individual cells. [W163510] Figure 3.2-60 is a photograph of a typical PP during construction.

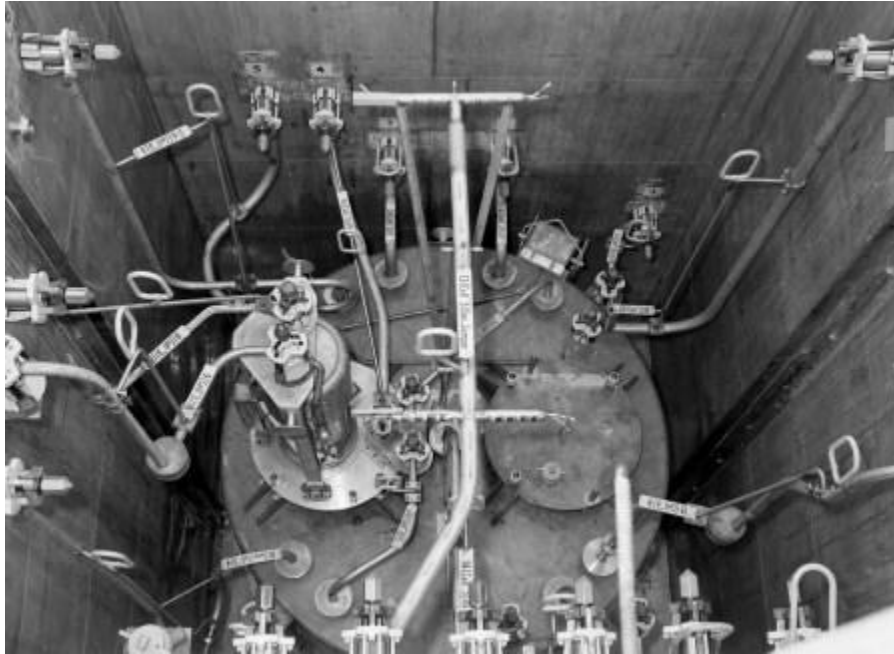
Figure 3.2-60: Construction of Typical HTF PP



All the PPs (except for HPP-1) contain a stainless steel pump tank. The PP tank vessels are 12 feet in diameter and 8 feet 6 inches high. [D116850] The PP provides secondary containment for the pump tank. The PPs have sumps have a conductivity probe, dip tube, and a transfer pump/jet for level detection and content transfer. Most PP locations have a flush water connection for flushing lines and vessels within the PP. The pump tanks have an approximately 7,200-gallon capacity and are equipped with dip-tubes for monitoring pump tank level. [PV179667]

There is not a pump tank in HPP-1 and it is used only for storage of old jumpers (rainwater that collects in the sump is pumped to HPT-3). A pump tank is within HPP-2, HPP-3, and HPP-4 (HPT-2, HPT-3, and HPT-4, respectively). Figure 3.2-61 shows the interior of HPP-3.

Figure 3.2-61: Interior View of HPP-3



HPP-5 and HPP-6/HPT-5 and HPT-6 - The walls of HPP-5 and HPP-6 are 2 feet 6 inches to 3 feet thick with sloped floors that are approximately 3 feet thick (2 feet 9 inches minimum). The cells are 18 feet x 15 feet and cell covers are concrete slabs 4 feet 3 inches thick. [W714951] Sheets of 11-gage stainless steel cover the walls and 0.375-inch thick sheets of stainless steel cover the floor and sump. [W714953] The PP tank vessels have sloped bottoms and are 12 feet in diameter, each with a capacity of 7,200 gallons. [PV179667]

HPP-7 through HPP-10/HPT-7 Through HPT-10 - HPP-7 through HPP-10 are 18 feet square, a height of 38 feet 8 inches, walls 3 feet to 3 feet 6 inches thick, and sloped floors approximately 3 feet thick. The cell covers are concrete slabs that are 4 feet 3 inches thick. [W778815] Sheets of 0.25-inch thick stainless steel cover the walls and 0.375-inch thick stainless steel sheets cover the floor and sump. [W778850] The tank vessels have sloped bottoms and are 12 feet in diameter, each with an approximate operating capacity of 6,000 gallons. [W752789]

CTS PP Building 242-3H (OLD) - 242-3H PP (Figure 3.2-62) is a 14-foot square cell with walls of reinforced concrete 1 foot 8 inches to 2 feet thick and sloped floors that are approximately 2 feet thick. The cell covers are reinforced concrete slabs with minimum thickness of 3 feet. [W238758] Sheets of stainless steel cover the walls, floor, and sump. [W238862] The PP tank vessel has a sloped bottom and is 8 feet in diameter with a capacity of approximately 3,000 gallons. [D139006] This PP was retired from service in 1979 and replaced with a new CTS PP to accommodate additional waste tanks.

Figure 3.2-62: Construction of HTF CTS PP Building 242-3H (Old)



CTS PP Building 242-18H (NEW) - 242-18H PP (Figure 3.2-63) is a 14-foot square cell with walls of reinforced concrete that are minimum 2 feet thick and sloped floors approximately 2 feet thick. [W702913] The cell covers are reinforced concrete slabs approximately 3 feet thick. [W702914] Sheets of 11-gage stainless steel cover the walls and 0.375-inch thick stainless steel sheets cover the floor and sump. [W702915] The PP tank vessel has a sloped bottom and is 8 feet in diameter with a capacity of approximately 3,000 gallons. [D139006]

Figure 3.2-63: Concentrate Transfer System PP and Pump Tank



3.2.2.3 Catch Tank

There is a single catch tank in HTF designed to collect drainage from HDB-1 and the Type I tank transfer line encasements. These transfer lines run primarily from Tanks 9 through 16 to HDB-1 and HDB-2. The transfer line encasement slopes towards the catch tank to collect leakage from the transfer line core pipe and in-leakage from ground water. The catch tank is located west of HDB-1. No significant contamination has been collected in this waste tank and it was not modeled as a source for contamination in the HTF PA; however, its description is provided for completeness.

The catch tank is a dished head stainless steel tank with a straight shell length of 30 feet and a diameter of 8 feet with a capacity of approximately 11,700 gallons. [D129961] It is located in an underground reinforced concrete cell with walls that are 2 feet 8 inches thick, a cover that is 2 feet 11 inches thick, and a floor that is 3 feet 10 inches thick. The floor of the catch tank is sloped to drain liquid into a sump and the bottom elevation of the floor, which is approximately at 241 feet above MSL, rests on a 4-inch thick base slab. [W149426]

3.2.2.4 Evaporator Systems

There are three evaporator systems in the HTF, the 242-H evaporator system (1H Evaporator), the 242-16H evaporator system (2H Evaporator), and the 242-25H evaporator system (3H Evaporator). The evaporators are used to reduce the amount of liquid volume of material resulting from nuclear processes. The evaporator systems are principally comprised of the evaporator, the overheads system, and the condenser. The 242-H evaporator system also includes the CTS, which was used to distribute evaporator bottoms throughout HTF (see Figure 3.2-54 for evaporator system locations within HTF). Table 3.2-7 provides evaporator system locations and elevations.

Table 3.2-7: Evaporator System Locations and Elevations

Evaporator System	North Location	East Location	Reference	Elevation of Cell Bottom (ft above MSL)	Top Elevation (ft above MSL)	Reference
242-H	71521	61716	W231132	314.5	348.5	W231299
242-16H	71173	62695	W702194	333.72 ^a	374.78 ^b	W702199
242-25H	71913	61398	W835332	295	345 ^c	SE5-2-2004313

Note Location is centerline of evaporator.

a Top of evaporator sump floor

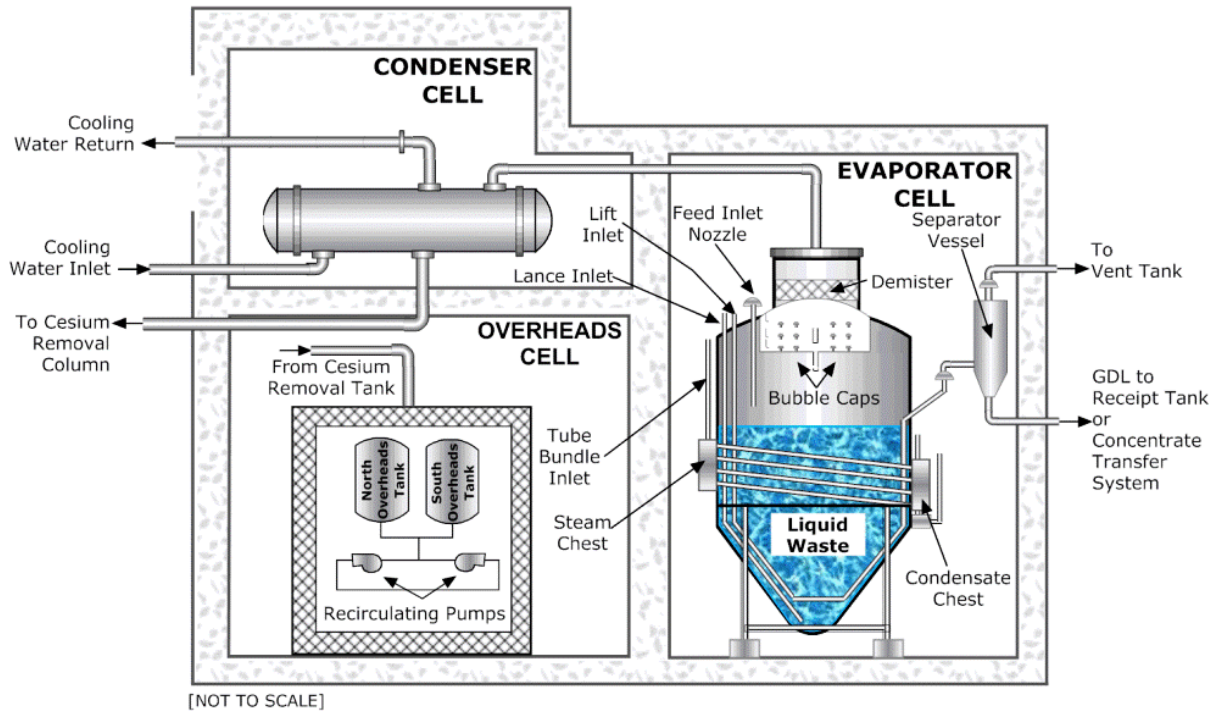
b Top of cell covers over condenser (N71191, E62691)

c Top of cell covers - does not include enclosure building.

3.2.2.4.1 242-H Evaporator System

The 242-H evaporator cell is a cuboid with a 16 foot x 15-foot base and a height of 25 feet. The cell includes a 2 foot x 2-foot floor sump with a depth of 2 foot 6 inches. The cell covers are 1-foot thick reinforced concrete. The cell provided containment for the evaporator and served as shielding for personnel protection. [W231299] Figure 3.2-64 is a sketch of the 242-H evaporator system.

Figure 3.2-64: 242-H Evaporator System Schematic



242-H Evaporator Vessel/Pot - The evaporator pot, located inside the 242-H evaporator cell, is a stainless steel cylindrical vessel with a conical bottom. The cylindrical portion is 8 feet in diameter and the overall height of the vessel is 15 feet. The evaporator was used to concentrate liquid in order to reduce liquid volumes. [W703006] Figure 3.2-65 is a view of the top of the evaporator.

Figure 3.2-65: 242-H Evaporator Vessel Top View

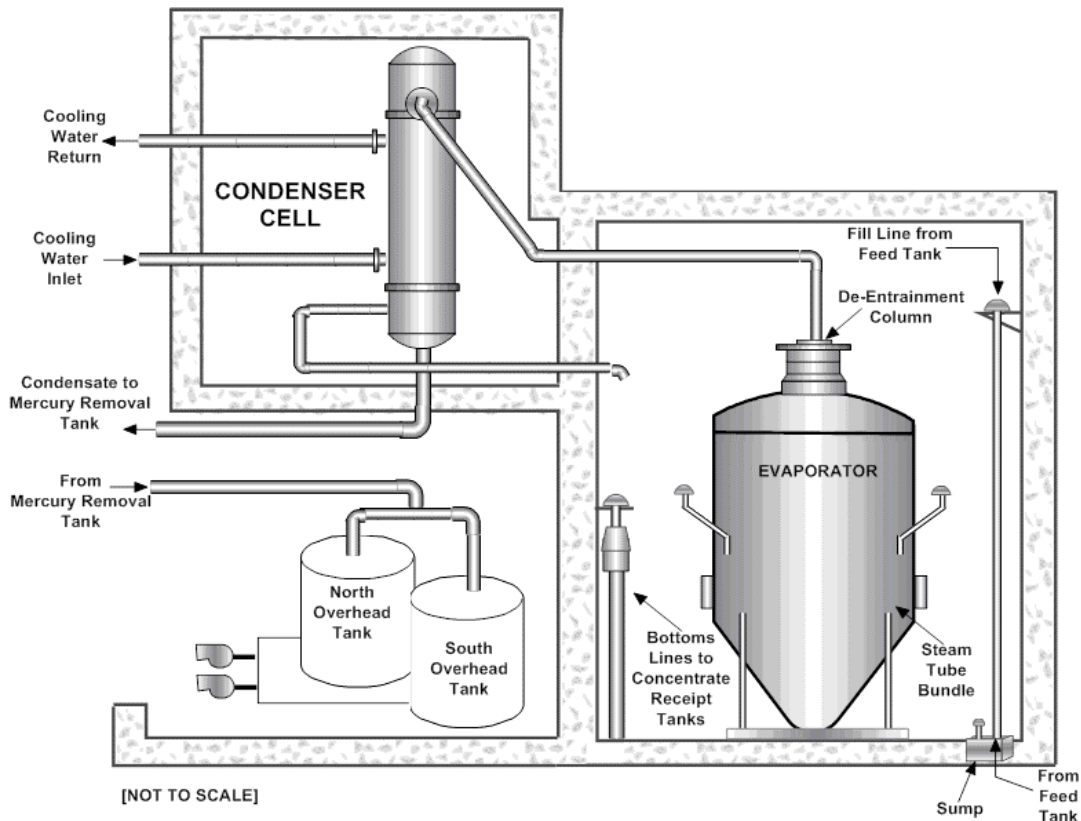


242-H Evaporator Overheads System - The receiver cell is a cuboid with a base 15 feet x 8 feet 10 inches and a height of 16 feet 6 inches. The receiver cell includes a floor sump, with the sump base 1 foot 6 inches square and a depth of 1 foot 6 inches. The receiver cell provided containment for the two overheads vessels. The overheads vessels functioned as receipt tanks for liquids condensed from evaporator vapors via the 242-H Condenser. [W231299]

3.2.2.4.2 242-16H Evaporator System

The 242-16H evaporator system is contained in three cells and a gang valve house. The evaporator cell contains the evaporator; the condenser cell contains the condenser; and an overheads cell contains overheads system components other than the condenser as shown in Figure 3.2-66.

Figure 3.2-66: 242-16H Evaporator System Schematic



242-16H Evaporator Cells - The evaporator cell is 16 feet x 16 feet and approximately 25 feet high. The walls are constructed of concrete that is 3 feet 6 inches thick and lined with 11-gage stainless steel. The floor is lined with 0.375-inch stainless steel plate. The roof consists of 1-foot thick concrete slab sections covered with a sloped galvanized steel rain cover with access ports. The evaporator cell collects leakage from equipment inside the evaporator or condenser cells, leakage from the lift/lance/evaporator cell sump-gang valve vent header, and liquid from cell spray operations. An evaporator underliner sump collects any leakage through the stainless steel liner. [W702199, W702678]

The condenser cell is 10 feet 6 inches x 9 feet 8 inches and 15 feet 6 inches high. The walls are 2-foot thick concrete. The roof is composed of 1-foot thick concrete slab sections and a sloped, galvanized steel rain cover with access ports. The condenser cell contains a 1-foot high stainless steel liner pan on a sloped floor. The condenser cell has an opening to the evaporator cell for the de-entrainment column piping and permits airflow to the evaporator cell. [W702199, W702678, W702679]

The overheads cell is 15 feet x 21 feet and is 21 feet high. The walls are constructed of concrete and the cell contains the following primary equipment: two overheads tanks, mercury removal tank, CRC feed tank, two CRC pumps, and two overheads pumps. This cell has a 14-inch high concrete curb and a sloped floor that are lined with 11-gage stainless steel. [W702199, W702678, W702679]

242-16H Evaporator Vessel/Pot - The 242-16H evaporator vessel is 8 feet in diameter and has a height of 19 feet from the top of the demister to the bottom of the conical shaped lower section. The vessel is constructed of 0.5-inch stainless steel. There are multiple evaporator vessel service/equipment lines installed in, or penetrating the vessel, including the feed inlet nozzle, steam tube bundle, warming coil, lift lines, de-entrainment column, lance lines, and the seal pot. Figure 3.2-67 provides a top view of the 242-16H evaporator vessel. [W449644]

Figure 3.2-67: 242-16H Evaporator Vessel Top View

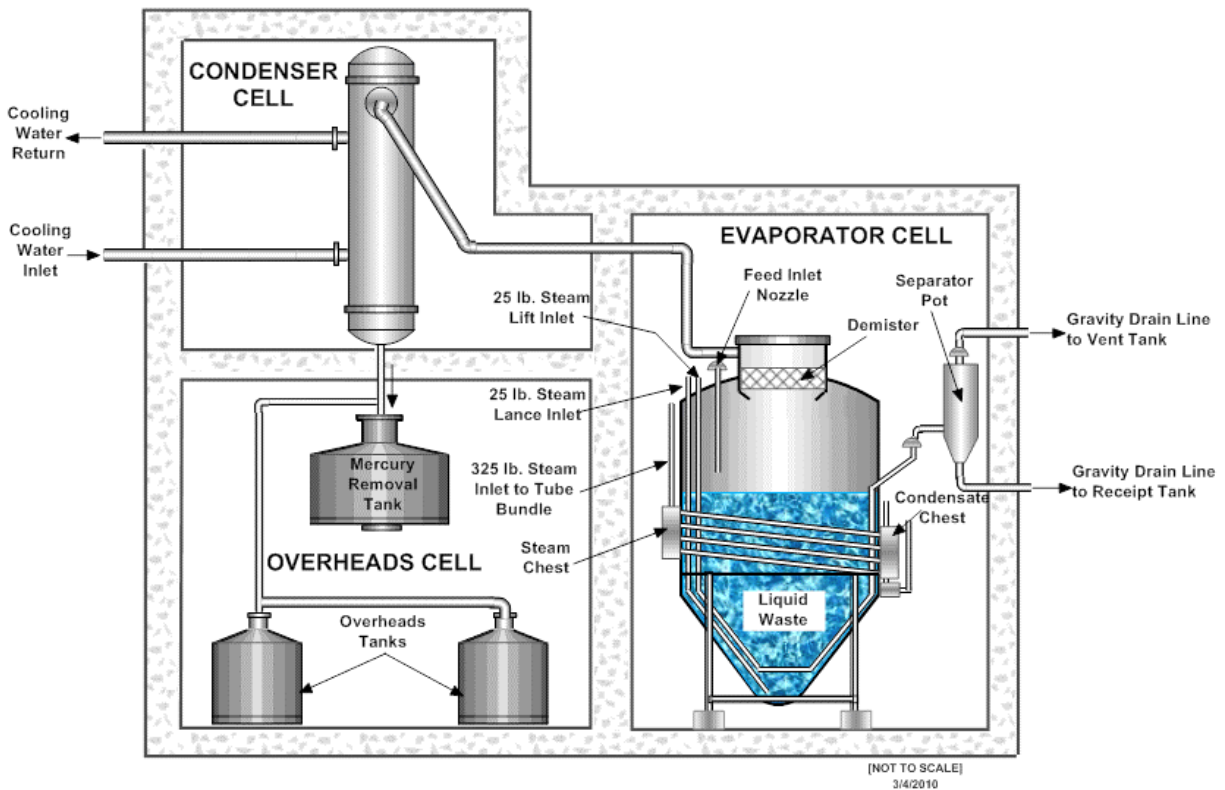


242-16H Evaporator Overheads System - The 242-16H overheads system includes the condenser, mercury removal tank; CRC feed tank, two CRC pumps, two overheads tanks, and two overheads pumps. The condenser is a vertical, single-pass, counter-flow tube, and shell type heat exchanger located in the condenser cell. The mercury removal tank receives condensed overheads from the condenser. When full, the stainless steel tank overflows to the CRC feed tank, permitting the heavier mercury to settle out and remain in the tank. The tank vents to the condenser cell, which vents and drains to the evaporator cell. The path from the evaporator vessel to the stainless steel overheads tanks travels through a stainless steel CRC feed tank. [W702199]

3.2.2.4.3 242-25H Evaporator System

The 242-25H evaporator facility includes the evaporator cell, which houses the evaporator vessel (pot), the condenser cell and condenser, and an overheads cell, which contains the overheads system (that includes the mercury removal tank, mercury removal station, two overheads tanks, and two overheads pumps). Figure 3.2-68 shows the (3H) 242-25H evaporator system arrangement. [SE5-2-2004260, W835332, W2010385]

Figure 3.2-68: 242-25H Evaporator System Schematic



242-25H Evaporator Building - The evaporator cell is 27 feet 6 inches x 20 feet with a height of 32 feet 9 inches. The concrete walls are 3 feet 6 inch thick and the roof is 3-foot 6-inch thick concrete slabs. The evaporator cell floor and sump are lined with 0.375-inch thick stainless steel and the walls are lined with 11-gage stainless steel. [W835332, W835333, W838269] Figure 3.2-69 provides a top view of the evaporator vessel and the evaporator cell.

Figure 3.2-69: 242-25H Evaporator Vessel and Cell Top View



The condenser cell is 10 feet 9 inches x 19 feet and 18 feet high. The concrete walls are a minimum of 2 feet thick and the roof is 2-foot thick concrete slabs. The condenser cell contains a 0.25-inch thick stainless steel liner pan on a sloped floor and 11-gage stainless steel wall liner 6 inches high. The condenser cell has an opening to the evaporator cell for de-entrainment column piping and airflow to the evaporator cell. [W835332, W835333, W838269]

The overheads cell is below grade and is 25 feet x 24 feet and 23 feet high. This cell contains a mercury removal tank, two overheads tanks, an overheads tank sample system, and two overheads pumps. The overheads cell contains a 0.25-inch thick stainless steel liner pan on a sloped floor and 14 inches high, 11-gage stainless steel wall liner. [SE5-2-2004260, W835335, W838269]

242-25H Evaporator Vessel/Pot - The 242-25H evaporator vessel has a capacity of approximately 19,000 gallons. The insulated vessel is 14 feet in diameter and 26 feet 6.375 inches in height from the top of the demister to the conical shaped bottom. The vessel shell is constructed of 0.5625-inch thick stainless steel and the cone is comprised of 0.4038-inch thick stainless steel. There are multiple evaporator vessel service/equipment lines installed in, or penetrating, the vessel, including the feed inlet nozzle, steam tube bundle, warming coil, lift lines, de-entrainment column, lance lines, and the seal pot. [AA98142C Sheets 31 and 40] Figure 3.2-70 provides a view of the bottom of the 242-25H evaporator vessel.

Figure 3.2-70: View of the Bottom of the 242-25H Evaporator Vessel



242-25H Evaporator Overheads System - The 242-25H overheads system includes the condenser, mercury removal tank, two overheads tanks, and two overheads pumps. The condenser is a vertical, single-pass, counter-flow tube, and shell type heat exchanger located in the condenser cell. The mercury removal tank receives condensed overheads from the condenser. A drain valve leads from the bottom of the removal tank to the mercury collection station located in the overheads receiver cell. The overheads are pumped to the Effluent Treatment Facility (ETF) by one of the two-recirculation pumps. The removal tank vents to the condenser cell, which vents and drains to the evaporator cell. Figure 3.2-71 provides a view of the overheads system condenser. [W835333]

Figure 3.2-71: 242-25H Evaporator Overheads System Condenser



3.2.2.5 Diversion Boxes and Valve Boxes

The HTF contains eight DBs (see Figure 3.2-54 for DB locations). Two of the DBs are incorporated with the design and construction of multiple PPs. Incorporated with HPP-1 through HPP-4 is HDB-2 and HDB-8 is incorporated with HPP-7 through HPP-10. [W163527, W778815]

The DBs are reinforced concrete structures that provide a central location for waste transfer lines. The DBs contain transfer line nozzles to which jumpers are connected in order to direct waste transfers to desired waste tanks and pump tanks. This reduces the number of transfer lines necessary to perform diverse transfers amongst tanks and other facilities. Each of the DBs are associated with, and provide connections to, a group of waste tanks that are categorized as shown in Table 3.2-8 (see Figure 3.2-54 for locations). Figure 3.2-72 shows the interior of HDB-1 and Figure 3.2-73 shows HDB-3 during the concrete cell and transfer pipe construction phase. [W147544, S5-2-1341]

Table 3.2-8: Diversion Boxes and Associated Service

Diversion Box	Associated Service
HDB-1	Type I Tanks 9 - 12
HDB-2	Type I Tanks 9 - 12, Type II Tanks 13 - 16
HDB-3	Type IV Tanks 21 - 24
HDB-4	Type III Tanks 29 - 32
HDB-5	Type IV Tanks 21 - 24
HDB-6	Type IIIA Tanks 35 - 37
HDB-7	Type IIIA Tanks 38 - 43, Tanks 48 - 51
HDB-8	Transfers to/from HDB-5, HDB-6, HDB-7 or transfers from FTF and the DWPF.

Figure 3.2-72: Interior of HDB-1

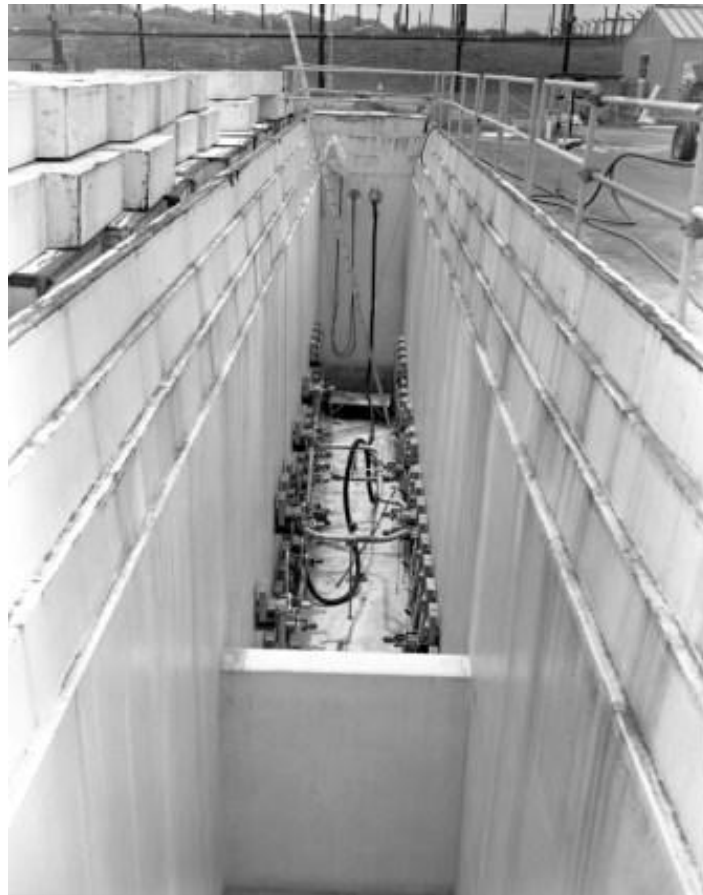


Figure 3.2-73: HDB-3 during Construction Phase



HDB-1 is 78 feet long x 7 feet wide and 21 feet high. The walls are reinforced concrete and are a minimum of 1 foot 6 inches thick and taper to accommodate the two layers of concrete slabs that form a roof approximately 2 feet 8 inches thick. The sloped, reinforced concrete floor is a minimum of 2 feet 6 inches thick. [W158080]

HDB-2 is 26 feet long x 15 feet wide that is incorporated with HPP-1 through HPP-4. The walls are reinforced concrete a minimum of 3 feet thick with a sloped floor of reinforced concrete approximately 4 feet 6 inches thick. The DB covers are concrete slabs and the walls and floor are lined with stainless steel. [W163386]

HDB-3 is a square with outside dimensions of 6 feet 8 inches. The concrete walls and floor are 10 inches thick and the concrete slabs that comprise the roof are 8 inches thick. [S5-2-1341]

HDB-4 is an octagon with an outer dimension of 10 feet and inside diameter of 7 feet. It is comprised of reinforced concrete walls a minimum of 18 inches thick and a sloped, reinforced concrete floor that is approximately 2 feet 6 inches thick. The cover is a reinforced concrete plug 7 feet 8 inches inside diameter and 3 feet thick. Stainless steel plate covers the walls, floor, and sump. [W236630]

HDB-5 is an octagon with an outer dimension of 10 feet and an inside diameter of 7 feet. It is comprised of reinforced concrete walls that are a minimum of 18 inches thick and a sloped, reinforced concrete floor that is approximately 2 feet 4 inches thick. The cover is a reinforced concrete plug with an inside diameter of 7 feet 8 inches and a thickness of 3 feet. Stainless steel plate covers the walls, floor, and sump. [S5-2-4262]

HDB-6 is a 15 foot square with walls and floor that are comprised of reinforced concrete. The walls are minimum 18 inches thick and the sloped floor is approximately 2 feet 11 inches thick. The cover for the DB is comprised of reinforced concrete slabs that are 3 feet thick. Stainless steel sheets cover the wall, floor, and sump. [W700547]

HDB-7 is a 25-foot long x 19-foot wide rectangle with walls and floor that are comprised of reinforced concrete. The walls are minimum 2 feet 6 inches thick and the sloped floor is approximately 3 feet 4 inches thick. The cover for the DB is comprised of reinforced concrete slabs that are 3 feet thick. Stainless steel covers the walls, floor, and sump. [W703874]

HDB-8 is a 20-foot long x 24-foot wide rectangle that is incorporated with HPP-7 through HPP-10. The HDB-8 walls are reinforced concrete with a minimum thickness of 3 feet. The floor is reinforced concrete that is 3 feet thick. The DB cover is comprised of reinforced concrete slabs approximately 4 feet 3 inches thick. The walls, floor, and sump are lined with stainless steel. [W778815, W778818]

3.2.2.5.1 Transfer Valve Boxes

Valve boxes provide passive containment for valve manifolds that allow waste to be transferred to one of several different locations using common transfer lines. Valve boxes house permanently installed valve manifolds within a heavily shielded box. The valves are manual ball valves installed within removable jumpers with flush water connections. The valve boxes serve specific transfers that are conducted as needed to support facility operations. Valve boxes are generally located adjacent to the tanks they provide transfer isolation capability for depending on the type of transfer being performed. [W2017867]

The valve boxes are constructed of stainless steel providing secondary containment for the valve manifolds they house. All valve boxes contain conductivity probes that actuate control room alarms if leakage is detected. Leakage that collects in the valve box will generally drain to the associated waste tank, DB or LDB. The valve boxes associated with HTF are further described below. [W2017867]

Valve Box 15/16 - Valve box for Tanks 15 and 16 contains a transfer line connection to HDB-2. Valve Box 15/16 design is shown on drawing S5-2-11980.

Tanks 21 and 22 Valve Boxes - Valve box design details for Tanks 21 and 22 are shown on drawings P-PM-H-7723 and P-PM-H-7726, respectively.

Tank 40 Valve Box and Tank 40 Drain Valve Box - Valve box and drain valve box design details for Tank 40 are shown on drawings W802781 and D199324, respectively.

Tank 42 Valve Box - Valve box design for Tank 42 is shown on drawing W740180.

Tank 49 Valve Box - Valve box design for Tank 49 is shown on drawing D189542.

Tank 50 Valve Box - Valve box design for Tank 50 is shown on drawing P-PJ-H-7973.

Tank 51 Valve Box and Tank 51 Drain Valve Box - The valve box for Tank 51 is used for transfers in and out of the waste tank. The design of the Tank 51 valve box and the Tank 51 drain valve box are shown on drawings W800445 and W807558, respectively.

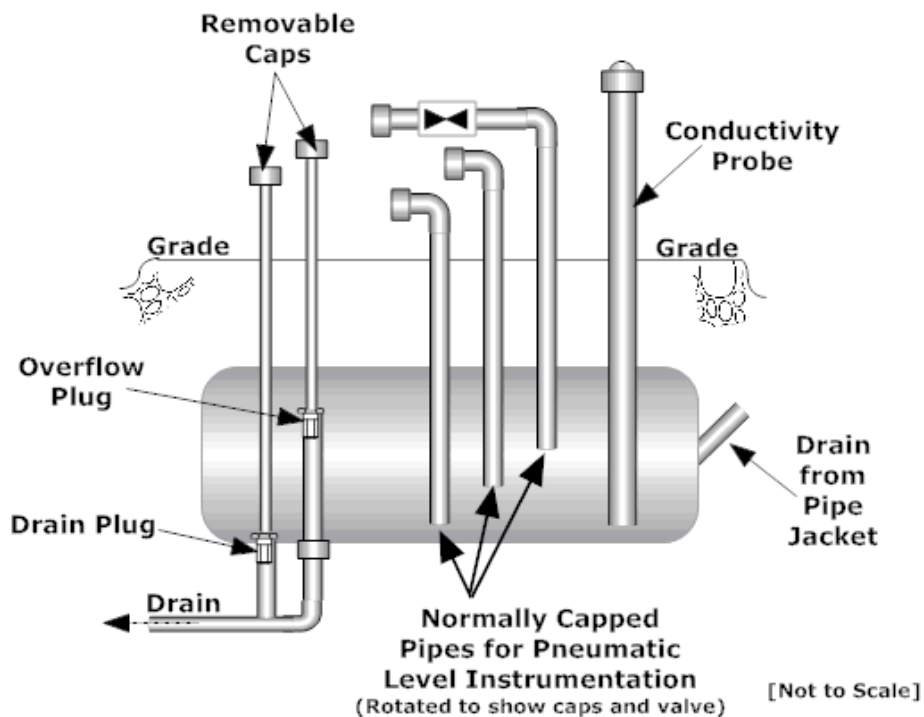
241-96H Valve Box - The 241-96H valve box allows transfers in and out of the Building 241- 96H MST strike tanks. This valve box design is shown on drawing C-CM-H-7026.

3.2.2.6 Other Ancillary Equipment

The LDBs are the primary means of detecting leaks from the waste transfer piping. The LDBs are situated at the low point of a transfer line, near a waste tank or DB where a transfer pipe penetrates the containment wall.

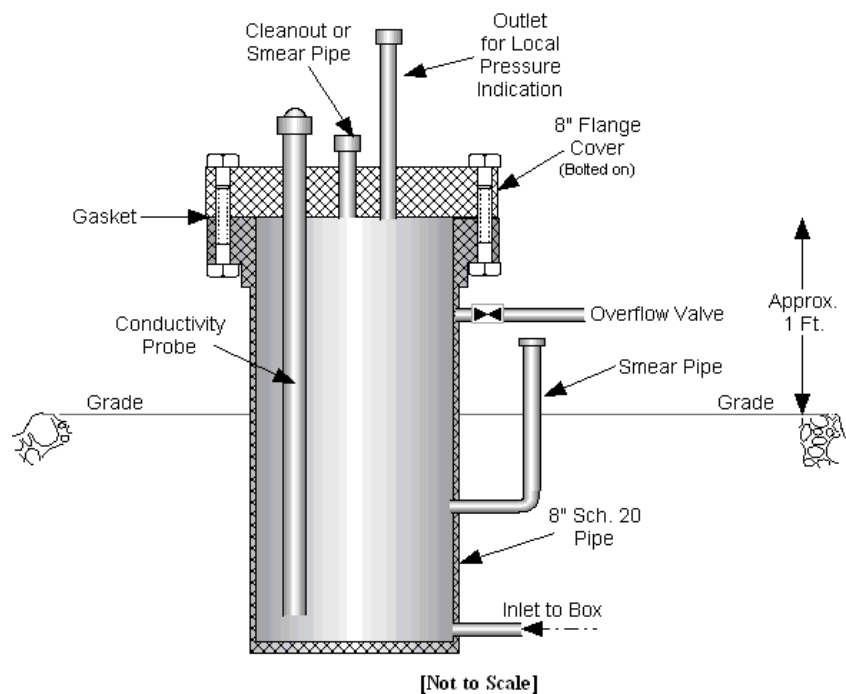
The LDBs are horizontal, carbon steel cylinders, with capped ends. They are located below grade level in proximity to a waste tank or DB that transfer lines penetrate. Each LDB is coated with protective coatings to protect it from corrosion. The components of a typical LDB include a conductivity probe, a set of dip tubes, an overflow line, and a drain line. The overflow plug is normally removed but is installed during pressure testing to ensure a pressure seal is maintained within the transfer piping and LDB. To support LDB conductivity probe operability, the drain plug is installed to prevent waste from draining past the probe undetected. The conductivity probe will annunciate a control room alarm if liquid is detected. Figure 3.2-74 shows a typical LDB. [W715343]

Figure 3.2-74: Typical Leak Detection Box



The MLDBs are used in place of LDBs in areas where the LDB cannot be gravity drained. Part of the MLDB extends above the ground. Each MLDB is coated with protective coating to protect it from corrosion. The MLDB consists of a vertical pipe flanged at the top with three 1 inch to 1.5-inch pipes extending out of the top flange. Level conductivity probe are located near the bottom of the MLDB. In addition to a conductivity probe, MLDBs also include an overflow line that is routed to a DB or PP, and an above ground pressure gauge to monitor for potential over-pressurization. A cleanout/smear pipe provides a means to sample, smear, or measure the contamination level of the MLDB. The cleanout/smear pipe also can be used to empty the MLDB, using a portable pump. Figure 3.2-75 shows a typical MLDB. [W702976]

Figure 3.2-75: Typical Modified Leak Detection Box



3.2.2.7 Water Infiltration through Ancillary Equipment

Multiple elements of the HTF design serve to minimize water infiltration through ancillary equipment. The steel wall liners will serve significantly to retard water flow into ancillary equipment. The design features assumed in HTF modeling are described in detail in Section 4.2.2.2. In addition, the ancillary equipment will be covered by the HTF closure cap (Section 3.2.4) which will further serve to limit the amount of water infiltration into any residual contamination remaining in the ancillary equipment.

3.2.2.7.1 Ancillary Equipment Structural Stability/Degradation

The structural stability of the ancillary equipment is provided by the steel wall liners and surrounding concrete vaults, (as applicable to the particular piece of ancillary equipment described previously). The impact of ancillary equipment degradation (e.g., corrosion

leading to failure of the stainless steel liner) was considered in HTF modeling and is described in detail in Section 4.2.2.

3.2.2.7.2 Ancillary Equipment as Inadvertent Intruder Barrier

The HTF closure cap, which covers all of the ancillary equipment, will serve as a deterrent to the inadvertent intruder, as will the concrete structures that house the ancillary equipment vessels (i.e., evaporator cells, PPs, catch tank cell) and the steel walls of the structures themselves. Section 4.2.3 contains a more detailed discussion of the inadvertent intruder and which exposure scenarios are considered credible based on the HTF ancillary equipment design.

3.2.3 Waste Tank Grouting

In May 2002, DOE issued an EIS on waste tank cleaning and stabilization alternatives. [DOE-EIS-0303] DOE studied five alternatives:

- Empty, clean, and fill waste tank with grout
- Empty, clean, and fill waste tank with sand
- Empty, clean, and fill waste tank with saltstone
- Clean and remove waste tanks
- No action

The EIS concluded the “empty, clean, and fill with grout” option under the Stabilize Tanks Alternative was preferred. The DOE also issued an EIS ROD selecting the “empty, clean, and fill with grout” alternative for SRS waste tank closure. [DOE-EIS-0303 ROD]

Evaluations described in the EIS showed the “empty, clean, and fill with grout” alternative to be the best approach to minimize human health and safety risks associated with closure of the tanks. [DOE-EIS-0303] This alternative offers several advantages over the other alternatives evaluated such as:

- Provides greater long-term stability of the tanks and their stabilized contaminants than the sand-fill approach
- Provides for retaining radionuclides within the tanks by use of reducing agents in a fashion that the sand-fill would not
- Avoids the technical complexities and additional worker radiation exposure that the fill-with-saltstone approach would entail
- Produces smaller impacts due to radiological contaminant transport than the sand- and saltstone-fill alternatives
- Avoids the excessive personnel radiation exposure and greater occupational safety impact that would be associated with the clean and remove alternative (DOE-EIS-0303)

Cementitious materials are often used to stabilize radioactive wastes. The purpose of this stabilization is to maintain waste tank structure and minimize water infiltration over an extended period, thereby impeding release of stabilized contaminants into the environment. Grout is a mixture of primarily cement and water proportioned to produce a pourable consistency. Grout studies focus on improving grout production and batching, grout flow,

measurement of the effective diffusion coefficients in grout and measurement of hydraulic properties. [WSRC-STI-2007-00369]

Filling a cleaned waste tank with grout prevents the walls and ceiling from possibly collapsing. The grout fill also helps to reduce water intrusion into the waste tank over time. Reducing the amount of water allowed to enter a closed waste tank retards the migration of residual radioactivity from the waste tank to the environment. Testing has demonstrated the chemical and physical characteristics of the grout formula used at SRS retards the movement of radioactivity. [WSRC-TR-97-0102]

The fill grout that shall be used to fill the waste tanks has low E_h (i.e., it is a reducing grout), which minimizes the mobility of radionuclides after closure. All grout formulas are alkaline because grout is a cement-based material that naturally has a high pH to be compatible with the carbon steel of the waste tank. Grout has a high compressive strength and low permeability, which limit the migration of contaminants after closure. The grout formulas must be flowable to allow a near level placement and pumpable to allow it to be pumped into the void spaces of in-place equipment that may be entombed within the grouted waste tanks.

3.2.3.1 Waste Tank Grouting Plan

Grout will be used to fill the entire volume of the Type I, II, III, IIIA, and IV tanks. Figures 3.2-76 through 3.2-80 illustrate the typical grouted configuration for Type I, II, III, IIIA, and IV tanks. For Type IV tanks, the formulation of reducing grout from SRNL-STI-2011-00551 meets the compressive strength requirements of strong grout such that it will discourage an intruder from drilling into the waste tank through the thin roof. For waste tanks with cooling coils and an annulus, the cooling coils and annulus are grouted to minimize void spaces and for stability. The capping of the cooling coil penetrations in the valve-house will be similar to the risers above the primary liner that will be detailed in the future closure modules. Equipment (jets, dip tubes, etc.) and voids inside the annulus will be filled with grout as possible. The annulus, risers, and ductwork will be filled with grout up to grade level and capped in the same manner as risers. Ancillary equipment such as DBs, PPs, and pump tanks will be grouted to prevent subsidence.

Figure 3.2-76: Typical Type I Tank Grouting Configuration

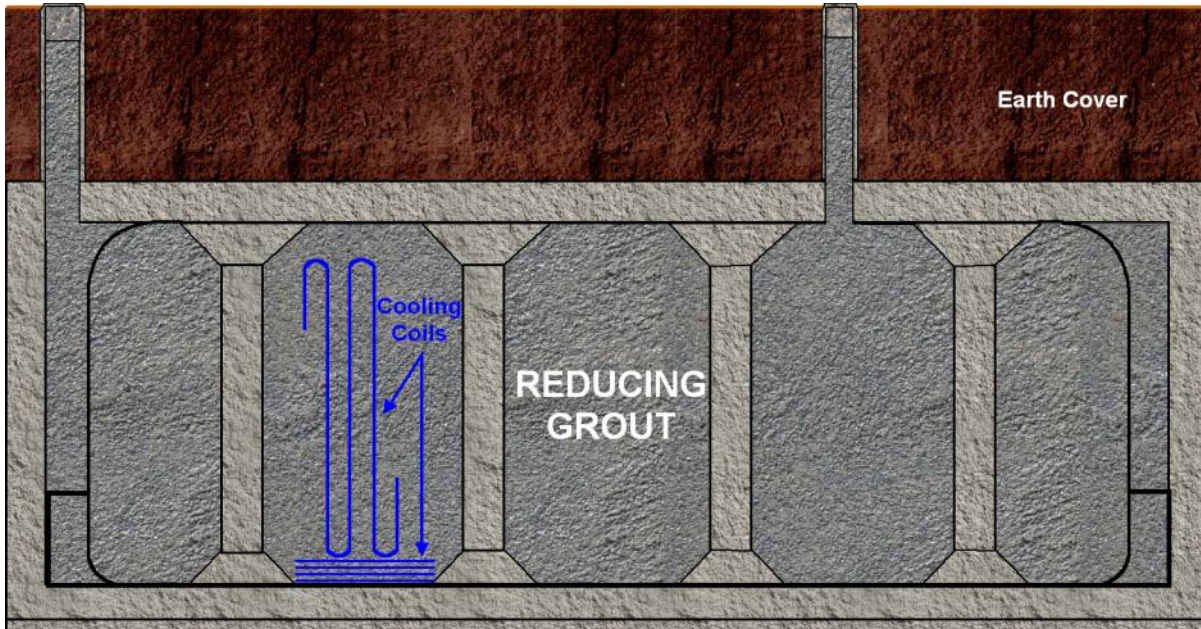


Figure 3.2-77: Typical Type II Tank Grouting Configuration

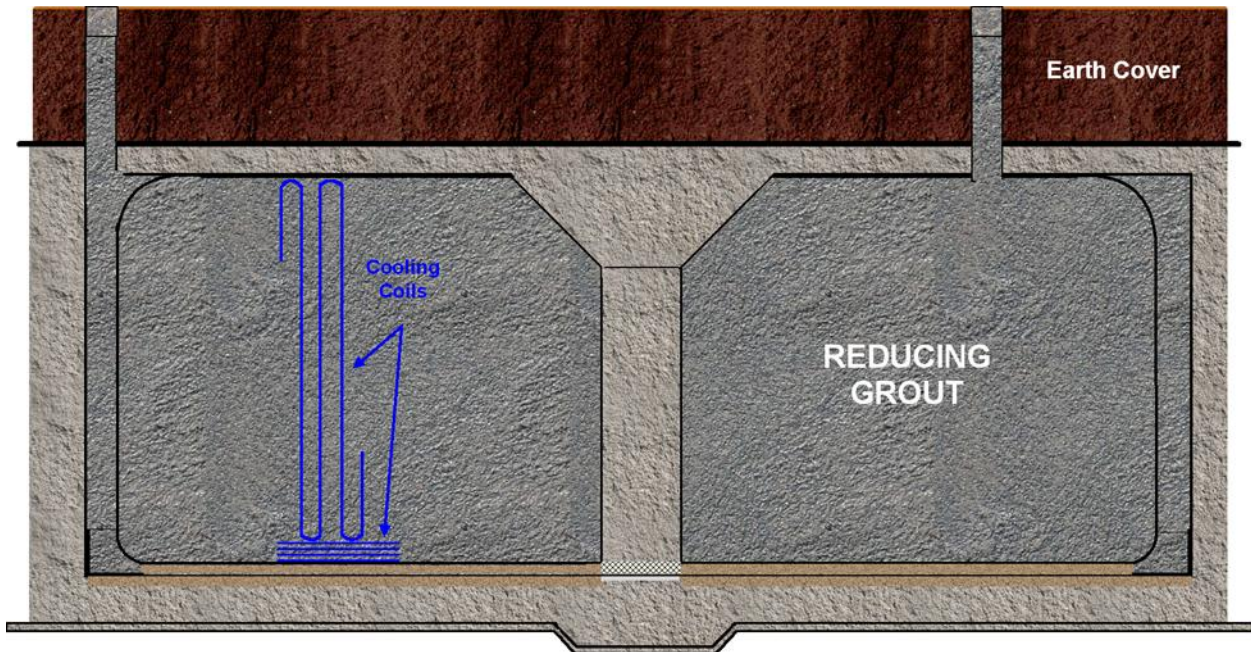


Figure 3.2-78: Typical Type III Tank Grouting Configuration

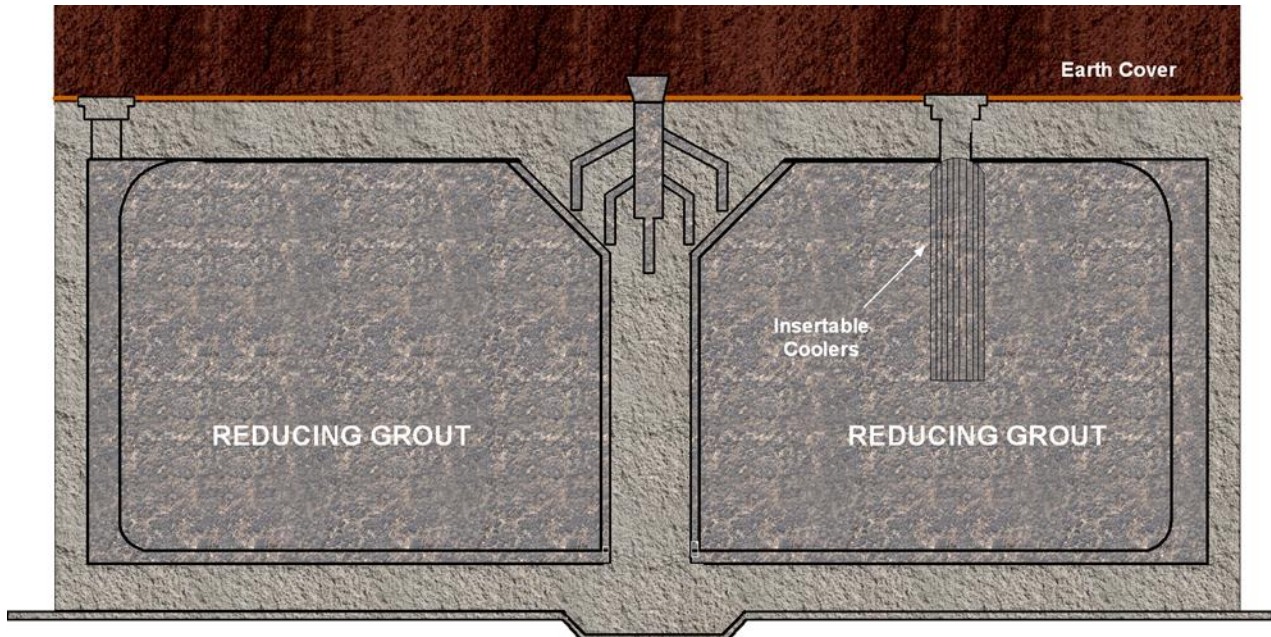


Figure 3.2-79: Typical Type IIIA Tank Grouting Configuration

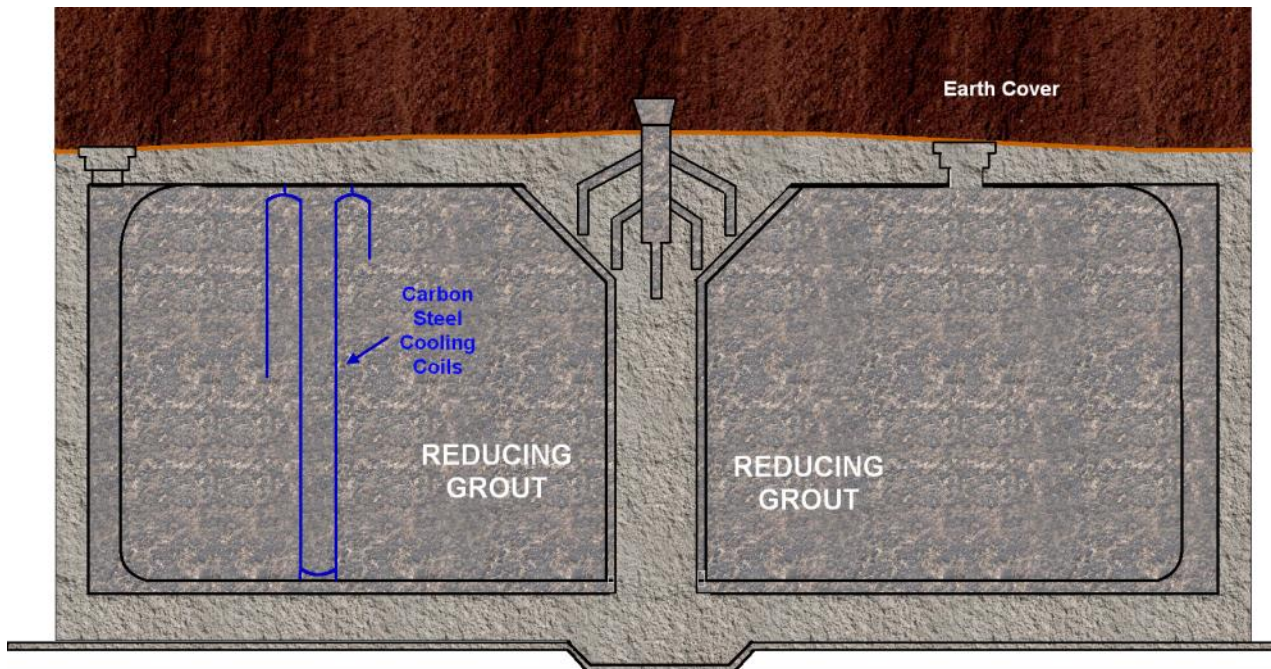
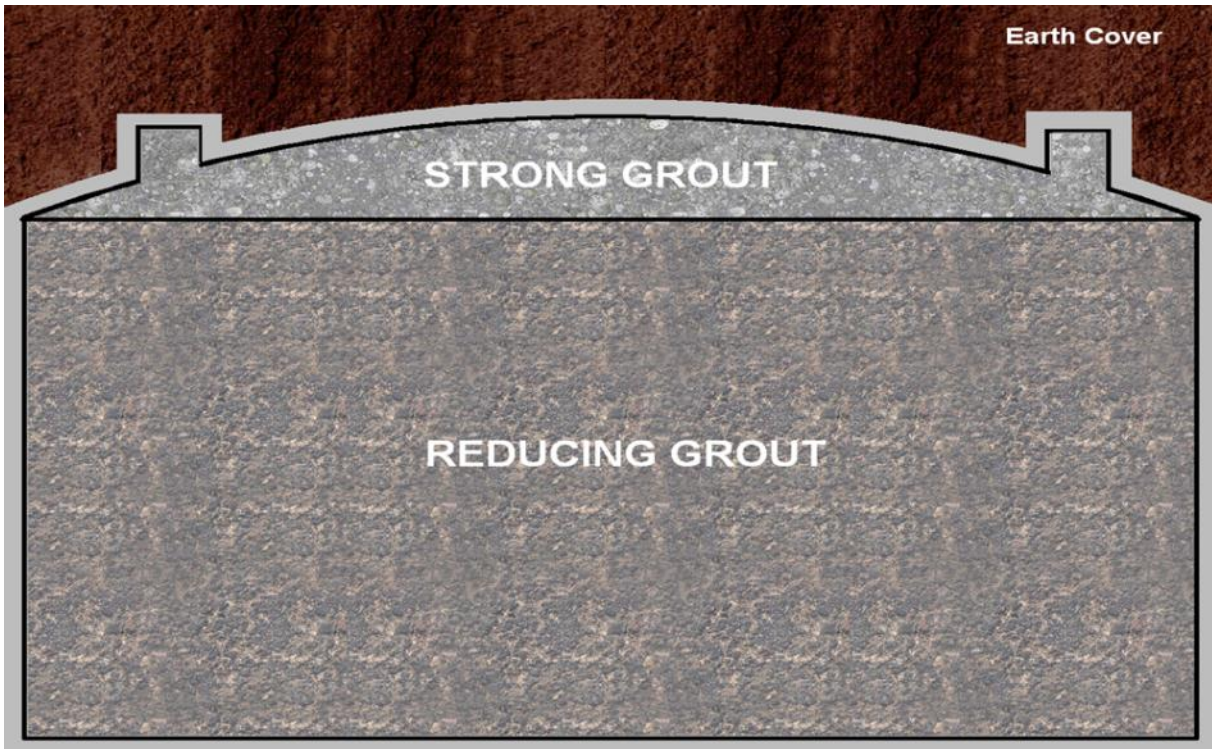


Figure 3.2-80: Typical Type IV Tank Grouting Configuration



Note: With a compressive strength of 2,000 psi, the reducing grout formula meets the requirements for a strong grout (i.e., it acts as a barrier by discouraging intruders from drilling).

The grout attributes important to waste tank final closure are:

- Low hydraulic conductivity
- High pH
- Low E_h
- High degradation resistance
- Highly flowable
- Self-leveling
- Low bleed water
- High compressive strength

Grout studies performed evaluated the chemical and mechanical properties of grout for waste tank closure. [SRNL-STI-2011-00551, WSRC-STI-2007-00369]

Grout is composed primarily of cement, sand, water, fly ash, slag, silica fume, viscosity modifier (Kelco-Crete or similar), and high range water reducer (ADVAFLOW or similar). The grout mix must be flowable, pumpable, and self-leveling. For grout formulations, future changes will be evaluated and used during final closure if further testing indicates the properties of the alternative mixes are superior to the current grout formula. While the admixtures have significant benefit in the early stages of grout placement, they are not expected to have any appreciable effect on the degradation analysis conducted in support of

the HTF PA based on the short effective life and the small quantity of the material added to the grout.

Most of the grout types studied consists of two major states, cured and fresh. [WSRC-STI-2007-00369] The major requirements for cured properties of grout include compressive strength, effective diffusion coefficient, hydraulic conductivity, porosity, and dry bulk density. The fresh grout properties include flow, bleed water, set time, air content, and wet unit weight (density). [SRNL-STI-2011-00551, WSRC-STI-2007-00641] The quality control of the grout production will be included as part of the grout procurement specification.

Grout requirements consist of both mechanical and chemical properties. The mechanical requirements of the grout consist of adequate compressive strength to withstand the overburden load and provide a physical barrier to discourage intruders. The chemical requirements of grout include high pH and a low oxidation potential. Table 3.2-9 outlines some of the key requirements.

Table 3.2-9: Mechanical and Chemical Requirements for Grout Material

Requirement / Properties	Attribute
Mechanical Requirements	
Rheology	ASTM D 6103 - 04
Cure Time	< 28 hours
Compressive Strength (nominal)	2,000 psi
Leveling Quality	Self
Segregation	Minimal
Heat of Hydration	Low Heat Mass Pour
Initial E_h	< 0 mV
Initial pH	> 12.5

[SRNL-STI-2011-00551, ASTM D 6103 - 04]

3.2.3.2 Grout Structural Stability/Degradation

During the grout degradation period, the permeability (hydraulic conductivity) increases from its initial permeability. Conceptually, the increasing permeability reflects an increase in the pathways available for water flow.

The most extensive attack comes from carbonation. The impact of carbonation on the permeability of cementitious barriers in the HTF closure concept depends on whether the barrier contains steel. The annulus and Type IV tanks do not contain rebar or steel, thus the overall effect of carbonation should be minimal regardless of the depth of the penetration.

Sulfate attack represents a complex set of chemical and physical processes that cannot be characterized by a single mechanism. Such type of degradation typically affects structures in contact with acidic flowing or percolating acidic water for long periods. [SRNL-STI-2010-00035]

The alkali-aggregate reactions take place in the concrete when alkalis in the pore solution or an alkali-rich external source react with carbonate or certain types of alkali to form hygroscopic gels that can imbibe water and expand.

The corrosion of steel reinforcement is the most common cause of degradation. Metal rebar oxidation in the presence of water results in the formation of iron hydroxide (rust). Progressive oxidations of steel rebar results in volumetric expansion as corrosion products are formed. This expansion causes de-bonding between the concrete and steel, and is responsible for micro cracking and a loss in tensile strength of the structural element. As the process progresses, continued expansion results in more cracking and spalling of the concrete cover, which exposes more steel rebar and accelerates corrosion and loss of mechanical properties.

Acid attack or decalcification of the calcium containing phases in the hydrated Portland cement paste plays a role in most of the chemical degradation processes affecting pastes and composite cementitious material. Decalcification also includes leaching of alkali ions from the cementitious material. Decalcification is a coupled dissolution/diffusion process. The simplest approach for simulating acid leaching is to assume a diffusion controlled process. The description of ionic transport phenomena at the pore scale has advanced considerably over the last 10 years. Most simulate acid attack as leaching of calcium hydroxide from the matrix. Some of these models also take into account the evolution of the porosity as the solid phases dissolve. [SRNL-STI-2010-00035]

A detailed explanation of degradation mechanisms is presented in SRNL-STI-2010-00035. Table 3.2-10 presents factors known to affect the physical stability of cementitious materials.

Table 3.2-10: Physical and Chemical Factors Related to Grout Stability

PHYSICAL FACTORS	CHEMICAL FACTORS
<p><u>Loss of Mass</u></p> <ul style="list-style-type: none"> - Erosion <ul style="list-style-type: none"> • Water • Wind <p><u>Mechanical Cracking</u></p> <ul style="list-style-type: none"> - Overload - Bio-intrusion - Freeze Thaw - Thermal Stress - Geological Stress <ul style="list-style-type: none"> • Earthquakes • Subsidence 	<p><u>Loss of Mass</u></p> <ul style="list-style-type: none"> - Desiccation (Early water loss) - Cracking - Dissolution/Leaching - Increased Porosity <ul style="list-style-type: none"> • Water • Acids • Microbial degradation <p><u>Addition of Mass (Expansion) - Cracking</u></p> <ul style="list-style-type: none"> - Sulfate (Ettringite) - Alkali (ASR hygroscopic gel) - Iron (rebar) + Oxygen, Carbonate, Chloride <p><u>Addition of Mass - Fill/Seal Cracks & Pores</u></p> <ul style="list-style-type: none"> - Carbonate (Calcium Carbonate Precipitation)

[WSRC-RP-2005-01675]

Mechanical cracking can be caused by overloading the waste tank and grout due to poor design or to geological events such as earthquakes or subsidence. Structural overload of the grout in the waste tank top is unlikely because the load requirement is the same as that of compacted soil. However, seismic events will not remove material on top of the waste tank, and the load bearing capacity of the unit is not expected to reduce to less than that of the surrounding soil. [WSRC-RP-2005-01675]

The grout is designed to minimize the chemical factors that can lead to cracking caused by shrinkage or expansion. In most cases, desiccation being the exception, cracking is due to the addition of mass rather than removal of mass. The reaction of carbon dioxide gas with the hydrated phases of the Portland cement in the grout is called carbonation. The products of carbonation block the pores in the grout. As the result of aging, carbonation will transform the grout from a man-made sandstone-like rock with a calcium silicate hydrate (CSH) matrix to a sandstone-like rock with a calcite-silicate (aged hydrated portland cement) matrix. For the grout, the specification requires Type I/II un-hydrated portland cement, which has a low to moderate (< 5 %) tricalcium aluminate concentration. [WSRC-TR-98-00271] With this relatively low percentage of reactive aluminum in the un-hydrated Portland cement, gypsum in the cement converts all the reactive alumina to ettringite. Ettringite is thermodynamically stable in a sulfate environment minimizing the potential for sulfate attack and sulfate degradation of the grout. [SRNL-STI-2010-00035]

If cracking does occur, the hydraulic conductivity of the grout will be affected, but even in a cracked state, the structural requirements are met because of the contained system. This is in contrast to structural concrete in which cracking will accelerate corrosion of rebar and the transmission of load to the rebar. For free standing reinforced structural concrete members and supported reinforced concrete slabs, transmission of load per the design requirements is critical because performance in tension, flexion and shear are typically required in addition to performance in compression. [SRNL-STI-2010-00035]

Finally, models/methodologies have been developed for predicting changes in physical properties of material in response to chemical and physical factors as a function of time. Empirical, theoretical, mechanistic, and probabilistic models are sometimes used in addition to analogies with geologic and ancient man-made materials. To date simpler models have been applied to the waste-tank closure grouts to describe the consequences of bounding (worst) cases. Initial mechanistic evaluations indicated that the grout would only be exposed to infiltrating rainwater and geologic forces. [SRNL-STI-2010-00035]

3.2.4 Closure Cap

An engineered closure cap will be installed over the HTF following the closure of the waste tanks and ancillary equipment. The HTF conceptual closure cap design is presented in SRNL-ESB-2008-00023. Because of the similar characteristics of the HTF design to the FTF design presented in the WSRC-STI-2007-00184, the FTF infiltration rates are considered applicable. The design information being provided is for planning purposes sufficient to support evaluation of the closure cap as part of the ICM being evaluated in this PA and is taken from the detailed FTF closure cap report WSRC-STI-2007-00184 for HTF. The closure cap design will be finalized closer to the time of HTF closure, to take advantage of possible advances in materials and closure cap technology that could be used to improve the design.

3.2.4.1 Closure Cap Background

An HTF engineered closure cap is anticipated to be necessary for several reasons. One, to provide physical stabilization of the closed site. Two, to minimize infiltration of surface water. Note that surface water that reaches stabilized contaminant wastes in the underground waste tanks and ancillary equipment could eventually lead to the contaminants reaching the underlying aquifer system. The third reason is to serve as an intruder deterrent to prevent a person who might inadvertently enter the area after active institutional controls preventing contact to buried residual radioactive material have ended. Intruder deterrence is provided by at least 10 feet of material above the waste tanks and significant ancillary equipment and the erosion barrier layer. Significant ancillary equipment is defined as equipment that requires intruder protection in association with the closure cap due to the anticipated residual radionuclide inventory. Significant ancillary equipment includes the evaporator facilities, PPs, and waste transfer lines.

3.2.4.1.1 HTF Layout Beneath the Closure Cap

The HTF encompasses approximately 45 acres. Within this area are the 29 underground waste tanks and ancillary equipment, including three evaporators housed in concrete enclosures, an underground catch tank, PPs, DBs, and various underground transfer lines.

The design of the closure cap is obviously influenced by HTF topography and equipment location that is evident by the aerial views of the HTF shown in Figures 3.2-81 through 3.2-83. The size and topography of the HTF influence the envisioned conceptual design of the closure cap concept to consist of three distinct areas, 1) known as the “West Hill” area (shown in Figure 3.2-82) will have its own closure cap, 2) known as the “East Hill” area (shown in Figure 3.2-83) will have its own closure cap, and 3) only encompasses HPP-5 and HPP-6 (shown in Figure 3.2-83) and warrants its own closure cap because of the topography of the area. [SRNL-ESB-2008-00023]

Figure 3.2-81: Aerial View of HTF



Figure 3.2-82: West Hill Area Aerial View

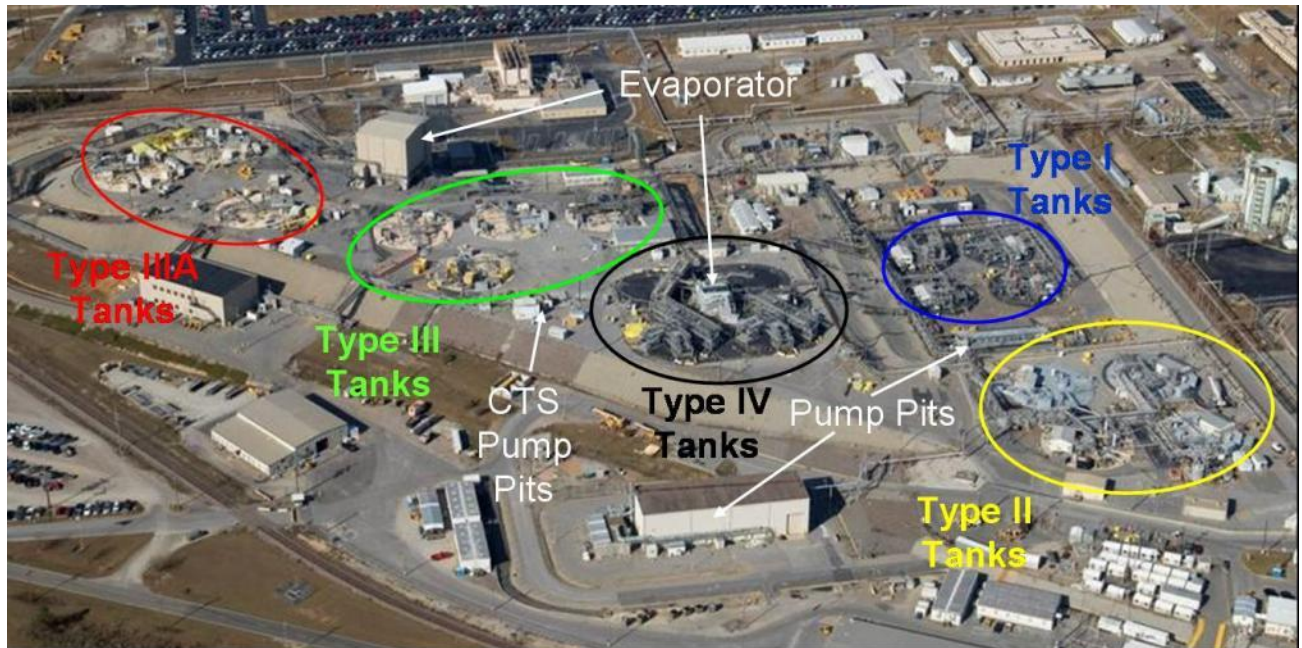


Figure 3.2-83: East Hill Area and HPP-5 and HPP-6 Aerial View



3.2.4.1.2 Key Time Period Assumptions

During the operational period (period during which waste is stored, processed, and removed from the waste tanks and then they are grouted), it is assumed that active HTF facility maintenance will be performed sufficient to prevent infiltration of rainwater into the waste tanks and subsurface discharge out of the waste tanks. After installation of the closure caps, a 100-year institutional control period will begin, during which time active HTF facility maintenance will be conducted sufficient to prevent pine forest succession and to repair any significant erosion. After the institutional control period ends, it is assumed that no active HTF facility maintenance will be conducted.

Currently no site-specific cap performance studies have been completed; therefore, conservative degradation assumptions have been made (e.g., pine tree root penetrations through the geosynthetic clay liner (GCL)). The closure caps are substantially degraded by approximately 2,600 years after closure.

3.2.4.1.3 Layouts Evaluated and Water Balances Analyzed

The current plan for HTF is to place a closure cap over all of HTF after operational period. The HTF conceptual closure cap design has a 2 % maximum surface slope that is less than 585 feet in length. Therefore, the calculations for the FTF conceptual closure cap design documented in WSRC-STI-2007-00184 are applicable for the HTF.

Using the 585 feet maximum slope length and 2 % maximum slope, initial infiltration estimates through the conceptual closure cap case were made utilizing the Hydrologic Evaluation of Landfill Performance (HELP) Model. Based upon the initial estimates, detailed water balances were produced. Table 3.2-11 presents the pertinent closure cap case for HTF modeling and the resulting average initial infiltration rate.

Table 3.2-11: Closure Cap Initial Configurations Evaluated and Condition Results

Parameter	Configuration
Layer (depth)	Topsoil (6 inches)
Layer (depth)	Upper Backfill (30 inches)
Layer (depth)	Erosion Barrier (12 inches) [soil infill]
Layer (depth)	Middle Backfill (12 inches)
Layer (depth)	Lateral Drainage Layer (12 inches) [soil infill]
Layer (depth)	High Density Polyethylene (HDPE) (0.06 inch)
Layer (depth)	GCL (0.2 inch)
Layer (depth)	Foundation Layer - Upper/Lower (84 inches)
Average infiltration rate	0.00088 in/yr (through the GCL)
Average change in water storage	0.06 in/yr

[WSRC-STI-2007-00184]

Note While the geotextile fabric layers are part of the cap design, they are not explicitly modeled in HELP.

Details on the input development required for the HELP modeling are provided in WSRC-STI-2007-00184. For the purposes of this modeling, synthetic daily weather data for precipitation, temperature, and solar radiation over 100 years was generated based upon the HELP data for Augusta, Georgia, and modified with SRS-specific average monthly precipitation and temperature data reported in WSRC-STI-2007-00184. Section 3.1.2 describes the collection process of weather data at SRS.

3.2.4.2 Ancillary Equipment Strategy

Underground piping will remain in place with a closure strategy consistent with other underground piping at a site that has been closed under CERCLA. Large diameter piping (greater than six inches in diameter) will be filled with a grout formulation or other materials, as appropriate, to prevent subsidence issues. The criterion for selecting piping size is based upon grouting practicality and elimination of subsidence potential. Ancillary equipment including the evaporator buildings, the catch tank, PPs, and DBs, to the extent practical, will remain in place and be filled with grout or other materials, as appropriate to eliminate subsidence potential. An exception to leaving ancillary equipment in place will be made for equipment that is significantly higher in elevation than the adjacent waste tanks, and would therefore result in a significant increase in the closure cap elevation. An example of structures needing elevation reduction would be the 242-16H Evaporator. Such ancillary equipment would undergo deactivation and decommissioning to reduce to an appropriate elevation for closure cap construction. Above grade structures, utilities, equipment, etc., (other than substantial above grade concrete associated with the waste tanks and ancillary equipment) that could interfere with closure cap construction will be removed from the HTF area prior to installation of the closure cap.

3.2.4.3 Closure Cap Installation Sequence

Design and installation of the final HTF closure cap will be coordinated with CERCLA closure activities in the area, and occur at a similar time as overall CERCLA closures as reported in Appendix E of the SRS FFA. [WSRC-OS-94-42] The final HTF closure cap will be designed with an appropriate interface with adjacent CERCLA closure systems.

3.2.4.4 Stability Analysis

Calculations to evaluate the physical stability of the closure cap design in relation to the erosion potential associated with a SRS-specific Probable Maximum Precipitation (PMP) event have been made using standard methodologies for a riprap design with a maximum 585 feet slope length. [NUREG-1623] While the methodology presented in NUREG-1623 specifically addresses a 1,000-year timeframe, the use of site-specific PMP event data (e.g., low frequency of occurrence and a bounding event of greater than 70 inches of rain in 1 hour) provides assurance of physical stability of the closure cap design for the 10,000-year evaluation period. A summary of this analysis is provided below, however details are presented in WSRC-STI-2007-00184.

- A 2 % slope over a length of 585 feet for the vegetative soil cover is considered physically stable (i.e., it would prevent the initiation of gully erosion during a PMP event). Maximum acceptable slopes for portions of the closure cap with slope lengths less than 585 feet may be greater than 2 %, if it were determined that they would be physically stable during the actual closure cap design process.
- An erosion barrier consisting of 12-inch thick riprap with a D50 (median size) of 2.5 inches on a 585-foot long, 2 % slope is considered physically stable (i.e., it would prevent any riprap movement during a PMP event). Based upon the D50 of 2.5 inch, rock consistent with Type B riprap from Table F-3 of NUREG-1623 or Size R-20 riprap from Table 1 of ASTM D 6092 - 97 is suitable for use in the erosion barrier.
- Side slope riprap that is 24 inches thick with a D50 of 9.1 inches on a 120-foot long, 33.3 % slope receiving drainage from a 585-foot long, 2 % slope is considered physically stable (i.e., it would prevent any riprap movement during a PMP event). Based upon the D50 of 9.1 inches, rock consistent with Type D riprap from Table F-3 of NUREG-1623 or Size R-150 riprap from Table 1 of ASTM D 6092 - 97 is suitable for use on the side slopes.
- The toe of side slope riprap that is 42 inches thick, extends out 20 feet from the side slope, and has a D50 of 11.6 inches is considered physically stable (i.e., it would prevent any riprap movement due to receiving runoff from the 2 %, 585 feet top slope and 33.3 %, 120-foot side slope during a PMP event). Based upon the D50 of 11.6 inches, rock consistent with Type D riprap from Table F-3 of NUREG-1623 or Size R-300 riprap from Table 1 of ASTM D 6092 - 97 is suitable for use on the toe.

Erosion barrier, side slope, and toe riprap size may be smaller for portions of the closure cap with shorter slope lengths than those used to determine these requirements if it is determined that the smaller sized riprap would be stable during a PMP event, during the actual closure cap design process.

3.2.4.5 Closure Cap General Design Features

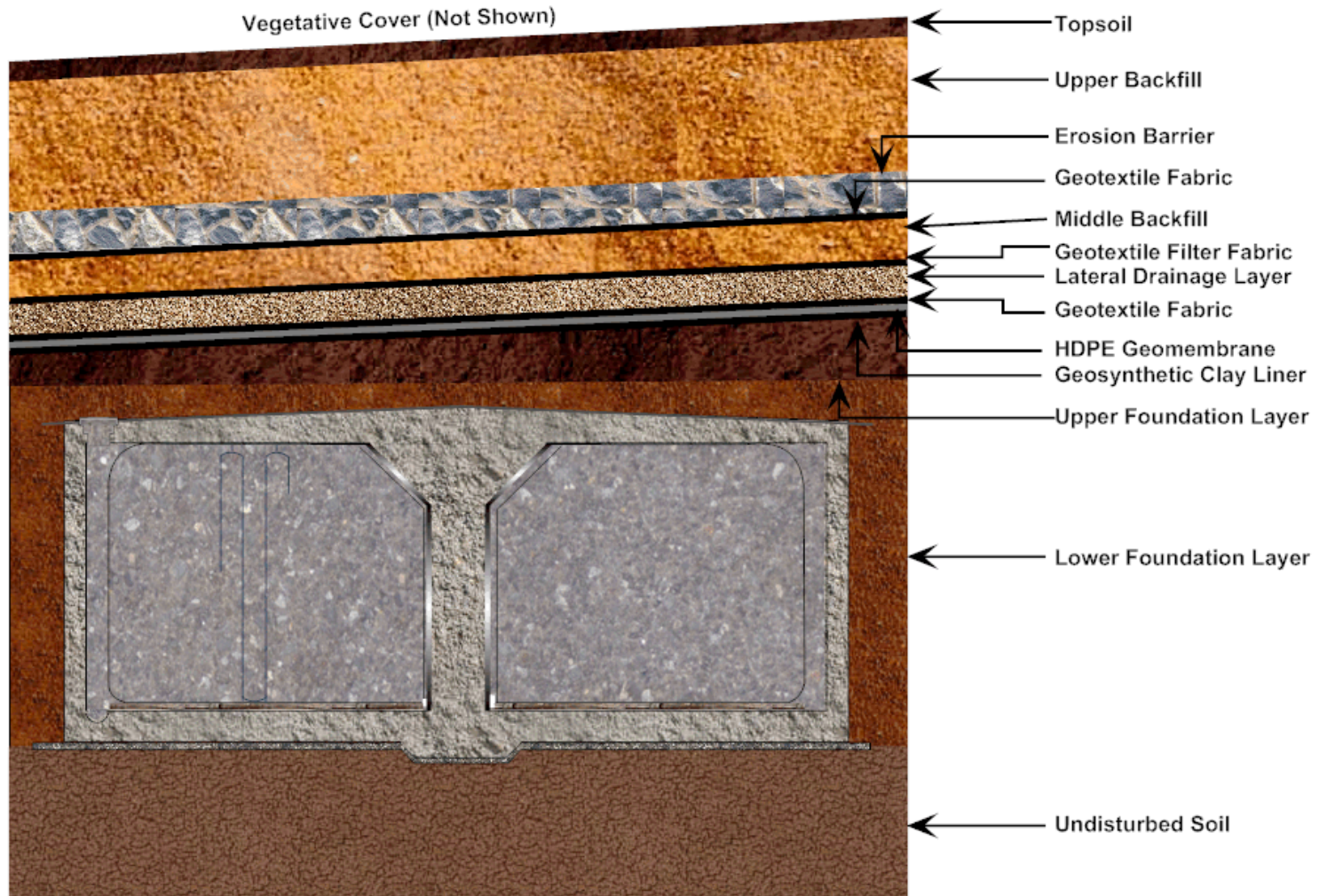
As noted previously, it is anticipated that the closure caps will be installed over all 29 waste tanks and associated ancillary equipment at the end of the operational period. The closure cap design and installation will take into account the waste tank and ancillary equipment characteristics and location, disposition of non-disposal structures and utilities, site topography and hydrogeology, potential exposure scenarios, and lessons learned implementing other closure systems, including those for other SRS facilities, uranium mill tailings sites and other DOE sites.

Figure 3.2-84 presents the general design of the closure cap above a closed waste tank. Figure 3.2-85 presents the closure cap footprint. Figures 3.2-86 to 3.2-89 present cross sections of the closure cap conceptual design. [SRNL-ESB-2008-00023] These figures represent the configuration identified in Table 3.2-11 with the inclusion of a geotextile fabric layer on top of the middle backfill layer, a geotextile filter fabric layer on top of the lateral drainage layer, and a geotextile fabric layer on top of the HDPE geomembrane layer.

3.2.4.5.1 Function of Closure Cap Layers

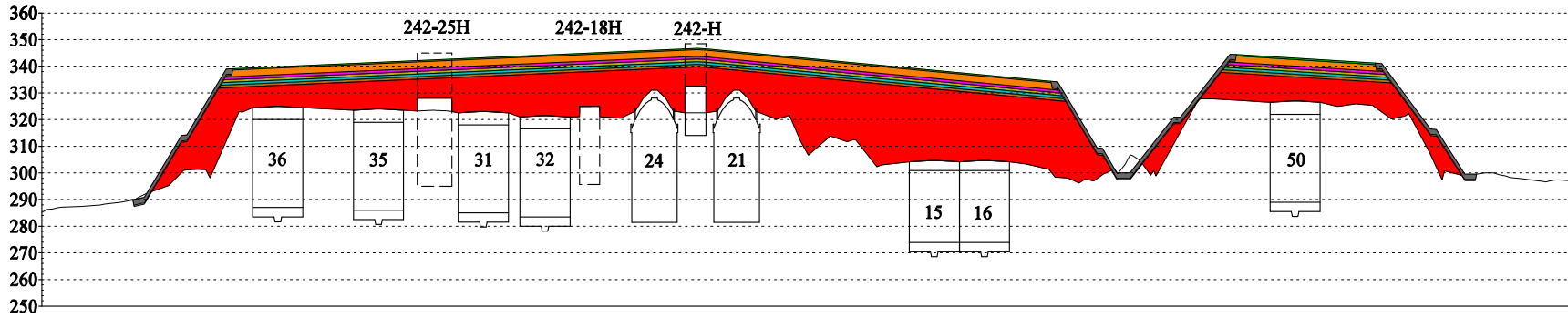
It is anticipated that the HTF closure cap will consist of the layers illustrated in Figure 3.2-84. Table 3.2-12 summarizes the function of each of these layers. Detailed discussion of each layer in the closure cap design is provided in WSRC-STI-2007-00184. The concepts for the side slopes and toes of the closure cap based upon the results of physical stability calculations referred to above are also detailed in WSRC-STI-2007-00184.

Figure 3.2-84: The HTF Closure Cap General Concept

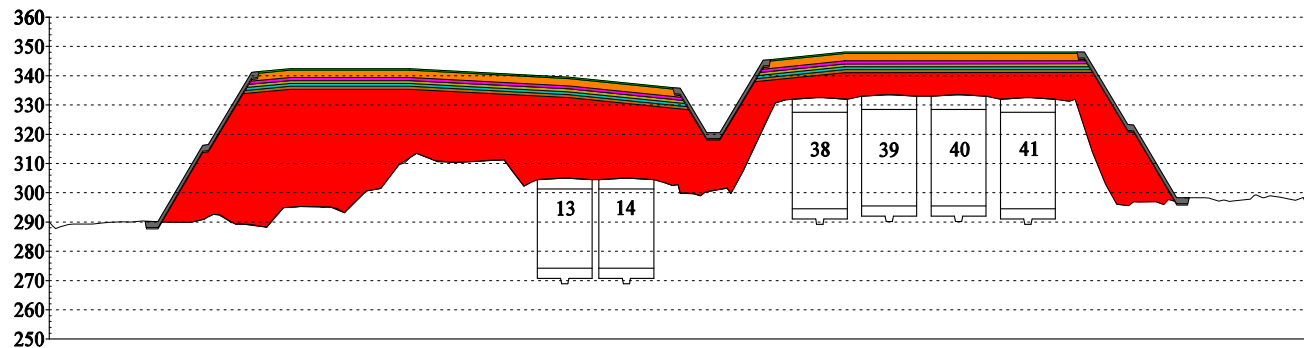


[NOT TO SCALE]

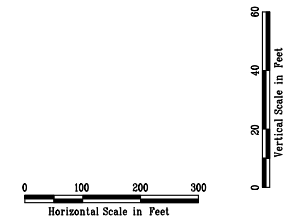
Figure 3.2-86: Closure Cap Conceptual Design, Sections A-A and B-B



Section A-A



Section B-B



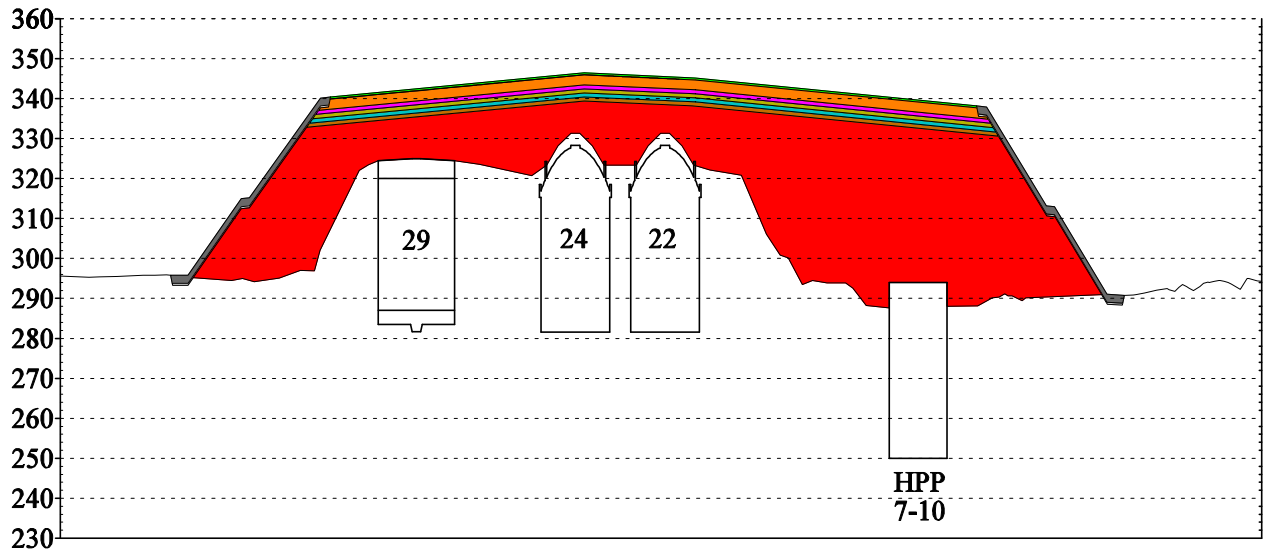
LEGEND:

Grey	RIPRAP
White	STONE BEDDING LAYER
Green	TOPSOIL
Orange	UPPER BACKFILL
Purple	EROSION BARRIER
Yellow	MIDDLE BACKFILL
Cyan	LATERAL DRAINAGE LAYER
Brown	UPPER FOUNDATION LAYER
Red	LOWER FOUNDATION LAYER
Dashed line	EXISTING GRADE

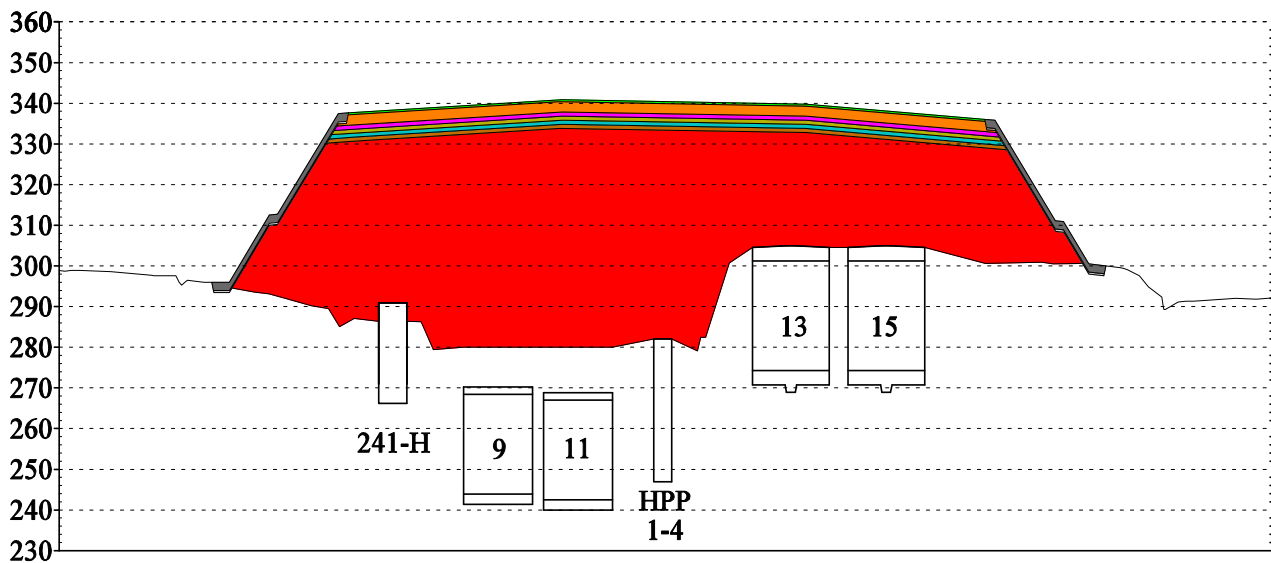
[SRNL-ESB-2008-00023 Figure 2]

NOTE Vertical scale of sections has been exaggerated five times in order to show all closure cap layers.

Figure 3.2-87: Closure Cap Conceptual Design, Sections C-C and D-D



Section C-C



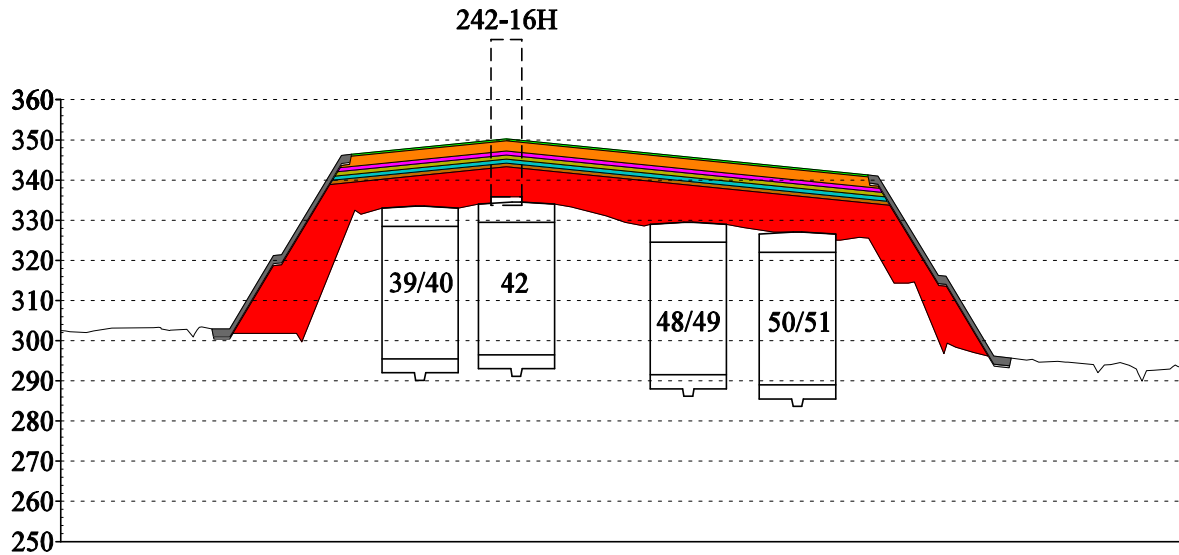
Section D-D

Legend on Figure 3.2-86

[SRNL-ESB-2008-00023 Figure 3]

Note Vertical scale of sections has been exaggerated five times in order to show all closure cap layers.

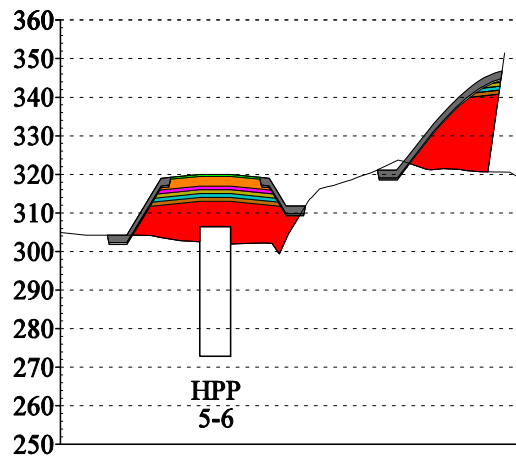
Figure 3.2-88: Closure Cap Conceptual Design, Section E-E



Section E-E

Legend on Figure 3.2-86

Figure 3.2-89: Closure Cap Conceptual Design, Section F-F



Section F-F

[SRNL-ESB-2008-00023 Figure 3]

NOTE Vertical scale of sections has been exaggerated five times in order to show all closure cap layers. See legend on Figure 3.2-86

Table 3.2-12: Function of the Conceptual Closure Cap Layers

Layer	Function
Vegetative Cover	The vegetative cover will promote runoff, minimize erosion, and promote evapotranspiration. The initial vegetative cover will be a persistent grass such as Bahia. If it is determined, that bamboo is a climax species that prevents or greatly slows the intrusion of pine trees, bamboo will be planted as the final vegetative cover at the end of the 100-year institutional control period. Bamboo is not assumed in present design calculations and modeling.
Topsoil	The topsoil is designed to support a vegetative cover, promote runoff, prevent the initiation of gully erosion, and provide water storage for the promotion of evapotranspiration.
Upper Backfill	The upper backfill is designed to increase the elevation of the closure cap to that necessary for placement of the topsoil and to provide water storage for the promotion of evapotranspiration.
Erosion Barrier	The erosion barrier is designed to prevent riprap movement during a PMP event and therefore form a barrier to further erosion and gully formation (i.e., provide closure cap physical stability). It is used to maintain a minimum 10 feet of clean material above the waste tanks and significant ancillary equipment to act as an intruder deterrent. It also provides minimal water storage for the promotion of evapotranspiration.
Geotextile Fabric	This geotextile fabric is designed to prevent the penetration of erosion barrier stone into the underlying middle backfill and to prevent piping of the middle backfill through the erosion barrier voids.
Middle Backfill	The middle backfill provides water storage for the promotion of evapotranspiration in the event that the topsoil and upper backfill are eroded away since the overlying erosion barrier provides only minimal water storage.
Geotextile Filter Fabric	This geotextile fabric is designed to provide filtration between the overlying middle backfill layer and the underlying lateral drainage layer. This filtration allows water to freely flow from the middle backfill to the lateral drainage layer while preventing the migration of soil from the middle backfill to the lateral drainage layer.
Lateral Drainage Layer	The lateral drainage layer is a coarse sand pad designed to divert infiltrating water away from the underlying waste tanks and ancillary equipment and transport the water to the perimeter drainage system, in conjunction with the underlying composite hydraulic barrier (i.e., HDPE geomembrane and GCL), and to provide the necessary confining pressures to allow the underlying GCL to hydrate properly.
Geotextile Fabric	This geotextile fabric is a non-woven geotextile fabric designed to protect the underlying HDPE geomembrane from puncture or tear during placement of the overlying lateral drainage layer.
HDPE Geomembrane	The HDPE geomembrane forms a composite hydraulic barrier in conjunction with the GCL. The composite hydraulic barrier is designed to promote lateral drainage through the overlying lateral drainage layer and minimize infiltration to the waste tanks and ancillary equipment.
GCL	The GCL forms a composite hydraulic barrier described above in conjunction with the HDPE geomembrane. As part of the composite hydraulic barrier, the GCL is designed to hydraulically-plug any holes that may develop in the HDPE geomembrane.
Upper Foundation Layer Lower Foundation Layer	The foundation layers are designed to provide structural support for the rest of the overlying closure cap, produce the required contours and a slope of 2 % for the overlying layers, produce the maximum 3:1 side slopes of the closure cap, provide a suitable surface for installation of the GCL (i.e., a soil with a moderately low permeability and a smooth surface, free from deleterious materials), promote drainage of infiltrating water away from and around the waste tanks and ancillary equipment, and contain utilities, equipment, facilities, etc., that are not removed from above current grade prior to installation of the closure cap.

[WSRC-STI-2007-00184, Table 12]

3.2.4.5.2 Site Preparation

The existing surfaces (i.e., soils, asphalt, riprap, concrete waste tank tops, and significant ancillary equipment) over which the closure cap will be constructed must be prepared prior to closure cap construction. It is anticipated that existing soil surfaces will have 3 to 6 inches of soil removed to eliminate any topsoil and vegetation present, will be rough graded to establish a base elevation, and will be compacted with a vibratory roller. Existing asphalt surfaces directly over waste tanks and significant ancillary equipment will likely be left in place; however such surfaces between waste tanks and significant ancillary equipment may need to be broken up or removed in order to prevent the asphalt from acting as a perched water zone within the closure cap and to promote downward infiltration around the waste tanks and significant ancillary equipment. It is anticipated that existing riprap will be removed or that the voids within the existing riprap surfaces will be filled to eliminate subsidence potential. It is anticipated that no preparatory actions will be required for the waste tank tops themselves other than that necessary to provide appropriate protection during closure cap construction. It is anticipated that the PPs, DBs, and catch tanks will require grouting in order to eliminate subsidence potential.

Detailed information regarding the purpose, design, and constructability of each of the closure cap layers is provided in WSRC-STI-2007-00184.

3.2.4.5.3 Vegetative Cover

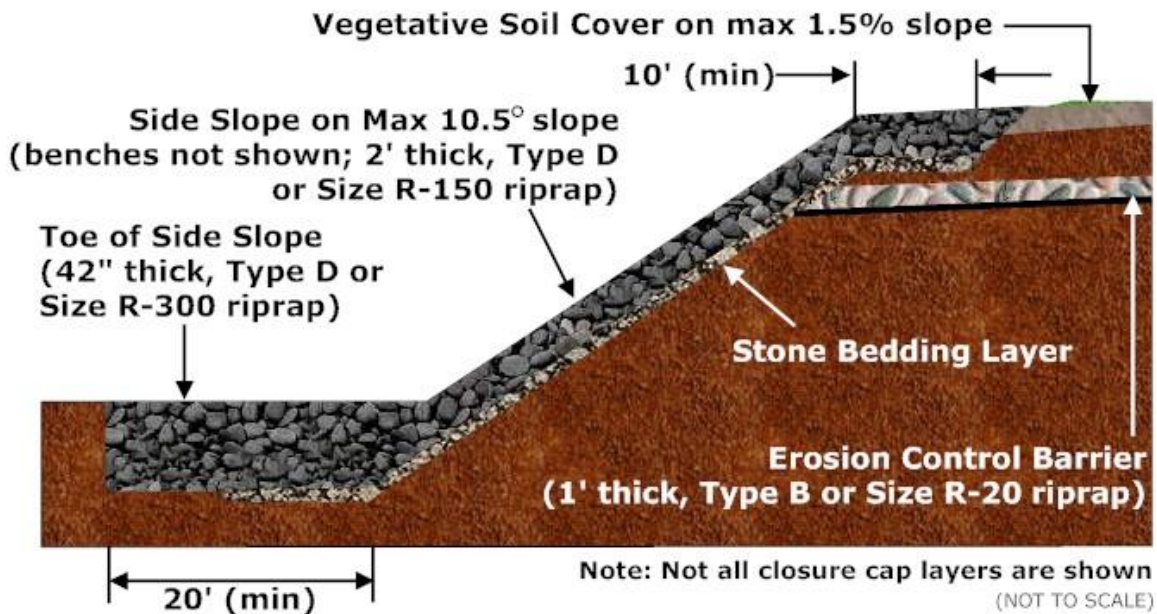
In addition to the modeled closure cap layers, a vegetative cover will promote runoff, minimize erosion, and promote evapotranspiration. The topsoil will be fertilized, seeded, and mulched to provide a vegetative cover. The initial vegetative cover shall be a persistent grass such as Bahia. During seeding and establishment of the initial grass, appropriate mulch, erosion control fabric, or similar substances will be used to protect the surface.

The area will be repaired through transplanting or replanting to ensure that a self maintaining cover is developed. If it is determined that bamboo is a climax species that prevents or greatly slows the intrusion of pine trees, it will be planted as the final vegetative cover at the end of the 100-year institutional control period. Pine trees are typically assumed to be the most deeply rooted naturally occurring climax plant species at SRS, which will degrade the GCL through root penetration. In contrast, bamboo is a shallow-rooted species, which will not degrade the GCL. Additionally, bamboo evapotranspires year-round in the SRS climate, minimizes erosion, and can sustain growth with minimal maintenance. A study conducted by USDA Soil Conservation Service (SCS) has shown that two species of bamboo will quickly establish a dense ground cover. [WSRC-MS-92-513] All work in association with the vegetative cover shall be performed in accordance with approved drawings, plans, and specifications of the final design, which will be produced near the end of the operational period.

3.2.4.5.4 Conceptual Closure Cap Slopes

The toe of the closure cap side slope will consist of a riprap layer to stabilize the side slope riprap, provide erosion protection at the toe, transition flow from the side slope to adjacent areas, and provide gully intrusion protection to the embankment. The toe riprap will extend from the toe of the side slope a minimum of 20 feet, as shown in Figure 3.2-90. Since the HTF maximum slope height is greater than FTF, the riprap size will have to be re-evaluated prior to final cap design but will not impact the infiltration rates. [SRNL-ESB-2008-00023]

Figure 3.2-90: Closure Cap Toe and Side Slope Configuration Concept



Note Not shown in the above figure is the bench for the side slopes of the caps covering the “West Hill” and “East Hill” areas.

The closure cap side slopes will be placed at a maximum three horizontal to one vertical (3H:1V, 33.3 %, or 19.5°) and have a riprap surface with an underlying gravel bedding layer to prevent gully formation on the side slopes and to provide long-term slope stability. The side slope riprap and underlying gravel bedding layer will extend from the toe of the side slope up the side slope to a minimum 10 feet onto the top slope, as shown in Figure 3.2-90. Details of the cap side slope design and construction is provided in WSRC-STI-2007-00184.

An integrated drainage system will be designed and built to handle the runoff from the closure caps and drainage from the closure cap lateral drainage layers. The runoff and lateral drainage will be directed to a system of riprap lined ditches, which will be designed in accordance with NUREG-1623. The riprap lined ditches will direct the water away from the closure cap as a whole and will be constructed around the perimeter of the closure caps. The ditches will discharge into sedimentation basins as necessary for sediment control. The riprap for the ditches has not been sized yet since the HTF is

currently in the operational period. Due to the early phase and lack of a detailed closure cap layout, a detailed drainage system can not yet be designed. Therefore drainage areas and flows cannot be currently assigned in order to size the riprap for various sized ditches.

3.2.4.6 Conceptual Closure Cap Case

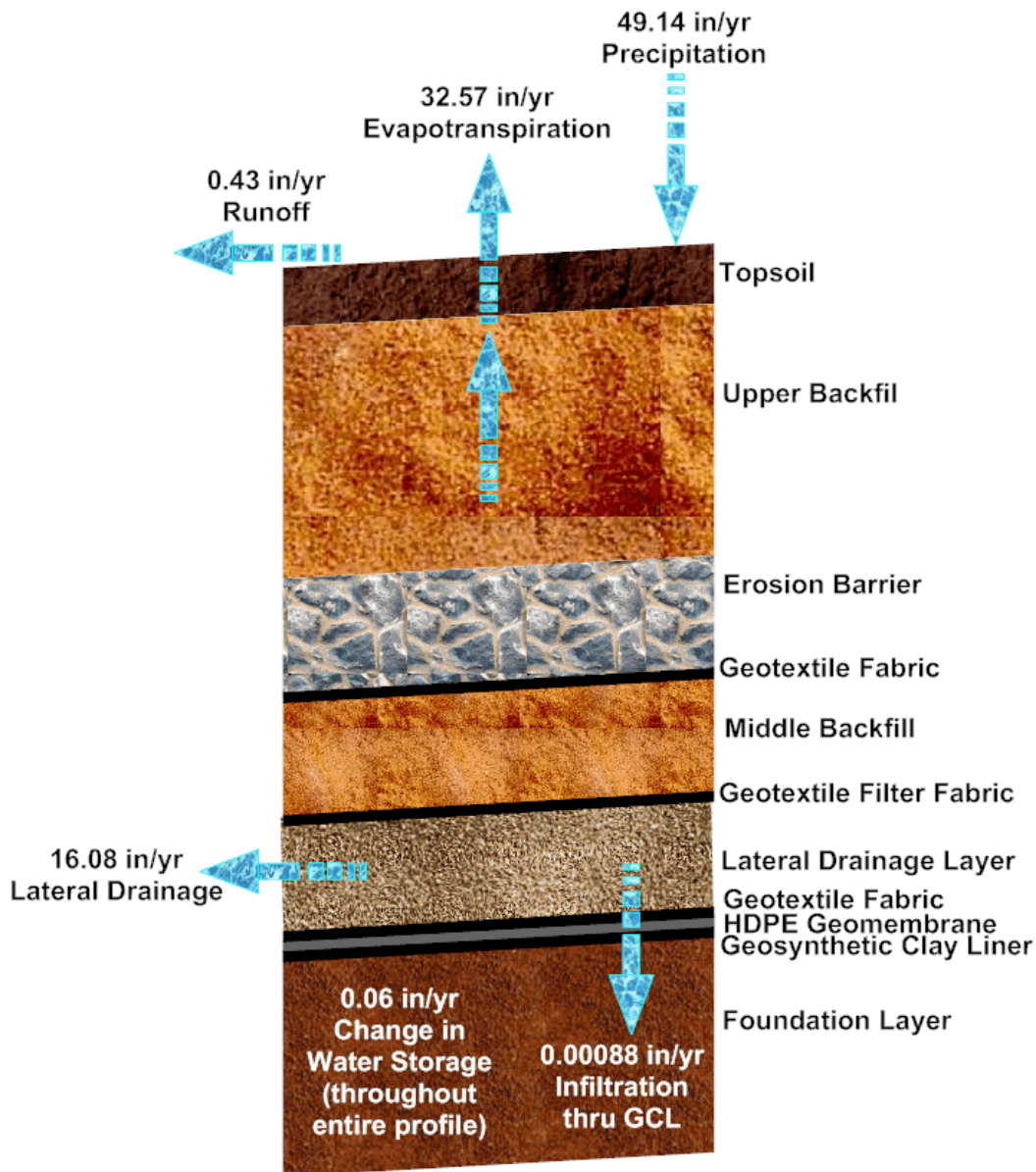
Based on the results from WSRC-STI-2007-00184, closure cap Configuration # 1a which consists of a composite hydraulic layer with an overlaying lateral drainage layer and an erosion barrier is the recommended closure cap configuration for FTF and is the proposed configuration for HTF. This configuration has the following advantages:

- Results in the least infiltration to the waste tanks
- The use of a composite hydraulic barrier (i.e., HDPE geomembrane underlain by a GCL) provides defense-in-depth by the providing a HDPE geomembrane with a significantly lower saturated hydraulic conductivity underlain by the GCL to plug any holes that may develop in the HDPE geomembrane
- The use of an erosion barrier provides long-term physical stability for the closure cap

(Note: Configuration # 1 in WSRC-STI-2007-00184, results in the lowest infiltration rate however, the selection of the material to infill the erosion barrier has not been determined and the use of soil as the infill material, used in Configuration # 1a results in a more conservative infiltration rate.)

Figure 3.2-91 depicts the HELP model scenario and results for the recommended closure cap design. The material properties utilized in this assessment of the closure cap configuration are provided in WSRC-STI-2007-00184.

Figure 3.2-91: The HELP Model Scenario and Results for Closure Cap Design Initial Conditions



[WSRC-STI-2007-00184]

3.2.4.7 Conceptual Closure Cap Degradation Mechanisms

Potential HTF closure cap degradation mechanisms are the same as presented and discussed in detail in WSRC-STI-2007-00184. This scenario assumes a 100-year institutional control period following closure cap construction during which the closure cap is maintained. At the end of institutional control, it is assumed that a pine forest succeeds the closure cap's original vegetative cover. A summary of the degradation mechanisms and proposed course of action to address each mechanism is provided in Table 3.2-13.

Table 3.2-13: Closure Cap Potential Degradation Mechanisms and Course of Action

Affected Layer	Potential Degradation Mechanism	Proposed Course of Action
All Layers	<ul style="list-style-type: none"> -Static loading induced settlement -Seismic induced liquefaction and subsequent settlement -Seismic induced slope instability 	Final design will appropriately consider and handle these mechanisms and thus are not considered for performance modeling purposes
	-Seismic induced lateral spread	Location of closure cap not conducive to lateral spreading - no action
	-Seismic induced direct rupture due to faulting	Surface faulting is non-existent in Southeastern United States - no action
	-Stabilized Contaminant Layer Subsidence	Not applicable - waste tanks and subsurface items containing significant void space will be filled with grout
Vegetative cover	<ul style="list-style-type: none"> -Succession -Stressors (droughts, disease, fire, and biological) 	Penetration of pine tree roots and the rate of pine tree succession from stressors are included in the performance modeling
Soil above the erosion barrier	-Erosion	Included in the performance modeling
	-Desiccation (wet-dry cycles)	Mineralogy and composition of topsoil and backfill and the controlled compaction of the backfill is expected to preclude significant cracking upon drying and thus is not considered for performance modeling purposes
Erosion barrier	-Weathering (dissolution)	Weathering will be appropriately considered in the final design and thus is not considered for performance modeling purposes
	-Biological (root penetration)	The hydraulic properties of the erosion barrier are not expected to be appreciably impacted by pine root penetration and thus root penetration is not considered for performance modeling purposes
	-Biological (burrowing animals)	Design precludes the intrusion of burrowing animals and thus this mechanism is not considered for performance modeling purposes
	-Chemical (stabilized contaminant leachate)	Not applicable - potential sources are located below this layer
Lateral drainage layer	-Siltin-in	Performance model includes the migration of colloidal clay from the middle backfill layer to this layer - affecting hydraulic properties
	-Biological (root penetration)	The presence of pine tree roots within this layer is included in the performance modeling

**Table 3.2-13: Closure Cap Potential Degradation Mechanisms and Course of Action
(Continued)**

Affected Layer	Potential Degradation Mechanism	Proposed Course of Action
HDPE Geomembrane	-Ultraviolet radiation	During construction, timely coverage of the geomembrane limits potential degradation from ultraviolet radiation thus not considered for performance modeling purposes
	-Antioxidant depletion	Included in the performance modeling in conjunction with tensile stress cracking (below)
	-Thermal oxidation	Included in the performance modeling in conjunction with tensile stress cracking (below)
	-High energy irradiation	Estimated dose rate and the 10,000 year integrated dose are not sufficient to cause degradation and are not considered for performance modeling purposes
	-Tensile stress cracking	Included in the performance modeling
	-Biological (microbial)	HDPE geomembrane insensitive to microbial biodegradation and is not considered for performance modeling purposes
	-Biological (root penetration)	Root penetration through existing holes caused by other degradation mechanisms is included in the performance modeling
	-Biological (burrowing animals)	Existence of erosion barrier above this layer precludes this mechanism and is not considered for performance modeling purposes
	-Chemical (stabilized contaminant leachate)	Not applicable - potential sources are located below this layer
GCL	-Slope stability	Placement is only on 2 % slope thus is not considered for performance modeling purposes
	-Freeze-thaw cycles	Depth of the layer precludes this degradation thus is not considered for performance modeling purposes
	-Dissolution	Degradation via this mechanism is not considered credible thus is not considered for performance modeling purposes
	-Divalent cations (Ca ⁺² , Mg ⁺² , etc.)	Included in the performance modeling
	-Desiccation (wet-dry cycles)	Selection of materials and 6 feet of soil materials preclude this damage thus is not considered for performance modeling purposes
	-Biological (root penetration)	Root penetration through existing holes in the HDPE geomembrane is included in the performance modeling
	-Biological (burrowing animals)	Existence of erosion barrier above this layer precludes this mechanism and is not considered for performance modeling purposes
	-Chemical (stabilized contaminant leachate)	Not applicable - potential sources are located below this layer

Based on the identified degradation mechanisms, Table 3.2-14 presents the estimated infiltration rate change over the compliance period.

Table 3.2-14: Conceptual Closure Cap Estimated Infiltration over Time

Time Interval (yr)	Average Annual Infiltration through the GCL (in/yr)
0	0.00088
100	0.010
180	0.17
290	0.37
300	0.50
340	1.00
380	1.46
560	3.23
1,000	7.01
1,800	10.65
2,623	11.47
3,200	11.53
5,600	11.63
10,000	11.67

[SRNL-ESB-2008-00023, Table 2]

The model results show that the degradation of the sand lateral drainage layer, GCL, and HDPE geomembrane proceed to a significantly degraded state at approximately 1,800 to 2,623 years causing infiltration to increase. At that time, the upper foundation layer typical of soil-bentonite blends becomes more important relative to infiltration. For the period 2,623 to 10,000 years, the infiltration rate is controlled by the combined saturated hydraulic conductivity of the sand lateral drainage layer, GCL, HDPE geomembrane, and upper foundation layer. [SRR-CWDA-2011-00054, Table RAI-IE-3.1] HELP model output associated with nominal saturation and head on the composite barrier shows that none of the individual closure cap layers are at the saturated state, except for the GCL, which the HELP model assigns the saturated state based upon its model designation as a barrier soil liner. [SRR-CWDA-2011-00054, Table RAI-IE-1.2]

The predicted HELP model average annual head on the HDPE geomembrane associated with each of the time steps increases with time through year 2,623, due to the assumed closure cap degradation, particularly that of the sand drainage layer. [SRR-CWDA-2011-00054, Table RAI-IE-1.3] After year 2,623, the head begins to decrease because complete degradation of the sand drainage layer has occurred while degradation of the HDPE geomembrane continues. At its greatest, the predicted HELP model HDPE geomembrane head extends partially into the erosion barrier. A significant build-up of head should not be possible within the side slopes due to their slope (i.e., maximum 33.3 % slope). [WSRC-STI-2007-00184]

The conservative assumptions utilized within the HELP modeling (i.e., silting-in without clay mobilization and deep root penetration of the HDPE) tend to restrict modeled lateral drainage from the closure cap and increase infiltration through the composite barrier layer. Therefore,

the HELP model saturation assumption should be greater than what would actually occur in the field. Since these saturations are typical conditions for many SRS surficial soils and do not represent saturated conditions, concerns relative to the potential impact of the closure cap saturation state on stability, vegetation, erosion, and the performance of cover materials under hydrostatic pressure should be minimal.

3.2.4.8 Open Issues for Further Design

Listed below are open issues related to the HTF closure cap concept which will be addressed as the design concept matures.

- Is bamboo a climax species that prevents or greatly slows the intrusion of pine trees?
- What are the requirements for the foundation layer particularly in terms of its ability to drain water away from and around the waste tanks and ancillary equipment?
- What is the estimated weathering rate of the erosion barrier stone (assumed granite) based upon natural or archaeological analogs and available literature?
- What material should be used to fill the stone voids of the erosion barrier to prevent loss of overlying material into the erosion barrier?
- Should a sodium bentonite or calcium bentonite GCL be utilized?
- The definition of a significant void requiring grouting in order to eliminate subsidence needs to be determined.
- Sizing of the side slope and toe riprap.

The current design concept makes conservative assumptions about these open issues, and is acceptable for use for PA modeling.

3.3 Evaluation of Inventory Constituents

3.3.1 Evaluation of Radionuclides in Principal Decay Chains

An initial radionuclide screening process, developed to support characterization efforts applicable for HTF PA modeling, evaluated 849 isotopes. Of the original 849 isotopes, 690 were excluded from further consideration using the following information as described in Appendix A of SRR-CWDA-2010-00023, Rev. 3 and detailed in CBU-PIT-2005-00228:

- Physical properties of each radioisotope (e.g., half-life and decay mechanism)
- Potential isotope production mechanisms and age of the waste
- Screening factors for ground disposal of radionuclides developed in NCRP-123, which convert a quantity of each radionuclide to a dose (CBU-PIT-2005-00228)

3.3.2 Evaluation of Remaining Radionuclides

Many of the remaining 159 isotopes from the initial screening were not created in SRS reactors and therefore further evaluation determined which isotopes could be screened from analyses as described in Appendix B of SRR-CWDA-2010-00023, Rev. 3. The isotopes to be used in further analyses are identified in Table 3.3-1 and will have initial inventory estimates developed.

Table 3.3-1: Radionuclides of Concern

Ac-227	Cl-36	Eu-152	Pa-231	Ra-226	Th-232
Al-26	Cm-243	Eu-154	Pd-107	Ra-228	U-232
Am-241	Cm-244	H-3	Pt-193	Se-79	U-233
Am-242m	Cm-245	I-129	Pu-238	Sm-151	U-234
Am-243	Cm-247	K-40	Pu-239	Sn-126	U-235
Ba-137m	Cm-248	Nb-94	Pu-240	Sr-90	U-236
C-14	Co-60	Ni-59	Pu-241	Tc-99	U-238
Cf-249	Cs-135	Ni-63	Pu-242	Th-229	Y-90
Cf-251	Cs-137	Np-237	Pu-244	Th-230	Zr-93

3.3.3 Evaluation of Chemicals

The list of chemical constituents that were included in the PA modeling was derived from a screening process consisting of several steps to arrive at an appropriate list of constituents to be included in the waste tank closure inventory estimates. The approach was developed for use in screening the chemicals of interest in Tanks 18 and 19; since the chemical constituents for FTF and HTF are assumed the same, using the developed list was appropriate. Table 3.3-2 lists the chemical constituents of concern for the HTF PA.

During the closure process for each waste tank, the actual tank inventory will be used to determine projected dose and risk impacts for that waste tank

Table 3.3-2: Chemical Inventory of Concern

Ag	Cd	F	Mo	PO ₄	U
Al	Cl	Fe	Ni	Sb	Zn
As	Co	Hg	NO ₂	Se	
B	Cr	I	NO ₃	SO ₄	
Ba	Cu	Mn	Pb	Sr	

Further information can be found on evaluation of the radiological and chemical constituents in the HTF closure inventory document. [SRR-CWDA-2010-00023, Rev. 3]

3.4 Inventory Methodology

The following general approach was used for estimating radiological and chemical inventories for use in the HTF PA modeling.

- The contaminant screening process discussed in Section 3.3 consisted of several steps to arrive at an appropriate list of radionuclides and chemicals to be included in the HTF waste tank closure inventory estimates.
- Both residual material concentrations and volumes were estimated to develop initial inventory estimates.

- Adjustments were made to the initial inventory estimates to add reasonable conservatism to the final inventory estimates. These adjustments included grouping the waste tanks according to use and design; inventory adjustment as applicable within that group; increasing initial individual waste tank inventories by one order of magnitude for the Type I, Type II, and Type IV waste tanks; and assigning the maximum concentration of each radiological or chemical constituent from each individual waste tank within a grouping.

Specific details of the methodology can be found in SRR-CWDA-2010-00023, Rev. 3.

At the time of waste tank closure, sampling and analyses will be performed. A statistically based sampling plan will be developed specifically for each waste tank. The plan will ensure samples are collected in a manner that provides the basis for the final waste tank residual characterization. The samples will be analyzed in accordance with the sample plan and the results used in the final waste tank residual inventory determination. Constituents listed in Tables 3.3-1 and 3.3-2 will be included in the basis for the final inventory determination. Although not all constituents will be included in the sampling analyses, those constituents not included in the sampling analyses will be justified (e.g., lack of risk significance, not detectable, below detection limits). These constituents will be determined via special methods (e.g., ratios to other radionuclides or fission yields) in order to conduct an appropriate comparison to the PA modeled residual inventory. Appendix B of SRNL-STI-2010-00439 contains a description of the various methodologies employed during final closure characterization.

3.4.1 Initial Waste Tank Inventory Estimates

The initial waste tank inventory estimates were based on WCS concentrations and volume estimates from waste tank cleaning history.

3.4.1.1 Initial Waste Tank Concentration Estimates

The majority of the radionuclide concentrations and the entire inventory of chemical constituents in the residual material are estimated using data from WCS.

3.4.1.1.1 The Waste Characterization System

The WCS is an electronic information system that tracks waste tank data, including projected radiological and chemical inventories, based on sample analyses, process histories, composition studies, and theoretical relationships. The system (initially developed in 1995) tracks the dry sludge concentrations of 40 radiological and of 37 chemical waste compounds in each of the SRS waste tanks. The 40 radionuclides tracked in the WCS were selected primarily based on their impact on waste-tank safety-basis source term, inhalation dose potential, or on the E-Area Vault Waste Acceptance Criteria (WAC). Further information concerning the use of the WCS and its maintenance is provided in SRR-CWDA-2010-00023, Rev. 3.

3.4.1.1.2 Other Constituents Not Addressed in the WCS

In the WCS, a subset of the 29 HTF waste tanks required additional estimating where no input was available for a particular radiological or non-radiological constituent. In

addition, updated special analysis methods provided estimates for additional isotopes generated as activation products. Affected constituents and the methods used to estimate their inventories are detailed in SRR-CWDA-2010-00023, Rev. 3.

3.4.1.1.3 Accounting for Zeolite

Certain waste tanks contain zeolite in addition to the sludge material. Liquid overheads from the evaporator systems were treated in the past using CRCs containing zeolite, which functioned as a molecular sieve. In HTF, these columns were located in Tanks 24, 32, and 42. The estimated radiological concentrations in Tanks 24, 32, 38, 40, 42, and 51 have been adjusted to account for the zeolite and corresponding captured cesium.

The solids (sludge and zeolite) concentrations assume that zeolite remains unchanged during the waste removal processes. Experience with Tanks 18 and 19 demonstrated that the only element that accumulated on zeolite under actual in-tank conditions was cesium.

3.4.1.2 Initial Waste Tank Volume Estimates

The initial inventory estimates were based on residual solids volume of 4,000 gallons. This reasonable conservative volume was based on waste removal experiences in Tanks 5, 6, 18, and 19. Table 3.4-1 shows the residual volumes from previous waste removal experiences. The residual volume in Tank 16 was estimated with a different volume (1,000 gallons) based on its waste removal history. A more in depth discussion is available in SRR-CWDA-2010-00023, Rev. 3.

Table 3.4-1: Waste Removal Process Residual Volumes

Tank	Residual Volume (gal)
5	1,900
6	3,000
16	220*
18	3,900
19	2,000

* Estimated

Inventories inside failed cooling coils, on the surface of waste tank walls, cooling coils, and columns are encompassed by the total estimated waste tank inventory.

3.4.2 Annulus and Type II Tank Sand Pad Inventory Estimates

Wall inspections of the waste tanks have found cracks where material has leaked in the secondary containment or annulus. The amount of material contained in the each tank's annulus has been estimated. Based on these estimates, inventories within the appropriate annuli were estimated.

All Type II tanks have both a primary and secondary sand layer. The 1-inch thick primary sand layer is between the primary and secondary liners and the 1-inch thick secondary sand layer is between the secondary liner and the basemat. Due to the material that leaked from the Type II tanks, residual material has been assumed present within these primary sand layers and within the secondary sand layer for Tank 16.

3.4.2.1 *Annulus Concentration Estimates*

Characterization of the material within the various annuli is limited. Few samples have been taken from annulus material and even when taken, constituents analyzed have been limited. Recently, samples were collected from the Tank 16 annulus. Four samples were taken around the annulus and numerous constituents analyzed. These sample results were used for all tanks with annulus material.

The constituent concentrations assumed for the annulus material was based on these recent samples. For those constituents analyzed, the concentration reported provided the estimate of that constituent's concentration. Since the sample analysis did not include all constituents of concern, the remaining constituents were estimated. For a description of the estimate methods, refer to SRR-CWDA-2010-00023.

3.4.2.2 *Annulus Volume Estimates*

Current estimates of the amount of material within the tank annuli were used to estimate the residual volumes at closure. The Type I and II tanks are known to have leaksites and material in their annuli. Table 3.4-2 shows the current material volume estimates and the assumed residual material volume estimates for estimating the annuli inventories. Type IV tanks do not have annuli and the Type III and IIIA tanks are assumed to have insignificant quantities of residual material within their annuli.

Table 3.4-2: Tank Annulus Material Volume Estimates

	Current Volume Estimate	Residual Volume Estimate (gal)
Tank 9	Material depth of 8 – 10 inches	3,300
Tank 10	Material depth of 2 – 3 inches	3,300
Tank 11	Trace	100
Tank 12	Trace	100
Tank 13	Trace	100
Tank 14	Material depth of 12 – 13 inches	3,300
Tank 15	Trace	100
Tank 16	3,300 gallons	3,300

The amount of material currently in the Tank 16 annulus has been most recently estimated to be 3,300 gallons. For other annuli with significant volume, this volume was also used. Except for Tank 16, the material in the annuli is expected to be highly soluble. This is due to the material originally being supernate that leaked into each annulus and dried. Therefore, the 3,300-gallon estimate for all other waste tanks is believed to be reasonably conservative. Tank 16 is expected to be an exception due to the mixture of silicon from sand blasting activities. This material is expected to limit the quantity of material removed and, is therefore the reason to use its volume as the reasonably conservative estimate for the appropriate annuli volume.

For those tanks annulus with a trace amount of material, a reasonably conservative volume of 100 gallons was used.

3.4.2.3 Annulus Inventory Estimates

The annulus inventories were estimated by multiplying the volume and concentration estimates. These are presented in Tables 3.4-3 and 3.4-4. The decay date for these inventories is 2032.

Table 3.4-3: Estimated Annulus Radiological Inventories (2032)

Radionuclide	Tank 9 (Ci)	Tank 10 (Ci)	Tank 11 (Ci)	Tank 12 (Ci)	Tank 13 (Ci)	Tank 14 (Ci)	Tank 15 (Ci)	Tank 16 (Ci)
Ac-227	1.0E+00	1.0E+00	1.0E+00	1.0E+00	1.0E+00	1.0E+00	1.0E+00	1.0E+00
Al-26	1.0E+00	1.0E+00	1.0E+00	1.0E+00	1.0E+00	1.0E+00	1.0E+00	1.0E+00
Am-241	7.0E+00	7.0E+00	2.1E-01	2.1E-01	2.1E-01	7.0E+00	2.1E-01	7.0E+00
Am-242m	1.0E+00	1.0E+00	1.0E+00	1.0E+00	1.0E+00	1.0E+00	1.0E+00	1.0E+00
Am-243	3.0E+00	3.0E+00	3.0E+00	3.0E+00	3.0E+00	3.0E+00	3.0E+00	1.0E+00
Ba-137m	1.1E+04	1.1E+04	3.5E+02	3.5E+02	3.5E+02	1.1E+04	3.5E+02	1.6E+04
C-14	1.0E+00	1.0E+00	1.0E+00	1.0E+00	1.0E+00	1.0E+00	1.0E+00	1.0E+00
Cf-249	1.0E+00	1.0E+00	1.0E+00	1.0E+00	1.0E+00	1.0E+00	1.0E+00	1.0E+00
Cf-251	1.0E+00	1.0E+00	1.0E+00	1.0E+00	1.0E+00	1.0E+00	1.0E+00	1.0E+00
Cl-36	1.7E-03	1.7E-03	5.3E-05	5.3E-05	5.3E-05	1.7E-03	5.3E-05	2.5E-03
Cm-243	1.0E+00	1.0E+00	1.0E+00	1.0E+00	1.0E+00	1.0E+00	1.0E+00	1.0E+00
Cm-244	2.1E-01	2.1E-01	6.4E-03	6.4E-03	6.4E-03	2.1E-01	6.4E-03	2.1E-01
Cm-245	1.0E+00	1.0E+00	1.0E+00	1.0E+00	1.0E+00	1.0E+00	1.0E+00	1.0E+00
Cm-247	1.0E+00	1.0E+00	1.0E+00	1.0E+00	1.0E+00	1.0E+00	1.0E+00	1.0E+00
Cm-248	1.0E+00	1.0E+00	1.0E+00	1.0E+00	1.0E+00	1.0E+00	1.0E+00	1.0E+00
Co-60	1.0E+00	1.0E+00	1.0E+00	1.0E+00	1.0E+00	1.0E+00	1.0E+00	1.0E+00
Cs-135	3.2E-03	3.2E-03	9.8E-05	9.8E-05	9.8E-05	3.2E-03	9.8E-05	3.2E-03
Cs-137	1.2E+04	1.2E+04	3.7E+02	3.7E+02	3.7E+02	1.2E+04	3.7E+02	1.7E+04
Eu-152	2.1E+01	2.1E+01	2.1E+01	2.1E+01	2.1E+01	2.1E+01	2.1E+01	1.0E+00
Eu-154	2.9E+00	2.9E+00	8.8E-02	8.8E-02	8.8E-02	2.9E+00	8.8E-02	2.9E+00
H-3	1.0E+00	1.0E+00	1.0E+00	1.0E+00	1.0E+00	1.0E+00	1.0E+00	1.0E+00
I-129	1.7E-04	1.7E-04	5.3E-06	5.3E-06	5.3E-06	1.7E-04	5.3E-06	1.7E-04
K-40	8.7E-04	8.7E-04	2.6E-05	2.6E-05	2.6E-05	8.7E-04	2.6E-05	1.2E-03
Nb-94	8.7E-02	8.7E-02	2.6E-03	2.6E-03	2.6E-03	8.7E-02	2.6E-03	1.2E-01
Ni-59	8.6E+00	8.6E+00	8.6E+00	8.6E+00	8.6E+00	8.6E+00	8.6E+00	1.0E+00
Ni-63	9.6E+00	9.6E+00	2.9E-01	2.9E-01	2.9E-01	9.6E+00	2.9E-01	9.6E+00
Np-237	2.6E-02	2.6E-02	7.9E-04	7.9E-04	7.9E-04	2.6E-02	7.9E-04	2.6E-02
Pa-231	1.7E-03	1.7E-03	5.3E-05	5.3E-05	5.3E-05	1.7E-03	5.3E-05	2.5E-03
Pd-107	1.7E-01	1.7E-01	5.3E-03	5.3E-03	5.3E-03	1.7E-01	5.3E-03	2.5E-01
Pt-193	1.7E-01	1.7E-01	5.3E-03	5.3E-03	5.3E-03	1.7E-01	5.3E-03	2.5E-01
Pu-238	2.5E+01	2.5E+01	7.6E-01	7.6E-01	7.6E-01	2.5E+01	7.6E-01	2.5E+01
Pu-239	3.6E+00	3.6E+00	1.1E-01	1.1E-01	1.1E-01	3.6E+00	1.1E-01	3.6E+00
Pu-240	4.2E+00	4.2E+00	1.3E-01	1.3E-01	1.3E-01	4.2E+00	1.3E-01	4.2E+00
Pu-241	1.3E+01	1.3E+01	3.9E-01	3.9E-01	3.9E-01	1.3E+01	3.9E-01	1.8E+01
Pu-242	1.0E+00	1.0E+00	1.0E+00	1.0E+00	1.0E+00	1.0E+00	1.0E+00	1.0E+00
Pu-244	1.0E+00	1.0E+00	1.0E+00	1.0E+00	1.0E+00	1.0E+00	1.0E+00	1.0E+00

Table 3.4-3: Estimated Annulus Radiological Inventories (2032) (Continued)

Radionuclide	Tank 9 (Ci)	Tank 10 (Ci)	Tank 11 (Ci)	Tank 12 (Ci)	Tank 13 (Ci)	Tank 14 (Ci)	Tank 15 (Ci)	Tank 16 (Ci)
Ra-226	1.7E-02	1.7E-02	5.3E-04	5.3E-04	5.3E-04	1.7E-02	5.3E-04	2.5E-02
Ra-228	1.7E+00	1.7E+00	5.3E-02	5.3E-02	5.3E-02	1.7E+00	5.3E-02	2.5E+00
Se-79	4.8E+00	4.8E+00	4.8E+00	4.8E+00	4.8E+00	4.8E+00	4.8E+00	1.0E+00
Sm-151	1.5E+02	1.5E+02	4.7E+00	4.7E+00	4.7E+00	1.5E+02	4.7E+00	1.5E+02
Sn-126	4.6E+00	4.6E+00	4.6E+00	4.6E+00	4.6E+00	4.6E+00	4.6E+00	1.0E+00
Sr-90	7.8E+03	7.8E+03	2.4E+02	2.4E+02	2.4E+02	7.8E+03	2.4E+02	7.8E+03
Tc-99	4.9E+00	4.9E+00	1.5E-01	1.5E-01	1.5E-01	4.9E+00	1.5E-01	4.9E+00
Th-229	1.7E-03	1.7E-03	5.3E-05	5.3E-05	5.3E-05	1.7E-03	5.3E-05	2.5E-03
Th-230	1.7E-02	1.7E-02	5.3E-04	5.3E-04	5.3E-04	1.7E-02	5.3E-04	2.5E-02
Th-232	2.4E-02	2.4E-02	7.1E-04	7.1E-04	7.1E-04	2.4E-02	7.1E-04	2.5E-02
U-232	1.7E-03	1.7E-03	5.3E-05	5.3E-05	5.3E-05	1.7E-03	5.3E-05	2.5E-03
U-233	1.4E-01	1.4E-01	4.3E-03	4.3E-03	4.3E-03	1.4E-01	4.3E-03	1.4E-01
U-234	9.1E-02	9.1E-02	2.8E-03	2.8E-03	2.8E-03	9.1E-02	2.8E-03	9.1E-02
U-235	2.6E-04	2.6E-04	7.9E-06	7.9E-06	7.9E-06	2.6E-04	7.9E-06	2.6E-04
U-236	1.2E-03	1.2E-03	3.6E-05	3.6E-05	3.6E-05	1.2E-03	3.6E-05	1.2E-03
U-238	1.0E-03	1.0E-03	3.2E-05	3.2E-05	3.2E-05	1.0E-03	3.2E-05	1.0E-03
Y-90	7.8E+03	7.8E+03	2.4E+02	2.4E+02	2.4E+02	7.8E+03	2.4E+02	7.8E+03
Zr-93	5.5E-03	5.5E-03	1.7E-04	1.7E-04	1.7E-04	5.5E-03	1.7E-04	5.5E-03

Table 3.4-4: Estimated Annulus Chemical Inventories

Chemical	Tank 9 (kg)	Tank 10 (kg)	Tank 11 (kg)	Tank 12 (kg)	Tank 13 (kg)	Tank 14 (kg)	Tank 15 (kg)	Tank 16 (kg)
Ag	2.1E+00	2.1E+00	6.5E-02	6.5E-02	6.5E-02	2.1E+00	6.5E-02	2.1E+00
Al	1.2E+03	1.2E+03	3.8E+01	3.8E+01	3.8E+01	1.2E+03	3.8E+01	1.2E+03
As	1.8E-02	1.8E-02	5.4E-04	5.4E-04	5.4E-04	1.8E-02	5.4E-04	1.8E-02
B	3.0E-01	3.0E-01	9.1E-03	9.1E-03	9.1E-03	3.0E-01	9.1E-03	3.0E-01
Ba	1.3E+00	1.3E+00	4.1E-02	4.1E-02	4.1E-02	1.3E+00	4.1E-02	1.3E+00
Cd	1.0E-01	1.0E-01	3.2E-03	3.2E-03	3.2E-03	1.0E-01	3.2E-03	1.0E-01
Cl	1.0E+01	1.0E+01	3.1E-01	3.1E-01	3.1E-01	1.0E+01	3.1E-01	1.0E+01
Co	1.5E-01	1.5E-01	4.6E-03	4.6E-03	4.6E-03	1.5E-01	4.6E-03	1.5E-01
Cr	3.7E+00	3.7E+00	1.1E-01	1.1E-01	1.1E-01	3.7E+00	1.1E-01	3.7E+00
Cu	1.6E+01	1.6E+01	4.9E-01	4.9E-01	4.9E-01	1.6E+01	4.9E-01	1.6E+01
F	7.7E+00	7.7E+00	2.3E-01	2.3E-01	2.3E-01	7.7E+00	2.3E-01	7.7E+00
Fe	6.2E+02	6.2E+02	1.9E+01	1.9E+01	1.9E+01	6.2E+02	1.9E+01	6.2E+02
Hg	4.3E+01	4.3E+01	1.3E+00	1.3E+00	1.3E+00	4.3E+01	1.3E+00	4.3E+01
I	2.0E-01	2.0E-01	6.0E-03	6.0E-03	6.0E-03	2.0E-01	6.0E-03	2.0E-01
Mn	5.3E+00	5.3E+00	1.6E-01	1.6E-01	1.6E-01	5.3E+00	1.6E-01	5.3E+00
Mo	5.5E-01	5.5E-01	1.7E-02	1.7E-02	1.7E-02	5.5E-01	1.7E-02	5.5E-01
Ni	1.4E+00	1.4E+00	4.3E-02	4.3E-02	4.3E-02	1.4E+00	4.3E-02	1.4E+00
NO ₂	1.2E+03	1.2E+03	3.8E+01	3.8E+01	3.8E+01	1.2E+03	3.8E+01	1.2E+03
NO ₃	2.4E+03	2.4E+03	7.3E+01	7.3E+01	7.3E+01	2.4E+03	7.3E+01	2.4E+03
Pb	2.1E+01	2.1E+01	6.5E-01	6.5E-01	6.5E-01	2.1E+01	6.5E-01	2.1E+01
PO ₄	4.6E+00	4.6E+00	1.4E-01	1.4E-01	1.4E-01	4.6E+00	1.4E-01	4.6E+00

Table 3.4-4: Estimated Annulus Chemical Inventories (Continued)

Chemical	Tank 9 (kg)	Tank 10 (kg)	Tank 11 (kg)	Tank 12 (kg)	Tank 13 (kg)	Tank 14 (kg)	Tank 15 (kg)	Tank 16 (kg)
Sb	1.9E+00	1.9E+00	5.7E-02	5.7E-02	5.7E-02	1.9E+00	5.7E-02	1.9E+00
Se	4.0E-03	4.0E-03	1.2E-04	1.2E-04	1.2E-04	4.0E-03	1.2E-04	4.0E-03
SO ₄	2.1E+01	2.1E+01	6.3E-01	6.3E-01	6.3E-01	2.1E+01	6.3E-01	2.1E+01
Sr	6.6E-01	6.6E-01	2.0E-02	2.0E-02	2.0E-02	6.6E-01	2.0E-02	6.6E-01
U	3.3E+00	3.3E+00	9.9E-02	9.9E-02	9.9E-02	3.3E+00	9.9E-02	3.3E+00
Zn	1.9E+01	1.9E+01	5.6E-01	5.6E-01	5.6E-01	1.9E+01	5.6E-01	1.9E+01

3.4.2.4 Type II Tank Sand Pad Concentration Estimates

The residual material within the sand layer was assumed to have the same concentrations as determined for the annulus material.

3.4.2.5 Type II Tank Sand Pad Volume Estimates

The quantity estimate within the Type II tank sand layers was based on the operational history of each tank. For Tanks 14 and 16, a significant quantity of material leaked from the primary tank into the secondary containment and was sufficient to deposit material at a depth of several inches. Due to the depth of material in the annulus and sand pad construction features, it was reasonably conservative to assume the sand pad was saturated with residual material. For Tanks 13 and 15, a minimal quantity of material has leaked from the primary tank. This is based on the inspections of the annulus floor where negligible quantities of material have been observed. Due to the minimal material amount in Tanks 13, 15 and sand pad construction features, a reasonably conservative amount of 100 gallons was assumed in these sand pads. For a more in-depth description, refer to SRR-CWDA-2010-00023, Rev. 3.

The Type II tanks also have a secondary sand layer that is beneath the secondary liner or annulus. Tank 16 experienced the largest quantity of material leaving the tank and gathering in the annulus. In 1960, enough material filled the annulus that tens of gallons overflowed the annulus pan. For the purpose of this inventory evaluation, it is conservatively assumed that all of the material (26 gallons) that overflowed the annulus pan entered the secondary sand layer below Tank 16. For Tanks 13 through 15, no material has leaked beyond the secondary containment; therefore, it is assumed that the secondary sand layers below these tanks contain no inventory.

3.4.2.6 Type II Tank Sand Pad Inventory Estimates

The primary and secondary sand layer inventories are presented in Tables 3.4-5 and 3.4-6; however, the secondary sand layer inventory only applies to Tank 16. The decay date for these inventories is 2032.

Table 3.4-5: Type II Sand Pad Radiological Inventory (2032)

Radionuclide	Tank 13 (Ci)	Tank 14 (Ci)	Tank 15 (Ci)	Tank 16 (Ci)	
	Primary	Primary	Primary	Primary	Secondary
Ac-227	1.0E+00	1.0E+00	1.0E+00	1.0E+00	1.0E+00
Al-26	1.0E+00	1.0E+00	1.0E+00	1.0E+00	1.0E+00
Am-241	2.1E-01	2.8E+00	2.1E-01	2.8E+00	5.5E-02
Am-242m	1.0E+00	1.0E+00	1.0E+00	1.0E+00	1.0E+00
Am-243	3.0E+00	3.0E+00	3.0E+00	1.0E+00	1.0E+00
Ba-137m	3.5E+02	4.5E+03	3.5E+02	4.5E+03	9.0E+01
C-14	1.0E+00	1.0E+00	1.0E+00	1.0E+00	1.0E+00
Cf-249	1.0E+00	1.0E+00	1.0E+00	1.0E+00	1.0E+00
Cf-251	1.0E+00	1.0E+00	1.0E+00	1.0E+00	1.0E+00
Cl-36	5.3E-05	6.9E-04	5.3E-05	6.9E-04	1.4E-05
Cm-243	1.0E+00	1.0E+00	1.0E+00	1.0E+00	1.0E+00
Cm-244	6.4E-03	8.3E-02	6.4E-03	8.3E-02	1.7E-03
Cm-245	1.0E+00	1.0E+00	1.0E+00	1.0E+00	1.0E+00
Cm-247	1.0E+00	1.0E+00	1.0E+00	1.0E+00	1.0E+00
Cm-248	1.0E+00	1.0E+00	1.0E+00	1.0E+00	1.0E+00
Co-60	1.0E+00	1.0E+00	1.0E+00	1.0E+00	1.0E+00
Cs-135	9.8E-05	1.3E-03	9.8E-05	1.3E-03	2.6E-05
Cs-137	3.7E+02	4.8E+03	3.7E+02	4.8E+03	9.5E+01
Eu-152	2.1E+01	2.1E+01	2.1E+01	1.0E+00	1.0E+00
Eu-154	8.8E-02	1.1E+00	8.8E-02	1.1E+00	2.3E-02
H-3	1.0E+00	1.0E+00	1.0E+00	1.0E+00	1.0E+00
I-129	5.3E-06	6.9E-05	5.3E-06	6.9E-05	1.4E-06
K-40	2.6E-05	3.4E-04	2.6E-05	3.4E-04	6.9E-06
Nb-94	2.6E-03	3.4E-02	2.6E-03	3.4E-02	6.9E-04
Ni-59	8.6E+00	8.6E+00	8.6E+00	1.0E+00	1.0E+00
Ni-63	2.9E-01	3.8E+00	2.9E-01	3.8E+00	7.6E-02
Np-237	7.9E-04	1.0E-02	7.9E-04	1.0E-02	2.1E-04

Table 3.4-5: Type II Sand Pad Radiological Inventory (2032) (Continued)

Radionuclide	Tank 13 (Ci)	Tank 14 (Ci)	Tank 15 (Ci)	Tank 16 (Ci)	
	Primary	Primary	Primary	Primary	Secondary
Pa-231	5.3E-05	6.9E-04	5.3E-05	6.9E-04	1.4E-05
Pd-107	5.3E-03	6.9E-02	5.3E-03	6.9E-02	1.4E-03
Pt-193	5.3E-03	6.9E-02	5.3E-03	6.9E-02	1.4E-03
Pu-238	7.6E-01	9.8E+00	7.6E-01	9.8E+00	2.0E-01
Pu-239	1.1E-01	1.4E+00	1.1E-01	1.4E+00	2.9E-02
Pu-240	1.3E-01	1.7E+00	1.3E-01	1.7E+00	3.3E-02
Pu-241	3.9E-01	5.1E+00	3.9E-01	5.1E+00	1.0E-01
Pu-242	1.0E+00	1.0E+00	1.0E+00	1.0E+00	1.0E+00
Pu-244	1.0E+00	1.0E+00	1.0E+00	1.0E+00	1.0E+00
Ra-226	5.3E-04	6.9E-03	5.3E-04	6.9E-03	1.4E-04
Ra-228	5.3E-02	6.9E-01	5.3E-02	6.9E-01	1.4E-02
Se-79	4.8E+00	4.8E+00	4.8E+00	1.0E+00	1.0E+00
Sm-151	4.7E+00	6.1E+01	4.7E+00	6.1E+01	1.2E+00
Sn-126	4.6E+00	4.6E+00	4.6E+00	1.0E+00	1.0E+00
Sr-90	2.4E+02	3.1E+03	2.4E+02	3.1E+03	6.3E+01
Tc-99	1.5E-01	1.9E+00	1.5E-01	1.9E+00	3.8E-02
Th-229	5.3E-05	6.9E-04	5.3E-05	6.9E-04	1.4E-05
Th-230	5.3E-04	6.9E-03	5.3E-04	6.9E-03	1.4E-04
Th-232	7.1E-04	9.3E-03	7.1E-04	6.9E-03	1.4E-04
U-232	5.3E-05	6.9E-04	5.3E-05	6.9E-04	1.4E-05
U-233	4.3E-03	5.6E-02	4.3E-03	5.6E-02	1.1E-03
U-234	2.8E-03	3.6E-02	2.8E-03	3.6E-02	7.2E-04
U-235	7.9E-06	1.0E-04	7.9E-06	1.0E-04	2.1E-06
U-236	3.6E-05	4.7E-04	3.6E-05	4.7E-04	9.4E-06
U-238	3.2E-05	4.1E-04	3.2E-05	4.1E-04	8.3E-06
Y-90	2.4E+02	3.1E+03	2.4E+02	3.1E+03	6.3E+01
Zr-93	1.7E-04	2.2E-03	1.7E-04	2.2E-03	4.3E-05

Table 3.4-6: Type II Sand Pad Chemical Inventory

Chemical	Tank 13 (kg)	Tank 14 (kg)	Tank 15 (kg)	Tank 16 (kg)	
	Primary	Primary	Primary	Primary	Secondary
Ag	6.5E-02	8.4E-01	6.5E-02	8.4E-01	1.7E-02
Al	3.8E+01	4.9E+02	3.8E+01	4.9E+02	9.8E+00
As	5.4E-04	7.1E-03	5.4E-04	7.1E-03	1.4E-04
B	9.1E-03	1.2E-01	9.1E-03	1.2E-01	2.4E-03
Ba	4.1E-02	5.3E-01	4.1E-02	5.3E-01	1.1E-02
Cd	3.2E-03	4.1E-02	3.2E-03	4.1E-02	8.3E-04
Cl	3.1E-01	4.1E+00	3.1E-01	4.1E+00	8.1E-02
Co	4.6E-03	6.0E-02	4.6E-03	6.0E-02	1.2E-03
Cr	1.1E-01	1.5E+00	1.1E-01	1.5E+00	2.9E-02
Cu	4.9E-01	6.4E+00	4.9E-01	6.4E+00	1.3E-01
F	2.3E-01	3.0E+00	2.3E-01	3.0E+00	6.1E-02
Fe	1.9E+01	2.4E+02	1.9E+01	2.4E+02	4.9E+00
Hg	1.3E+00	1.7E+01	1.3E+00	1.7E+01	3.4E-01
I	6.0E-03	7.9E-02	6.0E-03	7.9E-02	1.6E-03
Mn	1.6E-01	2.1E+00	1.6E-01	2.1E+00	4.2E-02
Mo	1.7E-02	2.2E-01	1.7E-02	2.2E-01	4.3E-03
Ni	4.3E-02	5.5E-01	4.3E-02	5.5E-01	1.1E-02
NO ₂	3.8E+01	4.9E+02	3.8E+01	4.9E+02	9.8E+00
NO ₃	7.3E+01	9.5E+02	7.3E+01	9.5E+02	1.9E+01
Pb	6.5E-01	8.4E+00	6.5E-01	8.4E+00	1.7E-01
PO ₄	1.4E-01	1.8E+00	1.4E-01	1.8E+00	3.6E-02
Sb	5.7E-02	7.5E-01	5.7E-02	7.5E-01	1.5E-02
Se	1.2E-04	1.6E-03	1.2E-04	1.6E-03	3.1E-05
SO ₄	6.3E-01	8.2E+00	6.3E-01	8.2E+00	1.6E-01
Sr	2.0E-02	2.6E-01	2.0E-02	2.6E-01	5.2E-03
U	9.9E-02	1.3E+00	9.9E-02	1.3E+00	2.6E-02
Zn	5.6E-01	7.3E+00	5.6E-01	7.3E+00	1.5E-01

3.4.3 Waste Tank Inventory Adjustments

Following the initial estimate of residual waste tank inventories, adjustments were performed based on experience with tank farm operations, previous inventory developments, and modeling efforts. Independent steps were developed to adjust systematically the HTF waste tank inventories, with each step adjusting the inventory either by waste tank or by constituent. The steps used in the inventory adjustment were as follows:

1. The inventory adjustment used the initial inventory estimates as the starting point (Section 3.4.1).
2. The waste tanks were grouped according to waste tank use and design (Section 3.4.3.2).
3. To account for uncertainty surrounding future operations and movement of material within the HTF, the maximum concentration of each radionuclide or chemical from any tank within a group was applied to the other tanks within the tank grouping (Section 3.4.3.2.1).

The adjustments summarized in this section are explained in further detail in SRR-CWDA-2010-00023, Rev. 3.

3.4.3.1 Nominal Activity (Radionuclides)

Allowing for more efficient and cost effective means of confirming radionuclide concentrations with a limited potential impact to dose, the inventories for a group of radionuclides were adjusted to either 1 curie, or used an analytical detection limit. If the radionuclide inventory estimated was less than the detection limit, then it was adjusted up to the detection limit. However, if the radionuclide inventory estimated was greater than the detection limit, then it was adjusted up to 1 curie. Recent sample analyses from Tanks 5, 18, and 19 were reviewed for appropriate detection limits. The adjustments to either the detection limit or to 1 curie exclusively increased residual inventories estimates. Inventory estimates were not adjusted lower, only higher.

For those radionuclides that have been observed (through previous analyses or scoping studies) to have greater potential impact on the overall dose, the inventory was adjusted to the analytical detection limit.

Note that those radionuclides with estimated inventories greater than 1 curie were not adjusted in this step. In addition, this adjustment only applied to the radiological inventories and not to the chemical inventories.

For the discussion on the specific detection limits used, refer to SRR-CWDA-2010-00023, Rev. 3.

3.4.3.2 Waste Tank Grouping

The waste tank type generally had an effect on the type of waste received and therefore guided the group selection. In general, each waste tank type was built at approximately the same time. The waste tanks were grouped based on use and design as presented in Table 3.4-7.

Table 3.4-7: Waste Tank Groupings

Types I & II	Type III/IIIA	Type IV
Tanks 9, 10, 11, 12, 13, 14, and 15	Tanks 29, 30, 31, 32, 35, 36, 37, 38, 39, 40, 41, 42, 43, 48, 49, 50, and 51	Tanks 21, 22, 23, and 24

Note Tank 16 is a special case with its own grouping

Based on experience with previous PAs, overestimating the Pu-238 inventories can ultimately exaggerate the projected overall dose. To reduce this exaggeration for estimating Pu-238 inventories in the Type III and IIIA tanks, the grouping was split based on the two different waste types (salt and sludge). The groupings of the waste tanks used for the Pu-238 inventory estimate is presented in Table 3.4-8

Table 3.4-8: Waste Tank Groupings for Pu-238

Types I and II	Type III/IIIA		Type IV
N/A*	Salt	Sludge	N/A*
Tanks 9 and 10, 11, 12, 13, 14, and 15	Tanks 29, 30, 31, 36, 37, 38, 41, 48, 49, and 50	Tanks 32, 35, 39, 40, 42, 43, and 51	Tanks 21, 22, 23, and 24

Note Tank 16 is a special case with its own grouping

* No additional criteria was attributed to this tank type group

3.4.3.2.1 Adjustments within Each Grouping

Within each grouping, adjustments were made to produce reasonably conservative waste tank inventory estimates. To account for the uncertainty in the waste tank order of waste removal, the maximum inventory within each grouping was assigned to each tank. Due to decreases in concentrations observed during the waste removal process, the cesium, strontium, and zirconium inventories were adjusted one order of magnitude lower. Based on a comparison of recent Tank 5 residual material sample results to the estimated inventories in the FTF PA (which used a similar inventory estimate methodology), it was determined that the Tc-99 and Zr-93 inventory estimates needed adjusting. Refer to SRR-CWDA-2010-00023, Rev. 3 for further details.

3.4.4 Final Waste Tank Inventory Estimates

The system plan calls for the last waste tank to be grouted at the end of fiscal year 2032. Therefore, all the radiological inventories have been decay corrected to 2032. After all waste inventory adjustments, the final radionuclide estimates are provided in Table 3.4-9. The estimated chemical constituent inventories are provided in Table 3.4-10.

In using the estimates of Tables 3.4-9 and 3.4-10 in the PA, it should be kept in mind that the curies of residual radiological and the mass of residual chemical waste constituents are important to the analyses, not the estimated residual waste volume. While the estimated solids volume was used to calculate the residual radiological and chemical waste constituent inventories, the volume estimate was not significant in its own right.

Estimate conservatism and uncertainty are addressed in Section 5.6.3.1. In addition, further details can be found in SRR-CWDA-2010-00023, Rev. 3.

Table 3.4-9: Estimated Radiological Inventory (Ci) at Closure

Tank	Ac-227	Al-26	Am-241	Am-242m	Am-243	Ba-137m	C-14	Cf-249	Cf-251	Cl-36	Cm-243	Cm-244	Cm-245
9	1.0E+00	1.0E+00	7.0E+02	1.0E+00	3.0E+00	7.4E+02	1.0E+00	1.0E+00	1.0E+00	2.1E-03	1.0E+00	2.0E+01	1.0E+00
10	1.0E+00	1.0E+00	7.0E+02	1.0E+00	3.0E+00	7.4E+02	1.0E+00	1.0E+00	1.0E+00	2.1E-03	1.0E+00	2.0E+01	1.0E+00
11	1.0E+00	1.0E+00	7.0E+02	1.0E+00	3.0E+00	7.4E+02	1.0E+00	1.0E+00	1.0E+00	2.1E-03	1.0E+00	2.0E+01	1.0E+00
12	1.0E+00	1.0E+00	7.0E+02	1.0E+00	3.0E+00	7.4E+02	1.0E+00	1.0E+00	1.0E+00	2.1E-03	1.0E+00	2.0E+01	1.0E+00
13	1.0E+00	1.0E+00	7.0E+02	1.0E+00	3.0E+00	7.4E+02	1.0E+00	1.0E+00	1.0E+00	2.1E-03	1.0E+00	2.0E+01	1.0E+00
14	1.0E+00	1.0E+00	7.0E+02	1.0E+00	3.0E+00	7.4E+02	1.0E+00	1.0E+00	1.0E+00	2.1E-03	1.0E+00	2.0E+01	1.0E+00
15	1.0E+00	1.0E+00	7.0E+02	1.0E+00	3.0E+00	7.4E+02	1.0E+00	1.0E+00	1.0E+00	2.1E-03	1.0E+00	2.0E+01	1.0E+00
16	1.0E+00	1.0E+00	8.1E+01	1.0E+00	1.0E+00	1.2E+02	1.0E+00	1.0E+00	1.0E+00	5.3E-04	1.0E+00	2.4E+00	1.0E+00
21	1.0E+00	1.0E+00	5.0E+00	1.0E+00	1.0E+00	2.3E+03	1.0E+00	1.0E+00	1.0E+00	2.1E-03	1.0E+00	4.6E+00	1.0E+00
22	1.0E+00	1.0E+00	5.0E+00	1.0E+00	1.0E+00	2.3E+03	1.0E+00	1.0E+00	1.0E+00	2.1E-03	1.0E+00	4.6E+00	1.0E+00
23	1.0E+00	1.0E+00	5.0E+00	1.0E+00	1.0E+00	2.3E+03	1.0E+00	1.0E+00	1.0E+00	2.1E-03	1.0E+00	4.6E+00	1.0E+00
24	1.0E+00	1.0E+00	5.0E+00	1.0E+00	1.0E+00	2.3E+03	1.0E+00	1.0E+00	1.0E+00	2.1E-03	1.0E+00	4.6E+00	1.0E+00
29	1.0E+00	1.0E+00	1.1E+03	1.0E+00	1.0E+00	5.2E+03	1.0E+00	1.0E+00	1.0E+00	2.1E-03	1.0E+00	2.2E+03	1.0E+00
30	1.0E+00	1.0E+00	1.1E+03	1.0E+00	1.0E+00	5.2E+03	1.0E+00	1.0E+00	1.0E+00	2.1E-03	1.0E+00	2.2E+03	1.0E+00
31	1.0E+00	1.0E+00	1.1E+03	1.0E+00	1.0E+00	5.2E+03	1.0E+00	1.0E+00	1.0E+00	2.1E-03	1.0E+00	2.2E+03	1.0E+00
32	1.0E+00	1.0E+00	1.1E+03	1.0E+00	1.0E+00	5.2E+03	1.0E+00	1.0E+00	1.0E+00	2.1E-03	1.0E+00	2.2E+03	1.0E+00
35	1.0E+00	1.0E+00	1.1E+03	1.0E+00	1.0E+00	5.2E+03	1.0E+00	1.0E+00	1.0E+00	2.1E-03	1.0E+00	2.2E+03	1.0E+00
36	1.0E+00	1.0E+00	1.1E+03	1.0E+00	1.0E+00	5.2E+03	1.0E+00	1.0E+00	1.0E+00	2.1E-03	1.0E+00	2.2E+03	1.0E+00
37	1.0E+00	1.0E+00	1.1E+03	1.0E+00	1.0E+00	5.2E+03	1.0E+00	1.0E+00	1.0E+00	2.1E-03	1.0E+00	2.2E+03	1.0E+00
38	1.0E+00	1.0E+00	1.1E+03	1.0E+00	1.0E+00	5.2E+03	1.0E+00	1.0E+00	1.0E+00	2.1E-03	1.0E+00	2.2E+03	1.0E+00
39	1.0E+00	1.0E+00	1.1E+03	1.0E+00	1.0E+00	5.2E+03	1.0E+00	1.0E+00	1.0E+00	2.1E-03	1.0E+00	2.2E+03	1.0E+00
40	1.0E+00	1.0E+00	1.1E+03	1.0E+00	1.0E+00	5.2E+03	1.0E+00	1.0E+00	1.0E+00	2.1E-03	1.0E+00	2.2E+03	1.0E+00
41	1.0E+00	1.0E+00	1.1E+03	1.0E+00	1.0E+00	5.2E+03	1.0E+00	1.0E+00	1.0E+00	2.1E-03	1.0E+00	2.2E+03	1.0E+00
42	1.0E+00	1.0E+00	1.1E+03	1.0E+00	1.0E+00	5.2E+03	1.0E+00	1.0E+00	1.0E+00	2.1E-03	1.0E+00	2.2E+03	1.0E+00
43	1.0E+00	1.0E+00	1.1E+03	1.0E+00	1.0E+00	5.2E+03	1.0E+00	1.0E+00	1.0E+00	2.1E-03	1.0E+00	2.2E+03	1.0E+00
48	1.0E+00	1.0E+00	1.1E+03	1.0E+00	1.0E+00	5.2E+03	1.0E+00	1.0E+00	1.0E+00	2.1E-03	1.0E+00	2.2E+03	1.0E+00
49	1.0E+00	1.0E+00	1.1E+03	1.0E+00	1.0E+00	5.2E+03	1.0E+00	1.0E+00	1.0E+00	2.1E-03	1.0E+00	2.2E+03	1.0E+00
50	1.0E+00	1.0E+00	1.1E+03	1.0E+00	1.0E+00	5.2E+03	1.0E+00	1.0E+00	1.0E+00	2.1E-03	1.0E+00	2.2E+03	1.0E+00
51	1.0E+00	1.0E+00	1.1E+03	1.0E+00	1.0E+00	5.2E+03	1.0E+00	1.0E+00	1.0E+00	2.1E-03	1.0E+00	2.2E+03	1.0E+00

Table 3.4-9: Estimated Radiological Inventory (Ci) at Closure (Continued)

Tank	Cm-247	Cm-248	Co-60	Cs-135	Cs-137	Eu-152	Eu-154	H-3	I-129	K-40	Nb-94	Ni-59	Ni-63	Np-237
9	1.0E+00	1.0E+00	1.0E+00	5.4E-03	7.9E+02	2.1E+01	2.9E+02	1.0E+00	2.8E-04	1.1E-03	1.1E-01	8.6E+00	6.3E+02	2.1E-01
10	1.0E+00	1.0E+00	1.0E+00	5.4E-03	7.9E+02	2.1E+01	2.9E+02	1.0E+00	2.8E-04	1.1E-03	1.1E-01	8.6E+00	6.3E+02	2.1E-01
11	1.0E+00	1.0E+00	1.0E+00	5.4E-03	7.9E+02	2.1E+01	2.9E+02	1.0E+00	2.8E-04	1.1E-03	1.1E-01	8.6E+00	6.3E+02	2.1E-01
12	1.0E+00	1.0E+00	1.0E+00	5.4E-03	7.9E+02	2.1E+01	2.9E+02	1.0E+00	2.8E-04	1.1E-03	1.1E-01	8.6E+00	6.3E+02	2.1E-01
13	1.0E+00	1.0E+00	1.0E+00	5.4E-03	7.9E+02	2.1E+01	2.9E+02	1.0E+00	2.8E-04	1.1E-03	1.1E-01	8.6E+00	6.3E+02	2.1E-01
14	1.0E+00	1.0E+00	1.0E+00	5.4E-03	7.9E+02	2.1E+01	2.9E+02	1.0E+00	2.8E-04	1.1E-03	1.1E-01	8.6E+00	6.3E+02	2.1E-01
15	1.0E+00	1.0E+00	1.0E+00	5.4E-03	7.9E+02	2.1E+01	2.9E+02	1.0E+00	2.8E-04	1.1E-03	1.1E-01	8.6E+00	6.3E+02	2.1E-01
16	1.0E+00	1.0E+00	1.0E+00	9.9E-04	1.3E+02	1.0E+00	3.3E+01	1.0E+00	5.3E-05	2.6E-04	2.6E-02	1.0E+00	1.1E+02	2.2E-02
21	1.0E+00	1.0E+00	1.0E+00	2.3E-02	2.4E+03	1.0E+00	8.3E+00	1.0E+00	2.1E-04	1.1E-03	1.1E-01	1.0E+00	9.1E+00	1.3E-02
22	1.0E+00	1.0E+00	1.0E+00	2.3E-02	2.4E+03	1.0E+00	8.3E+00	1.0E+00	2.1E-04	1.1E-03	1.1E-01	1.0E+00	9.1E+00	1.3E-02
23	1.0E+00	1.0E+00	1.0E+00	2.3E-02	2.4E+03	1.0E+00	8.3E+00	1.0E+00	2.1E-04	1.1E-03	1.1E-01	1.0E+00	9.1E+00	1.3E-02
24	1.0E+00	1.0E+00	1.0E+00	2.3E-02	2.4E+03	1.0E+00	8.3E+00	1.0E+00	2.1E-04	1.1E-03	1.1E-01	1.0E+00	9.1E+00	1.3E-02
29	1.0E+00	1.0E+00	1.0E+00	7.1E-03	5.5E+03	3.8E+01	9.2E+02	1.0E+00	6.7E-03	1.1E-03	1.1E-01	1.0E+00	7.9E+02	4.0E-01
30	1.0E+00	1.0E+00	1.0E+00	7.1E-03	5.5E+03	3.8E+01	9.2E+02	1.0E+00	6.7E-03	1.1E-03	1.1E-01	1.0E+00	7.9E+02	4.0E-01
31	1.0E+00	1.0E+00	1.0E+00	7.1E-03	5.5E+03	3.8E+01	9.2E+02	1.0E+00	6.7E-03	1.1E-03	1.1E-01	1.0E+00	7.9E+02	4.0E-01
32	1.0E+00	1.0E+00	1.0E+00	7.1E-03	5.5E+03	3.8E+01	9.2E+02	1.0E+00	6.7E-03	1.1E-03	1.1E-01	1.0E+00	7.9E+02	4.0E-01
35	1.0E+00	1.0E+00	1.0E+00	7.1E-03	5.5E+03	3.8E+01	9.2E+02	1.0E+00	6.7E-03	1.1E-03	1.1E-01	1.0E+00	7.9E+02	4.0E-01
36	1.0E+00	1.0E+00	1.0E+00	7.1E-03	5.5E+03	3.8E+01	9.2E+02	1.0E+00	6.7E-03	1.1E-03	1.1E-01	1.0E+00	7.9E+02	4.0E-01
37	1.0E+00	1.0E+00	1.0E+00	7.1E-03	5.5E+03	3.8E+01	9.2E+02	1.0E+00	6.7E-03	1.1E-03	1.1E-01	1.0E+00	7.9E+02	4.0E-01
38	1.0E+00	1.0E+00	1.0E+00	7.1E-03	5.5E+03	3.8E+01	9.2E+02	1.0E+00	6.7E-03	1.1E-03	1.1E-01	1.0E+00	7.9E+02	4.0E-01
39	1.0E+00	1.0E+00	1.0E+00	7.1E-03	5.5E+03	3.8E+01	9.2E+02	1.0E+00	6.7E-03	1.1E-03	1.1E-01	1.0E+00	7.9E+02	4.0E-01
40	1.0E+00	1.0E+00	1.0E+00	7.1E-03	5.5E+03	3.8E+01	9.2E+02	1.0E+00	6.7E-03	1.1E-03	1.1E-01	1.0E+00	7.9E+02	4.0E-01
41	1.0E+00	1.0E+00	1.0E+00	7.1E-03	5.5E+03	3.8E+01	9.2E+02	1.0E+00	6.7E-03	1.1E-03	1.1E-01	1.0E+00	7.9E+02	4.0E-01
42	1.0E+00	1.0E+00	1.0E+00	7.1E-03	5.5E+03	3.8E+01	9.2E+02	1.0E+00	6.7E-03	1.1E-03	1.1E-01	1.0E+00	7.9E+02	4.0E-01
43	1.0E+00	1.0E+00	1.0E+00	7.1E-03	5.5E+03	3.8E+01	9.2E+02	1.0E+00	6.7E-03	1.1E-03	1.1E-01	1.0E+00	7.9E+02	4.0E-01
48	1.0E+00	1.0E+00	1.0E+00	7.1E-03	5.5E+03	3.8E+01	9.2E+02	1.0E+00	6.7E-03	1.1E-03	1.1E-01	1.0E+00	7.9E+02	4.0E-01
49	1.0E+00	1.0E+00	1.0E+00	7.1E-03	5.5E+03	3.8E+01	9.2E+02	1.0E+00	6.7E-03	1.1E-03	1.1E-01	1.0E+00	7.9E+02	4.0E-01
50	1.0E+00	1.0E+00	1.0E+00	7.1E-03	5.5E+03	3.8E+01	9.2E+02	1.0E+00	6.7E-03	1.1E-03	1.1E-01	1.0E+00	7.9E+02	4.0E-01
51	1.0E+00	1.0E+00	1.0E+00	7.1E-03	5.5E+03	3.8E+01	9.2E+02	1.0E+00	6.7E-03	1.1E-03	1.1E-01	1.0E+00	7.9E+02	4.0E-01

Table 3.4-9: Estimated Radiological Inventory (Ci) at Closure (Continued)

Tank	Pa-231	Pd-107	Pt-193	Pu-238	Pu-239	Pu-240	Pu-241	Pu-242	Pu-244	Ra-226	Ra-228	Se-79	Sm-151	Sn-126
9	2.1E-03	2.1E-01	2.1E-01	6.5E+03	8.0E+01	5.0E+01	7.6E+02	1.0E+00	1.0E+00	2.1E-02	2.1E+00	4.8E+00	1.1E+04	4.6E+00
10	2.1E-03	2.1E-01	2.1E-01	6.5E+03	8.0E+01	5.0E+01	7.6E+02	1.0E+00	1.0E+00	2.1E-02	2.1E+00	4.8E+00	1.1E+04	4.6E+00
11	2.1E-03	2.1E-01	2.1E-01	6.5E+03	8.0E+01	5.0E+01	7.6E+02	1.0E+00	1.0E+00	2.1E-02	2.1E+00	4.8E+00	1.1E+04	4.6E+00
12	2.1E-03	2.1E-01	2.1E-01	6.5E+03	8.0E+01	5.0E+01	7.6E+02	1.0E+00	1.0E+00	2.1E-02	2.1E+00	4.8E+00	1.1E+04	4.6E+00
13	2.1E-03	2.1E-01	2.1E-01	6.5E+03	8.0E+01	5.0E+01	7.6E+02	1.0E+00	1.0E+00	2.1E-02	2.1E+00	4.8E+00	1.1E+04	4.6E+00
14	2.1E-03	2.1E-01	2.1E-01	6.5E+03	8.0E+01	5.0E+01	7.6E+02	1.0E+00	1.0E+00	2.1E-02	2.1E+00	4.8E+00	1.1E+04	4.6E+00
15	2.1E-03	2.1E-01	2.1E-01	6.5E+03	8.0E+01	5.0E+01	7.6E+02	1.0E+00	1.0E+00	2.1E-02	2.1E+00	4.8E+00	1.1E+04	4.6E+00
16	5.3E-04	5.3E-02	5.3E-02	2.9E+02	7.7E+00	3.7E+00	2.0E+01	1.0E+00	1.0E+00	5.3E-03	5.3E-01	1.0E+00	1.8E+03	1.0E+00
21	2.1E-03	2.1E-01	2.1E-01	7.2E+01	1.0E+00	3.6E-01	2.1E+00	1.0E+00	1.0E+00	2.1E-02	2.1E+00	1.0E+00	2.4E+02	1.0E+00
22	2.1E-03	2.1E-01	2.1E-01	7.2E+01	1.0E+00	3.6E-01	2.1E+00	1.0E+00	1.0E+00	2.1E-02	2.1E+00	1.0E+00	2.4E+02	1.0E+00
23	2.1E-03	2.1E-01	2.1E-01	7.2E+01	1.0E+00	3.6E-01	2.1E+00	1.0E+00	1.0E+00	2.1E-02	2.1E+00	1.0E+00	2.4E+02	1.0E+00
24	2.1E-03	2.1E-01	2.1E-01	7.2E+01	1.0E+00	3.6E-01	2.1E+00	1.0E+00	1.0E+00	2.1E-02	2.1E+00	1.0E+00	2.4E+02	1.0E+00
29	2.1E-03	2.1E-01	2.1E-01	2.8E+03	2.4E+02	1.5E+02	4.6E+03	1.0E+00	1.0E+00	2.1E-02	2.1E+00	1.0E+00	7.7E+04	1.0E+00
30	2.1E-03	2.1E-01	2.1E-01	2.8E+03	2.4E+02	1.5E+02	4.6E+03	1.0E+00	1.0E+00	2.1E-02	2.1E+00	1.0E+00	7.7E+04	1.0E+00
31	2.1E-03	2.1E-01	2.1E-01	2.8E+03	2.4E+02	1.5E+02	4.6E+03	1.0E+00	1.0E+00	2.1E-02	2.1E+00	1.0E+00	7.7E+04	1.0E+00
32	2.1E-03	2.1E-01	2.1E-01	1.5E+04	2.4E+02	1.5E+02	4.6E+03	1.0E+00	1.0E+00	2.1E-02	2.1E+00	1.0E+00	7.7E+04	1.0E+00
35	2.1E-03	2.1E-01	2.1E-01	2.8E+03	2.4E+02	1.5E+02	4.6E+03	1.0E+00	1.0E+00	2.1E-02	2.1E+00	1.0E+00	7.7E+04	1.0E+00
36	2.1E-03	2.1E-01	2.1E-01	2.8E+03	2.4E+02	1.5E+02	4.6E+03	1.0E+00	1.0E+00	2.1E-02	2.1E+00	1.0E+00	7.7E+04	1.0E+00
37	2.1E-03	2.1E-01	2.1E-01	2.8E+03	2.4E+02	1.5E+02	4.6E+03	1.0E+00	1.0E+00	2.1E-02	2.1E+00	1.0E+00	7.7E+04	1.0E+00
38	2.1E-03	2.1E-01	2.1E-01	2.8E+03	2.4E+02	1.5E+02	4.6E+03	1.0E+00	1.0E+00	2.1E-02	2.1E+00	1.0E+00	7.7E+04	1.0E+00
39	2.1E-03	2.1E-01	2.1E-01	1.5E+04	2.4E+02	1.5E+02	4.6E+03	1.0E+00	1.0E+00	2.1E-02	2.1E+00	1.0E+00	7.7E+04	1.0E+00
40	2.1E-03	2.1E-01	2.1E-01	1.5E+04	2.4E+02	1.5E+02	4.6E+03	1.0E+00	1.0E+00	2.1E-02	2.1E+00	1.0E+00	7.7E+04	1.0E+00
41	2.1E-03	2.1E-01	2.1E-01	2.8E+03	2.4E+02	1.5E+02	4.6E+03	1.0E+00	1.0E+00	2.1E-02	2.1E+00	1.0E+00	7.7E+04	1.0E+00
42	2.1E-03	2.1E-01	2.1E-01	1.5E+04	2.4E+02	1.5E+02	4.6E+03	1.0E+00	1.0E+00	2.1E-02	2.1E+00	1.0E+00	7.7E+04	1.0E+00
43	2.1E-03	2.1E-01	2.1E-01	1.5E+04	2.4E+02	1.5E+02	4.6E+03	1.0E+00	1.0E+00	2.1E-02	2.1E+00	1.0E+00	7.7E+04	1.0E+00
48	2.1E-03	2.1E-01	2.1E-01	2.8E+03	2.4E+02	1.5E+02	4.6E+03	1.0E+00	1.0E+00	2.1E-02	2.1E+00	1.0E+00	7.7E+04	1.0E+00
49	2.1E-03	2.1E-01	2.1E-01	2.8E+03	2.4E+02	1.5E+02	4.6E+03	1.0E+00	1.0E+00	2.1E-02	2.1E+00	1.0E+00	7.7E+04	1.0E+00
50	2.1E-03	2.1E-01	2.1E-01	1.5E+04	2.4E+02	1.5E+02	4.6E+03	1.0E+00	1.0E+00	2.1E-02	2.1E+00	1.0E+00	7.7E+04	1.0E+00
51	2.1E-03	2.1E-01	2.1E-01	1.5E+04	2.4E+02	1.5E+02	4.6E+03	1.0E+00	1.0E+00	2.1E-02	2.1E+00	1.0E+00	7.7E+04	1.0E+00

Table 3.4-9: Estimated Radiological Inventory (Ci) at Closure (Continued)

Tank	Sr-90	Tc-99	Th-229	Th-230	Th-232	U-232	U-233	U-234	U-235	U-236	U-238	Y-90	Zr-93
9	1.4E+04	8.1E+00	2.1E-03	2.1E-02	2.9E-02	2.1E-03	5.9E-01	9.6E-02	2.1E-02	2.1E-02	2.9E-02	1.4E+04	4.0E-01
10	1.4E+04	8.1E+00	2.1E-03	2.1E-02	2.9E-02	2.1E-03	5.9E-01	9.6E-02	2.1E-02	2.1E-02	2.9E-02	1.4E+04	4.0E-01
11	1.4E+04	8.1E+00	2.1E-03	2.1E-02	2.9E-02	2.1E-03	5.9E-01	9.6E-02	2.1E-02	2.1E-02	2.9E-02	1.4E+04	4.0E-01
12	1.4E+04	8.1E+00	2.1E-03	2.1E-02	2.9E-02	2.1E-03	5.9E-01	9.6E-02	2.1E-02	2.1E-02	2.9E-02	1.4E+04	4.0E-01
13	1.4E+04	8.1E+00	2.1E-03	2.1E-02	2.9E-02	2.1E-03	5.9E-01	9.6E-02	2.1E-02	2.1E-02	2.9E-02	1.4E+04	4.0E-01
14	1.4E+04	8.1E+00	2.1E-03	2.1E-02	2.9E-02	2.1E-03	5.9E-01	9.6E-02	2.1E-02	2.1E-02	2.9E-02	1.4E+04	4.0E-01
15	1.4E+04	8.1E+00	2.1E-03	2.1E-02	2.9E-02	2.1E-03	5.9E-01	9.6E-02	2.1E-02	2.1E-02	2.9E-02	1.4E+04	4.0E-01
16	2.2E+03	1.5E+00	5.3E-04	5.3E-03	5.3E-03	5.3E-04	8.7E-02	2.4E-02	5.3E-03	5.3E-03	5.3E-04	2.2E+03	6.3E-02
21	3.1E+02	1.6E-01	2.1E-03	2.1E-02	2.1E-02	2.1E-03	6.0E-02	2.2E-02	2.1E-02	2.1E-02	7.4E-03	3.1E+02	8.8E-03
22	3.1E+02	1.6E-01	2.1E-03	2.1E-02	2.1E-02	2.1E-03	6.0E-02	2.2E-02	2.1E-02	2.1E-02	7.4E-03	3.1E+02	8.8E-03
23	3.1E+02	1.6E-01	2.1E-03	2.1E-02	2.1E-02	2.1E-03	6.0E-02	2.2E-02	2.1E-02	2.1E-02	7.4E-03	3.1E+02	8.8E-03
24	3.1E+02	1.6E-01	2.1E-03	2.1E-02	2.1E-02	2.1E-03	6.0E-02	2.2E-02	2.1E-02	2.1E-02	7.4E-03	3.1E+02	8.8E-03
29	2.0E+04	9.7E+00	2.1E-03	2.1E-02	2.7E-02	2.1E-03	1.3E+00	6.6E-01	2.1E-02	1.1E-01	8.4E-02	2.0E+04	5.7E-01
30	2.0E+04	9.7E+00	2.1E-03	2.1E-02	2.7E-02	2.1E-03	1.3E+00	6.6E-01	2.1E-02	1.1E-01	8.4E-02	2.0E+04	5.7E-01
31	2.0E+04	9.7E+00	2.1E-03	2.1E-02	2.7E-02	2.1E-03	1.3E+00	6.6E-01	2.1E-02	1.1E-01	8.4E-02	2.0E+04	5.7E-01
32	2.0E+04	9.7E+00	2.1E-03	2.1E-02	2.7E-02	2.1E-03	1.3E+00	6.6E-01	2.1E-02	1.1E-01	8.4E-02	2.0E+04	5.7E-01
35	2.0E+04	9.7E+00	2.1E-03	2.1E-02	2.7E-02	2.1E-03	1.3E+00	6.6E-01	2.1E-02	1.1E-01	8.4E-02	2.0E+04	5.7E-01
36	2.0E+04	9.7E+00	2.1E-03	2.1E-02	2.7E-02	2.1E-03	1.3E+00	6.6E-01	2.1E-02	1.1E-01	8.4E-02	2.0E+04	5.7E-01
37	2.0E+04	9.7E+00	2.1E-03	2.1E-02	2.7E-02	2.1E-03	1.3E+00	6.6E-01	2.1E-02	1.1E-01	8.4E-02	2.0E+04	5.7E-01
38	2.0E+04	9.7E+00	2.1E-03	2.1E-02	2.7E-02	2.1E-03	1.3E+00	6.6E-01	2.1E-02	1.1E-01	8.4E-02	2.0E+04	5.7E-01
39	2.0E+04	9.7E+00	2.1E-03	2.1E-02	2.7E-02	2.1E-03	1.3E+00	6.6E-01	2.1E-02	1.1E-01	8.4E-02	2.0E+04	5.7E-01
40	2.0E+04	9.7E+00	2.1E-03	2.1E-02	2.7E-02	2.1E-03	1.3E+00	6.6E-01	2.1E-02	1.1E-01	8.4E-02	2.0E+04	5.7E-01
41	2.0E+04	9.7E+00	2.1E-03	2.1E-02	2.7E-02	2.1E-03	1.3E+00	6.6E-01	2.1E-02	1.1E-01	8.4E-02	2.0E+04	5.7E-01
42	2.0E+04	9.7E+00	2.1E-03	2.1E-02	2.7E-02	2.1E-03	1.3E+00	6.6E-01	2.1E-02	1.1E-01	8.4E-02	2.0E+04	5.7E-01
43	2.0E+04	9.7E+00	2.1E-03	2.1E-02	2.7E-02	2.1E-03	1.3E+00	6.6E-01	2.1E-02	1.1E-01	8.4E-02	2.0E+04	5.7E-01
48	2.0E+04	9.7E+00	2.1E-03	2.1E-02	2.7E-02	2.1E-03	1.3E+00	6.6E-01	2.1E-02	1.1E-01	8.4E-02	2.0E+04	5.7E-01
49	2.0E+04	9.7E+00	2.1E-03	2.1E-02	2.7E-02	2.1E-03	1.3E+00	6.6E-01	2.1E-02	1.1E-01	8.4E-02	2.0E+04	5.7E-01
50	2.0E+04	9.7E+00	2.1E-03	2.1E-02	2.7E-02	2.1E-03	1.3E+00	6.6E-01	2.1E-02	1.1E-01	8.4E-02	2.0E+04	5.7E-01
51	2.0E+04	9.7E+00	2.1E-03	2.1E-02	2.7E-02	2.1E-03	1.3E+00	6.6E-01	2.1E-02	1.1E-01	8.4E-02	2.0E+04	5.7E-01

Table 3.4-10: Estimated Chemical Inventory (kg) at Closure

Tank	Ag	Al	As	B	Ba	Cd	Cl	Cr	Cu	F	Fe	Hg	I
9	5.3E+00	2.5E+03	1.4E-01	3.6E+01	2.0E+01	1.5E+01	1.0E+02	2.1E-01	1.7E+01	5.1E+00	1.4E+01	3.0E+03	4.2E+02
10	5.3E+00	2.5E+03	1.4E-01	3.6E+01	2.0E+01	1.5E+01	1.0E+02	2.1E-01	1.7E+01	5.1E+00	1.4E+01	3.0E+03	4.2E+02
11	5.3E+00	2.5E+03	1.4E-01	3.6E+01	2.0E+01	1.5E+01	1.0E+02	2.1E-01	1.7E+01	5.1E+00	1.4E+01	3.0E+03	4.2E+02
12	5.3E+00	2.5E+03	1.4E-01	3.6E+01	2.0E+01	1.5E+01	1.0E+02	2.1E-01	1.7E+01	5.1E+00	1.4E+01	3.0E+03	4.2E+02
13	5.3E+00	2.5E+03	1.4E-01	3.6E+01	2.0E+01	1.5E+01	1.0E+02	2.1E-01	1.7E+01	5.1E+00	1.4E+01	3.0E+03	4.2E+02
14	5.3E+00	2.5E+03	1.4E-01	3.6E+01	2.0E+01	1.5E+01	1.0E+02	2.1E-01	1.7E+01	5.1E+00	1.4E+01	3.0E+03	4.2E+02
15	5.3E+00	2.5E+03	1.4E-01	3.6E+01	2.0E+01	1.5E+01	1.0E+02	2.1E-01	1.7E+01	5.1E+00	1.4E+01	3.0E+03	4.2E+02
16	4.5E-01	4.6E+02	4.5E-03	9.1E+00	1.7E+00	4.7E-01	2.6E+00	2.1E-02	2.1E+00	5.9E-01	1.9E+00	1.6E+02	5.0E+01
21	1.8E+00	3.8E+01	2.5E-02	3.6E+01	3.0E+00	2.7E+00	2.0E+01	8.5E-02	4.3E+00	6.0E-01	9.0E-01	6.2E+02	4.6E+01
22	1.8E+00	3.8E+01	2.5E-02	3.6E+01	3.0E+00	2.7E+00	2.0E+01	8.5E-02	4.3E+00	6.0E-01	9.0E-01	6.2E+02	4.6E+01
23	1.8E+00	3.8E+01	2.5E-02	3.6E+01	3.0E+00	2.7E+00	2.0E+01	8.5E-02	4.3E+00	6.0E-01	9.0E-01	6.2E+02	4.6E+01
24	1.8E+00	3.8E+01	2.9E-03	3.6E+01	3.0E+00	2.7E+00	2.0E+01	8.5E-02	4.3E+00	6.0E-01	9.0E-01	6.2E+02	4.6E+01
29	8.2E+00	2.3E+03	1.5E-01	3.6E+01	2.1E+01	1.6E+01	6.8E+01	3.7E-01	2.8E+01	8.0E+00	2.8E+01	1.7E+03	6.9E+02
30	8.2E+00	2.3E+03	1.5E-01	3.6E+01	2.1E+01	1.6E+01	6.8E+01	3.7E-01	2.8E+01	8.0E+00	2.8E+01	1.7E+03	6.9E+02
31	8.2E+00	2.3E+03	1.5E-01	3.6E+01	2.1E+01	1.6E+01	6.8E+01	3.7E-01	2.8E+01	8.0E+00	2.8E+01	1.7E+03	6.9E+02
32	8.2E+00	2.3E+03	1.5E-01	3.6E+01	2.1E+01	1.6E+01	6.8E+01	3.7E-01	2.8E+01	8.0E+00	2.8E+01	1.7E+03	6.9E+02
35	8.2E+00	2.3E+03	1.5E-01	3.6E+01	2.1E+01	1.6E+01	6.8E+01	3.7E-01	2.8E+01	8.0E+00	2.8E+01	1.7E+03	6.9E+02
36	8.2E+00	2.3E+03	1.5E-01	3.6E+01	2.1E+01	1.6E+01	6.8E+01	3.7E-01	2.8E+01	8.0E+00	2.8E+01	1.7E+03	6.9E+02
37	8.2E+00	2.3E+03	1.5E-01	3.6E+01	2.1E+01	1.6E+01	6.8E+01	3.7E-01	2.8E+01	8.0E+00	2.8E+01	1.7E+03	6.9E+02
38	8.2E+00	2.3E+03	1.5E-01	3.6E+01	2.1E+01	1.6E+01	6.8E+01	3.7E-01	2.8E+01	8.0E+00	2.8E+01	1.7E+03	6.9E+02
39	8.2E+00	2.3E+03	1.5E-01	3.6E+01	2.1E+01	1.6E+01	6.8E+01	3.7E-01	2.8E+01	8.0E+00	2.8E+01	1.7E+03	6.9E+02
40	8.2E+00	2.3E+03	1.5E-01	3.6E+01	2.1E+01	1.6E+01	6.8E+01	3.7E-01	2.8E+01	8.0E+00	2.8E+01	1.7E+03	6.9E+02
41	8.2E+00	2.3E+03	1.5E-01	3.6E+01	2.1E+01	1.6E+01	6.8E+01	3.7E-01	2.8E+01	8.0E+00	2.8E+01	1.7E+03	6.9E+02
42	8.2E+00	2.3E+03	1.5E-01	3.6E+01	2.1E+01	1.6E+01	6.8E+01	3.7E-01	2.8E+01	8.0E+00	2.8E+01	1.7E+03	6.9E+02
43	8.2E+00	2.3E+03	1.5E-01	3.6E+01	2.1E+01	1.6E+01	6.8E+01	3.7E-01	2.8E+01	8.0E+00	2.8E+01	1.7E+03	6.9E+02
48	8.2E+00	2.3E+03	1.5E-01	3.6E+01	2.1E+01	1.6E+01	6.8E+01	3.7E-01	2.8E+01	8.0E+00	2.8E+01	1.7E+03	6.9E+02
49	8.2E+00	2.3E+03	1.5E-01	3.6E+01	2.1E+01	1.6E+01	6.8E+01	3.7E-01	2.8E+01	8.0E+00	2.8E+01	1.7E+03	6.9E+02
50	8.2E+00	2.3E+03	1.5E-01	3.6E+01	2.1E+01	1.6E+01	6.8E+01	3.7E-01	2.8E+01	8.0E+00	2.8E+01	1.7E+03	6.9E+02
51	8.2E+00	2.3E+03	1.5E-01	3.6E+01	2.1E+01	1.6E+01	6.8E+01	3.7E-01	2.8E+01	8.0E+00	2.8E+01	1.7E+03	6.9E+02

Table 3.4-10: Estimated Chemical Inventory (kg) at Closure (Continued)

Tank	Mn	Mo	Ni	NO ₂	NO ₃	Pb	PO ₄	Sb	Se	SO ₄	Sr	U	Zn
9	5.7E+02	3.6E+01	6.3E+01	3.5E+03	3.2E+02	5.0E+01	8.8E+00	6.0E+00	1.1E-02	4.4E+01	5.6E+00	8.8E+01	6.0E+00
10	5.7E+02	3.6E+01	6.3E+01	3.5E+03	3.2E+02	5.0E+01	8.8E+00	6.0E+00	1.1E-02	4.4E+01	5.6E+00	8.8E+01	6.0E+00
11	5.7E+02	3.6E+01	6.3E+01	3.5E+03	3.2E+02	5.0E+01	8.8E+00	6.0E+00	1.1E-02	4.4E+01	5.6E+00	8.8E+01	6.0E+00
12	5.7E+02	3.6E+01	6.3E+01	3.5E+03	3.2E+02	5.0E+01	8.8E+00	6.0E+00	1.1E-02	4.4E+01	5.6E+00	8.8E+01	6.0E+00
13	5.7E+02	3.6E+01	6.3E+01	3.5E+03	3.2E+02	5.0E+01	8.8E+00	6.0E+00	1.1E-02	4.4E+01	5.6E+00	8.8E+01	6.0E+00
14	5.7E+02	3.6E+01	6.3E+01	3.5E+03	3.2E+02	5.0E+01	8.8E+00	6.0E+00	1.1E-02	4.4E+01	5.6E+00	8.8E+01	6.0E+00
15	5.7E+02	3.6E+01	6.3E+01	3.5E+03	3.2E+02	5.0E+01	8.8E+00	6.0E+00	1.1E-02	4.4E+01	5.6E+00	8.8E+01	6.0E+00
16	2.6E+01	9.1E+00	1.1E-01	1.2E+01	4.1E+01	1.4E+00	1.1E+00	1.9E-01	1.0E-03	5.2E+00	6.8E-01	2.5E-01	5.1E-01
21	8.5E+00	3.6E+01	4.6E+01	7.2E+02	2.6E+01	1.0E+01	4.8E+01	1.1E+00	2.0E-03	3.4E+01	6.0E-01	2.2E+01	1.5E+01
22	8.5E+00	3.6E+01	4.6E+01	7.2E+02	2.6E+01	1.0E+01	4.8E+01	1.1E+00	2.0E-03	3.4E+01	6.0E-01	2.2E+01	1.5E+01
23	8.5E+00	3.6E+01	4.6E+01	7.2E+02	2.6E+01	1.0E+01	4.8E+01	1.1E+00	2.0E-03	3.4E+01	6.0E-01	2.2E+01	1.5E+01
24	8.5E+00	3.6E+01	4.6E+01	7.2E+02	2.6E+01	1.0E+01	4.8E+01	1.1E+00	2.0E-03	3.4E+01	6.0E-01	2.2E+01	1.5E+01
29	3.6E+02	3.6E+01	1.3E+02	1.3E+03	6.1E+02	3.2E+01	1.7E+01	6.5E+00	1.2E-02	7.0E+01	9.4E+00	2.3E+02	1.0E+01
30	3.6E+02	3.6E+01	1.3E+02	1.3E+03	6.1E+02	3.2E+01	1.7E+01	6.5E+00	1.2E-02	7.0E+01	9.4E+00	2.3E+02	1.0E+01
31	3.6E+02	3.6E+01	1.3E+02	1.3E+03	6.1E+02	3.2E+01	1.7E+01	6.5E+00	1.2E-02	7.0E+01	9.4E+00	2.3E+02	1.0E+01
32	3.6E+02	3.6E+01	1.3E+02	1.3E+03	6.1E+02	3.2E+01	1.7E+01	6.5E+00	1.2E-02	7.0E+01	9.4E+00	2.3E+02	1.0E+01
35	3.6E+02	3.6E+01	1.3E+02	1.3E+03	6.1E+02	3.2E+01	1.7E+01	6.5E+00	1.2E-02	7.0E+01	9.4E+00	2.3E+02	1.0E+01
36	3.6E+02	3.6E+01	1.3E+02	1.3E+03	6.1E+02	3.2E+01	1.7E+01	6.5E+00	1.2E-02	7.0E+01	9.4E+00	2.3E+02	1.0E+01
37	3.6E+02	3.6E+01	1.3E+02	1.3E+03	6.1E+02	3.2E+01	1.7E+01	6.5E+00	1.2E-02	7.0E+01	9.4E+00	2.3E+02	1.0E+01
38	3.6E+02	3.6E+01	1.3E+02	1.3E+03	6.1E+02	3.2E+01	1.7E+01	6.5E+00	1.2E-02	7.0E+01	9.4E+00	2.3E+02	1.0E+01
39	3.6E+02	3.6E+01	1.3E+02	1.3E+03	6.1E+02	3.2E+01	1.7E+01	6.5E+00	1.2E-02	7.0E+01	9.4E+00	2.3E+02	1.0E+01
40	3.6E+02	3.6E+01	1.3E+02	1.3E+03	6.1E+02	3.2E+01	1.7E+01	6.5E+00	1.2E-02	7.0E+01	9.4E+00	2.3E+02	1.0E+01
41	3.6E+02	3.6E+01	1.3E+02	1.3E+03	6.1E+02	3.2E+01	1.7E+01	6.5E+00	1.2E-02	7.0E+01	9.4E+00	2.3E+02	1.0E+01
42	3.6E+02	3.6E+01	1.3E+02	1.3E+03	6.1E+02	3.2E+01	1.7E+01	6.5E+00	1.2E-02	7.0E+01	9.4E+00	2.3E+02	1.0E+01
43	3.6E+02	3.6E+01	1.3E+02	1.3E+03	6.1E+02	3.2E+01	1.7E+01	6.5E+00	1.2E-02	7.0E+01	9.4E+00	2.3E+02	1.0E+01
48	3.6E+02	3.6E+01	1.3E+02	1.3E+03	6.1E+02	3.2E+01	1.7E+01	6.5E+00	1.2E-02	7.0E+01	9.4E+00	2.3E+02	1.0E+01
49	3.6E+02	3.6E+01	1.3E+02	1.3E+03	6.1E+02	3.2E+01	1.7E+01	6.5E+00	1.2E-02	7.0E+01	9.4E+00	2.3E+02	1.0E+01
50	3.6E+02	3.6E+01	1.3E+02	1.3E+03	6.1E+02	3.2E+01	1.7E+01	6.5E+00	1.2E-02	7.0E+01	9.4E+00	2.3E+02	1.0E+01
51	3.6E+02	3.6E+01	1.3E+02	1.3E+03	6.1E+02	3.2E+01	1.7E+01	6.5E+00	1.2E-02	7.0E+01	9.4E+00	2.3E+02	1.0E+01

3.4.5 Ancillary Equipment Inventory Estimates

Ancillary equipment includes transfer lines, transfer line secondary containment, pump tanks, PPs, a catch tank, DBs, valve boxes, and the evaporator systems. Over the operating life of the facility, radioactive waste comes in physical contact with some of these components, leaving behind varying degrees of contamination depending on the service life of the component, the material of construction, and the type of waste that contacts the component. Components that directly contacted waste material have an estimated modeling inventory and are transfer lines, pump tanks, CTS tanks, and evaporator vessels.

The ancillary equipment estimates summarized in this section are explained in further detail in SRR-CWDA-2010-00023, Rev. 3. All estimates are at 2032 date of closure.

3.4.5.1 Transfer Line Inventory Estimate

The amount of residual material in the piping systems was determined analytically. [CBU-PIT-2005-00120] The methodology in the referenced document was used for transfer lines. The transfer line inventory estimate was based on estimating the particle residuals remaining after a transfer line is flushed. For more details into the estimates methodology, refer to SRR-CWDA-2010-00023, Rev. 3.

The total radiological inventory in the transfer lines is presented in Table 3.4-11. The total chemical inventory in the transfer lines is presented in Table 3.4-12.

Table 3.4-11: Estimated Radiological Inventory (Ci) in Transfer Lines at Closure

Radionuclide	Residual Radioactivity (Ci)	Radionuclide	Residual Radioactivity (Ci)	Radionuclide	Residual Radioactivity (Ci)
Ac-227	8.2E-09	Eu-152	1.2E+00	Ra-226	1.2E-08
Al-26	9.4E-04	Eu-154	4.8E+00	Ra-228	5.3E-05
Am-241	1.1E+01	H-3	4.1E-02	Se-79	7.9E-02
Am-242m	7.6E-03	I-129	1.4E-05	Sm-151	6.0E+02
Am-243	1.7E-01	K-40	9.8E-05	Sn-126	9.2E-02
Ba-137m	4.4E+02	Nb-94	3.0E-05	Sr-90	2.1E+03
C-14	1.3E-04	Ni-59	1.3E-01	Tc-99	1.2E+00
Cf-249	7.2E-12	Ni-63	9.4E+00	Th-229	9.8E-05
Cf-251	2.5E-13	Np-237	5.7E-03	Th-230	1.5E-06
Cl-36	2.0E-04	Pa-231	4.5E-08	Th-232	6.5E-04
Cm-243	4.1E-03	Pd-107	2.0E-02	U-232	5.3E-05
Cm-244	1.3E+00	Pt-193	2.0E-02	U-233	2.6E-02
Cm-245	5.6E-04	Pu-238	8.6E+01	U-234	5.5E-03
Cm-247	1.3E-12	Pu-239	1.4E+00	U-235	7.1E-05
Cm-248	1.3E-12	Pu-240	8.1E-01	U-236	5.4E-04
Co-60	2.8E-01	Pu-241	1.7E+01	U-238	6.3E-04
Cs-135	1.3E-03	Pu-242	2.3E-03	Y-90	2.1E+03
Cs-137	4.7E+02	Pu-244	1.1E-05	Zr-93	1.0E-01

Table 3.4-12: Estimated Chemical Inventory (kg) in Transfer Lines at Closure

Chemical	Residual Mass (kg)	Chemical	Residual Mass (kg)
Ag	2.3E-01	Mn	1.1E+01
Al	3.0E+01	Mo	3.3E+00
As	5.9E-03	Ni	3.9E+00
B	3.3E+00	NO ₂	6.0E+01
Ba	5.7E-01	NO ₃	4.6E+00
Cd	6.3E-01	Pb	1.5E+00
Cl	4.1E+00	PO ₄	4.8E-01
Co	1.1E-02	Sb	2.5E-01
Cr	4.6E-01	Se	4.8E-03
Cu	1.5E-01	SO ₄	1.5E+00
F	2.7E-01	Sr	1.5E-01
Fe	8.7E+01	U	1.8E+00
Hg	9.5E+00	Zn	2.1E-01
I	3.4E-02		

3.4.5.2 Pump Tank and CTS Inventory

Pump tanks differ from piping systems with respect to such features as geometry and usage. Only residue left behind after rinsing and flushing was considered for these components. All of these pump tanks are accessible for waste removal and cleaning resulting in a very low residual inventory. The HTF has two CTS tanks. The CTS tanks are comparable in capacity to the pump tanks, thus a similar residual inventory is expected. Therefore, the source term and residual volumes are assumed the same for each pump tank and CTS tank resulting in the same estimated inventory for each. The pump tank radiological inventory is presented in Table 3.4-13 and the chemical inventory is presented in Table 3.4-14.

Table 3.4-13: Estimated Radiological Inventory in Pump Tanks and CTS Tank at Closure

Radionuclide	HPT and CTS (Ci)						
Ac-227	1.0E-11	Cm-248	3.3E-15	Pd-107	4.8E-05	Sr-90	3.0E+00
Al-26	2.3E-06	Co-60	4.2E-05	Pt-193	3.6E-05	Tc-99	3.1E-03
Am-241	2.5E-02	Cs-135	3.1E-06	Pu-238	1.8E-01	Th-229	2.4E-07
Am-242m	1.7E-05	Cs-137	7.0E-01	Pu-239	3.3E-03	Th-230	3.7E-09
Am-243	4.0E-04	Eu-152	9.5E-04	Pu-240	2.0E-03	Th-232	1.6E-06
Ba-137m	6.6E-01	Eu-154	2.1E-03	Pu-241	1.4E-02	U-232	1.0E-07
C-14	3.2E-07	H-3	3.0E-05	Pu-242	5.7E-06	U-233	6.4E-05
Cf-249	1.7E-14	I-129	3.4E-08	Pu-244	2.6E-08	U-234	1.3E-05
Cf-251	6.0E-16	K-40	2.4E-07	Ra-226	2.9E-11	U-235	1.7E-07
Cl-36	4.8E-07	Nb-94	7.2E-08	Ra-228	1.0E-08	U-236	1.3E-06
Cm-243	6.0E-06	Ni-59	3.2E-04	Se-79	1.9E-04	U-238	1.5E-06
Cm-244	1.4E-03	Ni-63	2.0E-02	Sm-151	1.2E+00	Y-90	3.0E+00
Cm-245	1.4E-06	Np-237	1.4E-05	Sn-126	2.2E-04	Zr-93	2.5E-04
Cm-247	3.2E-15	Pa-231	1.1E-10				

Table 3.4-14: Estimated Chemical Inventory in Pump Tanks and CTS Tank at Closure

Chemical	HPT and CTS (kg)	Chemical	HPT and CTS (kg)
Ag	5.7E-04	Mn	2.7E-02
Al	7.4E-02	Mo	8.0E-03
As	1.4E-05	Ni	9.5E-03
B	8.0E-03	NO ₂	1.5E-01
Ba	1.4E-03	NO ₃	1.1E-02
Cd	1.5E-03	Pb	3.6E-03
Cl	1.0E-02	PO ₄	1.2E-03
Co	2.6E-05	Sb	6.2E-04
Cr	1.1E-03	Se	1.2E-05
Cu	3.7E-04	SO ₄	3.7E-03
F	6.6E-04	Sr	3.7E-04
Fe	2.1E-01	U	4.5E-03
Hg	2.3E-02	Zn	5.1E-04
I	8.3E-05		

3.4.5.3 Evaporator System Inventory

Field characterization data for the FTF 242-F Evaporator was used to estimate the residual material in each evaporator in HTF (no field data for HTF evaporator residual material is currently available). Further details on the estimated inventories for the evaporator systems are in the HTF closure inventory document. [SRR-CWDA-2010-00023, Rev. 3] The inventories are presented in Tables 3.4-15 and 3.4-16.

Table 3.4-15: Estimated Radiological Inventory (Ci) in Evaporator Vessels at Closure

Radionuclide	Inventory in Evaporator Vessels (Ci)	Radionuclide	Inventory in Evaporator Vessels (Ci)
Am-241	3.9E-03	Pu-242	4.5E-06
Ba-137m	4.7E-01	Se-79	7.7E-09
Co-60	3.0E-05	Sr-90	2.8E-02
Cs-137	5.0E-01	Tc-99	1.3E-03
H-3	3.0E-06	U-233	1.1E-05
Np-237	3.6E-06	U-234	7.1E-06
Pu-238	4.3E-03	U-235	8.1E-08
Pu-239	1.4E-02	U-236	1.4E-07
Pu-240	3.1E-03	U-238	7.5E-06
Pu-241	1.1E-02	Y-90	2.8E-02

Table 3.4-16: Estimated Chemical Inventory (kg) in Evaporator Vessels at Closure

Chemical	Inventory in Evaporator Vessel (kg)
Ag	2.2E-04
Al	1.3E-02
As	2.0E-05
B	8.5E-05
Ba	7.4E-04
Cd	3.0E-04
Cr	2.5E-03
Cu	8.3E-04
Fe	2.2E-01
Hg	1.0E-03
Mn	8.7E-03
Mo	1.0E-03
Ni	3.0E-03
Pb	1.6E-03
Sb	8.2E-04
Se	2.0E-05
Sr	4.0E-03
U	2.2E-02
Zn	2.8E-03

3.4.5.4 Other Ancillary Equipment

The PPs are stainless steel lined reinforced concrete structures located below grade at the low points of transfer lines. These structures are secondary containments that house the pump tanks and are accessible for cleaning at the time of closure. No inventory was assigned to these structures.

There is a single catch tank in HTF designed to collect drainage from HDB-1 and the Type I tank transfer line encasements. No significant contamination has been collected in this catch tank. Therefore, no inventory was assigned to this catch tank.

The DBs are shielded reinforced concrete structures containing transfer line nozzles to which jumpers are connected in order to direct waste transfers to the desired location. The majority of DBs are located below ground and are either stainless steel lined or sealed with water proofing compounds to prevent ground contamination. These structures are accessible for cleaning at the time of closure. No inventory was assigned to these structures.

Transfer valve boxes facilitate specific waste transfers that are conducted frequently. The valves are generally manual ball valves in removable jumpers with flush water connections on the transfer lines. The valve boxes provide secondary containment. These structures are accessible for cleaning at the time of closure. No inventory was assigned to these structures.

Various ancillary equipment serves as transfer line secondary containment (e.g., transfer line jackets, LDB, encasements). No leakage of waste from primary core pipe into secondary containment has been identified. The core transfer line inner surface area is 99 % stainless steel and is not expected to corrode significantly prior to end of operations. Therefore, no inventory will be assigned to the jackets.

It is expected that ARP/MCU facilities will be completely cleaned so that no inventory remains or any contaminated components will be removed prior to the placement of the closure cap. No inventory has been assigned to these facilities.

4.0 ANALYSIS OF PERFORMANCE

The purpose of this section is to provide the technical basis for the analyses of performance for the closed HTF facilities over time based on the total remaining inventory.

Section 4.1 provides an overview of the ICM comprised of three components: 1) closure cap, 2) vadose zone, and 3) saturated zone.

Section 4.2 describes the ICM approach for contaminant release.

- 4.2.1 presents details of the source term release, the analyses performed to estimate the leaching of contaminants from the CZ by the pore fluid, based on solubility controls used for modeling the transport of contaminants from their initial closure locations within the waste tanks and ancillary equipment to the underground aquifers.
- 4.2.2 describes the assumed radionuclide transport mechanisms and parameters used for groundwater pathways modeling to estimate exposures to MOP and the inadvertent intruder for various scenarios.
- 4.2.3 defines MOP and intruder exposure pathways used for dose calculation.

Section 4.3 describes various computer codes, their purpose, and integration utilized in this PA.

Section 4.4 describes the integrated closure system, including the assumed waste tank modeling dimensions, scenarios of potential conditions of the waste tanks, and scenarios of potential conditions of ancillary equipment. The modeling processes used in PORFLOW and GoldSim are detailed in this section.

Section 4.5 describes the ICM and modeling assumptions to estimate the potential flux of gaseous radionuclides at the ground surface for the air pathway analyses. Results are provided based on the assumed inventory of radionuclides susceptible to volatilization. A radon analysis is also completed by presenting the ICM, modeling assumptions, and the results of the radon (Rn-222) surface flux analysis based on source inventories of the parent radionuclides that generate Rn-222.

Section 4.6 presents the factors for each element necessary in the biotic dose pathway model.

- 4.6.1 presents the bioaccumulation factors used in the analysis.
- 4.6.2 presents consumption rates for human health exposure.

Section 4.7 presents the internal and external Dose Conversion Factors (DCFs) utilized in the various dose pathway models.

Section 4.8 describes the risk evaluation, including the ICM and protocols for the assessment of human health and ecological risk from radioactive and chemical contaminants contained within the closed HTF.

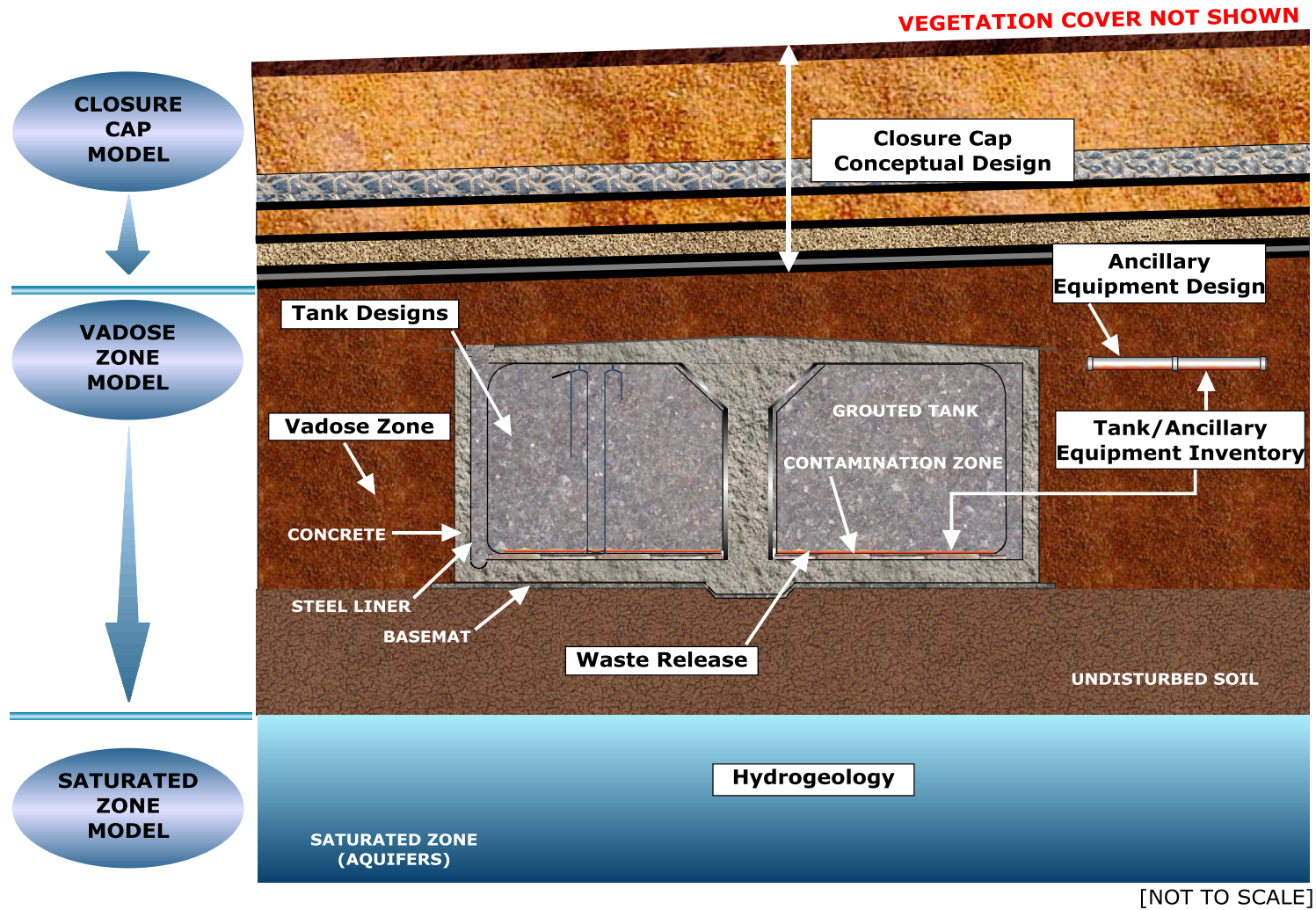
4.1 Overview of Analyses

The purpose of this section is to describe the ICM to be used for evaluating the performance of the HTF closure system during the period following closure.

This ICM is used to evaluate the migration of contaminants from the HTF and is illustrated in Figure 4.1-1. It comprises three related conceptual models that represent the HTF closure system and the environmental media through which contaminants may migrate, 1) the conceptual closure cap model, 2) the vadose zone model, and 3) the saturated zone model. This section compiles and organizes relevant data associated with these three component conceptual models to facilitate use of mathematical models to implement the ICM in the evaluation of potential HTF impacts.

The ICM described in this section is for use in simulating the release of radiological and chemical contaminants and their migration through soil and groundwater from the 29 underground waste tanks of the HTF and the associated ancillary equipment. The ancillary equipment of interest includes three evaporators, nine pump tanks, and the network of waste transfer lines in the area. The ICM focuses on contaminant migration via groundwater. The model output is used to predict effects of contaminants on human receptors through various pathways and exposure routes. Although the ICM focuses primarily on the groundwater exposure pathway, the air pathway is also taken into account (e.g., inhalation of volatile radioactive contaminants in water taken from a contaminated well or stream is accounted for in the inputs related to human receptor impacts). This section does not address inadvertent intrusion into the CZ, nor does it describe the mathematical models of the various computer codes used to implement the ICM to predict future behavior of the contaminants. Figure 4.1-1 graphically depicts the relationship between the HTF modeling inputs.

Figure 4.1-1: H-Area Tank Farm Modeling Input Relationships



4.2 Integrated Conceptual Model of Facility Performance

The ICM simulates radiological and chemical contaminant release from the 29 waste tanks and associated ancillary equipment in the HTF. An independent conceptual waste release model was used to simulate stabilized contaminant release from the grouted waste tanks based on various chemical phases in the waste tank controlling solubility and thereby affecting the timing and rate of release from the CZ.

Due to the complex nature of this model, a structured methodology is necessary to ensure that relevant components and assumptions are adequately addressed during model development. The relevant features, events, and processes (FEPs) analysis confirmed that the ICM was developed within defined boundaries and with appropriate consideration. [SRR-CWDA-2012-00044]

This ICM approach considers the integrity of the waste tank steel liners and cementitious barriers in waste tank modeling. In the ICM, steel liner failure triggers waste release from the waste tanks. After failure, the carbon steel liner is assumed to be absent, or otherwise not a hindrance to advection and diffusion.

With this approach, the time of initial waste release is tied to the integrity of the waste tank primary liners (waste tank secondary liners were assumed to fail at the same time as the primary liner). This time calculation is based on steel corrosion rates under different conditions (e.g., differing diffusion coefficients for CaO_2). The failure times varied with waste tank design, owing to differences in liner properties. [WSRC-STI-2007-00061, SRNL-STI-2010-00047] The failure analyses considered general and localized corrosion mechanisms of the waste tank steel. Consumption of the waste tank steel encased in grouted conditions was estimated due to carbonation of the concrete leading to low pH conditions, or the chloride-induced depassivation of the steel leading to accelerated corrosion. The modeling approach used for predicting steel liner failure is discussed in Section 4.2.2.2.6. Steel liner failure for four waste tanks (Type I, Tank 12 and Type II, Tanks 14, 15, and 16) does not utilize data from the liner degradation reports. Instead, these waste tanks are assumed to have liner degradation at the time of HTF closure, based on present leak site numbers and physical locations. [C-ESR-G-00003]

The time of initial waste release from the closed waste tanks was caused by through-wall thinning due to general corrosion. Since corrosion was assumed to occur uniformly, liner failure occurs when the thinnest segment has been completely corroded. Under conservative diffusion coefficient conditions (i.e., when holes from pitting begin to occur), the earliest liner failures are predicted to occur 75 years after HTF closure for the Type IV tanks. The latest liner failures were predicted to occur 12,751 years after HTF closure in the Type III and IIIA tanks, through general corrosion under grouted conditions. Prior to failure, the primary liner is considered impermeable with respect to both advection and diffusion. After failure, the liner is not a hindrance to advection and diffusion (i.e., there would be no retardation).

Flow in-to and out-of the CZ is controlled by the material properties of the waste tank cementitious materials. The expected degradation rate and timing for the waste tank cementitious materials is based on SRNL-STI-2010-00035 and SRR-CWDA-2010-00019, and can vary dependent on waste tank type. The waste tank grout can begin degrading as early as year 800 (Type IV tanks) with full degradation being reached as early as year 13,200 (Type I

tanks). The waste tank concrete can begin degrading as early as year 400 (Type IV tanks) with full degradation occurring as early as year 800 (Type IV tanks).

Soil-solute K_d s for the cementitious materials depend on pore water flow through the material. These values will increase over time in stages as the concrete ages with increasing pore water flow. The infiltrating liquid will initially be characterized as Region I, it will transition to Region II, then Region III as the pH of the liquid changes over time. Because each individual waste tank grout and concrete will be aged at the time of overall HTF closure, none of the waste tank cementitious materials were characterized as young (Region I). The differences between the chemical phases are summarized in Table 4.2-1. The waste tank concrete properties are originally characterized as Oxidizing Region II transitioning to Oxidizing Region III. The waste-tank grout properties are initially characterized as Reduced Region II, then transition to Oxidized Region II after 523 pore volumes and to Oxidizing Region III after 2,119 pore volumes. [ISSN 1019-0643, SRNL-STI-2012-00404] This aging process is directly related to flow through the grout, and is therefore accelerated when liner failure allows additional liquid to encounter the cementitious materials inside the waste tank liner.

Table 4.2-1: Summary of Chemical Phases

Chemical Phase	Description
Region I	The pH lies between approximately 13.3 and 12.5. The pore water composition is dominated by potassium, sodium, and hydroxide. The solution is saturated with respect to portlandite ($\text{Ca}(\text{OH})_2$ approximately $2.0\text{E}-03$ moles). The major solid phases present in cement have already formed, though hydration may be continuing.
Region II	Contact with “flowing” groundwater has removed virtually all of the highly soluble (potassium, sodium) hydroxide. The pore water composition is now dominated by portlandite ($\text{Ca}(\text{OH})_2$ approximately $2.0\text{E}-03$ moles) which fixes the pH at approximately 12.5. The portlandite is also being slowly removed by groundwater flow but the quantities contained in the cement are so large that this phase buffers the system over very long periods. There are no significant changes in the major solid phases present in Region I and II.
Region III	The removal of $\text{Ca}(\text{OH})_2$ has become significant and the pH falls continuously. The CSH gel is no longer stable and begins to dissolve incongruently. The Ca^2 concentration decreases continuously to approximately 1.0 to $5.0\text{E}-03$ moles at pH of approximately 11.

[ISSN 1019-0643]

The pump tanks (HPT-2 through HPT-10) and evaporators (242-H, 242-16H, and 242-25H) are modeled as point sources located in the HTF at a central point of the individual components. Transfer line inventory is modeled by distributing the assumed inventory equally over the entire HTF. Other ancillary equipment is not modeled explicitly.

Based on stainless steel corrosion rate calculations, the earliest failure of a stainless steel transfer line is predicted to occur 510 years after HTF closure. [WSRC-STI-2007-00460] Failure is assumed after 25 % pitting penetration of the transfer line wall. Predicted failure times are dependent on the thickness of the transfer lines. A more detailed discussion of ancillary equipment corrosion failure is provided in Section 4.2.2.2.6.

4.2.1 Source Term Release

The work described in this section (Section 4.2.1) is directly from the *Evolution of Chemical Conditions and Estimated Solubility Controls on Radionuclides in the Residual Waste Layer During Post-Closure Aging of High-Level Waste Tanks* (SRNL-STI-2012-00404) report.

Release of contaminants from residual waste remaining in closed waste tanks will depend on the chemical composition of pore fluids passing through the residual waste layer. The composition of these fluids will vary, causing solubilities of key radionuclides to vary, as infiltration water flows through the waste tank reducing grout. Geochemical modeling is described here that enables a flow and transport model with limited chemical capabilities to simulate this. The simplifications that allow implementation of the model are documented and justified. In the most general sense, the model assumes that the residual waste remains as a discrete layer at the bottom of the waste tanks after they are filled with reducing grout. Henceforth, this discrete layer is referred to as the residual waste layer. Infiltration from the surface or groundwater that passes through the waste tanks interacts with the grout driving changes to grout mineralogy and causing fluids emerging from the grout into the residual waste layer to have a composition that reflects these interactions. Release of contaminants from the waste tanks is controlled primarily by solubility of assumed contaminant-bearing solid phases in the varying fluid composition. Hence, this waste release model imposes chemical constraints on contaminant release that vary as the grout degrades. Varying physical controls such as hydraulic driving forces and hydraulic conductivity can be imposed by the flow and transport model that draws input from this waste release model.

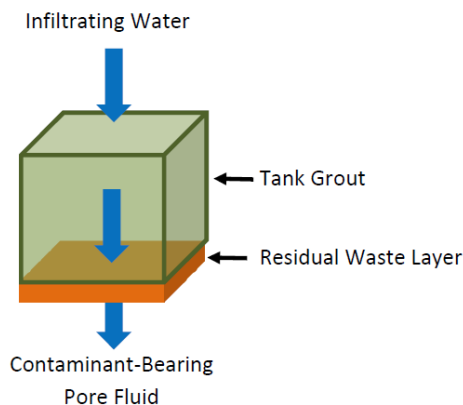
Development of the waste release model was done in two stages, the modeling of the grout degradation and the estimation of solubilities of 27 elements at the various chemical conditions suggested by the grout modeling. Of the 27 elements, neptunium, plutonium, technetium, and uranium are considered the most likely risk drivers based on process knowledge and previous PA modeling. These are given extra attention in development of the waste release model.

4.2.1.1 Simulations of Tank Grout Degradation

4.2.1.1.1 Estimated Chemical Evolution of Reducing Grout

Figure 4.2-1 shows a diagram depicting the conceptual model of waste release from HLW waste tanks. Water infiltrating through the cover system enters the grout, reacts with grout minerals, and ultimately passes through the residual waste layer beneath the grout. As reactions in the grouting progress and minerals dissolve or precipitate, the pore water chemistry exiting the grout changes. The changing pore water chemistry passing through the residual waste layer results in varying solubility of contaminants.

Figure 4.2-1: Conceptual Model of Pore Fluid Evolution and Plutonium Dissolution from the Residual Waste Layer



The simulation treats the tank grout as a porous, unsaturated medium. It is recognized that fracturing could lead to heterogeneous flow patterns and that “fast” flow paths might occur within the tank. Yet, there is very little certainty about the nature and effects of fracturing over the thousands of years of tank aging. In particular, there is uncertainty surrounding the extent to which water passing through fractures interacts with the grout and, importantly, how water that reaches the residual layer through a fracture interacts with that layer. The differing effects of fractures and fast flow paths are addressed in sensitivity analyses within the PA using information selected from the waste release model and implemented with the flow and transport modeling.

The Geochemist’s Workbench (GWB) was used to simulate the major changes in pore fluid chemistry by modeling infiltrating fluid passing through a hypothetical 1 cubic meter block of waste tank grout. The simulations were done in the “flush” mode to simulate plug flow through a porous medium. Each pore volume of fluid that enters the grout block completely replaces the previous reacted pore volume of fluid. This results in a reaction path model in which each pore volume of reacting fluid changes the mineralogy of the grout. The changes are reflected in the chemical composition of the fluid exiting the grout. The nature of this type of modeling produces step changes in the major chemical parameters of interest such as E_h and pH. These occur when a mineral that exerts the dominant control on a parameter is completely dissolved from the grout. Minor changes in these parameters may occur when a previously stable mineral begins to dissolve or a mineral begins to precipitate.

The advantage of this type of modeling is its flexibility. The only grout properties required are the mineralogy and the porosity. This frees the flow and transport model to run numerous simulations varying flow conditions without the immense computational burden of solving the equilibrium chemistry at each node.

The initial mineralogy of the hypothetical grout block was estimated from the proposed grout formulation (Table 4.2-2) using a normative calculation. The normative mineralogy is simply a way to assign the chemical components of the bulk composition of the grout to mineral phases. The actual mineralogy is unknown so representative

phases used in published cement simulations were chosen for the normative mineralogy. The effect of small deviations from these nominal values on rates of grout degradation would be small relative to the effects of other uncertainties. Chemical analyses of each of the major cementitious constituents in the formulation are shown in Table 4.2-2 along with the calculated bulk composition of the proposed grout are shown in Table 4.2-3.

Table 4.2-2: Proposed Tank 18 Grout Formulation

Grout Component	Concentrations (lb/yd ³)
Cement	125
Slag Grade 100	210
Fly Ash Class F	363
Quartz Sand	1790
Gravel No. 8	800
Water	405

Table 4.2-3: Chemical Compositions of Major Grout Constituents and Bulk Composition of Proposed Grout

Component	Cement (wt %)	Slag Grade 100 (x _B %)	Fly Ash Class F (wt %)	Proposed Grout (g/m ³)
Al ₂ O ₃	4.91	10.1	28.4	77388
CaO	64.3	35.8	1.41	95326
Fe ₂ O ₃	3.5	0.36	7.99	20252
K ₂ O	0.37	0.27	2.99	7050
MgO	0.95	12.6	1.0	18557
Na ₂ O	0.09	0.22	0.44	1288
SO ₃	2.64	1.99	0.1	4653
SiO ₂	21.0	39.1	53.1	178647

The normative mineralogy of the grout was calculated by assigning major chemical components to cementitious minerals:

- All SO₃ was assigned to gypsum (CaSO₄·2H₂O) with the requisite CaO
- All remaining CaO was assigned to JenH (Ca_{1.33}Si_{1.0}O_{3.33}·2.17H₂O) with the requisite SiO₂
- All MgO was assigned to OH-Hydrotalcite (Mg₄Al₂(OH)₁₄·2H₂O) with the requisite Al₂O₃
- All remaining Al₂O₃ was assigned to gibbsite (Al(OH)₃)
- All Fe₂O₃ into was assigned to magnetite (Fe₃O₄)
- All remaining SiO₂ was assigned to amorphous silica (SiO₂)

The alkalis were assumed to remain soluble in the pore fluid to be leached out with the first pore volume of infiltrating fluid.

The normative mineralogy is shown in Table 4.2-4. The normative mineralogy is assumed completely hydrated because of the time lag between closure cap degradation and breaching of the liner. Amorphous silica in the mineralogy represents the silica glass associated with blast furnace slag and fly ash. There is an excess of silica relative to

portlandite ($\text{Ca}(\text{OH})_2$), and thus all portlandite is assumed to react to the CSH phase JenH. Iron likely exists in several phases, but magnetite was chosen here because it is a common phase in fly ash and the portland cement has a measured reduction capacity. Nevertheless, only one gram of magnetite was put in the “Basis” mineralogy for the grout simulations so that only reduction capacity from the slag would be considered, a bias toward a shorter duration of reducing conditions. Pyrite (FeS_2) was assigned to account for this because pyrrhotite, which has been observed in various types of slag quickly oxidizes to pyrite during grout simulations.

Table 4.2-4: Calculated Normative Mineralogy of Proposed Grout and Equilibrium Mineralogy as Recalculated by GWB

Minerals in System	Normative Mineralogy (g/m^3)	Recalculated (g/m^3)
Calcite	--	2.82E-01
Ettringite	--	2.58E+04
Gibbsite	1.01E+05	9.72E+04
Gypsum	1.00E+04	--
JenH	2.15E+05	9.69E+04
TobD	--	1.21E+05
Magnetite	1.96E+04*	1.04E+00
OH-Hydrotalcite	5.10E+04	5.10E+04
SiO2	1.05E+05*	--
Pyrite	8.16E+02	8.16E+02
Inert	1.54E+06	1.54E+06

* Not used in Base Case simulation (see uncertainty section)

When setting up a simulation in GWB the normative mineralogy and pore fluid are entered into the “basis.” From this starting point, GWB recalculates the basis so that the fluid and minerals are in equilibrium. This may involve precipitation or dissolution of minerals. In the recalculated mineralogy in Table 4.2-4, a small amount of calcite and larger amounts of ettringite ($\text{Ca}_6\text{Al}_2(\text{SO}_4)_3(\text{OH})_{12}\cdot 26\text{H}_2\text{O}$) and TobD ($\text{Ca}_{0.88}\text{Si}_{0.67}\text{O}_{2.22}\cdot 1.83\text{H}_2\text{O}$) were added at the expense of carbonate in the original pore fluid and minerals containing calcium, sulfur, aluminum, and silica.

Pyrite was included in the mineralogy to account for the reducing capacity of the grout. It is important to note that pyrite is used simply as a method to account for the measured reducing capacity of the grout and is not meant to imply that grains of pyrite in the grout are the primary source of reducing capacity. To the contrary, the main source of reducing capacity is likely reduced sulfur incorporated in the silica glass of the blast furnace slag. However, this cannot be represented in the model in a way that is mechanistically true. So, a distinct solid phase, in this case pyrite, is used to account for the reducing capacity.

The reducing capacity of the grout was calculated from the amount of slag in the formulation and the measured reducing capacity of slag. This was done as described in the detailed list below.

- measured reducing capacity of slag = 819 $\mu\text{eq/g}$
- pyrite oxidation reaction: $\text{FeS}_2 + 3.75\text{O}_2 + 0.5\text{H}_2\text{O} = \text{Fe}^{+3} + 2\text{SO}_4^{-2} + \text{H}^+$
- 15 moles electrons exchanged/mole pyrite oxidized: $\text{MW}_{\text{pyrite}} = 119.967 \text{ g/mol}$
- $15/119.967 = 0.125$ moles electrons exchanged/gram pyrite oxidized
- reduction capacity of pyrite = 125,000 $\mu\text{eq/g}$
- 124,591 grams slag/ m^3 of reducing grout
- total reduction capacity = $124,591 \text{ g slag/m}^3 \text{ grout} \times 819 \mu\text{eq/g slag} = 1.02\text{E}8 \mu\text{eq/m}^3 \text{ grout}$
- total reduction capacity expressed as grams pyrite = $1.02\text{E}8 \mu\text{eq/m}^3 \text{ grout} \div 1.25\text{E}5 \mu\text{eq/g pyrite} = 816 \text{ grams pyrite/m}^3 \text{ grout}$

Other iron was left out of the mineralogy with the exception of 1 gram of magnetite to hold a place for iron in the basis.

The chemical composition of the infiltrating water that was reacted with the tank grout is shown in Table 4.2-5. It was derived by equilibrating an average rainwater composition with kaolinite and amorphous silica using GWB. This was used to simulate rainwater that had passed through soil and the closure cap. The dissolved oxygen and carbon dioxide concentrations were calculated by equilibrating this water with atmospheric oxygen ($P_{\text{O}_2} = 0.2$ atmospheres) and carbon dioxide ($P_{\text{CO}_2} = 3.2\text{E-}4$ atmospheres). It is assumed here that the pore water composition remains constant throughout the grout aging simulation. At some point, perhaps within the modeling period, the infiltration would revert to the composition of rainwater. Assuming rainwater composition in the SRS area in the future is similar to the composition, the primary difference would be lower dissolved aluminum and silica concentrations. The rainwater pH and the dissolved gas concentrations would be the same. Reaction of the infiltrating water with grout was closed with respect to atmospheric gases. A porosity of 21 % defined the pore volume of the grout block.

Table 4.2-5: Infiltrating Water Composition Used in Grout Evolution Simulations

Constituent	Concentration
pH	4.68
$\text{O}_2(\text{aq})$	$2.19\text{E-}4 \text{ mol/L}$
$\text{CO}_2(\text{aq})$	$1.07\text{E-}5 \text{ mol/L}$
Cl^-	$2.74\text{E-}5 \text{ mol/L}$
Na^+	$8.69\text{E-}6 \text{ mol/L}$
Ca^{+2}	$2.06\text{E-}6 \text{ mol/L}$
Mg^{+2}	$1.34\text{E-}6 \text{ mol/L}$
Al^{+3}	$8.43\text{E-}7 \text{ mol/L}$
$\text{H}_4\text{SiO}_4(\text{aq})$	$1.90\text{E-}3 \text{ mol/L}$
SO_4^{-2}	$1.35\text{E-}5 \text{ mol/L}$

The simulations of the chemical evolution of tank grout were run using The GWB, with some notable exceptions. The current simulations used a different set of cementitious minerals with different thermodynamic data as described in SRNL-STI-2012-00404. The PHREEQC thermodynamic database (provided with GWB as “thermo_phreeqc”) was

used as the framework to build a thermodynamic database suitable for simulations of cementitious materials. In addition to cementitious minerals, the thermodynamic data for the iron minerals pyrite, magnetite, and maghemite were updated. The minerals allowed in the simulations are shown in Table 4.2-6.

Table 4.2-6: Minerals Allowed in Simulations of Tank Grout Chemical Evolution

Brucite	Gibbsite	Monocarboaluminate
C4AH13	Gypsum	OH-Hydrotalcite
Calcite	JenD	Portlandite
Ettringite	JenH	SiO2(am)
Fe(OH) ₃ (am)	Maghemite	TobD
Fe-Ettringite	Magnetite	TobH

It should be noted that an inherent assumption in these simulations is that the minerals that make up the residual waste layer do not strongly influence the composition of the pore fluids. Gibbsite, hematite, cejkaite, calcite, a nitrated sodium aluminum silicate, and a uranyl hydrogen fluoride hydrate have been observed in Tank 18 residual waste. The hematite is assumed here to convert to magnetite prior to the tank liner breaching because of contact with the reducing grout pore fluids. The grout pore-fluids are in equilibrium with gibbsite and calcite throughout the simulation, so the presences of these in the residual waste layer do not affect the pore fluid composition. The effect of the other phases is unknown. Nonetheless, the residual waste layer is approximately 2.9 centimeters thick on average compared to the approximate 10-meter thick layer of grout above it. Hence, one pore volume of fluid passing through the grout equates to approximately 345 pore volumes of the residual waste layer (assuming a similar porosity). The mineralogy of the residual waste layer should quickly approach equilibrium with the grout pore fluids.

Figures 4.2-2 and 4.2-3 show the evolution of E_h and pH in fluids eluting from the tank grout over 2,500 pore volumes. Figure 4.2-4 shows the evolution of the mineralogy of the grout that dictates the pH and E_h transitions. A nomenclature modified to include redox aspects of the grout is used to describe the chemical evolution of the tank grout. The grout evolves through three distinct regions beginning with Reduced Region II (Figure 4.2-2). In this region, the E_h is predominantly -0.47 volts and is poised by the presence of pyrite. When pyrite is completely oxidized at pore volume 523, there is a step change to Oxidized Region II with an E_h of +0.56 volts. The mineral JenH initially controlled pH at 11.6 but is converted to TobD by 67 pore volumes of fluid reacted. Throughout the remainder of Reduced Region II and all of Oxidized Region II, TobD controls pH at a value of 11.1 (Figures 4.2-3 and 4.2-4). At pore volume 2,119, the mass of TobD is exhausted and the grout moves into Oxidized Region III. This region has an E_h of +0.68 volts and a pH of 9.2. The E_h is poised by equilibrium with dissolved oxygen and the pH is controlled by OH-hydrotalcite. An increase in dissolved inorganic carbon also occurs in Oxidized Region III as calcite begins to dissolve.

Figure 4.2-2: E_h Evolution during Simulated Grout Aging

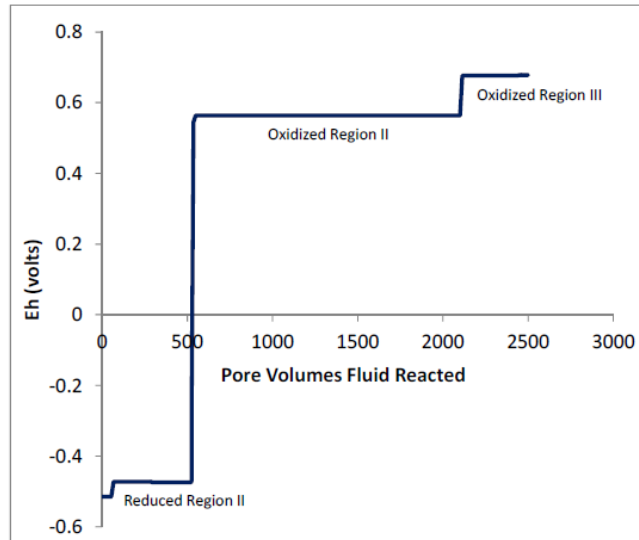


Figure 4.2-3: Simulated Evolution of pH in Grout Pore Fluids Entering Residual Waste Layer

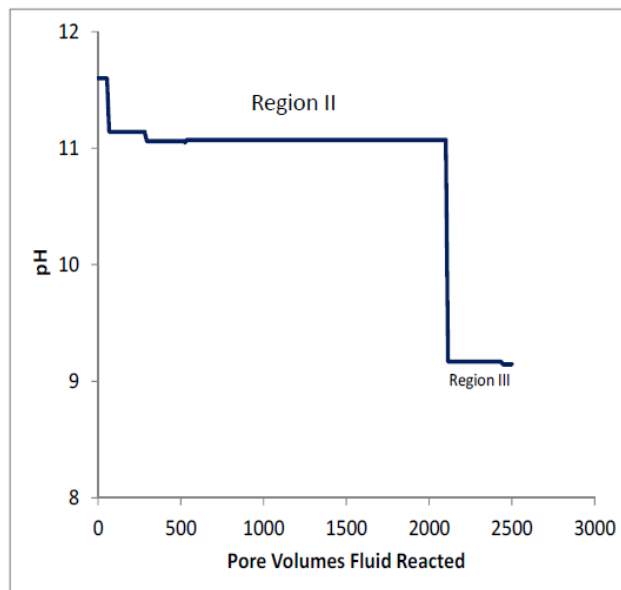
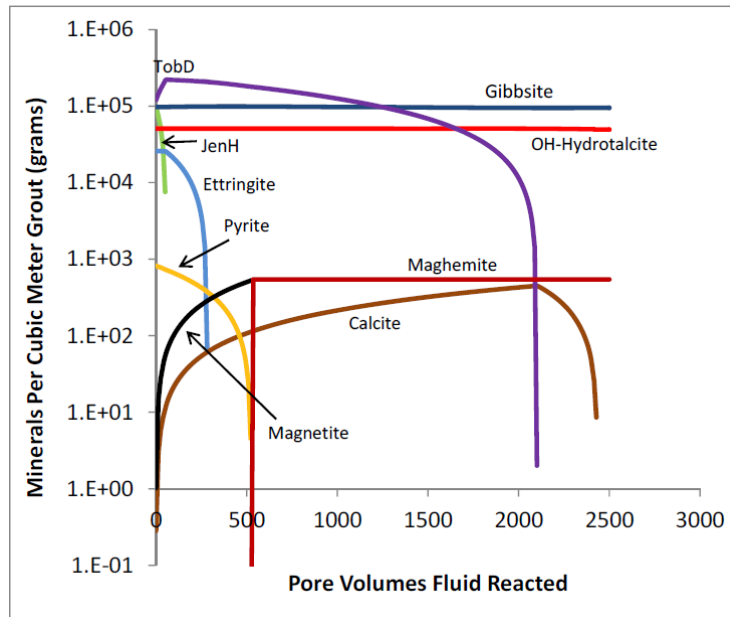


Figure 4.2-4: Simulated Evolution of Mineralogy in Tank Grout



The simulation results provide the basis for choosing chemical conditions for calculating solubility of various radionuclides throughout the PA modeling period. These are shown in Table 4.2-7.

Table 4.2-7: E_h , pH, and Dissolved Inorganic Carbon at Different Chemical Conditions during Simulated Evolution of Tank Grout

Chemical Condition	E_h (v)	pH	Ca (molar)	Total Carbonate (molar)
Reduced Region II	-0.47	11.1	4.0E-03	6.7E-07
Oxidized Region II	+0.56	11.1	4.0E-03	6.9E-07
Oxidized Region III	+0.68	9.2	6.6E-05	7.5E-05

4.2.1.1.2 Pore Fluid Conditions for Submerged Waste Tanks

For several tanks in H Area, the residual waste layer is below the water table. For the purposes of this analysis all waste tanks that have a portion of the residual waste layer at or below the water table are called “submerged tanks.” In submerged tanks, once the tank liner fails the pore fluid passing through the waste layer will be influenced by the chemistry of groundwater. For these waste tanks, it was conservatively assumed that lateral flow of groundwater through the waste tank grout would predominate over vertical flow from infiltrate. To evaluate the potential influence of groundwater on radionuclide solubility, four different chemical conditions were simulated that show varying degrees of groundwater influence. The basis for these is shown in Figure 4.2-5. The groundwater composition used (Table 4.2-8) is from a background water table well (designated P27D), approximately 450 meters east of Tank 43.

Condition A: Groundwater flows laterally directly into the residual waste layer with no effect of outer concrete.

Condition B: Groundwater equilibrates with outer concrete, assumed fully carbonated, before passing through the residual waste layer where it mixes with a small amount of Oxidized Region II grout pore fluid

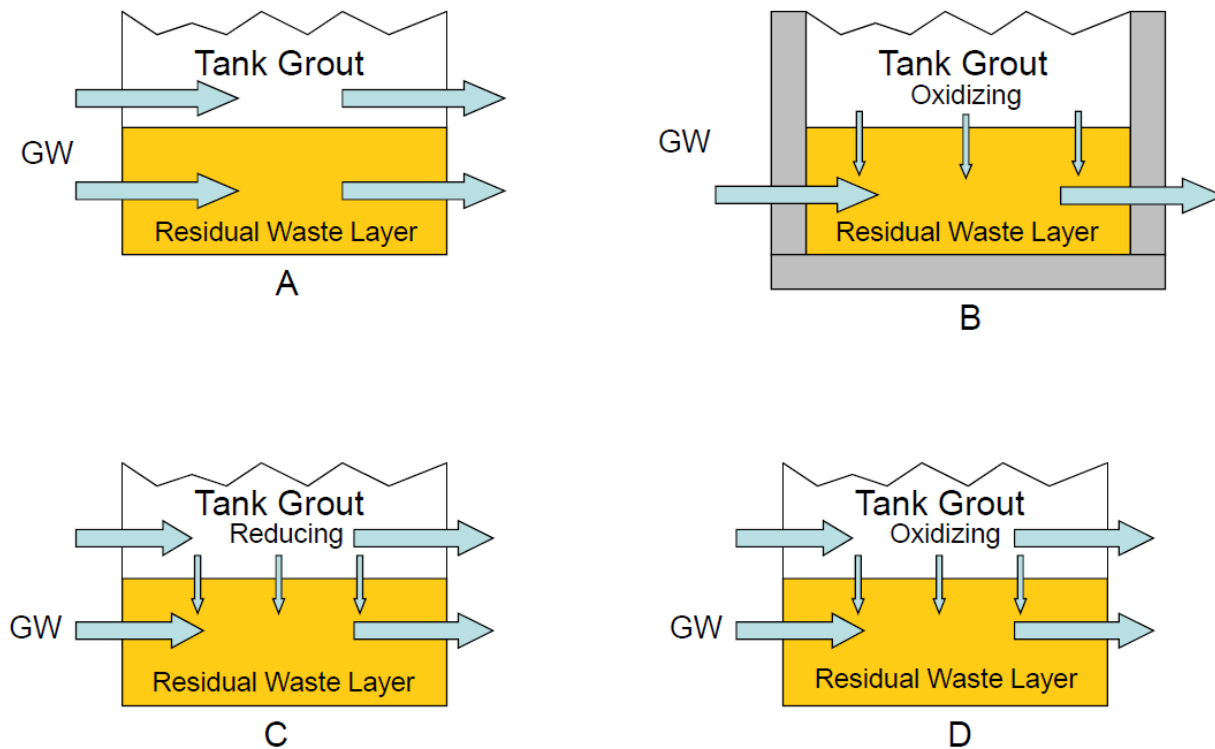
Condition C: Groundwater flows laterally directly into the residual waste layer with no effect of outer concrete and mixes with a small amount of Reducing Region II grout pore fluid

Condition D: Groundwater flows laterally directly into the residual waste layer with no effect of outer concrete and mixes with a small amount of Oxidizing Region II grout pore fluid

Table 4.2-8: Groundwater Composition Used to Mix with Grout Pore Fluids to Produce Conditions B, C, and D

Parameter	P27D Groundwater
pH	5.4
Eh (v)	0.37
Ca ⁺² (mol/L)	6.2E-05
DIC	9.8E-05
SO ₄ ⁻²	6.3E-06
Na ⁺	4.4E-05
Cl ⁻	8.5E-05

Figure 4.2-5: Basis for Four Conditions Controlling Pore Fluid Chemistry in Residual Waste Layer of Partially Submerged Waste Tanks



To calculate the compositions for Conditions B, C, and D, the GWB was used in the “Flush” mode to mix the two-endmember fluid compositions. The E_h of the Oxidizing Region II endmember was set to 0.24 volts for reasons discussed below. Mixing of compositions using E_h to represent the redox state can lead to spurious results, the endmember E_h values can be altered in the final mixing results. To overcome this, the fugacities of oxygen in equilibrium with the E_h were used to account for the redox state of the endmembers.

Figure 4.2-6 shows pH and E_h mixing curves for Conditions B, C, and D and Table 4.2-9 shows the compositions of the pore fluids for each Condition. Composition of 90 % groundwater and 10 % grout pore fluid were chosen for Conditions B, C, and D, consistent with the flow and transport modeling. Equilibrium with precipitating calcite causes similarity in pH, calcium concentrations, and dissolved inorganic carbon concentrations between Conditions B, C, and D.

Figure 4.2-6: pH and E_h Curves Resulting from Mixing End-member Pore Fluid Compositions for Conditions B, C, and D

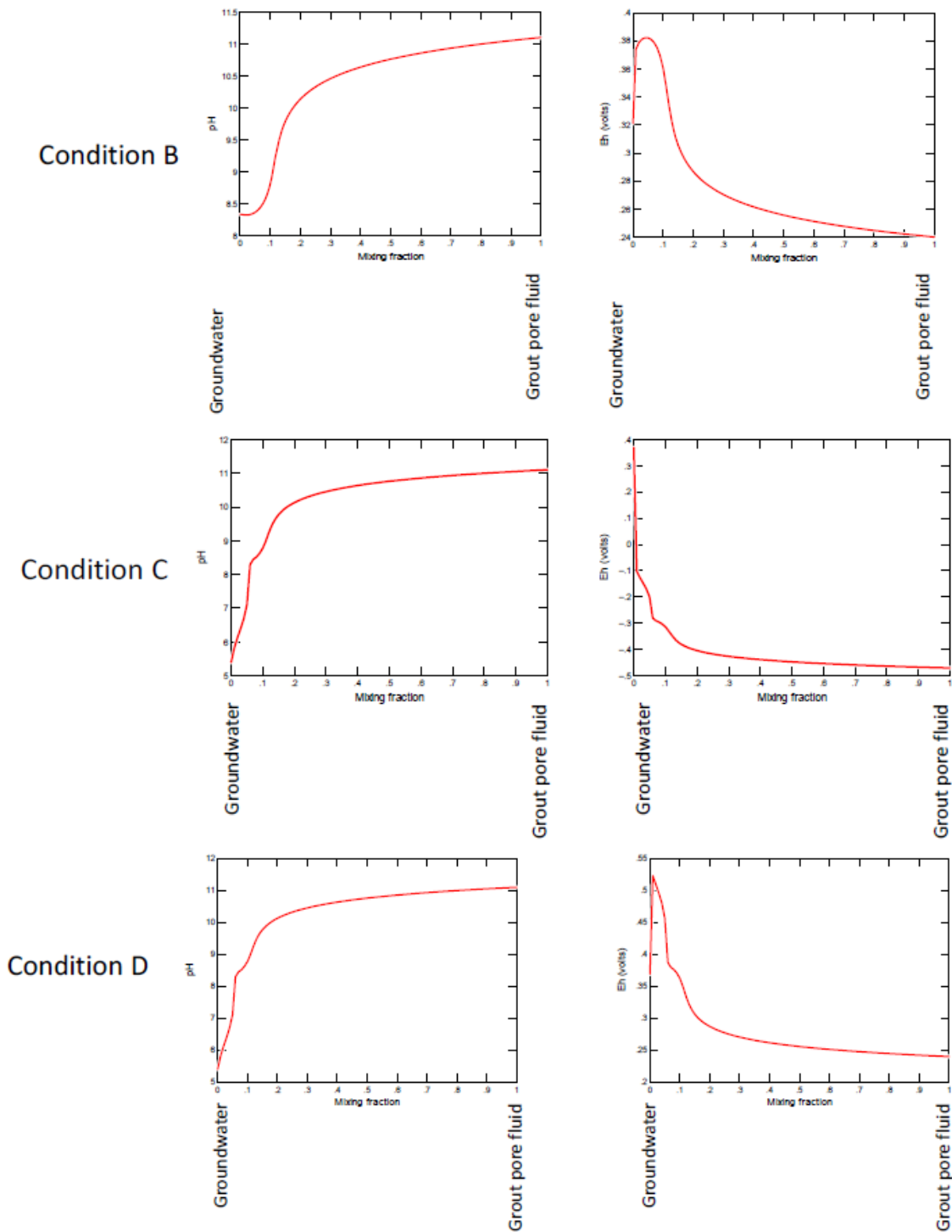


Table 4.2-9: Chemical Compositions of Contaminated Zone Pore Fluids for Conditions A, B, C, and D

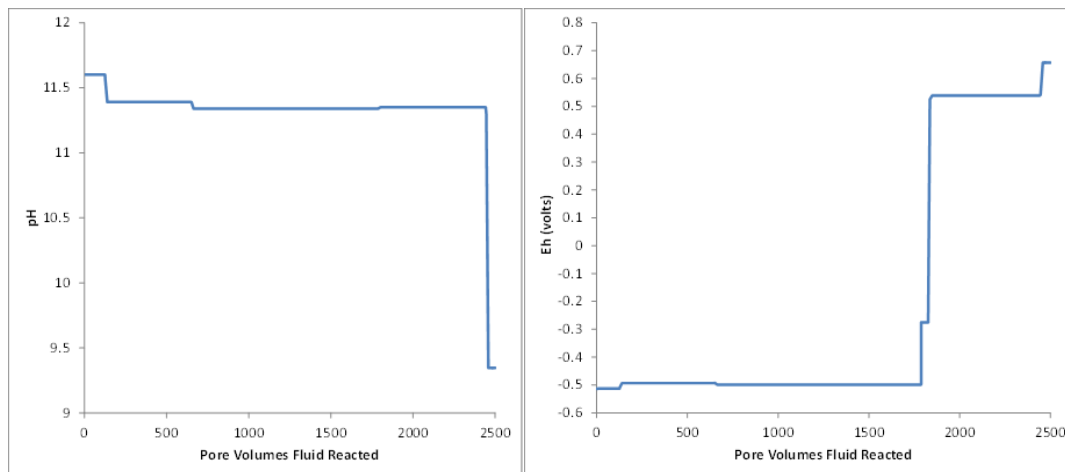
Parameter	Condition A	Condition B	Condition C	Condition D
pH	5.4	8.8	8.8	8.8
E_h (v)	0.37	0.36	-0.31	0.36
Ca^{+2} (mol/L)	6.2E-05	4.0E-04	3.9E-04	3.9E-04
DIC	9.8E-05	2.8E-05	3.2E-05	3.0E-05
SO_4^{-2}	6.3E-06	1.5E-05	2.0E-05	6.9E-06
Na^+	4.4E-05	3.9E-05	4.0E-05	4.0E-05
Cl^-	8.5E-05	8.1E-04	7.8E-04	8.0E-04

DIC dissolved inorganic carbon

4.2.1.1.3 Grout Degradation in Submerged Tanks

The evolution from one condition to another during grout degradation of the submerged tanks is not as straightforward as for the non-submerged tanks. The most probable progression would be from Condition C to Condition D to Oxidized Region III and eventually to Condition A. The number of pore volumes of infiltrating fluid used in the grout simulations was insufficient for the grout to evolve to Condition A and no specific transition is listed. Solubilities are included for Condition A for comparison to the other conditions. Grout degradation simulations were run for submerged tanks using The GWB and the same conceptual model as for the non-submerged tanks, but with a different infiltrating fluid. For these simulations, the infiltrating fluid for the non-submerged tanks was mixed with groundwater using the “Flash” mode in GWB. The mix composition for 90 % groundwater and 10 % original infiltrate was used as the grout degrading fluid. Figure 4.2-7 shows the pH and E_h transitions from the simulations. E_h transitioned from -0.47 volts to 0.54 volts after 1,826 pore-volumes. The reason for the longer transition time compared to the non-submerged tanks is the low dissolved oxygen concentration (3.8E-05 molar) in the background well nearest the HTF. The pH transitioned from 11.3 to 9.3 at 2,445 pore volumes of fluid reacted. Within the waste layer, a pore fluid composition of Condition C would be applicable to 1,826 pore volumes fluid reacted Condition D would be applicable to 2,445, followed by Oxidized Region III.

Figure 4.2-7: pH and E_h Transitions in Grout Pore Fluid as Grout Degrades in Submerged Waste Tanks



4.2.1.1.4 Uncertainties

This simulation of the chemical evolution of tank grout is meant to provide a basis for PA modeling to reflect potential changes in the solubility of radionuclides in the residual waste layer in response to evolution of the layers pore-fluid composition as tank grout ages. There is uncertainty in this approach that is primarily driven by the uncertainty regarding the physical condition of the grout at the time the liner is breached and thereafter. To date PA modeling has nominally treated the grout as a porous medium and the variable effect of fast flow paths and other phenomena have been assessed in sensitivity analyses. The simulation of the chemical evolution of waste tank grout presented here is to support flow and transport modeling of the grout as a porous medium and does not explicitly account for physical degradation of grout or heterogeneity in chemical or flow properties, including fracturing.

Uncertainty in simulations of chemical degradation of grout persists because of a lack of pertinent experimental data. Yet, it is worth considering the validity of extrapolating short-term grout degradation experiments to the very long frames of time involved in PA modeling. In a detailed study of the microfabric and chemistry of 20-year old cement blends stored at 98 % relative humidity, indications were that the blends had not yet reached “‘steady-state’ equilibrium.” Most experimental studies are done on cements aged a fraction of that time. In contrast, the grout in tanks will age at 100 % relative humidity for several hundred to thousands of years before the steel liner will be breached and radionuclides released. For these simulations, it is assumed that the grout is fully hydrated and at equilibrium and is likely to behave differently than cementitious materials in short-term laboratory experiments. Likewise, it is difficult to extrapolate results from column studies to actual flow through the tank grout. This is because the contact time with cementitious material for any aliquot of effluent in a column study is typically much shorter than the contact time infiltration will have with tank grout materials. This is not an argument against experiments, but rather a caution that it is very

difficult to extrapolate experimental results to the actual processes that will control grout degradation over very long timeframes.

There are multiple sources of uncertainty in simulating chemical degradation of the reducing tank grout. Some of these such as variations in dissolved oxygen and CO₂ in the infiltrate, thermodynamic uncertainty, and disposition of silica can be quantified. Others such as the effective reactivity of the grout minerals are difficult to quantify. Some of the assumptions used in the simulations bias the results toward shorter durations of Reduced Region II and Oxidized Region II (Conditions C and D for submerged waste tanks). Yet, quantifying the uncertainty in these durations was not attempted. Instead, rather large uncertainties were incorporated into the probabilistic analyses as bounding values. An uncertainty of $\pm 30\%$ of pore volumes was used for the duration of Reduced Region II and an uncertainty of $\pm 50\%$ was used for the duration of Oxidized Region II.

4.2.1.2 Solubility Estimations

Radionuclide solubility estimations were done using GWB. This involved selecting an appropriate thermodynamic database, selecting an appropriate solubility-controlling phase for each radionuclide, and then equilibrating these phase(s) with the fluid compositions from Tables 4.2-5 and 4.2-8.

For the elements americium, nickel, neptunium, plutonium, uranium, technetium, and thorium thermodynamic data for aqueous hydroxyl and carbonate complexes, as well as appropriate solid phases, were obtained by direct download from the Nuclear Energy Agency. The Nuclear Energy Agency is part of the Organization for Economic Co-Operation and Development and has published several thorough reviews of thermodynamic data for radionuclides and compiled internally consistent traceable datasets. The data was converted to a format suitable for use by GWB using the Gibbs free energies of the solids and aqueous complexes of interest and their associated components to calculate LogK values for dissociation constants. These were entered into the “thermo_phreeqc” database available with GWB. For the other elements, the thermodynamic database available from the Japanese Atomic Energy Agency was used. It uses Nuclear Energy Agency data for some elements but includes many more elements than the Nuclear Energy Agency database. The Japanese Atomic Energy Agency database is also well reviewed, internally consistent, and traceable. For a few specific calculations, other sources of thermodynamic data were used and these are noted in the text.

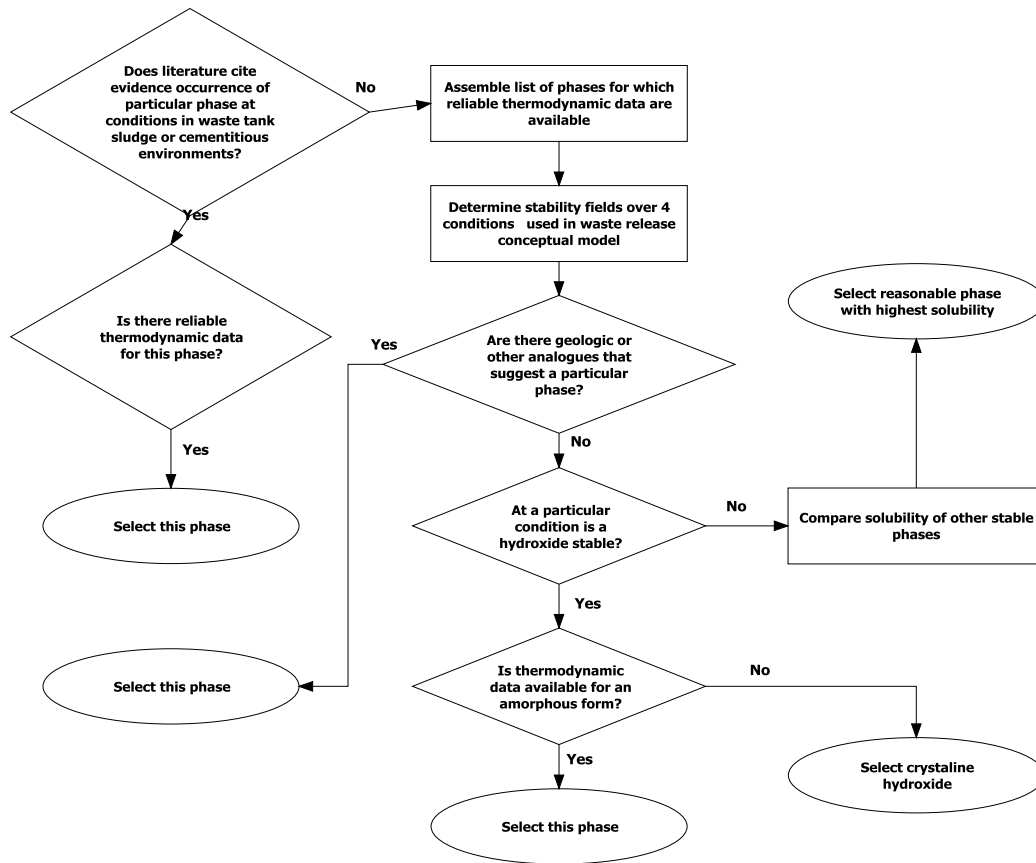
4.2.1.2.1 Selecting Solubility Controlling Phases

A fundamental part of establishing solubility controlled waste release rates is selection of a solubility-controlling phase for each radionuclide. For some of the radionuclides of interest there are studies in the literature that can guide selection of solubility controls. For other radionuclides, selection of solubility controlling phases was generally conservative, meaning that where multiple phases of a radionuclide were possible, selection was biased toward higher solubilities.

Two factors that determine the solubility of a phase, the composition, and the structure. For phases with the same composition, amorphous forms usually have higher solubilities than crystalline forms. Thus, where thermodynamic data existed, the amorphous forms were selected for solubility controls. For most, hydroxides were chosen over oxides because the hydroxide of an element usually has a higher solubility than the oxide. Carbonate phases were selected for strontium, calcium, and some trivalent species under relatively high carbonate conditions. Carbonate phases normally precipitate easily from solution and their occurrence in the grouted tanks was considered plausible.

The selection of solubility controlling phases followed the general process shown in Figure 4.2-8. For each radionuclide, the process began with an examination of the literature for occurrence of a stable phase with reliable thermodynamic data at conditions prevalent in the tanks or cementitious systems. If one was found, it was selected. If none was found, a list of other phases that contain components found in the tanks and having reliable thermodynamic data was assembled. The stability fields of these phases were examined and phases stable at conditions corresponding to those of the conceptual model were retained. If there were appropriate geologic or industrial process analogues cited in the literature, they were considered. Examples are radium sulfate and strontium carbonate. If there were no analogues cited in the literature, but the hydroxide was stable, it was retained. If reliable thermodynamic data was available for the amorphous hydroxide then it was selected. The process attempted to balance scientific knowledge with the need to be cautious and biased toward higher solubilities.

Figure 4.2-8: General Flow for Selection of Solubility Controlling Phases



4.2.1.2.2 Solubility Estimates

Solubility estimates for 16 elements were calculated using GWB by equilibrating a selected solubility-controlling phase with the composition of the pore fluid representing each chemical condition. The pore fluid compositions are listed in Table 4.2-10. Not all of the elements that were in the pore fluid compositions produced by the grout modeling were used in the solubility estimates. Therefore, the compositions listed in Table 4.2-10 are not in perfect charge balance. This was accounted for in the solubility estimates for all conditions except Condition A by adjusting the chloride concentration to achieve charge balance. Charge balance could not be achieved for Condition A by varying chloride, sulfate, or sodium. So, solubility estimates in Condition A were run without balancing charge. To test whether this made a difference, a more complete composition was used for Condition A and charge balanced using chloride. There were no significant differences in solubilities between the estimates with or without charge balance.

Table 4.2-10: Pore Fluid Compositions Used for Solubility Estimates for Each Chemical Condition

Parameter	Red. Reg. II	Ox. Reg. II	Ox. Reg. III	Condition A	Condition B	Condition C	Condition D
pH	11.1	11.1	9.2	5.4	8.8	8.8	8.8
E _h (volts)	-0.47	0.24	0.29	0.37	0.36	-0.31	0.36
Ca ⁺² (molar)	4.0E-03	4.0E-03	6.6E-05	6.2E-05	4.0E-04	3.9E-04	3.9E-04
DIC	6.7E-07	6.9E-07	7.5E-05	9.8E-05	2.8E-05	3.2E-05	3.0E-05
SO ₄ ⁻²	1.0E-05	1.0E-05	1.0E-05	6.3E-06	1.5E-05	2.0E-05	6.9E-06
Na ⁺	1.0E-03	1.0E-03	1.0E-03	4.4E-05	3.9E-05	4.0E-05	4.0E-05
Cl ⁻	1.0E-03	1.0E-03	1.0E-03	8.5E-05	8.1E-04	7.8E-04	8.0E-04
Oxalate	4.1E-06	4.1E-06	4.4E-05	4.2E-05	9.5E-06	9.5E-06	9.5E-06

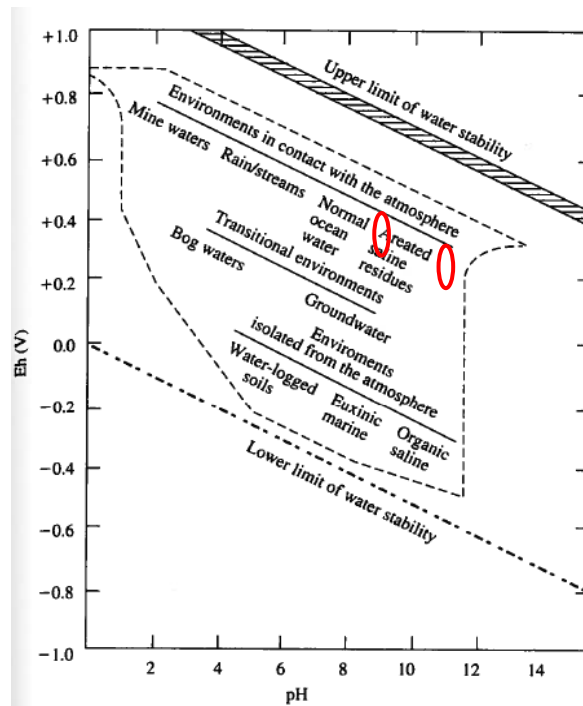
DIC dissolved inorganic carbon

For relatively soluble elements, here defined as greater than 1E-05 mol/L, a different approach was used for calculating solubilities. Rather than equilibrating a solubility-controlling phase with a pore fluid composition, the element was added to the pore fluid composition until saturation with a controlling phase was reached.

4.2.1.2.3 E_h Values Used in Solubility Estimates

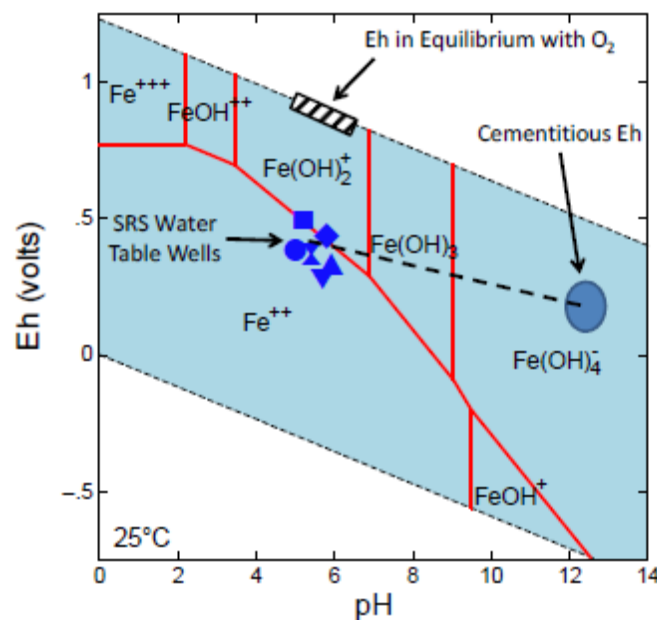
In the grout degradation simulations the E_h at oxidizing conditions is controlled by equilibrium with the dissolved oxygen. Yet, E_h values of natural waters are rarely in equilibrium with dissolved oxygen despite being exposed to oxygenated groundwater for thousands of years. This may be due to predominantly slow reaction kinetics for oxidation by dissolved oxygen. Figure 4.2-9 shows E_h-pH regimes for different types of natural waters. The added red ovals are at pH values of approximately 9.2 and 11.1 and suggest the range of E_h values that would be reasonable for calculating solubilities at these pH values. The disparity between measured E_h and that in equilibrium with dissolved oxygen is also observed in SRS groundwater. Measurements of the groundwater E_h from six water table wells are shown on an E_h-pH diagram in Figure 4.2-10. The E_h values are lower than would be expected for equilibrium with dissolved oxygen (crosshatched region) and their position suggests they reflect the ferric-ferrous iron couple. Others have suggested that E_h values used for modeling metal solubility and speciation in cements at pH = 12.5 should be near + 0.2 volts, rather than the + 0.48 volts that would be in equilibrium with dissolved oxygen. It has been reported that E_h values of ordinary portland cement should be between 0 and + 0.1 volts. Likewise, E_h values for a West Valley grout measured approximately + 0.15 volts. Therefore, it is reasonable to assume that E_h values controlling solubility in the oxidized regions simulated here would be lower than those resulting from the grout simulations (i.e., lower than equilibrium with the dissolved oxygen).

Figure 4.2-9: E_h -pH Diagram Showing Typical Regimes for Various Natural Waters



Note Red ovals are overlaid to suggest the range of realistic E_h values for calculating solubilities in Oxidized Region II and III.

Figure 4.2-10: E_h -pH Diagram Showing E_h of SRS Background Water Table Wells in Relation to Iron Speciation



Here, E_h values of + 0.24 and + 0.29 volts were chosen for Oxidized Regions II and III. This was based on extrapolating the groundwater values from Figure 4.2-10 to the appropriate pH values of 11.1 and 9.2 along a line intersecting the point pH = 12.5, E_h = + 0.2 volts.

4.2.1.2.4 Oxalate in the Residual Waste

Washing the waste tank with oxalic acid is the baseline for tank closure. The oxalate ion can chelate some radionuclides, enhancing their solubility. Thus, oxalate was considered in the estimates of contaminant solubilities. An oxalate concentration of 1,000 mg/L was measured in the final wash Tank 5F. However, calcium oxalate has a relatively low solubility and will control the solubility of oxalate in the calcium-rich pore fluids associated with the waste tank grout. Thus, the solubility of calcium oxalate was estimated for each pore fluid condition by equilibrating it with the composition of the various pore fluids using GWB. Table 4.2-10 lists the pore fluid compositions, including oxalate, used for solubility estimates at each chemical condition.

4.2.1.2.5 Estimated Solubilities

Table 4.2-11 shows solubility values and controlling phases for all of the elements of interest at each of the chemical states of interest. Several of the elements have either a very small inventory or a short half-life and are unlikely to be an issue at exposure points. In addition, some of the elements have no identified solubility controls and it is recommended that their release be modeled as instantaneous (within the first pore volume). Solubilities for six conditions are shown because the composition of the Condition B pore fluid is so similar to that of Condition D that only solubilities for Condition D are reported.

Table 4.2-11: Calculated Solubility and Controlling Phases of Radionuclides of Interest

Element	Reduced Region II		Oxidized Region II	
	Controlling Phase	Solubility (mol/L)	Controlling Phase	Solubility (mol/L)
Ac	Ac(OH) ₃ (am)	1E-09	Ac(OH) ₃ (am)	1E-09
Am	Am(OH) ₃ (am)	1E-09	Am(OH) ₃ (am)	1E-09
Ba	BaSO ₄ (barite)	3E-05	BaSO ₄ (barite)	3E-05
Bk	Short half-life	-	Short half-life	-
C	CaCO ₃ (calcite)	2E-06	CaCO ₃ (calcite)	2E-06
Cf	Small inventory	-	Small inventory	-
Cm	Cm(OH) ₃ (am)	1E-09	Cm(OH) ₃ (am)	1E-09
Co	CoS (beta)	3E-02	No solubility control	-
Cs	No solubility control	-	No solubility control	-
Eu	Eu(OH) ₃ (am)	8E-07	Eu(OH) ₃ (am)	8E-07
I	No solubility control	-	No solubility control	-
Nb	No solubility control	-	No solubility control	-
Ni	NiS (c, alpha)	2E-09 ¹	Ni(OH) ₂ (beta)	1E-07
Np	NpO ₂ (am, hyd)	1E-09	NpO ₂ (am, hyd)	3E-07
Pa	No solubility control	-	No solubility control	-
Pu	PuO ₂ (am, hyd)	3E-11	PuO ₂ (am, hyd)	3E-11
Ra	RaSO ₄	3E-05	RaSO ₄	3E-05
Rh	Short half-life	-	Short half-life	-
Se	FeSe ₂ (cr)	2E-05	No solubility control	-
Sm	Sm(OH) ₃ (am)	1E-09	Sm(OH) ₃ (am)	1E-09
Sn	SnO ₂ (am)	4E-04	SnO ₂ (am)	4E-04
Sr	SrCO ₃ (strontianite)	3E-03	SrCO ₃ (strontianite)	3E-03
Tc	TcO ₂ · 1.6H ₂ O	1E-08	No solubility control	-
Te	Short half-life	-	Short half-life	-
Th	ThO ₂ (am, hyd, aged)	1E-09	ThO ₂ (am, hyd, aged)	1E-09
U	UO ₂ (am, hyd)	5E-09	UO ₃ · 2H ₂ O	5E-05
Y	Y(OH) ₃ (c)	4E-13 ²	Y(OH) ₃ (c)	4E-13 ²
Element	Oxidized Region III		Condition A	
Ac	Ac(OH) ₃ (am)	6E-08	No solubility control	-
Am	Am(OH) ₃ (am)	2E-09 ³	AmOHCO ₃	3E-04
Ba	BaSO ₄ (barite)	1E-05	BaCO ₃ (Witherite)	3E-05
Bk	Short half-life	-	Short half-life	-
C	CaCO ₃ (calcite)	1E-03	No solubility control	-
Cf	Small inventory	-	Small inventory	-
Cm	CmCO ₃ OH · 0.5H ₂ O (c)	2E-09	Cm(OH) ₃	3E-04
Co	No solubility control	-	No solubility control	-
Cs	No solubility control	-	No solubility control	-
Eu	EuOHCO ₃ (cr)	3E-08	Eu ₂ (CO ₃) ₃ · 8H ₂ O	2E-03
I	No solubility control	-	No solubility control	-
Nb	No solubility control	-	No solubility control	-
Ni	NiCO ₃ (c)	1E-05	No solubility control	-
Np	NpO ₂ (am, hyd)	2E-06	NpO ₂ (am, hyd)	3E-05
Pa	No solubility control	-	No solubility control	-

**Table 4.2-11: Calculated Solubility and Controlling Phases of Radionuclides of Interest
(Continued)**

Element	Oxidized Region III		Condition A	
	Controlling Phase	Solubility (mol/L)	Controlling Phase	Solubility (mol/L)
Pu	PuO ₂ (am, hyd)	3E-11	PuO ₂ (am, hyd)	2E-10
Ra	RaSO ₄	1E-05	RaSO ₄	3E-05
Rh	Short half-life	-	Short half-life	-
Se	No solubility control	-	No solubility control	-
Sm	SmCO ₃ OH·0.5H ₂ O (c)	2E-09	SmCO ₃ OH·0.5H ₂ O	3E-04
Sn	SnO ₂ (am)	7E-07	SnO ₂ (am)	3E-08
Sr	SrCO ₃ (strontianite)	1E-04	No solubility control	-
Tc	No solubility control	-	No solubility control	-
Te	Short half-life	-	Short half-life	-
Th	ThO ₂ (am, hyd, aged)	1E-09	ThO ₂ (am, aged)	2E-05
U	UO ₃ ·2H ₂ O	4E-06	UO ₃ ·2H ₂ O	4E-05
Y	Y(OH) ₃ (c)	2E-09	No solubility control	-
Element	Condition C		Condition D	
Ac	Ac(OH) ₃ (am)	2E-07	Ac(OH) ₃ (am)	2E-07
Am	AmCO ₃ OH·0.5H ₂ O	4E-09	AmCO ₃ OH·0.5H ₂ O	4E-09
Ba	BaSO ₄	7E-06	BaSO ₄	2E-05
Bk	Short half-life	-	Short half-life	-
C	CaCO ₃ (calcite)	4E-04	CaCO ₃ (calcite)	4E-04
Cf	Small inventory	-	Small inventory	-
Cm	CmCO ₃ OH·0.5H ₂ O	4E-09	CmCO ₃ OH·0.5H ₂ O	4E-09
Co	beta-CoS	1E-04	No solubility control	-
Cs	No solubility control	-	No solubility control	-
Eu	EuOHCO ₃ (c)	3E-08	EuOHCO ₃ (c)	4E-08
I	No solubility control	-	No solubility control	-
Nb	No solubility control	-	No solubility control	-
Ni	alpha-NiS	6E-11	beta-Ni(OH) ₂	6E-07
Np	NpO ₂ (am, hyd)	1E-09	NpO ₂ (am, hyd)	2E-05
Pa	No solubility control	-	No solubility control	-
Pu	PuO ₂ (am, hyd)	3E-11	PuO ₂ (am, hyd)	3E-11
Ra	RaSO ₄	7E-06	RaSO ₄	2E-05
Rh	Short half-life	-	Short half-life	-
Se	FeSe ₂	5E-08	No solubility control	-
Sm	SmCO ₃ OH·0.5H ₂ O	4E-09	SmCO ₃ OH·0.5H ₂ O	4E-09
Sn	SnO ₂ (am)	3E-07	SnO ₂ (am)	3E-07
Sr	SrCO ₃ (strontianite)	1E-03	SrCO ₃ (strontianite)	1E-03
Tc	No solubility control	-	No solubility control	-
Te	Short half-life	-	Short half-life	-
Th	ThO ₂ (am, aged)	1E-09	ThO ₂ (am, aged)	1E-09
U	UO ₂ (am)	4E-09	UO ₃ ·2H ₂ O	2E-06
Y	Y(OH) ₃	1E-08	Y(OH) ₃	1E-08

1 An alternate value is 1E-07 mol/L because NiS (alpha) is sensitive to E_h in Reduce Region II

2 Note the Y-90 is the yttrium isotope of concern and its transport is controlled by the transport and decay of Sr-90

3 An alternative value is 6E-08 mol/L for Am(OH)³ (am) as the controlling phase

4 For technetium, iron co-precipitated solubilities from Table 4.2-14 were used for deterministic modeling

4.2.1.2.6 Solubilities of Neptunium, Plutonium, and Uranium at E_h in Equilibrium with Dissolved Oxygen

Table 4.2-12 shows the estimated solubilities and controlling phases for neptunium, plutonium, and uranium for E_h values in equilibrium with dissolved oxygen in Oxidized Regions II and III. Plutonium is the only one significantly affected by the assumption that E_h is not in equilibrium with dissolved oxygen.

Table 4.2-12: Estimated Solubilities of Neptunium, Plutonium, and Uranium in Oxidized Regions II and III at E_h Values in Equilibrium with Dissolved Oxygen

Element	Oxidized Region II		Oxidized Region III	
	Phase	Solubility (mol/L)	Phase	Solubility (mol/L)
Np	NpO ₂ OH (am, aged)	7E-07	NpO ₂ OH (am, aged)	5E-05
Pu	PuO ₂ (am, hyd)	5E-08	PuO ₂ (am, hyd)	8E-08
U	UO ₃ ·2H ₂ O	6E-05	UO ₃ ·2H ₂ O	4E-06

4.2.1.2.7 Apparent Solubilities for Coprecipitated Elements

The term coprecipitated here includes radionuclides bound in the crystal lattice of solid iron phases and mixed with iron phases such that the access of pore fluids to the plutonium is occluded by the host phase. Technetium is very soluble at the conditions of waste tank washing, and thus it is suspected that technetium that remains in the residual waste after the washing process is co-precipitated with iron or other phases. Several studies provide evidence of technetium co-precipitated with iron phases. A significant fraction of Tc-99 in Hanford Site waste tank sludge was observed to be relatively insoluble, 20 % in one sample and 80 % in another, and that the insoluble Tc-99 was correlated with iron oxides in selective extraction experiments. It was also observed that technetium co-precipitated with ferric iron phases in Hanford Site tank waste. They conducted experiments with perrhenate, an analogue for pertechnetate, under Hanford Site tank sludge conditions and concluded that up to 14 % of the Tc-99 in waste tank sludges may be irreversibly sorbed, possibly coprecipitated, in iron and aluminum solids. It was also hypothesized that Tc-99 was removed from solution during titration experiments of acidic groundwater by co-precipitation with iron and aluminum phases.

There is indirect evidence to suggest that plutonium would be coprecipitated with iron phases. Co-precipitation with ferric iron phases has been the basis for various methods of removal of plutonium from solution. Site-specific evidence is presented in a review of F-Area Tank 18 history and chemistry. It is likely that a portion of plutonium remaining in the residual waste after cleaning is coprecipitated.

There is also evidence in the literature that neptunium may readily coprecipitated with ferric iron oxides. It was found that Np(V) and Np(VI) sorb strongly to ferric oxyhydroxides at high pH, while Np(IV) forms true mixed oxide co-precipitates. If neptunium sorbed strongly to ferric iron phases as they formed, and these particles settled to the bottom of the waste tanks to form a lithified heel, the neptunium would be effectively co-precipitated. Its release to pore fluids would require dissolution of the ferric iron phases. Likewise, it was observed that Np(IV) sorbed strongly on magnetite in anaerobic conditions, while Np(V) sorbed strongly to hematite under aerobic conditions.

An apparent solubility of a coprecipitated radionuclide can be estimated if it is assumed that a coprecipitated radionuclide would be released as the host iron phase dissolved at the same molar X:Fe ratio at which it exists in the solid. Molar ratios of neptunium, plutonium, technetium, and uranium in HTF waste tanks were calculated from the estimated final inventories. These and the solubilities of an assumed host iron phase were used to estimate apparent solubilities for neptunium, plutonium, technetium, and uranium. A similar method was used to calculate release of Tc-99 from an iron phase.

The iron phases used here to estimate the apparent solubility of co-precipitated plutonium throughout the post-closure aging of the waste tanks are magnetite (Fe_3O_4) and maghemite (Fe_2O_3). Tank 18 residual waste samples X-ray diffraction analysis shows that hematite is a dominant iron phase in the tank today. For the grout simulations presented here it is assumed that exposure to reducing pore fluids after closure, but before the liner is breached, would convert the hematite to magnetite. Magnetite is assumed prevalent in Reducing Region II and oxidizes to maghemite at the transition to Oxidized Region II. Hematite could be assumed prevalent in Oxidized Region II and III, but maghemite is a more likely oxidation product of magnetite because of their similar crystal structures. In addition, maghemite is more soluble than hematite and biases the apparent solubilities of plutonium to higher values.

The solubilities of magnetite and maghemite were calculated at the chemical conditions of Reduced Region II, Oxidized Region II, and Oxidized Region III using The GWB. Thermodynamic data for magnetite was obtained from the HATCHES database. For comparison, the solubility of magnetite using a value for logK from the HATCHES Version 7 database was slightly higher ($6.8\text{E}-06$ versus $4.0\text{E}-06$) than that GWB. The value from the HATCHES database was used because it is expected to be more consistent with the Nuclear Energy Agency thermodynamic data. Neither the HATCHES nor the Nuclear Energy Agency databases contain data for maghemite. Thus, the thermodynamic data for this phase was obtained from the HATCHES Version 7 database. Table 4.2-13 shows the solubility of the iron host phase and Table 4.2-14 shows the estimated apparent solubilities of neptunium, plutonium, technetium, and uranium.

Table 4.2-13: Solubility of Host Iron Phases the Pore Fluids of the Different Chemical Conditions

Condition	Phase	Fe Solubility (mol/L)
Reducing Region II	Magnetite	7.30E-11
Oxidized Region II	Maghemite	7.10E-10
Oxidized Region III	Maghemite	1.40E-11
Condition A	Maghemite	1.11E-08
Condition C	Magnetite	2.27E-08
Condition D	Maghemite	8.54E-12

Table 4.2-14: Apparent Solubilities (mol/L) of Potentially Coprecipitated Elements

Condition	Pu	Np	U	Tc ^a
Reducing Region II	8E-13	5E-15	2E-12	1E-14
Oxidized Region II	7E-12	4E-14	2E-11	1E-13
Oxidized Region III	2E-13	9E-16	5E-13	2E-15
Condition A	2E-10	3E-13	9E-11	1E-12
Condition C	3E-10	6E-13	2E-10	3E-12
Condition D	1E-13	2E-16	7E-14	1E-15

a Iron co-precipitated solubility for technetium used in deterministic modeling

4.2.1.2.8 Uncertainties in Solubility Estimates

Several sources contribute to uncertainty in the solubility estimates presented here. Uncertainty in the thermodynamic data and choice of solubility controlling phase are inherent to any solubility estimate. Uncertainty in the solubility-controlling phase primarily reflects lack of available information on kinetics of nucleation and is the reason the choices here are mostly biased toward higher solubilities. Most other sources relate to the uncertainty in the chemical conditions of the fluid in which the solubility-controlling phase is dissolving. This section presents some of these uncertainties and their effect on solubility values. The first subsection examines uncertainty in solubilities of neptunium, plutonium, uranium, and technetium introduced by uncertainty in the thermodynamic data. The following subsection summarizes sensitivities to choice of controlling phase, pH, E_h , dissolved inorganic carbon, and oxalate for each element.

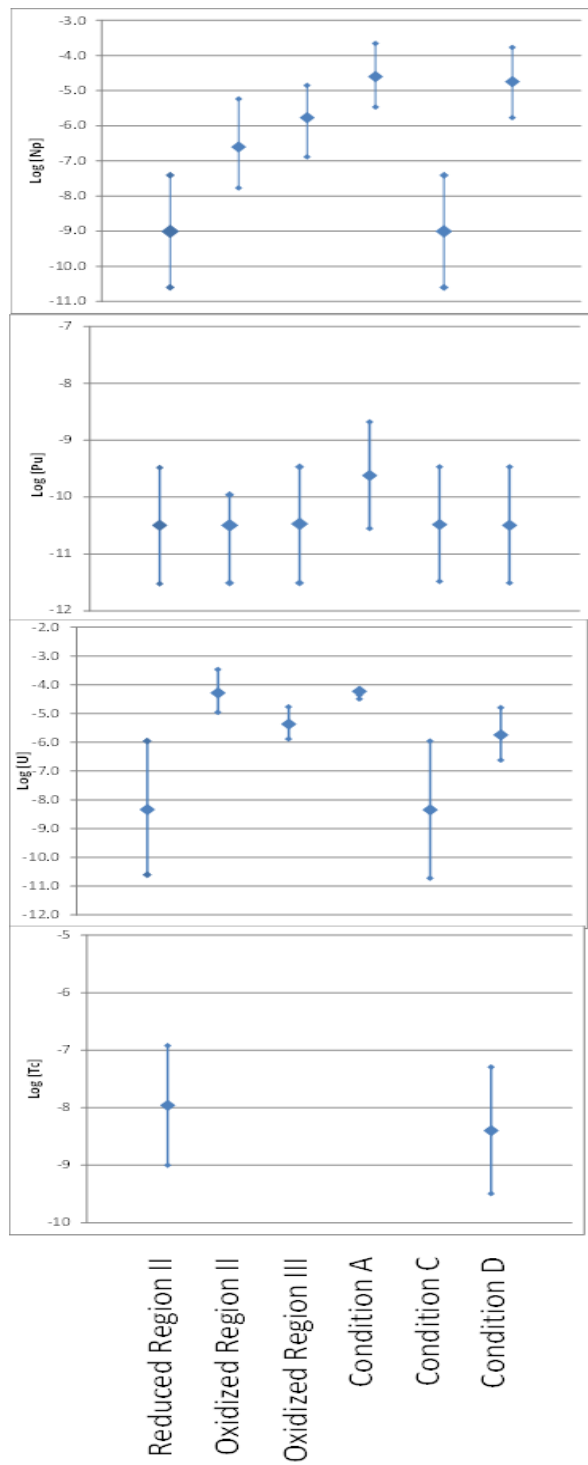
Thermodynamic Data

Uncertainty in thermodynamic data is the product of uncertainty in experimental results from which the thermodynamic data is derived. In many cases, equilibrium constants for aqueous species and solid phases are estimated from measurement of an equilibrium constant of a related entity. In these cases, uncertainty is introduced by the estimation method. For the Nuclear Energy Agency database, uncertainties for all reactions were estimated from evaluation of the experimental data by the Nuclear Energy Agency.

Four elements, neptunium, plutonium, uranium, and technetium, are considered most likely to contribute to significant doses based on inventories, knowledge of their behavior, and previous PA modeling. Uncertainties in the solubilities for these were estimated here using the uncertainties listed by the Nuclear Energy Agency for the formation reactions of the solubility-controlling phase and the dominant aqueous species. The dominant aqueous species were defined from the solubility runs of GWB as the species with the highest concentrations and those with concentrations within an order of magnitude of the highest. Solubility runs were then done in which the equilibrium constants of the formation reactions for the controlling solid and the aqueous species were varied in opposite directions by the uncertainty listed by the Nuclear Energy Agency for each reaction. In other words to estimate the maximum solubility within the uncertainty, the solid phase was made less stable and the dominant aqueous species were made more stable. The opposite was done to estimate the minimum solubility. This gives a range that can be considered the maximum uncertainty in solubility.

Uncertainties were estimated for the four elements in the six different pore fluid compositions and are shown in Figure 4.2-11. In general, the uncertainties are between 1 and 2 orders of magnitude. The uncertainties in solubilities for other elements addressed in this report are probably similar, though uncertainties for elements that have a long history of experiments may be less.

Figure 4.2-11: Uncertainty in Solubility Estimations for Neptunium, Plutonium, Uranium, and Technetium under the Six CZ Pore Fluid Conditions



Additional Sources of Solubility Uncertainty

There is uncertainty associated with the composition of the pore fluids in Table 4.2-10 contacting the residual waste as the tanks age, which introduces uncertainty into the solubility estimates. Solubilities may be particularly sensitive to pH, E_h , dissolved inorganic carbon, and oxalate concentration. The sensitivities of neptunium, plutonium, uranium, and technetium solubilities to these parameters were examined using diagrams that plot the solubility of a controlling phase against the parameter of interest. Some general trends observed are:

- In reducing conditions technetium is the only element that is sensitive to pH - increased pH causes increased solubility
- In oxidizing conditions neptunium and uranium are sensitive to pH
- For neptunium, plutonium, technetium, and uranium, E_h changes produce near step changes in solubility
 - For neptunium, plutonium, and uranium in reduced phases, as E_h increases to a threshold value and over a narrow range of E_h the solubility of the reduced phase increases and a more soluble oxidized phase becomes stable
 - For technetium at E_h values greater than the threshold value, solubility increases over a narrow E_h range to a point where no solubility control is exerted
- Pu(IV) is insensitive to E_h up to values of $E_h = +0.45$ volts in Region II conditions
- Np(IV) is insensitive to E_h up to values of $E_h = +0.10$ volts
- The elements are most sensitive to dissolved inorganic carbon in Oxidized Region III and Condition A pore fluids
- Uranium is most sensitive to oxalate concentrations
- Neptunium is sensitive in oxidized regions at oxalate concentration greater than used for estimating solubilities
- Plutonium and technetium solubilities are not sensitive to oxalate concentration

4.2.2 Radionuclide Transport

Over the course of time, the mobile contaminants in the closed waste tanks and ancillary equipment are likely to release and gradually migrate downward through unsaturated soil to the hydrogeologic units comprising the shallow aquifers underlying the HTF. Some contaminants will be transported via groundwater through near surface aquifers and discharge to either Fourmile Branch or UTR streams. Exposure to contaminants could occur through various pathways associated with groundwater, surface water uses, and air exposure. Figure 3.1-4 shows the location of the HTF within the GSA, which is bounded by UTR to the north and by Fourmile Branch to the south.

In model simulations, HTF contaminant transport processes in cementitious materials and soils included advection, dispersion, and sorption. Contaminant transport through the cementitious materials and soils is impeded by sorption, as represented through the K_d of the soils (Section 4.2.2.2.2) and cementitious materials (Section 4.2.2.2.4). The K_d values used

are based primarily on SRS site-specific experimental data, some central value of literature, or on expert judgment, with SRS site-specific experimental data being the preferred information source.

Colloidal transport is not included as a HTF contaminant transport process in model simulations. A University of Georgia/SRNL study conducted in 1994 discusses field studies of colloid facilitated transport of plutonium that were conducted at SRS by two groups, the University of Georgia/SRNL and Woods Hole Oceanographic Institution. Together their results indicate little or perhaps no colloidal transport of plutonium occurring within the GSA of the SRS, which includes both HTF and FTF.

In the University of Georgia/SRNL study, plutonium associated with a filterable fraction was measured in groundwater recovered in F Area, near the E-Area burial grounds and the SDF. This filterable fraction was presumed to be a colloidal fraction based on specialized low-flow collection and filtering techniques. Minimal plutonium was found in association with colloids, 0.003 pCi/L Pu-239/240 (5,000 times less than the MCL).

The percent of plutonium retained by filters, increased as the pH of the plume increased, which was also coincidental with distance from the point source. Inversely, the percent of plutonium that passed through the smallest membrane, 500 MWCO or approximately 0.5 nanometer decreases with an increase in distance from the point source. The ratio between the plutonium concentration of colloids in well water and liquid in the source zone did not change in a systematic manner with distance (or pH) in the field.

A colloid study conducted in F Area by the Woods Hole Oceanographic Institution in 1998 concluded that colloids were not involved in plutonium transport. The difference between these two studies (1994 study and 1998 study) is that one reported little colloidal plutonium and the other reported no colloidal plutonium. These results may be attributed to sampling 8 years later in a more basic pH plume and with significant differences in sampling and analytical techniques. The study reporting no colloidal plutonium used more sensitive analytical methods but larger MWCO membranes permitting larger particles to pass through (1,000 MWCO or approximately 1 nanometer) to separate colloidal from the dissolved fractions).

Woods Hole Oceanographic Institution and the SRNL returned to F Area in 2004 to characterize changes in plutonium oxidation states and plutonium association with colloids in groundwater samples collected 6 years earlier. They reported small concentrations of plutonium associated with colloids. The percentage of plutonium associated with colloids, 1.0 to 23 %, fell between the results of the previous two studies. They concluded that plutonium moved primarily in the dissolved state (and in the higher plutonium oxidation states). They reported that colloidal plutonium increased systematically with decreases in redox conditions. They observed greater dynamic shifts in plutonium speciation, colloid association, and transport in groundwater on both seasonal and decadal time scales and over short field spatial scales than commonly believed.

These results are supported by a series of laboratory experiments that were conducted to determine the effects of ionic strength (the amount of salts in solution), pH, and soil type on the colloidal dispersion of SRS sediments. At background sediment pH values (pH 4.2 to

5.9), there was minimal tendency for clays to disperse. Iron oxides generated from corrosion would not be any more dispersive than the nanoparticles in soils, and as such, would not tend to be dispersive under ambient groundwater conditions. The results also showed that as the pH was increased there was generally a critical pH above which clay dispersion occurred. This critical pH was between 5.7 and 6.2. These findings also have implications to waste disposal facilities where cementitious materials are present.

Cementitious materials will likely generate leachate that will elevate pH, calcium, and ionic strength levels; an increase in pH will promote dispersion, whereas an increase in the latter two parameters promotes colloid settling. These offsetting factors between SRS groundwater and cement leachate make it difficult to predict a priori whether colloids would remain in suspension. A recent SRNL study sought to determine whether cementitious leachates would promote the *in situ* mobilization of natural colloidal particles from SRS sandy sediment. The intent was to determine if a cementitious surface or subsurface structure would create plumes that could produce conditions conducive to sediment dispersion and mobile colloid generation, either by 1) mineral precipitation of the cement leachate interacting with SRS groundwater, or 2) the release of colloidal particles from SRS sandy sediment.

The results of the laboratory study demonstrate that *in situ* homogeneous precipitation, which is simply the mixing of cement leachate with SRS groundwater (without a solid present), is not likely to result in the formation of a large amount of precipitated solid phases. Additionally, it was shown that a SRS subsurface system is not spontaneously dispersive, meaning that the subsurface clays tend to remain immobile due to natural electrostatic forces. When a cementitious leachate (pH 12.80 to pH approximately 8) encounters the sediment, dispersion will occur as a sharp peak, containing a relatively high percentage of the clay-size particles in the sediment (approximately 13 %). Subsequently, few colloids enter the mobile phase, although the aqueous chemical conditions of the system remain unchanged. Finally, within the cementitious plume *in situ* precipitates, specifically a Na-CO₃ phase, were collected. Once the cement leachate was diluted 1000 times with a groundwater or if the pH dropped below approximately 8, colloid release was undetectable.

Based on the information available to date, colloid-facilitated radionuclide transport would not have a significant effect on contaminant movement in the HTF transport models. Potential effects on radionuclide transport as modeled due to colloid-facilitated transport is addressed indirectly through varying various inputs related to transport in the UA/SA (e.g., by varying radionuclide inventory and K_d values as described in Sections 5.6.3.1 and 5.6.3.4, respectively).

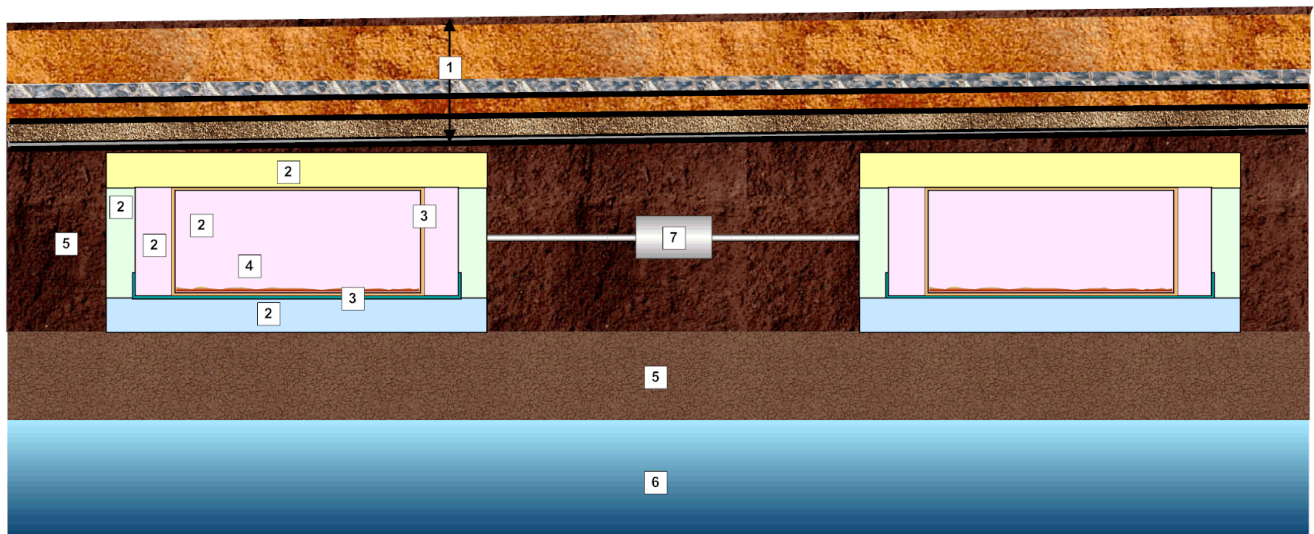
4.2.2.1 Model Approach

The ICM modeling domain is organized vertically from top to bottom as shown in Figure 4.2-12. For the purposes of this document, the ICM has been broken up into its three component conceptual models:

- Conceptual closure cap
- Vadose zone
- Saturated zone (i.e., the aquifers)

Simplifying model assumptions have been made for each of these distinct zones or layers and are summarized below and discussed in detail in Section 4.4.

Figure 4.2-12: Conceptual Closure Model for HTF



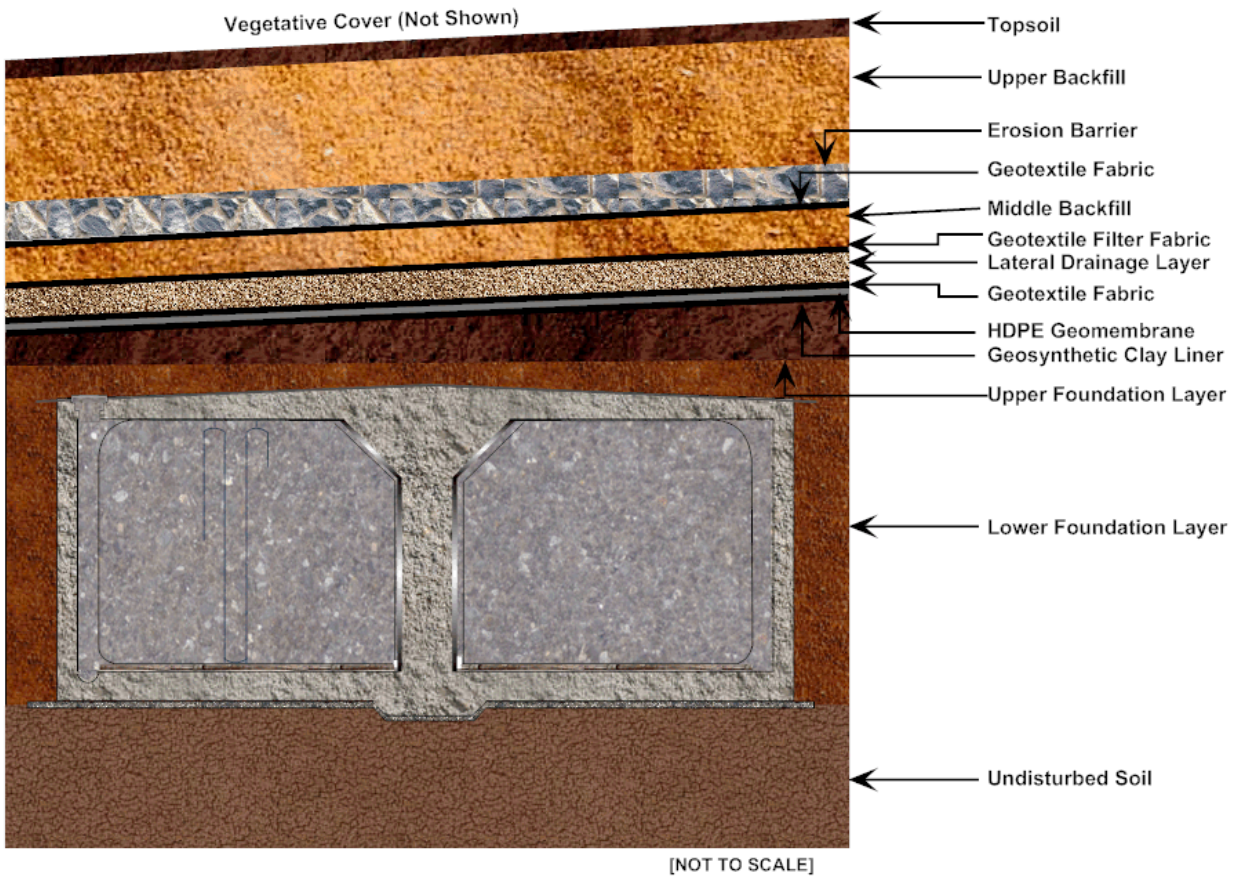
[NOT TO SCALE]

- 1 **Closure Cap** - Provides water flux to the top of tank from infiltrating rainwater.
- 2 **Vault Concrete and Tank Fill Grout** - Provides degradation description of the concrete and grout based materials in the tank system.
- 3 **Carbon Steel Tank Liner (Primary and Secondary)** - Provides degradation description of the carbon steel liners in the tank system.
- 4 **Waste Release** - Provides waste contamination release rates of residual inventory based on solubility and sorption rates per nuclide.
- 5 **Vadose Zone and Backfill** - Provides hydraulic related values for the unsaturated undisturbed soil beneath the tanks and the backfill soil surrounding the tanks.
- 6 **Hydrogeology** - Provides hydraulic related values for the saturated soil beneath the tanks.
- 7 **Ancillary Equipment** - Provides waste contamination release rates of residual waste associated with ancillary equipment.

4.2.2.1.1 Conceptual Closure Cap

The design concept for the HTF assumes it will be covered by two large closure caps, one over the “West Hill” area and one over the “East Hill” area, and a small closure cap over PPs 5 and 6. The conceptual design and expected performance of the closure caps are described in Section 3.2.4. Figure 4.2-13 illustrates the conceptual design of the HTF closure caps.

Figure 4.2-13: Closure Cap Concept for HTF



4.2.2.1.2 Vadose Zone

Although the conceptual closure cap has a certain physical thickness (a minimum of 10 feet), the cap is viewed as a surface feature in the ICM, as it is simulated separately. The area directly beneath the conceptual closure cap in the ICM is considered the vadose zone. The vadose zone and the surrounding soil, both undisturbed and backfill, contain the majority of the potential contamination sources in HTF (i.e., 21 waste tanks and ancillary equipment). In addition, eight waste tanks, along with some ancillary equipment, are either fully submerged or partially submerged in the saturated zone. The residual inventories are classified as waste tanks or ancillary equipment. Table 4.2-15 shows the thickness of the vadose zone under each of the 29 HTF waste tanks.

Table 4.2-15: Vadose Zone Thickness beneath HTF Waste Tanks

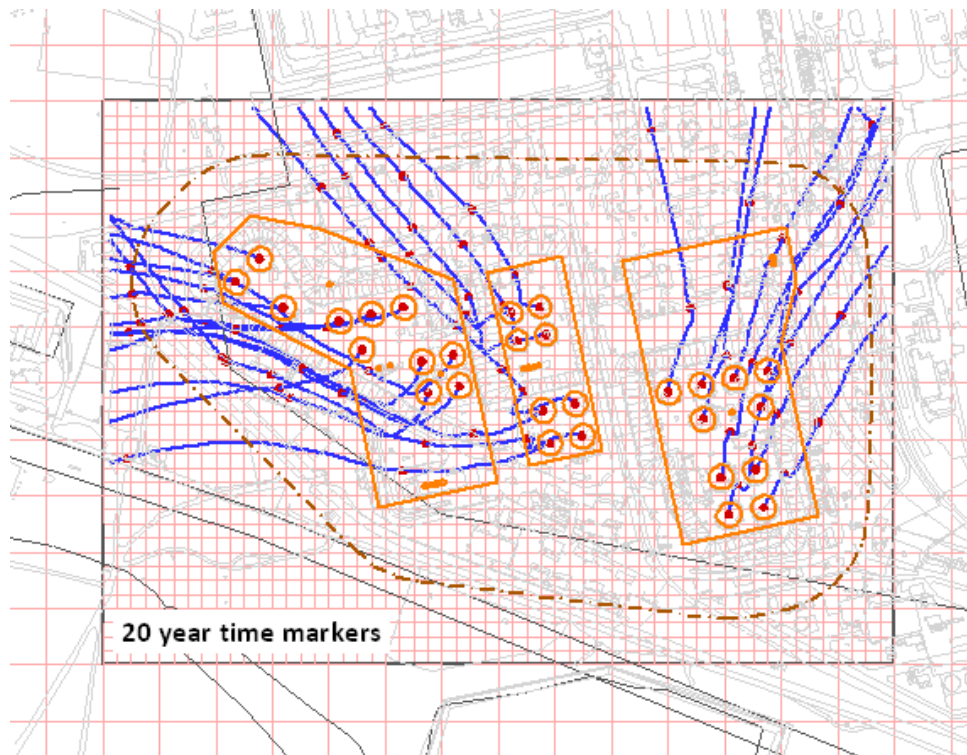
Tank Group Numbers	Tank Type	Average Concrete Working Slab Top Elevation (ft above MSL)	Group Median Water Table Elevation (ft above MSL)	Distance from Working Slab to Water Table (ft)
9 - 12	I	240.65	276.14	-35.5
13 - 16	II	270.33	276.93	-6.6
21 - 24	IV	281.75	274.65	7.1
29 - 32	III	281.88	273.80	8.1
35 - 37	IIIA	283.37	268.98	14.4
38 - 43	IIIA	292.09	273.93	18.2
48 - 51	IIIA	286.89	274.40	12.5

[SRNL-STI-2010-00148, Table 4]

The waste tanks will be modeled slightly differently, depending on the type. The segmentation approach and a discussion of different model elements for each waste tank type are described in Section 4.4.1. The material properties of waste tank and waste tank system behavior over time are discussed in later sections.

The transfer lines in the HTF are not concentrated in any geographical area, but transverse under all areas between waste tanks and transfer facilities. Therefore, the transfer line inventory was modeled by distributing the assumed inventory equally over all of the HTF area around the waste tanks and transfer facilities as indicated by the orange solid lines presented in Figure 4.2-14. Pump tanks (HPT 2 through 10), CTS pump tanks (242-3H and 242-18H), and evaporator pots (242-H, 242-16H, and 242-25H) were modeled as point sources located in the HTF at a central point of an individual component. The inventory associated with these waste sources was assumed to have had contact with the soil (so that any waste release is direct) after an assumed transfer line/waste tank degradation time. Other ancillary equipment was not modeled, based on the assumed inventories being insignificant or not inventory containment (e.g., catch tank).

Figure 4.2-14: HTF PORFLOW Model Stream Traces and 100-Meter Boundary



4.2.2.1.3 Saturated Zone

After contaminants have left the vadose zone, they will be transported into the aquifers beneath the HTF. A description of the HTF hydrogeology is provided in SRNL-STI-2010-00148 and states that the GSAD and WSRC-STI-2006-00198 soil data should be applied for the HTF. The GSAD, comprising SRS characterization and monitoring data and interpretations, will be used as the basis of hydrogeologic input values into the computational model for groundwater flow and contaminant transport. The GSAD was developed using field data and interpretations for the GSA and vicinity and is documented in WSRC-TR-96-0399, Volumes 1 and 2.

The aquifers of primary interest for HTF modeling are the UTRA and Gordon Aquifer. Potential contamination from the HTF is not expected to enter the deeper Crouch Branch Aquifer because an upward hydraulic gradient exists between the Crouch Branch and Gordon Aquifers near UTRA. [SRNL-STI-2010-00148]

Groundwater flow in the UTRA is predominantly horizontal with a smaller, vertically downward component. Near groundwater divides located between surface water drainages, the vertical component of groundwater flow is stronger and downward due to the decreasing hydraulic head with increasing depth. In areas along Fourmile Branch, shallow groundwater moves generally in a horizontal direction and deeper groundwater has vertically upward potential to the shallow aquifers. In these areas, hydraulic heads increase with depth. To the north of HTF, however, the rising elevation of the UTRA and the deep incision of UTR stream result in truncation of the entire aquifer. In these

areas, shallow groundwater may seep out along the major tributaries to UTRs above the valley floor or may seep downward to the next underlying aquifer zone and discharge along the stream valley.

The Gordon Aquifer is overlain by the UTRA-LZ along the valley of Fourmile Branch. Along UTRA, the Gordon Aquifer has been partially eroded by the deep streambed incision. The aquifer discharges to UTRA and is locally recharged by leakage from overlying aquifers near the HTF. A southeast-to-northwest hydraulic gradient is observed for this aquifer layer in the GSA.

Because the HTF is located over a groundwater divide between UTR and Fourmile Branch streams, contaminants could eventually discharge to both, depending on the contaminant origination point.

Within the GSA, for defining transport properties, soils with a saturated hydraulic conductivity greater than 1.0E-07 cm/s are defined as sandy and those with a saturated hydraulic conductivity less than 1.0E-07 cm/s are defined as clay. Within the GSA model the saturated zone soils that are defined as sandy will be assigned the effective diffusion coefficient of the upper vadose zone (i.e., 5.3E-06 cm²/s) and those soils defined as clay will be assigned that of the vadose zone clay (i.e., 4.0E-06 cm²/s). These property definitions are done to remain consistent with the soils of the vadose zone. [WSRC-STI-2006-00198]

Table 4.2-16 provides a summary of the saturated zone soils hydraulic properties (as represented by the vadose zone soil properties) and the model input used to represent these values.

Table 4.2-16: Upper Vadose Zone and Effective Saturated Zone Soil Properties

Actual/Model	η (%)	ρ_h (g/cm ³)	ρ_n (g/cm ³)	Saturated D_e (cm ² /s)
Upper Vadose Zone	39 (total)	1.65	2.70	5.3E-06
Saturated Zone Soil (Effective Properties for Modeling Purposes)	25 (effective)	1.04 (effective)	1.39 (effective)	Sandy: 5.3E-06 Clay: 4.0E-06

[WSRC-STI-2006-00198]

η = Porosity

ρ_h = Dry Bulk Density

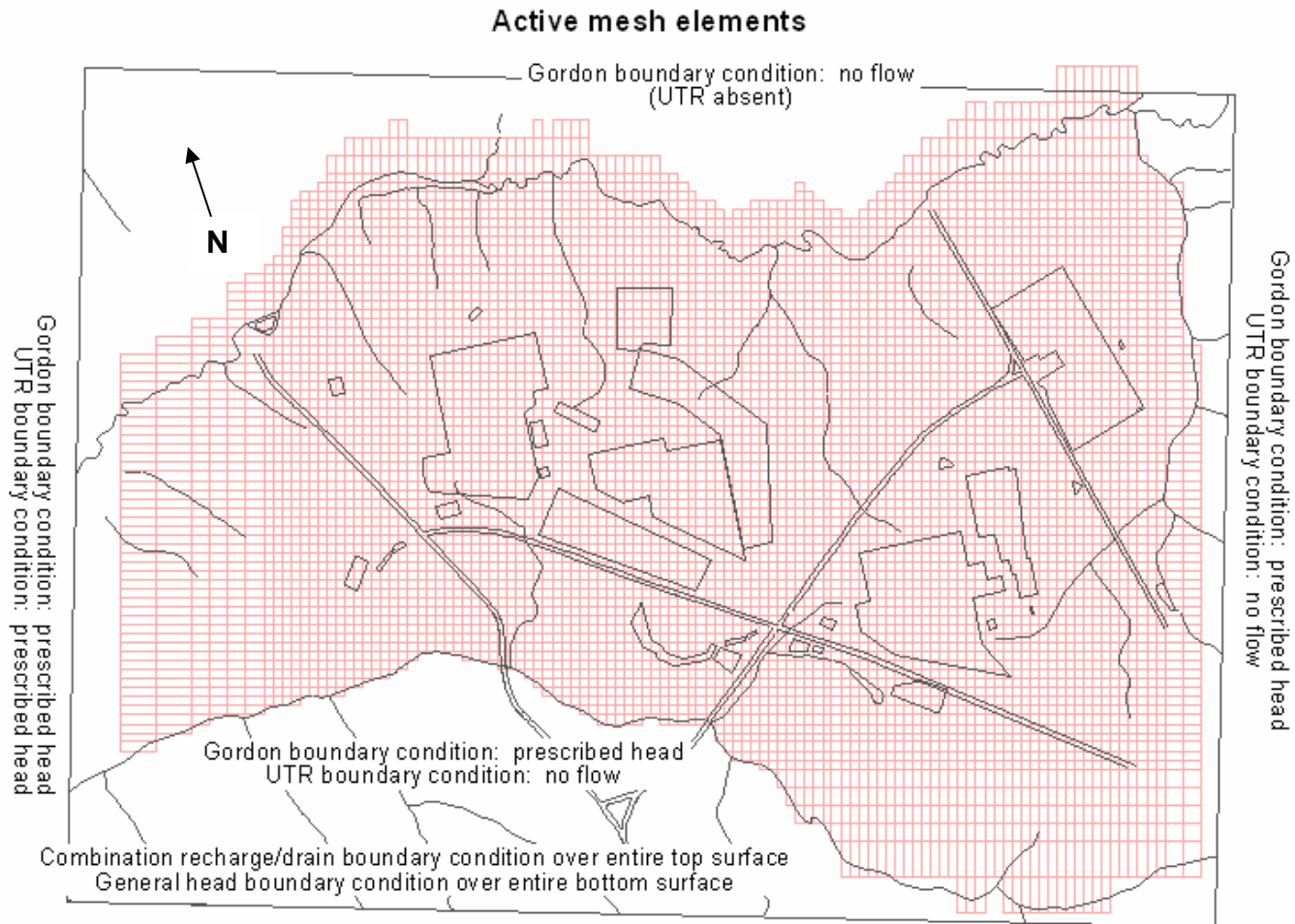
ρ_n = Particle Density

D_e = Effective Diffusion Coefficient

4.2.2.1.4 Groundwater Flow Simulation

The simulation model for groundwater flow constructed from the GSAD using the PORFLOW code is referred to as the GSA/PORFLOW Model. In the model, groundwater from the UTRA-UZ and UTRA-LZ assumed to discharge equally from each side to UTR and Fourmile Branch aquifers in the GSA. Therefore, these streams provide natural, no-flow boundary conditions for most of the UTR Aquifer Unit. The GSA boundary conditions are graphically displayed in Figure 4.2-15. On the west side of the unit, hydraulic head values from a contour map of measured water elevations are prescribed. The Gordon Aquifer is assumed to discharge equally from both sides of UTRA-UZ, UTRA-LZ and a no-flow boundary condition is specified over the north face of the model. Lacking natural boundary conditions, hydraulic heads are specified over the west, south, and east faces of the model within the Gordon Aquifer. Areas of groundwater recharge and discharge consistent with computed hydraulic head at ground surface are computed as part of the model solution using a combined recharge/drain boundary condition applied over the entire top surface of the model. Using this hybrid boundary condition, groundwater discharges to surface water in regions where the computed head is above ground elevation. Flows across the Crouch Branch Confining Unit are small compared to surface recharge and flow across the Gordon Confining Unit, and are neglected in the model.

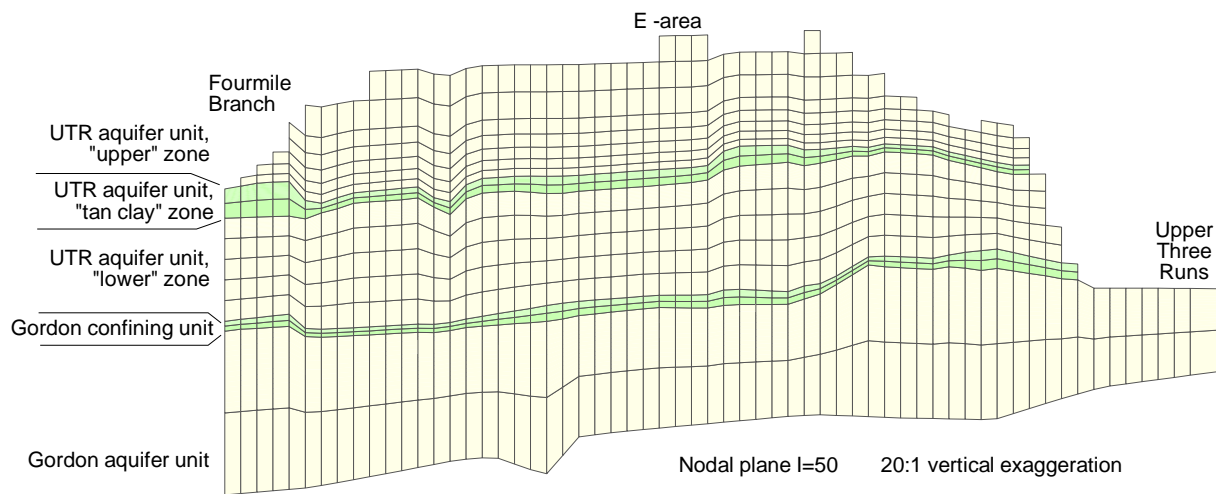
Figure 4.2-15: GSA Boundary Conditions



[WSRC-TR-2004-00106]

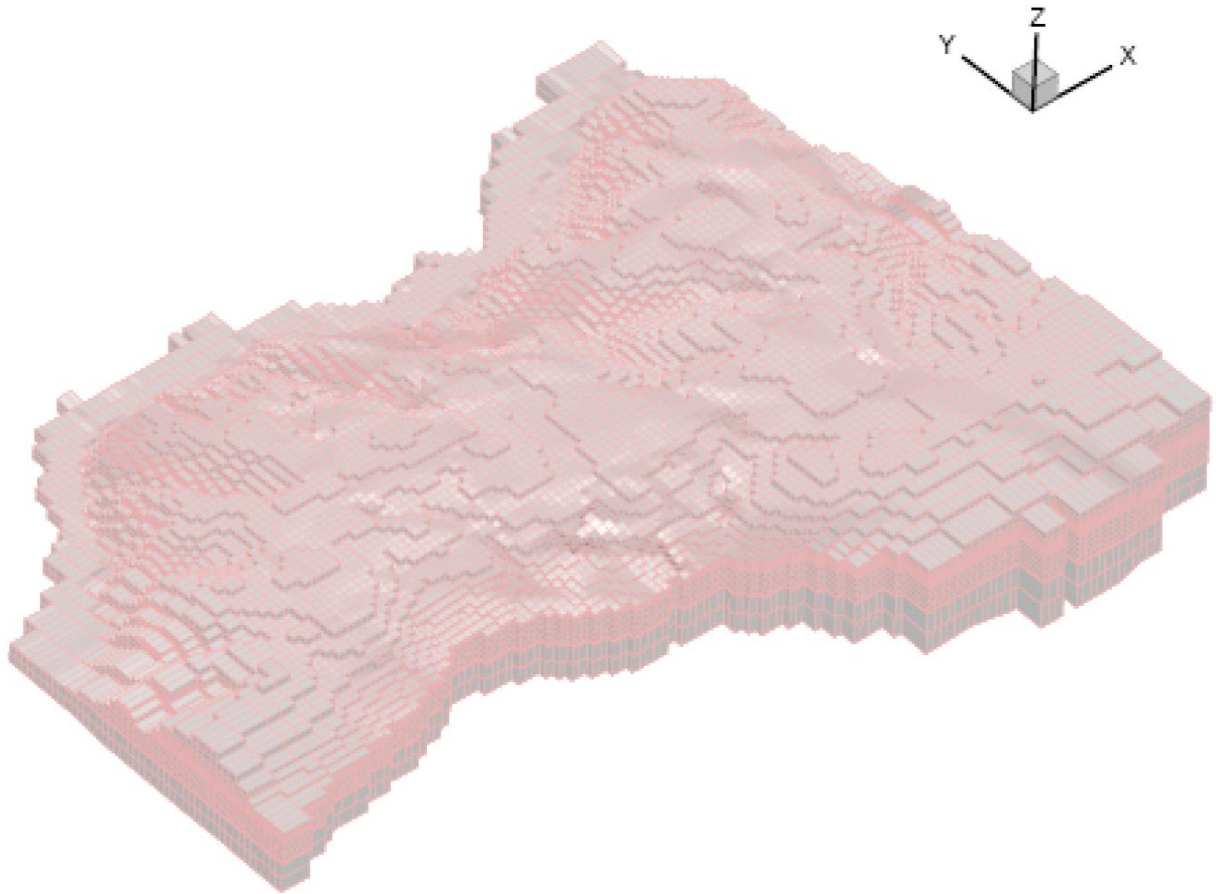
The area resolution of the GSA aquifer model is 200 square feet except in peripheral areas. There are 108 grid blocks along the east-west axis, and 77 blocks along the north-south axis. The vertical resolution varies depending on hydrogeologic unit and terrain/hydrostratigraphic surface variations as depicted in Figure 4.2-16. Each hydrostratigraphic surface is defined by numerous "picks" ranging in number from approximately 52 to 225 depending on the surface. The UTRA-UZ represented with up to 10 finite elements in the vertical direction. The vadose zone is included in the model. The UTRA-LZ contains five finite-elements while the TCCZ separating the aquifer zones is modeled with two vertical elements. The Gordon Confining Unit and Gordon Aquifer each contain two elements, totaling 21 vertical elements from ground surface to the bottom of the Gordon Aquifer. The 3-D grid comprises 102,295 active cells as depicted in Figure 4.2-17. [WSRC-TR-2004-00106]

Figure 4.2-16: North-South Cross-Section of GSA/PORFLOW Computational Mesh



[WSRC-TR-2004-00106]

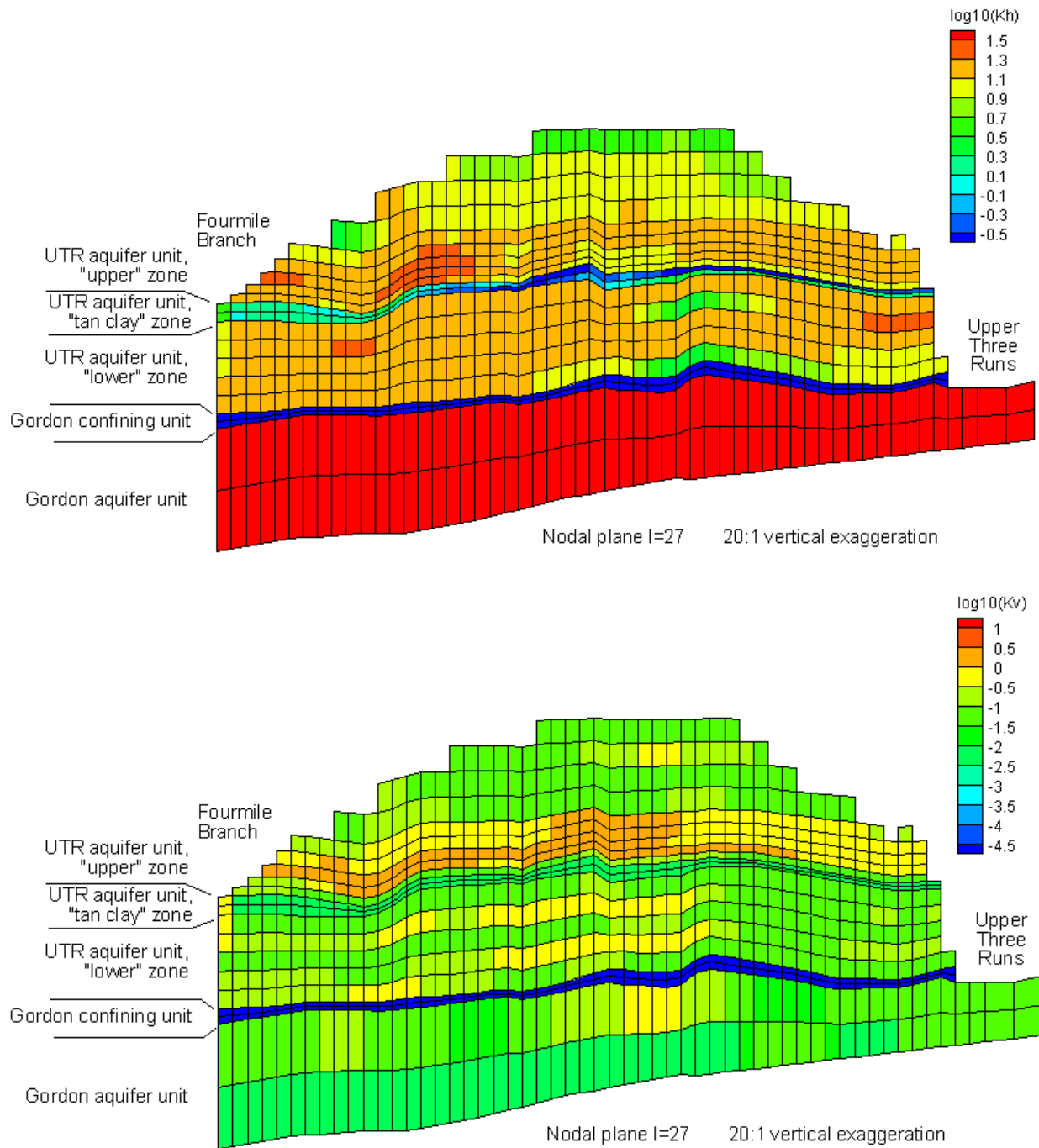
Figure 4.2-17: Perspective View of GSA/PORFLOW Computational Mesh



[WSRC-TR-2004-00106]

Hydraulic conductivity values in the model are based on a characterization GSAD discussed in Section 3.1.5. The conductivity field is heterogeneous within hydrogeologic units and reflects variations present in the characterization data. The average horizontal conductivities in the saturated UTRA-UZ, UTRA-LZ, and Gordon Aquifer are approximately 10, 13, and 38 ft/d, respectively. The average vertical conductivities for the TCCZ and the Gordon Confining Unit are $6.0E-03$ and $1.0E-05$ ft/d, respectively. [WSRC-TR-96-0399] Figure 4.2-18 illustrate typical horizontal and vertical model hydraulic conductivity fields, respectively, along a representative cross-section through the GSA. The GSA/PORFLOW Model calibration and validation used measured, well water levels.

Figure 4.2-18: North-South Cross Sections of GSA/PORFLOW Model - Horizontal and Vertical Hydraulic Conductivity Variations Views

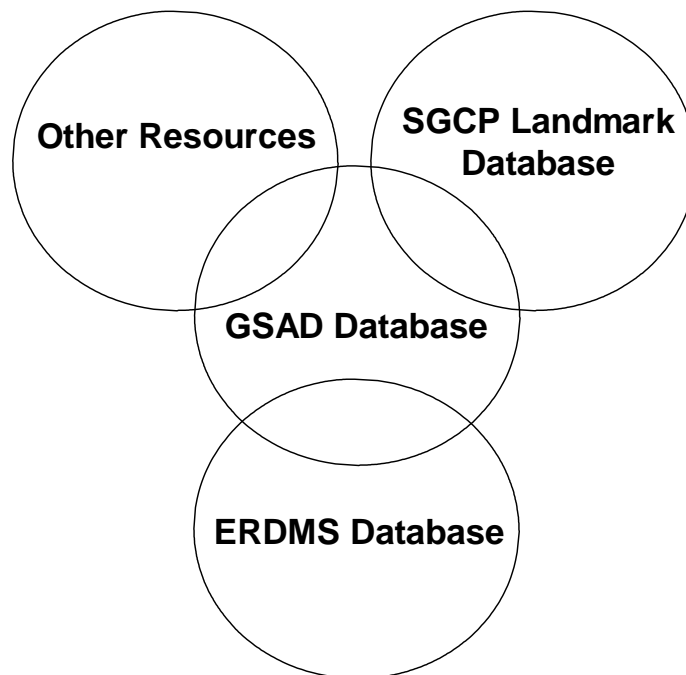


The average natural recharge over the entire model domain is 14.7 in/yr compared to approximately 15 in/yr from prior groundwater budget studies. [WSRC-TR-2004-00106] Various man-made features (e.g., basins) provide additional recharge in localized areas. The estimated discharge rates to UTR and Fourmile Branch, within the model domain, are 18.2 and 2.6 ft³/s, respectively. [WSRC-TR-2004-00106] The simulated discharge rates are 11.4 and 3.8 ft³/s, respectively. Predicted seepage faces are consistent with field observations. Simulated hydraulic heads, vertically averaged over the entire thickness of the UTRA-LZ, UTRA-UZ, and Gordon Aquifer, agree with potentiometric maps based on measured heads. The evaluation of simulated versus measured heads utilized GSA/PORFLOW results for the vertically averaged head and the residuals between computed and measured heads. [WSRC-TR-2004-00106] Simulated flow directions vertically averaged over the entire thickness of the aquifer zones agree with conceptual models of groundwater flow.

Adequacy of GSAD Data Set for Groundwater Flow Simulation

The GSAD includes field data and interpretations collected in the GSA through 1996. Although characterization and monitoring have been ongoing, the additional data has not altered fundamental understanding of groundwater flow patterns and gradients in the GSA. The GSAD is a subset of site-wide data sets of soil lithology and groundwater information. These larger sets of data are captured in the Environmental Restoration Data Management System (ERDMS) database, ACP landmark database and other resources. The relationship between GSAD and the full set of data is pictured in Figure 4.2-19.

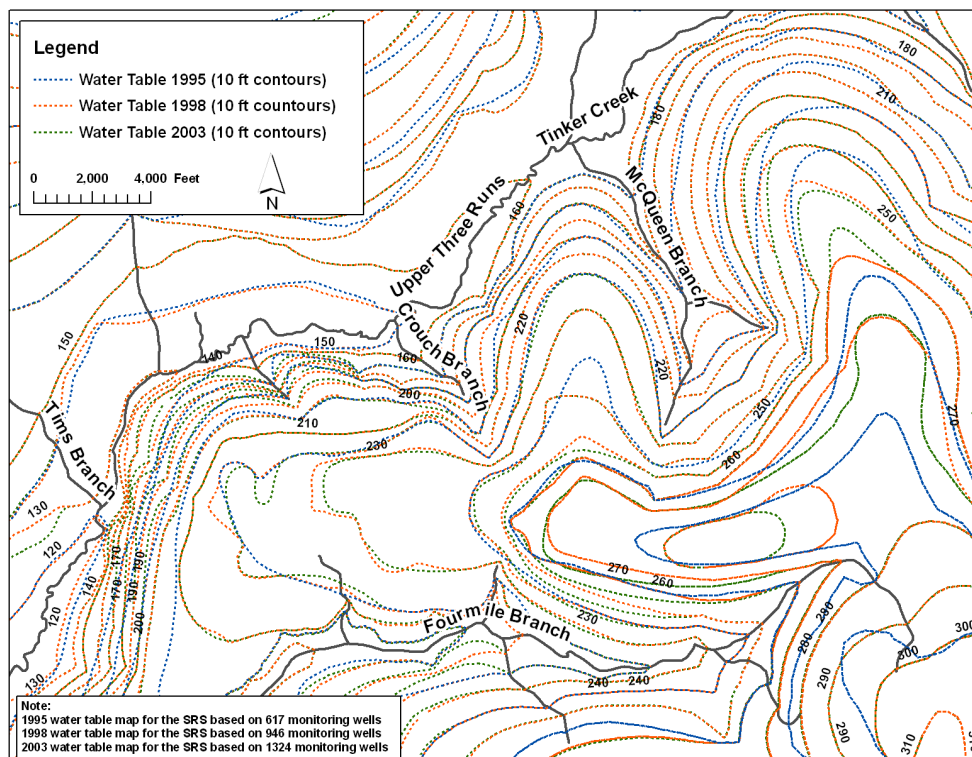
Figure 4.2-19: The GSAD Database Relationship



The more recent field data (i.e., 1996-2006) is limited to CPT picks and a few geophysical logs with no new HTF foot-by-foot core descriptions. During the 1980s and early 1990s, significant work was conducted within the GSA to better define the hydrogeology including installation of well clusters and continuous core descriptions and geophysical logs associated with the deepest well in the cluster. At that point, the hydrostratigraphy of the GSA was considered sufficiently defined, and no additional characterization was planned. Since the mid-1990s, wells have been installed to better define plumes and CPT logs have been generated for structural, seismic, and vadose zone monitoring purposes. Most of the new data are shallow and consist of CPT or geophysical logs. Most of the new data may provide picks for the top two aquifers surfaces only. [SRNL-STI-2010-00148]

In order to evaluate the need to update the original GSAD to incorporate new hydrogeologic information, two evaluations were identified. Figure 4.2-20 shows recent water table contour maps for the GSA based on water level data collected in 1995, 1998, and 2003. Contours were developed using mean water levels from SRS wells, field verification of perennial stream reaches, and the USGS 1:24000 scale topography data. [WSRC-MS-95-0524, WSRC-TR-98-00045, WSRC-TR-2003-00250] These contour maps are consistent with each other indicating that there has not been a significant change in our understanding of long-term average water table conditions in the GSA since the mid-1990s.

Figure 4.2-20: Water Table Contour Maps for GSA



A report was prepared in 2010 (*Hydrogeologic Data Summary in Support of the H-Area Tank Farm Performance Assessment*) to provide a summary of recent available geotechnical data for the HTF vicinity. This report focused on sediment descriptions, geotechnical data (e.g., grain size analyses), and interpretations for the vadose zone from historical and recent studies. The report also included potentially significant findings regarding the saturated zone (e.g., existence/thickness of the TCCZ). Review of the data collected in SRNL-STI-2010-00148 showed that the available data is consistent with the assumptions made for vadose zone sediments in the HTF PA modeling effort. [SRNL-STI-2010-00148]

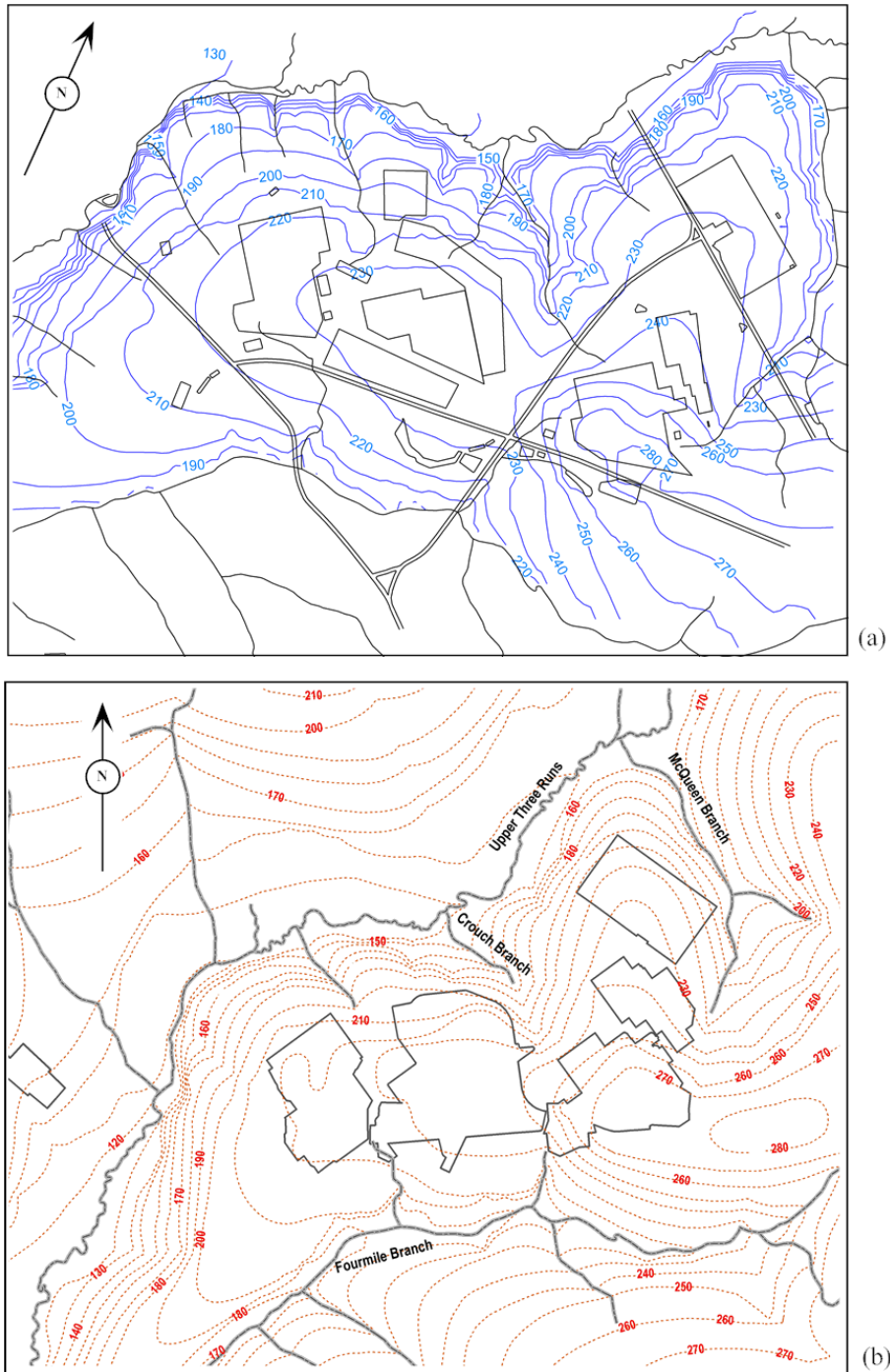
One area of particular interest in the SRNL-STI-2010-00148 data review was the TCCZ. Measurements of the TCCZ thickness were compared within the HTF to the TCCZ thickness as represented in the GSA/PORFLOW Model, which was developed from data lying outside the HTF. Generally, the two values are close, and uncertainty in data quality interpretation is not exceeded by the differences. The study indicates that the TCCZ exhibits spatial correlation across HTF, such that interpolation-using data outside the HTF produces reasonable estimates of actual thickness. The GSA/PORFLOW Model representation of the TCCZ is judged reasonable for HTF PA modeling.

Best-estimate predictions and field monitoring indicate that plume migration can be expected to occur through the UTRS-UZ and UTRA-LZ for travel distances through at least 100 meters. Contamination may or may not pass through the UTRA, TCCZ before reaching the 100-meter perimeter. In PORFLOW modeling, the TCCZ is assigned the same geochemical properties (K_d) as the aquifer zones for UTRA-UZ and UTRA-LZ (no credit is taken for the TCCZ as a potential chemical barrier to plume migration laterally and downward). Hydraulically, the TCCZ is assigned a vertical conductivity of $2.1E-06$ cm/s (26 in/yr) in H Area. Thus, the confining zone is also relatively ineffective as a flow barrier.

Although the Gordon Confining Unit may not be completely continuous in all areas of the GSA, the formation has sufficient continuity to function as a significant flow barrier, and be classified as a “confining unit” as opposed to a “confining zone” (e.g., TCCZ). Variation in leakance through the Gordon Confining Unit would lead to somewhat faster and/or slower travel within the UTRA. Uncertainty in aquifer velocity/travel time is considered in GoldSim modeling. Higher leakance would increase peak concentration in the Gordon Aquifer, but decrease the overall peak, which occurs in the UTRA. The GSA/PORFLOW representation of the green clay as a confining unit is viewed as reasonable for HTF PA modeling.

Figure 4.2-21 provides a comparison of the GSA 2003 water table map developed using median water levels from SRS wells (bottom) and the water table predicted by the GSA/PORFLOW model.

Figure 4.2-21: Comparison of (a) GSA/PORFLOW Model Predicted and (b) 2003 Water Table Maps



[SRNL-STI-2010-00148]

Table 4.2-17 summarizes hydraulic head residuals between the model and the field data. [WSRC-TR-2004-00106 Section 3.1] Table 4.2-17 also summarizes more recent well water level data through 2006 (available because of well installations and continued monitoring). The agreement between the model and the data set through 2006 is similar to that of the original data set. [SRNL-STI-2010-00148]

Table 4.2-17: Hydraulic Head Residuals - GSA/PORFLOW Model and Field Data through 2006

Aquifer Zone	Number of Wells	Median Residual (ft)	Average Residual (ft)	Root-Mean-Square Residual (ft)	Minimum Residual (ft)	Maximum Residual (ft)
Up to 1995 Data	638					
Gordon	79	-0.0	-0.5	1.7	-4.7	2.5
UTRA-LZ	173	+0.8	+0.6	4.6	-9.4	27.0
UTRA-UZ	386	-0.1	-0.5	3.4	-15.2	10.0
Up to 2006 Data	917					
Gordon	94	+0.3	-0.0	1.5	-3.8	2.6
UTRA-LZ	272	+1.1	+1.0	4.7	-11.9	27.0
UTRA-UZ	551	+0.8	+0.1	3.5	-16.8	14.5

[SRNL-STI-2010-00148]

4.2.2.1.5 Transport Model Interfaces

As noted earlier, the ICM of subsurface water flow and contaminant transport comprises three principal elements, 1) the closure cap, 2) the vadose zone, and 3) the saturated aquifer zone, as illustrated in Figure 4.2-12.

The prescribed rainfall condition, in the form of daily rainfall values over an extended period, is the primary input or external boundary condition to the closure-cap flow analysis. The closure cap model produces a net infiltration rate at the bottom of the closure cap that becomes a flow boundary condition to the adjoining vadose zone. The assumption is water infiltration to the closure cap is free of contaminants, so the concentration is set to zero at the top boundary of the vadose zone.

Groundwater flow in the much larger scale saturated zone, or aquifer model, is controlled by net infiltration or recharge over a broad area surrounding the HTF. Rather than using the flow exiting the vadose zone at the water table as a direct input to the aquifer model, an average recharge value is applied to the aquifer flow model based on field studies. [WSRC-TR-96-0399 Volume 2] For saturated zone contaminant transport, the contaminant flux leaving the bottom of the vadose zone model becomes the source of contamination entering the aquifer.

Each water table flux contribution from an individual waste tank is assigned to the aquifer transport grid by uniformly distributing the flux to those water table cells with centroids lying within the footprint of the waste tank. Each flux originating from discrete

ancillary equipment is assigned to the cell with the closest centroid. Flux from transfer lines is spread uniformly over the facility footprint.

4.2.2.2 Material Properties

Material properties of interest appear in technical reports including:

- The conceptual closure cap layers (SRNL-ESB-2008-00023)
- The vadose zone soil (SRNL-STI-2010-00148)
- The cementitious materials for example waste tank top and sides, basemat, and grout (WSRC-STI-2006-00198, WSRC-STI-2007-00369, SRNL-STI-2012-00404)
- The CZ (SRNL-STI-2012-00404)
- The carbon steel waste tank liner (WSRC-STI-2007-00061, SRNL-STI-2010-00047)
- The stainless steel ancillary equipment (WSRC-STI-2007-00460)
- The soil and groundwater in the saturated zone, for example the aquifers underlying the waste tank systems (SRNL-STI-2010-00148)

Because material properties form a key part of the ICM, some data from other technical reports identified above are duplicated in this section for completeness. Material properties for carbon steel, cementitious material, and stainless steel are also provided. The only relevant information for both carbon and stainless steel is the projected time of failure under different conditions. The assumption for this material is it is impermeable until the time of steel failure, and then becomes sufficiently permeable that it is not a barrier to contaminant migration.

4.2.2.2.1 Conceptual Closure Cap Material Properties

Preliminary values for conceptual closure cap layer thickness and infiltration rate changes with time from the predicted degradation of the conceptual closure cap are provided in SRNL-ESB-2008-00023.

Tables 4.2-18 and 4.2-19 provide the conceptual closure-cap layer thicknesses and infiltration rates, respectively. These values are considered preliminary values for the HTF closure cap conceptual design.

Table 4.2-18: Conceptual Closure Cap Layers Top to Bottom

Layer	Layer Thickness (in)
Vegetative Cover	N/A
Topsoil	6
Upper Backfill	30
Erosion Barrier	12
Geotextile Fabric	NC
Middle Backfill	12
Geotextile Filter Fabric	NC
Lateral Drainage Layer	12
Geotextile Fabric	NC
HDPE Geomembrane	0.06 (60 mil)
GCL	0.2
Upper Foundation Layer	12
Lower Foundation Layer	72 (min.)

[SRNL-ESB-2008-00023, Table 1]

NC = Not Calculated

Table 4.2-19: Conceptual Closure Cap Infiltration over Time

Time Interval (yr)	Average Annual Infiltration Through GCL (in/yr)
0	0.00088
100	0.010
180	0.17
290	0.37
300	0.50
340	1.00
380	1.46
560	3.23
1,000	7.01
1,800	10.65
2,623	11.47
3,200	11.53
5,600	11.63
10,000	11.67

[SRNL-ESB-2008-00023, Table 2]

4.2.2.2.2 Vadose Zone Material Properties

In this section, the focus of this portion of the overall HTF closure input conceptual model (Figure 4.2-12) is on the region between the existing grade (prior to closure cap installation) and the top of the water table, excluding the waste tanks themselves. This area (number 5 in Figure 4.2-12) includes the concrete working slab on which the waste tanks were built, the undisturbed, unsaturated soil under this slab, and the existing backfill soil around the waste tanks. Note that the modeling properties of procured sand used in the waste tank liner systems are also discussed herein. The parameters that comprise this section include:

- Vadose zone thickness under each of the 29 waste tanks
- Saturated effective diffusion coefficient
- Average total porosity
- Average dry bulk density
- Average particle density
- Saturated horizontal hydraulic conductivity
- Saturated vertical hydraulic conductivity
- K_d values
- Characteristic curves (suction head, saturation, and relative permeability)

Vadose Zone Background

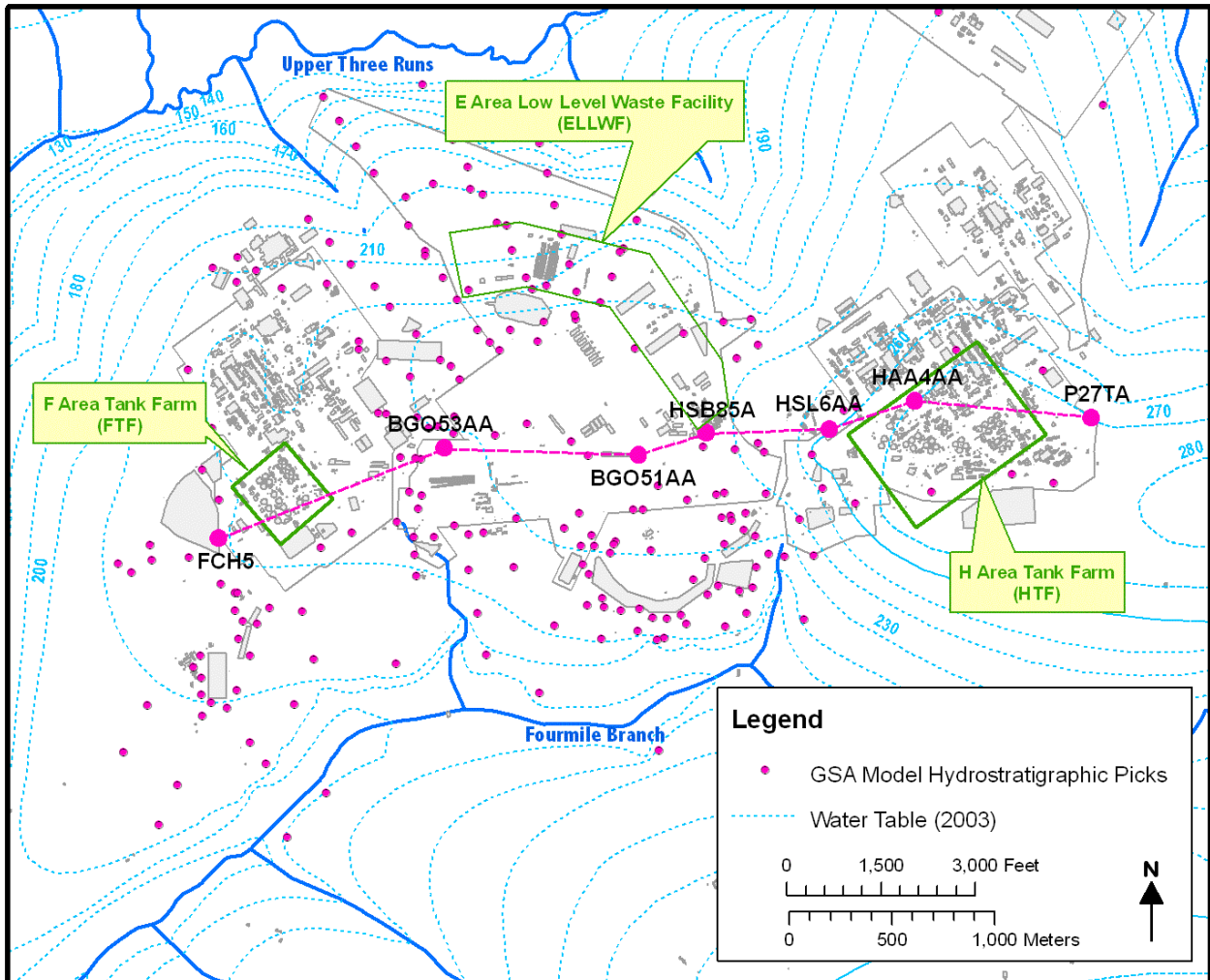
Section 3.2.1 provides a detailed description of the construction of the various waste tank groups situated in HTF. The general construction approach for each waste tank group involved four major steps:

1. Excavating an area below grade and stockpiling the excavated soil
2. Laying an non-reinforced concrete working slab at the bottom of the excavation to provide a stable platform for construction activities
3. Constructing the waste tanks
4. Backfilling around the waste tanks with the previously removed soil

A substantial body of vadose zone characterization data is available for the GSA, especially for the E-Area LLW Disposal Facilities, which are located approximately 3,000 feet northwest of the HTF. Available data show that the vadose zone at HTF is similar to the vadose zones in both E Area and F Area. [SRNL-STI-2010-00148] Figure 4.2-22 is a location map for borings across the GSA, including borings from F Area, E Area, and H Area. The GSA is located on a topographic high between two streams, UTR to the north and Fourmile Branch to the south. Figure 4.2-23 shows a geologic cross-section across the GSA, based on the core descriptions and gamma ray logs from seven boring locations (three from H Area, three from E Area, and one from F Area) specified on Figure 4.2-23. Across the GSA, marker bed relations (i.e., vertical occurrences of the TCCZ and Gordon Confining Unit), are identified and appear similar in nature. [SRNL-STI-2010-00148]

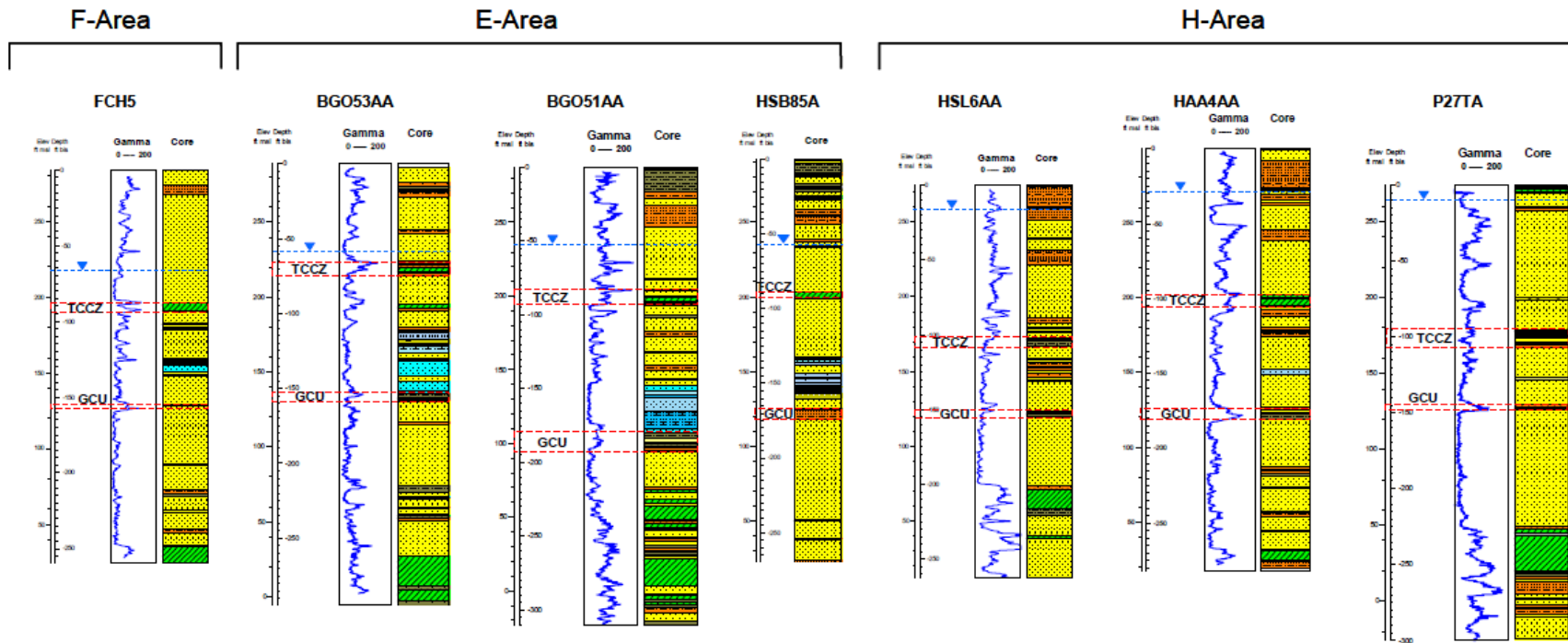
A review of the recent and historical water level data in the HTF indicates that the Type I tanks (Tanks 9 through 12) are submerged, Type II tanks (Tanks 13 through 16) are partially submerged, and all the remaining waste tanks have a negligible to relatively thin vadose zone (< 20 feet). The vadose zone is thickest beneath the northern Type IIIA tanks (Tanks 38 through 43). In the HTF, the undisturbed vadose zone beneath the waste tanks appears to correspond to the “Upland Unit” and Tobacco Road Sand Formation [SRNL-STI-2010-00148], according to existing hydrogeologic interpretations of CPT logs presented in Figure 4.2-24. The properties of this zone most likely represent the upper vadose zone properties as identified in WSRC-STI-2006-00198. [SRNL-STI-2010-00148]

Figure 4.2-22: The GSA Geologic Cross-Section Location Map



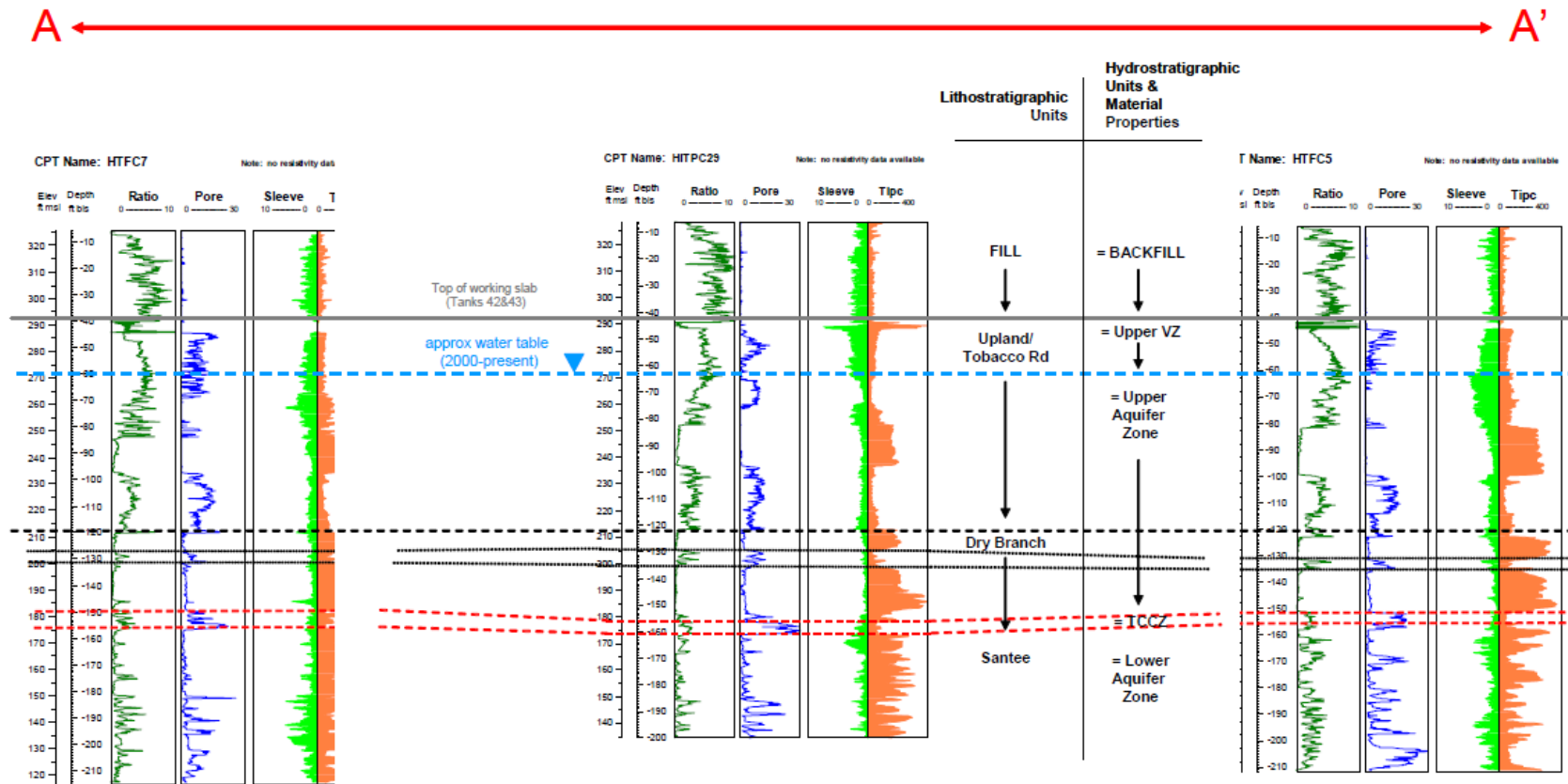
[SRNL-STI-2010-00148]

Figure 4.2-23: Comparison of E-Area, F-Area, and H-Area Vadose Zone Using Core Descriptions and Gamma Ray Logs



NOTES: MSL = mean sea level; bls = below land surface; ft = feet; Gamma is shown in American Petroleum Institute units; TCCZ = Tan Clay Confining Zone as defined in the GSA/PORFLOW Model database; color coated lithology columns are based on foot by foot core descriptions; in general colors correspond to the following: yellows = sands, grays and greens = clays, oranges = clayey sands, blues = calcitic sections/limestones (SRNL-STI-2010-00148)

Figure 4.2-24: Comparison of H-Area Vadose Zone Using CPT Logs



NOTES: msl = mean sea level; bls = below land surface; ft = feet; TCCZ = Tan Clay Confining Zone; Upper VZ = Upper Vadose Zone;
FOR CPT LOGS: sleeve = sleeve resistance (tsf); tip = tip resistance (tsf); ratio = friction ratio (reflects sleeve/tip); pore = pore pressure (psi)
[SRNL-STI-2010-00148]

Concrete Working Slab

As described in Section 3.2.1, all the HTF waste tanks have a working slab below their basemat except the Type IV tanks (Tanks 21 through 24), which have a maintenance slab between them. Table 4.2-20 summarizes available information on the design of the working slabs for the different HTF waste tank types. Figure 4.2-25 shows a typical working slab under Tanks 13 through 16 (Type II tanks). The working slabs for the Type IIIA tanks were broken up or perforated with holes before backfilling, and this condition is assumed to exist between the waste tanks, but not underneath the waste tanks.

Table 4.2-20: Waste Tank Working Slab Information by Type

Tank Type	Working Slab Design
I	A 4 inches thick slab with a 42 foot 5-inch radius, and a wire mesh layered in the middle (W145225)
II	A 6 inches thick slab, with the four waste tanks placed within a 255 foot x 274 foot rectangle (W163048)
IV	A 3-inch drainage and maintenance slab between waste tanks (W230826)
III	A 6 inches thick slab that slopes away from the waste tanks extending at least 30 feet beyond waste tank vault (W236439)
IIIA	A minimum 4-inch thick working slab filling the entire excavation, extending at least 25 feet beyond the waste tank vaults and was either broken up or punched with holes (4-inch diameter on 18-inch center) prior to backfilling as shown in Figure 3.2-30 (W449843, W700834, W706301)

Figure 4.2-25: Working Slab for Tanks 13 through 16



Table 4.2-21 shows estimated material properties for the working slabs. Figure 4.2-26 provides the characteristic curves (suction head, and relative permeability) for the working slab.

Table 4.2-21: Estimated Working Slab Material Properties of Interest

Material	Saturated D_e (cm ² /s)	η_e (%)	ρ_h (g/cm ³)	ρ_n (g/cm ³)	K_{sat} (cm/s)
Low Quality Concrete	8.0E-07	16.8	2.06	2.51	3.5E-08

[WSRC-STI-2007-00369, Table 20 for basemat surrogate]

D_e = Effective Diffusion Coefficient

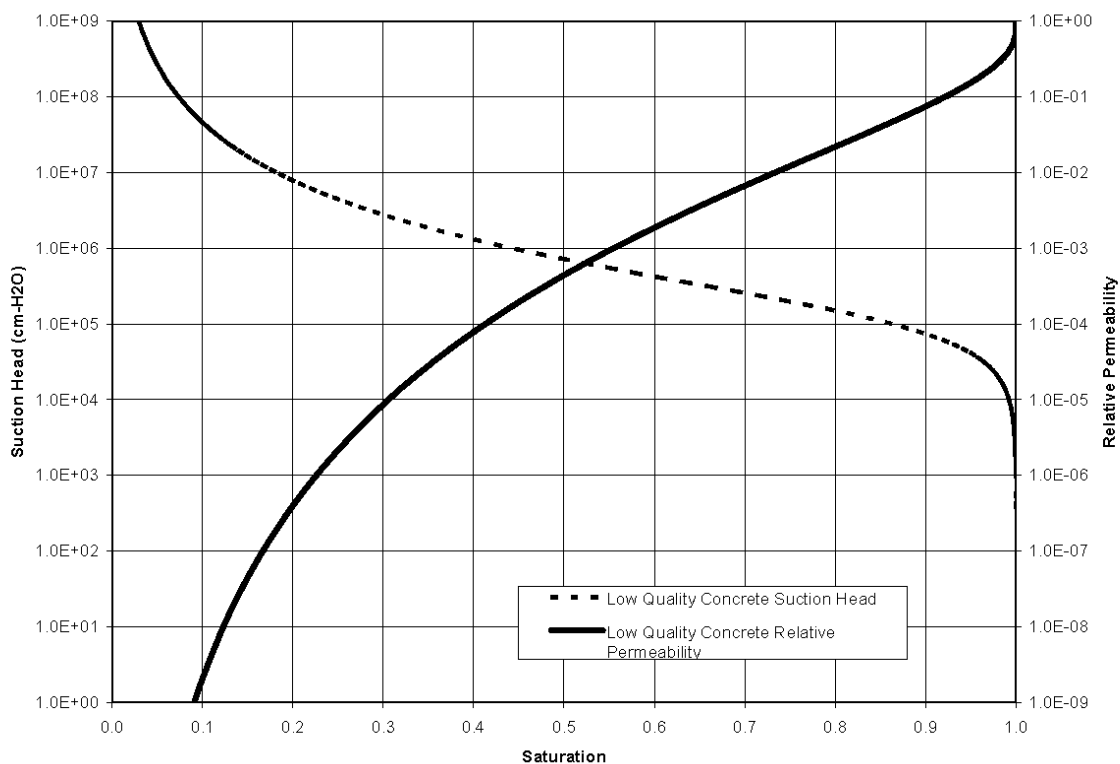
η_e = Effective Porosity

ρ_h = Dry Bulk Density

ρ_n = Particle Density

K_{sat} = Saturated Hydraulic Conductivity

Figure 4.2-26: Working Slab (Low Quality Concrete) Characteristic Curves



[WSRC-STI-2007-00369]

Given the minimal thickness of the working slabs compared to the waste tank basemats, the slabs were ignored in modeling contaminant transport through the waste tank bottom and basemat into the vadose zone for all waste tank types except for the Type II tanks. For the Type II tanks, there is inventory modeled in the sand pads and the working slab is 6 inches thick.

Vadose Zone and Backfill Material Properties

The physical and chemical properties of the vadose zone soils surrounding and below the contamination sources are needed for the ICM. Data tables are presented for several vadose zone material properties: saturated effective diffusion coefficients, average total porosity, average dry bulk density, saturated horizontal hydraulic conductivity, saturated vertical hydraulic conductivity, and K_d values. The properties are assumed not to change over time because of the stability of the soil and soil structure. These material properties are summarized in Tables 4.2-22, 4.2-23, and 4.2-24. Figures 4.2-27 and 4.2-28 illustrate the vadose zone and backfill characteristic curves, showing suction head, saturation, and relative permeability.

Table 4.2-22: Estimated Vadose Zone Material Properties of Interest

Material	Saturated D_e (cm ² /s)	Average η_T (%)	Average ρ_h (g/cm ³)	Average ρ_n (g/cm ³)	Horizontal K_{sat} (cm/s)	Vertical K_{sat} (cm/s)
Upper Vadose Zone	5.3E-06	39	1.65	2.70	6.2E-05	8.7E-06
Lower Vadose Zone	5.3E-06	39	1.62	2.66	3.3E-04	9.1E-05

[WSRC-STI-2006-00198]

D_e = Effective Diffusion Coefficient

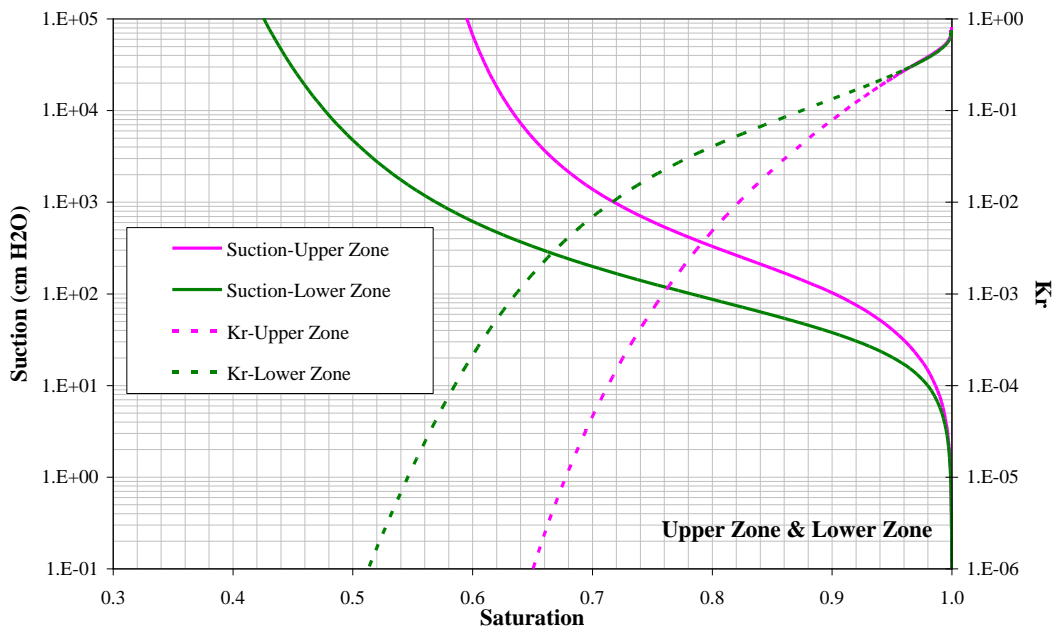
η_T = Total Porosity

ρ_h = Dry Bulk Density

ρ_n = Particle Density

K_{sat} = Saturated Hydraulic Conductivity

Figure 4.2-27: Upper and Lower Vadose Zone Characteristic Curves



[WSRC-STI-2006-00198]

Table 4.2-23: Estimated Backfill Material Properties of Interest

Material	Saturated D_e (cm ² /s)	Average η_T (%)	Average ρ_h (g/cm ³)	Average ρ_n (g/cm ³)	Horizontal K_{sat} (cm/s)	Vertical K_{sat} (cm/s)
Backfill	5.3E-06	35	1.71	2.63	7.6E-05	4.1E-05

Note For controlled compacted backfill; all property values except for saturated D_e are based on laboratory data for samples of similar backfill from the GSA; saturated D_e values are based on literature values.

[WSRC-STI-2006-00198, Table 5-18]

D_e = Effective Diffusion Coefficient

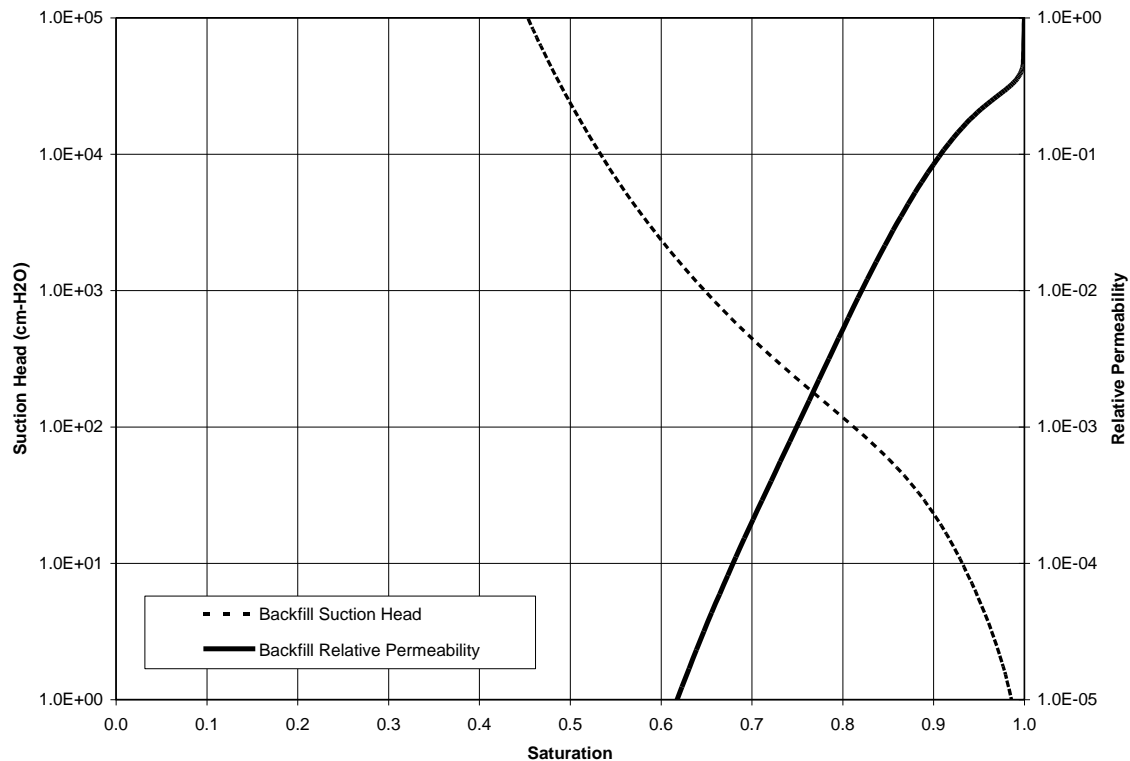
η_T = Total Porosity

ρ_h = Dry Bulk Density

ρ_n = Particle Density

K_{sat} = Saturated Hydraulic Conductivity

Figure 4.2-28: Backfill Characteristic Curves



[WSRC-STI-2006-00198]

Table 4.2-24 summarizes available information about the backfill that is present around the waste tanks and, in some cases, also over the tanks.

Table 4.2-24: Waste Tank Backfill Information by Type

Tank Type	Backfill Information
I	Excavated soil was compacted around and over the waste tanks. The backfill was installed per W145225. Nine feet of backfill was emplaced over the waste tank tops extending to a finish grade of approximately 300 feet above MSL. [W146377]
II	Backfill around the waste tanks was installed per drawing W163048 specifications. The backfill below the working slab is test controlled compacted backfill not to contain more than 7 % material passing through a #200 sieve (0.0029-inch sieve opening). The backfill around the waste tanks was placed in successive, uniform layers, with a compacted thickness no more than 12 inches. It was then brought to an elevation level with the top of the waste tanks (approximately 325 feet above MSL) and extended laterally for a minimum of 21 feet then sloped down at an angle less than 1:1 for a lateral distance of 31 feet, reaching final grade at an elevation of 300 feet above MSL. [W163048]
IV	Earth was excavated from the area surrounding the waste tanks to a depth of 17 feet below existing grade. [W230826] Vermiculite bags (minimum 8 inches thick) were installed immediately adjacent to the waste tank walls to provide cushion layer for expansion voids behind and between bags were filled with earth backfill. [DP-478] Standard compaction of excavated soil (sandy clay) was placed around and over waste tanks. [W231221, W230976, W231023]
III/IIIA	All areas receiving backfill (including sloped areas) were prepared per W700834. Excavated soil was compacted around and over the waste tanks. Prior to placing backfill, either the working slab was broken up or 4-inch holes, 18 inches on center were punched in the slab. In other areas receiving backfill, the soil cover (e.g., vegetation, top soil, soil-erosion protection layer) was removed and the ground scarified to a depth of 4 inches. Backfill with the amount (percent) of water most favorable to achieve not less than 95 % of the maximum dry density was used. [W701036]. Backfill was placed to within 1 foot of the elevation of the top of the Type III/IIIA tanks. [W231220, W700242, W701036, W704700]

As indicated in Table 4.2-24, the excavated soil was used for backfilling around the waste tanks. Excavated soil was also used to cover the tops of the waste tanks, except for the Type IIIA tanks, as shown in this table. The cover soil consisted predominately of upper vadose zone soil (i.e., sand with a significant silt and clay content) with some lower vadose zone soil (i.e., a coarser-grained soil). Soil considered too sandy was not utilized as backfill. [WSRC-STI-2006-00198]

The backfill was placed either by standard compaction or by test-controlled compaction. Standard compaction consisted of rolling damp, maximum 12-inch lifts of soil with mechanical compaction equipment until a visually uniform compaction was obtained. Test-controlled compaction consisted of compacting moisture-conditioned soil with mechanical compaction equipment until densities greater than or equal to 95 % of maximum dry soil density was obtained as determined by testing. One exception to this general rule was the use of bags of vermiculite around Tanks 21 through 24. It was assumed that the presence of the material would have an insignificant effect on modeling.

Recommended K_d values for the vadose zone and backfill soil are primarily taken from recent compilation of geotechnical data prepared in support of site PA modeling

and supplemented by any recent element-specific reports as noted in Table 4.2-25. [SRNL-STI-2009-00473] Estimates of the K_d values were provided for each element and soil type. These values are based primarily on SRS site-specific experimental data, some central value of literature, or on expert judgment, with the site-specific experimental data being the preferred information source. It is not clear if the compilation of data included values from any calcareous strata or soft zones. There is no SRS chemical, mineralogical, or sorption data available known to be specifically representative of the soft zones. The silty and clayey fine sands, fine-grained clays, and calcareous shell fragments, which comprise the soft zones, would tend to raise the pH in the groundwater and introduce minor amounts of carbonate into the aqueous phase. If literature K_d values representative of the soft zones were included, the stochastic distributions for the vadose zone and backfill soil would likely spread, but would have minimal impact on recommended values.

Table 4.2-25 identifies K_d values of the vadose zone and backfill soils. The K_d values for each radionuclide in Table 4.2-25 were used in deterministic analysis and the UA/SA in the PA. SRNL-STI-2009-00473 provides information for soil K_d values when influenced by the high pH of cementitious material leachate. The values are applicable to vadose (unsaturated) zone soils and are not applicable to waste tanks in the water table (Type I and II tanks). The transition to non-cement leachate impacted K_d value will coincide with the transition of the CZ to Oxidized Region III.

The conceptual model also assumes that plutonium sorption is primarily controlled by solubility at the high pH levels of cementitious environments. Due to the high surface area and the very low solubility of plutonium, the K_{ds} for plutonium are also very high. This assumption stems from the experimental evidence and the extremely high tendency for plutonium to sorb even under very low plutonium concentrations to SRS sediments. [SRNL-STI-2009-00636] As discussed from lab testing, Pu(V) was added to SRS sandy subsurface sediment at plutonium concentration below Pu(V) solubility and analyzed after 33 days. The results show that the Pu(V) sorbed to the sediment under oxidizing conditions, in a manner similar to the plutonium geochemical behaving as Pu(IV). In the presence of cementitious materials, where much greater surface areas and higher pH levels exist, the K_{ds} are expected to increase significantly compared to the SRS sediments. [WSRC-TR-2003-00035]

Table 4.2-25: Recommended K_d Values for the Vadose Zone

Element	Soils Media		Cement Leachate Impacted Soils Media	
	Backfill Soil (mL/g)*	Vadose Zone Soil (mL/g)**	Backfill Soil (mL/g)*	Vadose Zone Soil (mL/g)**
Ac	8,500	1,100	12,750	1,650
Ag	30 ^b	10 ^b	480	192
Al	1,300	1,300	1,950	1,950
Am	8,500	1,100	12,750	1,650
Ar	0	0	0	0
As	200	100	280	140
At	0.9	0.3	0.1	0
B ^a	0	0	0	0
Ba ^c	101	15	303	45
Bi	8,500	1,100	12,750	1,650
Bk	8,500	1,100	12,750	1,650
C	400	10	2,000	50
Ca	17	5	51	15
Cd	30	15	90	45
Ce	8,500	1,100	12,750	1,650
Cf	8,500	1,100	12,750	1,650
Cl	8 ^b	1 ^b	0 ^a	0 ^a
Cm	8,500	1,100	12,750	1,650
Co	100	40	320	128
Cr	400 ^b	1,000 ^b	14	6
Cs	50	10	50	10
Cu	70	50	224	160
Eu	8,500	1,100	12,750	1,650
F	0	0	0	0
Fe	400	200	600	300
Fr	50	10	50	10
Gd	8,500	1,100	12,750	1,650
H	0	0	0	0
Hg	1,000	800	3,200	2,560
I	0.9	0.3	0.1	0
K	25	5	25	5
Lu	8,500	1,100	12,750	1,650
Mn	200	15	280	21
Mo	1,000	1,000	1,400	1,400
N	0	0	0	0

Table 4.2-25: Recommended K_d Values for the Vadose Zone (Continued)

Element	Soils Media		Cement Leachate Impacted Soils Media	
	Backfill Soil (mL/g)*	Vadose Zone Soil (mL/g)**	Backfill Soil (mL/g)*	Vadose Zone Soil (mL/g)**
Na	25	5	25	5
Nb	0	0	0	0
Ni	30	7	96	22
Np	9	3	14	5
PO ₄ ^a	0	0	0	0
Pa	9	3	14	5
Pb	5,000	2,000	16,000	6,400
Pd	30	7	96	22
Pm ^a	0	0	0	0
Po	5,000	2,000	10,000	4,000
Pr ^a	0	0	0	0
Pt	30	7	96	22
Pu	5,950	650 ^d	11,900	580
Ra ^b	185	25	555	75
Rb	50	10	50	10
Re	1.8	0.6	0.2	0.1
Rh ^a	0	0	0	0
Rn	0	0	0	0
Ru ^a	0	0	0	0
SO ₄ ^a	0	0	0	0
Sb	2,500	2,500	3,500	3,500
Se	1,000	1,000	1,400	1,400
Sm	8,500	1,100	12,750	1,650
Sn	5,000	2,000	15,000	6,000
Sr	17	5	51	15
Tc	1.8	0.6	0.2	0.1
Te	1,000	1,000	1,400	1,400
Th	2,000	900	4,000	1,800
Tl	70 ^b	25 ^b	0 ^a	0 ^a
U	400 ^b	300 ^b	900	600
V ^a	0	0	0	0
Y	8,500	1,100	12,750	1,650
Zn	30	15	90	45
Zr	2,000	900	4,000	1,800

- * Backfill soil represented by clayey sediment
- ** Vadose zone soil represented by sandy sediment
- Note: Values from SRNL-STI-2009-00473 unless otherwise noted
- a Assigned a value of zero
- b SRNL-STI-2010-00493
- c SRNL-STI-2011-00011
- d SRNL-STI-2011-00672

4.2.2.2.3 Procured Sands

Type II tanks were constructed above a 1-inch sand pad contained within a circular pan. An additional 1-inch sand pad is located under the secondary liner. In accordance with the requirements of site specifications, the consistency of sand in both of the 1 inch layers consists of clean, hard, durable, siliceous particles free from foreign material (i.e., procured and washed sand free of silt or clay), and uniformly graded from standard sieves #16 and #100. The size of the sand grain ranges from 0.15 millimeter (#100 sieve) to 1 millimeter (#16 sieve), and is classified as fine to medium sand per the Unified Soil Classification System (USCS), and fine to coarse per the USDA classification. [W163018]

Table 4.2-26 provides the estimated materials properties for the sand. Figure 4.2-29 provides the characteristic curves (suction head, saturation, and relative permeability) for the sand.

Table 4.2-26: Estimated Sand Material Properties of Interest

Material	Saturated D_e (cm ² /s)	Average η_T (%)	Average ρ_n (g/cm ³)	Average ρ_n (g/cm ³)	Horizontal K_{sat} (cm/s)	Vertical K_{sat} (cm/s)
Sand	8E-06	38	1.65	2.66	5E-04	2.8E-04

[WSRC-STI-2006-00198, Table 5-18]

D_e = Effective Diffusion Coefficient

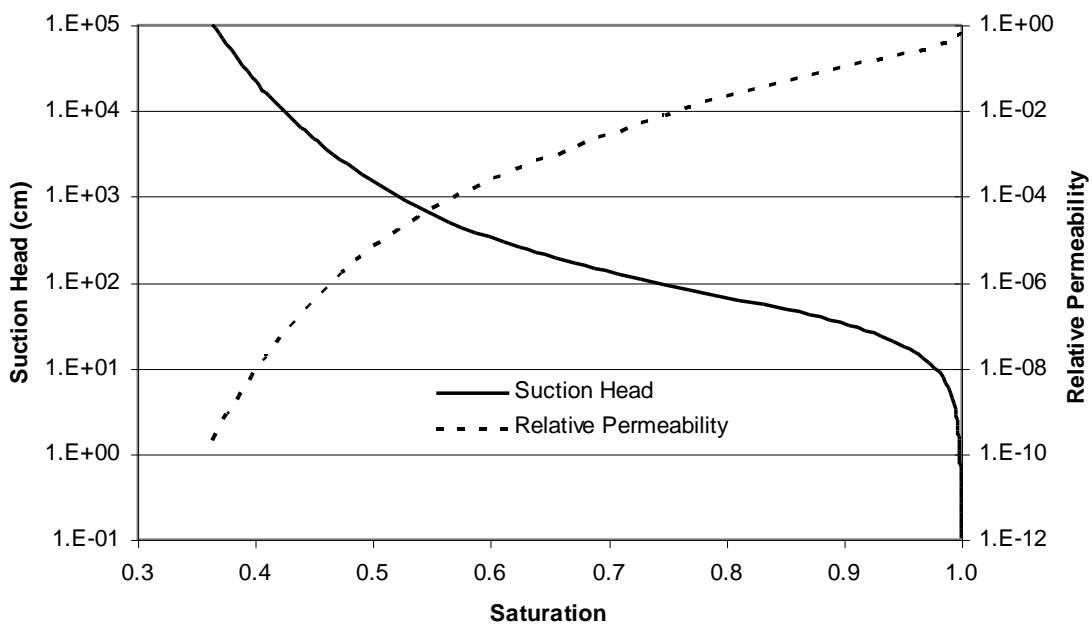
η_T = Total Porosity

ρ_h = Dry Bulk Density

ρ_n = Particle Density

K_{sat} = Saturated Hydraulic Conductivity

Figure 4.2-29: Procured Sand Characteristic Curves



[WSRC-STI-2006-00198]

Table 4.2-27 presents the thickness of the vadose zone beneath each of the waste tanks. The thicknesses of the vadose zone below the different waste tanks range from approximately -35.5 to 18.2 feet with negative values indicating the base of the tank is below the water table.

Table 4.2-27: Vadose Zone Thickness for HTF

Tank Type	Waste Tank	Working Slab Top Elevation (ft above MSL)	Approximate Water Table Elevation (ft above MSL)	Vadose Zone Thickness (ft)
I	9	241.4	276.9	-35.5
	10	241.4	276.3	-35.5
	11	241.4	277.2	-35.5
	12	241.4	276.6	-35.5
II	13	270.3	276.9	-6.6
	14	270.3	276.9	-6.6
	15	270.3	276.9	-6.6
	16	270.3	276.9	-6.6
IV	21	281.8	274.7	7.1
	22	281.8	274.7	7.1
	23	281.8	274.7	7.1
	24	281.8	274.7	7.1
III	29	283.5	275.4	8.1
	30	283.5	275.4	8.1
	31	283.5	275.4	8.1
	32	283.5	275.4	8.1
IIIA	35	282.7	268.3	14.4
	36	283.7	269.3	14.4
	37	283.7	269.3	14.4
	38	291.1	272.9	18.2
	39	291.1	272.9	18.2
	40	291.1	272.9	18.2
	41	291.1	272.9	18.2
	42	291.1	272.9	18.2
	43	291.1	272.9	18.2
	48	288.1	275.6	12.5
49	288.1	275.6	12.5	
50	288.1	275.6	12.5	
51	288.1	275.6	12.5	

[SRNL-STI-2010-00148]

4.2.2.2.4 Cementitious Material Properties

The physical and chemical properties of the cementitious materials associated with the waste tanks after closure (i.e., waste tank top and sides, basemat, grout fill) are needed for the ICM. Property estimates for cementitious materials associated with the HTF will be utilized as input to deterministic, sensitivity, and uncertainty modeling. This section will provide initial properties, hydraulic conductivity, K_d s, and degradation timing. Some properties are expected to remain constant over time. These include porosity, dry bulk density, particle density, and the water retention curves. Because the form of cementitious material degradation is cracking and not the dissolving of the cement paste, for the porosity, bulk density, and particle density of the cementitious material a marginal impact is expected. While it is recognized that some variability exists, it was judged a reasonable modeling simplification to hold porosity, dry bulk density, particle density, and the water retention curves constant. Section 4.4.2 describes additional cases employed in the model, which include the existence of fast flow paths, which could be attributed to cracked cementitious materials.

Estimates for these properties for the cementitious materials associated with the HTF waste tanks have been provided in SRNL-STI-2011-00551 and WSRC-STI-2007-00369. The cementitious materials in the HTF can be grouped into two types, 1) the grout used to fill the waste tanks, and 2) the concrete in the waste tank vault roof, basemat, and walls. The properties associated with the waste tank grout are taken from the specification reducing grout properties in SRNL-STI-2011-00551, which are based on testing of the grout formula planned to be used for waste tank fill. The properties associated with the waste tank concrete are taken from the basemat surrogate properties in WSRC-STI-2007-00369, which are based on testing of similar vintage SRS concrete (concrete from a P-Area foundation slab that is over 30 years old). The properties from SRNL-STI-2011-00551 and WSRC-STI-2007-00369 are shown in Table 4.2-28 and Figure 4.2-30.

Table 4.2-28: Cementitious Material Initial Properties

Material	η (%)	ρ_h (g/cm ³)	ρ_n (g/cm ³)	D_e (cm ² /s)	K (cm/s)
Vault Concrete (Basemat, Roof and Walls)	16.8	2.06	2.51	8.0E-07	3.4E-08
Grout Fill	21.0	1.97	2.49	5.0E-08	2.1E-09

D_e = Effective Diffusion Coefficient

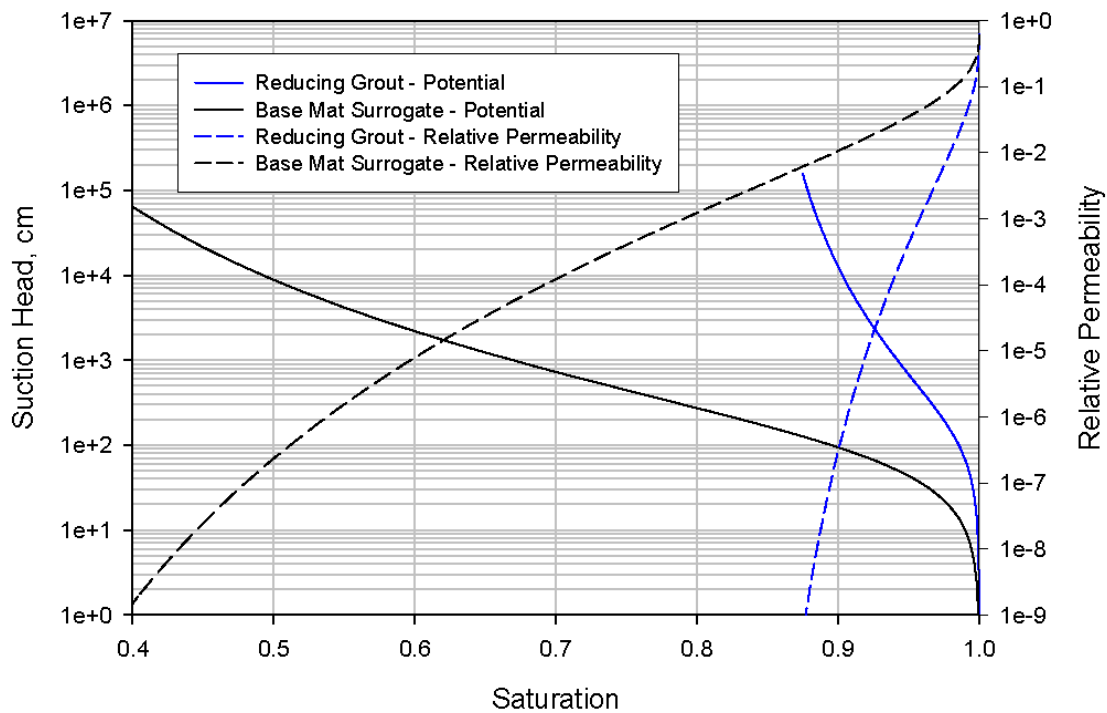
η = Porosity

ρ_h = Dry Bulk Density

ρ_n = Particle Density

K = Saturated Hydraulic Conductivity

Figure 4.2-30: Recommended Characteristic Curves for Waste Tank Grout and Concrete



[WSRC-STI-2007-00369]

As described in Section 3.2.3.1, some equipment will be left in place within the waste tanks and entombed within the grout. Despite the potential presence of cooling coils and other equipment, HTF PA modeling assumes that the grouted interiors of the waste tanks are homogenous. Columns, cooling coils, in-place mixers, and other equipment likely to be left within the tanks are not explicitly modeled; rather the interior of each waste tank is modeled as a single grouted monolith. As the grout is assumed both flowable and pumpable, due diligence shall be exercised to fill any void spaces associated with in-place equipment. Potential impacts from leaving this incidental equipment in place, with respect to grout performance (i.e., waste tank stability, reducing capacity, and flow), were evaluated for FTF and determined to be negligible. [SRR-CWDA-2012-00051]

Cementitious Material Hydraulic Conductivity

The cementitious barriers identified in the HTF closure concept are either reinforced concrete (waste tank vault and basemat) or non-reinforced grout (annulus and waste tank fill). The hydraulic conductivities of the initial state (non-degraded) materials were obtained from a concrete sample collected from a slab constructed in 1978 that was used as a surrogate for the vault and basemat concrete, and a laboratory sample of grout that was prepared by the current specification for waste tank operational closure. [WSRC-STI-2007-00369, SRNL-STI-2011-00551]

The saturated hydraulic conductivities of the concrete barriers after degradation by the various mechanisms were estimated. The discussion of the modeling approach and parameters will be detailed in Section 4.4.4.1.

Cementitious Materials K_d s

The K_d values are necessary for cementitious materials through which contaminants have the potential to travel. Table 4.2-29, provides K_d values for cementitious materials as a function of aging. The K_d values in Table 4.2-29 are based on SRS site-specific data, values from literature, or on engineering judgment, with the site-specific data being the preferred information source. [SRNL-STI-2009-00473] The K_d for an element is dependent on the pH of the pore water, which in turn is dependent upon the amount of water (number of pore water volumes) that has passed through the cementitious material over time. The water chemistry for the testing reported in SRNL-STI-2009-00473 is found in Table 9 of WSRC-STI-2007-00640. The experimental information for the aged concrete from P Area is used as the basemat surrogate. Because the foundation slab of non-slag containing concrete from P Area was exposed to natural environmental conditions, the early pore volumes of rainwater would have “aged” the concrete. The experimental results of K_d testing with the concrete are thus applicable to oxidizing K_d conditions. [WSRC-STI-2007-00640] To account for other important aspects of aged cement, such as mineralogical changes that exist in thousands of year old concrete, K_d values were further adjusted. The experimental results are similar to the values for oxidized concrete contained in NUREG_CR-6377 except for a non-zero technetium K_d . The experimental values reported in SRNL-STI-2009-00473 are used in conjunction with like element experimental values and previously reported K_d work in SRNL-STI-2010-00493 and SRNL-STI-2010-00667 in the determination of the recommended K_d values reported in Table 4.2-29.

Table 4.2-29: Recommended K_d Values for Cementitious Materials

Element	Oxidizing Cementitious Media			Reducing Cementitious Media		
	Young-Age (mL/g)	Middle-Age (mL/g)	Old-Age (mL/g)	Young-Age (mL/g)	Middle-Age (mL/g)	Old-Age (mL/g)
Ac	6,000	6,000	600	7,000	7,000	1,000
Ag	4,000	4,000	400	5,000	5,000	1,000
Al	6,000	6,000	600	7,000	7,000	1,000
Am	6,000	6,000	600	7,000	7,000	1,000
Ar	0	0	0	0	0	0
As	320	320	100	200	200	100
At	8	15	4	5	9	4
Au ^a	0	0	0	0	0	0
B ^a	0	0	0	0	0	0
Ba ^c	100	100	70	100	100	70
Be ^a	0	0	0	0	0	0
Bi	6,000	6,000	600	7,000	7,000	1,000
Bk	6,000	6,000	600	7,000	7,000	1,000
C	3,000	3,000	300	3,000	3,000	300
Ca	15	15	5	15	15	5
Cd	4,000	4,000	400	5,000	5,000	1,000
Ce	6,000	6,000	600	7,000	7,000	1,000
Cf	6,000	6,000	600	7,000	7,000	1,000
Cl	10	10	1	10	10	1
Cm	6,000	6,000	600	7,000	7,000	1,000
Co	4,000	4,000	400	5,000	5,000	1,000
Cr	10	10	1	1,000	1,000	1,000
Cs	2	20	10	2	20	10
Cu	4,000	4,000	400	5,000	5,000	1,000
Es ^a	0	0	0	0	0	0
Eu	6,000	6,000	600	7,000	7,000	1,000
F	10	10	1	10	10	1
Fe	6,000	6,000	600	7,000	7,000	1,000
Fr	2	20	10	2	20	10
Ga ^a	0	0	0	0	0	0
Gd	6,000	6,000	600	7,000	7,000	1,000
Ge ^a	0	0	0	0	0	0
H	0	0	0	0	0	0

Table 4.2-29: Recommended K_d Values for Cementitious Materials (Continued)

Element	Oxidizing Cementitious Media			Reducing Cementitious Media		
	Young-Age (mL/g)	Middle-Age (mL/g)	Old-Age (mL/g)	Young-Age (mL/g)	Middle-Age (mL/g)	Old-Age (mL/g)
Hf ^a	0	0	0	0	0	0
Hg	300	300	100	5,000	5000	1,000
Ho ^a	0	0	0	0	0	0
I	8	15	4	5	9	4
In ^a	0	0	0	0	0	0
Ir ^a	0	0	0	0	0	0
K	2	20	10	2	20	10
Kr	0	0	0	0	0	0
La ^a	0	0	0	0	0	0
Lu	6,000	6,000	600	7,000	7,000	1,000
Mn	100	100	10	100	100	10
Mo	300	300	150	300	300	150
N	10	10	1	10	10	1
Na	0.5	1	0.5	0.5	1	0.5
Nb	1,000	1,000	500	1,000	1,000	500
Ni	4,000	4,000	400	4,000	4,000	400
Np	10,000	10,000	5,000	10,000	10,000	5,000
P ^a	0	0	0	0	0	0
Pa	10,000	10,000	5,000	10,000	10,000	5,000
Pb	300	300	100	5,000	5,000	1,000
Pd	4,000	4,000	400	5,000	5,000	1,000
Pm ^a	0	0	0	0	0	0
Po	300	300	100	5,000	5,000	500
PO ₄ ^a	0	0	0	0	0	0
Pr ^a	0	0	0	0	0	0
Pt	4,000	4,000	400	5,000	5,000	1,000
Pu	10,000	10,000	2,000	10,000	10,000	2,000
Pu_4	10,000	10,000	2,000	10,000	10,000	2,000
Pu_5	1,000	1,000	100	1,000	1,000	100
Ra	100	100	70	100	100	70
Rb	2	20	10	2	20	10
Re	0.8	0.8	0.5	5,000	5,000	1,000
Rh ^a	0	0	0	0	0	0
Rn	0	0	0	0	0	0
Ru ^a	0	0	0	0	0	0
Sb	1,000	1,000	100	1,000	1,000	100
Sc ^a	0	0	0	0	0	0
Se	300	300	150	300	300	150

Table 4.2-29: Recommended K_d Values for Cementitious Materials (Continued)

Element	Oxidizing Cementitious Media			Reducing Cementitious Media		
	Young-Age (mL/g)	Middle-Age (mL/g)	Old-Age (mL/g)	Young-Age (mL/g)	Middle-Age (mL/g)	Old-Age (mL/g)
Si ^a	0	0	0	0	0	0
Sm	6,000	6,000	600	7,000	7,000	1,000
Sn	4,000	4,000	2,000	5,000	5,000	500
SO ₄ ^a	0	0	0	0	0	0
Sr ^c	15	15	5	15	15	5
Ta ^a	0	0	0	0	0	0
Tc ^c	0.8	0.8	0.5	1,000	1,000	1,000
Te	300	300	150	300	300	150
Th	10,000	10,000	2,000	5,000	5,000	500
Ti ^a	0	0	0	0	0	0
Tl	150	150	150	2	20	10
U	1,000 ^b	1,000 ^b	100 ^b	2,500	2,500	2,500
V ^a	0	0	0	0	0	0
Y	6,000	6,000	600	7,000	7,000	1,000
Zn	4,000	4,000	400	5,000	5,000	2,000
Zr	10,000	10,000	2,000	5,000	5,000	500

Note: Values from SRNL-STI-2009-00473 unless otherwise noted

a Assigned a value of zero

b SRNL-STI-2010-00493

c SRNL-STI-2010-00667

The number of pore water volumes passing through the waste tank and the corresponding transitions to different waste tank chemistry conditions is included in the HTF modeling. As part of the waste release modeling (discussed in detail in Section 4.2.1), the estimated transition times between various chemical phases was calculated for the waste tank pore water. The waste tank pore water chemistry for non-submerged waste tanks was calculated to change from Region II Reduced conditions (middle age reducing) to Region II Oxidized conditions (middle age oxidizing) after 523 pore volumes pass through the grout. The change from Region II conditions (middle age) to Region III conditions (old age) was calculated to occur after 2,119 pore volumes. [ISSN 1019-0643, SRNL-STI-2012-00404]

The waste tank pore water chemistry for submerged waste tanks was calculated to change from Condition C to Condition D after 1,787 pore volumes pass through the grout. The change from Condition D to Oxidized Region III was calculated to occur after 2,442 pore volumes pass through the grout. [SRNL-STI-2012-00404]

As a modeling simplification, the pore volume transition times for the Base Case were determined assuming the representative grout formula was present throughout the waste tank interior.

As part of the UA/SA, the transition times between chemical states was varied in the stochastic analyses as described in Section 5.6.3.8.

Based on changes in the pH with aging, the K_d values for concrete have been divided into three stages as shown in Table 4.2-29. [SRNL-STI-2009-00473] The young, middle, and old ages correspond to Regions I, II, and III. Waste tank grout and concrete are initially characterized as middle aged (Region II) and transition to Region III over time as the material properties change. Because the waste tank grout and cement in individual waste tanks will be aged at the time of overall HTF closure, none of the waste tank cementitious materials were characterized as young (Region I). [ISSN 1019-0643]

Grout and Concrete Degradation

The current SRS HTF disposal environment is very benign with respect to chemical degradation of the reinforced concrete vaults and the waste tank grout material. Consequently, the degradation due to chemical processes is expected to progress at a very slow rate. An evaluation of the HTF grout and concrete degradation is presented in more detail in SRNL-STI-2010-00035.

The penetration depth of the chemical species responsible for the degradation was assumed as equivalent to the depth of degradation. The consequences of the degradation depended on the material porosity and if the material contained steel reinforcement because carbon-steel rebar introduces an additional degradation process (i.e., concrete cracking due to formation of expansive metal corrosion products). [SRNL-STI-2010-00035]

Porosity and diffusion coefficient data for two representative materials were used in calculations to predict the depth of penetration of the various forms of chemical attack. These materials were a surrogate foundation slab of concrete (3,000-psi concrete from P Area that was poured in 1978) which represented the vault and basemat concrete and a waste tank grout that represented all of the grout in the waste tanks and the annulus spaces.

For saturated concrete and grout, acid leaching (i.e., decalcification) was the most aggressive degradation mechanism. The depth of severe decalcification at 1,000-years exposure was 6.5 and 8.2 centimeters for the surrogate vault concrete and waste tank grout, respectively. The effect of decalcification is to increase porosity and permeability and to decrease the pH of the pore solution from approximately 12.5 to lower values depending on the evolution of the mineral phase assemblages as a function of calcium concentration in the pore solution. [SRNL-STI-2010-00035]

For unsaturated concrete and grout in the vadose zone, the most extensive cementitious penetration as a function of time was found to be from carbonation. For material with the porosity of the surrogate basemat concrete (volume fraction of 16.8 %), the depth of penetration from carbonation was estimated to be 21 centimeters (8.27 inches) after 1,000 years. The estimated depth of penetration for the representative grout from carbonation reactions was 36 centimeters (14.17 inches) after 1,000 years. These values were applied to Type I, II, III, and IIIA tanks. Because Type IV tanks contain no cooling coils in the grout and are therefore not affected by steel expansive phase corrosion impacts, the estimated depth of

penetration for the representative reducing grout was 8.2 centimeters (3.23 inches) after 1,000 years. [SRNL-STI-2010-00035]

The effect of carbonation on the permeability of the cementitious barriers in the HTF closure concept depends on whether the barrier contains steel. Carbonation in itself may actually reduce permeability by plugging pores with calcium carbonate. However, it will affect the permeability of reinforced concrete because the concrete will crack due to formation of expansive iron hydroxide phases that form when steel corrodes. Steel passivation is lost when the pH of the pore solution is in equilibrium with calcium carbonate (a pH of approximately 8.4) rather than calcium hydroxide (a pH of approximately 12.5). [SRNL-STI-2010-00035]

The consequences of carbonation with respect to the permeability of the cementitious barriers in the HTF depend on the assumptions made to link depth of penetration with formation of expansive iron hydroxide phase from associated rebar corrosion and the assumptions linking corrosion with concrete cracking. For the reinforced vault concrete, the assumption that cracking occurs simultaneously with carbonation is unrealistic. Cracking will lag the carbonation by a considerable time especially in the absence of other corrodents such as chloride ions. When cracking from expansion does occur, the permeability will increase.

Because the annulus grout and grout in the waste tanks without cooling coils do not contain rebar or steel, the overall effect of carbonation should be minimal regardless of the depth of penetration. The permeability of these materials is not expected to change significantly as the result of carbonation. This is the case even though the rate of carbonate penetration is faster due to the higher porosity of the reducing grout (a volume fraction of 26.6 %). [SRNL-STI-2010-00035]

Carbonation of the grout will not commence until the waste tank is breached due to corrosion or development of a fast pathway. Based on calculated waste-tank corrosion rates a lengthy lag time is anticipated before carbonate actually contacts the grout and the carbonation front advances to the cooling coils. The corrosion rate is expected to be very slow in the absence of additional corrodents. The effect of carbonation on cracking when it does occur is expected to be the same as described above. However, the possibility exists that expansive reactions occurring under the somewhat constrained conditions of the buried waste tank could result in very little change in permeability. [SRNL-STI-2010-00035]

The use of a compressive strength of 1,800 psi as a long-term degraded cement property is the design strength of the cement neglecting any further increase in strength. Justification that 1,800 psi bounds the concrete strength and is an appropriate lower bound for use as the long-term material strength of concrete and grout is provided in T-CLC-F-00421.

The radiological effects on degradation of grouted waste tank residuals are estimated as bounded by the modeled degradation mechanism based on data from a study on solidification of SRS HLW sludge in portland cement matrices. In this study, simulated high-level cementitious waste forms were gamma-irradiated to 1,010

radiation-absorbed doses. After irradiation, compressive strength and the strontium leachability of the cementitious waste forms were measured and compared to samples that were not irradiated. No significant reductions of compressive strength or increase in strontium leaching, which are degradation metrics, were attributed to the radiological exposure. [DP-1448] The effects of the alpha radiation on the degradation properties of grout are expected to be less than the effects of the gamma radiation because the alpha dose rates that the grout will be exposed to are lower than the gamma dose rates. [SRNL-PSE-2006-00097]

Consideration of the lack of HTF ground motion and soil-structure interaction studies for low probability of exceedance events at SRS led to adoption of the same bounding criteria for the HTF structural assessment as that described in *Structural Assessment of F-Area Tank Farm After Final Closure* (T-CLC-F-00421). The impact from seismic effects on grout and concrete degradation is implicitly considered in the conceptual model. To simulate potential conditions in the HTF closure system, multiple waste tank cases were evaluated in the stochastic modeling.

As the grout-filled waste tank is essentially a monolithic block, only extremely large ground motions would have significant effects. As a buried monolith, no amplification will occur in the structure, so a convenient method of determining the peak ground acceleration from the design response spectra is to determine a value at very high frequencies or very low periods, often referred to as the zero period acceleration, where period is the reciprocal of the frequency. Based on extrapolation from SRS PC-3 ($P = 4.0E-04$) and PC-4 ($P = 1.0E-4$) site design response spectra, the horizontal and vertical peak ground accelerations are 0.45g and 2.0g respectively for an event with a probability of exceedance of $1.0E-06$. [T-CLC-F-00421] It is recognized that 2.0 grams vertical acceleration is a bounding number for ground acceleration at SRS since it is extrapolated from the peak of the SRS horizontal design spectra. At the nearby Vogtle Electric Generating Plant, the vertical/horizontal ratio for the maximum considered event was 1.0, so a similar ratio should be considered acceptable for the SRS tank farms. [NUREG-1923] Based on a vertical/horizontal ratio of 1.0, the maximum vertical acceleration would be 0.45 grams, much less than 2.0 grams assumed. The grout monolith is not expected to crack from these accelerations.

The timing of the degradation of the waste tank cementitious materials is detailed in Table 4.2-30 for the various waste tank types. The table provides the point in time the applicable cementitious material (grout or concrete) transitions from the initial state, to a degrading state, to a fully degraded state.

Table 4.2-30: Cementitious Material Degradation Transition Times (Yrs) by Waste Tank Type

Cementitious Material Stages	Type I	Type II	Type III	Type IIIA	Type IV
HTF Reducing grout (Initial Properties)	0 - 2,700	0 - 5,100	0 - 5,100	0 - 5,000	0 - 800
Degrading HTF Reducing grout	2,700 - 13,200	5,100 - 16,700	5,100 - 19,200	5,000 - 19,100	800 - 64,400
Fully Degraded HTF Reducing grout	13,200	16,700	19,200	19,100	64,400
HTF Concrete (Initial Properties)	0 - 1,350	0 - 2,550	0 - 2,550	0 - 2,500	0 - 400
Degrading HTF Aged Concrete	1,350 - 2,700	2,550 - 5,100	2,550 - 5,100	2,500 - 5,000	400 - 800
Fully Degraded HTF Aged Concrete	2,700	5,100	5,100	5,000	800

[SRR-CWDA-2010-00019]

4.2.2.2.5 Contamination Zone Properties

A waste release study describing the component of the CZ conceptual model related to the waste release approach (i.e., contaminant leaching) was prepared for the HTF PA. This study describes the methods used to estimate solubility and sorption controls on contaminant release, and provides specific calculations for uranium and technetium as examples of the process used. [SRNL-STI-2012-00404]

4.2.2.2.6 Carbon and Stainless Steel Material Properties

Material properties for carbon steel used in the liner and stainless steel used in the ancillary equipment are expressed as predicted times of failure due to corrosion under different conditions or as being initially failed based on current waste-tank liner conditions. Prior to failure, steel is assumed as impermeable with respect to both advection and diffusion. After failure, steel is assumed to be absent, or otherwise not a hindrance to advection and diffusion (i.e., there would be no retardation). In the steel liner failure analyses, there was not an independent assessment of the secondary liner. It is explicitly modeled and fails at the same time as the primary liner.

Carbon Steel

Predictions for failure of the carbon steel liners are based on the results of two studies. [WSRC-STI-2007-00061, SRNL-STI-2010-00047] These studies developed estimates for corrosion-induced failure of the steel liners. These estimates considered general and localized corrosion mechanisms of the waste tank steel exposed to the CZ, to grout, and to soil conditions for the Type I, II, III, IIIA, and IV tanks in HTF.

SRNL-STI-2010-00047 focused specifically on the degradation of the Type I and II tanks and transfer lines in groundwater.

Degradation of the waste tank steel encased in grouted conditions was estimated due to carbonation of the concrete leading to low pH conditions, or the chloride-induced depassivation of the steel leading to accelerated corrosion. Chloride-induced corrosion was determined to be the more aggressive phenomenon.

The time of liner failure is calculated based on steel corrosion rates under different conditions (e.g., differing diffusion coefficients). These failure times vary with waste tank design, owing to differences in construction. The timing of consumption of the waste tank steel encased in grouted conditions is estimated due to carbonation of the concrete leading to low pH conditions, and the chloride-induced depassivation of the steel leading to accelerated corrosion.

The liner failure analyses considered the current condition of the HTF waste tanks, with the relevant parameters being known leak sites, their location, and whether they led to accumulation on the annulus floor. All HTF Type I and Type II tanks (Tanks 9 through 16) have documented leak sites.

In-leakage of liquid into the annulus space by rainwater entering through riser opening plugs, transfer line openings, or past tank-top cover plates would be sporadic, linked to ambient conditions, and of limited duration due to operation of the annulus ventilation system. Any rainwater that might leak into the waste tanks before grouting should be inhibited by a small heal of alkaline waste that should minimize the amount of corrosion.

The liner failure study considered the condition of the HTF waste tanks to be closed when determining the liner failure times. Since the transport model is most concerned with waste tank failures that could allow significant flow through and away from the CZ, the failure mechanisms of primary concern are those near or at the bottom of the waste tanks that cause significant through-wall flow. Data on waste tank conditions is compiled and updated annually through a waste-tank inspection program. The leak site information in C-ESR-G-00003 is updated as needed to reflect any changes to conditions. C-ESR-G-00003 documents the number of leak sites and their location on the liner. As noted above, Tanks 9 through 16 have leak sites as documented in C-ESR-G-00003. Waste tanks with only a small number of leak sites that are located near the top of the liner and away from the CZ are modeled as failing per the information provided in SRNL-STI-2010-00047, which includes Tanks 9, 10, 11, and 13. Tanks 12, 14, 15, and 16 have either many leak sites and/or leak sites located near the bottom of the liner, thus near the CZ. Tanks 12, 14, 15, and 16 are therefore modeled with liner failure at the time of closure and the liner is not assumed as a barrier to flow. The Type III, IIIA, and Type IV tanks have not experienced any service-induced pitting or cracking and are assumed in the same condition as when put into service. There are not any waste tanks believed to have experienced general corrosion based on the results of ultrasonic inspections.

The liner studies considered that the waste tank steel liner thicknesses at the time of closure may be different from the nominal thicknesses per specifications used for this analysis. Specifically, chemical cleaning utilizing OA has been proposed to remove the last remnants of waste in the waste tank prior to operational closure. An analysis of the waste tank chemical cleaning was completed to determine any major influence on the initial thickness.

Corrosion testing has been done to determine the effects of the OA cleaning process on the carbon steel. Corrosion rates during OA chemical cleaning depend on the concentration of the chemical cleaning agent, the temperature of the cleaning solution, and if the solution is agitated. Based on the results for the mass fraction of 1 % and 8 % OA, the corrosion rate increased from 21 mils/yr to 45 mils/yr, respectively. Above 30°C, corrosion rate dramatically increases, up 100 mils/yr at 60°C. Agitation increases the chemical cleaning effectiveness to dissolve sludge solids and increases the steel corrosion rate by several orders of magnitude. Localized corrosion (i.e., pitting) would not reach 50 % through wall during OA sludge cleaning. The risk of significant corrosion may be reduced by minimizing the exposure time and the length of time that the chemical solution is agitated, reducing the temperature, and the presence of a head of inhibited water. The calculated results indicate that the maximum metal loss due to the cleaning process is minimal (less than 10 mils, or 0.01 inch). Thus, OA cleaning does not affect the liner failure model.

A stochastic approach is used to estimate the distributions of failures based upon the differing mechanisms of corrosion, but accounting for variances in each of the independent variables. It is assumed that life of the waste tank liners is a function of the time to corrosion initiation plus the time for corrosion to propagate through the liner. The corrosion proceeds under grouted conditions until chloride can induce depassivation of the surface or carbonation can reduce the pH of the surrounding concrete, thereby negating the high pH “protection” of the steel liner.

The failure time of the liner is defined to be:

$$t_{failure} = t_{initiation} + \frac{Thickness}{CorrosionRate}$$

where:

$t_{failure}$	=	time to complete consumption of the waste tank wall by general corrosion
$t_{initiation}$	=	time to chloride induced depassivation or carbonation front
$Thickness$	=	initial thickness of liner (mils)
$CorrosionRate$	=	dependent upon condition (i.e., chloride or carbonation in mils/yr)

The time to failure of the primary liner by general corrosion can be due to the following:

- General corrosion in grouted conditions
- Chloride induced depassivation, followed by general corrosion
- Carbonation induced loss of protective capacity of the concrete
- A combination of items 1 through 3

The corrosion rate, once chloride induced depassivation occurs, is calculated based upon oxygen diffusion through the concrete. Given the low passive current densities, the amount of waste tank liner wall loss due to corrosion is expected to be relatively minor during the initiation phase. Wall loss is accelerated during the time that corrosion mechanisms are most active. Carbonation proceeds more rapidly at the higher humidity found in the concrete pores exposed to soil, as opposed to the humidity of ventilated annulus or sealed tank interiors. Thus, the aggressive corrosion species are migrating primarily from the exterior side of the waste tank steel as the rate of diffusion of carbon dioxide or calcium hydroxide into the saturated pore spaces increases. The corrosion rate assumption once the carbonation front reaches the liner is 10 mils/yr. Thus, the system is modeled from a single side as a competition between the initiation time to chloride-induced depassivation and the initiation time to carbonation induced corrosion rates. The system also addresses the issue of the carbonation front reaching the waste tank liner prior to complete failure by chloride-induced corrosion.

Localized corrosion mechanisms are accounted for in the comprehensive stochastic model. Pit growth contributes to the corrosion rate; however, the rate of pit growth decreases with time by nearly two orders of magnitude after the first 50 years. This decrease is typical for carbon steels and is associated with the build-up of corrosion products that inhibit the availability of aggressive species at the steel surface.

The stochastic analysis elucidated insights into the controlling mechanisms of failure for each of the waste tank types. The failure times are a function of the diffusion coefficients, thereby controlling the failure times. The analyses are based upon the assumption that carbonation was the most aggressive mechanism of corrosion of the waste tank liner due to the loss of the high pH environment, and that chloride may induce depassivation on the steel surface, but is still dependent upon the oxygen diffusion to drive the corrosion reaction. The relative effects of carbonation and chloride induced corrosion as a function of diffusion coefficient can be examined by comparing the median values of failure for each of the conditions. The results suggest that the carbonation rates are the critical factor in controlling the life estimation. Once the carbonation front has reached the steel liner, the liner is essentially consumed within a nominal time of 50 years. As such, the recommendations for failure time used in stochastic modeling for contaminant escape are critically linked to the diffusion coefficients. The diffusion coefficient for oxygen through the concrete is not as critical.

The failure distributions for a diffusion coefficient of $1.0E-06 \text{ cm}^2/\text{s}$ are used in the stochastic modeling analyses. The distributions reflect the results of the statistical corrosion analysis using site-specific water and soil conditions. [WSRC-STI-2007-00061, SRNL-STI-2010-00047] These diffusion rates are considered bounding (i.e., faster than rates that are typically reported). Typically, the diffusion rates of each are calculated and/or measured to be approximately $1.0E-08 \text{ cm}^2/\text{s}$. The results indicate that the majority of the statistical observations convert to carbonation related initiation/failure when carbonation diffusion coefficients are greater than $1.0E-05 \text{ cm}^2/\text{s}$.

A failure analysis was performed to incorporate a diffusion coefficient distribution and a more bounding corrosion rate distribution into a single waste tank life, liner distribution. The additional waste-tank liner failure analysis considers the passive current density along with other potential corrosion mechanisms with uncertainty included. The parameters included in the analysis take into account:

- Grout may provide less corrosion protection than high quality concrete
- Potential for galvanic corrosion with stainless steel
- Initial failures by stress corrosion cracking
- Variability in the passive current density
- Potential rapid gaseous transport pathways leading to small regions with carbonation reaching the waste tank liner at early periods
- Spatially variant corrosion rate at different locations on the same waste tank
- Potential for more rapid corrosion of welds

This analysis incorporated a wider range of outcomes into a single distribution, so that the possible liner failure dates and probabilities across the entire spectrum of scenarios could be observed at one time. The results of this sensitivity study are shown in Table 4.2-31. The liner failure distributions can be interpreted in two ways, with the specified failure probability and calculated year representing either:

The year in which the stated percentage of waste tanks will have their primary liners totally fail (e.g., 25 % of all the Type IV tanks will have their primary waste tank liners completely fail at year 90)

The year in which a given percentage of an individual waste tank primary liner fails (e.g., 25 % of the Tank 21 primary liner will fail at year 90)

Table 4.2-31: Comprehensive Sensitivity Analysis of Carbon Steel Liner

Tank Type	Years Following HTF Tank Closure		
	25 % Failure Probability	50 % Failure Probability	75 % Failure Probability
Type I	2,097	4,183	6,153
Type II	2,461	4,890	6,283
Type III/IIIA	3,397	8,272	15,289
Type IV	90	2,010	8,104

For the failure analysis presented in SRNL-STI-2010-00047, HTF Type I and II tanks were exposed to soils with significant amounts of groundwater. The groundwater can increase the general corrosion rate due to higher electrolyte mobility and higher conductivity that can increase corrosion. Differences in oxygen concentration at the interface where soil with groundwater meets soil without groundwater can cause galvanic cells that increase the corrosion rate. The Type I tanks in the HTF are submerged more than 50 % in groundwater. Type II tanks in the HTF have some exposure of the concrete vault bottom to soil with groundwater. The effect of groundwater on the waste tank corrosion can be seen by comparing this simulation with the simulation for Type I tanks in Table 40 of WSRC-STI-2007-00061 Rev. 2. The median time to failure of the waste tank decreased to 4,183 years in the presence of groundwater from 7,630 years in soils with no significant groundwater. The decrease in the time to failure is mainly due to the higher corrosion rate of the waste tank liner after it has gone through depassivation from chloride attack.

Although Type II tanks are primarily in soil without groundwater, some Type II tanks are partially submerged in groundwater. The median time to failure of the waste tank decreased to 4,890 years in the presence of groundwater from 13,600 years in soils with no significant groundwater.

The cases are meant to represent conditions that may be present without regard to the mechanism that led to those conditions. There are varieties of mechanisms that can lead to earlier degradation times than those modeled in the Base Case. In the closed HTF conditions, some mechanisms may be possible although not likely. The cases should not be interpreted as representing a specific mechanism for liner degradation. The liner failure times modeled in Cases B, C, D, and E are meant to encompass various mechanisms and provide information on the risk significance of earlier liner failure than that modeled in the Base Case.

This showed that if differences between expected waste tank modeling cases (Section 4.4.1) are disregarded, and all liner failure mechanisms are considered simultaneously, the liner life could be shortened. Utilizing different scenarios for modeling is still preferred for the ICM Base Case since independently moving the liner failure date forward can decrease the peak dose. Early liner failure tends to allow the closure cap to reduce infiltration into the waste tank during release of radionuclides that are not significantly affected by either the waste release solubility limits and/or concrete/soil retardation (e.g., with low soil/concrete K_d values). The early liner failure can, therefore spread the releases out over a longer period.

Table 4.2-32 presents a summary of the deterministic (i.e., single value) and probabilistic (i.e., distribution) values that are used to determine liner failure during modeling. The deterministic values utilize the median values from the stochastic analysis. The results corresponding to the reasonably bounding carbon dioxide diffusion rates ($1.0E-06 \text{ cm}^2/\text{s}$) were utilized for baseline modeling and a bounding oxygen diffusion rate of $1.0E-04 \text{ cm}^2/\text{s}$ for submerged waste tanks and $1.0E-06 \text{ cm}^2/\text{s}$ for non-submerged waste tanks. The results corresponding to the maximum evaluated carbon dioxide diffusion rates ($1.0E-04 \text{ cm}^2/\text{s}$) were utilized for fast flow

case modeling and for the rising aquifer modeling case, where the loss of reducing capability for the cementitious materials might be expected to occur sooner but the oxygen diffusion rates are not changed from the Base Case. As discussed previously, Tanks 12, 14, 15, and 16 were modeled with a liner failure at the time of waste tank operational closure based on the number and/or location of existing leak sites.

Table 4.2-32: Carbon Steel Liner Life Estimates by Waste Tank Type

Waste Tank Type	Applicable Cases ^a	Grouted Waste Tank Liner Condition ^f	Liner Failure Year for Modeling	
			Deterministic	Probabilistic
Type I	A	D_i 1.0E-06 CO ₂ , 1.0E-04 O ₂	11,397 ^b	Figure 43 ^c
	B, C, D, E	D_i 1.0E-04 CO ₂ , 1.0E-04 O ₂	1,142 ^b	Figure 44 ^c
Type II	A	D_i 1.0E-06 CO ₂ , 1.0E-04 O ₂	12,687 ^b	Figure 46 ^c
	B, C, D, E	D_i 1.0E-04 CO ₂ , 1.0E-04 O ₂	2,506 ^b	Figure 47 ^c
Type III/IIIA	A	D_i 1.0E-06 CO ₂ , 1.0E-06 O ₂	12,751 ^d	Table 34 ^e
	B, C, D, E	D_i 1.0E-04 CO ₂ , 1.0E-06 O ₂	2,077 ^d	Table 35 ^e
Type IV	A	D_i 1.0E-06 CO ₂ , 1.0E-06 O ₂	3,638 ^d	Table 37 ^e
	B, C, D, E	D_i 1.0E-04 CO ₂ , 1.0E-06 O ₂	75 ^d	Table 38 ^e

- a Conditions are from Table 4.4-1.
- b Median value from same figures as (c) below $D_i(O_2) = 1.0E-04$
- c Figures from SRNL-STI-2010-00047
- d Median value from same tables as (e) below $D_i(O_2) = 1.0E-06$
- e Tables from WSRC-STI-2007-00061
- f Diffusion coefficient reported in cm²/s
- D_i Intrinsic diffusion coefficient

Prior to failure, the liner is assumed impermeable with respect to both advection and diffusion. After failure, the liner is assumed to not be a hindrance to advection and diffusion (i.e., retardation due to the presence of corrosion products is not included in the model).

The failure years associated with Table 4.2-32 represent median values used to represent failure, which as discussed previously, was modeled as the date from which the steel liner is absent or otherwise not a hindrance to advection and diffusion. The conceptual model is a reasonable simplification, utilizing a “simultaneous” liner failure model, which assumes the entire liner fails in a given year. The simultaneous liner failure model was used instead of using a patch model, which would add percentages of each waste tank failing each year (i.e., leak sites in the liner appearing at different waste tank locations, percent of through wall leakage increasing, and the waste tank gradually failing over time). Although not an exact simulation of the expected primary liner failure mechanism, the conceptual-model liner failure approach is reasonable for the following reasons:

The CZ of concern is located essentially across the waste tank bottoms, making failure of most liner sections unimportant, since they would not result in flow through or contaminant release from the CZ.

Modeling the entire primary liner to fail concurrently would have a tendency to maximize the flow path simultaneously into and away from the CZ, which would in turn has a tendency to maximize peak doses. Allowing the entire liner to fail early or

allowing small flow paths through the CZ as the patch model approach would simulate, can have the tendency to decrease the resulting peak doses (as detailed in the Section 5.6.7 comprehensive sensitivity analysis discussion).

Though not independently addressed in the carbon steel failure analysis, in addition to the primary liner, there is a full secondary steel liner for the Type III and IIIA tanks and a 5-foot high secondary liner near the CZ for the Type I and II tanks. In the analyses, these secondary liners are assumed to fail at the same time as the primary steel liner. If the patch model were used, failure of a single patch near the CZ might not result in contaminant release if the nearby secondary liner patches were still intact.

Stainless Steel

Two conditions were analyzed in WSRC-STI-2007-00460 for situations without significant groundwater, general corrosion, and pitting penetration. Table 4.2-33 presents the results of the FTF study for these two conditions in soil for various stainless steel wall thicknesses. Pitting corrosion was found to be the controlling mechanism for the degradation of the stainless steel transfer-line core piping and its consequent ability to maintain confinement of contaminants. It is assumed that if 75 % of the transfer line is intact, the line is capable of providing this confinement function (i.e., once 25 % of the line wall has been penetrated, the lines are considered incapable of confining contaminants). The probabilistic analysis for the HTF is discussed further in Section 4.4.2 of this PA.

Table 4.2-33: Corrosion Induced Failure Times for Stainless Steel Transfer Lines

SRS Soil Conditions	Years Following Waste Tank Closure		
	3-in dia (0.19-in min wall thickness)	2-in dia (0.14-in min wall thickness)	1-in dia (0.12-in min wall thickness)
Failure: steel consumption	4,725	3,375	2,900
Failure: 25 % pitting penetration	532	515	510
First pit penetration	189	135	116

[WSRC-STI-2007-00460]

These estimates can be applied to general and localized corrosion mechanisms of the stainless steel exposed to SRS soil conditions for the stainless steel core transfer lines in HTF. Section 3.2.2.1 describes the different types of transfer lines used in the HTF. The vast majority of the piping is stainless steel, either encased in concrete, inside a carbon-steel jacket, or surrounded by a cement-asbestos jacket. The core pipe has a diameter ranging from 1 inch to 3 inches with minimum wall thicknesses from 0.12 inch to 0.19 inch (minimum wall thicknesses are 87.5 % of nominal wall thicknesses). [WSRC-STI-2007-00460] The lifetime of the transfer lines is shortened by both general corrosion and pitting corrosion. The life of the stainless steel transfer lines was estimated for general corrosion based upon 0.04 mils/yr bounding. Pitting of the stainless steel transfer lines starts faster than general

corrosion, but the pitting rate decreases significantly and the pitting depth is less than the depth of general corrosion by 500 years after soil with groundwater exposure. The failures of the lines due to general corrosion are between 2,900 to 4,725 years for various diameter stainless steel pipes. [WSRC-STI-2007-00460]

These estimates considered general and localized corrosion mechanisms of the stainless steel exposed to SRS soil conditions for the stainless steel core transfer lines in HTF. Section 3.2.2.1 describes the different types of transfer lines used in the HTF. The vast majority of the piping is stainless steel, either encased in concrete, inside a carbon-steel jacket, or surrounded by a cement-asbestos jacket. The core pipe has a diameter ranging from 1 inch to 3 inches with minimum wall thicknesses from 0.12 inch to 0.19 inch (minimum wall thicknesses are 87.5 % of nominal wall thicknesses). [WSRC-STI-2007-00460]

The pitting model assumes formation of a hemispherical pit and estimates the area breached based on the maximum pit depth, the thickness of the pipe, and the number of pits per given surface area. [WSRC-STI-2007-00460] The amount of ingress and egress of liquid is proportional to the area breached. It is assumed that once pitting corrosion forms on 25 % of the outer surface of the stainless steel transfer line, enough of the pits would be deep enough to penetrate the line wall such that the line can no longer contain the contents or prevent ingress or egress of water. Using the percentage breached curves; the earliest pitting corrosion failure time is 510 years. [WSRC-STI-2007-00460]

Within H Area, many transfer lines are exposed to soils with significant amounts of groundwater. Predictions for failure of the stainless steel transfer-line core piping are based on the results of a recent study specific to HTF closure. [SRNL-STI-2010-00047] The results of the stochastic failure analysis for the stainless steel transfer lines exposed to significant groundwater are presented in Table 4.2-34. Pitting corrosion was found to be the controlling mechanism for the degradation of the stainless steel transfer-line core piping and its consequent ability to maintain confinement of contaminants. It is assumed that if 75 % of the transfer line is intact, the line is capable of providing this confinement function (i.e., once 25 % of the line wall has been penetrated, the lines are considered incapable of confining contaminants). The pitting model assumes formation of a hemispherical pit and estimates the area breached based on the maximum pit depth, the thickness of the pipe, and the number of pits per given surface area. [WSRC-STI-2007-00460] It is assumed that once pitting corrosion forms on 25 % of the outer surface of the stainless steel transfer line, enough of the pits would be deep enough to penetrate the line wall such that the line can no longer contain the contents or prevent ingress or egress of water. The 25 % time to failure for an H Area 1-inch diameter transfer line with a minimum thickness of 120 mils (0.12 inch) and has been exposed to soils with significant amount of water was 6,000 years.

Table 4.2-34: Analysis of Stainless Steel Transfer Lines Submerged in Groundwater

Wall Thickness	Years Following HTF Waste Tank Closure		
	25 % Failure Probability	50 % Failure Probability	75 % Failure Probability
3-in dia pipe (avg) 216 mils (0.216 in)	10,797	27,001	36,016
1-in. dia pipe (min) 120 mils (0.120 in)	5,999	15,001	20,009

[SRNL-STI-2010-00047]

The long failure times (compared to the results in Table 4.2-33) are predicted due to the low rate of general corrosion and pitting rates for stainless steel samples tested by the National Bureau of Standards. One of the primary causes for the shift in failures time is a change in the pitting rate equation to a power law expression from a constant rate. Due to this change, general corrosion has limited transfer line lifetime instead of pitting. Due to the varying degradation times calculated, a failure time of 510 years is assumed in HTF PA modeling for all ancillary equipment to maximize the dose contributions of the ancillary inventory. [SRNL-STI-2010-00047]

4.2.2.2.7 Saturated Zone Hydraulic Properties

Within the GSAD, soils with a saturated hydraulic conductivity greater than 1.0E-07 cm/s are defined as sandy and those with a saturated hydraulic conductivity less than 1.0E-07 cm/s are defined as clay when defining transport properties (i.e., K_d and effective diffusion coefficient). [WSRC-STI-2006-00198] For consistency with the vadose zone soils, the saturated zone soils within the GSA model that are defined as sandy are assigned the effective diffusion coefficient of the upper vadose zone (i.e., 5.3E-06 cm²/s) and those defined as clay are assigned that of the vadose zone clay (i.e., 4.0E-06 cm²/s).

Table 4.2-35 provides a summary of the saturated zone soils hydraulic and the model input used to represent these values. The properties of the upper vadose zone are representative of sandy soil and the saturated zone soil is representative of both sandy soil and clayey soil (dependent on location). Thus, the K_d values used for transport of contaminants through the upper vadose zone and the sandy soil regions of the saturated zone are assigned the K_d values for sandy soil that are presented in Table 4.2-35 for vadose zone soil. For those regions within the saturated zone that are representative of clayey soil, the K_d values used for transport of contaminants through these regions are assigned the K_d values for clayey soil that are presented in Table 4.2-35 for backfill soil.

Table 4.2-35: Upper Vadose Zone and Effective Saturated Zone Soil Properties

Actual/Model	η (%)	ρ_h (g/cm ³)	ρ_n (g/cm ³)	Saturated D_e (cm ² /s)
Upper Vadose Zone	39 (total)	1.65	2.70	5.3E-06
Saturated Zone Soil (Effective Properties for Modeling Purposes)	25 (effective)	1.04 (effective)	1.39 (effective)	Sandy: 5.3E-06 Clay: 4.0E-06

[WSRC-STI-2006-00198 Section 5.6.1]

η = Porosity

ρ_h = Dry Bulk Density

ρ_n = Particle Density

D_e = Effective Diffusion Coefficient

4.2.3 Exposure Pathways and Scenarios

Intruder and MOP exposure pathways must be defined to calculate receptor doses. The primary mechanism for transport of radionuclides from the HTF is expected to be leaching to the groundwater, groundwater transport to the well and the stream, and subsequent human consumption or exposure. The scenarios are not assumed to occur until after the 100-year institutional control period ends, after which time it is assumed that no active HTF facility maintenance will be conducted. All potential exposure pathways are identified in Tables 4.2-36 and 4.2-37 for MOP and intruder, respectively. Tables 4.2-36 and 4.2-37 identify the individual assumed pathways and whether quantified dose calculations are required for the individual pathways. Tables 4.2-36 and 4.2-37 also identify the individual pathways that are not assumed to occur. The consumption rates, bioaccumulation factors, transfer factors, and exposure times that are used in conjunction with the pathways are discussed in detail in Section 4.6. The DCFs used in conjunction with the pathways are discussed in detail in Section 4.7.

Table 4.2-36: Potential MOP Stabilized Contaminant Exposure Pathways

Primary Stabilized Contaminant Source	Stabilized Contaminant Release Mechanism	Primary Pathway	Secondary Pathway	Tertiary Pathway	Exposure Route	MOP at Well	MOP at Stream
Waste Tank & Ancillary Equipment	Groundwater release at Stream	Domestic Use of Stream water	Drinking Water	N/A	Ingestion	N/A	X
Waste Tank & Ancillary Equipment	Groundwater release at Stream	Domestic Use of Stream water	Showering	N/A	Dermal	N/A	O
Waste Tank & Ancillary Equipment	Groundwater release at Stream	Domestic Use of Stream water	Showering	N/A	Inhalation	N/A	X
Waste Tank & Ancillary Equipment	Groundwater release at Stream	Domestic Use of Stream water	Showering	N/A	Ingestion (incidental)	N/A	X
Waste Tank & Ancillary Equipment	Groundwater release at Stream	Stream water	Swimming	N/A	Inhalation	X	X
Waste Tank & Ancillary Equipment	Groundwater release at Stream	Stream water	Swimming	N/A	Dermal	O	O
Waste Tank & Ancillary Equipment	Groundwater release at Stream	Stream water	Swimming	N/A	Ingestion (incidental)	X	X
Waste Tank & Ancillary Equipment	Groundwater release at Stream	Stream water	Swimming	Direct Rad Emissions	External Exposure	X	X
Waste Tank & Ancillary Equipment	Groundwater release at Stream	Stream water	Fishing, Boating	Direct Rad Emissions	External Exposure	X	X
Waste Tank & Ancillary Equipment	Groundwater release at Stream	Stream water	Fishing, Boating	N/A	Dermal	O	O
Waste Tank & Ancillary Equipment	Groundwater release at Stream	Stream water	Fish Biotic Uptake	Fish	Ingestion	X	X
Waste Tank & Ancillary Equipment	Groundwater release at Stream	Stream water	Shellfish Biotic Uptake	Shellfish	Ingestion	O	O
Waste Tank & Ancillary Equipment	Groundwater release at Stream	Stream water to Livestock	Livestock Biotic Uptake	Meat	Ingestion	N/A	X

Table 4.2-36: Potential MOP Stabilized Contaminant Exposure Pathways (Continued)

Primary Stabilized Contaminant Source	Stabilized Contaminant Release Mechanism	Primary Pathway	Secondary Pathway	Tertiary Pathway	Exposure Route	MOP at Well	MOP at Stream
Waste Tank & Ancillary Equipment	Groundwater release at Stream	Stream water to Livestock	Livestock Biotic Uptake	Milk	Ingestion	N/A	X
Waste Tank & Ancillary Equipment	Groundwater release at Stream	Stream water to Poultry	Poultry Biotic Uptake	Meat	Ingestion	N/A	X
Waste Tank & Ancillary Equipment	Groundwater release at Stream	Stream water to Poultry	Poultry Biotic Uptake	Eggs	Ingestion	N/A	X
Waste Tank & Ancillary Equipment	Groundwater release at Stream	Stream Water Irrigation	Garden Vegetables Biotic Uptake	Vegetables	Ingestion	N/A	X
Waste Tank & Ancillary Equipment	Groundwater release at Stream	Stream Water Irrigation	Fodder Biotic Uptake	Livestock Biotic Uptake - Meat	Ingestion	N/A	X
Waste Tank & Ancillary Equipment	Groundwater release at Stream	Stream Water Irrigation	Fodder Biotic Uptake	Livestock Biotic Uptake - Milk	Ingestion	N/A	X
Waste Tank & Ancillary Equipment	Groundwater release at Stream	Stream Water Irrigation	Fodder Biotic Uptake	Poultry Biotic Uptake - Meat	Ingestion	N/A	X
Waste Tank & Ancillary Equipment	Groundwater release at Stream	Stream Water Irrigation	Fodder Biotic Uptake	Poultry Biotic Uptake - Eggs	Ingestion	N/A	X
Waste Tank & Ancillary Equipment	Groundwater release at Stream	Stream Water Irrigation	Fugitive Dust Generation during Irrigation	Ambient Air (particulates)	Inhalation	N/A	X
Waste Tank & Ancillary Equipment	Groundwater release at Stream	Stream Water Irrigation	Vapor Generation during Irrigation	Ambient Air (vapors)	Inhalation	N/A	X
Waste Tank & Ancillary Equipment	Groundwater release at Stream	Stream Water Irrigation	Direct Soil Contact	N/A	Ingestion (incidental)	N/A	X
Waste Tank & Ancillary Equipment	Groundwater release at Stream	Stream Water Irrigation	Direct Soil Contact	N/A	Dermal	N/A	O

Table 4.2-36: Potential MOP Stabilized Contaminant Exposure Pathways (Continued)

Primary Stabilized Contaminant Source	Stabilized Contaminant Release Mechanism	Primary Pathway	Secondary Pathway	Tertiary Pathway	Exposure Route	MOP at Well	MOP at Stream
Waste Tank & Ancillary Equipment	Groundwater release at Stream	Stream Water Irrigation	Direct Rad Emissions from soil	N/A	External Exposure	N/A	X
Waste Tank & Ancillary Equipment	Volatilization	Ambient Air (vapors)	N/A	N/A	Inhalation	X	X
Waste Tank & Ancillary Equipment	Volatilization	Ambient Air (vapors)	Plume Rad Exposure	N/A	External Exposure	X	X
Waste Tank & Ancillary Equipment	Volatilization	Ambient Air (vapors)	Livestock Biotic Uptake	Meat	Ingestion	X	X
Waste Tank & Ancillary Equipment	Volatilization	Ambient Air (vapors)	Livestock Biotic Uptake	Milk	Ingestion	X	X
Waste Tank & Ancillary Equipment	Volatilization	Ambient Air (vapors)	Poultry Biotic Uptake	Meat	Ingestion	X	X
Waste Tank & Ancillary Equipment	Volatilization	Ambient Air (vapors)	Poultry Biotic Uptake	Eggs	Ingestion	X	X
Waste Tank & Ancillary Equipment	Volatilization	Ambient Air (vapors)	Garden Vegetables Biotic Uptake	Vegetables	Ingestion	X	X
Waste Tank & Ancillary Equipment	Volatilization	Ambient Air (vapors)	Fodder Biotic Uptake	Livestock Biotic Uptake - Meat	Ingestion	X	X
Waste Tank & Ancillary Equipment	Volatilization	Ambient Air (vapors)	Fodder Biotic Uptake	Livestock Biotic Uptake - Milk	Ingestion	X	X
Waste Tank & Ancillary Equipment	Volatilization	Ambient Air (vapors)	Fodder Biotic Uptake	Poultry Biotic Uptake - Meat	Ingestion	X	X
Waste Tank & Ancillary Equipment	Volatilization	Ambient Air (vapors)	Fodder Biotic Uptake	Poultry Biotic Uptake - Eggs	Ingestion	X	X

Table 4.2-36: Potential MOP Stabilized Contaminant Exposure Pathways (Continued)

Primary Stabilized Contaminant Source	Stabilized Contaminant Release Mechanism	Primary Pathway	Secondary Pathway	Tertiary Pathway	Exposure Route	MOP at Well	MOP at Stream
Waste Tank & Ancillary Equipment	Groundwater Withdrawal at Well	Domestic Use of Well Water	Drinking Water	N/A	Ingestion	X	N/A
Waste Tank & Ancillary Equipment	Groundwater Withdrawal at Well	Domestic Use of Well Water	Showering	N/A	Dermal	O	N/A
Waste Tank & Ancillary Equipment	Groundwater Withdrawal at Well	Domestic Use of Well Water	Showering	N/A	Inhalation	X	N/A
Waste Tank & Ancillary Equipment	Groundwater Withdrawal at Well	Domestic Use of Well Water	Showering	N/A	Ingestion (incidental)	X	N/A
Waste Tank & Ancillary Equipment	Groundwater Withdrawal at Well	Well Water to Livestock	Livestock Biotic Uptake	Meat	Ingestion	X	N/A
Waste Tank & Ancillary Equipment	Groundwater Withdrawal at Well	Well Water to Livestock	Livestock Biotic Uptake	Milk	Ingestion	X	N/A
Waste Tank & Ancillary Equipment	Groundwater Withdrawal at Well	Well Water to Poultry	Poultry Biotic Uptake	Meat	Ingestion	X	N/A
Waste Tank & Ancillary Equipment	Groundwater Withdrawal at Well	Well Water to Poultry	Poultry Biotic Uptake	Eggs	Ingestion	X	N/A
Waste Tank & Ancillary Equipment	Groundwater Withdrawal at Well	Well Water Irrigation	Garden Vegetables Biotic Uptake	Vegetables	Ingestion	X	N/A

Table 4.2-36: Potential MOP Stabilized Contaminant Exposure Pathways (Continued)

Primary Stabilized Contaminant Source	Stabilized Contaminant Release Mechanism	Primary Pathway	Secondary Pathway	Tertiary Pathway	Exposure Route	MOP at Well	MOP at Stream
Waste Tank & Ancillary Equipment	Groundwater Withdrawal at Well	Well Water Irrigation	Fodder Biotic Uptake	Livestock Biotic Uptake - Meat	Ingestion	X	N/A
Waste Tank & Ancillary Equipment	Groundwater Withdrawal at Well	Well Water Irrigation	Fodder Biotic Uptake	Livestock Biotic Uptake - Milk	Ingestion	X	N/A
Waste Tank & Ancillary Equipment	Groundwater Withdrawal at Well	Well Water Irrigation	Fodder Biotic Uptake	Poultry Biotic Uptake - Meat	Ingestion	X	N/A
Waste Tank & Ancillary Equipment	Groundwater Withdrawal at Well	Well Water Irrigation	Fodder Biotic Uptake	Poultry Biotic Uptake - Eggs	Ingestion	X	N/A
Waste Tank & Ancillary Equipment	Groundwater Withdrawal at Well	Well Water Irrigation	Fugitive Dust Generation during Irrigation	Ambient Air (particulates)	Inhalation	X	N/A
Waste Tank & Ancillary Equipment	Groundwater Withdrawal at Well	Well Water Irrigation	Vapor Generation during Irrigation	Ambient Air (vapors)	Inhalation	X	N/A
Waste Tank & Ancillary Equipment	Groundwater Withdrawal at Well	Well Water Irrigation	Direct Soil Contact	N/A	Ingestion (incidental)	X	N/A
Waste Tank & Ancillary Equipment	Groundwater Withdrawal at Well	Well Water Irrigation	Direct Soil Contact	N/A	Dermal	O	N/A
Waste Tank & Ancillary Equipment	Groundwater Withdrawal at Well	Well Water Irrigation	Direct Rad Emissions from Soil	N/A	External Exposure	X	N/A

X = addressed quantitatively, O = addressed qualitatively, N/A = not applicable

Table 4.2-37: Potential Intruder Waste Exposure Pathways

Primary Stabilized Contaminant Source	Stabilized Contaminant Release Mechanism	Primary Pathway	Secondary Pathway	Tertiary Pathway	Exposure Route	Acute Intruder	Chronic Intruder
Ancillary Equipment	Drill Cuttings brought to Surface	Fugitive Dust Generation during drilling	Ambient Air (particulates)	N/A	Inhalation	X	N/A
Ancillary Equipment	Drill Cuttings brought to Surface	Drill Cuttings dropped on surface	Direct Soil Contact	N/A	Ingestion	X	N/A
Ancillary Equipment	Drill Cuttings brought to Surface	Drill Cuttings dropped on surface	Direct Soil Contact	N/A	Dermal	O	N/A
Ancillary Equipment	Drill Cuttings brought to Surface	Drill Cuttings dropped on surface	Direct Rad Emissions	N/A	External Exposure	X	N/A
Ancillary Equipment	Drill Cuttings brought to Surface	Drill Cuttings mixed in Garden	Garden Vegetables Biotic Uptake	Vegetables	Ingestion	N/A	X
Ancillary Equipment	Drill Cuttings brought to Surface	Drill Cuttings mixed in Garden	Fodder Biotic Uptake	Livestock Biotic Uptake - Meat	Ingestion	N/A	N/A
Ancillary Equipment	Drill Cuttings brought to Surface	Drill Cuttings mixed in Garden	Fodder Biotic Uptake	Livestock Biotic Uptake - Milk	Ingestion	N/A	N/A
Ancillary Equipment	Drill Cuttings brought to Surface	Drill Cuttings mixed in Garden	Fodder Biotic Uptake	Poultry Biotic Uptake - Meat	Ingestion	N/A	N/A
Ancillary Equipment	Drill Cuttings brought to Surface	Drill Cuttings mixed in Garden	Fodder Biotic Uptake	Poultry Biotic Uptake - Eggs	Ingestion	N/A	N/A
Ancillary Equipment	Drill Cuttings brought to Surface	Drill Cuttings mixed in Garden	Direct Soil Contact	N/A	Ingestion	N/A	X
Ancillary Equipment	Drill Cuttings brought to Surface	Drill Cuttings mixed in Garden	Direct Soil Contact	N/A	Dermal	N/A	O
Ancillary Equipment	Drill Cuttings brought to Surface	Drill Cuttings mixed in Garden	Direct Rad Emissions	N/A	External Exposure	N/A	X

Table 4.2-37: Potential Intruder Waste Exposure Pathways (Continued)

Primary Stabilized Contaminant Source	Stabilized Contaminant Release Mechanism	Primary Pathway	Secondary Pathway	Tertiary Pathway	Exposure Route	Acute Intruder	Chronic Intruder
Ancillary Equipment	Drill Cuttings brought to Surface	Drill Cuttings mixed in Garden	Fugitive Dust Generation during Irrigation	Ambient Air (particulates)	Inhalation	N/A	X
Waste Tank & Ancillary Equipment	Groundwater release at Stream	Domestic use of Stream water	Drinking Water	N/A	Ingestion	N/A	N/A
Waste Tank & Ancillary Equipment	Groundwater release at Stream	Domestic use of Stream water	Showering	N/A	Dermal	N/A	N/A
Waste Tank & Ancillary Equipment	Groundwater release at Stream	Domestic use of Stream water	Showering	N/A	Inhalation	N/A	N/A
Waste Tank & Ancillary Equipment	Groundwater release at Stream	Domestic use of Stream water	Showering	N/A	Ingestion (incidental)	N/A	N/A
Waste Tank & Ancillary Equipment	Groundwater release at Stream	Stream water	Swimming	N/A	Inhalation	N/A	X
Waste Tank & Ancillary Equipment	Groundwater release at Stream	Stream water	Swimming	N/A	Dermal	N/A	O
Waste Tank & Ancillary Equipment	Groundwater release at Stream	Stream water	Swimming	N/A	Ingestion (incidental)	N/A	X
Waste Tank & Ancillary Equipment	Groundwater release at Stream	Stream water	Swimming	Direct Rad Emissions	External Exposure	N/A	X

Table 4.2-37: Potential Intruder Waste Exposure Pathways (Continued)

Primary Stabilized Contaminant Source	Stabilized Contaminant Release Mechanism	Primary Pathway	Secondary Pathway	Tertiary Pathway	Exposure Route	Acute Intruder	Chronic Intruder
Waste Tank & Ancillary Equipment	Groundwater release at Stream	Stream water	Fishing, Boating	Direct Rad Emissions	External Exposure	N/A	X
Waste Tank & Ancillary Equipment	Groundwater release at Stream	Stream water	Fishing, Boating	N/A	Dermal	N/A	O
Waste Tank & Ancillary Equipment	Groundwater release at Stream	Stream water	Fish Biotic Uptake	Fish	Ingestion	N/A	X
Waste Tank & Ancillary Equipment	Groundwater release at Stream	Stream water	Shellfish Biotic Uptake	Shellfish	Ingestion	N/A	O
Waste Tank & Ancillary Equipment	Groundwater release at Stream	Stream water to Livestock	Livestock Biotic Uptake	Meat	Ingestion	N/A	N/A
Waste Tank & Ancillary Equipment	Groundwater release at Stream	Stream water to Livestock	Livestock Biotic Uptake	Milk	Ingestion	N/A	N/A
Waste Tank & Ancillary Equipment	Groundwater release at Stream	Stream water to Poultry	Poultry Biotic Uptake	Meat	Ingestion	N/A	N/A
Waste Tank & Ancillary Equipment	Groundwater release at Stream	Stream water to Poultry	Poultry Biotic Uptake	Eggs	Ingestion	N/A	N/A
Waste Tank & Ancillary Equipment	Groundwater release at Stream	Stream Water Irrigation	Garden Vegetables Biotic Uptake	Vegetables	Ingestion	N/A	N/A

Table 4.2-37: Potential Intruder Waste Exposure Pathways (Continued)

Primary Stabilized Contaminant Source	Stabilized Contaminant Release Mechanism	Primary Pathway	Secondary Pathway	Tertiary Pathway	Exposure Route	Acute Intruder	Chronic Intruder
Waste Tank & Ancillary Equipment	Groundwater release at Stream	Stream Water Irrigation	Fodder Biotic Uptake	Livestock Biotic Uptake - Meat	Ingestion	N/A	N/A
Waste Tank & Ancillary Equipment	Groundwater release at Stream	Stream Water Irrigation	Fodder Biotic Uptake	Livestock Biotic Uptake - Milk	Ingestion	N/A	N/A
Waste Tank & Ancillary Equipment	Groundwater release at Stream	Stream Water Irrigation	Fodder Biotic Uptake	Poultry Biotic Uptake - Meat	Ingestion	N/A	N/A
Waste Tank & Ancillary Equipment	Groundwater release at Stream	Stream Water Irrigation	Fodder Biotic Uptake	Poultry Biotic Uptake - Eggs	Ingestion	N/A	N/A
Waste Tank & Ancillary Equipment	Groundwater release at Stream	Stream Water Irrigation	Fugitive Dust Generation during Irrigation	Ambient Air (particulates)	Inhalation	N/A	N/A
Waste Tank & Ancillary Equipment	Groundwater release at Stream	Stream Water Irrigation	Vapor Generation during Irrigation	Ambient Air (vapors)	Inhalation	N/A	N/A
Waste Tank & Ancillary Equipment	Groundwater release at Stream	Stream Water Irrigation	Direct Soil Contact	N/A	Ingestion (incidental)	N/A	N/A
Waste Tank & Ancillary Equipment	Groundwater release at Stream	Stream Water Irrigation	Direct Soil Contact	N/A	Dermal	N/A	N/A
Waste Tank & Ancillary Equipment	Groundwater release at Stream	Stream Water Irrigation	Direct Rad Emissions from Soil	N/A	External Exposure	N/A	N/A

Table 4.2-37: Potential Intruder Waste Exposure Pathways (Continued)

Primary Stabilized Contaminant Source	Stabilized Contaminant Release Mechanism	Primary Pathway	Secondary Pathway	Tertiary Pathway	Exposure Route	Acute Intruder	Chronic Intruder
Waste Tank & Ancillary Equipment	Volatilization	Ambient Air (vapors)	N/A	N/A	Inhalation	N/A	X
Waste Tank & Ancillary Equipment	Volatilization	Ambient Air (vapors)	Plume Rad Exposure	N/A	External Exposure	N/A	X
Waste Tank & Ancillary Equipment	Volatilization	Ambient Air (vapors)	Livestock Biotic Uptake	Meat	Ingestion	N/A	O
Waste Tank & Ancillary Equipment	Volatilization	Ambient Air (vapors)	Livestock Biotic Uptake	Milk	Ingestion	N/A	O
Waste Tank & Ancillary Equipment	Volatilization	Ambient Air (vapors)	Poultry Biotic Uptake	Meat	Ingestion	N/A	O
Waste Tank & Ancillary Equipment	Volatilization	Ambient Air (vapors)	Poultry Biotic Uptake	Eggs	Ingestion	N/A	O
Waste Tank & Ancillary Equipment	Volatilization	Ambient Air (vapors)	Garden Vegetables Biotic Uptake	Vegetables	Ingestion	N/A	O
Waste Tank & Ancillary Equipment	Volatilization	Ambient Air (vapors)	Fodder Biotic Uptake	Livestock Biotic Uptake - Meat	Ingestion	N/A	O
Waste Tank & Ancillary Equipment	Volatilization	Ambient Air (vapors)	Fodder Biotic Uptake	Livestock Biotic Uptake - Milk	Ingestion	N/A	O

Table 4.2-37: Potential Intruder Waste Exposure Pathways (Continued)

Primary Stabilized Contaminant Source	Stabilized Contaminant Release Mechanism	Primary Pathway	Secondary Pathway	Tertiary Pathway	Exposure Route	Acute Intruder	Chronic Intruder
Waste Tank & Ancillary Equipment	Volatilization	Ambient Air (vapors)	Fodder Biotic Uptake	Poultry Biotic Uptake - Meat	Ingestion	N/A	O
Waste Tank & Ancillary Equipment	Volatilization	Ambient Air (vapors)	Fodder Biotic Uptake	Poultry Biotic Uptake - Eggs	Ingestion	N/A	O
Waste Tank & Ancillary Equipment	Groundwater Withdrawal at Well	Domestic Use of Well Water	Drinking Water	N/A	Ingestion	N/A	X
Waste Tank & Ancillary Equipment	Groundwater Withdrawal at Well	Domestic Use of Well Water	Showering	N/A	Dermal	N/A	O
Waste Tank & Ancillary Equipment	Groundwater Withdrawal at Well	Domestic Use of Well Water	Showering	N/A	Inhalation	N/A	X
Waste Tank & Ancillary Equipment	Groundwater Withdrawal at Well	Domestic Use of Well Water	Showering	N/A	Ingestion (incidental)	N/A	X
Waste Tank & Ancillary Equipment	Groundwater Withdrawal at Well	Well Water to Livestock	Livestock Biotic Uptake	Meat	Ingestion	N/A	X
Waste Tank & Ancillary Equipment	Groundwater Withdrawal at Well	Well Water to Livestock	Livestock Biotic Uptake	Milk	Ingestion	N/A	X
Waste Tank & Ancillary Equipment	Groundwater Withdrawal at Well	Well Water to Poultry	Poultry Biotic Uptake	Meat	Ingestion	N/A	X
Waste Tank & Ancillary Equipment	Groundwater Withdrawal at Well	Well Water to Poultry	Poultry Biotic Uptake	Eggs	Ingestion	N/A	X

Table 4.2-37: Potential Intruder Waste Exposure Pathways (Continued)

Primary Stabilized Contaminant Source	Stabilized Contaminant Release Mechanism	Primary Pathway	Secondary Pathway	Tertiary Pathway	Exposure Route	Acute Intruder	Chronic Intruder
Waste Tank & Ancillary Equipment	Groundwater Withdrawal at Well	Well Water Irrigation	Garden Vegetables Biotic Uptake	Vegetables	Ingestion	N/A	X
Waste Tank & Ancillary Equipment	Groundwater Withdrawal at Well	Well Water Irrigation	Fodder Biotic Uptake	Livestock Biotic Uptake - Meat	Ingestion	N/A	X
Waste Tank & Ancillary Equipment	Groundwater Withdrawal at Well	Well Water Irrigation	Fodder Biotic Uptake	Livestock Biotic Uptake - Milk	Ingestion	N/A	X
Waste Tank & Ancillary Equipment	Groundwater Withdrawal at Well	Well Water Irrigation	Fodder Biotic Uptake	Poultry Biotic Uptake - Meat	Ingestion	N/A	X
Waste Tank & Ancillary Equipment	Groundwater Withdrawal at Well	Well Water Irrigation	Fodder Biotic Uptake	Poultry Biotic Uptake - Eggs	Ingestion	N/A	X
Waste Tank & Ancillary Equipment	Groundwater Withdrawal at Well	Well Water Irrigation	Fugitive Dust Generation during Irrigation	Ambient Air (particulates)	Inhalation	N/A	X
Waste Tank & Ancillary Equipment	Groundwater Withdrawal at Well	Well Water Irrigation	Vapor Generation during Irrigation	Ambient Air (vapors)	Inhalation	N/A	X
Waste Tank & Ancillary Equipment	Groundwater Withdrawal at Well	Well Water Irrigation	Direct Soil Contact	N/A	Ingestion (incidental)	N/A	X
Waste Tank & Ancillary Equipment	Groundwater Withdrawal at Well	Well Water Irrigation	Direct Soil Contact	N/A	Dermal	N/A	O
Waste Tank & Ancillary Equipment	Groundwater Withdrawal at Well	Well Water Irrigation	Direct Rad Emissions from Soil	N/A	External Exposure	N/A	X

X = addressed quantitatively, O = addressed qualitatively, N/A = not applicable

4.2.3.1 Member of the Public Exposure Pathways

Table 4.2-36 presents, and this section discusses, MOP exposure pathways used in the PA analyses. Table 4.2-36 also indicates whether quantitative dose calculations are included as part of the PA analyses. The assumption is that these scenarios occur after the end of the 100-year institutional control period and discontinuation of the active HTF facility maintenance. Section 4.6 discusses in detail the consumption rates and bioaccumulation factors used in conjunction with the pathways.

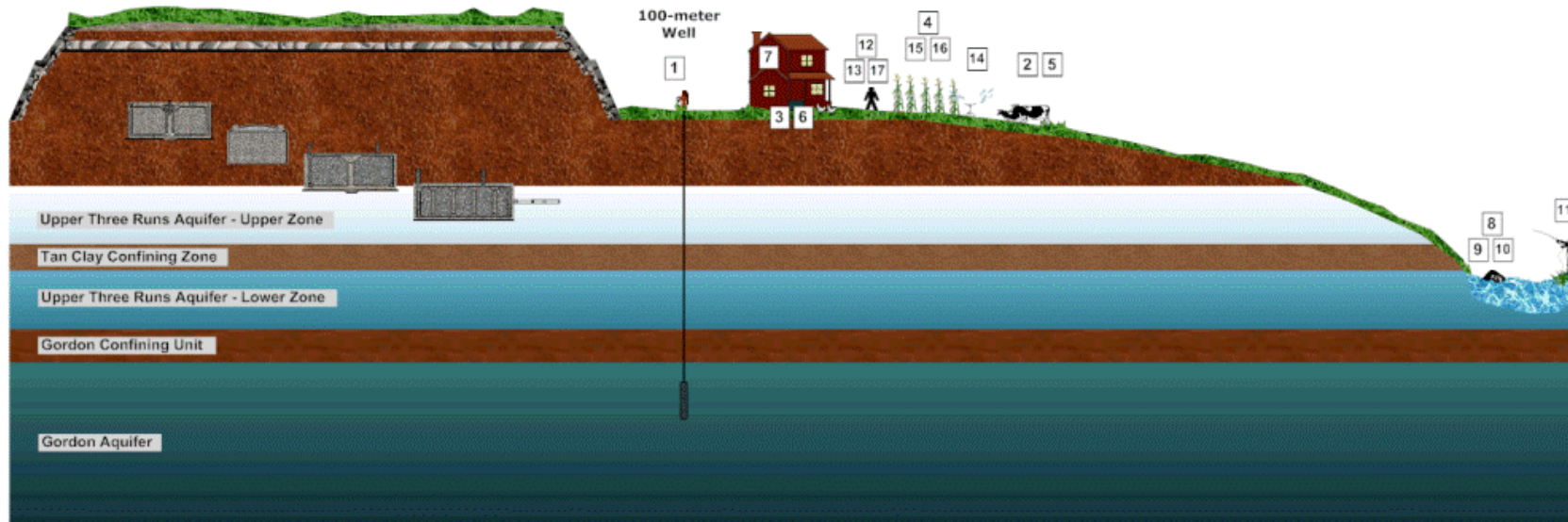
4.2.3.1.1 Scenario with Well Water as Primary Water Source

The primary water source for MOP exposure pathways is a well drilled into the groundwater aquifers. A GSA stream is the secondary water source for recreational use pathways and the fish ingestion pathway.

In the groundwater well-dose analyses, doses are calculated using water from a well for domestic purposes (e.g., drinking water, irrigation). The following exposure pathways involving the use of contaminated well water are assumed to occur as presented in Table 4.2-36 and Figure 4.2-31.

- Direct ingestion of well water
- Ingestion of milk and meat from livestock (e.g., dairy and beef cattle) that drink well water
- Ingestion of meat and eggs from poultry that drink well water
- Ingestion of vegetables grown in garden soil irrigated with well water
- Ingestion of milk and meat from livestock (e.g., dairy and beef cattle) that eat fodder from pasture irrigated with well water
- Ingestion of meat and eggs from poultry that eat fodder from pasture irrigated with well water
- Ingestion and inhalation of well water while showering

Figure 4.2-31: Scenario with Well Water as Primary Water Source



SCENARIO WITH WELL WATER AS PRIMARY WATER SOURCE

1. Direct ingestion of well water
2. Ingestion of milk and meat from livestock (e.g., dairy and beef cattle) that drink well water
3. Ingestion of meat and eggs from poultry that drink well water
4. Ingestion of vegetables grown in garden soil irrigated with well water
5. Ingestion of milk and meat from livestock (e.g., dairy and beef cattle) that eat fodder from a pasture irrigated with well water
6. Ingestion of meat and eggs from poultry that eat fodder from a pasture irrigated with well water
7. Ingestion and inhalation of well water while showing
8. Direct irradiation during recreational activities (e.g., swimming, fishing, boating) from stream water
9. Dermal contact with stream water during recreational activities (e.g., swimming, fishing)
10. Incidental ingestion and inhalation of stream water during recreational activities
11. Ingestion of fish from the stream water
12. Direct plume shine
13. Inhalation
14. Inhalation of well water used for irrigation
15. Inhalation of dust from the soil that was irrigated with well water
16. Ingestion of or dermal contact with soil that was irrigated with well water
17. Direct radiation exposure from radionuclides deposited on the soil that was irrigated with well water

The following exposure pathways involving the use of contaminated surface water (from the applicable stream) for recreational use are assumed to occur:

- Direct irradiation during recreational activities (e.g., swimming, fishing, boating) from stream water
- Dermal contact with stream water during recreational activities (e.g., swimming, fishing)
- Incidental ingestion and inhalation of stream water during recreational activities
- Ingestion of fish from the stream water

Additional exposure pathways could involve releases of radionuclides into the air from the water taken from the well (i.e., volatile radionuclides such as H-3, C-14, I-129). Exposures from the air pathway in this PA:

- Direct plume shine
- Inhalation

Other secondary and indirect pathways contribute relatively minor doses to a receptor (e.g., MOP) when compared to direct pathways such as ingestion of milk and meat. These pathways include:

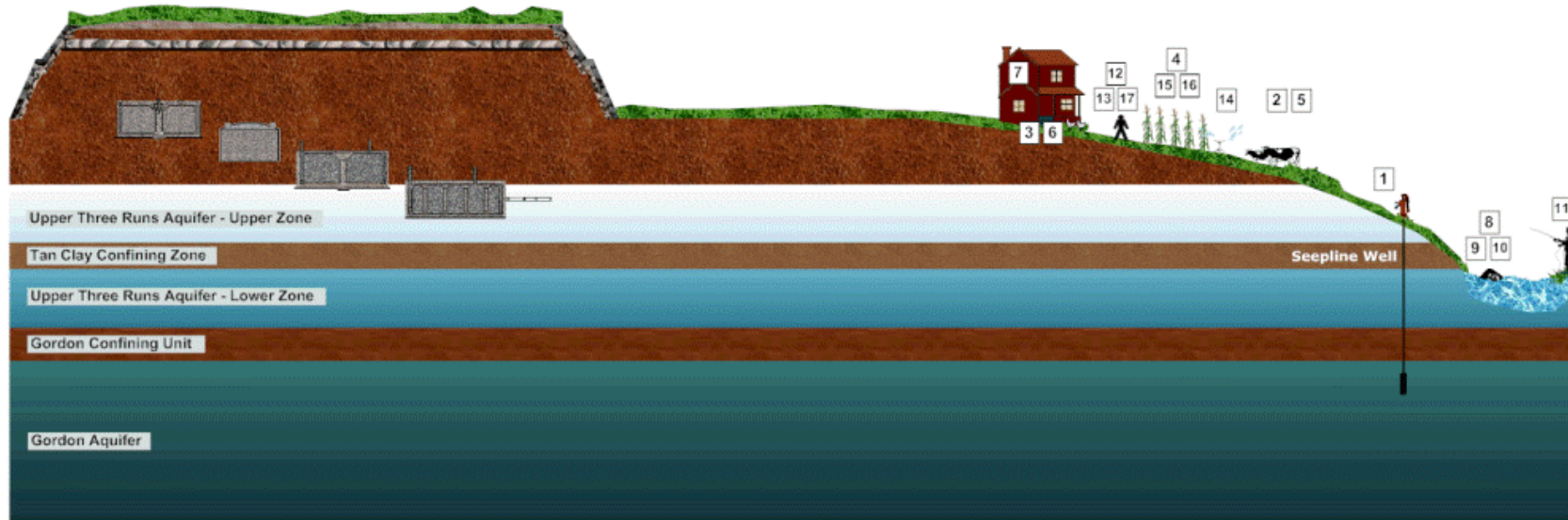
- Inhalation of well water used for irrigation
- Inhalation of dust from the soil irrigated with well water
- Ingestion of or dermal contact with soil irrigated with well water
- Direct radiation exposure from radionuclides deposited on the soil irrigated with well water

4.2.3.1.2 Scenario with Stream Water as Primary Water Source

In the stream dose analyses, doses are calculated using water from the applicable stream (Fourmile Branch or UTR) for domestic and recreational purposes. The following exposure pathways involving the use of surface water (from the applicable stream) are assumed to occur as presented in Table 4.2-36 and Figure 4.2-32.

- Direct ingestion of stream water
- Ingestion of milk and meat from livestock (e.g., dairy and beef cattle) that drink stream water
- Ingestion of meat and eggs from poultry that drink stream water
- Ingestion of vegetables grown in garden soil irrigated with stream water
- Ingestion of milk and meat from livestock (e.g., dairy and beef cattle) that eat fodder from pasture irrigated with stream water
- Ingestion of meat and eggs from poultry that eat fodder from pasture irrigated with stream water
- Ingestion and inhalation of stream water while showering

Figure 4.2-32: Scenario with Stream Water as Primary Water Source



DOSE ANALYSES USING STREAM WATER AS PRIMARY WATER SOURCE

1. Direct ingestion of stream water
2. Ingestion of milk and meat from livestock (e.g., dairy and beef cattle) that drink stream water
3. Ingestion of meat and eggs from poultry that drink stream water
4. Ingestion of vegetables grown in garden soil irrigated with stream water
5. Ingestion of milk and meat from livestock (e.g., dairy and beef cattle) that eat fodder from a pasture irrigated with stream water
6. Ingestion of meat and eggs from poultry that eat fodder from a pasture irrigated with stream water
7. Ingestion and inhalation of stream water while showing
8. Direct irradiation during recreational activities (e.g., swimming, fishing, boating) from stream water
9. Dermal contact with stream water during recreational activities (e.g., swimming, fishing)
10. Incidental ingestion and inhalation of stream water during recreational activities
11. Ingestion of fish from the stream water
12. Direct plume shine
13. Inhalation
14. Inhalation of well water used for irrigation
15. Inhalation of dust from the soil that was irrigated with stream water
16. Ingestion of or dermal contact with soil that was irrigated with stream water
17. Direct radiation exposure from radionuclides deposited on the soil that was irrigated with stream water

The following exposure pathways involving the use of contaminated surface water (from the applicable stream) for recreational use are assumed to occur:

- Direct irradiation during recreational activities from stream water (e.g., swimming, fishing, boating)
- Dermal contact with stream water during recreational activities (e.g., swimming, fishing)
- Incidental ingestion and inhalation of stream water during recreational activities
- Ingestion of fish from the stream water

Additional exposure pathways could involve releases of radionuclides into the air from the water taken from the stream (i.e., volatile radionuclides such as H-3, C-14, I-129). Exposures from the air pathway in this PA:

- Direct plume shine
- Inhalation

Other secondary and indirect pathways contribute relatively minor doses to a receptor when compared to direct pathways such as ingestion of milk and meat. These pathways include:

- Inhalation of stream water used for irrigation
- Inhalation of dust from the soil that was irrigated with stream water
- Ingestion of or dermal contact with soil that was irrigated with stream water

Direct radiation exposure from radionuclides deposited on the soil that was irrigated with stream water

4.2.3.1.3 Basis for Public Release Pathways

Table 4.2-36 was prepared to provide a list of the HTF exposure pathways identified as candidates for detailed analyses. The list of candidates was developed based on a review of SRS PA analyses and NRC documents. [SRS-REG-2007-00002, SRR-CWDA-2009-00017, NUREG-0782, NUREG-0945, NUREG-1573] Those activities at SRS that could bring humans in contact with stabilized contaminants (e.g., water use, hunting, fishing, recreational activities such as swimming and boating, habitation in dwellings, other unique activities that involve water use or ground disturbance) were considered (with emphasis on local practices), to ensure that any pathways unique to SRS were taken into account. The *SRS Ecology Environmental Information Document* (WSRC-TR-2005-00201) was used as a source of relevant environmental information and conditions at SRS. For example, WSRC-TR-2005-00201 was used to identify potential wild game available on-site, potential bio-intrusion candidates (flora and fauna), and the potential for the presence of fish and/or shellfish in the creeks bordering the HTF.

Those potential pathways denoted with an “X” had quantified analysis for the various receptors. Potential pathways denoted with an “O” did not have quantified analysis performed based on the applicable justifications provided throughout this section (Table 4.2-36). The guidance found in NUREG-1854 indicates that transport pathways may be excluded from PA if it can be demonstrated that either there is limited potential for

radionuclide releases into a particular pathway, or the pathway is not viable (e.g., water is not potable). Other pathways were marked as “N/A” because of the nature of the scenario making the interaction of two or more pathways impossible (e.g., a garden that receives 100 % of its irrigation water from a well cannot also receive water from a stream).

Pathways related to MOP resident scenario using water from a well or stream had the following assumptions made:

- The stabilized contaminants release mechanisms to the MOP are leaching of stabilized contaminants to the groundwater and volatilization of the stabilized contaminants to the surface. Well drilling is not a release mechanism since any well drilling associated with the MOP scenarios would be outside the HTF buffer zone and therefore stabilized contaminants remain undisturbed.
- Bio-intrusion and/or erosion are not considered credible mechanisms for significant stabilized contaminant disturbance based on the depth and form of the stabilized contaminant. The stabilized contaminants will be significantly below ground, from at least 10 feet for ancillary equipment to approximately 40 feet for stabilized contaminant waste tank heels. Stabilized contaminants are contained within stainless steel or carbon steel equipment and stabilized via grouting as part of waste-tank system closures. No mechanism was identified that would result in stabilized contaminant disturbance and dispersal that would affect the dose to the MOP (outside the HTF buffer zone).
- In the well water as primary water source scenario, well water will be used as a primary potable water source for a residence near the well (e.g., drinking water, showering) and will be used by the resident as a primary water source for agriculture (e.g., irrigation, livestock water).
- In the MOP near a stream scenario, stream water will be used as a primary potable water source for a residence near the stream (e.g., drinking water, showering) and will be used by the resident as a primary water source for agriculture (e.g., irrigation, livestock water).
- In both MOP scenarios, the resident (near the well and/or near a stream) can use a stream for recreational activities (e.g., swimming, fishing, boating).
- Any wild game ingested (deer, wild pigs) would merely offset ingested livestock, and would result in a lower total dose since the livestock raised near HTF would be more affected by HTF stabilized contaminants than transient wild game.
- A survey of land and water usage characteristics within a 50-mile region of SRS was conducted and documented in WSRC-RP-91-17. The results of this study found that hogs are raised on farms within 50 miles of the SRS; however, hogs eat commercial feed. Thus, the consideration of local consumption of hogs is not in the determination of “meat” production or consumption.
- There are two streams (UTR and Fourmile Branch) from which ingestion of finfish with significant contamination is possible. The assumption for these streams as a source of dietary fish was conservative, and the two streams are not significant sources of edible shellfish, and shellfish play an insignificant role in

local diets in relation to other ingested dose contributors such as livestock, milk, and vegetables, thus shellfish were excluded (local invertebrate consumption total is 2 kg/yr). [WSRC-TR-2005-00201, WSRC-STI-2007-00004]

- Since there is no substantial water source at the well site, there was no consideration for pathways related to water-related commercial activities. Based on the relative proximity of a large, natural water source (i.e., the Savannah River), there is no assumption that a man-made body of water would be created at the MOP resident site.
- The consideration for the dose associated with dermal absorption of radionuclides is insignificant because, unlike some chemicals, radionuclides generally adsorb poorly into the body. The one exception is tritium, where the concentrations found are small enough in groundwater rendering it an insignificant contributor to dose.
- The quantities of water ingested during the relatively short activities of showering (10 min/d) and swimming (7 hr/yr) are negligible and not addressed independently. The impact of these activities is addressed with the “direct ingestion of well water” pathway (i.e., they are included in the 337 liters of water that is assumed to be ingested every year). [SRNL-STI-2010-00447]

4.2.3.2 Intruder Exposure Pathways

After HTF closure, the stabilized contaminant materials will be primarily located in material protected areas (e.g., grouted waste tanks, DB covers, and valve box shielding). These are clearly distinguishable from the surrounding soil and make drilling an impractical scenario based on regional drilling practices. Regional drilling conditions indicate that a barrier (closure-cap erosion barrier, waste tank top, or grout fill) would cause drillers to stop operations and move drilling location. Transfer lines containing stabilized contaminants are highly vulnerable to intrusion because they are near grade-level prior to facility closure and a size (typically 3-inch diameter or less) that will reduce detection capability and increases intruder drilling operation encounter potential. However, even with their increased risk of encroachment, the probability is low due to the minimal surface area of the transfer lines within the entire HTF footprint. The analysis in support of this considered 82 % of the transfer line length having a 3-inch diameter, 0.24 % with a 4-inch diameter, and the balance of the lines having a diameter less than 3 inches.

Table 4.2-37 presents the dose pathways for an inadvertent intruder and intruder scenarios are discussed in Section 4.2.3.2.1. Additionally, Table 4.2-37 indicates if detailed dose calculations are required. The assumption is that intruder release scenarios will occur after the 100-year institutional control period ends (after which active HTF facility maintenance has concluded). Because of the longevity of stainless steel transfer line integrity, (see Section 4.2.2.2.6) this is considered a conservative scenario. Natural processes such as erosion (addressed in Sections 3.2.4.4 and 3.2.4.5), seismic activity (addressed in Section 3.1.4.3), and flooding (addressed in Section 3.1.5.4) were considered and will not have an impact on the modeled intruder scenarios.

4.2.3.2.1 Intruder Release Scenarios

The consumption rates and bioaccumulation factors that were used in conjunction with the Table 4.2-37 proposed pathways are discussed in detail in Section 4.6. The following intruder scenarios were considered for the calculation of the dose to an inadvertent intruder.

- Acute Intruder-Drilling Scenario
- Acute Intruder-Construction Scenario
- Acute Intruder-Discovery Scenario
- Chronic Intruder-Agricultural (Post-Drilling) Scenario
- Chronic Intruder-Resident Scenario
- Chronic Intruder-Recreational Hunting Fishing Scenario
- Bio-intrusion Scenario

4.2.3.2.2 Acute Intruder-Drilling Scenario

The assumption in this scenario is that a well is drilled into the closure site sometime after the end of active institutional controls. The assumed well uses are domestic water and irrigation. Based on the geologic characterization data for the HTF area contained in the GSAD database, discussed in Section 3.1.4, there do not appear to be any unique geologic natural resources in the HTF area. Lacking identification of additional natural resources in the HTF, additional drilling scenarios are not considered. The person or persons who perform the well installation are the acute intruder in a drilling scenario and exposure to drill cuttings during installation is anticipated.

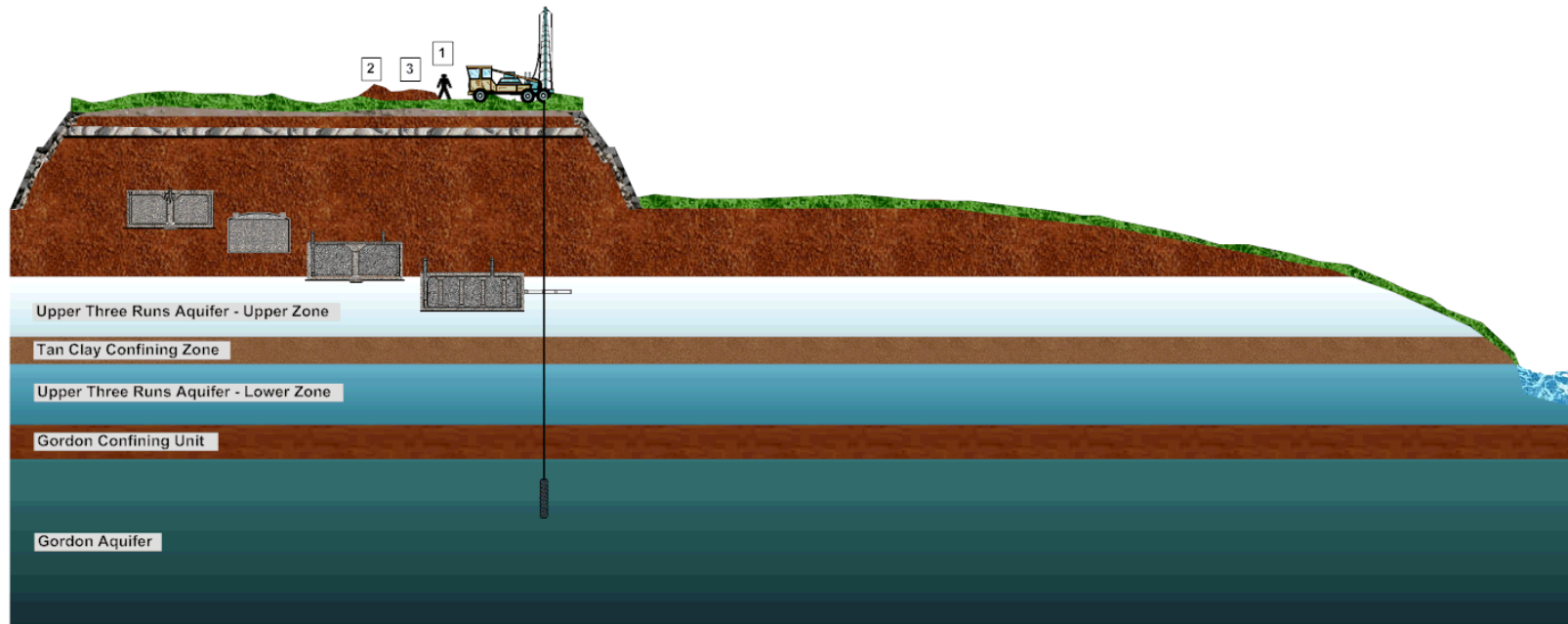
The assumption is that a drilling borehole will penetrate the closure site. This scenario involves stabilized contaminants below the depth of typical construction excavations. The acute drilling scenario assumes that an inadvertent intruder drills a well into a transfer line, but not into a waste tank. Although the probability of hitting a transfer line within the area may be small, it is assumed that this occurs for the drilling scenario. The intruder is exposed to contaminated drill cuttings spread over the ground and contaminated airborne dust.

Exposure of a resident or farmer to drill cuttings left on the land surface after the installation of a well was considered under the intruder-resident scenario or intruder-agricultural scenarios.

The exposure pathways for this acute drilling scenario include (Figure 4.2-33):

- Inhalation of re-suspended drill cuttings
- External exposure to the drill cuttings
- Inadvertent drill cuttings ingestion

Figure 4.2-33: Acute Intruder Drilling Scenario



ACUTE INTRUDER-DRILLING SCENARIO

1. Inhalation of resuspended drill cuttings
2. External exposure to drill cuttings
3. Inadvertent drill cuttings ingestion

4.2.3.2.3 Acute Intruder-Construction Scenario

In this scenario, it is assumed that after the end of active institutional controls, a construction project begins at the site with associated earthmoving activities. The intruder-construction scenario involves an inadvertent intruder who chooses to excavate or construct a building on the closure site. The intruder is assumed to dig a basement excavation to a depth of approximately 10 feet. It is assumed that the intruder does not recognize the hazardous nature of the material excavated. During the excavation of the basement, the intruder is exposed to the exhumed stabilized contaminants by inhalation of re-suspended contaminated soil and external irradiation from contaminated soil. Due to the disposal depth of the stabilized contaminants in the waste tanks and in ancillary equipment (from a minimum of 10 feet to approximately 40 feet below the HTF closure cap), the intruder-construction scenario is not considered applicable. The intruder-construction scenario could also apply to an industrial facility that would require a deeper foundation excavation. While the *Savannah River Site Long Range Comprehensive Plan* (PIT-MISC-0041) and *Savannah River Site End State Vision* (PIT-MISC-0089) identify the GSA as an industrial zone, this is only in relation to future DOE activities. The institutional DOE knowledge would preclude building on top of the closed HTF. While the site is currently planned to be “federally owned, controlled, and maintained in perpetuity” (PIT-MISC-0089), the area surrounding the SRS in South Carolina do not currently support heavy industrial facilities. The main industrial resource would be the Savannah River and building an industrial facility miles away from the river is not expected. Due to these considerations, the intruder-construction scenario at the HTF is also not considered applicable for an industrial intruder.

4.2.3.2.4 Acute Intruder-Discovery Scenario

The intruder-discovery scenario is a modification of the intruder-construction scenario. The basis for the intruder-discovery scenario is the same as the intruder-construction scenario except that the exposure time is reduced. The scenario involves the intruder excavating a basement to a depth of approximately 10 feet. The intruder is assumed to recognize that he or she is digging into very unusual soil immediately upon encountering the waste tank/piping system and leaves the site. Consequently, the exposure time is reduced. Similar to the intruder-construction scenario, the intruder-discovery scenario was not considered for further analysis due to the disposal depth of the stabilized contaminants in the waste tanks and in ancillary equipment (from a minimum of 10 feet to approximately 40 feet below the HTF closure cap).

4.2.3.2.5 Chronic Intruder-Agricultural (Post-Drilling) Scenario

In the chronic intruder-agriculture scenario, it is assumed that after the end of active institutional controls, a farmer lives on, and consumes food crops grown and animals reared on the closure site, and performs recreational activities on the site. The chronic intruder-agriculture scenario is an extension of the Acute Intruder-Drilling Scenario. It is assumed, in this scenario, that an intruder lives in a building near the well drilled as part of the intruder-drilling scenario and engages in agricultural and recreational activities on

the contaminated site and stream. Excavation to the surface of the stabilized contaminants in the waste tanks was not considered credible due to its depth of more than 40 feet below the closure cap. Therefore, the chronic intruder-agriculture scenario was retained for the ancillary equipment inventory and specifically a waste transfer line because it is less protected than a DB, valve box, or PP (each shielded with thick shield covers of several feet of concrete as noted in Section 3.2.2).

The primary water source for the chronic intruder-agriculture scenario is a well drilled into the groundwater aquifers through a transfer line. The stream is the secondary water source for recreational use pathways and the fish ingestion pathway. The assumption for soil used for gardening purposes is that it is contaminated by both drill cuttings and irrigation well water. The intruder is exposed to (Figure 4.2-34):

- Direct ingestion of well water
- Ingestion and inhalation of well water while showering
- Ingestion of milk and meat from livestock (e.g., dairy and beef cattle) that drink well water
- Ingestion of meat and eggs from poultry that drink well water
- Ingestion of vegetables grown in garden soil irrigated with well water and containing contaminated drill cuttings
- Ingestion of milk and meat from livestock (e.g., dairy and beef cattle) that eat fodder from pasture irrigated with well water
- Ingestion of meat and eggs from poultry that eat fodder from pasture irrigated with well water
- Inhalation of well water used for irrigation
- Inhalation of dust from the soil that was contaminated by drill cuttings and irrigated with well water
- Ingestion of soil that was contaminated by drill cuttings and irrigated with well water
- Direct radiation exposure from radionuclides on the soil that was contaminated by drill cuttings and irrigated with well water

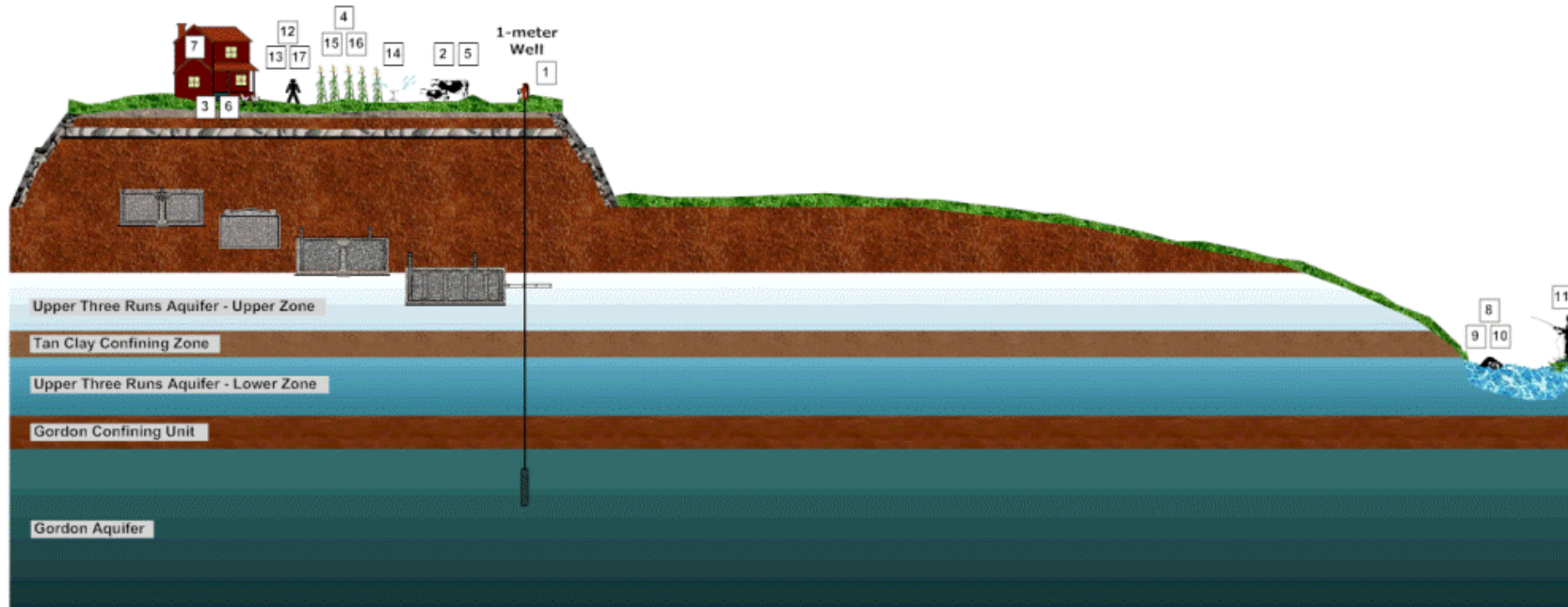
The following exposure pathways involving the use of contaminated surface water (from the applicable stream) for recreational use are assumed to occur:

- Direct irradiation during recreational activities (e.g., swimming, fishing, boating) from stream water
- Dermal contact with stream water during recreational activities (e.g., swimming, fishing)
- Incidental ingestion and inhalation of stream water during recreational activities
- Ingestion of fish from the stream water

The intruder may also be exposed to a release of volatile radionuclides (e.g., H-3, C-14, I-129) from the drill cuttings and contaminated well water. These pathways include:

- Direct plume shine
- Inhalation

Figure 4.2-34: Chronic Intruder Agricultural (Post-Drilling) Scenario



CHRONIC INTRUDER-AGRICULTURAL (POST-DRILLING) SCENARIO

1. Direct ingestion of well water
2. Ingestion of milk and meat from livestock (e.g., dairy and beef cattle) that drink well water
3. Ingestion of meat and eggs from poultry that drink well water
4. Ingestion of vegetables grown in garden soil irrigated with well water and containing contaminated drill cuttings
5. Ingestion of milk and meat from livestock (e.g., dairy and beef cattle) that eat fodder from a pasture irrigated with well water
6. Ingestion of meat and eggs from poultry that eat fodder from a pasture irrigated with well water
7. Ingestion and inhalation of well water while showing
8. Direct irradiation during recreation activities (e.g., swimming, fishing, boating) from stream water
9. Dermal contact with stream water during recreational activities (e.g., swimming, fishing)
10. Incidental ingestion and inhalation of stream water during recreational activities
11. Ingestion of fish from the stream water
12. Direct plume shine
13. Inhalation
14. Inhalation of well water used for irrigation
15. Inhalation of dust from the soil that was contaminated by drill cuttings and irrigated with well water
16. Ingestion of soil that was contaminated by drill cuttings and irrigated with well water
17. Direct radiation exposure from radionuclides on the soil that was contaminated by drill cuttings and irrigated with well water

4.2.3.2.6 Chronic Intruder-Resident Scenario

In this scenario, it is assumed that after the end of active institutional controls, an intruder (i.e., the resident intruder) inadvertently constructs a house at, and lives on, the closure site. The intruder-resident scenario involves the same pathways as the Chronic Intruder Agricultural (Post-Drilling) Scenario, with the potential for additional pathways associated with a house constructed over stabilized contaminants. The pathways uniquely associated with construction of a residence over stabilized contaminants were considered insignificant because of the depth of the stabilized contaminants under the closure cap and the shielding provided by the waste tank and ancillary equipment containment shielding. This shielding would reduce the external dose rates to very low levels. The intruder resident scenario did not require a unique analysis because it was addressed by the Chronic Intruder Agricultural (Post-Drilling) Scenario.

4.2.3.2.7 Chronic Intruder-Recreational Hunting/Fishing Scenario

In this scenario, the assumption is a hunter/fisher inadvertently visits the site, perhaps on a periodic basis, and consumes game and fish taken from the site. For the Chronic Intruder-Agricultural (Post-Drilling) Scenario, the intruder is assumed to perform similar recreational activities as the hunter/fisher who inadvertently visits the site, except for hunting wild game. As discussed in Section 4.2.3.3, the livestock raised near HTF would be more affected by HTF stabilized contaminants than transient wild game. Given the other significant exposure pathways the inadvertent intruder is considered to experience as part of the Chronic Intruder-Agricultural (Post-Drilling) Scenario (e.g., use of well water as potable water, ingestion of livestock and vegetables raised using well water), the intruder-recreational scenario is bounded by the Chronic Intruder Agricultural (Post-Drilling) Scenario and does not require unique analysis.

4.2.3.2.8 Bio-Intrusion Scenario

The bio-intrusion scenario assumes that an intruder moves onto the site but does not excavate into the stabilized contaminants. Rather, radioactivity is brought to the surface by plants through root uptake and by burrowing animals. Bio-intrusion is not considered a credible mechanism for significant stabilized contaminant disturbance, based on the stabilized contaminant depth and form. The stabilized contaminants will be significantly below ground, from at least 10 feet for ancillary equipment to at least 40 feet for stabilized contaminant tank heels. The stabilized contaminant is contained within closed waste tanks or equipment of either stainless steel or carbon steel and will be stabilized and/or grouted as part of the waste tank closure. Of the likely burrowing animal residents at SRS, only one burrower, the Florida Harvester Ant, is expected to burrow below 2 meters, and then, only 5 % of its burrows are expected to be that deep. [WSRC-RP-92-1360] Assuming the HTF cover reverts to pine forest in the future, the pine trees could also pose a bio-intrusion risk, with a mature pine having roots from 6-feet to 12-feet deep. [WSRC-TR-2003-00436] These bio-intrusion depths are not deep enough to reach the principal HTF stabilized contaminant inventory at closure (stabilized contaminant tank heels), and are unlikely to reach any ancillary equipment inventory, which in almost

all cases will be more than 12-feet deep. Even if a pine tree root were to reach the ancillary equipment containment, no significant stabilized contaminant dispersal would be anticipated. The amount of contamination excavated from animal burrows or vegetative intrusion is far less than that involved in the agricultural (intruder-drilling) scenarios for drilling a domestic well into the underlying aquifers. Therefore, this scenario is bounded by the Chronic Intruder-Agricultural (Post-Drilling) Scenario and the bio-intrusion scenario does not require further analysis.

4.2.3.3 Basis for Intruder Pathways

Table 4.2-37 was prepared to provide a list of all the HTF exposure pathways identified as candidates for detailed analysis. The list of candidates was developed based on a review of SRS PA analyses and NRC documents. [SRS-REG-2007-00002, SRR-CWDA-2009-00017, NUREG-0782, NUREG-0945, NUREG-1573] Those human activities at SRS that could bring humans in contact with stabilized contaminants (e.g., water use, hunting, fishing, recreational activities such as swimming and boating, habitation in dwellings, other unique activities that involve water use or ground disturbance) were considered (with emphasis on local practices), to ensure that any pathways unique to SRS were taken into account. Those potential pathways that have quantitative analysis are denoted with an “X” for the various receptors. Quantitative analysis was not performed for potential pathways denoted with an “O”, based on the applicable justifications provided throughout this section. NUREG-1854 states that transport pathways may be excluded from performance analysis if it can be demonstrated that either there is limited potential for radionuclides to be released into a particular pathway, or the pathway is not viable (e.g., water is not potable). Other pathways were excluded due to the nature of the scenario making them impossible (e.g., a garden that receives 100 % irrigation from well water does not receive water from a stream).

The following inputs and assumptions were made regarding the intruder release pathways scenario using water from a well or stream.

- The stabilized contaminant release mechanisms to the intruder are well installation and inadvertent drilling into ancillary equipment, leaching of stabilized contaminants to the groundwater, and volatilization of the stabilized contaminants to the surface. Drilling a well into a waste tank is not considered a credible release mechanism since local practices would cause a well driller to choose a new location before the stabilized contaminant waste tank inventory was disturbed. The local well drillers expect to reach good drinking water aquifers at 150 to 200 feet while drilling through sandy soil (no drilling through high-strength geologic materials). A driller would not expend the effort and equipment damage required to drill through the concrete/grout/steel covering the stabilized contaminant, waste tank inventory. Even if the driller did not realize that he had struck a waste tank, and simply thought he had merely hit a layer of high-strength geologic materials, local experience would tell him that moving the drill site a short distance would avoid the impediment. Similarly, well drilling through a transfer line is also unlikely, especially while the line maintains some structural integrity. Nevertheless, as a bounding case for the purposes of this exercise, it has been assumed that a well driller could drill through an intact transfer line immediately after the end of institutional control.

- Well water will be used by the inadvertent intruder as a primary potable water source (e.g., drinking water, showering) and is used as a primary water source for agriculture (e.g., irrigation, livestock water).
- The inadvertent intruder can use a nearby stream for recreational activities (e.g., swimming, fishing, and boating).
- Any wild game ingested (deer, wild pigs) would merely offset ingested livestock, and would result in a lower total dose since the livestock raised near HTF would be more affected by HTF stabilized contaminants than transient wild game.
- A survey of land and water usage characteristics within a 50-mile region of SRS was conducted and documented in WSRC-RP-91-17. The results of this study found that hogs are raised on farms within 50 miles of the SRS; however, hogs eat commercial feed. Thus, the local consumption of hogs is not considered in the determination of “meat” production or consumption.
- There are two streams (UTR and Fourmile Branch) from which ingestion of finfish with significant contamination is possible. These streams were conservatively assumed a source of dietary fish, excluding shellfish because the streams are not significant sources of edible shellfish and it plays an insignificant role in local diets when considered with other ingested contributors to dose (livestock, milk, and vegetables). [WSRC-TR-2005-00201, WSRC-STI-2007-00004]
- Since there is no substantive water source readily available at the well site, pathways related to water-related commercial activities were not considered. Based on the relative proximity of a large, natural water source (i.e., the Savannah River), it is not assumed that a man-made body of water would be created at the MOP resident site.
- The quantities of water ingested during the relatively short activities of showering (10 min/d) and swimming (7 hr/yr) are negligibly small and are not be addressed independently. The impact of these activities is addressed by the “direct ingestion of well water” pathway (i.e., they are included in the 337 liters of water that is assumed to be ingested every year). [SRNL-STI-2010-00447]
- The dose associated with dermal absorption of radionuclides is insignificant because, unlike some chemicals, radionuclides are generally adsorbed into the body very poorly. Tritium is an exception to this rule, but tritium is found in such relatively small concentrations in the groundwater that it would not be a significant contributor to dose.

4.2.4 Summary of Key Transport Assumptions

The following are the key transport analyses assumptions associated with contaminant release, groundwater transport, and dose.

4.2.4.1 Key Assumptions for Contaminant Release

- An independent conceptual waste release model was used to simulate stabilized contaminant release from the grouted tanks based on various chemical phases in the tank controlling solubility.

- Steel liner failure triggers contaminant release from the tanks. After failure, the carbon steel liner is assumed to be absent, or otherwise not a hindrance to advection and diffusion.
- The steel liner failure analyses considered general and localized corrosion mechanisms of the tank steel.
- Four waste tanks (Type I, Tank 12 and Type II, Tanks 14, 15, and 16) are assumed to have liner degradation at the time of HTF closure, based on present leak site numbers and physical locations.
- Tank concrete properties are originally characterized as Oxidizing Region II transitioning to Oxidizing Region III.
- The reducing grout properties are initially characterized as Reduced Region II, then transition to Oxidized Region II and Oxidized Region III.
- Transfer line inventory is modeled by distributing the assumed inventory over the HTF footprint. Other ancillary equipment is not modeled explicitly.
- Eight waste tanks, along with some ancillary equipment, are either fully submerged or partially submerged in the saturated zone.
- Leaching of contaminants is modeled as a non-uniform leaching process that depends on the chemical state of pore fluid contacting the stabilized contaminant at any given time.
- The calculation of radionuclide solubility in the CZs is done under the assumption of thermodynamic equilibrium using the geochemical modeling program, GWB.

In this analysis, the key conservatism introduced into the analysis was the decision to model only solubility controls to account for stabilized contaminant release in fate and transport models. Contaminant transport outside of the CZ was modeled using soil K_d values taken from compilations of geotechnical data in support of site PA modeling. The selection of solubility controlling phases is very conservative, meaning that where multiple phases of a radionuclide were possible, that with the highest solubility is selected. The process attempted to balance scientific knowledge with the need to be cautious and biased toward higher solubility. Some contaminants were simulated as having no identified solubility controls, with their releases modeled as instantaneous.

In an equilibrium model, the assumption that solubility rather than adsorption controls contaminant release results in faster overall release of radionuclides. This is because the maximum concentration that can desorb is controlled by solubility. In effect, if the K_d is low enough that a concentration is released that exceeds solubility, some of the radionuclide will precipitate bringing the concentration down to solubility. The stabilized contaminant release rate will drop below that dictated by solubility when the radionuclide inventory is depleted to where the concentration released is below solubility. At higher K_d values the concentration released at any given time will always be below the concentration dictated by solubility. Thus, time until complete release of a radionuclide using adsorption controls will always be longer than when only solubility controls are used.

4.2.4.2 Key Assumptions for Groundwater Transport

- HTF contaminant transport processes in cementitious materials and soils include advection, dispersion, and sorption, but not colloidal transport.
- Although the conceptual closure cap has a certain physical thickness (a minimum of 10 feet), the cap is viewed as a surface feature in the ICM and is simulated separately. The closure cap model produces a net infiltration rate at the bottom of the closure cap that becomes a flow boundary condition to the adjoining vadose zone.
- For saturated zone contaminant transport, the contaminant flux leaving the bottom of the vadose zone model becomes the source of contamination entering the aquifer.
- The aquifers of primary interest for HTF modeling are the UTR and Gordon Aquifers. Potential contamination from the HTF is not expected to enter the deeper Crouch Branch Aquifer.
- Because the HTF is located over a groundwater divide between UTR and Fourmile Branch, contaminants could eventually discharge to both streams, depending on the contaminant's origination point.
- The simulation model for groundwater flow constructed from the GSAD using the PORFLOW code is referred to as the GSA/PORFLOW Model. The 3-D grid comprises 102,295 active cells.
- Some cementitious properties are expected to remain constant over time. These include porosity, dry bulk-density and particle density. Because the form of cementitious material degradation is cracking and not the dissolving the cement paste, the porosity, bulk density, and particle density of the cementitious material, a marginal impact is expected.
- The most extensive cementitious material attack was found to be from carbonation on unsaturated concrete and grout. Carbonation was found to result in the greatest penetration as a function of time. The effect of carbonation on the permeability of the cementitious barriers depends on whether the barrier contains steel.

In this analysis, several conditions introduce conservatism into the flow calculations. Of particular importance is the approach to handling loss of containment after failure of the steel liner. Immediately after failure, the liner is assumed as not a hindrance to advection or diffusion, which allows the immediate release of non-adsorbing contaminants and hastens the geochemical transition of the waste form from reducing to oxidizing conditions accompanied by a general increase in contaminant release rates.

4.2.4.3 Key Assumptions for Dose Calculations

- The primary mechanism for transport of radionuclides is expected to be leaching to the groundwater, groundwater transport to the well/stream, and subsequent human consumption or exposure.
- The scenarios are not assumed to occur until after the 100-year institutional control period ends, after which time it is assumed that no active HTF facility maintenance will be conducted.
- Pathways related to MOP resident scenario using water from a well or stream incorporated the following key assumptions:

- The stabilized contaminants release mechanisms to MOP are leaching of stabilized contaminants to the groundwater and volatilization of the stabilized contaminants to the surface. Well drilling is not a release mechanism.
- Bio-intrusion and/or erosion are not considered credible mechanisms. The stabilized contaminants will be significantly below ground, from at least 10 feet for ancillary equipment to approximately 40 feet for stabilized contaminants.
- In the well water as primary water source scenario, well water will be used as a primary potable water source for a residence near the well.
- In the MOP near a stream scenario, stream water will be used as a primary potable water source for a residence near the stream.
- There are two streams (UTR and Fourmile Branch) from which ingestion of finfish with significant contamination is possible. The assumption for these streams as a source of dietary fish was conservative, and the two streams are not significant sources of edible shellfish.
- Since there is no substantial water source at the well site, there was no consideration for pathways related to water-related commercial activities.
- The quantities of water ingested during the relatively short activities of showering (10 min/d) and swimming (7 hr/yr) are negligible and not addressed independently.
- The scenario involves the intruder excavating a basement to a depth of approximately 10 feet. The intruder is assumed to recognize that he or she is digging into very unusual soil immediately upon encountering the waste tank/piping system and leaves the site.
- The chronic intruder-agriculture scenario is an extension of the Acute Intruder-Drilling Scenario. It is assumed in this scenario that an intruder lives in a building near the well drilled as part of the intruder-drilling scenario and engages in agricultural and recreational activities on the contaminated site and stream.

Key conservatisms incorporated into the calculation of dose include that all groundwater concentrations used for dose calculations are maximum values. For example, a dose computed for Sector A, at the maximum hypothetical 100-meter well location, uses for each contaminant the maximum concentration from any of the wells within the sector. This maximum is selected for each time step in the simulation. The dose provided is the maximum of the sectors, A through F.

4.2.4.4 Key Assumptions for Air and Radon Pathways

The following are the key air and radon pathway analyses assumptions:

- The stabilized contaminant layer was represented as a 1-foot layer of material located at the bottom of the waste tank.
- The stabilized contaminant layer, reducing grout, and concrete roof were assumed saturated at 50 %.
- The stabilized contaminant layer is assumed to have properties similar to reducing grout.

- Exclusion of the top soil, upper backfill, HDPE geomembrane, GCL, and primary steel liner of the waste tank make the model conservative.
- The final closure cap as outlined with exclusions was assumed to remain intact for the duration of the simulation.

In this analysis, several conditions introduce conservatism into the calculations. These include:

- Using boundary conditions that force all gaseous radionuclides to move upward from the stabilized CZ to the land surface - some gaseous radionuclides diffuse sideways and downward in air-filled pores surrounding the stabilized CZ; therefore, ignoring this has the effect of increasing flux at the land surface.
- Not taking credit for removal of radionuclides via pore water moving vertically downward through the model domain - this mechanism would likely remove some dissolved radionuclides therefore its omission had the effect of increasing the estimate of instantaneous radionuclide flux at the land surface in simulations.
- Exclusion of the HDPE geomembrane, GCL, and the primary steel liner of the waste tank - inclusion of these materials in the model would significantly reduce the gaseous flux at land surface due to material properties (i.e., low air-filled porosity).
- Excluding cover materials above the erosion barrier (i.e., top soil and upper backfill layers) - this material exclusion shortens the diffusion pathway and could increase flux at the land surface.
- Assuming stabilized contaminant layer, reducing grout and the concrete roof are only 50 % saturated - these materials are likely at or near saturation making the air-filled porosity equal to one-half the total porosity and increasing diffusive transport through the materials since gaseous flux is through air-filled porosity.
- Using Type I and II tanks with minimum closure cap thickness.
- Concentrating entire estimated HTF residual inventory to a 1-foot stabilized contaminant layer to determine maximum dose and flux.

4.3 Modeling Codes

In the process of completing the PA for the HTF, a variety of modeling codes were utilized to perform various media transport, radiological dose, and groundwater concentrations calculations. The purpose of this section is to present the modeling codes used and describe the modeling code integration. A brief description is provided for each modeling code, which includes the function of the code, available code manuals or technical documents for the applicable code revision, reasons for selection of the particular code, and available QA documentation for the code. The results of the HTF PA will be used during the CERCLA closure process and complement any additional evaluations necessary using existing ACP modeling methods for residual materials other than those in the waste tanks and ancillary equipment.

4.3.1 Modeling Codes Used

Five primary modeling codes were used to support the HTF PA, as discussed below. These are HELP, PORFLOW, GoldSim, CAP-88 (Clean Air Act Assessment Package), and GWB.

4.3.1.1 *Hydrologic Evaluation of Landfill Performance Model*

The HELP model is a quasi, 2-D water balance model designed to conduct landfill-water balance analyses. The HELP model was used to generate water infiltration estimates through the closure cap, for use in PA calculations. HELP model infiltration estimates form the input to subsequent flow and contaminant transport models.

The HELP model requires the input of weather, soil, and design data. It provides estimates of runoff, evapotranspiration, lateral drainage, vertical percolation (i.e., infiltration), hydraulic head, and water storage for the evaluation of various landfill designs. U.S. Army Corps of Engineers (USACE) personnel at the Waterways Experiment Station (WES) in Vicksburg, Mississippi developed the HELP model, under an interagency agreement with the EPA. [EPA-600-R-94-168b] As such, the HELP model is an EPA sanctioned model for conducting landfill-water balance analyses. HELP model version 3.07, issued on November 1, 1997, is the latest version of the model and was the version used for the HTF PA calculations. The HELP model was used at SRS in the development of calculations supporting the SDF PA and was the code used by ACP during CERCLA closure evaluations. [SRR-CWDA-2009-00017] While other infiltration calculation codes for the closure cap exist, the HELP model is a proven code that is appropriate for use at SRS. It is public domain software available from Environmental Laboratory's models and tools. EPA and the USACE have provided a user's guide that provides instruction documentation associated with the HELP model. [EPA-600-R-94-168a] Figures 4.3-1 and 4.3-2 illustrate the integration of the HELP model in HTF PA modeling.

Figure 4.3-1: Modeling Code Integration for HTF PA

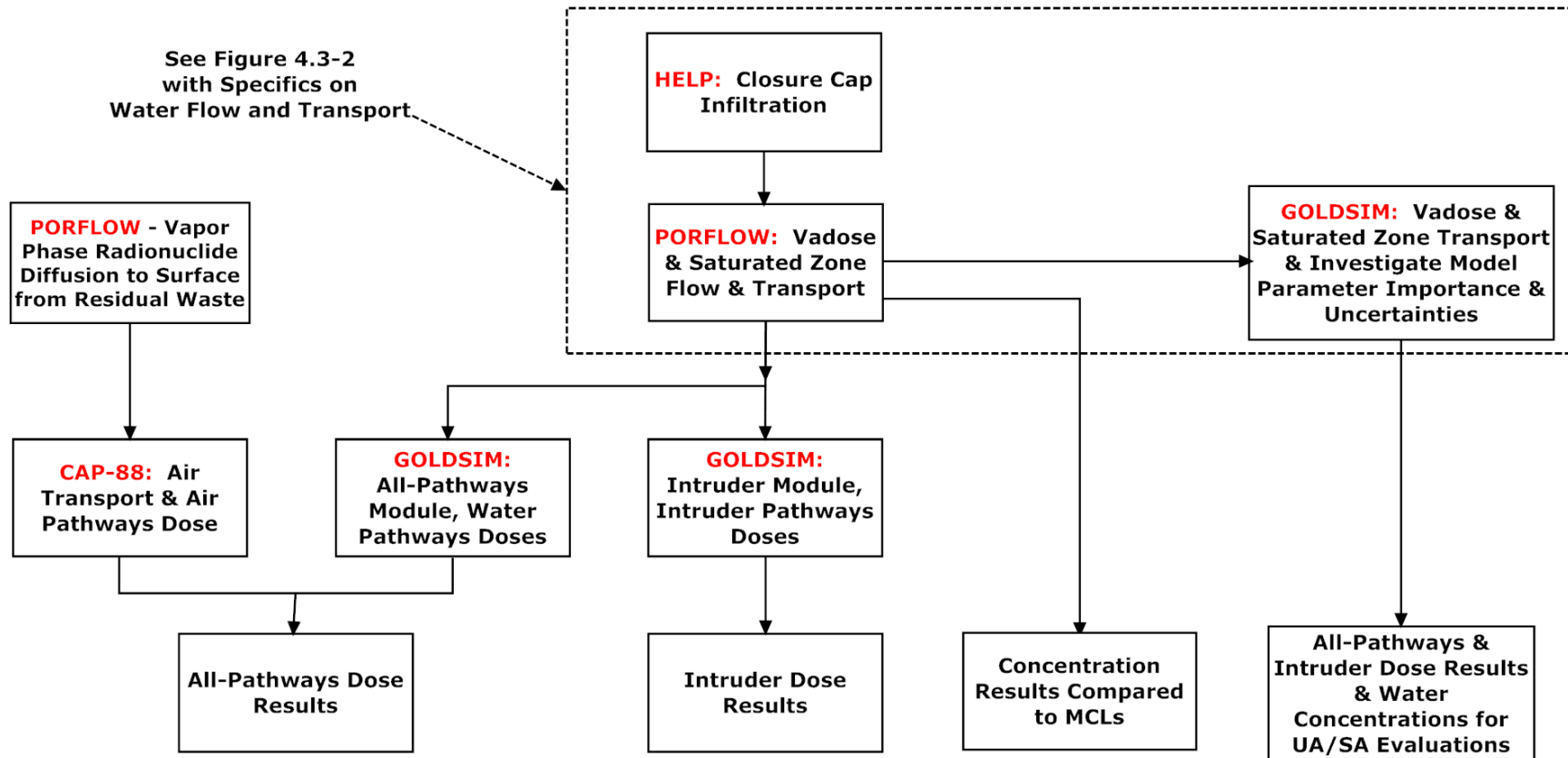
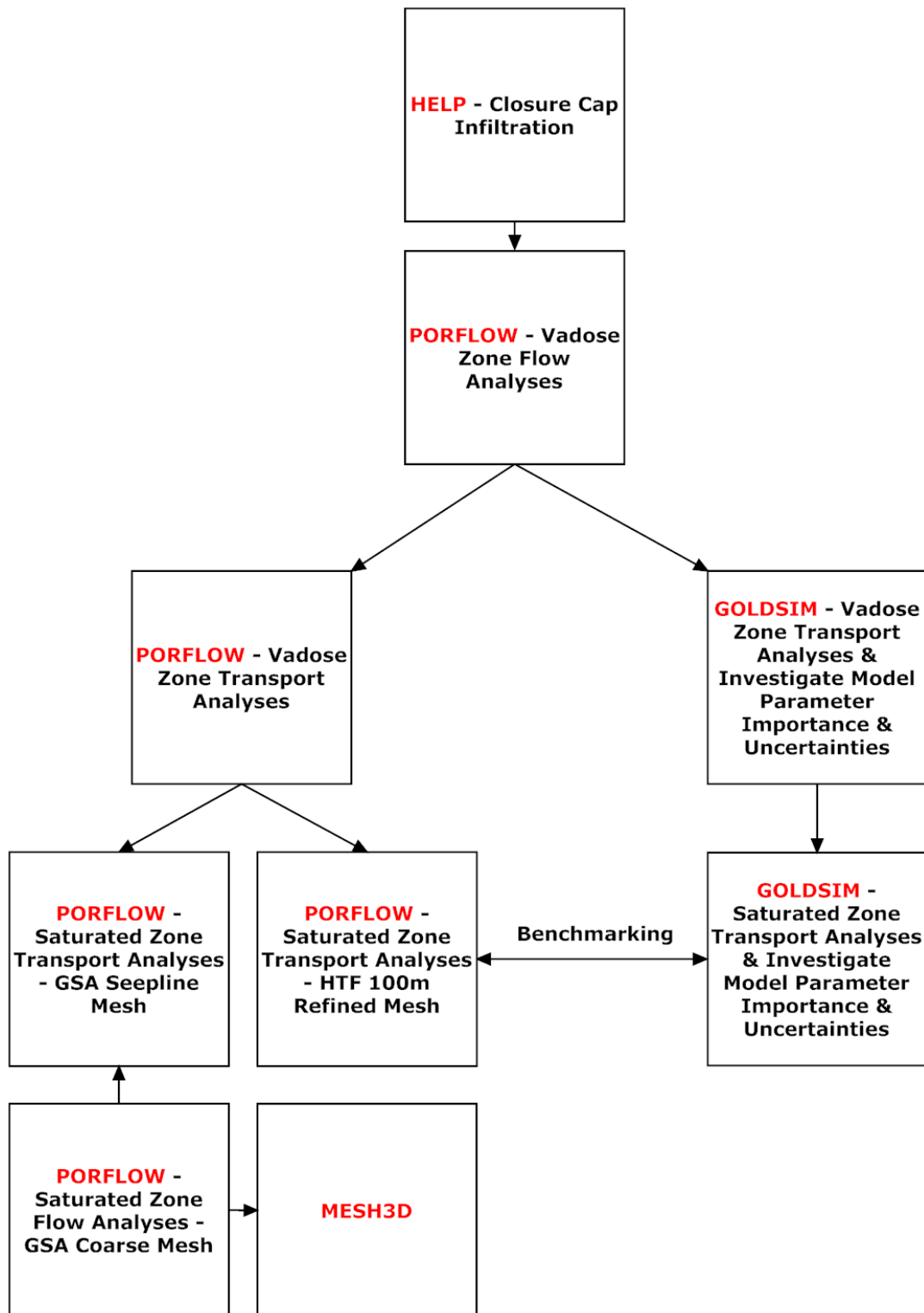


Figure 4.3-2: Modeling Code Integration for HTF PA
(Details of Water Flow and Transport)



Engineering documentation provides information on the source language used to write the code, the hardware necessary to operate the code, data generation methodologies available for use, and the methods of solution. [EPA-600-R-94-168b]

HELP verification test reports exist which compare the model's drainage layer estimates to the results of large-scale physical models and compare the model's water balance estimates to "field data from 20 landfill cells at seven sites in the United States." [EPA-600-2-87-049, EPA-600-2-87-050]

The *FTF Closure Cap Concept and Infiltration Estimates* (WSRC-STI-2007-00184) report discusses eight water balance and infiltration studies that have been conducted in and around SRS by various organizations, including SRNL, USGS, State University of New York at Brockport, Pennsylvania State University, University of Arizona, and the Desert Research Institute. Findings from these studies are reported in the closure cap report. The HELP model results compare very well with the background water balance and infiltration studies, indicating that use of the HELP model produces reasonable and acceptable results. The closure cap report (WSRC-STI-2007-00184) shows that evapotranspiration dominates the water balance distribution of precipitation at SRS in both the background water balance and infiltration studies and in the results from the HELP model. Based upon these evaluations, use of the HELP model to establish the upper boundary condition infiltration for a 2-D PORFLOW vadose zone flow model is appropriate. [WSRC-STI-2007-00184]

The HELP model was used to evaluate seven infiltration cases for the closure cap. Case #6 is a soils only closure cap, with no barrier, drainage, or erosion control layers. As such, the water balance, HELP model results from Case #6 are most applicable for comparison to the background water balance and infiltration studies. The average HELP model Case #6 infiltration (16.45 in/yr) is slightly greater than the median infiltration of the background studies (14.85 in/yr); indicating that the HELP model infiltration results are conservative. [WSRC-STI-2007-00184]

In summary, additional studies for comparison to support HELP appropriateness in humid environments are not needed since the limitations of the software result in conservative infiltration estimates.

The Software Quality Assurance Plan (SQAP) for the HELP model version used for the HTF PA calculations is documented within Q-SQA-A-00005.

4.3.1.2 PORFLOW

PORFLOW is a commercial Computational Fluid Dynamics (CFD) tool developed by Analytic & Computational Research, Inc. PORFLOW numerically solves problems involving transient or steady state fluid flow, heat, salinity and mass transport in multi-phase, variably saturated, porous or fractured media with dynamic phase change. PORFLOW was used in the HTF PA modeling to calculate fluid flow and contaminant transport in the vadose and saturated zones. PORFLOW transport results were utilized by subsequent modeling codes to calculate radiological doses and perform human health and ecological risk evaluations. PORFLOW flow results were also used to conduct probabilistic simulations of contaminant transport via GoldSim, another computational tool. In addition, PORFLOW

was used to calculate vapor phase radionuclide diffusion to the ground surface from stabilized contaminant material for use in air transport calculations. Figures 4.3-1 and 4.3-2 illustrate the integration of PORFLOW in the HTF PA modeling and provide additional detail of the integration and steps of PORFLOW calculations for fluid flow and contaminant transport.

PORFLOW accommodates alternate fluid and media property relations, and complex and arbitrary boundary conditions. The geometry may be 2-D or 3-D, Cartesian, or cylindrical, and the mesh may be structured or unstructured, giving maximum flexibility to the user. Version 6.30.2 of PORFLOW was used to accomplish HTF PA simulations. Version 6.30.2 is the latest site version of PORFLOW and contains the “STRATified” aquifer dispersion model and the greater limit on the number of “STATistics” files, which were identified as necessary for the prior work. PORFLOW was used at SRS for calculations supporting the FTF and SDF PAs, and used by Idaho National Laboratory for analyses supporting operational closure of the tank farm facility. [SRS-REG-2007-00002, SRR-CDWA-2009-00017, DOE-ID-10966] For the HTF PA, PORFLOW is an appropriate code because it can accommodate calculations in both the saturated and unsaturated zones and has the ability to simulate first-order decay and progeny in-growth associated with radionuclide chains, which is necessary for calculations involving radioactive stabilized contaminant disposal.

Analytic & Computational Research, Inc. has provided the following documentation for use the PORFLOW CFD tool:

- A user’s guide (ACRi-2008)
- Validation data (ACRi-1994)
- Software verification for PORFLOW Version 6.30.2 (SRNL-TR-2010-00213)

The SQAP for the PORFLOW version used for the HTF PA calculations is covered by G-SQP-A-00012.

MESH3D is a grid refinement tool developed by SRNL for extracting a portion of a PORFLOW model grid and flow solution, and optionally refining the cutout grid by subdividing cells. [Q-SQP-G-00003] The velocity and saturation fields are refined using a mass-conserving interpolation method. MESH3D is used to extract and refine a portion of the GSA/PORFLOW flow model of the vicinity of HTF for performing higher resolution transport simulations of plume migration from waste tank sources out to 100 meters. Software design, use, testing, and QA plan for MESH3D are addressed by Q-SQP-G-00003.

The design check of the data used to perform the PORFLOW modeling is documented in SRNL-L3200-2012-00023, and all technical findings have been satisfactorily resolved. The scope of the design check includes

- Vadose zone flow input
- Vadose zone transport input
- Aquifer transport input

4.3.1.3 GoldSim

GoldSim is a commercial program developed by GoldSim Technology Group LLC. It is a user-friendly, graphical Windows-based program for carrying out dynamic probabilistic simulations of complex systems to support management and decision-making in engineering, science, and business.

GoldSim was used to assist in developing uncertainty analyses for the HTF PA. The parameters modeled in GoldSim identified important input parameters in the groundwater transport model. GoldSim utilized the flow field outputs from PORFLOW to perform transport calculations and subsequent dose calculations for evaluation of input parameter importance and calculation uncertainties. GoldSim was used to evaluate parameter importance while developing the initial model for PORFLOW and provide feedback to the PORFLOW modelers on focus areas requiring additional attention. GoldSim was also employed for the performance of the all-pathways and intruder analyses by using the contaminant transport results from PORFLOW to calculate groundwater pathways and inadvertent intruder doses. Figures 4.3-1 and 4.3-2 illustrate the integration of GoldSim in the modeling efforts and provide additional detail of the integration and steps of GoldSim calculations for fluid flow and contaminant transport.

GoldSim was designed to facilitate the construction of large, complex models. The user can build a model of a system in a hierarchical, modular manner, such that the model can evolve and add detail as more knowledge regarding the system is obtained. Other features, such as the ability to manipulate arrays, the ability to “localize” parts of a model, and the ability to assign version numbers to a model that is constantly being modified and improved, further facilitate the construction and management of large models. GoldSim has an extensive internal database of units and conversion factors allowing the user to enter data and display results in any units and/or define customized units. GoldSim ensures dimensional consistency in models and carries out all of the unit conversions internally, eliminating the need to carry out (error-prone) unit conversions. The user can dynamically link external programs or spreadsheets directly into a HTF GoldSim Model. In addition, GoldSim was specifically designed to support the addition of customized modules (program extensions) to address specialized applications, such as contaminant transport.

GoldSim, Version 10.50, Service Pack 2 is used for the PA porous medium transport and dose analyses because 1) its capabilities meet program needs, 2) it allows for ease of input changes and output visualization, and 3) it is used by other DOE sites (e.g., Nevada Test Site, Yucca Mountain Project) and the NRC.

The GoldSim Technology Group LLC provides a user’s guide (GTG-2010d) and a separate guide for contaminant transport calculations (GTG-2010e). The SQAP for the GoldSim software is covered by B-SQP-C-00002. Data verification for the HTF GoldSim model is covered under SRR-CWDA-2012-00070.

A dynamic link library, *ReadFlowFields.DLL*, was designed for use in conjunction with the area-specific GoldSim models. [B-SQP-C-00003] Functionally, this software is used to read data into a GoldSim model file from an external input file. In the HTF GoldSim Model the dynamic link library is used to read in flow data from files generated using HTF PORFLOW Flow Model. [SRR-CWDA-2012-00093] The SQAP for the *ReadFlowFields.DLL* is covered by B-SQP-C-00003.

4.3.1.4 CAP-88

The CAP-88 computer model is a set of computer programs, databases, and associated utility programs developed by the EPA for estimating dose and risk from radionuclide emissions to air. The CAP-88 model was used in the HTF PA to estimate annual dose to maximally exposed individuals (MEI) considering plume and ground gamma-shine, inhalation and foodstuff ingestion pathways using the vapor-phase radionuclide diffusion to the surface results from PORFLOW.

The CAP-88 model was developed by the EPA and used to demonstrate compliance with 40 CFR 61-Subpart H, emission standards. The CAP-88 model uses a modified Gaussian plume equation to estimate the average dispersion of radionuclides released from up to six sources at the same release location with different release heights. Assessments are done for a circular grid with a radius up to 50 miles. Figure 4.3-1 illustrates the integration of CAP-88 in the HTF PA.

The CAP-88 program was written in FORTRAN77 (Formula Translating System) and was compiled to run on an IBM (International Business Machine) 3090 mainframe under OS/VS2 (Operating System/Virtual Storage 2), using the IBM FORTRAN77 (1978 FORTRAN ANSI standard compliant revision) compiler (computer source code translator), at the EPA National Computer Center in the Research Triangle Park, North Carolina.

A user's guide for CAP-88 is available. [CAP-88] The SQAP for CAP-88 used for the HTF PA calculations is covered by Q-SQP-A-00002.

4.3.1.5 The Geochemist's Workbench

The GWB, Release 8.0, is a geochemical modeling software developed by the University of Illinois for manipulating chemical reactions, calculating stability diagrams and the equilibrium states of natural waters, tracing reaction processes, modeling reactive transport, plotting the results of these calculations, and storing the related data. The software contains tools for balancing reactions, calculating activity diagrams, computing speciation in aqueous solutions, plotting the results of these calculations, and storing the related data. [SRR-CWDA-2010-00105] The SQAP for GWB is covered by SRR-CWDA-2010-00154.

As described in Section 4.2.1.1, this code was used to estimate chemical conditions, such as the effects of the partial pressure of carbon dioxide. These calculations supported the conceptual model of contaminant releases from the CZ of the waste tanks. [WSRC-STI-2007-00544]

4.3.2 Software QA

The hierarchy of the SRS quality documents is described in this section.

Management Policies (MP), 1-01, Policy 4.2 contains the SRS policy statement regarding the company's commitment to provide products and services that meet or exceed the requirements and expectations of our customers. The Quality Assurance Program is to be implemented in a manner to support implementation of the SRS imperatives of safety, disciplined operations, cost effectiveness, continuous improvement, and teamwork. The SRS has established and implemented an Integrated Safety Management System (ISMS). The QA program is consistent with, and an integral part, of the SRS ISMS. The MP requires the QA program to include appropriate quality procedures for compliance with legal, regulatory, contractual, and corporate quality requirements. The MP stipulates that the SRS QA program comply with 10 CFR 830 *Nuclear Safety Management* and DOE O 414.1, *Quality Assurance*. Application of the QA program contributes to the safe, reliable, and environmentally sound operation of the SRS. It incorporates a graded approach commensurate QA/Quality Control (QC) risk definition and application requirements. Application of the Quality Assurance Management Plan (QAMP) enables error prevention, detection and correction of deficient conditions and the incorporation of an assessment process for identifying continuous improvement opportunities. The focus of quality improvement is to reduce the variability of every process that influences the quality and value of SRS products or services. [MP 1-01, Policy 4.2]

Quality Assurance Manual 1-Q provides the structure and procedures for achieving and verifying the SRS requirements for quality. The manual consists of a series of QA procedures that describe applicable QA requirements. 1Q Manual, Procedure 2-1, *Quality Assurance Program*, Section B states that the QA program has been developed to be responsive to the requirements of DOE O 414.1D, and DOE *Nuclear Safety Management*, Title 10 CFR 830, Subpart A, *Quality Assurance Requirements*. Because of the size and complexity of SRS and its varied products, services, and missions, the program has been defined in a standard framework of company policy, procedures, and instructions to be used by the implementing organizations to perform quality-related activities. [1Q Manual, Procedure 2-1] Software QA is conducted in accordance with the requirements of the 1Q Manual, Procedure 20-1 through the development and execution of the SQAPs. The SQAPs for the specific software codes used in the HTF PA are identified in Section 4.3.1. [1Q Manual, Procedure 20-1]

4.3.3 Model Checking

The E7 Manual, *Conduct of Engineering Manual*, E7, Procedure 2.60, *Technical Reviews* is the QA implementing procedure for performing technical reviews. This procedure defines the processes used by SRS to verify the inputs and outputs for the different modeling codes. The end use of data drives the level of review required. Design Verification, the highest-level review, must be performed for work affecting Safety Significant/Safety Class systems. Design Check is the next lower level of review and is required for all Production Support and General Service design output documents. Because the work associated with the PA and associated documents are not associated with Safety Significant or Safety Class systems, the Design Check represents the appropriate level of rigor.

During a Design Check, the technical accuracy of the design document is assured by performing the following activities:

- A mathematical check, if appropriate
- A review for correct use of technical input, including quality requirements
- A review of the approach used and reasonableness of the output
- An administrative check (e.g., page numbers, format)

To perform a Design Check the following criteria must be met:

- Cannot be a participant in the development of the portion of the document being checked
- Must be knowledgeable in the area of the design or analysis for which they review
- Must be capable of performing similar design or analysis activities
- Must have the security clearance for access to sufficient information to perform the Design Check

Between 2002 and 2004 SRNL developed, piloted, and implemented technical review guidelines incorporating the E7 Manual, Procedure 2.60 requirements for performing Design Checks and Design Verification by document review. These guidelines also meet the requirements for review of Type 2 Calculations contained in E7 Manual, Procedure 2.31, *Engineering Calculations*. The guidelines provide a flowchart to map the SRNL technical review process, lines of inquiry for performing reviews, a checklist for communicating instructions, and best management practices to set a benchmark for management expectations.

Figures 4.3-1 and 4.3-2 present the approach to modeling code integration used for the HTF PA. Important to the implementation of the modeling integration shown in Figures 4.3-1 and 4.3-2 is assurance that the input data to the various codes is verified to be accurate. Documentation of the verification for the model input traced from source documents, to modeling input, and to appropriate sections within the PA has been performed and is described in *H-Area Tank Farm (HTF) Performance Assessment (PA) Model Quality Assurance (QA) Report*, SRR-CWDA-2012-00070. Model inputs are implemented as components to the model files (i.e., they are “hardwired” into the models). Consequently, inputs are controlled in accordance with the quality assurance requirements of the respective

model(s) and any changes to the inputs result in a change to the model, thus requiring re-checking of the affected model file(s).

4.4 Closure System Modeling

This section describes how the HTF design elements and their associated properties were represented in the computer modeling codes. The closed waste tank system conceptual design was an aphysical simplification of the actual system design for the waste tank, which is required for analytical modeling. Certain waste tank features and design elements are by necessity omitted in the conceptual model and are discussed in Section 4.4.1.

This section also describes how the HTF closure cap system is expected to behave in the future, and what modeling scenarios were used to depict system behavior over time. Because it is difficult to predict with a high level of certainty just what changes may occur to a closed, grouted waste tank system over time, this section describes a range of potential conditions that a closed waste tank or ancillary system may be subjected. While the baseline analysis (represented through the HTF PORFLOW Model) reflected the best estimate of future behavior of the closed system, the probabilistic analyses (represented through the HTF GoldSim Model) considered a variety of possible scenarios. In addition to analyzing differing scenarios, the transport models were all run to at least 100,000 years in order to determine peak concentrations.

4.4.1 Individual Waste Tank Modeling

Certain waste tank features and design elements were omitted in the initial conceptual model. The waste tank design features not included in the initial conceptual design will be addressed in subsequent conceptual models (e.g., cooling coils and rebar as fast flow paths). A number of general modeling decision guidelines were followed for the initial design:

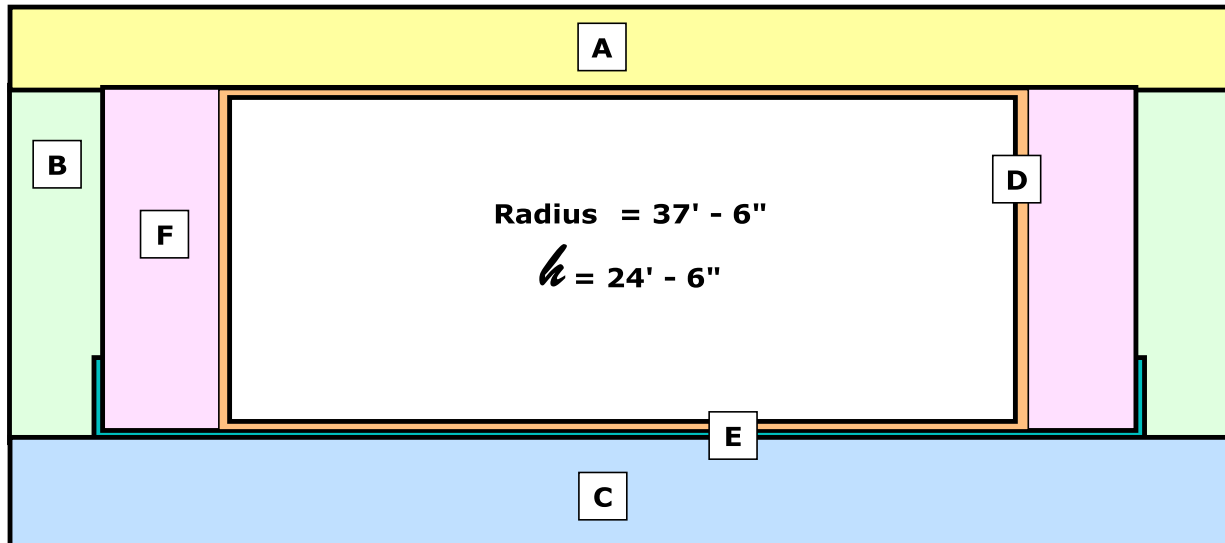
- The intent of the initial conceptual model was to capture waste tank dimensions and relative material differences for each discrete waste tank segment.
- Each discrete waste tank segment/area was represented as homogeneous, ignoring interior elements (e.g., rebar, cooling coils) and/or penetrations through the area (e.g., waste tank risers, transfer lines).
- Minimum segment thicknesses were used where an area had variable thickness (e.g., waste tank walls, waste tank tops).
- Grouting of void areas in the waste tanks (e.g., primary liner tank interior, waste tank annulus) was assumed to have occurred as planned.

4.4.1.1 Type I Tank Modeling

The Type I tank dimensions are presented in Figure 4.4-1. Specific areas where these modeling decisions are implemented for the Type I tanks are as follows:

- The basemat segment of the waste tank was derived from basemat thickness, without consideration for other material layers below the waste tank (i.e., concrete working slab, grout layer, lean concrete layer, and waterproofing layer).
- The primary liner and secondary liner are explicitly modeled.
- The primary and secondary liner assumed thicknesses were based on the minimum thicknesses only.
- Penetrations of the waste tank wall and liner (e.g., transfer lines) were not modeled.
- The primary liner encased waste tank cavity, considered filled with grout, was treated as a discrete area.
- The 12 waste-tank support columns and cooling coils were not modeled and not included in the primary liner waste tank interior. The waste tank annulus, assumed filled with grout, was treated as a discrete area.
- The roof penetrations of the waste tank (e.g., risers) were not modeled.
- Concrete supporting rebar in the waste tank top, walls, and basemat was not modeled, and concrete was considered a homogenous material.
- The waste-tank underliner sump was not modeled.
- The waterproofing, brick wall, and bituminous grout layers outside the concrete vault were not modeled and considered as soil.

Figure 4.4-1: Typical Type I Tank Modeling Dimensions



[NOT TO SCALE]

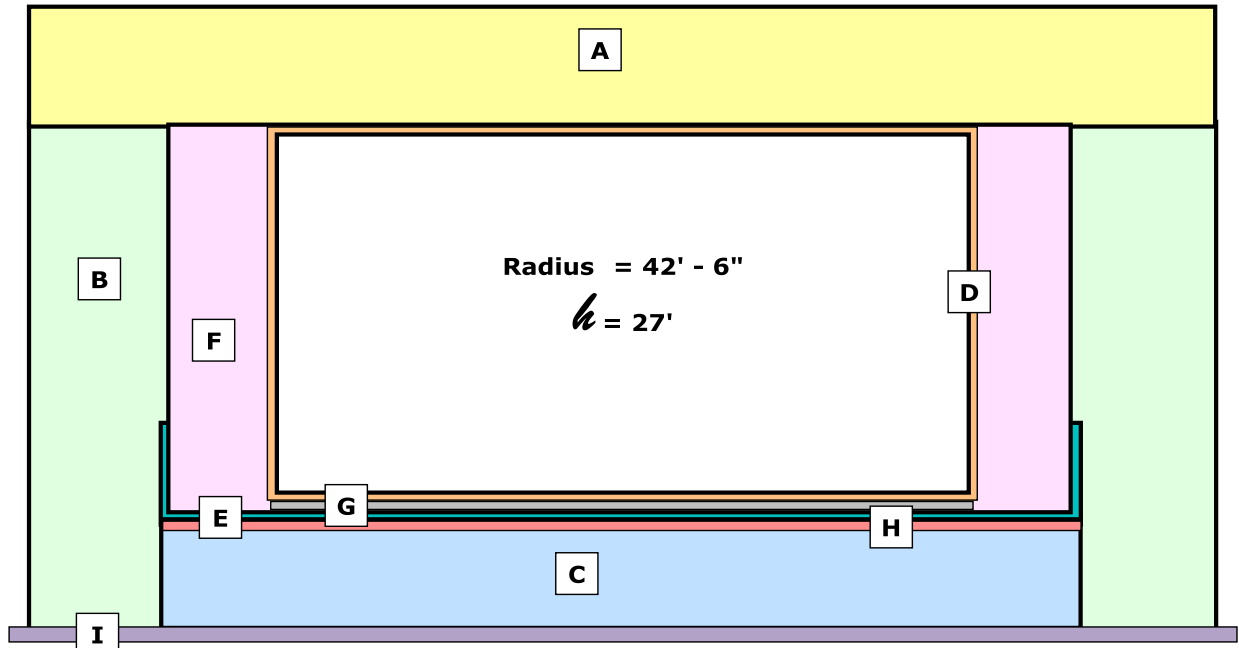
LABEL	THICKNESS	MATERIAL
A Roof	22"	Concrete
B Wall	22"	Concrete
C Basemat	30"	Concrete
D Primary Liner	0.5"	Carbon Steel
E Secondary Liner	5' x 0.5"	Carbon Steel
F Grouted Annulus	30"	Reducing Grout

4.4.1.2 Type II Tank Modeling

The Type II tank dimensions are presented in Figure 4.4-2. Specific areas where these modeling decisions are implemented for the Type II tanks are highlighted below:

- The basemat segment was based on the basemat thickness disregarding other material layers below the waste tank (e.g., grout layer, and waterproofing layer).
- Primary and secondary liner assumed thicknesses were based on minimum thicknesses only.
- Penetrations of the waste tank wall and liner (e.g., transfer lines) were not modeled.
- The primary liner, waste tank cavity was considered as filled with grout and was treated as a discrete area.
- The support column and cooling coils were not modeled, and were not included in the primary liner. The waste tank annulus was treated as a discrete area because the assumption that it will be filled with grout.
- The roof penetrations (e.g., risers) were not modeled.
- Concrete rebar in the waste tank top, walls, and basemat was not modeled, such that concrete is considered a homogenous material.
- The soil hydration system was not modeled.

Figure 4.4-2: Typical Type II Tank Modeling Dimensions



[NOT TO SCALE]

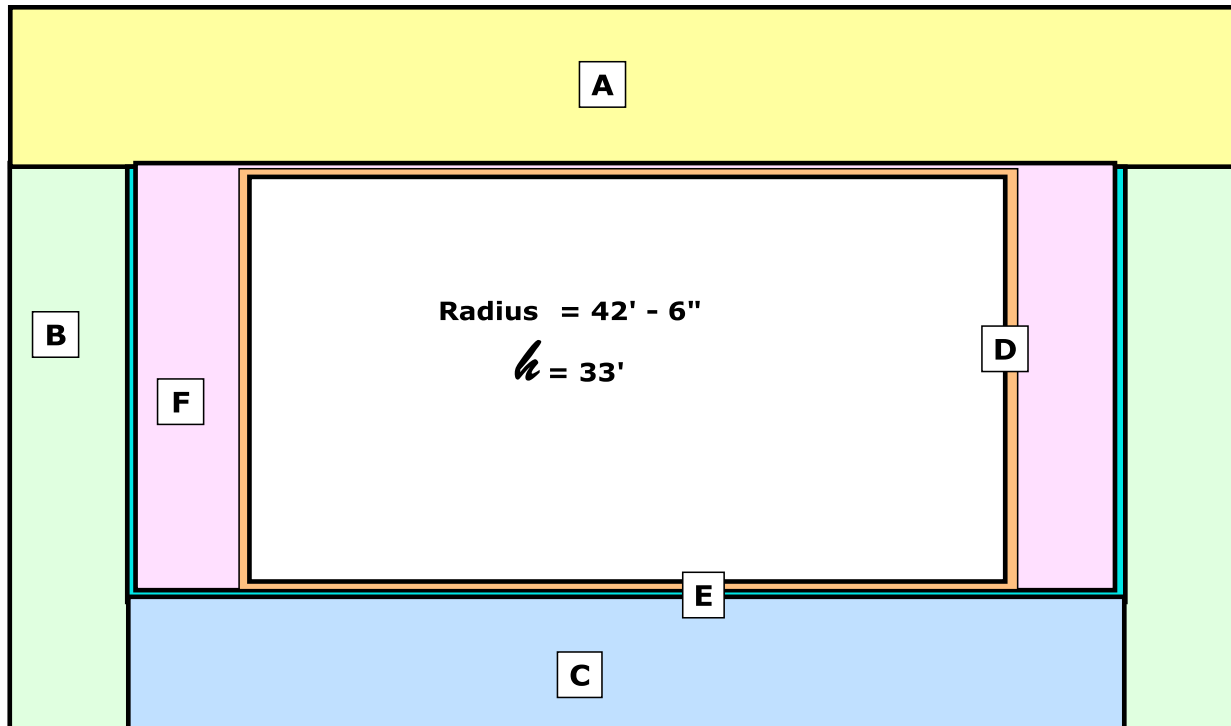
LABEL	THICKNESS	MATERIAL
A Roof	45"	Concrete
B Wall	33"	Concrete
C Basemat	42"	Concrete
D Primary Liner	0.5"	Carbon Steel
E Secondary Liner	5' X 0.5"	Carbon Steel
F Grouted Annulus	30.625"	Reducing Grout
G Primary Sand Pad	1"	Procured Washed Sand
H Secondary Sand Pad	1"	Procured Washed Sand
I Working Slab	6"	Concrete

4.4.1.3 Type III and IIIA Tank Modeling

The Type III and Type IIIA tank dimensions are presented in Figures 4.4-3 and 4.4-4, respectively. Specific areas where these modeling decisions are implemented for the Type III and IIIA tanks are highlighted below:

- Type IIIA tank basemat thickness has 2 inches subtracted to reflect the 2-inch leak detection slots cut into the basemat. [W701336, W707253]
- Thermocouple piping running through the waste tank walls and basemat was not modeled.
- The primary liner, waste tank cavity was considered as filled with grout and treated as a discrete area.
- The center column, center annulus, ventilation ductwork, and cooling coils were not modeled.
- The waste tank annulus was assumed as filled with grout and was treated as a discrete area.
- The primary liner and secondary liner assumed thicknesses were based on the minimum thicknesses only (e.g., extra thickness at knuckle not modeled).
- Penetrations through the waste tank wall and primary liner (e.g., transfer lines) were not modeled.
- The roof penetrations for the waste tanks (e.g., risers) were not modeled.
- Concrete rebar in the waste tank top, walls, and basemat were not modeled, such that concrete is considered a homogenous material.
- The underliner sump for the waste tank was not modeled.

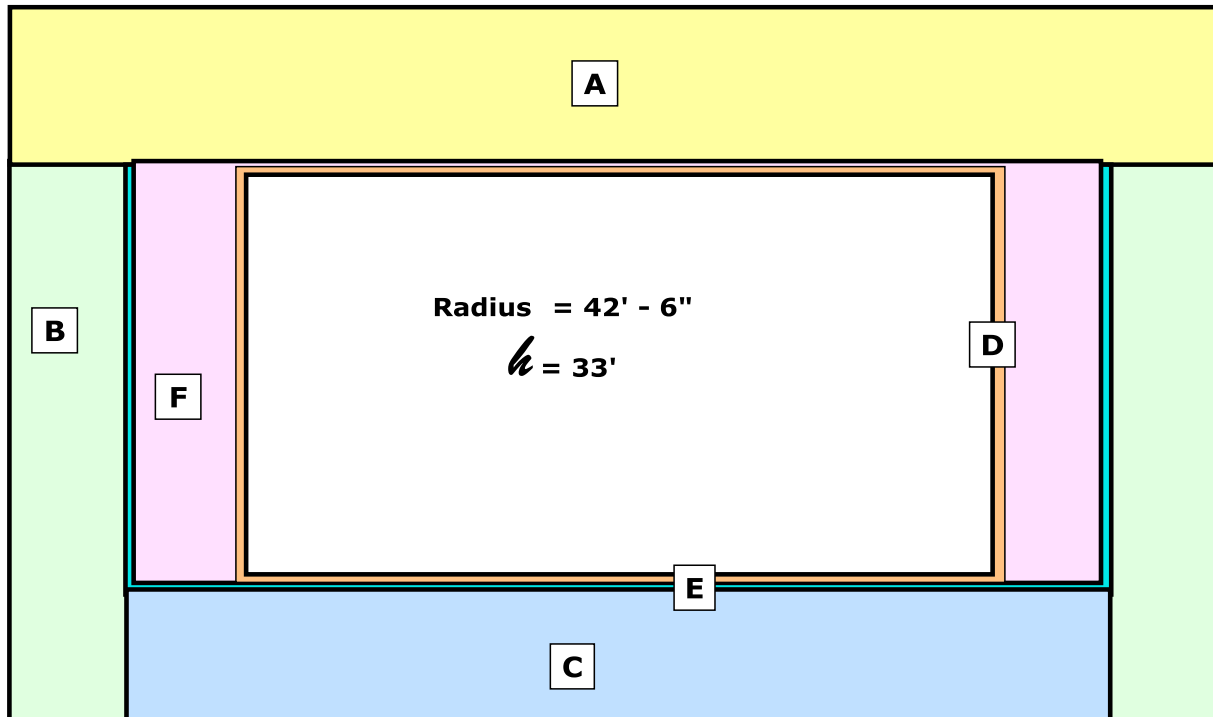
Figure 4.4-3: Typical Type III Tank Modeling Dimensions



[NOT TO SCALE]

LABEL	THICKNESS	MATERIAL
A Roof	48"	Concrete
B Wall	30"	Concrete
C Basemat	42"	Concrete
D Primary Liner	0.5"	Carbon Steel
E Secondary Liner	0.375"	Carbon Steel
F Grouted Annulus	30"	Reducing Grout

Figure 4.4-4: Typical Type IIIA Tank Modeling Dimensions



[NOT TO SCALE]

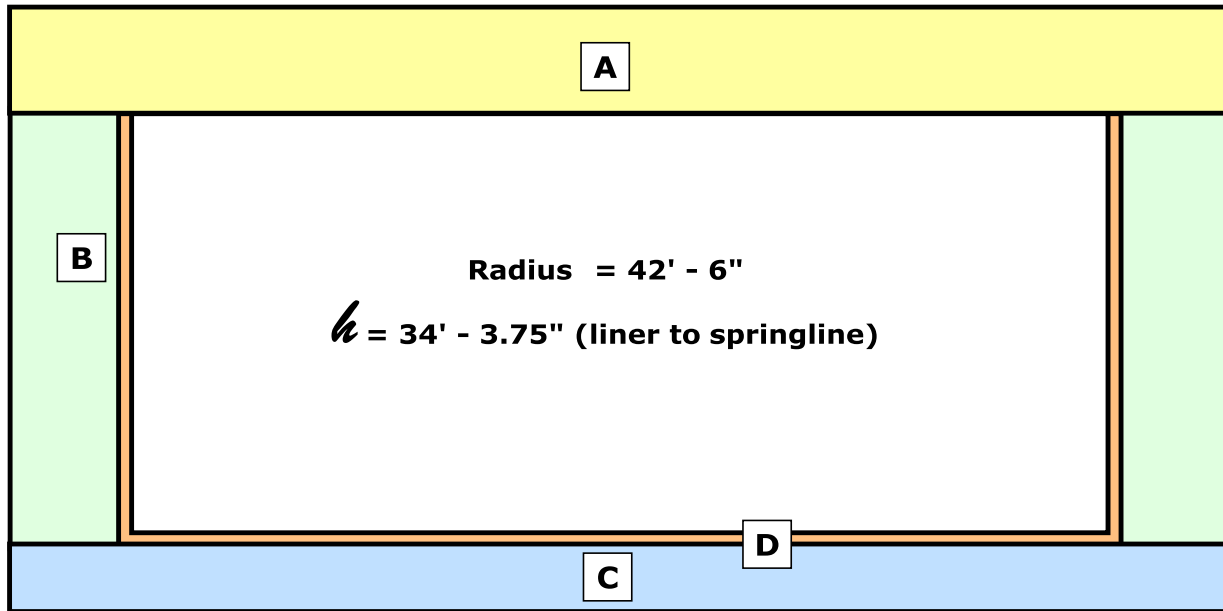
LABEL	THICKNESS	MATERIAL
A Roof	48"	Concrete
B Wall	30"	Concrete
C Basemat	41" (Typical) (43" - Tanks 35 - 37)	Concrete
D Primary Liner	0.5"	Carbon Steel
E Secondary Liner	0.375"	Carbon Steel
F Grouted Annulus	30"	Reducing Grout

4.4.1.4 Type IV Tank Modeling

The Type IV tank dimensions are presented in Figure 4.4-5. Specific areas where Type IV tank modeling decisions of interest are implemented are highlighted below:

- The basemat segment of the waste tank was based on the basemat thickness and the cement topping placed over the basemat. An approximately thickness of 0.1 inch was subtracted to account for the drainage grooves cut into the cement topping. The effective 0.1-inch groove thickness is based on the grooves being 1.625-inch deep and covering less than 6 % of the waste tank footprint. The wall footing of the waste tank and the grouted segment between the wall footing and the basemat were not modeled.
- The primary liner, waste tank cavity was assumed as filled with grout and treated as a discrete area.
- The primary liner assumed thickness was based on the minimum thicknesses only (e.g., extra thickness at knuckle not modeled).
- Penetrations of the waste tank wall and tank liner (e.g., transfer lines) were not modeled.
- The wall thickness of the waste tank is the minimum wall thickness and does not reflect the variable thickness of the wall.
- The thickness of the waste tank roof is the minimum thickness of the dome and does not reflect the variable thickness of the roof.
- The waste-tank roof penetrations (e.g., risers) were not modeled.
- Concrete rebar in the waste tank top, wall, and basemat was not modeled such that concrete is considered a homogenous material.
- The waste-tank underliner sump was not modeled.

Figure 4.4-5: Typical Tank IV Tank Modeling Dimensions



[NOT TO SCALE]

LABEL	THICKNESS	MATERIAL
A Roof	7"	Concrete
B Wall	7"	Concrete
C Basemat	6.9025"	Concrete
D Primary Liner	0.375"	Carbon Steel

4.4.2 Systems and Potential Degradation

There are 29 underground waste tanks and 18 ancillary equipment sources (11 pump tanks, 3 evaporators, and 4 groups of piping) identified and modeled in the operational closure of HTF. Each of these systems will initially be placed in a controlled condition at closure.

The HTF closure system is designed to contain the residual waste. However, the waste tanks themselves, the ancillary equipment, and the closure system will degrade over time, eventually releasing contaminants to the environment.

To simulate potential conditions in the HTF closure system over the modeling period, five waste tank cases have been identified for analyses. Each case starts out with the system closed as planned, with the waste tanks and ancillary equipment filled with grout and the

closure cap in place. In the time frames discussed, year zero is taken to be the year during which the HTF is closed (current estimated closure date is 2032).

Waste tank Cases A through E begin with the engineered closure cap in place as planned. In the analyses of Cases A through E, expected degradation over time of the closure cap materials was simulated using the increasing infiltration rates shown in Table 3.2-14. The waste release process described in Section 4.2.1 and the conceptual model material properties described in Section 4.2.2.2 were employed in each waste-tank case evaluation. The differences between the five waste tank cases are summarized in Table 4.4-1 and are discussed in detail in the following sections.

Table 4.4-1: Waste Tank Case Summary

Case	Assumed Fast Flow Paths	Degradation of Cementitious Materials	Liner Failure Time ^a	CZ/Chemical Transition Driver
A	None	Degradation curve based on Table 4.2-30	Later failure date (based on grouted D of $1.0E-06$ CO ₂) in Table 4.2-32	Full Grout Capacity
B	Channel with no flow impedance through grout	Degradation assumed to be a step change at year 501	Early failure date (based on grouted D of $1.0E-04$ CO ₂) in Table 4.2-32	Full Grout Capacity
C	Channel with no flow impedance through grout	Degradation curve based on Table 4.2-30	Early failure date (based on grouted D of $1.0E-04$ CO ₂) in Table 4.2-32	CZ Reducing Capacity
D	Channel with no flow impedance through grout and basemat	Degradation assumed to be a step change at year 501	Early failure date (based on grouted D of $1.0E-04$ CO ₂) in Table 4.2-32	Full Grout Capacity
E	Channel with no flow impedance through grout and basemat	Degradation curve based on Table 4.2-30	Early failure date (based on grouted D of $1.0E-04$ CO ₂) in Table 4.2-32	CZ Reducing Capacity

Note Case E is a combination of Cases C and D. Case E uses flow path from Case D and remaining transitions from Case C.

D diffusion coefficient

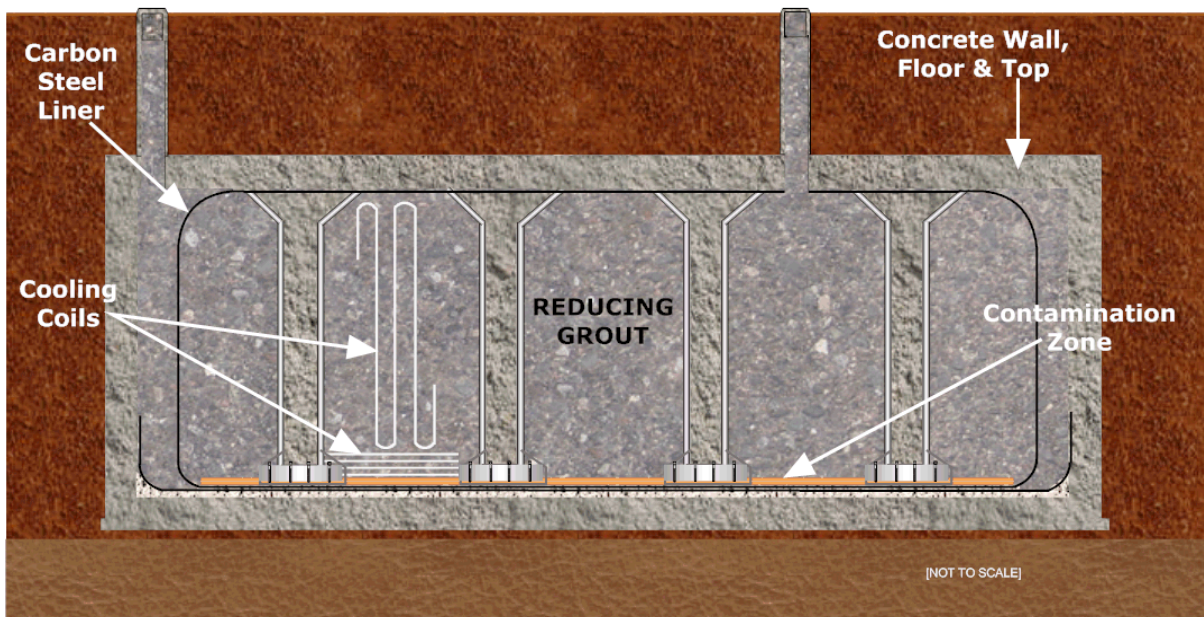
a Grouted D reported in cm²/s and Tanks 12, 14, 15, and 16 were modeled with a failed liner at the time of HTF facility closure for all cases.

4.4.2.1 Waste Tank Case A

Case A is the HTF Base Case for waste tank operational closure. Figure 4.4-6 represents waste tank Base Case. In the Base Case, no fast flow path exists from outside the waste tank system, through the waste tank, and exiting the system. In the Base Case, it was assumed that the cementitious material that makes up the walls, waste tank grout, and basemat concrete degrades over time (with these changes simulated by increasing hydraulic conductivity). Degradation of waste tank cementitious materials (degradation rate and timing) was based on SRNL-STI-2010-00035 and SRR-CWDA-2010-00019, and can vary dependent on waste tank type. The timing of the degradation of the waste tank cementitious materials is detailed in Table 4.2-30 for the various waste tank types.

Under the Base Case, the assumption for the entire primary (carbon steel) liner is impermeable, with the liner in direct contact with intact grout or concrete on all sides. Under these conditions, the liner was expected to remain impermeable until several thousand years after the waste tank operational closure as detailed in SRNL-STI-2010-00047, (except for Type I Tank 12 and Type II Tanks 14, 15, and 16, which have an assumed liner failure at HTF facility closure). After the liner fails, it was assumed, in the Base Case, that contaminants begin to leach from the degraded system based on changes to the pH and redox potential of the residual contamination on the floor of the waste tank system. The reducing capacity of the full volume of grout is available to affect the infiltrating water. Individual radionuclide leach rates will vary over time based on solubility and adsorption controls. In this condition, it was assumed that no fast flow exits through the concrete basemat. Rather, it was assumed that contaminants were transported through the concrete basemat.

Figure 4.4-6: Base Case Modeling Conditions



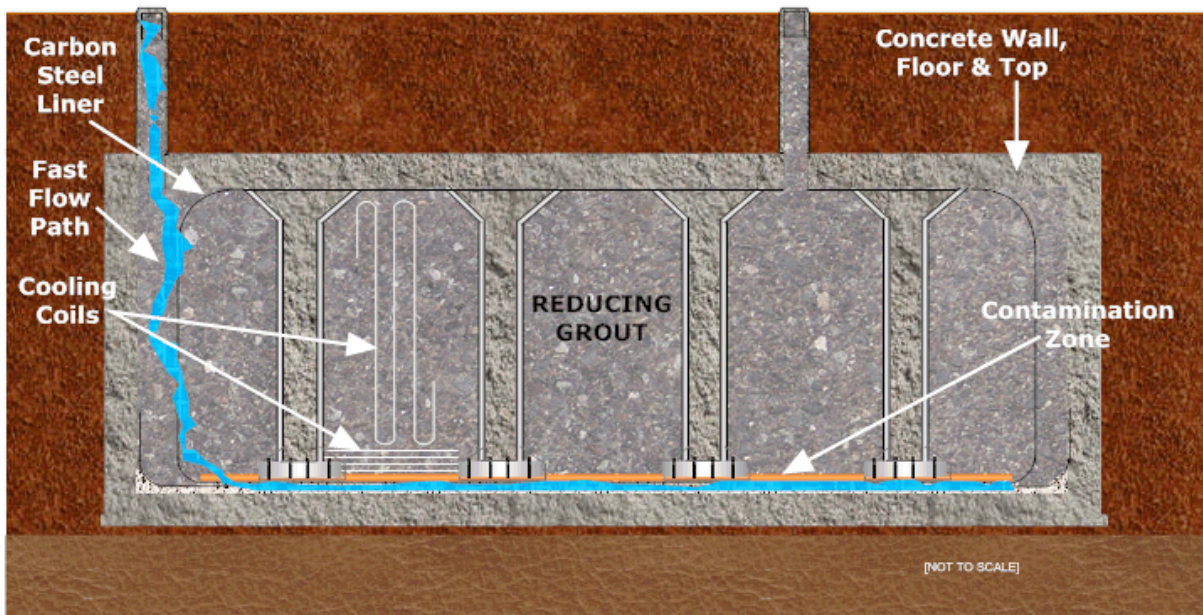
4.4.2.2 Waste Tank Case B

Figure 4.4-7 represents waste tank Case B. In Case B, it was assumed that a fast flow path exists between the waste tank top and CZ, (e.g., from riser through cooling coil). The fast flow path through the grout was represented in the conceptual design by modeling a channel through the grout with full flow. Sorption is not considered in the fast flow path. The presence of the channel in the model is not ascribed to a particular cause, but is used to reflect the fact that various mechanisms have been postulated that could result in a significantly increased hydraulic conductivity (e.g., grout shrinkage, seismic induced fractures). The concrete walls, waste tank grout, and basemat degrade over time (as simulated by increasing hydraulic conductivity). The waste tank cementitious materials were assumed to begin to degrade at year 500, with degradation occurring essentially instantaneously.

It is assumed that concrete/grout pore water with relatively high oxygen concentration and low pH is in contact with the steel liner. In this condition, the diffusion coefficients (which control the failure times) are higher ($1.0\text{E-}04 \text{ cm}^2/\text{s}$) than in the Base Case ($1.0\text{E-}06 \text{ cm}^2/\text{s}$) and thus the steel liner will fail earlier than in the Base Case. Under these conditions, the steel liner was expected to remain impermeable until the analyzed failure times from SRNL-STI-2010-00047 were reached (Type I Tank 12 and Type II Tanks 14, 15, and 16, have an assumed steel liner failure at HTF facility closure).

After liner failure, it was assumed in Case B that contaminants begin to leach from the degraded system based on changes to the pH and redox potential of the residual contamination on the floor of the waste tank system. The reducing capacity of the full volume of grout is available to influence the infiltrating water. Individual radionuclide leach rates will vary over time based on solubility and adsorption controls. In Case B, it was assumed that no fast flow path exists through the concrete basemat. In fact, it was assumed that the concrete basemat had an increase in permeability based on concrete degradation. Whether the grout fast flow path is active during any period of time was dependent on the availability of sufficiently high infiltration through the conceptual closure cap.

Figure 4.4-7: Case B Modeling Conditions



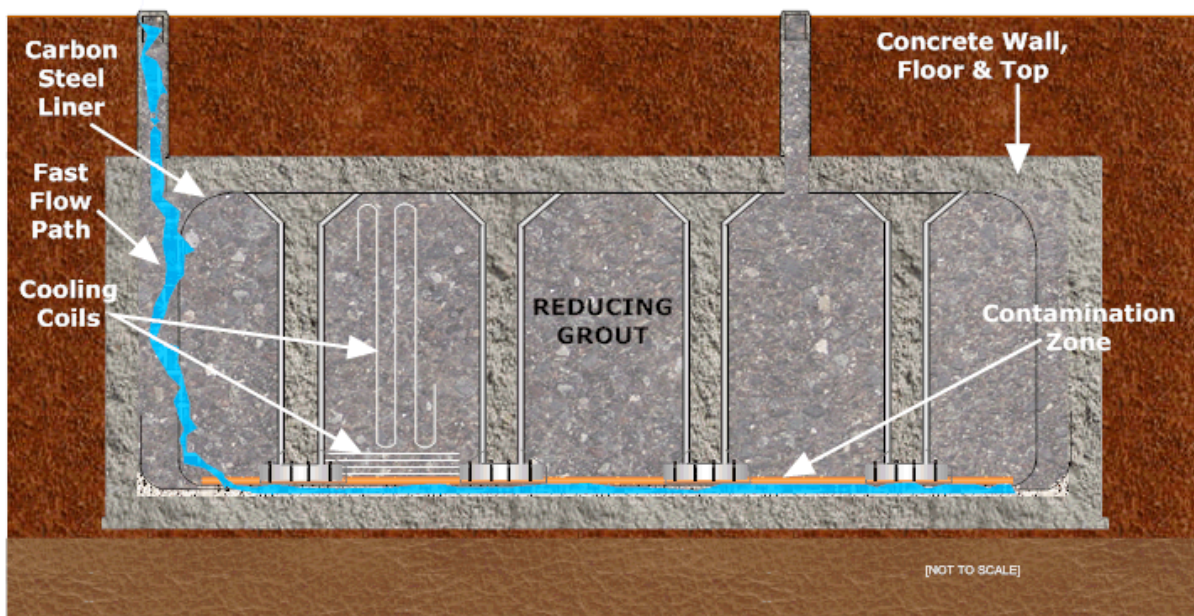
4.4.2.3 Waste Tank Case C

Figure 4.4-8 represents waste tank Case C. In Case C, it was assumed that a fast flow path exists between the waste tank top and CZ (e.g., from riser through cooling coil). The fast flow path through the grout was represented in the conceptual design by modeling a channel through the grout with full flow. Sorption is not considered in the fast flow path. The presence of the channel in the model is not ascribed to a particular cause, but is used to reflect the fact that various mechanisms have been postulated that could result in a significantly increased hydraulic conductivity (e.g., grout shrinkage, seismic induced fractures). The concrete walls, waste tank grout, and basemat degrade over time (as simulated by increasing hydraulic conductivity). Degradation of waste tank cementitious materials (degradation rate and timing) was based on SRNL-STI-2010-00035 and SRR-CWDA-2010-00019, and can vary dependent on waste tank type. The timing of the degradation of the waste tank cementitious materials is detailed in Table 4.2-30 for the various waste tank types.

It is assumed that concrete/grout pore water with relatively high oxygen concentration and low pH is in contact with the steel liner. In this condition, the diffusion coefficients (which control the failure times) are higher ($1.0E-04 \text{ cm}^2/\text{s}$) than in the Base Case ($1.0E-06 \text{ cm}^2/\text{s}$) and thus the liner will fail earlier than the Base Case. Under these conditions, the carbon steel liner was expected to remain impermeable until the analyzed failure times from SRNL-STI-2010-00047 are reached (Type I Tank 12 and Type II Tanks 14, 15, and 16 have an assumed carbon steel liner failure at HTF facility closure).

After the steel liner failure in Case C, it was assumed that contaminants began to leach from the degraded system based on changes to the pH and redox potential of the residual contamination on the floor of the waste tank system. The reducing capacity of the full volume of grout is not available to influence the infiltrating water. The infiltrating water chemistry is driven by the volume of the CZ due to the assumption that the fast flow bypasses the full grout volume and therefore the grout does not impart any chemistry changes to the water. Individual radionuclide leach rates will vary over time based on solubility and adsorption controls. In Case C, it was assumed that no fast flow path exists through the concrete basemat. Rather, the assumption was that the basemat has had an increase in permeability based on concrete degradation. Whether the grout fast flow path is active during any period was dependent on the availability of sufficiently high infiltration through the conceptual closure cap.

Figure 4.4-8: Case C Modeling Conditions



4.4.2.4 Waste Tank Case D

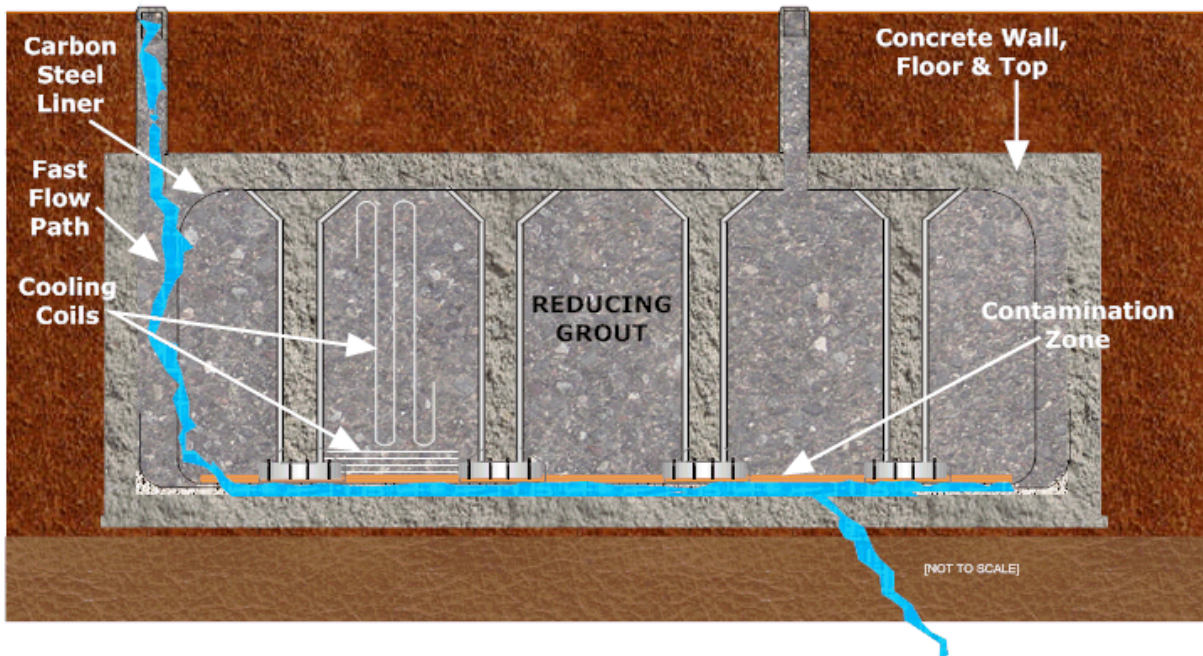
Figure 4.4-9 represents waste tank Case D. In Case D, it was assumed that a fast flow path exists through the entire operationally closed system (e.g., through a riser, through a cooling coil, through the waste tank grout, and through the concrete basemat). The fast flow path through the grout and basemat was represented in the conceptual design by modeling a channel through the grout and basemat with full flow. Sorption is not considered in the fast flow path. The presence of the channel in the model is not ascribed to a particular cause, but is used to reflect the fact that various mechanisms have been postulated that could result in a significantly increased hydraulic conductivity (e.g., grout shrinkage, seismic induced fractures). The concrete walls, waste tank grout, and basemat degrade over time (as simulated by increasing hydraulic conductivity). The waste tank cementitious materials were assumed to begin to degrade at year 500 with degradation occurring essentially instantaneously.

It is assumed that concrete/grout pore water with relatively high oxygen concentration and low pH is in contact with the steel liner. In this condition, the diffusion coefficients (which control the failure times) are higher ($1\text{E-}04 \text{ cm}^2/\text{s}$) than in the Base Case ($1\text{E-}06 \text{ cm}^2/\text{s}$) and thus the liner will fail earlier than the Base Case. In these conditions the steel liner was expected to remain impermeable until the analyzed failure times from SRNL-STI-2010-00047 are reached (Type I Tank 12 and Type II Tanks 14, 15, and 16, have an assumed liner failure at HTF facility closure).

After steel liner failure, it was assumed in Case D that contaminants begin to leach from the degraded system based on changes to the pH and redox potential of the residual contamination on the floor of the waste tank system. The reducing capacity of the full volume of grout is available to influence the infiltrating water. Individual radionuclide leach

rates will vary over time based on solubility and adsorption controls. In Case D, it was assumed that a fast flow path exists through the concrete basemat. Whether the fast flow path is active during any period depended on the availability of sufficiently high infiltration through the closure cap.

Figure 4.4-9: Case D Modeling Conditions



4.4.2.5 Waste Tank Case E

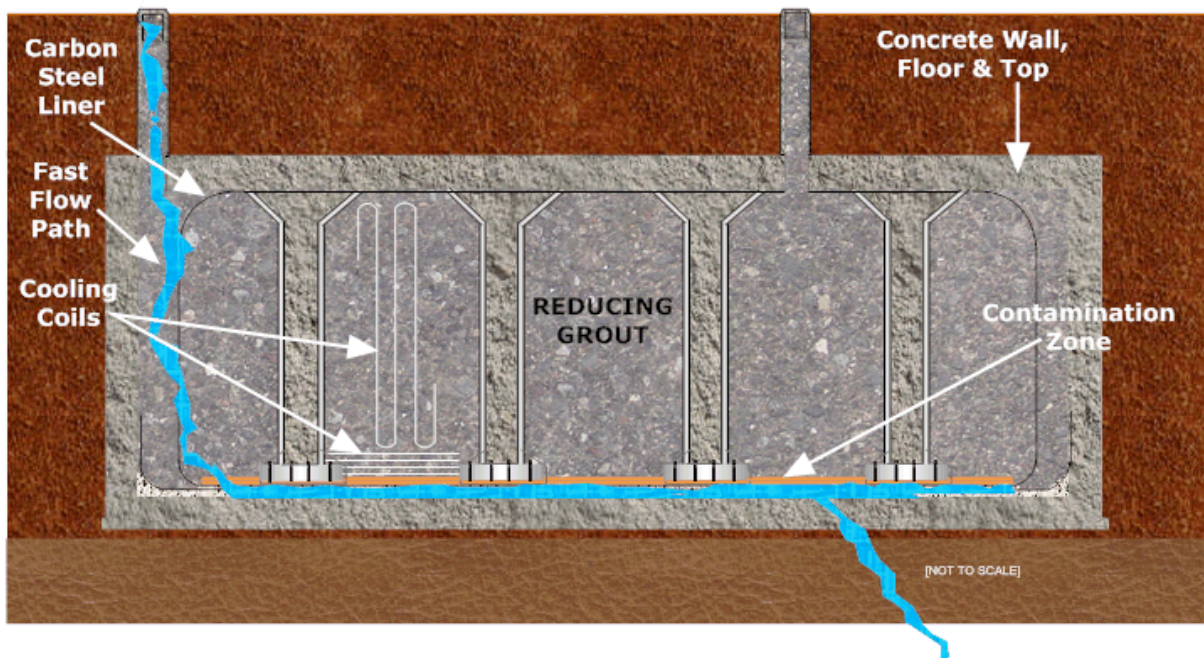
Figure 4.4-10 represents waste tank Case E. In Case E, it was assumed that a fast flow path exists through the entire operationally closed waste tank system (e.g., through riser due to incomplete filling with grout during operational closure, through a cooling coil, through the waste tank grout, and through the concrete basemat). The fast flow path through the grout and concrete basemat was represented in the conceptual design by modeling a channel through the grout and concrete basemat with full flow. Sorption is not considered in the fast flow path. The presence of the channel in the model is not ascribed to a particular cause, but is used to reflect the fact that various mechanisms have been postulated that could result in a significantly increased hydraulic conductivity (e.g., grout shrinkage, seismic induced fractures). The cementitious materials that make up the walls (grout and concrete basemat) degrade over time (as simulated by increasing hydraulic conductivity). The degradation of waste tank cementitious material (degradation rate and timing) was based on SRNL-STI-2010-00035 and SRR-CWDA-2010-00019, and varied depending on waste tank type. The timing of the degradation of waste tank cementitious materials is detailed in Table 4.2-34 for the various waste tank types.

It is assumed that concrete/grout pore water with relatively high oxygen concentration and low pH is in contact with the carbon steel liner. In this condition, the diffusion coefficients (which control failure times) are higher ($1.0\text{E-}04 \text{ cm}^2/\text{s}$) than in the Base Case ($1.0\text{E-}06$

cm^2/s) and thus the liner will fail earlier than in the Base Case. Under these conditions, the carbon steel liner was expected to remain impermeable until the analyzed failure times from SRNL-STI-2010-00047 are reached (Type I Tank 12 and Type II Tanks 14, 15, and 16 have an assumed primary steel liner failure at HTF facility closure).

After liner failure, it was assumed in Case E that contaminants begin to leach from the degraded system based on changes to the pH and redox potential of the residual contamination on the floor of the waste tank system. The reducing capacity of the full volume of the grout is not available to influence the infiltrating water. The infiltrating water chemistry is driven by the volume of the CZ due to the assumption that the fast flow bypasses the full grout volume and therefore the grout does not impart any chemistry changes to the water. Individual radionuclide leach rates will vary over time based on solubility and adsorption controls. In Case E, it was assumed that a fast flow path exists through the concrete basemat. Whether the fast flow path is active during any period is dependent on the availability of sufficiently high infiltration through the conceptual closure cap.

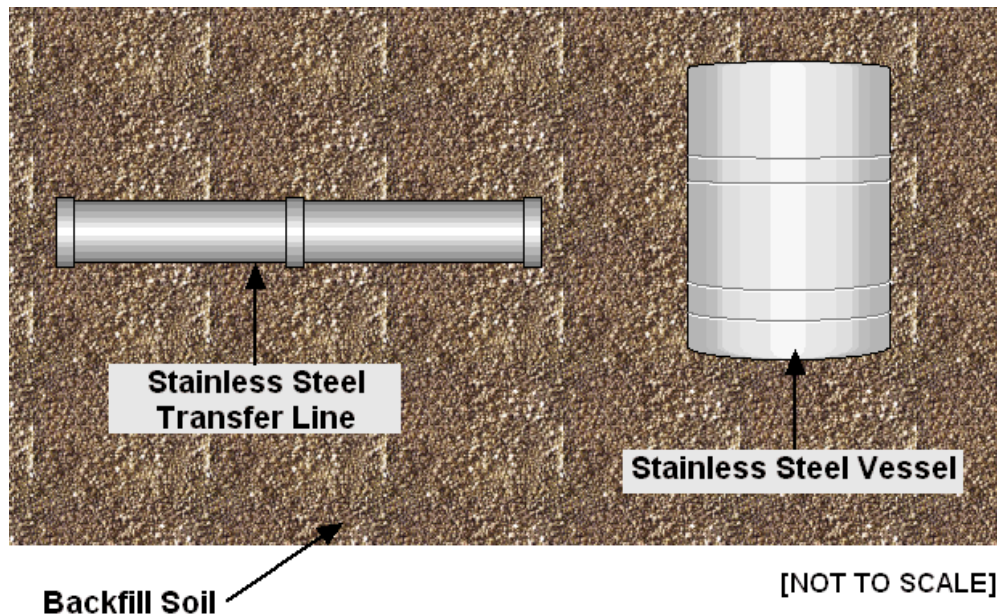
Figure 4.4-10: Case E Modeling Conditions



4.4.2.6 Ancillary Equipment Case

In the Ancillary Equipment Case (Figure 4.4-11) the conceptual closure cap degradation occurs as shown in Table 3.2-13. The ancillary equipment was located below grade in HTF (Section 3.2.2 provides details on HTF ancillary equipment) and was covered by the conceptual closure cap. Modeling consisted of source geometry of 14 separate point sources (HPT-2 through HPT-10, Old and New CTS pump tanks (242-3H and 242-18H), Evaporators 242-H, 242-16H, and 242-25H) and a network of waste transfer lines represented by stabilized contaminants distributed over four zones in the HTF facility.

Figure 4.4-11: Ancillary Equipment Case Modeling Conditions



At the time of operational closure, it is assumed that the ancillary equipment will be intact. Contaminant release for this case was assumed to occur when the stainless steel fails. As discussed in Section 4.2.2.2, predictions for core piping failure of the stainless steel transfer lines were based on results of recent studies specific to the application of the HTF closure PA. [WSRC-STI-2007-00460, SRNL-STI-2010-00047] These estimates considered general and localized corrosion mechanisms of the stainless steel exposed to SRS soil conditions for the stainless steel core transfer lines in HTF. The results of these studies were incorporated by assuming that the applicable ancillary equipment containment (e.g., pump tanks, evaporators, and transfer line core pipe) failed and released the associated inventory into the surrounding soil at year 510 (the earliest time of 25 % pitting penetration for “in soil” 0.116-inch thick stainless steel). This simplification of the modeling was considered reasonable for all ancillary equipment containment because at closure, the ancillary equipment containments will not be directly in soil, (the pump tanks and evaporators are in concrete cells that will be filled with grout, and the transfer lines are typically contained within a secondary jacket). Additionally, only insignificant quantities of the HTF transfer lines are carbon steel rather than stainless steel (six carbon-steel lines equal to 1,313 feet out of the facility total 74,800 feet). This simplification was important for transfer line modeling since the transfer line inventory was not modeled as point sources but spread throughout the entire HTF modeling area. The transfer line inventory is minor relative to the waste tank inventories. Once the stainless steel containment for ancillary equipment fails, the associated source term was assumed available for release directly into the soil surrounding the ancillary equipment. It is assumed that no hold up or containment of the source term is provided by any of the cementitious materials surrounding the vessels, pits, and waste lines (such as the secondary containment structures). After container failure for ancillary equipment, the flow through the CZ was set equal to the conceptual closure cap driven infiltration rate.

4.4.3 Evaluation of Integrated System Behavior

Upon operational closure of the HTF, it is necessary to evaluate the integrated system behavior. The various individual system behaviors that are evaluated have been presented for waste tank Cases A through E (Figures 4.4-6 through 4.4-10) and the Ancillary Equipment Case (Figure 4.4-11). The analysis of the Base Case, HTF PORFLOW Model results reflected the best estimate of closure system behavior. These independent modeling scenarios for the HTF waste tanks and ancillary equipment are melded together in the probabilistic analysis to produce integrated results.

The saturated zone is laid out on a grid so that individual waste tanks and ancillary equipment point sources can be individually resolved. Explicit representation of individual sources enables investigation of potential plume overlap from separate sources. Integrated system behavior, as measured by concentration at exposure points, was simulated by applying contaminant flux transients for various inventory sources and cases to appropriately located grid cells.

Provided below is a short description of the ICM process flow for the conceptual closure cap and vadose zone. The ICM consists of different segments, some represented by independent sub-models. For example, the waste release model developed different solubility limits for different chemical states; the chemical state used in the model was determined in PORFLOW based on the calculated pore volumes. It should be noted that since the sub-models were developed independently and may have different levels of conservatism, some shared input parameters might have different values from sub-model to sub-model. For example, the diffusion coefficient is different between the concrete degradation evaluation and waste tank liner failure evaluation. While the coefficient in the Base Case waste tank liner evaluation (Section 4.2.2.2.6) is a more expected value, the concrete degradation evaluation (Section 4.2.2.2.4) chose a high coefficient to estimate degradation rates conservatively. Emphasis was placed on ensuring that individual sub-models are defensible, and the fact that two model segments may assume different values for the same parameter was not considered significant if the sub-models are valid and defensible.

The model process-flow explanation below describes how each individual model segment is integrated into the entire model and how its behavior is depicted. Timelines for the Base Case and alternate cases (Case B through E) associated with the various model segments for the different waste tank types are provided in Tables 4.4-2 through 4.4-9.

The simplified model flow process for a single waste tank is provided in the following sections.

Table 4.4-2: Type I Tank Process Change Timeline

Change in Model Parameters	Year of Occurrence				
	Base Case	Case B	Case C	Case D	Case E
Concrete (waste tank top, sides, basemat, etc.) starts to degrade hydraulically	1,350	500	1,350	500	1,350
Waste tank wall concrete transitions from Oxidized Region II to Oxidized Region III	2,139	529	2,396	529	2,400
Waste tank basemat concrete transitions from Oxidized Region II to Oxidized Region III	2,210	558	1,707	558	1,660
Waste tank roof concrete transitions from Oxidized Region II to Oxidized Region III	2,237	546	2,073	546	2,057
Closure cap reaches approximate steady state infiltration rate (11.5 in/yr)	2,625	2,625	2,625	2,625	2,625
Concrete fully degraded hydraulically	2,700	529	2,700	529	2,700
Waste tank grout starts to degrade hydraulically	2,700	500	2,700	500	2,700
Waste tank annulus grout transitions from Reducing Region II to Oxidized Region II	7,265	562	6,811	562	6,814
Waste tank annulus grout transitions from Oxidized Region II to Oxidized Region III	7,811	585	7,075	585	7,076
Waste tank steel liner fails hydraulically	11,397	1,142	1,142	1,142	1,142
Waste tank grout transitions from Reducing Region II to Oxidized Region II	11,684	1,560	8,501	1,560	8,501
CZ transitions from Reducing Region II to Oxidized Region II	11,684	1,560	1,180	1,560	1,145
Waste tank grout transitions from Oxidized Region II to Oxidized Region III	11,881	1,713	8,890	1,713	8,890
CZ transitions from Oxidized Region II to Oxidized Region III	11,881	1,713	1,194	1,713	1,146
Waste tank grout fully degraded hydraulically	13,200	529	13,200	529	13,200

Table 4.4-3: Type I Tank (No Liner) Process Change Timeline

Change in Model Parameters	Year of Occurrence				
	Base Case	Case B	Case C	Case D	Case E
Waste tank steel liner fails hydraulically	0	0	0	0	0
Concrete (waste tank top, sides, basemat, etc.) starts to degrade hydraulically	1,350	500	1,350	500	1,350
Waste tank wall concrete transitions from Oxidized Region II to Oxidized Region III	2,140	546	2,392	546	2,399
Waste tank basemat concrete transitions from Oxidized Region II to Oxidized Region III	2,212	538	1,476	533	1,350
Waste tank roof concrete transitions from Oxidized Region II to Oxidized Region III	2,239	541	2,072	541	2,053
Closure cap reaches approximate steady state infiltration rate (11.5 in/yr)	2,625	2,625	2,625	2,625	2,625
Concrete fully degraded hydraulically	2,700	538	2,700	533	2,700
Waste tank grout starts to degrade hydraulically	2,700	500	2,700	500	2,700
Waste tank annulus grout transitions from Reducing Region II to Oxidized Region II	6,612	545	6,794	545	6,803
Waste tank annulus grout transitions from Oxidized Region II to Oxidized Region III	6,909	562	7,066	562	7,071
Waste tank grout transitions from Reducing Region II to Oxidized Region II	7,718	927	8,501	927	8,501
CZ transitions from Reducing Region II to Oxidized Region II	7,718	927	39	927	3
Waste tank grout transitions from Oxidized Region II to Oxidized Region III	8,130	1,082	8,890	1,082	8,890
CZ transitions from Oxidized Region II to Oxidized Region III	8,130	1,082	54	1,082	4
Waste tank grout fully degraded hydraulically	13,200	538	13,200	533	13,200

Table 4.4-4: Type II Tank Process Change Timeline

Change in Model Parameters	Year of Occurrence				
	Base Case	Case B	Case C	Case D	Case E
Concrete (waste tank top, sides, basemat, etc.) starts to degrade hydraulically	2,550	500	2,550	500	2,550
Closure cap reaches approximate steady state infiltration rate (11.5 in/yr)	2,625	2,625	2,625	2,625	2,625
Waste tank basemat concrete transitions from Oxidized Region II to Oxidized Region III	3,785	588	2,670	591	3,092
Waste tank wall concrete transitions from Oxidized Region II to Oxidized Region III ^a	4,573	1,927	7,925	1,927	8,055
Waste tank roof concrete transitions from Oxidized Region II to Oxidized Region III	5,016	2,458	4,750	2,458	4,744
Concrete fully degraded hydraulically	5,100	588	5,100	591	5,100
Waste tank grout starts to degrade hydraulically	5,100	500	5,100	500	5,100
Waste tank annulus grout transitions from Reducing Region II to Oxidized Region II	9,040	1,201	15,107	1,201	15,145
Waste tank annulus grout transitions from Oxidized Region II to Oxidized Region III	10,903	2,382	20,982	2,382	21,013
Waste tank steel liner fails hydraulically	12,687	2,506	2,506	2,506	2,506
Waste tank grout transitions from Reducing Region II to Oxidized Region II	14,846	5,318	10,494	5,317	10,493
CZ transitions from Reducing Region II to Oxidized Region II	14,846	5,318	2,523	5,317	2,512
Waste tank grout fully degraded hydraulically	16,700	500	16,700	500	16,700
Waste tank grout transitions from Oxidized Region II to Oxidized Region III	24,876	14,220	20,054	14,218	20,053
CZ transitions from Oxidized Region II to Oxidized Region III	24,876	14,220	2,564	14,218	2,532

^a Includes basemat concrete under wall

Table 4.4-5: Type II Tank (No Liner) Process Change Timeline

Change in Model Parameters	Year of Occurrence				
	Base Case	Case B	Case C	Case D	Case E
Waste tank steel liner fails hydraulically	0	0	0	0	0
Concrete (waste tank top, sides, basemat, etc.) starts to degrade hydraulically	2,550	500	2,550	500	2,550
Closure cap reaches approximate steady state infiltration rate (11.5 in/yr)	2,625	2,625	2,625	2,625	2,625
Waste tank basemat concrete transitions from Oxidized Region II to Oxidized Region III	3,524	173	173	573	2,110
Waste tank wall concrete transitions from Oxidized Region II to Oxidized Region III ^a	4,562	5,757	7,672	5,765	8,054
Waste tank roof concrete transitions from Oxidized Region II to Oxidized Region III	5,005	2,462	4,737	2,462	4,689
Concrete fully degraded hydraulically	5,100	600	5,100	573	5,100
Waste tank grout starts to degrade hydraulically	5,100	500	5,100	500	5,100
Waste tank annulus grout transitions from Reducing Region II to Oxidized Region II	8,507	2,894	14,867	2,898	15,140
Waste tank grout transitions from Reducing Region II to Oxidized Region II	9,222	3,961	10,491	3,960	10,483
CZ transitions from Reducing Region II to Oxidized Region II	9,222	3,961	341	3,960	340
Waste tank annulus grout transitions from Oxidized Region II to Oxidized Region III	16,509	8,546	20,793	8,461	21,009
Waste tank grout fully degraded hydraulically	16,509	500	16,700	500	16,700
Waste tank grout transitions from Oxidized Region II to Oxidized Region III	19,414	12,872	20,052	12,870	20,045
CZ transitions from Oxidized Region II to Oxidized Region III	19,414	12,872	484	12,870	480

^a Includes basemat concrete under wall

Table 4.4-6: Type III Tank Process Change Timeline

Change in Model Parameters	Year of Occurrence				
	Base Case	Case B	Case C	Case D	Case E
Concrete (waste tank top, sides, basemat, etc.) starts to degrade hydraulically	2,550	500	2,550	500	2,550
Closure cap reaches approximate steady state infiltration rate (11.5 in/yr)	2,625	2,625	2,625	2,625	2,625
Waste tank wall concrete transitions from Oxidized Region II to Oxidized Region III ^a	4,776	6,238	23,156	6,238	23,486
Waste tank roof concrete transitions from Oxidized Region II to Oxidized Region III	5,066	2,558	4,833	2,558	4,817
Concrete fully degraded hydraulically	5,100	600	5,100	600	5,100
Waste tank grout starts to degrade hydraulically	5,100	500	5,100	500	5,100
Waste tank steel liner fails hydraulically	12,751	2,077	2,077	2,077	2,077
Waste tank basemat concrete transitions from Oxidized Region II to Oxidized Region III	13,936	3,394	3,655	3,436	4,955
Waste tank annulus grout transitions from Reducing Region II to Oxidized Region II	15,116	1,324	19,838	1,324	20,022
Waste tank grout transitions from Reducing Region II to Oxidized Region II	16,463	6,123	11,026	6,123	11,022
CZ transitions from Reducing Region II to Oxidized Region II	16,463	6,123	2,090	6,123	2,083
Waste tank grout fully degraded hydraulically	19,200	500	19,200	500	19,200
Waste tank annulus grout transitions from Oxidized Region II to Oxidized Region III	24,125	9,020	33,138	9,020	33,322
Waste tank grout transitions from Oxidized Region II to Oxidized Region III	27,831	18,324	23,518	18,324	23,511
CZ transitions from Oxidized Region II to Oxidized Region III	27,831	18,324	2,132	18,324	2,104

^a Includes basemat concrete under wall

Table 4.4-7: Type IIIA Tank Process Change Timeline

Change in Model Parameters	Year of Occurrence				
	Base Case	Case B	Case C	Case D	Case E
Concrete (waste tank top, sides, basemat, etc.) starts to degrade hydraulically	2,500	500	2,500	500	2,500
Closure cap reaches approximate steady state infiltration rate (11.5 in/yr)	2,625	2,625	2,625	2,625	2,625
Waste tank wall concrete transitions from Oxidized Region II to Oxidized Region III ^a	4,753	6,226	20,498	6,226	21,567
Concrete fully degraded hydraulically	5,000	600	5,000	600	5,000
Waste tank grout starts to degrade hydraulically	5,000	500	5,000	500	5,000
Waste tank roof concrete transitions from Oxidized Region II to Oxidized Region III	5,165	2,734	4,978	2,734	4,960
Waste tank steel liner fails hydraulically	12,751	2,077	2,077	2,077	2,077
Waste tank basemat concrete transitions from Oxidized Region II to Oxidized Region III	13,914	3,368	3,629	3,410	4,960
Waste tank annulus grout transitions from Reducing Region II to Oxidized Region II	14,756	1,328	18,908	1,328	18,993
Waste tank grout transitions from Reducing Region II to Oxidized Region II	16,284	6,064	10,941	6,064	10,938
CZ transitions from Reducing Region II to Oxidized Region II	16,284	6,064	2,090	6,064	2,083
Waste tank grout fully degraded hydraulically	19,100	500	18,908	500	18,993
Waste tank annulus grout transitions from Oxidized Region II to Oxidized Region III	21,305	8,770	31,614	8,770	31,685
Waste tank grout transitions from Oxidized Region II to Oxidized Region III	27,625	18,089	23,234	18,089	23,195
CZ transitions from Oxidized Region II to Oxidized Region III	27,625	18,089	2,132	18,089	2,104

^a Includes basemat concrete under wall

Table 4.4-8: Type IIIA Tank West Process Change Timeline

Change in Model Parameters	Year of Occurrence				
	Base Case	Case B	Case C	Case D	Case E
Concrete (waste tank top, sides, basemat, etc.) starts to degrade hydraulically	2,500	500	2,500	500	2,500
Closure cap reaches approximate steady state infiltration rate (11.5 in/yr)	2,625	2,625	2,625	2,625	2,625
Waste tank wall concrete transitions from Oxidized Region II to Oxidized Region III ^a	4,747	6,225	21,804	6,225	21,076
Concrete fully degraded hydraulically	5,000	600	5,000	600	5,000
Waste tank grout starts to degrade hydraulically	5,011	500	5,000	500	5,000
Waste tank roof concrete transitions from Oxidized Region II to Oxidized Region III	5,011	2,558	4,810	2,558	4,793
Waste tank steel liner fails hydraulically	12,751	2,077	2,077	2,077	2,077
Waste tank basemat concrete transitions from Oxidized Region II to Oxidized Region III	13,958	3,421	3,711	3,465	5,097
Waste tank annulus grout transitions from Reducing Region II to Oxidized Region II	14,722	1,324	19,115	1,324	19,432
Waste tank grout transitions from Reducing Region II to Oxidized Region II	16,190	6,024	10,900	6,024	10,897
CZ transitions from Reducing Region II to Oxidized Region II	16,190	6,024	2,091	6,024	2,083
Waste tank grout fully degraded hydraulically	19,100	500	19,100	500	19,100
Waste tank annulus grout transitions from Oxidized Region II to Oxidized Region III	20,411	8,764	31,926	8,770	32,243
Waste tank grout transitions from Oxidized Region II to Oxidized Region III	27,343	17,928	22,987	17,927	23,014
CZ transitions from Oxidized Region II to Oxidized Region III	27,343	17,928	2,134	17,927	2,104

^a Includes basemat concrete under wall

Table 4.4-9: Type IV Tank Process Change Timeline

Change in Model Parameters	Year of Occurrence				
	Base Case	Case B	Case C	Case D	Case E
Concrete (waste tank top, sides, basemat, etc.) starts to degrade hydraulically	400	500	400	500	400
Waste tank roof concrete transitions from Oxidized Region II to Oxidized Region III	686	1,018	689	1,018	689
Concrete fully degraded hydraulically	800	600	800	600	800
Waste tank grout starts to degrade hydraulically	800	500	800	500	800
Waste tank wall concrete transitions from Oxidized Region II to Oxidized Region III	1,400	2,708	3,105	2,708	3,105
Closure cap reaches approximate steady state infiltration rate (11.5 in/yr)	2,625	2,625	2,625	2,625	2,625
Waste tank steel liner fails hydraulically	3,638	75	75	75	75
Waste tank basemat concrete transitions from Oxidized Region II to Oxidized Region III	3,927	993	1,338	999	1,338
Waste tank grout transitions from Reducing Region II to Oxidized Region II	7,961	5,867	7,418	5,867	7,418
CZ transitions from Reducing Region II to Oxidized Region II	7,961	5,867	391	5,867	391
Waste tank grout transitions from Oxidized Region II to Oxidized Region III	21,824	20,468	22,135	20,468	22,118
CZ transitions from Oxidized Region II to Oxidized Region III	21,824	20,468	531	20,468	531
Waste tank grout fully degraded hydraulically	64,400	500	64,400	500	64,400

4.4.3.1 Closure Cap

A flow rate leaving the closure cap over time was determined in the closure cap sub-model. The infiltration rate into the closure cap top was based on the rainfall rates and closure-cap material properties (which are discussed in detail in Section 4.2.2.2.1). The flow rate out of the closure cap was calculated using the HELP code, with the closure cap modeled as degrading over time. The flow rate through the closure cap reached a steady state value at approximately year 2,600. Table 3.2-14 provides the time-variant infiltration rates based on the closure cap analysis presented in Section 3.2.4.

4.4.3.2 Waste Tank Top

The flow leaving the closure cap will travel to the waste tank, with the flow rate being affected by the concrete waste tank top. Based on the relative hydraulic properties of the two materials (soil vs. concrete), some flow will be directed around the waste tank into the surrounding soil, while some flow will travel downward through the concrete. The concrete material properties (which are discussed in detail in Section 4.2.2.2.4) were modeled as changing over time. The only waste tank top material properties of concern was the hydraulic properties, since the waste tank top impacts flow but will not retard contaminant transport (since no inventory was modeled at the top). The waste tank top hydraulic properties were defined initially and in a fully degraded state, and cementitious materials degradation analysis was performed to determine the time it would take to reach the fully degraded state (Table 4.2-30). Once the initial and end state times were set, the model assumed linear degradation of the hydraulic properties over time.

4.4.3.3 Waste Tank Liner Top

After passing through the concrete waste tank top, flow leaving the cap will travel into the grout (for Type IV tanks and after liner failure for Type I, II, III, and IIIA tanks) or reach the top of the steel liner (for Type I, II, III, and IIIA tanks before liner failure) and be deflected away from the waste tank. The liner failure time was determined by an independent sub-model analysis (described in Section 4.2.2.2.6) for each waste tank type except for the Type IV tanks (Type IV tanks do not have a top liner). Tank 12 (Type I) and Tanks 14, 15, and 16 (Type II) have liner failure at the time of operational closure. Prior to failure, the liner was modeled as being effectively impermeable to both advection and diffusion. After failure, the liner was not a hindrance to flow and transport.

4.4.3.4 Waste Tank Grout

Water will enter the top of the waste tank grout and travels downward to the CZ at the bottom of the waste tank. The waste tank, grout material properties (e.g., hydraulic conductivity, K_{dS} , which are discussed in detail in Section 4.2.2.2.4) were modeled as changing over time. Some scenarios used in the SA (Section 4.4.2) fast flow paths through the grout were modeled resulting in a higher flow rate around the grout. The hydraulic properties were defined initially and in fully degraded state, and a cementitious materials degradation analysis was performed to determine the time it would take to reach the fully degraded state (Table 4.2-30). Once the initial and end state times were set, the model assumed linear degradation of the grout hydraulic properties over time.

Table 4.2-29, provides K_d values for cementitious materials as a function of chemical reduction ability and aging, with the grout “age” dependent on the pH of the concrete pore water, which in turn, is dependent upon the amount of water (number of pore volumes) that has passed through the concrete over time. A description of chemistry modeling for the pore water is provided in the Section 4.4.3.5.

The properties of the waste-tank grout material of principal concern are the hydraulic properties, but the K_{ds} , which control the waste tank grout, radionuclide storage capacity, may also play a role in the release of radionuclides over time. Radionuclides may diffuse from the CZ upwards into the waste tank grout and be released over time after liner failure. In addition, because the Type IV tanks do not have a liner at the top, a circulation pattern with upward flow at the outer edge of the waste tank may occur in the waste tank grout and CZ prior to liner failure. The storage of radionuclides in the waste tank grout can delay the release of radionuclides after liner failure due to sorption. In addition, changes in K_{ds} associated with chemistry changes can be reflected in radionuclide release rates from the grout. The grout hydraulic properties influence the water flow rate through the waste tank. The earlier the grout degrades, the earlier the flow rate through the waste tank reaches a steady state maximum flow.

4.4.3.5 Contamination Zone

In the model, the assumption for the waste tank residual inventory was that it is contained within a thin layer (i.e., the CZ) at the bottom of the waste tank. The release rate of contaminants from the CZ is solubility controlled, and is tied to the chemical properties (e.g., oxidation potential, pH) of the waste-tank pore water. The release rate from the CZ is independent of the grout or CZ K_{ds} . The assumed solubility limit varies depending on waste tank pore water chemistry and the controlling phase of the radionuclide being released. Different solubility limits for different waste tank chemistries were derived for the radionuclides in the CZ (as discussed in Section 4.2.1). Additional emphasis was placed on those radionuclides shown during initial modeling to have the most impact on peak dose (plutonium, neptunium, uranium, technetium), including an uncertainty study and development of stochastic distributions for alternative controlling phases (Section 4.2.1.3).

As pore volumes pass through the waste tank, the pH and reducing capability of the grout will be affected. The number of pore water volumes passing through the waste tank and the corresponding transitions to different waste tank chemistry conditions was included in the HTF modeling. As part of the waste release modeling (discussed in detail in Section 4.2.1), the estimated transition times between various chemical phases was calculated for the waste tank pore water. The waste-tank pore water chemistry was calculated to change from Reducing Region II conditions (middle age reducing) to Oxidizing Region II conditions (middle age oxidizing) after 523 pore-volumes had passed through the grout. The change from Oxidizing Region II conditions (middle age oxidizing) to Oxidizing Region III conditions (old age oxidizing) was calculated to occur after 2,119 pore volumes. For submerged waste tanks, pore water chemistry was calculated to change from Reducing Region II conditions (middle age reducing) to Oxidizing Region II conditions (middle age oxidizing) after 1,787 pore-volumes passed through the grout. The change from Oxidizing

Region II conditions (middle age oxidizing) to Oxidizing Region III conditions (old age oxidizing) was calculated to occur after 2,442 pore volumes.

4.4.3.6 Waste Tank Liner Sides and Floor

After leaving the CZ and entering the waste tank pore water, the contaminants will not leave the waste tank until the steel liner fails (with the exception of liners of Tank 12 (Type I) and Tanks 14, 15, and 16 (Type II), which are assumed to fail at the time of HTF facility closure). Note that a minimal release can occur prior to liner failure because the HTF PORFLOW Model uses non-zero (but extremely small) pre-liner-failure hydraulic conductivities and diffusion coefficients for the liners. For the Type IV tanks (which do not have a top liner) waste leaving the CZ can migrate into the waste tank grout and transport upward. The liner failure time was determined by analyses for each waste tank type, with both the primary and secondary liner (where applicable) failing at the same time. While it utilizes many of the same assumptions, the analyses of the waste tank liner calculate failure times independent of the flow and transport models. As discussed in Section 4.4.3.3, when the liner fails, it is assumed to fail completely with the modeled, failed liner having no further impact to flow and transport.

4.4.3.7 Basemat

After contaminants exit the waste tank liner, they are expected to enter the concrete waste tank basemat located directly below the liner. The waste tank, grout material properties (which are discussed in detail in Section 4.2.2.2.4) were modeled as changing over time. The material properties of the concrete affect both the flow rate through the basemat and the K_d value. The hydraulic properties were defined 1) initially with intact conditions and 2) in a fully degraded state. A cementitious materials degradation analysis was performed to determine the time it would take to reach the fully degraded state (Table 4.2-30). Once the initial and end state times were set, the model assumed linear degradation of the basemat hydraulic properties over time. In some sensitivity scenarios, fast flow paths through the basemat were modeled resulting in a higher flow rate through the basemat concrete.

Contaminant transport is retarded by basemat concrete with some radionuclides slowing greatly depending on their K_d s. Table 4.2-29, provides K_d values for cementitious materials as a function of aging, with the grout "age" dependent on the pH of the concrete pore water, which in turn is dependent upon the amount of water (number of pore water volumes) that has passed through the concrete over time. A description of pore-water chemistry modeling is provided in the Section 4.4.3.5. As the waste tank chemistry changes, the concrete transitions from Oxidizing Region II conditions (middle age oxidizing) to Oxidizing Region III conditions (old age oxidizing), and the associated material properties were modeled as changing (Region I is not considered because the waste tanks would have already reached Region II by the time of HTF facility closure).

4.4.3.8 Vadose Zone beneath the Waste Tank

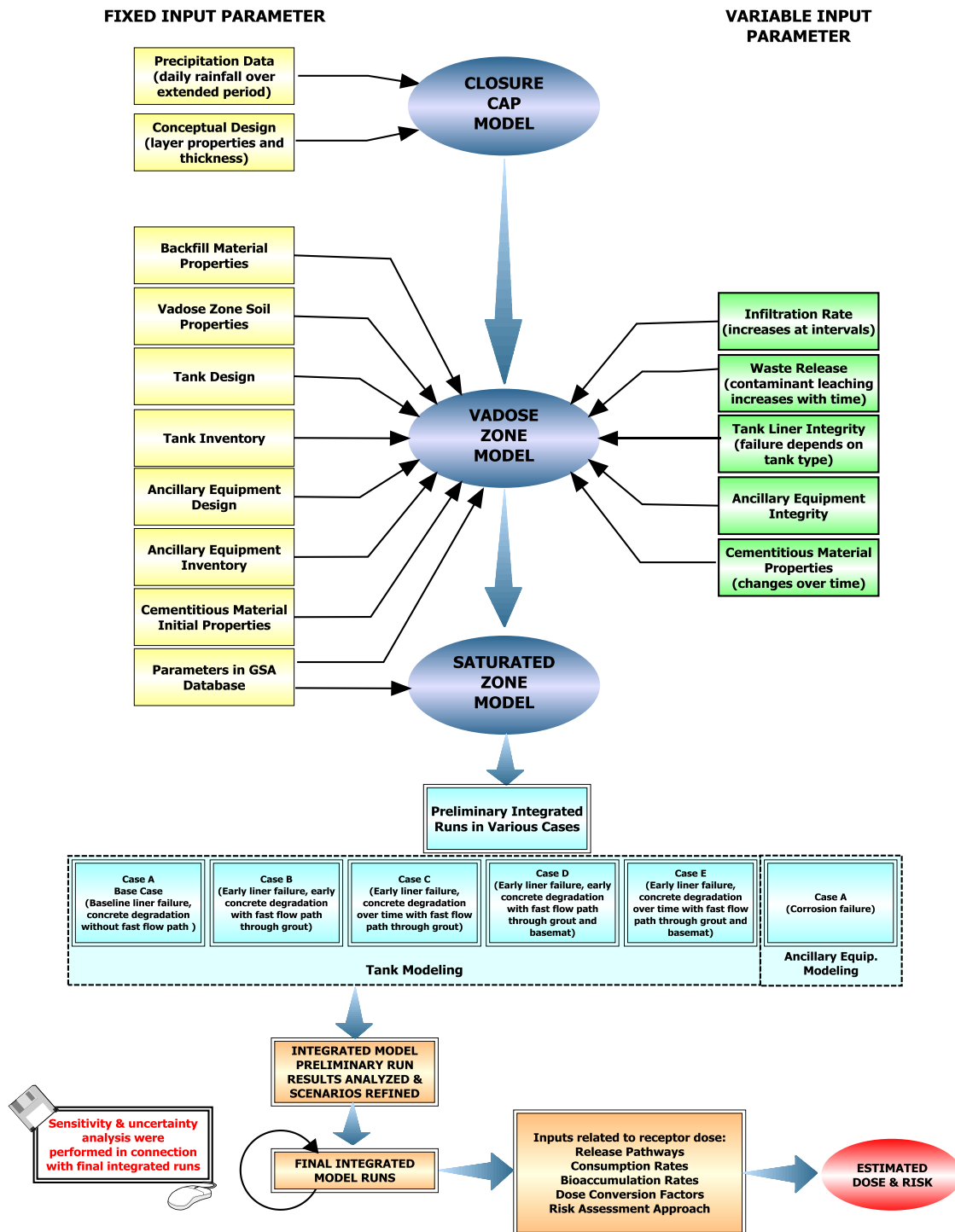
After contaminants exit the basemat, they will enter the vadose zone (e.g., soil) beneath the waste tank (with the exception of the submerged waste tanks where contaminants would pass directly into the saturated zone, which is discussed in detail in Section 4.2.2.2.2). The vadose zone material properties affect both the flow rate through the soil and the associated K_d values, with both being important to the model. The vadose zone K_d s can vary over time as a function of the redox state of the water coming from the grout. When the CZ water chemistry (based upon the grout water chemistry) is considered a function of Reducing Region II or Oxidizing Region II conditions (see Section 4.4.3.5), the vadose zone uses the leachate influenced values presented in Table 4.2-25. After the grout water chemistry was considered a function of Oxidizing Region III conditions, the non-impacted K_d values were used. Note that the leachate affected K_d s were not used in Cases C and E, where a fast flow path that bypasses the grout at its outer edge of the grout was assumed to supply much of the water entering the vadose zone. The vadose zone thickness below each waste tank can vary depending on the waste tank involved, as shown in Table 4.2-27. In the probabilistic model, the vadose zone thickness does not vary, only the saturated thickness is sampled. The working slabs under waste tank basemats were not explicitly modeled but were modeled as soil. Given the minimal thickness of the working slabs relative to the waste tank basemats, as well as the possibility of cracks in the working slabs, it was appropriate to disregard the working slabs in modeling contaminant transport through the waste tank bottom and basemat into the vadose zone.

4.4.4 Modeling Process

Figure 4.4-12 illustrates the general process to be followed in implementing the ICM. This figure shows the three component models and their key inputs.

Some inputs involve fixed parameters that do not change over time. These are generally shown on the left side of the figure. The inputs on the right side of the figure do change over time.

Figure 4.4-12: Model Process Flow



As shown in Figure 4.4-12, and as explained previously, five waste tank cases were identified for the preliminary model runs, which were accomplished using the applicable computer codes. These cases were analyzed by running the model using different combinations as discussed above.

The results of the preliminary model runs were analyzed. Based on analysis results the model was refined as indicated. Such refinements could involve eliminating one or more waste tank cases used in the preliminary analyses or the revision of a waste tank case.

After refinements were made, the final model runs were performed. The UA/SAs were performed in connection with the final model runs, with results being assessed with the last of the final model runs.

The result of this process provided the predicted contaminant concentrations in groundwater and surface water. The data for radiological contaminants was then used in combination with the inputs related to receptor dose shown on Figure 4.4-12.

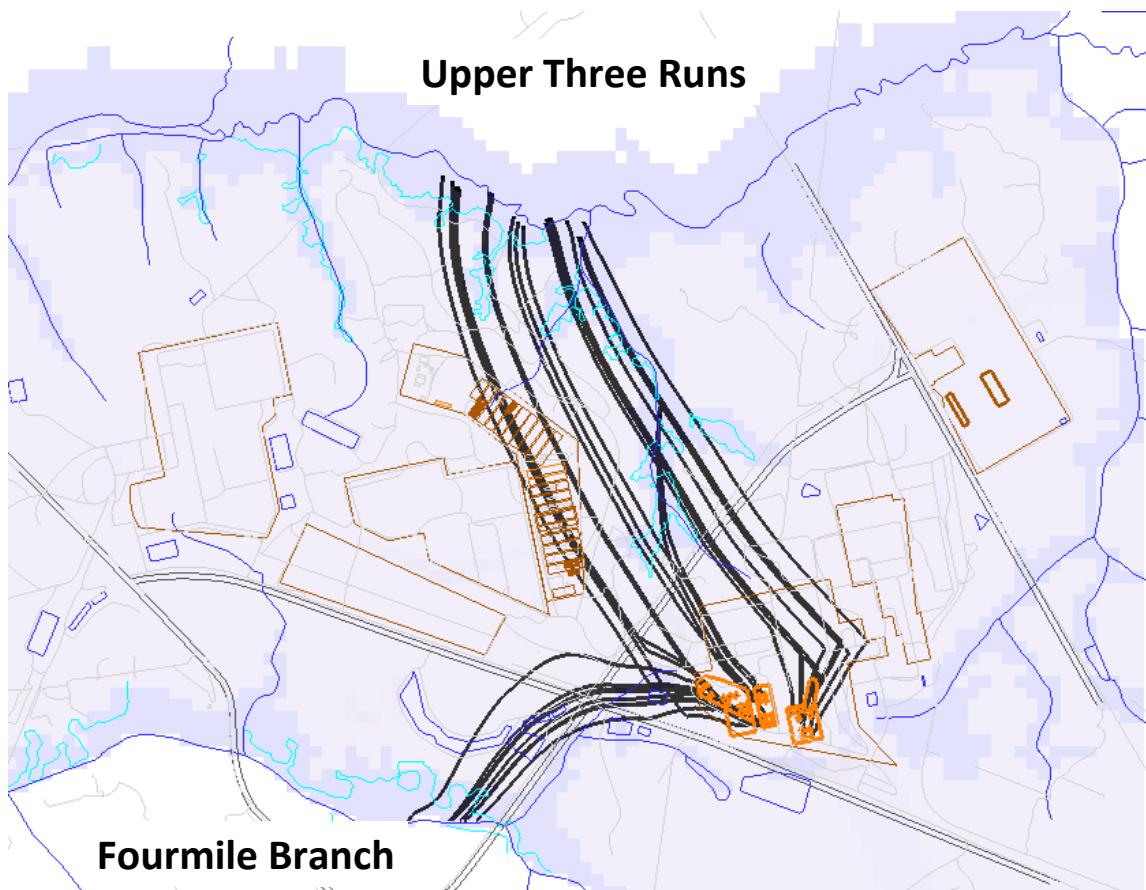
4.4.4.1 *PORFLOW Modeling Process*

A description of the HTF PORFLOW Model is contained in SRNL-STI-2012-00465.

4.4.4.1.1 Regional GSA and Local HTF Modeling in PORFLOW

The PORFLOW computer code was used to model HTF flow and transport for all cases. Regional GSA modeling in PORFLOW was developed using a 200-foot x 200-foot grid with primary focus on seepage concentration (Figure 4.4-13). Most of the groundwater flow paths discharge to the UTR seepage, which more deeply incises the terrain in comparison to Fourmile Branch. The abrupt counter-clockwise turn in some path lines coincides with passage through the Gordon Confining Unit from the UTRA to the Gordon Aquifer. The two aquifers exhibit different flow directions in this area.

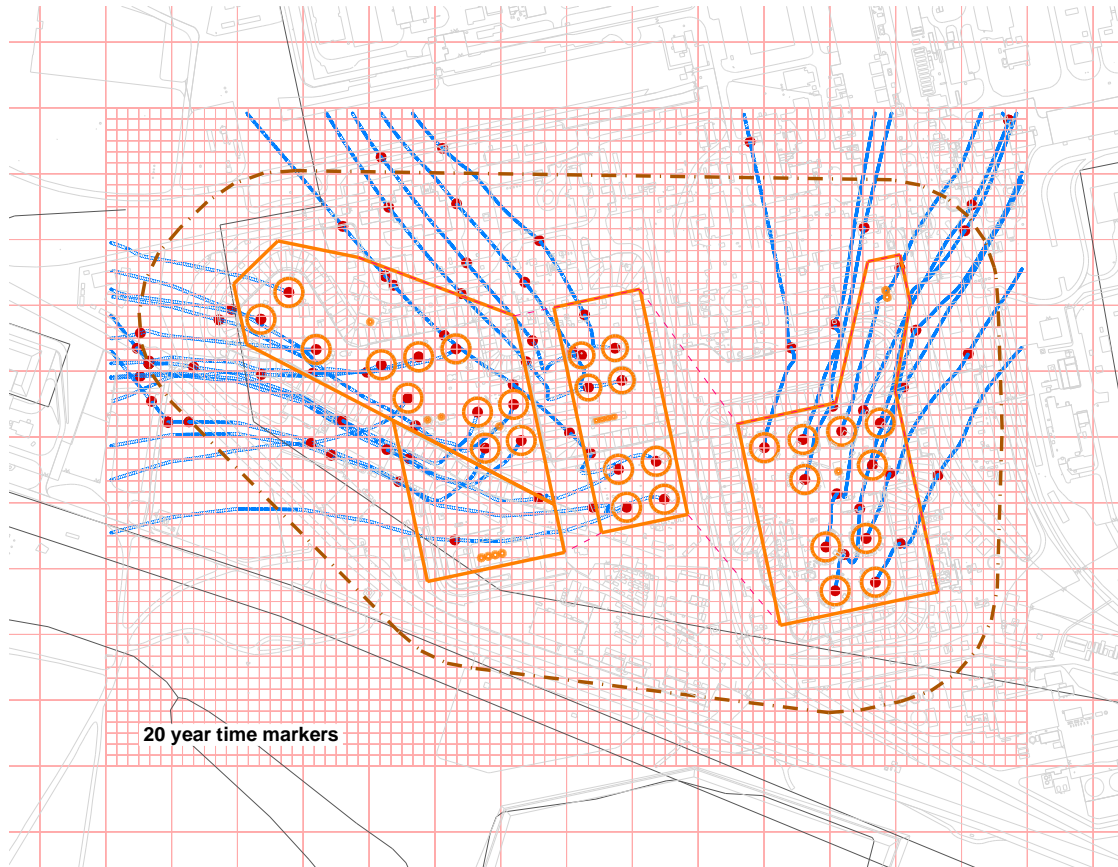
Figure 4.4-13: PORFLOW GSA Modeling



The HTF modeling was developed from the GSA scale model using a 33 foot x 33-foot grid refinement, with the primary focus being on the 1-meter and 100-meter concentrations (Figure 4.4-14). [SRNL-STI-2012-00465] To avoid excessive numerical dispersion at the 100-meter scale, a grid resolution finer than 200 feet x 200 feet was required. The HTF velocity field was generated directly from the coarser scale GSA velocity model using a mass-conserving linear interpolation scheme, rather than a separate flow model requiring its own boundary conditions and properties. This approach ensured strict consistency between the two-aquifer flow fields, apart from resolution. The HTF velocity field includes the entire vertical extent of the GSA model within the horizontal confines of the HTF domain. The stream traces from the HTF waste tanks are shown in Figure 4.4-14 as blue lines emanating from the waste tank centerlines (red dots). Twenty-year time markers (red dots located along the stream traces) indicate travel time in the saturated zone between waste tanks and the 100-meter perimeter (dash-dot line). In aquifer transport modeling, hydrodynamic dispersion is represented by a stratified dispersion model (WSRC-TR-99-00282) defined by longitudinal horizontal, longitudinal vertical, transverse horizontal and transverse vertical dispersivities of 3.16 meter, 0.316 meter, 0.316 meter, and 0.0316 meter, respectively, which are 3.28 %, 0.328 %, 0.328 %, and 0.0328 % of a nominal 100-meter plume travel distance. Plume spreading in PORFLOW model simulations is influenced by A) physical

dispersion (specified by two or more longitudinal and transverse dispersivities), B) numerical dispersion (dependent on the solution algorithm, and spatial and temporal step sizes), and C) heterogeneity in the permeability field. A longitudinal dispersivity of 3.2 meters is specified in modeling based on SRNL-STI-2012-00465. Lower dispersivities most often produce higher groundwater concentrations. [SRNL-STI-2012-00465] In addition, the GSA scale model has been shown to preserve mass to adequate tolerances. [WSRC-TR-2004-00106, Q-SQP-G-00003]

Figure 4.4-14: HTF PORFLOW Model Stream Traces and 100-Meter Boundary



4.4.4.1.2 General Vadose Zone Waste Tank Modeling in PORFLOW

The waste tanks, surrounding vadose zone soils, and any saturated soils at or above the waste tank bottom were modeled in PORFLOW using an axisymmetric, 2-D, radial slice (unit radian pie wedge). For waste tanks above the water table, the bottom boundary of the modeling domain coincides with the water table, and the contaminant flux leaving the model domain is the aquifer transport source-term. For submerged or partially submerged waste tanks, the modeling domain extends below the water table, and the contaminant flux leaving the waste tank boundary becomes the aquifer source term. In the flow model, infiltration from the HELP cover system model was prescribed along the top boundary, a fixed pressure head consistent with the water table elevation was imposed along the bottom boundary, and no flow was allowed to cross the waste tank centerline or the outer radius of the model domain. In transport simulations, zero concentration was prescribed at the top boundary, zero diffusive flux along the bottom boundary, and no flux along the sides.

Because no flow/flux boundary conditions were applied to the sides of the model domain, lateral flow and transport in the saturated zone was not explicitly addressed in near-field PORFLOW simulations for submerged and partially submerged waste tanks. A modeling experiment conducted during the conceptual model development phase indicated that lateral flow has a negligible impact on advective contaminant release from the CZ (because of its minimal thickness) provided the lateral flow does not exceed roughly 100 times the downward flow. [SRNL-STI-2012-00465] Portage (PORTAGE-08-022) developed a fully 3-D, combined vadose zone and aquifer model of the H-Tank Farm based on a regional scale model of the GSA. The Portage model provides important insights into the aquifer flow field surrounding submerged waste tanks in H Area. This prior modeling indicates generally smaller lateral to downward flow ratios in HTF (around ten times). Aquifer crossflow in near-field modeling could thus be neglected. Another consideration for submerged and partially submerged waste tanks is the effect of lateral flow in the aquifer on the chemical state of components, such as the waste tank grout, specifically oxidation potential, and the pH transition times, which are a function of pore volume counts. For an approximate account of aquifer crossflow, pore volume counts from the near-field flow model were inflated using a “crossflow factor” for computing chemical transitions, as discussed later in this section.

Up to 25 distinct material zones were used in PORFLOW to represent different materials and to reflect different flow scenarios (e.g., fast flow paths) for a given waste tank type. Approximately 5,000 to 7,000 grid blocks were used to represent each of the four different waste tank types (grids vary with waste tank type). A graphic depiction of the PORFLOW modeling grids for the various waste tank types, including a lower corner detail, is provided in Figures 4.4-15 through 4.4-22 (the Type IIIA tanks are similar to the Type III tanks, so no separate graphic is shown). It should be noted that the color variations within Figures 4.4-15 through 4.4-22 denote the various distinct modeled material zones. Figure 4.4-23 shows a portion of the fast flow path (when activated) for a Type IV tank. Waste tank depth to the vadose zone was modeled as uniform for a particular waste tank type (i.e., one depth for all Type I tanks) using an average of the

values in Table 4.2-27 for the associated waste tank type. The chosen grid resolution was a compromise between two competing objectives, 1) resolution of thin geometric features (e.g., CZ, waste tank liners) and sharp flow field transitions (e.g., pooled water flowing over roof edge), and 2) achieving reasonable computer storage and runtimes. Each grid extends 30 feet beyond the outside radius of a waste tank to represent average conditions. At certain angles, obstructions such as adjacent waste tanks are present at shorter distances. A sensitivity study indicated insignificant impact on water table flux for a grid extending to the shorter half-distance between waste tanks. PORFLOW material properties for native soil utilize Section 4.2.2.2.2 parameters for vadose zone soil and for backfill utilize Section 4.2.2.2.2 parameters for backfill soil. Figures 4.4-24 through 4.4-39 display the flow fields for the various waste tank types over time. The figures are color coded to show the areas of highest saturation (dark blue) and have arrows, which denote the flow magnitude. The head of the arrows point in the flow direction, and the size of the head denotes relative flow magnitude (i.e., the larger the arrowhead, the larger the flow magnitude). Dotted or dashed lines represent infiltration and minimal flow in the downward direction. The figures show how PORFLOW simulated flow and how flow changes over time due to waste tank changes (e.g., cap degradation, grout degradation, liner failure).

Figure 4.4-15: PORFLOW Type I Tank Model

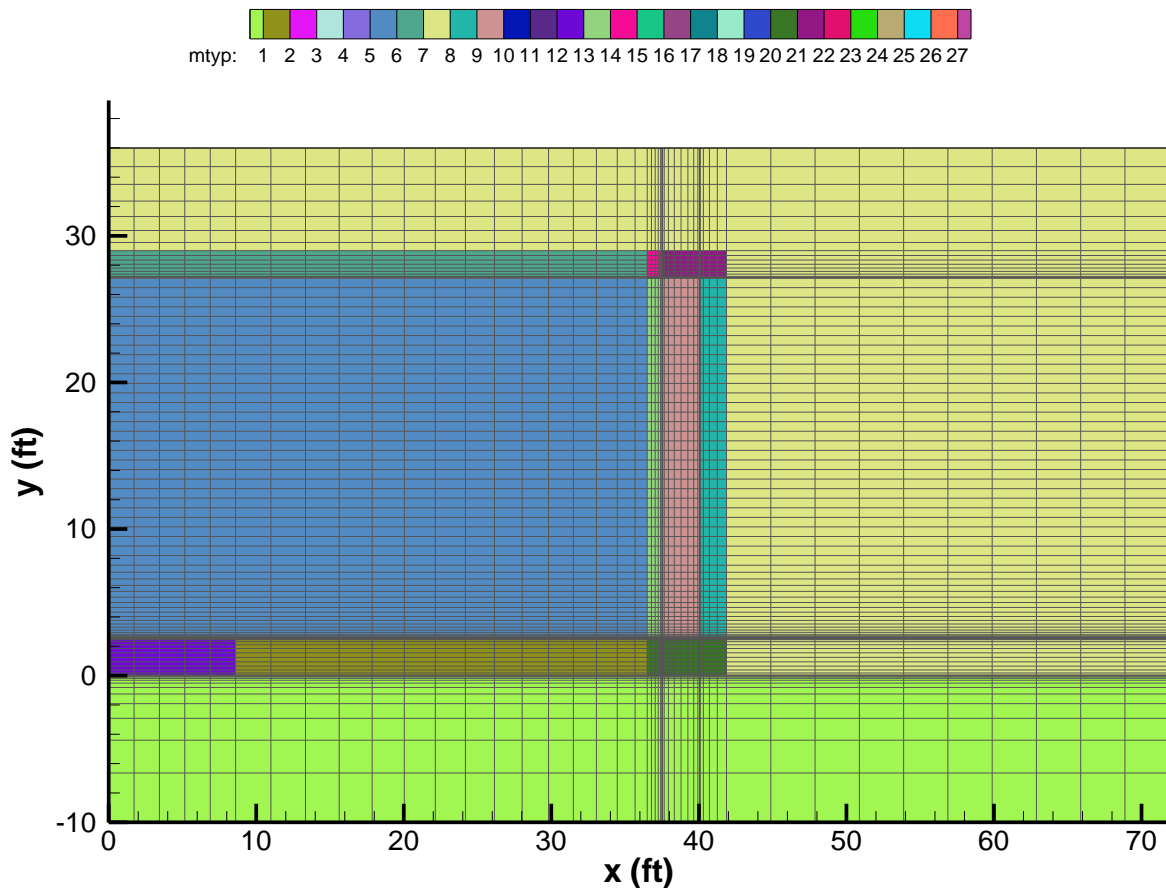


Figure 4.4-16: PORFLOW Type I Tank Model, Lower Corner Detail

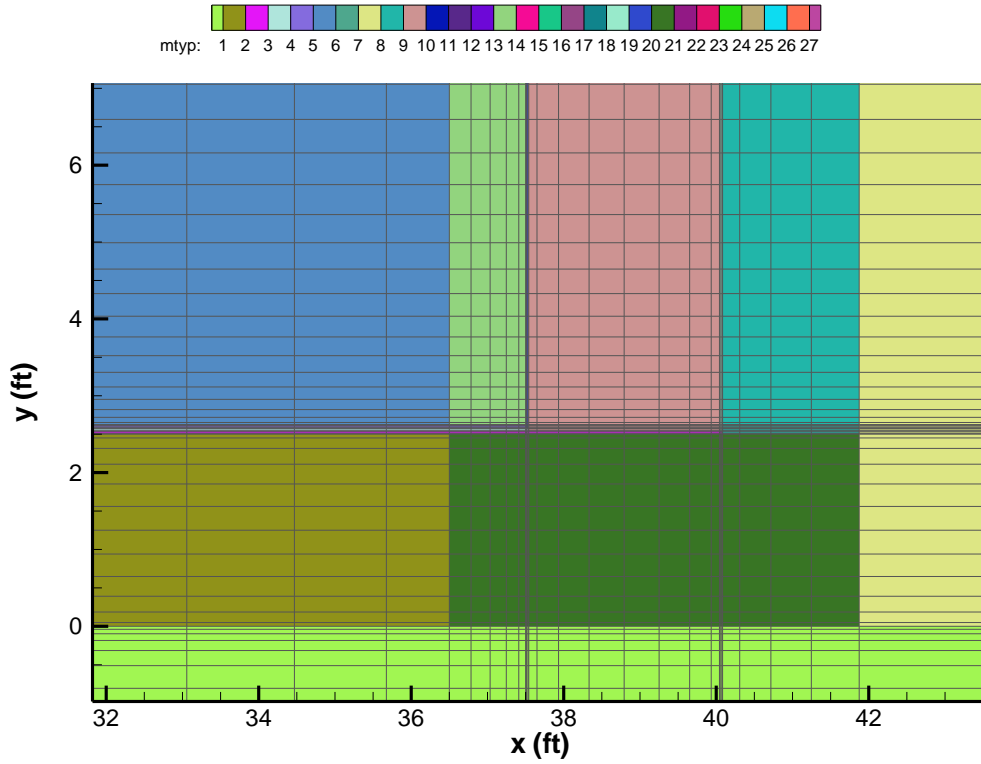


Figure 4.4-17: PORFLOW Type II Tank Model

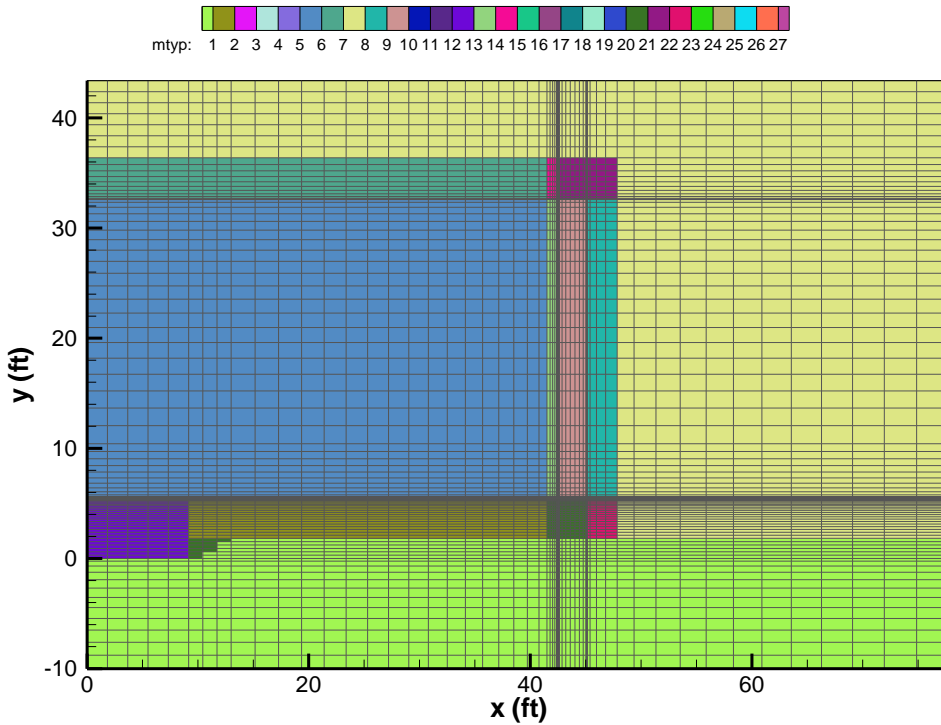


Figure 4.4-18: PORFLOW Type II Tank Model, Lower Corner Detail

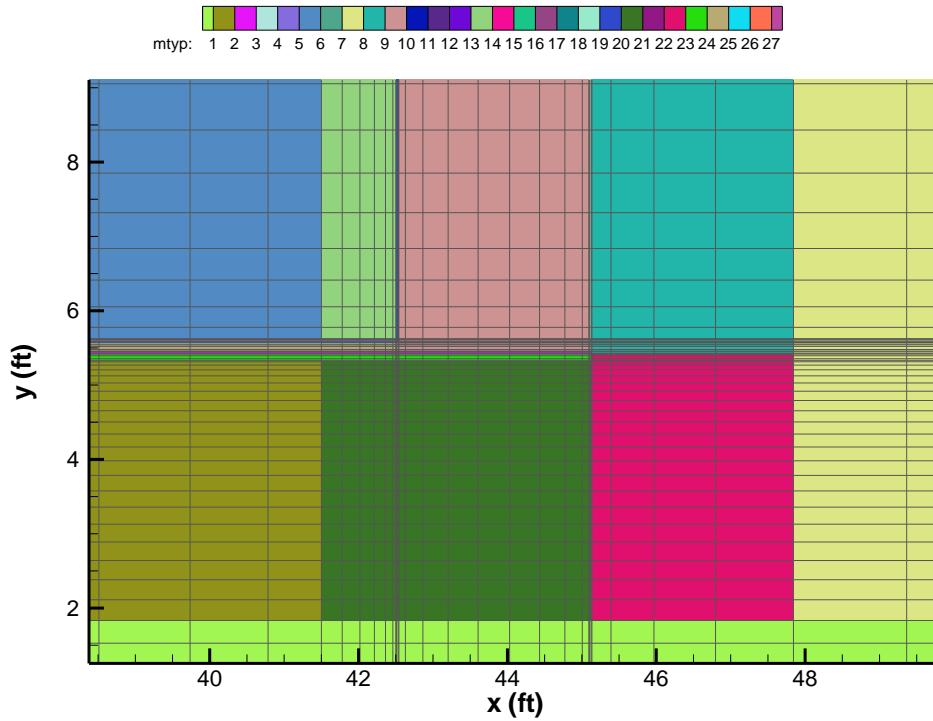


Figure 4.4-19: PORFLOW Type III Tank Model Detail

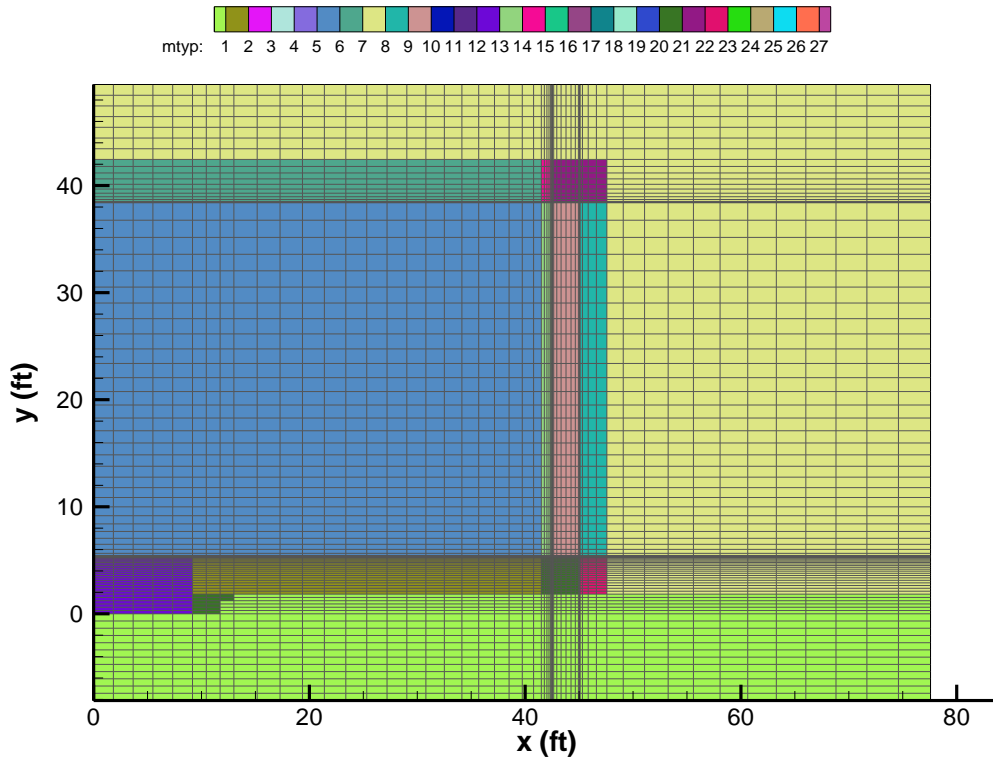


Figure 4.4-20: PORFLOW Type III Tank Model, Lower Corner Detail

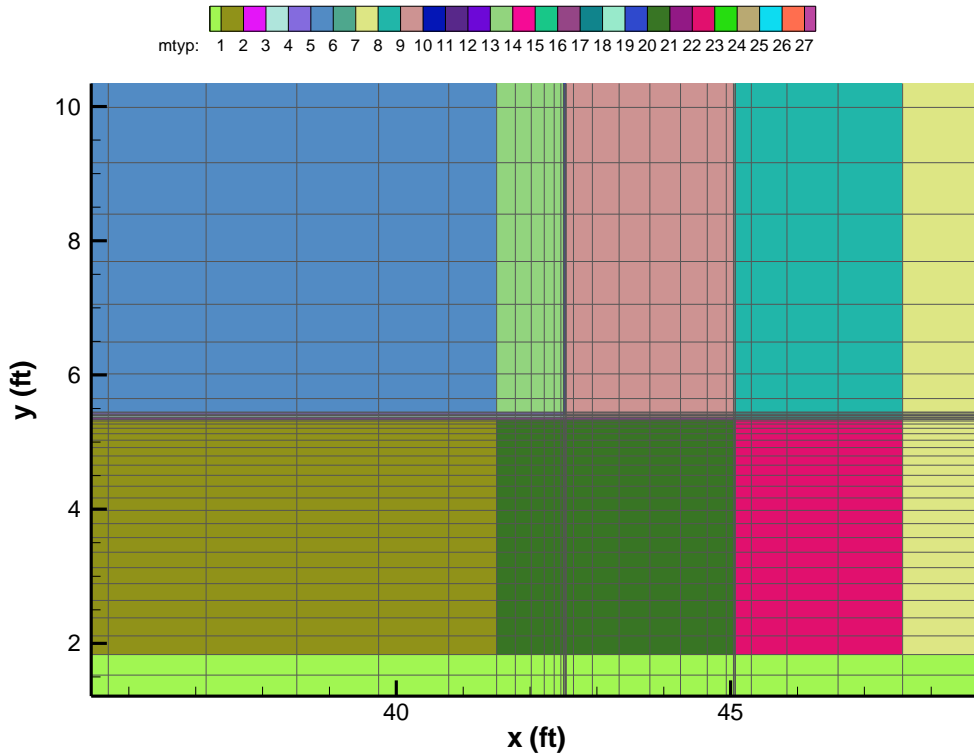


Figure 4.4-21: PORFLOW Type IV Tank Model, Domed Roof Explicitly Modeled

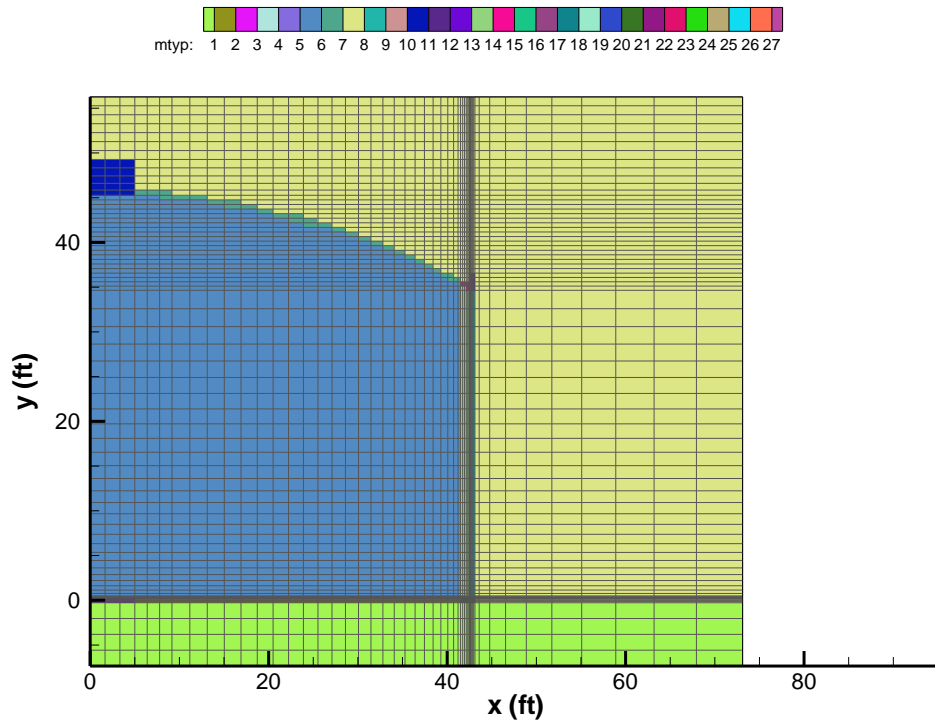


Figure 4.4-22: PORFLOW Type IV Tank Model, Lower Corner Detail

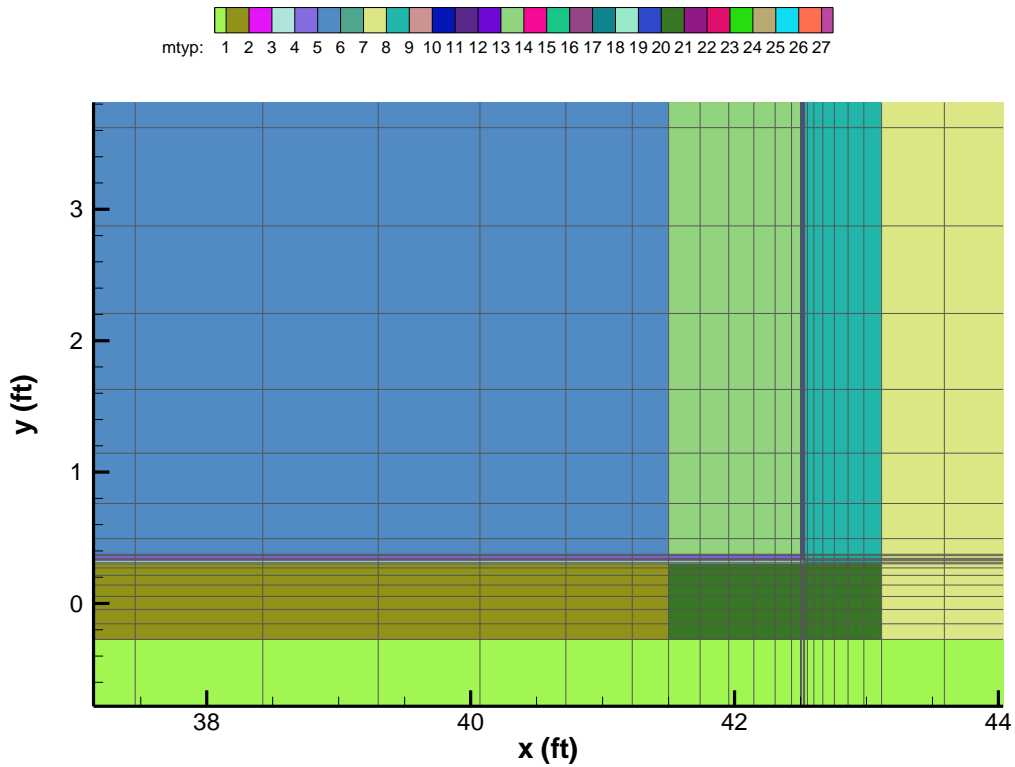


Figure 4.4-23: PORFLOW Type IV Tank Model, Tank Top Corner Detail

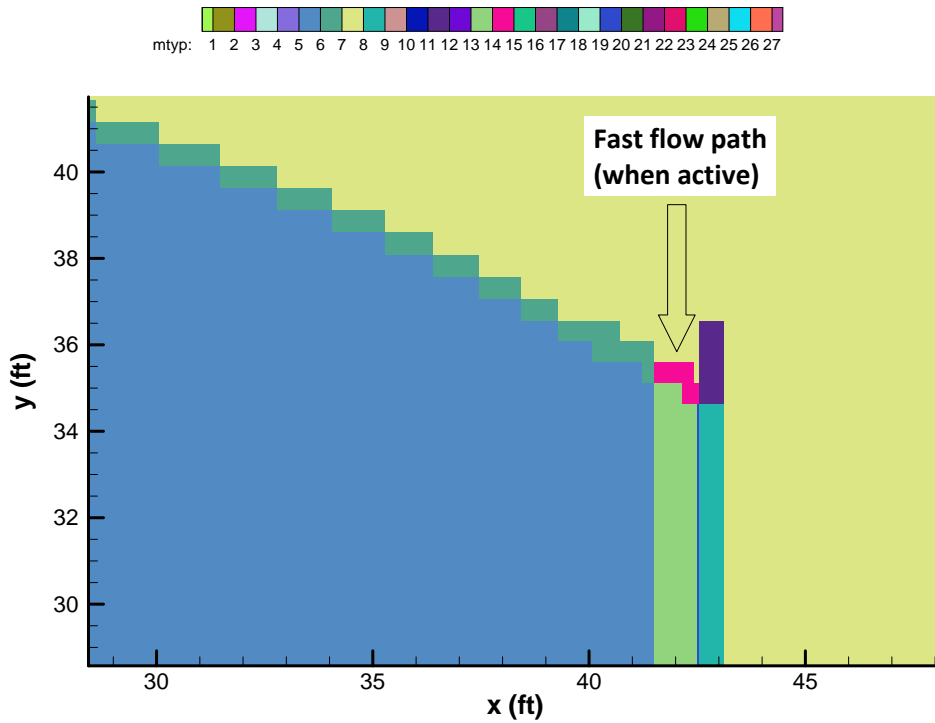
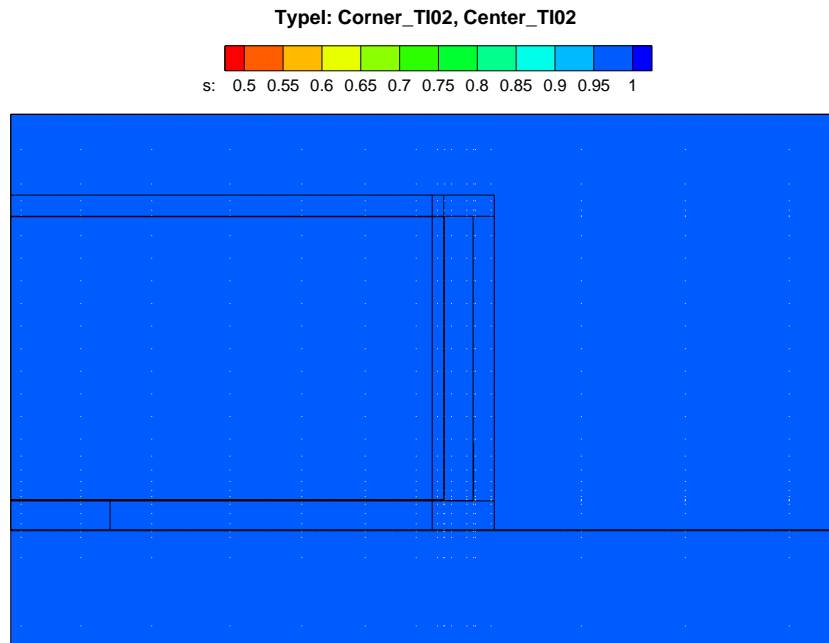
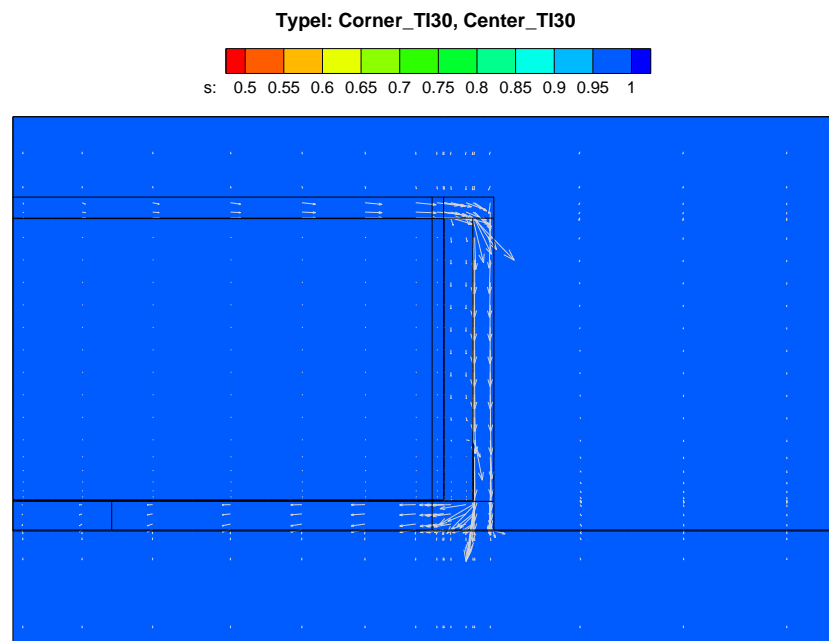


Figure 4.4-24: Type I Tank Flow Field - Year 100



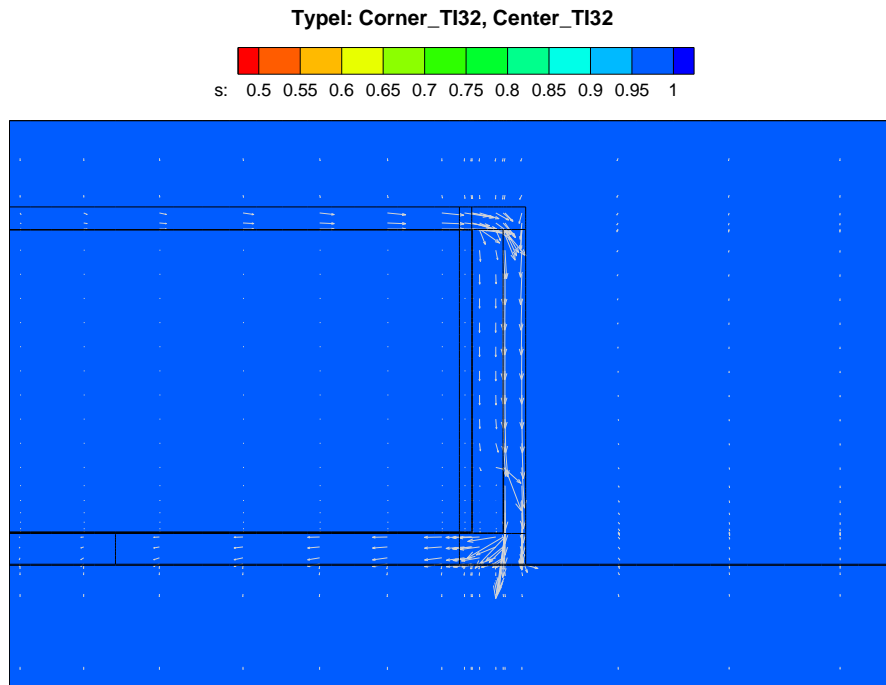
(s: = saturation)

Figure 4.4-25: Type I Tank Flow Field - Year 10,000



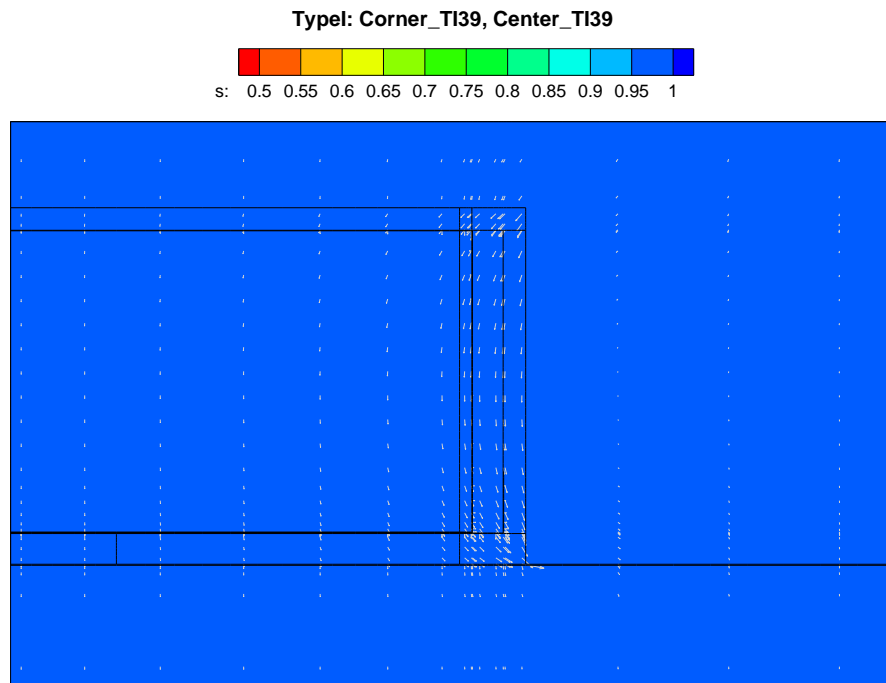
(s: = saturation)

Figure 4.4-26: Type I Tank Flow Field (Immediately Prior to Liner Failure) - Year 11,397



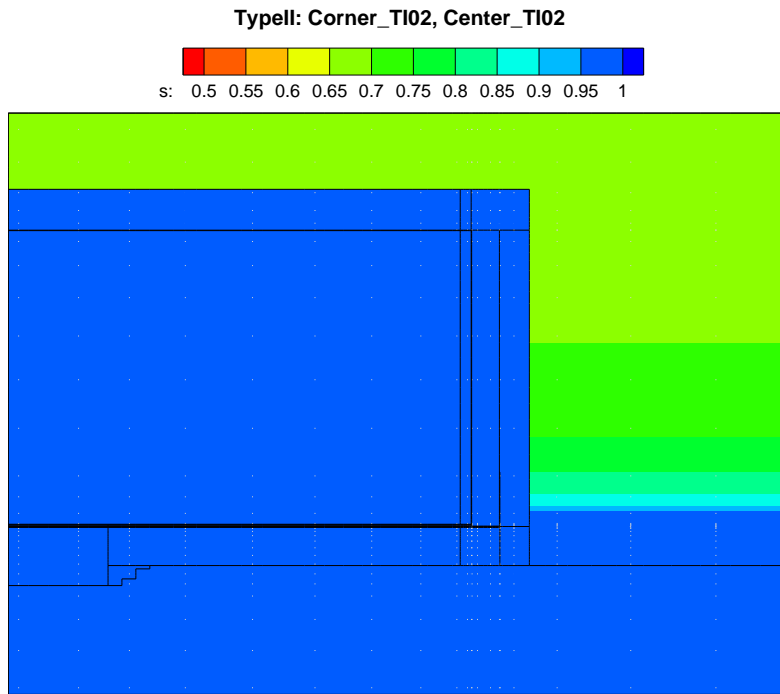
(s: = saturation)

Figure 4.4-27: Type I Tank Flow Field - Year 20,000



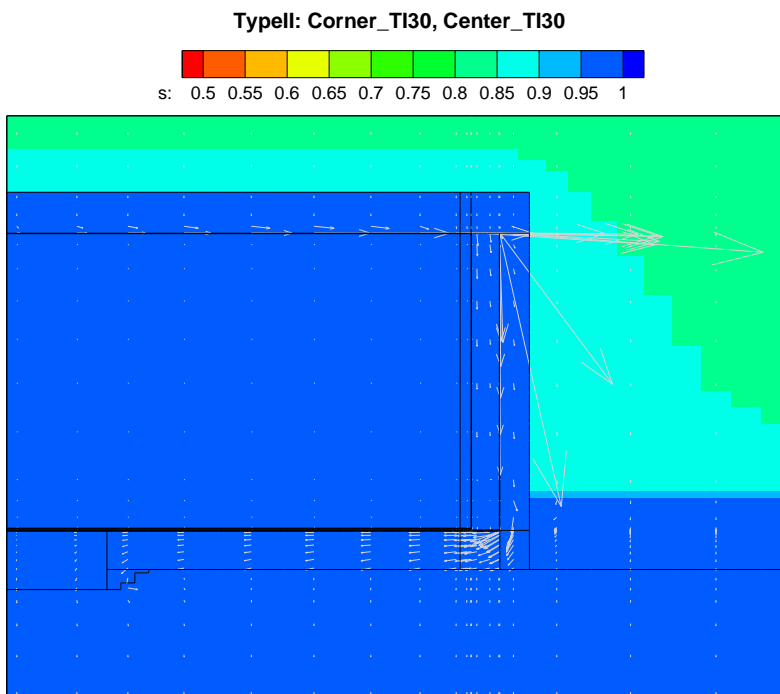
(s: = saturation)

Figure 4.4-28: Type II Tank Flow Field - Year 100



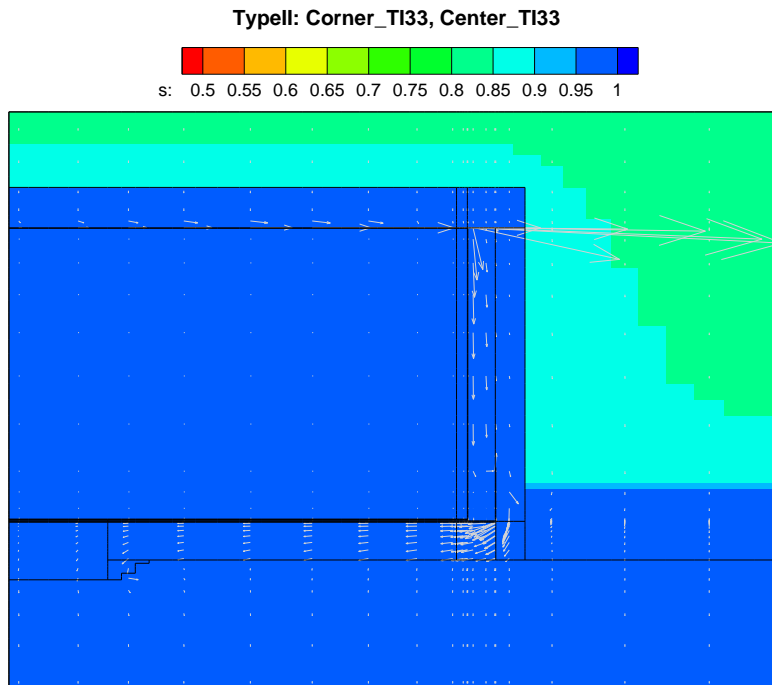
(s: = saturation)

Figure 4.4-29: Type II Tank Flow Field - Year 10,000



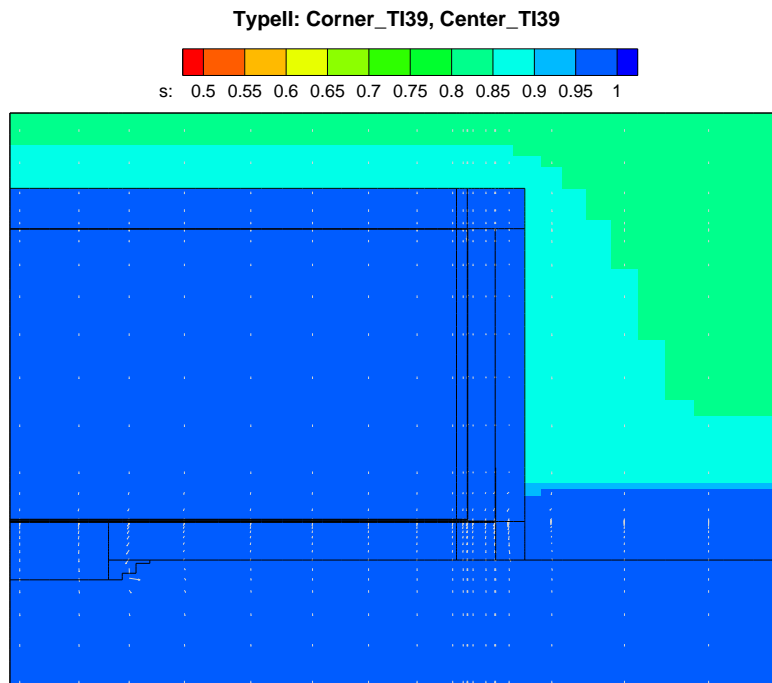
(s: = saturation)

Figure 4.4-30: Type II Tank Flow Field (Immediately Prior to Liner Failure) - Year 12,687



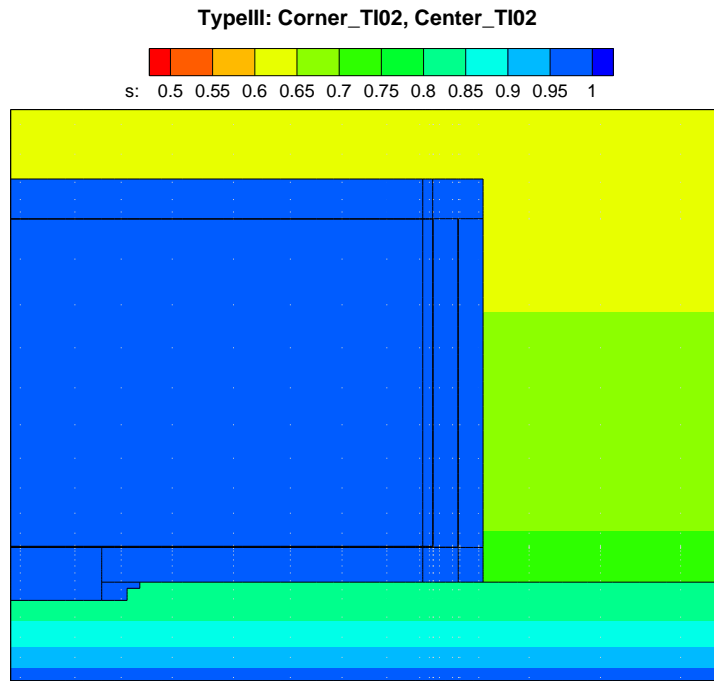
(s: = saturation)

Figure 4.4-31: Type II Tank Flow Field - Year 20,000



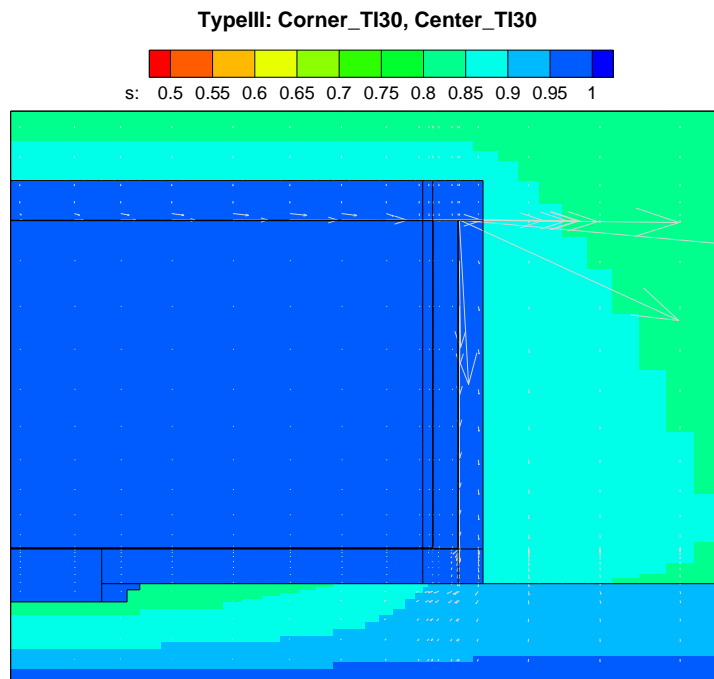
(s: = saturation)

Figure 4.4-32: Type III Tank Flow Field - Year 100



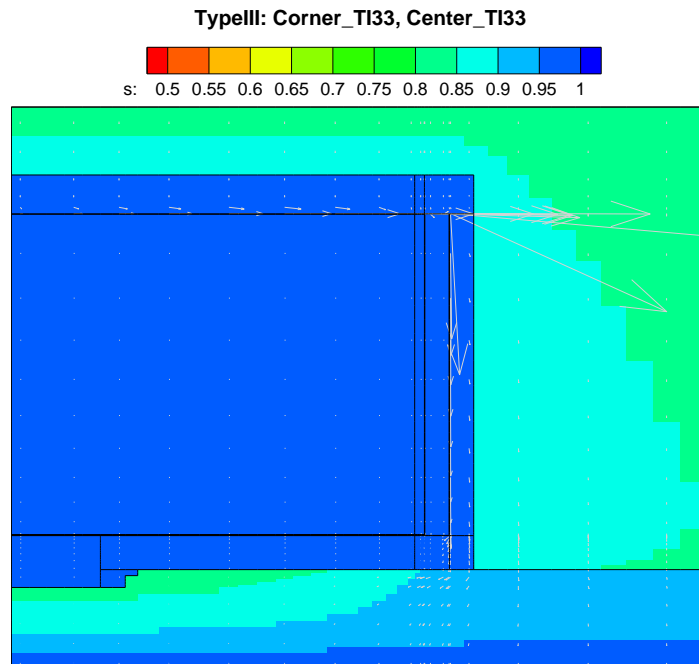
(s: = saturation)

Figure 4.4-33: Type III Tank Flow Field - Year 10,000



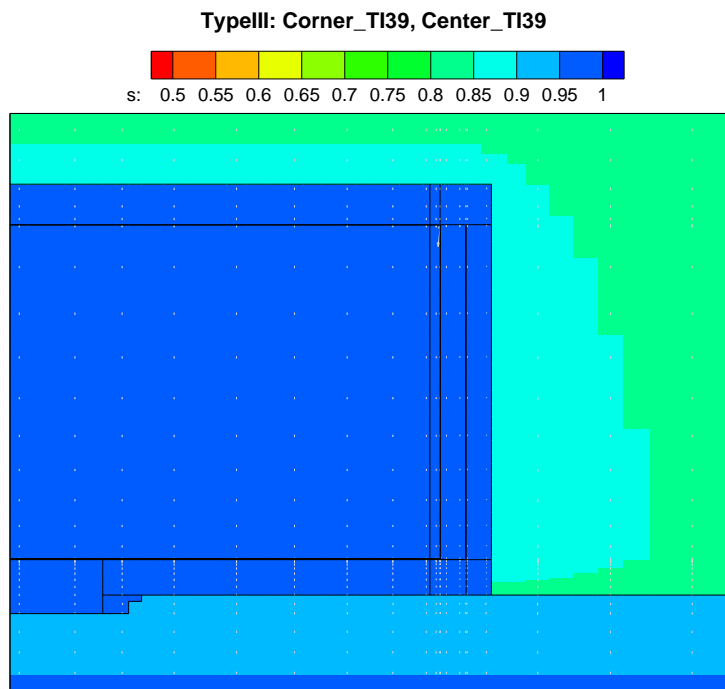
(s: = saturation)

Figure 4.4-34: Type III Tank Flow Field (Immediately Prior to Liner Failure) - Year 12,751



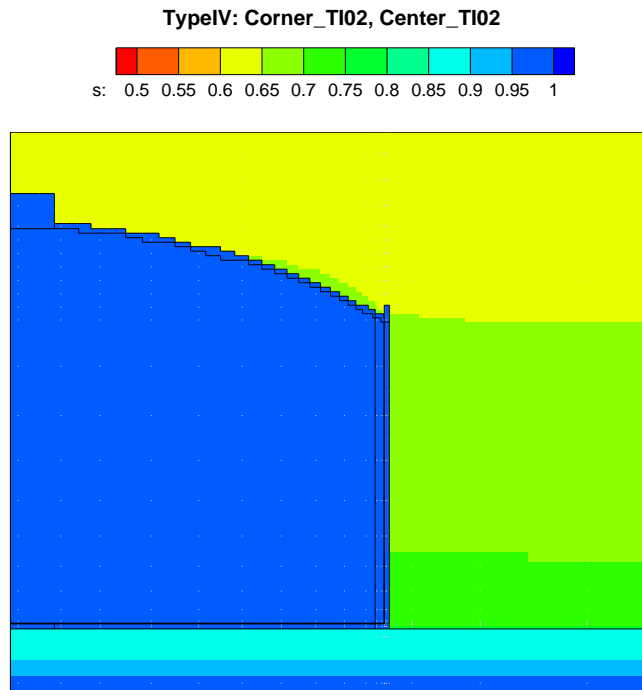
(s: = saturation)

Figure 4.4-35: Type III Tank Flow Field - Year 20,000



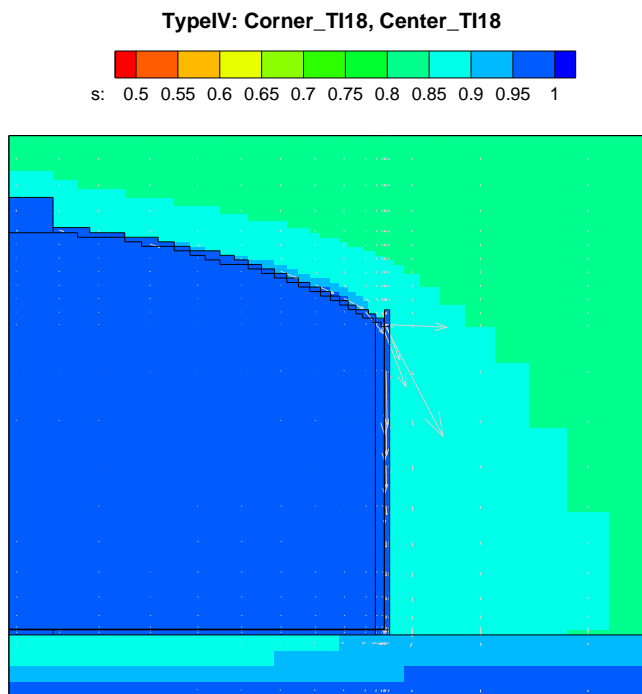
(s: = saturation)

Figure 4.4-36: Type IV Tank Flow Field - Year 100



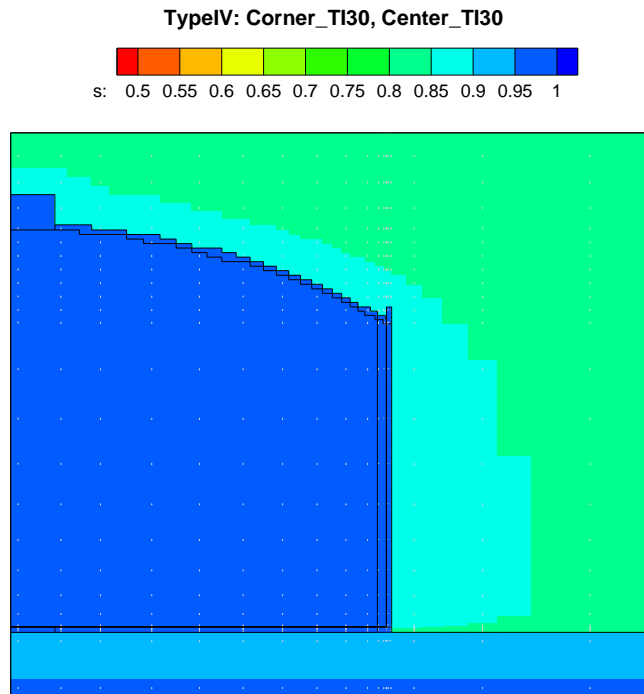
(s: = saturation)

Figure 4.4-37: Type IV Tank Flow Field (Immediately Prior to Liner Failure) - Year 3,638



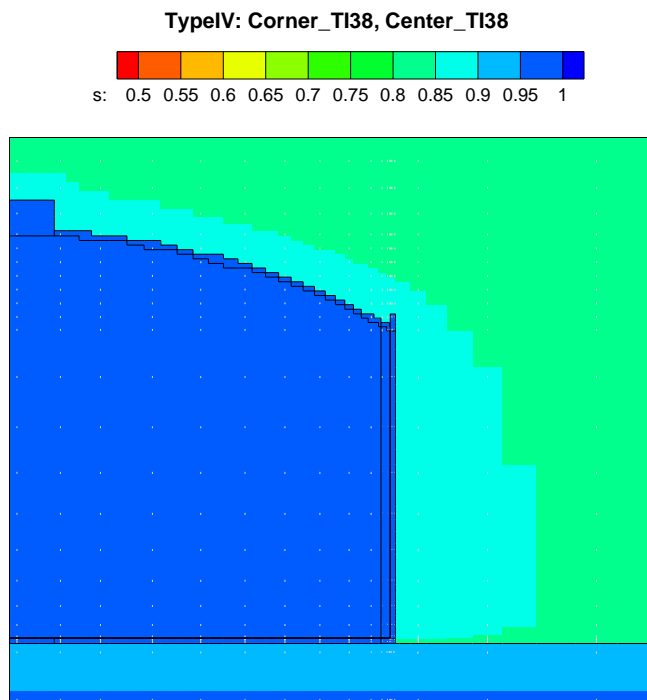
(s: = saturation)

Figure 4.4-38: Type IV Tank Flow Field - Year 10,000



(s: = saturation)

Figure 4.4-39: Type IV Tank Flow Field - Year 20,000



(s: = saturation)

Hydrodynamic dispersion was neglected in vadose transport modeling because most materials are homogeneous (e.g., concrete) or relatively so (e.g., backfilled soil). Preferential flow pathways through cracks, fractures, or other discrete features were modeled using one of two methods, depending on scale. Even though there is an increase in saturated hydraulic conductivity and modified characteristic curves, small-scale features are implicitly represented within a porous medium formulation. Large-scale features are explicitly represented in a porous medium formulation as discrete zones of high permeability (e.g., sand seam). A porous, rather than fractured, medium approach was preferred for smaller scale fracture scenarios because, 1) smaller scale crack/fracture geometry and other properties have not been defined for the degraded material of interest and 2) the scenarios of interest for the HTF PA can be adequately represented in the simpler porous medium approach.

Material properties are independently defined for each grid zone, but are not necessarily different (depending on the scenario). Properties are defined as the product of these factors:

- Base value from a materials palette, a time-invariant constant
- Time-dependent factor #1, intended to represent baseline physical changes
- Time-dependent factor #2, intended for UA/SA perturbations

The latter two factors defining the properties can be arbitrary piecewise-linear functions. They are functionally identical and differ only in intended usage. Material properties can change in the HTF PORFLOW Model over time. In PORFLOW modeling, infiltrate pore volume as a function of time is calculated outside of PORFLOW after flow simulations have been completed. Chemical transitions in subsequent transport modeling are based on these calculations, oxidation potential, and pH transitions as a function of pore volumes from SRNL-STI-2012-00404. In general, chemical transitions for a material zone are based on infiltrate pore volumes for that same zone. For example, at the time when the calculated volume of pore water flowing through the grout zone equals the transition volume, the materials in the grout zone are subsequently modeled as having the properties associated with the new chemical phase (Table 4.2-1).

For some materials and cases, chemical transitions for a particular zone are tied to the transition in another zone. For example, the basemat of Type II tanks is divided into three sub-zones, 1) a thicker disk at the waste tank centerline, 2) an outer ring beneath the annulus space, and 3) the remaining center ring. The transition times for all three regions are tied to the pore volume count through the center ring. Thus, no credit is taken for the thicker inner disk, nor is the pore volume count biased by faster flows rounding the outside corner of the overall basemat.

A second example of the chemical transition for a particular zone being tied to the transition is the CZ in the Base Case. In this case, infiltrate flowed downward through the waste tank grout and the pore water chemistry of the overlying grout is assumed imparted on the very thin CZ in intimate contact with grout. Therefore, the chemical transition times are considered identical for the two materials. Cases B and D initially had a fast flow path around the grout, but the grout degraded hydraulically at year 501,

after which infiltrate flowed downward through the grout. In these cases, the chemical transition of the CZ is also based on the overlying grout. For Cases C and E, a fast flow path through the grout existed, but the grout failed hydraulically as it did in the Base Case. Since the overlying grout remains intact longer, the infiltrate was able to bypass the waste tank grout (via the fast flow path) and flow through the CZ. For these cases, the CZ is based on its own pore water count.

Chemical degradation is indirectly coupled to hydraulic degradation through infiltrate pore volumes. Chemical transitions are a function of infiltrate pore volumes. Hydraulic degradation that alters the flow field may affect the infiltrate pore volume count, and thus oxidation potential and pH transitions occur in time.

Type III, IIIA, and IV tanks in H Area reside above the water table and are subject to a downward flow gradient, similar to tanks in F Area. The resulting axi-symmetric flow around the circular tanks can be efficiently handled by a 2-D (r,z) PORFLOW model. However, Type I tanks are fully submerged and Type II tanks are partially submerged. These tanks may be affected by lateral flow in the saturated zone, in addition to the downward flow component from infiltrating soil moisture. Explicit simulation of aquifer crossflow would require a three-dimensional numerical model because conditions are no longer axi-symmetric. The additional computational burden of 3-D simulations was judged as impractical considering the large number of tanks, configurations, scenarios, and species to be modeled. Instead, 2-D axi-symmetric PORFLOW models are used for all tank types, and the effects of aquifer crossflow are accounted for in an approximate manner for Type I and II tanks. Crossflow influences three aspects of PORFLOW simulation, which are discussed in turn below.

When tank steel and concrete components are largely intact and function as the primary barrier to waste release, the main effect of aquifer crossflow is to sweep away contamination that might otherwise build up in soil surrounding the tank, reducing the concentration gradient across the barrier and hindering diffusional releases, if any. Contaminant releases prior to barrier degradation are zero (e.g., prior to liner failure) or small compared to later releases. The effect of any artificial contaminant buildup in PORFLOW simulations is considered insignificant to peak flux results and neglected.

After the primary barrier degrades, advection is the primary release mechanism and crossflow directly contributes to waste release from the contamination zone. However, the relative contribution of the latter can be small or negligible depending on the magnitude of the crossflow and the geometry of the waste zone.

For submerged and partially submerged waste tanks, the raw pore volume counts from near-field PORFLOW modeling were inflated for material zones to account for aquifer crossflow by using a ‘crossflow factor’ defined as:

$$\frac{F}{D} = 1 + \frac{C}{I}$$

where:

<i>F</i>	=	total flow considering crossflow
<i>D</i>	=	downward flow from near-field PORFLOW modeling
<i>C</i>	=	crossflow rate
<i>I</i>	=	infiltration rate in near-field PORFLOW modeling

The adjusted total flow is used to count pore volumes flushed through a material zone. The crossflow rate is assumed to be $C = 480$ cm/yr, which corresponds to a crossflow ratio of ten times based on simulations in PORTAGE-08-022, and a nominal present day infiltration rate of 48 cm/yr. The crossflow factor is generally applied to waste tank components that are fully submerged. Further information is provided in SRNL-STI-2012-00465. The materials palette used in HTF PORFLOW modeling is provided in Table 4.4-10.

Table 4.4-10: PORFLOW Materials Palette

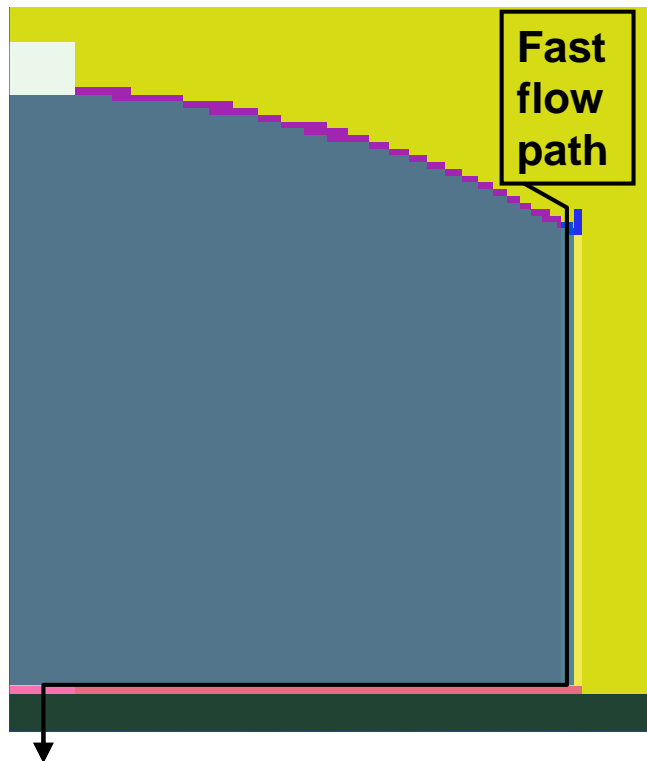
Material ID	K_{sat} Horizontal (cm/s)	K_{sat} Horizontal (cm/yr)	K_{sat} Vertical (cm/s)	K_{sat} Vertical (cm/yr)	Saturated D_e (cm ² /s)	Saturated D_e (cm ² /yr)	η_T (unitless)	ρ_h (g/cm ³)	ρ_n (g/cm ³)	Characteristic Curve
<i>native_soil</i>	6.2E-05	2.0E+03	8.7E-06	2.7E+02	5.3E-06	167.26	0.39	1.65	2.70	<i>UpperVz</i>
<i>LowerVz</i>	3.3E-04	1.0E+04	9.1E-05	2.9E+03	5.3E-06	167.26	0.39	1.62	2.66	<i>LowerVz</i>
<i>OscBefore</i>	1.2E-04	3.8E+03	1.2E-04	3.8E+03	5.3E-06	167.26	0.46	1.44	2.65	<i>OscBefore</i>
<i>OscAfter</i>	1.4E-05	4.4E+02	1.4E-05	4.4E+02	4.0E-06	126.23	0.27	1.92	2.65	<i>OscAfter</i>
<i>backfill</i>	7.6E-05	2.4E+03	4.1E-05	1.3E+03	5.3E-06	167.26	0.35	1.71	2.63	<i>CcBackfill</i>
<i>IlyPermeable Backfill</i>	1.4E-03	4.4E+04	7.6E-04	2.4E+04	8.0E-06	252.46	0.41	1.56	2.64	<i>IlyPermeableBack fill</i>
<i>SingleVadose Zone</i>	1.9E-04	6.0E+03	3.0E-05	9.5E+02	5.3E-06	167.26	0.39	1.63	2.67	<i>SingleVadoseZone</i>
<i>Sand</i>	5.0E-04	1.6E+04	2.8E-04	8.8E+03	8.0E-06	252.46	0.38	1.65	2.66	<i>Sand</i>
<i>ClaySand</i>	8.3E-05	2.6E+03	2.1E-05	6.6E+02	5.3E-06	167.26	0.37	1.68	2.67	<i>ClaySand</i>
<i>Clay</i>	2.0E-06	6.3E+01	9.5E-07	3.0E+01	4.0E-06	126.23	0.43	1.52	2.67	<i>Clay</i>
<i>Gravel</i>	1.5E-01	4.7E+06	1.5E-01	4.7E+06	9.4E-06	296.64	0.30	1.82	2.60	<i>Gravel</i>
<i>basemat</i>	3.4E-08	1.10E+00	3.4E-08	1.10E+00	8.0E-07	25.25	0.168	2.06	2.51	<i>fractured_basemat</i>
<i>grout</i>	2.1E-09	6.63E-02	2.1E-09	6.63E-02	5.0E-08	25.25	0.21	1.97	2.49	<i>fractured_grout</i>
<i>wall_roof</i>	3.4E-08	1.10E+00	3.4E-08	1.10E+00	8.0E-07	25.25	0.168	2.06	2.51	<i>fractured_basemat</i>
<i>contaminated _zone</i>	2.1E-09	6.63E-02	2.1E-09	6.63E-02	5.0E-08	25.25	0.21	1.97	2.49	<i>fractured_grout</i>
<i>liner</i>	5.0E-15	1.6E-07	5.0E-15	1.6E-07	1.0E-13	3.16E-06	0.39	N/A	2.70	<i>Concrete_Qlow_N ewCigGrout</i>
<i>vertical_liner</i>	5.0E-15	1.6E-07	5.0E-15	1.6E-07	1.0E-13	3.16E-06	0.39	N/A	2.70	<i>Concrete_Qlow_N ewCigGrout</i>
<i>fast_flow</i>	1.5E-01	4.7E+06	1.5E-01	4.7E+06	9.4E-06	296.64	0.30	1.82	2.60	<i>Gravel</i>

K_{sat} = Saturated Hydraulic Conductivity
 η_T = Total Porosity
 ρ_h = Dry Bulk Density
 ρ_n = Particle Density
 D_e = Effective Diffusion Coefficient

4.4.4.1.3 Fast Flow Path Modeling in PORFLOW

To represent the effect of a hypothetical fast flow path through a waste tank (Figure 4.4-40), the HTF PORFLOW Model assumed all water being shed from the tank roof was intercepted by a high conductivity vertical leg encircling the waste tank perimeter just inside the primary liner. Horizontal flow then takes place through the CZ, which was also assigned a high conductivity, with the entire CZ allowed to contact infiltrating water. Contaminant transport was then assumed to take place through a high conductivity center “donut” hole in the waste tank basemat. The hole was sized to allow high flow through the fast flow path and contamination layer in particular. The materials occupying the fast flow zones were assumed to have high conductivity and diffusion coefficient relative to backfilled and native soils, but no adsorption was assumed (i.e., $K_d = 0$ for all radiological and chemical transport).

Figure 4.4-40: PORFLOW Type IV Tank Fast Flow Path Model



4.4.4.1.4 Vadose and Aquifer Model Validation in PORFLOW

Additional PORFLOW validation was performed beyond code verification exercises and GSA/HTF model development. Using characterization and monitoring data, aspects of the PORFLOW vadose zone and aquifer models have been compared to independent field data, as identified below. Additional detail can be obtained in the associated references.

Vadose Zone

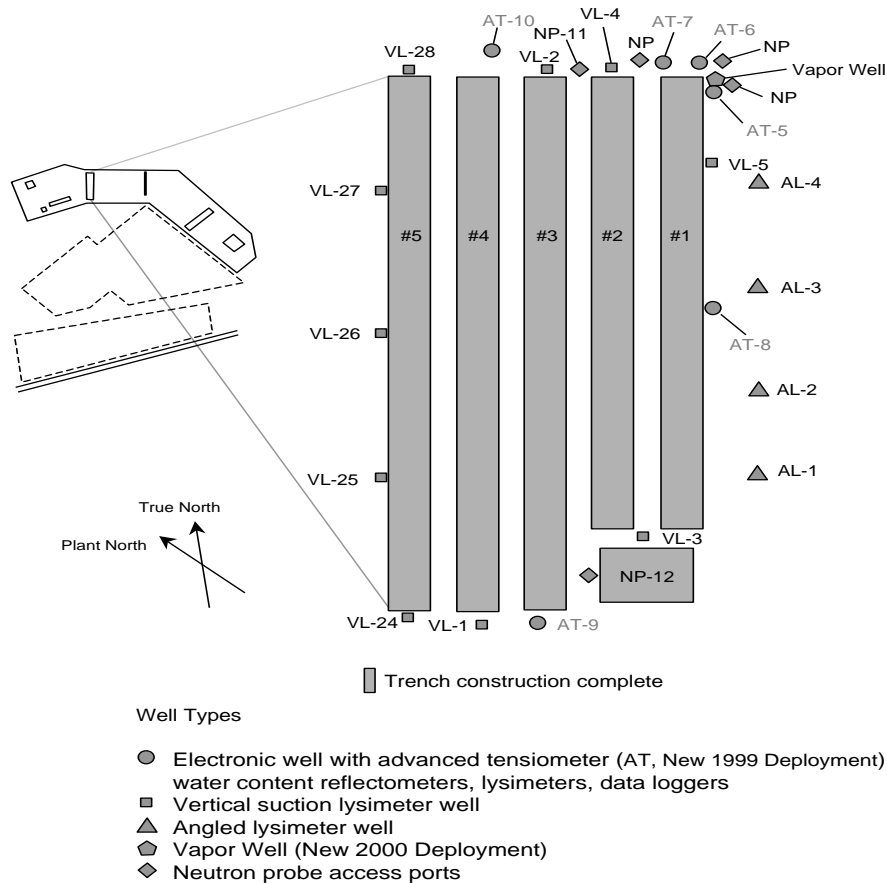
- Soil suction and water content from Vadose Zone Monitoring System (VZMS) in E Area (WSRC-STI-2006-00198 Section 5.8)
- Tracer test pore velocity (WSRC-TR-2007-00283 Section 4.0)
- Tritium migration beneath the E-Area Slit Trenches (herein)

Aquifer

- Surveyed seepines (WSRC-TR-2004-00106)
- Pathline comparisons to existing plumes (herein)

The VZMS monitors soil conditions beneath and alongside the solid waste disposal trenches (slit trenches) in E Area under uncapped infiltration conditions (Figure 4.4-41). E Area is located in the GSA adjacent to H Area. Field measurements using tensiometers and neutron probes indicate that soil suction ranges from approximately 50 to 200 centimeters, while water content varies between about 0.15 and 0.30. The latter values suggest water saturation between 35 % and 75 %. Infiltration over the affected area is estimated to be 30 cm/yr (12 in/yr). Using the upper vadose zone and lower vadose zone soil properties recommended in WSRC-STI-2006-00198 and adopted for HTF PA modeling, a PORFLOW representation of E-Area conditions produced suction head and saturation values of 83 centimeters and 91 % in the upper vadose zone, and 170 centimeters and 72 % in the lower vadose zone.

Figure 4.4-41: Layout and Instrumentation for VZMS at Slit Trenches



A series of field and laboratory tracer experiments have been conducted at SRS under uncapped (normal infiltration) conditions. The HTF PORFLOW Model described above produced pore velocities of approximately 34 in/yr and 43 in/yr for upper and lower vadose zones, respectively. Together, the tracer test data indicate a pore velocity of about 45 in/yr for the same infiltration, which is similar to the model simulations.

A PORFLOW vadose zone model, similar to that used for HTF PA simulations was compared to tritium concentration data from the VZMS (Figure 4.4-41). Concentration data was grouped according to elevation (high/low) and location (center/edge) relative to a disposal trench (Figure 4.4-42). The concentration data exhibits large variability, as is commonly observed with point measurements (Figure 4.4-43). The “Generic” and “Concrete” labels in Figure 4.4-43 refer to the waste form(s) containing tritium contamination. “Generic” designates general waste of a variety of forms, whereas “concrete” is reserved for concrete rubble waste generated from demolition of Building 232-F. In model simulations, tritium in “generic” waste is immediately available for transport. Tritium embedded in concrete is released more slowly by diffusion. The HTF PORFLOW Model has a homogeneous conductivity field and no dispersion was prescribed during transport simulations. Thus, the simulations may have under-predicted lateral plume spreading compared to actual conditions. For example, sediment layering

can cause contamination to migrate outside the footprint of the trench. Small changes in the degree of lateral plume dispersion can lead to large changes in “edge” concentration, whereas the “center” (plume centerline) concentration would be less affected. Given uncertainty in the tritium source strength and distribution, and PORFLOW simplification of natural subsurface heterogeneity, close agreement between the data and model was not expected. Rather than representing a definitive validation of the model, DOE believes the comparison does not provide evidence of model invalidation. Being equivalent to a spatial average representation, the PORFLOW predictions do not reflect the data scatter, but do appear to be generally consistent with the measurement trends. In general, the lateral dispersion during the dominantly vertical vadose zone seepage will lead to a spreading of the source that will be reflected in higher edge concentrations and slightly lower peak concentrations at down gradient locations. It will also tend to lead to contaminants reaching points of assessment sooner than would be expected given less lateral dispersion.

Figure 4.4-42: Basis for HTF PORFLOW Model and VZMS Data Comparison

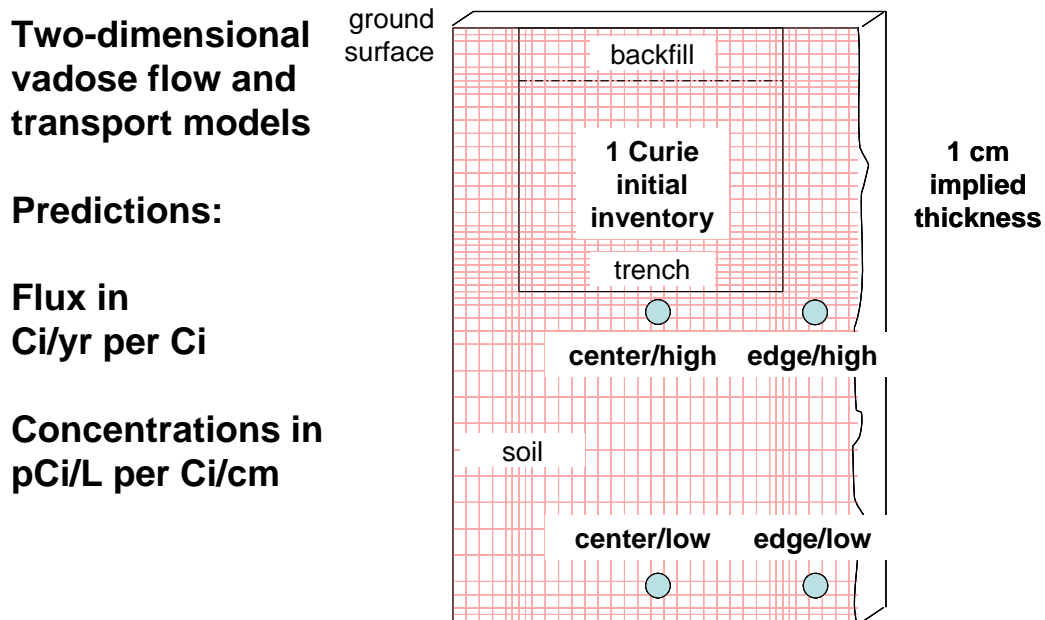
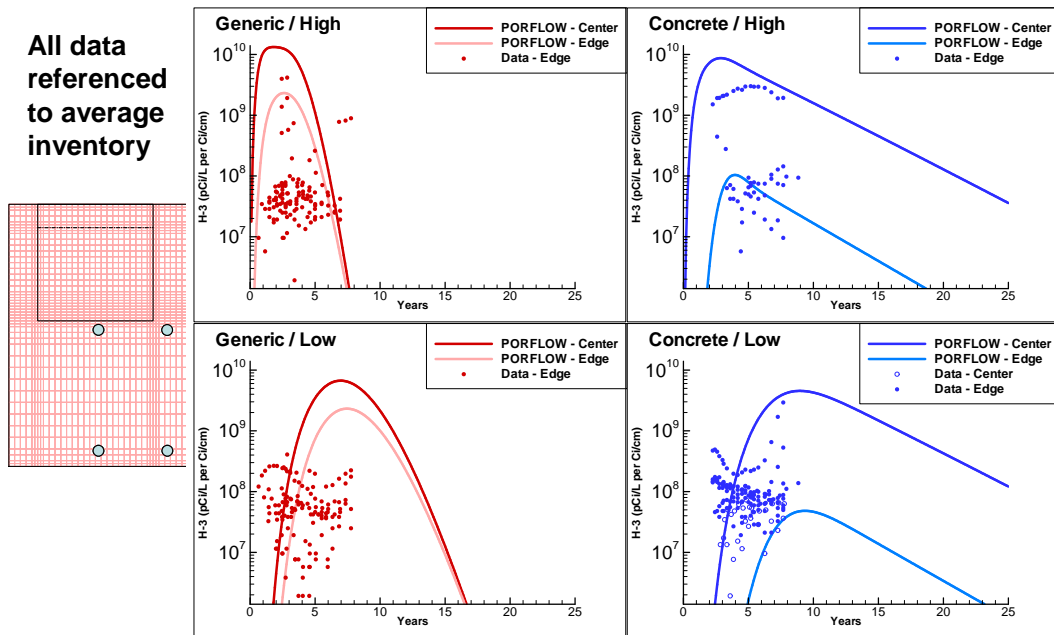
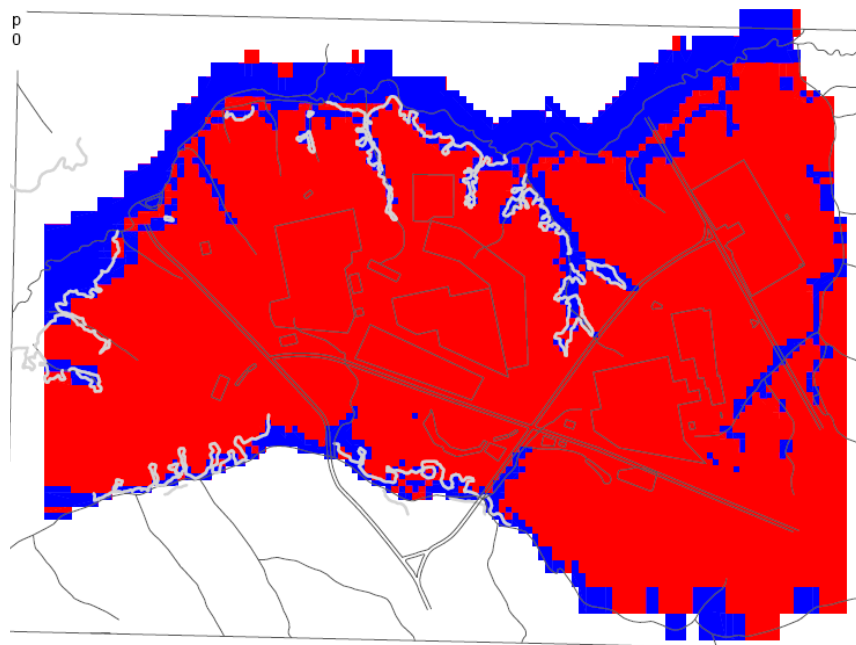


Figure 4.4-43: HTF PORFLOW Model and VZMS Tritium Data Comparison



The GSA/PORFLOW Model predictions of seepines bordering the GSA have been compared to field surveys (Figure 4.4-44). [WSRC-TR-2004-00106] The seepine data was not used in model development or calibration. The simulated seepage faces are generally consistent with the field observations.

Figure 4.4-44: Surveyed Seepines Compared to GSA/PORFLOW Model Simulation



Note: Seepine predicted at interface of recharge (red) areas and discharge (blue) areas with surveyed seepine location shown in white trace lines. [WSRC-TR-2004-00106 Figure 3-6]

The GSA contains a number of tritium plumes, typically associated with E-Area solid waste disposal facilities. Being un-retarded, tritium is an ideal tracer of groundwater flow. Groundwater pathlines from the GSA/PORFLOW Model were compared to an existing tritium plume map. The model pathlines were observed to be consistent with plume trajectory deduced from monitoring well data (Figure 4.4-45). Simulated pathlines have also been compared to F-Area plumes, with good agreement (Figure 4.4-46). The plume distributions depicted in Figures 4.4-45 and 4.4-46 were generated from field measurements. Simulated pathlines are also compared to an H-Area plume in Figure 4.4-47 with similar paths although the plume data is limited. The plume distribution depicted in Figure 4.4-47 was generated from field measurements. The GSA/PORFLOW Model was not calibrated to these data.

Figure 4.4-45: Comparison of GSA/PORFLOW Groundwater Pathlines to Tritium Plume Emanating from E-Area Mixed Waste Management Facility

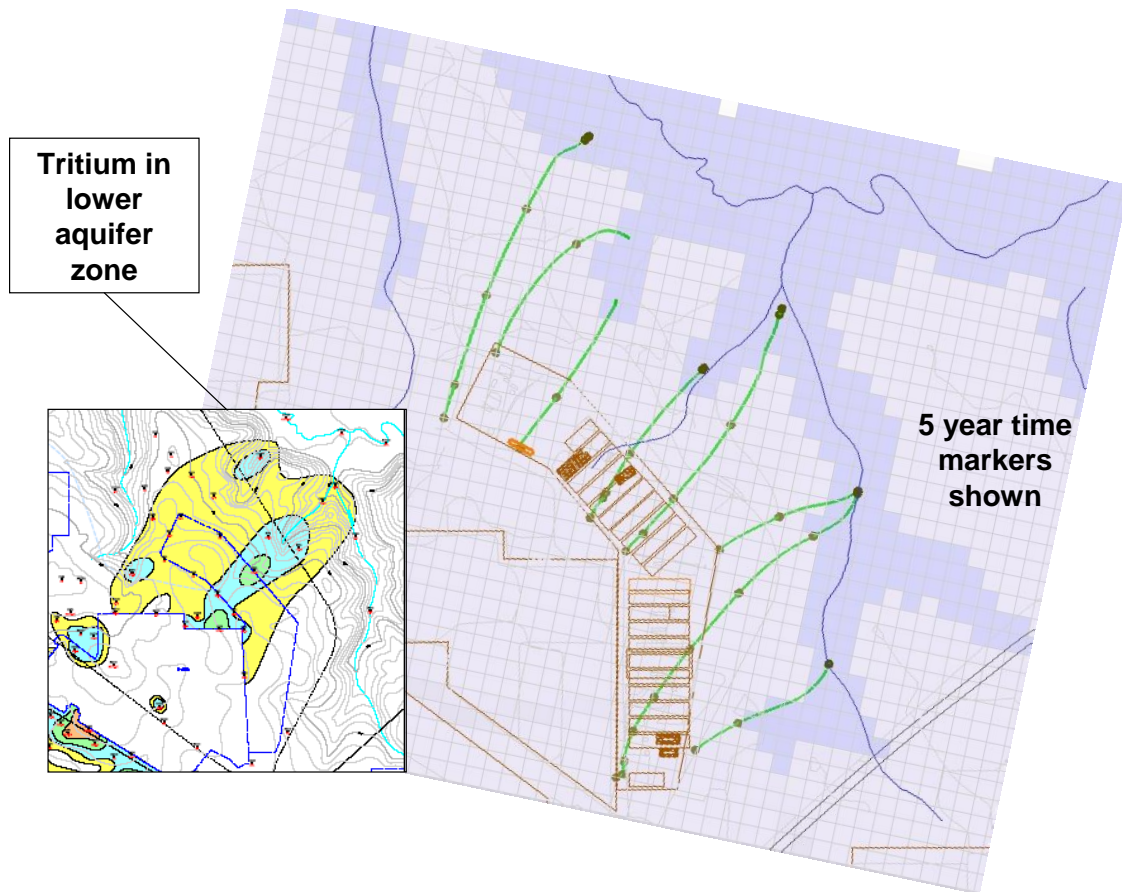
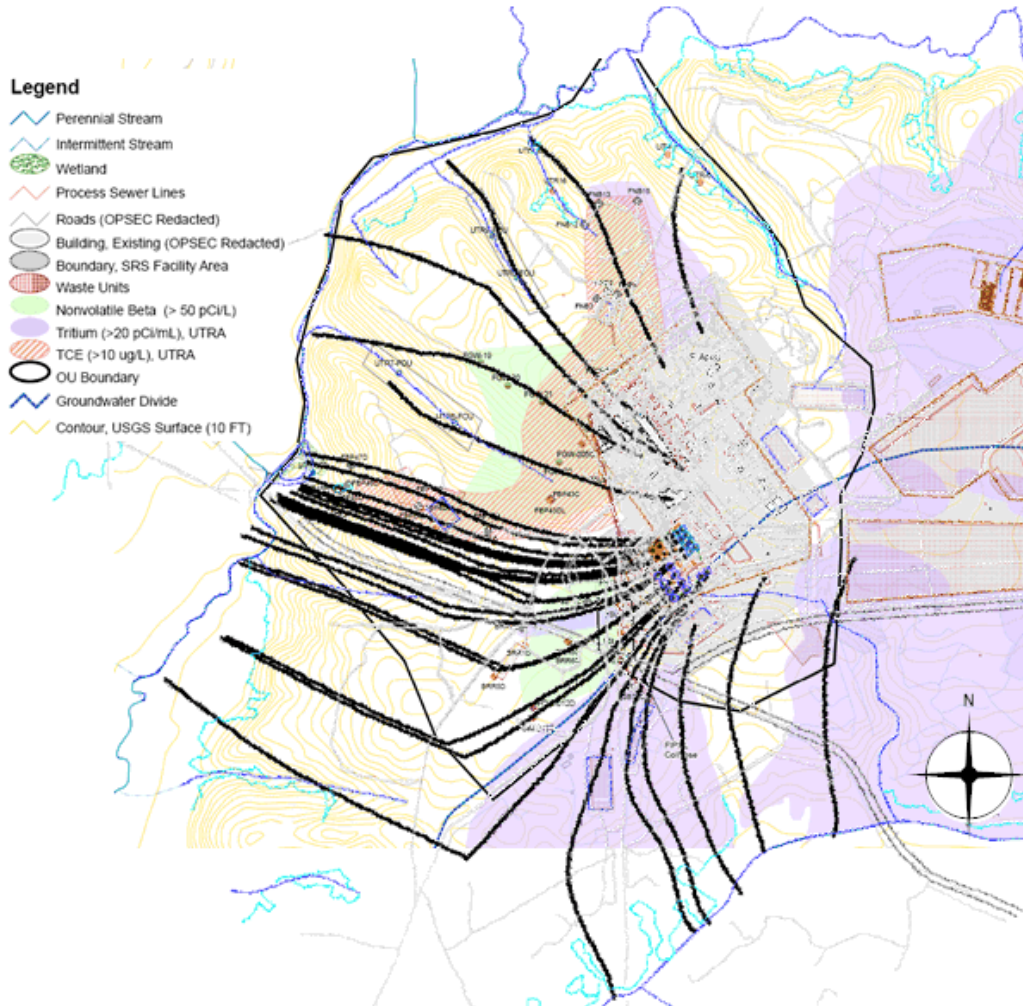


Figure 4.4-46: Comparison of GSA/PORFLOW Groundwater Pathlines to Contaminant Plumes Emanating from F Area



4.4.4.1.5 PORFLOW Parametric Study

A flow parametric study was conducted for the HTF based on the Case-A scenario. Flow rates and associated parameters generated during the study were output in a form that the HTF GoldSim model could utilize in stochastic fate and transport simulations as discussed in Sections 4.4.4.2 and 6.3.3. The study included running 72 parametric cases with varying flow field cases for each of four waste tank types. The following attributes were varied in the study:

- 3 fast flow cases (none, partial, full)
- 4 liner failure times (time zero, early, moderate, late)
- 3 cementitious material degradation rates (fast, nominal, slow)
- 2 infiltration cases (nominal, no-cap)
- 72 total parametric cases
- 4 tank types (Type I, II, IIIA, and IV tanks)

PORFLOW simulations were only performed for Type I, II, IIIA, and IV tanks. Type III and IIIA West tanks were not simulated considering their close similarity to Type IIIA tanks.

Fast Flow Path Cases

The “partial” fast flow path will breach the roof and grout, but not the basemat/floor (as in Cases B and C). The “full” fast flow path will breach the roof, grout, and basemat/floor (as in Cases D and E). The HTF Stochastic Model is designed to sample for conditions based on five cases (Cases A through E). For compatibility, when the sampled condition is the Base Case, the first fast flow case (none) is used. When the sampled condition is either Case B or Case C, the second fast flow case (partial) is used and when the sampled condition is Case D or E, the third fast flow case (full) is used.

Liner Failure Times

The parametric study also included the four liner-failure times presented in Table 4.4-11. Since the HTF Stochastic Model, sampling procedure chooses a specific failure time. That specific time dictates which set of flow data based on the liner failure times presented in Table 4.4-11 is used. The criteria for choosing the liner failure time from Table 4.4-11 is based on which time in the table (for the specified waste tank type), the sampled time is closest to. In the HTF GoldSim Model simulation, the sampled liner failure time is used. Since the liner failure times differ, the flow data time series from the parametric study data is scaled from time-zero to the liner failure time to fit the time span from time-zero to the sampled liner failure time. The component of the time series following liner failure is then shifted so that it is consistent with the sampled time failure (scaling is not considered). In this way, the influence of liner failure time can be evaluated and a degree of consistency between liner failure time and degradation is imposed.

Table 4.4-11: Liner Failure Times

Label	No Fast Flow				Partial or Full Fast Flow			
	Type I Liner Failure Year	Type II Liner Failure Year	Type III Liner Failure Year	Type IV Liner Failure Year	Type I Liner Failure Year	Type II Liner Failure Year	Type III Liner Failure Year	Type IV Liner Failure Year
0	0	0	0	0	0	0	0	0
Early	2,100	2,506	3,100	500	100	100	100	75
Moderate	11,397	12,687	12,751	3,638	1,142	2,506	2,077	1,000
Late	15,000	14,500	14,500	8,000	11,000	12,000	12,000	3,638

The selected failure times align with existing breaks between flow time intervals; therefore, no changes were made to time intervals TI01 through TI40.

Cementitious Material Variation

Degradation times for concrete and grout were rescaled (expanded or contracted) by multiplying and dividing by a factor of 2 to create two off-nominal cases:

- Fast degradation times = nominal degradation times divided by 2
- Slow degradation times = nominal degradation time multiplied by 2

The rescaled degradation times generally did not align with existing breaks between flow time intervals; however, no changes were made to time intervals TI01 through TI40 to achieve matches (as was done for the Base Case).

Infiltration variation

For conceptual closure cap conditions, a nominal infiltration rate of 11.67 in/yr was used (See Table 4.2-19). A “no-cap” infiltration rate of 16.45 in/yr for all time was used as an alternative to the nominal infiltration rate.

Parametric matrix

The parametric cases from which the flow fields are sampled are listed below in Tables 4.4-12 through 4.4-14.

Table 4.4-12: Parametric Cases (No Fast Flow Zones)

Flow Run	Fast Flow	Liner Failure (varies by tank type)	Infiltration Rate (in/yr)	Hydraulic Conductivity Curve
1	None (Case A)	0	Nominal (11.67)	Normal degradation
2	None (Case A)	Early	Nominal (11.67)	Normal degradation
3	None (Case A)	Moderate	Nominal (11.67)	Normal degradation
4	None (Case A)	Late	Nominal (11.67)	Normal degradation
5	None (Case A)	0	Nominal (11.67)	Faster degradation
6	None (Case A)	Early	Nominal (11.67)	Faster degradation
7	None (Case A)	Moderate	Nominal (11.67)	Faster degradation
8	None (Case A)	Late	Nominal (11.67)	Faster degradation
9	None (Case A)	0	Nominal (11.67)	Slower degradation
10	None (Case A)	Early	Nominal (11.67)	Slower degradation
11	None (Case A)	Moderate	Nominal (11.67)	Slower degradation
12	None (Case A)	Late	Nominal (11.67)	Slower degradation
13	None (Case A)	0	No cap (16.45)	Normal degradation
14	None (Case A)	Early	No cap (16.45)	Normal degradation
15	None (Case A)	Moderate	No cap (16.45)	Normal degradation
16	None (Case A)	Late	No cap (16.45)	Normal degradation
17	None (Case A)	0	No cap (16.45)	Faster degradation
18	None (Case A)	Early	No cap (16.45)	Faster degradation
19	None (Case A)	Moderate	No cap (16.45)	Faster degradation
20	None (Case A)	Late	No cap (16.45)	Faster degradation
21	None (Case A)	0	No cap (16.45)	Slower degradation
22	None (Case A)	Early	No cap (16.45)	Slower degradation
23	None (Case A)	Moderate	No cap (16.45)	Slower degradation
24	None (Case A)	Late	No cap (16.45)	Slower degradation

Case A = Base Case

Table 4.4-13: Parametric Cases (Partial Fast Flow Zones)

Flow Run	Fast Flow (Case)	Liner Failure (varies by tank type)	Infiltration Rate (in/yr)	Hydraulic Conductivity Curve
25	Partial (Case B and C)	0	Nominal (11.67)	Normal degradation
26	Partial (Case B and C)	Early	Nominal (11.67)	Normal degradation
27	Partial (Case B and C)	Moderate	Nominal (11.67)	Normal degradation
28	Partial (Case B and C)	Late	Nominal (11.67)	Normal degradation
29	Partial (Case B and C)	0	Nominal (11.67)	Faster degradation
30	Partial (Case B and C)	Early	Nominal (11.67)	Faster degradation
31	Partial (Case B and C)	Moderate	Nominal (11.67)	Faster degradation
32	Partial (Case B and C)	Late	Nominal (11.67)	Faster degradation
33	Partial (Case B and C)	0	Nominal (11.67)	Slower degradation
34	Partial (Case B and C)	Early	Nominal (11.67)	Slower degradation
35	Partial (Case B and C)	Moderate	Nominal (11.67)	Slower degradation
36	Partial (Case B and C)	Late	Nominal (11.67)	Slower degradation
37	Partial (Case B and C)	0	No cap (16.45)	Normal degradation
38	Partial (Case B and C)	Early	No cap (16.45)	Normal degradation
39	Partial (Case B and C)	Moderate	No cap (16.45)	Normal degradation
40	Partial (Case B and C)	Late	No cap (16.45)	Normal degradation
41	Partial (Case B and C)	0	No cap (16.45)	Faster degradation
42	Partial (Case B and C)	Early	No cap (16.45)	Faster degradation
43	Partial (Case B and C)	Moderate	No cap (16.45)	Faster degradation
44	Partial (Case B and C)	Late	No cap (16.45)	Faster degradation
45	Partial (Case B and C)	0	No cap (16.45)	Slower degradation
46	Partial (Case B and C)	Early	No cap (16.45)	Slower degradation
47	Partial (Case B and C)	Moderate	No cap (16.45)	Slower degradation
48	Partial (Case B and C)	Late	No cap (16.45)	Slower degradation

Table 4.4-14: Parametric Cases (Full Fast Flow Zones)

Flow Run	Fast Flow (Case)	Liner Failure (varies by tank type)	Infiltration Rate (in/yr)	Hydraulic Conductivity Curve
49	Full (Case D and E)	0	Nominal (11.67)	Normal degradation
50	Full (Case D and E)	Early	Nominal (11.67)	Normal degradation
51	Full (Case D and E)	Moderate	Nominal (11.67)	Normal degradation
52	Full (Case D and E)	Late	Nominal (11.67)	Normal degradation
53	Full (Case D and E)	0	Nominal (11.67)	Faster degradation
54	Full (Case D and E)	Early	Nominal (11.67)	Faster degradation
55	Full (Case D and E)	Moderate	Nominal (11.67)	Faster degradation
56	Full (Case D and E)	Late	Nominal (11.67)	Faster degradation
57	Full (Case D and E)	0	Nominal (11.67)	Slower degradation
58	Full (Case D and E)	Early	Nominal (11.67)	Slower degradation
59	Full (Case D and E)	Moderate	Nominal (11.67)	Slower degradation
60	Full (Case D and E)	Late	Nominal (11.67)	Slower degradation
61	Full (Case D and E)	0	No cap (16.45)	Normal degradation
62	Full (Case D and E)	Early	No cap (16.45)	Normal degradation
63	Full (Case D and E)	Moderate	No cap (16.45)	Normal degradation
64	Full (Case D and E)	Late	No cap (16.45)	Normal degradation
65	Full (Case D and E)	0	No cap (16.45)	Faster degradation
66	Full (Case D and E)	Early	No cap (16.45)	Faster degradation
67	Full (Case D and E)	Moderate	No cap (16.45)	Faster degradation
68	Full (Case D and E)	Late	No cap (16.45)	Faster degradation
69	Full (Case D and E)	0	No cap (16.45)	Slower degradation
70	Full (Case D and E)	Early	No cap (16.45)	Slower degradation
71	Full (Case D and E)	Moderate	No cap (16.45)	Slower degradation
72	Full (Case D and E)	Late	No cap (16.45)	Slower degradation

Application of Parametric Study Results

A detailed discussion of the parametric study is presented in SRNL-STI-2012-00465, Section 2.3, and the outputs are utilized in the HTF GoldSim Fate and Transport modeling process discussed below.

4.4.4.2 GoldSim Modeling Process

The HTF Stochastic Model is an object-oriented probabilistic model designed to evaluate parameter sensitivity and the influence of parameter uncertainty on the potential for the radiological and chemical contaminants located within HTF for migration to the accessible environment. A detailed description of the HTF Stochastic model development and input parameters can be found in the H-Area Tank Farm Stochastic Fate and Transport Model (SRR-CWDA-2010-00093, Rev. 1). The following sections describe the stochastic modeling process. To support the preparation of the HTF PA, Rev. 1, the HTF GoldSim Model was revised to reflect changes made to the HTF PORFLOW Model as well as to capture updates in the structure of the HTF GoldSim Model that allows the model to represent more rigorously the waste tanks, auxiliary sources, and the saturated zone. [SRR-CWDA-2010-

00093, Rev. 2] While discussing the GoldSim modeling process, the PORFLOW deterministic model is frequently referenced for comparison purposes. Please refer to Section 4.4.4.1 for an expanded explanation of the PORFLOW deterministic implementation.

The stochastic model is, by necessity, simpler than the PORFLOW groundwater model in its environmental transport calculations, but includes additional calculations that cannot be performed in PORFLOW. The HTF GoldSim Model is a 1-D model as opposed to the 3-D HTF PORFLOW Model. Therefore, to replicate the 3-D processes represented in PORFLOW, some additional tasks, such as implementing a plume function, were required during GoldSim modeling. In addition, the HTF GoldSim Model does not model flow velocity independent but uses input flow profiles generated by PORFLOW (see SRR-CWDA-2010-00093, Rev. 2, for the input flow profiles used in the HTF GoldSim Model). Ultimately, to use the stochastic model with confidence, validation of the 1-D HTF GoldSim Model versus the 3-D HTF PORFLOW Model is required and this validation has been explicitly addressed in the GoldSim benchmarking discussion (Section 5.6.2).

The HTF GoldSim Model is comprised of two sub-models, 1) an abstraction of the HTF PORFLOW Model and 2) a dose calculator. Where necessary, the HTF GoldSim Model discussion will differentiate these two sub-models as the transport sub-model and the dose calculator sub-model. The transport sub-model of the HTF GoldSim Model is further divided into two models, one for waste tank types where the mass releases are completely controlled by the liners (Tank Types III, IIIA, and IV), and a separate transport model for waste tank types where mass can be released from sand pads and the annulus prior to liner failure (Tank Types I and II). The abstraction is specifically designed to approximate the process of radionuclide transport from tanks and ancillary equipment sources in a manner that would allow for UA/SA to be performed in a time-efficient manner, while still allowing the influence of parameters on the transport processes to be examined.

The HTF GoldSim Model also includes a dose calculator, which can be used to evaluate dose at points of compliance based on the concentrations generated by the transport abstraction sub-model or generated by the HTF PORFLOW Model. The dose calculator sub-model will be discussed in Section 4.4.4.2.3, while the description below pertains to the GoldSim HTF transport sub-model.

4.4.4.2.1 HTF GoldSim Model Features

The HTF stochastic model was developed using GoldSim (Version 10.5, SP2), which is a graphics based object-oriented computer program designed to carry out dynamic, probabilistic simulations. [GTG-2010d] In addition to its use as a generalized stochastic analysis program, GoldSim contains contaminant and radionuclide transport modules that can be used to develop probabilistic simulations of the release of contaminants from engineered barriers, and the fate and transport of contaminants through natural barriers. GoldSim contaminant and radionuclide transport modules approximate contaminant or radionuclide transport processes analytically (or semi-analytically) using pipe elements (or networks of pipe elements) or numerically using networks of mixing cells (cell pathway elements). [GTG-2010e]

To minimize computation time, the 3-D conceptual model simulated by the HTF PORFLOW Model is compartmentalized into simplified 1-D legs comprised of GoldSim cell pathway elements in the HTF transport model. Each leg is comprised of one or more mixing cells linked in series. When needed to reproduce specific effects in specific waste tank types (Tank Types II and IV), communication between parallel strings of cells was allowed.

In the HTF GoldSim Transport Model, the waste tank structure was divided into several groups of cells, representing the various components of the waste tank structure (e.g., grout, CZ, steel liners, concrete basemat, sand pads, and the annulus grout). Figures 4.4-1 through 4.4-5 display a simplification of the various components that exist for each waste tank type. PORFLOW discretely represents these components, as illustrated in Figures 4.4-15 through 4.4-22. In contrast to the HTF GoldSim Model, certain design elements, such as the concrete roof, and for some waste tanks (Type I, III, and IIIA tanks) the concrete wall, were not represented in the GoldSim HTF transport model.

The unsaturated zone (for non-submerged waste tanks), the saturated zone beneath the contaminant sources (waste tanks and ancillary equipment), and the saturated zone, downgradient from the contaminant sources simulated using GoldSim pipe elements.

Cell Pathway

As noted in the *GoldSim Contaminant Transport Module User's Guide* (GTG-2010e), the cell pathway elements represent discrete, well-mixed environmental compartments or "mixing cells" that can be used to describe the environmental system being simulated. A cell pathway element represents a specific volume of reference fluid (water for the HTF model) and mass of solid(s). Within the cell, complete mixing takes place so there is no spatial differentiation of concentration within any phase. The dissolved species migrate between cells via advection or diffusion.

The GoldSim cell-pathway elements can simulate the transport processes within the waste tanks because the HTF GoldSim Model is designed to evaluate the fate and transport of radionuclide decay chains and can consider the influence of solubility controls on isotopes as well as sorption on the radionuclide transport process. GoldSim allows for two types of mass links between cells, advective links, and diffusive links.

Pipe Elements

The GoldSim pipe elements are based on 1-D analytical solutions to advective-dispersive transport in a constant flow field. The pipe elements are appropriate for the saturated zone analysis because properties, such as K_d s, diffusion coefficients, and velocities are held constant in the saturated zone.

Sub-Models and Looping Structure

The transport modules take advantage of GoldSim sub-model elements to define the transport abstraction as a separate "inner model" which was fed data from the main

model. The sub-models can be switched on when performing GoldSim transport simulations and switched off when using PORFLOW concentration results. In addition, the transport modules take advantage of GoldSim Looping Containers to allow the sub-models to be run in a looping mode for the 47 different contaminant sources (29 waste tanks and 18 ancillary equipment sources). For additional information regarding the looping architecture implemented in the HTF GoldSim Model, refer to Section 3.2 of SRR-CWDA-2010-00093, Rev. 1.

Plume Function

The HTF GoldSim transport sub-models provide a built-in function that can be used to impose the influence of horizontal transverse (lateral) and vertical transverse dispersion on the results generated by a 1-D transport analysis. Designed for use as a multiplier of concentration (or fluxes) at the end of pipe pathway elements to reflect the influence of transverse dispersion on the results, the plume function returns a value between zero and one. It was used in the transport sub-models of the HTF GoldSim Model to account for the influence of lateral and vertical dispersion on the 1-D transport analysis through the chain of cells representing the saturated zone.

For additional details regarding the analytical solutions used in the plume function, see Section 3.1 of SRR-CWDA-2010-00093, Rev. 1.

Monte Carlo Method and Stochastic Elements

The HTF GoldSim Model uses a Latin Hypercube sampling method and stochastic elements to propagate uncertainty in the future performance of the HTF as a barrier to contaminant transport. GoldSim stochastic elements are designed explicitly to represent uncertainty in input parameters within a model. Each uncertain parameter is represented by a range of possible values. The traditional Monte-Carlo method randomly samples the data over the complete probabilistic range at each realization. The Latin Hypercube sampling approach divides each stochastic element's distribution $P\{0,1\}$ into up to 10,000 strata of equal probability. The actual number used is the smaller of the number of realizations and 10,000 strata. The strata are then randomly "shuffled" into a new order and a random value is then picked from each stratum. The application of the Latin Hypercube sampling process ensures that a uniform spanning of sampling occurs. [GTG-2010d]

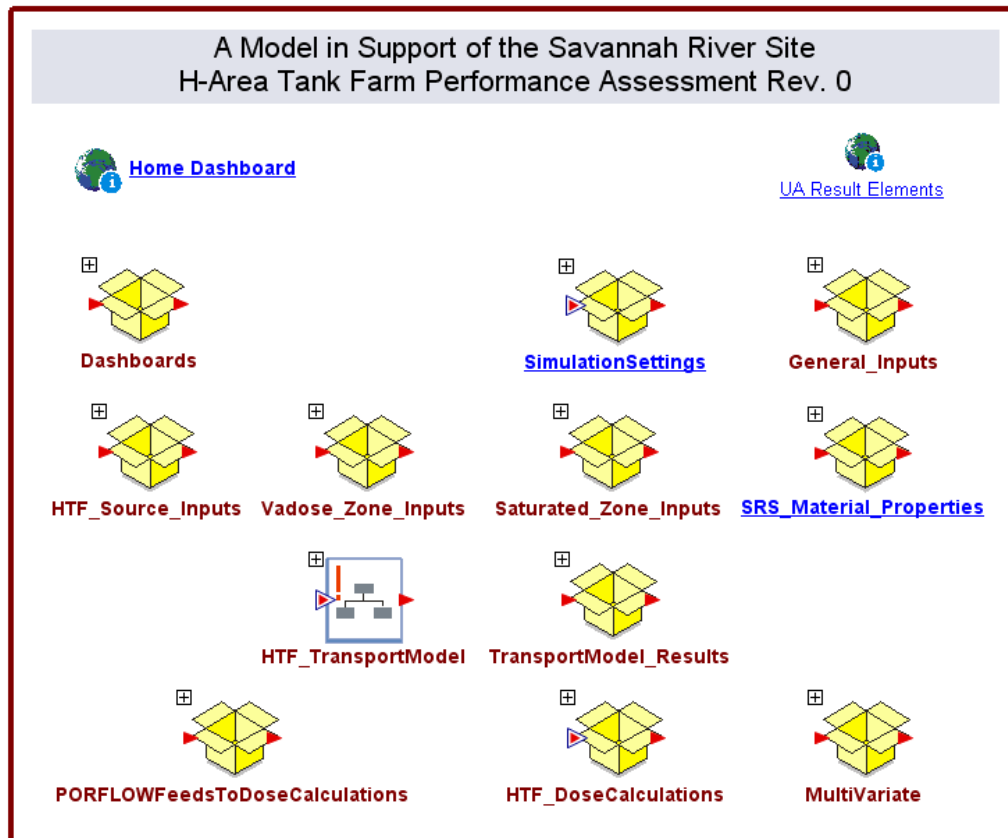
The stochastic parameters implemented within the HTF GoldSim Model are presented in Section 5.6.3, while a discussion of the UA/SAs is provided in Sections 5.6.4 and 5.6.5.

4.4.4.2.2 Transport Model Layout and Structure

Upper Level Model Organization

The HTF GoldSim Model is comprised of three sub-models; the first two represent the abstraction of the HTF PORFLOW Model and the third is the dose calculator. Figure 4.4-48 displays the upper level HTF GoldSim Model organization.

Figure 4.4-48: Top Level of the HTF Stochastic Model



The dose calculator sub-model consisted of the following containers:

- *HTF_DoseCalculations*
- *PORFLOWFeedsToDoseCalculations*

The content of the dose calculator sub-model will be discussed in more detail in Section 4.4.4.2.3.

The following describes the contents of the transport sub-model. As shown in Figure 4.4-48, the static “outer” portion of the transport sub-model, in which all of the control elements and data input elements are assembled, was comprised of the following GoldSim containers:

- *General_Inputs* - contains globally used parameters, such as constants
- *HTF_Source_Inputs* - contains waste tank and ancillary equipment initial inventories
- *Vadose_Zone_Inputs* - contains vadose zone flow and geometry input parameters
- *Saturated_Zone_Inputs* - contains saturated zone properties
- *SRS_Material_Properties* - contains soil, cementitious, and liner material properties

These static “outer” model containers include parameters describing the model domain, (i.e. physical and chemical properties, the model flow system, and model geometry). The deterministic values assigned to the physical and chemical properties were set equal to the values used in the PORFLOW deterministic model. These properties are described in Section 4.2. Stochastic ranges applied to these parameters when the model was simulated in the probabilistic mode are presented in Section 5.6.3. Additional details on the HTF GoldSim Model inputs are included in SRR-CWDA-2010-00093, Rev. 2.

The “inner” portion of the model was defined in:

- *HTF_TransportModel*
- *TransportModel_Results*

The “inner model,” or sub-model, performs all of the dynamic transport calculations for mass transport associated with contaminant source releases. The sub-model was embedded within a series of containers, the uppermost being the *HTF_TransportModel* container (Figure 4.4-48), which deactivates when the time stepping begins for the dose calculator sub-model.

The *TransportModel_Results* container passed results from *HTF_TransportModel* to the main model. Details regarding the internal looping structure of the sub-models are provided in SRR-CWDA-2010-00093, Rev. 1.

The upper level container *MultiVariate* included elements used specifically for the UA/SA, the results of which are discussed in Section 5.6.4 and Section 5.6.5.

The remaining upper level container *Dashboards* provided user controls for users viewing the model with a GoldSim Player.

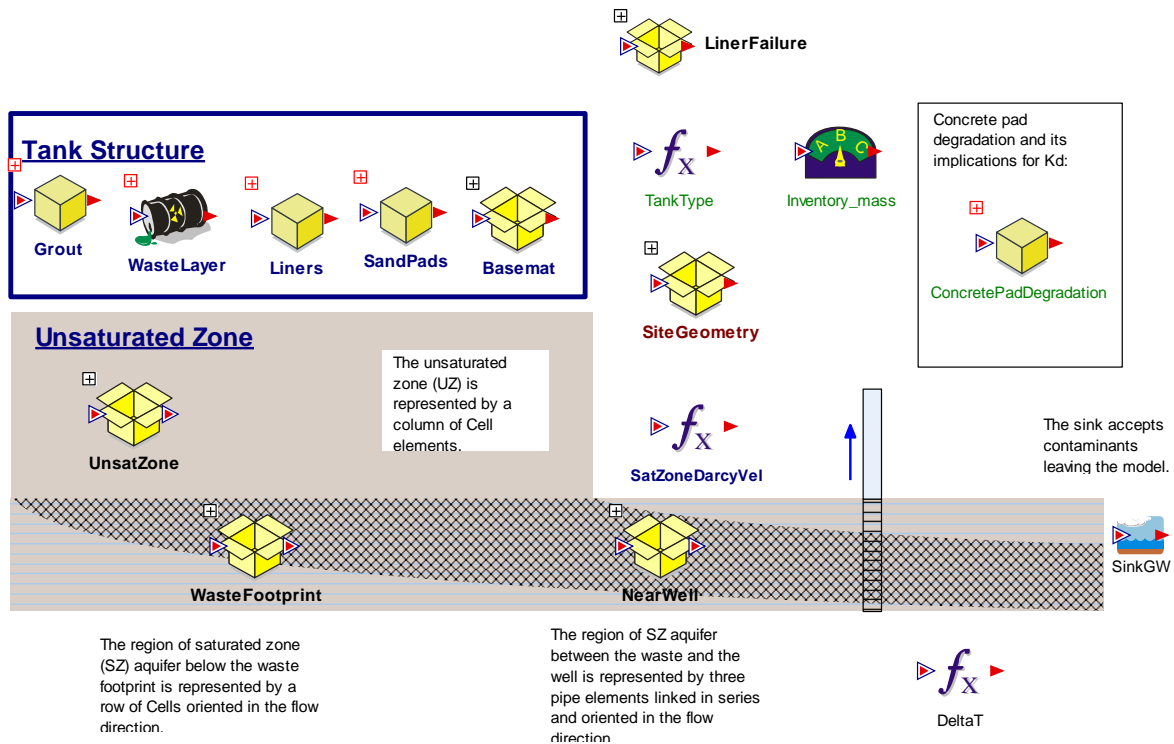
Transport Model Overview

Transport for waste tanks and ancillary equipment are performed separately. Embedded within the *HTF_TransportModel* container (Figure 4.4-48) are the containers, *HTFTanks_Transport_Model* (HTF Tank transport sub-model), *HTFTanks_Transport_Model_TII* (HTF Tank transport sub-model), and *HTFAncillary_Equipment_Model* (HTF Ancillary Equipment transport sub-model).

Tanks

Figure 4.4-49 displays the contents of *HTFTanks_Transport_Model_TII*. The container, *HTFTanks_Transport_Model_TII* contains strings of mixing cells that can be used to evaluate transport of inventory initialized in the annulus (for Type I and II tanks) or in the sand pads (for Type II tanks). The transport element networks found in the container *HTFTanks_Transport_Model* can also be used to evaluate Type I tank releases if it is assumed that there is no initial inventory in the annulus.

Figure 4.4-49: Contents of the Container *HTFTanks_Transport_Model*



Waste Tank Transport

Below is a general overview of the components explicitly modeled in the *HTFTanks_Transport* sub-model.

In the *HTFTanks_Transport* sub-model, also known as the *Vadose_Zone_Inputs* model, the cell networks are distributed within five upper level containers and a source element. The source element is a specialized type of container that is capable of performing functions associated with engineered barrier capabilities. Based upon these functions, this container executes a controlled release into associated cells, which are defined by inserting them into the source element. [GTG-2010d] In the waste tank model, the cell associated with the source element (e.g., *WasteLayer*) represents the CZ in the engineered waste tank structure. In the ancillary equipment model, the cell associated with the source element represents the contaminated soil at the ancillary equipment location.

The upper level containers in the HTF Tank transport sub-model (*HTFTanks_Transport_Model*) that contain segments of the cell network are:

- *Grout*
- *WasteLayer*
- *Liners*
- *SandPads* (for Type II tanks, including annulus and walls for Type I and II tanks)
- *Basemat* (concrete)
- *UnsatZone*
- *WasteFootprint*
- *NearWell*

The transport relationships between these components are simplified in schematic diagrams, presented in Figures 4.4-50 and 4.4-51. Type I and II tanks are identified separately (Figure 4.4-50) because the Type I and Type II tanks have initial inventories at the bottom of the annulus. The occurrence of annulus inventories makes the annulus to wall pathway the controlling release pathway prior to liner failure. After liner failure, the remainder of mass in the annulus is released through the basemat underlying the annulus. In addition, Type II tanks contain initial inventories in the primary (Tanks 13, 14, and 15) or primary and secondary (Tank 16) sand pads. Prior to liner failure, some of the primary sand pad inventory will diffuse into the annulus with some remaining in the annulus and some migrating to wall and out. In evaluating mass release from the Type I and Type II tanks, the annulus and wall are explicitly modeled. Type III, IIIA, and IV tank simulations are based on a simpler abstraction that does not explicitly consider the annulus and wall (Figure 4.4-51). Note that the annulus and wall transport containers are located in the *SandPads* container. This organization is based on an earlier conceptual model that assumed that only the Type II tanks contained an initial inventory outside of the contaminant zone.

Also included in the schematics are the unsaturated and saturated zone model components and the outputs used for dose calculations. Each cell in the diagrams presented in Figures 4.4-50 and 4.4-51 represent a separate domain in the HTF Tank transport sub-model. The arrows indicate the direction of transport and the type of transport, advective or diffusive. The numbered arrows indicate the points at which PORFLOW generated flow fields were used as input to calculate movement of the radionuclides from one domain to another. The thick arrows indicate *HTFTanks_Transport* sub-model output that fed the dose calculator sub-model. Specifically, radionuclide concentrations calculated in the Footprint Cell network and the *NearWell* pipe network are output to the dose calculator sub-model (Section 4.4.4.2.3).

Figure 4.4-50: Schematic of Modeled Components for Type I and II Tanks

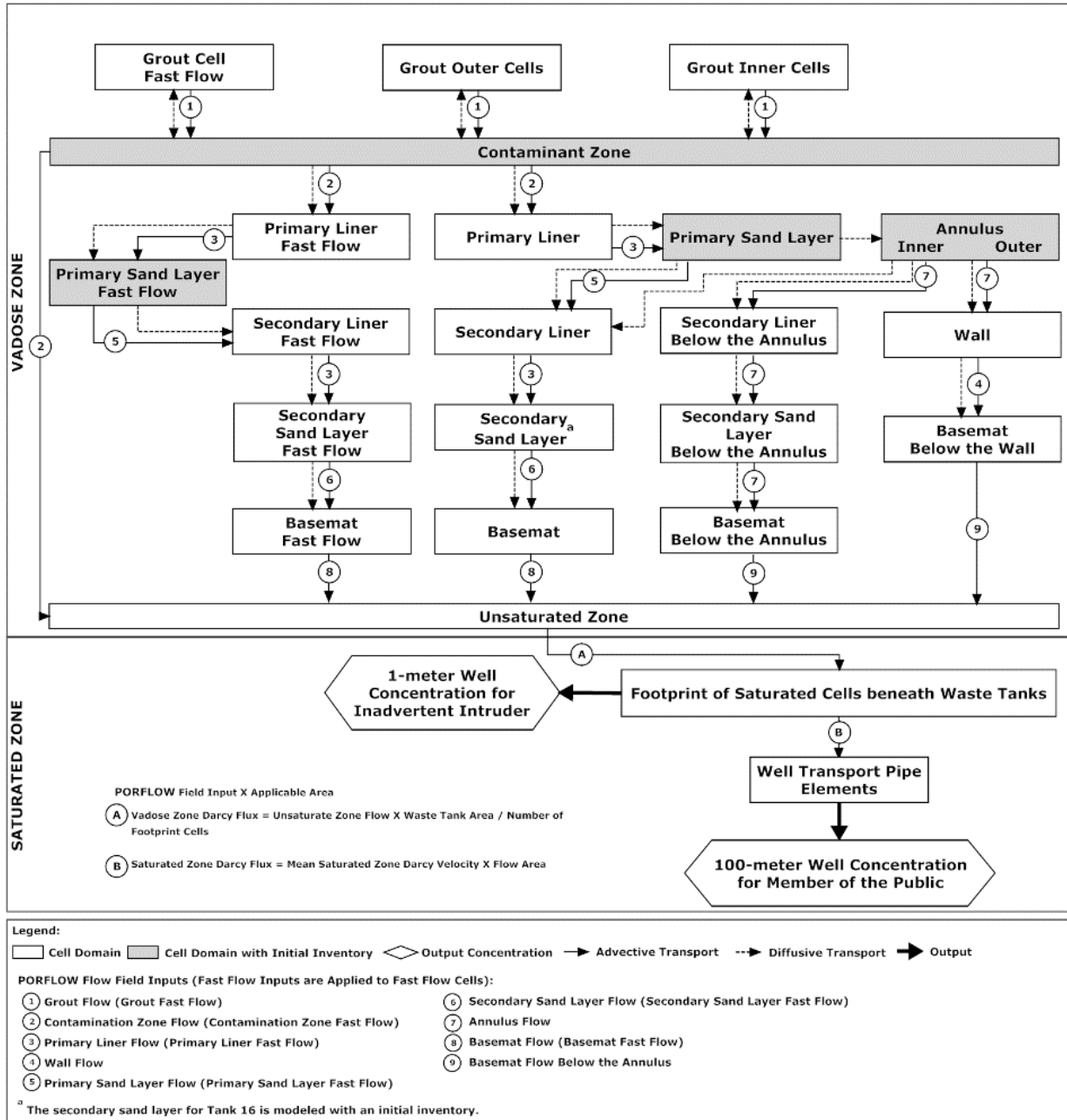
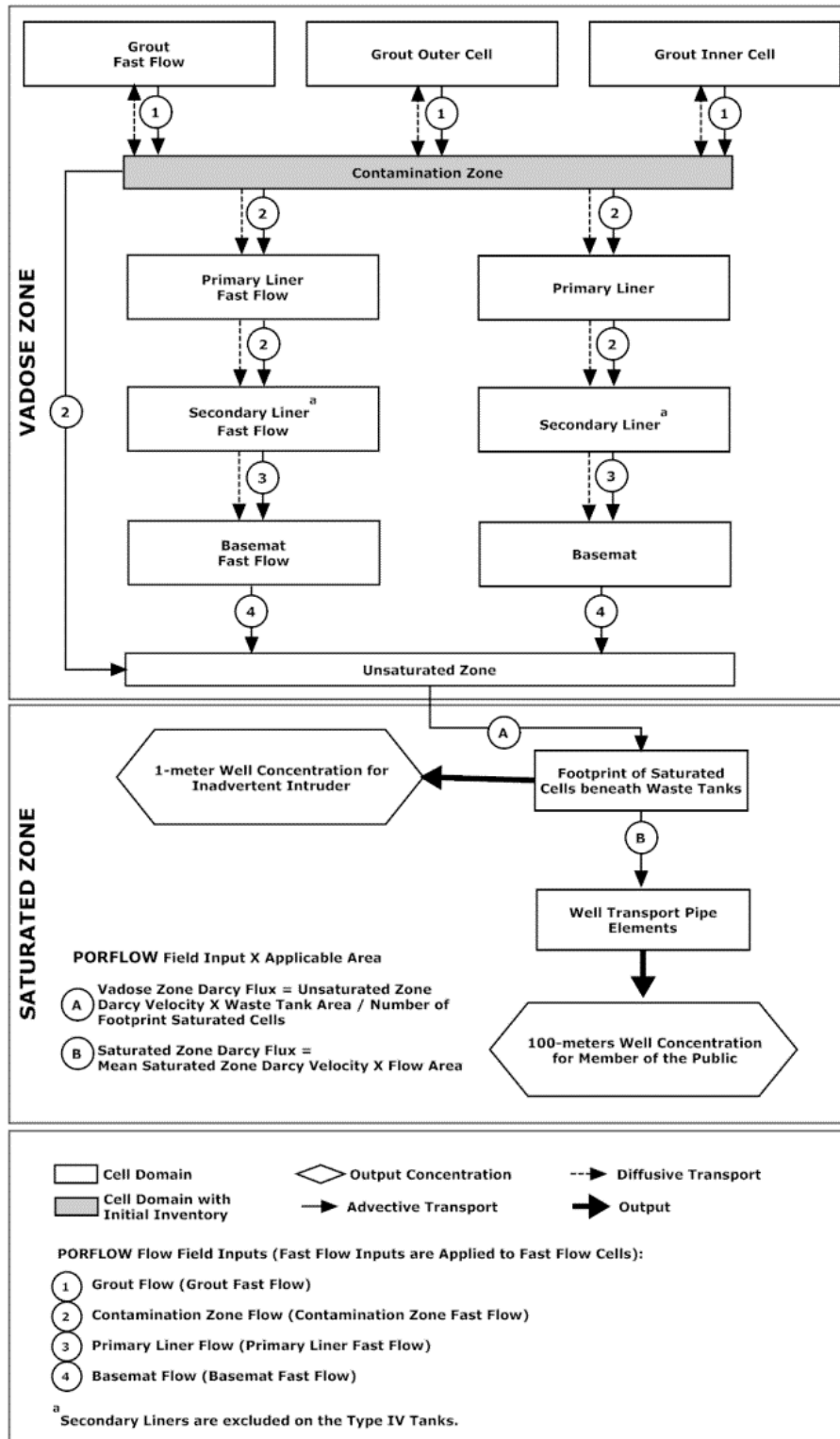


Figure 4.4-51: Schematic of Modeled Components for Type III, IIIA, and IV Tanks



[SRR-CWDA-2010-00093, Rev. 2]

In addition to cells representing the different sections of the tank structure (tank grout, CZ, liners, basemat, unsaturated zone, sand pads, annulus, and wall) separate cell pathways are used to model the fast flow through the grout, liners (and for Type II tanks, the sand pads and secondary liners), and concrete basemat. These fast flow cells are represented in Figure 4.4-50 and 4.4-51 with the suffix, “fast flow.” The fast flow cells are similar in construct to their nominal transport cell counterpart; however, the fast flow area is a fraction of the area of the normal transport cell (set based on the geometry of the different waste tank types). Additionally, a separate PORFLOW generated fast flow flow field was applied to the fast flow cells and sorption is neglected. Transport through these cells was enabled during simulation of the alternative Cases B through E (see Table 4.4-1 for the Waste Tank Case Summary). In the Base Case flow simulations, fast flow cells are simulated using the same flow properties as used in the remainder of the zone in which they occurs. In HTF Transport Model Base Case simulations, sorption is simulated in the fast flow cells. As implemented in the HTF PORFLOW and HTF GoldSim Models, but not evident in the schematics (Figures 4.4-50 and 4.4-51), the fast flow path through the grout is located on the outer ring of the grout. However, upon entering the CZ, the fast flow moved laterally (Figures 4.4-7 through Figure 4.4-10) and then vertically downward through a fast flow path in the basemat in Cases D and E.

Grout

The grout, which fills the space overlying the CZ, is included in the model to simulate the effects of advection (this is mainly important for Type IV tanks) and diffusion of radionuclides and chemical constituents from the CZ upwards into the grout prior to liner failure. This process can be important at early times prior to liner failure when the downward flow in the grout and CZ is very low. Migration of mass upwards into the grout allows for a delaying of the mass released from the grout. The grout is represented by three sets of 20 mixing cells (cell pathway elements) connected in series. The three sets of mixing cells represent an inner cylinder used to capture downward flow, an outer cylinder used to capture upward flow prior to liner failure, and the fast zone between the tank grout and the vertical primary liner. [SRR-CWDA-2010-00093, Rev. 2] All mass that enters the grout originates in the CZ.

Also considered in the model was the influence of water leaching from the grout on the chemistry within the grout, the CZ, and the unsaturated zone. The K_d s within the grout are modeled as a function of the number of pore volumes of water that passed through the grout. The relationship between the number of pore volumes flushed through the grout and the chemistry of the water passing through the grout is discussed in Section 4.2.1 and 5.6.3. Table 5.6-16 (Section 5.6.3) summarizes the number of pore water volumes (deterministic and stochastic ranges) required to flush through the grout before the chemical transition is achieved. The chemical transition times for each waste tank, are calculated by the HTF GoldSim Model and closely match the data provided in Tables 4.4-2 through 4.4-9 (Section 4.4.3). The basis of these calculations, is the PORFLOW based grout volume and either the PORFLOW generated volumetric flow rate through the pore volume (for unsubmerged-grout

conditions in Type II, III, IIIA, and IV tanks) or the vertical Darcy velocity and crossflow factor (see Section 4.4.4.1.2) for submerged-grout conditions found at Type I tanks. The chemical transition times control the K_d s. The timing of physical degradation of the grout and cementitious materials for each waste tank type is given in Table 4.2-30 (Section 4.2.2).

For Cases A, B, and D, solubilities, within the CZ are based on the above chemical transition times calculated for the overlying waste tank reducing grout. Flow through the CZ forms the basis of calculations for Cases C and E. The above chemical transition times, calculated for the overlying waste tank reducing grout, also control the K_d s within the unsaturated zone where present (Type III, IIIA, and IV tanks). In Cases C and E the reducing capacity of the full volume of grout are not considered available to affect the infiltrating water and therefore the K_d s in the unsaturated zone are not controlled by chemical transitions.

Waste Layer/CZ

In the HTF Tank transport sub-model (*HTFTanks_Transport_Model_TII*), the CZ was simulated using the source element, *WasteLayer*. The only barrier considered in the source element, the outer-barrier, failed immediately. Although the steel liner failure may not have occurred yet, the mass was released so that processes, such as upward diffusion from the CZ into the grout and minor leakage through the steel liner, could be considered. Two sources were defined in the source element, *WasteLayer*, the first source term was comprised of the radionuclide species, and the second source term was comprised of the chemical species. A baseline inventory of radionuclides and chemical contaminants were developed for each waste tank and component of ancillary equipment and a detailed description is presented in Sections 3.3.2 and 3.3.3. The source terms represent the median inventory multiplied by a factor that was set to one for deterministic runs and defines the influence of uncertainty for stochastic runs (See Section 5.6.3 for the inventory uncertainty distributions). The source element *WasteLayer* executes a controlled release into the associated cell *WasteCell*, which is located in the source element and represents the CZ in the engineered waste tank structure. Note that in the *HTFTanks_Transport* sub-model *HTFTanks_Transport_Model* the source element has been replaced by a container. Although the source element can be a powerful tool, it is not needed for the simple release model applied here. The structure and the contents within the source element and the container are similar.

Within the CZ, the releases are controlled by solubility limits for species, which readily precipitate under the specified chemical conditions. As described above in the section for waste tank grout, the waste-tank grout transition times control the time-dependent chemical conditions for Cases A, B, and D and the CZ transition times control the time-dependent chemical conditions for Cases C and E.

Liners (and where applicable Sand Pads, Lower Annulus, and Wall)

The timing of contaminant release below the waste tanks is largely a function of the effectiveness of the steel liners. The HTF GoldSim model used the PORFLOW generated primary liner flow field as input. Prior to liner failure, the flow fields generated by PORFLOW indicate very little flow, in general. Type IV tanks, however, have a relatively thin primary liner (0.375 inch compared to 0.5 inch for Type I, II, III, and IIIA tanks, see Figures 4.4-1 through 4.4-5, Section 4.4.1) and no secondary liner. As a result, prior to liner failure, flow through the Type IV liner was greater relative to the other waste tank types.

In contrast, in the HTF GoldSim Model, the onset of diffusive transport through the liners for all waste tank types occurs only after liner failure. This was accomplished by setting the area of diffusion to zero prior to liner failure. Setting the diffusive area to zero is consistent with the HTF PORFLOW Model, which multiplied the liner diffusion coefficient by a factor of 1.0E-6 prior to liner failure. The timing of liner failure for each waste tank type is listed in Table 5.6-6 (Section 5.6.3). The deterministic value (or baseline value) is equal to the median probability value.

Although the liners are thin, relative to the other waste tank components, and do not represent a zone with sorptive capacity, they are very important in limiting diffusive transport. For instance, in Type II tanks, the primary liner limits upward diffusion from the primary sand pad (which has an initial inventory) to the CZ. This is significant because the addition of solubility-limited radionuclides, such as Tc-99, to the CZ could result in underestimated releases of the solubility controlled species. This was avoided by explicitly modeling the liners. The liner (for Type IV tanks) or liners (primary and secondary for Type I, II, III, and IIIA tanks) were each accounted for by a single cell pathway element. Additional complexity was added in the HTF GoldSim Model for Type I and II tanks for adequate replication of the transport results from PORFLOW. For Type II tanks, primary and secondary sand pads are added to the structure and for Type I and II tanks, the section of the annulus and wall located, at/or below the secondary liner was also explicitly simulated. [SRR-CWDA-2010-00093, Rev. 1]

When simulating releases from Type II tanks, sand pads were represented by two cell pathway elements, the *PrimarySandLayer* and *SecondarySandLayer* (and their fast flow counterparts). These sand pads are separated by the cell pathway *SecondaryLiner*. At the time of operational closure, the primary sand pad in the four Type II tanks (Tanks 13 through 16) are considered to have an initial inventory. In addition, the annulus in the Type I and II tanks, and the secondary sand pad in Tank 16 were assigned an initial inventory. For a description of the initial inventory estimates used in the HTF GoldSim Model for the sand pads and waste tanks annulus, refer to Section 3.4.2.

The grouted annulus and wall are important to transport because some of the inventory that is initialized at the bottom of the annulus may be released through the annulus to wall pathway prior to liner failure and the remainder, may be released as a

pulse when the liner fails. The mass initialized within the primary sand pad may also diffuse into the annulus supplementing the mass originating within the annulus.. Because certain chemical species have extremely different K_d s under various chemical conditions in these cementitious barriers, large releases may occur at chemical transition times. Radionuclides controlled by high K_d s under Reducing Region II conditions in the annulus and relatively low K_d s under Oxidizing Region II conditions, such as Tc-99 will rapidly move out of the annulus upon the annulus chemical transition, potentially leading to a pulse in dose. The chemical transition times in the annulus is controlled by the number of pore volumes that will have flushed through the annulus. Radionuclide transport in the wall was also controlled by sorption onto concrete for the different species, however, the initial chemical state of the wall material is Oxidizing Region II, and therefore had less impact on the overall transport as compared to the grouted annulus.

The abstraction of the annulus/vertical-liner/wall system used for Type I and II tanks in the HTF GoldSim Model prepared to support the HTF PA Rev. 1 considers only the segments of the annulus and wall that are located below the vertical liner separating the two zones (see Figures 4.4-1 and 4.4-2). It is assumed that the transport between the annulus and wall takes place in a small area just above the liner prior to liner failure. Therefore, prior to liner failure flow and diffusion take place between the top of the abbreviated annulus and wall zones. After liner failure, it is assumed that the major process controlling vertical transport is downward flow in the wall and annulus and transfer of mass between the annulus and wall is small enough to be neglected. In the original HTF GoldSim Model, movement of radionuclides within the annulus is controlled by diffusion and to a degree upward flow associated with a circulation cell that forms within the localized section of the annulus, prior to liner failure and by downward flow after liner failure.

Prior to liner failure, diffusion from the top of the annulus into a sink cell designed to maintain a near-zero concentration is allowed. The diffusive flux into the sink cell is applied to the top of the wall section in the form of the integrated release from the diffusive link between the top cell of the annulus and the sink cell. In addition to diffusion from the top of the model into the sink cell, to avoid underestimating the release to the wall, the advection associated with a water circulation pattern within the volume of the annulus below the secondary liner is allowed to influence the mass migration into the wall. Because the influence associated with advection in a circulation cell would entail the use of a complex model, the advection is considered in an ad hoc manner. Within the annulus, an abstraction of the circulation pattern seen in the HTF PORFLOW Model prior to liner failure is applied.

The abstraction is implemented by dividing the annulus into two concentric cylinders, which represent an inner and outer zone. When the PORFLOW velocities averaging process is applied to two zones, vertically downward flow occurs in the inner zone and vertically upward flow in the outer zone prior to liner failure. The upward flow is applied to the annulus prior to liner failure and downward flow based on averaging the flow rate over both zones is used after failure. Since a rigorous determination of

how much mass leaves the annulus and enters the wall due to advection cannot be made, the upward flow rate is weighted based upon an analysis comparing GoldSim and PORFLOW peak results prior to liner failure. A multiplier of 0.08 provided a reasonable fit. [SRR-CWDA-2010-00093, Rev. 2]

Basemat (Concrete)

The concrete basemat was represented by a series of five cell pathway elements. Mass entered the concrete at the *ConcretePadIn* cell pathway element from the secondary liner for Type I, III, and IIIA tanks, and from the single liner of the Type IV tanks whereas it entered the Type II tanks from the secondary sand pad. The mass moved downwards through the series of five cell pathway elements representing the basemat, exiting the basemat from *ConcretePadOut*. As with the rest of the waste tank structure mixing cells, transport through the basemat cells is a function of advection and diffusion. Note that because diffusion is simulated, the mass can also diffuse back upwards if the concentration gradient dictates. Similar to the other cementitious barriers, radionuclide transport in the basemat concrete is controlled by sorption and is species and chemical environment dependent.

Type I and II tanks required additional cells to model the section of the concrete basemat below the annulus and wall. The concrete basemat below the annulus (*Basemat_np*), and concrete basemat below the wall (*Basemat_npw*) were each represented by five cell pathway elements. These containers can be found in *SandPads* container (Figure 4.4-49), under *Basemat2*. As with the nominal basemat cells that were discussed in the preceding paragraph, mass transport is a function of advection and diffusion, and is controlled via K_dS under the various chemical environments. The chemical transition times were based on the PORFLOW transition times. The K_dS in the basemat beneath the annulus were controlled by the general basemat transition times and the K_dS beneath the wall were controlled by the wall transition times.

In the HTF GoldSim Model, the basemat is divided into, up to, four cylindrical zones (two for Type III, IIIA, and IV tanks, three for Type I, and four for Type II). The zones are defined outwardly from the center of the waste tank as the fast flow zone at the center of waste tank foot print, a cylinder that underlies the rest of the waste tank footprint, a third cylinder that underlies the annulus, and a fourth cylinder that underlies the wall. [SRR-CWDA-2010-00093, Rev. 2] The vertical discretization of the basemat is the same for all four of its segments. The main reason for rediscrretizing the basemat was to minimize the numerical dispersion seen when simulating the transport of highly sorbing species, such as Np-237.

In order to help reduce numerical dispersion and correlate GoldSim and PORFLOW model results, the vertical linkage of cells from top to bottom is based upon utilizing a string of up to 30 cells. The model gives the user the capability to choose the number of cells (in groups of 5) that represent the basemat for each waste tank type. The choice of the number of cells used in the HTF GoldSim Model to represent the basemat (see Table 4.4-15) is based on the benchmarking analysis comparing the

HTF GoldSim Model with HTF PORFLOW Model results. [SRR-CWDA-2010-00093, Rev. 2]

Table 4.4-15: Vertical Discretization of the Basemat by Waste Tank Type

Waste Tank Type	Number of Cells
Type I	30
Type I (no liner)	30
Type II	30
Type II (no liner)	30
Type III	30
Type IIIA	25
Type IIIA West	25
Type IV	5

Note: That the Type IV tanks use only five cells. This difference is consistent with the smaller number of cells used in the discretization of the HTF PORFLOW Model.

Unsaturated Zone

For waste tank releases, for tanks underlain by an unsaturated zone, a string of 20 mixing cells was used to represent the unsaturated zone. The partially and fully submerged cells still use a set of 10 cells of 0.001-foot total thickness to represent the non-existent unsaturated zone.

Tank Submodel Flow Fields

For the tanks, the HTF GoldSim Model is designed to read in flow data from external files containing PORFLOW generated time series assembled in table form. In addition, a set of flow fields and associated data for 72 possible flow scenarios was generated using the HTF PORFLOW Model (Section 4.4.4.1.5) and assembled in a single file from which the HTF GoldSim Model reads the data associated with the flow scenario that best fits the parameters it has chosen for a specific realization. The logic implemented for the sampling process is discussed in this section and the data used with this new implementation is discussed in Section 5.6.3.

The process of reading in the data is performed using a dynamic link library containing a FORTRAN based function that accepts instructions from the HTF GoldSim Model and returns the data needed which it reads from an external file as per the instructions. The dynamic link library, *ReadFlowFields.DLL* (B-SQP-C-00003), is integrated into the HTF GoldSim Model using GoldSim External elements. Through the external element interface, instructions are passed to the dynamic link library. The instructions and their variable names are listed in Table 4.4-16. The instructions passed to the dynamic link library include:

1. the location of the desired table in the file containing the desired data
2. the location of the data file name in the control file
3. the number of dependent variables in the table from which the data is to be read

4. a file extension number for the control file (set to zero if not used)
5. the number of columns containing the Darcy velocity, volumetric flows and saturations to be returned to the GoldSim model (time series data)
6. the position of the infiltration data in the list of outputs to be read
7. a variable name and column number for each data parcel to be read

For more detailed instructions on data column locations see Table 4.4-16. ReadFlowFields.dll will then return either 1-D tables of time versus dependent variable or scalar variables to the GoldSim-based model. The data passed back from the DLL to the HTF GoldSim Model (as listed in Table 4.4-17) include time series of zone-based Darcy velocities, volumetric flows, saturations, and infiltration rates, as well as scalar values of zone based pore volumes, pH transition times, E_h transition times, and cross-flow rates for fully or partially submerged tanks.

Table 4.4-16: Instruction Data Passed to ReadFlowFields.DLL

Number	Variable Name	Variable Meaning
1	<i>LocNumber</i>	The location of the desired table in a file of ordered 2-D tables each table representing a PORFLOW flow simulation.
2	<i>File Number</i>	The position of the required input file name in a ReadFlowFields.dll control file
3	<i>szTable</i>	The number of dependent-variable columns in the referenced table
4	<i>FileExt</i>	File extension number if desired (normally set to zero)
5	<i>NTimeD</i>	The number of the columns containing Darcy velocity, volumetric flows and saturations to be returned to the HTF GoldSim Model
6	<i>InfilIndex</i>	The position of the infiltration data in the output returned to the HTF GoldSim Model
7 thru the number of variables -1	<i>Variable Names</i>	The position of dependent-variable column in the referenced table for each 1-D table or scalar variable to be returned is found (note that the column number is based on the dependent variables only so that the first three columns representing the run index and time are not considered in determining the position of the columns)
Final Line	<i>Blank</i>	A zero indicating that no more data is requested

[SRR-CWDA-2010-00093, Rev. 2]

Table 4.4-17: Data Extracted from the Flow Field Files

Data	Form	Units
Darcy Velocities	1-D Table	cm/yr
Volumetric Flows	1-D Table	cm ³ /yr
Saturations	1-D Table	N/A
Pore Volumes	Scalar	cm ³
pH Transition Times	Scalar	yr
E_h Transition Times	Scalar	yr
Infiltration Rate	1-D Table	cm/yr
Cross Flow Rate	Scalar	cm/yr

[SRR-CWDA-2010-00093, Rev. 2]

The control file used in the model must be named *ReadFlowFiles.in* or *ReadFlowFilesXX.in* where *XX* is the file extension number passed through the external function interface (see Table 4.4-16). A sample control file is presented in Figure 4.4-52 (the sample file is the file used in the benchmarking study described below). Line by line this control file contains:

1. the number of flow data files that can be chosen from
2. a file name for each flow data file
3. the number of descriptive lines found at the top of the data file (not including the descriptive lines described below)
4. the number of descriptive lines preceding each table (this number is the same for each table)
5. the number of time-specific rows in each table (this number is the same for each table)

Figure 4.4-52: Sample Control File for *ReadFlowFields.DLL*

```
6                ! number of data files to be read
GoldSim_StochasticFlowFields.txt  !
GoldSim_CaseAFlowFields.txt      !
GoldSim_CaseBFlowFields.txt      !
GoldSim_CaseCFlowFields.txt      !
GoldSim_CaseDFlowFields.txt      !
GoldSim_CaseEFlowFields.txt      !
0                ! number of lines in the top-of-file header
1                ! number of rows in the header for each data table
40               ! number of rows in each data table
```

[SRR-CWDA-2010-00093, Rev. 2]

Note there are six data files listed in this control file. The first file contains the flow data for stochastic runs and the other five files contain the flow data for Cases A through E. Note the first file contains 72 x 4 (288) tables for 72 parametric samples and 4 waste tank types (Type I, II, IIIA, and IV). Type III and IIIA West are not included because their results are so similar to the Type IIIA results. The other files each contain 8 tables representing the 8 included waste tank types (Type I, I no-liner, II, II no-liner, IIIA, IIIA West, and IV).

In addition to the file name data, the control file includes the number of text lines at the top of each file, and the number of header lines for each flow data table within a file. The final number in the control file is the number of rows (time steps) in each table.

The flow-field tables included in the file, *GoldSim_StochasticFlowFields.txt*, are based on a parametric study performed using the HTF PORFLOW Model. See Section 4.4.4.1.5 for a discussion of the parametric study.

Saturated Zone Pipe Elements

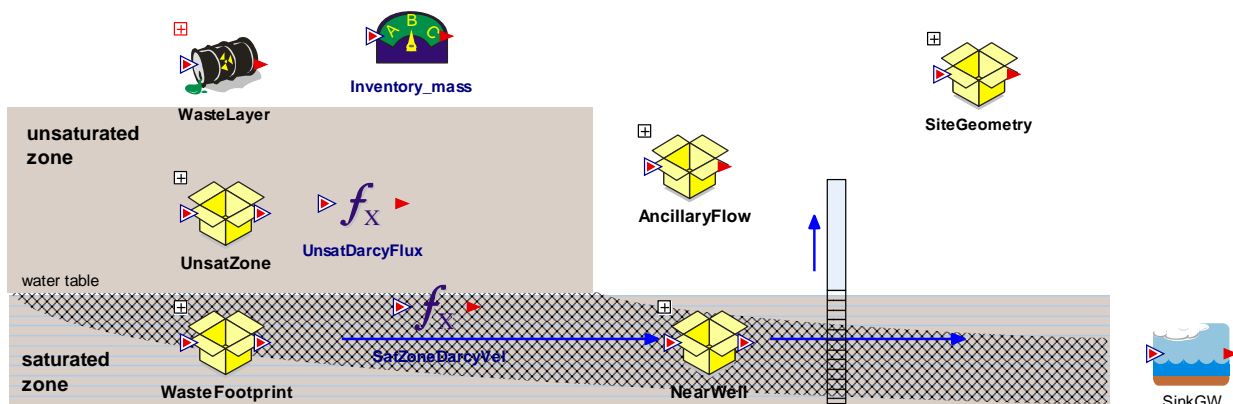
To allow the HTF GoldSim Model user to simulate the effects of longitudinal dispersivity, GoldSim pipe elements are used to simulate radionuclide and chemical constituent fate and transport through the saturated zone. Since the saturated zone properties and flow rates do not change over time, the use of pipes is appropriate. The saturated zone submodel is comprised of three pipes linked in series to allow the

user to experiment with spatially based changes in transport parameters if desired. The mass flux boundary condition for the saturated zone is defined by the output from an integrator element that provides the boundary condition for the pipe element in the form of a cumulative mass release curve generated by the releases from the unsaturated zone to the footprint cells. The boundary condition is applied to the upgradient section of the first pipe with the length of the waste tank diameter. [SRR-CWDA-2010-00093, Rev. 2]

Ancillary Equipment Transport

Figure 4.4-53 displays the components of the HTF Ancillary Equipment transport sub-model. The HTF Ancillary Equipment transport sub-model is represented by two sets of mixing cells linked in series, which release radionuclides and chemical constituents into a single pipe element representing the saturated zone transport leg. The first set of cells represents the backfill containing the ancillary equipment and the second set of cells represents the unsaturated zone beneath. The backfill cells are located within a GoldSim source element and the source term is represented by an instantaneous release of the inventory to a number of cells representing the backfill. The number of cells used to represent the backfill is based on the equipment type and is consistent with the backfill cells used in the PORFLOW simulations. The transfer line zones are represented by 20 cells, and the other ancillary equipment by 4 cells. The conceptual model, for ancillary equipment failure, has the failure occurring at 510 years. Evidence discussed in Section 4.4.2.6 indicates this is a conservative (and simplifying) assumption. The source model immediately applies the inventory to the backfill cells, and the failure timing is implemented by not allowing flow out of the backfill until 510 years have passed. Note that since flow rates are already 5.6 cm/yr by 510 years, the influence of diffusion is disregarded in the ancillary equipment transport calculations and only advective transport is considered.

Figure 4.4-53: Contents of the Container *HTFAncillary_Equipment_Model*



For the ancillary equipment releases, the unsaturated zone is also discretized in a manner that is consistent with the discretization used in the HTF PORFLOW Model. A flexible discretization system allowing the unsaturated zone to be discretized into as many as 60 cells was implemented. To simplify the logic, the discretization allows for the use of multiple sets of 10 cells using from 1 to 6 sets. The number of cells representing the unsaturated zone for each ancillary equipment source is presented in Table 4.4-18.

Table 4.4-18: Vertical Discretization of the Unsaturated Zone by Ancillary Equipment Source

Ancillary Equipment Source	HTF GoldSim Model Unsaturated Zone Cells	HTF PORFLOW Model Unsaturated Zone Cells
HPT 2	10	9
HPT 3	10	9
HPT 4	10	9
HPT 5	10	13
HPT 6	10	13
HPT 7	10	9
HPT 8	10	9
HPT 9	10	9
HPT 10	10	9
E242-H	40	36
E242-16H	50	46
E242-25H	30	25
Transfer-Line 1	40	36
Transfer-Line 2	10	8
Transfer-Line 3	40	36
Transfer-Line 4	10	11
CTS (New)	20	21
CTS (Old)	20	21

4.4.4.2.3 GoldSim Dose Calculator Sub-Model

Because of residual waste in HTF, contaminants may be released to the environment and in turn provide a dose to a potential receptor. Section 4.2.3 identifies the different exposure pathways that contaminants may travel to reach each receptor and Sections 4.6 and 4.7 provide the parameters used to estimate the dose to the receptors. The dose calculator sub-model calculates the dose to each of these receptors via the identified biotic pathways. Table 4.4-19 links the different biotic pathways contributing to the dose to each receptor with the contaminant source. The dose calculator applies an effective dose factor for a given biotic pathway to the identified contaminant concentration in order to calculate the dose to the receptor. The equations defining the dose to each receptor, which is equal to the product of the effective dose factor and the appropriate water or soil contaminant concentration, are detailed in Section 5.4 or Section 6.2 and 6.3 for the intruder. The dose calculator was used to calculate dose for all modeling cases.

Table 4.4-19: Summary of Biotic Pathways by Receptor

Receptor	Path	Biotic Pathway	Contaminant Concentration Source
MOP - Well	Ingestion	Drinking Water	100m water well
		Eating Chicken	100m water well
		Eating Chicken	Fodder (calculated from 100m water well)
		Eating Egg	100m water well
		Eating Egg	Fodder (calculated from 100m water well)
		Eating Beef	100m water well
		Eating Beef	Fodder (calculated from 100m water well)
		Drinking Milk	100m water well
		Drinking Milk	Fodder (calculated from 100m water well)
		Eating Vegetables	Leaf (calculated from 100m water well)
		Eating Vegetables	Root (calculated from 100m water well)
		Eating Fish	Stream (Seepline)
		Eating Soil	Irrigated Soil (calculated from 100m water well)
	Exposure	Irrigated Soil	Irrigated Soil (calculated from 100m water well)
		Swimming	Stream (Seepline)
		Boating	Stream (Seepline)
	Inhalation	Irrigation Water	100m water well
Showering		100m water well	
Dust		Irrigated Soil (calculated from Seepline)	
Swimming		Stream (Seepline)	
MOP - Stream	Ingestion	Drinking Water	100m water well
		Eating Chicken	100m water well
		Eating Chicken	Fodder (calculated from Seepline)
		Eating Egg	100m water well
		Eating Egg	Fodder (calculated from Seepline)
		Eating Beef	100m water well
		Eating Beef	Fodder (calculated from Seepline)
		Drinking Milk	100m water well
		Drinking Milk	Fodder (calculated from Seepline)
		Eating Vegetables	Leaf (calculated from Seepline)
		Eating Vegetables	Root (calculated from Seepline)
		Eating Fish	Stream (Seepline)
		Eating Soil	Irrigated Soil (calculated from Seepline)
	Exposure	Irrigated Soil	Irrigated Soil (calculated from Seepline)
		Swimming	Stream (Seepline)
		Boating	Stream (Seepline)
	Inhalation	Irrigated Soil	Stream (Seepline)
Showering		Stream (Seepline)	
Dust		Irrigated Soil (calculated from stream)	
Swimming		Stream (Seepline)	

Table 4.4-19: Summary of Biotic Pathways by Receptor (Continued)

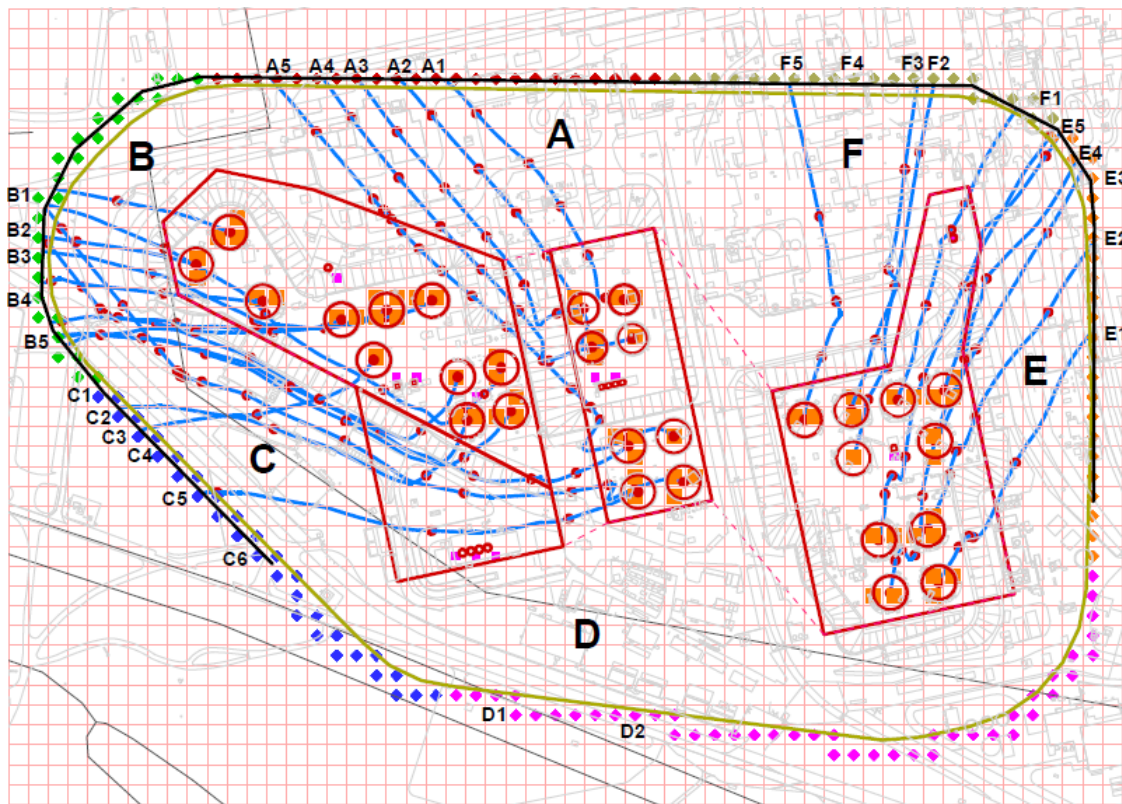
Receptor	Path	Biotic Pathway	Contaminant Concentration Source
Acute – Intruder	Ingestion	Drill Cuttings	Drill Cuttings (calculated from transfer line source)*
	Exposure	Drill Cuttings	Drill Cuttings (calculated from transfer line source)*
	Inhalation	Drill Cuttings	Drill Cuttings (calculated from transfer line source)*
Chronic – Intruder	Ingestion	Drinking Water	1m water well
		Eating Chicken	1m water well
		Eating Chicken	Fodder (calculated from 1m water well)
		Eating Egg	1m water well
		Eating Egg	Fodder (calculated from 1m water well)
		Eating Beef	1m water well
		Eating Beef	Fodder (calculated from 1m water well)
		Drinking Milk	1m water well
		Drinking Milk	Fodder (calculated from 1m water well)
		Eating Vegetables	Leaf (calculated from 1m water well)
		Eating Vegetables	Root (calculated from 1m water well)
		Eating Vegetables	Root (calculated from Drill Cuttings spread around a garden)*
		Eating Fish	Stream (Seepline)
		Eating Soil	Irrigated Soil (calculated from 1m water well)
		Eating Soil	Drill Cuttings spread around garden*
	Exposure	Irrigated Soil	Irrigated Soil (calculated from 1m water well)
		Soil	Drill Cuttings spread around garden*
		Swimming	Stream (Seepline)
		Boating	Stream (Seepline)
	Inhalation	Irrigated Soil	1m water well
Showering		1m water well	
Dust		Irrigated Soil (calculated from 1m water well)	
Dust		Drill Cuttings spread around garden*	
Swimming		Stream (Seepline)	

* Indicates unique contaminant concentration source-specific to the intruder receptor.

GoldSim Calculated Sources by Receptor

MOP Dose from Well Pathways - The MOP is assumed to have access to groundwater via a drinking water well located approximately 100 meters from the HTF boundary. In order to estimate the location that could result in the highest dose, a line of hypothetical wells were placed at the intersection of the 100-meter boundary and the PORFLOW generated stream traces (Figure 4.4-54). The projected dose estimate incurred by the MOP was calculated using groundwater from each well. (Note: HTF GoldSim Model concentrations were evaluated at these same hypothetical 100-meter well locations.)

Figure 4.4-54: HTF Waste Tank Sources with Hypothetical 100-Meter Well Location



Light blue lines = PORFLOW generated stream traces from waste tank sources (circles)

Colored stipple = 100-meter boundary, colored by Sector A through F

A1 through A5, etc. = hypothetical 100-meter well location

Note: The grid used in the Figure 4.4-54 background is coarser than the grid used in the HTF PORFLOW Model, but, the figure was not revised since the locations of the wells and positions of the stream traces associated with the grid refinement are not impacted.

Figure 4.4-54 illustrates the hypothetical 100-meter well locations. A centerline distance and an offset distance along the PORFLOW stream trace was measured from each of the waste tanks to each of the hypothetical wells, and these lengths were input into the HTF GoldSim Model (see Section 4.4 of SRR-CWDA-2010-00093, Rev. 1). Each well receives contaminant contributions from each waste tank (and ancillary equipment), depending on its proximity to the plume emanating from each contaminant source. For a discussion of the plume function, which is used in the calculation of the concentration at each well, see Section 4.4.4.2.1. The GoldSim calculated well concentrations were taken from the container, *ExposureMediaConc*.

MOP Dose from Stream Pathways - Transport assumptions for mobile contaminants are from the HTF area by groundwater through the aquifers underlying the HTF to the outcrops at Fourmile Branch and UTR. Upon reaching the surface water, the contaminants could be present at the seepline, in sediments at the bottom of streams, and at the shoreline. Human receptors could be exposed to contaminants through various pathways associated with the aquifers.

The transport sub-model estimates the concentration of contaminants at the seepline by applying a species dependent ratio ranging from 1 % and 10 % to the GoldSim calculated concentration at the 100-meter well. The data element, *SeeptoWellRatio_vec* contains the individual ratios applied to the 100-meter concentration in order to estimate the seepline concentration for each radionuclide. Although the ratios could have been assigned by element, it was more conservative to evaluate the ratio for the individual radionuclide. Table 4.4-20 displays the ratios used as input to the HTF GoldSim Model. The ratios were based on an analysis documented in Appendix F.

Table 4.4-20: Contaminant-Specific 100-Meter Concentration to Seepage Concentration Ratio

Contaminant	Ratio	Contaminant	Ratio
Ac-227	0.1	Nb-93m	0.1
Ag	0.1	Nb-94	0.1
Ag-108m	0.1	Ni	0.1
Al-26	0.1	Ni-59	0.02
Am-241	0.01	Ni-63	0.1
Am-242m	0.1	NO2	0.1
Am-243	0.01	NO3	0.1
As	0.1	Np-237	0.1
Ba	0.1	Pa-231	0.1
Bi-210m	0.1	Pb	0.1
C-14	0.1	Pb-210	0.1
Ca-41	0.1	Pd-107	0.1
Cd	0.1	Pt-193	0.1
Cf-249	0.1	Pu-238	0.01
Cf-251	0.1	Pu-239	0.01
Cl-36	0.1	Pu-240	0.1
Cm-243	0.1	Pu-241	0.1
Cm-244	0.1	Pu-242	0.1
Cm-245	0.1	Pu-244	0.1
Cm-246	0.1	Ra-226	0.05
Cm-247	0.1	Ra-228	0.1
Cm-248	0.1	Sb	0.1
Co-60	0.1	Se	0.1
Cr	0.1	Se-79	0.1
Cs-135	0.02	Sm-147	0.1
Cs-137	0.1	Sm-151	0.1
Cu	0.1	Sn-126	0.1
Eu-152	0.1	Sr-90	0.1
Eu-154	0.1	Tc-99	0.06
Eu-155	0.1	Th-229	0.1
F	0.1	Th-230	0.02
Fe	0.1	Th-232	0.1
Gd-152	0.1	U-232	0.1
H-3	0.1	U-233	0.1
Hg	0.1	U-234	0.03
I-129	0.02	U-235	0.1
K-40	0.1	U-236	0.1
Lu-174	0.1	U-238	0.1
Mn	0.1	Zn	0.1
Mo-93	0.1	Zr-93	0.1

The individual contaminant ratio (Table 4.4-20) was estimated using PORFLOW Base Case simulated concentrations and was assumed the same for the alternative Cases B through E. Because the alternative cases only change the time of the waste release from the engineered barrier, it was assumed the physical processes within the vadose and saturated zones remain unchanged; therefore using the same ratio for the alternative cases is justified.

Chronic Intruder - The chronic intruder is exposed to contaminants in a drinking water well located 1 meter from a waste tank and from contaminated soil in a garden. In PORFLOW calculations, the concentrations used for the chronic intruder dose calculations are taken at a 1-meter perimeter boundary that surrounds the whole HTF (see Figure 4.4-55). In the HTF GoldSim Model, the chronic intruder analysis is performed by choosing one of seven possible well locations defined by yellow squares in Figure 4.4-55 and evaluating the concentration at that location. The well locations and waste tanks they are adjacent to are identified in Table 4.4-21, along with the PORFLOW grid locations. In addition, the HTF GoldSim Model also considers contributions from upgradient waste tanks to the specified wells. For waste tanks likely to influence concentrations at the specified wells, GoldSim pipe-model analyses are performed to evaluate the contributions to the wells. Lists of the upgradient waste tanks contributing to each of the specified wells are presented in Table 4.4-21. For the present model, the well analyzed is Well 3 (Table 4.4-21), which is adjacent to Tank 12. This choice is based on a comparison of PORFLOW Case-A dose results evaluated at the seven possible wells. For the Base Case, Well 3 showed the highest dose.

Figure 4.4-55: PORFLOW Generated Stream Traces from Waste Tanks with Hypothetical 1-Meter and 100-Meter Boundaries

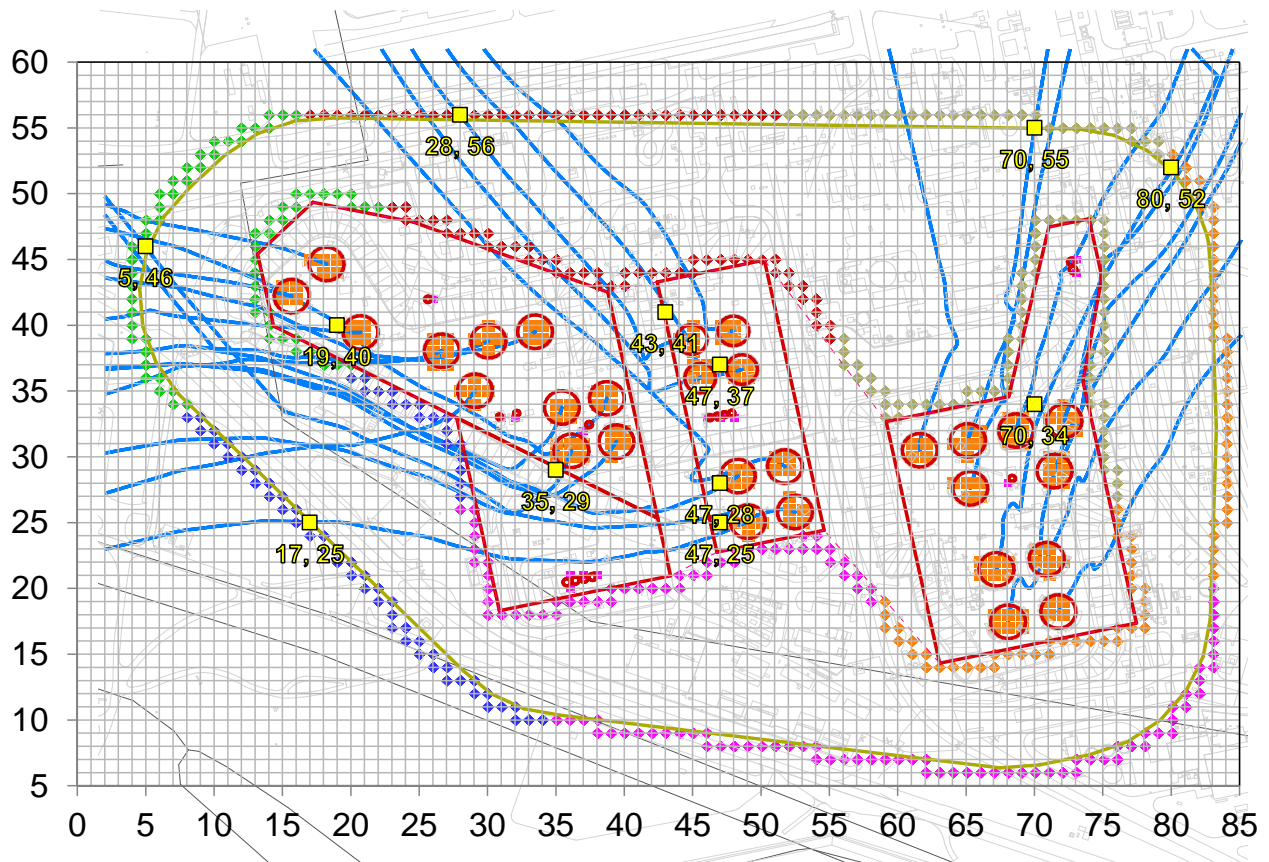


Table 4.4-21: Inadvertent Intruder Analysis Wells

Well Number	Adjacent Waste Tank Number	PORFLOW Model Grid Location (X-Index, Y-Index)	Upgradient Waste Tanks Contributing to Well Concentration
1	40	70, 31	38, 39, 41, 42, 43, 48, 49, 50, 51
2	9	43, 41	10, 11, 12, 14
3	12	47, 37	10, 14
4	13	47, 26	14, 15, 16
5	15	47, 25	13, 14, 16
6	22	35, 29	13, 14, 15, 16, 21, 23, 24, 29, 30, 31
7	35	19, 40	10, 11, 12, 13, 14, 15, 16, 21, 22, 23, 24, 29, 30, 32

[SRR-CWDA-2010-00093, Rev. 2]

For certain pathways, the chronic intruder obtains the additional dose from exposure to contaminated soil (See Table 4.4-19) calculated in the *Intruder_Drilling_Source* container.

Acute Intruder - The acute intruder is exposed to contaminated drill cuttings brought to the surface at the time of drilling. *DrillCuttings_Conc*, also located within *Intruder_Drilling_Source* container, calculates the concentration in the discrete amount of soil brought up during drilling. This concentration was applied to the effective dose factors to calculate the dose to the acute intruder only, while the *CuriesinGarden* represents the drill cuttings spread across a garden of a known volume, and was only applied to the dose of the chronic intruder.

PORFLOW Input Concentrations

The dose calculator sub-model has the functionality of either calculating dose based on concentrations calculated in the GoldSim transport model or from concentrations calculated in the PORFLOW transport model. The concentrations used for PORFLOW dose calculations are housed in container *PORFLOWFeedstoDoseCalculations*. These concentrations are case dependent, and were replaced when calculating PORFLOW dose for the alternative cases, Cases B through E.

Similar to the GoldSim concentrations, the PORFLOW concentrations are evaluated for each sector at the 100-meter water well (Figure 4.4-54) and at the 1-meter water well. A single seepline concentration is used, as opposed to individual sector concentrations. The seepline concentration used here is the maximum radionuclide concentration of the Fourmile Branch or UTR aquifers at each time step.

4.5 Airborne and Radon Analyses

The air and radon pathway analysis was conducted for post-closure time periods. The air and radon pathway PORFLOW transport model had imbedded biases that where possible were conservative in intent (See Section 4.5.3). The same conceptualization was used for both the air and radon pathways analyses. The PORFLOW transport model utilized the same input files for both pathways.

Of the available four waste tank types, the Type I and II tanks were conservatively chosen as representative of all waste tank types for this analysis. This analysis did not consider any associated piping or ancillary equipment. The two waste tank types (out of the four types) chosen were selected because they will have the least grout and concrete thickness above the stabilized CZ (which is located at the bottom of the waste tank). Additionally, for conservatism the minimum closure cap thickness over the waste tanks was assumed. These assumptions were anticipated to produce the maximum flux of gaseous radionuclides at the ground surface.

4.5.1 Air and Radon Pathway Conceptual Model

The approach taken focused primarily on the Base Case where nominal settings for many of the input parameters were conservatively chosen. The main analysis tool employed was the PORFLOW code that simulates the transport of radionuclide chains (i.e., parents and daughters) in porous media. The flux of radioactive gasses at the land surface above the HTF was evaluated for the assumed closure scenarios. Gaseous radionuclides within the CZ diffuse outward into the air-filled pore space of the overlying materials. Ultimately, some of the radionuclides emanate at the land surface. As such, air is the medium through which they diffuse. It was assumed that fluctuations in atmospheric pressure at the land surface that are capable of inducing small pulses of air movement into and out of the shallow soil profile over relatively short periods would have a net zero effect when averaged over longer periods. Thus, advective transport of radionuclides in air-filled soil pores was not considered a significant process when compared to the rate of air diffusion.

The closure cap, as described in SRNL-ESB-2008-00023, consists of a top soil layer, an upper backfill layer, an erosion barrier layer, middle backfill layer, lateral drainage layer, a HDPE geomembrane, a GCL, an upper foundation layer, and a lower foundation layer. The top soil layer, upper backfill layer, HDPE geomembrane and the GCL are excluded from these analyses. By excluding these materials, the baseline air analysis was more conservative as these materials have the expectation of significantly reducing the gaseous flux at the land surface. The HDPE geomembrane would have very low water vapor transmission; the GCL would have high porosity, low hydraulic conductivity, and swell when wet hydraulically plugging any holes that may develop in the HDPE membrane. [WSRC-STI-2007-00184] The HDPE geomembrane and GCL were included in the simulations of water infiltration through the closure cap, as discussed in Sections 3.2.4.1.3 and 4.2.2.2.1. The top soil layer and the upper backfill layer were also excluded from the baseline analysis, since they are located above the erosion barrier and are therefore subject to erosion. The assumption for this analysis was that the components situated below the top of the erosion barrier (soil layers) remain intact for the duration of the simulation (10,000 years).

The Type I and Type II tanks include primary and secondary steel liners situated above a layer of basemat concrete. The top of the waste tank is covered with a concrete roof. For the baseline analysis, the model domain begins at the top surface of the lower primary liner and extends through the stabilized contaminants to the top of the erosion barrier. The baseline model excluded the upper primary steel liner. As with the exclusion of the geomembrane and GCL, excluding the steel liner would make the model more conservative because if included, the expectation is the steel liner would significantly reduce the gaseous flux at the land surface.

The total modeled thickness for a Type I tank and cover materials (excluding the top soil, upper backfill, geomembrane, GCL, and steel liner), including a 1.0-foot (0.3 meter) modeled, stabilized contaminant layer thickness, is 36.33 feet (11.07 meters). Total modeled thickness for the Type II tank waste tank and cover materials (excluding the top soil, upper backfill, geomembrane, GCL, and steel liner), including a 1.0-foot (0.3 meter) thick modeled, stabilized contaminant layer is 41.75 feet (12.73 meters).

The uniform, 1-foot thick, stabilized contaminant layer only applies to the airborne pathway and radon release analyses and was assumed as a conservative modeling simplification. The stabilized contaminant layer thickness in this model differs from the residual solids volume used in the groundwater model to provide a shorter pathway to the surface, thus increasing the gaseous flux to the surface. Table 4.5-1 lists the analysis individual components for the Type I and II tanks (closure cap included). Materials are indicated with the associated thickness in inches, feet, and meters.

Table 4.5-1: Layers and Thicknesses for Type I and II Tanks and Cover Material

Layer	Thickness (in)	Thickness (ft)	Thickness (m)
Erosion Barrier	12	1.00	0.30
Middle Backfill	12	1.00	0.30
Lateral Drainage	12	1.00	0.30
Upper Foundation	12	1.00	0.30
Lower Foundation	72 (min)	6.00	1.83
Type I Concrete Roof	22	1.83	0.56
Type I Grout	282	23.50	7.16
Type II Concrete Roof	45	3.75	1.14
Type II Grout	312	26.00	7.92
Modeled Stabilized Contaminants Layer	12	1.00	0.30

[SRNL-STI-2010-00135]

4.5.2 Air and Radon Pathway Diffusive Transport Model

A 1-D PORFLOW based diffusive transport model Base Case was created for the HTF Type I and II tanks.

The governing equation for mass transport of species k in the fluid phase is given by:

$$\frac{\partial C_k}{\partial t} + \frac{\partial}{\partial x_i} \left(\frac{V_i}{R_f} C_k \right) = \frac{\partial}{\partial x_i} \left(\frac{D_{ij}}{R_f} \frac{\partial C_k}{\partial x_j} \right) + \gamma_k$$

where:

- C_k = concentration of species k , Ci/m³
- V_i = fluid velocity in the i^{th} direction, m/yr
- D_{ij} = effective diffusion coefficient for the species, m²/yr
- R_f = retardation factor
- γ_k = net decay of species k , Ci/m³ yr
- i, j = direction index
- t = time, yr
- x = distance coordinate, m

This equation is solved within PORFLOW to evaluate transient radionuclide transport above the waste tank and to determine gaseous radionuclide flux at the land surface over time. For this analysis, the advection term was disabled within PORFLOW and only the diffusive and net decay terms were evaluated.

The boundary conditions imposed on the entire model domain included:

- No-flux specified for all radionuclides along sides and bottom

$$(\partial C/\partial X = 0 \text{ at } x = 0, x = 1 \text{ and } \partial C/\partial Y = 0 \text{ at } y = 0)$$

- Species concentration set to zero at land surface (top of erosion barrier)

$$(C = 0 \text{ at } y = y_{\max})$$

These boundary conditions force all of the gaseous radionuclides to move upward from the stabilized CZ to the land surface. In reality, some lateral and downward diffusion occurs in the air-filled pores surrounding the stabilized CZ; hence ignoring this lateral and downward movement has the effect of increasing the flux at the land surface. This introduced some conservatism in the calculated results. Simulations were conducted in transient mode for diffusive transport in air, with results being obtained over 10,000 years.

The initial condition imposed on the domain, except for the stabilized CZ, included:

- Species concentration set to zero at time = 0

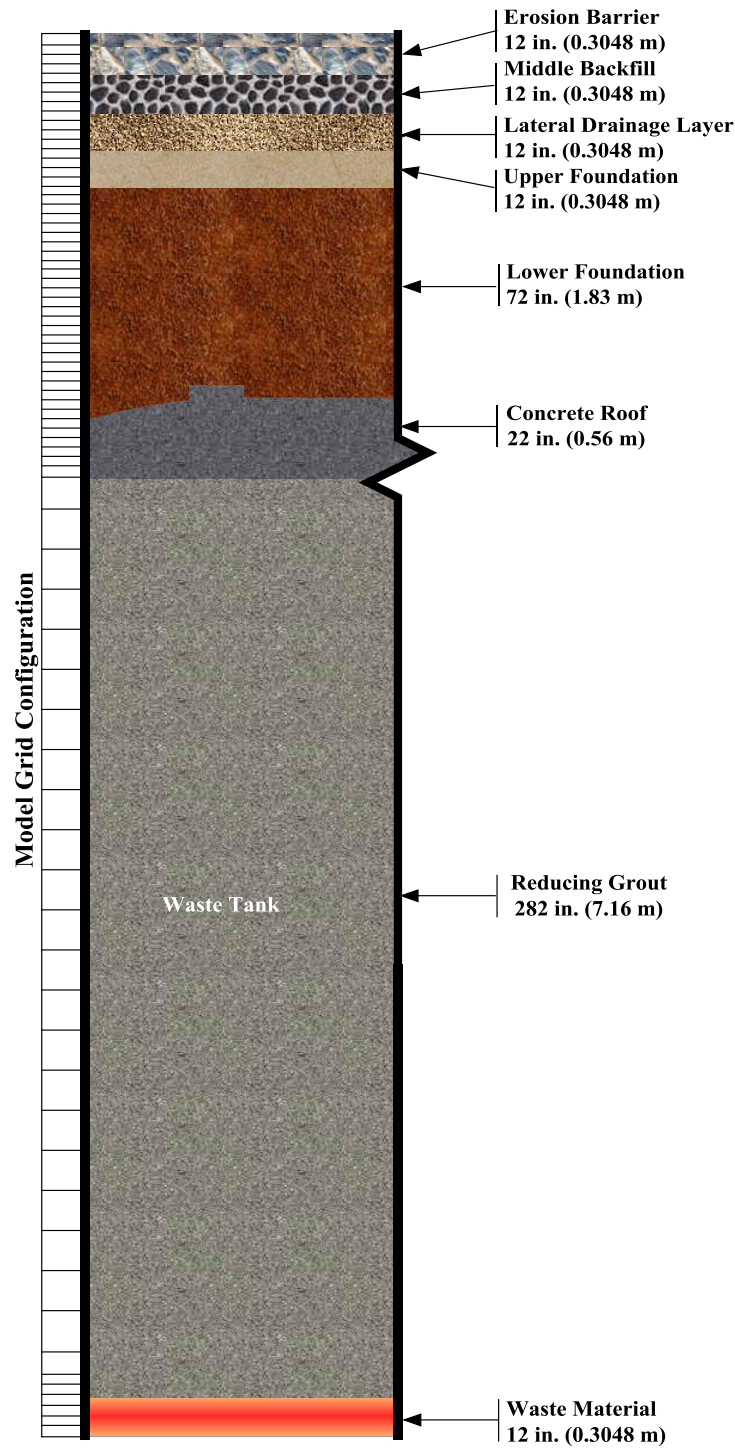
$$(C = 0 \text{ for } 0 \leq x \leq 1 \text{ at } t = 0 \text{ and } C = 0 \text{ for } 0 \leq y \leq y_{\max} \text{ at } t = 0)$$

For the air pathway analysis, the initial conditions for the model assumed a 1-curie inventory uniformly spread over the stabilized CZ for each radionuclide. The radon pathway analysis had an emanation factor of 0.25 applied resulting in an initial inventory of 0.25 curie uniformly spread over the stabilized CZ for each parent radionuclide. The emanation factor for the radon pathway analysis is explained more detail in Section 4.5.6.

4.5.2.1 Grid Construction

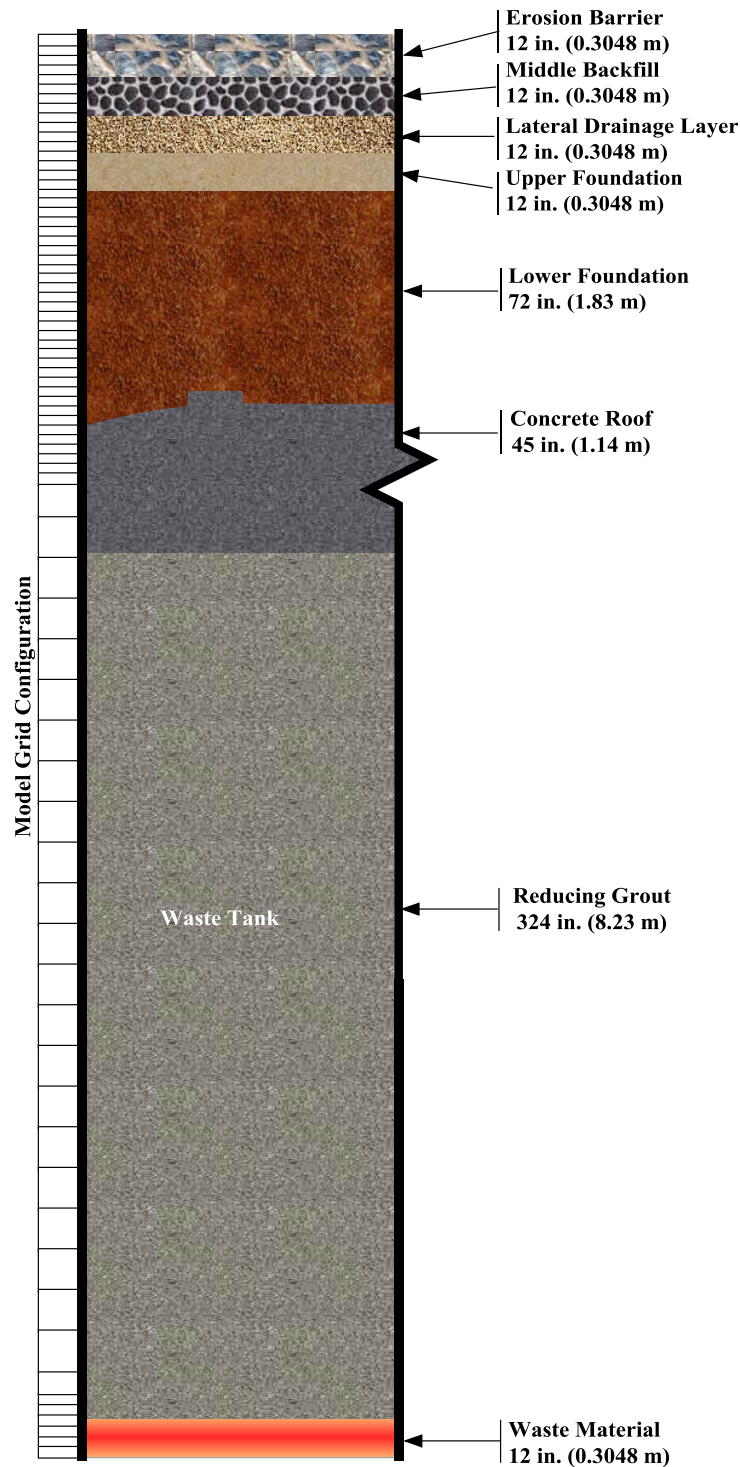
The model grid for the waste tank and overlying cover materials was constructed as a node mesh. This mesh creates a vertical stack of 78 model elements. Figure 4.5-1 shows a schematic of the PORFLOW Type I tank model grid. Figure 4.5-2 shows a schematic of the PORFLOW Type II tank model grid. The minimum possible cover thickness that could exist during the simulation period, the grid extends upward to the top of the erosion barrier. A set of consistent units was employed in the simulations for length, mass, and time, these being meters, grams and years, respectively.

Figure 4.5-1: Schematic of HTF PORFLOW Model Grid for Air and Radon Pathway Analyses for Type I Tanks



Note For conservatism, the model grid does not include the following layers: topsoil, upper backfill, HPDE geomembrane, and GCL.

Figure 4.5-2: Schematic of HTF PORFLOW Model Grid for the Air and Radon Pathway Analyses for Type II Tanks



Note For conservatism, the model grid does not include the following layers: topsoil, upper backfill, HPDE geomembrane, and GCL.

4.5.2.2 Material Zone Properties and Other Input Parameters

Material properties utilized within the 1-D numerical model were specified for eight material zones defined within the model domain. Each material zone was assigned values of particle density, total porosity, average saturation, air-filled porosity, air density, and an effective air diffusion coefficient for each source element or compound. An effective air diffusion coefficient was used for each radionuclide and material layer, therefore tortuosity was assigned a unit value in each material zone. An air fluid density of $1.24\text{E}+03 \text{ g/m}^3$ at standard atmospheric conditions was used in the transport simulations. [SRNL-STI-2010-00135]

The stabilized 1-foot thick contaminant layer was assumed to behave as a non-ideal fluid and confined to the bottom of the waste tank. The waste tank is to be filled with a grout from the existing specification. It was assumed that little to no mixing would occur between the grout and residual materials, and that the stabilized contaminant layer would have similar properties as the grout. The hydraulic and physical properties of this mix are reported in WSRC-STI-2007-00369. Based on the results of this testing, the stabilized contaminant layer and the grout layer were assigned a particle density of 2.51 g/cm^3 and a total and air-filled porosity of 0.266. The concrete roof layer was assumed similar to the basemat surrogate tested and reported in WSRC-STI-2007-00369. This layer was assigned a particle density of 2.51 g/cm^3 and a total air-filled porosity of 0.168. The stabilized contaminant layer and grout were expected to be at or near saturation due to short curing time and material water-retention properties. [WSRC-STI-2007-00369] The concrete roof layer is likely to be at or near saturation, due to infiltration through the closure cap materials over time as the closure cap degrades. [WSRC-STI-2007-00184] For this analysis, a saturation of 50 % was conservatively assumed. Therefore, the air-filled porosity was set equal to 50 % for the total porosity for the waste layer, grout, and concrete roof.

The foundation layer was divided into the upper and lower foundation layers. [WSRC-STI-2007-00184] It is anticipated that the lower foundation layer will need to promote drainage of infiltrating water away from and around the waste tanks, requiring a relatively high-saturated conductivity such as $1.0\text{E}-03 \text{ cm/s}$. It is anticipated that the upper foundation layer will consist of soil with a moderately low permeability (i.e., $\leq 1.0\text{E}-06 \text{ cm/s}$) produced by blending typical SRS backfill with a small weight percent bentonite. The particle density of the lower and upper foundation layers was assigned as 2.63 g/cm^3 that of control compacted backfill from WSRC-STI-2006-00198.

The particle density of the middle backfill layer was also assigned that of control compacted backfill from WSRC-STI-2006-00198 (i.e., 2.63 g/cm^3). The lateral drainage and erosion barrier layers were assigned a particle density typical of quartz (i.e., 2.65 g/cm^3).

Infiltration through the closure cap materials over time, as the closure cap degraded was evaluated using the HELP model. [WSRC-STI-2007-00184] Values for total porosity and volumetric moisture content for the closure cap materials and foundation layers were taken from this analysis. These values were used to calculate the average saturation and the air-filled porosity for the closure cap materials. The maximum air-filled porosity for each

material layer over the 10,000-year simulation was utilized, since this represented the greatest air-filled porosity in which a gas could diffuse.

Table 4.5-2 provides the values of particle density (ρ_n), total porosity (η_T), average saturation (S_a), and air-filled porosity (η_a) utilized for the layers used in the baseline scenario (i.e., waste material layer to the erosion barrier) for the simulation period.

Table 4.5-2: Particle Density, Total Porosity, Average Saturation, and Air-Filled Porosity by Layer for Type I and II Tanks Baseline Scenario

Layer	ρ_n (g/cm ³)	η_T	S_a	η_a
Erosion barrier layer ^{a, c}	2.65	0.150	0.84	0.024
Middle backfill layer ^{b, c}	2.63	0.371	0.82	0.067
Lateral drainage layer ^{a, c}	2.65	0.417	0.61	0.162
Upper Foundation layer ^{b, c}	2.63	0.35	0.72	0.098
Lower Foundation Layer ^{b, c}	2.63	0.457	0.28	0.328
Concrete Roof ^{d, f}	2.51	0.168	0.50	0.084
Grout ^{e, g}	2.51	0.266	0.50	0.133
Stabilized Contaminant Layer ^{f, g}	2.51	0.266	0.50	0.133

- a ρ_n assumed to be that typical of quartz (SRNL-STI-2010-00135)
- b Values for ρ_n taken as that of control compacted backfill from WSRC-STI-2006-00198
- c η_T , S_a , and η_a values derived from WSRC-STI-2007-00184
- d The concrete roof is assumed similar to the basemat surrogate as given by WSRC-STI-2007-00369 ρ_n and porosity(η) is taken from WSRC-STI-2007-00369
- e ρ_n and η of grout is taken from WSRC-STI-2007-00369
- f The stabilized contaminant is assumed to have the properties of grout
- g The concrete roof, grout, and stabilized contaminant layer are assumed conservatively as partially saturated; therefore, the S_a is taken as 50 % and the η_a is taken as one-half η_T

4.5.3 Summary of Key Air and Radon Pathway Assumptions

The following are the key air and radon pathway analyses assumptions associated with the HTF baseline scenario:

- The stabilized contaminant layer was represented as a 1-foot layer of material located at the bottom of the waste tank
- The stabilized contaminant layer, grout, and concrete roof were assumed saturated at 50 %
- The stabilized contaminant layer was assumed to have properties similar to grout
- Exclusion of the top soil, upper backfill, HDPE geomembrane, GCL, and primary steel liner of the waste tank make the model more conservative
- The final closure cap as outlined with exclusions was assumed to remain intact for the duration of the simulation

In this analysis, several conditions introduce conservatism into the calculations. These include:

- Using boundary conditions that force all gaseous radionuclides to move upward from the stabilized CZ to the land surface - some gaseous radionuclides diffuse sideways and downward in air-filled pores surrounding the stabilized CZ; therefore, ignoring this has the effect of increasing flux at the land surface
- Not taking credit for removal of radionuclides via pore water moving vertically downward through the model domain - this mechanism would likely remove some dissolved radionuclides therefore its omission had the effect of increasing the estimate of instantaneous radionuclide flux at the land surface in simulations
- Exclusion of the HDPE geomembrane, GCL, and the primary steel liner of the waste tank - inclusion of these materials in the model would significantly reduce the gaseous flux at land surface due to material properties (i.e., low air-filled porosity)
- Excluding cover materials above the erosion barrier (i.e., top soil and upper backfill layers) - this material exclusion shortens the diffusion pathway and could increase flux at the land surface
- Assuming stabilized contaminant layer, grout, and the concrete roof are only 50 % saturated - these materials are likely at or near saturation making the air-filled porosity equal to one-half the total porosity and increasing diffusive transport through the materials since gaseous flux is through air-filled porosity
- Using Type I and Type II tanks with minimum closure cap thickness
- Concentrating entire estimated HTF residual inventory to a 1-foot stabilized contaminant layer to determine maximum dose and flux
- The minimum apparent inverse Henry's Law coefficients for all possible conditions for a particular radionuclide was used to calculate the partitioning coefficient
- The parent radionuclides would be leached and transported downward from the stabilized CZ by pore water movement, and this potential downward migration of the parent radionuclides was not considered in the radon analysis

4.5.4 Air Pathway Analysis

For the air pathway analysis, a list of radionuclides of interest was chosen based on a NCRP atmospheric screening methodology. [NCRP-123] The radionuclides of concern for the airborne pathway are constrained by the actual waste tank inventory and the limited number of radionuclides susceptible to volatilization. These radionuclides included C-14, Cl-36, I-129, Se-79, Sb-125, Sn-126, H-3, and Tc-99. In accordance with DOE O 435.1 Chg.1, Rn-222 is addressed separately. A summary of the radionuclides and compounds of interest is presented in Table 4.5-3.

Table 4.5-3: Radionuclides and Compounds of Interest for Air and Radon Pathway Analyses

Radionuclide	Half-life (yr)	A_r	Mol in Gas Phase	M_r
C-14	5.70E+03	14	CO ₂	45.99
Cl-36	3.01E+05	36	Cl ₂	72
I-129	1.57E+07	129	I ₂	258
Sb-125	2.76E+00	125	Sb	125
Se-79	2.95E+05	79	Se	79
Sn-126	2.30E+05	126	Sn	126
H-3	1.23E+01	3	H ₂	6
Tc-99	2.11E+05	99	Tc	99
Rn-222	1.05E-02	222	Rn	222

A_r – approximate atomic weight

M_r – molecular weight

[SRNL-STI-2010-00135]

4.5.4.1 Source Term Development

The assumed source term for the simulations was 1 curie of each radionuclide, which was distributed uniformly throughout the liquid filled porosity of the stabilized contaminant layer. The radionuclides were allowed to partition between the pore fluid and the air-filled porosity. Apparent inverse Henry's Law coefficients for each radionuclide for several possible pore fluids for both submerged and non-submerged waste tanks are estimated. [SRNL-TR-2010-00096] Apparent inverse Henry's Law coefficients with units of kilogram atmospheres per mole are reported so that a large value indicates the constituent partitions strongly in the liquid phase. They are also considered apparent because most of the gases dissociate in solution to species other than the aqueous species of the gas. [SRNL-TR-2010-00096] These coefficients are presented in Table 4.5-4. The minimum apparent inverse Henry's Law coefficients for all possible conditions for a particular radionuclide was used to calculate the partitioning coefficient used in the air pathway modeling.

Table 4.5-4: Apparent Inverse Henry’s Law Coefficients for Various Pore Solutions for Waste Tanks

Isotope	Non-Submerged Waste Tank			Submerged Waste Tank				Minimum ^e
	Reducing Region II	Oxidizing Region II	Oxidizing Region III	Condition A ^a	Condition B ^b	Condition C ^c	Condition D ^d	
	H	H	H	H	H	H	H	H
C-14	7.966E+04	8.138E+04	2.807E+00	3.790E-02	3.586E+01	1.569E+02	1.617E+02	3.790E-02
Cl-36	2.961E+17	3.211E+17	3.580E+14	5.160E+11	4.147E+15	1.406E+16	1.439E+16	5.160E+11
I-129	3.632E+20	1.068E+33	1.346E+29	6.329E+14	5.089E+18	1.725E+19	6.959E+29	6.329E+14
Sb-125	1.785E+35	8.726E+70	4.883E+38	6.868E+32	4.294E+44	3.509E+34	9.862E+44	6.868E+32
Se-79	1.789E+06	2.505E+101	3.798E+87	2.822E+25	2.356E+44	8.525E+04	1.594E+96	8.525E+04
Sn-126	1.262E+61	1.806E+71	6.086E+61	9.597E+53	5.115E+69	4.728E+60	4.787E+98	9.597E+53
H-3	2.139E+03	2.139E+03	2.138E+03	2.138E+03	2.138E+03	2.138E+03	2.138E+03	2.138E+03
Tc-99	4.831E+67	5.741E+51	7.168E+45	1.490E+40	9.625E+47	2.108E+68	1.159E+49	1.490E+40

- a Condition A = groundwater
 - b Condition B = groundwater equilibrated with calcite
 - c Condition C = mixture 0.9 groundwater + 0.1 Reduced Region II
 - d Condition D = mixture 0.9 groundwater + 0.1 Oxidized Region II
 - e The minimum apparent $k_{H,inv}$ is for all pore solutions (submerged and non-submerged)
- SRNL-STI-2010-00135 (Table 4)

4.5.4.2 Implementation of Partitioning Coefficients in PORFLOW

PORFLOW has the capability of partitioning radionuclides between the solid and liquid phases through a K_d . However, PORFLOW does not have the capability of directly partitioning radionuclides between the liquid and gas phases through Henry’s Law. Therefore, in order to use PORFLOW to represent transport of radionuclides through the gas phase while considering liquid-gas partitioning, Henry’s Law constants must be converted to equivalent K_d .

The minimum apparent inverse Henry’s Law coefficient for each radionuclide was converted into pseudo-partitioning coefficients for use in PORFLOW. The conventional application of partitioning in PORFLOW involves the transfer of contaminant from solid to liquid phase via a linear and completely reversible reaction. The reaction is represented in the form of K_d , which is used in the calculation of the retardation factor (equation in Section 4.5.2, retardation factor). The K_d is the concentration of contaminants in the solid phase relative to the concentration of contaminant in solution with typical units of milliliter per gram. The air pathway analysis partitioned contaminants from the liquid to the gas phase rather than from the solid to the liquid phase. Therefore, it was necessary to develop a relationship between the apparent inverse Henry’s Law coefficients and the K_d concept used in PORFLOW. The resulting partitioning coefficients used in the PORFLOW air pathway analysis are given in Table 4.5-5.

Table 4.5-5: Apparent Inverse Henry's Law Coefficients and K_d by Radionuclide (Type I and II Tanks)

Radionuclide	$k_{H,inv}$ (mol/atm·kg)	K_d (mL/g)
C-14	3.790E-02	9.111E-01
Cl-36	5.160E+11	1.241E+13
I-129	6.329E+14	1.522E+16
Sb-125, 126	6.868E+32	1.651E+34
Se-79	8.525E+04	2.050E+06
Sn-121m, 126	9.597E+53	2.307E+55
Tc-99	1.490E+40	3.582E+41
Tritium	2.138E+03	5.141E+04

[SRNL-STI-2010-00135]

To implement the partitioning coefficients correctly in PORFLOW it was necessary to redefine the material properties of the stabilized CZ. The typical simulation in PORFLOW involves a solid, liquid, and a gas, with partitioning of contaminants between the solid and liquid phase (via K_d) and advective or diffusive transport occurring through the liquid phase. Inputs include the bulk density of the solid phase and the porosity of the gas-liquid phase. For gaseous diffusion problems, the particle density is that of the solid material, the porosity is the void space occupied by the gas (air-filled porosity), and the fluid density is the density of air. If the gaseous contaminants are assumed to be totally in the gas phase and the waste is assumed dry, then the air-filled porosity equals the total porosity and there is no partitioning. For this air pathway analysis, the waste was assumed to be 50 % saturated with the radionuclides of interest partitioned between the gas and liquid phase based on the material properties presented in Table 4.5-2.

In order to implement the K_d approach to partitioning, the liquid takes on the role usually played by the solid in a typical groundwater transport problem. Likewise, the gas takes on the role usually played by the liquid. The solid phase can be thought of as having the role typically played by gas where it is not involved in the transport process. In this implementation, the total porosity is the content of the solid and gas phases. The air-filled porosity, which is the porosity used in the transport analysis, is determined by multiplying the total porosity by the gas saturation.

Air is the fluid through which the radioactive gasses diffuse to the ground surface. As such, the fluid density input to PORFLOW was the density of air. For each simulation, a 1-curie inventory of each radionuclide was placed in the waste layer and partitioned between the liquid and gas phases according to the partitioning coefficients presented in Table 4.5-5. Once in the gas phase, the radionuclides diffused to the land surface based on the effective diffusion coefficients presented in Table 4.5-6 and the transport equation provided in Section 4.5.2.

4.5.4.3 Effective Air Diffusion Coefficients

The effective air diffusion coefficient of each radionuclide or compound within each material zone was determined. A relationship was established between moisture saturation and the radon effective air-diffusion coefficient for various pore sizes of earthen materials. Using

this method, a radon effective air-diffusion coefficient was determined for each material type based upon the average moisture saturation for the material. [SRNL-STI-2010-00135] Subsequently, using Graham's Law, the effective air-diffusion coefficient of each radionuclide or compound evaluated was determined for each material type based on the radon effective air-diffusion coefficient using the following relationship:

$$D = D' \sqrt{\frac{MWT'}{MWT}}$$

Where:

- D = the effective diffusion coefficient of the radionuclide of interest (m^2/yr) within the material zone of interest
- D' = the effective diffusion coefficient of Rn-222 (m^2/yr) within the material zone of interest
- MWT' = the molecular weight of the reference radionuclide (Rn-222)
- MWT = the molecular weight of the element or compound of interest

A summary of the radon effective air-diffusion coefficients and the calculated effective air-diffusion coefficients for each radionuclide/compound by material zone are presented in Table 4.5-6.

Table 4.5-6: Effective Air-Diffusion Coefficients by Radionuclide/Compound and Material for Type I and II Tanks and Closure Cap

Radionuclide	Tank Stabilized Contaminants, Grout, and Concrete Roof Layer (m^2/yr)	Lower Foundation Layer (m^2/yr)	Upper Foundation Layer (m^2/yr)	Lateral Drainage Layer (m^2/yr)	Middle Backfill Layer (m^2/yr)	Erosion Barrier Layer (m^2/yr)
C-14	1.358E+01	2.658E+01	5.752E+00	9.213E+00	3.196E+00	2.858E+00
Cl-36	1.085E+01	2.124E+01	4.597E+00	7.364E+00	2.555E+00	2.284E+00
H-3	3.760E+01	7.359E+01	1.593E+01	2.551E+01	8.850E+00	7.912E+00
I-129	5.734E+00	1.122E+01	2.429E+00	3.890E+00	1.350E+00	1.207E+00
Rn-222	6.181E+00	1.210E+01	2.618E+00	4.194E+00	1.455E+00	1.301E+00
Sb-125	8.237E+00	1.612E+01	3.489E+00	5.589E+00	1.939E+00	1.734E+00
Se-79	1.036E+01	2.028E+01	4.389E+00	7.030E+00	2.439E+00	2.181E+00
Sn-126	8.205E+00	1.606E+01	3.475E+00	5.567E+00	1.931E+00	1.727E+00
Tc-99	9.256E+00	1.812E+01	3.921E+00	6.280E+00	2.179E+00	1.948E+00

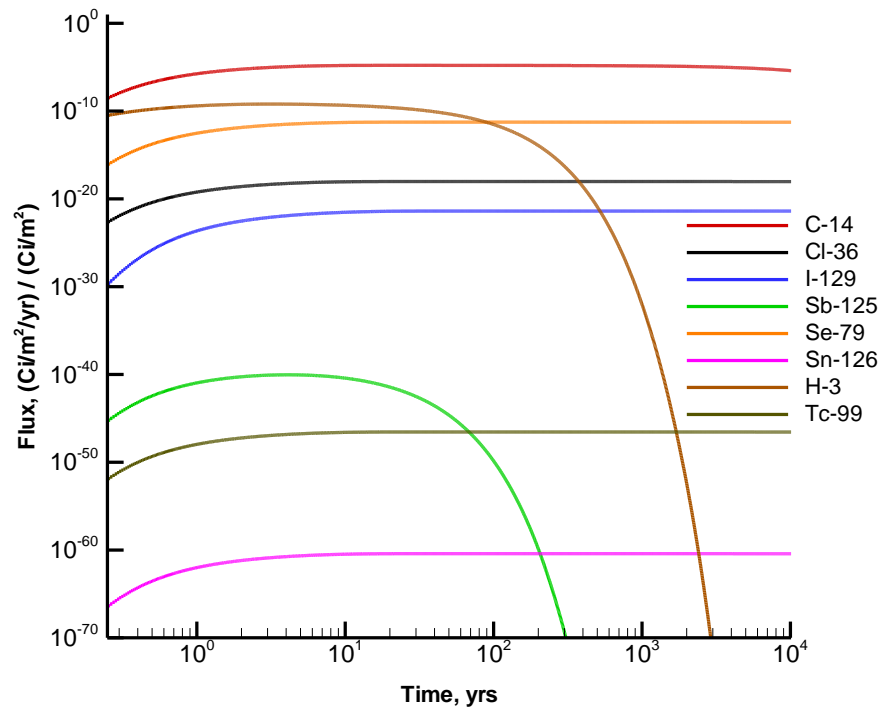
Note The effective diffusion coefficient for Rn-222 was used to determine the effective air diffusion coefficient of each radionuclide/compound based on Graham's Law (Graham's Law states that the rate of diffusion of a gas is inversely proportional to the square root of its molecular weight). [SRNL-STI-2010-00135]

4.5.5 Air Pathway Model Factors for a Unit Curie

4.5.5.1 Air Pathway Flux to Ground Surface

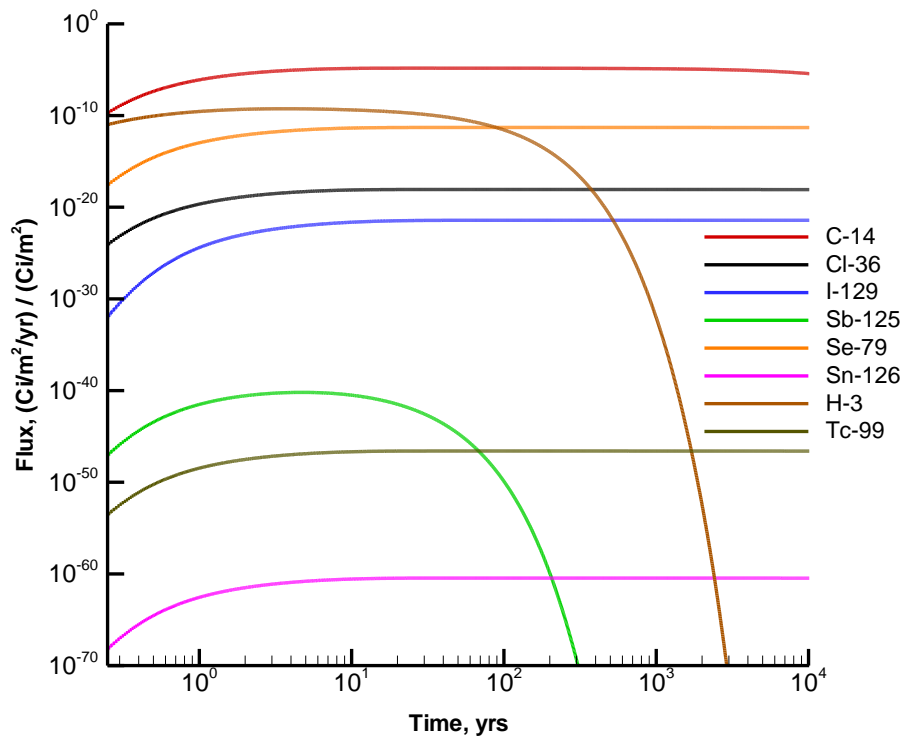
Model simulations were conducted to evaluate the peak flux of each radionuclide (other than radon) emanating from the top of the model domain. A unit inventory of 1 curie was assigned to the HTF Type I and Type II tanks stabilized CZ for each radionuclide considered in the analysis. Results were output in curies per year, consistent with the set of units employed in the model, and are presented for each radionuclide in Figure 4.5-3 for Type I tanks and in Figure 4.5-4 for Type II tanks. The peak fluxes emanating at the land surface are presented for Type I tanks in Table 4.5-7 and for Type II tanks in Table 4.5-8 for each period. The results are reported in this way to facilitate calculation of human exposure at the SRS boundary, at 100 meters from HTF, and at 2,360 meters from HTF (i.e., UTR representative seepline distance).

Figure 4.5-3: Flux at Land Surface per Curie of Radionuclide Remaining Type I Tanks



[SRNL-STI-2010-00135]

Figure 4.5-4: Flux at Land Surface per Curie of Radionuclide Remaining in Type II Tanks



[SRNL-STI-2010-00135]

Table 4.5-7: Peak Fluxes for Each Radionuclide for Type I Tanks

Radionuclide	Activity in Residual Waste (Ci)	Peak Flux (Ci/yr/Ci)	
		0 - 100 Yrs	100 - 10,000 Yrs
C-14	1.0	1.62E-05	1.60E-05
Cl-36	1.0	9.53E-19	9.53E-19
H-3	1.0	6.33E-10	2.93E-12
I-129	1.0	4.11E-22	4.11E-22
Sb-125	1.0	9.10E-41	1.31E-50
Se-79	1.0	5.51E-12	5.51E-12
Sn-126	1.0	3.88E-61	3.88E-61
Tc-99	1.0	2.82E-47	2.82E-47

[SRNL-STI-2010-00135]

Table 4.5-8: Peak Fluxes for Each Radionuclide for Type II Tanks

Radionuclide	Activity in Residual Waste (Ci)	Peak Flux (Ci/yr/Ci)	
		0 - 100 Yrs	100 - 10,000 Yrs
C-14	1.0	1.47E-05	1.45E-05
Cl-36	1.0	8.65E-19	8.64E-19
H-3	1.0	5.53E-10	2.66E-12
I-129	1.0	3.73E-22	3.73E-22
Sb-125	1.0	6.35E-41	1.19E-50
Se-79	1.0	5.00E-12	5.00E-12
Sn-126	1.0	3.52E-61	3.52E-61
Tc-99	1.0	2.56E-47	2.55E-47

[SRNL-STI-2010-00135]

4.5.5.2 Air Pathway Unit Dose Calculations

An evaluation was conducted to assess the potential unit dose to a MEI located 100 meters from HTF, the UTR seepline, and Fourmile Branch seepline. [SRNL-STI-2010-00135] The DRFs were calculated for each radionuclide potentially released from the HTF using CAP-88, the EPA model for NESHAP. The unit dose to the receptor exposed to 1 curie of the specified radionuclide potentially released to the atmosphere is represented by DRFs. For the receptor located at the seepline locations, the distance from the HTF is sufficient for an assumption of a point source. However, the DRFs for the 100-meter receptor required evaluation of an area source because of the close proximity of HTF to the 100-meter receptor. For radionuclides not contained within the CAP-88 library (Se-79, Cl-36) atmospheric transport was estimated by assigning the surrogate Sn-126, which has a similar half-life to Se-79 and Cl-36. [SRNL-STI-2010-00018] Unit doses for radionuclides not contained within the CAP-88 library were estimated by applying their dosimetric properties to the surrogate's relative air concentrations estimated by the model.

The SRS-specific 100-meter DRFs and the calculated Type I and Type II tank exposure levels for the MEI within 10,000-years are presented in Table 4.5-9 and Table 4.5-10. Site-specific seepline DRFs and the calculated Type I and Type II tank exposure levels for the MEI within 10,000-years at the seepline locations are presented in Table 4.5-11 through Table 4.5-14. Assuming that the entire HTF inventory is evenly distributed within either a representative Type I or Type II tank, the dose to the MEI can be calculated to conservatively bound the dose from airborne radionuclides (as further described in Section 5.3).

Table 4.5-9: 100-Meter DRFs and Type I Tank Exposure Levels within 10,000 Years

Radionuclide	Peak Flux (Ci/yr/Ci)	SRS 100m DRF ^a (mrem/Ci)	Unit Dose to MEI at 100m Boundary ^b (mrem/yr/Ci)
C-14	1.60E-05	8.1E-03	1.3E-07
Cl-36	9.53E-19	1.7E-02	1.6E-20
H-3	2.93E-12	1.7E-04	5.0E-16
I-129	4.11E-22	1.2E+01	4.9E-21
Sb-125	1.31E-50	2.3E-01	3.0E-51
Se-79	5.51E-12	2.3E-02	1.3E-13
Sn-126	3.88E-61	1.1E+01	4.3E-60
Tc-99	2.82E-47	6.4E-02	1.8E-48

a SRNL-STI-2010-00018

b Unit dose to MEI at 100 meters = Peak Flux × DRF (SRNL-STI-2010-00135)

Table 4.5-10: 100-Meter DRFs and Type II Tank Exposure Levels within 10,000 Years

Radionuclide	Peak Flux (Ci/yr/Ci)	SRS 100m DRF ^a (mrem/Ci)	Unit Dose to MEI at 100m Boundary ^b (mrem/yr/Ci)
C-14	1.45E-05	8.1E-03	1.2E-07
Cl-36	8.64E-19	1.7E-02	1.5E-20
H-3	2.66E-12	1.7E-04	4.5E-16
I-129	3.73E-22	1.2E+01	4.5E-21
Sb-125	1.19E-50	2.3E-01	2.7E-51
Se-79	5.00E-12	2.3E-02	1.1E-13
Sn-126	3.52E-61	1.1E+01	3.9E-60
Tc-99	2.55E-47	6.4E-02	1.6E-48

a SRNL-STI-2010-00018

b Unit dose to MEI at 100 meters = Peak Flux × DRF (SRNL-STI-2010-00135)

Table 4.5-11: UTR Seepline (2,360 Meter) DRFs and Type I Tank Exposure Levels within 10,000 Years

Radionuclide	Peak Flux (Ci/yr/Ci)	UTR 2,360m DRF ^a (mrem/Ci)	Unit Dose to MEI at 2,360m Boundary ^b (mrem/yr/Ci)
C-14	1.60E-05	1.2E-03	1.9E-08
Cl-36	9.53E-19	3.2E-03	3.0E-21
I-129	4.11E-22	9.3E-01	3.8E-22
Sb-125	1.31E-50	5.2E-02	6.8E-52
Se-79	5.51E-12	4.8E-03	2.6E-14
Sn-126	3.88E-61	2.4E+00	9.3E-61
H-3	2.93E-12	2.5E-05	7.3E-17
Tc-99	2.82E-47	1.4E-02	3.9E-49

a SRNL-STI-2010-00018

b Unit dose to MEI at 2,360 meters = Peak Flux × DRF (SRNL-STI-2010-00135)

Table 4.5-12: UTR Seepage (2,360 Meter) DRF and Type II Tank Exposure Levels within 10,000 Years

Radionuclide	Peak Flux (Ci/yr/Ci)	UTR 2,360m DRF ^a (mrem/Ci)	Unit Dose to MEI at 2,360m Boundary ^b (mrem/yr/Ci)
C-14	1.45E-05	1.2E-03	1.7E-08
Cl-36	8.64E-19	3.2E-03	2.8E-21
I-129	3.73E-22	9.3E-01	3.5E-22
Sb-125	1.19E-50	5.2E-02	6.2E-52
Se-79	5.00E-12	4.8E-03	2.4E-14
Sn-126	3.52E-61	2.4E+00	8.4E-61
H-3	2.66E-12	2.5E-05	6.7E-17
Tc-99	2.55E-47	1.4E-02	3.6E-49

^a SRNL-STI-2010-00018

^b Unit dose to MEI at 2,360 meters = Peak Flux × DRF (SRNL-STI-2010-00135)

Table 4.5-13: Fourmile Branch Seepage (1,170 Meter) DRFs and Type I Tank Exposure Levels within 10,000 Years

Radionuclide	Peak Flux (Ci/yr/Ci)	Fourmile Branch 1,170m DRF ^a (mrem/Ci)	Unit Dose to MEI at 1,170m Boundary ^b (mrem/yr/Ci)
C-14	1.60E-05	3.9E-03	6.2E-08
Cl-36	9.53E-19	9.5E-03	9.1E-21
I-129	4.11E-22	3.6E+00	1.5E-21
Sb-125	1.31E-50	1.5E-01	2.0E-51
Se-79	5.51E-12	1.4E-02	7.7E-14
Sn-126	3.88E-61	6.6E+00	2.6E-60
H-3	2.93E-12	8.0E-05	2.3E-16
Tc-99	2.82E-47	4.0E-02	1.1E-48

^a SRNL-STI-2010-00018

^b Unit dose to MEI at 1,170 meters = Peak Flux × DRF (SRNL-STI-2010-00135)

Table 4.5-14: Fourmile Branch Seepage (1,170 Meter) DRFs and Type II Tank Exposure Levels within 10,000 Years

Radionuclide	Peak Flux (Ci/yr/Ci)	Fourmile Branch 1,170m DRF ^a (mrem/Ci)	Unit Dose to MEI at 1,170m Boundary ^b (mrem/yr/Ci)
C-14	1.45E-05	3.9E-03	5.7E-08
Cl-36	8.64E-19	9.5E-03	8.2E-21
I-129	3.73E-22	3.6E+00	1.3E-21
Sb-125	1.19E-50	1.5E-01	1.8E-51
Se-79	5.00E-12	1.4E-02	7.0E-14
Sn-126	3.52E-61	6.6E+00	2.3E-60
H-3	2.66E-12	8.0E-05	2.1E-16
Tc-99	2.55E-47	4.0E-02	1.0E-48

^a SRNL-STI-2010-00018

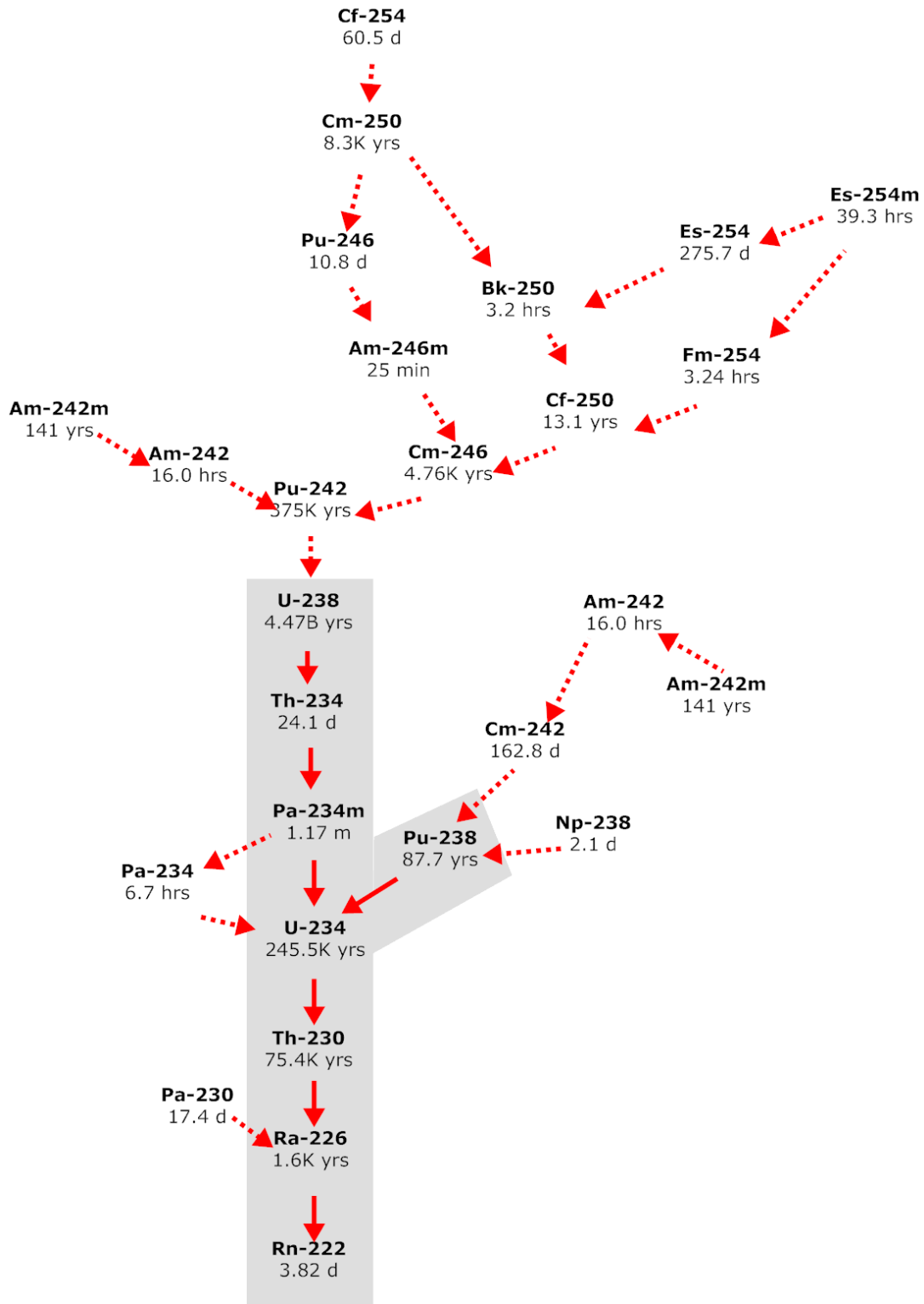
^b Unit dose to MEI at 1,170 meters = Peak Flux × DRF (SRNL-STI-2010-00135)

4.5.6 Radon Analysis

The permissible radon flux for DOE facilities is addressed in DOE M 435.1-1 IV.P.(c) stating the radon flux requirement is that the release of radon shall be less than an average yearly flux of 20 pCi/m²/s at the surface of the facility. The performance objective refers only to radon, and the correct species must be analyzed depending on the characteristics of the residual waste stream. The instantaneous Rn-222 flux at the land surface was evaluated for 10,000-years.

The potential parent radionuclides that can contribute to the creation of Rn-222 are illustrated in Figure 4.5-5. The diagram indicates the specific decay chains that lead to the formation of Rn-222, as well as the half-lives for each radionuclide. The extremely long half-life of U-238 (4.468E+9 years) causes the other radionuclides higher up on the chain of parents to be of little concern with regard to their potential to contribute significantly to the Rn-222 flux at the land surface over the period of interest. In Figure 4.5-5, the parent radionuclides that were individually evaluated are indicated with the gray shaded area (i.e., beginning with Pu-238 and U-238). Generated within the stabilized CZ, Rn-222 is in the gaseous phase and diffuses outward from this zone into the air-filled soil pores surrounding the HTF, eventually resulting in some of the radon emanating at the land surface. As such, air is the fluid through which Rn-222 diffuses, although some Rn-222 may dissolve in residual pore water.

Figure 4.5-5: Radioactive Decay Chains Leading to Rn-222



The parent radionuclides are assumed to exist in the solid phase and therefore do not migrate upward through the air-filled pore space, although they could be leached and transported downward from the stabilized CZ by pore water movement. This potential downward migration of the parent radionuclides was not considered in the radon analysis.

Decay chains evaluated were $U-238 \rightarrow Th-234 \rightarrow Pa-234m \rightarrow U-234 \rightarrow Th-230 \rightarrow Ra-226 \rightarrow Rn-222$ and $Pu-238 \rightarrow U-234 \rightarrow Th-230 \rightarrow Ra-226 \rightarrow Rn-222$. Each parent in these chains, except Th-234 and Pa-234m, was simulated separately as the starting point of the decay chain. [SRNL-STI-2010-00135] Compared to the other parent radionuclides in these chains, Th-234 and Pa-234m have extremely short half-lives. Only a fraction of the Rn-222 generated by the decay of each parent is available for migration away from its source and into open pore space. Since the Rn-222 parent radionuclides exist as oxides or in other crystalline forms, only a fraction of Rn-222 generated by decay of Ra-226 has sufficient energy to migrate away from its original location into adjacent pore space before further decay occurs (3.82-day half-life for Rn-222).

The emanation coefficient is generally defined as the fraction of the total amount of Rn-222 produced by radium decay that escapes from soil particles and enters the pore space of the medium (the fraction of the Rn-222 that is available for transport). In the case of the HTF, the parent radionuclides are not embedded in soil but are contained within stabilized contaminants entombed in concrete/grout. Literature values for the Rn-222 emanation factor for these conditions are not available. Studies have shown the emanation factor to vary between 0.02 and 0.7 for various soil types depending primarily on moisture content. Generally, higher emanation factors are associated with higher moisture contents. [SRNL-STI-2010-00135]

RESidual RADioactivity (RESRAD) computer software is a model used to estimate radiation dose and risk from residual radioactive materials. [ANL-EAD-4] This DOE and NRC approved code assumes an emanation factor of 0.25 for Rn-222, which is representative of a silty, loam soil with low moisture content. For the HTF radon pathway analysis, the RESRAD default emanation factor of 0.25 was chosen recognizing that literature values for residual wastes similar to the HTF are not available. [SRNL-STI-2010-00135] The use of 0.25 was conservative since the assumption is that the stabilized contaminant is partially saturated and emanation factors reported in the literature for drier soils are much lower. To account for the emanation factor in the model, an effective source term of 0.25 curie of parent radionuclide was utilized for each curie disposed within the facility. [SRNL-STI-2010-00135]

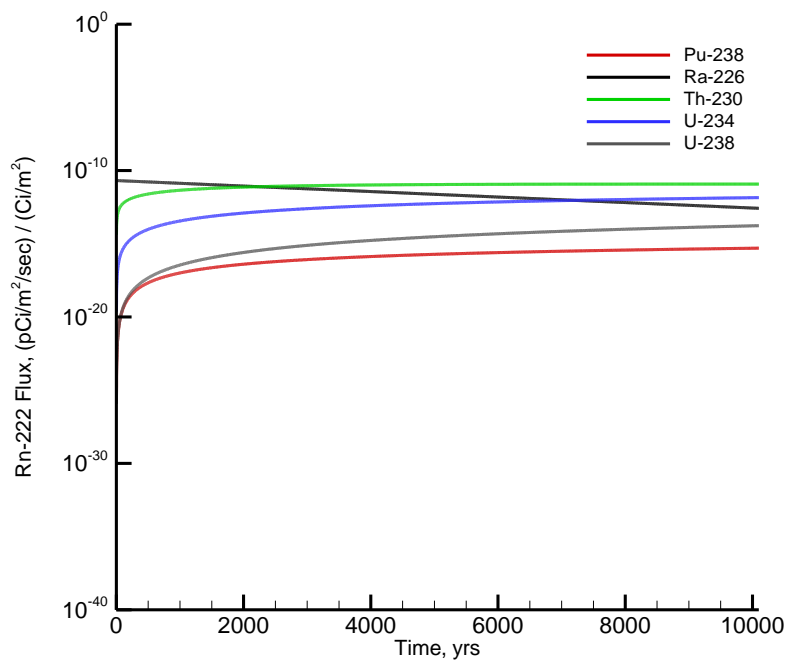
Some radon dissolves in pore water, but since diffusion proceeds slower in fluid, air diffusion was the only transport process by which Rn-222 was allowed to reach the land surface of the HTF. The molecular diffusion coefficient of Rn-222 in open air is $347 \text{ m}^2/\text{yr}$ ($1.1E-05 \text{ m}^2/\text{s}$). [SRNL-STI-2010-00135] A relationship between moisture saturation and the radon effective air-diffusion coefficient for various pore sizes of earthen materials was established. This method was used to calculate a radon effective air-diffusion coefficient for each material type based upon the average moisture saturation for the material. Tortuosity was assigned a unit value for each material type. A summary of the radon air-diffusion coefficients by material type are presented in Table 4.5-6.

4.5.7 Radon Pathway Model Results

Model simulations were conducted to evaluate the peak instantaneous Rn-222 flux at the land surface for the compliance period for Type I and Type II tanks. Unlike the air pathway analysis presented in PA Section 4.5.5, which computes a unit dose from all HTF sources at surface locations away from the closed HTF, the radon analysis evaluates the peak radon flux at a surface location of expected maximum flux within the confines of the HTF. Because of the greater amount of cementitious material in Type III, IIIA, and IV tanks, the expected maximum radon flux would be less than either a Type I or Type II tank.

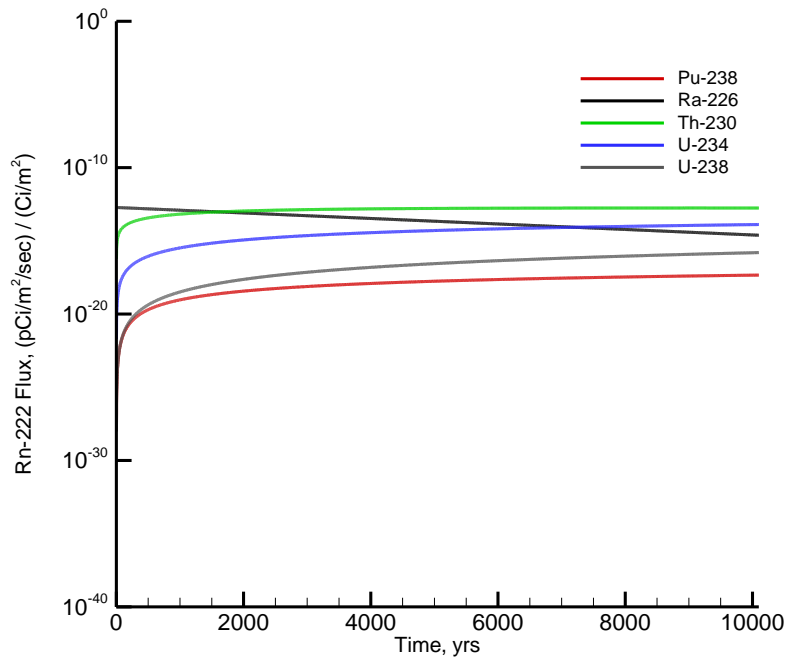
Model results were output in curie per meter squared per year for each curie of inventory per meter squared, consistent with the set of units employed in the model. A graph of these results is shown in Figure 4.5-6 for Type I tanks and in Figure 4.5-7 for Type II tanks. The units are converted to picocurie per squared meter per second ($\text{pCi}/\text{m}^2/\text{s}$) for each curie per squared meter (Ci/m^2), which are the units used to define the regulatory flux limit in DOE M 435.1-1. The peak fluxes represent the peak flux Rn-222 Ci/m^2 at the land surface, and are given in Table 4.5-15 for Type I tanks and in Table 4.5-16 for Type II tanks.

Figure 4.5-6: Rn-222 Flux at Land Surface Resulting from Unit Source Term for Type I Tanks



[SRNL-STI-2010-00135]

Figure 4.5-7: Rn-222 Flux at Land Surface Resulting from Unit Source Term for Type II Tanks



[SRNL-STI-2010-00135]

Table 4.5-15: Simulated Peak Instantaneous Rn-222 Flux over 10,000 Years at the Land Surface for Type I Tanks

Parent Rn-222 Source (1 Ci/m ²)	Flux (pCi/m ² /s) / (Ci/m ²)
Pu-238	5.01E-16
Ra-226	2.08E-11
Th-230	1.19E-11
U-234	1.42E-12
U-238	1.72E-14

[SRNL-STI-2010-00135 Table 25]

Table 4.5-16: Simulated Peak Instantaneous Rn-222 Flux over 10,000 Years at the Land Surface for Type II Tanks

Parent Rn-222 Source (1 Ci/m ²)	Flux (pCi/m ² /s) / (Ci/m ²)
Pu-238	4.59E-18
Ra-226	1.91E-13
Th-230	1.75E-13
U-234	1.30E-14
U-238	1.58E-16

[SRNL-STI-2010-00135 Table 26]

4.6 Biotic Pathways

The purpose of this section is to document the Bioaccumulation Factors and Human Health Exposure parameters used in the HTF PA modeling effort. Exposure pathways for the HTF PA are discussed in Section 4.2.3. Bioaccumulation Factors and Human Health Exposure parameters are used to calculate doses for each of the pathways.

4.6.1 Bioaccumulation Factors

For PA analyses at SRS, soil-to-vegetable (also known as soil-to-plant ratios or plant-to-soil ratios), feed-to-milk, feed-to-beef, water-to-fish, feed-to-poultry, and feed-to-egg transfer factors are the bioaccumulation factors considered. Soil-to-vegetable transfer factors determine the fraction of an element that is drawn from the soil into the edible plant. Feed-to-milk transfer factors represent the element-specific fraction transferred from fodder to milk. Feed-to-beef transfer factors represent the element-specific fraction transferred from fodder-to-beef. Water-to-fish transfer factors are the equilibrium ratios between concentration in finfish and concentration in water. Feed-to-poultry transfer factors represent the element-specific fraction transferred from fodder to poultry. Feed-to-egg transfer factors represent the element-specific fraction transferred from fodder to eggs.

The factors utilized were developed based on comparison to a number of other DOE facilities and generic national and international references to establish relevance of the parameters selected and as needed, verify the regional differences for the Southeastern United States.

4.6.1.1 *Bioaccumulation Factor Methodology*

A report entitled *Land and Water Use Characteristics and Human Health Input Parameters for use in Environmental Dosimetry and Risk Assessments at the Savannah River Site* documents the SRS evaluation and reviews of transfer factors. [SRNL-STI-2010-00447] This report presents additional details on factors utilized in the past and discussion on factors developed for SRS use. This report also established a standardized source for bioaccumulation factor parameters that represent current data.

In developing SRNL-STI-2010-00447, a comprehensive literature review was completed and references were updated to include the latest available information. These values from the more recent compilations were recommended, rather than those in older publications. The general hierarchy on document use at SRS for bioaccumulation factors is listed below:

- Site-specific
 - WSRC-TR-96-0231
 - SRT-EST-2003-00134
 - SRNL-STI-2009-00178
- IAEA-472
- PNNL-13421
- ORNL-5786
- NCRP-123, Volume 1

Issued in 2010, the *Handbook of Parameter Values for the Prediction of Radionuclide Transfer in Terrestrial and Freshwater Environments* (IAEA-472) provides parameter values for radionuclide, bioaccumulation, and transfer in terrestrial and freshwater environments. This report supersedes IAEA-364 (*Handbook of Parameter Values for the Prediction of Radionuclide Transfer in Temperate Environments*) which was a key source of data in previous PA models.

Baseline Parameter Update for Human Health Input and Transfer Factors for Radiological Performance Assessments at the Savannah River Site (WSRC-STI-2007-00004) provides an evaluation of several sources of transfer factors and recommends values for use at SRS. WSRC-STI-2007-00004 recommends PNNL-13421 as the secondary source of values if site-specific values are not available. The hierarchy of documents in PNNL-13421 used to establish transfer factors is IAEA-364, NUREG_CR-5512, and NCRP-123 Volume 1. IAEA-364 encompasses a variety of plant types however; it has been superseded by IAEA-472. Residual Radioactive Contamination from Decommissioning: Technical Basis for Translating Contamination Levels to Annual Total Effective Dose Equivalent, NUREG_CR-5512, is frequently referenced because it contains a large set of data and traceable references. Screening Models for Releases of Radionuclides to Atmosphere, Surface Water, and Ground, NCRP-123, is chosen because it is a generally accepted reference for a generic model. WSRC-STI-2007-00004 also recommended values from ORNL-5786 as a third source. In ORNL-5786, the hierarchy of documents used to establish transfer factors is Regulatory Guide 1.109, then the TERRA code values.

A survey of land and water usage characteristics within a 50-mile region of the SRS was conducted and documented in WSRC-RP-91-17. The results indicate that chickens are raised on farms within 50 miles of SRS; however, chickens eat commercial feed. Since poultry production is an indoor operation with feed provided by the parent companies responsible for marketing the final product, SRNL-STI-2010-00447 did not include feed-to-poultry and feed-to-egg transfer factors. In order to account for local poultry and egg farmers that use free-range methods or home-grown fodder as feed, a methodology similar to that described above for SRNL-STI-2010-00447 was used to determine the feed-to-poultry and feed-to-egg transfer factors. The PNNL-13421 transfer factors were used and updated with the transfer factors from the IAEA-472. Five elements (aluminum, carbon, hydrogen, lutetium, and platinum) in the model that feed-to-poultry or feed-to-egg transfer factors were not found were assigned a zero value.

4.6.1.1.1 Bioaccumulation Parameters

The transfer factors that SRS utilized for the PA appear in Tables 4.6-1 through 4.6-6. The data in these tables was taken from SRNL-STI-2010-00447, PNNL-13421, and IAEA-472.

Table 4.6-1: Soil-to-Vegetable Transfer Factors (Unitless)

Atomic No.	Element	Value	Atomic No.	Element	Value	Atomic No.	Element	Value
89	Ac	6.11E-05	32	Ge	1.56E-02	84	Po	4.30E-04
47	Ag	1.19E-04	1	H	4.80E+00	59	Pr	3.90E-03
13	Al	1.27E-04	108	Ha	2.00E-03	78	Pt	4.88E-03
95	Am	7.33E-05	2	He	1.00E-20	94	Pu	1.97E-05
18	Ar	1.00E-20	72	Hf	1.95E-04	88	Ra	1.19E-02
33	As	2.73E-03	80	Hg	9.03E-02	37	Rb	1.39E-01
85	At	2.93E-02	67	Ho	3.90E-03	75	Re	1.21E-01
79	Au	2.64E-03	53	I	1.32E-02	104	Rf	3.00E-03
5	B	3.90E-01	49	In	2.43E-04	45	Rh	1.76E-01
56	Ba	9.75E-04	77	Ir	4.76E-03	86	Rn	1.00E-20
4	Be	6.83E-04	19	K	2.54E-01	44	Ru	6.29E-03
83	Bi	9.75E-02	36	Kr	1.00E-20	16	S	2.93E-01
97	Bk	1.00E-03	57	La	9.09E-04	51	Sb	2.61E-04
35	Br	2.93E-01	3	Li	7.80E-04	21	Sc	4.24E-04
6	C	1.37E-01	103	Lr	2.00E-03	34	Se	1.89E-02
20	Ca	3.90E+00	71	Lu	7.80E-04	14	Si	2.65E-02
48	Cd	1.49E-01	101	Md	2.00E-03	62	Sm	3.90E-03
58	Ce	1.63E-03	12	Mg	1.28E-01	50	Sn	2.27E-03
98	Cf	6.11E-05	25	Mn	6.39E-02	38	Sr	1.23E-01
17	Cl	3.49E+00	42	Mo	8.71E-02	73	Ta	4.88E-03
96	Cm	1.27E-04	7	N	7.43E-03	65	Tb	3.90E-03
27	Co	2.48E-02	11	Na	5.85E-03	43	Tc	1.79E+01
24	Cr	1.95E-04	41	Nb	2.18E-03	52	Te	5.85E-02
55	Cs	6.85E-03	60	Nd	3.90E-03	90	Th	3.14E-04
29	Cu	1.56E-01	10	Ne	1.00E-20	22	Ti	5.85E-04
66	Dy	3.90E-03	28	Ni	2.18E-02	81	Tl	2.43E-04
68	Er	3.90E-03	102	No	2.00E-03	69	Tm	7.80E-04
99	Es	1.00E-03	93	Np	3.91E-03	92	U	6.69E-03
63	Eu	3.90E-03	8	O	6.00E-01	23	V	5.85E-04
9	F	3.65E-03	76	Os	6.45E-03	74	W	1.95E-02
26	Fe	1.10E-02	15	P	1.95E-01	54	Xe	1.00E-20
100	Fm	2.00E-03	91	Pa	6.11E-05	39	Y	3.90E-04
87	Fr	5.85E-03	82	Pb	5.18E-03	70	Yb	7.80E-04
31	Ga	2.43E-04	46	Pd	1.28E-02	30	Zn	1.71E-01
64	Gd	3.90E-03	61	Pm	2.32E-02	40	Zr	7.80E-04

Table 4.6-2: Feed-to-Milk Transfer Factors (d/L)

Atomic No.	Element	Value	Atomic No.	Element	Value	Atomic No.	Element	Value
89	Ac	2.00E-05	32	Ge	7.21E-02	59	Pr	3.00E-05
47	Ag	1.58E-03	1	H	1.50E-02	78	Pt	5.15E-03
13	Al	2.06E-04	105	Ha	5.00E-06	94	Pu	1.00E-05
95	Am	4.20E-07	2	He	1.00E-20	88	Ra	3.80E-04
33	As	6.00E-05	72	Hf	5.50E-07	37	Rb	1.20E-02
85	At	1.03E-02	80	Hg	4.70E-04	75	Re	1.50E-03
79	Au	5.50E-06	67	Ho	3.00E-05	104	Rf	2.00E-05
5	B	1.55E-03	53	I	5.40E-03	45	Rh	1.00E-02
56	Ba	1.60E-04	49	In	2.00E-04	86	Rn	1.00E-20
4	Be	8.30E-07	77	Ir	2.00E-06	44	Ru	9.40E-06
83	Bi	5.00E-04	19	K	7.20E-03	16	S	7.90E-03
97	Bk	2.00E-06	57	La	2.00E-05	51	Sb	3.80E-05
35	Br	2.00E-02	3	Li	2.06E-02	21	Sc	5.00E-06
6	C	1.20E-02	103	Lr	5.00E-06	34	Se	4.00E-03
20	Ca	1.00E-02	71	Lu	2.06E-05	14	Si	2.00E-05
48	Cd	1.90E-04	101	Md	5.00E-06	62	Sm	3.00E-05
58	Ce	2.00E-05	12	Mg	3.90E-03	50	Sn	1.00E-03
98	Cf	1.50E-06	25	Mn	4.10E-05	38	Sr	1.30E-03
17	Cl	1.70E-02	42	Mo	1.10E-03	73	Ta	4.10E-07
96	Cm	2.00E-05	7	N	2.50E-02	65	Tb	3.00E-05
27	Co	1.10E-04	11	Na	1.30E-02	43	Tc	1.87E-03
24	Cr	4.30E-04	41	Nb	4.10E-07	52	Te	3.40E-04
55	Cs	4.60E-03	60	Nd	3.00E-05	90	Th	5.00E-06
29	Cu	2.00E-03	28	Ni	9.50E-04	22	Ti	7.53E-05
66	Dy	3.00E-05	102	No	5.00E-06	81	Tl	2.00E-03
68	Er	3.00E-05	93	Np	5.00E-06	69	Tm	2.06E-05
99	Es	2.00E-06	76	Os	5.00E-03	92	U	1.80E-03
63	Eu	3.00E-05	15	P	2.00E-02	23	V	2.06E-05
9	F	1.00E-03	91	Pa	5.00E-06	74	W	1.90E-04
26	Fe	3.50E-05	82	Pb	1.90E-04	39	Y	2.00E-05
87	Fr	2.06E-02	46	Pd	1.00E-02	70	Yb	2.06E-05
31	Ga	5.00E-05	61	Pm	3.00E-05	30	Zn	2.70E-03
64	Gd	3.00E-05	84	Po	2.10E-04	40	Zr	3.60E-06

Table 4.6-3: Feed-to-Beef Transfer Factors (d/kg)

Atomic No.	Element	Value	Atomic No.	Element	Value	Atomic No.	Element	Value
89	Ac	4.00E-04	64	Gd	2.00E-05	78	Pt	4.00E-03
47	Ag	3.00E-03	32	Ge	7.00E-01	94	Pu	1.10E-06
13	Al	1.50E-03	1	H	0.00E+00	88	Ra	1.70E-03
95	Am	5.00E-04	105	Ha	5.00E-06	37	Rb	1.00E-02
33	As	2.00E-03	72	Hf	3.16E-05	75	Re	8.00E-03
85	At	1.00E-02	80	Hg	2.50E-01	45	Rh	2.00E-03
79	Au	5.00E-03	67	Ho	3.00E-04	86	Rn	1.00E-20
5	B	8.00E-04	53	I	6.70E-03	44	Ru	3.30E-03
56	Ba	1.40E-04	49	In	8.00E-03	16	S	2.00E-01
4	Be	1.00E-03	77	Ir	1.50E-03	51	Sb	1.20E-03
83	Bi	4.00E-04	19	K	2.00E-02	21	Sc	1.50E-02
97	Bk	2.50E-05	57	La	1.30E-04	34	Se	1.50E-02
35	Br	2.50E-02	3	Li	1.00E-02	14	Si	4.00E-05
6	C	3.10E-02	103	Lr	2.00E-04	62	Sm	3.16E-04
20	Ca	1.30E-02	71	Lu	4.50E-03	50	Sn	8.00E-02
48	Cd	5.80E-03	12	Mg	2.00E-02	38	Sr	1.30E-03
58	Ce	2.00E-05	25	Mn	6.00E-04	73	Ta	1.34E-05
98	Cf	4.00E-05	42	Mo	1.00E-03	65	Tb	2.00E-05
17	Cl	1.70E-02	7	N	7.50E-02	43	Tc	6.32E-03
96	Cm	4.00E-05	11	Na	1.50E-02	52	Te	7.00E-03
27	Co	4.30E-04	41	Nb	2.60E-07	90	Th	2.30E-04
24	Cr	9.00E-03	60	Nd	2.00E-05	22	Ti	1.73E-04
55	Cs	2.20E-02	28	Ni	5.00E-03	81	Tl	4.00E-02
29	Cu	9.00E-03	102	No	2.00E-04	69	Tm	4.50E-03
66	Dy	2.00E-05	93	Np	1.00E-03	92	U	3.90E-04
68	Er	2.00E-05	76	Os	4.00E-01	23	V	2.50E-03
99	Es	2.50E-05	15	P	5.50E-02	74	W	4.00E-02
63	Eu	2.00E-05	91	Pa	4.47E-04	39	Y	1.00E-03
9	F	1.50E-01	82	Pb	7.00E-04	70	Yb	4.00E-03
26	Fe	1.40E-02	46	Pd	4.00E-03	30	Zn	1.60E-01
100	Fm	2.00E-04	61	Pm	2.00E-05	40	Zr	1.20E-06
87	Fr	2.50E-03	84	Po	5.00E-03			
31	Ga	5.00E-04	59	Pr	2.00E-05			

Table 4.6-4: Water-to-Fish Bioaccumulation Factors (L/kg)

Atomic No.	Element	Value	Atomic No.	Element	Value	Atomic No.	Element	Value
89	Ac	2.50E+01	64	Gd	3.00E+01	78	Pt	3.50E+01
47	Ag	1.10E+02	32	Ge	4.00E+03	94	Pu	3.00E+01
13	Al	5.10E+01	2	He	1.00E+00	88	Ra	4.00E+00
95	Am	2.40E+02	1	H	1.00E+00	37	Rb	4.90E+03
33	As	3.30E+02	72	Hf	1.10E+03	75	Re	1.20E+02
85	At	1.50E+01	80	Hg	6.10E+03	45	Rh	1.00E+01
79	Au	2.40E+02	67	Ho	3.00E+01	45	Rn	7.55E-10
56	Ba	1.20E+00	53	I	3.00E+01	44	Ru	5.50E+01
4	Be	1.00E+02	49	In	1.00E+04	16	S	8.00E+02
83	Bi	1.50E+01	77	Ir	1.00E+01	51	Sb	3.70E+01
97	Bk	2.50E+01	19	K	3.20E+03	21	Sc	1.90E+02
35	Br	9.10E+01	57	La	3.70E+01	34	Se	6.00E+03
6	C	3.00E+00	71	Lu	2.50E+01	14	Si	2.00E+01
20	Ca	1.20E+01	12	Mg	3.70E+01	62	Sm	3.00E+01
48	Cd	2.00E+02	25	Mn	2.40E+02	50	Sn	3.00E+03
58	Ce	2.50E+01	42	Mo	1.90E+00	38	Sr	2.90E+00
98	Cf	2.50E+01	7	N	2.00E+05	73	Ta	3.00E+02
17	Cl	4.70E+01	11	Na	7.60E+01	65	Tb	4.10E+02
96	Cm	3.00E+01	41	Nb	3.00E+02	43	Tc	2.00E+01
27	Co	7.60E+01	60	Nd	3.00E+01	52	Te	1.50E+02
24	Cr	4.00E+01	28	Ni	2.10E+01	90	Th	6.00E+00
55	Cs	3.00E+03	93	Np	2.10E+01	22	Ti	1.90E+02
29	Cu	2.30E+02	8	O	1.00E+00	81	Tl	9.00E+02
66	Dy	6.50E+02	76	Os	1.00E+03	92	U	9.60E-01
68	Er	3.00E+01	15	P	1.40E+05	23	V	9.70E+01
99	Es	2.50E+01	91	Pa	1.00E+01	74	W	1.00E+01
63	Eu	1.30E+02	82	Pb	2.50E+01	39	Y	4.00E+01
9	F	1.00E+01	46	Pd	1.00E+01	30	Zn	3.40E+03
26	Fe	1.70E+02	61	Pm	3.00E+01	40	Zr	2.20E+01
87	Fr	3.00E+01	84	Po	3.60E+01			
31	Ga	4.00E+02	59	Pr	3.00E+01			

Table 4.6-5: Feed-to-Poultry Transfer Factors (d/kg)

Atomic No.	Element	Value	Atomic No.	Element	Value	Atomic No.	Element	Value
89	Ac	6.00E-03	63	Eu	2.00E-03	78	Pt	0.00E+00
47	Ag	2.00E+00	9	F	1.40E-02	94	Pu	3.00E-03
13	Al	0.00E+00	26	Fe	1.00E+00	88	Ra	3.00E-02
95	Am	6.00E-03	64	Gd	2.00E-03	51	Sb	6.00E-03
33	As	8.30E-01	1	H	0.00E+00	34	Se	9.70E+00
56	Ba	1.90E-02	80	Hg	3.00E-02	62	Sm	2.00E-03
83	Bi	9.80E-02	53	I	8.70E-03	50	Sn	8.00E-01
6	C	0.00E+00	19	K	4.00E-01	38	Sr	2.00E-02
20	Ca	4.40E-02	71	Lu	0.00E+00	43	Tc	3.00E-02
48	Cd	1.70E+00	25	Mn	1.90E-03	90	Th	6.00E-03
98	Cf	6.00E-03	42	Mo	1.80E-01	92	U	7.50E-01
17	Cl	3.00E-02	41	Nb	3.00E-04	30	Zn	4.70E-01
96	Cm	6.00E-03	28	Ni	1.00E-03	40	Zr	6.00E-05
27	Co	9.70E-01	93	Np	6.00E-03			
24	Cr	2.00E-01	91	Pa	6.00E-03			
55	Cs	2.70E+00	82	Pb	8.00E-01			
29	Cu	5.00E-01	46	Pd	3.00E-04			

Table 4.6-6: Feed-to-Egg Transfer Factors (d/kg)

Atomic No.	Element	Value	Atomic No.	Element	Value	Atomic No.	Element	Value
89	Ac	4.00E-03	63	Eu	4.00E-05	78	Pt	0.00E+00
47	Ag	5.00E-01	9	F	2.70E+00	94	Pu	1.20E-03
13	Al	0.00E+00	26	Fe	1.80E+00	88	Ra	3.10E-01
95	Am	3.00E-03	64	Gd	4.00E-05	51	Sb	7.00E-02
33	As	2.60E-01	1	H	0.00E+00	34	Se	1.60E+00
56	Ba	8.70E-01	80	Hg	5.00E-01	62	Sm	4.00E-05
83	Bi	2.60E-01	53	I	2.40E+00	50	Sn	1.00E+00
6	C	0.00E+00	19	K	1.00E+00	38	Sr	3.50E-01
20	Ca	4.40E-01	71	Lu	0.00E+00	43	Tc	3.00E+00
48	Cd	1.00E-01	25	Mn	4.20E-02	90	Th	4.00E-03
98	Cf	4.00E-03	42	Mo	6.40E-01	92	U	1.10E+00
17	Cl	2.70E+00	41	Nb	1.00E-03	30	Zn	1.40E+00
96	Cm	4.00E-03	28	Ni	1.00E-01	40	Zr	2.00E-04
27	Co	3.30E-02	93	Np	4.00E-03			
24	Cr	9.00E-01	91	Pa	4.00E-03			
55	Cs	4.00E-01	82	Pb	1.00E+00			
29	Cu	5.00E-01	46	Pd	4.00E-03			

4.6.2 Human Health Exposure Parameters (Consumption Rates)

This section documents the human health exposure parameters (i.e., consumption rates) used in the HTF PA modeling effort. The factors utilized were developed based on comparison to a number of other DOE facilities and generic national and international references to establish relevance of the parameters selected and as needed, verify the regional differences for the Southeastern United States. The parameter values recommended were based on expected values along with a range for these values versus providing parameters for estimating an annual dose to the MEI. The consumption rates that SRS utilized for the PA appear in Tables 4.6-7 through 4.6-9. Distribution ranges for Tables 4.6-7 through 4.6-9 are presented in Section 5.6.3 tables.

Table 4.6-7: Crop Exposure Times and Productivity

Parameter	GoldSim Parameter Name	Value	
Vegetable crop exposure times to irrigation (d)	VeggieExposureTime	70	
Buildup time of radionuclides in soil (d) ^a	SoilBuildupTime	9,125	
Agricultural productivity (kg/m ²) ^a	VegetationProductionYield	2.2	
Fraction of Foodstuff Produced Locally		All-Pathway	Intruder
Leafy vegetables and produce	LocalGrown and LocalGrown_Intr	0.173	0.308
Meat	FracLocalBeef_MOP and FracLocalBeef_Intr	0.306	0.319
Milk	FracLocalMilk_MOP and FracLocalMilk_Intr	0.207	0.254
Poultry and Eggs ^b	FracLocalChic_MOP and FracLocalChic_Intr	0.306	0.319

[WSRC-STI-2007-00004, Table 3-1 except as noted]

a SRNL-STI-2010-00447

b ML083190829, Table A-1

Table 4.6-8: Physical Parameters

Parameter	GoldSim Parameter Name	Value
Water Density (g/ml)	<i>WaterDens</i>	1.0
Areal surface density of soil (kg/m ²)	<i>SurfaceSoilDensity</i>	240
Density of Sandy Soil (kg/m ³) ^a	<i>DryBulkDensity_SandySoil</i>	1,650
Airborne release fraction ^b	<i>ARF</i>	1.0E-04
Soil loading in air (kg/m ³)	<i>AirMassLoadingSoil</i>	1.0E-07
Depth of garden (cm)	<i>TillDepth and SoilThickness</i>	15
Water contained in air at ambient conditions (g/m ³) ^c	<i>AirWaterContent</i>	10
Water contained in air at shower conditions (g/m ³) ^c	<i>ShowerAirWaterContent</i>	41
Soil moisture content ^d	<i>SoilMoistureContent</i>	0.2086
Precipitation rate (in/yr) ^d	<i>PR</i>	49.1
Evapotranspiration rate (in/yr) ^d	<i>ER</i>	32.6
Irrigation rate (in/yr)	<i>IR</i>	52*
Irrigation rate (L/d/m ²)	<i>IrrigationRate</i>	3.6*
Fraction of the time that vegetation is irrigated	<i>FracYearIrrigate</i>	0.2
Weathering decay constant (1/d)	<i>WeatheringDecayConst</i>	0.0495
Fraction of material deposited on leaves that is retained	<i>LeafRetention</i>	0.25
Fraction of material deposited on leaves that is retained after washing	<i>WashingFactor</i>	1.0
Area of garden for family of four (m ²)	<i>GardenSize</i>	100
Well diameter (ft) ^e	<i>WellDiameter</i>	0.667
Transfer line circumference (ft) ^e	<i>PipeAreaperLength</i>	0.803
Well depth (ft) ^e	<i>WellDepth</i>	100

[WSRC-STI-2007-00004, Table 3-2 except as noted]

a WSRC-STI-2006-00198, Table 5-18

b DOE-HDBK-3010-94

c HNF-SD-WM-TI-707

d WSRC-STI-2007-00184

e SRR-CWDA-2010-00054

* Based on an assumption of 1-in/wk = 0.36 cm/d. A 1m² area, 0.36 cm/d x 10,000 cm²/m² x 1L/1,000 cm³=3.6 L/d/m².

Table 4.6-9: Individual Exposure Times and Consumption Rates

Parameter	GoldSim Parameter Name	Value
Breathing rate (m ³ /yr)	<i>AirIntake</i>	5,548
Consumption Rate		
Soil (kg/year)	<i>SoilConsumptionRate</i>	0.0365
Leafy vegetable (kg/yr)	<i>Leafy</i>	21
Other vegetable (kg/yr)	<i>Veg</i>	163
Meat (kg/yr)	<i>BeefConsumptionRate</i>	43
Poultry (kg/yr) ^a	<i>ChicConsumptionRate</i>	25
Eggs (kg/yr) ^a	<i>EggConsumptionRate</i>	19
Finfish (kg/yr)	<i>FishConsumptionRate</i>	9
Milk (L/yr)	<i>MilkConsumptionRate</i>	120
Water (L/yr)	<i>WaterConsumptionRate</i>	337
Fodder-Beef cattle (kg/d)	<i>ConsumptionFodderBeef</i>	36
Fodder-Milk cattle (kg/d)	<i>ConsumptionFodderMilk</i>	52
Fodder-Poultry (kg/d) ^a	<i>ConsumptionFodderChic and ConsumptionFodderEgg</i>	0.1
Fraction of milk-cow feed is from pasture (fodder)	<i>FodderFractionMilk</i>	0.56
Fraction of beef-cow feed is from pasture (fodder)	<i>FodderFractionBeef</i>	0.75
Fraction of poultry feed is from pasture (fodder)	<i>FodderFractionChic and FodderFractionEgg</i>	1
Water (beef cow) (L/d)	<i>CattleWaterConsumptionBeef</i>	28
Water (milk cow) (L/d)	<i>CattleWaterConsumptionMilk</i>	50
Water (poultry) (L/d) ^a	<i>ChicWaterConsumption and EggWaterConsumption</i>	0.3
Exposure Time		
Swimming (hr/yr) ^b	<i>AnnualSwimming</i>	7
Boating (hr/yr) ^b	<i>AnnualBoating</i>	22
Showering (min/d)	<i>ExposureFractionShower</i>	10
Fraction of time spent working in garden	<i>ExposureFractionGarden</i>	0.01
Boating geometry factor ^c	<i>BoatingGF</i>	0.5
Swimming geometry factor ^c	<i>SwimmingGF</i>	1
Fraction of year acute intruder is exposed to drill cuttings ^d	<i>FractionExposedtoCuttings</i>	0.0023

[WSRC-STI-2007-00004, Table 4-1 except as noted]

a ML083190829, Table A-1

b SRNL-STI-2010-00447

c Conservative assumption

d Assumes 20 hours to complete well drilling

4.6.2.1 Human Health Exposure Parameters Methodology

Baseline Parameter Update for Human Health Input and Transfer Factors for Radiological Performance Assessments at the Savannah River Site (WSRC-STI-2007-00004) documents the results of the SRS evaluation and reviews of consumption rates. The report includes

information to establish a range of values for each parameter that was used to perform the uncertainty analyses. Refer to this report for additional discussion on parameters such as water ingestion rates, crop yields, garden fractions, and sizes along with soil exposure times. *Land and Water Use Characteristics and Human Health Input Parameters for use in Environmental Dosimetry and Risk Assessments at the Savannah River Site* (SRNL-STI-2010-00447) relies heavily on WSRC-STI-2007-00004, and reproduces nearly all of the human health exposure parameters from that report. Since WSRC-STI-2007-00004 also provides a range of values used to perform uncertainty analyses, the human health exposure parameters and ranges used in the HTF PA were taken from WSRC-STI-2007-00004 with a few parameters updated by SRNL-STI-2010-00447 as noted in the tables.

In developing WSRC-STI-2007-00004, a comprehensive literature review was completed. A hierarchy of data sources was established to select values for human health exposure parameters. The utilization of site-specific values from the most recent and comprehensive references are given priority. Values promulgated by national or international organizations were used as representative of the SRS area practices in the absence of site-specific values. The *Risk-Based Screening of Radionuclide Releases from the Savannah River Site* was used as a source to validate the receptor practices in the areas surrounding SRS. [CDC-2006] The values given for the parameters are given as expected values, together with an observed range.

Site-specific information is available for most of the human health exposure parameters required to estimate doses. Report WSRC-RP-91-17, *Land and Water-Use Characteristics in the Vicinity of the Savannah River Site and Site-Specific Parameter Values for the Nuclear Regulatory Commission's Food Pathway Dose Model*, surveyed county agents in South Carolina and Georgia and compiled county-specific statistics on land and water use within a 50 mile radius of SRS. When the report does not provide site-specific information for physical parameters and consumption rates, global data are used. The EPA report *Exposure Factors Handbook, National Center for Environmental Assessment*, summarizes and recommends parameter data for human health exposure and human exposure to environmental contaminants based on studies published through August 30, 1997. [EPA-600-P-95-002Fa-c] Documents ANL-EAD-4 and ANL-EAIS-8 provide data for use in RESRAD, DOE, and NRC supported dose model based on literature review of standard values and publications. NUREG_CR-5512 provides generic and site-specific human health data for estimating dose from exposure to residual radioactive contamination.

4.7 Dose Analysis

Over time, the mobile contaminants in the HTF waste tanks and ancillary equipment will gradually migrate downward through unsaturated soil to the hydrogeologic units comprising the shallow aquifer underlying the HTF. Some contaminants will be transported via groundwater through the aquifers, to the outcrops at Fourmile Branch and UTR. Upon reaching the surface water, the contaminants could be present at the seepage line, in sediments at the bottom of streams, and at the shoreline. Human receptors could be exposed to contaminants through various pathways associated with the aquifers and surface water as described in Section 4.2.3.

The potential dose to MOP via the air pathway was also evaluated as described in Section 5.3.

4.7.1 Dose Conversion Factors

The purpose of this section is to present the set of DCFs used in dose calculations for the HTF PA modeling effort. Table 4.7-1 presents the list of internal and external DCFs for the 63 radionuclides identified in the inventory screening process for use in the PA modeling.

Table 4.7-1: Internal and External DCFs

Rad	Internal DCFs (rem/ μ Ci)		External DCFs (rem/yr per μ Ci/m ³)		
	Ingestion	Inhalation	Infinite Depth	15 cm	Water Immersion
Ac-227 ^a	4.47E+00	2.10E+03	1.26E-03	1.18E-03	4.74E-03
Ag-108m	8.51E-03	2.74E-02	6.02E-03	5.38E-03	1.97E-02
Al-26	1.30E-02	7.40E-02	1.09E-02	9.03E-03	3.43E-02
Am-241	7.40E-01	1.55E+02	2.73E-05	2.73E-05	2.20E-04
Am-242m ^a	7.41E-01	1.53E+02	4.25E-05	4.10E-05	2.03E-04
Am-243 ^a	7.43E-01	1.52E+02	5.59E-04	5.44E-04	2.57E-03
Bi-210m ^a	5.55E-02	1.26E+01	8.65E-04	8.14E-04	3.14E-03
C-14	2.15E-03	7.40E-03	8.41E-09	8.41E-09	5.13E-08
Ca-41	7.03E-04	3.52E-04	0.00E+00	0.00E+00	0.00E+00
Cf-249	1.30E+00	2.59E+02	1.16E-03	1.07E-03	4.03E-03
Cf-251	1.33E+00	2.63E+02	3.29E-04	3.22E-04	1.45E-03
Cl-36	3.44E-03	2.70E-02	1.49E-06	1.42E-06	5.23E-06
Cm-243	5.55E-01	1.15E+02	3.64E-04	3.53E-04	1.52E-03
Cm-244	4.44E-01	9.99E+01	7.87E-08	7.87E-08	1.34E-06
Cm-245	7.77E-01	1.55E+02	2.13E-04	2.10E-04	1.03E-03
Cm-246	7.77E-01	1.55E+02	7.26E-08	7.26E-08	1.23E-06
Cm-247 ^a	7.03E-01	1.44E+02	1.16E-03	1.08E-03	4.09E-03
Cm-248	2.85E+00	5.55E+02	5.49E-08	5.49E-08	9.30E-07
Co-60	1.26E-02	3.70E-02	1.01E-02	8.47E-03	3.20E-02
Cs-135	7.40E-03	2.55E-03	2.39E-08	2.39E-08	1.28E-07
Cs-137 ^a	4.81E-02	1.70E-02	2.13E-03	1.89E-03	6.92E-03
Eu-152	5.18E-03	1.55E-01	4.38E-03	3.76E-03	1.44E-02
Eu-154	7.40E-03	1.96E-01	4.80E-03	4.11E-03	1.55E-02
Eu-155	1.18E-03	2.55E-02	1.14E-04	1.14E-04	6.55E-04
Gd-152	1.52E-01	7.03E+01	0.00E+00	0.00E+00	0.00E+00
H-3	6.66E-05	1.67E-04	0.00E+00	0.00E+00	0.00E+00
I-129	4.07E-01	1.33E-01	8.09E-06	8.09E-06	1.04E-04
K-40	2.29E-02	7.77E-03	6.50E-04	5.34E-04	2.03E-03
Lu-174	9.99E-04	1.55E-02	3.58E-04	3.09E-04	1.40E-03
Mo-93	1.15E-02	2.18E-03	3.69E-07	3.69E-07	6.91E-06
Nb-93m	4.44E-04	1.89E-03	6.50E-08	6.50E-08	1.21E-06
Nb-94	6.29E-03	4.07E-02	6.05E-03	5.29E-03	1.95E-02
Ni-59	2.33E-04	4.81E-04	0.00E+00	0.00E+00	0.00E+00
Ni-63	5.55E-04	1.78E-03	0.00E+00	0.00E+00	0.00E+00
Np-237 ^a	4.10E-01	8.51E+01	6.86E-04	6.52E-04	2.66E-03
Pa-231	2.63E+00	5.18E+02	1.19E-04	1.12E-04	4.41E-04

Table 4.7-1: Internal and External DCFs (Continued)

Rad	Internal DCFs (rem/ μ Ci)		External DCFs (rem/yr per μ Ci/m ³)		
	Ingestion	Inhalation	Infinite Depth	15 cm	Water Immersion
Pb-210 ^a	7.00E+00	1.66E+01	3.81E-06	3.73E-06	2.28E-05
Pd-107	1.37E-04	2.18E-03	0.00E+00	0.00E+00	0.00E+00
Pt-193	1.15E-04	7.77E-05	3.54E-09	3.54E-09	1.08E-07
Pu-238	8.51E-01	1.70E+02	9.46E-08	9.42E-08	1.33E-06
Pu-239	9.25E-01	1.85E+02	1.84E-07	1.77E-07	1.12E-06
Pu-240	9.25E-01	1.85E+02	9.17E-08	9.15E-08	1.30E-06
Pu-241	1.78E-02	3.33E+00	3.69E-09	3.68E-09	1.89E-08
Pu-242	8.88E-01	1.78E+02	8.00E-08	8.00E-08	1.09E-06
Pu-244 ^a	8.92E-01	1.74E+02	1.26E-03	1.11E-03	4.11E-03
Ra-226 ^a	1.04E+00	1.31E+01	6.99E-03	5.89E-03	2.25E-02
Ra-228 ^a	3.08E+00	1.70E+02	1.01E-02	8.37E-03	3.25E-02
Se-79	1.07E-02	4.07E-03	1.16E-08	1.16E-08	6.92E-08
Sm-147	1.81E-01	3.55E+01	0.00E+00	0.00E+00	0.00E+00
Sm-151	3.63E-04	1.48E-02	6.15E-10	6.15E-10	9.92E-09
Sn-126 ^a	1.88E-02	1.05E-01	7.40E-03	6.61E-03	2.45E-02
Sr-90 ^a	1.14E-01	1.39E-01	1.54E-05	1.44E-05	4.41E-05
Tc-99	2.37E-03	1.48E-02	7.85E-08	7.82E-08	3.67E-07
Th-229 ^a	2.27E+00	3.17E+02	9.98E-04	9.21E-04	3.83E-03
Th-230	7.77E-01	5.18E+01	7.56E-07	7.46E-07	4.60E-06
Th-232	8.51E-01	9.25E+01	3.26E-07	3.25E-07	2.32E-06
U-232 ^a	1.75E+00	1.89E+02	6.37E-03	5.15E-03	2.04E-02
U-233	1.89E-01	1.33E+01	8.73E-07	8.45E-07	4.25E-06
U-234	1.81E-01	1.30E+01	2.51E-07	2.50E-07	2.04E-06
U-235 ^a	1.75E-01	1.15E+01	4.73E-04	4.61E-04	1.99E-03
U-236	1.74E-01	1.18E+01	1.34E-07	1.33E-07	1.35E-06
U-238 ^a	1.79E-01	1.08E+01	9.49E-05	8.48E-05	3.45E-04
Zr-93	4.07E-03	3.70E-02	0.00E+00	0.00E+00	0.00E+00

a Based on the parent radionuclide plus daughter products

Radiation doses to humans may result from internal inhalation or ingestion of radionuclides by or from external exposure to radionuclides present in the environment. Dose assessment at SRS is carried out by considering radionuclide concentrations in environmental media, factoring in human exposure conditions, and performing the conversion of exposure to dose. For internal exposure, radionuclide activity intake is calculated by combining the radioactivity concentration in environmental media (e.g., food, soil, air, and water) with the amount of environmental medium taken into the body. Then, using internal DCFs, radionuclide intake is converted into dose. To assess exposure from external sources, SRS uses external DCFs that convert radionuclide concentrations in environmental media to doses for the duration of exposure.

4.7.1.1 Internal DCFs

Previous SRS PA analyses utilized the DCFs from EPA Federal Guidance Report 11, published in 1988. [EPA-520-1-88-020] The International Commission on Radiological

Protection (ICRP) published new DCFs based upon updated dosimetric models in ICRP Publication 72 in 1996. The DOE has begun using the ICRP models for occupational exposure internal dose assessments at different sites including SRS. In addition and they are used for SRS safety basis calculations. Safety basis documents, as defined in 10 CFR 830, Subpart B, are the DSA and hazard controls that provide reasonable assurance that a DOE nuclear facility can be operated safely in a manner that adequately protects workers, the public, and the environment. Only internal DCFs for adults, as opposed to internal DCFs for children or infants, were utilized in the HTF PA, consistent with guidance in DOE Guide 435.1-1, Section IV.P.(2).

The DCFs are converted to standard units for input into the calculations by multiplying the ICRP-72 DCFs by $3.7E+06$ (Sv/Bq/rem/ μ Ci). The internal DCFs are expressed in rem divided by microcurie and presented in Table 4.7-1 for the various radionuclides. For inhalation DCFs, the most likely lung absorption type from Table 2 of ICRP-72 was used if available, and if not available, the most conservative type was assumed.

For radionuclides with daughter products that are expected to be in secular equilibrium with the parent radionuclide, the DCFs of the daughter products are summed with the DCF of the parent radionuclide to match the modeling code transport output. The equilibrium is calculated using the individual ICRP-72 DCF and adjusted by the branching fraction for the daughter products to the parent. For example, the ICRP-72 ingestion DCF for Pb-210, Bi-210, and Po-210 is 2.6 rem/ μ Ci ($6.9E-07$ Sv/Bq), $4.8E-03$ rem/ μ Ci ($1.3E-09$ Sv/Bq), and 4.4 rem/ μ Ci ($1.2E-06$ Sv/Bq) respectively. Based on a branching fraction of 1.0 for Bi-210 and 1.0 for Po-210, the adjusted Pb-210 DCF is $2.6 \text{ rem}/\mu\text{Ci} + 4.8E-03 \text{ rem}/\mu\text{Ci} + 4.4 \text{ rem}/\mu\text{Ci} = 7.0 \text{ rem}/\mu\text{Ci}$. Radionuclides that have short-lived daughter product DCFs included in the parent DCF are noted in Table 4.7-1.

Because the ICRP data is the most recent data available and is based on the most recent dosimetric models, the ICRP-72 DCFs were used for this HTF PA analyses and have been approved for use by DOE Office of Health Safety and Security. [ICRP-72, DOE_02-23-2011]

4.7.1.2 External DCFs

External DCFs for uniformly distributed contamination in soil at an infinite depth with no shielding and at 15 cm are taken from EPA Federal Guidance Report 12. [EPA-402-R-93-081] The external DCFs in EPA-402-R-93-081 represent the dose rate per unit of activity of soil contaminated at various depths, reported in sievert (Sv) divided by second divided by becquerel (Bq) divided by meter cubed ($\text{Sv/s per Bq}/\text{m}^3$). The DCFs are converted to standard units for input into PA calculations by multiplying the EPA-402-R-93-081 DCFs by $1.168E+14$ ($(\text{rem}/\text{yr} / \mu\text{Ci}/\text{m}^3) / (\text{Sv/s per Bq}/\text{m}^3)$). External DCFs are presented in Table 4.7-1 for various radionuclides for both contaminated soil and for immersion in contaminated water. [EPA-402-R-93-081]

For radionuclides with daughter products that are expected to be in secular equilibrium with the parent radionuclide, the DCFs of the daughter products are summed with the DCF of the parent radionuclide to match the modeling code transport output. The equilibrium is calculated using the individual EPA-402-R-93-081 DCF and adjusted by the branching

fraction for the daughter products to the parent, similar to the calculation described for the internal DCFs. Radionuclides, which have short-lived daughter product DCFs included in the parent DCFs are noted in Table 4.7-1.

4.7.2 MOP Dose Analysis

Two distinct release scenarios were analyzed to assess the potential MOP doses associated with the HTF. The difference in the scenarios was the primary water source, 1) a well drilled into the groundwater aquifers and 2) an HTF stream. The MOP dose pathways used in the PA analyses are discussed in detail in Section 4.2.3.1.

The consumption rates and bioaccumulation factors that are used in conjunction with the proposed pathways are discussed in detail in Section 4.6.

4.7.3 Intruder Dose Analysis

Two distinct release scenarios were analyzed to assess the potential intruder doses associated with the HTF. The intruder scenarios of concern are the Acute Intruder-Drilling Scenario and the Chronic Intruder Agricultural (Post-Drilling) Scenario. The intruder dose pathways used in the PA analyses are discussed in detail in Section 4.2.3.2.

The consumption rates and bioaccumulation factors that are used in conjunction with the proposed pathways are discussed in detail in Section 4.6.

4.7.4 Analysis Approach

The MOP and intruder exposure scenarios were analyzed for HTF to provide results to demonstrate compliance with the performance criteria. The analysis provides not only the maximum projected dose and time of occurrence, but also the dominant pathway contributing to the dose and the radionuclides responsible for the maximum dose.

The groundwater and surface water concentrations and resulting human health impacts are calculated for the Base Case using the PORFLOW computer code. The analysis approaches used for HTF are based upon the radionuclide inventories (Sections 3.3.2 and 3.3.3), stabilized contaminant release mechanisms (Section 4.2.1), and radionuclide transport models (Section 4.2.2) as described previously in this document.

4.8 RCRA/CERCLA Risk Evaluation

Protocols have been developed, with approval of SCDHEC and the EPA to support the SRS ACP remediation activities. The protocols provide instructions for the development of conceptual site models used in the RCRA Facility Investigation Work Plan and CERCLA Remedial Investigation (RI) process. [ERD-AG-003_F.17, ERD-AG-003_P.1.4, ERD-AG-003_P.1.5, ERD-AG-003_P.5.2, and ERD-AG-003_P.10.1] These same protocols were used to evaluate the potential for adverse effects associated with exposure to constituents present at the HTF in the stabilized contaminants. Groundwater concentrations at the HTF were compared to the SDWA MCLs. In the absence of MCLs, groundwater radionuclide concentrations were compared to PRGs, and non-radionuclide concentrations were compared to RSLs.

The PRGs are risk-based tools used to evaluate and clean up contaminated sites. The use of PRGs to evaluate risk/hazard is a simple and accepted method; however, this method does not

replace the current Constituent of Potential Concern (COPC) identification process that considers the residential soil PRGs in the initial screening step. [EPA-PRGs_11-13-2007]

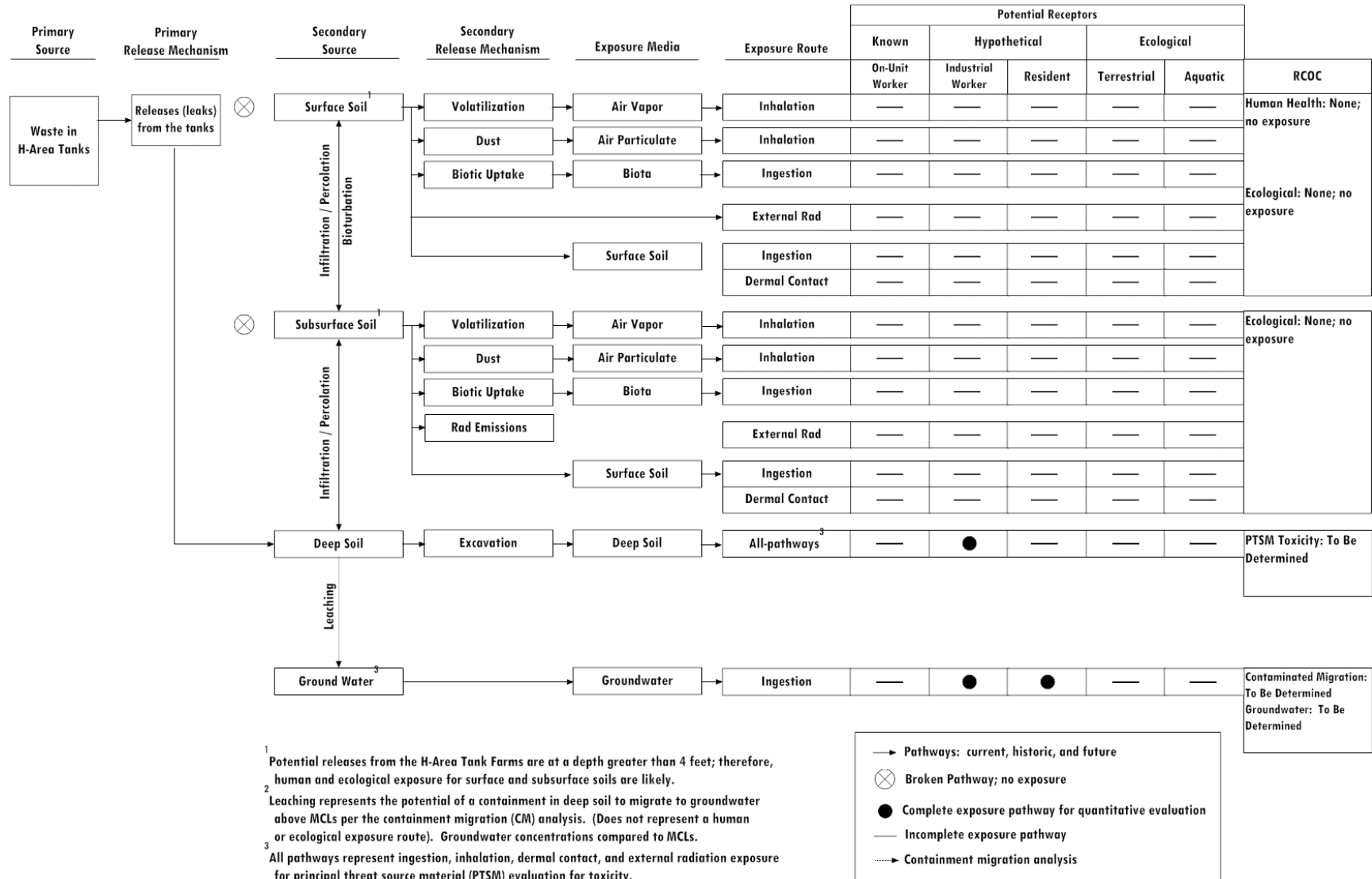
The May 2010 version of the EPA RSL tables is the source of RSLs for non-radiological constituents. It combines current EPA toxicity values with standard exposure factors to estimate contaminant concentrations in environmental media (soil, air, and water) that the agency considers protective of humans (including sensitive groups), over a lifetime. Region 3 RSL concentrations are based on direct contact pathways for which generally accepted methods, models, and assumptions have been developed (i.e., quantitative ingestion, dermal contact, and inhalation factors) for specific land use conditions.

Oak Ridge National Laboratory (ORNL) has derived risk-based radiological PRG values using default parameters and the latest toxicity values. The EPA website provides specific details regarding use of the database tool to calculate the PRGs and generic tables that were used for comparison to the modeled radionuclide concentrations evaluated in this PA. [EPA-PRGs_11-13-2007]

4.8.1 Integrated Conceptual Model

The ICM for HTF (Figure 4.8-1) depicts the understanding of the site and focuses on identifying potential contaminant migration from the sources to potential receptors. The ICM identifies potential sources of contamination, release mechanisms, media of concern, exposure routes, and potential receptors. For the purposes of the ICM, the surface soil interval is defined as the 0 to 0.3-meter (0 to 1-foot) interval and is evaluated for human and ecological exposure. The subsurface soil interval is the 0.3 to 1.2-meter (1 to 4-foot) interval and is evaluated for ecological exposure. The deep soil interval (> 1.2 meters) is defined on a subunit specific basis and is evaluated for Principal Threat Source Material (PTSM) (future excavation scenario) and contaminant migration potential. The approved risk evaluation approach used in the RCRA Facility Investigation and CERCLA RI process differs slightly from the general analysis approach used in calculating the PA dose results in Sections 5 and 6, such that there will be some differences between the risk analyses release scenarios (shown in Figure 4.8-1), and the dose analyses pathways and scenarios (Section 4.2.3). The RCRA/CERCLA risk approach uses MCLs, RSLs, and PRGs to determine constituents of concern in the ACP protocols, which are calculated using generally accepted EPA water consumption rates. The general analysis approach used in the PA uses various exposure pathways and consumption rates to calculate MOP radiological doses. The placement of a low permeability closure cap will ensure that the surface (i.e., 0 to 0.3 meter) and subsurface (i.e., 0.3 to 1.2 meter) soils will not be contaminated and that there is no pathway for ecological risk.

Figure 4.8-1: Integrated Conceptual Site Model for HTF



Initially, the ICM provides a representation of the contamination source. It also includes potential release mechanisms and exposure routes based on existing understanding of the nature and extent of contamination. For this evaluation, because the HTF will remain operational while the individual waste tanks are closed, only the stabilized contamination in the waste tanks is considered. Final facility closure of the HTF will include the evaluation of potential surface soil contamination.

4.8.1.1 Primary Source of Contamination

The primary source of contamination was the stabilized contaminants in the HTF waste tanks and ancillary equipment. Contaminants may be released from primary sources through release (migration) of contaminants from the waste tanks and ancillary equipment.

4.8.1.2 Secondary Sources of Contamination

Environmental media impacted by the release of primary source contamination becomes a secondary source. After grouting the waste tanks and ancillary equipment, at least 10 feet of material will be placed as backfill. Potential releases from the HTF are then at depths greater than 1.2 meters; therefore human and ecological exposure for surface or subsurface soils is unlikely (incomplete pathway). Secondary sources of contamination include deep soils beneath the waste tanks and groundwater.

Environmental media may serve as both a contaminant reservoir, via chemical bonding and biotic uptake, and/or secondary release mechanism of contaminants. Secondary release mechanisms include, leaching of constituents from deep soils to groundwater and excavation of deep soils.

4.8.1.3 Exposure Pathways (Media)

Contact with contaminated environmental media creates exposure pathways for human receptors. Potential exposure media includes excavation of deep soil and groundwater.

4.8.1.4 Exposure Routes

Potential exposure routes for human receptors may include the following:

- Ingestion of excavated soil
- Inhalation of air vapor and particulates from excavated soil
- Dermal contact with excavated soil
- External radiation exposure from radiological constituents in excavated soil
- Ingestion of groundwater

4.8.1.5 Receptors

Potential releases from the HTF are at a depth greater than 1.2 meters (4 feet); therefore, the standard human and ecological receptor scenarios do not apply. A future industrial worker scenario is considered for deep soils at the PTSM toxicity threshold to take into account potential exposure through excavation.

4.8.2 Risk Assessment

The risk assessment for the HTF closure follows the ACP protocols for human health and ecological risk assessments. [ERD-AG-003_F.17, ERD-AG-003_P.1.4, ERD-AG-003_P.1.5] Based on available characterization data and estimated volume of residual material expected to remain in each of the waste tanks and ancillary equipment, the chemical and radiological inventory used for PA modeling has been calculated for HTF as discussed in Section 3.3. Modeling was conducted to determine the peak concentrations of the non-radiological contaminants in the groundwater over the 1,000 years following closure, and radiological contaminants in the groundwater over the 10,000 years following closure. Comparison of actual waste tank residual inventory versus the calculated values used in the modeling will occur prior to each waste tank closure in a Special Analysis for the HTF PA. The SA includes documentation of checking the residual waste tank inventory-data inputs, formulas, and calculations, to ensure that the results in the HTF PA Model are validated.

4.8.2.1 Human Health Risk Assessment

The SRS ACP protocols call for evaluation of surface soils for exposure to a future industrial worker from 0 to 1 foot. Some of the ancillary equipment may currently be within the 0 to 1-foot depth. However, since the waste tanks and ancillary equipment will be stabilized and covered with at least 10 feet of backfill, there will be no pathway for future industrial worker exposure. Therefore, based on the evaluation using the SRS ACP protocols, no human health risk assessment is required at this time. [ERD-AG-003_F.17, ERD-AG-003_P.1.4, ERD-AG-003_P.1.5]

4.8.2.2 Ecological Risk Assessment

The ACP protocols call for evaluation of surface soils for ecological exposure from 0 to 4 feet. Some of the ancillary equipment may currently be within the 0 to 4-foot depth. However, since the waste tanks and ancillary equipment will be stabilized and covered with at least 10 feet of backfill, there will be no pathway for ecological exposure. Therefore, based on the evaluation using the ACP protocols, no ecological risk assessment is required at this time. [ERD-AG-003_F.17, ERD-AG-003_P.1.4, ERD-AG-003_P.1.5]

4.8.2.3 Principal Threat Source Materials

The PTSM are those materials that include or contain hazardous substances, pollutants, or contaminants that act as a reservoir for migration of contamination to groundwater, surface water, or air, or that act as a source for direct exposure. [OSWER 9380.3-06FS] Source characterizations are necessary to determine whether the source(s) can be designated as PTSM, Low-Level Threat Source Material, or non-hazardous materials.

The closed HTF waste tanks and ancillary equipment are, by definition, PTSM. The waste tanks and the residue remaining in the waste tanks will be stabilized and then covered with at least 10 feet of backfill. This approach is consistent with ACP remediation of reactor seepage basins, which contained contaminated soils determined to be PTSM. [ERD-AG-003_F.17, ERD-AG-003_P.1.4, ERD-AG-003_P.1.5, ERD-AG-003_P.10.1]

4.8.2.4 Contaminant Migration Constituents of Concern

Contaminant migration constituents of concern (CMCOC) were identified through a system that is consistent with both the ACP protocols and the HTF PA. The CMCOC were identified by modeling the release of contaminants and their travel through the vadose zone. The same model utilized in the HTF PA to meet 10 CFR 61 requirements is used as the basis of the CMCOC evaluation. Peak concentrations, incorporating the full contaminant inventory and consideration of various fate and transport uncertainties, of any radiological contaminants that are modeled to reach the water table are compared to MCL, PRG, or other appropriate standards in cases where the constituent does not have an MCL. Non-radiological contaminants are compared to MCLs or RSLs. Any constituents that are predicted to exceed these standards in the groundwater directly beneath HTF (within the 1-meter boundary) in 10,000 years for radiological contaminants and 1,000 years for non-radiological contaminants are identified as CMCOC. The CMCOC are often addressed by the placement of a low permeability cap such as is planned for the HTF closure. [ERD-AG-003_F.17, ERD-AG-003_P.1.4, ERD-AG-003_P.1.5, ERD-AG-003_P.5.2] Values for CMCOC are included for 10,000 years at both the HTF 100-meter boundary and the seepage line. Risk Assessment modeling results and uncertainties are discussed in detail in Section 5.7.

5.0 RESULTS OF ANALYSIS

The purpose of this section is to present the results for the analyses described in Section 4 of this PA.

- Section 5.1 presents the Source Term Analysis and Release results process.
- Section 5.2 presents peak groundwater concentrations for the radionuclides and chemicals discussed in Section 3.3.
- Section 5.3 presents the Air Pathway and Radon release results.
- Section 5.4 presents individual Biotic Pathway formulas used to calculate the doses to MOP.
- Section 5.5 presents the results of MOP Dose Analyses.
- Section 5.6 presents the UA/SA.
- Section 5.7 presents the Risk Analyses.
- Section 5.8 presents the As Low As Reasonably Achievable (ALARA) Analyses.

5.1 Source Term Analysis and Release Results Process

The purpose of this section is to describe the process of evaluating modeled concentrations and dose and risk at exposure points for various pathways and exposure groups.

In the source term analyses, the release of radionuclides from the waste tanks was controlled, in most cases, by solubility, which will vary with the pH and/or with E_h . All chemicals and some radionuclides are modeled as being released instantaneously from the CZ. In addition to solubility, the stabilized contaminant release rate for waste tanks was also impacted by the water flow through the waste tank, which varied by waste tank type and changed over time as the hydraulic properties of the waste tank materials changed. Results of the radionuclide and chemical environmental transport modeling to the HTF 100-meter boundary are summarized by aquifer in Section 5.2.1. These data are presented in either picocurie per liter for radionuclides or in microgram per liter for chemicals. In addition, the overall maximum concentrations for sensitivity run radionuclides by aquifer are provided.

Detailed modeling was performed on radionuclides determined to have the largest impact on dose and are discussed in Section 5.2.2 as “sensitivity run” radionuclides. Radionuclides are designated as sensitivity run radionuclides if 1) the radionuclides contributes greater than 0.25 mrem/yr to the MOP dose or 2) those radionuclides have a significant impact on progeny of the radionuclides that contributed greater than 0.25 mrem/yr to the MOP dose. Sensitivity run radionuclides were then modeled to determine concentration and dose to the MOP at the seep lines of UTR and Fourmile Branch.

The waste tank and ancillary equipment inventory of potentially airborne isotopes is used in conjunction with the methodology described in Section 4.5 to conservatively bound the air pathway dose. The air pathway dose at 100 meter and at the UTR and Fourmile Branch seep lines and the radon peak flux are calculated and presented in Section 5.3. The specific dose calculation formulas for the individual elements of the biotic pathways for the MOP scenarios

discussed in Section 4.2.3 are provided in Section 5.4. This includes the scenarios with the MOP at the 100-meter location as well as at the stream seepines.

The peak total groundwater pathway doses are calculated using the pathway formulas discussed in Section 5.4 for the MOP at 100 meters and at the seepines. The groundwater pathway doses are calculated utilizing the peak groundwater concentrations identified in Section 5.2 and presented in Section 5.5.

The purpose of the UA/SA in Section 5.6 is to consider the effects of uncertainties in the conceptual models and sensitivities in the parameters used in the mathematical modeling. The uncertainty analysis was performed using the probabilistic model (i.e., the HTF GoldSim Model) discussed in Section 5.6.1. The probabilistic model provides the capability to vary multiple parameters simultaneously, so the concurrent effect of changes can be analyzed and the potential impacts of changes can be assessed. This capability allows for identification of parameters that are only of significance when varied at the same time as another parameter. This section also includes the deterministic sensitivity analyses and the barrier analyses performed using the HTF GoldSim Model, which provide additional information concerning which parameters are important to the HTF model.

The risk analysis discussed in Section 5.7 is based on ACP protocols for evaluating human health and ecological risk. The CMCOC were established by comparing modeled radionuclide activities and chemical concentrations at the 1-meter boundary to established regulatory limits. Modeled values for CMCOC at both the 100-meter boundary and the seepines were used to determine risk to the MEI.

Section 5.8 presents the ALARA Analysis.

5.2 Environmental Transport of Radionuclides

The purpose of this section is to present the groundwater concentrations for all of the radionuclides and chemicals discussed in the source term screening section of the PA (Section 3.3). Maximum groundwater concentrations are presented for two exposure points, 1) 100 meters from the HTF and 2) the seepines (UTR and Fourmile Branch). Results are presented for the three distinct aquifers modeled (UTRA-UZ, UTRA-LZ, and Gordon Aquifer).

The groundwater concentrations at 100 meters and at the seepine were calculated using the HTF PORFLOW Model for the Base Case discussed in Section 4.4.2.1. A summary of several key parameters used in the baseline HTF PORFLOW Modeling case are provided in Table 5.2-1.

Table 5.2-1: Baseline Case

HTF Parameter	Baseline
Radiological inventory	Table 3.4-9
Chemical inventory	Table 3.4-10
Solubilities (reduced and oxidized)	Table 4.2-10 and 4.2-11
Vadose K_d values	Table 4.2-25
Cementitious K_d values	Table 4.2-29
Cementitious material degradation times	Table 4.2-30
Type I basemat thickness (in)	30
Type II basemat Thickness (in)	42
Type III basemat thickness (in)	42
Type IIIA basemat thickness (in)	41
Type IV basemat thickness (in)	6.9025
Bypass fraction (% basemat with $K_d = 0$, represents fast flow path in GoldSim)	0 %
Waste tank degradation case	Case A (Base Case) (Section 4.4.2.1)
Vadose zone thickness	Table 4.2-15
Type I tank liner failure (yr) ^a	11,397
Type II tank liner failure (yr) ^b	12,687
Type III and IIIA tank liner failure (yr)	12,751
Type IV tank liner failure (yr)	3,638
Ancillary equipment containment failure (yr)	510
Chemical transition of waste tank grout from reduced to oxidized (pore volumes)	523
Chemical transition of waste tank grout from Region II to Region III (pore volumes)	2,119

a Type I Tank 12 is modeled to have liner failure at the time of HTF closure

b Type II Tanks 14, 15, and 16 are modeled to have liner failure at the time of HTF closure

The uncertainties and sensitivities associated with the Base Case are discussed in detail in Section 5.6.

5.2.1 Groundwater Concentrations at 100 Meters

The 100-meter groundwater concentrations were calculated using the HTF PORFLOW Model, which divides the area around HTF into computational cells. The red line in Figure 5.2-1 is the demarcation line from which the 1-meter and 100-meter concentrations are calculated. The orange squares in Figure 5.2-1 identify aquifer source nodes that receive contaminant flux from vadose zone, waste tank modeling. Source nodes are defined as cells within the footprint for each waste tank. Typically, three to four cells are identified as source nodes. With respect to area, two computational cells come closest to matching the physical waste tank area. Once source node (closest to the center of the waste tank footprint) concentrates the vadose zone flux, while additional source nodes dilute the source. Sixteen (55 %) waste tanks utilize two source nodes, while five (17 %), seven (24 %), and one (3 %) waste tanks have one, three, and four source nodes, respectively. A sensitivity case using a conservative tracer species and exactly two sources for each waste tank indicates a modest impact on 1-meter and 100-meter concentrations. At 100 meters, peak concentrations

differed by less than 10 % for 11 waste tanks, and 10 to 20 % for the remaining two waste tanks. At 1-meter nodes, peak concentrations differed by less than 10 % for six waste tanks, 10 to 20 % for five waste tanks, and 20 to 30 % for two waste tanks. The average peak concentration for all waste tanks together was nearly identical for the two cases at both 1 meter and 100 meters. The smaller magenta squares indicate the source nodes of certain ancillary (point) sources, such as pump tanks and evaporators.

Figure 5.2-1: 100 Meter Distance from HTF



Red Line = Demarcation line from which the 1-meter and 100-meter concentrations are calculated.
Red Diamonds = 1-meter distance from HTF
Green Diamonds = 100-meter distance from HTF

The green diamonds in Figure 5.2-1 show the 100-meter distance from HTF. Figure 5.2-2 illustrates the contaminant flow from the waste tanks using centerline stream traces. Since contaminant transport is not via a straight line, but by the applicable aquifers, the actual travel distance to reach 100 meters from the HTF boundary is greater than 100 meters for some sources. Table 5.2-2 shows the approximate distances a contaminant has to travel from each waste tank to reach a point 100 meters from the HTF boundary in the direction of the flow. The aquifer travel distances to the 100-meter boundary were scaled from the center of the waste tank location along the stream traces to the 100-meter boundary using information presented in Figure 5.2-2. The aquifer travel distances to the 100-meter boundary were measured from the center of the waste tank location along the 2-D stream trace to the center of the hypothetical wells along the 100-meter boundary. A string was laid along the stream traces on Figure 5.2-2 scaled in feet and converted to meters.

Figure 5.2-2: Stream Traces from HTF



Table 5.2-2: Approximate Aquifer Travel Distance to HTF 100-Meter Boundary

Waste Tank	100m Boundary (m)	Waste Tank	100m Boundary (m)
9	269	31	234
10	220	32	181
11	308	35	164
12	284	36	113
13	504	37	128
14	454	38	259
15	327	39	253
16	574	40	240
21	379	41	216
22	291	42	287
23	399	43	247
24	336	48	346
29	280	49	249
30	253	50	370
		51	234

The groundwater concentrations at 100 meters are assumed as the highest concentration in the range 100 meters or farther from the HTF. This assumption is supported by Figures 5.2-3 and 5.2-4, which present the plume that would result from a continuous (non-depleting) source of tracer (no decay, nor sorption). Figure 5.2-3 is a projection of plume centerline concentration onto a map view that displays the highest concentration at any location, irrespective of depth/aquifer. The waste tanks in HTF are shown as the small red circles. Similarly, Figure 5.2-4 is a projection of plume centerline onto the cross-sectional slice A-A shown in Figure 5.2-3. Scale bars indicate groundwater concentration is in moles divided by liter. The plume was generated from a hypothetical constant source of 1 mol/yr of a non-sorbing, non-decaying tracer placed in the waste tank source zones. The tracer plume illustrates groundwater flow directions and dispersion.

Peak concentration is observed to decrease monotonically with travel distance from the source zone, because of hydrodynamic dispersion. No physical mechanism exists to concentrate contamination beyond the source zone in the fully 3-D PORFLOW simulations. Hence, calculating the concentrations at 100 meters is adequate to capture the peak concentration that can occur at any location beyond 100 meters.

Figure 5.2-3: Contaminant Plume Leaving HTF (Aerial View)

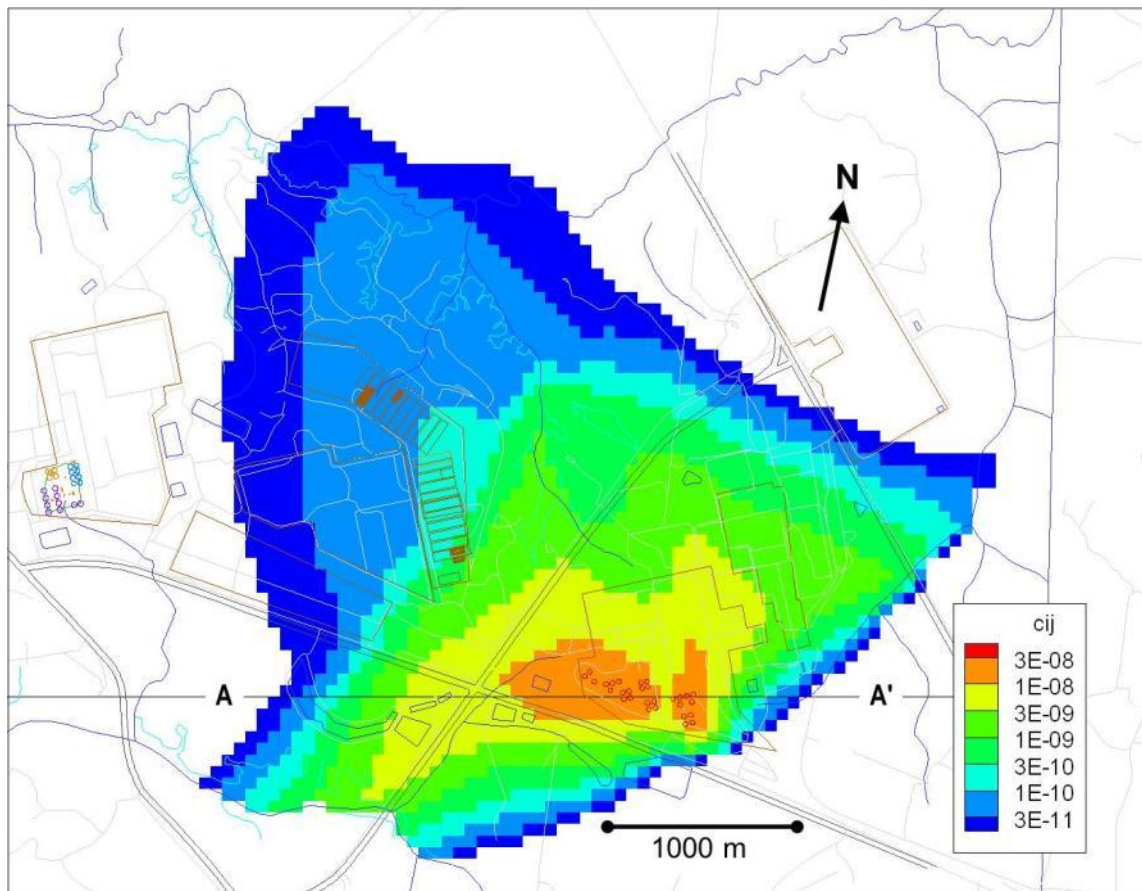
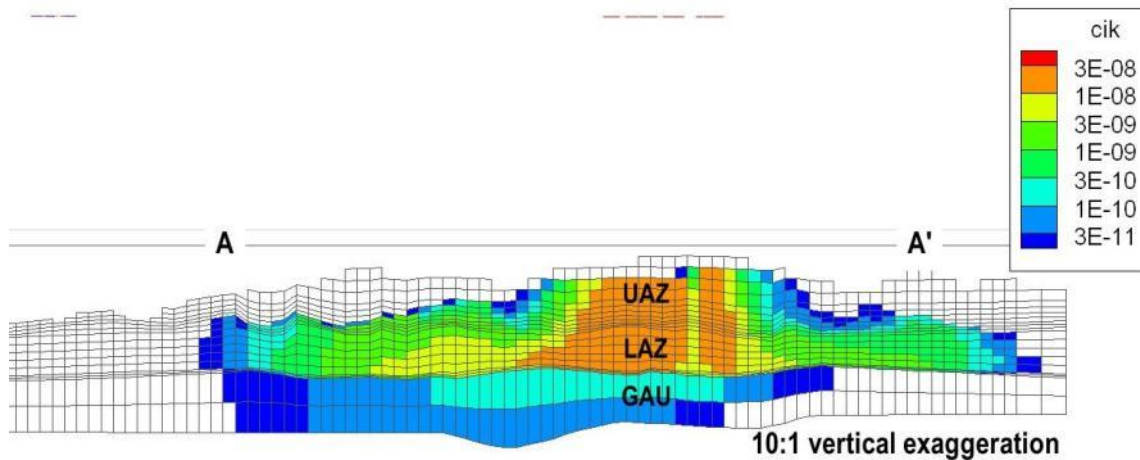


Figure 5.2-4: Contaminant Plume Leaving HTF (Cross Section View)



The PORFLOW 100-meter concentrations were calculated for six sectors (Sectors A through F) as shown on Figure 5.2-5. The peak concentration values for the 100-meter results are recorded for the depths of the three aquifer of concern (i.e., UTRA-UZ, UTRA-LZ, and Gordon Aquifer). The concentration for each aquifer represents peak concentration in any vertical computational mesh within the aquifer. The mesh vertical thicknesses (heights) in the computational model are less than 10 feet in the UTRA-UZ, and less than 15 feet in the UTRA-LZ. No well screen averaging was used in determining the concentrations for dose calculations because the typical well screen length of 20 feet is similar to the computational mesh height. Dividing the results into sectors was necessary to allow the large amount of concentration data to be stored from PORFLOW and used by the GoldSim dose calculator model, but also allowed variability in peak concentration for different areas of the HTF to be more easily evaluated. The six sectors were analyzed for each radionuclide and chemical to find the maximum groundwater concentrations at 100 meters from the HTF. The PORFLOW 1-meter concentrations were calculated for six sectors (Sectors A through F), as shown in Figure 5.2-5. Using the sectors to determine the highest groundwater concentrations causes the calculated peak doses to be higher than they actually are, since the peak concentrations are determined for each radionuclide independent of the location within the sector.

Figure 5.2-5: HTF PORFLOW 1-Meter and 100-Meter Model Evaluation Sectors



Note: The individual sectors at the 1-meter and 100-meter boundaries are indicated by unique diamond colors.

Tables 5.2-3 through 5.2-5 present the peak 100-meter radionuclide concentrations (picocurie divided by liter) in each sector for the three aquifers. These radionuclide concentrations reflect the peak concentrations for each radionuclide in the sector. These values are conservatively high for the radionuclides present in multiple decay chains because the totals are simply the sum of the individual peaks within that sector for a given radionuclide, without regard to time or location. For example, if Pb-210 were present as a daughter product in six decay chains, those six concentrations would all be added (along with the initial Pb-210) together to arrive at a single Pb-210 concentration for that sector, even though the peaks for six daughters might have occurred at different times and at different locations within the sector. Tables 5.2-3 through 5.2-5 also list the MCL for each constituent with the derived values for beta and photo emitters from EPA 815-R-02-001. The MCLs provided in the reference are derived for 4 mrem/yr beta-gamma dose. The peak concentration from any time in 1,000 years for each beta-gamma emitter is compared to a specific MCL to determine their fraction. This was a conservative approach since peaks may occur at different times. To determine if the 4 mrem/yr beta-gamma limit is met, the sum of the fractions must be less than 1.0. The total alpha MCL includes Ra-226, but does not include radon or uranium. The radium MCL includes both Ra-226 and Ra-228. [SCDHEC R.61-58] The MCL for total uranium, in units of microgram divided by liter, is compared to the chemical concentration of uranium in the groundwater.

Table 5.2-3: Radiological 100-Meter Concentrations for UTRA-UZ

Rad	MCL (pCi/L)*	Sector A Concentration		Sector B Concentration		Sector C Concentration		Sector D Concentration		Sector E Concentration		Sector F Concentration	
		(pCi/L)	Yr Peak Occurs	(pCi/L)	Year Peak Occurs								
Ac-227	N/A	3.7E-08	1,000	3.7E-09	1,000	1.1E-07	1,000	5.1E-10	1,000	1.0E-08	808	2.0E-08	790
Al-26	N/A	<1E-30	1,000	<1E-30	1,000	<1E-30	1,000	<1E-30	1,000	<1E-30	1,000	<1E-30	1,000
Am-241	Total α	2.1E-27	1,000	<1E-30	1,000	5.4E-30	1,000	1.2E-28	1,000	<1E-30	1,000	2.3E-30	1,000
Am-242m	Total α	<1E-30	1,000	<1E-30	1,000	<1E-30	1,000	<1E-30	1,000	<1E-30	1,000	<1E-30	1,000
Am-243	Total α	1.5E-28	1,000	<1E-30	1,000	<1E-30	1,000	8.8E-30	1,000	<1E-30	1,000	<1E-30	1,000
C-14	2,000	8.9E-06	1,000	4.0E-13	1,000	7.8E-05	1,000	5.1E-07	1,000	9.6E-07	1,000	1.1E-05	1,000
Cf-249	Total α	<1E-30	1,000	<1E-30	1,000	<1E-30	1,000	<1E-30	1,000	<1E-30	1,000	<1E-30	1,000
Cf-251	Total α	<1E-30	1,000	<1E-30	1,000	<1E-30	1,000	<1E-30	1,000	<1E-30	1,000	<1E-30	1,000
Cl-36	700	7.0E-03	858	1.2E-02	966	1.1E-02	998	1.5E-03	1,000	4.1E-03	1,000	4.8E-03	1,000
Cm-243	Total α	<1E-30	1,000	<1E-30	1,000	<1E-30	884	<1E-30	498	<1E-30	1,000	<1E-30	1,000
Cm-244	Total α	<1E-30	390	<1E-30	1,000	<1E-30	362	<1E-30	312	<1E-30	850	<1E-30	440
Cm-245	Total α	<1E-30	1,000	<1E-30	1,000	<1E-30	1,000	<1E-30	1,000	<1E-30	1,000	<1E-30	1,000
Cm-247	Total α	<1E-30	1,000	<1E-30	1,000	<1E-30	1,000	<1E-30	1,000	<1E-30	1,000	<1E-30	1,000
Cm-248	Total α	<1E-30	1,000	<1E-30	1,000	<1E-30	1,000	<1E-30	1,000	<1E-30	1,000	<1E-30	1,000
Co-60	100	1.2E-30	110	<1E-30	340	1.3E-28	138	1.8E-29	112	<1E-30	234	<1E-30	122
Cs-135	900	9.7E-05	1,000	6.2E-12	1,000	5.8E-03	1,000	5.6E-06	1,000	8.0E-05	1,000	5.0E-04	1,000
Cs-137	200	9.9E-09	846	6.4E-16	742	5.5E-07	854	3.7E-10	890	1.7E-09	1,000	1.2E-08	962
Eu-152	200	<1E-30	290	<1E-30	808	<1E-30	272	<1E-30	232	<1E-30	600	<1E-30	328
Eu-154	60	<1E-30	186	<1E-30	474	<1E-30	174	<1E-30	148	<1E-30	346	<1E-30	210
H-3	20,000	6.4E+00	78	6.4E-02	80	1.3E+00	62	1.3E-01	60	3.9E-07	80	3.7E-02	80
I-129	1	1.9E-03	656	3.2E-03	682	2.7E-03	716	5.4E-04	738	1.6E-03	754	1.6E-03	704
K-40	N/A	2.0E-04	1,000	4.3E-07	1,000	1.3E-03	848	6.8E-06	984	2.3E-04	946	4.6E-04	918
Nb-93m	1,000	8.2E+00	562	1.3E+01	836	3.5E+01	820	1.8E+00	844	8.2E+00	840	1.1E+01	838
Nb-94	N/A	9.8E-03	578	1.5E-02	582	1.9E-02	542	2.9E-03	600	8.8E-03	606	9.4E-03	586

Table 5.2-3: Radiological 100-Meter Concentrations for UTRA-UZ (Continued)

Rad	MCL (pCi/L)*	Sector A Concentration		Sector B Concentration		Sector C Concentration		Sector D Concentration		Sector E Concentration		Sector F Concentration	
		(pCi/L)	Year Peak Occurs										
Ni-59	300	7.0E-02	1,000	1.5E-06	1,000	1.3E+00	954	4.5E-03	1,000	1.7E-01	1,000	4.7E-01	1,000
Ni-63	50	5.1E-03	990	8.5E-08	1,000	1.5E-01	876	3.2E-04	998	1.1E-02	1,000	3.0E-02	976
Np-237	Total α	1.0E-01	1,000	1.4E-02	1,000	2.5E-01	1,000	1.1E-03	1,000	3.1E-02	776	6.0E-02	758
Pa-231	Total α	1.4E-05	1,000	1.8E-06	1,000	4.3E-05	1,000	1.9E-07	1,000	4.0E-06	780	7.9E-06	764
Pb-210	N/A	2.9E-12	1,000	2.2E-26	1,000	6.2E-11	1,000	3.9E-14	1,000	8.0E-17	1,000	2.2E-12	1,000
Pd-107	N/A	1.1E-02	1,000	2.2E-07	1,000	2.0E-01	954	6.8E-04	1,000	2.6E-02	1,000	7.1E-02	1,000
Pt-193	3,000	1.6E-08	902	1.4E-13	1,000	7.9E-07	828	9.4E-10	912	2.1E-08	966	7.8E-08	924
Pu-238	Total α	7.0E-26	1,000	<1E-30	1,000	3.1E-27	1,000	8.2E-27	1,000	<1E-30	1,000	2.1E-28	1,000
Pu-239	Total α	3.2E-24	1,000	<1E-30	1,000	1.7E-25	1,000	4.4E-25	1,000	<1E-30	1,000	9.6E-27	1,000
Pu-240	Total α	1.7E-24	1,000	<1E-30	1,000	9.5E-26	1,000	2.4E-25	1,000	<1E-30	1,000	5.3E-27	1,000
Pu-241	300	1.4E-30	1,000	<1E-30	1,000								
Pu-242	Total α	5.5E-27	1,000	<1E-30	1,000	3.1E-28	1,000	7.8E-28	1,000	<1E-30	1,000	1.7E-29	1,000
Pu-244	Total α	2.5E-29	1,000	<1E-30	1,000	1.4E-30	1,000	3.6E-30	1,000	<1E-30	1,000	<1E-30	1,000
Ra-226	Total α /Ra	3.8E-10	1,000	3.5E-24	1,000	8.3E-09	1,000	5.2E-12	1,000	1.7E-14	1,000	3.0E-10	1,000
Ra-228	Total Ra	4.1E-20	1,000	<1E-30	1,000	4.1E-19	1,000	8.5E-21	1,000	8.1E-30	1,000	3.8E-21	1,000
Se-79	N/A	3.2E-28	1,000	<1E-30	1,000	1.5E-30	1,000	2.4E-29	1,000	<1E-30	1,000	<1E-30	1,000
Sm-151	1,000	2.5E-28	1,000	<1E-30	1,000	<1E-30	1,000	1.2E-29	1,000	<1E-30	1,000	<1E-30	1,000
Sn-126	N/A	<1E-30	1,000										
Sr-90	8	3.7E-06	764	3.5E-10	1,000	2.4E-04	724	2.1E-07	778	3.3E-06	830	1.4E-05	800
Tc-99	900	1.0E+02	732	1.6E+02	774	1.4E+02	824	2.7E+01	882	8.4E+01	906	8.1E+01	848
Th-229	Total α	1.9E-09	1,000	4.9E-11	1,000	1.4E-08	1,000	5.4E-11	1,000	1.2E-09	1,000	2.5E-09	1,000
Th-230	Total α	1.1E-24	1,000	<1E-30	1,000	2.0E-24	1,000	3.6E-25	1,000	<1E-30	1,000	1.4E-26	1,000
Th-232	Total α	1.3E-29	1,000	<1E-30	1,000	<1E-30	1,000	1.2E-30	1,000	<1E-30	1,000	<1E-30	1,000
U-232	Total U	4.2E-28	1,000	<1E-30	1,000	6.5E-28	1,000	1.0E-28	1,000	<1E-30	1,000	5.7E-30	1,000

Table 5.2-3: Radiological 100-Meter Concentrations for UTRA-UZ (Continued)

Rad	MCL (pCi/L)*	Sector A Concentration		Sector B Concentration		Sector C Concentration		Sector D Concentration		Sector E Concentration		Sector F Concentration	
		(pCi/L)	Year Peak Occurs										
U-233	Total U	6.5E-07	1,000	3.7E-08	1,000	2.7E-06	1,000	1.2E-08	1,000	1.8E-07	1,000	4.5E-07	1,000
U-234	Total U	7.2E-21	1,000	<1E-30	1,000	8.7E-21	1,000	1.6E-21	1,000	<1E-30	1,000	9.9E-23	1,000
U-235	Total U	1.4E-23	1,000	<1E-30	1,000	2.8E-23	1,000	4.4E-24	1,000	<1E-30	1,000	2.0E-25	1,000
U-236	Total U	1.1E-22	1,000	<1E-30	1,000	2.2E-22	1,000	3.4E-23	1,000	<1E-30	1,000	1.5E-24	1,000
U-238	Total U	1.3E-22	1,000	<1E-30	1,000	2.5E-22	1,000	3.9E-23	1,000	<1E-30	1,000	1.8E-24	1,000
Zr-93	2,000	1.9E-27	1,000	<1E-30	1,000	1.7E-29	1,000	1.7E-28	1,000	<1E-30	1,000	3.1E-30	1,000
Total Alpha	15	1.0E-01	NA	1.4E-02	NA	2.5E-01	NA	1.1E-03	NA	3.1E-02	NA	6.0E-02	NA
Total Ra	5	3.8E-10	NA	3.5E-24	NA	8.3E-09	NA	5.2E-12	NA	1.7E-14	NA	3.0E-10	NA
Sum of beta-gamma MCL fractions		1.2E-01	NA	1.9E-01	NA	1.9E-01	NA	3.2E-02	NA	1.0E-01	NA	1.0E-01	NA

* MCL values for beta and photon emitters are calculated in EPA 815-R-02-001 based on 4 mrem/yr beta-gamma dose.
N/A = Not Applicable

Table 5.2-4: Radiological 100-Meter Concentrations for UTRA-LZ

Rad	MCL (pCi/L)*	Sector A Concentration		Sector B Concentration		Sector C Concentration		Sector D Concentration		Sector E Concentration		Sector F Concentration	
		(pCi/L)	Year Peak Occurs										
Ac-227	N/A	9.3E-09	1,000	9.1E-09	1,000	9.0E-08	1,000	2.0E-09	1,000	3.6E-09	832	5.6E-09	836
Al-26	N/A	<1E-30	1,000										
Am-241	Total α	<1E-30	1,000										
Am-242m	Total α	<1E-30	1,000										
Am-243	Total α	<1E-30	1,000										
C-14	2,000	4.2E-10	1,000	2.9E-12	1,000	4.3E-05	1,000	2.1E-07	1,000	3.3E-08	1,000	5.7E-08	1,000
Cf-249	Total α	<1E-30	1,000										
Cf-251	Total α	<1E-30	1,000										
Cl-36	700	1.0E-02	930	9.1E-03	1,000	9.1E-03	1,000	2.7E-04	674	4.6E-03	1,000	4.8E-03	1,000
Cm-243	Total α	<1E-30	1,000										
Cm-244	Total α	<1E-30	724	<1E-30	1,000	<1E-30	690	<1E-30	662	<1E-30	1,000	<1E-30	776
Cm-245	Total α	<1E-30	1,000										
Cm-247	Total α	<1E-30	1,000										
Cm-248	Total α	<1E-30	1,000										
Co-60	100	<1E-30	200	<1E-30	384	<1E-30	194	<1E-30	166	<1E-30	316	<1E-30	214
Cs-135	900	3.5E-08	1,000	3.0E-11	1,000	3.4E-03	1,000	2.7E-06	1,000	2.9E-06	1,000	5.2E-06	1,000
Cs-137	200	1.1E-12	1,000	2.1E-15	798	1.5E-07	900	9.1E-11	972	5.7E-11	1,000	1.0E-10	1,000
Eu-152	200	<1E-30	542	<1E-30	1,000	<1E-30	518	<1E-30	494	<1E-30	848	<1E-30	580
Eu-154	60	<1E-30	344	<1E-30	688	<1E-30	330	<1E-30	308	<1E-30	506	<1E-30	370
H-3	20,000	1.2E+01	84	4.0E+00	90	1.3E+01	74	9.2E-01	72	3.9E-07	118	2.5E-01	92
I-129	1	2.4E-03	686	2.6E-03	736	2.0E-03	598	2.3E-04	852	1.9E-03	736	1.9E-03	730
K-40	N/A	1.6E-05	1,000	1.1E-06	1,000	1.4E-03	900	2.5E-05	1,000	7.9E-05	986	1.2E-04	992
Nb-93m	1,000	5.0E+00	584	8.7E+00	852	2.7E+01	546	3.4E-01	896	7.2E+00	850	7.9E+00	846
Nb-94	N/A	1.2E-02	590	1.2E-02	604	1.5E-02	544	1.2E-03	648	1.0E-02	598	1.0E-02	596

Table 5.2-4: Radiological 100-Meter Concentrations for UTRA-LZ (Continued)

Rad	MCL (pCi/L)*	Sector A Concentration		Sector B Concentration		Sector C Concentration		Sector D Concentration		Sector E Concentration		Sector F Concentration	
		(pCi/L)	Year Peak Occurs										
Ni-59	300	7.4E-04	1,000	3.1E-06	1,000	1.4E+00	1,000	6.3E-03	1,000	2.9E-02	1,000	4.3E-02	1,000
Ni-63	50	5.0E-05	1,000	1.7E-07	1,000	1.2E-01	920	4.4E-04	1,000	1.8E-03	1,000	2.6E-03	1,000
Np-237	Total α	3.2E-02	1,000	3.8E-02	1,000	1.9E-01	1,000	4.7E-03	964	1.0E-02	800	1.6E-02	804
Pa-231	Total α	4.2E-06	1,000	4.8E-06	1,000	3.4E-05	1,000	7.1E-07	1,000	1.4E-06	804	2.2E-06	808
Pb-210	N/A	3.5E-20	1,000	6.5E-27	1,000	1.4E-12	1,000	1.9E-15	1,000	1.7E-20	1,000	5.0E-20	1,000
Pd-107	N/A	1.1E-04	1,000	4.7E-07	1,000	2.1E-01	1,000	9.6E-04	1,000	4.4E-03	1,000	6.5E-03	1,000
Pt-193	3,000	1.0E-10	1,000	2.8E-13	1,000	4.3E-07	868	9.3E-10	990	3.1E-09	1,000	4.6E-09	1,000
Pu-238	Total α	<1E-30	1,000										
Pu-239	Total α	<1E-30	1,000										
Pu-240	Total α	<1E-30	1,000										
Pu-241	300	<1E-30	1,000										
Pu-242	Total α	<1E-30	1,000										
Pu-244	Total α	<1E-30	1,000										
Ra-226	Total α /Ra	6.6E-18	1,000	1.1E-24	1,000	2.4E-10	1,000	2.9E-13	1,000	3.9E-18	1,000	1.1E-17	1,000
Ra-228	Total Ra	<1E-30	1,000	<1E-30	1,000	3.5E-25	1,000	8.8E-27	1,000	<1E-30	1,000	<1E-30	1,000
Se-79	N/A	<1E-30	1,000										
Sm-151	1,000	<1E-30	1,000	<1E-30	1,000	<1E-30	1,000	<1E-30	1,000	<1E-30	1,000	<1E-30	1,000
Sn-126	N/A	<1E-30	1,000										
Sr-90	8	2.7E-08	932	7.3E-10	1,000	1.1E-04	752	1.6E-07	836	4.3E-07	868	6.4E-07	864
Tc-99	900	2.0E+02	858	1.7E+02	722	1.9E+02	690	1.3E+01	1,000	9.9E+01	876	9.9E+01	870
Th-229	Total α	2.2E-10	1,000	1.1E-10	1,000	1.2E-08	1,000	1.4E-10	1,000	3.7E-10	1,000	5.7E-10	1,000
Th-230	Total α	<1E-30	1,000										
Th-232	Total α	<1E-30	1,000										
U-232	Total U	<1E-30	1,000										

Table 5.2-4: Radiological 100-Meter Concentrations for UTRA-LZ (Continued)

Rad	MCL (pCi/L) *	Sector A Concentration		Sector B Concentration		Sector C Concentration		Sector D Concentration		Sector E Concentration		Sector F Concentration	
		(pCi/L)	Year Peak Occurs										
U-233	Total U	1.1E-07	1,000	8.8E-08	1,000	2.4E-06	1,000	4.1E-08	1,000	6.2E-08	1,000	9.9E-08	1,000
U-234	Total U	<1E-30	1,000	<1E-30	1,000	2.4E-29	1,000	1.2E-29	1,000	<1E-30	1,000	<1E-30	1,000
U-235	Total U	<1E-30	1,000										
U-236	Total U	<1E-30	1,000										
U-238	Total U	<1E-30	1,000										
Zr-93	2,000	<1E-30	1,000										
Total Alpha	15	3.2E-02	NA	3.8E-02	NA	1.9E-01	NA	4.7E-03	NA	1.0E-02	NA	1.6E-02	NA
Total Ra	5	6.6E-18	NA	1.1E-24	NA	2.4E-10	NA	2.9E-13	NA	3.9E-18	NA	1.1E-17	NA
Sum of beta-gamma MCL fractions		2.2E-01	NA	2.0E-01	NA	2.4E-01	NA	1.5E-02	NA	1.2E-01	NA	1.2E-01	NA

* MCL values for beta and photon emitters are calculated in EPA 815-R-02-001 based on a 4 mrem/yr beta-gamma dose.
N/A = Not Applicable

Table 5.2-5: Radiological 100-Meter Concentrations for the Gordon Aquifer

Rad	MCL (pCi/L)*	Sector A Concentration		Sector B Concentration		Sector C Concentration		Sector D Concentration		Sector E Concentration		Sector F Concentration	
		(pCi/L)	Year Peak Occurs										
Ac-227	N/A	3.2E-14	1,000	1.8E-13	1,000	1.7E-13	1,000	1.8E-16	1,000	5.9E-17	1,000	2.1E-16	1,000
Al-26	N/A	<1E-30	1,000										
Am-241	Total α	<1E-30	1,000										
Am-242m	Total α	<1E-30	1,000										
Am-243	Total α	<1E-30	1,000										
C-14	2,000	3.0E-20	1,000	5.3E-18	1,000	7.3E-17	1,000	1.6E-20	1,000	3.6E-22	1,000	8.7E-22	1,000
Cf-249	Total α	<1E-30	1,000										
Cf-251	Total α	<1E-30	1,000										
Cl-36	700	5.5E-07	1,000	7.5E-07	1,000	1.9E-07	1,000	2.4E-10	1,000	3.1E-10	1,000	1.0E-09	1,000
Cm-243	Total α	<1E-30	1,000										
Cm-244	Total α	<1E-30	900	<1E-30	1,000	<1E-30	918	<1E-30	822	<1E-30	1,000	<1E-30	952
Cm-245	Total α	<1E-30	1,000										
Cm-247	Total α	<1E-30	1,000										
Cm-248	Total α	<1E-30	1,000										
Co-60	100	<1E-30	242	<1E-30	394	<1E-30	240	<1E-30	226	<1E-30	364	<1E-30	256
Cs-135	900	7.1E-17	1,000	1.3E-14	1,000	3.7E-13	1,000	1.6E-17	1,000	2.0E-18	1,000	5.6E-18	1,000
Cs-137	200	4.9E-21	682	6.3E-19	682	7.4E-18	1,000	4.1E-22	1,000	3.2E-23	1,000	9.1E-23	1,000
Eu-152	200	<1E-30	674	<1E-30	1,000	<1E-30	690	<1E-30	616	<1E-30	982	<1E-30	712
Eu-154	60	<1E-30	430	<1E-30	768	<1E-30	442	<1E-30	394	<1E-30	592	<1E-30	454
H-3	20,000	1.0E-03	114	2.0E-03	106	7.5E-04	100	1.8E-06	100	2.6E-12	142	1.7E-06	124
I-129	1	1.4E-06	876	1.5E-06	868	2.4E-07	788	6.2E-09	1,000	6.7E-08	968	4.3E-07	1,000
K-40	N/A	1.2E-12	1,000	5.2E-11	1,000	6.7E-11	1,000	4.1E-14	1,000	3.0E-14	1,000	9.2E-14	1,000
Nb-93m	1,000	1.8E-03	952	2.6E-03	982	9.9E-04	996	2.3E-06	960	4.3E-05	928	2.0E-04	938
Nb-94	N/A	1.1E-05	642	1.1E-05	640	1.9E-06	604	5.1E-08	708	5.1E-07	676	3.6E-06	698

Table 5.2-5: Radiological 100-Meter Concentrations for the Gordon Aquifer (Continued)

Rad	MCL (pCi/L)*	Sector A Concentration		Sector B Concentration		Sector C Concentration		Sector D Concentration		Sector E Concentration		Sector F Concentration	
		(pCi/L)	Year Peak Occurs										
Ni-59	300	1.3E-11	1,000	1.6E-09	1,000	5.6E-09	1,000	8.1E-13	1,000	6.2E-13	1,000	1.7E-12	1,000
Ni-63	50	7.7E-13	1,000	9.0E-11	1,000	3.3E-10	1,000	5.4E-14	1,000	3.5E-14	1,000	9.4E-14	1,000
Np-237	Total α	1.4E-07	1,000	7.3E-07	1,000	6.0E-07	1,000	6.8E-10	1,000	1.8E-10	1,000	6.4E-10	1,000
Pa-231	Total α	1.8E-11	1,000	9.4E-11	1,000	7.9E-11	1,000	8.8E-14	1,000	2.5E-14	1,000	8.9E-14	1,000
Pb-210	N/A	<1E-30	1,000	1.5E-28	1,000	1.4E-25	1,000	8.6E-30	1,000	<1E-30	1,000	<1E-30	1,000
Pd-107	N/A	2.0E-12	1,000	2.4E-10	1,000	8.5E-10	1,000	1.2E-13	1,000	9.4E-14	1,000	2.5E-13	1,000
Pt-193	3,000	1.3E-18	1,000	1.5E-16	1,000	5.8E-16	1,000	1.0E-19	1,000	5.9E-20	1,000	1.6E-19	1,000
Pu-238	Total α	<1E-30	1,000										
Pu-239	Total α	<1E-30	1,000										
Pu-240	Total α	<1E-30	1,000										
Pu-241	300	<1E-30	1,000										
Pu-242	Total α	<1E-30	1,000										
Pu-244	Total α	<1E-30	1,000										
Ra-226	Total α /Ra	4.4E-29	1,000	2.4E-26	1,000	2.1E-23	1,000	1.4E-27	1,000	<1E-30	1,000	<1E-30	1,000
Ra-228	Total Ra	<1E-30	1,000										
Se-79	N/A	<1E-30	1,000										
Sm-151	1,000	<1E-30	1,000	<1E-30	1,000	<1E-30	1,000	<1E-30	1,000	<1E-30	1,000	<1E-30	1,000
Sn-126	N/A	<1E-30	1,000										
Sr-90	8	1.9E-15	1,000	8.5E-14	960	1.6E-13	898	7.3E-17	994	4.7E-17	982	1.4E-16	986
Tc-99	900	3.6E-01	1,000	3.9E-01	1,000	5.9E-02	1,000	1.7E-04	1,000	1.2E-03	1,000	5.0E-03	1,000
Th-229	Total α	3.6E-16	1,000	3.5E-15	1,000	3.6E-15	1,000	3.2E-18	1,000	1.6E-18	1,000	5.5E-18	1,000
Th-230	Total α	<1E-30	1,000										
Th-232	Total α	<1E-30	1,000										
U-232	Total U	<1E-30	1,000										

Table 5.2-5: Radiological 100-Meter Concentrations for the Gordon Aquifer (Continued)

Rad	MCL (pCi/L)*	Sector A Concentration		Sector B Concentration		Sector C Concentration		Sector D Concentration		Sector E Concentration		Sector F Concentration	
		(pCi/L)	Year Peak Occurs										
U-233	Total U	3.0E-13	1,000	2.0E-12	1,000	2.0E-12	1,000	2.0E-15	1,000	7.9E-16	1,000	2.7E-15	1,000
U-234	Total U	<1E-30	1,000										
U-235	Total U	<1E-30	1,000										
U-236	Total U	<1E-30	1,000										
U-238	Total U	<1E-30	1,000										
Zr-93	2,000	<1E-30	1,000										
Total Alpha	15	1.4E-07	NA	7.3E-07	NA	6.0E-07	NA	6.8E-10	NA	1.8E-10	NA	6.4E-10	NA
Total Ra	5	4.4E-29	NA	2.4E-26	NA	2.1E-23	NA	1.4E-27	NA	<1E-30	NA	<1E-30	NA
Sum of beta- gamma MCL fractions		4.1E-04	NA	4.3E-04	NA	6.7E-05	NA	2.0E-07	NA	1.4E-06	NA	6.2E-06	NA

* MCL values for beta and photon emitters are calculated in EPA 815-R-02-001 based on a 4 mrem/yr beta-gamma dose.

N/A = Not Applicable

If the sum of the beta-gamma ratios is greater than 1.0, the total beta-gamma for the sector is calculated to be greater than the MCL. The highest predicted ratio was in Table 5.2-4 for Sector C of the UTRA-LZ with a summed ratio of 2.4E-01, which is below the total beta-gamma MCL.

In addition, as indicated in Table 5.2-3 through 5.2-5, on an individual constituent basis none of the radionuclides in any sector or aquifer at the 100-meter boundary exceeded their respective MCL. Total alpha values, which are determined by summing individual radionuclide alpha values by sector, are below the MCL for gross alpha of 15 pCi/L. The radionuclides used in this calculation are Am-241, Am-242m, Am-243, Cf-249, Cf-251, Cm-243, Cm-244, Cm-245, Cm-247, Cm-248, Np-237, Pa-231, Pu-238, Pu-239, Pu-240, Pu-242, Pu-244, Ra-226, Th-229, Th-230, and Th-232.

Tables 5.2-6 through 5.2-8 show the peak 100-meter chemical concentrations in each sector for the three aquifers. Nitrate and nitrite are modeled as nitrogen, therefore, the MCL for nitrate and nitrite (10,000 µg/L) is compared to the total nitrogen concentration. Total uranium includes all of the uranium isotopes as determined by inductively coupled plasma mass spectrometry (ICP-MS). The total uranium concentration is expressed in units of microgram per liter therefore; the MCL for total uranium (30 µg/L) is compared to the total uranium chemical concentration for compliance. On an individual constituent basis, none of the chemicals in any sector or aquifer at the 100-meter boundary exceeded their respective MCL.

Table 5.2-6: Chemical 100-Meter Concentrations for UTRA-UZ

Constituent	MCL (µg/L)	Sector A Concentration		Sector B Concentration		Sector C Concentration		Sector D Concentration		Sector E Concentration		Sector F Concentration	
		(µg/L)	Year Peak Occurs										
Ag	100	1.8E-05	1,000	1.4E-12	1,000	1.5E-03	1,000	1.0E-06	1,000	2.3E-05	1,000	1.4E-04	1,000
Al	200	2.4E-30	1,000	<1E-30	1,000								
As	10	6.9E-18	1,000	<1E-30	1,000	1.8E-16	1,000	2.2E-18	1,000	3.0E-30	1,000	7.5E-19	1,000
B	N/A	1.7E+01	114	1.7E+00	582	2.5E+00	540	3.3E-01	600	1.0E+00	606	1.1E+00	586
Ba	2,000	2.1E-06	1,000	6.8E-15	1,000	1.4E-04	1,000	6.7E-08	1,000	6.2E-08	1,000	2.1E-06	1,000
Cd	5	2.3E-06	1,000	6.9E-15	1,000	4.4E-04	1,000	1.0E-07	1,000	2.2E-07	1,000	4.4E-06	1,000
Cl	250,000	1.5E-01	858	2.6E-01	966	2.3E-01	1,000	3.2E-02	1,000	8.7E-02	1,000	1.0E-01	1,000
Co	N/A	1.6E-12	1,000	2.3E-29	1,000	1.5E-10	1,000	1.2E-13	1,000	2.2E-19	1,000	8.0E-13	1,000
Cr	100	1.9E-30	1,000	<1E-30	1,000								
Cu	1,300	1.5E-12	1,000	<1E-30	1,000	2.1E-10	1,000	3.4E-13	1,000	1.0E-20	1,000	5.3E-13	1,000
F	4,000	9.1E-02	578	1.4E-01	582	1.7E-01	542	2.7E-02	600	8.2E-02	606	8.7E-02	586
Fe	300	6.1E-18	1,000	<1E-30	1,000	4.2E-17	1,000	1.7E-18	1,000	<1E-30	1,000	1.8E-19	1,000
Hg	2	1.0E-27	1,000	<1E-30	1,000	1.8E-29	1,000	1.2E-28	1,000	<1E-30	1,000	2.1E-30	1,000
I	N/A	4.7E-03	656	7.9E-03	682	6.7E-03	716	1.3E-03	738	4.0E-03	754	4.0E-03	704
Mn	50	3.9E-05	1,000	1.3E-13	1,000	1.3E-03	1,000	1.3E-06	1,000	6.0E-07	1,000	4.0E-05	1,000
Mo	N/A	1.3E-29	1,000	<1E-30	1,000	<1E-30	1,000	1.0E-30	1,000	<1E-30	1,000	<1E-30	1,000
N	10,000	6.5E+00	578	9.7E+00	582	1.2E+01	542	1.9E+00	600	5.8E+00	606	6.2E+00	586
Ni	N/A	2.1E-03	1,000	4.5E-08	1,000	4.1E-02	956	1.4E-04	1,000	5.1E-03	1,000	1.4E-02	1,000
Pb	15	<1E-30	1,000										
PO ₄	N/A	4.1E+00	114	2.4E-01	582	4.3E-01	542	4.9E-02	600	1.5E-01	606	1.6E-01	586
Sb	6	<1E-30	1,000										
Se	50	<1E-30	1,000										
SO ₄	250,000	2.1E+01	114	7.7E-01	582	2.0E+00	166	1.5E-01	164	4.6E-01	606	4.9E-01	586
Sr	N/A	4.3E-04	1,000	8.3E-07	1,000	2.2E-03	822	1.2E-05	1,000	4.2E-04	928	8.2E-04	900
U	30	3.7E-22	1,000	<1E-30	1,000	7.4E-22	1,000	1.1E-22	1,000	<1E-30	1,000	5.1E-24	1,000
Zn	5,000	7.7E-07	1,000	2.3E-15	1,000	1.5E-04	1,000	3.4E-08	1,000	7.3E-08	1,000	1.5E-06	1,000

Table 5.2-7: Chemical 100-Meter Concentrations for UTRA-LZ

Constituent	MCL (µg/L)	Sector A Concentration		Sector B Concentration		Sector C Concentration		Sector D Concentration		Sector E Concentration		Sector F Concentration	
		(µg/L)	Year Peak Occurs										
Ag	100	1.1E-08	1,000	5.6E-12	1,000	9.3E-04	1,000	5.3E-07	1,000	8.9E-07	1,000	1.6E-06	1,000
Al	200	<1E-30	1,000										
As	10	<1E-30	1,000	<1E-30	1,000	4.1E-21	1,000	3.6E-23	1,000	<1E-30	1,000	<1E-30	1,000
B	N/A	5.2E+01	132	1.9E+01	210	2.3E+01	194	1.3E+00	186	1.1E+00	598	1.2E+00	596
Ba	2,000	1.1E-11	1,000	1.5E-14	1,000	2.8E-05	1,000	1.3E-08	1,000	2.9E-10	1,000	5.8E-10	1,000
Cd	5	3.9E-11	1,000	1.5E-14	1,000	9.4E-05	1,000	3.4E-08	1,000	1.1E-09	1,000	2.2E-09	1,000
Cl	250,000	2.2E-01	930	1.9E-01	1,000	1.9E-01	1,000	5.8E-03	676	9.8E-02	1,000	1.0E-01	1,000
Co	N/A	4.8E-22	1,000	1.8E-30	1,000	2.4E-13	1,000	4.3E-16	1,000	1.8E-23	1,000	6.4E-23	1,000
Cr	100	<1E-30	1,000										
Cu	1,300	6.2E-23	1,000	<1E-30	1,000	8.8E-14	1,000	1.9E-16	1,000	3.0E-25	1,000	2.0E-24	1,000
F	4,000	1.1E-01	590	1.1E-01	604	1.4E-01	544	1.1E-02	648	9.4E-02	598	9.5E-02	596
Fe	300	<1E-30	1,000	<1E-30	1,000	4.1E-24	1,000	3.7E-25	1,000	<1E-30	1,000	<1E-30	1,000
Hg	2	<1E-30	1,000										
I	N/A	5.9E-03	686	6.5E-03	736	4.9E-03	598	5.8E-04	852	4.6E-03	738	4.6E-03	732
Mn	50	1.0E-10	1,000	2.8E-13	1,000	2.7E-04	1,000	1.5E-07	1,000	2.8E-09	1,000	5.5E-09	1,000
Mo	N/A	<1E-30	1,000										
N	10,000	7.6E+00	590	7.9E+00	604	1.0E+01	544	8.1E-01	648	6.7E+00	598	6.8E+00	596
Ni	N/A	2.3E-05	1,000	9.3E-08	1,000	4.2E-02	1,000	1.9E-04	1,000	8.8E-04	1,000	1.3E-03	1,000
Pb	15	<1E-30	1,000										
PO ₄	N/A	1.3E+01	138	7.5E+00	212	8.8E+00	198	5.1E-01	186	1.7E-01	598	5.9E-01	226
Sb	6	<1E-30	1,000										
Se	50	<1E-30	1,000										
SO ₄	250,000	6.8E+01	138	3.6E+01	212	4.2E+01	196	2.4E+00	186	5.3E-01	598	2.8E+00	226
Sr	N/A	3.4E-05	1,000	2.1E-06	1,000	2.4E-03	870	4.0E-05	1,000	1.4E-04	966	2.2E-04	974
U	30	<1E-30	1,000	<1E-30	1,000	2.4E-30	1,000	1.1E-30	1,000	<1E-30	1,000	<1E-30	1,000
Zn	5,000	1.3E-11	1,000	4.9E-15	1,000	3.1E-05	1,000	1.1E-08	1,000	3.6E-10	1,000	7.4E-10	1,000

Table 5.2-8: Chemical 100-Meter Concentrations for Gordon Aquifer

Constituent	MCL (µg/L)	Sector A Concentration		Sector B Concentration		Sector C Concentration		Sector D Concentration		Sector E Concentration		Sector F Concentration	
		(µg/L)	Year Peak Occurs										
Ag	100	5.5E-17	1,000	1.0E-14	1,000	3.0E-13	1,000	9.8E-18	1,000	1.7E-18	1,000	5.3E-18	1,000
Al	200	<1E-30	1,000										
As	10	<1E-30	1,000										
B	N/A	1.1E-01	350	1.1E-01	350	1.8E-02	314	3.2E-05	314	5.7E-05	676	4.7E-04	704
Ba	2,000	3.4E-20	1,000	4.4E-18	1,000	7.7E-17	1,000	2.8E-21	1,000	4.8E-24	1,000	1.7E-23	1,000
Cd	5	3.7E-19	1,000	4.9E-17	1,000	2.6E-15	1,000	9.5E-20	1,000	1.7E-22	1,000	9.6E-22	1,000
Cl	250,000	1.2E-05	1,000	1.6E-05	1,000	4.1E-06	1,000	5.0E-09	1,000	6.5E-09	1,000	2.2E-08	1,000
Co	N/A	<1E-30	1,000	4.8E-30	1,000	3.5E-25	1,000	2.3E-29	1,000	<1E-30	1,000	<1E-30	1,000
Cr	100	<1E-30	1,000										
Cu	1,300	<1E-30	1,000	<1E-30	1,000	1.0E-25	1,000	1.0E-29	1,000	<1E-30	1,000	<1E-30	1,000
F	4,000	9.9E-05	642	1.1E-04	640	1.8E-05	604	4.7E-07	708	4.7E-06	676	3.3E-05	698
Fe	300	<1E-30	1,000										
Hg	2	<1E-30	1,000										
I	N/A	3.4E-06	880	3.7E-06	870	5.9E-07	790	1.5E-08	1,000	1.6E-07	968	1.1E-06	1,000
Mn	50	1.7E-19	1,000	2.2E-17	1,000	2.3E-16	1,000	7.9E-21	1,000	1.4E-23	1,000	4.5E-23	1,000
Mo	N/A	<1E-30	1,000										
N	10,000	7.0E-03	642	7.6E-03	640	1.3E-03	604	3.4E-05	708	3.4E-04	676	2.4E-03	698
Ni	N/A	4.0E-13	1,000	4.8E-11	1,000	1.7E-10	1,000	2.5E-14	1,000	1.9E-14	1,000	5.1E-14	1,000
Pb	15	<1E-30	1,000										
PO ₄	N/A	4.5E-02	350	4.5E-02	348	6.4E-03	314	1.4E-05	312	8.4E-06	676	1.1E-04	402
Sb	6	<1E-30	1,000										
Se	50	<1E-30	1,000										
SO ₄	250,000	2.2E-01	348	2.2E-01	348	3.1E-02	312	6.5E-05	314	2.6E-05	676	5.2E-04	408
Sr	N/A	4.4E-12	1,000	2.2E-10	1,000	2.8E-10	1,000	1.4E-13	1,000	1.4E-13	1,000	4.3E-13	1,000
U	30	<1E-30	1,000										
Zn	5,000	1.2E-19	1,000	1.6E-17	1,000	8.6E-16	1,000	3.2E-20	1,000	5.8E-23	1,000	3.2E-22	1,000

The 100-meter radionuclide and chemical concentration curves (for 20,000 years) associated with the six sectors and three aquifers for the Base Case, as described in Section 4.4.2.1, are captured in Appendix B as follows:

- Appendix B.1 - 100-meter Radiological and Chemical Concentrations at the UTRA-UZ (Sectors A through F)
- Appendix B.2 - 100-meter Radiological and Chemical Concentrations at the UTRA-LZ (Sectors A through F)
- Appendix B.3 - 100-meter Radiological and Chemical Concentrations at the Gordon Aquifer (Sectors A through F)

To support further evaluation of sensitivity run radionuclides (e.g., individual waste tank contributions), additional 100-meter groundwater concentrations were calculated using the HTF PORFLOW Model. Appendix D contains 100,000-year curves for the 100-meter radionuclide concentrations for all of HTF (waste tank and ancillary inventories). Appendix E contains 20,000-year data curves for the 100-meter radionuclide concentrations for selected HTF sources, which included individual waste tanks and waste tank and ancillary equipment source groupings. The individual waste tank source runs were for Tanks 12, 13, 16, 22, 32, 36, 39, and 40. The waste tank and ancillary equipment source group model runs were for Type I (Tanks 9, 10, and 11), Type II (Tanks 14 and 15), Type IV (Tanks 21, 23, and 24), and Type III and IIIA (Tanks 29, 30, 31, 35, and 37). The transfer lines source for the “West Hill” was represented by the piping for Type III and IIIA tanks. The transfer lines source for the Type I and Type II tanks was represented by the piping for the Type II tanks. The remaining waste tanks and ancillary equipment were evaluated as a single group. The Base Case concentration results are for sensitivity run radionuclides only and are presented from the three aquifers of concern (UTRA-UZ, UTRA-LZ, and Gordon Aquifer) for Sectors A through F.

5.2.2 Sensitivity Run Radionuclide Determination

The purpose of this section is to present the methodology used to determine which radionuclides were most significant and to document which radionuclides would be considered a sensitivity run radionuclide. While all radionuclides identified in the HTF waste tank inventory (Section 3.3.2) were included in 100-meter groundwater modeling efforts, narrowing the catalog of radionuclides down to a sensitivity run radionuclide list allowed the analysis to concentrate on the few radionuclides that posed more risk and concentrated modeling efforts on the areas of greatest concern.

The sensitivity run radionuclides were determined based on the peak 100-meter groundwater concentrations by radionuclide provided in Tables 5.2-3 through 5.2-5 (it should be noted that the peak concentration for each individual radionuclide is not necessarily in the same year). These concentrations were then run through the GoldSim dose calculator to determine dose rates by sector. Any radionuclide in a given sector with greater than 0.25 mrem/yr dose (assuming the Base Case pathways and assumptions) anytime within 20,000 years at the 100-meter boundary was considered a sensitivity run radionuclide. The 0.25 mrem/yr screening threshold (100 times less than the 25 mrem/yr performance objective) was considered sufficiently low, such that the seepline contribution of the radionuclides that were screened

out would not appreciably affect the peak dose results, even accounting for cumulative pathway effects. In order to fully evaluate the contribution of the sensitivity run radionuclides, some radionuclides with a contribution of less than 0.25 mrem/yr at the 100-meter boundary were included because they had a significant (i.e., > 0.25 mrem/yr) impact on progeny; Am-241 (for Np-237), Pu-238 (for Ra-226), Pu-239 (for Pa-231), Th-230 (for Pb-210 and Ra-226), U-234 (for Pb-210 and Ra-226), and U-235 (for Pa-231). The resulting sensitivity run radionuclides are Am-241, I-129, Ni-59, Np-237, Pu-238, Pu-239, Tc-99, Th-230, U-234, and U-235. The screening conclusions are provided in Table 5.2-9.

Table 5.2-9: Determination of Sensitivity Run Radionuclides for the 100-Meter Boundary

Radionuclide ^a	20,000 Peak Dose (mrem/yr)						Basis
	Sector A	Sector B	Sector C	Sector D	Sector E	Sector F	
Ac-227	0.00	0.00	0.00	0.00	0.00	0.00	
Al-26	0.00	0.00	0.00	0.00	0.00	0.00	
Am-241	0.00	0.00	0.00	0.00	0.00	0.00	Np-237 parent
Am-242m	0.00	0.00	0.00	0.00	0.00	0.00	
Am-243	0.00	0.00	0.00	0.00	0.00	0.00	
C-14	0.07	0.11	0.12	0.01	0.01	0.01	
Cf-249	0.00	0.00	0.00	0.00	0.00	0.00	
Cf-251	0.00	0.00	0.00	0.00	0.00	0.00	
Cl-36	0.02	0.02	0.02	0.00	0.01	0.01	
Cm-243	0.00	0.00	0.00	0.00	0.00	0.00	
Cm-244	0.00	0.00	0.00	0.00	0.00	0.00	
Cm-245	0.00	0.00	0.00	0.00	0.00	0.00	
Cm-247	0.00	0.00	0.00	0.00	0.00	0.00	
Cm-248	0.00	0.00	0.00	0.00	0.00	0.00	
Co-60	0.00	0.00	0.00	0.00	0.00	0.00	
Cs-135	0.02	0.06	0.06	0.00	0.01	0.01	
Cs-137	0.00	0.00	0.00	0.00	0.00	0.00	
Eu-152	0.00	0.00	0.00	0.00	0.00	0.00	
Eu-154	0.00	0.00	0.00	0.00	0.00	0.00	
H-3	0.00	0.00	0.00	0.00	0.00	0.00	
I-129	1.25	8.52	5.44	0.29	5.62	5.52	Dose > 0.25
K-40	0.03	0.02	0.02	0.01	0.01	0.01	
Nb-93m	0.21	0.03	0.05	0.00	0.01	0.01	
Nb-94	0.14	0.11	0.11	0.00	0.03	0.03	
Ni-59	0.73	0.16	0.15	0.01	0.01	0.01	Dose > 0.25

**Table 5.2-9: Determination of Sensitivity Run Radionuclides for the 100-Meter Boundary
(Continued)**

Radionuclide ^a	20,000 Peak Dose (mrem/yr)						Basis
	Sector A	Sector B	Sector C	Sector D	Sector E	Sector F	
Ni-63	0.00	0.00	0.00	0.00	0.00	0.00	
Np-237	0.83	0.18	0.17	0.01	0.03	0.03	Dose > 0.25
Pa-231	0.80	0.52	0.50	0.02	0.40	0.39	Dose > 0.25
Pb-210	0.33	0.49	0.50	0.03	0.29	0.29	Dose > 0.25
Pd-107	0.01	0.00	0.00	0.00	0.00	0.00	
Pt-193	0.00	0.00	0.00	0.00	0.00	0.00	
Pu-238	0.00	0.00	0.00	0.00	0.00	0.00	Pb-210 and Ra-226 parent
Pu-239	0.00	0.00	0.00	0.00	0.00	0.00	Pa-231 parent
Pu-240	0.00	0.00	0.00	0.00	0.00	0.00	
Pu-241	0.00	0.00	0.00	0.00	0.00	0.00	
Pu-242	0.00	0.00	0.00	0.00	0.00	0.00	
Pu-244	0.00	0.00	0.00	0.00	0.00	0.00	
Ra-226	3.90	5.77	4.70	0.30	3.35	3.42	Dose > 0.25
Ra-228	0.00	0.00	0.00	0.00	0.00	0.00	
Se-79	0.00	0.00	0.00	0.00	0.00	0.00	
Sm-151	0.00	0.00	0.00	0.00	0.00	0.00	
Sn-126	0.00	0.00	0.00	0.00	0.00	0.00	
Sr-90	0.00	0.00	0.00	0.00	0.00	0.00	
Tc-99	3.83	0.48	0.27	0.04	0.14	0.14	Dose > 0.25
Th-229	0.00	0.00	0.00	0.00	0.00	0.00	
Th-230	0.00	0.00	0.00	0.00	0.00	0.00	Pb-210 and Ra-226 parent
Th-232	0.00	0.00	0.00	0.00	0.00	0.00	
U-232	0.00	0.00	0.00	0.00	0.00	0.00	
U-233	0.00	0.00	0.00	0.00	0.00	0.00	
U-234	0.00	0.00	0.00	0.00	0.00	0.00	Ra-226 parent
U-235	0.00	0.00	0.00	0.00	0.00	0.00	Pa-231 parent
U-236	0.00	0.00	0.00	0.00	0.00	0.00	
U-238	0.00	0.00	0.00	0.00	0.00	0.00	
Y-90	0.00	0.00	0.00	0.00	0.00	0.00	
Zr-93	0.00	0.00	0.00	0.00	0.00	0.00	

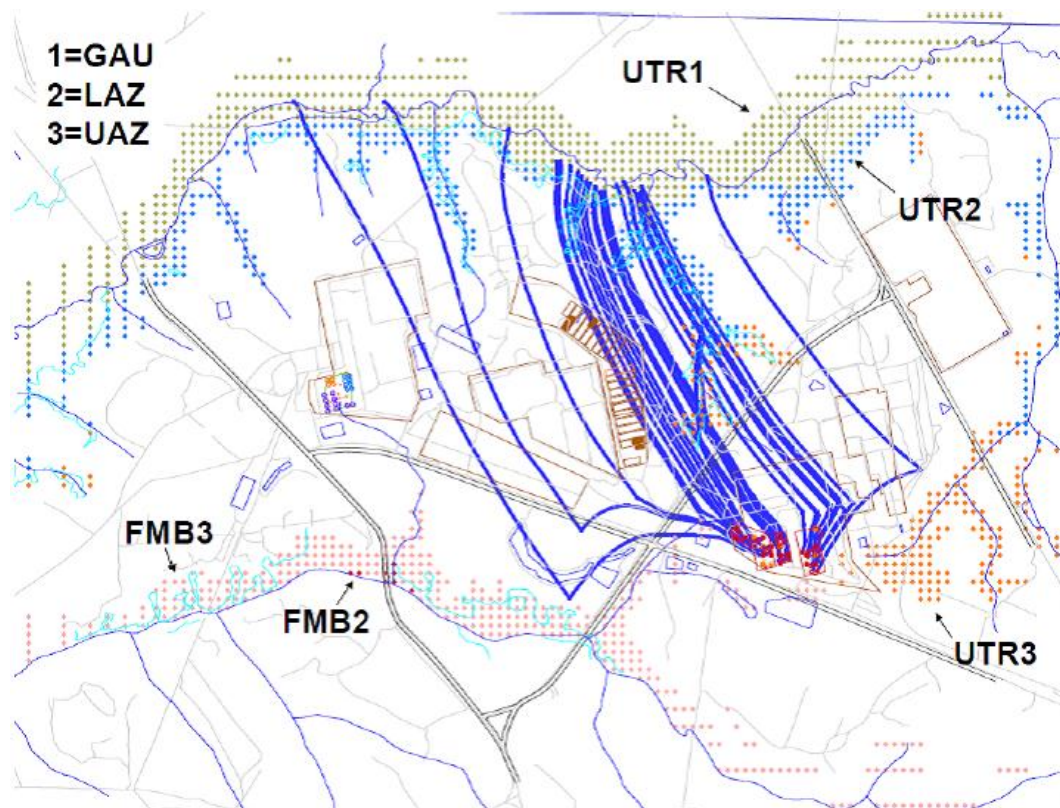
^a Sensitivity run radionuclides are shaded gray.

Only the sensitivity run radionuclides were included in the initial seepline PORFLOW modeling run to determine seepline concentrations. The modeling was performed to 20,000 years and it included all aquifer and discharge locations for the Base Case. The maximum concentration per sensitivity run radionuclide at the seepline in 20,000 years was compared to the corresponding maximum 100-meter concentration in 20,000 years for the same radionuclide. The resulting ratios were averaged for the sensitivity run radionuclides (see Appendix F.1). The overall average ratio for the sensitivity run radionuclides was 2.4 %; however, the ratio for the radionuclide that had the highest dose at the seepline, Ra-226, has a ratio of 6.9 % (see Appendix F.1). Therefore, a ratio of 10 % was chosen for conservatism. The 10 % ratio was then multiplied by the 100-meter concentration for the remaining radionuclides not modeled to get an estimated seepline concentration. The ratios are presented in Table 4.4-20. The concentrations at the seepline for the sensitivity run radionuclides and the weighted concentrations for the remaining radionuclides were then run through the GoldSim dose calculator to determine individual radionuclide dose at the seepline.

5.2.3 Groundwater Concentrations at the Seeplines

The seepline groundwater concentrations for sensitivity run radionuclides were calculated using the HTF PORFLOW Model, which grids the GSA surrounding the HTF. Figure 5.2-6 shows the HTF seeplines in relation to the HTF. The PORFLOW seepline concentrations are provided for two sectors (UTR and Fourmile Branch) and five aquifers (three outcropping to UTR and two outcropping to Fourmile Branch) as shown on Figure 5.2-6. The peak concentration values for the seepline results were recorded for the depths of the three aquifers of concern (i.e., UTRA-UZ, UTRA-LZ, and Gordon Aquifer). The diamond shapes on Figure 5.2-6 correspond to the PORFLOW calculated location where the applicable aquifer is outcropping. For example, the green diamonds represent the location where the Gordon Aquifer outcrops to UTR. For Fourmile Branch, there are only two sets of diamonds, since the Gordon Aquifer does not outcrop to Fourmile Branch.

Figure 5.2-6: HTF PORFLOW Seepline Evaluation Sectors



UTR1 = Gordon Aquifer Unit (GAU) outcropping to UTR
UTR2 = UTRA-LZ (LAZ) outcropping to UTR
UTR3 = UTRA-UZ (UAZ) outcropping to UTR
FMB2 = LAZ outcropping to Fourmile Branch
FMB3 = UAZ outcropping to Fourmile Branch

The five aquifers were analyzed for each sensitivity run radionuclide to find the maximum groundwater concentrations at each seepline. PORFLOW modeling point sources included individual waste tanks and waste tank and/or ancillary equipment groupings. The individual waste tank sources included Tanks 12, 13, 16, 22, 32, 36, 39, and 40. The waste tank source group modeling point that were run included Type I (Tanks 9, 10, and 11), Type II (Tanks 14 and 15), Type IV (Tanks 21, 23, and 24), and Type III and IIIA (Tanks 29, 30, 31, 35, and 37). The transfer lines source for the West Hill was represented by the piping for Type III and IIIA tanks. The transfer lines source for Type I and II tanks was represented by the piping for the Type II tanks. All remaining waste tanks and ancillary equipment were evaluated as a single group. The PORFLOW seepline concentrations were then modeled with the GoldSim dose calculator in order to derive doses for applicable dose pathways (e.g., swimming, boating, and fishing).

Tables 5.2-10 and 5.2-11 show the overall peak seepline radionuclide concentrations in 10,000 years and to 20,000 years for the sensitivity run radionuclides by aquifer for the Base Case for UTR and Fourmile Branch, respectively. These values are conservatively high for

the radionuclides present in multiple decay chains because the totals are simply the sum of the individual peaks from all sources for a given radionuclide for the Base Case.

Table 5.2-10: Seepline Sensitivity Run Radionuclide Concentrations for UTR

Rad	Peak Seepline Concentration 10,000 Years (pCi/L)	Location of Largest Contributor (Aquifer)	Year of Largest Contribution 10,000 Years	Peak Seepline Concentration 20,000 Years (pCi/L)	Location of Largest Contributor (Aquifer)	Year of Largest Contribution 20,000 Years
Ac-227	7.96E-06	UTRA-LZ	10,000	5.36E-05	UTRA-LZ	20,000
Am-241	5.87E-22	UTRA-UZ	6,324	5.87E-22	UTRA-UZ	6,324
I-129	9.92E-03	UTRA-LZ	3,882	9.94E-01	UTRA-LZ	13,070
Ni-59	1.72E+00	UTRA-LZ	10,000	5.92E+01	UTRA-LZ	15,856
Np-237	8.40E-03	UTRA-LZ	2,044	3.22E-02	UTRA-LZ	20,000
Pa-231	2.76E-03	UTRA-LZ	10,000	1.82E-02	UTRA-LZ	20,000
Pb-210	2.30E-06	UTRA-LZ	10,000	3.66E-03	UTRA-UZ	16,992
Pu-238	1.11E-26	UTRA-UZ	1,746	1.11E-26	UTRA-UZ	1,746
Pu-239	2.00E-14	UTRA-UZ	10,000	2.88E-11	UTRA-UZ	20,000
Ra-226	1.88E-04	UTRA-LZ	10,000	2.90E-01	UTRA-UZ	16,940
Tc-99	2.26E+01	UTRA-LZ	8,938	2.26E+01	UTRA-LZ	8,938
Th-230	1.79E-14	UTRA-UZ	10,000	2.23E-08	UTRA-UZ	20,000
U-234	5.89E-12	UTRA-LZ	10,000	4.42E-06	UTRA-UZ	20,000
U-235	1.23E-14	UTRA-LZ	10,000	8.20E-09	UTRA-UZ	20,000

Table 5.2-11: Seepline Sensitivity Run Radionuclide Concentrations for Fourmile Branch

Rad	Peak Seepline Concentration 10,000 Years (pCi/L)	Location of Largest Contributor (Aquifer)	Year of Largest Contribution 10,000 Years	Peak Seepline Concentration 20,000 Years (pCi/L)	Location of Largest Contributor (Aquifer)	Year of Largest Contribution 20,000 Years
Ac-227	3.02E-05	UTRA-UZ	10,000	7.56E-05	UTRA-UZ	19,978
Am-241	2.60E-18	UTRA-UZ	5,752	2.60E-18	UTRA-UZ	5,752
I-129	3.60E-02	UTRA-UZ	3,802	1.92E+00	UTRA-UZ	12,908
Ni-59	1.16E+01	UTRA-UZ	10,000	4.83E+01	UTRA-UZ	14,782
Np-237	3.12E-02	UTRA-UZ	1,234	3.12E-02	UTRA-UZ	1,234
Pa-231	1.03E-02	UTRA-UZ	10,000	2.57E-02	UTRA-UZ	19,972
Pb-210	2.86E-04	UTRA-UZ	10,000	1.21E-02	UTRA-UZ	16,748
Pu-238	1.34E-22	UTRA-UZ	1,620	1.34E-22	UTRA-UZ	1,620
Pu-239	3.60E-11	UTRA-UZ	10,000	3.38E-08	UTRA-UZ	20,000
Ra-226	2.29E-02	UTRA-UZ	10,000	9.59E-01	UTRA-UZ	16,714
Tc-99	1.34E+01	UTRA-UZ	738	1.34E+01	UTRA-UZ	738
Th-230	2.61E-11	UTRA-UZ	10,000	8.60E-07	UTRA-UZ	20,000
U-234	7.44E-09	UTRA-UZ	10,000	1.47E-04	UTRA-UZ	20,000
U-235	1.92E-11	UTRA-UZ	10,000	4.16E-07	UTRA-UZ	20,000

Appendix C contains data curves showing the far-field (i.e., seepline) radionuclide concentrations (sensitivity run radionuclides for 20,000 years) for all of HTF (waste tank and ancillary inventories) for the Base Case.

5.3 Air Pathway and Radon Analyses

Section 4.5 describes the methods used to conservatively bound the dose from airborne radionuclides. The results in that section provided a dose to the MEI per curie of inventory for Type I and Type II tank cases out to 10,000 years. These waste tank types were selected because they will have the least grout and concrete thickness above the stabilized CZ, the minimum assumed closure cap thickness over the waste tanks, and therefore, should produce the maximum flux of gaseous radionuclides at the ground surface.

Assuming that the entire HTF inventory is evenly distributed within either a representative Type I or Type II tank, the dose to the MEI can be calculated to conservatively bound the dose from airborne radionuclides. For the air pathway, the flux of eight radionuclides was modeled using PORFLOW. The DRFs that represent the dose to the receptor exposed to 1 curie of the specified radionuclide potentially released from the waste tank to the atmosphere were calculated at 100 meters, the Fourmile Branch seepline, and the UTR seepline. The estimated total waste tank and ancillary equipment inventory of selected potentially airborne isotopes at closure is summarized in Table 5.3-1.

Table 5.3-1: Projected Total HTF Inventory of Gaseous Radionuclides

Radionuclide	C-14	Cl-36	I-129	Se-79	Sn-126	H-3	Tc-99
Total HTF Inventory^a (Ci)	4.20E+01	6.89E-02	1.18E-01	1.06E+021	1.04E+02	4.21E+01	2.51E+02

^a SRR-CWDA-2010-00023, Rev. 3

Calculated exposure levels for Type I and Type II tanks to the MEI within 10,000 years at 100 meters are presented in Tables 5.3-2 and 5.3-3, respectively. Calculated exposure levels for Type I and Type II tanks to the MEI within 10,000 years at the Fourmile Branch (1,170 meter) seepline are presented in Tables 5.3-4 and 5.3-5, respectively. Calculated exposure levels for Type I and Type II tanks to the MEI within 10,000 years at the UTR (2,360 meter) seepline are presented in Tables 5.3-6 and 5.3-7, respectively. The contribution of Sb-125 to the air pathways dose is insignificant based on the waste tank inventory and Sb-125 short half-life and is not included in the tables. As indicated in Figures 4.5-3 and 4.5-4, the maximum calculated fluxes occur within the first 1,000 years following facility closure.

Table 5.3-2: 100-Meter Boundary DRFs and Type I Tank Dose within 10,000 Years

Radionuclide	Peak Flux ^a (Ci/yr/Ci)	SRS 100m DRF ^a (mrem/Ci)	Dose to MEI at 100m Boundary ^a (mrem/yr/Ci)	HTF Inventory ^b (Ci)	MEI Dose at 100m Boundary (mrem/yr)
C-14	1.60E-05	8.1E-03	1.3E-07	4.20E+01	5.46E-06
Cl-36	9.53E-19	1.7E-02	1.6E-20	6.89E-02	1.10E-21
I-129	4.11E-22	1.2E+01	4.9E-21	1.18E-01	5.78E-22
Sb-125	1.31E-50	2.3E-01	3.0E-51	N/A	N/A
Se-79	5.51E-12	2.3E-02	1.3E-13	1.06E+02	1.38E-11
Sn-126	3.88E-61	1.1E+01	4.3E-60	1.04E+02	4.47E-58
H-3	2.93E-12	1.7E-04	5.0E-16	4.21E+01	2.11E-14
Tc-99	2.82E-47	6.4E-02	1.8E-48	2.51E+02	4.52E-46
Total Dose					5.46E-06

a SRNL-STI-2010-00135 (Table 10)

b Table 5.3-1

Table 5.3-3: 100-Meter Boundary DRFs and Type II Tank Dose within 10,000 Years

Radionuclide	Peak Flux ^a (Ci/yr/Ci)	SRS 100m DRF ^a (mrem/Ci)	Dose to MEI at 100m Boundary ^a (mrem/yr/Ci)	HTF Inventory ^b (Ci)	Dose to MEI at 100m Boundary (mrem/yr)
C-14	1.45E-05	8.1E-03	1.20E-07	4.20E+01	5.04E-06
Cl-36	8.64E-19	1.7E-02	1.50E-20	6.89E-02	1.03E-21
I-129	3.73E-22	1.2E+01	4.50E-21	1.18E-01	5.31E-22
Sb-125	1.19E-50	2.3E-01	2.70E-51	N/A	N/A
Se-79	5.00E-12	2.3E-02	1.10E-13	1.06E+02	1.17E-11
Sn-126	3.52E-61	1.1E+01	3.90E-60	1.04E+02	4.06E-58
H-3	2.66E-12	1.7E-04	4.50E-16	4.21E+01	1.89E-14
Tc-99	2.55E-47	6.4E-02	1.60E-48	2.51E+02	4.02E-46
Total Dose					5.04E-06

a SRNL-STI-2010-00135 (Table 18)

b Table 5.3-1

Table 5.3-4: Fourmile Branch Seepline DRFs and Type I Tank Dose within 10,000 Years

Radionuclide	Peak Flux ^a (Ci/yr/Ci)	Fourmile Branch 1,170m DRF ^a (mrem/Ci)	Dose to MEI at 1,170m ^a (mrem/yr/Ci)	HTF Inventory ^b (Ci)	Dose to MEI at 1,170m Seepline (mrem/yr)
C-14	1.60E-05	3.9E-03	6.2E-08	4.20E+01	2.60E-06
Cl-36	9.53E-19	9.5E-03	9.1E-21	6.89E-02	6.27E-22
I-129	4.11E-22	3.6E+00	1.5E-21	1.18E-01	1.77E-22
Sb-125	1.31E-50	1.5E-01	2.0E-51	N/A	N/A
Se-79	5.51E-12	1.4E-02	7.7E-14	1.06E+02	8.16E-12
Sn-126	3.88E-61	6.6E+00	2.6E-60	1.04E+02	2.70E-58
H-3	2.93E-12	8.0E-05	2.3E-16	4.21E+01	9.68E-15
Tc-99	2.82E-47	4.0E-02	1.1E-48	2.51E+02	2.76E-46
Total Dose					2.60E-06

a SRNL-STI-2010-00135 (Table 11)

b Table 5.3-1

Table 5.3-5: Fourmile Branch Seepline DRFs and Type II Tank Dose within 10,000 Years

Radionuclide	Peak Flux ^a (Ci/yr/Ci)	FMB 1,170m DRF ^a (mrem/Ci)	Dose to MEI at 1,170m ^a (mrem/yr/Ci)	HTF Inventory ^b (Ci)	Dose to MEI at 1,170m Seepline (mrem/yr)
C-14	1.45E-05	3.9E-03	5.7E-08	4.20E+01	2.39E-06
Cl-36	8.64E-19	9.5E-03	8.2E-21	6.89E-02	5.65E-22
I-129	3.73E-22	3.6E+00	1.3E-21	1.18E-01	1.53E-22
Sb-125	1.19E-50	1.5E-01	1.8E-51	N/A	N/A
Se-79	5.00E-12	1.4E-02	7.0E-14	1.06E+02	7.42E-12
Sn-126	3.52E-61	6.6E+00	2.3E-60	1.04E+02	2.39E-58
H-3	2.66E-12	8.0E-05	2.1E-16	4.21E+01	8.84E-15
Tc-99	2.55E-47	4.0E-02	1.0E-48	2.51E+02	2.51E-46
Total Dose					2.39E-06

a SRNL-STI-2010-00135 (Table 19)

b Table 5.3-1

Table 5.3-6: UTR Seepline DRFs and Type I Tank Dose within 10,000 Years

Radionuclide	Peak Flux ^a (Ci/yr/Ci)	UTR 2,360m DRF ^a (mrem/Ci)	Dose to MEI at 2,360m ^a (mrem/yr/Ci)	HTF Inventory ^b (Ci)	Dose to MEI at 2,360m Seepline (mrem/yr)
C-14	1.60E-05	1.2E-03	1.9E-08	4.20E+01	7.98E-07
Cl-36	9.53E-19	3.2E-03	3.0E-21	6.89E-02	2.07E-22
I-129	4.11E-22	9.3E-01	3.8E-22	1.18E-01	4.48E-23
Sb-125	1.31E-50	5.2E-02	6.8E-52	N/A	N/A
Se-79	5.51E-12	4.8E-03	2.6E-14	1.06E+02	2.76E-12
Sn-126	3.88E-61	2.4E+00	9.3E-61	1.04E+02	9.67E-59
H-3	2.93E-12	2.5E-05	7.3E-17	4.21E+01	3.07E-15
Tc-99	2.82E-47	1.4E-02	3.9E-49	2.51E+02	9.79E-47
Total Dose					7.98E-07

a SRNL-STI-2010-00135 (Table 16)

b Table 5.3-1

Table 5.3-7: UTR Seepline DRFs and Type II Tank Dose within 10,000 Years

Radionuclide	Peak Flux ^a (Ci/yr/Ci)	UTR 2,360m DRF ^a (mrem/Ci)	Does to MEI at 2,360m ^a (mrem/yr/Ci)	HTF Inventory ^b (Ci)	Dose to MEI at 2,360m Seepline (mrem/yr)
C-14	1.45E-05	1.2E-03	1.7E-08	4.20E+01	7.14E-07
Cl-36	8.64E-19	3.2E-03	2.8E-21	6.89E-02	1.93E-22
I-129	3.73E-22	9.3E-01	3.5E-22	1.18E-01	4.13E-23
Sb-125	1.19E-50	5.2E-02	6.2E-52	N/A	N/A
Se-79	5.00E-12	4.8E-03	2.4E-14	1.06E+02	2.54E-12
Sn-126	3.52E-61	2.4E+00	8.4E-61	1.04E+02	8.74E-59
H-3	2.66E-12	2.5E-05	6.7E-17	4.21E+01	2.82E-15
Tc-99	2.55E-47	1.4E-02	3.6E-49	2.51E+02	9.04E-47
Total Dose					7.14E-07

a SRNL-STI-2010-00135 (Table 24)

b Table 5.3-1

For the radon air pathway, the Rn-222 flux which resulted from five radionuclides, Pu-238, Ra-226, Th-230, U-234, and U-238. Table 5.3-8 was developed from Table 3.4-9 by selecting the highest possible inventory for each radionuclide from either a Type I or Type II tank. As shown in Figure 4.5-6, with the exception of Ra-226, the peak flux of Rn-222 occurs at the end of the 10,000-year evaluation period. This is due to the long half-life for each of the parent radionuclides. For Ra-226, the peak flux of Rn-222 occurs within the first year of the simulation and declines gradually. Therefore, the peak dose of radon for the modeling period is assumed to be at 10,000 years. Section 4.5.3 describes other factors contributing to the conservative nature of the results.

Table 5.3-8: Projected Type I or II Tanks Inventory of Isotopes Producing Rn-222

Radionuclide	Pu-238	U-238	U-234	Th-230	Ra-226
Type I or II Inventory ^a (Ci)	6.49E+03	3.09E-02	2.23E-01	4.56E-02	4.56E-02

a SRR-CWDA-2010-00023, Rev. 3

The peak instantaneous radon flux is found by multiplying the unit flux by the Type I or II tanks radon inventory then divided by the Type I or II tanks surface area. The inventory of isotopes contributing to the radon flux based on Type I or II tanks case is summarized in Tables 5.3-9 and 5.3-10, respectively. The peak instantaneous radon flux for Type I or II tanks, using the Type I and II tank inventory, is 1.23E-14 pCi/m²/s and 9.37E-17 pCi/m²/s, respectively.

The permissible radon flux for DOE facilities is addressed in DOE M 435.1-1 IV.P.(c) and states the radon flux requirement is that the release of radon shall be less than an average flux of 20 pCi/m²/s at the surface of the facility. The peak instantaneous radon flux for Type I and Type II tanks is below the regulatory limits. These results are conservative because of the selection of the Type I or Type II tank will have the least grout and concrete thickness above the stabilized 1-foot CZ resulting in a shorter pathway to the surface. Exclusion of the top soil, upper backfill, HDPE geomembrane, GCL, and primary steel liner of the waste tank, which have the expectation of significantly reducing the gaseous radon flux at the land surface, contributes to the model conservatism.

Table 5.3-9: Peak Instantaneous Rn-222 Flux at Land Surface from Type I Tanks

Parent Source	Type I or II Inventory ^a (Ci)	Type I Inventory ^b (Ci/m ²)	Rn-222 Flux at Land Surface ^c (pCi/m ² /s)/(Ci/m ²)	Peak Instantaneous Flux at Land Surface (pCi/m ² /s)
Pu-238	6.49E+03	1.58E+01	5.01E-16	7.92E-15
U-238	3.09E-02	7.53E-05	1.72E-14	1.29E-18
U-234	2.23E-01	5.43E-04	1.42E-12	7.72E-16
Th-230	4.56E-02	1.11E-04	1.19E-11	1.32E-15
Ra-226	4.56E-02	1.11E-04	2.08E-11	2.31E-15
Total				1.23E-14

a Table 5.3-8

b Total surface area of HTF Type I tank is 410.43 m² (75-foot diameter waste tank)

c SRNL-STI-2010-00135 (Table 25)

Table 5.3-10: Peak Instantaneous Rn-222 Flux at Land Surface from Type II Tanks

Parent Source	Type II Inventory ^a (Ci)	Type II Inventory ^b (Ci/m ²)	Rn-222 Flux at Land Surface ^c (pCi/m ² /s)/(Ci/m ²)	Peak Instantaneous Flux at Land Surface (pCi/m ² /s)
Pu-238	6.49E+03	1.23E+01	4.59E-18	5.65E-17
U-238	3.09E-02	5.86E-05	1.58E-16	9.26E-21
U-234	2.23E-01	4.23E-04	1.30E-14	5.50E-18
Th-230	4.56E-02	8.65E-05	1.75E-13	1.51E-17
Ra-226	4.56E-02	8.65E-05	1.91E-13	1.65E-17
Total				9.37E-17

a Table 5.3-8

b Total surface area of HTF Type II tank is 527.18 m² (85-foot diameter waste tank)

c SRNL-STI-2010-00135 (Table 26)

The estimated annual dose from the inhalation of Rn-222 would be highest to an inadvertent intruder inhabiting the residence built directly above the waste tank. The dose to the MOP from the inhalation of Rn-222 would be significantly less than the estimated dose to the intruder because the residence of the MOP is at least 100 meters away from any waste tank. This intruder analysis assumes the peak Rn-222 concentration to be in equilibrium within the controlled volume of the basement of the residence built directly above the waste tank with the highest peak radon flux.

The estimated annual dose to an intruder from the inhalation of Rn-222 is dependent on the following:

- Concentration of Rn-222 in a controlled volume occupied by the intruder
- Intruder occupancy (fraction of year) in the controlled volume
- Breathing rate
- Rn-222 DCF

The controlled volume assumed in this analysis is a basement in a residential home that has a floor area of 200m² and 2.43-meter ceilings for a total volume of approximately 488m³. The size of this controlled volume is based on the assumed values presented in NUREG_CR-4370, *Update of Part 61 Impacts Analysis Methodology* (Section 4.2.5.2). It is assumed that this controlled volume is situated above a Type I tank, which has the highest peak radon flux.

The buildup of Rn-222 in the basement is dependent on the production rate (P) and removal rate (R) of Rn-222. Based on Table 5.3-9, the peak instantaneous Rn-222 flux is 1.23E-14 pCi/m²/s. Taking no credit for intervening materials of construction (concrete, block, etc.) the production rate of Rn-222 entering the controlled volume is assumed to be at a constant rate equal to the peak flux times the basement floor area of 200m². Thus, P = 7.78E-05 pCi/yr. Assuming an air exchange rate of 1.0 V/hr taken from NUREG_CR-4370, Section 4.2.5.2, the removal rate is 8,760 V/yr. The greatest Rn-222 concentration is when the buildup is at equilibrium, which

equals P/R, or 8.88E-09 picocurie. The peak Rn-222 concentration in the controlled volume is then estimated to be 2.51E-12 pCi/m³ (1.30E-09 pCi/488m³).

For this analysis, the intruder is assumed to occupy the controlled volume 100 % of the time. The assumed nominal breathing rate is 5,548 m³/yr. The DCF for Rn-222 inhalation is estimated based on 10 CFR 20. Assuming the occupational dose limit of 0.05 sieverts (5,000 millirem) specified in 10 CFR 20 and dividing by the annual limits on intake for Rn-222 of 100 microcuries (1.0E+08 pCi) in air from Table 1, Column 2 of Appendix B; the Rn-222 DCF is therefore estimated to be 5.0E-05 mrem/pCi.

The estimated dose to the intruder from the inhalation of Rn-222 is then calculated by the Rn-222 concentration in the controlled volume times the breathing rate times the DCF. Based on the inputs, the estimated annual dose from the inhalation of Rn-222 equals 1.82E-11 pCi/m³ x 5,548 m³/yr x 5.0E-05 mrem/pCi, or 5.05E-12 mrem/yr.

5.4 Biotic Pathways

The MOP exposure pathways are discussed in detail in Section 4.2.3.1. The HTF MOP scenario with 100-meter well water as a primary water source is graphically represented in Figure 4.2-31. The HTF MOP scenario with stream water as a primary water source is graphically represented in Figure 4.2-32. The individual elements of the MOP biotic pathways that were identified for analyses and inclusion in the two MOP scenarios are provided in this section. The GoldSim computer code was used to calculate doses utilizing the dose formulas provided below and utilizing the PORFLOW or GoldSim calculated 100-meter and seepage concentrations as inputs. Unless otherwise noted, formulas were based on those used in LADTAP or in the PA for the INL waste tank farm facility. [WSRC-STI-2006-00123, DOE-ID-10966] While these documents were used as guides for the formulas, ultimately the basis for all the formulas can be traced to Regulatory Guide 1.109.

5.4.1 MOP at the 100-Meter Well Dose Pathways

The following MOP exposure pathways were used in calculating the dose to the MOP receptor with 100-meter well water as a primary water source. The stream is the secondary water source for the pathways involving swimming, fishing/boating, and fish ingestion. The stream concentrations used in the dose calculations for those secondary water source pathways are the peak aquifer concentrations (as discussed in Section 5.2.3), and conservatively assume no stream dilution. All transfer times are assumed negligible due to the half-lives of the radionuclides and the long-term analysis of the PA. Unit conversions are not explicitly stated in the equations, but are coded into GoldSim.

5.4.1.1 MOP at the 100-Meter Well Ingestion Dose Pathways

5.4.1.1.1 Ingestion of Water

Exposure route for water ingestion assumes the receptor uses a well as a drinking water source that is located 100 meters from the HTF waste tanks. The incidental ingestion of water from showering and during recreational activities is assumed negligible when compared to ingestion of drinking water. The dose from consumption of drinking water was calculated using the following formula.

$$D = C_{GW} \times U_w \times DCF$$

where:

- D = dose from 1-year consumption of contaminated groundwater (rem/yr)
- C_{GW} = radionuclide concentration in groundwater from the 100-meter well (pCi/L)
- U_w = human consumption rate of water (L/yr), Table 4.6-9
- DCF = ingestion DCF (rem/μCi), Table 4.7-1

5.4.1.1.2 Ingestion of Beef and Milk

Beef and dairy exposure route assumes cattle drink contaminated stock water and consume fodder irrigated with contaminated water. The stock water and irrigation water is from the 100-meter well. The fodder is contaminated from direct deposition of contaminated irrigation water on plants and from deposition of contaminated irrigation water in soil followed by root uptake by plants. The buildup of radionuclide concentration in the soil from successive years of irrigation is accounted for. The radionuclide concentration in fodder from deposition and root uptake is calculated using the following formulas.

$$C_f = C_{GW} \times I \times (LEAF + SOIL \times T_{StV}) \times F_I$$

$$LEAF = \frac{r \times (1 - e^{-\lambda_e t_v})}{Y_v \times \lambda_e}$$

$$\lambda_e = \lambda_i + \lambda_w$$

$$SOIL = \frac{1 - e^{-\lambda_B t_b}}{\rho_S \times \lambda_B}$$

$$\lambda_L = \frac{P_R + I_R \times F_I - E_R}{S_D \times (S_M + \rho_{SS} \times K_d)}$$

$$\lambda_B = \lambda_i + \lambda_L$$

where:

C_f	=	radionuclide concentration in fodder (pCi/kg)
C_{GW}	=	radionuclide concentration in groundwater from the 100-meter well (pCi/L)
I	=	irrigation rate (L/m ² -d), Table 4.6-8
$LEAF$	=	radionuclide deposition and retention on the vegetation leaves (m ² d/kg)
$SOIL$	=	radionuclide deposition and buildup rate in the soil (m ² d/kg)
T_{SV}	=	soil to vegetation ratio (unitless), Table 4.6-1
F_I	=	fraction of the time vegetation is irrigated (unitless), Table 4.6-8
r	=	fraction of material deposited on leaves that is retained (unitless), Table 4.6-8
λ_e	=	weathering and radiological decay constant (1/d)
t_V	=	time vegetation is exposed to irrigation (d), Table 4.6-7
Y_V	=	vegetation production yield (kg/m ²), Table 4.6-7
λ_i	=	radiological decay constant (1/d) [ln2/half-life of radionuclide i]
λ_w	=	weathering decay constant (1/d), Table 4.6-8
ρ_S	=	areal surface density of soil (kg/m ²), Table 4.6-8
t_b	=	buildup time of radionuclides in soil (d), Table 4.6-7
λ_B	=	soil buildup rate (1/d)
λ_L	=	soil retention rate (1/d)
P_R	=	precipitation rate (in/yr), Table 4.6-8
I_R	=	irrigation rate (in/yr), Table 4.6-8
E_R	=	evapotranspiration rate (in/yr), Table 4.6-8
S_D	=	depth of garden (cm), Table 4.6-8
S_M	=	soil moisture content (unitless), Table 4.6-8
ρ_{SS}	=	density of sandy soil (g/cm ³), Table 4.6-8
K_d	=	distribution coefficient (mL/g), Table 4.2-25

Following the cattle consumption of the contaminated water and fodder, the receptor consumes the contaminated beef and milk from the cattle. Beef and milk are treated separately. The dose is calculated using the following formulas.

Beef:

$$D = T_B \times (FF_B \times C_f \times Q_{FB} + C_{GW} \times Q_{WB}) \times DCF \times U_B \times F_B$$

Milk:

$$D = T_M \times (FF_M \times C_f \times Q_{FM} + C_{GW} \times Q_{WM}) \times DCF \times U_M \times F_M$$

where:

D	=	dose from 1-year consumption of contaminated beef or milk (rem/yr)
T_B	=	beef transfer coefficient (d/kg), Table 4.6-3
T_M	=	milk transfer coefficient (d/L), Table 4.6-2
FF_i	=	beef or milk cattle intake fraction from irrigated field/pasture (unitless), Table 4.6-9
C_f	=	radionuclide concentration in fodder, as defined above (pCi/kg)
Q_{Fi}	=	consumption rate of fodder by beef or milk cattle (kg/d), Table 4.6-9
C_{GW}	=	radionuclide concentration in groundwater from the 100-meter well (pCi/L)
Q_{Wi}	=	consumption rate of water by beef or milk cattle (L/d), Table 4.6-9
DCF	=	ingestion DCF (rem/ μ Ci), Table 4.7-1
U_B	=	human consumption rate of beef (kg/yr), Table 4.6-9
U_M	=	human consumption rate of milk (L/yr), Table 4.6-9
F_B	=	fraction of meat produced locally (unitless), Table 4.6-7
F_M	=	fraction of milk produced locally (unitless), Table 4.6-7

5.4.1.1.3 Ingestion of Vegetables

The dose to humans from ingestion of contaminated leafy vegetables and produce is calculated assuming two contamination routes, 1) direct deposition of contaminated irrigation water on plants, and 2) deposition of contaminated irrigation water on soil followed by root uptake by plants. The buildup of radionuclide concentration in the soil from successive years of irrigation is accounted for. Leafy vegetables and produce are treated separately. The irrigation water is from the 100-meter well. The dose is calculated using the following formula.

$$D = C_{GW} \times I \times (LEAF + SOIL \times T_{SV}) \times DCF \times (U_{LV} \times k + U_{OV}) \times F_V \times F_I$$

where:

- D = dose from 1-year consumption of contaminated vegetables (rem/yr)
- C_{GW} = radionuclide concentration in groundwater from the 100-meter well (pCi/L)
- I = irrigation rate (L/m²-d), Table 4.6-8
- $LEAF$ = radionuclide deposition and retention rate on the vegetable's leaves, as defined in Section 5.4.1.1.2 (m²d/kg)
- $SOIL$ = radionuclide deposition and buildup rate in the soil, as defined in Section 5.4.1.1.2 (m²d/kg)
- T_{SV} = soil to vegetation ratio (unitless), Table 4.6-1
- DCF = ingestion DCF (rem/μCi), Table 4.7-1
- U_{LV} = human consumption rate of leafy vegetables (kg/yr), Table 4.6-9
- U_{OV} = human consumption rate of other vegetables (produce) (kg/yr), Table 4.6-9
- k = fraction of material deposited on leaves that is retained after washing (unitless), Table 4.6-8
- F_V = fraction of leafy vegetables and produce produced locally (unitless), Table 4.6-7
- F_I = fraction of the time vegetables are irrigated (unitless), Table 4.6-8

5.4.1.1.4 Ingestion of Fish

Exposure route from fish ingestion assumes fish are caught from a stream contaminated from the aquifer, and the receptor in turn consumes the contaminated fish. The dose is calculated using the following formula.

$$D = C_{SW} \times U_F \times T_F \times DCF$$

where:

- D = dose from 1-year consumption of contaminated fish (rem/yr)
- C_{SW} = radionuclide concentration in water from the stream (undiluted aquifer) (pCi/L)
- U_F = human consumption rate of finfish (kg/yr), Table 4.6-9
- T_F = fish bioaccumulation factor (L/kg), Table 4.6-4
- DCF = ingestion DCF (rem/μCi), Table 4.7-1

5.4.1.1.5 Ingestion of Soil

Exposure route from ingestion of soil assumes the soil is irrigated with groundwater from the 100-meter well and the receptor in turn consumes the contaminated soil. This formula was derived following the approach of the previous pathway calculations. A soil buildup factor was applied to account for the buildup of radionuclide concentration in the soil from successive years of irrigation. The radionuclide concentration in the soil and the dose is calculated using the following formulas.

$$D = C_D \times DCF \times U_D$$

$$C_D = C_{GW} \times I \times F_I \times SOIL$$

where:

D	=	dose from 1-year consumption of contaminated soil (rem/yr)
C_D	=	radionuclide concentration in soil irrigated with water from the 100-meter well (pCi/kg)
DCF	=	ingestion DCF (rem/ μ Ci), Table 4.7-1
U_D	=	human consumption rate of dirt (kg/yr), Table 4.6-9
C_{GW}	=	radionuclide concentration in groundwater from the 100-meter well (pCi/L)
I	=	irrigation rate (L/m ² -d), Table 4.6-8
F_I	=	fraction of the time soil is irrigated (unitless), Table 4.6-8
$SOIL$	=	radionuclide deposition and buildup rate in the soil, as defined in Section 5.4.1.1.2 (m ² d/kg)

5.4.1.1.6 Ingestion of Poultry and Eggs

The poultry and egg exposure route assumes poultry drink contaminated stock water and consume fodder irrigated with contaminated water. The stock water and irrigation water is from the 100-meter well. The fodder is contaminated from direct deposition of contaminated irrigation water on plants and from deposition of contaminated irrigation water in soil followed by root uptake by plants. Following the poultry consumption of the contaminated water and fodder, the receptor consumes the contaminated poultry and eggs. Poultry and eggs are treated separately. The concentration in fodder and the dose is calculated using the following formulas.

$$C_f = C_{GW} \times I \times (LEAF + SOIL \times T_{SIV}) \times F_I$$

Poultry:

$$D = T_P \times (FF_P \times C_f \times Q_{FP} + C_{GW} \times Q_{WP}) \times DCF \times U_P \times F_P$$

Eggs:

$$D = T_E \times (FF_P \times C_f \times Q_{FP} + C_{GW} \times Q_{WP}) \times DCF \times U_E \times F_E$$

where:

D	=	dose from 1-year consumption of contaminated poultry or eggs (rem/yr)
C_f	=	radionuclide concentration in fodder (pCi/kg)
C_{GW}	=	radionuclide concentration in groundwater from the 100-meter well (pCi/L)
I	=	irrigation rate (L/m ² -d), Table 4.6-8
$LEAF$	=	radionuclide deposition and retention rate on the vegetation leaves, as defined in Section 5.4.1.1.2 (m ² d/kg)
$SOIL$	=	radionuclide deposition and buildup rate in the soil, as defined in Section 5.4.1.1.2 (m ² d/kg)
T_{SV}	=	soil to vegetation ratio (unitless), Table 4.6-1
F_I	=	fraction of the time vegetation is irrigated (unitless), Table 4.6-8
T_P	=	poultry transfer coefficient (d/kg), Table 4.6-5
T_E	=	egg transfer coefficient (d/kg), Table 4.6-6
FF_P	=	poultry or egg intake fraction from irrigated field/pasture (unitless), Table 4.6-9
Q_{FP}	=	consumption rate of fodder by poultry (kg/d), Table 4.6-9
Q_{WP}	=	consumption rate of water by poultry (L/d), Table 4.6-9
DCF	=	ingestion DCF (rem/μCi), Table 4.7-1
U_P	=	human consumption rate of poultry (kg/yr), Table 4.6-9
U_E	=	human consumption rate of eggs (kg/yr), Table 4.6-9
F_P	=	fraction of poultry produced locally (unitless), Table 4.6-7
F_E	=	fraction of eggs produced locally (unitless), Table 4.6-7

5.4.1.2 MOP at the 100-Meter Well Direct Exposure Dose Pathways

5.4.1.2.1 Direct Exposure from Irrigated Soil

Exposure route from direct contact to soil assumes the soil is irrigated with groundwater from the 100-meter well and the receptor in turn is exposed during time spent caring for a garden. The dose is calculated using the following formula.

$$D = C_D \times F_G \times DCF \times \rho_{SS}$$

where:

D	=	dose from 1-year direct exposure to contaminated soil (rem/yr)
C_D	=	radionuclide concentration in soil irrigated with water from the 100-meter well, as defined in Section 5.4.1.1.5 (pCi/kg)
F_G	=	fraction of time spent in garden (unitless), Table 4.6-9
DCF	=	external DCF, 15cm (rem/yr per $\mu\text{Ci}/\text{m}^3$), Table 4.7-1
ρ_{SS}	=	density of sandy soil (g/cm^3), Table 4.2-39

5.4.1.2.2 Direct Exposure from Swimming

Direct contact exposure route from swimming assumes the receptor receives dose from swimming in a stream contaminated from the aquifer. The dose is calculated using the following formula.

$$D = GF_S \times t_S \times C_{SW} \times DCF$$

where:

D	=	dose from 1-year direct exposure to contaminated stream water (rem/yr)
GF_S	=	swimming geometry factor (unitless), Table 4.6-9
t_S	=	time per year spent swimming (hr/yr), Table 4.6-9
C_{SW}	=	radionuclide concentration in water from the stream (undiluted aquifer) (pCi/L)
DCF	=	external DCF, water immersion (rem/yr per $\mu\text{Ci}/\text{m}^3$), Table 4.7-1

5.4.1.2.3 Direct Exposure from Fishing/Boating

Direct contact exposure route for fishing/boating assumes the receptor receives dose from fishing or boating in a stream contaminated from the aquifer. The dose is calculated using the following formula.

$$D = GF_B \times t_B \times C_{SW} \times DCF$$

where:

D	=	dose from 1-year direct exposure to contaminated stream water (rem/yr)
GF_B	=	boating geometry factor (unitless), Table 4.6-9
t_B	=	time per year spent boating (hr/yr), Table 4.6-9
C_{SW}	=	radionuclide concentration in water from the stream (undiluted aquifer) (pCi/L)
DCF	=	external DCF, water immersion (rem/yr per $\mu\text{Ci}/\text{m}^3$), Table 4.7-1

5.4.1.3 MOP at the 100-Meter Well Inhalation Dose Pathways

5.4.1.3.1 Inhalation during Irrigation

Exposure route from inhalation during irrigation assumes soil is irrigated with groundwater from the 100-meter well and the receptor in turn is exposed by breathing while the garden is irrigated but only during time spent caring for a garden. To account for the quantity of contaminants released into the air and available for inhalation, an Airborne Release Fraction (ARF) is included in the pathway formula. This ARF is conservatively assumed to be 1E-04 taken from DOE-HDBK-3010-94 and is used for all subsequent MOP water inhalation pathway calculations. This formula was derived following the approach of the previous pathway calculations. The dose is calculated using the following formula.

$$D = \frac{C_{GW} \times DCF \times U_A \times F_G \times C_{WA} \times ARF}{\rho_W}$$

where:

- D = dose from 1-year inhalation of contaminated groundwater in the air from irrigation (rem/yr)
- C_{GW} = radionuclide concentration in groundwater from the 100-meter well (pCi/L)
- DCF = inhalation DCF (rem/ μ Ci), Table 4.7-1
- U_A = air intake (m^3 /yr), Table 4.6-9
- F_G = fraction of time spent in garden exposed to soil irrigated with contaminated groundwater (unitless), Table 4.6-9
- C_{WA} = water contained in air at ambient conditions (g/m^3), Table 4.6-8
- ARF = airborne release fraction (unitless), Table 4.6-8
- ρ_W = water density (g/mL), Table 4.6-8

5.4.1.3.2 Inhalation during Showering

Exposure route from inhalation while showering assumes the receptor is exposed by breathing humid air within the shower. The source of water for the shower is the 100-meter well. This formula was derived following the approach of the previous pathway calculations. The dose is calculated using the following formula.

$$D = \frac{C_{GW} \times DCF \times U_A \times t_S \times C_{WS} \times ARF}{\rho_W}$$

where:

- D = dose from 1-year inhalation of contaminated groundwater while showering (rem/yr)

C_{GW}	=	radionuclide concentration in groundwater from the 100-meter well (pCi/L)
DCF	=	inhalation DCF (rem/ μ Ci), Table 4.7-1
U_A	=	air intake (m^3 /yr), Table 4.6-9
t_S	=	fraction of time spent in shower (unitless), Table 4.6-9
C_{WS}	=	water contained in air at shower conditions (g/m^3), Table 4.6-8
ARF	=	airborne release fraction (unitless), Table 4.6-8
ρ_W	=	water density (g/mL), Table 4.6-8

5.4.1.3.3 Inhalation of Dust from Irrigated Soil

Exposure route from inhalation of irrigation soil assumes soil is irrigated with groundwater from the 100-meter well and the receptor is exposed by breathing dust during time spent caring for a garden. This formula was derived following the approach of the previous pathway calculations. The dose is calculated using the following formula.

$$D = U_A \times L_{SiA} \times C_D \times DCF \times F_G$$

where:

D	=	dose from 1-year inhalation of contaminated dust (rem/yr)
U_A	=	air intake (m^3 /yr), Table 4.6-9
L_{SiA}	=	soil loading in air while working in a garden (kg/m^3), Table 4.6-8
C_D	=	radionuclide concentration in soil irrigated with water from the 100-meter well, as defined in Section 5.4.1.1.5 (pCi/kg)
DCF	=	inhalation DCF (rem/ μ Ci), Table 4.7-1
F_G	=	fraction of time spent in garden exposed to soil irrigated with contaminated groundwater (unitless), Table 4.6-9

5.4.1.3.4 Inhalation While Swimming

Exposure route from inhalation while swimming assumes a stream contaminated from the aquifer and the receptor inhales saturated air. The dose is calculated using the following formula.

$$D = \frac{U_A \times GF_S \times t_S \times C_{SW} \times DCF \times C_{WA} \times ARF}{\rho_W}$$

where:

D	=	dose from 1-year inhalation of contaminated stream water while swimming (rem/yr)
U_A	=	air intake (m^3 /yr), Table 4.6-9
GF_S	=	swimming geometry factor (unitless), Table 4.6-9

t_s	=	time per year spent swimming (hr/yr), Table 4.6-9
C_{SW}	=	radionuclide concentration in water from the stream (undiluted aquifer) (pCi/L)
DCF	=	inhalation DCF (rem/ μ Ci), Table 4.7-1
C_{WA}	=	water contained in air at ambient conditions (g/m^3), Table 4.6-8
ARF	=	airborne release fraction (unitless), Table 4.6-8
ρ_w	=	water density (g/mL), Table 4.6-8

5.4.2 MOP at the Stream Dose Pathways

The MOP exposure pathways detailed below are used in calculating the dose to the HTF MOP receptor with stream water as a primary water source. The stream concentrations used in the dose calculations are the peak aquifer concentrations (as discussed in Section 5.2.3), and conservatively assume no stream dilution. All transfer times are assumed negligible due to the half-lives of the radionuclides and the long-term analysis of the PA. Unit conversions are not explicitly stated in the equations, but are coded into GoldSim.

5.4.2.1 MOP at the Stream Ingestion Dose Pathways

5.4.2.1.1 Ingestion of Water

Exposure route from ingestion of drinking water assumes the receptor uses water from a stream contaminated from the aquifer, as a drinking water source. The incidental ingestion of water from showering and during recreational activities is assumed negligible when compared to ingestion of drinking water. The dose from consumption of drinking water is calculated using the following formula.

$$D = C_{SW} \times U_w \times DCF$$

where:

D	=	dose from 1-year consumption of contaminated stream water (rem/yr)
C_{SW}	=	radionuclide concentration in water from the stream (undiluted aquifer) (pCi/L)
U_w	=	human consumption rate of water (L/yr), Table 4.6-9
DCF	=	ingestion DCF (rem/ μ Ci), Table 4.7-1

5.4.2.1.2 Ingestion of Beef and Milk

Exposure route from ingestion of beef and dairy assumes cattle drink contaminated stream water and consume fodder irrigated with contaminated stream water. The fodder is contaminated from direct deposition of irrigation water on plants and from deposition of irrigation water on soil followed by root uptake by plants. The receptor in turn consumes the contaminated beef and milk from the cattle. Beef and milk are treated separately. The concentration in fodder and the dose is calculated using the following formulas.

$$C_f = C_{SW} \times I \times (LEAF + SOIL \times T_{SV}) \times F_I$$

Beef:

$$D = T_B \times (FF_B \times C_f \times Q_{FB} + C_{SW} \times Q_{WB}) \times DCF \times U_B \times F_B$$

Milk:

$$D = T_M \times (FF_M \times C_f \times Q_{FM} + C_{SW} \times Q_{WM}) \times DCF \times U_M \times F_M$$

where:

D	=	dose from 1-year consumption of contaminated beef or milk (rem/yr)
C_f	=	radionuclide concentration in fodder (pCi/kg)
C_{SW}	=	radionuclide concentration in water from the stream (undiluted aquifer) (pCi/L)
I	=	irrigation rate (L/m ² -d), Table 4.6-8
$LEAF$	=	radionuclide deposition and retention rate on the vegetation's leaves, as defined in Section 5.4.1.1.2 (m ² d/kg)
$SOIL$	=	radionuclide deposition and buildup rate in the soil, as defined in Section 5.4.1.1.2 (m ² d/kg)
T_{SV}	=	soil to vegetation ratio (unitless), Table 4.6-1
F_I	=	fraction of the time vegetation is irrigated (unitless), Table 4.6-8
T_B	=	beef transfer coefficient (d/kg), Table 4.6-3
T_M	=	milk transfer coefficient (d/L), Table 4.6-2
FF_i	=	beef or milk cattle intake fraction from irrigated field/pasture (unitless), Table 4.6-9
Q_{Fi}	=	consumption rate of fodder by beef or milk cattle (kg/d), Table 4.6-9
Q_{Wi}	=	consumption rate of water by beef or milk cattle (L/d), Table 4.6-9
DCF	=	ingestion DCF (rem/μCi), Table 4.7-1

U_B	=	human consumption rate of beef (kg/yr), Table 4.6-9
U_M	=	human consumption rate of milk (L/yr), Table 4.6-9
F_B	=	fraction of beef produced locally (unitless), Table 4.6-7
F_M	=	fraction of milk produced locally (unitless), Table 4.6-7

5.4.2.1.3 Ingestion of Vegetables

The dose to humans from ingestion of contaminated leafy vegetables and produce is calculated assuming two-contamination routes 1) direct deposition of contaminated irrigation water on plants and 2) deposition of contaminated irrigation water on soil followed by root uptake by plants. The irrigation water is from a stream contaminated from the aquifer. Leafy vegetables and produce are treated separately. The dose is calculated using the following formula.

$$D = C_{SW} \times I \times (LEAF + SOIL \times T_{SV}) \times DCF \times (U_{LV} \times k + U_{OV}) \times F_V \times F_I$$

where:

D	=	dose from 1-year consumption of contaminated vegetables (rem/yr)
C_{SW}	=	radionuclide concentration in water from the stream (undiluted aquifer) (pCi/L)
I	=	irrigation rate (L/m ² -d), Table 4.6-8
$LEAF$	=	radionuclide deposition and retention rate on the vegetable's leaves, as defined in Section 5.4.1.1.2 (m ² d/kg)
$SOIL$	=	radionuclide deposition and buildup rate in the soil, as defined in Section 5.4.1.1.2 (m ² d/kg)
T_{SV}	=	soil to vegetation ratio (unitless), Table 4.6-1
DCF	=	ingestion DCF (rem/μCi), Table 4.7-1
U_{LV}	=	human consumption rate of leafy vegetables (kg/yr), Table 4.6-9
U_{OV}	=	human consumption rate of other vegetables (produce) (kg/yr), Table 4.6-9
k	=	fraction of material deposited on leaves that is retained after washing (unitless), Table 4.6-8
F_V	=	fraction of leafy vegetables and produce produced locally (unitless), Table 4.6-7
F_I	=	fraction of the time vegetables are irrigated (unitless), Table 4.6-8

5.4.2.1.4 Ingestion of Fish

Exposure route from ingestion of fish assumes fish are caught from a stream contaminated from the aquifer, and the receptor in turn consumes the contaminated fish. The dose is calculated using the following formula.

$$D = C_{SW} \times U_F \times T_F \times DCF$$

where:

- D = dose from 1-year consumption of contaminated fish (rem/yr)
- C_{SW} = radionuclide concentration in water from the stream (undiluted aquifer) (pCi/L)
- U_F = human consumption rate of finfish (kg/yr), Table 4.6-9
- T_F = fish bioaccumulation factor (L/kg), Table 4.6-4
- DCF = ingestion DCF (rem/ μ Ci), Table 4.7-1

5.4.2.1.5 Ingestion of Soil

Exposure route from soil ingestion assumes soil is irrigated with water from a stream contaminated from the aquifer, and the receptor in turn consumes the contaminated soil. This formula was derived following the approach of the previous pathway calculations. The radionuclide concentration in the soil and the dose is calculated using the following formulas.

$$D = C_D \times DCF \times U_D$$
$$C_D = C_{SW} \times I \times F_I \times SOIL$$

where:

- D = dose from 1-year consumption of contaminated soil (rem/yr)
- C_D = radionuclide concentration in soil irrigated with stream water (undiluted aquifer) (pCi/kg)
- DCF = ingestion DCF (rem/ μ Ci), Table 4.7-1
- U_D = human consumption rate of dirt (kg/yr), Table 4.6-9
- C_{SW} = radionuclide concentration in water from the stream (undiluted aquifer) (pCi/L)
- I = irrigation rate (L/m²-d), Table 4.6-8
- F_I = fraction of the time soil is irrigated (unitless), Table 4.6-8
- $SOIL$ = radionuclide deposition and buildup rate in the soil, as defined in Section 5.4.1.1.2 (m²d/kg)

5.4.2.1.6 Ingestion of Poultry and Eggs

The poultry and egg exposure route assumes poultry drink contaminated stream water and consume fodder irrigated with contaminated stream water. The fodder is contaminated from direct deposition of irrigation water on plants and from deposition of irrigation water on soil followed by root uptake by plants. The receptor in turn consumes the contaminated poultry and eggs. Poultry and eggs are treated separately. The concentration in fodder and the dose is calculated using the following formulas.

$$C_f = C_{SW} \times I \times (LEAF + SOIL \times T_{SV}) \times F_I$$

Poultry:

$$D = T_P \times (FF_P \times C_f \times Q_{FP} + C_{SW} \times Q_{WP}) \times DCF \times U_P \times F_P$$

Eggs:

$$D = T_E \times (FF_P \times C_f \times Q_{FP} + C_{SW} \times Q_{WP}) \times DCF \times U_E \times F_E$$

where:

D	=	dose from 1-year consumption of contaminated poultry or eggs (rem/yr)
C_f	=	radionuclide concentration in fodder (pCi/kg)
C_{SW}	=	radionuclide concentration in water from the stream (undiluted aquifer) (pCi/L)
I	=	irrigation rate (L/m ² -d), Table 4.6-8
$LEAF$	=	radionuclide deposition and retention rate on the vegetation's leaves, as defined in Section 5.4.1.1.2 (m ² d/kg)
$SOIL$	=	radionuclide deposition and buildup rate in the soil, as defined in Section 5.4.1.1.2 (m ² d/kg)
T_{SV}	=	soil to vegetation ratio (unitless), Table 4.6-1
F_I	=	fraction of the time vegetation is irrigated (unitless), Table 4.6-8
T_P	=	poultry transfer coefficient (d/kg), Table 4.6-5
T_E	=	egg transfer coefficient (d/kg), Table 4.6-6
FF_P	=	poultry intake fraction from irrigated field/pasture (unitless), Table 4.6-9
Q_{FP}	=	consumption rate of fodder by poultry (kg/d), Table 4.6-9
Q_{WP}	=	consumption rate of water by poultry (L/d), Table 4.6-9
DCF	=	ingestion dose conversion factor (rem/μCi), Table 4.7-1
U_P	=	human consumption rate of poultry (kg/yr), Table 4.6-9

- U_E = human consumption rate of eggs (kg/yr), Table 4.6-9
 F_P = fraction of poultry produced locally (unitless), Table 4.6-7
 F_E = fraction of eggs produced locally (unitless), Table 4.6-7

5.4.2.2 MOP at the Stream Direct Exposure Dose Pathways

5.4.2.2.1 Direct Exposure from Irrigated Soil

Exposure route from direct contact with irrigated soil assumes soil is irrigated with water from a stream contaminated from the aquifer and the receptor in turn is exposed during time spent caring for a garden. The dose is calculated using the following formula.

$$D = C_D \times F_G \times DCF \times \rho_{SS}$$

where:

- D = dose from 1-year direct exposure to contaminated soil (rem/yr)
 C_D = radionuclide concentration in soil irrigated with stream water, as defined in Section 5.4.2.1.5 (undiluted aquifer) (pCi/kg)
 F_G = fraction of time spent in garden (unitless), Table 4.6-9
 DCF = external DCF, 15 cm (rem/yr per $\mu\text{Ci}/\text{m}^3$), Table 4.7-1
 ρ_{SS} = density of sandy soil (g/cm^3), Table 4.6-8

5.4.2.2.2 Direct Exposure from Swimming

Exposure route from direct contact while swimming assumes the receptor receives dose from swimming in a stream contaminated from the aquifer. The dose is calculated using the following formula.

$$D = GF_S \times t_S \times C_{SW} \times DCF$$

where:

- D = dose from 1-year direct exposure to contaminated stream water (rem/yr)
 GF_S = swimming geometry factor (unitless), Table 4.6-9
 t_S = time per year spent swimming (hr/yr), Table 4.6-9
 C_{SW} = radionuclide concentration in water from the stream (undiluted aquifer) (pCi/L)
 DCF = external DCF, water immersion (rem/yr per $\mu\text{Ci}/\text{m}^3$), Table 4.7-1

5.4.2.2.3 Direct Exposure from Fishing/Boating

Exposure route from direct contact while fishing/boating assumes the receptor receives dose from fishing or boating in a stream contaminated from the aquifer. The dose is calculated using the following formula.

$$D = GF_B \times t_B \times C_{SW} \times DCF$$

where:

- D = dose from 1-year direct exposure to contaminated stream water (rem/yr)
- GF_B = boating geometry factor (unitless), Table 4.6-9
- t_B = time per year spent boating (hr/yr), Table 4.6-9
- C_{SW} = radionuclide concentration in water from the stream (undiluted aquifer) (pCi/L)
- DCF = external DCF, water immersion (rem/yr per $\mu\text{Ci}/\text{m}^3$), Table 4.7-1

5.4.2.3 MOP at the Stream Inhalation Dose Pathways

5.4.2.3.1 Inhalation during Irrigation

Exposure route from inhalation during irrigation assumes soil is irrigated with water from a stream contaminated from the aquifer, and the receptor in turn is exposed by breathing contaminated air only during the time spent caring for a garden while the garden is irrigated. This formula was derived following the approach of the previous pathway calculations.

$$D = \frac{C_{SW} \times DCF \times U_A \times F_G \times C_{WA} \times ARF}{\rho_W}$$

where:

- D = dose from 1-year inhalation of contaminated stream water in the air from irrigation (rem/yr)
- C_{SW} = radionuclide concentration in water from the stream (undiluted aquifer) (pCi/L)
- DCF = inhalation DCF (rem/ μCi), Table 4.7-1
- U_A = air intake (m^3/yr), Table 4.6-9
- F_G = fraction of time spent in garden exposed to soil irrigated with water from the stream (undiluted aquifer) (unitless), Table 4.6-9
- C_{WA} = water contained in air at ambient conditions (g/m^3), Table 4.6-8
- ARF = airborne release fraction (unitless), Table 4.6-8
- ρ_W = water density (g/mL), Table 4.6-8

5.4.2.3.2 Inhalation While Showering

The exposure route for inhalation during showering assumes receptor exposed by breathing humid air within the shower. The source of water for the shower is a stream contaminated from the aquifer. This formula was derived following the approach of the previous pathway calculations. The dose is calculated using the following formula.

$$D = \frac{C_{SW} \times DCF \times U_A \times t_S \times C_{WS} \times ARF}{\rho_W}$$

where:

- D = dose from 1-year inhalation of contaminated stream water while showering (rem/yr)
- C_{SW} = radionuclide concentration in water from the stream (undiluted aquifer) (pCi/L)
- DCF = inhalation DCF (rem/ μ Ci), Table 4.7-1
- U_A = air intake (m^3 /yr), Table 4.6-9
- t_S = fraction of time spent in shower (unitless), Table 4.6-9
- C_{WS} = water contained in air at shower conditions (g/m^3), Table 4.6-8
- ARF = airborne release fraction (unitless), Table 4.6-8
- ρ_W = water density (g/mL), Table 4.6-8

5.4.2.3.3 Inhalation of Dust from Irrigated Soil

The exposure route for irrigated soil inhalation assumes soil is irrigated with water from a stream contaminated from the aquifer, and the receptor in turn is exposed by breathing contaminated dust during the time spent caring for a garden. This formula was derived following the approach of the previous pathway calculations. The dose is calculated using the following formula.

$$D = U_A \times L_{SiA} \times C_D \times DCF \times F_G$$

where:

- D = dose from 1-year inhalation of contaminated dust (rem/yr)
- U_A = air intake (m^3 /yr), Table 4.6-9
- L_{SiA} = soil loading in air while working in a garden (kg/m^3), Table 4.6-8
- C_D = radionuclide concentration in soil irrigated with stream water, as defined in Section 5.4.2.1.5 (undiluted aquifer) (pCi/kg)
- DCF = inhalation DCF (rem/ μ Ci), Table 4.7-1
- F_G = fraction of time spent in garden exposed to soil irrigated with water from the stream (undiluted aquifer) (unitless), Table 4.6-9

5.4.2.3.4 Inhalation While Swimming

The exposure route for inhalation during swimming assumes a stream contaminated from the aquifer and the receptor inhales saturated air. This formula was derived following the approach of the previous pathway calculations. The dose is calculated using the following formula.

$$D = \frac{U_A \times GF_S \times t_S \times C_{SW} \times DCF \times C_{WA} \times ARF}{\rho_w}$$

where:

D	=	dose from 1-year inhalation of contaminated stream water while swimming (rem/yr)
U_A	=	air intake (m ³ /yr), Table 4.6-9
GF_S	=	swimming geometry factor (unitless), Table 4.6-9
t_S	=	time per year spent swimming (hr/yr), Table 4.6-9
C_{SW}	=	radionuclide concentration in water from the stream (undiluted aquifer) (pCi/L)
DCF	=	inhalation DCF (rem/μCi), Table 4.7-1
C_{WA}	=	water contained in air at ambient conditions (g/m ³), Table 4.6-8
ARF	=	airborne release fraction (unitless), Table 4.6-8
ρ_w	=	water density (g/mL), Table 4.6-8

5.5 Dose Analysis

The total peak doses are calculated utilizing the pathways identified in Section 5.4 for the MOP at the 100-meter boundary and the MOP at applicable streams (either UTR or Fourmile Branch) for the Base Case (Section 4.4.2). The peak doses are calculated using the peak groundwater concentrations identified in Section 5.2 for different time-periods. In addition, a peak dose associated with the sensitivity-run radionuclides is calculated through 100,000 years.

5.5.1 MOP at 100-Meter Groundwater Pathway Dose Results

The groundwater pathway, peak doses for the six 100-meter sectors are calculated using the peak concentration for each radionuclide in the sector (a discussion of how peak concentrations are determined by sector is provided in Section 5.2). The groundwater pathway peak doses are the total dose associated with all the individual 100-meter well pathways identified in Section 5.4.

5.5.1.1 MOP 100-Meter Peak Annual Groundwater Pathway Dose

Table 5.5-1 presents a comparison of the 100-meter peak, groundwater pathway doses for the different 100-meter sectors within 1,000, 10,000, and 100,000 years. In calculating the peak groundwater pathway dose, the highest radionuclide concentration within the vertical computational meshes is used from any of the three distinct aquifers modeled (UTRA-UZ, UTRA-LZ, and Gordon Aquifer).

Table 5.5-1: MOP at 100-Meter Peak Groundwater Pathways Dose by Sector

Sector ^a	Peak Dose in 1,000 Years	Peak Dose in 10,000 Years	Peak Dose in 100,000 Years
A	0.3 mrem/yr (year 860) Principal Radionuclide: Tc-99 (96 %) Principal Pathways: Water Ingestion (57 %) Vegetable Ingestion (35 %)	4.0 mrem/yr (year 8,790) Principal Radionuclide: Tc-99 (96 %) Principal Pathways: Water Ingestion (58 %) Vegetable Ingestion (35 %)	120 mrem/yr (year 90,800) Principal Radionuclide: Ra-226 (85 %) Principal Pathways: Water Ingestion (85 %) Vegetable Ingestion (14 %)
B	0.2 mrem/yr (year 730) Principal Radionuclide: Tc-99 (99 %) Principal Pathways: Water Ingestion (56 %) Vegetable Ingestion (36 %)	1.5 mrem/yr (year 8,860) Principal Radionuclides: Tc-99 (31 %) Ra-226 (31 %) Pa-231 (23 %) Principal Pathways: Water Ingestion (76 %) Vegetable Ingestion (20 %)	73 mrem/yr (year 70,380) Principal Radionuclide: Ra-226 (79 %) Principal Pathways: Water Ingestion (85 %) Vegetable Ingestion (14 %)
C	0.3 mrem/yr (year 700) Principal Radionuclide: Tc-99 (88 %) Principal Pathways: Water Ingestion (60 %) Vegetable Ingestion (33 %)	2.2 mrem/yr (year 10,000) Principal Radionuclides: Ra-226 (58 %) Pa-231 (19 %) Principal Pathways: Water Ingestion (85 %) Vegetable Ingestion (14 %)	69 mrem/yr (year 68,500) Principal Radionuclide: Ra-226 (78 %) Principal Pathways: Water Ingestion (85 %) Vegetable Ingestion (14 %)
D	0.04 mrem/yr (year 880) Principal Radionuclide: Tc-99 (96 %) Principal Pathways: Water Ingestion (55 %) Vegetable Ingestion (34 %)	0.1 mrem/yr (year 10,000) Principal Radionuclide: Ra-226 (79 %) Principal Pathways: Water Ingestion (83 %) Vegetable Ingestion (14 %)	7.1 mrem/yr (year 83,440) Principal Radionuclide: Ra-226 (85 %) Principal Pathways: Water Ingestion (85 %) Vegetable Ingestion (14 %)
E	0.1 mrem/yr (year 870) Principal Radionuclide: Tc-99 (98 %) Principal Pathways: Water Ingestion (56 %) Vegetable Ingestion (35 %)	0.1 mrem/yr (year 870) Principal Radionuclide: Tc-99 (98 %) Principal Pathways: Water Ingestion (56 %) Vegetable Ingestion (35 %)	91 mrem/yr (year 89,560) Principal Radionuclide: Ra-226 (85 %) Principal Pathways: Water Ingestion (85 %) Vegetable Ingestion (14 %)
F	0.2 mrem/yr (year 870) Principal Radionuclide: Tc-99 (93 %) Principal Pathways: Water Ingestion (58 %) Vegetable Ingestion (34 %)	0.2 mrem/yr (year 870) Principal Radionuclide: Tc-99 (93 %) Principal Pathways: Water Ingestion (58 %) Vegetable Ingestion (34 %)	99 mrem/yr (year 87,080) Principal Radionuclide: Ra-226 (85 %) Principal Pathways: Water Ingestion (85 %) Vegetable Ingestion (14 %)

a Sectors illustrated in Figure 5.2-5

Figures 5.5-1 and 5.5-2 present the peak doses to the 100-meter MOP receptor over time during the 1,000 and 10,000 time-periods for the 100-meter sectors. The peak 100-meter MOP groundwater pathway dose within 1,000 years is 0.3 mrem/yr in Sectors A (at year 860) and C (at year 700), and within 10,000 years is 4.0 mrem/yr at year 8,790 in Sector A. Figure 5.5-3 presents the 100-meter MOP receptor doses within 100,000 years for the 100-meter sectors with a peak of approximately 120 mrem/yr in Sector A (at year 90,800).

An overview of the modeling results indicate:

- Contaminant water concentrations and dose are directly influenced by flow direction (see Figures 5.2-2 and 5.2-5), timing of the loss of contaminant containment, and inventory location with respect to the 100-meter boundary.
- Early dose peaks (prior to year 2,500) are associated with the inventory from ancillary equipment (including transfer lines), from sand pads under Type II tanks, and tanks assumed to have failed steel liners at the time of closure (Tanks 12, 14, 15 and 16).
- Later dose peaks result from the loss of containment due to failure of the steel liner (Type IV tanks at year 3,638; Type I tanks at year 11,397; Type II tanks at year 12,687; and Type III and IIIA tanks at year 12,751). Loss of the steel liner initiates changes to the chemistry and radionuclide holding capability of the grout, which directly affects radionuclide release rates, as illustrated by the dose peaks.
- Peak doses to the MOP within 10,000 years at the 100-meter boundary are primarily from Tc-99, Pa-231, and Ra-226 (see Figures 5.5-5, 5.5-8, and 5.5-11) from the groundwater pathways in Sectors A, B, and C.
- Peak dose to the MOP within 100,000 years at the 100-meter boundary is primarily from Ra-226 (see Figures 5.5-6, 5.5-9, and 5.5-12) from the groundwater pathways in Sectors A, B, and C.
- The all-pathways dose is the same as the groundwater pathways dose due to the negligible dose contribution from the air pathway, as presented in Section 5.3.

Figure 5.5-1: 100-Meter Sector MOP Peak Groundwater Pathway Dose Results within 1,000 Years

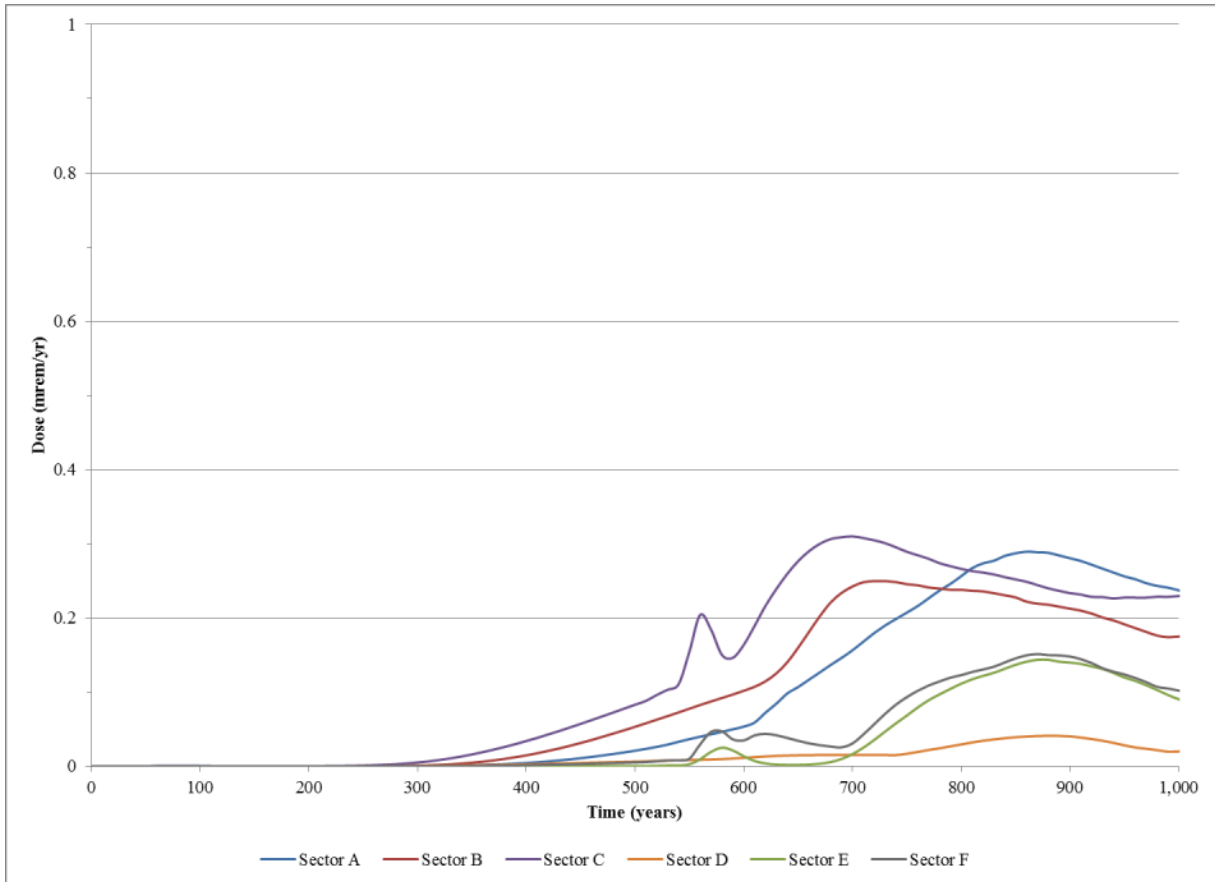


Figure 5.5-2: 100-Meter Sector MOP Peak Groundwater Pathway Dose Results within 10,000 Years

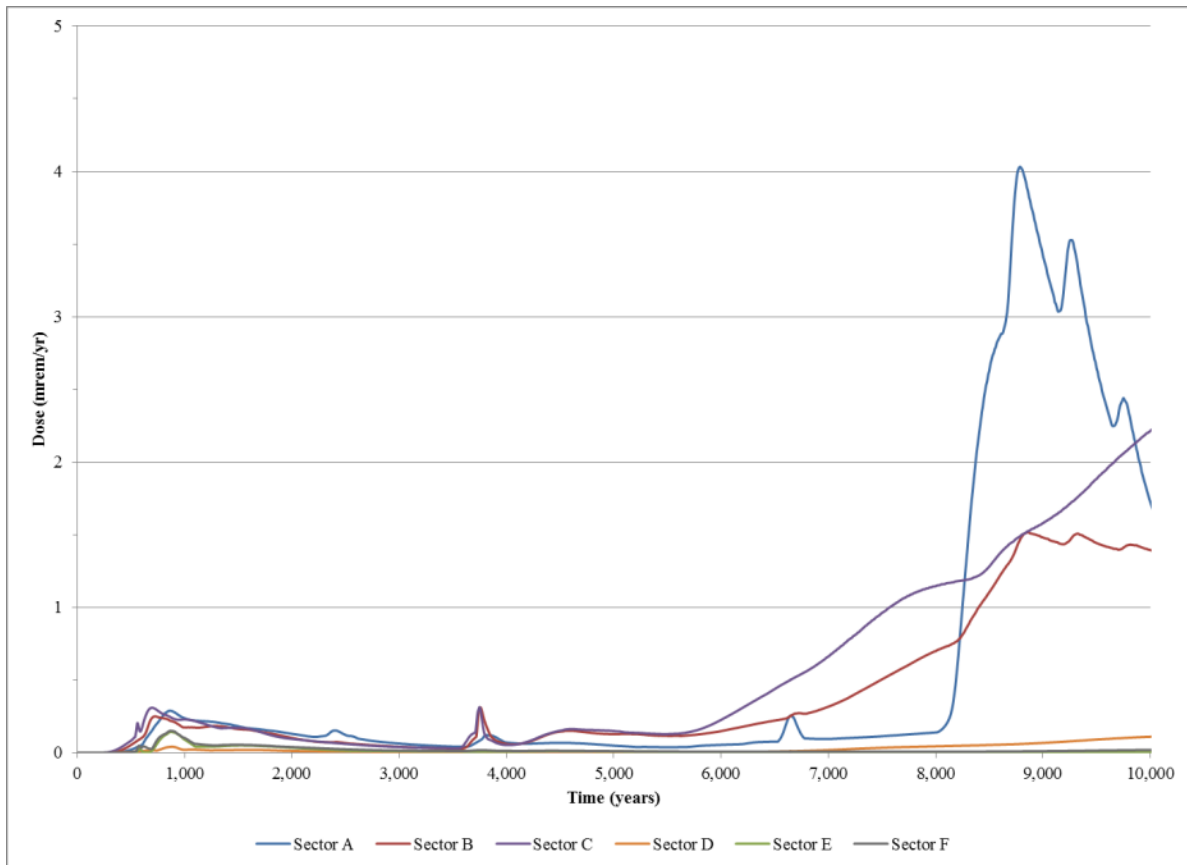
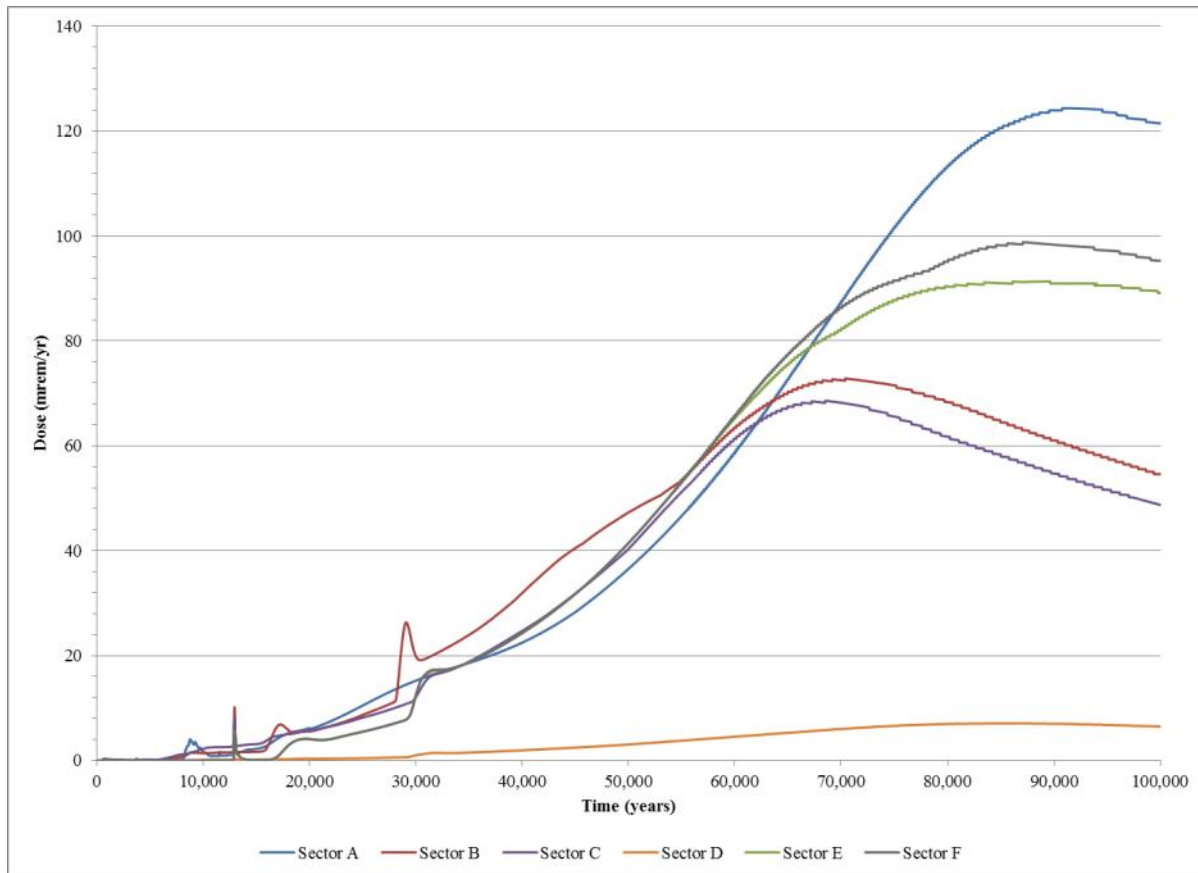


Figure 5.5-3: 100-Meter Sector MOP Peak Groundwater Pathway Dose Results within 100,000 Years



Provided below is a more detailed discussion of the peaks that appear in Figures 5.5-1 through 5.5-3. The discussion also relies upon information from Figures 5.5-4 through 5.5-12 relating to the individual radionuclide contributors to the groundwater pathway doses.

- The dose peaks prior to year 2,500 are influenced by ancillary equipment releases, in particular the transfer lines, which are distributed throughout the HTF and therefore affect all sectors. The timing of the ancillary equipment peaks is fairly consistent for all sectors, with the magnitude of the peak vary depending on what ancillary equipment other than the transfer lines are contributing to the peak (i.e., Sectors A, B, and C have more inventory sources, such as the PP and evaporators nearby). The ancillary equipment releases start when containment fails (at year 510). In contrast to the waste tanks (where solubility control was modeled as controlling waste release), the ancillary equipment releases were modeled as instantaneous, so the entire inventory in each ancillary equipment location is available for release at year 510.
- The peaks in the first 1,500 years after HTF closure are associated with Tc-99 and Np-237 from ancillary equipment (including transfer lines), from sand pads under Type II tanks, and from waste tanks that are assumed to have failed steel liners at the time of closure (Tanks 12, 14, 15, and 16). The Tc-99 travels quickly (K_d in soil of

- 0.6 mL/g) to the 100-meter boundary after the ancillary equipment containment fails (at year 510). The Tc-99 inventory in the sand pads under the Type II tanks is available for transport and contributes to a single peak soon thereafter. The Np-237 travels relatively quickly (K_d in soil of 3 mL/g), but does not travel as quickly as the Tc-99 due to soil retardation being greater for neptunium, so the peak associated with Np-237 is later and less acute. The basemat transitions from Oxidized Region II to Oxidized Region III at year 109 for the Type II tanks with a failed liner, and at year 1,350 for the Type I tanks with a failed liner.
- The small dose increase near year 3,700 is associated with I-129. This release is primarily associated with liner degradation of Type IV tanks. The contribution of I-129 to dose is quick because it travels rapidly (K_d in basemat of 15 mL/g, K_d in soil of 0.3 mL/g).
 - There is a dose spike associated with I-129 at approximately 13,000 years. This is due to the waste-tank liner failures for Tank 13 (12,700 years) and Type III and IIIA tanks (at approximately 12,700 years).
 - The behavior between year 3,700 and 11,300 is tied to releases from the Type IV tanks and from waste tanks with initial liner failure. The Type IV tank liners are considered to fail at approximately year 3,700 while the Types I, II, III, and IIIA tanks do not fail until approximately years 11,400, 12,700, and 12,750, respectively (excepting those waste tanks, Tanks 12, 14, 15, and 16, that are modeled as being failed at the time of HTF facility closure). The releases from the CZs are potentially solubility limited, such that release fluxes from tank liners may vary by radionuclide dependent on its individual solubility controlled release rate from the CZ.
 - The Sectors B and C doses between approximately year 6,000 and 10,000 years have a significant Ra-226 contribution. Although there is some initial Ra-226 inventory, this dose is primarily due to the decay of Ra-226 parent radionuclides (Pu-238, U-234, and Th-230) wherein Pu-238 comprises approximately 85 % of the Ra-226 contribution; therefore, the radium travel time is tied to plutonium. Radium moves faster through concrete than plutonium (i.e., the radium K_d in concrete of 100 mL/g is much lower than the plutonium K_d in concrete of 10,000 mL/g). Further, once the radium is released from the basemat, it moves even faster through the soil (K_d in soil of 25 mL/g), however it lags behind the Np-237 because radium is still being released primarily as a daughter product of Pu-238. The Ra-226 contribution starts ramping up almost as soon as the Type IV tank liners fail and steadily increases as more Ra-226 is produced from decay. The Ra-226 releases in Sector A increase at a slower rate than in Sectors B and C because the Type IV tanks have a thinner basemat for radium to travel through than the Type I and II tanks that primarily influence Sector A.
 - There is a dose spike in Sectors A and B after year 8,000 associated with Tc-99. These dose peaks are tied to waste tank grout and annulus grout degradation in the Type I and II tanks that are modeled as having initially failed steel liners (Tanks 12, 14, 15 and 16). At this time, the waste tank and annulus grout transitions from reduced to oxidized conditions. As the annulus grout transitions to oxidizing grout, the relative Ra-226 doses from each respective waste tank type increases. When this

- transition occurs, the K_d for both radium and plutonium in the grout decreases (from 100 mL/g to 70 mL/g for radium and from 10,000 mL/g to 2,000 mL/g for plutonium). These changes result in faster transport of Ra-226 and its parent radionuclide (Pu-238). This is best depicted in Figure 5.5-6, which presents a series of “step” increases in the Ra-226 dose for Sector C, although Sectors A and B also experience significant contributions. The first step (between about 6,000 and 9,000 years) corresponds to the annulus transition in Tank 12, which occurs at 6,549 years.
- The next step (between 9,000 years and about 15,000 years) corresponds to the other Type I tanks and the Type II tanks, which experience transitions between 7,453 and 9,126, at which point the increase in Ra-226 becomes relatively steady. Starting around year 15,000, Sectors B and C see large increases in Ra-226 doses. These are tied to Type III and IIIA tank liner failures (which occur at approximately 12,750 years) as Ra-226 travels through the waste tank basemats. The concrete basemats have a relatively low K_d for radium (basemat K_d 70 to 100 mL/g) but are thick (41 to 43 inches for Type III and IIIA tanks). The differences in the release times are due to variation in the thicknesses of the basemats.
 - Near the 30,000-year frame of time, there is a peak due to Ra-226 in all sectors. The peak source is the Type III and IIIA tanks. Sectors E and F mirror the dose profiles from Sector A in many ways but always with a smaller magnitude dose. Sectors E and F are both tied to Type IIIA tanks, which experience liner failure at approximately 12,750 years.
 - Sector D is nearest to the Type II tanks. Tanks 14, 15, and 16 are modeled as having initially failed liners (at the time of HTF closure) whereas the liner for Tank 13 fails later at 12,700 years. However, the flow path’s direction generally draws contaminants away from the Sector D 100-meter boundary. Therefore, results from Sector D are negligible, relative to the other sectors.
 - The peak dose for each sector is shown to peak after 70,000 years and to be decreasing within 100,000 years.

5.5.1.2 Individual Radionuclide Contributions to the MOP 100-Meter Peak Annual Groundwater Pathway Dose

For the individual radionuclide contributions analyses, Sectors A, B, and C were selected for discussion. Sectors A, B, and C were the highest contributors to dose within 10,000 years, as seen in Figures 5.5-1 and 5.5-2.

Figures 5.5-4 through 5.5-6 present the relative contribution from individual radionuclides to the Sector A 100-meter groundwater pathway dose over time (1,000, 10,000 and 100,000 years respectively). Figures 5.5-7, 5.5-8, and 5.5-9 present the relative contribution from individual radionuclides to the Sector B 100-meter groundwater pathway dose over time (1,000, 10,000, and 100,000 years respectively). Figures 5.5-10, 5.5-11, and 5.5-12 present the relative contribution from individual radionuclides to the Sector C 100-meter groundwater pathway dose over time (1,000, 10,000, and 100,000 years respectively). During the 1,000-year period, Sector C has the peak, groundwater pathway dose to the MOP at 100 meters and the peak dose is primarily associated with Tc-99 (88 %). During the 10,000-year period, Sector A has the peak, groundwater pathway dose to the MOP at 100

meters and the 10,000-year peak dose is primarily associated with Tc-99 (96 %). The top individual radionuclide contributors (> 5 % contribution) to the MOP peak, groundwater pathway dose at 100 meters are Tc-99 and Np-237 as shown in Table 5.5-2.

Figure 5.5-4: Individual Radionuclide Contributors to the Sector A 100-Meter Peak Groundwater Pathway Dose - 1,000 Years

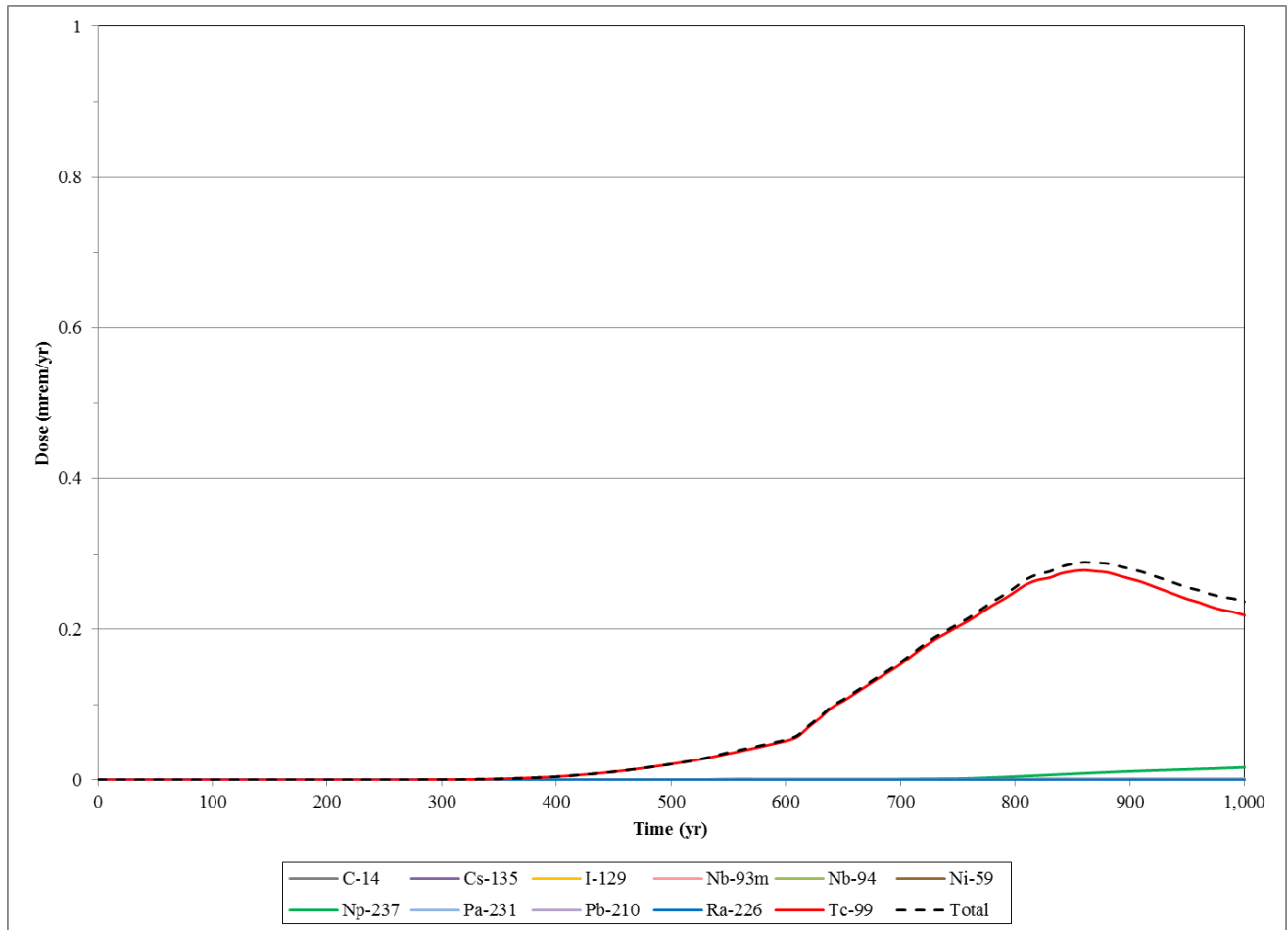


**Figure 5.5-5: Individual Radionuclide Contributors to the Sector A 100-Meter Peak
Groundwater Pathway Dose - 10,000 Years**

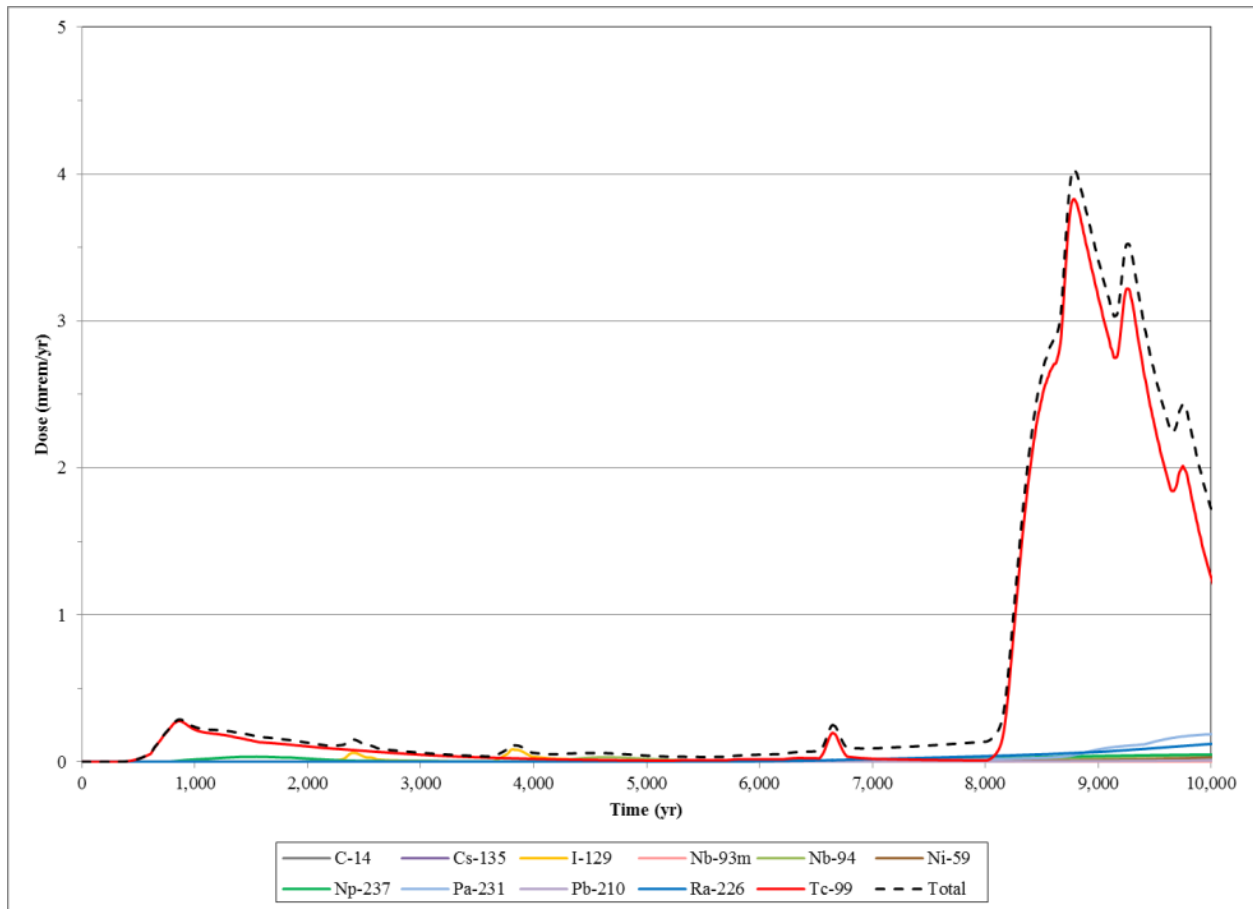


**Figure 5.5-6: Individual Radionuclide Contributors to the Sector A 100-Meter Peak
Groundwater Pathway Dose - 100,000 Years**

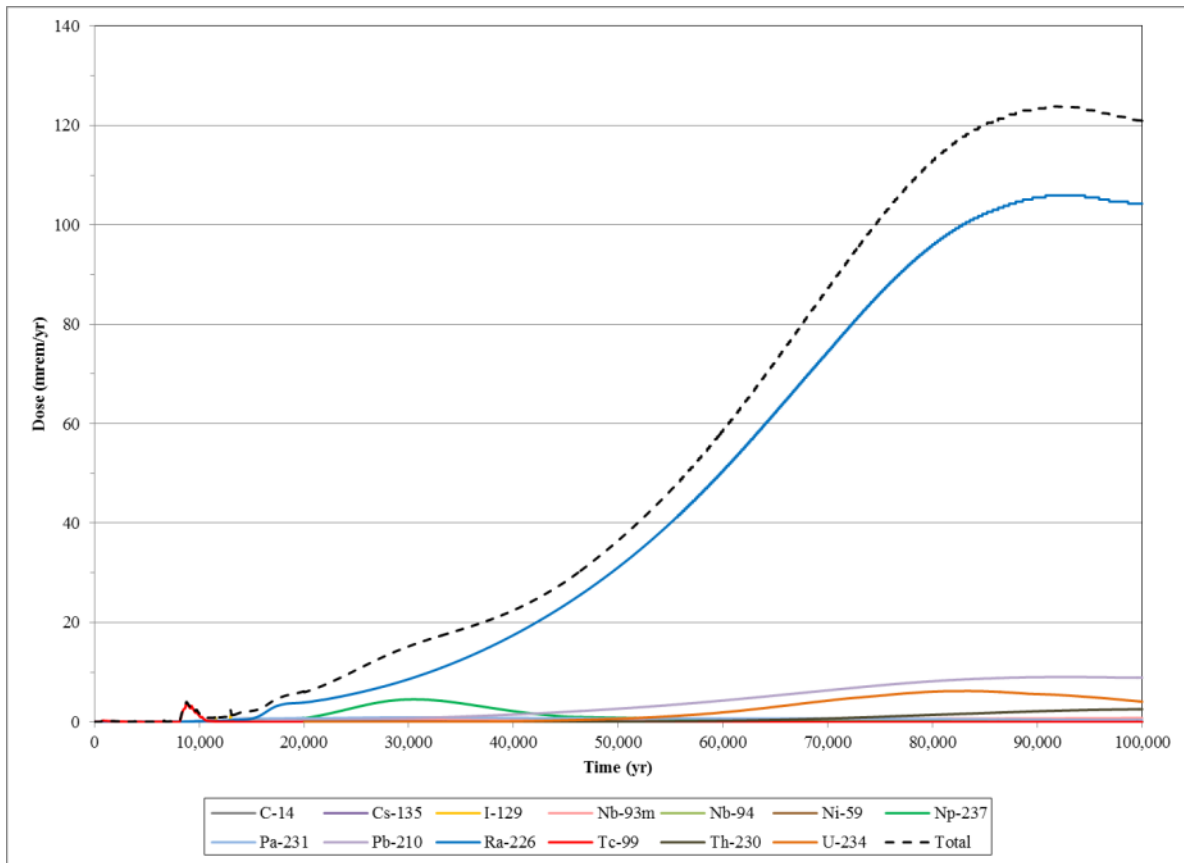


Figure 5.5-7: Individual Radionuclide Contributors to the Sector B 100-Meter Peak
Groundwater Pathway Dose - 1,000 Years

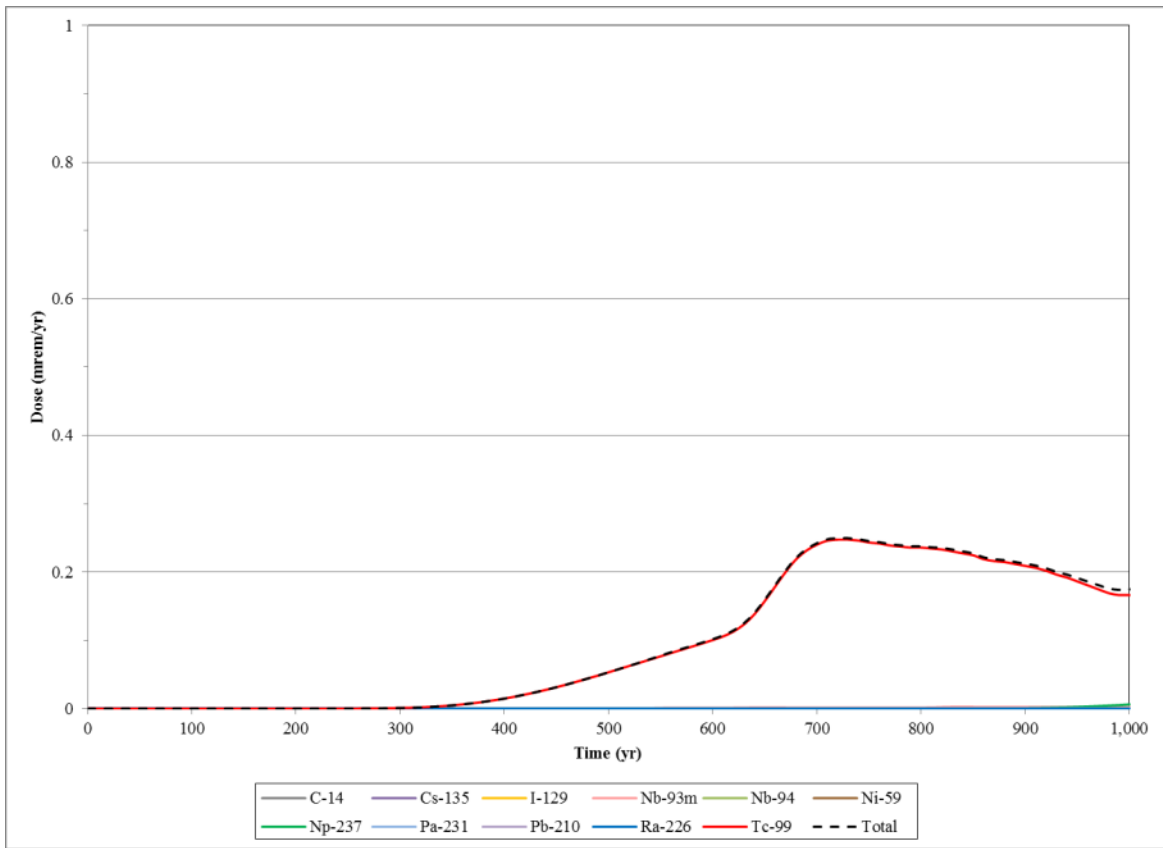


Figure 5.5-8: Individual Radionuclide Contributors to the Sector B 100-Meter Peak
Groundwater Pathway Dose - 10,000 Years

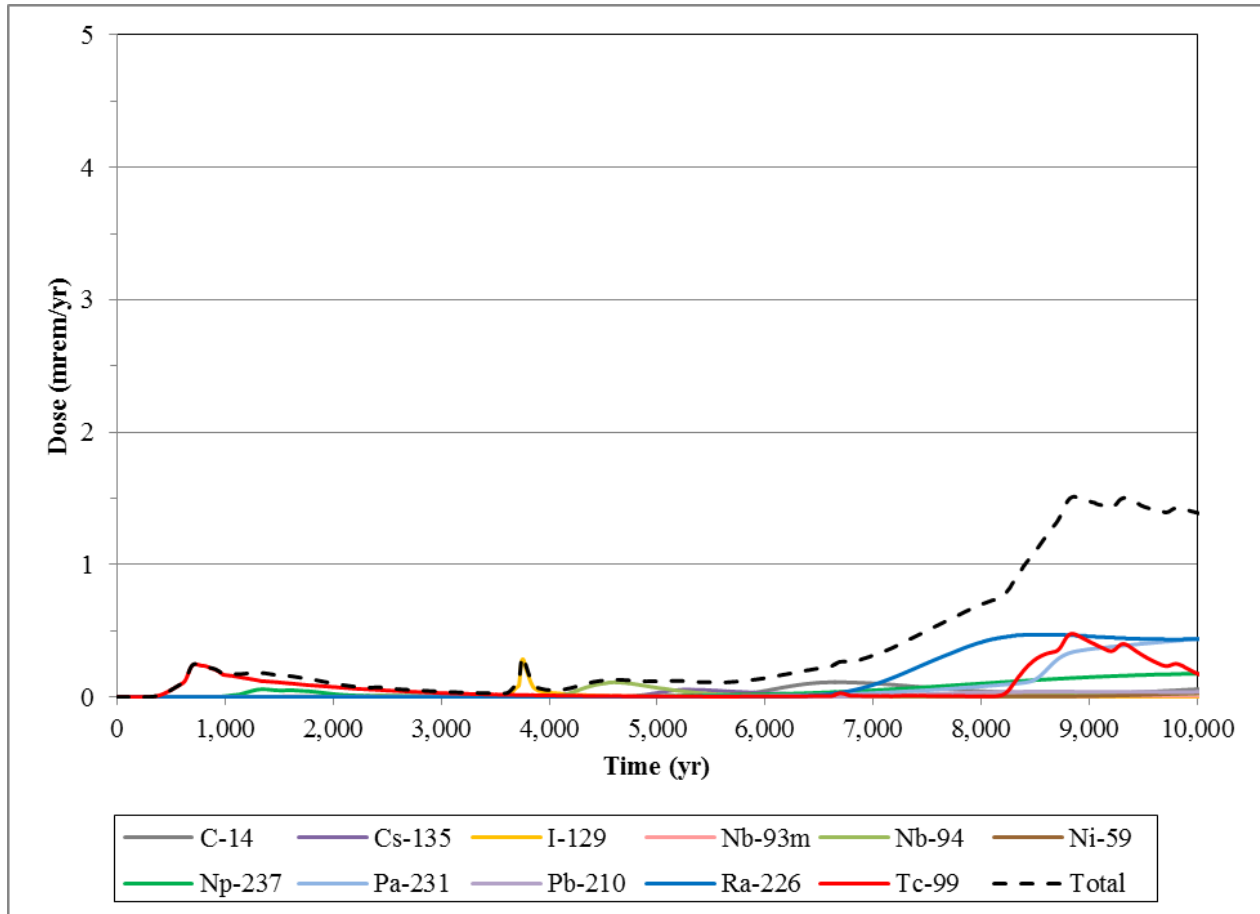


Figure 5.5-9: Individual Radionuclide Contributors to the Sector B 100-Meter Peak
Groundwater Pathway Dose - 100,000 Years

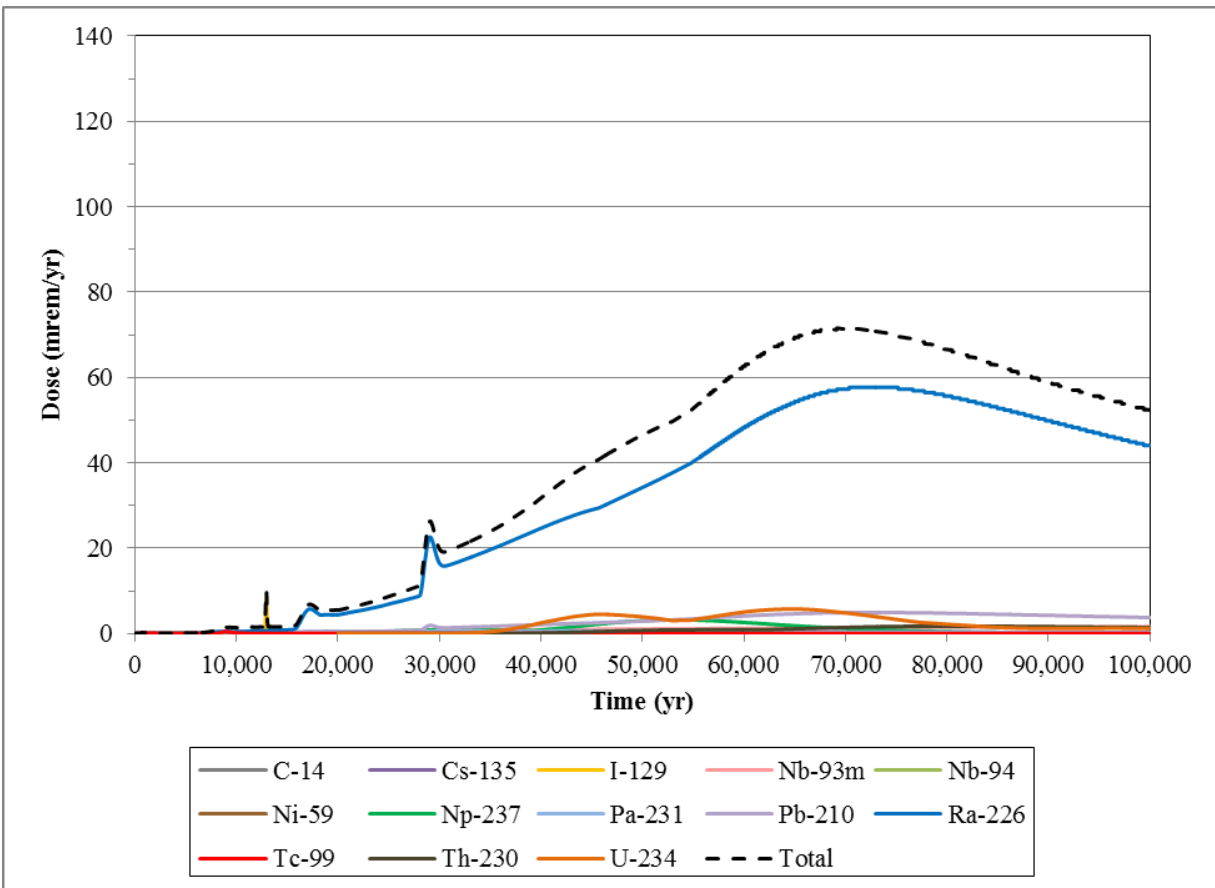


Figure 5.5-10: Individual Radionuclide Contributors to the Sector C 100-Meter Peak
Groundwater Pathway Dose - 1,000 Years

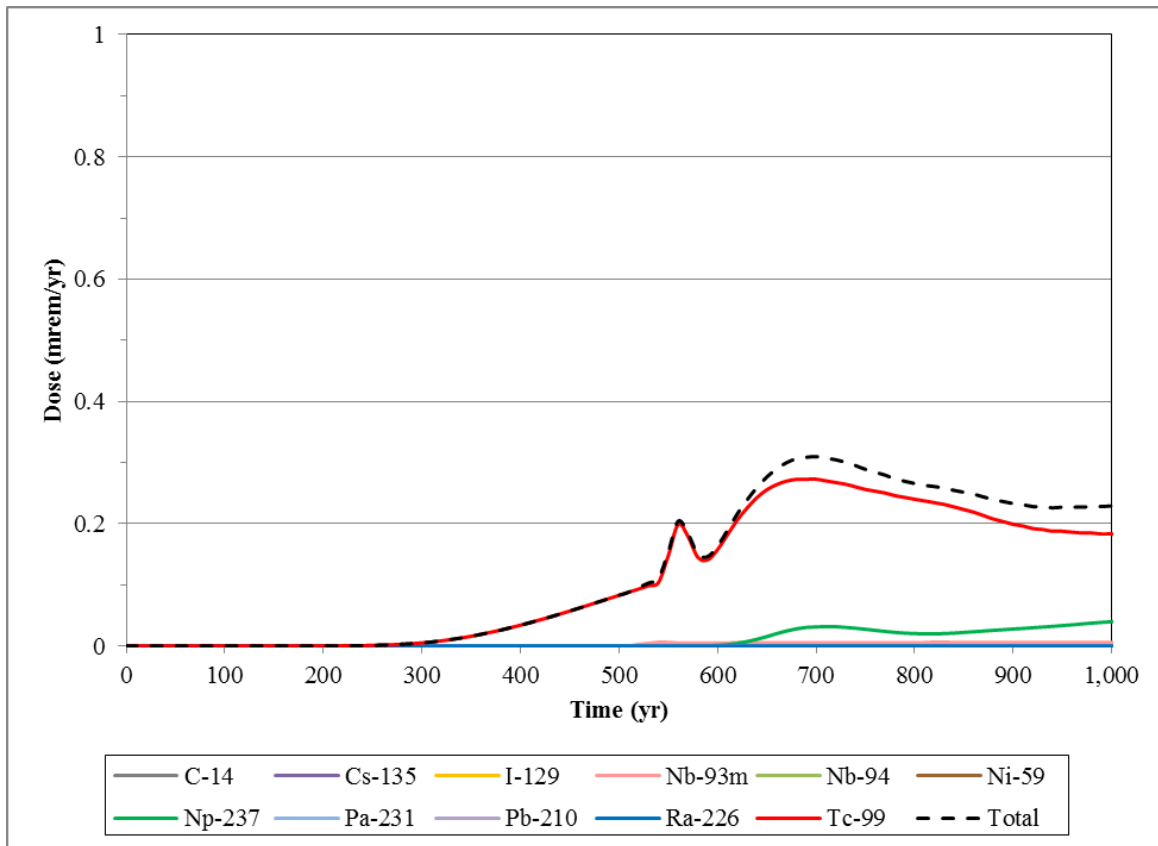


Figure 5.5-11: Individual Radionuclide Contributors to the Sector C 100-Meter Peak
Groundwater Pathway Dose - 10,000 Years

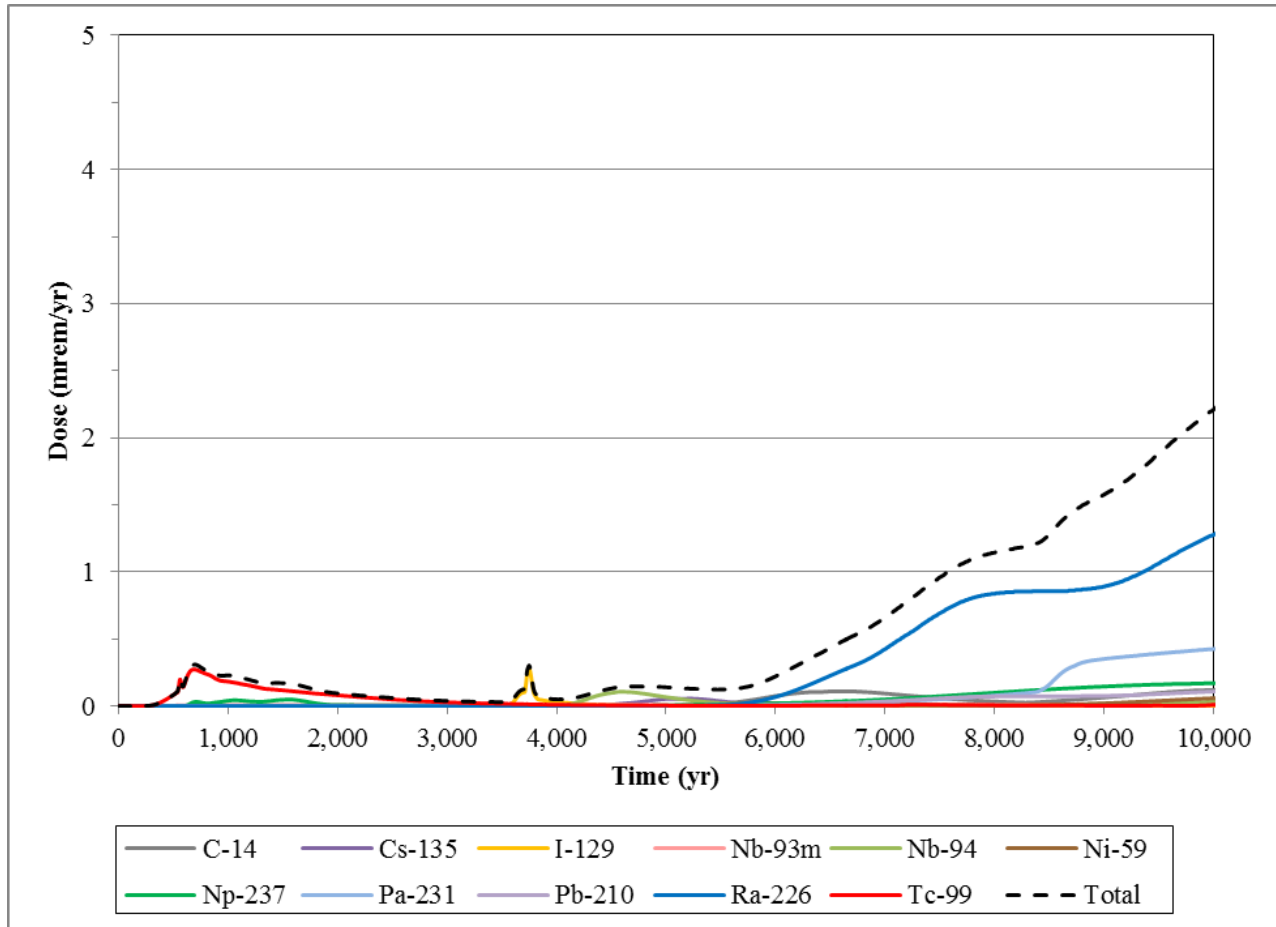


Figure 5.5-12: Individual Radionuclide Contributors to the Sector C 100-Meter Peak Groundwater Pathway Dose - 100,000 Years

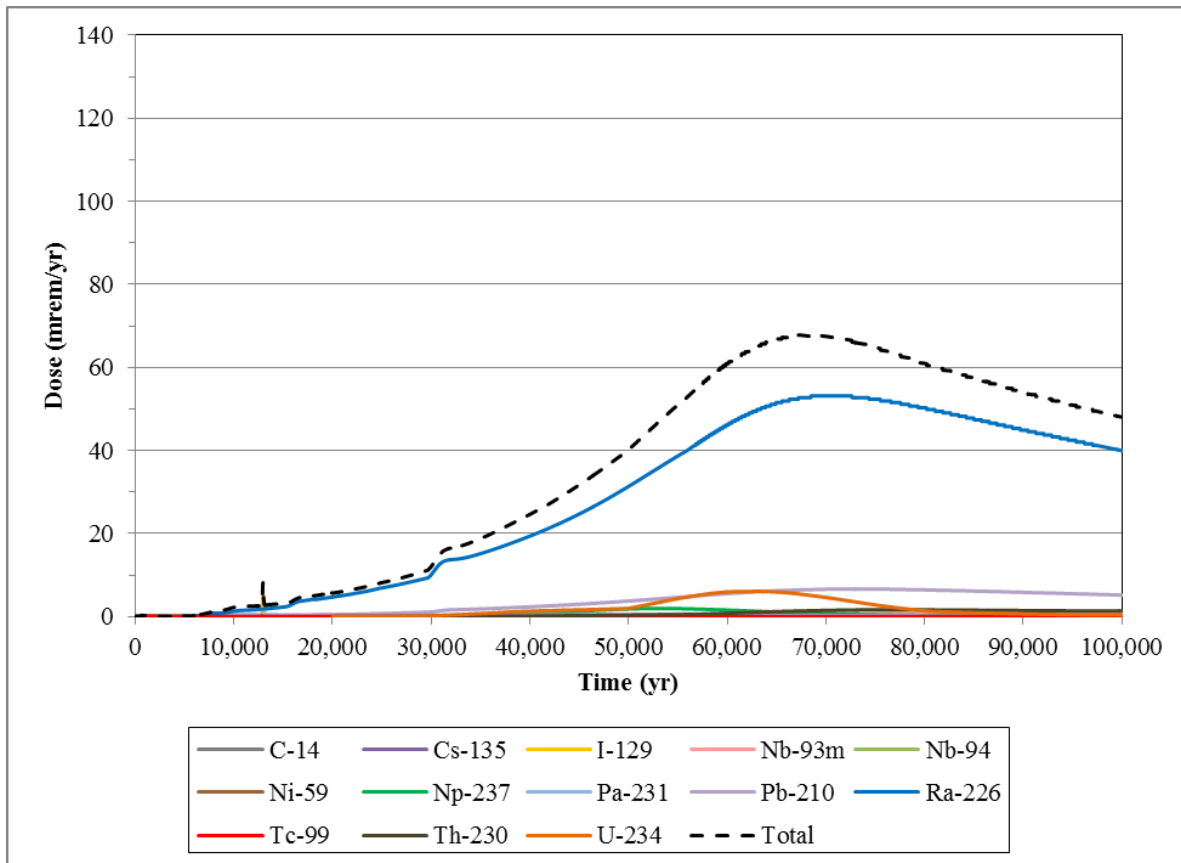


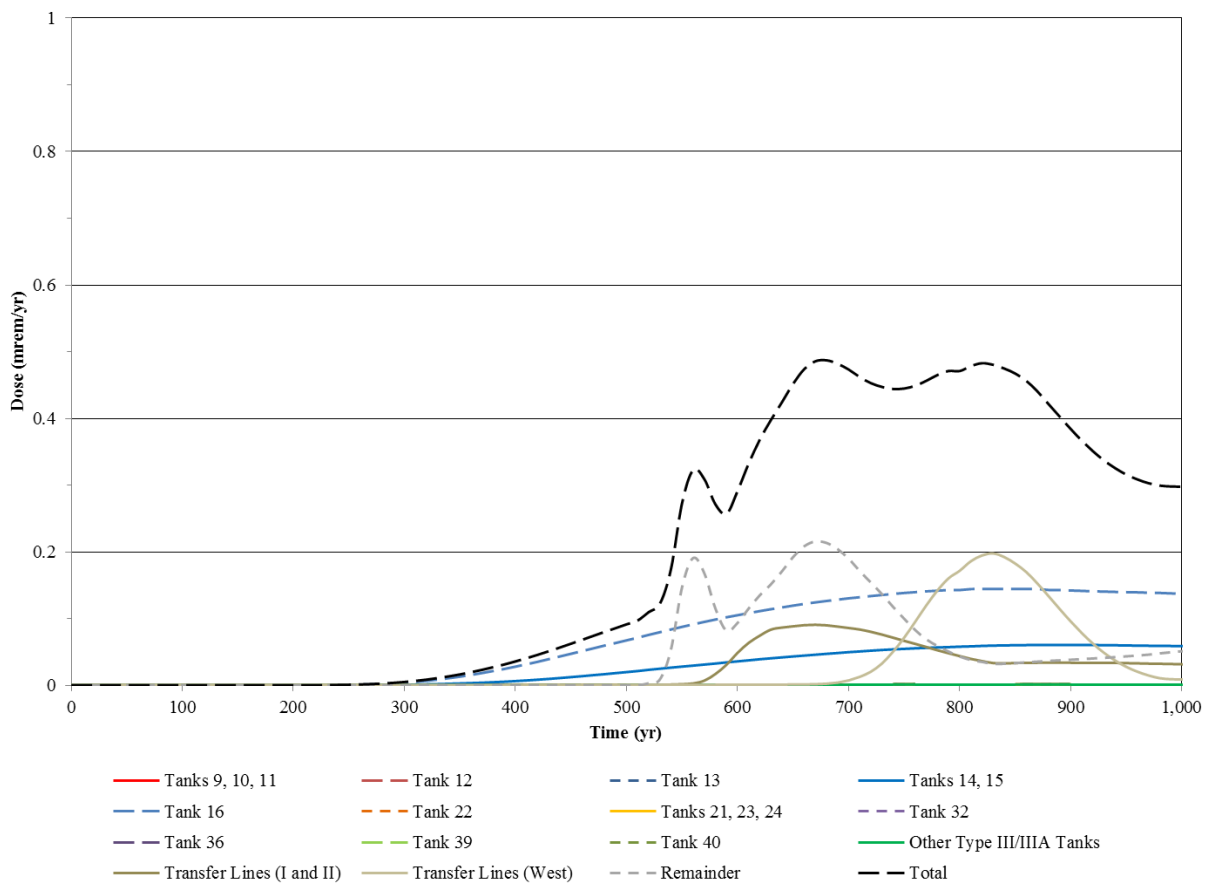
Table 5.5-2: MOP at 100-Meter Peak Groundwater Pathway Dose Individual Radionuclide Contributions at Peak Years – Sectors C (1,000 years) and A (10,000 years)

Radionuclide	Contribution to Sector C Peak dose at year 700 (mrem/yr)	Percentage of Total Peak Dose	Contribution to Sector A Peak dose at year 8,790 (mrem/yr)	Percentage of Total Peak Dose
I-129	< 0.01	< 0.5 %	< 0.01	< 0.5 %
Nb-93m	0.01	1.7 %	< 0.01	< 0.5 %
Nb-94	< 0.01	< 0.5 %	0.02	0.6 %
Np-237	0.03	10 %	0.04	0.9 %
Pa-231	< 0.01	< 0.5 %	0.05	1.2 %
Pu-239	< 0.01	< 0.5 %	< 0.01	< 0.5 %
Ra-226	< 0.01	< 0.5 %	0.06	1.5 %
Tc-99	0.27	88 %	3.8	96 %
Others	< 0.01	< 0.5 %	< 0.01	< 0.5 %
TOTAL	0.31	100 %	4.0	100 %

5.5.1.3 Individual Waste Tank Contributions to MOP 100-Meter Peak Annual Groundwater Pathway Dose

Table 5.5-3 presents the relative contributions from the waste sources, which will contribute to the Sectors C and A 100-meter MOP groundwater pathway doses at the year of the peak dose (700 years and 8,790 years, respectively). At year 700, the 100-meter peak groundwater, pathway dose in Sector C is dominated by contributions from the ancillary equipment (which contribute 44 % of the dose), followed by doses from Tanks 14, 15, and 16, which contribute about 38 % of the dose. Figure 5.5-13 shows the Sector C 100-meter MOP groundwater pathway doses by source for the 1,000-year frame of time.

Figure 5.5-13: Individual Radionuclide Contributors to the Sector C 100-Meter Peak Groundwater Pathway Dose - 1,000 Years



Tanks 9, 10, and 11 are the primary contributors (95 %) to the 100-meter peak, groundwater pathway dose in Section A at year 8,790. Tanks 9, 10, and 11 have intact liners during the 10,000-year period, so this contribution is attributed to the inventory available in each waste tank's annulus (mainly Tanks 9 and 10). Tank 12 (also a Type I tank) make up most of the remaining contribution (2 %) to the 100-meter peak groundwater pathway dose in Section A at year 8,790. The Type I tanks with intact liners and the Type III and IIIA tanks do not fail prior to 10,000 years and therefore do not contribute to dose within 10,000-year period. Appendix E contains the 100-meter radionuclide concentration curves (20,000 years) for Tanks 12, 13, 16, 22, 32, 36, 39, and 40, the transfer lines, and all other sources combined. Figure 5.5-14 shows the Sector-A 100-meter MOP groundwater pathway doses by source for the 10,000-year time frame. The individual source contributions in Sectors B and C are shown in Figures 5.5-15 and 5.5-16, respectively.

Figure 5.5-14: Individual Source Contributors to the Sector A 100-Meter Peak Groundwater Pathway Dose - 10,000 Years

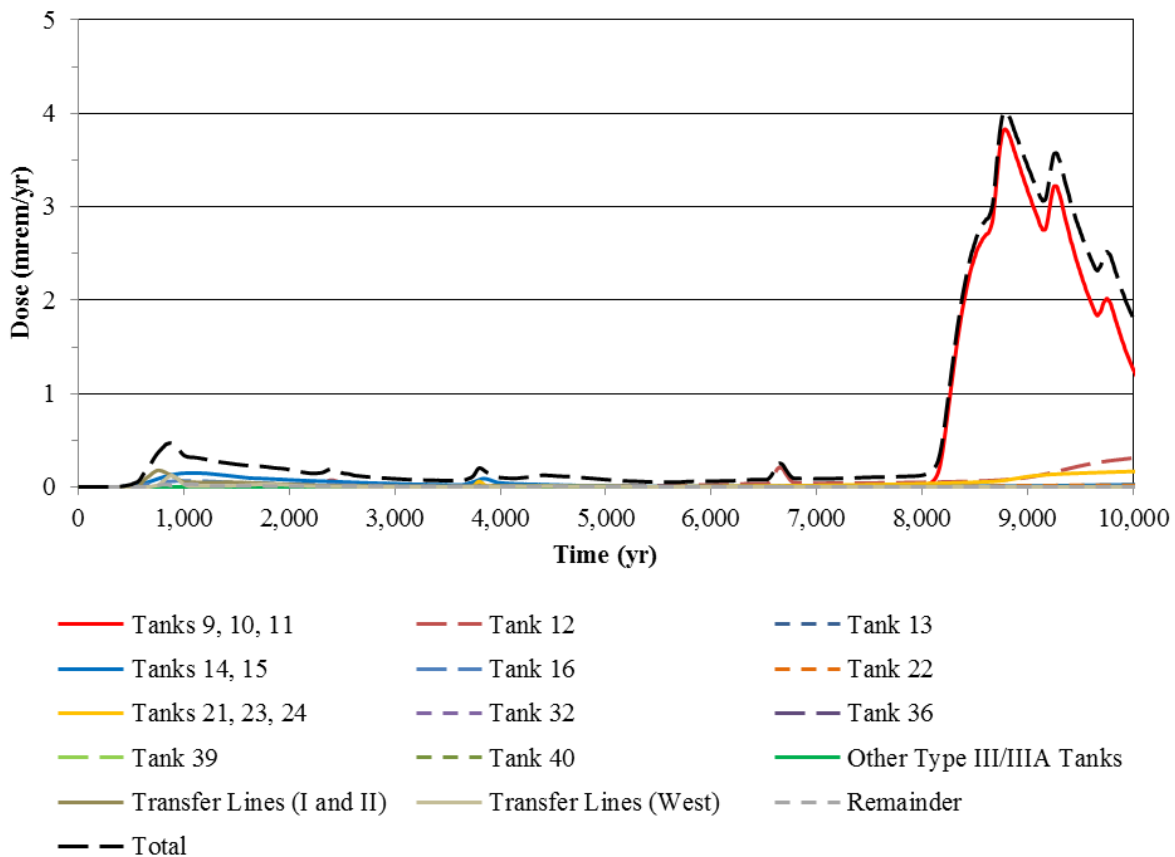


Figure 5.5-15: Individual Source Contributors to the Sector B 100-Meter Peak Groundwater Pathway Dose - 10,000 Years

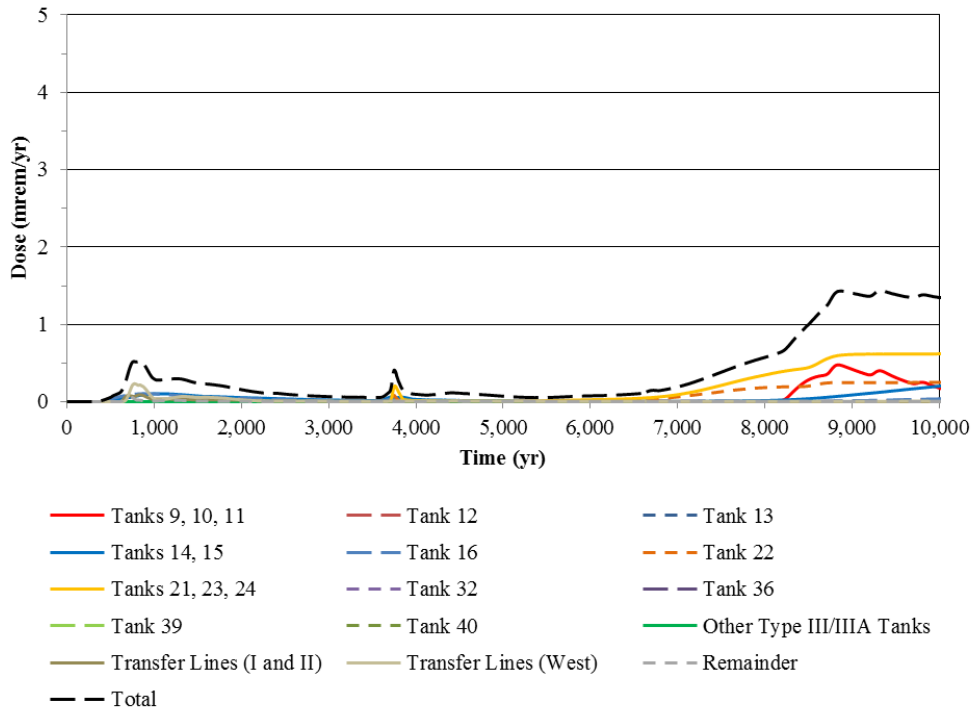


Figure 5.5-16: Individual Source Contributors to the Sector C 100-Meter Peak Groundwater Pathway Dose - 10,000 Years

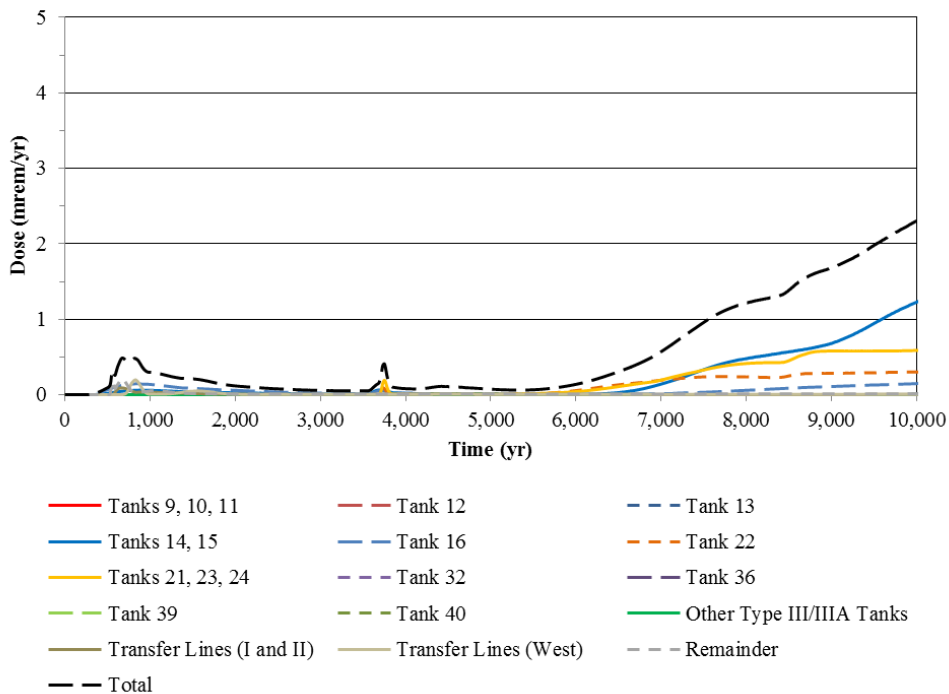


Table 5.5-3: MOP at 100-Meter Peak Groundwater Pathway Dose Individual Source Contributions at Peak Years - Sectors A and C Peak

Waste Source ^a	Contribution to Sector C Peak Dose at year 700 (mrem/yr)	Percentage of Total Peak Dose	Contribution to Sector A Peak Dose at year 8,790 (mrem/yr)	Percentage of Total Peak Dose
Tanks 9, 10, and 11	< 0.01	< 0.5 %	3.8	95 %
Tank 12	< 0.01	< 0.5 %	0.08	2.0 %
Tank 13	< 0.01	< 0.5 %	< 0.01	< 0.5 %
Tanks 14 and 15	0.05	10 %	0.01	< 0.5 %
Tank 16	0.13	28 %	< 0.01	< 0.5 %
Tank 22	< 0.01	< 0.5 %	0.01	< 0.5 %
Tanks 21, 23, and 24	< 0.01	< 0.5 %	0.07	1.9 %
Transfer Line, Group 2 (Type I and Type II)	0.09	18 %	< 0.01	< 0.5 %
Transfer Line, Group 3 (West Hill)	< 0.01	< 0.5 %	< 0.01	< 0.5 %
All Other Sources	0.19	40 %	< 0.01	< 0.5 %
TOTAL	0.47	100 %	4.0	100 %

^a The Type III and IIIA tanks (Tanks 29, 30, 31, 32, 35, 36, 37, 38, 39, 40, 41, 42, 43, 48, 49, 50, and 51) do not fail prior to 10,000 years and are excluded from this table because their contributions to peak doses is 0 %.

5.5.1.4 Individual Pathway Contributions to MOP 100-Meter Peak Annual Groundwater Pathway Dose

As stated previously, the total peak groundwater-pathway dose results are the summation of the doses associated with all the individual 100-meter well pathways identified in Section 5.4. Table 5.5-4 presents the relative contributions from the individual groundwater pathways to the Sector C 100-meter MOP receptor dose at 700 years (the year of the peak dose). The primary contributors are water ingestion (60 % of peak dose) and vegetable ingestion (33 % of peak dose). Similarly, Table 5.5-5 presents the relative contributions from the individual groundwater pathways to the Sector A, 100-meter MOP receptor dose at 8,790 years (the year of the peak dose). Like Sector C, the primary contributors for Sector A are water ingestion (58 % of peak dose) and vegetable ingestion (35 % of peak dose).

Table 5.5-4: MOP at 100-Meter Peak Groundwater Pathway Dose Individual Contributions at Peak Years - Sector C

Pathway	Associated Contribution at year 700 (mrem/yr)	Percentage of Total Peak Dose	Principal Radionuclide Pathway Dose
Water Ingestion	1.9E-01	60 %	Tc-99 (83 %)
Vegetable Ingestion	1.0E-01	33 %	Tc-99 (95 %)
Beef Ingestion	8.0E-03	2.6 %	Tc-99 (99 %)
Egg Ingestion	7.8E-03	2.5 %	Tc-99 (~100 %)
Other Pathways	6.3E-03	2.0 %	N/A
Summary			
Pathway	Associated Contribution at year 700 (mrem/yr)	Percentage of Total Peak Dose	
Total Inhalation	4.3E-06	0 %	
Total Ingestion	3.1E-01	100 %	
Total Exposure	2.7E-06	0 %	
TOTAL	0.31	100 %	

Table 5.5-5: MOP at 100-Meter Peak Groundwater Pathway Dose Individual Contributions at Peak Years - Sector A

Pathway	Associated Contribution at year 8,790 (mrem/yr)	Percentage of Total Peak Dose	Principal Radionuclide Pathway Dose
Water Ingestion	2.3E+00	58 %	Tc-99 (93 %)
Vegetable Ingestion	1.4E+00	35 %	Tc-99 (98 %)
Beef Ingestion	1.1E-01	2.8 %	Tc-99 (99 %)
Egg Ingestion	1.1E-01	2.7 %	Tc-99 (~100 %)
Other Pathways	7.8E-02	1.9 %	N/A
Summary			
Pathway	Associated Contribution at year 8,790 (mrem/yr)	Percentage of Total Peak Dose	
Total Inhalation	1.9E-05	0 %	
Total Ingestion	4.0E+00	100 %	
Total Exposure	1.8E-04	0 %	
TOTAL	4.0	100 %	

Table 5.5-6 presents a comparison of the 100-meter peak, water ingestion doses for the different 100-meter sectors. Figure 5.5-17 presents the water ingestion doses to the 100-meter MOP receptor over time during the 1,000-year time period for the 100-meter sectors. Figure 5.5-18 presents the water ingestion doses to the 100-meter MOP receptor over time

during the 10,000-year time period for the 100-meter sectors. The highest 100-meter MOP water ingestion dose in the 10,000-year period is a 2.3 mrem/yr dose in Sector A at year 8,790. Figure 5.5-19 presents the 100-meter MOP receptor, water ingestion doses within 100,000 years for the 100-meter sectors. Figures 5.5-20, 5.5-21, and 5.5-22 show the vegetable ingestion doses to the 100-meter MOP receptor for the 100-meter sectors.

Table 5.5-6: MOP at 100-Meter Peak Water Ingestion Doses by Sector

Sector	Peak Water Ingestion Dose in 1,000 years (mrem/yr)	Principal Radionuclide	Peak Water Ingestion Dose in 10,000 years (mrem/yr)	Principal Radionuclide
A	0.17 (year 860)	Tc-99 (95 %)	2.3 (year 8,790)	Tc-99 (93 %)
B	0.14 (year 720)	Tc-99 (99 %)	1.2 (year 9,330)	Ra-226 (32 %) Pa-231 (29 %) Tc-99 (19 %)
C	0.19 (year 700)	Tc-99 (83 %)	1.9 (year 10,000)	Ra-226 (58 %) Pa-231 (20 %)
D	0.023 (year 880)	Tc-99 (96 %)	0.091 (year 10,000)	Ra-226 (81 %)
E	0.081 (year 870)	Tc-99 (97 %)	0.081 (year 870)	Tc-99 (97 %)
F	0.087 (year 870)	Tc-99 (91 %)	0.087 (year 870)	Tc-99 (91 %)

Figure 5.5-17: MOP at 100-Meter Peak Water Ingestion Dose within 1,000 Years for the 100-Meter Sectors

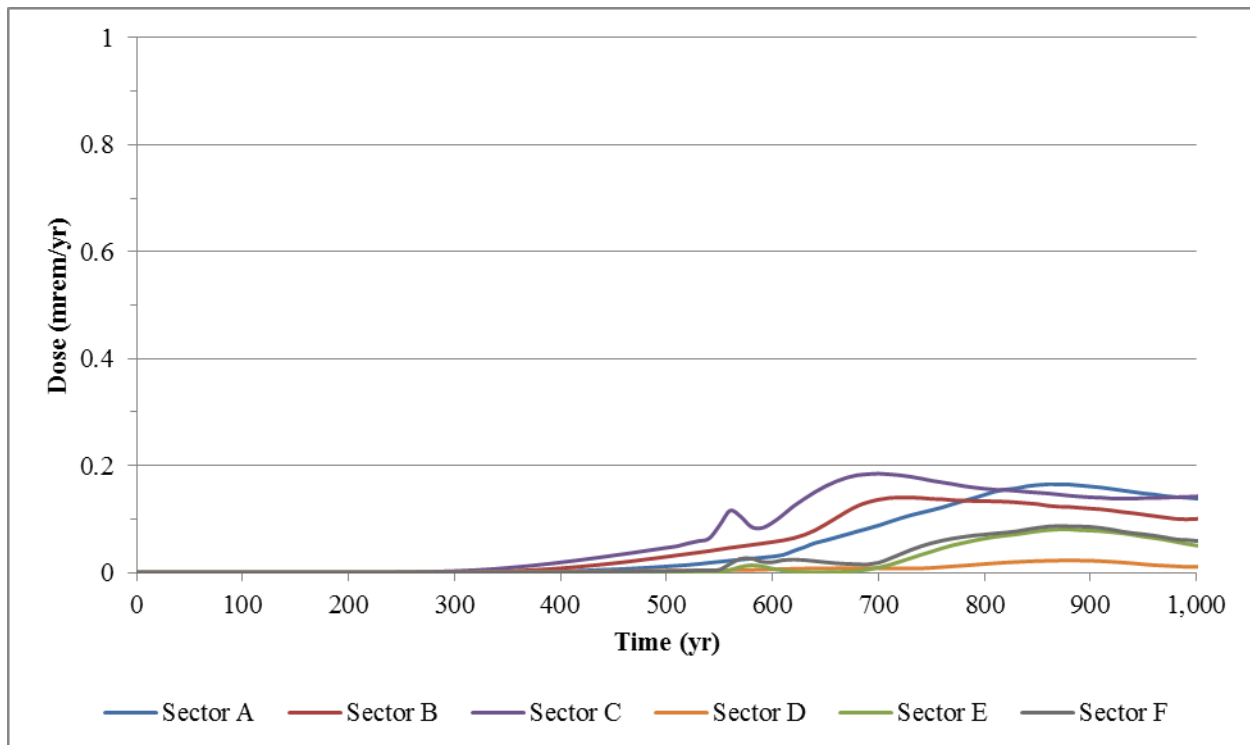


Figure 5.5-18: MOP at 100-Meter Peak Water Ingestion Dose within 10,000 Years for the 100-Meter Sectors

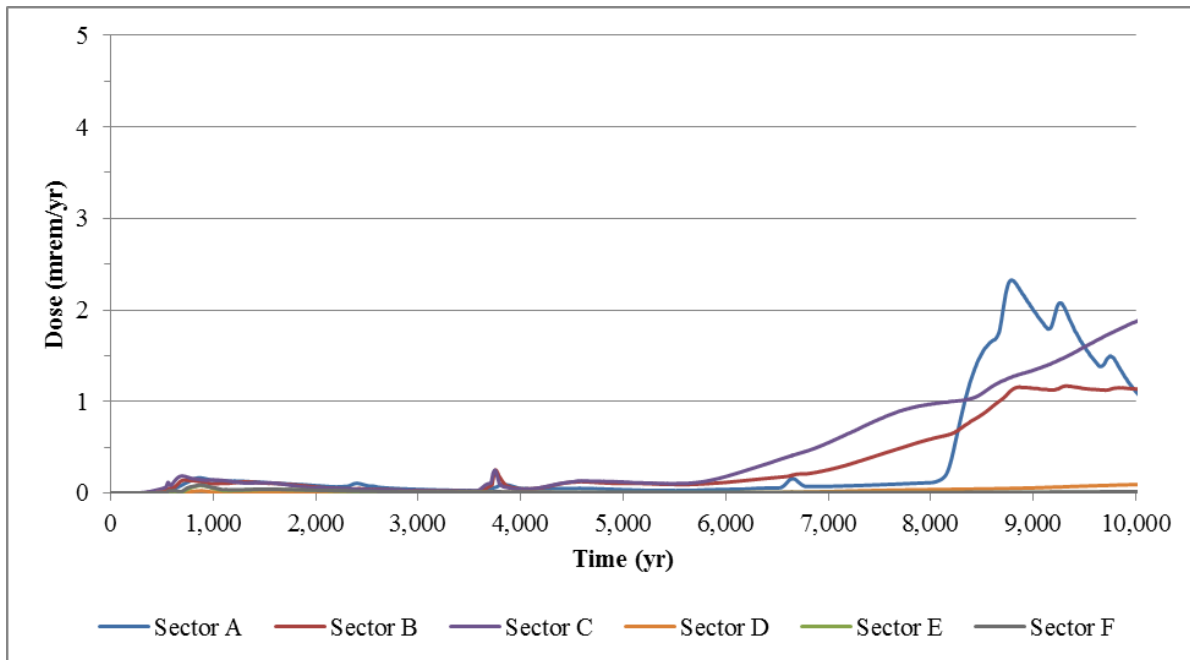


Figure 5.5-19: MOP at 100-Meter Peak Water Ingestion Dose within 100,000 Years for the 100-Meter Sectors

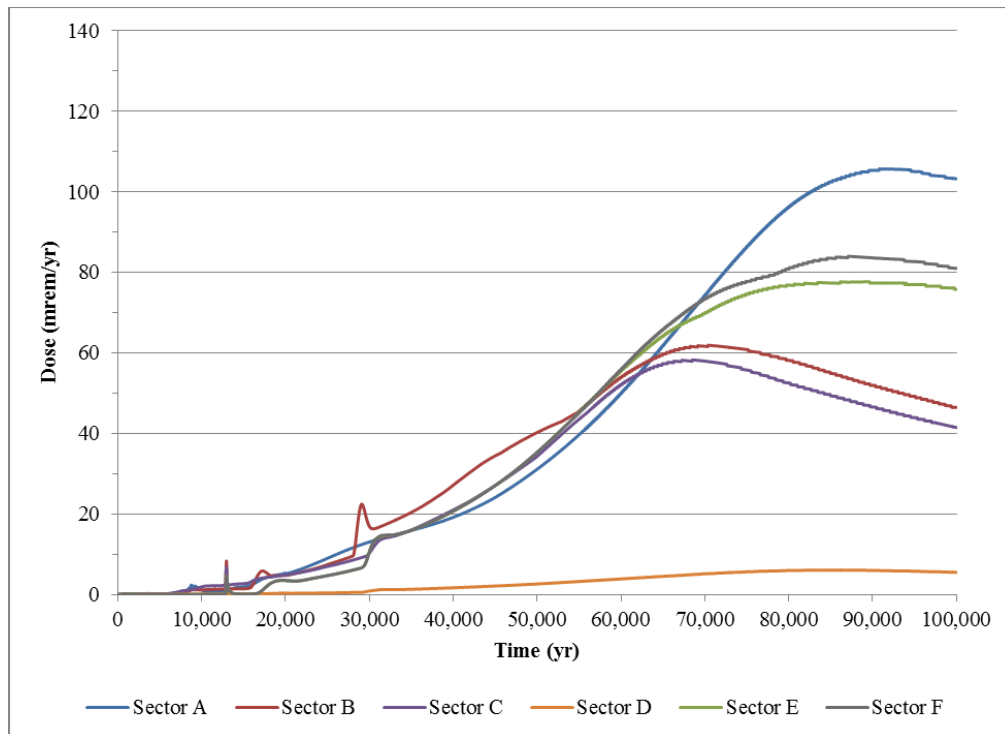


Figure 5.5-20: MOP at 100-Meter Peak Vegetable Ingestion Dose within 1,000 Years for the 100-Meter Sectors

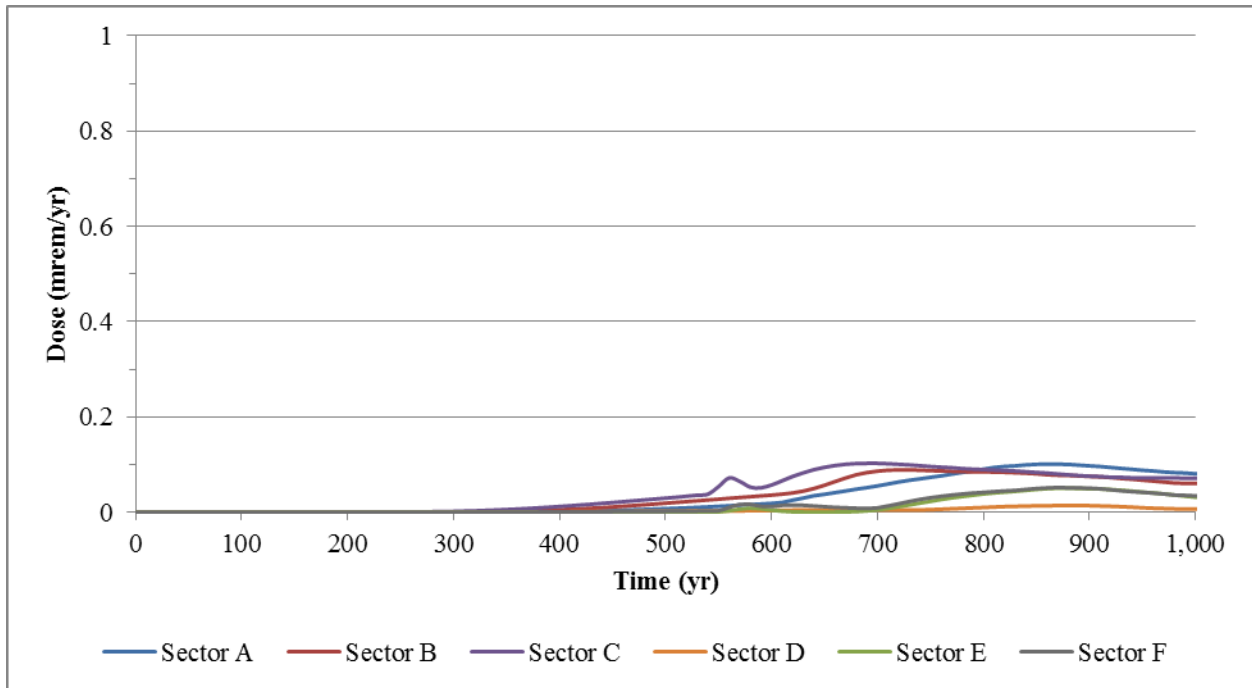


Figure 5.5-21: MOP at 100-Meter Peak Vegetable Ingestion Dose within 10,000 Years for the 100-Meter Sectors

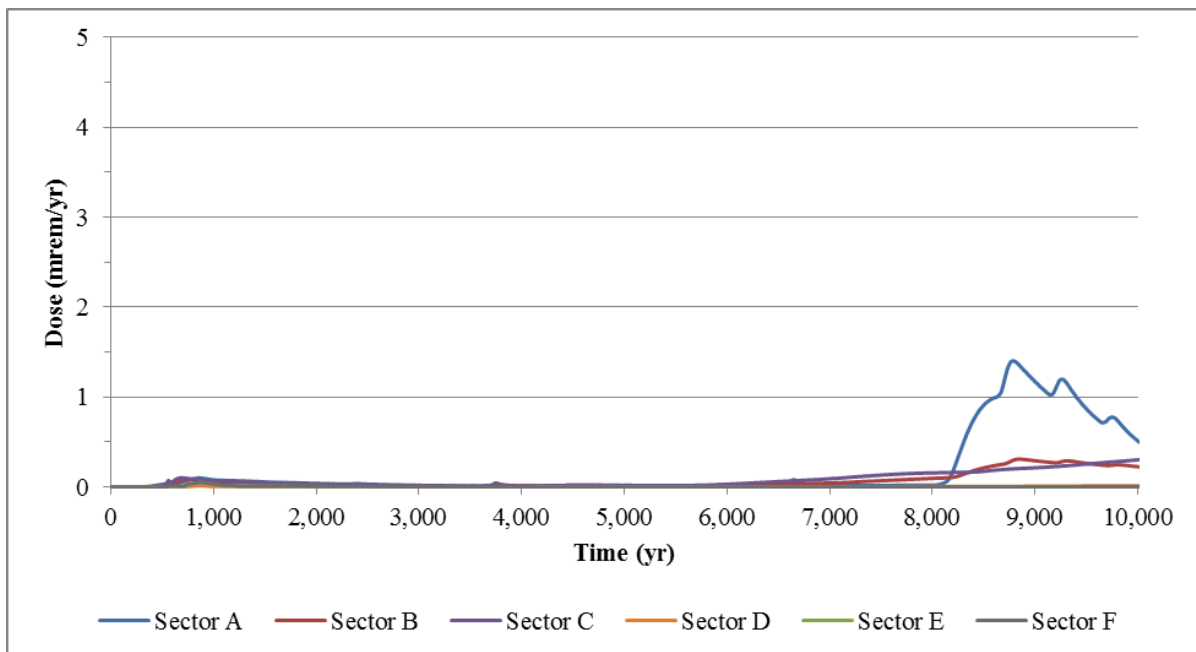
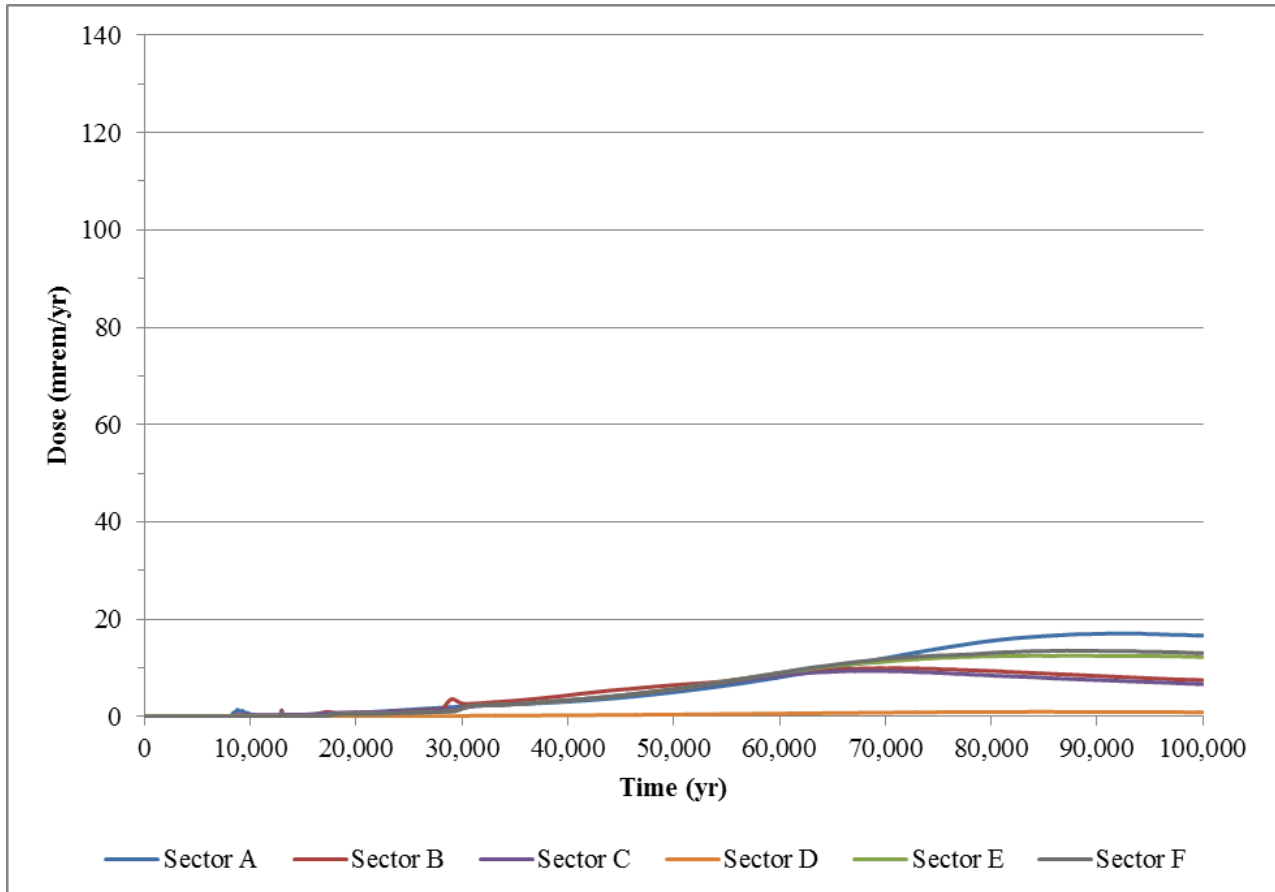


Figure 5.5-22: MOP at 100-Meter Peak Vegetable Ingestion Dose within 100,000 Years for the 100-Meter Sectors



5.5.2 MOP at Stream Groundwater Pathway Dose Results

The peak, groundwater pathway doses for two stream seepines (Fourmile Branch and UTR) are calculated using the highest concentration for each radionuclide in the seepine sector (a discussion of how peak concentrations are determined by sector is provided in Section 5.2). In calculating the peak groundwater pathway dose, the highest radionuclide concentration is used from each of the distinct aquifers modeled (the UTRA-UZ, UTRA-LZ, and the Gordon Aquifer) for the two seepine sectors. The concentration for each aquifer represents peak concentration in any vertical computational mesh within the aquifer. The mesh vertical thicknesses (heights) in the computational model are less than 10 feet in the UTRA-UZ, and less than 15 feet in the UTRA-LZ. No well screen averaging was used in determining the concentrations for dose calculations because the typical well screen length of 20 feet is approximate to the computational mesh height. As discussed in Section 4.2.3.1.2, the stream dose analysis assumes direct ingestion of water from the stream location with no stream dilution assumed. These peak-groundwater pathway doses are the total dose associated with all the individual MOP stream pathways identified in Section 5.4.

5.5.2.1 MOP at Stream Peak Annual Dose

Table 5.5-7 presents a comparison of the MOP stream, peak groundwater pathway doses for the two sectors. The peak, groundwater pathway dose in the 10,000-year period is associated with the Fourmile Branch. Figure 5.5-23 presents the peak, groundwater pathway doses over time during the 10,000-year period for the two streams of concern (UTR and Fourmile Branch). The MOP at the stream, peak groundwater pathway dose in the 10,000-year period is a 0.044 mrem/yr groundwater pathway dose at year 8,960. Figure 5.5-24 presents the peak, groundwater pathway stream doses within 20,000 years.

Table 5.5-7: MOP at Stream Peak Groundwater Pathways Dose

Stream ^a	Peak Dose in 10,000 Years	Principal Radionuclides	Principal Pathways
Fourmile Branch	0.039 mrem/yr (year 9,990)	Pa-231 (33 %) Ra-226 (26 %) Np-237 (16 %)	Water Ingestion (62 %) Fish Ingestion (25 %) Vegetable Ingestion (12 %)
UTR	0.044 mrem/yr (year 8,960)	Tc-99 (95 %)	Water Ingestion (44 %) Vegetable Ingestion (27 %) Fish Ingestion (24 %)

a Stream seepelines illustrated in Figure 5.2-6.

Figure 5.5-23: MOP at Stream Peak Groundwater Pathway Dose within 10,000 Years

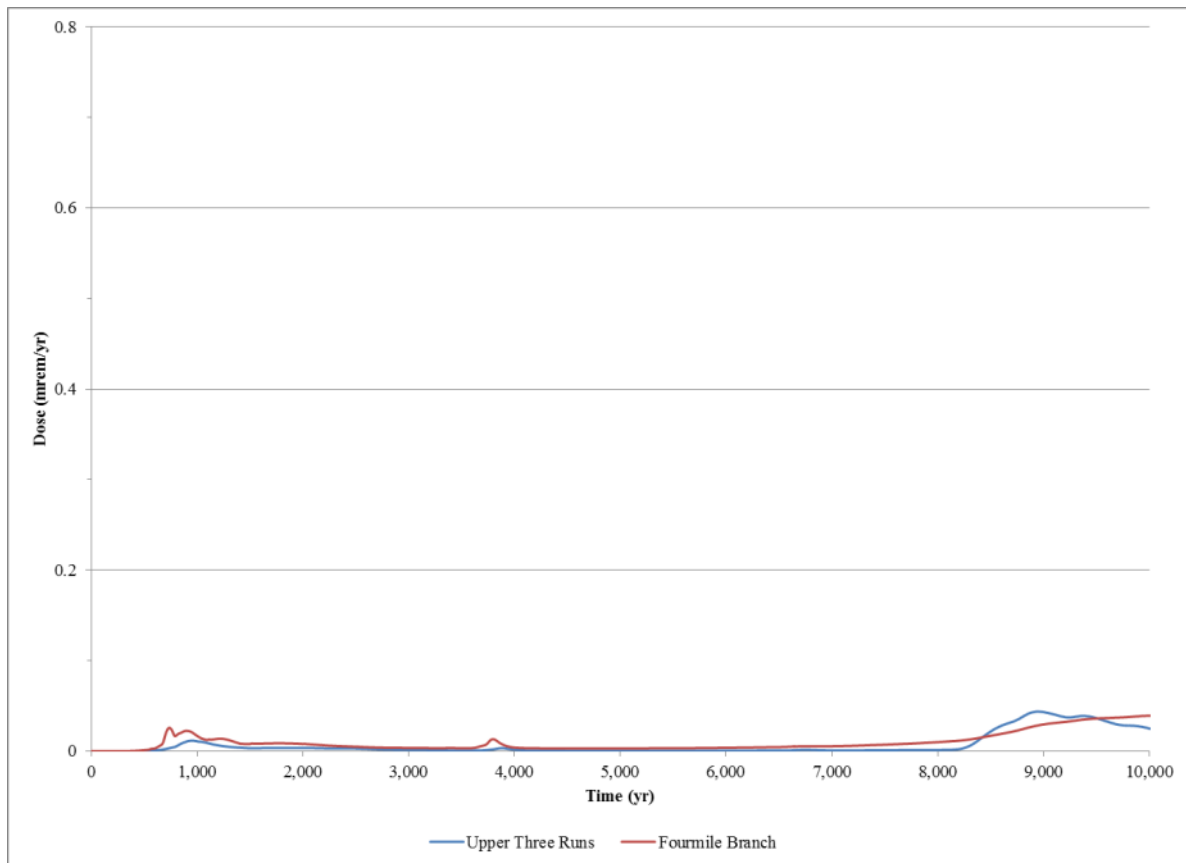
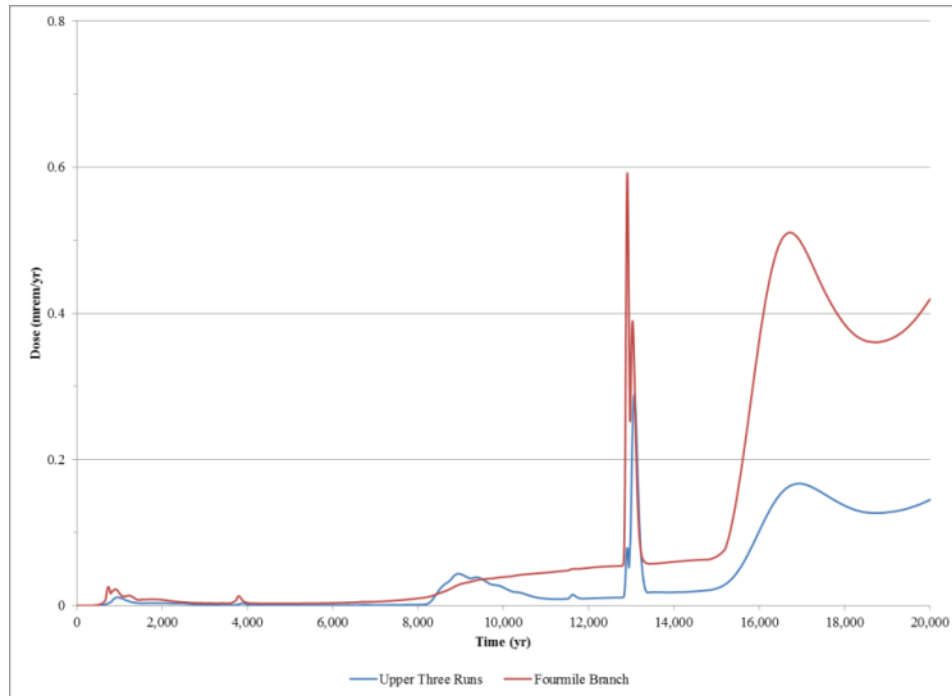
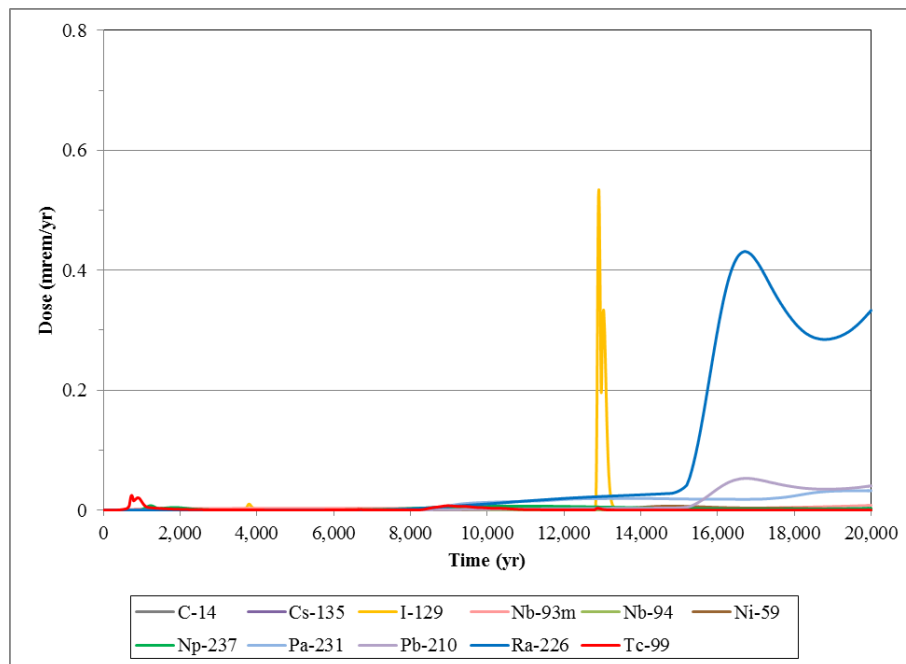


Figure 5.5-24: MOP at Stream Peak Groundwater Pathway Dose within 20,000 Years

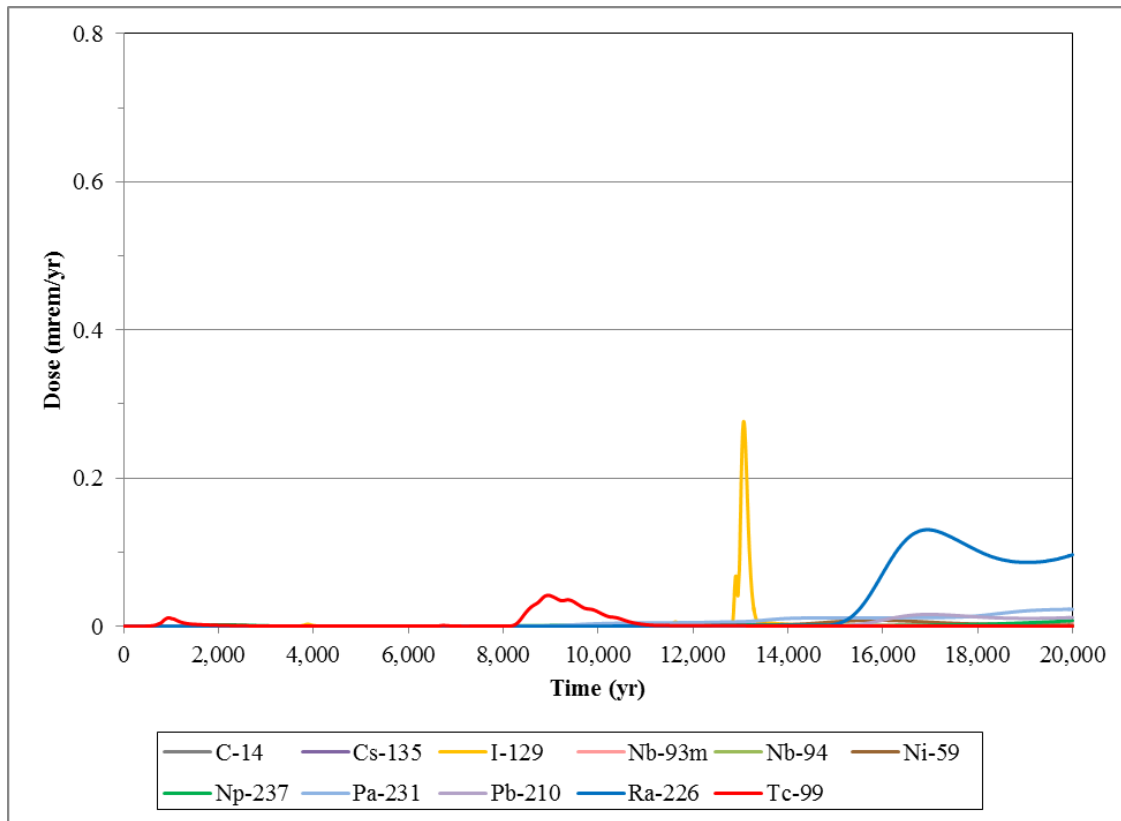


Figures 5.5-25 and 5.5-26 show the relative contribution from individual radionuclides to the groundwater pathway MOP dose at the stream within 20,000 years (Fourmile Branch and UTR, respectively).

Figure 5.5-25: Individual Radionuclide Contributors to the Fourmile Branch Groundwater Pathway Dose - 20,000 Years



**Figure 5.5-26: Individual Radionuclide Contributors to the UTR Groundwater Pathway
Dose - 20,000 Years**



5.5.2.2 MOP at Stream Individual Pathway Contributors

Table 5.5-8 presents the relative contributions from the individual groundwater pathways to the Fourmile Branch MOP receptor dose at 9,990 years (the year of the peak Fourmile Branch dose). The primary contributors are water ingestion (62 %), followed by fish ingestion (25 %), and vegetable ingestion (12 %). Table 5.5-9 presents the relative contributions from the individual groundwater pathways to the UTR MOP receptor dose at 8,960 years (the year of the peak UTR dose). The primary contributor to the UTR peak is water ingestion (44 %), followed by vegetable ingestion (27 %), and fish ingestion (24 %).

Table 5.5-8: MOP at Stream Peak Groundwater Pathway Dose Individual Contributions for Fourmile Branch

Pathway	Associated Contribution at year 9,990 (mrem/yr)	Percentage of Total Peak Dose	Principal Radionuclide Pathway Dose
Water Ingestion	0.024	62 %	Pa-231 (37 %)
Fish Ingestion	0.010	25 %	Nb-93m (26 %)
Vegetable Ingestion	0.005	12 %	Pa-231 (30 %)
All Others	< 0.001	1 %	N/A
TOTAL	0.039	100 %	

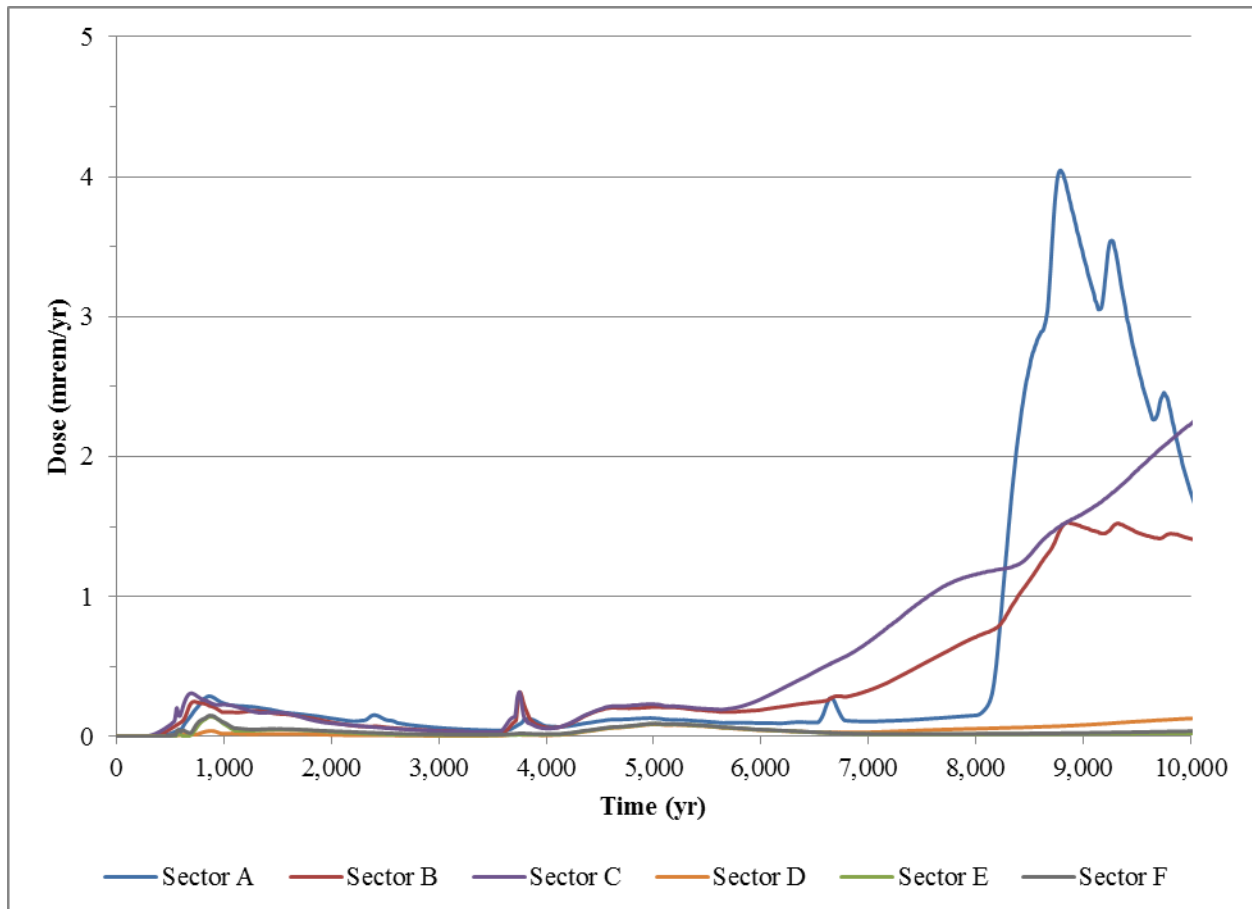
Table 5.5-9: MOP at Stream Peak Groundwater Pathway Dose Individual Contributions for UTR

Pathway	Associated Contribution at year 8,960 (mrem/yr)	Percentage of Total Peak Dose	Principal Radionuclide Pathway Dose
Water Ingestion	0.019	44 %	Tc-99 (94 %)
Vegetable Ingestion	0.012	27 %	Tc-99 (99 %)
Fish Ingestion	0.010	24 %	Tc-99 (93 %)
All Others	< 0.02	6 %	N/A
TOTAL	0.044	100 %	

5.5.3 MOP All-Pathway Dose Results

The purpose of this section is to present the total all-pathway peak doses for both the MOP at 100 meters and the MOP at the stream. The total all-pathway doses include both the groundwater and air pathway contributors. As calculated in Section 5.3, the air pathway dose is negligible; therefore, the all-pathway dose is the same as the groundwater pathway dose. Figure 5.5-27 presents the all-pathway dose to the MOP at the 100-meter sectors.

Figure 5.5-27: MOP Peak 100-Meter Sector All-Pathway Dose within 10,000 Years



5.6 Uncertainty and Sensitivity Analyses

The purpose of the UA/SA is to consider the effects of uncertainties in the conceptual models used and examine model sensitivity to the parameters used in the mathematical models. This evaluation was conducted for analyses related to the MOP as well as those related to inadvertent intruders. These evaluations focused on key uncertainties and key sensitivities identified during modeling.

The UA/SA were primarily performed using a probabilistic model (i.e., the HTF GoldSim Model), as discussed in Sections 5.6.1 through 5.6.5. Section 5.6.1 summarizes the purpose, the key assumptions, and the approach used to develop the HTF Stochastic Fate and Transport Model. The abstracted probabilistic model is benchmarked against the deterministic HTF PORFLOW Model in Section 5.6.2. Section 5.6.3 identifies and defines the stochastic parameters applied in the probabilistic model. The analysis to evaluate how the uncertainty in model input parameters is propagated through the model to the selected model results, or endpoints, is detailed in Section 5.6.4. Section 5.6.5 documents the SAs, which identifies the stochastic model input parameters most influential in determining the results (e.g., concentrations and potential dose). The barrier analyses documented in Section 5.6.6 compares the fluxes beneath the containment structures for several deterministic PORFLOW simulations, each representing a different barrier failure mode. The objective of this section is to evaluate the barrier's importance to releases to the saturated zone. Section 5.6.7 contains deterministic sensitivity analysis, including comparison of the deterministic PORFLOW Base Case (Case A) dose time histories to the alternative Cases B through E, and to the no closure cap case. Section 5.6.8 contains additional SA performed using GoldSim.

The probabilistic model allows for varying multiple parameters simultaneously, so concurrent effects of changes in the model can be analyzed, and the potential impact of changes can be assessed. This assessment allows for identification of parameters that are only of significance when varied simultaneously with another parameter. The deterministic model single parameter analysis provides a method to evaluate parametric effects in isolation, so the importance of the uncertainty around a parameter of concern can be more effectively evaluated. Using both probabilistic and deterministic models for SAs versus a single approach provides additional information concerning which parameters are of most importance to the HTF model.

5.6.1 Uncertainty and Sensitivity Analyses using Probabilistic Modeling

Uncertainty is inherent in simplified numeric models that attempt to replicate engineered or natural systems. Different types of uncertainty exist in modeling complex systems: uncertainty in possible future outcomes, uncertainty in the consequences of future outcomes, and uncertainty in the parameters used as input to these models. The objective of the probabilistic model is to provide the vehicle to quantify parameter uncertainty explicitly as a probability in order to bound the range of possible receptor dose outcomes, and to enable identification of those parameters strongly influencing dose.

5.6.1.1 *HTF GoldSim Stochastic Fate and Transport Model*

A probabilistic model was constructed to replicate fate and transport of HTF contaminant releases modeled using PORFLOW, in order to characterize parameter uncertainty and

sensitivity (see Section 5.6.2 on benchmarking). The probabilistic model is necessarily simpler than the PORFLOW groundwater model in its environmental transport calculations, but includes additional calculations that cannot be performed in PORFLOW. The probabilistic model is described in more detail in Section 4.4.4.2 and in the report *H-Area Tank Farm Stochastic Fate and Transport Model*. [SRR-CWDA-2010-00093, Rev. 2]

The probabilistic model, developed using the GoldSim systems analysis software, accepts uncertainty and variability in the input parameters, the values of which can be defined using probability distributions. If a given model input (e.g., the porosity of sandy soil) is given a distribution, or range of values, then this distribution is sampled in the collection of Monte Carlo runs that constitutes a probabilistic analysis. The collective uncertainty of all stochastic (probabilistic) inputs is reflected in the range and distribution of modeled results, such as water concentrations or dose to hypothetical future human receptors. If an input parameter is given no range of input values, that is, if it is defined deterministically, then it contributes nothing to the overall uncertainty in the results. Few parameters have zero uncertainty. An example of a parameter without a defined range is the half-life of radionuclides.

5.6.1.2 HTF GoldSim Model Assumptions

A number of assumptions are necessary when simplifying complex engineered and natural systems for modeling purposes. The key model assumptions for the probabilistic model are summarized below:

Inventory Assumptions:

- The transfer line inventory used to calculate the “drill-cuttings” concentration for the acute and chronic intruder dose calculations is a projected inventory. [SRR-CWDA-2010-00023, Rev. 3]

Transport Assumptions:

- At the intersection of PORFLOW stream traces and the 100-meter boundary surrounding the HTF, a line of hypothetical evaluation wells are located (See Figure 4.4-54 in Section 4.4.4.2). These evaluation wells are grouped based on their location in Sectors A through E. These “100-meter wells” are a point at which contaminant concentrations are evaluated for use in dose calculations compared with relevant performance measures. The assumption was made that contaminant transport distance is equal to the distance between the contaminant sources and these 100-meter wells along the stream trace.
- The MOP and intruder dose calculations require as input the contaminant concentration in the stream (Table 4.4-20, Section 4.4.4.2) to calculate the dose to the receptor from certain activities (e.g., fishing, swimming, and boating). The probabilistic model does not explicitly calculate stream concentrations. The probabilistic model estimates the concentration of contaminants in the stream by applying a species dependent ratio to the GoldSim calculated concentration at the 100-meter well. This ratio is the ratio between the PORFLOW stream (e.g., seep line) concentrations for each radionuclide to the PORFLOW 100-meter well

concentrations. Applying these ratios to estimate the stream concentrations is reasonably conservative because the water in the stream pathways would be subject to stream dilution, however, this is not accounted for when the raw seepage concentration from PORFLOW is used. Therefore, the ratio, which is based on the raw seepage concentration from PORFLOW, does not account for stream dilution. The calculation of this ratio is documented in Appendix F.1.

Dose Calculator Assumptions:

- The chronic intruder (Section 6.3) resides next to a Type I tank and uses water from a well, drilled 1 meter from this waste tank. This waste tank was selected because it has the highest chronic intruder dose of the 7 wells tested in the PORFLOW model analysis described in Section 6.5.1.3.
- The drill-cuttings concentration used in the acute and chronic intruder dose calculations assume the intruder drills into a 3-inch transfer line.

5.6.2 GoldSim Benchmarking

The HTF PORFLOW Model is a 3-D flow and transport model designed to simulate rigorously the transport and fate of radionuclides and non-radioactive species released from waste tanks and associated ancillary equipment located in the HTF. The HTF GoldSim Model is an abstraction of the HTF PORFLOW Model designed to perform UA/SA that would be prohibitive using a computationally intensive model like the HTF PORFLOW Model. The HTF PORFLOW Model is a deterministic model, in that it assumes single values for parameters used in the flow and transport calculations. One of the drawbacks to this type of model is that the selected parameter value may be conservative in most situations, but under a unique set of conditions, the selected parameter value may actually force a non-conservative result. The HTF GoldSim Model offers the ability to test the sensitivity of the system to a range of parameter values. Therefore, the HTF GoldSim Model is necessarily a simplification of the HTF PORFLOW Model.

In abstract, spatially averaged flow rates from the HTF PORFLOW Model were used as input to the HTF GoldSim Model and controlled the transport of radionuclides and non-radioactive species through a simplified assemblage of the containment features (e.g., liner, basemat). While 3-D flow can take place within the containment structures, the HTF GoldSim Model is limited to 1-D flow through these features. In the saturated zone, the complex 3-D PORFLOW flow fields are represented by 1-D flow along PORFLOW generated stream traces. The 1-D GoldSim flow paths emanate from the upgradient edge of the containment feature's footprint with the source term, defined by the unsaturated zone releases, applied to the segment of the stream trace under the tank (or ancillary equipment) footprint. In the saturated zone, the timing of concentration breakthrough curve peaks generated by PORFLOW (for a conservative tracer) and the stream trace lengths were used to determine the flow velocities along the stream traces. Concentrations derived at the 100-meter boundary are adjusted to reflect any differences between the averaged flow velocities and the PORFLOW generated velocities at the 100-meter boundary. For a more detailed description of the abstracted model, refer to Section 4.4.4.2.

The section presented below describes the process used to evaluate how well the GoldSim abstraction replicates the HTF PORFLOW Model. This process is referred to as “benchmarking” and is done to ensure the validity of the GoldSim abstraction. The benchmarking is necessary to provide justification for the assumption that when the HTF GoldSim Model is simulated stochastically (e.g., multi-realizations are performed to test ranges of variable values), the results approximate the results of the HTF PORFLOW Model. Although key results of this evaluation are presented here, the detailed results can be found in the report, *H-Area Tank Farm Stochastic Fate and Transport Model* (SRR-CWDA-2010-00093, Rev. 2).

5.6.2.1 Benchmarking Process Description

In the benchmarking effort, PORFLOW/GoldSim comparisons were performed in four phases. The first phase focuses on how well the abstraction model approximates the radionuclide releases from the waste tanks and ancillary equipment. The radionuclide releases to the saturated zone are used for this comparison, and are referred to below as “vadose zone mass release.” The second phase focused on how well the abstraction model approximated the radionuclide transport behavior in the saturated zone. The sector-based (see Figure 4.4-54) radionuclide species-specific dose contributions are examined for this task. The third phase compared PORFLOW dose results with GoldSim dose results, evaluating how well the timing and magnitude of the time histories matched. This third step verified that the physical and radiological processes controlling radionuclide transport were translated to the dose results, which is the metric used to evaluate whether HTF meets the dose performance objectives. The fourth phase used a comparison of inadvertent human intrusion (IHI) total dose results, based on concentrations solved for adjacent to Tank 12.

The benchmarking evaluation was conducted for the Base Case results. Table 4.4-1 (in Section 4.4.2) presents a summary of the various waste tank cases modeled.

The HTF Model is based on 47 different source release locations, 8 different waste tank types (counting “no liner” waste tanks and western Type IIIA tanks separately), 80-modeled radionuclides, and 28 hypothetical observation wells. In deterministic mode, the model is set up to consider five different modeling cases, Cases A through E, and all 8 waste tank types. In stochastic mode, the HTF Model considers 4 different waste tank types (Type I, II, IIIA, and IV). In addition, for each waste tank type, there are 72 data sets to sample from (see Sections 4.4.4.2.2 and 5.6.3.2). For the benchmarking effort, a comparison of results for every radionuclide, at all locations for every scenario would be quite extensive. A selection process was devised to narrow the number of comparisons required, but would still ensure adequate model representation.

5.6.2.1.1 Representative Contaminant Sources

Of the 29 waste tanks in the HTF, 9 representative waste tanks were selected for evaluation dependent on waste tank type, condition of the liner, and other specific reasons for inclusion. The Table 5.6-1 summarizes the selected waste tanks and the rationale for their selection. A single ancillary equipment location was selected for each ancillary equipment unit type. Table 5.6-2 lists the representative ancillary equipment locations.

Table 5.6-1: Summary of Selected Waste Tanks

Representative Waste Tank	Waste Tank Type	Initial Liner Failed	Additional Reason for Inclusion?
Tank 9	Type I	N	N/A
Tank 12	Type I	Y	N/A
Tank 13	Type II	N	N/A
Tank 15	Type II	Y	N/A
Tank 16	Type II	Y	Initial inventory in the secondary sand pad
Tank 24	Type IV	N	N/A
Tank 31	Type III	N	N/A
Tank 36	Type IIIA	N	Located on west side of HTF
Tank 40	Type IIIA	N	Located on east side of HTF

N/A = Not Applicable

Table 5.6-2: Summary of Selected Ancillary Equipment

Representative	Type
HPT-7	Pump Tank
242-25H	Evaporator
Transfer Line Zone 3 or HTF-T-Line3	Transfer Line

5.6.2.1.2 Representative Radionuclides

Of the 80 radionuclides modeled in GoldSim, five were selected for the benchmarking comparison (Ra-226, Tc-99, I-129, Cs-135, and Np-237). Evaluation of individual radionuclides, as opposed to total dose, is important because each radionuclide behaves differently in the engineered and natural system. Because the HTF GoldSim Model is trying to replicate the transport system, evaluating individual radionuclides provides validation that the different modeling components are responding appropriately. Based on results from PORFLOW, the main contributors to total dose within 10,000 years include Ra-226 and Tc-99 (See Section 5.5, Table 5.5-1). These radionuclides were included in the benchmarking evaluation for this reason, but also because they (or their parent radionuclide) are affected by solubility controls in GoldSim.

The HTF GoldSim Model handles the influence of solubility limits in a more refined manner than PORFLOW. In the GoldSim simulations, all isotopes of uranium, for example, are considered simultaneously in the analysis. This means that GoldSim sums the concentration for each isotope of uranium together and evaluates if the solubility limit is reached at each time step. If the summed uranium concentration is higher than the

solubility limit, uranium will precipitate out, thus limiting the amount of uranium released to the saturated zone. In the PORFLOW simulations, the isotopes are not summed together, but are considered separately for the duration of the simulation. PORFLOW therefore, is more likely to overestimate the mass released from the CZ.

Because their transport is not subject to solubility control, Cs-135 and I-129 were chosen as benchmarking species. In the unsaturated zone, Cs-135 is more strongly sorbed than I-129, therefore they were both included for comparison. Because it is strongly sorbed to cementitious material and only slightly sorbed to soils in the unsaturated zone, Np-237 was selected.

5.6.2.1.3 Representative Observation Wells

Of the 6 sectors presented in Figure 4.4-54, five were selected based on the locations where stream traces crossed the 100-meter boundary and their relative importance to peak dose. The Sectors used for the comparison are A, B, C, E, and F and are shown in Figure 4.4-54 (in Section 4.4.4.2). Sector D was ignored because stream traces do not cross the segment of the 100-meter boundary defining Sector D.

5.6.2.2 Benchmarking Results

The Base Case (Case A) represents what is considered the most likely scenario for the time-based degradation of the waste tank structure, including the degradation of the cementitious materials and the steel liner. For brevity, this “benchmarking” section presents the Base Case mass release results for Tanks 9 (submerged Type I, no initial liner damage), 12 (submerged Type I, initial liner failed), 13 (submerged Type II, no initial liner damage), 24 (Type IV, no initial liner damage) and the saturated zone concentrations at Observation Well A3 only. To review all benchmarking results, refer to SRR-CWDA-2010-00093, Rev. 2. Note that the mass releases from waste tanks as presented here represent the source terms applied to the saturated zone. Their determination includes the influence of transport in the unsaturated zone for non-submerged waste tanks.

5.6.2.2.1 Tank 9 Mass Release from a Type I Tank with Intact Liner

Tank 9 is a submerged Type I tank with an initially intact liner that failed at year 11,397. Figures 5.6-1 through 5.6-5 display PORFLOW/GoldSim comparison plots of the mass released (mole per year) from Tank 9 for the following radionuclides, Ra-226, Tc-99, I-129, Np-237, and Cs-135. The curves indicate that the HTF GoldSim Model reproduces the HTF PORFLOW Model releases well.

Figure 5.6-1: Mass Release from Type I Tank 9 - Ra-226 (Base Case)

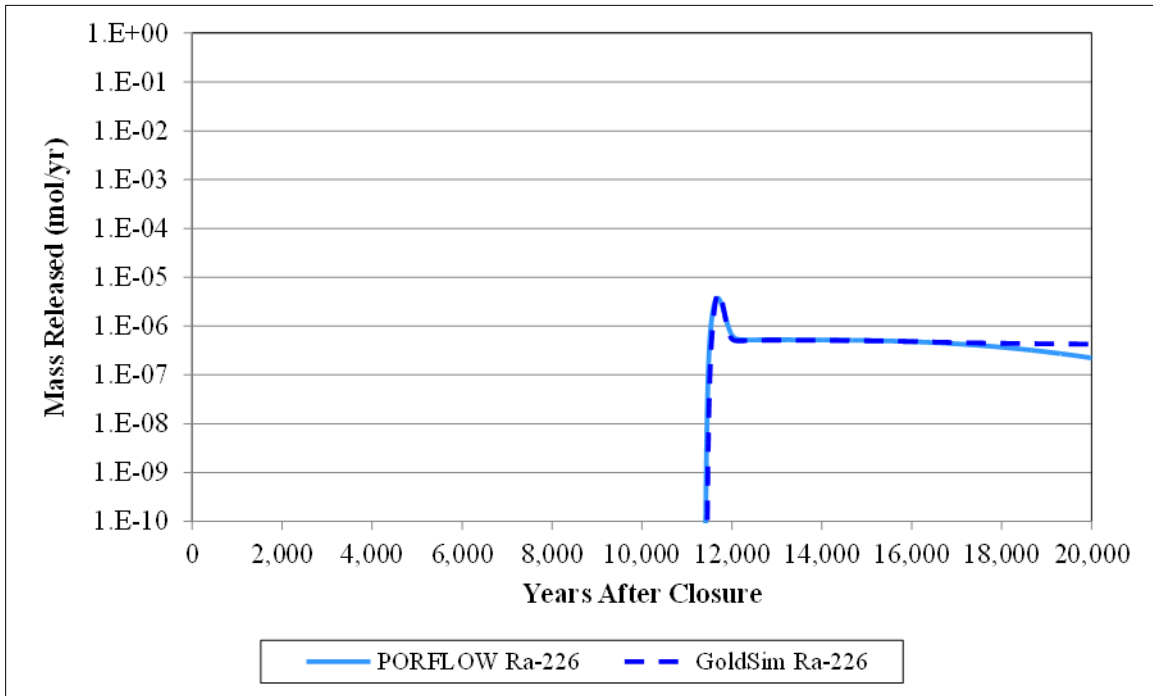


Figure 5.6-2: Mass Release from Type I Tank 9 - Tc-99 (Base Case)

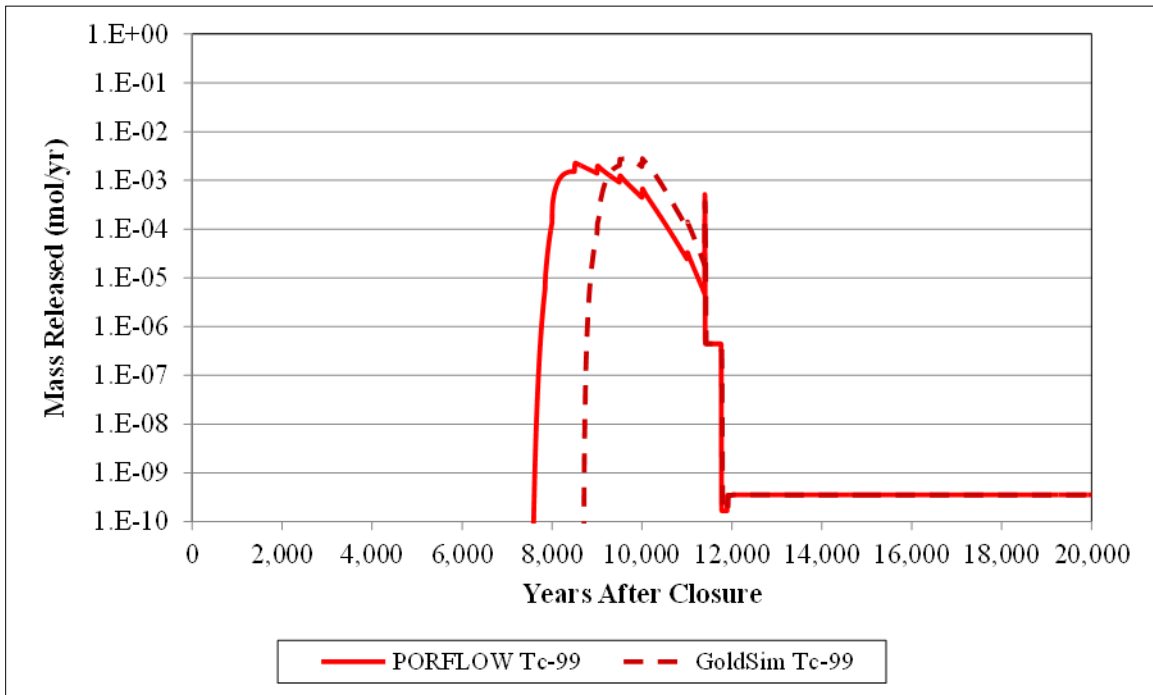


Figure 5.6-3: Mass Release from Type I Tank 9 - I-129 (Base Case)

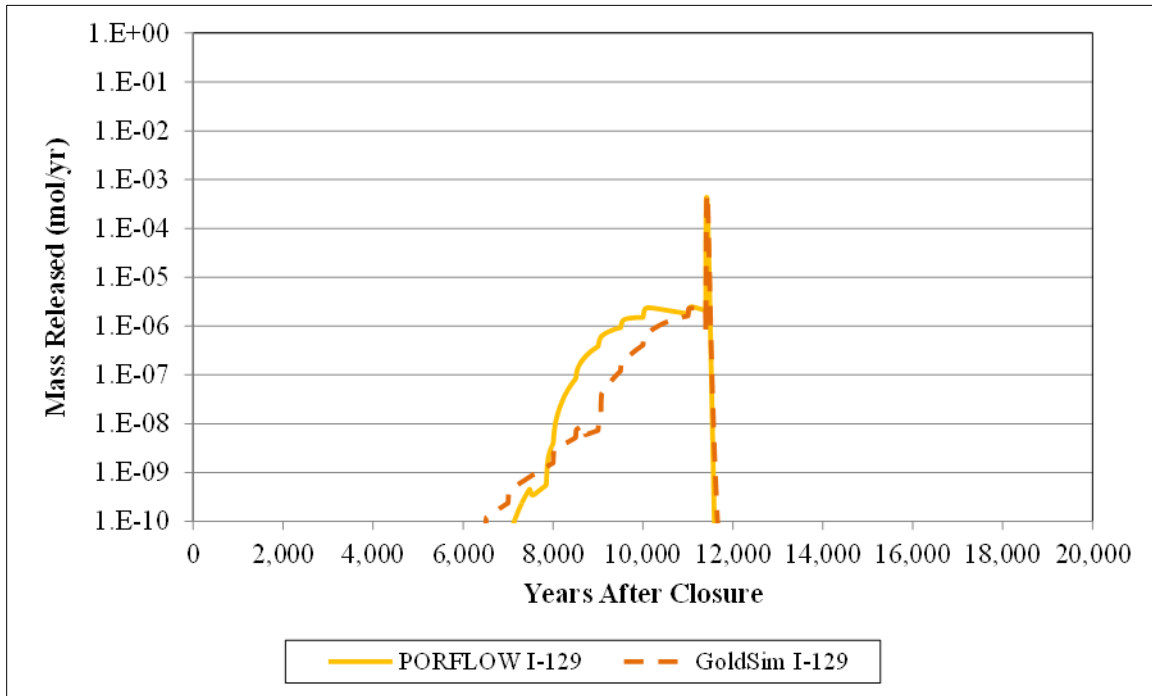


Figure 5.6-4: Mass Release from Type I Tank 9 - Np-237 (Base Case)

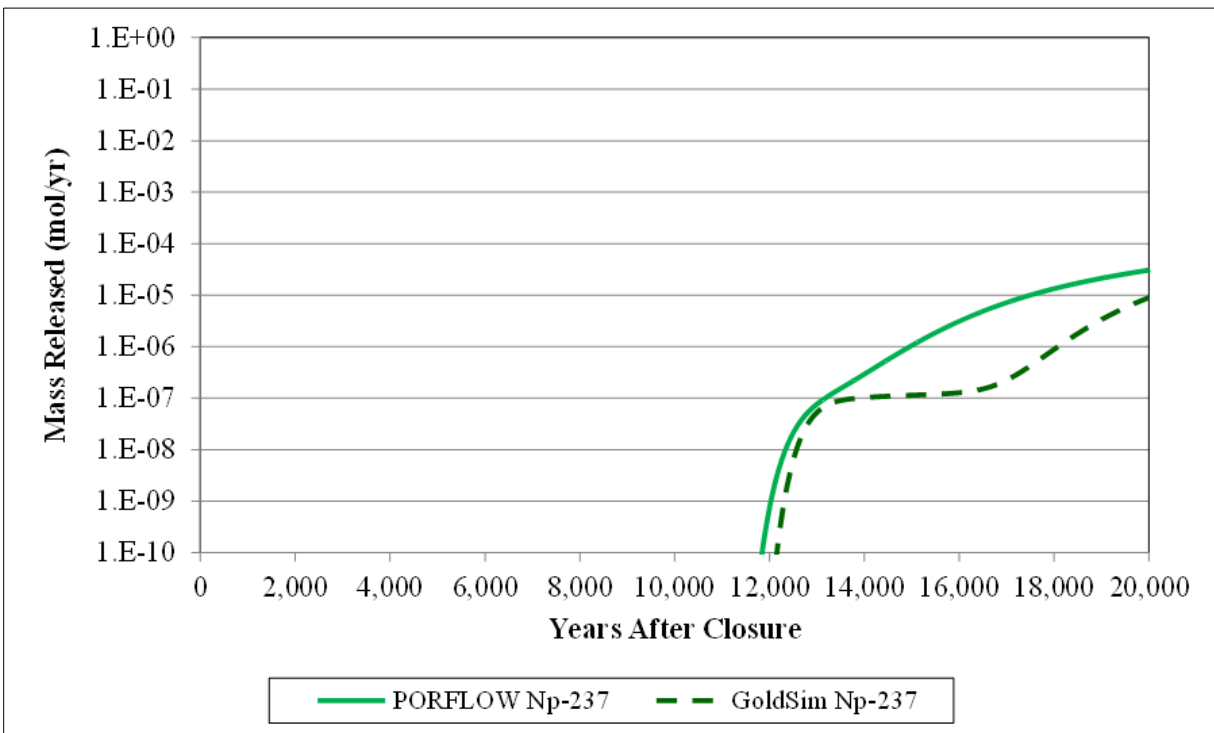
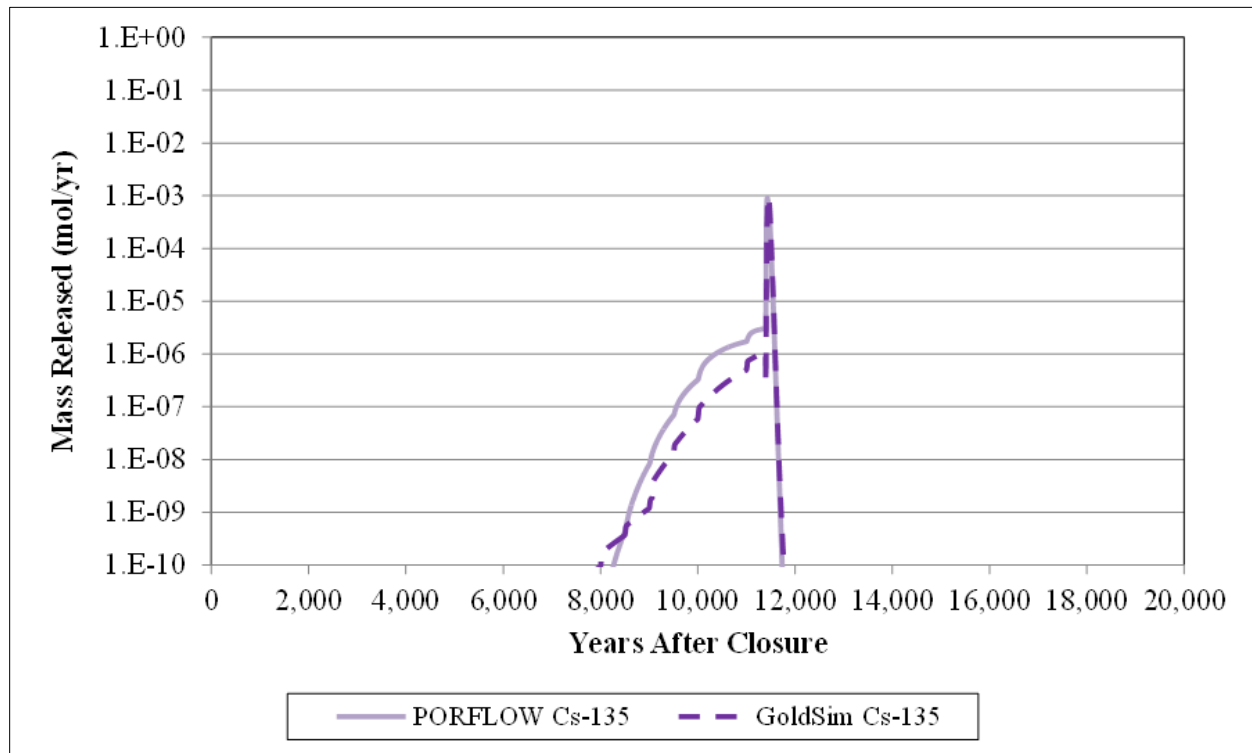


Figure 5.6-5: Mass Release from Type I Tank 9 - Cs-135 (Base Case)



The close match between the curves representing Tank 9 Ra-226 releases (Figure 5.6-1) is significant because it indicates GoldSim also adequately represents the transport of the parents of Ra-226. The initial inventory of Ra-226 is relatively small. The majority of Ra-226 is generated through in-growth from the Pu-238→U-234→Th-230→Ra-226 chain making the initial inventory of Pu-238 important to the dose results and not the initial inventory of Ra-226.

In addition to being a major dose contributor, Tc-99 is strongly controlled by solubility limits. As Figure 5.6-2 illustrates, after liner failure, the GoldSim Tc-99 release overlies the PORFLOW release, indicating that the solubility control associated with the CZ is being accurately approximated in the HTF GoldSim Model. Prior to liner failure, the Tc-99 release is dominated by the release of an inventory initialized at the bottom of the annulus. The differences between the two curves prior to liner failure are caused by differences in the manner that the annulus chemistry transition times are evaluated in the two models. In the PORFLOW model, the transition times are based on the pore volume of the entire annulus and the volumetric flow through that pore volume. In the GoldSim model, the transition times are based on the pore volume of the annulus located below the secondary liner and the volumetric flow through that abbreviated pore volume.

Both the timing and the magnitude of the PORFLOW I-129 peak release displayed in Figure 5.6-3 are similar to the GoldSim results. The match is especially good at the higher concentrations. Note that the GoldSim results prior to the liner failure are influenced by the differences in the transition-time calculations.

The Np-237 releases from Tank 9 are plotted in Figure 5.6-4 with the PORFLOW results showing an earlier breakthrough for the mass initialized as Np-237.

Because its transport is not subject to solubility control and it is more strongly sorbed than I-129 in the unsaturated zone, Cs-135 was chosen as a benchmarking species. Figure 5.6-5 shows that there is a good match between the PORFLOW results and the GoldSim results for Cs-135 releases from Tank 9. The match is especially good at the higher concentrations.

5.6.2.2.2 Tank 13 Mass Release from a Type II Tank with an Intact Liner

Tank 13 is a submerged Type II tank with an intact liner. Type II tanks have a more complex engineered system, due in large part from the inclusion of the sand pads (primary and secondary) located beneath the primary and secondary liners (e.g., Figure 4.4-50 in Section 4.4.4.2), therefore flow and transport is consequently more complex for these waste tanks. For Type II tanks, it is assumed some contaminant exists in the primary sand pad and annulus at the time of closure. It is also assumed for Tank 16 that some contaminant exists in the secondary sand pad. The mass in the primary sand pad, which is sandwiched between the primary and secondary liners, is capable of migrating out of the engineered barrier prior to liner failure, a process that is observed in the PORFLOW simulations. For Tank 13, a Type II tank with an intact liner, the initial exit route is from the sand pad to the annulus and upward through the annulus. The mass must first migrate above the 5-foot secondary liner vertical extension, before it can leave the system by migrating through the wall, into the concrete basemat, and finally into the saturated zone.

Although the HTF GoldSim Model simulates vertical flow and diffusion along the pathways described above, it assumes that matrix diffusion controls the migration of radionuclides and chemical constituents from the primary sand pad to the annulus. Prior to liner failure, diffusion is considered a dominant process in moving mass upwards through the annulus to the top of the secondary liner where the mass can enter the wall. Since advection associated with a circulation cell in the annulus can cause upward movement of radionuclides in the annulus, advection is also considered in a simplified manner (see Section 4.4.4.2.2). After liner failure, downward vertical flow through the annulus is assumed as the critical process for transporting any mass that enters the annulus from the primary sand pad.

Figures 5.6-6 through 5.6-10 display PORFLOW/GoldSim comparison plots of the mass released (mole per year) from Tank 13 for radionuclides Ra-226, Tc-99, I-129, Np-237, and Cs-135. Comparisons of the curves indicate that the HTF GoldSim Model adequately approximates the magnitude and the timing of the HTF PORFLOW Model releases for Type II tanks, with only small discrepancies.

Figure 5.6-6: Mass Release from Type II Tank 13 - Ra-226 (Base Case)

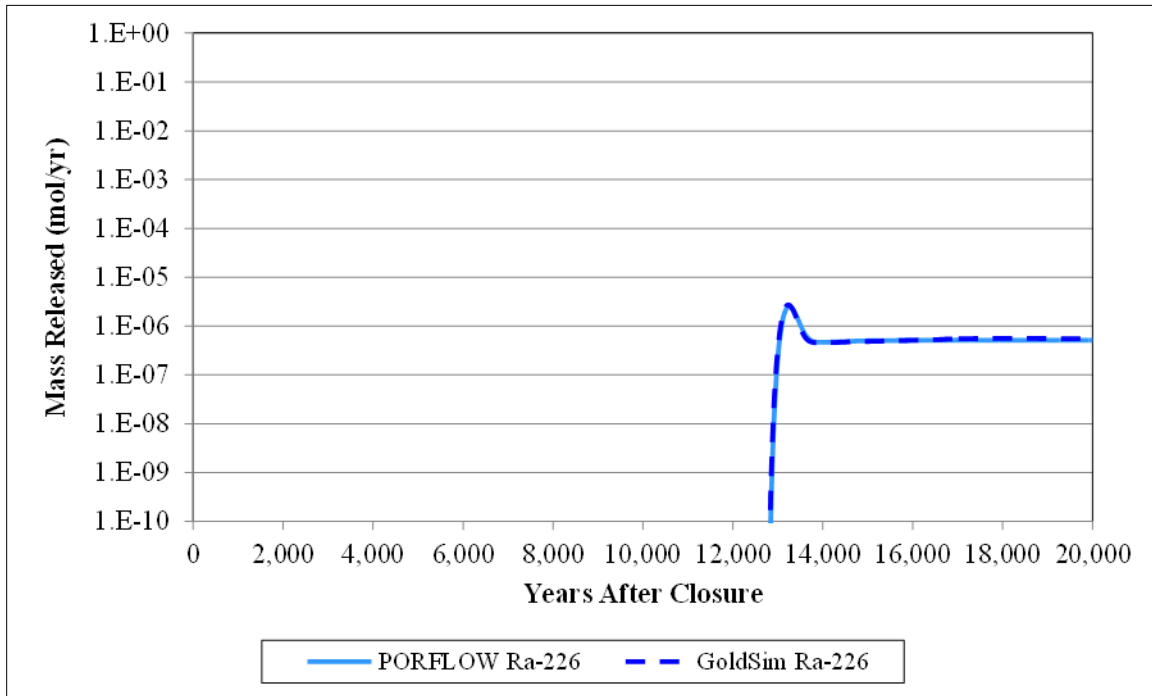


Figure 5.6-7: Mass Release from Type II Tank 13 - Tc-99 (Base Case)

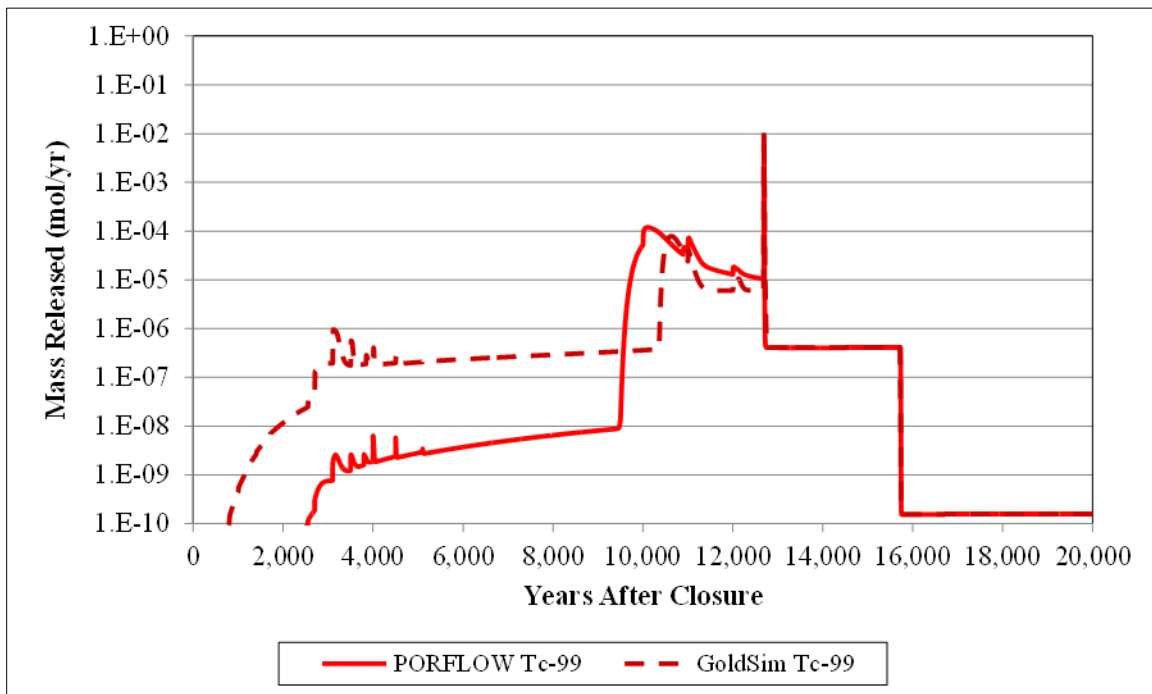


Figure 5.6-8: Mass Release from Type II Tank 13 - I-129 (Base Case)

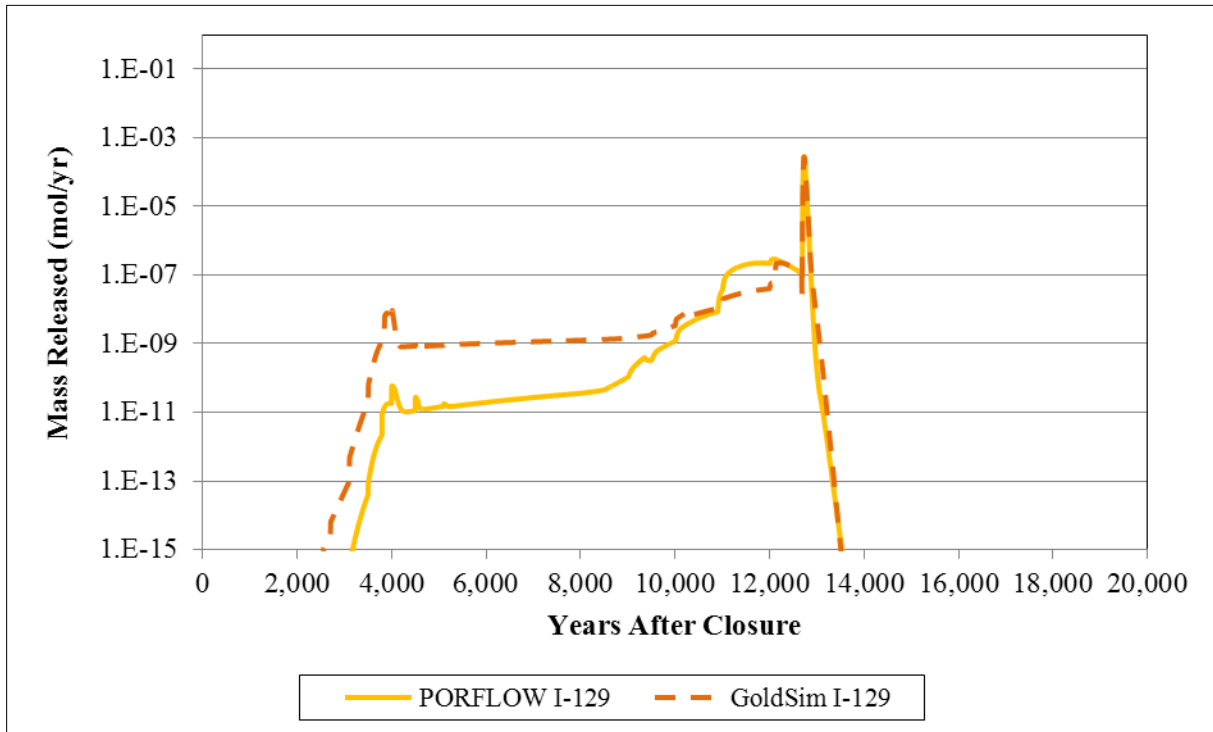


Figure 5.6-9: Mass Release from Type II Tank 13 - Np-237 (Base Case)

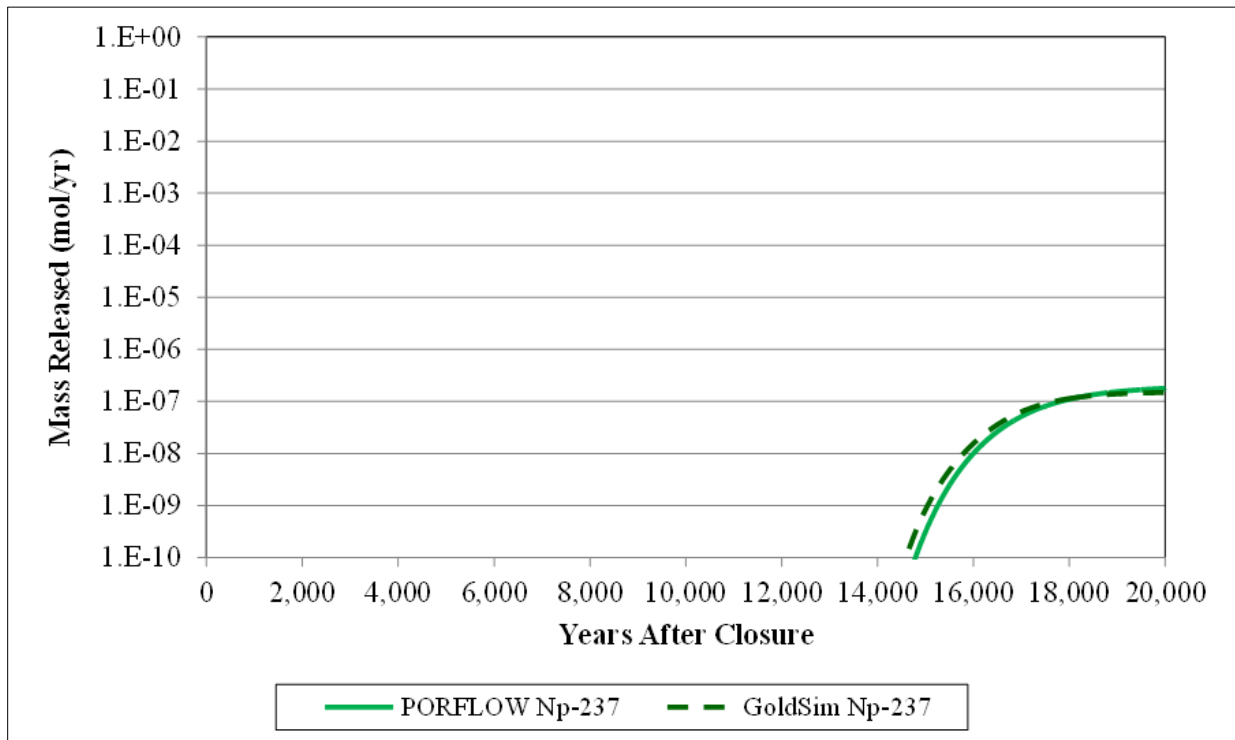


Figure 5.6-10: Mass Release from Type II Tank 13 - Cs-135 (Base Case)

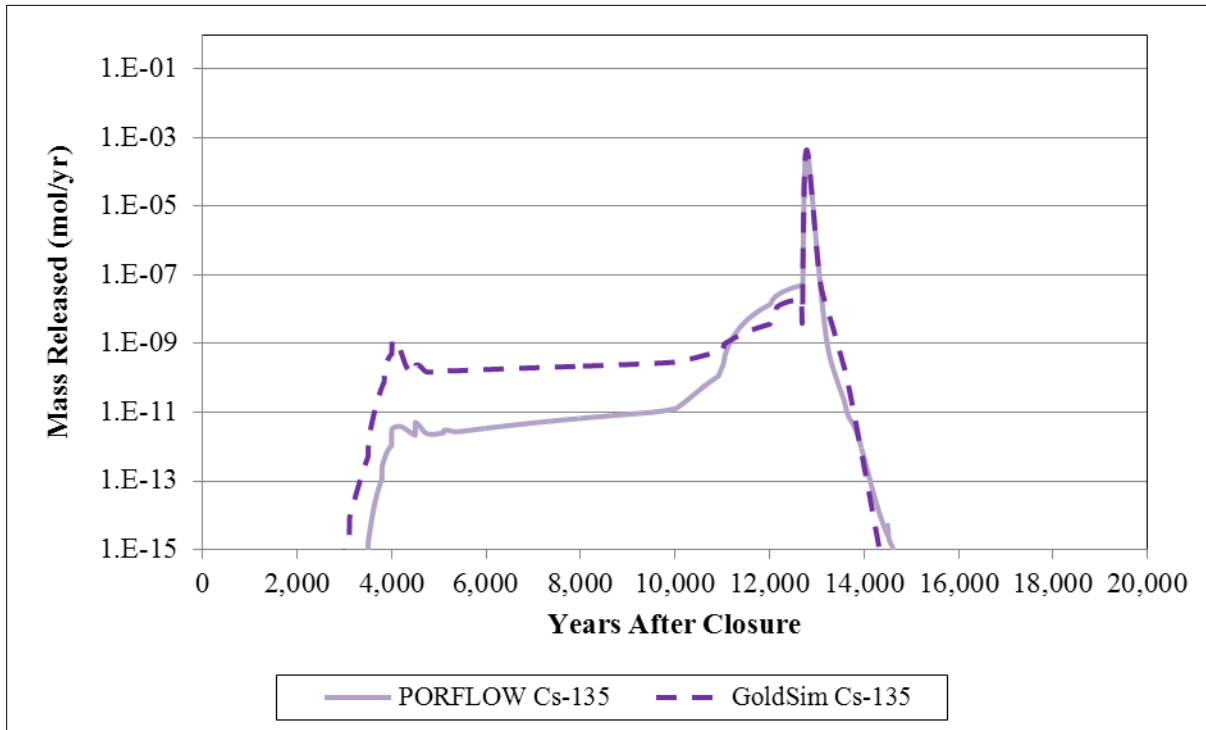


Figure 5.6-6 illustrates that GoldSim is able to replicate Ra-226 mass release from a Type II tank with an intact liner.

A noticeable increase in Tc-99 mass release is observed in Figure 5.6-7 just after 9,000 years in the PORFLOW model results and after 10,000 years in the GoldSim model results. This pulse corresponds to the chemical transitions of the annulus concrete from Reducing Region II to Oxidizing Region II. Prior to the chemical transition, the Tc-99 mass release from the HTF GoldSim Model reflects the general trends, but tends to overestimate the release. The difference between transition times in the two models again reflects the difference between how the two models calculate transition times in the annulus (and wall). After the liner failure, the two models show very similar behavior.

Figure 5.6-8 presents a good match between the PORFLOW results and the GoldSim results for I-129 releases from Tank 13 after liner failure. Prior to liner failure, the GoldSim model overestimates the release from the annulus. The match is especially good at the high peak concentration associated with the liner failure.

Figure 5.6-9 indicates that releases of Np-237 predicted by the GoldSim model accurately reflect the releases predicted by the PORFLOW model.

Figure 5.6-10 shows that for Cs-135, the match between the PORFLOW results and the GoldSim results is very good after liner failure. Prior to liner failure, the GoldSim model overestimates the release from the annulus. The match is especially good at the high peak concentration associated with the liner failure.

5.6.2.2.3 Tank 15 Mass Release from a Type II Tank with Initial Liner Damage

Tank 15 is a submerged Type II tank with initial liner damage that is simulated as complete liner failure at the start of the simulation. Figures 5.6-11 through 5.6-15 display PORFLOW/GoldSim comparison plots of the mass released (mol/yr) from Tank 15 for the following radionuclides, Ra-226, Tc-99, I-129, Np-237, and Cs-135.

Figure 5.6-11: Mass Release from Type II Tank 15 - Ra-226 (Base Case)

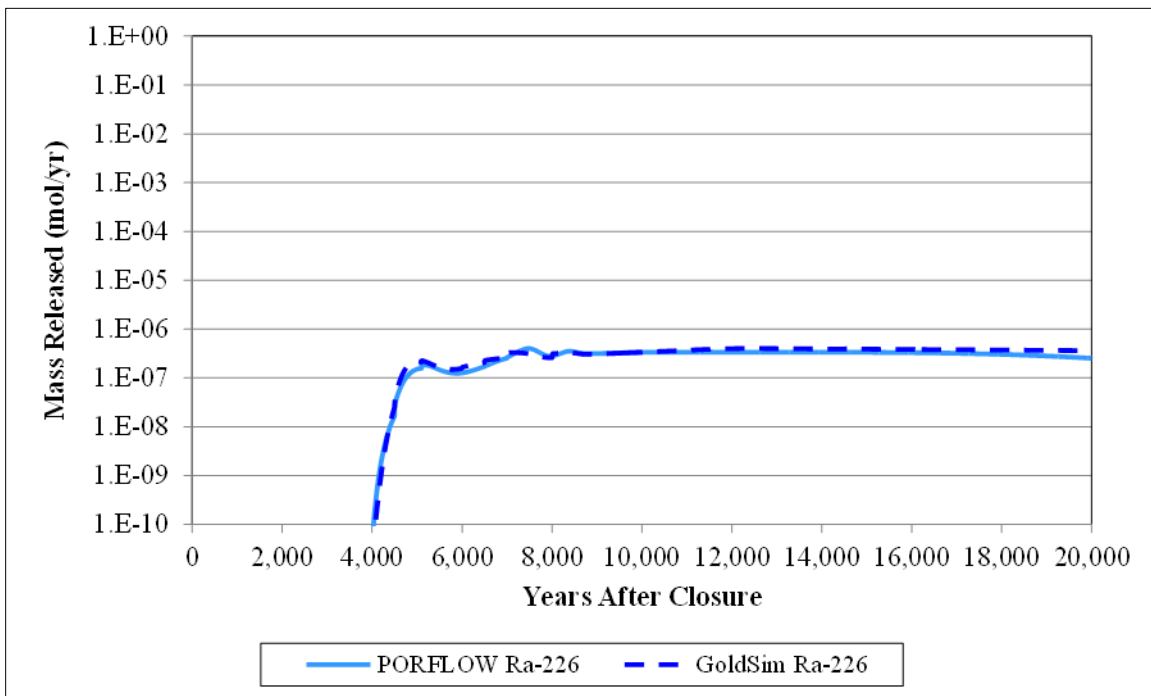


Figure 5.6-12: Mass Release from Type II Tank 15 - Tc-99 (Base Case)

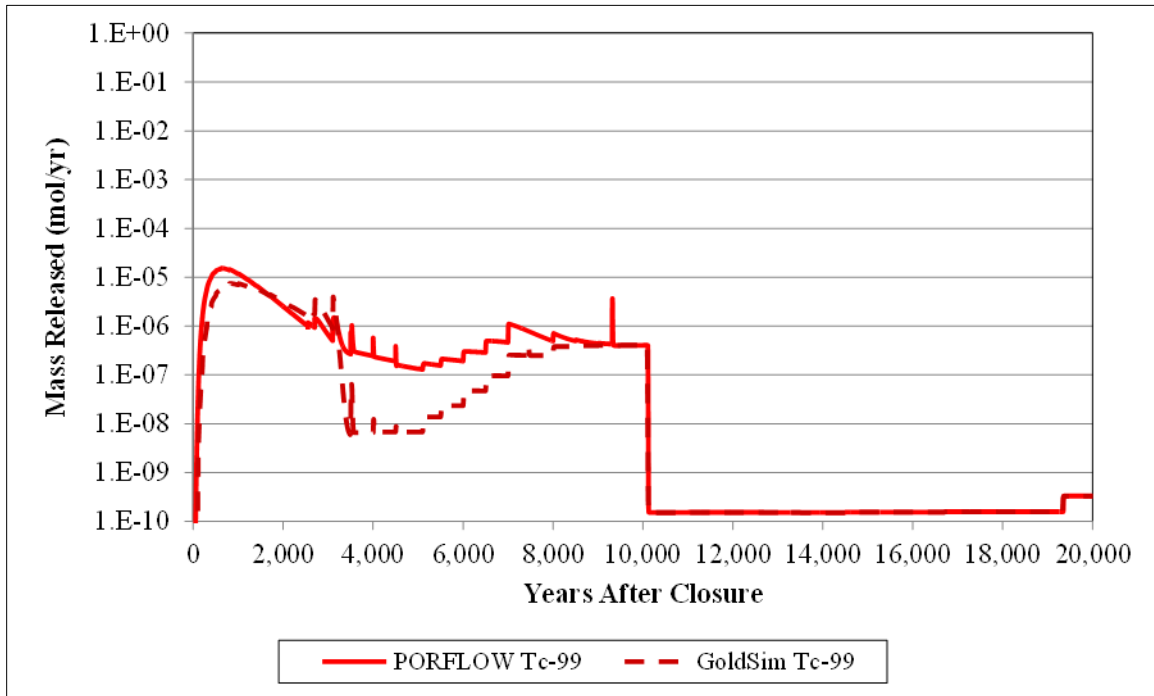


Figure 5.6-13: Mass Release from Type II Tank 15 - I-129 (Base Case)

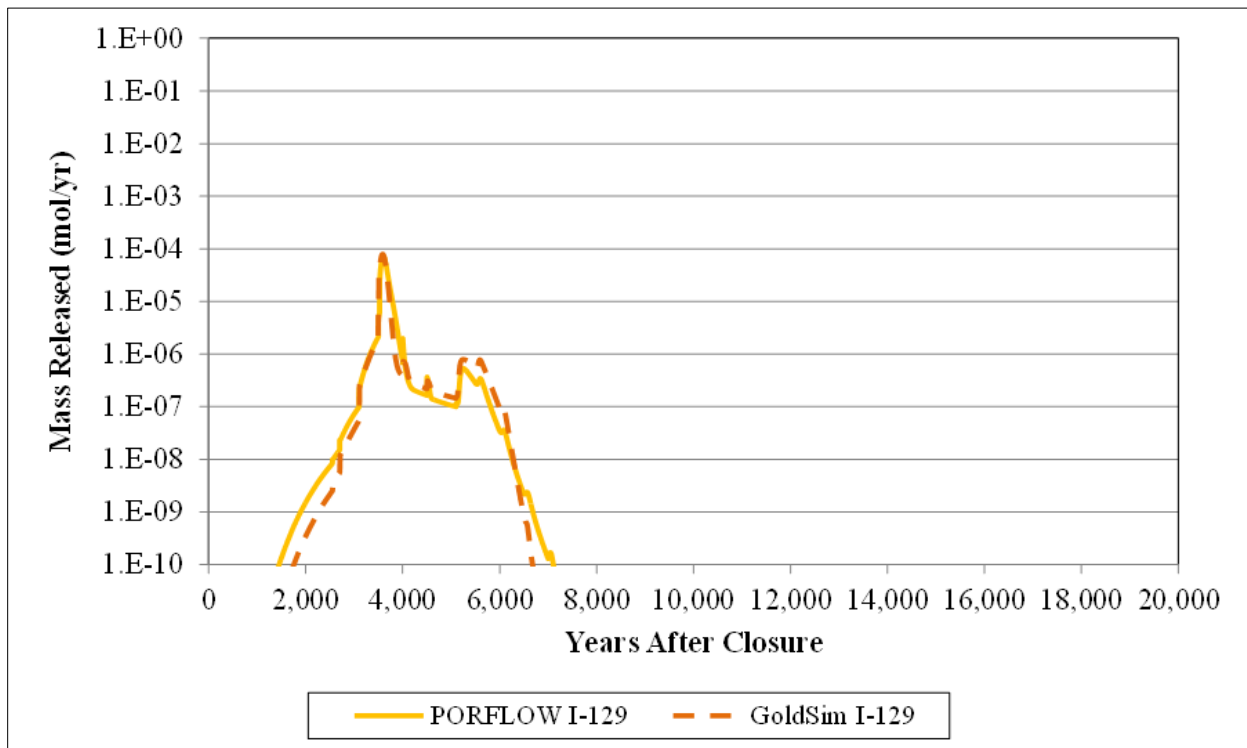


Figure 5.6-14: Mass Release from Type II Tank 15 - Np-237 (Base Case)

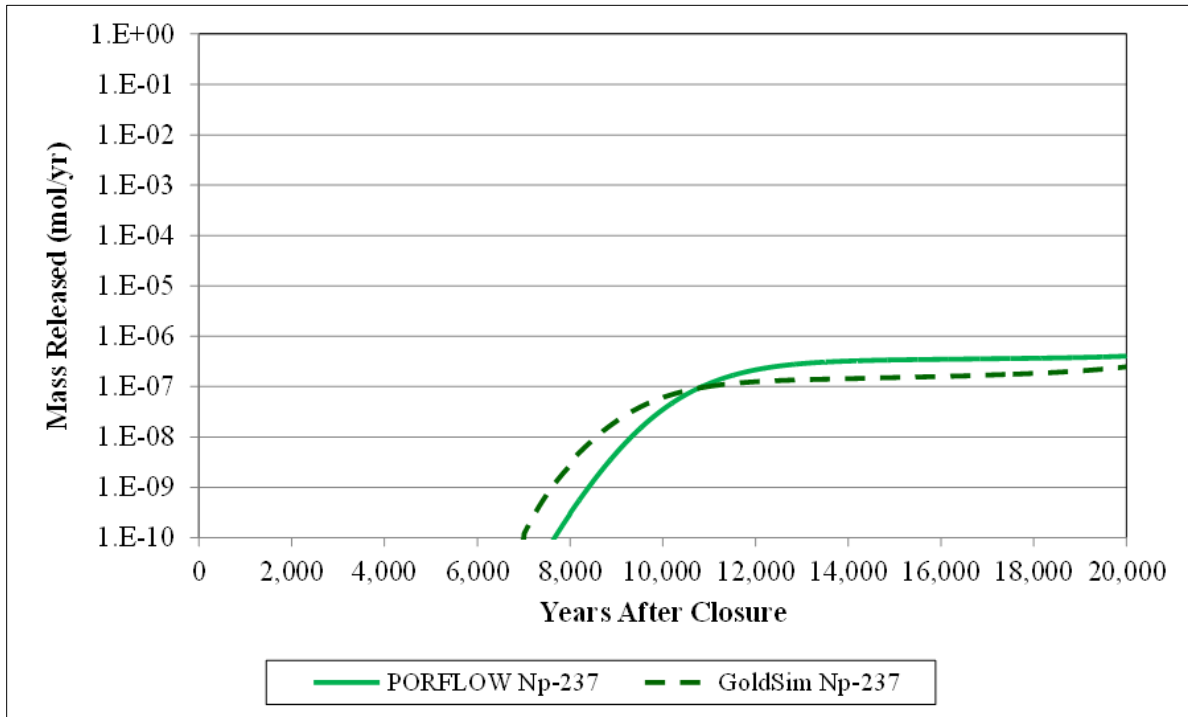


Figure 5.6-15: Mass Release from Type II Tank 15 - Cs-135 (Base Case)

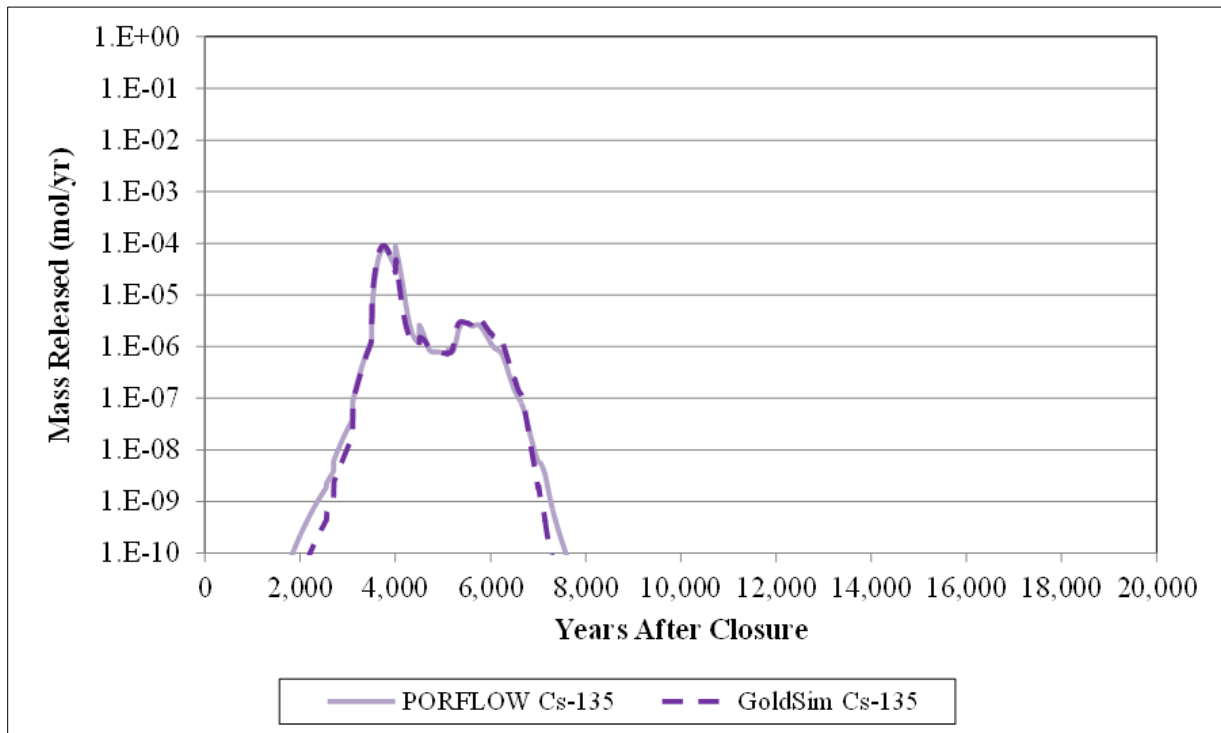


Figure 5.6-11 plots Tank 15 Ra-226 releases from PORFLOW and GoldSim. The general trend of the release and release rates are very consistent between the two models.

As Figure 5.6-12 illustrates, the GoldSim model does a good job of reproducing the trends in the release of Tc-99 to the saturated zone from Tank 15. Prior to 10,000 years, differences between the way the annulus and sandpads are handled in the radial versus 1-D analysis can be seen. The later trends found in the PORFLOW simulations are reproduced very well by the GoldSim model. After 10,000 years the GoldSim model release curve overlies the PORFLOW model release curve, indicating that the solubility control associated with the CZ is being accurately approximated in the HTF GoldSim Model for the Type II tank. The more subtle changes in plateau levels reflect the changes in PORFLOW flow rates in conjunction with constant solubility limits. The dramatic decrease in the release rate of Tc-99 around 10,000 years reflects the transition of the waste tank grout and CZ from submerged Condition C (Reducing Region II), where Tc-99 has a high solubility limit, to submerged Condition D (Oxidizing Region II), where Tc-99 has a lower solubility limit. Dropping the solubility limit forces Tc-99 to precipitate, thus reducing the dissolved concentrations in the CZ and the associated releases. At around 19,350 years, the solubility limit doubles as reflected in Figure 5.6-12.

Both the timing and the magnitude of the PORFLOW I-129 peak release displayed in Figure 5.6-13 are similar to the GoldSim results. The match is especially good at the peak concentrations, which occur around 3,500 years and correspond to the chemical transition of the concrete basemat from Oxidized Region II to Oxidized Region III. Iodine has a greater affinity to sorb to cementitious materials under the Region II conditions (I-129 $K_d = 15$ mL/g) than under Oxidized Region III conditions (I-129 $K_d = 4$ mL/g), therefore the transition results in an immediate addition of mass to the water resulting in the peak I-129 release rates. The similarities in the curves indicate that GoldSim replicates the sorption processes in the cementitious materials for this radionuclide.

Figure 5.6-14 displays the PORFLOW and GoldSim Np-237 releases from Tank 15. The GoldSim Np-237, Tank 15 releases begin slightly earlier and are of lower magnitude for the first 20,000 years. However, the general trends of the curves are quite similar.

Figure 5.6-15 shows that there is a good match between the PORFLOW results and the GoldSim results for Cs-135 releases from Tank 15. Similar to the release of I-129 (Figure 5.6-13), the match reflects the trends well and is especially good at the higher concentrations.

5.6.2.2.4 Tank 24 Mass Release from a Type IV Tank with an Intact Liner

Tank 24 is a non-submerged Type IV tank with an intact liner that fails at 3,638 years. Figures 5.6-16 through 5.6-20 display PORFLOW/GoldSim comparison plots of the mass released (mole per year) from Tank 24 for the following radionuclides, Ra-226, Tc-99, I-129, Np-237, and Cs-135. The curves indicate that the HTF GoldSim Model reproduces the HTF PORFLOW Model releases very well.

Figure 5.6-16: Mass Release from Type IV Tank 24 - Ra-226 (Base Case)

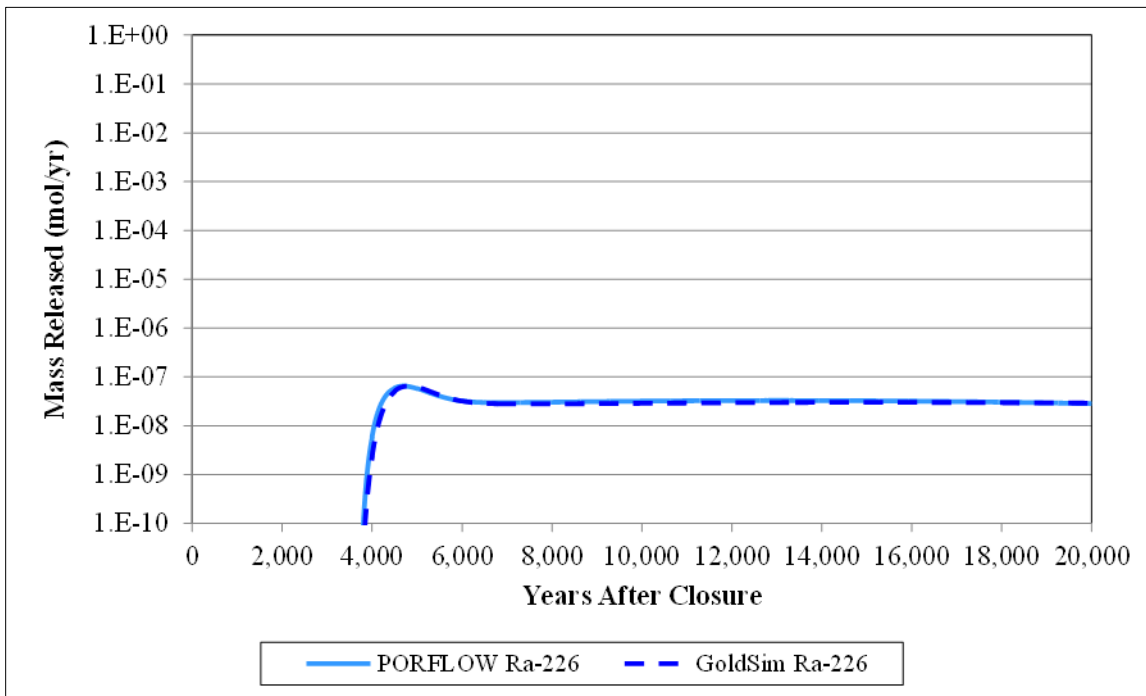


Figure 5.6-17: Mass Release from Type IV Tank 24 - Tc-99 (Base Case)

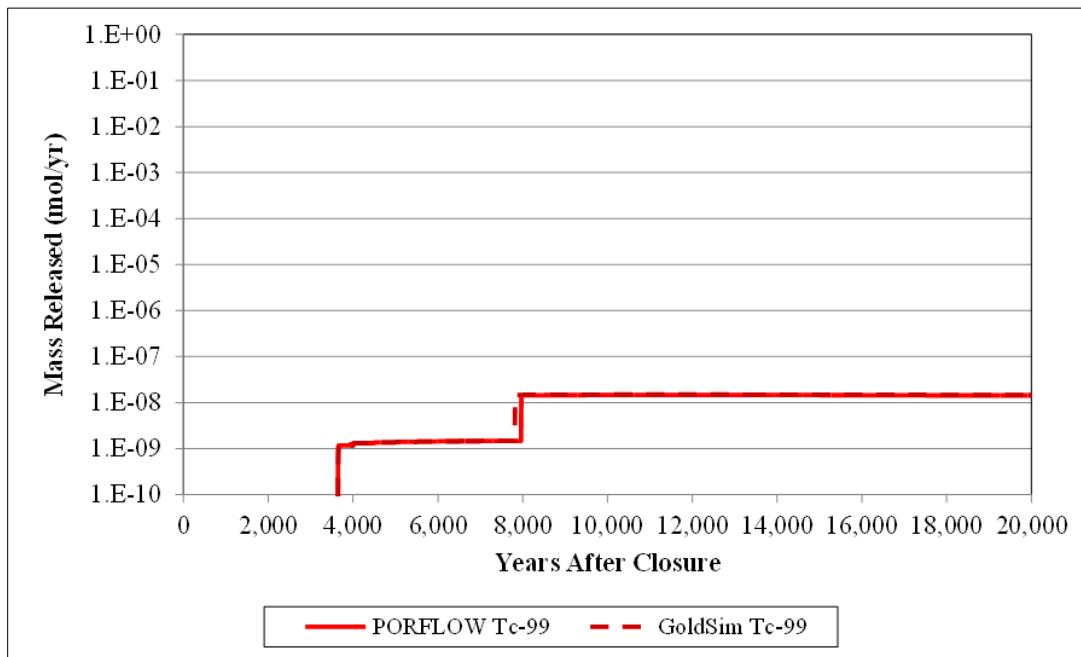


Figure 5.6-18: Mass Release from Type IV Tank 24 - I-129 (Base Case)

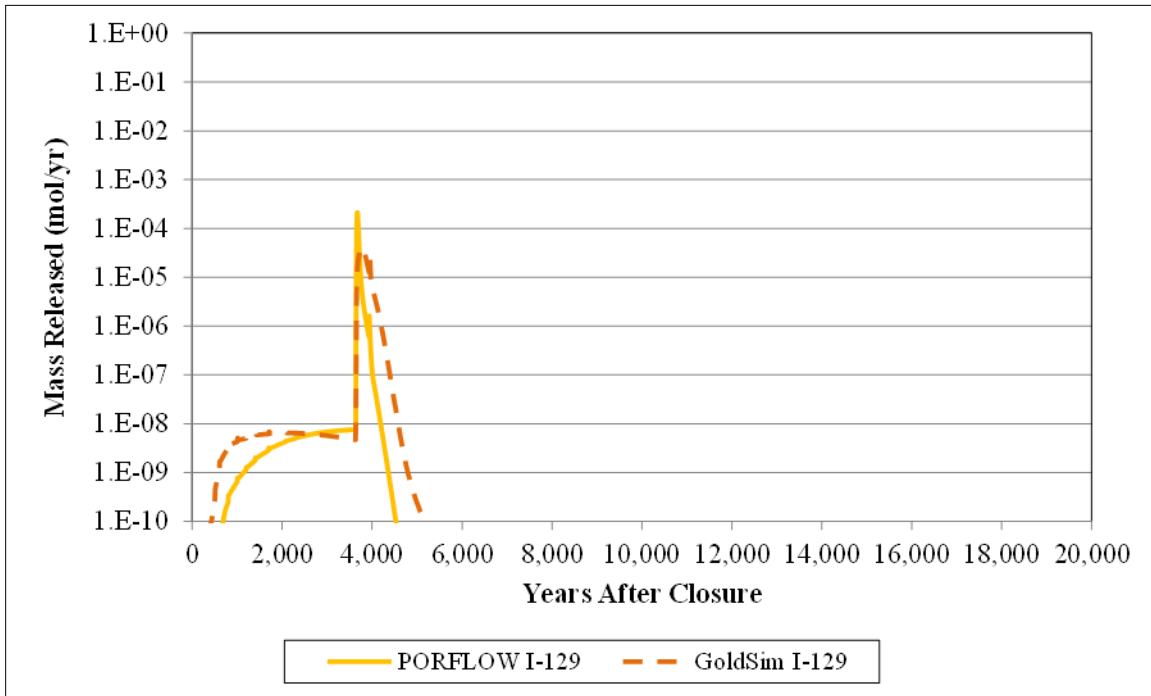


Figure 5.6-19: Mass Release from Type IV Tank 24 - Np-237 (Base Case)

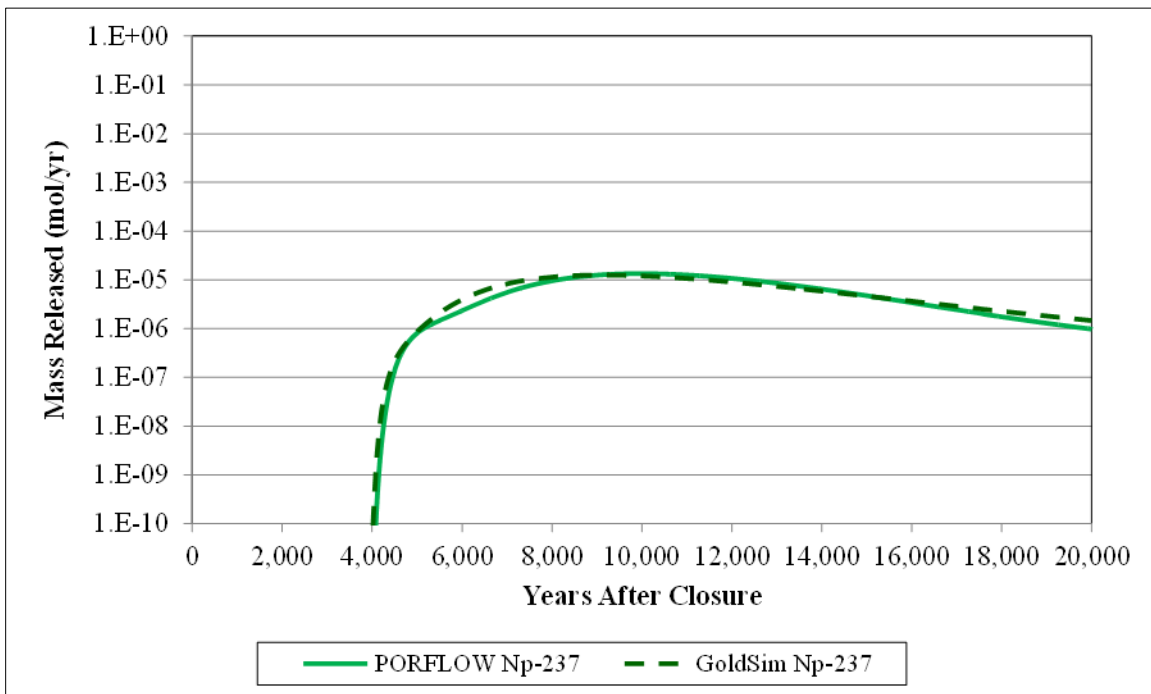
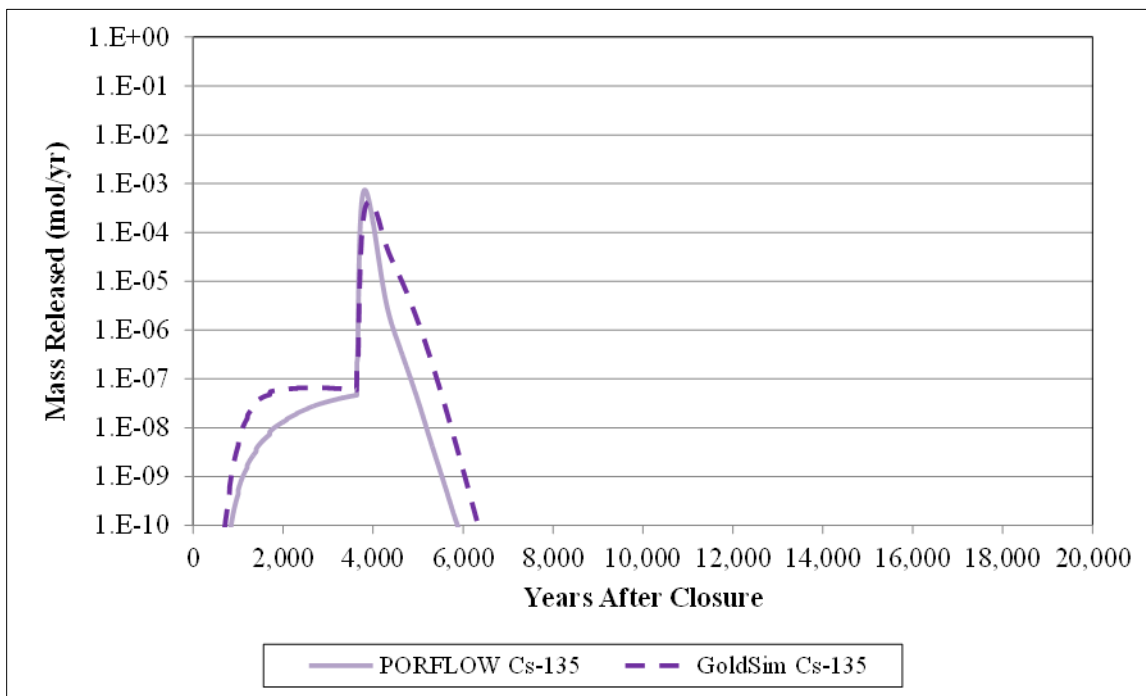


Figure 5.6-20: Mass Release from Type IV Tank 24 - Cs-135 (Base Case)



The comparison between PORFLOW and GoldSim model results presented in Figure 5.6-16 shows that The GoldSim model results closely match the PORFLOW model results. The close match between the curves representing Tank 24 Ra-226 releases (Figure 5.6-16) is significant because it indicates GoldSim adequately represents the transport of Ra-226 and its predecessors in the decay chain.

As Figure 5.6-17 illustrates, the GoldSim Tc-99 release closely overlies the PORFLOW release, indicating that the solubility control associated with the CZ is being accurately approximated in the HTF GoldSim Model. The CZ transition from Reducing Region II to Oxidizing Region II occurs at around 8,000 years.

The trends of the PORFLOW I-129 peak release curve, displayed in Figure 5.6-18 are similar to the GoldSim results. The breakthrough curve is a little more dispersed in the GoldSim results giving it a lower peak. Because the GoldSim model peak is wider, peak results at the 100-meter boundary should be similar.

Figure 5.6-19 indicates that Np-237 releases match very well between the PORFLOW and GoldSim models for this non-submerged Type IV tank.

Figure 5.6-20 shows that there is a good match between the PORFLOW results and the GoldSim results for Cs-135 releases from Tank 24. As with I-129 (Figure 5.6-18), the Cs-135 release is slightly more dispersed in the GoldSim results, although the difference in the peaks for the Cs-135 results is a little less than for the I-129 results.

5.6.2.2.5 Sector A Saturated Zone Transport Behavior

The second phase of the benchmarking process focuses on how well the abstraction model approximates the radionuclide transport behavior in the saturated zone. The radionuclide dose contributions for five sectors were examined for this task. The sectors used for the comparison are A, B, C, E, and F. The locations of the sectors and associated GoldSim model observation wells and the PORFLOW generated stream traces are shown in Figure 4.4-54 (Section 4.4.4.2). For clarity, in this analysis, results are presented for Sector A, and only the larger dose contributors, C-14, I-129, Nb-93m, Nb-94, Ni-59, Np-237, Pa-231, Pb-210, Ra-226, and Tc-99. More extensive results for the other Sectors are provided in SRR-CWDA-2010-00093, Rev. 2.

Based on the PORFLOW generated stream traces, Tank 9, Tank 10, Tank 11, Tank 12, and Tank 14 releases will dominate the doses and radionuclide-specific dose contributions for Sector A. An examination of PORFLOW and GoldSim model generated radionuclide-specific dose contributions presented in Figures 5.6-21 and 5.6-22 indicate that the GoldSim model can provide a computationally efficient approximation of the 100-meter boundary concentrations. There is consistency in the trends observed in the two sets of breakthrough curves. In addition, the peak values controlled by Tc-99, and for later times Ra-226, are similar. Peak breakthrough curve values for many of the other plotted species, such as I-129, Nb-93m, Nb-94, Ni-59, and Pb-210 are also similar. Certain specific differences seen in the breakthrough curve trends can be attributed to differences in the dimensionality of the model flow fields and the number of observation points used to determine the sector-based results. For example, in the PORFLOW model with its fully 3-D saturated zone flow field, in addition to the influence of mechanical dispersion, plume spreading is strongly controlled by the diverging flow field. This phenomenon is typified by the results presented in Figure 5.6-23, which depict a PORFLOW model generated plume emanating from a steady release of a conservative species from Tank 13. As can be seen by comparing this with Figure 4.4-54, which shows the streamtraces on which the GoldSim abstraction is based, it is unlikely that mechanical dispersion alone would cause the plume to spread that much. As can be seen comparing Figures 5.6-21 and 5.6-22, in the PORFLOW results, two large I-129 peaks occur after 10,000 years while only one peak occurs in the GoldSim results. This difference indicates that the release from Tank 13 does not influence the results for Sector A in the GoldSim model but does in the PORFLOW model. A second difference between the two models is in the number of observation points used to evaluate the peak results. In the PORFLOW model, concentrations at any grid node within a sector may be a potential definer of dose contribution for the sector (the highest concentration decides). In the GoldSim model, only a few observation points in the area where stream traces cross the 100-meter boundary are considered. Therefore as mass reaches the 100-meter boundary, the results are coming from PORFLOW will change location over time more than the GoldSim results. This and contributions from more tanks will help smooth out the PORFLOW model results as can be seen by comparing the Tc-99 results presented in Figures 5.6-21 and 5.6-22. As can be seen in Figures 5.6-21 and 5.6-22, this smoothing process has little influence on the determination of peak dose.

Figure 5.6-21: PORFLOW Model Species-Specific Dose Contributions for Sector A

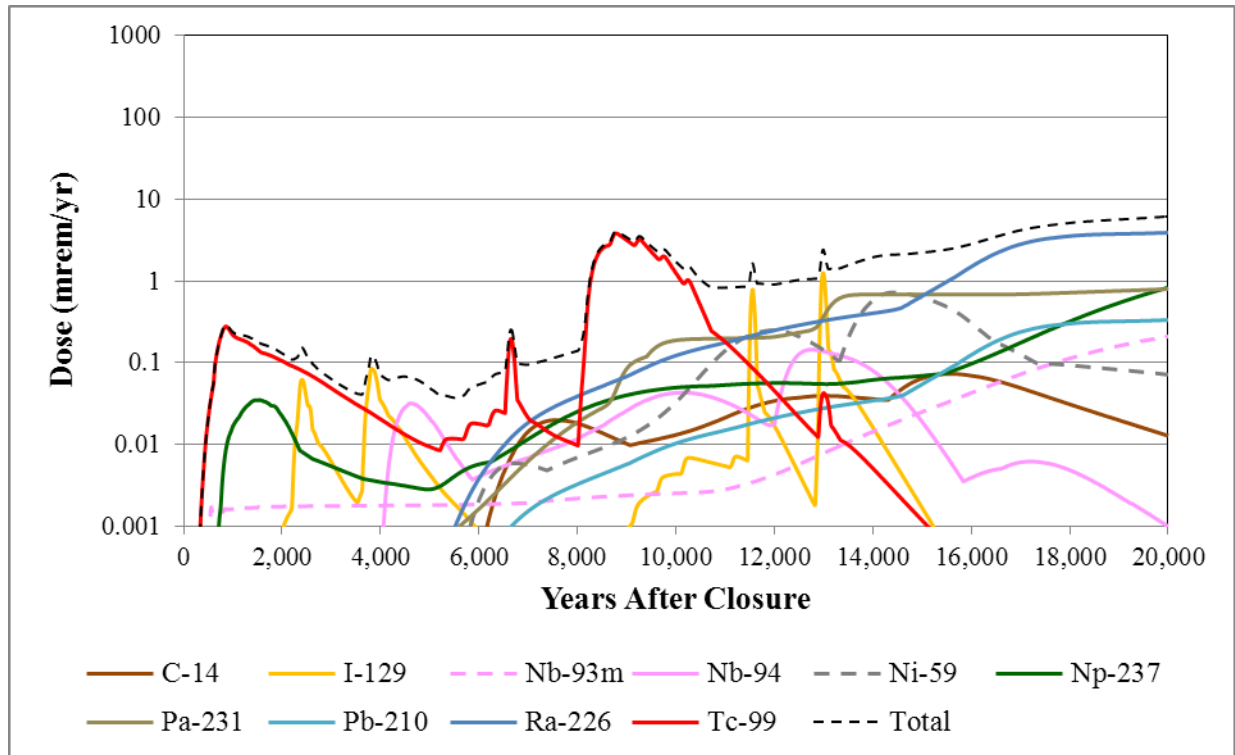


Figure 5.6-22: GoldSim Model Species-Specific Dose Contributions for Sector A

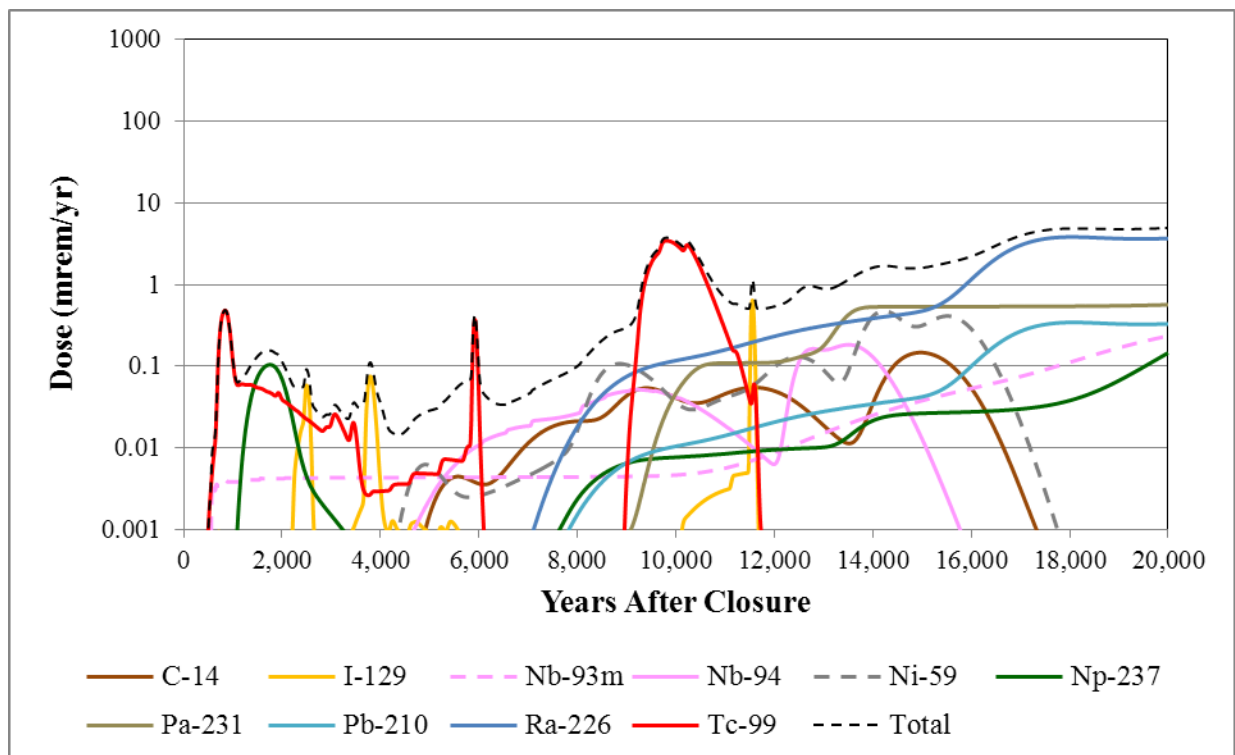
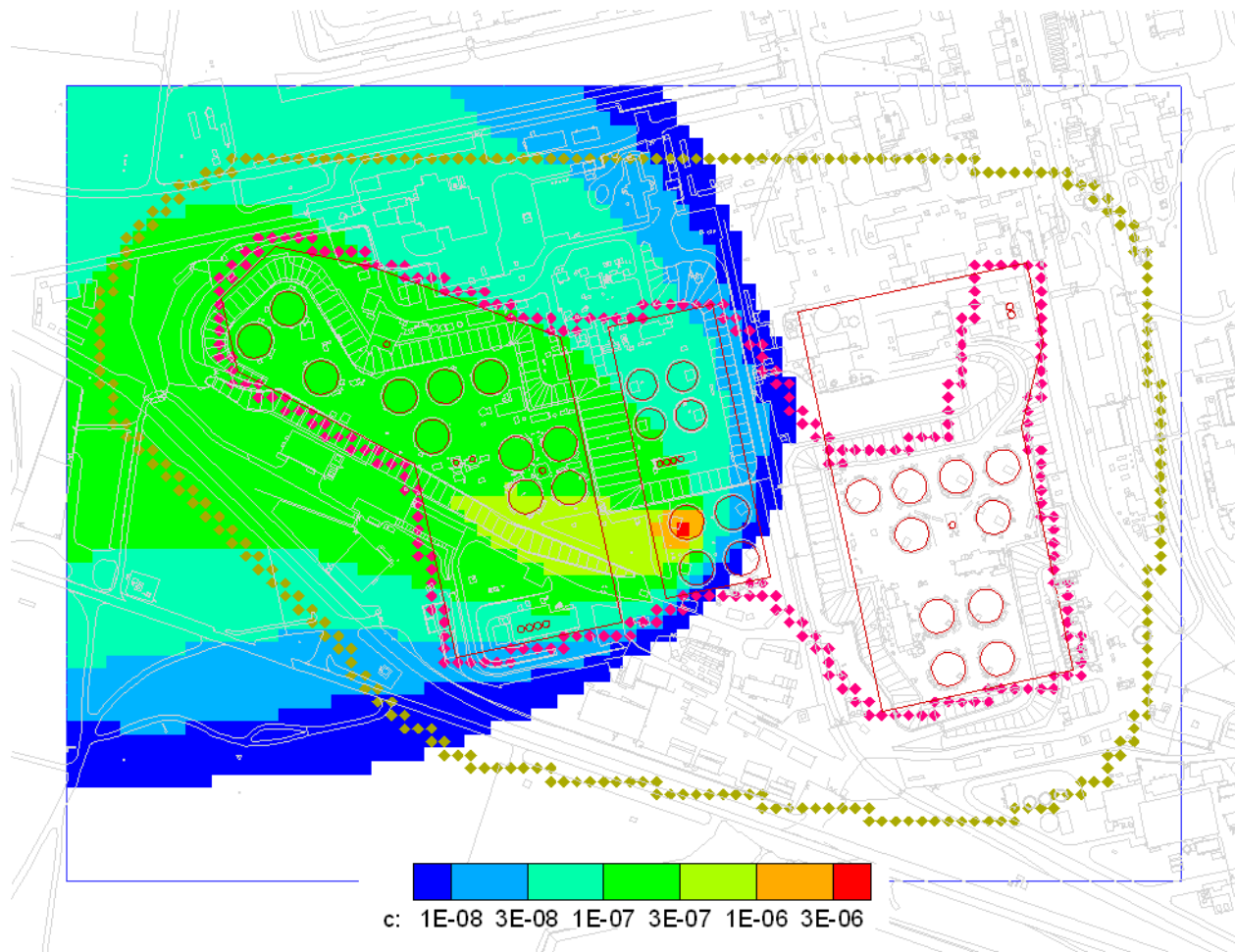


Figure 5.6-23: Plume Formed by a Steady Release of a Conservative Constituent from Tank 13



Note: Units on scale bar are in mol/L and the concentrations were produced by a hypothetical constant source of 1 mol/yr.

5.6.2.2.6 Total Dose Comparison for Base Case (Case A)

A third check on the appropriateness of the GoldSim model as a surrogate for the fully 3-D PORFLOW model is a comparison between total doses generated using PORFLOW and the GoldSim model. For the Base Case, the comparison between the PORFLOW and GoldSim results are presented in Figures 5.6-24 through 5.6-28. The results presented in Figures 5.6-24 through 5.6-28 indicate that the GoldSim model approximates the general trends quite well, including capturing the peaks.

Figure 5.6-24: Comparison between PORFLOW and GoldSim Total Dose Results for Base Case, Sector A

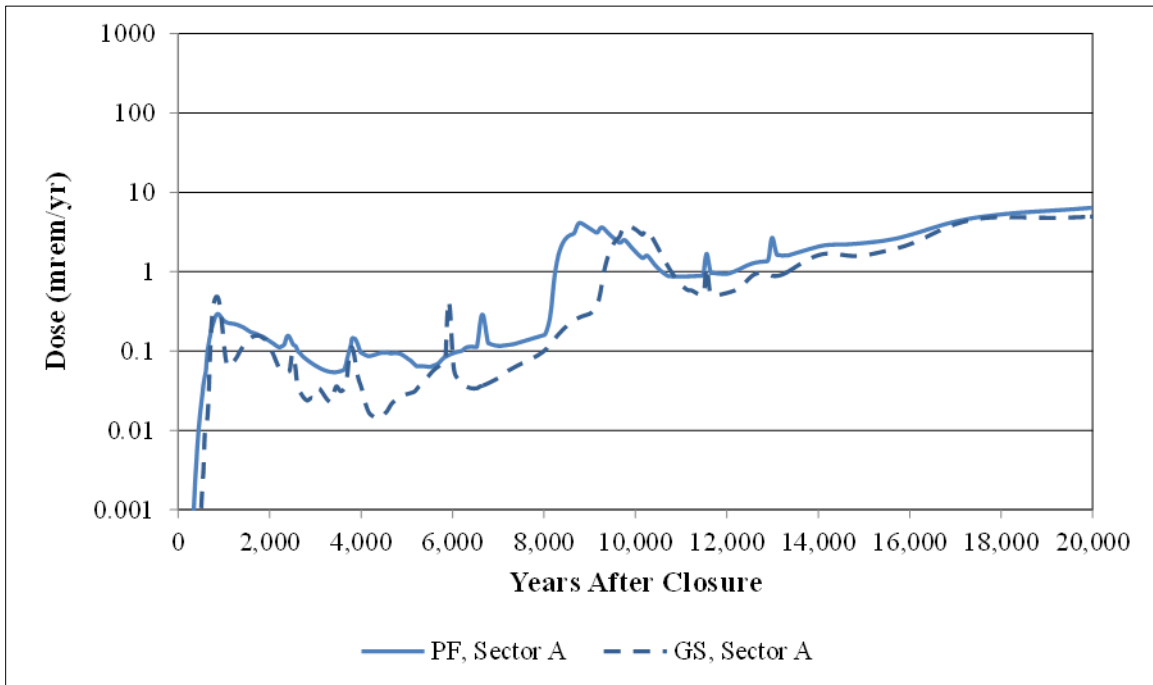


Figure 5.6-25: Comparison between PORFLOW and GoldSim Total Dose Results for Base Case, Sector B

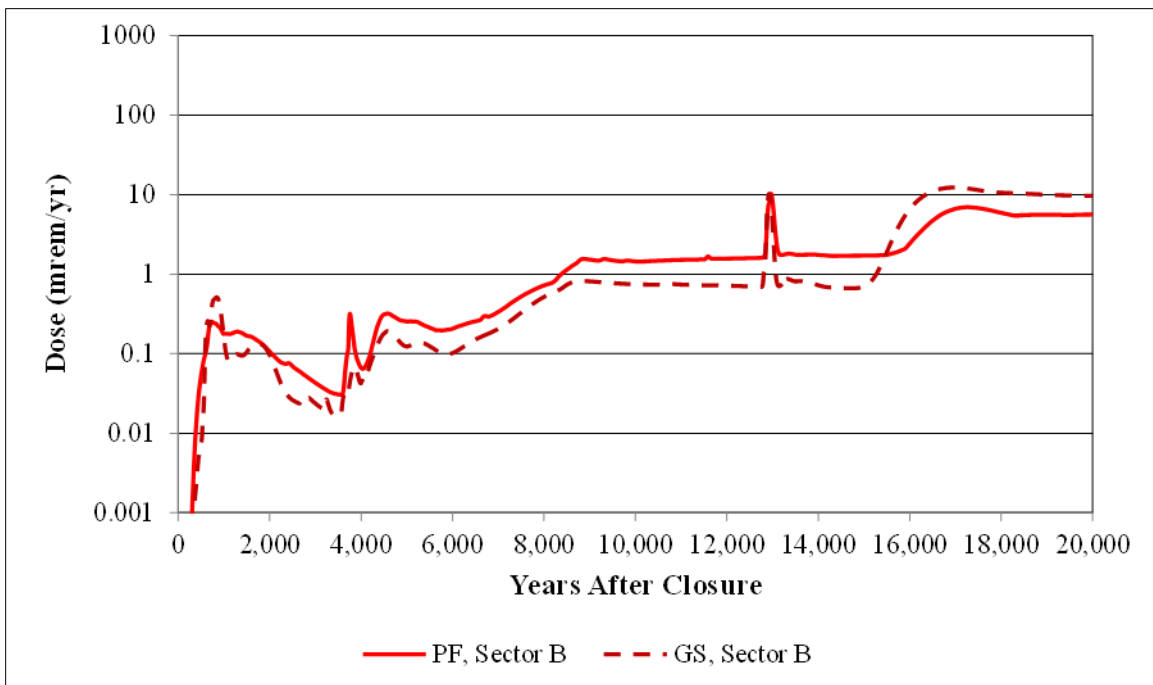


Figure 5.6-26: Comparison between PORFLOW and GoldSim Total Dose Results for Base Case, Sector C

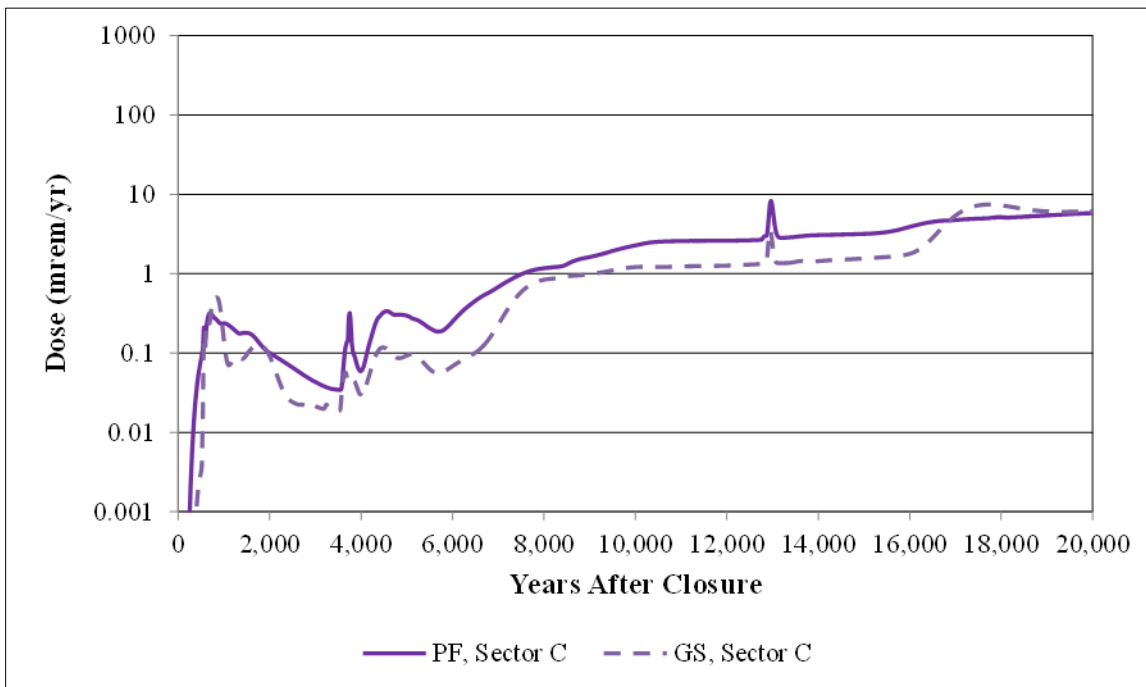


Figure 5.6-27: Comparison between PORFLOW and GoldSim Total Dose Results for Base Case, Sector E

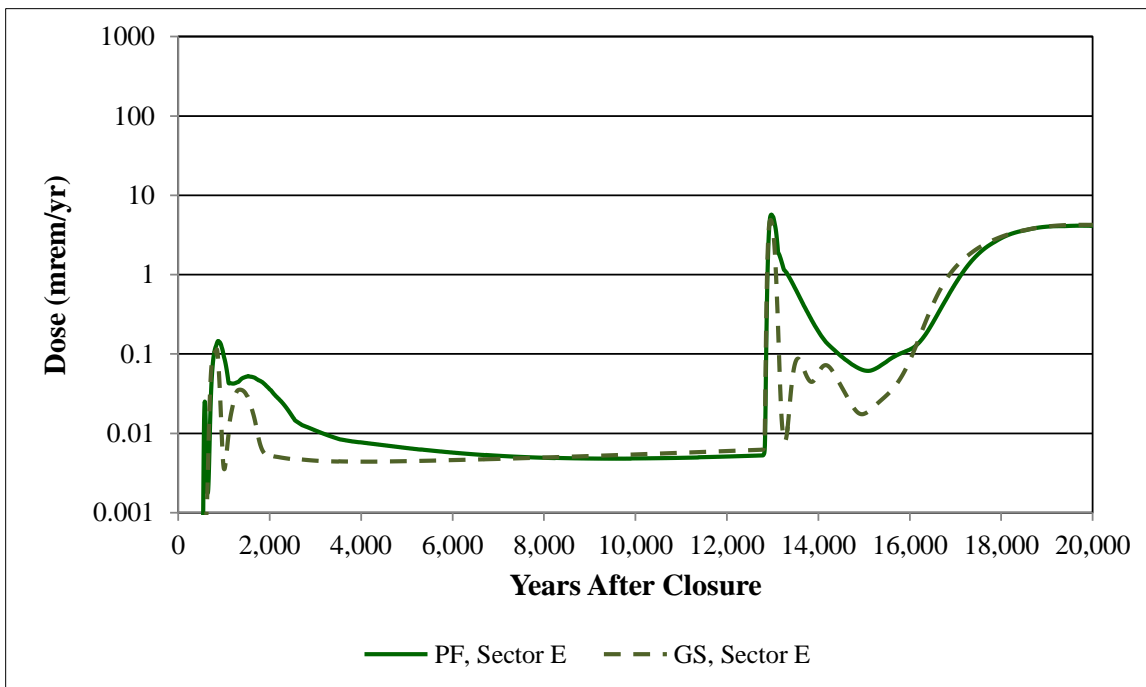
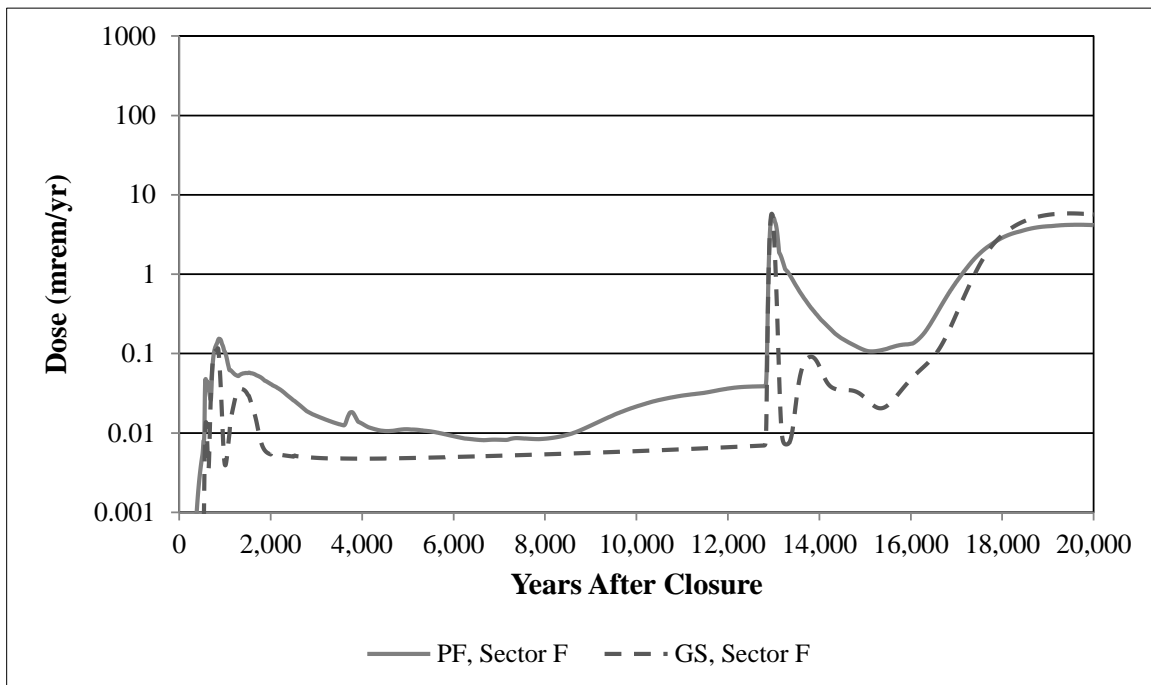


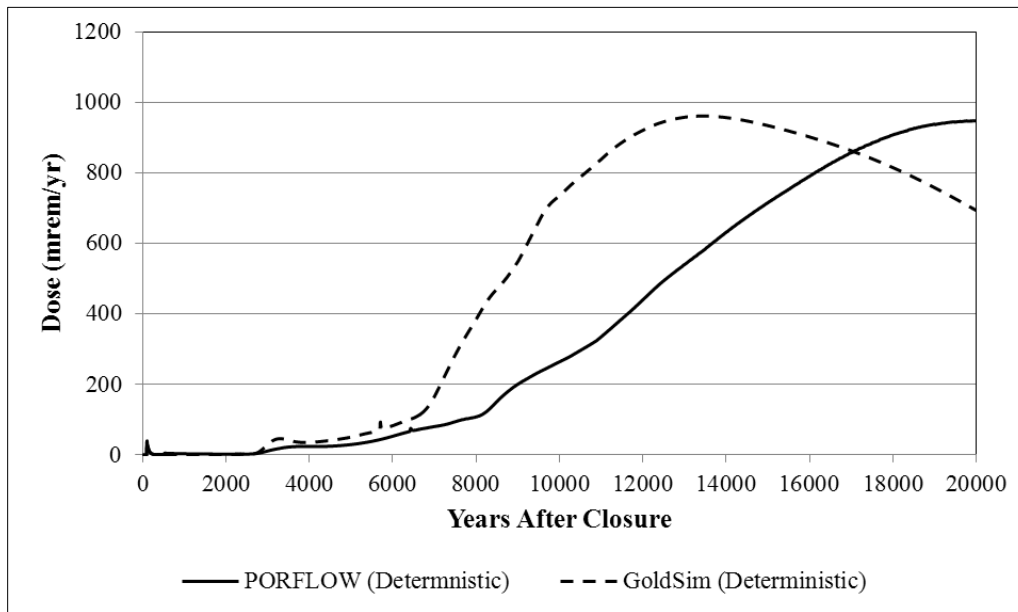
Figure 5.6-28: Comparison between PORFLOW and GoldSim Total Dose Results for Base Case, Sector F



5.6.2.2.7 Inadvertent Human Intrusion Case

In addition, to 100-meter boundary results, PORFLOW provides 1-meter boundary results for use in the IHI case. The GoldSim model does not consider a 1-meter boundary but assumes that the intruder drills a well just outside of a waste tank. Based on PORFLOW results adjacent to specified waste tanks (see, SRR-CWDA-2010-00093, Rev. 2, Section 3.1.1.6 and Table 3.1-9) showing a maximum IHI dose adjacent to Tank 12 (see Figure 3.1-5), the GoldSim model assumes that the well is drilled next to Tank 12. A comparison, between GoldSim and PORFLOW results for a well drilled next to Tank 12, presented in Figure 5.6-29, shows a peak 10,000-year dose of 735 mrem/yr, at a well adjacent to Tank 12. This is about 2.8 times higher than the deterministic PORFLOW result (264 mrem/yr). Over a 20,000-year period, the GoldSim results for the well drilled next to Tank 12 show a peak dose of 961 mrem/yr, within 20,000 years for a well adjacent to Tank 12. This is just 1.7 % more than the deterministic PORFLOW result (945 mrem/yr). Although the two models show very similar peak results, there is a large difference in breakthrough times. This large difference in breakthrough times is associated with the influence of horizontal flow in the PORFLOW model, which lengthens the pathway taken by radionuclides initialized in the annulus as they pass through the basemat into the unsaturated zone.

Figure 5.6-29: Comparison between PORFLOW and GoldSim IHI Results



5.6.2.2.8 Benchmarking Summary

The radionuclides used for benchmarking the waste tank releases, were selected based on the magnitude of their contributions to total dose in the PORFLOW and their individual transport characteristics. The chosen radionuclides are either fast moving (e.g., I-129 is not subject to solubility controls and is only slightly sorbed), slow moving (e.g., Tc-99 is greatly influenced by solubility limits in the CZ), or produced by in-growth of slow-moving radionuclides (e.g., Ra-226 occurs mostly as in-growth from Pu-238, U-234, and Th-230, all controlled by solubility and sorption processes). By verifying the transport behavior of representative radionuclides, this verifies, by extension, other radionuclides included in the inventory that have similar transport characteristics. By using the major dose contributors as indicators, confidence in the GoldSim model could be built.

The results of the four phase benchmarking analysis provide validation that radionuclide release and transport, as simulated in the GoldSim model, mirror the deterministic PORFLOW release and transport behavior. Comparison of the final dose results further verify the agreement between the PORFLOW 3-D transport model and the simplified 1-D GoldSim model, providing confidence that the HTF GoldSim Model UA/SA results presented in Section 5.6.4 and Section 5.6.5 successfully propagate model uncertainty, and identify the most dose sensitive parameters. For additional benchmarking results, refer to SRR-CWDA-2010-00093, Rev. 2.

5.6.3 Parameters Evaluated in the HTF Probabilistic Model

A separate HTF Fate and Transport Model (e.g., also referred to as the HTF GoldSim Model, the stochastic model, or probabilistic model) was developed using the GoldSim software program to evaluate parameter sensitivity and the influence of parameter uncertainty on the migration of radionuclides and non-radioactive contaminants from the closed HTF to the accessible environment (see Section 4.4.4.2). The parameters selected for evaluation in the stochastic analyses were based on modeling experience, and the availability of generic and site-specific data to provide a basis for parameter ranges. For a complete description of the HTF GoldSim Model and the input stochastic data used in the model, refer to the report *H-Area Tank Farm Stochastic Fate and Transport Model* (SRR-CWDA-2010-00093 Rev. 2).

This section summarizes the probabilistic distributions used in the HTF GoldSim Model. The stochastic parameters are organized by HTF GoldSim Model type. The HTF GoldSim Model contains both a transport sub-model as well as a dose calculator sub-model. The transport sub-model is an abstraction of the HTF PORFLOW flow and transport model, while the dose calculator sub-model takes the calculated contaminated concentrations at points of assessment, and applies exposure pathways and parameters (e.g., bioaccumulation factors, ingestion rates, DCFs, etc.) to determine the dose to the receptor (see Section 4.4.4.2). Uncertainty distributions have been applied to parameters within the transport sub-model as well as in the dose calculator sub-model, and the basis and distribution type are discussed in the specific sections. Sections 5.6.3.1 through Section 5.6.3.11 describe the specific parameter distributions used in the transport sub-model. Section 5.6.3.12 presents the stochastic parameters applied in the dose calculator sub-model.

5.6.3.1 Radiological Inventory

The waste tank and ancillary equipment inventories in the HTF GoldSim Model control the total amount of contaminants available for release. Section 3.4 describes the basis for estimates of residual radiological inventory in the HTF waste tanks and ancillary equipment. The baseline, or deterministic, inventory used for each radionuclide is listed in Table 3.3-9. SRR-CWDA-2010-00023, Rev. 3 details the process for selecting the baseline inventory. This report also includes a section on the selection of inventory distributions for probabilistic modeling.

The process used to estimate the waste tank residual material at operational closure created estimates that were both bounding and reasonable. Estimates were developed for all chemicals and radionuclides expected to occur in HTF, but those components expected to affect dose are closely scrutinized, and the values selected are intended to provide conservatism over what is expected to remain at operational closure.

The initial inventories are considered conservative estimates. For instance, in estimating residuals from reprocessed reactor spent fuel, maximum burn-up is assumed, consequently certain radionuclide byproducts are also maximized. An unknown amount of residual material characterized as fission products bearing Plutonium-Uranium Extraction Process (PUREX) low heat waste actually originated as cladding waste or other low radionuclide bearing wastes that contain relatively small amounts of fission products. [LWO-PIT-2007-00025] Additional conservatism is added to the estimate of residuals assumed to remain in the waste tanks after cleaning. It is probable that less residuals thus a lower inventory of contaminants will actually remain. These process-related uncertainties have not been quantified; instead, this uncertainty is accounted for by applying a lower and upper bound to the initial inventory estimates, using a log uniform distribution. The log uniform distribution is expected to conservatively bound all uncertainties related to various historical processes at SRS.

In the HTF GoldSim Model, a minimum and maximum multiplier (selected to be reasonably conservative based on scatter plots of sampled data from FTF Tanks 5, 18, and 19 presented in SRR-CWDA-2010-00023, Rev. 3) is applied (between 0.01 and 10 are applied to both radionuclide and non-radiological chemical elements) to the initial inventory for each isotope and chemical constituent. The multipliers are presented in Table 5.6-3 and 5.6-4 and are based on the confidence in the initial estimate. The inventory multipliers were chosen based on the inventory estimate for each constituent and are listed in Tables 5.6-3 and 5.6-4. Below is description of basis for each multiplier. For radionuclides estimated by the nominal activity adjustment (1 curie or the detection limit), a maximum multiplier of one was used. Since the actual inventory is expected not to exceed the estimate, a multiplier was selected to reflect that idea. The minimum multiplier was set at two orders of magnitude below the estimate. There is uncertainty in the value for this multiplier because many of the radionuclides are based on the reaching the detection limits. For those constituents that were not adjusted to the nominal activities (1 curie or the detection limit), a maximum of 10 were chosen based on SRR-CWDA-2010-00023, Rev. 3. In Figure 9.1-1 of SRR-CWDA-2010-00023, Rev. 3, three waste tanks sample results are compared to predicted values. In general, the predicted values were within one order of magnitude of the sample results. Given that there are estimates that varied greater than one order of magnitude from actual, the maximum multipliers could have been increased to reflect each constituents range. Although due to the limited data set (i.e., sample results from only three waste tanks), the fact that zeolite was not accounted for in the original WCS sludge solids estimate (i.e., impacting Cs-137 estimates) and the fact that Tanks 18 and 19 do not reflect chemical cleaning impacts, a more generalized value was selected. The minimum of 0.01 was generally selected based on Figure 9.1-1 of SRR-CWDA-2010-00023, Rev. 3. While the lower end of the range of data extended to less than 0.01, generally the values of only one of the waste tanks were less than 0.01. Therefore, a minimum of 0.01 was conservatively selected. For those waste tanks that were not adjusted by the residual volume uncertainty step, a minimum of 0.1 was selected.

The multipliers used were based on SRR-CWDA-2010-00023, Rev. 1. There is no difference between the current and previous multiplier estimate for a majority of the constituents. [SRR-CWDA-2010-00023, Rev. 1 and 3] In the limited number of differences, the difference is generally conservative. With respect to the minimum multipliers, the current value (0.01) for several radionuclides (Am-241, Cm-244, Cs-135, Cs-137, Eu-154, Ni-63, Np-237, Pu-238, Pu-239, Pu-240, Pu-241, Sm-151, Sr-90, Tc-99, Th-232, U-233, and U-234) in the Type III and IIIA tanks is lower than the value used in the model (0.1). With respect to the maximum multiplier, the multiplier for Th-229 (in Tanks 11, 12, 13, 14, and 15), Th-232 (in Tank 16), and U-235 (in Tanks 11, 12, 13, 14, 15, and the Type III and IIIA tanks) is currently estimated (1) lower than the previous estimate (10). There is a non-conservatism associated with the use of the previous maximum values but it is insignificant. For Pu-241 (in Tanks 9 and 10), Th-232 (in Tanks 9 and 10), U-236 (in the Type III and IIIA tanks), and U-238 (in Tanks 21, 22, and 23), the current estimate (10) is higher than the previous value (1).

Table 5.6-3: Radiological Inventory Multipliers

Rad	^a Waste Tanks - Log Uniform Distribution - Minimums																												
	9	10	11	12	13	14	15	16	21	22	23	24	29	30	31	32	35	36	37	38	39	40	41	42	43	48	49	50	51
Ac-227	0.01	0.01	0.01	0.01	0.01	0.01	0.01	0.01	0.01	0.01	0.01	0.01	0.01	0.01	0.01	0.01	0.01	0.01	0.01	0.01	0.01	0.01	0.01	0.01	0.01	0.01	0.01	0.01	0.01
Al-26	0.01	0.01	0.01	0.01	0.01	0.01	0.01	0.01	0.01	0.01	0.01	0.01	0.01	0.01	0.01	0.01	0.01	0.01	0.01	0.01	0.01	0.01	0.01	0.01	0.01	0.01	0.01	0.01	0.01
Am-241	0.01	0.01	0.01	0.01	0.01	0.01	0.01	0.01	0.01	0.01	0.01	0.01	0.1	0.1	0.1	0.1	0.1	0.1	0.1	0.1	0.1	0.1	0.1	0.1	0.1	0.1	0.1	0.1	0.1
Am-242m	0.01	0.01	0.01	0.01	0.01	0.01	0.01	0.01	0.01	0.01	0.01	0.01	0.01	0.01	0.01	0.01	0.01	0.01	0.01	0.01	0.01	0.01	0.01	0.01	0.01	0.01	0.01	0.01	0.01
Am-243	0.01	0.01	0.01	0.01	0.01	0.01	0.01	0.01	0.01	0.01	0.01	0.01	0.01	0.01	0.01	0.01	0.01	0.01	0.01	0.01	0.01	0.01	0.01	0.01	0.01	0.01	0.01	0.01	0.01
C-14	0.01	0.01	0.01	0.01	0.01	0.01	0.01	0.01	0.01	0.01	0.01	0.01	0.01	0.01	0.01	0.01	0.01	0.01	0.01	0.01	0.01	0.01	0.01	0.01	0.01	0.01	0.01	0.01	0.01
Cf-249	0.01	0.01	0.01	0.01	0.01	0.01	0.01	0.01	0.01	0.01	0.01	0.01	0.01	0.01	0.01	0.01	0.01	0.01	0.01	0.01	0.01	0.01	0.01	0.01	0.01	0.01	0.01	0.01	0.01
Cf-251	0.01	0.01	0.01	0.01	0.01	0.01	0.01	0.01	0.01	0.01	0.01	0.01	0.01	0.01	0.01	0.01	0.01	0.01	0.01	0.01	0.01	0.01	0.01	0.01	0.01	0.01	0.01	0.01	0.01
Cl-36	0.01	0.01	0.01	0.01	0.01	0.01	0.01	0.01	0.01	0.01	0.01	0.01	0.01	0.01	0.01	0.01	0.01	0.01	0.01	0.01	0.01	0.01	0.01	0.01	0.01	0.01	0.01	0.01	0.01
Cm-243	0.01	0.01	0.01	0.01	0.01	0.01	0.01	0.01	0.01	0.01	0.01	0.01	0.01	0.01	0.01	0.01	0.01	0.01	0.01	0.01	0.01	0.01	0.01	0.01	0.01	0.01	0.01	0.01	0.01
Cm-244	0.01	0.01	0.01	0.01	0.01	0.01	0.01	0.01	0.01	0.01	0.01	0.01	0.1	0.1	0.1	0.01	0.1	0.1	0.1	0.1	0.1	0.1	0.1	0.1	0.1	0.1	0.1	0.1	0.1
Cm-245	0.01	0.01	0.01	0.01	0.01	0.01	0.01	0.01	0.01	0.01	0.01	0.01	0.01	0.01	0.01	0.01	0.01	0.01	0.01	0.01	0.01	0.01	0.01	0.01	0.01	0.01	0.01	0.01	0.01
Cm-247	0.01	0.01	0.01	0.01	0.01	0.01	0.01	0.01	0.01	0.01	0.01	0.01	0.01	0.01	0.01	0.01	0.01	0.01	0.01	0.01	0.01	0.01	0.01	0.01	0.01	0.01	0.01	0.01	0.01
Cm-248	0.01	0.01	0.01	0.01	0.01	0.01	0.01	0.01	0.01	0.01	0.01	0.01	0.01	0.01	0.01	0.01	0.01	0.01	0.01	0.01	0.01	0.01	0.01	0.01	0.01	0.01	0.01	0.01	0.01
Co-60	0.01	0.01	0.01	0.01	0.01	0.01	0.01	0.01	0.01	0.01	0.01	0.01	0.01	0.01	0.01	0.01	0.01	0.01	0.01	0.01	0.01	0.01	0.01	0.01	0.01	0.01	0.01	0.01	0.01
Cs-135	0.01	0.01	0.01	0.01	0.01	0.01	0.01	0.01	0.01	0.01	0.01	0.01	0.1	0.1	0.1	0.1	0.1	0.1	0.1	0.1	0.1	0.1	0.1	0.1	0.1	0.1	0.1	0.1	0.1
Cs-137	0.01	0.01	0.01	0.01	0.01	0.01	0.01	0.01	0.01	0.01	0.01	0.01	0.1	0.1	0.1	0.1	0.1	0.1	0.1	0.1	0.1	0.1	0.1	0.1	0.1	0.1	0.1	0.1	0.1
Eu-152	0.01	0.01	0.01	0.01	0.01	0.01	0.01	0.01	0.01	0.01	0.01	0.01	0.1	0.1	0.1	0.1	0.1	0.1	0.1	0.01	0.01	0.01	0.01	0.01	0.01	0.01	0.01	0.01	0.01
Eu-154	0.01	0.01	0.01	0.01	0.01	0.01	0.01	0.01	0.01	0.01	0.01	0.01	0.1	0.1	0.1	0.1	0.1	0.1	0.1	0.1	0.1	0.1	0.1	0.1	0.1	0.1	0.1	0.1	0.1
H-3	0.01	0.01	0.01	0.01	0.01	0.01	0.01	0.01	0.01	0.01	0.01	0.01	0.01	0.01	0.01	0.01	0.01	0.01	0.01	0.01	0.01	0.01	0.01	0.01	0.01	0.01	0.01	0.01	0.01
I-129	0.01	0.01	0.01	0.01	0.01	0.01	0.01	0.01	0.01	0.01	0.01	0.01	0.01	0.01	0.01	0.01	0.01	0.01	0.01	0.01	0.01	0.01	0.01	0.01	0.01	0.01	0.01	0.01	0.01
K-40	0.01	0.01	0.01	0.01	0.01	0.01	0.01	0.01	0.01	0.01	0.01	0.01	0.01	0.01	0.01	0.01	0.01	0.01	0.01	0.01	0.01	0.01	0.01	0.01	0.01	0.01	0.01	0.01	0.01
Nb-94	0.01	0.01	0.01	0.01	0.01	0.01	0.01	0.01	0.01	0.01	0.01	0.01	0.01	0.01	0.01	0.01	0.01	0.01	0.01	0.01	0.01	0.01	0.01	0.01	0.01	0.01	0.01	0.01	0.01
Ni-59	0.01	0.01	0.01	0.01	0.01	0.01	0.01	0.01	0.01	0.01	0.01	0.01	0.01	0.01	0.01	0.01	0.01	0.01	0.01	0.01	0.01	0.01	0.01	0.01	0.01	0.01	0.01	0.01	0.01
Ni-63	0.01	0.01	0.01	0.01	0.01	0.01	0.01	0.01	0.01	0.01	0.01	0.01	0.1	0.1	0.1	0.1	0.1	0.1	0.1	0.1	0.1	0.1	0.1	0.1	0.1	0.1	0.1	0.1	0.1
Np-237	0.01	0.01	0.01	0.01	0.01	0.01	0.01	0.01	0.01	0.01	0.01	0.01	0.1	0.1	0.1	0.1	0.1	0.1	0.1	0.1	0.1	0.1	0.1	0.1	0.1	0.1	0.1	0.1	0.1

Table 5.6-3: Radiological Inventory Multipliers (Continued)

Rad	^a Waste Tanks - Log Uniform Distribution - Minimums																												
	9	10	11	12	13	14	15	16	21	22	23	24	29	30	31	32	35	36	37	38	39	40	41	42	43	48	49	50	51
Pa-231	0.01	0.01	0.01	0.01	0.01	0.01	0.01	0.01	0.01	0.01	0.01	0.01	0.01	0.01	0.01	0.01	0.01	0.01	0.01	0.01	0.01	0.01	0.01	0.01	0.01	0.01	0.01	0.01	0.01
Pd-107	0.01	0.01	0.01	0.01	0.01	0.01	0.01	0.01	0.01	0.01	0.01	0.01	0.01	0.01	0.01	0.01	0.01	0.01	0.01	0.01	0.01	0.01	0.01	0.01	0.01	0.01	0.01	0.01	0.01
Pt-193	0.01	0.01	0.01	0.01	0.01	0.01	0.01	0.01	0.01	0.01	0.01	0.01	0.01	0.01	0.01	0.01	0.01	0.01	0.01	0.01	0.01	0.01	0.01	0.01	0.01	0.01	0.01	0.01	0.01
Pu-238	0.01	0.01	0.01	0.01	0.01	0.01	0.01	0.01	0.01	0.01	0.01	0.01	0.1	0.1	0.1	0.1	0.1	0.1	0.1	0.1	0.1	0.1	0.1	0.1	0.1	0.1	0.1	0.1	0.1
Pu-239	0.01	0.01	0.01	0.01	0.01	0.01	0.01	0.01	0.01	0.01	0.01	0.01	0.1	0.1	0.1	0.1	0.1	0.1	0.1	0.1	0.1	0.1	0.1	0.1	0.1	0.1	0.1	0.1	0.1
Pu-240	0.01	0.01	0.01	0.01	0.01	0.01	0.01	0.01	0.01	0.01	0.01	0.01	0.1	0.1	0.1	0.1	0.1	0.1	0.1	0.1	0.1	0.1	0.1	0.1	0.1	0.1	0.1	0.1	0.1
Pu-241	0.01	0.01	0.01	0.01	0.01	0.01	0.01	0.01	0.01	0.01	0.01	0.01	0.1	0.1	0.1	0.1	0.1	0.1	0.1	0.1	0.1	0.1	0.1	0.1	0.1	0.1	0.1	0.1	0.1
Pu-242	0.01	0.01	0.01	0.01	0.01	0.01	0.01	0.01	0.01	0.01	0.01	0.01	0.01	0.01	0.01	0.01	0.01	0.01	0.01	0.01	0.01	0.01	0.01	0.01	0.01	0.01	0.01	0.01	0.01
Pu-244	0.01	0.01	0.01	0.01	0.01	0.01	0.01	0.01	0.01	0.01	0.01	0.01	0.01	0.01	0.01	0.01	0.01	0.01	0.01	0.01	0.01	0.01	0.01	0.01	0.01	0.01	0.01	0.01	0.01
Ra-226	0.01	0.01	0.01	0.01	0.01	0.01	0.01	0.01	0.01	0.01	0.01	0.01	0.01	0.01	0.01	0.01	0.01	0.01	0.01	0.01	0.01	0.01	0.01	0.01	0.01	0.01	0.01	0.01	0.01
Ra-228	0.01	0.01	0.01	0.01	0.01	0.01	0.01	0.01	0.01	0.01	0.01	0.01	0.01	0.01	0.01	0.01	0.01	0.01	0.01	0.01	0.01	0.01	0.01	0.01	0.01	0.01	0.01	0.01	0.01
Se-79	0.01	0.01	0.01	0.01	0.01	0.01	0.01	0.01	0.01	0.01	0.01	0.01	0.01	0.01	0.01	0.01	0.01	0.01	0.01	0.01	0.01	0.01	0.01	0.01	0.01	0.01	0.01	0.01	0.01
Sm-151	0.01	0.01	0.01	0.01	0.01	0.01	0.01	0.01	0.01	0.01	0.01	0.01	0.1	0.1	0.1	0.1	0.1	0.1	0.1	0.1	0.1	0.1	0.1	0.1	0.1	0.1	0.1	0.1	0.1
Sn-126	0.01	0.01	0.01	0.01	0.01	0.01	0.01	0.01	0.01	0.01	0.01	0.01	0.01	0.01	0.01	0.01	0.01	0.01	0.01	0.01	0.01	0.01	0.01	0.01	0.01	0.01	0.01	0.01	0.01
Sr-90	0.01	0.01	0.01	0.01	0.01	0.01	0.01	0.01	0.01	0.01	0.01	0.01	0.1	0.1	0.1	0.1	0.1	0.1	0.1	0.1	0.1	0.1	0.1	0.1	0.1	0.1	0.1	0.1	0.1
Tc-99	0.01	0.01	0.01	0.01	0.01	0.01	0.01	0.01	0.01	0.01	0.01	0.01	0.1	0.1	0.1	0.1	0.1	0.1	0.1	0.1	0.1	0.1	0.1	0.1	0.1	0.1	0.1	0.1	0.1
Th-229	0.01	0.01	0.01	0.01	0.01	0.01	0.01	0.01	0.01	0.01	0.01	0.01	0.01	0.01	0.01	0.01	0.01	0.01	0.01	0.01	0.01	0.01	0.01	0.01	0.01	0.01	0.01	0.01	0.01
Th-230	0.01	0.01	0.01	0.01	0.01	0.01	0.01	0.01	0.01	0.01	0.01	0.01	0.01	0.01	0.01	0.01	0.01	0.01	0.01	0.01	0.01	0.01	0.01	0.01	0.01	0.01	0.01	0.01	0.01
Th-232	0.01	0.01	0.01	0.01	0.01	0.01	0.01	0.01	0.01	0.01	0.01	0.01	0.1	0.1	0.1	0.01	0.1	0.1	0.1	0.1	0.1	0.1	0.1	0.1	0.1	0.1	0.1	0.1	0.1
U-232	0.01	0.01	0.01	0.01	0.01	0.01	0.01	0.01	0.01	0.01	0.01	0.01	0.01	0.01	0.01	0.01	0.01	0.01	0.01	0.01	0.01	0.01	0.01	0.01	0.01	0.01	0.01	0.01	0.01
U-233	0.01	0.01	0.01	0.01	0.01	0.01	0.01	0.01	0.01	0.01	0.01	0.01	0.1	0.1	0.1	0.01	0.1	0.1	0.1	0.1	0.1	0.1	0.1	0.1	0.1	0.1	0.1	0.1	0.1
U-234	0.01	0.01	0.01	0.01	0.01	0.01	0.01	0.01	0.01	0.01	0.01	0.01	0.1	0.1	0.1	0.1	0.1	0.1	0.1	0.1	0.1	0.1	0.1	0.1	0.1	0.1	0.1	0.1	0.1
U-235	0.01	0.01	0.01	0.01	0.01	0.01	0.01	0.01	0.01	0.01	0.01	0.01	0.1	0.1	0.1	0.1	0.1	0.1	0.1	0.1	0.1	0.1	0.1	0.1	0.1	0.1	0.1	0.1	0.1
U-236	0.01	0.01	0.01	0.01	0.01	0.01	0.01	0.01	0.01	0.01	0.01	0.01	0.01	0.01	0.01	0.01	0.01	0.01	0.01	0.01	0.01	0.01	0.01	0.01	0.01	0.01	0.01	0.01	0.01
U-238	0.01	0.01	0.01	0.01	0.01	0.01	0.01	0.01	0.01	0.01	0.01	0.01	0.1	0.1	0.1	0.01	0.1	0.1	0.1	0.1	0.1	0.1	0.1	0.1	0.1	0.1	0.1	0.1	0.1
Zr-93	0.01	0.01	0.01	0.01	0.01	0.01	0.01	0.01	0.01	0.01	0.01	0.01	0.1	0.1	0.1	0.1	0.1	0.1	0.1	0.1	0.1	0.1	0.1	0.1	0.1	0.1	0.1	0.1	0.1

Table 5.6-3: Radiological Inventory Multipliers (Continued)

Rad	^b Waste Tank - Log Uniform Distribution - Maximums																													
	9	10	11	12	13	14	15	16	21	22	23	24	29	30	31	32	35	36	37	38	39	40	41	42	43	48	49	50	51	
Ac-227	1	1	1	1	1	1	1	1	1	1	1	1	1	1	1	1	1	1	1	1	1	1	1	1	1	1	1	1	1	
Al-26	1	1	1	1	1	1	1	1	1	1	1	1	1	1	1	1	1	1	1	1	1	1	1	1	1	1	1	1	1	1
Am-241	10	10	10	10	10	10	10	10	10	10	10	10	10	10	10	10	10	10	10	10	10	10	10	10	10	10	10	10	10	10
Am-242m	1	1	1	1	1	1	1	1	1	1	1	1	1	1	1	1	1	1	1	1	1	1	1	1	1	1	1	1	1	1
Am-243	1	1	1	1	1	1	1	1	1	1	1	1	1	1	1	1	1	1	1	1	1	1	1	1	1	1	1	1	1	1
C-14	1	1	1	1	1	1	1	1	1	1	1	1	1	1	1	1	1	1	1	1	1	1	1	1	1	1	1	1	1	1
Cf-249	1	1	1	1	1	1	1	1	1	1	1	1	1	1	1	1	1	1	1	1	1	1	1	1	1	1	1	1	1	1
Cf-251	1	1	1	1	1	1	1	1	1	1	1	1	1	1	1	1	1	1	1	1	1	1	1	1	1	1	1	1	1	1
Cl-36	1	1	1	1	1	1	1	1	1	1	1	1	1	1	1	1	1	1	1	1	1	1	1	1	1	1	1	1	1	1
Cm-243	1	1	1	1	1	1	1	1	1	1	1	1	1	1	1	1	1	1	1	1	1	1	1	1	1	1	1	1	1	1
Cm-244	10	10	10	10	10	10	10	10	10	10	10	10	10	10	10	1	10	10	10	10	10	10	10	10	10	10	10	10	10	10
Cm-245	1	1	1	1	1	1	1	1	1	1	1	1	1	1	1	1	1	1	1	1	1	1	1	1	1	1	1	1	1	1
Cm-247	1	1	1	1	1	1	1	1	1	1	1	1	1	1	1	1	1	1	1	1	1	1	1	1	1	1	1	1	1	1
Cm-248	1	1	1	1	1	1	1	1	1	1	1	1	1	1	1	1	1	1	1	1	1	1	1	1	1	1	1	1	1	1
Co-60	1	1	1	1	1	1	1	1	1	1	1	1	1	1	1	1	1	1	1	1	1	1	1	1	1	1	1	1	1	1
Cs-135	10	10	10	10	10	10	10	10	10	10	10	10	10	10	10	10	10	10	10	10	10	10	10	10	10	10	10	10	10	10
Cs-137	10	10	10	10	10	10	10	10	10	10	10	10	10	10	10	10	10	10	10	10	10	10	10	10	10	10	10	10	10	10
Eu-152	10	10	10	10	10	10	10	1	1	1	1	1	10	10	10	10	10	10	10	1	1	1	1	1	1	1	1	1	1	1
Eu-154	10	10	10	10	10	10	10	10	10	10	10	10	10	10	10	10	10	10	10	10	10	10	10	10	10	10	10	10	10	10
H-3	1	1	1	1	1	1	1	1	1	1	1	1	1	1	1	1	1	1	1	1	1	1	1	1	1	1	1	1	1	1
I-129	1	1	1	1	1	1	1	1	1	1	1	1	1	1	1	1	1	1	1	1	1	1	1	1	1	1	1	1	1	1
K-40	1	1	1	1	1	1	1	1	1	1	1	1	1	1	1	1	1	1	1	1	1	1	1	1	1	1	1	1	1	1
Nb-93m	1	1	1	1	1	1	1	1	1	1	1	1	1	1	1	1	1	1	1	1	1	1	1	1	1	1	1	1	1	1
Nb-94	10	10	1	1	1	1	1	1	1	1	1	1	1	1	1	1	1	1	1	1	1	1	1	1	1	1	1	1	1	1
Ni-59	10	10	10	10	10	10	10	1	1	1	1	1	1	1	1	1	1	1	1	1	1	1	1	1	1	1	1	1	1	1
Ni-63	10	10	10	10	10	10	10	10	10	10	10	10	10	10	10	10	10	10	10	10	10	10	10	10	10	10	10	10	10	10
Np-237	10	10	10	10	10	10	10	10	10	10	10	10	10	10	10	10	10	10	10	10	10	10	10	10	10	10	10	10	10	10

Table 5.6-3: Radiological Inventory Multipliers (Continued)

Rad	^b Waste Tank - Log Uniform Distribution - Maximums																													
	9	10	11	12	13	14	15	16	21	22	23	24	29	30	31	32	35	36	37	38	39	40	41	42	43	48	49	50	51	
Pa-231	1	1	1	1	1	1	1	1	1	1	1	1	1	1	1	1	1	1	1	1	1	1	1	1	1	1	1	1	1	
Pd-107	1	1	1	1	1	1	1	1	1	1	1	1	1	1	1	1	1	1	1	1	1	1	1	1	1	1	1	1	1	1
Pt-193	1	1	1	1	1	1	1	1	1	1	1	1	1	1	1	1	1	1	1	1	1	1	1	1	1	1	1	1	1	1
Pu-238	10	10	10	10	10	10	10	10	10	10	10	10	10	10	10	10	10	10	10	10	10	10	10	10	10	10	10	10	10	10
Pu-239	10	10	10	10	10	10	10	10	10	10	10	10	10	10	10	10	10	10	10	10	10	10	10	10	10	10	10	10	10	10
Pu-240	10	10	10	10	10	10	10	10	10	10	10	10	10	10	10	10	10	10	10	10	10	10	10	10	10	10	10	10	10	10
Pu-241	1	1	10	10	10	10	10	10	10	10	10	10	10	10	10	10	10	10	10	10	10	10	10	10	10	10	10	10	10	10
Pu-242	1	1	1	1	1	1	1	1	1	1	1	1	1	1	1	1	1	1	1	1	1	1	1	1	1	1	1	1	1	1
Pu-244	1	1	1	1	1	1	1	1	1	1	1	1	1	1	1	1	1	1	1	1	1	1	1	1	1	1	1	1	1	1
Ra-226	1	1	1	1	1	1	1	1	1	1	1	1	1	1	1	1	1	1	1	1	1	1	1	1	1	1	1	1	1	1
Ra-228	1	1	1	1	1	1	1	1	1	1	1	1	1	1	1	1	1	1	1	1	1	1	1	1	1	1	1	1	1	1
Se-79	10	10	10	10	10	10	10	1	1	1	1	1	1	1	1	1	1	1	1	1	1	1	1	1	1	1	1	1	1	1
Sm-151	10	10	10	10	10	10	10	10	10	10	10	10	10	10	10	10	10	10	10	10	10	10	10	10	10	10	10	10	10	10
Sn-126	10	10	10	10	10	10	10	1	1	1	1	1	1	1	1	1	1	1	1	1	1	1	1	1	1	1	1	1	1	1
Sr-90	10	10	10	10	10	10	10	10	10	10	10	10	10	10	10	10	10	10	10	10	10	10	10	10	10	10	10	10	10	10
Tc-99	10	10	10	10	10	10	10	10	10	10	10	10	10	10	10	10	10	10	10	10	10	10	10	10	10	10	10	10	10	10
Th-229	1	1	10	10	10	10	10	1	1	1	1	1	1	1	1	1	1	1	1	1	1	1	1	1	1	1	1	1	1	1
Th-230	1	1	1	1	1	1	1	1	1	1	1	1	1	1	1	1	1	1	1	1	1	1	1	1	1	1	1	1	1	1
Th-232	1	1	10	10	10	10	10	10	1	1	1	1	10	10	10	1	10	10	10	10	10	10	10	10	10	10	10	10	10	10
U-232	1	1	1	1	1	1	1	1	1	1	1	1	1	1	1	1	1	1	1	1	1	1	1	1	1	1	1	1	1	1
U-233	10	10	10	10	10	10	10	10	10	10	10	10	10	10	10	1	10	10	10	10	10	10	10	10	10	10	10	10	10	10
U-234	10	10	10	10	10	10	10	10	10	10	10	10	10	10	10	10	10	10	10	10	10	10	10	10	10	10	10	10	10	10
U-235	1	1	10	10	10	10	10	1	1	1	1	1	10	10	10	10	10	10	10	10	10	10	10	10	10	10	10	10	10	10
U-236	1	1	1	1	1	1	1	1	1	1	1	1	1	1	1	1	1	1	1	1	1	1	1	1	1	1	1	1	1	1
U-238	10	10	10	10	10	10	10	1	1	1	1	10	10	10	10	1	10	10	10	10	10	10	10	10	10	10	10	10	10	10
Zr-93	10	10	10	10	10	10	10	10	10	10	10	10	10	10	10	10	10	10	10	10	10	10	10	10	10	10	10	10	10	10

a Shaded cells indicate radionuclides and waste tanks which apply 0.1 (as opposed to 0.01) as the minimum multiplier

b Shaded cells indicate radionuclides and waste tanks which apply 10 (as opposed to 1) as the maximum multiplier.

Table 5.6-4: Chemical Inventory Multipliers for All Waste Tank Types

	Probability	Multiplier
Chemicals	0.25	0.01
	0.25	0.1
	0.25	1
	0.25	10

Several radionuclides listed in Table 5.6-3 have maximum multipliers equal to one, indicating that the initial inventory will not go above the deterministic baseline inventory. This was done for radionuclides where the inventory projections indicate they would remain below the detection limit (1.0E-4 curie), or where the adjusted inventory was 1.0 curie (Section 3.4.2.3) when the baseline inventory was set equal to the detection limit or 1.0 curie, it was a conservative adjustment of these inventory estimates. Therefore, an upper multiplier of 1.0 would be appropriate. The HTF GoldSim Model then adjusts the value to lower, more realistic values. As Tables 5.6-3 and 5.6-4 indicate, the lower limit is either one order or two orders of magnitude less than the baseline inventory. For those components of the initial inventory expected to have a large impact on dose, and that had projected inventories greater than the detection limit, a multiplier of 10 is used for the upper bound. An example is Pu-238, which has a lower and upper multiplier equal to 0.01 and 10. Pu-238 decays to Ra-226, which is the radionuclide that drives peak dose in 20,000 years (Section 5.5). The initial inventory of Ra-226 is insignificant; rather it is the radioactive decay from its many parent radionuclides that control the concentration of Ra-226 and ultimately the dose from Ra-226. Because Pu-238 decay to Ra-226 is the largest contributor to the concentration of Ra-226, it was considered conservative to provide an upper bound an order of magnitude higher than the already conservative baseline estimate.

An initial inventory is assumed to exist in the Type I annulus and the Type II sand pads and annulus. An initial inventory is also assumed to exist in the ancillary equipment including the transfer lines. Both the sand pad and annulus initial inventory estimates were considered extremely conservative due to the residual volume assumed relative to the amount anticipated as described in SRR-CWDA-2010-00023, Rev. 3, therefore, an uncertainty of zero was applied.

5.6.3.2 Waste Tank Cases

This section specifically considers the uncertainty accounted for by simulating different waste tank cases. As presented in Section 4.4.2, five different waste tank cases (Cases A through E) were simulated deterministically using the PORFLOW flow and transport model. The differences in the five conceptual models include 1) the existence of fast flow paths, 2) the timing of cementitious material degradation, 3) the timing of liner failure, and 4) the influence of the reducing capacity of the grout on the CZ. The differences between the five cases are summarized in Table 4.4-1 (Section 4.4.2).

A probability is applied to each case according to its likelihood of occurrence. The discrete distribution applied to the five scenarios presented in Table 5.6-5 is meant only to enable evaluation of the sensitivity of the case on dose. The applied values are not based on quantified data, but are instead relative relationships based on engineering judgment.

Table 5.6-5: Case Probability for All Waste Tank Types

Case	Probability ^a
A	75 %
B	5 %
C	15 %
D	1.25 %
E	3.75 %

a Discrete distribution chosen using engineering judgment.

The following assumptions were used to inform the probability values:

- Fast flow paths, in the form of cracks through the cement barriers of the waste tanks (as represented by Cases B, C, D and E), are not likely to occur immediately at the time of closure. Therefore, the Base Case was applied a 75 % probability of occurrence, and the remaining fast flow cases a collective probability of 25 %.
- Case B and C can be loosely grouped into a subgroup of fast flow paths through the grout but not the basemat. The grout is considered more likely to have a fast flow path (e.g., shrinkage gap) compared to the basemat, therefore a much smaller probability is applied to Cases D and E. Case B and C are given a probability of occurrence equal to 20 %, while D and E have the collective probability equal to 5 %.
- The 20 % applied collectively to B and C and the 5 % applied collectively to D and E are further refined by the likelihood of having instantaneous degradation of the cementitious materials at year 501. It was considered more likely that cementitious degradation would be gradual; therefore, B and D were given lower probabilities of occurrence than their counterparts were.

The impact of fast flow paths, the timing of liner failure, and cementitious material degradation time are represented both implicitly in the HTF GoldSim Model using case dependent flow fields and explicitly using stochastic parameters. Both are described in the following sections.

The HTF GoldSim Model was used to model only contaminant transport and therefore, flow is not calculated independently. Instead, the flow fields calculated in PORFLOW for each model component (e.g., grout, CZ, basemat, primary, and secondary liner, annulus) were used as input to the HTF GoldSim Model. There is a unique set of PORFLOW flow-fields used in the HTF GoldSim Model for deterministic runs for each of the five failure cases. Also, with the stochastic simulations, there is an alternate set of flow-fields that can be sampled from. The flow-fields included as tables in the file, *GoldSim_StochasticFlowFields.txt*, are based on a parametric study performed using the HTF PORFLOW Model. The flow parametric study was based on the Base Case scenario with the following attributes varied:

- 3 fast flow cases (none, partial, full)
- 4 liner failure times (time zero, early, moderate, late)
- 3 cementitious material degradation rates (fast, nominal, and slow)
- 2 infiltration cases (nominal, no-cap)

The “partial” fast flow path will breach the roof and grout, but not the basemat/floor (as in Cases B and C). The “full” fast flow path will breach the roof, grout, and basemat/floor (as in Cases D and E). The HTF Stochastic Fate and Transport Model is designed to sample for condition based on 5 cases (Cases A through E). For compatibility, when the sampled condition is the Base Case, the first fast flow case (none) is used. When the sampled condition is either Case B or Case C, the second fast flow case (partial) is used and when the sampled condition is Case D or E, the third fast flow case (full) is used.

The parametric study also included four liner failure times, which are presented in Table 5.6-6. The HTF Stochastic Model sampling procedure chooses a specific failure time. That specific time is used to choose which set of flow data based on the liner failure times presented in Table 5.6-6 is to be used. The criteria for choosing the liner failure time from Table 5.6-6 is which time in the table for the specified waste tank type, the sampled time is closest to. In the GoldSim model simulation, the sampled liner failure time is used. Since the liner failure times differ, the flow data time series from the parametric study data is scaled from time-zero to the liner failure time to fit the time span from time-zero to the sampled liner failure time. The component of the time series following liner failure is then shifted so that it is consistent with the sampled time failure (no scaling is considered). In this way, any the effect of any liner failure time can be evaluated and a degree of correlation between liner failure time and concrete degradation is imposed.

Uncertainty in the concrete and grout degradation rates is also considered using a scaling factor. The three cementitious material degradation rates considered are the Base Case degradation times, fast (Base Case degradation times divided by two), and slow (Base Case degradation times multiplied by two).

Table 5.6-6: Liner Failure Times

Fast Flow Path:	None				Partial and Full			
	Type I Liner Failure Year	Type II Liner Failure Year	Type III/IIIA Liner Failure Year	Type IV Liner Failure Year	Type I Liner Failure Year	Type II Liner Failure Year	Type III/IIIA Liner Failure Year	Type IV Liner Failure Year
0	0	0	0	0	0	0	0	0
Early	2,100	2,506	3,100	500	100	100	100	75
Moderate	11,397	12,687	12,751	3,638	1,142	2,506	2,077	1,000
Late	15,000	14,500	14,500	8,000	11,000	12,000	12,000	3,638

The other parameter evaluated in the parametric study is the infiltration rate. A “no-cap” infiltration rate of 16.45 in/yr for all time was used as an alternative to the nominal infiltration curve.

The parametric cases from which the flow fields are sampled are listed below in Tables 5.6-7 to 5.6-9.

Table 5.6-7: Parametric Cases (No Fast Flow Zones)

Flow Run	Fast Flow	Liner Failure (see table)	Infiltration Rate (in/yr)	Hydraulic Conductivity Curve
1	None (Case A)	0	Nominal (11.67)	Normal degradation
2	None (Case A)	Early	Nominal (11.67)	Normal degradation
3	None (Case A)	Moderate	Nominal (11.67)	Normal degradation
4	None (Case A)	Late	Nominal (11.67)	Normal degradation
5	None (Case A)	0	Nominal (11.67)	Faster degradation
6	None (Case A)	Early	Nominal (11.67)	Faster degradation
7	None (Case A)	Moderate	Nominal (11.67)	Faster degradation
8	None (Case A)	Late	Nominal (11.67)	Faster degradation
9	None (Case A)	0	Nominal (11.67)	Slower degradation
10	None (Case A)	Early	Nominal (11.67)	Slower degradation
11	None (Case A)	Moderate	Nominal (11.67)	Slower degradation
12	None (Case A)	Late	Nominal (11.67)	Slower degradation
13	None (Case A)	0	No cap (16.45)	Normal degradation
14	None (Case A)	Early	No cap (16.45)	Normal degradation
15	None (Case A)	Moderate	No cap (16.45)	Normal degradation
16	None (Case A)	Late	No cap (16.45)	Normal degradation
17	None (Case A)	0	No cap (16.45)	Faster degradation
18	None (Case A)	Early	No cap (16.45)	Faster degradation
19	None (Case A)	Moderate	No cap (16.45)	Faster degradation
20	None (Case A)	Late	No cap (16.45)	Faster degradation
21	None (Case A)	0	No cap (16.45)	Slower degradation
22	None (Case A)	Early	No cap (16.45)	Slower degradation
23	None (Case A)	Moderate	No cap (16.45)	Slower degradation
24	None (Case A)	Late	No cap (16.45)	Slower degradation

Case A = Base Case

Table 5.6-8: Parametric Cases (Partial Fast Flow Zones)

Flow Run	Fast Flow (Case)	Liner Failure (see table)	Infiltration Rate (in/yr)	Hydraulic Conductivity Curve
25	Partial (Case B and C)	0	Nominal (11.67)	Normal degradation
26	Partial (Case B and C)	Early	Nominal (11.67)	Normal degradation
27	Partial (Case B and C)	Moderate	Nominal (11.67)	Normal degradation
28	Partial (Case B and C)	Late	Nominal (11.67)	Normal degradation
29	Partial (Case B and C)	0	Nominal (11.67)	Faster degradation
30	Partial (Case B and C)	Early	Nominal (11.67)	Faster degradation
31	Partial (Case B and C)	Moderate	Nominal (11.67)	Faster degradation
32	Partial (Case B and C)	Late	Nominal (11.67)	Faster degradation
33	Partial (Case B and C)	0	Nominal (11.67)	Slower degradation
34	Partial (Case B and C)	Early	Nominal (11.67)	Slower degradation
35	Partial (Case B and C)	Moderate	Nominal (11.67)	Slower degradation
36	Partial (Case B and C)	Late	Nominal (11.67)	Slower degradation
37	Partial (Case B and C)	0	No cap (16.45)	Normal degradation
38	Partial (Case B and C)	Early	No cap (16.45)	Normal degradation
39	Partial (Case B and C)	Moderate	No cap (16.45)	Normal degradation
40	Partial (Case B and C)	Late	No cap (16.45)	Normal degradation
41	Partial (Case B and C)	0	No cap (16.45)	Faster degradation
42	Partial (Case B and C)	Early	No cap (16.45)	Faster degradation
43	Partial (Case B and C)	Moderate	No cap (16.45)	Faster degradation
44	Partial (Case B and C)	Late	No cap (16.45)	Faster degradation
45	Partial (Case B and C)	0	No cap (16.45)	Slower degradation
46	Partial (Case B and C)	Early	No cap (16.45)	Slower degradation
47	Partial (Case B and C)	Moderate	No cap (16.45)	Slower degradation
48	Partial (Case B and C)	Late	No cap (16.45)	Slower degradation

Table 5.6-9: Parametric Cases (Full Fast Flow Zones)

Flow Run	Fast Flow (Case)	Liner Failure (see table)	Infiltration Rate (in/yr)	Hydraulic Conductivity Curve
49	Full (Cases D and E)	0	Nominal (11.67)	Normal degradation
50	Full (Cases D and E)	Early	Nominal (11.67)	Normal degradation
51	Full (Cases D and E)	Moderate	Nominal (11.67)	Normal degradation
52	Full (Cases D and E)	Late	Nominal (11.67)	Normal degradation
53	Full (Cases D and E)	0	Nominal (11.67)	Faster degradation
54	Full (Cases D and E)	Early	Nominal (11.67)	Faster degradation
55	Full (Cases D and E)	Moderate	Nominal (11.67)	Faster degradation
56	Full (Cases D and E)	Late	Nominal (11.67)	Faster degradation
57	Full (Cases D and E)	0	Nominal (11.67)	Slower degradation
58	Full (Cases D and E)	Early	Nominal (11.67)	Slower degradation
59	Full (Cases D and E)	Moderate	Nominal (11.67)	Slower degradation
60	Full (Cases D and E)	Late	Nominal (11.67)	Slower degradation
61	Full (Cases D and E)	0	No cap (16.45)	Normal degradation
62	Full (Cases D and E)	Early	No cap (16.45)	Normal degradation
63	Full (Cases D and E)	Moderate	No cap (16.45)	Normal degradation
64	Full (Cases D and E)	Late	No cap (16.45)	Normal degradation
65	Full (Cases D and E)	0	No cap (16.45)	Faster degradation
66	Full (Cases D and E)	Early	No cap (16.45)	Faster degradation
67	Full (Cases D and E)	Moderate	No cap (16.45)	Faster degradation
68	Full (Cases D and E)	Late	No cap (16.45)	Faster degradation
69	Full (Cases D and E)	0	No cap (16.45)	Slower degradation
70	Full (Cases D and E)	Early	No cap (16.45)	Slower degradation
71	Full (Cases D and E)	Moderate	No cap (16.45)	Slower degradation
72	Full (Cases D and E)	Late	No cap (16.45)	Slower degradation

The inclusion points for the flow data in the HTF GoldSim Model is schematically depicted in Figure 4.4-50 for Type I and II tanks and Figure 4.4-51, for the other waste tank types (see Section 4.4.4.2). Having different flow fields for the various cases is the method by which uncertainties in parameters affecting flow (e.g., liner failure time and cementitious materials degradation time) are incorporated into the UA/SA.

5.6.3.3 Solubility

The solubility values applied to the CZ in the HTF GoldSim Model control contaminant release, with different solubility values resulting in different release rates. Table 4.2-10 and Table 4.2-11 (from Section 4.2.1) present the deterministic solubility values by controlling phase for all elements of interest at each of the chemical states of interest. For plutonium, neptunium, technetium, and uranium, the solubility values listed correspond to iron co-precipitation as the controlling mechanism.

As discussed in Section 4.2.1, there is large uncertainty in the calculation of solubility values within the waste cell. Much of the uncertainty is because of unknowns related to the CZ and how the conditions in this domain will evolve with time. Some of the uncertainty is due to the limited amount of thermodynamic data available for many of the radionuclides of interest. Uncertainty associated with the solubility model was managed largely through applying conservative modeling assumptions, specifically in determining the controlling phase for the element of interest.

For those radionuclides which have historically been of most concern at SRS (plutonium, uranium, neptunium, and technetium), distributions were assigned for Reducing Region II, Oxidizing Region II, and Oxidizing Region III conditions. Tables 5.6-10 through 5.6-12 present the discrete distributions applied to the controlling phases for plutonium, uranium, neptunium, and technetium. The probabilities are weighted to account for the likelihood of the different controlling phases. The possibility of iron co-precipitation as a controlling phase was included in the probability distributions. The probabilities chosen are based on observations in the literature and expected thermodynamic stability. [SRNL-STI-2012-00404]

Table 5.6-10: Probability Distributions for Various Phases Controlling Reduced Region II Solubility

	Controlling Phase	Solubility (mol/L)	Probability
Plutonium	PuO ₂ (am, hyd)	3.2E-11	0.5
	Iron co-precipitation	7.6E-13	0.5
Neptunium	NpO ₂ (am, hyd)	9.9E-10	0.5
	Iron co-precipitation	4.6E-15	0.5
Technetium	TcO ₂ ·1.6H ₂ O	1.1E-08	0.5
	Iron co-precipitation ^a	1.1E-14	0.5
Uranium	UO ₂ (am, hyd)	4.6E-09	0.5
	Iron co-precipitation	2.4 E-12	0.5

^a Iron co-precipitation values used for deterministic simulations.

Table 5.6-11: Probability Distributions for Various Phases Controlling Oxidized Region II Solubility

	Controlling Phase	Solubility (mol/L)	Probability
Plutonium	PuO ₂ (am, hyd)	3.2E-11	0.5
	Iron co-precipitation	7.4E-12	0.5
Neptunium	NpO ₂ (am, hyd)	2.5E-07	0.5
	Iron co-precipitation	4.4E-14	0.5
Technetium	No solubility control	instantaneous release	0.5
	Iron co-precipitation ^a	1.1E-13	0.5
Uranium	UO ₃ ·2H ₂ O	5.1E-05	0.5
	Iron co-precipitation	2.3E-11	0.5

^a Iron co-precipitation values used for deterministic simulations.

Table 5.6-12: Probability Distributions for Various Phases Controlling Oxidized Region III Solubility

Element	Controlling Phase	Solubility (mol/L)	Probability
Plutonium	PuO _{2(am,hyd)}	3.2E-11	0.5
	Iron co-precipitation	1.5E-13	0.5
Neptunium	NpO _{2(am,hyd)}	1.7E-06	0.5
	Iron co-precipitation	8.8E-16	0.5
Technetium	no solubility limit	Modeled as instantaneous release	0.5
	Iron co-precipitation ^a	2.1E-15	0.5
Uranium	UO ₃ ·2H ₂ O	4.3E-06	0.5
	Iron co-precipitation	4.5E-13	0.5

a Iron co-precipitation values used for deterministic simulations

Uncertainties in predicting the controlling phase accounts for a large portion of the uncertainty in calculating the appropriate solubility. Uncertainties in the thermodynamic quantities also play an important role (Section 4.2.1). [SRNL-STI-2012-00404] Uncertainty in the controlling phase is presented above, while uncertainty in thermodynamic quantities is addressed by implementing four bounding conditions discussed in detail in Section 4.2.2. Changing the chemical conditions in the grout and CZ are implemented in GoldSim by modifying the chemical transition times in the CZ. This is discussed in Section 5.6.3.8.

5.6.3.4 Distribution Coefficient Values

The cementitious material (both concrete and grout) comprising the engineered barrier and the soil underlying the HTF have a propensity to slow the transport of certain radionuclides through the environment, thus retarding their arrival to a potential receptor. The ability of the cementitious materials or the soils to sorb the different radionuclides is represented using K_d s. The ability of the material to sorb the radionuclide is dependent on the chemical condition of the environment. Tables 4.2-25 and 4.2-29 (Section 4.2.2) show the deterministic K_d values for the soils, for soils impacted by reducing cement leachate, and for the cementitious materials. The K_d values are element dependent and they vary depending on the chemical state of the system (e.g., young/old age; reducing/oxidizing regions). The bases for deterministic values are presented in Section 4.2.2 and in the report, *Geochemical Data Package for Performance Assessment Calculations Related to the Savannah River Site*. [SRNL-STI-2009-00473]

Groupings for the K_d values used in the HTF GoldSim Model were based on the approach described in SRNL-STI-2009-00150. This report recommends applying a lognormal distribution with maximum and minimum values based on the material under consideration. The shape of the lognormal distribution is based on the geometric standard deviation (GSD) that differs by the material under consideration and the magnitude of the deterministic value for the K_d . Table 5.6-13 provides the distributions used in the HTF GoldSim Model for each of the materials. In Table 5.6-13, in the “Lognormal GSD” column certain conditions are defined to calculate the GSD. Here, the geometric mean (GM) is equal to the deterministic

(baseline) value. For example, for clayey soils (and cement leachate impacted clayey soils), radionuclides with a deterministic K_d value less than 4 mL/g will have a lognormal GSD equal to 1.001, but for radionuclides with deterministic K_d values greater than 4 mL/g, the lognormal GSD is calculated as the product of 0.25 and the deterministic value. While a GSD of 1.001 results in a small distribution around the GM, this is only for elements that already have a low deterministic value and thus have low retardation which for soil include technetium, iodine, and astatine. Of particular interest is the technetium, which has a deterministic value in sandy soil of 0.6 mL/g and a small distribution around this value. The dispersion of technetium K_d values was evaluated in SRNS-STI-2008-00286 and the mean was 3.4 mL/g with a 95th percentile range of 2.4 to 4.4 mL/g. The deterministic value was already a pessimistic value based on the site-specific data and therefore, it would be inappropriate to allow the distribution around the modeled value to range lower.

Table 5.6-13: K_d Variability in the HTF GoldSim Model

Material Zone	Min	Max	Lognormal GSD	
			GM < 4.0 mL/g	GM = 4.0 mL/g or greater
Clayey Soils ^b and Cement Leachate Impacted Clayey Soils	0.5xGM ^a	1.5xGM	GM < 2.7 mL/g	GM = 2.7 mL/g or greater
			1.001 mL/g	0.25 x GM
Sandy Soils ^c and Cement Leachate Impacted Sandy Soils	0.25xGM	1.75xGM	GM < 2.7 mL/g	GM = 2.7 mL/g or greater
			1.001 mL/g	0.375 x GM
Cementitious Materials	0.25xGM	1.75xGM	GM < 2.7 mL/g	GM = 2.7 mL/g or greater
			1.001 mL/g	0.375 x GM

a GM = geometric mean of the lognormal distribution defined as the baseline value presented in Table 4.2-25 for soils, and cement leachate impacted soils and Table 4.2-29 for cementitious materials.

b Backfill layer

c Vadose zone and saturated zone

5.6.3.5 Basemat Thickness

The concrete floor thickness, also known as the basemat thickness in the HTF GoldSim Model, retards contaminant transport with its effectiveness related to the basemat K_d values and the basemat thickness. Section 4.4.1 shows the design dimensions used in the baseline modeling for the various waste tank types, including concrete basemat thickness. Section 3.2.1 provides design details for the various waste tank types, including details regarding the concrete basemat designs. The basemat thickness specified on construction drawings is used as the most likely basemat thickness, with other design details used to determine a probable maximum and minimum thickness of basemat concrete. A triangular distribution using these maximum, minimum, and the most likely value as the peak was utilized for basemat thickness in the stochastic analyses. Table 5.6-14 summarizes the values used in the HTF GoldSim Model.

Table 5.6-14: Basemat Thickness Variability in the HTF GoldSim Model

Tank Type	Deterministic (in)	Triangular	
		Min (in)	Max (in)
Type I	30	29	37
Type II	42	41.5	48.5
Type III	42	41.5	48.5
Type IIIA	41	40.5	45.5
Type IV	6.9025	6.7775	7.0275

The design details used as the basis for the various thicknesses are described below for each waste tank type.

5.6.3.5.1 Type IV Tank Concrete Floor Thickness

As described in Section 3.2, a Type IV tank basemat was specified to be 4-inches thick. A 3-inch cement topping was then poured over the basemat and given a float and trowel finish having a maximum tolerance of plus or minus 0.125 inch from a true level. Drainage channels, 1.625-inches deep and approximately 3.5-inches wide (3.625 inches at the top and 3.125 inches at the bottom), for use in leak detection were formed in the 3-inch deep basemat cement topping. The drainage channels cover less than 6 % of the total foundation area.

Thickness Calculations

- Minimum at channel location - 5.25 inches (4 + 2.875 - 1.625)
- Minimum without channel - 6.875 inches (4 + 2.875)
- Median at channel location - 5.375 inches (3 + 4 - 1.625)
- Median without channel - 7 inches (3 + 4)
- Maximum at channel location - 5.5 inches (4 + 3.125 - 1.625)
- Maximum without channel - 7.125 inches (4 + 3.125)

Modeling Values Used

	<u>Inches:</u>	<u>Basis:</u>
Most likely:	6.9025	Weighted median (0.06 (5.375) + 0.94 (7))
Minimum:	6.7775	Weighted minimum (0.06 (5.25) + 0.94 (6.875))
Maximum:	7.0275	Weighted maximum (0.06 (5.5) + 0.94 (7.125))
Mean:	6.9025	Based on triangular distribution

5.6.3.5.2 Type I Tank Concrete Floor Thickness

As presented in Section 3.2, the working slab for a Type I tank is 4-inches thick. A 30-inch reinforced concrete base (i.e., the basemat) sits on top of the working slab. The basemat assumed tolerance is ± 1 inch based on the construction specification requirement of no visual variance in concrete level. [Spec-3019] A 3-inch layer of grout sits on top of the basemat, and the primary container sits above the grout.

Modeling Values Used

	<u>Inches:</u>	<u>Basis:</u>
Most likely:	30.0	30-inch basemat
Minimum:	29.0	30-inch basemat - 1-inch tolerance on basemat
Maximum:	37.0	4-inch working slab + 30-inch basemat + 3-inch grout layer
Mean:	32.0	Based on triangular distribution

5.6.3.5.3 Type II Tank Concrete Floor Thickness

The modeling values used for Type II tanks are the same as for Type III tanks described in Section 3.2.

Modeling Values Used

	<u>Inches:</u>	<u>Basis:</u>
Most likely:	42.0	42-inch basemat (ignore drop panel)
Minimum:	41.5	42-inch basemat - 0.5-inch tolerance on basemat
Maximum:	48.5	6-inch working slab + 42-inch basemat + 0.5-inch tolerance on basemat (ignore drop panel)
Mean:	44.0	Based on triangular distribution

5.6.3.5.4 Type III Tank Concrete Floor Thickness

As described in Section 3.2, Type III tanks have a 6-inch working slab. The Type III tank basemat, made of reinforced concrete, has a 3 foot 6-inch minimum thickness (5 feet 4 inches at drop panel at waste tank center). The concrete finish shall have a tolerance of 0.125-inch per 10 feet. The basemats in Type III tanks do not have leak detection slots.

Modeling Values Used

	<u>Inches:</u>	<u>Basis:</u>
Most likely:	42.0	42-inch basemat (ignore drop panel)
Minimum:	41.5	42-inch basemat - 0.5-inch tolerance on basemat
Maximum:	48.5	6-inch working slab + 42-inch basemat + 0.5-inch tolerance on basemat (ignore drop panel)
Mean:	44.0	Based on triangular distribution

5.6.3.5.5 Type IIIA Tank Concrete Floor Thickness

As described in Section 3.2, Type IIIA tanks have a 4-inch working slab. The Type IIIA tank basemat has a 3-foot 7-inch minimum thickness (6 feet 4 inches at drop panel at waste tank center). The concrete finish shall have a tolerance of 0.125-inch per 10 feet. A grid of 2-inch deep interconnected radial channels is grooved into the concrete basemat upon which the secondary liner rests.

Modeling Values Used

	<u>Inches:</u>	<u>Basis:</u>
Most likely:	41.0	43-inch basemat - 2-inch drainage channels (ignore drop panel)
Minimum:	40.5	43-inch basemat - 2 inch drainage channels - 0.5-inch tolerance on basemat
Maximum:	45.5	4-inch working slab + 43 inch basemat - 2-inch drainage channels + 0.5-inch tolerance on basemat (ignore drop panel)
Mean:	42.3	Based on triangular distribution

5.6.3.6 Basemat Fast Flow

Cases A through E are differentiated, in part, by the presence or absence of a fast flow path, as well as a number of other parameters (Table 4.4-1, Section 4.4.2). Using separate model cases run deterministically enables evaluation of the sensitivity of the system to a fast flow path. However, a stochastic parameter was developed in the HTF GoldSim Model specifically to address the uncertainty associated with the existence of a fast flow path through the basemat, regardless of case. In other words, although the Cases A, B, and C do not have a fast flow path through the basemat, when run stochastically, a “basemat bypass factor” is applied to allow a fraction of flow to bypass the basemat. This bypass factor is implemented by setting the K_d for all radionuclides in the basemat equal to zero, effectively eliminating any retardation affects the basemat concrete provides.

The bypass fraction distribution is represented by a triangular distribution with zero being set as the most likely value (meaning 0 % of flow bypasses the basemat) and the upper bound set at 0.1 % (meaning 10 % of flow bypasses the basemat). The distribution is based on the assumption that cracking in the basemat is not predicted to occur during the performance period. Although, some uncertainty was applied to represent void spaces forming all the way through the basemat, it was judged much more likely that the cracking would have a tendency to be self-sealing and would not create full channels; therefore, only 10 % of flow bypasses the basemat.

5.6.3.7 Waste Tank and Ancillary Equipment Containment Failure Times

The containment failure times in the HTF GoldSim Model control initial contaminant release from the associated location (waste tank or ancillary equipment). Table 4.2-32 presents the deterministic liner failure times used in the HTF PA, while Table 5.6-15 shows the probabilistic distributions applied during stochastic modeling. The waste tank steel life estimates assume general corrosion and pitting (leading to stress corrosion cracking) are the primary corrosion mechanisms acting on the waste tank liners, as they are exposed to the CZ, grouted, and soil conditions. [SRNL-STI-2010-00047] Results used in the HTF GoldSim Model for Type I and II tanks partially submerged in groundwater are based on analyses presented in *Life Estimation of High Level Waste Tank Steel For H-Tank Farm Closure Performance Assessment* (SRNL-STI-2010-00047). In order to represent submerged waste tank conditions, which can have increased galvanic corrosion due to increased oxygen concentrations in wet soil, a high oxygen diffusion rate was selected ($1.0\text{E-}4 \text{ cm}^2/\text{s}$). The Base Case assumes there are no fast flow paths through the containment barriers. Under these conditions, it is reasonably bounding to assume carbon dioxide diffusion rates will be faster in the fast flow Cases B through E. Therefore, results corresponding to lower ($1.0\text{E-}6 \text{ cm}^2/\text{s}$) carbon dioxide diffusion rates were used to represent the Base Case. The results corresponding to the maximum evaluated carbon dioxide diffusion rates ($1.0\text{E-}4 \text{ cm}^2/\text{s}$) were selected for the remaining fast flow modeling cases (Cases B through E).

Table 5.6-15: Probability Distribution of Liner Failure Times by Waste Tank Types and Case

Case A		Case B,C,D, & E		Case A		Case B,C,D, & E		Case A		Case B,C,D, & E	
Type I ^{a,k}		Type I ^{b,k}		Type II ^{c,k}		Type II ^{d,k}		Type IV ^e		Type IV ^f	
Probability level	Value (yrs)	Probability level	Value (yrs)	Probability level	Value (yrs)	Probability level	Value (yrs)	Probability level	Value (yrs)	Probability level	Value (yrs)
0	3,452	0	85	0	7,443	0	123	0	152	0	38
0.005	8,497	0.005	175	0.005	11,358	0.005	330	0.005	444	0.005	42
0.025	8,946	0.025	238	0.025	11,796	0.025	473	0.025	655	0.025	45
0.1	9,518	0.1	364	0.1	12,272	0.1	757	0.1	1,071	0.1	49
0.25	10,182	0.25	587	0.25	12,425	0.25	1,258	0.25	1,805	0.25	56
0.5	11,397	0.5	1,142	0.5	12,687	0.5	2,506	0.5	3,638	0.5	75
0.75	12,626	0.75	2,703	0.75	12,960	0.75	6,018	0.75	8,819	0.75	126
0.9	12,994	0.9	7,310	0.9	13,131	0.9	12,408	0.9	9,639	0.9	280
0.975	13,185	0.975	12,265	0.975	13,220	0.975	13,017	0.975	10,012	0.975	1,050
0.995	13,237	0.995	13,033	0.995	13,244	0.995	13,201	0.995	10,102	0.995	5,107
1	13,250	1	13,250	1	13,250	1	13,250	1	10,125	1	10,125
Case A		Case B,C,D, & E		Case A		Case B,C,D, & E		From SRNL-STI-2010-00047: D _i units (cm ² /s): a Figure 43 D _i (CO ₂) = 1.0E-6, and D _i (O ₂) = 1.0E-4 b Figure 44 D _i (CO ₂) = 1.0E-4, and D _i (O ₂) = 1.0E-4 c Figure 46 D _i (CO ₂) = 1.0E-6, and D _i (O ₂) = 1.0E-4 d Figure 47 D _i (CO ₂) = 1.0E-4, and D _i (O ₂) = 1.0E-4 From WSRC-STI-2007-00061: D _i units (cm ² /s): e Table 37 D _i (CO ₂) = 1.0E-6, and D _i (O ₂) = 1.0E-6 f Table 38 D _i (CO ₂) = 1.0E-4, and D _i (O ₂) = 1.0E-6 g Table 34 D _i (CO ₂) = 1.0E-6, and D _i (O ₂) = 1.0E-6 h Table 35 D _i (CO ₂) = 1.0E-4, and D _i (O ₂) = 1.0E-6 i Table 34 D _i (CO ₂) = 1.0E-6, and D _i (O ₂) = 1.0E-6 j Table 35 D _i (CO ₂) = 1.0E-4, and D _i (O ₂) = 1.0E-6 k NOTE: Tank 12 (Type I) and Tanks 14, 15, and 16 (Type II) have no liner, therefore are set to fail at time = 0.01 years Case A = Base Case			
Type III ^g		Type III ^h		Type IIIA West ⁱ		Type IIIA West ^j					
Probability level	Value (yrs)	Probability level	Value (yrs)	Probability level	Value (yrs)	Probability level	Value (yrs)				
0	6,789	0	117	0	6,789	0	117				
0.005	12,255	0.005	281	0.005	12,255	0.005	281				
0.025	12,275	0.025	400	0.025	12,275	0.025	400				
0.1	12,351	0.1	634	0.1	12,351	0.1	634				
0.25	12,500	0.25	1,047	0.25	12,500	0.25	1,047				
0.5	12,751	0.5	2,077	0.5	12,751	0.5	2,077				
0.75	13,000	0.75	4,986	0.75	13,000	0.75	4,986				
0.9	13,150	0.9	12,341	0.9	13,150	0.9	12,341				
0.975	13,225	0.975	13,010	0.975	13,225	0.975	13,010				
0.995	13,245	0.995	13,201	0.995	13,245	0.995	13,201				
1	13,250	1	13,250	1	13,250	1	13,250				

The liner failure distributions used for the remaining waste tank types, Type III, IIIA, and IV, were taken directly from the probabilistic analyses presented in WSRC-STI-2007-00061. Similar to the submerged and partially submerged Tank I and Tank II analysis presented in SRNL-STI-2010-00047, the waste tank steel life estimates assume general corrosion and pitting are the main corrosion mechanisms degrading the liners as they are exposed to the CZ, grout, and soil conditions. Appropriate probability distributions were selected to represent Cases A through E, again, based on the oxygen and carbon dioxide diffusion rates. Fast flow Cases B through E applied the probabilities associated with faster carbon dioxide diffusion rates ($1.0\text{E-}4 \text{ cm}^2/\text{s}$) to maximize transport conditions, and the Base Case applied the probabilities associated with the slower carbon dioxide diffusion rates ($1.0\text{E-}6 \text{ cm}^2/\text{s}$). Because Type III, IIIA, and IV tanks are considered unsaturated, the slower oxygen ($1.0\text{E-}6 \text{ cm}^2/\text{s}$) diffusion rate is considered adequate.

Each piece of ancillary equipment (with the transfer lines being treated as a collective inventory) was assumed in the HTF GoldSim Model to fail independently, with the failure time occurring between the time of first pit penetration (116 years) and 100 % pitting penetration (approximately 1,000 years). The most probable time of ancillary equipment failure in the probabilistic HTF analyses assumed 25 % pitting penetration time (510 years). Uncertainty is not considered with respect to the ancillary equipment, containment failure time.

The diffusion rates utilized for all cases are considered bounding (i.e., faster than are typically reported).

5.6.3.8 Transition Times between Chemical States

One of the key factors controlling the dose to downstream receptors is the chemical degradation of the grout and the chemical evolution in the CZ. The chemical state, defined in the HTF GoldSim Model as Region II or Region III, oxidizing or reducing, controls the selection of the solubilities and K_d s applied to the different radionuclides in the engineered system, thus controlling their release rates. Section 4.2.1 discusses the model used to calculate the number of pore volumes required to pass through the waste tank before the grout transitions to different waste tank chemistry. The results of this model are summarized in Section 4.2.1. Table 5.6-16 presents the deterministic pore volumes required to cause a step change to a different chemical state, used as input to the HTF GoldSim Model. The timing of the various chemical transitions can be determined based on the flow rates through the system (which vary by component and by model case), and the waste tank pore volume. The calculated chemical transition times by waste tank are presented in Table 4.2-30 (Section 4.2.2).

Table 5.6-16: Pore Volume Distribution for Chemical Condition Step Change

Waste Tank Position	Transition ^a	Number of Pore Volumes Required		
		Deterministic (Most Likely)	Triangular Distribution	
			Minimum	Maximum
Non Submerged	Reduced Region II to Oxidized Region II (Step 1)	523	366	680
	Oxidized Region II to Oxidized Region III (Step 2)	2,119	1,060	3,179
Submerged	Condition C ^b to Condition D ^b (Step 1)	1,787	1,251	2,323
	Condition D ^b to Oxidized Region III (Step 2)	2,442	1,221	3,663

Based on results from SRNL-STI-2012-00404

a Step 1 = +/- 30 % of most likely; Step 2 = +/- 50 % of most likely

b Where Condition C = water flowing into the CZ is small fraction of groundwater mixed with the Reduced Region II grout pore fluid, and Condition D = water flowing into CZ is small fraction of groundwater mixed with Oxidized Region II grout pore fluid.

Uncertainty in the timing of the chemical transitions is captured by sampling the number of pore volumes required to cause a step change to a different chemical state, instead of using the set deterministic value presented in Table 5.6-16. A triangular distribution is applied to each chemical transition using the range with the minimum and maximum values indicated in Table 5.6-16. The Step 1 minimum and maximum pore flush volumes are set based on $\pm 30\%$ of the deterministic value, and Step 2 is set equal to $\pm 50\%$ of the deterministic value. The variation provided by these values was judged reasonable to provide a distribution that showed the effects of uncertainty. Varying the transition time via the number of pore volumes required enables non-mechanistic probabilistic modeling of the multiple factors that could cause early or late transition (e.g., uncertainty in the initial grout formulation, flow differences, chemistry changes). The transition times can have a significant impact on results, as documented in Section 5.6.4.

5.6.3.9 HTF Lower Vadose Zone Thickness

The lower vadose zone is a natural barrier that slows the transport of certain contaminants. Table 4.2-27 presents the spatially variable lower vadose zone thicknesses below the waste tanks used in the deterministic (baseline) analysis. [SRNL-STI-2010-00148] Negative values indicate the top of the slab is below the water table. The depth of the vadose zone beneath each waste tank is simulated as a constant in HTF GoldSim Model.

5.6.3.10 Saturated Zone Flow Modeling Parameters

For source term releases, the modeling domain for the saturated zone begins at the upgradient edge of the waste tank and extends to the 100-meter boundary. Data input specific to the saturated zone includes, 1) data that describes the flow fields controlling the transport of mass released from the waste tanks and ancillary equipment and 2) data describing the

geometry of the saturated zone and the spatial relationships between the sources (waste tanks and ancillary equipment) and the 100-meter boundary.

The HTF GoldSim Model flow fields were extracted from the HTF PORFLOW Model (see Figures 4.4-50 and 4.4-51 for input points, presented in Section 4.4.4.2). The flow fields vary by component and through time, and therefore reflect degradation of the barrier. The uncertainty associated with the flow fields is represented using different model cases, as described in Section 5.6.3.2.

Three modeling parameters of particular importance in describing the saturated zone geometry and spatial relationships are the Saturated Zone Darcy Velocity, Saturated Zone Thickness, and the Saturated Zone Width. Uncertainty was applied to the saturated zone model by applying probabilistic distributions to these parameters.

5.6.3.10.1 Saturated Zone Darcy Velocity

Groundwater flow in the saturated zone is approximated as a unidirectional flow field of constant Darcy velocity. The flow velocity is derived from a PORFLOW simulation where stream traces were generated based on a particle released at the center of each source (waste tank or ancillary equipment). A particle path length to the 100-meter boundary from the stream trace simulation and the time it took for the peak value of the breakthrough curves to reach the boundary were translated into averaged transport velocities. Darcy velocities were in turn derived from the transport velocities and the saturated zone porosity used in the HTF GoldSim Model as follows:

$$DarcyVelocity = TransportVelocity \times Porosity$$

The waste tank-specific mean Darcy velocities in the saturated zone are presented in Table 5.6-17. These values are used in the HTF GoldSim Model.

Table 5.6-17: Mean Darcy Velocity from Waste Tanks

Waste Tank	Mean Darcy Velocity (ft/yr)
Tank 9	4.01
Tank 10	3.62
Tank 11	4.1
Tank 12	3.93
Tank 13	12.15
Tank 14	4.26
Tank 15	10.62
Tank 16	14.39
Tank 21	10.52
Tank 22	9.24
Tank 23	8.65
Tank 24	8.87
Tank 29	6.25
Tank 30	6.1
Tank 31	6.5
Tank 32	5.88
Tank 35	8.12
Tank 36	9.1
Tank 37	8.73
Tank 38	6.28
Tank 39	7.1
Tank 40	8.37
Tank 41	8.66
Tank 42	6.26
Tank 43	6.82
Tank 48	5.61
Tank 49	10.68
Tank 50	4.74
Tank 51	4.26

[SRR-CWDA-2010-00093 Rev. 1]

The ancillary equipment-specific mean Darcy velocities in the saturated zone are presented in Table 5.6-18, and were derived using the same methodology as was for the waste tank-specific mean Darcy velocities. These values were used in the HTF GoldSim Model.

Table 5.6-18: Mean Darcy Velocity from Ancillary Equipment

Ancillary Equipment	Mean Darcy Velocity (ft/yr)
HPT2	4.31
HPT3	4.2
HPT4	4.13
HPT5	11.21
HPT6	10.71
HPT7	10.38
HPT8	10.1
HPT9	10.59
HPT10	10.41
E242_H	10.73
E242_16H	6.97
E242_25H	7.15
HTF_T_Line1	22.55
HTF_T_Line2	4.94
HTF_T_Line3	15.66
HTF_T_Line4	10.7
CTSO	6.13
CTSN	7.76

[SRR-CWDA-2010-00093 Rev. 1]

Uncertainty associated with variable velocities in the saturated zone presented in Table 5.6-17 and Table 5.6-18 is accounted for by applying a uniform distribution with minimum values set equal to half the mean Darcy velocities and 1.5 times the mean Darcy velocities for the maximum values.

5.6.3.10.2 Saturated Zone Thickness

In the HTF GoldSim Model, water leaving the unsaturated zone enters the saturated zone (i.e., the aquifer) as recharge, and this infiltrating water is mixed into the volume of aquifer water. The concentration in the cell at a given time is determined by the flow rate and mixing volume (flow face area times flow velocity time) in the aquifer. The aquifer thickness is therefore important to the receptor dose calculation, because it defines the cell volume, which directly affects the concentration.

Based on the estimates for the combined thickness of the UTRA-LZ and UTRA-UZ of the UTRA reported in Table 7 of *Hydrogeologic Data Summary in Support of the H-Area Tank Farm Performance Assessment*, the deterministic saturated zone thickness value applied to the HTF GoldSim Model was fixed at 130 feet. Because it falls within the range indicated from existing well data and it is in agreement with modeled PORFLOW values, 130 feet is selected.

The uncertainty associated with the variability in saturated zone thickness, presented in Table 5.6-19, is accounted for by applying a triangular distribution, with the deterministic value of 130 feet representing the most likely value. The minimum value is set equal to 110 feet, while the maximum is set equal to 170 feet. The minimum and maximum values are based on the measured range reported for the combined thicknesses of the UTRA-LZ and UTRA-UZ in the HTF area. [SRNL-STI-2010-00148]

Table 5.6-19: Distribution for Saturated Zone Thickness

	Triangular Distribution		
	Deterministic	Minimum	Maximum
Thickness (ft)	130	110	170

[Table 7, SRNL-STI-2010-00148]

5.6.3.10.3 Saturated Zone Width

The cross-sectional area of the cell network (representing the saturated zone) perpendicular to flow is defined as the product of the saturated zone width and the saturated zone thickness. The saturated zone width for waste tanks is defined as the diameter of the waste tank (Table 5.6-20). Because the waste tank diameter is known, the uncertainty is not considered for the waste tanks.

Table 5.6-20: Saturated Zone Width for Waste Tanks

Tank Type	Saturated Zone Width (ft)
Type I	75
Type II	85
Type III/IIIA	85
Type IV	85

[SRR-CWDA-2010-00093 Rev. 1 Table 4.4-5]

For the ancillary equipment sources, the square root of the source area is used as the saturated zone width (Table 5.6-21). Because the mass released from the ancillary equipment sources is considered to be immediately applied to the unsaturated zone (or saturated zone if applicable) at a specific time, uncertainty on its distribution is considered. The uncertainty in the saturated zone width below ancillary equipment sources is described by a uniform distribution between 0.8 and 1.2 times the deterministic value of the saturated zone width.

Table 5.6-21: Saturated Zone Width for Ancillary Equipment

Ancillary Equipment	Saturated Zone Width (ft)
HPT2	10.63
HPT3	10.63
HPT4	10.63
HPT5	10.63
HPT6	10.63
HPT7	10.63
HPT8	10.63
HPT9	10.63
HPT10	10.63
E242_H	7.09
E242_16H	7.09
E242_25H	12.41
Transfer Lines 1	609.30
Transfer Lines 2	432.32
Transfer Lines 3	621.92
Transfer Lines 4	371.80
CTSO	7.09
CTSN	7.09

[SRR-CWDA-2010-00093 Rev. 1 Table 4.4-6]

5.6.3.11 Well Depth

As discussed in the exposure pathways section of this PA (Section 4.2.3), the well water (located at the 100-meter boundary or seep line) may be used as a primary potable water source for a future resident (e.g., drinking water, showering) and may be used by the resident as a primary water source for agriculture (e.g., irrigation, livestock water). The hypothetical impacts to the MOP can be highly dependent on which aquifer the water is drawn. The report, *Evaluation of Well Drilling Records in the Vicinity of SRS from CY2005 Through CY2009* (SRR-CWDA-2010-00054), examines available on-site well drilling data, and information from regional commercial well drillers to determine probabilities associated with a future resident drilling into a particular aquifer. The deterministic HTF GoldSim Model assumes the water wells are drilled into the UTRA-LZ.

The report SRR-CWDA-2010-00054 concludes that water wells drilled in the SRS area have a high probability of being located in the UTRA-LZ or the deeper Gordon Aquifer (Table 5.6-22).

Table 5.6-22: Probability of Drilling into the Aquifers

Aquifer (Depth)	% of Total in GSA	Dilution Multiplier
UTRA-UZ	4 %	1
UTRA-LZ	52 %	1
Gordon Aquifer	44 %	0.01

To simulate the probability that the well source might be drilled into a lower aquifer (UTRA-LZ or the Gordon Aquifer), the well depth probabilities in Table 5.6-22 were used as a stochastic in the HTF GoldSim Model. During the HTF GoldSim Model multi-realization simulation, 44 % of the realizations used well water drilled from the Gordon Aquifer. For those realizations that drill into the Gordon Aquifer, a dilution multiplier was applied to the GoldSim calculated concentration values (Table 5.6-22). The dilution multiplier was set to 0.01, based on comparison of PORFLOW peak concentrations between the UTRA-LZ and the Gordon Aquifer (Appendix F.2).

5.6.3.12 Bioaccumulation Factors and Human Health Exposure Parameters

The bioaccumulation factors (Section 4.6.1) and human health exposure (Section 4.6.2) parameters were used to calculate dose to the MOP and intruder in the dose calculator module of the HTF GoldSim Model for the different exposure pathways. Other human health exposure factors, described in the following sections, were given a probabilistic distribution in the HTF GoldSim Model in order to evaluate the model’s sensitivity to their uncertainty. The stochastic distributions applied to the human health exposure factors are presented in Tables 5.6-23 through 5.6-29.

Table 5.6-23: Stochastic Crop Exposure Times and Productivity

Parameter	GoldSim Parameter Name	Value	Min	Max	
Vegetable crop exposure times to irrigation (d)	<i>VeggieExposureTime</i>	70	60	90	
Buildup time of radionuclides in soil (d) ^a	<i>SoilBuildupTime</i>	9,125	N/A	N/A	
Agricultural productivity (kg/m ²) ^a	<i>VegetationProductionYield</i>	2.2	0.7	4	
Fraction of Foodstuff Produced Locally		All-Pathway	Intruder	Min	Max
Leafy vegetables and produce	<i>LocalGrown</i> and <i>LocalGrown_Intr</i>	0.173	0.308	0.1	0.5
Meat	<i>FracLocalBeef_MOP</i> and <i>FracLocalBeef_Intr</i>	0.306	0.319	0.1	0.5
Milk	<i>FracLocalMilk_MOP</i> and <i>FracLocalMilk_Intr</i>	0.207	0.254	0.1	0.5
Poultry and Egg ^b	<i>FracLocalChic_MOP</i> and <i>FracLocalChic_Intr</i>	0.306	0.319	0.1	0.5

[WSRC-STI-2007-00004, Table 3-1 except as noted]

a SRNL-STI-2010-00447

b ML083190829, Table B-1

N/A = Not applicable

Table 5.6-24: Stochastic Physical Parameters

Parameter	GoldSim Parameter Name	Value	Min	Max
Water Density (g/mL)	<i>WaterDens</i> (kg/m ³)	1	N/A	N/A
Areal surface density of soil (kg/m ²)	<i>SurfaceSoilDensity</i>	240	180	270
Density of Sandy Soil (kg/m ³) ^a	<i>DryBulkDensity_SandySoil</i>	1,650	N/A	N/A
Airborne release fraction ^b	<i>ARF</i>	1.00E-04	N/A	N/A
Soil loading in air	<i>AirMassLoadingSoil</i>	1.00E-07	1.00E-09	3.00E-07
Depth of garden (cm)	<i>TillDepth and SoilThickness</i>	15	15	61
Water contained in air at ambient conditions (g/m ³) ^c	<i>AirWaterContent</i>	10	N/A	N/A
Water contained in air at shower conditions (g/m ³) ^c	<i>ShowerAirWaterContent</i>	41	N/A	N/A
Soil moisture content ^d	<i>SoilMoistureContent</i>	0.2086	N/A	N/A
Precipitation rate (in/yr) ^d	<i>PR</i>	49.1	N/A	N/A
Evapotranspiration rate (in/yr) ^d	<i>ER</i>	32.6	N/A	N/A
Irrigation rate (in/yr)	<i>IR</i>	52 ^e	N/A	N/A
Irrigation rate (L/d/m ²)	<i>IrrigationRate</i>	3.6 ^e	2.08	5.5
Fraction of the time that vegetation or soil is irrigated	<i>FracYearIrrigate</i>	0.2	0.2	0.25
Weathering decay constant (1/d)	<i>WeatheringDecayConst</i>	0.0495	0.03	0.0495
Fraction of material deposited on leaves that is retained	<i>LeafRetention</i>	0.25	0.2	0.25
Fraction of material deposited on leaves that is retained after washing	<i>WashingFactor</i>	1	N/A	N/A
Area of garden for family of four (m ²)	<i>GardenSize</i>	100	100	500
Well diameter (ft)	<i>WellDiameter</i>	0.667	N/A	N/A
Transfer line circumference (ft)	<i>PipeAreaperLength</i>	0.803	N/A	N/A
Well depth (ft)	<i>WellDepth</i>	100	N/A	N/A

[WSRC-STI-2007-00004, Table 3-2 except as noted]

a WSRC-STI-2006-00198, Table 5-18

b DOE-HDBK-3010-94

c HNF-SD-WM-TI-707

d WSRC-STI-2007-00184

e Based on an assumption of 1 in/wk = 0.36 cm/d. For a 1m² area, 0.36 cm/d x 10,000 cm²/m² x 1L/1,000 cm³=3.6 L/d/m².

N/A = Not applicable

Table 5.6-25: Stochastic Individual Exposure Times and Consumption Rates

Parameter	GoldSim Parameter Name	Recommendation		
		Value	Min	Max
Breathing rate (m ³ /yr)	<i>AirIntake</i>	5,548	1,267	11,600
Consumption Rate				
Soil (kg/yr)	<i>SoilConsumptionRate</i>	0.0365	N/A	N/A
Leafy vegetable (kg/yr)	<i>Leafy</i>	21	18	43
Other vegetable (kg/yr)	<i>Veg</i>	163	90	276
Meat (kg/yr)	<i>BeefConsumptionRate</i>	43	26	81
Poultry (kg/yr) ^d	<i>ChicConsumptionRate</i>	25	Table 5.6-26	
Egg (kg/yr) ^d	<i>EggConsumptionRate</i>	19	Table 5.6-26	
Finfish (kg/yr)	<i>FishConsumptionRate</i>	9	2.2	19
Milk (L/yr)	<i>MilkConsumptionRate</i>	120	73.7	230
Water (L/yr)	<i>WaterConsumptionRate</i>	337	184	730
Fodder-Beef cattle (kg/d)	<i>ConsumptionFodderBeef</i>	36	27	50
Fodder-Milk cattle (kg/d)	<i>ConsumptionFodderMilk</i>	52	36	55
Fodder-Poultry (kg/d) ^d	<i>ConsumptionFodderChic and ConsumptionFodderEgg (clone)</i>	0.1	NA	NA
Fraction of milk-cow feed is from pasture (fodder)	<i>FodderFractionMilk</i>	0.56	0.5	1
Fraction of beef-cow feed is from pasture (fodder)	<i>FodderFractionBeef</i>	0.75	0.5	1
Fraction of Poultry-feed is from pasture (fodder)	<i>FodderFractionChic and FodderFractionEgg (clone)</i>	1	NA	NA
Water (beef cow) (L/d)	<i>CattleWaterConsumptionBeef</i>	28	28	50
Water (milk cow) (L/d)	<i>CattleWaterConsumptionMilk</i>	50	50	60
Water (Poultry) (L/d) ^d	<i>ChicWaterConsumption and EggWaterConsumption (clone)</i>	0.3	NA	NA
Exposure Time				
Swimming (hr/yr) ^a	<i>AnnualSwimming</i>	7	N/A	N/A
Boating (hr/yr) ^a	<i>AnnualBoating</i>	22	N/A	N/A
Showering (min/d)	<i>ExposureFractionShower</i>	10	10	30
Fraction of time spent working in garden	<i>ExposureFractionGarden</i>	0.01	0.01	0.08
Boating geometry factor ^b	<i>BoatingGF</i>	0.5	N/A	N/A
Swimming geometry factor ^b	<i>SwimmingGF</i>	1	N/A	N/A
Fraction of year acute intruder is exposed to drill cuttings ^c	<i>FractionExposedtoCuttings</i>	0.0023	0.0011	0.0046

[WSRC-STI-2007-00004, Table 4-1 except as noted]

a SRNL-STI-2010-00447

b Conservative assumption

c Assumes 20 hours to complete well drilling, for baseline, 10 hours for minimum, and 40 hours for maximum

N/A = Not applicable

Table 5.6-26: Stochastic Human Consumption Rates for Poultry and Eggs

Parameter	GoldSim Parameter Name	Cumulative Probability	Value (kg/yr)
Human Consumption Rate of Poultry Mean Value = 25 kg/yr	<i>ChicConsumptionRate</i>	0	3.85
		0.01	3.85
		0.05	4.18
		0.1	5.94
		0.25	9.57
		0.5	19.85
		0.75	38.22
		0.9	50.83
		0.95	58.52
		0.99	72.81
		1	72.81
Parameter	GoldSim Parameter Name	Cumulative Probability	Value (kg/yr)
Human Consumption Rate of Eggs Mean Value = 19 kg/yr	<i>EggConsumptionRate</i>	0	2.8
		0.01	2.8
		0.05	4.5
		0.1	5.3
		0.25	8.23
		0.5	12.36
		0.75	21.35
		0.9	35.9
		0.95	47.35
		0.99	120.71
		1	120.71

[ML083190829, Table A-1]

Table 5.6-27: Stochastic Transfer Factors for Milk

Milk Transfer Factors		Triangular Distribution	
Element	Recommended Value (d/L)	Min (d/L)	Max (d/L)
Ac	2.00E-05	2.00E-06	2.06E-05
Ag	1.58E-03	5.00E-05	5.00E-02
Al	2.06E-04	2.00E-04	2.06E-04
Am	4.20E-07	4.00E-07	5.00E-06
As	6.00E-05	6.00E-05	1.00E-04
At	1.03E-02	1.00E-02	1.03E-02
Au	5.50E-06	5.00E-06	1.00E-05
B	1.55E-03	1.50E-03	3.00E-03
Ba	1.60E-04	1.60E-04	8.00E-03
Be	8.30E-07	8.30E-07	2.00E-06
Bi	5.00E-04	5.00E-04	1.00E-03
Bk	2.00E-06	4.00E-07	2.00E-06
Br	2.00E-02	2.00E-02	2.06E-02
C	1.20E-02	1.05E-02	1.20E-02
Ca	1.00E-02	3.00E-03	1.03E-02
Cd	1.90E-04	1.20E-04	2.00E-03
Ce	2.00E-05	2.00E-05	1.00E-04
Cf	1.50E-06	7.50E-07	2.00E-06
Cl	1.70E-02	1.50E-02	2.00E-02
Cm	2.00E-05	2.00E-06	2.06E-05
Co	1.10E-04	1.10E-04	2.06E-03
Cr	4.30E-04	1.00E-05	2.20E-03
Cs	4.60E-03	4.60E-03	1.20E-02
Cu	2.00E-03	1.50E-03	1.40E-02
Dy	3.00E-05	2.00E-05	6.00E-05
Er	3.00E-05	2.00E-05	6.00E-05
Es	2.00E-06	4.00E-07	2.00E-06
Eu	3.00E-05	2.00E-05	6.00E-05
F	1.00E-03	1.00E-03	7.00E-03
Fe	3.50E-05	3.00E-05	1.20E-03
Fr	2.06E-02	8.00E-03	2.06E-02
Ga	5.00E-05	1.00E-05	5.15E-05
Gd	3.00E-05	2.00E-05	6.00E-05
Ge	7.21E-02	1.00E-02	7.21E-02
H	1.50E-02	1.00E-20	1.50E-02

Table 5.6-27: Stochastic Transfer Factors for Milk (Continued)

Milk Transfer Factors		Triangular Distribution	
Element	Recommended Value (d/L)	Min (d/L)	Max (d/L)
Ha	5.00E-06	5.00E-06	5.00E-06
He	1.00E-20	1.00E-20	1.00E-20
Hf	5.50E-07	5.50E-07	2.50E-05
Hg	4.70E-04	4.50E-04	5.00E-04
Ho	3.00E-05	2.00E-05	6.00E-05
I	5.40E-03	5.40E-03	1.20E-02
In	2.00E-04	1.00E-04	2.00E-04
Ir	2.00E-06	2.00E-06	2.06E-06
K	7.20E-03	7.00E-03	7.21E-03
La	2.00E-05	5.00E-06	6.00E-05
Li	2.06E-02	2.06E-02	5.00E-02
Lr	5.00E-06	5.00E-06	5.00E-06
Lu	2.06E-05	2.00E-05	6.00E-05
Md	5.00E-06	5.00E-06	5.00E-06
Mg	3.90E-03	3.90E-03	8.00E-03
Mn	4.10E-05	3.00E-05	3.61E-04
Mo	1.10E-03	1.10E-03	7.50E-03
N	2.50E-02	1.00E-02	2.58E-02
Na	1.30E-02	1.30E-02	4.00E-02
Nb	4.10E-07	4.10E-07	2.06E-02
Nd	3.00E-05	5.00E-06	6.00E-05
Ni	9.50E-04	9.50E-04	2.00E-02
No	5.00E-06	5.00E-06	5.00E-06
Np	5.00E-06	5.00E-06	1.00E-05
Os	5.00E-03	1.00E-04	3.50E+00
P	2.00E-02	1.50E-02	2.50E-02
Pa	5.00E-06	5.00E-06	5.15E-06
Pb	1.90E-04	1.90E-04	3.00E-04
Pd	1.00E-02	1.00E-04	1.03E-02
Pm	3.00E-05	2.00E-05	6.00E-05
Po	2.10E-04	2.10E-04	4.00E-04
Pr	3.00E-05	5.00E-06	6.00E-05
Pt	5.15E-03	1.00E-04	5.15E-03
Pu	1.00E-05	1.00E-07	1.00E-05

Table 5.6-27: Stochastic Transfer Factors for Milk (Continued)

Milk Transfer Factors		Triangular Distribution	
Element	Recommended Value (d/L)	Min (d/L)	Max (d/L)
Ra	3.80E-04	3.80E-04	1.30E-03
Rb	1.20E-02	1.00E-02	3.00E-02
Re	1.50E-03	1.40E-04	2.00E-03
Rf	2.00E-05	2.00E-05	2.00E-05
Rh	1.00E-02	5.00E-04	1.03E-02
Rn	1.00E-20	1.00E-20	1.00E-20
Ru	9.40E-06	6.00E-07	2.00E-05
S	7.90E-03	7.90E-03	2.00E-02
Sb	3.80E-05	2.50E-05	1.50E-03
Sc	5.00E-06	5.00E-06	6.00E-05
Se	4.00E-03	4.00E-03	4.50E-02
Si	2.00E-05	2.00E-05	2.06E-05
Sm	3.00E-05	5.00E-06	6.00E-05
Sn	1.00E-03	1.00E-03	2.50E-03
Sr	1.30E-03	8.00E-04	2.80E-03
Ta	4.10E-07	4.10E-07	5.00E-06
Tb	3.00E-05	2.00E-05	6.00E-05
Tc	1.87E-03	2.30E-05	2.50E-02
Te	3.40E-04	2.00E-04	1.00E-03
Th	5.00E-06	5.00E-06	5.15E-06
Ti	7.53E-05	5.50E-07	1.03E-02
Tl	2.00E-03	1.00E-03	1.00E-02
Tm	2.06E-05	2.06E-05	6.00E-05
U	1.80E-03	4.00E-04	1.80E-03
V	2.06E-05	2.00E-05	5.00E-04
W	1.90E-04	1.90E-04	5.00E-04
Y	2.00E-05	1.00E-05	2.00E-03
Yb	2.06E-05	2.06E-05	6.00E-05
Zn	2.70E-03	2.70E-03	3.90E-02
Zr	3.60E-06	5.50E-07	3.09E-05

[SRNL-STI-2010-00447, Table 3, WSRC-STI-2007-00004, Table B-2 and IAEA-472 Table 26]

Table 5.6-28: Stochastic Transfer Factors for Beef

Beef Transfer Factors		Triangular Distribution	
Element	Recommended Value (d/kg)	Min (d/kg)	Max (d/kg)
Ac	4.00E-04	2.00E-05	4.00E-04
Ag	3.00E-03	3.00E-03	1.70E-02
Al	1.50E-03	5.00E-04	1.50E-03
Am	5.00E-04	3.50E-06	5.00E-04
As	2.00E-03	1.50E-03	2.00E-02
At	1.00E-02	1.00E-02	1.00E-02
Au	5.00E-03	2.00E-04	8.00E-03
B	8.00E-04	8.00E-04	8.00E-04
Ba	1.40E-04	1.40E-04	3.00E-02
Be	1.00E-03	1.00E-03	5.00E-03
Bi	4.00E-04	4.00E-04	2.00E-03
Bk	2.50E-05	2.00E-05	4.00E-05
Br	2.50E-02	2.00E-02	5.00E-02
C	3.10E-02	3.10E-02	4.89E-02
Ca	1.30E-02	7.00E-04	1.30E-02
Cd	5.80E-03	4.00E-04	5.80E-03
Ce	2.00E-05	2.00E-05	1.20E-03
Cf	4.00E-05	4.00E-05	5.00E-03
Cl	1.70E-02	1.70E-02	8.00E-02
Cm	4.00E-05	3.50E-06	2.00E-04
Co	4.30E-04	4.30E-04	3.00E-02
Cr	9.00E-03	2.40E-03	3.00E-02
Cs	2.20E-02	4.00E-03	5.00E-02
Cu	9.00E-03	8.00E-03	1.00E-02
Dy	2.00E-05	2.00E-05	5.50E-03
Er	2.00E-05	2.00E-05	4.00E-03
Es	2.50E-05	2.00E-05	2.50E-05
Eu	2.00E-05	2.00E-05	5.00E-03
F	1.50E-01	2.00E-02	1.50E-01
Fe	1.40E-02	1.40E-02	4.00E-02
Fm	2.00E-04	2.00E-04	2.00E-04
Fr	2.50E-03	2.50E-03	3.00E-02
Ga	5.00E-04	3.00E-04	5.00E-04
Gd	2.00E-05	2.00E-05	3.50E-03
Ge	7.00E-01	2.00E-01	7.00E-01

Table 5.6-28: Stochastic Transfer Factors for Beef (Continued)

Beef Transfer Factors		Triangular Distribution	
Element	Recommended Value (d/kg)	Min (d/kg)	Max (d/kg)
H	0.00E+00	0.00E+00	1.20E-02
Ha	5.00E-06	5.00E-06	5.00E-06
Hf	3.16E-05	1.00E-06	1.00E-03
Hg	2.50E-01	1.00E-02	2.50E-01
Ho	3.00E-04	2.00E-05	4.50E-03
I	6.70E-03	2.90E-03	4.00E-02
In	8.00E-03	4.00E-03	8.00E-03
Ir	1.50E-03	1.50E-03	2.00E-03
K	2.00E-02	2.00E-02	2.00E-02
La	1.30E-04	1.30E-04	2.00E-03
Li	1.00E-02	1.00E-02	2.00E-02
Lr	2.00E-04	2.00E-04	2.00E-04
Lu	4.50E-03	2.00E-03	4.50E-03
Mg	2.00E-02	3.00E-03	2.00E-02
Mn	6.00E-04	4.00E-04	1.00E-03
Mo	1.00E-03	1.00E-03	8.00E-03
N	7.50E-02	1.00E-02	7.50E-02
Na	1.50E-02	1.50E-02	8.00E-02
Nb	2.60E-07	2.60E-07	2.80E-01
Nd	2.00E-05	2.00E-05	3.30E-03
Ni	5.00E-03	5.00E-03	5.30E-02
No	2.00E-04	2.00E-04	2.00E-04
Np	1.00E-03	5.50E-05	1.00E-03
Os	4.00E-01	2.00E-03	4.00E-01
P	5.50E-02	4.60E-02	2.00E-01
Pa	4.47E-04	5.00E-06	5.00E-03
Pb	7.00E-04	3.00E-04	8.00E-04
Pd	4.00E-03	2.00E-04	4.00E-03
Pm	2.00E-05	2.00E-05	5.00E-03
Po	5.00E-03	9.50E-05	5.00E-03
Pr	2.00E-05	2.00E-05	4.70E-03
Pt	4.00E-03	2.00E-04	4.00E-03
Pu	1.10E-06	5.00E-07	1.00E-04
Ra	1.70E-03	2.50E-04	1.70E-03
Rb	1.00E-02	1.00E-02	3.10E-02

Table 5.6-28: Stochastic Transfer Factors for Beef (Continued)

Beef Transfer Factors		Triangular Distribution	
Element	Recommended Value (d/kg)	Min (d/kg)	Max (d/kg)
Re	8.00E-03	1.00E-04	1.00E-02
Rh	2.00E-03	1.00E-03	2.00E-03
Rn	1.00E-20	1.00E-20	1.00E-20
Ru	3.30E-03	2.00E-03	4.00E-01
S	2.00E-01	1.00E-01	2.00E-01
Sb	1.20E-03	4.00E-05	4.00E-03
Sc	1.50E-02	2.00E-03	1.50E-02
Se	1.50E-02	1.50E-02	1.00E-01
Si	4.00E-05	4.00E-05	3.00E-04
Sm	3.16E-04	2.00E-05	5.00E-03
Sn	8.00E-02	1.00E-02	8.00E-02
Sr	1.30E-03	3.00E-04	1.00E-02
Ta	1.34E-05	3.00E-07	6.00E-04
Tb	2.00E-05	2.00E-05	4.50E-03
Tc	6.32E-03	1.00E-04	4.00E-01
Te	7.00E-03	7.00E-03	7.70E-02
Th	2.30E-04	6.00E-06	2.30E-04
Ti	1.73E-04	1.00E-06	3.00E-02
Tl	4.00E-02	2.00E-03	4.00E-02
Tm	4.50E-03	2.00E-03	4.50E-03
U	3.90E-04	2.00E-04	8.00E-04
V	2.50E-03	2.50E-03	1.00E-02
W	4.00E-02	1.30E-03	4.50E-02
Y	1.00E-03	3.00E-04	8.00E-03
Yb	4.00E-03	2.00E-03	4.00E-03
Zn	1.60E-01	3.00E-02	1.60E-01
Zr	1.20E-06	1.00E-06	3.40E-02

[SRNL-STI-2010-00447, Table 4, WSRC-STI-2007-00004, Table B-3 and IAEA-472 Table 30]

Table 5.6-29: Stochastic Transfer Factors for Fish

Fish Transfer Factors		Triangular Distribution	
Element	Recommended Value (L/kg)	Min (L/kg)	Max (L/kg)
Ac	2.50E+01	1.50E+01	2.50E+01
Ag	1.10E+02	2.30E+00	1.10E+02
Al	5.10E+01	1.00E+01	5.00E+02
Am	2.40E+02	2.10E+01	2.40E+03
As	3.30E+02	1.00E+02	1.70E+03
At	1.50E+01	1.50E+01	1.50E+01
Au	2.40E+02	3.30E+01	2.40E+02
Ba	1.20E+00	1.20E+00	2.00E+02
Be	1.00E+02	2.00E+00	1.00E+02
Bi	1.50E+01	1.00E+01	1.50E+01
Bk	2.50E+01	2.50E+01	2.50E+01
Br	9.10E+01	9.10E+01	4.20E+02
C	3.00E+00	3.00E+00	5.00E+04
Ca	1.20E+01	1.20E+01	1.00E+03
Cd	2.00E+02	2.00E+02	2.00E+02
Ce	2.50E+01	1.00E+00	5.00E+02
Cf	2.50E+01	2.50E+01	2.50E+01
Cl	4.70E+01	4.70E+01	1.00E+03
Cm	3.00E+01	2.10E+01	2.50E+02
Co	7.60E+01	5.00E+01	3.30E+02
Cr	4.00E+01	4.00E+00	2.00E+02
Cs	3.00E+03	2.00E+03	4.70E+03
Cu	2.30E+02	5.00E+01	2.30E+02
Dy	6.50E+02	3.00E+01	6.50E+02
Er	3.00E+01	3.00E+01	3.00E+01
Es	2.50E+01	1.00E+01	2.50E+01
Eu	1.30E+02	2.50E+01	1.30E+02
F	1.00E+01	1.00E+01	1.00E+01
Fe	1.70E+02	1.00E+02	2.00E+03
Fr	3.00E+01	3.00E+01	3.00E+01
Ga	4.00E+02	3.33E+02	4.00E+02
Gd	3.00E+01	2.50E+01	3.00E+01
Ge	4.00E+03	3.33E+03	4.00E+03
He	1.00E+00	1.00E+00	1.00E+00
H	1.00E+00	9.00E-01	1.00E+00

Table 5.6-29: Stochastic Transfer Factors for Fish (Continued)

Fish Transfer Factors		Triangular Distribution	
Element	Recommended Value (L/kg)	Min (L/kg)	Max (L/kg)
Hf	1.10E+03	3.33E+00	1.10E+03
Hg	6.10E+03	1.00E+03	6.10E+03
Ho	3.00E+01	2.50E+01	3.00E+01
I	3.00E+01	1.50E+01	5.00E+02
In	1.00E+04	1.00E+04	1.00E+05
Ir	1.00E+01	1.00E+01	1.00E+01
K	3.20E+03	1.00E+03	1.00E+04
La	3.70E+01	2.50E+01	3.70E+01
Lu	2.50E+01	2.50E+01	2.50E+01
Mg	3.70E+01	3.70E+01	5.00E+01
Mn	2.40E+02	1.00E+02	4.00E+02
Mo	1.90E+00	1.90E+00	1.00E+01
N	2.00E+05	1.50E+05	2.00E+05
Na	7.60E+01	8.00E+00	1.00E+02
Nb	3.00E+02	2.00E+02	3.00E+04
Nd	3.00E+01	2.50E+01	1.00E+02
Ni	2.10E+01	2.10E+01	1.00E+02
Np	2.10E+01	1.00E+01	2.50E+02
O	1.00E+00	1.00E+00	1.00E+00
Os	1.00E+03	1.00E+01	1.00E+05
P	1.40E+05	1.50E+03	1.40E+05
Pa	1.00E+01	1.00E+01	1.13E+01
Pb	2.50E+01	2.50E+01	3.00E+02
Pd	1.00E+01	1.00E+01	1.00E+01
Pm	3.00E+01	2.50E+01	3.00E+01
Po	3.60E+01	3.60E+01	5.00E+02
Pr	3.00E+01	2.50E+01	1.00E+02
Pt	3.50E+01	3.50E+01	1.00E+02
Pu	3.00E+01	3.50E+00	4.70E+03
Ra	4.00E+00	4.00E+00	7.00E+01
Rb	4.90E+03	2.00E+03	4.90E+03
Re	1.20E+02	1.19E+02	1.20E+04
Rh	1.00E+01	1.00E+01	1.00E+01
Rn	7.55E-10	7.55E-10	5.70E+01
Ru	5.50E+01	1.00E+01	1.00E+02

Table 5.6-29: Stochastic Transfer Factors for Fish (Continued)

Fish Transfer Factors		Triangular Distribution	
Element	Recommended Value (L/kg)	Min (L/kg)	Max (L/kg)
S	8.00E+02	7.50E+02	1.00E+03
Sb	3.70E+01	1.00E+00	2.00E+02
Sc	1.90E+02	1.00E+02	1.90E+02
Se	6.00E+03	1.70E+02	6.00E+03
Si	2.00E+01	2.50E+00	2.00E+01
Sm	3.00E+01	2.50E+01	3.00E+01
Sn	3.00E+03	3.00E+03	3.00E+03
Sr	2.90E+00	2.90E+00	5.01E+02
Ta	3.00E+02	1.00E+02	3.00E+04
Tb	4.10E+02	2.50E+01	4.10E+02
Tc	2.00E+01	1.50E+01	2.00E+01
Te	1.50E+02	1.50E+02	4.00E+02
Th	6.00E+00	6.00E+00	1.00E+02
Ti	1.90E+02	1.90E+02	1.00E+03
Tl	9.00E+02	9.00E+02	1.00E+04
U	9.60E-01	9.60E-01	5.00E+01
V	9.70E+01	1.00E+01	2.00E+02
W	1.00E+01	1.00E+01	1.20E+03
Y	4.00E+01	2.50E+01	4.00E+01
Zn	3.40E+03	3.50E+02	3.40E+03
Zr	2.20E+01	3.30E+00	3.00E+02

[SRNL-STI-2010-00447, Table 5, WSRC-STI-2007-00004, Table B-4 and IAEA-472 Table 57]

Where available, site-specific values and distribution information obtained from WSRC-STI-2007-00004 and SRNL-STI-2010-00447 was used in determining the values and stochastic range to be evaluated. Where no specific guidance was available, a triangular distribution using maximum and minimum values from WSRC-STI-2007-00004 was implemented. The value used in the deterministic analysis was applied to the most likely value as defined in SRNL-STI-2010-00447. For cases where site-specific distribution data was not available, it was judged reasonable to use the maximum and minimum values suggested in WSRC-STI-2007-00004. Where applicable, limits were adjusted based upon values presented in IAEA-472. Although the data distributions may not be site-specific and have not been weighted for the purpose of the stochastic analysis, they provide a wide range of possible outcomes and are therefore better able to identify parameters of potential concern.

The documents WSRC-STI-2007-00004 and SRNL-STI-2010-00447 do not present human health exposure factors related to the dose from eating poultry and eggs. Therefore, the values related to the chicken and the egg dose pathways presented in Tables 5.6-23, 5.6-25

and 5.6-26 are based on parameter sets presented in *Description of Methodology for Biosphere Dose Model BDOSE*. [ML083190829] Lacking specific site information for the fraction of poultry and eggs produced locally, ML083190829 assumes the same fraction used for locally produced beef for the SRS site, and this fraction was applied for the HTF dose to the receptors. Note a different value was used for the all-pathways dose versus the intruder dose (Table 5.6-23). Similarly, the minimum and maximum values used for SRS-specific fraction of locally produced beef were used for the minimum and maximum fraction of locally produced egg and poultry. The values representing the fraction of locally produced beef was selected for use in the chicken and egg pathway because out of the different food products produced locally, beef had the highest, most conservative fraction. The other various chicken and egg parameter values identified in Tables 5.6-25 and 5.6-26 were extracted from Table A-1 of ML083190829 and based on national averages. Further information regarding most of the distributions presented in the summary tables is provided in WSRC-STI-2007-00004.

5.6.3.12.1 Drinking Water Ingestion

Ingestion of water is a key usage factor for the all-pathway and inadvertent intruder analyses. The rate of contaminated water consumption can vary by exposure scenario based on assumed access to the water supply. For the inadvertent intruder where the contaminated water is expected to come from a well, an assumption can be made that water from the well is only used for cooking. Likewise, for the all-pathway analyses the assumption could be made that total water intake comes from the community water supply. However, in the absence of site and/or regional specific surveys, national estimates are appropriate.

The RESRAD 511 L/yr (1.4 L/d) average water ingestion rate updated for use in the all-pathway analyses is based on EPA surveys published in the early 1990s. [ANL-EAD-4] The 730 L/yr (2 L/d) water ingestion rates for the inadvertent intruder are taken from *Site-Specific Parameter Values for the Nuclear Regulatory Commission's Food Pathway Dose Model* (ISSN 0017-9078 - Volume 62), and are based on 10 CFR 50, Appendix I rates for the MEI. The average rate for ingestion of drinking water listed in those sources is 370 L/yr (1 L/d). These publications consider indirect ingestion of water but do not consider whether the water was bottled or if it came from a community or commercial source.

An EPA drinking water survey estimates per capita ingestion of water using data from the combined 1994, 1995, 1996, and 1998 *Continuing Survey of Food Intakes by Individuals*, (EPA-822-R-00-001) conducted by the USDA. This publication considers indirect ingestion of water from food with water added at the final phase of food preparation and reports water consumption from community water, bottled water, water from other sources, missing source, and total water. Summary data found in EPA-822-R-00-001 Executive Summary provided a 337 L/yr water ingestion rate.

According to the EPA, direct water is plain water ingested directly, as a beverage, and indirect water is water added to foods and beverages during final preparation at home, or by food service establishments, such as school cafeterias and restaurants. An example of

indirect water is water added to dry cake mix. Community water is tap water from the community water supply. Bottled water is purchased, plain water. Other water is water obtained from a well or rain cistern (household's), spring (household's or public), or other source. Preparation water is water used to prepare foods and includes the water used to prepare foods at home and by local food service establishments (indirect water), as well as water added by commercial food manufacturers. Missing water source indicates that a survey participant responded, "don't know" or "not ascertained" to the survey question regarding the source of water. Total water is the sum of direct and indirect water from all sources, which includes community water, bottled water, other water, and missing sources. [EPA-822-R-00-001]

The EPA drinking water survey reports the mean per capita total water ingestion is 1,233 mL/person/d (450 L/yr) when viewed across genders and all age categories with 75% from community water, 13% from bottled water, 10% from other sources (well, spring and cistern, etc.), and 2% from non-identified sources. This yields a per person mean of 924 mL/d (337 L/yr) from community water and 12.3 mL/d (4.5 L/yr) from other sources. [EPA-822-R-00-001]

A value of 337 L/yr is used as the nominal water ingestion rate for all MOP and inadvertent intruder pathway analysis. In the stochastic analyses of this parameter, the water ingestion rate range was assumed to be as high as 730 L/yr (2 L/d), which, as discussed above, is a maximum evaluation point provided by the NRC. [Regulatory Guide 1.109] The lower range of the water ingestion rate range was set at 184 L/yr the minimum recommended water ingestion rate is cut in half (e.g., water or other liquids from a clean source are used instead of drinking water from a contaminated source). A triangular distribution is used in the stochastic analysis, which causes the mean value for this parameter to rise well above the most likely value (417 L/yr versus 337 L/yr).

5.6.4 HTF Probabilistic UA/SA Model

A separate model was developed for performing the probabilistic UA/SA of the HTF PA calculations using the GoldSim system analysis software (Section 4.4.4.2). This model is intended to address the levels of uncertainty and sensitivity surrounding the PA calculations. The probabilistic UA/SA results can be used to place the deterministic analyses results (which are used to demonstrate compliance with the performance objectives) into context (i.e., to risk inform the deterministic results).

This model was run multiple times to develop results to support the probabilistic UA/SA. These modeling runs use the Monte Carlo method to sample uncertain parameters. Each run performed multiple realizations, where each realization represents a unique possible future outcome. The Monte-Carlo method samples values from each of the uncertain parameters during each realization. Collectively, all of the runs and realizations cover the complete probabilistic range for each parameter. The results of the independent realizations are assembled into probability distributions of possible outcomes. The following sections summarize these results.

The uncertainty analyses are concerned with how the uncertainty in model input parameters is propagated through the model to the selected model results, or endpoints. These model

endpoints are potential radiological doses to hypothetical human receptors and aqueous concentrations of specific radionuclide contaminants. (Note that the endpoints selection was based on previous HTF PA modeling results from Revision 0.) In contrast, the SA, discussed in Section 5.6.5, is focused on determining which of the many input parameters are most responsible for determining the endpoint values.

The probabilistic results of the HTF PA GoldSim Model are used to characterize uncertainty manifested in the model input distributions. Some of these distributions are parameter values, such as material properties or water flow rates. Others are more oriented toward model uncertainty, such as the parameter that selects the waste tank case to choose for a specific waste tank in a given realization. Collectively, the distributions of the uncertainty parameters in GoldSim are intended to capture the overall uncertainty in the model. These probabilistic model uncertainty analyses are not intended to quantify conceptual model uncertainty or uncertainty induced by model structure. Identification of conceptual model areas of importance is primarily accomplished throughout the combined sensitivity analyses (both probabilistic and single-parameter sensitivities). The SA (in Section 5.6.5) highlights the portions of the conceptual model that most influence the model results.

The HTF UA/SA is based on inputs and results for the HTF GoldSim Model using version *HTF Transport Model v0.025.gsm*. Three modeling cases were performed for use in the uncertainty analyses. Results presented for the Base Case and Case D are generated from 3,000 realizations that were performed using GoldSim probabilistic capability. These realizations were run in sets of 1,000 realizations, with Latin Hyper Cube sampling enabled and using different sampling seeds for each set. The sensitivity analysis (in Section 5.6.5) uses all 3,000 realizations, combined into one dataset.

In addition to the examination of the Base Case and Case D, a set of realizations was performed to collectively evaluate the effects of all waste tank cases (i.e., Cases A through E). In this “All Cases” run, every waste tank independently sampled the possible waste tank cases during each realization. As there are multiple waste tank cases to be considered, more realizations were required. The probabilistic uncertainty and sensitivity analyses consider 5,000 realizations, combined from five sets of 1,000 realizations.

Like the Base Case and Case D, the All Cases run was performed over a span of 20,000-years. In addition, another 1,000 realizations of the All Cases run was performed over a 100,000-year period, with modified time steps (to conserve computational efficiency). This additional run provides additional insight into the timing and magnitude of peak doses over all time. Table 5.6-30 presents the time stepping scheme used in both the 20,000-year duration and the 100,000-year duration modeling runs.

Table 5.6-30: Time Stepping for Probabilistic (Uncertainty and Sensitivity) Modeling

Duration of Model (years)	Time Range (years)	Number of Time Steps	Length (years)
20,000	0 to 20,000	2,000	10
100,000	0 to 10,000	1,000	10
	10,000 to 20,000	500	20
	20,000 to 30,000	200	50
	30,000 to 100,000	700	100

The Base Case (Case A) was selected because it is representative of the Base Case and, therefore, reflects the most probable and defensible values. Case D was selected as a representative “fast flow path” configuration (i.e., a channel with no flow impedance through the grout and the basemat, coupled with the early failure of the waste tank liner) to demonstrate low probability, but high-risk values. These modeling configurations are described in Section 4.4.2. The names of the GoldSim model files used in the probabilistic uncertainty and sensitivity analyses are listed in Table 5.6-31.

Table 5.6-31: GoldSim Model Files Used in the Probabilistic UA/SA

Waste Tank Configuration	GoldSim Model Files	Sampling Seed	Duration of Model (years)	Number of Realizations
Case A	<i>HTF Transport Model v0.025 CaseA r1000 s1.gsm</i>	1	20,000	1,000
Case A	<i>HTF Transport Model v0.025 CaseA r1000 s2t.gsm^a</i>	2	20,000	1,000
Case A	<i>HTF Transport Model v0.025 CaseA r1000 s3.gsm</i>	3	20,000	1,000
Case D	<i>HTF Transport Model v0.025 CaseD r1000 s1.gsm</i>	1	20,000	1,000
Case D	<i>HTF Transport Model v0.025 CaseD r1000 s2t.gsm^a</i>	2	20,000	1,000
Case D	<i>HTF Transport Model v0.025 CaseD r1000 s3.gsm</i>	3	20,000	1,000
All Cases	<i>HTF Transport Model v0.025 CaseAll r1000 s01.gsm</i>	1	20,000	1,000 (996) ^b
All Cases	<i>HTF Transport Model v0.025 CaseAll r1000 s02.gsm</i>	2	20,000	1,000
All Cases	<i>HTF Transport Model v0.025 CaseAll r1000 s03.gsm</i>	3	20,000	1,000
All Cases	<i>HTF Transport Model v0.025 CaseAll r1000 s04t.gsm^a</i>	4	20,000	1,000
All Cases	<i>HTF Transport Model v0.025 CaseAll r1000 s05t.gsm</i>	5	20,000	1,000
All Cases (100ky)	<i>HTF Transport Model v0.025 100ky CaseAll r1000 s1.gsm</i>	1	100,000	1,000

a Models used for uncertainty analysis figures, below.

b During sensitivity analysis investigation of the All Cases run performed with a sampling seed value of 1 and 1,000 realizations, it was determined that the last four realizations showed that the GoldSim model output spurious results (e.g., 0 mrem/yr for the peak doses); therefore, these last four realizations were ignored for analysis.

Case A = Base Case

When reviewing results from the probabilistic UA/SA, it should be noted that model variability is limited by which model parameters are defined as uncertain variables (which are sampled during each realization) as opposed to those parameters defined as known quantities (i.e., input parameters that remain unchanged regardless of sampling). From the model’s perspective, the definition of an input variable as a single value implies that the value is known perfectly. Uncertainty shown in the results does not take into account any contributions from these static (or deterministic) inputs, thereby underestimating potential uncertainty.

5.6.4.1 Uncertainty Analysis Summary Results

The most direct way to communicate the uncertain nature of the model results is to show graphs of certain key model endpoints. Statistics for peak values (e.g., mean of the peaks) are summarized in Table 5.6-32 for any time step within 10,000 years, plus the peak values from the All Cases run for any time step within 100,000 years.

The table focuses on peak doses to the MOP at the 100-meter boundary of the HTF because this is the relevant performance metric with respect to regulatory compliance. The study, therefore, focuses on the peak doses achieved within the 10,000-year period. Table 5.6-32 also provides peak doses over the 100,000-year time frame (for robustness).

Table 5.6-32: Statistics of the Peak Doses within Any Time Step

Endpoint Evaluated	Number of Realizations	Mean of the Peaks (mrem/yr)	Median of the Peaks (50 th Percentile) (mrem/yr)	95 th Percentile of the Peaks (mrem/yr)
MOP dose from Case A within 10,000 years	3,000	85	9	520
MOP dose from Case D within 10,000 years	3,000	210	31	980
MOP dose from All Cases within 10,000 years	5,000	220	28	1,000
MOP Dose from All Cases within 100,000 years	1,000	530	310	1,900

The values presented in Table 5.6-32 do not reflect the same statistical data as the statistical values and time histories shown in the following table and figures, although these are complementary of one another. The difference between information presented in the table above and information below is important to understand. The previous table shows summary statistics for peak MOP doses achieved at any time within the given time frames (e.g., 0 years to 10,000 years after closure). These are *statistics of the peak values* (e.g., mean of the peaks), regardless of when the peaks were achieved within the specific time frames. Alternatively, the information provided below examines statistics relative to each time step and offers *peak values of the statistics* (e.g., peak of mean). Figure 5.6-30, illustrates the difference between the mean of the peaks and the peak of the mean. This figure also demonstrates that the mean of the peaks can exceed the peak of the mean, as reflected in these uncertainty results. For example, the All Cases *mean of the peaks* of the MOP dose within 100,000 years is about 530 mrem/yr and reflects data over the entire range of the time frame (see Table 5.6-33), whereas the *peak of the mean* is only about 200 mrem/yr and occurs at 67,300 years after closure (see Table 5.6-34).

Figure 5.6-30: Difference between the Mean of Peaks and the Peak of Means

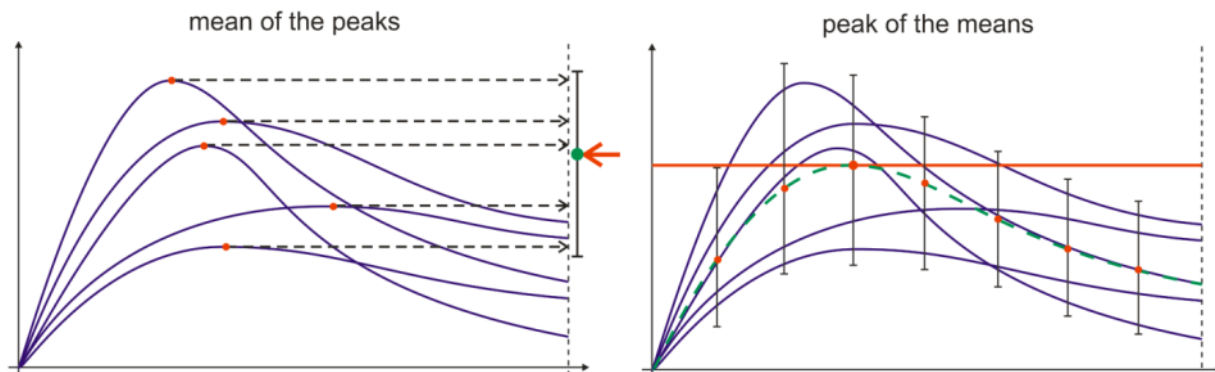


Table 5.6-33: Peak Doses of the Statistics

Endpoint Evaluated	Peak of the Means (mrem/yr)	Peak of the Medians (50 th Percentile) (mrem/yr)	Peak of the 95 th Percentiles (mrem/yr)
MOP dose from Case A within 10,000 years ^a	13 (at time step = 8,240 years)	2.3 (at time step = 9,950 years)	24 (at time step = 9,850 years)
MOP dose from Case D within 10,000 years ^b	35 (at time step = 9,620 years)	12 (at time step = 9,990 years)	112 (at time step = 9,960 years)
MOP dose from All Cases within 10,000 years ^c	15 (at time step = 9,750 years)	5.6 (at time step = 9,990 years)	58 (at time step = 1,470 years)
MOP dose from All Cases within 100,000 years ^d	205 (at time step = 67,300 years)	168 (at time step = 55,800 years)	684 (at time step = 77,100 years)

a From GoldSim model file: HTF Transport Model v0.025 CaseA r1000 s2t.gsm.

b From GoldSim model file: HTF Transport Model v0.025 CaseD r1000 s2t.gsm.

c From GoldSim model file: HTF Transport Model v0.025 CaseAll r1000 s04t.gsm.

d From GoldSim model file: HTF Transport Model v0.025 100ky CaseAll r1000 s1.gsm.

Figures 5.6-31 and 5.6-32 present the statistical time histories of the MOP doses based on the sector of highest dose within a 10,000-year period for the Base Case and Case D, respectively. Figures 5.6-33 and Figure 5.6-34 present similar time histories for the All Cases runs, over 10,000 year and 100,000 years, respectively. Each of these figures provides the results for a single set of 1,000 realization runs from the respective modeling cases.

In all four figures, the 5th and 95th percentiles are significantly below and above the median value, respectively. The mean values are driven higher, approaching the 75th percentile, by the uncertainty distributions of the modeled parameters. This indicates that the model applies distributions with long tails (e.g., lognormal distributions) or extreme values are inherent in these distributions. It is somewhat expected that the mean value is higher than the median because many of the dominant distributions were established to be reasonably conservative, resulting in the distributions being skewed to the high end. This approach inflates the variance in the uncertainty analyses, resulting in a few realizations dominating the uncertainty analyses results. The intent of Section 5.6.4.2 is to investigate which parameters are having the most impact on this aspect of the uncertainty analyses.

Figure 5.6-31: Statistical Time History of MOP Doses for Base Case (0 to 10,000 Years)

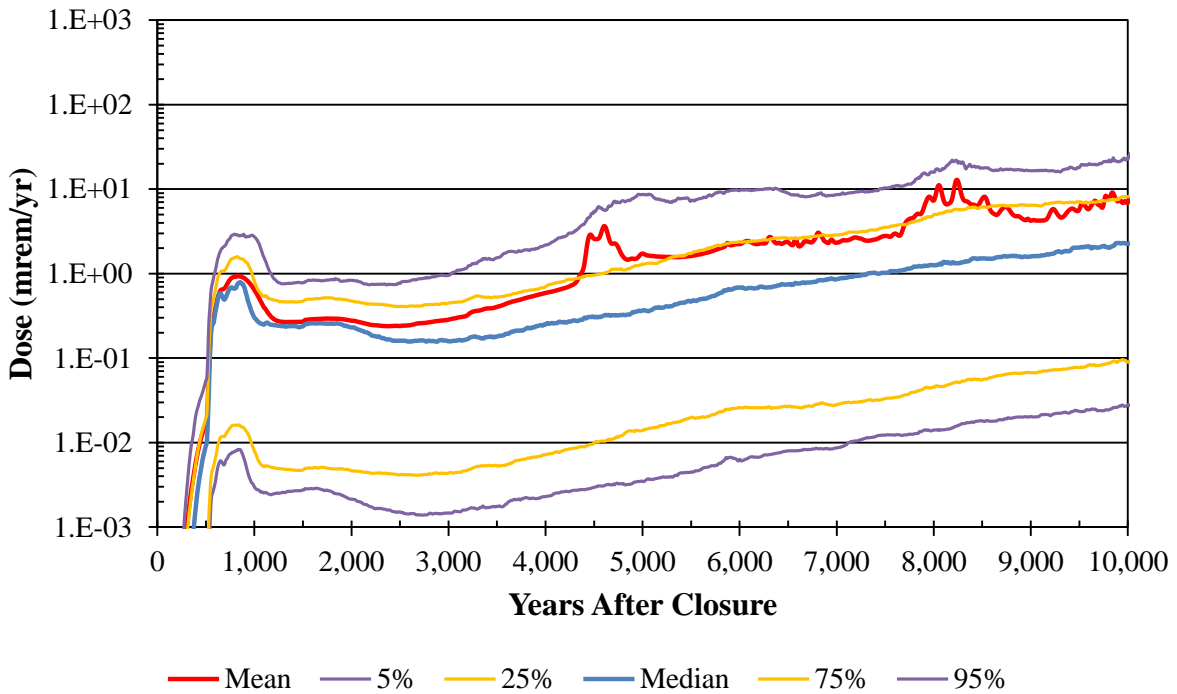


Figure 5.6-32: Statistical Time History of MOP Doses for Case D (0 to 10,000 Years)

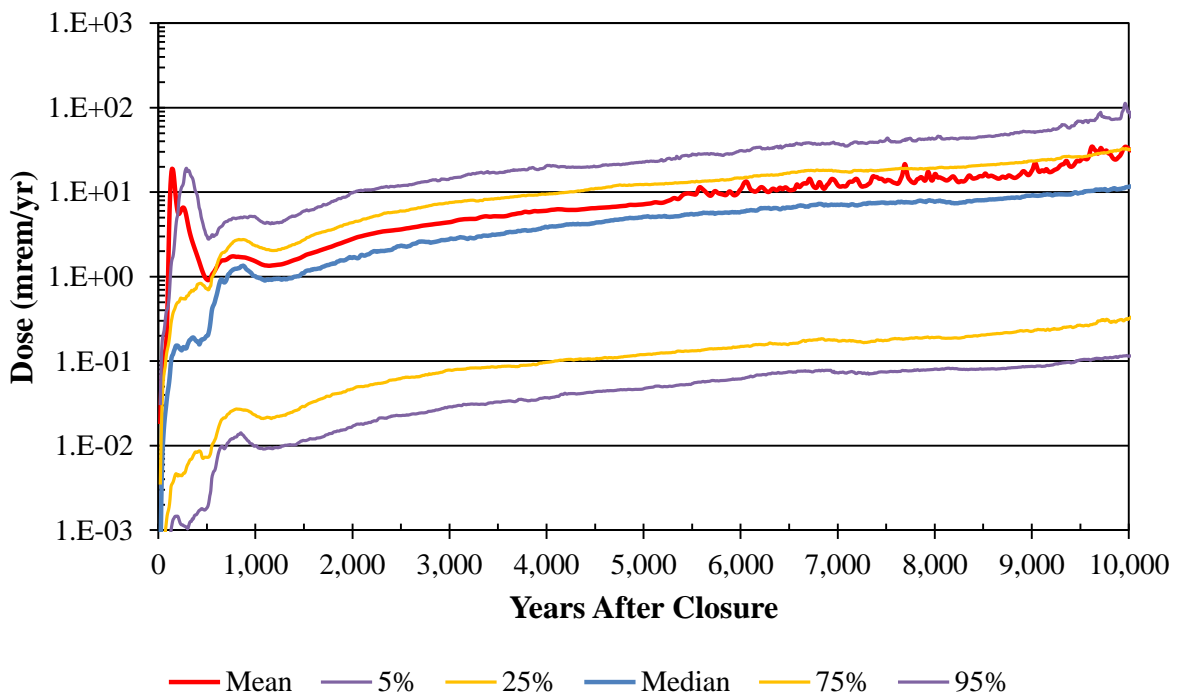


Figure 5.6-33: Statistical Time History of MOP Doses for All Cases (0 to 10,000 Years)

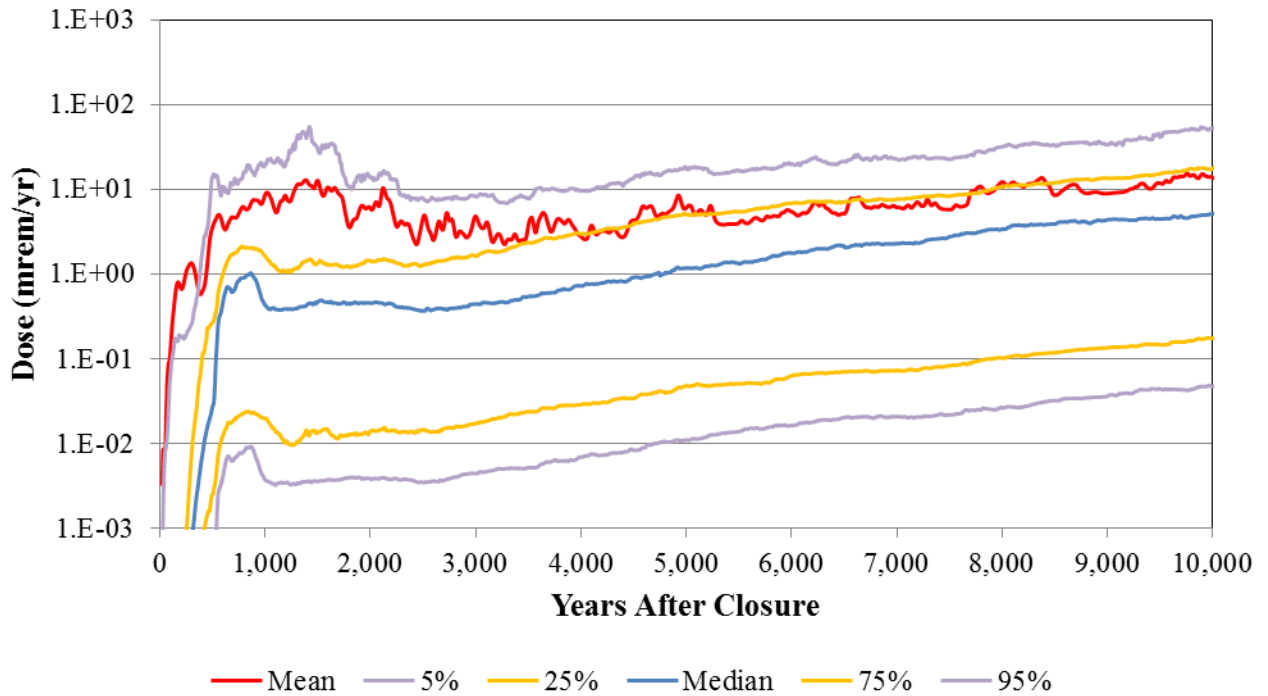
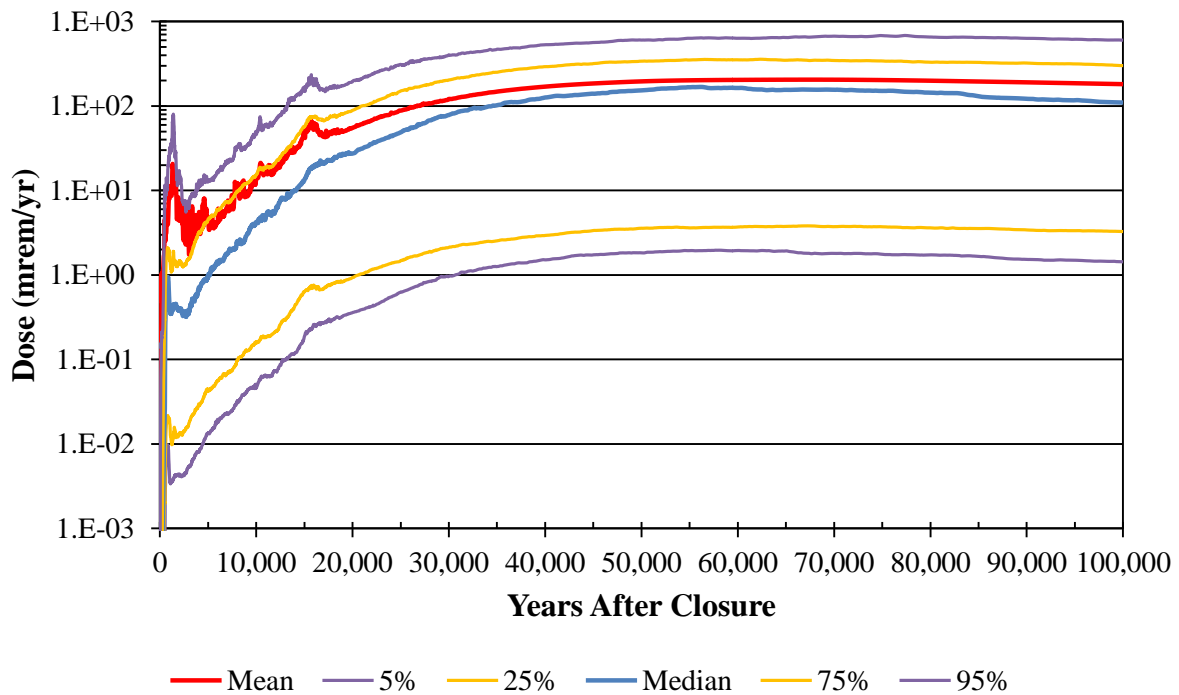


Figure 5.6-34: Statistical Time History of MOP Doses for All Cases (0 to 100,000 Years)



The “choppy” behavior in the mean and the 95th percentile doses are due to Tc-99 releases that “spike” when specific model conditions are met (e.g., chemical transitions in the CZ). As seen in Figure 5.6-34, after 20,000 years, the impact of Tc-99 is overcome by the releases from longer-lived, slower-moving radionuclides (such as Ra-226).

5.6.4.2 *Uncertainty Analysis Insights*

Based on the information presented in the uncertainty analyses section, the following general insights regarding the uncertainty analyses can be drawn.

- For the Base Case within 10,000 years, the mean of the peaks of the MOP doses is 85 mrem/yr and the peak of the means is lower at 13 mrem/yr.
- For the Base Case within 10,000 years, the 95th percentile of the peaks of the MOP doses is 520 mrem/yr and the peak of the 95th percentiles is lower at 24 mrem/yr.
- Based on the dose statistics reported in Tables 5.6-32 and 5.6-33, the Base Case uncertainty analysis dose results are lower than the dose results from the other uncertainty cases.
- The dose results from the Case D and All Cases realizations are not significantly greater than the Base Case results.
- The means are higher than the medians because many of the dominant distributions were established to be reasonably conservative, resulting in the distributions being skewed to the high end. This conservative bias can lead to misleading analyses if only the means are considered.

5.6.4.3 *Uncertainty Analysis Realizations of Interest*

This section identifies individual parameters that significantly impact uncertainty analyses by investigating realizations that significantly affect the overall results. Recognizing that the realizations with the highest dose to the MOP may have the most significant impact on the uncertainty analyses, the top five realizations from each of the uncertainty analysis models (Cases A, Case D and the All Cases run) were used for this evaluation. For each of these three cases, the evaluation was conducted by analyzing the five realizations (from the 1,000 realization sets used in Figures 5.6-31 through 5.6-33) that produce the highest peak doses to the MOP within 10,000 years. The highest dose consequences are those that have a combination of parameters with values significantly different from what is expected (i.e., the deterministic Base Case values) such that when they occur concurrently they produce dose results that are significantly higher than others. Parameters of interest are identified that have the greatest potential to influence the results.

5.6.4.3.1 Base Case (Case A) Realizations

The GoldSim model, *HTF Transport Model v0.025 CaseA r1000 s2t.gsm*, was used to generate 1,000 realizations. These 1,000 realizations are used here to identify the five realizations with the highest peak doses within the performance period for the Base Case. The results of this review are shown in Table 5.6-34. The Base Case peak dose from the deterministic PORFLOW model is also included for comparison.

Table 5.6-34: Five Highest MOP Dose Results from 1,000 Base Case Realizations within 10,000 Years

Realization	Peak Dose (mrem/yr)	Time of Peak Dose (yr)	Sector of Peak Dose	Major Pathway Contributors	Major Radionuclide Contributors
Deterministic Case ^a	4.0	8,790	A	Water Ingestion (58 %) Veg. Ingestion (35 %)	Tc-99 (100 %)
R 12 ^b	3,483	8,240	A	Beef Ingestion (68 %) Veg. Ingestion (13 %)	Tc-99 (100 %)
R 844 ^b	2,093	8,040	A	Beef Ingestion (72 %) Veg. Ingestion (12 %)	Tc-99 (100 %)
R 691 ^b	1,841	8,240	A	Beef Ingestion (53 %) Veg. Ingestion (33 %)	Tc-99 (100 %)
R 126 ^b	1,742	8,060	A	Beef Ingestion (72 %) Veg. Ingestion (12 %)	Tc-99 (100 %)
R 245 ^b	1,673	7,930	A	Beef Ingestion (73 %) Veg. Ingestion (15 %)	Tc-99 (100 %)

a From GoldSim model file: *HTF DoseCalculator Model v0.019_100K_07122012.gsm* (Case A deterministic model)

b From GoldSim model file: *HTF Transport Model v0.025 CaseA r1000 s2t.gsm*

Inspection of Table 5.6-34 indicates that even though the peak dose from the individual realizations are significantly higher than the deterministic case, the location (Sector A) and the identification of the major radionuclide contributor to the dose (Tc-99) are not different from the deterministic case. However, the major pathway contributors differ from the deterministic case.

The individual realizations are analyzed below by identifying those uncertainty parameters that have a direct impact on the magnitude or timing of the peak dose. Some initial interpretations of the deterministic model are required in order to do a detailed single realization analysis. Specifically, by identifying the individual waste tanks influencing the timing and magnitude of the deterministic peak dose, the number of key uncertainty parameters can be narrowed down. For example, the steel liner failure times for the Base Case deterministic simulation are as follows:

- Type I (intact liner) - 11,397 years
- Type II (intact liner) - 12,687 years
- Type IV (intact liner) - 3,638 years
- Type IIIA (intact liner) - 12,751 years

The timings of peak doses are between years 7,930 and 8,790 for the top realizations, therefore, the liner failures occurring after the end of the performance period are not driving the Tc-99 peaks for these realizations. In the GoldSim HTF Transport Model, releases from the Type IV waste tanks all feed to Sectors B and C; however, as the peak dose always occurs in Sector A, it was more likely that the peak doses are driven by releases from the Type I and Type II waste tanks that are modeled with degraded liners at the beginning of the simulation (i.e., Tanks 12, 14, 15, and 16). Finally, due to the closer proximity to the 100-meter boundary in Sector A, Tank 12 was the most likely contributor. Each realization was run again, using only Tank 12 as the only contaminant source; the results confirmed that Tank 12 is the driving dose contributor for all five Base Case realizations analyzed.

Two of the uncertainty parameters discussed below require additional explanation to ensure clarity: the selector for the well completion stratum and the selector for the infiltration rate. The completion stratum selector chooses between three potential well depths for the hypothetical well at the 100-meter boundary: UTRA-UZ (selector value of 1), UTRA-LZ (selector value of 2), or the Gordon Aquifer (selector value of 3). Note that mathematically there is no difference in the modeling impact between the two UTRA zones, as both result in a concentration multiplier of 100 %, whereas the Gordon Aquifer results in a concentration multiplier of 1 %. The infiltration rate selector determines whether the GoldSim realization will read flow data sets that are consistent with the presence of a closure cap (selector value of 1) or flow data sets that are consistent with the absence of a closure cap (selector value of 2).

Realization R 12

As indicated in Table 5.6-34, the major radionuclide contributor to the peak MOP dose is Tc-99 (100 %) with the major pathway contributors being beef ingestion (68 %) and vegetable ingestion (13 %). Additionally, for this realization, milk ingestion also shows significance (12 %). Uncertainty parameters influencing the release of Tc-99 with respect to the deterministic case are identified below, along with their respective sampled values. The deterministic (Base Case) value is presented within parentheses.

- Inventory multiplier for Tc-99 in Tank 12 = 9.9 (1.0)
- Infiltration rate selector = 2 [no closure cap] (1 [closure cap])
- Number of pore volume flushes to transition from Submerged Condition D to Oxidized Region III = 2,227 (2,442)
 - Results in transition at 8,070 years (8,103 years)
- Solubilities (in mol/L) of technetium in:
 - Submerged Condition C = 4.0E-09 (2.7E-12)
 - Submerged Condition D = 1.0E-15 (1.0E-15)
 - Oxidized Region III = -1 [no solubility control] (2.1E-15)
- Well completion stratum selector = 2 [UTR, Lower] (1 [UTR, Upper])

Parameters affecting the estimate of the dose by pathway are identified below. The deterministic value is presented within parentheses.

- Beef consumption rate = 67 kg/yr (43 kg/yr)
- Transfer factor for technetium beef ingestion = 2.6E-01 d/kg (6.32E-03 d/kg)
- Vegetable consumption rate = 199 kg/yr (163 kg/yr)
- Leafy vegetable consumption rate = 27 kg/yr (21 kg/yr)
- Fraction of vegetables grown locally = 0.22 (0.17)
- Milk consumption rate 225 L/yr (120 L/yr)

Realization R 844

As indicated in Table 5.6-34, the major radionuclide contributor to the peak MOP dose is Tc-99 (100 %) with the major pathway contributors being beef ingestion (72 %) and vegetable ingestion (12 %). Uncertainty parameters influencing the release of Tc-99 with respect to the deterministic case are identified below, along with their respective sampled values. The deterministic (Base Case) value is presented within parentheses.

- Inventory multiplier for Tc-99 in Tank 12 = 7.5 (1.0)
- Number of pore volume flushes to transition from Submerged Condition C to Submerged Condition D = 1,824 (1,787)
 - Results in transition at 7,850 years (7,438 years)
- Solubilities (in mol/L) of technetium in:
 - Submerged Condition C = 2.7E-12 (2.7E-12)
 - Submerged Condition D = -1 [no solubility control] (1.0E-15)
- Well completion stratum selector = 2 [UTR, Lower] (1 [UTR, Upper])

Parameters affecting the estimate of the dose by pathway are identified below. The deterministic value is presented within parentheses.

- Beef consumption rate = 70 kg/yr (43 kg/yr)
- Transfer factor for technetium beef ingestion = 2.3E-01 d/kg (6.32E-03 d/kg)
- Vegetable consumption rate = 93 kg/yr (163 kg/yr)
- Leafy vegetable consumption rate = 26 kg/yr (21 kg/yr)
- Fraction of vegetables grown locally = 0.24 (0.17)

Realization R 691

As indicated in Table 5.6-34, the major radionuclide contributor to the peak MOP dose is Tc-99 (100 %) with the major pathway contributors being beef ingestion (53 %) and vegetable ingestion (33 %). Uncertainty parameters influencing the release of Tc-99 with respect to the deterministic case are identified below, along with their respective sampled values. The deterministic (Base Case) value is presented within parentheses.

- Inventory multiplier for Tc-99 in Tank 12 = 6.8 (1.0)
- Infiltration rate selector = 2 [no closure cap] (1 [closure cap])

- Number of pore volume flushes to transition from Submerged Condition C to Submerged Condition D = 1,926 (1,787)
 - Results in transition at 7,890 years (7,438 years)
- Solubilities (in mol/L) of technetium in:
 - Submerged Condition C = 2.7E-12 (2.7E-12)
 - Submerged Condition D = -1 [no solubility control] (1.0E-15)
- Well completion stratum selector = 2 [UTR, Lower] (1 [UTR, Upper])

Parameters affecting the estimate of the dose by pathway are identified below. The deterministic value is presented within parentheses.

- Beef consumption rate = 71 kg/yr (43 kg/yr)
- Transfer factor for technetium beef ingestion = 2.8E-01 d/kg (6.32E-03 d/kg)
- Vegetable consumption rate = 202 kg/yr (163 kg/yr)
- Leafy vegetable consumption rate = 25 kg/yr (21 kg/yr)
- Fraction of vegetables grown locally = 0.38 (0.17)

Realization R 126

As indicated in Table 5.6-34, the major radionuclide contributor to the peak MOP dose is Tc-99 (100 %) with the major pathway contributors being beef ingestion (72 %) and vegetable ingestion (12 %). Uncertainty parameters influencing the release of Tc-99 with respect to the deterministic case are identified below, along with their respective sampled values. The deterministic (Base Case) value is presented within parentheses.

- Inventory multiplier for Tc-99 in Tank 12 = 9.6 (1.0)
- Number of pore volume flushes to transition from Submerged Condition D to Oxidized Region III = 1,899 (2,442)
 - Results in transition at 7,910 years (8,103 years)
- Solubilities (in mol/L) of technetium in:
 - Submerged Condition D = 1.0E-15 (1.0E-15)
 - Oxidized Region III = -1 [no solubility control] (2.1E-15)
- Well completion stratum selector = 2 [UTR, Lower] (1 [UTR, Upper])

Parameters affecting the estimate of the dose by pathway are identified below. The deterministic value is presented within parentheses.

- Beef consumption rate = 78 kg/yr (43 kg/yr)
- Transfer factor for technetium beef ingestion = 2.6E-01 d/kg (6.32E-03 d/kg)
- Vegetable consumption rate = 111 kg/yr (163 kg/yr)
- Leafy vegetable consumption rate = 41 kg/yr (21 kg/yr)
- Fraction of vegetables grown locally = 0.18 (0.17)

Realization R 245

As indicated in Table 5.6-34, the major radionuclide contributor to the peak MOP dose is Tc-99 (100 %) with the major pathway contributors being beef ingestion (73 %) and vegetable ingestion (15 %). Uncertainty parameters influencing the release of Tc-99 with respect to the deterministic case are identified below, along with their respective sampled values. The deterministic (Base Case) value is presented within parentheses.

- Inventory multiplier for Tc-99 in Tank 12 = 7.7 (1.0)
- Number of pore volume flushes to transition from Submerged Condition C to Submerged Condition D = 1,583 (1,787)
 - Results in transition at 7,660 years (7,438 years)
- Solubilities (in mol/L) of technetium in:
 - Submerged Condition C = 2.7E-12 (2.7E-12)
 - Submerged Condition D = -1 [no solubility control] (1.0E-15)
- Well completion stratum selector = 2 [UTR, Lower] (1 [UTR, Upper])

Parameters affecting the estimate of the dose by pathway are identified below. The deterministic value is presented within parentheses.

- Beef consumption rate = 62 kg/yr (43 kg/yr)
- Transfer factor for technetium beef ingestion = 2.4E-01 d/kg (6.32E-03 d/kg)
- Vegetable consumption rate = 136 kg/yr (163 kg/yr)
- Leafy vegetable consumption rate = 21 kg/yr (21 kg/yr)
- Fraction of vegetables grown locally = 0.22 (0.17)

5.6.4.3.2 Case D Realizations

The GoldSim model, *HTF Transport Model v0.025 CaseD r1000 s2t.gsm*, was used to generate 1,000 realizations. These 1,000 realizations are used here to identify the five realizations with the highest peak doses within the performance period for Case D. The results of this review are shown in Table 5.6-35. The Case D peak dose from the deterministic PORFLOW model is also included for comparison.

Table 5.6-35: Five Highest MOP Dose Results from 1,000 Case D Realizations within 10,000 Years

Realization	Peak Dose (mrem/yr)	Time of Peak Dose (yr)	Sector	Major Pathway Contributors	Major Radionuclide Contributors
Deterministic Case ^a	15	6,340	B	Water Ingestion (86 %) Veg Ingestion (13 %)	Np-237 (91 %) Ra-226 (6 %)
R 650 ^b	15,363	140	C	Water Ingestion (73 %) Fish Ingestion (15 %) Veg Ingestion (11 %)	Sr-90 (100 %)
R 664 ^b	6,131	9,620	B	Water Ingestion (9 %) Beef Ingestion (71 %) Veg. Ingestion (17 %)	Tc-99 (100 %)
R 913 ^b	5,962	7,690	B	Water Ingestion (8 %) Beef Ingestion (66 %) Veg. Ingestion (27 %) Milk Ingestion (8 %)	Tc-99 (100 %)
R 430 ^b	5,616	9,040	B	Beef Ingestion (65 %) Veg. Ingestion (17 %)	Tc-99 (100 %)
R 133 ^b	4,277	170	C	Water Ingestion (69 %) Fish Ingestion (8 %) Veg. Ingestion (23 %)	Sr-90 (100 %)

a From GoldSim model file: *HTF DoseCalculator Model v0.019_CaseD100K_07162012.gsm* (Case D deterministic model)

b From GoldSim model file: *HTF Transport Model v0.025 CaseD r1000 s2t.gsm*

Inspection of Table 5.6-35 indicates that the peak dose from the individual realizations is significantly higher than the deterministic Case D model. Each individual realization is further analyzed below by identifying those stochastic elements that have a direct impact on the peak dose. Based on Table 5.6-35, peak doses are driven by the release of either Sr-90 (if the peak occurs within the first 1,000 years) or Tc-99 (after the first 1,000 years).

The realizations of interest with peak doses that occur within Sector C (i.e., R 650 and R 133) both have a high Sr-90 dose contributions. The short half-life of Sr-90 does not allow it to affect the dose at much later dates, thus, these contributions are likely originating from those waste tanks that are initially failed (i.e., Tanks 12, 14, 15, or 16). For realizations R 650 and R 133, it was determined that the primary source of the Sr-90 release was from Tank 15.

The realizations of interest with peak doses that occur within Sector B (i.e., R 664, R 914, and R 430) each have high Tc-99 dose contributions. Investigation of these realizations determined that these Tc-99 releases originated from Tank 36 in all three of these realizations.

Realization R 650

As indicated in Table 5.6-35, the major radionuclide contributor to the peak MOP dose is Sr-90 (100 %), with the major pathway contributors being water ingestion (73 %), fish ingestion (15 %), and vegetable ingestion (11 %). Uncertainty parameters influencing the release of Sr-90 with respect to the deterministic case are identified below, along with their respective sampled values. The deterministic (Base Case) value is presented within parentheses.

- Inventory multiplier for Sr-90 in Tank 15 = 5.1 (1.0)
- Infiltration rate selector = 2 [no closure cap] (1 [closure cap])
- Sandy soil K_d for strontium = 1.5 mL/g (5 mL/g)
- Clayey soil K_d for strontium = 18.1 mL/g (17 mL/g)
- Well completion stratum selector = 2 [UTR, Lower] (1 [UTR, Upper])

Parameters influencing the estimate of the dose by pathway are identified below. The deterministic value is presented within parentheses.

- Water consumption rate = 413 L/yr (337 L/yr)
- Transfer factor for strontium fish ingestion = 71 L/kg (2.9 L/kg)
- Vegetable consumption rate = 121 kg/yr (163 kg/yr)
- Leafy vegetable consumption rate = 28 kg/yr (21 kg/yr)
- Fraction of vegetables grown locally = 0.34 (0.17)

Realization R 664

As indicated in Table 5.6-35, the major radionuclide contributor to the peak MOP dose is Tc-99 (100 %) with the major pathway contributors being beef ingestion (71 %) vegetable ingestion (17 %), and water ingestion (9 %). Uncertainty parameters influencing the release of Tc-99 with respect to the deterministic case are identified below, along with their respective sampled values. The deterministic (Base Case) value is presented within parentheses.

- Inventory multiplier for Tc-99 in Tank 36 = 5.0 (1.0)
- Infiltration rate selector = 2 [no closure cap] (1 [closure cap])
- Number of pore volume flushes to transition from Reduced Region II to Oxidized Region II = 413 (523)
 - Results in transition at 9,550 years (6,024 years)
- Solubilities (in mol/L) of technetium in:
 - Reduced Region II = 1.1E-14 (1.1E-14)
 - Oxidized Region II = -1 [no solubility control] (1.1E-13)
- Well completion stratum selector = 2 [UTR, Lower] (1 [UTR, Upper])

Parameters affecting the estimate of the dose by pathway are identified below. The deterministic value is presented within parentheses.

- Beef consumption rate = 70 kg/yr (43 kg/yr)
- Transfer factor for technetium beef ingestion = 2.4E-01 d/kg (6.32E-03 d/kg)

- Vegetable consumption rate = 155 kg/yr (163 kg/yr)
- Leafy vegetable consumption rate = 37 kg/yr (21 kg/yr)
- Fraction of vegetables grown locally = 0.24 (0.17)
- Water consumption rate = 493 L/yr (337 L/yr)

Realization R 913

As indicated in Table 5.6-35, the major radionuclide contributor to the peak MOP dose is Tc-99 (100 %) with the major pathway contributors being beef ingestion (66 %) and vegetable ingestion (27 %). Uncertainty parameters influencing the release of Tc-99 with respect to the deterministic case are identified below, along with their respective sampled values. The deterministic (Base Case) value is presented within parentheses.

- Inventory multiplier for Tc-99 in Tank 36 = 3.5 (1.0)
- Number of pore volume flushes to transition from Reduced Region II to Oxidized Region II = 490 (523)
 - Results in transition at 7,640 years (6,024 years)
- Solubilities (in mol/L) of technetium in:
 - Reduced Region II = 1.1E-14 (1.1E-14)
 - Oxidized Region II = -1 [no solubility control] (1.1E-13)
- Well completion stratum selector = 2 [UTR, Lower] (1 [UTR, Upper])

Parameters affecting the estimate of the dose by pathway are identified below. The deterministic value is presented within parentheses.

- Beef consumption rate = 79 kg/yr (43 kg/yr)
- Transfer factor for technetium beef ingestion = 2.8E-01 d/kg (6.32E-03 d/kg)
- Vegetable consumption rate = 233 kg/yr (163 kg/yr)
- Leafy vegetable consumption rate = 25 kg/yr (21 kg/yr)
- Fraction of vegetables grown locally = 0.44 (0.17)

Realization R 430

As indicated in Table 5.6-35, the major radionuclide contributor to the peak MOP dose is Tc-99 (100 %) with the major pathway contributors being beef ingestion (65 %) vegetable ingestion (17 %), milk ingestion (8 %), and water ingestion (8 %). Uncertainty parameters influencing the release of Tc-99 with respect to the deterministic case are identified below, along with their respective sampled values. The deterministic (Base Case) value is presented within parentheses.

- Inventory multiplier for Tc-99 in Tank 36 = 8.1 (1.0)
- Number of pore volume flushes to transition from Reduced Region II to Oxidized Region II = 625 (523)
 - Results in transition at 8,970 years (6,024 years)

- Solubilities (in mol/L) of technetium in:
 - Reduced Region II = $1.1\text{E-}14$ ($1.1\text{E-}14$)
 - Oxidized Region II = -1 [no solubility control] ($1.1\text{E-}13$)
- Well completion stratum selector = 2 [UTR, Lower] (1 [UTR, Upper])

Parameters affecting the estimate of the dose by pathway are identified below. The deterministic value is presented within parentheses.

- Beef consumption rate = 57 kg/yr (43 kg/yr)
- Transfer factor for technetium beef ingestion = $3.2\text{E-}01$ d/kg ($6.32\text{E-}03$ d/kg)
- Vegetable consumption rate = 135 kg/yr (163 kg/yr)
- Leafy vegetable consumption rate = 27 kg/yr (21 kg/yr)
- Fraction of vegetables grown locally = 0.24 (0.17)
- Water consumption rate = 271 L/yr (337 L/yr)
- Milk consumption rate = 98 L/yr (120 L/yr)
- Fraction of milk produced locally = 0.31 (0.207)

Realization R 133

As indicated in Table 5.6-35, the major radionuclide contributor to the peak MOP dose is Sr-90 (100 %), with the major pathway contributors being water ingestion (69 %), vegetable ingestion (23 %), and fish ingestion (8 %). Uncertainty parameters influencing the release of Sr-90 with respect to the deterministic case are identified below, along with their respective sampled values. The deterministic (Base Case) value is presented within parentheses.

- Inventory multiplier for Sr-90 in Tank 15 = 2.2 (1.0)
- Sandy soil K_d for strontium = 1.5 mL/g (5 mL/g)
- Clayey soil K_d for strontium = 15.8 mL/g (17 mL/g)
- Infiltration rate selector = 2 [no closure cap] (1 [closure cap])
- Well completion stratum selector = 2 [UTR, Lower] (1 [UTR, Upper])

Parameters influencing the estimate of the dose by pathway are identified below. The deterministic value is presented within parentheses.

- Water consumption rate = 494 L/yr (337 L/yr)
- Vegetable consumption rate = 185 kg/yr (163 kg/yr)
- Leafy vegetable consumption rate = 33 kg/yr (21 kg/yr)
- Fraction of vegetables grown locally = 0.43 (0.17)
- Transfer factor for strontium fish ingestion = 135 L/kg (2.9 L/kg)

5.6.4.3.3 All Cases Realizations

The GoldSim model, *HTF Transport Model v0.025 CaseAll r1000 s03t.gsm*, was used to generate 1,000 realizations. These 1,000 realizations are used here to identify the five realizations with the highest peak doses within the performance period for the All Cases runs. The results of this review are shown in Table 5.6-36.

Table 5.6-36: Five Highest MOP Dose Results from 1,000 All Cases Realizations within 10,000 Years

Realization	Peak Dose (mrem/yr)	Time of Peak Dose (yr)	Sector of Peak Dose	Major Pathway Contributors	Major Radionuclide Contributors
R 260 ^a	3,040	670	B	Beef Ingestion (72 %) Veg. Ingestion (12 %)	Tc-99 (100 %)
R 66 ^a	2,941	2,880	B	Veg. Ingestion (56 %) Beef Ingestion (19 %)	Tc-99 (100 %)
R 59 ^a	2,547	6,000	B	Beef Ingestion (44 %) Veg. Ingestion (22 %)	Tc-99 (100 %)
R 550 ^a	2,536	2,010	E	Beef Ingestion (47 %) Veg. Ingestion (39 %)	Tc-99 (100 %)
R 560 ^a	2,527	3,620	B	Beef Ingestion (49 %) Veg. Ingestion (28 %)	Tc-99 (100 %)

a From GoldSim model file: *HTF Transport Model v0.025 CaseAll r1000 s03t.gsm*

Inspection of Table 5.6-36 indicates that Tc-99 is the primary radionuclide influencing the peak dose, and beef and vegetable ingestion are the typical biotic pathways that influence this peak dose. In addition, as Sector B is the controlling sector for four out of the five top realizations, and given the timing of these peaks, the releases from the Type IV tanks are likely source contributors to these peak doses.

Realization R 260

As indicated in Table 5.6-36, the major radionuclide contributor to the peak MOP dose is Tc-99 (100 %) with the major pathway contributors being beef ingestion (72 %) and vegetable ingestion (12 %). Uncertainty parameters influencing the release of Tc-99 with respect to the deterministic case are identified below, along with their respective sampled values. The deterministic (Base Case) value is presented within parentheses.

- Configuration selection for Tank 37 = 3 [Case C, fast flow path / early liner failure waste tank configuration] (1, Base Case)
- Tank 37 liner failure time = 528 year, 140 years before peak dose
- Inventory multiplier for Tc-99 in Tank 37 = 8.5 (1.0)
- Infiltration rate selector = 2 [no closure cap] (1 [closure cap])
- Solubilities of technetium in Oxidized Region III = -1 [no solubility control] (2.1E-15 mol/L)
- Well completion stratum selector = 2 [UTR, Lower] (1 [UTR, Upper])

Parameters affecting the estimate of the dose by pathway are identified below. The deterministic value (from the Base Case) is presented within parentheses.

- Transfer factor for technetium beef ingestion = 3.5E-01 d/kg (6.32E-03 d/kg)
- Vegetable consumption rate = 174 kg/yr (163 kg/yr)
- Leafy vegetable consumption rate = 25 kg/yr (21 kg/yr)
- Fraction of vegetables grown locally = 0.18 (0.17)

Realization R 66

As indicated in Table 5.6-36, the major radionuclide contributor to the peak MOP dose is Tc-99 (100 %) with the major pathway contributors being vegetable ingestion (56 %) and beef ingestion (19 %). For this realization, water ingestion was also significant (15 %). Uncertainty parameters influencing the release of Tc-99 with respect to the deterministic case are identified below, along with their respective sampled values. The deterministic (Base Case) value is presented within parentheses.

- Configuration selection for Tank 36 = 5 [Case E, fast flow path / early liner failure waste tank configuration] (1, Base Case)
- Tank 36 liner failure time = 2793 year, about 90 years before peak dose
- Inventory multiplier for Tc-99 in Tank 36 = 8.5 (1.0)
- Solubilities of technetium in Oxidized Region II = -1 [no solubility control] (1.1E-13 mol/L)
- Well completion stratum selector = 2 [UTR, Lower] (1 [UTR, Upper])

Parameters affecting the estimate of the dose by pathway are identified below. The deterministic value (from the Base Case) is presented within parentheses.

- Transfer factor for technetium beef ingestion = 4.7E-02 d/kg (6.32E-03 d/kg)
- Vegetable consumption rate = 198 kg/yr (163 kg/yr)
- Leafy vegetable consumption rate = 18 kg/yr (21 kg/yr)
- Fraction of vegetables grown locally = 0.39 (0.17)

Realization R 59

As indicated in Table 5.6-36, the major radionuclide contributors to the peak MOP dose is Tc-99 (100 %) with the major pathway contributors being beef ingestion (44 %) and vegetable ingestion (22 %). For this realization, water and milk ingestion were also significant biotic pathways (17 % and 16 % of dose, respectively). Uncertainty parameters influencing the release of Tc-99 with respect to the deterministic case are identified below, along with their respective sampled values. The deterministic (Base Case) value is presented within parentheses.

- Configuration selection for Tank 35 = 3 [Case C, fast flow path / early liner failure waste tank configuration] (1, Base Case)
- Tank 35 liner failure time = 5,835 year, about 165 years before peak dose
- Inventory multiplier for Tc-99 in Tank 35 = 9.7 (1.0)
- Solubilities of technetium in Oxidized Region II = -1 [no solubility control] (1.1E-13 mol/L)
- Well completion stratum selector = 2 [UTR, Lower] (1 [UTR, Upper])

Parameters affecting the estimate of the dose by pathway are identified below. The deterministic value (from the Base Case) is presented within parentheses.

- Transfer factor for technetium beef ingestion = 1.6E-01 d/kg (6.32E-03 d/kg)
- Vegetable consumption rate = 127 kg/yr (163 kg/yr)

- Leafy vegetable consumption rate = 20 kg/yr (21 kg/yr)
- Fraction of vegetables grown locally = 0.34 (0.17)
- Water consumption rate = 419 L/yr (337 L/yr)
- Milk consumption rate = 223 L/yr (120 L/yr)

Realization R 550

As indicated in Table 5.6-36, the major radionuclide contributor to the peak MOP dose is Tc-99 (100 %) with the major pathway contributors being beef ingestion (47 %) vegetable ingestion (39 %). Uncertainty parameters influencing the release of Tc-99 with respect to the deterministic case are identified below, along with their respective sampled values. The deterministic (Base Case) value is presented within parentheses.

- Configuration selection for Tank 41 = 3 [Case C, fast flow path / early liner failure waste tank configuration] (1, Base Case)
- Tank 41 liner failure time = 1,830 year, about 180 years before peak dose
- Inventory multiplier for Tc-99 in Tank 41 = 8.3 (1.0)
- Infiltration rate selector = 2 [no closure cap] (1 [closure cap])
- Solubilities of technetium in Oxidized Region III = -1 [no solubility control] (2.1E-15 mol/L)
- Well completion stratum selector = 2 [UTR, Lower] (1 [UTR, Upper])

Parameters affecting the estimate of the dose by pathway are identified below. The deterministic value (from the Base Case) is presented within parentheses.

- Transfer factor for technetium beef ingestion = 1.8E-01 d/kg (6.32E-03 d/kg)
- Vegetable consumption rate = 218 kg/yr (163 kg/yr)
- Leafy vegetable consumption rate = 33 kg/yr (21 kg/yr)
- Fraction of vegetables grown locally = 0.29 (0.17)

Realization R 560

As indicated in Table 5.6-36, the major radionuclide contributor to the peak MOP dose is Tc-99 (100 %) with the major pathway contributors being beef ingestion (49 %) and vegetable ingestion (28 %). For this realization, water ingestion was also significant (16 %). Uncertainty parameters influencing the release of Tc-99 with respect to the deterministic case are identified below, along with their respective sampled values. The deterministic (Base Case) value is presented within parentheses.

- Configuration selection for Tank 36 = 3 [Case C, fast flow path / early liner failure waste tank configuration] (1, Base Case)
- Tank 36 liner failure time = 3,532 year, about 90 years before peak dose
- Inventory multiplier for Tc-99 in Tank 36 = 7.2 (1.0)
- Solubilities of technetium in Oxidized Region II = -1 [no solubility control] (1.1E-13 mol/L)
- Well completion stratum selector = 2 [UTR, Lower] (1 [UTR, Upper])

Parameters affecting the estimate of the dose by pathway are identified below. The deterministic value (from the Base Case) is presented within parentheses.

- Transfer factor for technetium beef ingestion = 1.4E-01 d/kg (6.32E-03 d/kg)
- Vegetable consumption rate = 161 kg/yr (163 kg/yr)
- Leafy vegetable consumption rate = 24 kg/yr (21 kg/yr)
- Fraction of vegetables grown locally = 0.21 (0.17)
- Water consumption rate = 426 L/yr (337 L/yr)

5.6.4.3.4 Insights from the Realization Study

A review of the fifteen realizations indicates that the parameters most significant to highest peak doses for the Base Case, Case D, and the All Cases runs are parameters that control the release and dose of Tc-99 (and Sr-90 to a lesser degree). Specific parameters of importance include the technetium solubility controls within the CZ and parameters related to Tc-99 doses via the beef and vegetable ingestion pathways.

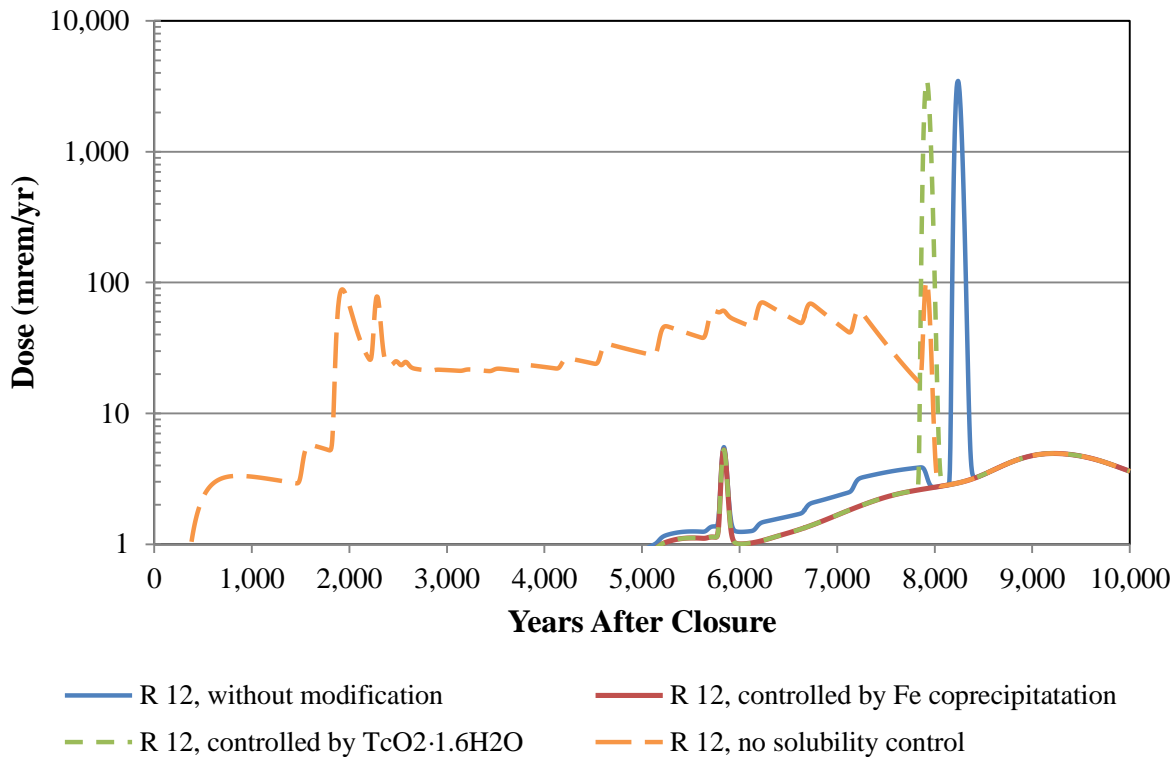
Realizations that remove solubility limits from technetium within the CZ result in greater Tc-99 releases, and therefore greater peak doses. When the solubility limit is removed, all available Tc-99 becomes soluble and is released for transport, and flushes through the system, thus maximizing Tc-99 releases.

Consistent with the controlling phase of iron co-precipitation for technetium, the deterministic cases allowed dissolved Tc-99 concentrations up to 1.1E-14 mol/L under Reduced Region II conditions, 1.1E-13 mol/L under Oxidized Region II conditions, and 2.1E-15 mol/L under Oxidized Region III conditions. For the submerged waste tanks, the deterministic cases allowed dissolved Tc-99 concentrations up to 2.7E-12 mol/L under Submerged Condition C and 1.0E-15 mol/L under Submerged Condition D.

For conservatism, the probabilistic model allows technetium solubility controls to sample between values for an iron co-precipitation-controlling phase and the values for a $\text{TcO}_2 \cdot 1.6\text{H}_2\text{O}$ -controlling phase. This alternative controlling phase allows dissolved concentrations of Tc-99 up to 1.0E-8 mol/L under Reduced Region II conditions, 4.0E-09 mol/L under Submerged Condition C, and applied no solubility controls under other conditions.

To illustrate the significance of this conservatism, the Base Case realization R 12 was run with modified technetium solubility controls. Figure 5.6-35 shows the Realization R 12 peak dose results from: 1) applying the sampled values as discussed above, 2) applying a controlling phase of iron co-precipitation only, 3) applying a controlling phase of $\text{TcO}_2 \cdot 1.6\text{H}_2\text{O}$ only, and 4) removing all solubility controls.

Figure 5.6-35: Illustration of the Effects of Modified Solubility Controls on Technetium in Tank 12, Base Case, Realization R 12



This figure illustrates that the TcO₂·1.6H₂O-controlled solubility (green-dashed curve) results in a dose with a similar magnitude to that of the sampled R 12 dose (blue curve), but which occurs at the first transition time (around 7,900 years after closure). Alternatively, the iron co-precipitation-controlled solubility (red curve, obscured by the green curve) results in a peak dose of 5 mrem/yr around 5,800 years after closure (two to three orders of magnitude lower than the sampled R 12 dose). Finally, removal of all solubility controls (orange-dashed curve) allows Tc-99 mass to “bleed” off from Tank 12, reducing the inventory available to impact peak doses, thus resulting in a peak dose of 103 mrem/yr around 7,900 years after closure (one to two orders of magnitude lower than the sampled R 12 peak dose).

Of the 15 realizations investigated 12 showed beef ingestion as the dominant biotic pathway. Variability in the Tc-99 dose through the beef ingestion pathway is strongly influenced by the transfer factor, as this multiplier has a range that spans three to four orders of magnitude (from 0.0001 d/kg to 0.4 d/kg). Due to a lack of available information regarding the behavior of this variable, the minimum, maximum, and deterministic values were sampled along a triangular distribution curve. This distribution curve was selected for conservatism, however it is possible, even likely, that beef transfer factor uncertainty would fit better to a less conservative distribution curve (such as a log-normal or normal distribution), thus reducing this artificial conservatism. The 12 realizations with peak doses dominated by the beef ingestion pathway all sampled the

beef transfer factor with values above 0.14 d/kg (22 times higher than the deterministic value of 0.00632 d/kg). An alternative distribution curve could reduce the likelihood of sampling values that are orders of magnitude above the deterministic value, thus reducing the significance of this parameter.

The two realizations of interest with peak doses dominated by Sr-90 both sampled high inventory multipliers within waste tanks that were modeled with degraded liners at the beginning of the simulation (Tanks 12, 14, 15, and 16). A high Sr-90 inventory can drive the peak dose early on, however the relatively short half-life of Sr-90 makes the Sr-90 dose contribution insignificant in later years. For the high inventory dose contribution to be maximized it had to occur in conjunction with a waste tank with an initially failed liner and a low K_d within sandy soil. The low K_d values for Sr-90 attributed to sandy soils (1.7 mL/g or less versus the deterministic value of 5 mL/g) allows for the rapid transport of Sr-90, such that the peak dose is achieved prior to the short Sr-90 half-life mitigating the Sr-90 dose contribution. The high inventory multiplier and low K_d values in sandy soil work together to allow Sr-90 to become more important than the other radionuclides, and drives the peak dose.

In summary, the parameters that influence the peak realizations can be significant and lead to higher dose if they occur simultaneously. These scenarios are not likely because the parameters that lead to the high dose realizations do not have a common mode initiator that would have the tendency to have these independent parameters occur simultaneously. The high dose realizations do not have any “critical” parameters in common. However, some multiple parameters have strong influence, and a smaller set of parameters with a very strong influence. Depending upon the alignment and number of parameters, these can combine to cause the peak dose to trend higher for a given realization.

5.6.5 Sensitivity Analysis using HTF Probabilistic Model

Given the uncertainties presented in Section 5.6.4, the next step was to identify those input parameters and other parameters in the model that led to the uncertainties. Even in complex models, the results are often strongly dependent on only a handful of parameters. What is important for one result (e.g., the Ra-226 concentration in well water) may be insignificant for another (e.g., the maximum dose achieved within a 10,000-year period). In fact, the maximum dose to the MOP will have different sensitivities at different times, since it is driven by the presence of different radionuclides. For example, a MOP dose may be dominated by Tc-99 at one time and by Ra-226 at another time, and these doses will be determined by different aspects of the model (different K_d s, containment failure modes, etc.) Extracting the important model inputs for results of interest is the subject of this probabilistic SA.

5.6.5.1 Introduction to HTF Probabilistic Model Sensitivity Analysis

Complex modeling is needed to explore the dynamics of systems where multiple variables interact in a nonlinear manner. The probabilistic simulation approach used in the HTF PA GoldSim Model propagates uncertainty from the sampled uncertainty parameters, through the model, to the predicted responses (e.g., doses or concentrations). Quantitative assessment

of the importance of inputs is necessary when the level of uncertainty in the system response exceeds the acceptable threshold specified in the decision-making framework. One of the goals of sensitivity analysis is to identify which variables have distributions that exert the greatest influence on the response.

Sensitivity analysis deals with estimating influence measures for input variables. Influence measures can be estimated in either a qualitative or a quantitative context. A qualitative SA provides a relative ranking of the importance of input factors without incurring the computational cost of quantitatively estimating the percentage of the output variation accounted for by each input factor. For both approaches, the estimates can be obtained either locally or globally within the parameter space. A local SA involves varying one explanatory variable while holding all other explanatory variables constant, and assessing the impact on the model response. This is local in the sense that only a minimal portion of the full explanatory variable space is explored (i.e., the point at which the explanatory variables are held constant). Although local SA is useful in some applications, the region of possible realizations for the model of interest is left largely unexplored.

Global SA attempts to explore the possible realizations of the model more completely. The space of possible realizations for the model can be explored using search curves or evaluation of multi-dimensional integrals using Monte Carlo methods. However, these approaches to global sensitivity analysis become more computationally intensive as the dimensionality of the model (i.e., the number of model parameters) increases. In this case, the HTF PA GoldSim Model includes nearly 2,800 uncertainty parameters, a very large dimensionality.

Because of the computational cost, SAs of high-dimensional probabilistic models requires efficient algorithms for practical application. In this work, datasets of 3,000 and 5,000 probabilistic model realizations, each with nearly 2,800 columns for the uncertainty parameters and one column for the peak MOP dose, were analyzed using Gradient Boosting Models (GBM). The GBM analysis provides a global sensitivity analysis that quantifies the importance of explanatory variables using sensitivity indices (SIs), which are metrics based on the explained variance in the response. These analyses were performed on results from the models identified in Table 5.6-31. [ISSN 0167-9473, ISSN 0885-6125-Vol 40 No 2, ISSN 0885-6125 Vol 24 No 2]

5.6.5.2 Model Fitting and Validation

This section discusses the statistical methods used in these SAs. Global sensitivity is estimated here as the proportion of the variance of the response accounted for by each explanatory variable. This estimation is conducted by fitting GBM predictions to realizations from the GoldSim model. Variance decomposition of the fitted GBM analysis is then used to estimate SIs. Under this decomposition approach, the most influential uncertainty parameters are identified. The necessary degree of model complexity is assessed using validation metrics, based on comparison of model predictions, with randomly selected subsets of the data. This approach uses the “deviance” of the model as a measure of goodness of fit. The concept of deviance is fundamental to classical statistical hypothesis testing (e.g., the common *t*-test can be derived using a deviance-based framework) and guides the model selection process applied here.

The GBM model-fitting approach is based on finding those values of each sampled parameter that result in the greatest difference in mean for the corresponding subsets of the response. For example, if there were only a single variable, the GBM would identify the value of that variable that corresponds to a split of the response into two parts. This will ensure that no other split would result in corresponding groups of the response variable with a greater difference in means. When multiple sampled variables are present, these multiple splits are referred to as “trees.” Each tree results in an estimate (e.g., prediction) of the response. As multiple potential trees are evaluated, they are compared to the observed data using a loss function. The selection of the loss function is an influential aspect of the GBM process, and depends on the distribution of the response. For data that are sufficiently skewed (e.g., non-normal), the absolute error loss function typically produces more reliable results.

A trade-off exists when considering which loss function to use. The squared-error loss function results in better fitting models, but can do so at the expense of introducing spurious variables into the model selection process when the response distribution is sufficiently skewed. The absolute error loss function produces model predictions with more variability, but is less likely to result in the selection of spurious variables in the model. For this application, the focus has been on using a deviance-based method to obtain models that identify the most important sampled variables with respect to the observed variability in the response. Therefore, the squared-error function was used in these applications.

Once a GBM model is constructed, each of the sampled variables that exist in the model can be assigned an SI. The SI is obtained through variance decomposition and can be interpreted as the percentage of variability explained in the model by a given explanatory variable. The sum of the SIs across the entire set of sampled variables in the model will approximately equal the coefficient of determination (R^2) of the linear regression of the GoldSim output versus the GBM predictions. The R^2 values for this version of the HTF model indicate an acceptable degree of predictive power of the GBM in fitting the GoldSim model. For the Base Case endpoints, the R^2 values range from 0.98 to 0.99, indicating excellent fits. For the Case D endpoints, the R^2 values range from 0.93 to 0.98, and for the All Cases endpoints, which are the most challenging, 0.75 to 0.94.

With standard linear regression techniques, it is assumed that the relationship between the response and the sampled variable is a constant. With the GBM approach, this relationship is not constrained by assumptions of linearity, and the partial dependence plots show the data based estimate of the relationship between the response and the sampled variable. This is useful for understanding the influence of changes in a single variable parameter, when integrating across all other variable parameters.

5.6.5.3 Summary Statistics for Endpoints

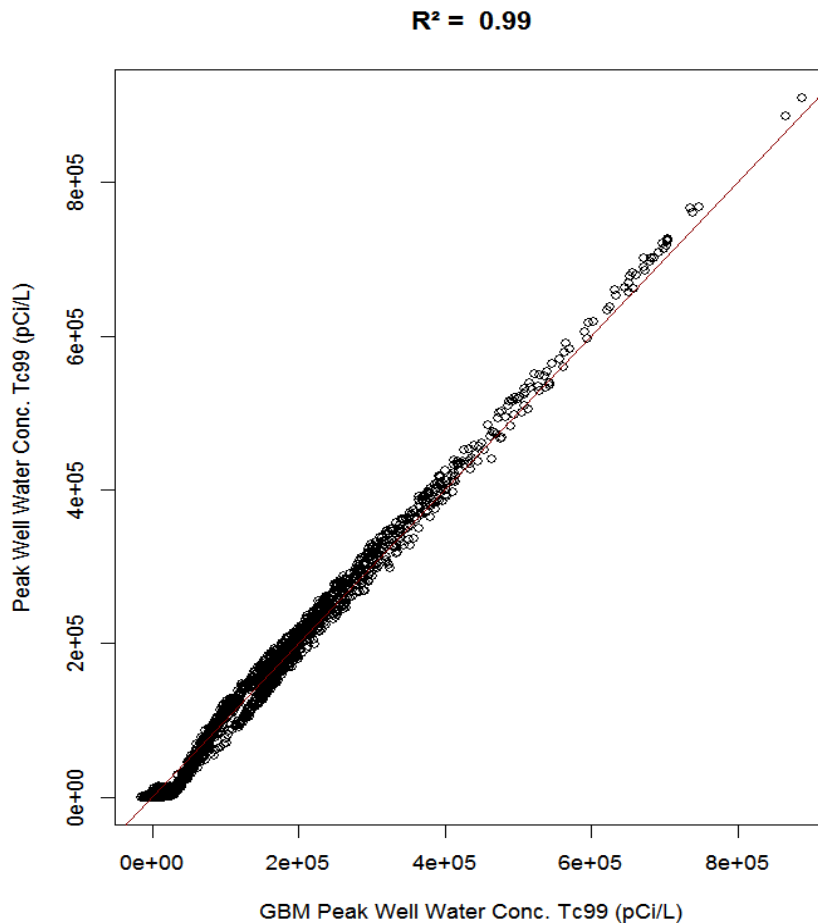
This SA used three GoldSim models, run in sets of 1,000 realizations (listed in Table 5.6-31): Base Case, Case D, and All Cases (as described in Section 5.6.4).

Endpoints were selected for total effective dose equivalents (TEDE) to the MOP, as well as groundwater concentrations of selected radionuclides. (Note that endpoint selection was based on previous HTF PA Rev. 0 modeling.) Doses are examined for peak values within

different periods of time (10,000 years and 20,000 years after closure). These are hypothetical doses from contaminated well water, wherein the maximum total dose from any sector (each with a number of wells arranged along the 100-meter boundary), is recorded at each time step. The conceptual model for exposure to well water is such that at any time step, the MOP is exposed to water from the well of highest concentration of certain radionuclides. This would be possible in reality only if the wells coexisted and if the receptor deliberately selected the most concentrated water, so it is an unrealistic bounding case. This is different from the concept that the MOP would be exposed to water from a single well that would produce the highest dose, which would be a more reasonable bounding case, and one that would yield results that would exist in statistically more stable modeling space.

In general, the GBM fits were acceptable, with estimated R^2 values ranging from 0.75 to 0.99. In the sample GBM fit plot given in Figure 5.6-36, the R^2 is reported as 0.99. This tells us that the GBM statistical predictive model is able to reproduce the GoldSim modeled results quite well, giving us confidence in the statistical analysis. Other GBM fits had values of R^2 as noted in the tables.

Figure 5.6-36: Example of a GBM Model Fit Plot



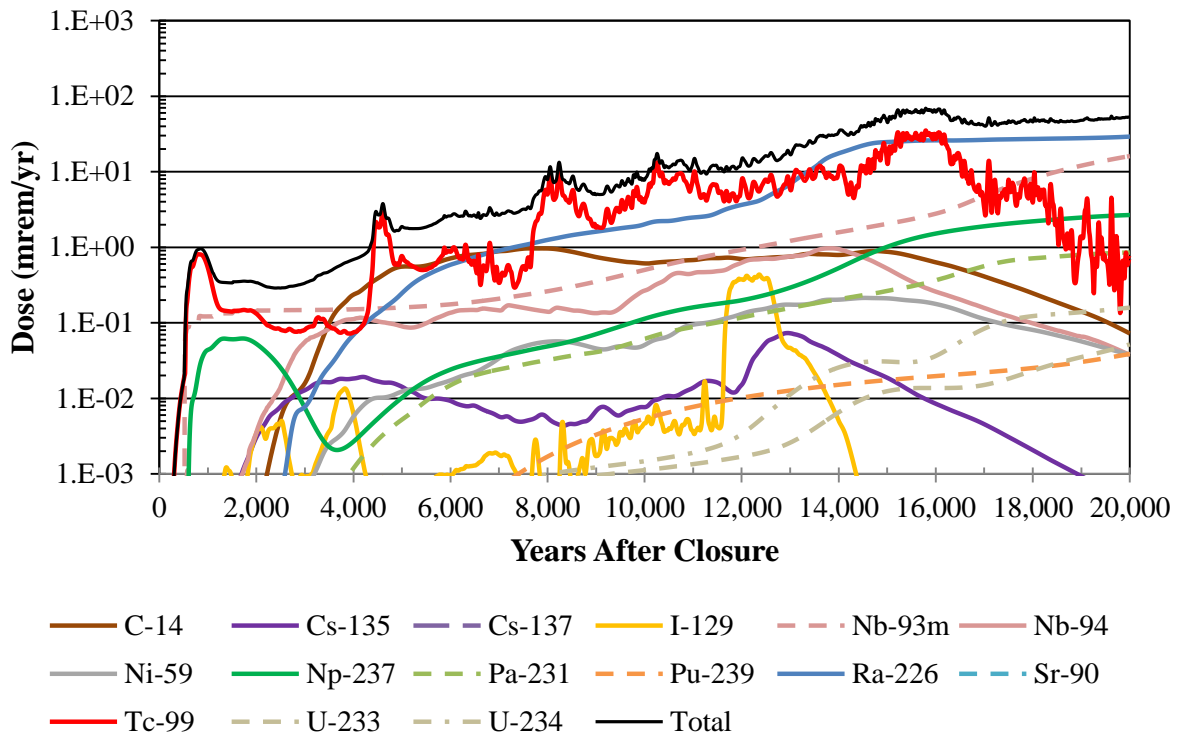
For each endpoint, as shown in Tables 5.6-37 through 5.6-39, for Cases A, D, and All Cases, the most significant uncertainty parameters identified by the SAs are presented, along with the SI for each. Parameters with SI values below 5 (explaining 5 % of the variation in the endpoint) are not included because their contributions to the given endpoint are relatively low. Following each table is a figure showing the mean dose results, by radionuclide, of each of the three modeling cases.

Table 5.6-37: Most Sensitive Parameters for the Endpoints of Interest for Base Case

Endpoint	SI Rank	Input Parameter	SI
Peak MOP dose at max sector within 10,000 yr $R^2 = 0.98$	1	Tank 12 inventory multiplier for Tc-99	16.9
	2	Water well completion stratum selector	9.28
Peak MOP dose at max sector within 20,000 yr $R^2 = 0.99$	1	Water well completion stratum selector	23.4
	2	Technetium solubility in Oxidizing Region II cementitious materials	14.0
	3	Tank 36 inventory multiplier for Tc-99	8.74
	4	Beef transfer factor for technetium	5.81
Peak conc. of I-129 at max sector within 20,000 yr $R^2 = 0.99$	1	Water well completion stratum selector	52.4
	2	Tank 36 inventory multiplier for I-129	8.65
	3	Iodine K_d in Oxidizing Region II cementitious materials	6.19
Peak conc. of Np-237 at max sector within 20,000 yr $R^2 = 0.99$	1	Water well completion stratum selector	15.6
	2	Neptunium K_d in Oxidizing Region III cementitious materials	13.7
	3	Tank 9 inventory multiplier for Np-237	6.32
Peak conc. of Ra-226 at max sector within 20,000 yr $R^2 = 0.99$	1	Water well completion stratum selector	33.5
	2	Radium K_d in sandy soil	27.7
	3	Tank 32 inventory multiplier for Pu-238	7.19
	4	Radium K_d in leachate-impacted sandy soil	6.39
Peak conc. of Tc-99 at max sector within 20,000 yr $R^2 = 0.99$	1	Water well completion stratum selector	35.4
	2	Technetium solubility in Oxidizing Region II cementitious materials	24.5
	3	Tank 36 inventory multiplier for Tc-99	16.1

The most significant parameter in determining the value of the 10,000-yr peak MOP dose endpoint from the Base Case is of a type that often recurs in throughout the HTF PA SAs: a log-normally distributed value that is used as a multiplier for the inventory of Tc-99 in Tank 12. Note that this parameter is positively correlated to dose, as expected. Higher inventories generally result in higher doses. Figure 5.6-37 shows that the mean of the Tc-99 dose (red curve) is prevalent throughout a large part of simulated period.

Figure 5.6-37: Radionuclide-Specific MOP Dose from any Sector within 20,000 Years, Base Case



The second most significant parameter is the selector for water well completion stratum. This parameter has three discrete values used to identify which aquifer a well is likely to be completed in (described in Section 5.6.3). The great difference in concentrations in the upper and lower aquifers is naturally a strong discriminator for dose thus this parameter is strongly influential in the dose and is commonly seen as a sensitive parameter for many of these endpoints. No other parameters have an influence of over 5 % (and SI value of 5) on this endpoint.

Table 5.6-38: Most Sensitive Parameters for the Endpoints of Interest for Case D

Endpoint	SI Rank	Input Parameter	SI
Peak MOP dose at max sector within 10,000 yr $R^2 = 0.93$	1	Tank 36 inventory multiplier for Tc-99	6.62
Peak MOP dose at max sector within 20,000 yr $R^2 = 0.97$	1	Water well completion stratum selector	18.5
	2	Lead K_d in Oxidizing Region III cementitious materials	11.2
	3	Technetium solubility in Oxidizing Region II cementitious materials	7.48
	4	Tank 36 inventory multiplier for Tc-99	5.49
Peak conc. of I-129 at max sector within 20,000 yr $R^2 = 0.97$	1	Water well completion stratum selector	29.3
Peak conc. of Np-237 at max sector within 20,000 yr $R^2 = 0.99$	1	Water well completion stratum selector	36.9
	2	Neptunium K_d in Oxidizing Region III cementitious materials	6.98
Peak conc. of Ra-226 at max sector within 20,000 yr $R^2 = 0.99$	1	Water well completion stratum selector	32.5
	2	Radium K_d in sandy soil	25.2
Peak conc. of Tc-99 at max sector within 20,000 yr $R^2 = 0.99$	1	Water well completion stratum selector	34.2
	2	Technetium solubility in Oxidizing Region II cementitious materials	18.5
	3	Tank 36 inventory multiplier for Tc-99	14.4

Similar to the Base Case, the Case D doses are dominated by the selector for the well completion stratum. The second-most important variable (within the 20,000-year time frame) is the K_d for lead in Oxidizing Region III cementitious materials, is likely to be spurious, since it is driven strongly by a single point of correlation, and since lead, while not insignificant, is not one of the top dose drivers. The variables ranked third and fourth are related to technetium as expected based on the role of Tc-99 as seen in Figure 5.6-38.

Figure 5.6-38: Radionuclide-Specific MOP Dose from any Sector within 20,000 Years, Case D

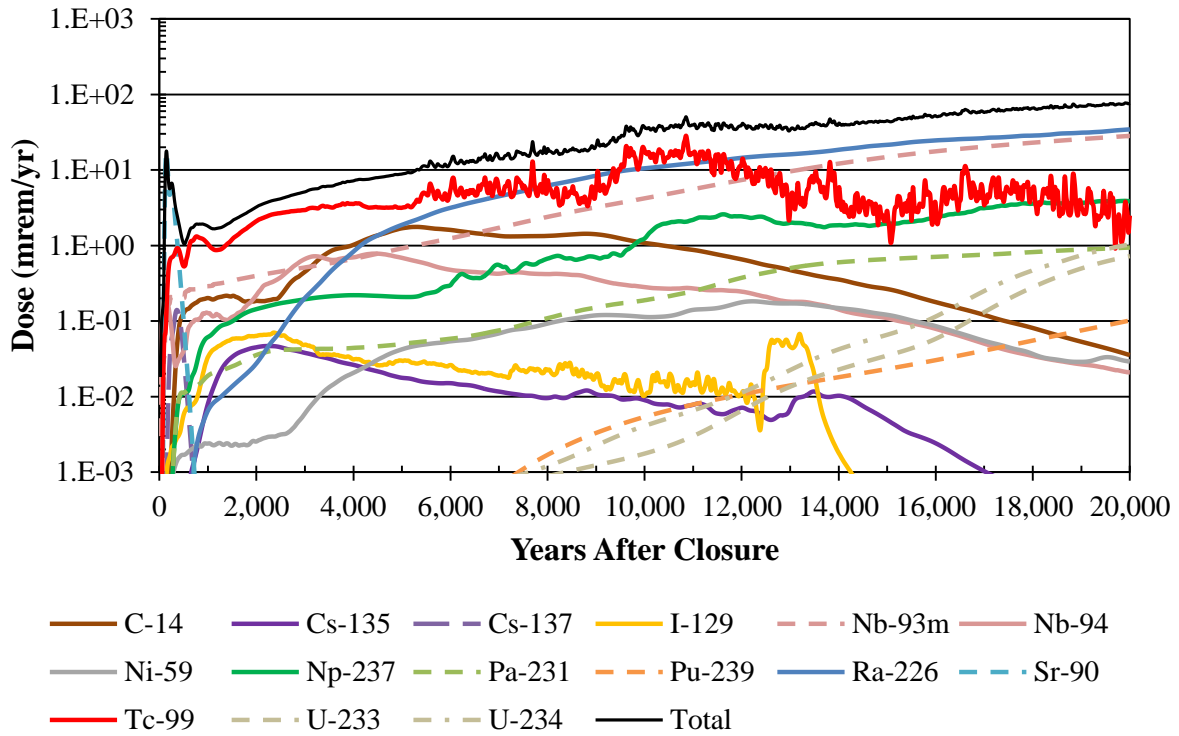
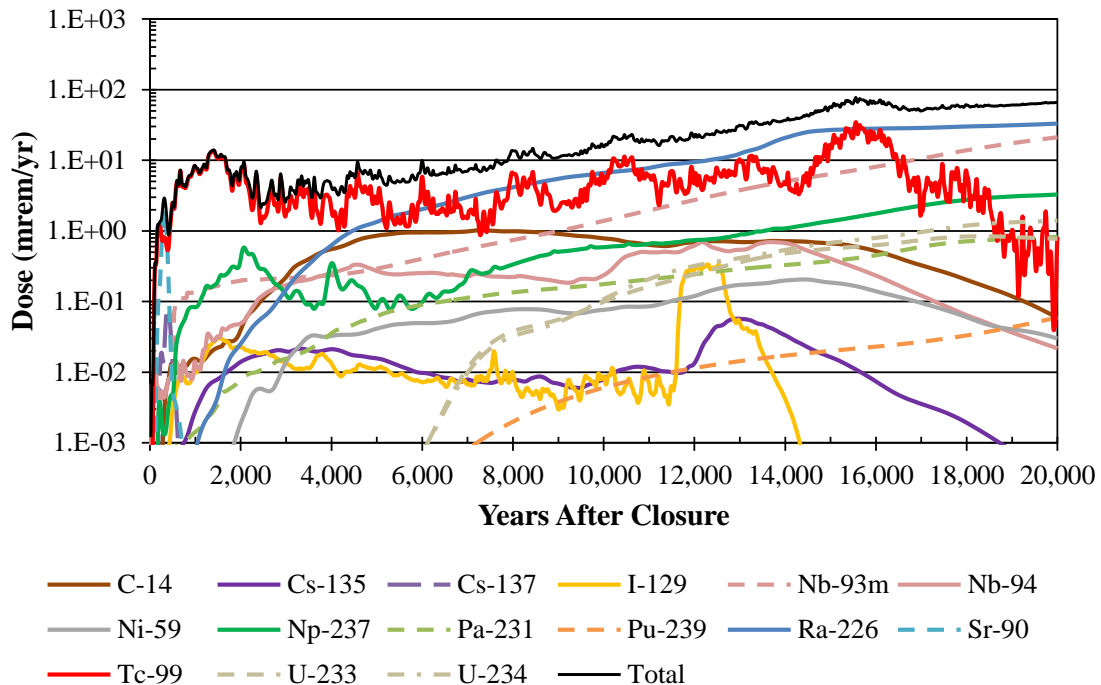


Table 5.6-39: Most Sensitive Parameters for the Endpoints of Interest for All Cases

Endpoint	SI Rank	Input Parameter	Sensitivity Index
Peak MOP dose at max sector within 10,000 yr $R^2 = 0.75$	1	Water well completion stratum selector	20.6
Peak MOP dose at max sector within 20,000 yr $R^2 = 0.88$	1	Water well completion stratum selector	29.0
	2	Technetium solubility in Oxidizing Region II cementitious materials	13.6
	3	Tank 36 inventory multiplier for Tc-99	10.1
	4	Beef transfer factor for technetium	7.12
Peak conc. of I-129 at max sector within 20,000 yr $R^2 = 0.90$	1	Water well completion stratum selector	55.8
	2	Tank 36 inventory multiplier for I-129	8.92
	3	Iodine K_d in Oxidizing Region II cementitious materials	6.96
Peak conc. of Np-237 at max sector within 20,000 yr $R^2 = 0.81$	1	Water well completion stratum selector	16.6
	2	Neptunium K_d in Oxidizing Region III cementitious materials	13.2
	3	Neptunium solubility in Oxidizing Region III cementitious materials	8.79
Peak conc. of Ra-226 at max sector within 20,000 yr $R^2 = 0.94$	1	Water well completion stratum selector	39.8
	2	Radium K_d in sandy soil	29.8
	3	Tank 32 inventory multiplier for Pu-238	6.28
Peak conc. of Tc-99 at max sector within 20,000 yr $R^2 = 0.92$	1	Water well completion stratum selector	40.5
	2	Technetium solubility in Oxidizing Region II cementitious materials	20.5
	3	Tank 36 inventory multiplier for Tc-99	15.7

For the All Cases analysis, the peak dose to a MOP within 10,000 years, using the highest estimated dose from any of the five failure scenarios, is also strongly influenced by the selector for the well completion stratum. This one variable is the only model variable with an SI value greater than 5 (i.e., this is the only variable that explains more than 5 % of the variation in the endpoint). The GBM fit R^2 of 0.75 indicates that noise in the model made for a challenging fit. The results for mean dose from each radionuclide are shown in Figure 5.6-39.

Figure 5.6-39: Radionuclide-Specific MOP Dose from any Sector within 20,000 Years, All Cases



5.6.5.4 Summary of the Sensitivity Analysis

The SA of the HTF GoldSim Model was very successful in identifying significant parameters for the selected endpoints. In the present analysis, GBM fitting has very high coefficient determination values, and relationships between input variables and result endpoint variations are clear.

Several recurring themes appeared in the SAs:

- The water well completion stratum parameter appeared in the top three sensitive parameters in almost every aqueous concentration and MOP dose endpoint.
- Specific K_d values are generally significant. More than half of the endpoints were dependent on the K_d s of radium in sandy soil, or of iodine or neptunium in Oxidizing Region III cements.
- Aqueous solubilities of technetium (and to a lesser degree, neptunium), in Oxidizing Region III cementitious materials are quite significant in determining well water concentrations and doses.
- A common influential variable type is an inventory multiplier parameter. Specific common inventory multipliers are for Tc-99 in Tanks 12 and 36, Np-237 in Tank 9, Pu-238 in Tank 32, and I-129 in Tank 36. These suggest that reducing uncertainty in inventory estimates could improve the defensibility of the model. The Tc-99 in Tank 36 has an especially strong influence on one third of all endpoints.
- In the Case-A MOP dose endpoint, the transfer factor for beef ingestion is also significant.

The water well completion stratum parameter is described in Section 5.6.3.11 and is based on well drilling records in counties bordering the SRS and concentration ratios developed from PORFLOW results.

The importance of K_d values in the HTF PA has been recognized and is an area of continued testing and analysis. Section 5.6.3.8 provides the results of current testing and analysis to develop the uncertainty parameters used within the model.

The representation of element-specific solubilities in cementitious materials is based on analyses reported in Section 4.2.1 and the uncertainty parameters are described in Section 5.6.3.3.

The strong and persistent influence of the inventory parameter on radionuclide concentrations, for various radionuclides in various waste tanks was anticipated. The basis for the initial residual inventories in the various waste tanks is provided in Section 3.3 and the development of the inventory multiplier parameter is described in Section 5.6.3.1.

The peak MOP dose within 20,000 years for the Base Case is influenced by the Tc-99 from beef ingestion, which is subject to influences from multiple uncertainty parameters, but is most strongly influenced by the transfer factor. This parameter is described in Section 5.6.3.12.

The SAs performed two important functions 1) it provided important feedback about which input parameters (and over what ranges) are most significant to specific endpoints, and 2) it identified parts of the model for which improved modeling implementation could prove most beneficial.

5.6.6 Barrier Analysis using the PORFLOW Deterministic Model

The *Barrier Analysis Report for the H-Area Tank Farm Performance Assessment* (SRR-CWDA-2012-00080) compared the fluxes beneath the containment structures for several deterministic PORFLOW simulations, each representing a different barrier failure mode. The objective of this report was to evaluate the importance of each barrier with respect to contaminant releases to the saturated zone.

The purpose of this section is to summarize the total barrier capability offered by each of the barriers as determined through the systematic analysis discussed in SRR-CWDA-2012-00080. The barrier analyses assessed the contribution of individual barriers (e.g., closure cap, grout, CZ, waste tank liner, and the vadose zone) by comparing contaminant flux results under various barrier conditions. The barrier analyses compared the differences in flux between intact and degraded barriers, while minimizing the contributions of the other barriers to the extent possible.

5.6.6.1 Barrier Analysis Scope

Barrier analyses were carried out for the waste tanks listed in Table 5.6-40. Each waste tank type is represented in this list, as well as representative Type I and II tanks with initially degraded liners (e.g., Tank 12 and Tank 15). Table 5.6-41 lists the radionuclides selected for barrier analyses, along with a description of their significance. The radionuclides chosen for analysis were the radionuclides with the greatest impact on dose and those possessing

differing transport characteristics (e.g., K_d values, solubility limits). The analysis point for each barrier is the radionuclide flux below the waste tank (i.e., at the water table for unsaturated waste tanks and exiting the basemat for submerged waste tanks). The Base Case initial inventory for each waste tank from HTF PA, Rev. 0 was used for all barrier analyses cases and alternative cases (e.g. the inventory estimates are the same).

A selection of the barrier analysis results is presented. Type II (both initially degraded and initially intact) and IV tanks are predominant dose contributors within 10,000 years of closure. Thus, the time histories of these waste tank types, displaying radionuclide fluxes, were the focus of the analyses (except for the vadose zone analysis which investigated effects on Type IV and IIIA tanks because submerged waste tanks were not a part of that analysis). The Type II tanks are unique in that they were modeled with an initial radionuclide inventory in their primary sand pad and annulus (Tank 16 also includes an initial inventory in the secondary sand pad).

Table 5.6-40: Summary of Waste Tanks Selected for Barrier Analysis

Representative Waste Tank	Waste Tank Type	Initially Failed Liner?
Tank 9	Type I (submerged)	N
Tank 12	Type I (submerged)	Y
Tank 13	Type II (submerged)	N
Tank 15	Type II (submerged)	Y
Tank 21	Type IV	N
Tank 36	Type IIIA	N

Table 5.6-41: Summary of Radionuclides Selected for Barrier Analysis

Radionuclide of Interest	Half-Life (yrs)	Significant Characteristics
Tc-99	2.11E+05	Significant dose contributor, long-lived, redox sensitive, K_d /solubility controlled
Ra-226	1.60E+03	Significant dose contributor, short-lived, not redox sensitive, K_d /solubility controlled, generated through ingrowth from the Pu-238→U-234→Th-230 chain
Pu-239	2.41E+04	Long-lived, redox sensitive, K_d /solubility controlled
I-129	1.57E+07	Significant dose contributor, long-lived, not redox sensitive, no solubility controls
Np-237	2.14E+06	Long-lived, K_d /solubility controlled, generated through ingrowth from Cm-245→Pu-241→Am-241 chain

The 10 run cases considered in the barrier analyses are detailed in Tables 5.6-42 and 5.6-43. In addition, waste tank releases generated using the alternative scenario settings for Cases B and C were also be evaluated (see Section 4.4.2 and Table 4.4-1 for a summary of the conceptual models for these two cases). Table 5.6-42 identifies the barrier analysis parameters for the five PORFLOW material zones that are varied (vadose zone, closure cap, CZ, waste tank liner, and cementitious materials including waste tank grout, basemat, wall,

and roof). Table 5.6-42 also describes the nominal (N), partially degraded (P), and fully degraded (F) conditions for each material zone. Table 5.6-43 lists the physical conditions of the material zone for each of the ten run configurations. The barrier analyses included the HTF PORFLOW Base Case, which uses the nominal barrier properties and a degraded run scenario (run 2) where every zone other than the CZ is modeled as fully degraded. There are also specific barrier cases associated with each material zone to evaluate the capabilities of each barrier configuration by holding other material zone conditions constant while varying the condition of the zone being assessed. Additional information regarding the material zones for the various barriers is provided in Sections 4.2.1 and 4.2.2.

Table 5.6-42: Barrier Analysis Variability

Material Zone	N (Nominal)	P (Partially Degraded)	F (Fully Degraded)
Closure Cap	Infiltration profile per Base Case (Table 4.2-23)	N/A	Infiltration constant at 16.45 in/yr (WSRC-STI-2007-00184)
Grout (K_d controlled)	Hydraulic properties (e.g., failure date) and chemical properties unchanged per Base Case	N/A	Hydraulic properties failed grout time 0, chemical properties unchanged, high flow throughout grout causes impart reducing capacity onto CZ.
CZ (Solubility controlled)	CZ initial solubility limits associated with Base Case	N/A	Solubility controls removed for Tc-99 and Ra-226 and set at very high levels for remaining radionuclides.
Waste Tank Liner ^a	Later liner failure (grouted CO ₂ diffusion coefficient of 1E-06)	Early liner failure (grouted CO ₂ diffusion coefficient 1E-04)	No waste tank liner at time = 0 years.
Waste Tank Concrete ^c (K_d controlled)	Hydraulic properties (e.g., failure date) and chemical properties unchanged per Base Case.	N/A	Hydraulic properties of failed concrete, initial chemical properties unchanged. Chemical transitions are function of “failed” flow fields.
Vadose Zone ^b (K_d controlled)	Native soil K_d values equal Base Case values	N/A	Native soil K_d values are as defined in SRR-CWDA-2012-00080.

a The liner barrier analysis does not apply to waste tanks with initially failed waste tank liners (e.g., Tanks 12 and 15 for this analysis).

b The vadose zone is the unsaturated native soil zone below the basemat of the waste tanks, therefore, this analysis only applies to the unsaturated waste tanks, which include Type III, IIIA and IV tanks.

c Includes basemat, wall, and roof cementitious materials.

N/A = Not applicable

Table 5.6-43: Barrier Analyses Configuration Case Summary by Material Zone

Configuration		PORFLOW Case A	Fully Degraded	Waste Tank Liner ^a			CZ		Natural Barrier		Closure Cap
Barrier Case		N/A	2	3	4	5	6	7	8	9	N/A
Material Zone	Closure Cap	N	F	F	F	N	F	N	N	F	F
	Grout and Concrete (basemat, wall, roof)	N	F	F	F	N	F	N	N	F	N
	CZ	N	N	N	N	N	F	F	N	N	N
	Liner	N	F	N	P	P	F	N	N	F	N
	Vadose Zone	N	F	F	F	N	F	N	F	N	N

a For Tank 12 and 15, liner is failed at time zero, therefore partial liner barrier analysis and liner barrier analysis are not applicable.

N = Nominal
P = Partially degraded
F = Fully degraded
N/A = Not applicable
Case A = Base Case

The results of the barrier analyses are presented in the *Barrier Analysis Report for the H-Area Tank Farm Performance Assessment* and summarized in Section 5.6.6.2. Although these barrier analyses were performed for Revision 0 of the HTF PA, the underlying model assumptions and performance-affecting properties of the barriers have not greatly changed therefore, the conclusions from these analyses remain applicable for Revision 1 of the HTF PA.

5.6.6.2 Barrier Analysis General Conclusions

The barriers with the most impact on releases from the source waste tanks are the liners, the CZ, and the waste tank grout, in this order. The closure cap and the vadose zone have less of an impact on radionuclide fluxes.

For the CZ, the waste tank grout, and the vadose zone, the importance of the barrier on radionuclide transport is element specific whereas the liner and closure cap are inclined to have similar effects on all radionuclides. Although an independent barrier analysis of the annulus grout was not performed, it is apparent from the interpretation of other analyses that the timing of annulus grout transition (in Type I and Type II waste tanks) greatly influences the timing of Tc-99 peak doses. The annulus transition triggers a large decrease in Tc-99 sorption onto the annulus grout (from a K_d of 5,000 mL/g to 0.8 mL/g). This transition combined with a significant inventory in the annulus (some initiated in the sand pads) produces significant releases prior to liner failure.

Liner failure has the largest impact on the timing of peak flux for the different radionuclides. The earlier a waste tank liner fails, the earlier the peak release for that radionuclide. Depending on the time of early failure, the peak flux can occur earlier by thousands of years. The change in the magnitude of the peaks varies by waste tank type and radionuclide. The

liner is an effective barrier to radionuclide migration because it is designed to prevent flow and mass transport out of the waste tanks. Failure of the liner allows mass built up behind the liner to be rapidly flushed from the bottom of the waste tanks. Secondary effects of liner failure include increased physical degradation of the grout, which influences the timing of solubility changes in the CZ and K_d transitions in the cementitious materials and vadose zone. In this way, the timing of liner failure strongly controls peak flux.

The CZ, which mostly impacts peak Tc-99 and Pu-239 releases (and Np-237 in later years), acts to delay and dampen the peak fluxes by one or more orders of magnitude, however it has no apparent impact on the transport of I-129 and Ra-226. The CZ effectively dampens the flux of Tc-99 and Pu-239 out of the waste tanks because 1) these radionuclides are strongly controlled by solubility, and 2) their aqueous concentration in the CZ remains at or close to the solubility limit. If their aqueous concentrations were less, the CZ would be less effective at limiting the release of these radionuclides.

The integrity of the waste tank grout plays an important role in delaying the releases of I-129, Ra-226, Np-237, and Pu-239 although the effects on magnitude are not significant. The integrity of the waste tank grout indirectly affects the Tc-99 releases, in that degraded waste tank grout has the ability to impart its reducing capacity onto the CZ, which causes the CZ chemical transitions to occur later. The impact of the grout on Type II tanks (both with and without a liner) is more difficult to discern because the radionuclide releases are overprinted by the inventory coming from the sand pads and annulus. More specifically, the large fluctuations in the hydraulic conductivity through the grout can greatly change the flow fields through the waste tank system, including redirecting flow through the annulus, which acts as a sink/source of inventory prior to liner failures.

The closure cap plays an important role in that it limits flow into and through the tanks, at least in the first few thousand years. The impact of the faster flow in the first few thousand years from removal of this barrier results in greater Np-237 and Pu-239 releases by as much as two orders of magnitude. The natural barrier dampens radionuclide releases especially for those radionuclides with higher soil K_d s (e.g., plutonium and radium, as well as the parents of radium and neptunium); however, this barrier plays a lesser role in controlling peak releases.

5.6.7 Sensitivity Analysis using the HTF Deterministic Model

This section presents the sensitivity of the HTF closure system to alternative waste tank cases, and the sensitivity of the system to key parameter variability. Although certain conditions used in the alternative cases and sensitivity studies are either non-mechanistic or not supported by experimental data (e.g., complete degradation of cementitious material in one time step at 501 years), sensitivity studies and simulation of alternative scenarios with pessimistic and/or variable settings provides insight into parameter importance to groundwater dose. For example, simulating the Base Case with the closure cap material zone set equal to the estimated natural infiltration rate (e.g., 16.45 in/yr) provides insight into the importance of this feature on the 100-meter groundwater pathway dose.

Section 5.6.7.1 contains alternative scenario analysis using the PORFLOW deterministic model, with the results summarized in Table 5.6-44. The scenarios considered in Section 5.6.7.1 include the impact of the various waste tank scenarios (i.e., Cases B through E) on

dose, the impact of assuming a no closure cap condition on dose, and impact on dose of a synergistic case that evaluates multiple pessimistic assumptions regarding three key modeling parameters. Sections 5.6.7.2 through 5.6.7.8 contain individual sensitivity studies of key parameter variability performed using the HTF PORFLOW Deterministic Model. The 100-meter radionuclide concentrations for each of the alternative scenarios and individual sensitivity studies (documented in Appendices H through U) are used to calculate the total dose associated with the individual MOP peak 100-meter groundwater pathways identified in Section 5.4. The sensitivity studies analyzed the impact of variability on the following:

- Grout transition times
- Key radionuclide solubility values
- Calcareous zones, soil K_d values
- Waste tank liner failure times
- Cementitious degradation rate
- Water ingestion rate

Table 5.6-44: Base Case and Alternative Cases Peak Doses

Case	1,000-Year Peak Dose	10,000-Year Peak Dose	100,000-Year Peak Dose
A	0.3 mrem/yr at year 700	4 mrem/yr at year 8,790	124 mrem/yr at year 90,800
B	12 mrem/yr at year 1,000	14 mrem/yr at year 1,060	125 mrem/yr at year 81,260
C	2.1 mrem/yr at year 480	16 mrem/yr at year 7,030	124 mrem/yr at year 84,040
D	12 mrem/yr at year 1,000	18 mrem/yr at year 6,340	123 mrem/yr at year 82,160
E	3.7 mrem/yr at year 840	239 mrem/yr at year 2,320	239 mrem/yr at year 2,320
NoCap	0.7 mrem/yr at year 690	4.7 mrem/yr at year 8,770	N/A* 9.4 mrem/yr at year 16,410
Synergistic Case	2.7 mrem/yr at year 970	5.7 mrem/yr at year 10,000	N/A* 12.5 mrem/yr at year 20,000

* Only calculated to 20,000 years

5.6.7.1 Alternative Scenario Analysis using the PORFLOW Deterministic Model

To simulate potential conditions in the HTF closure system over the modeling period, seven alternate modeling scenarios are analyzed. The seven scenarios include five waste tank cases (Cases A through E), a no closure cap scenario, and a “synergistic” waste tank case.

Base Case (Case A) through E Discussion

Case A results are considered the Base Case and are presented in Section 5.5. The alternate cases allow evaluation of system behavior while varying key components of the conceptual model. Section 4.4.2 describes the different cases in detail.

Each case starts out with the system closed as planned, with waste tanks and ancillary equipment filled with grout and the closure cap in place. Expected degradation of the closure cap materials over time are simulated using the increasing infiltration rates shown in Table 3.2-14 (and are the same for all five cases). Each waste tank case is simulated using the waste release process described in Section 4.2.1 and the material properties described in Section 4.2.2.2.

The differences between the seven waste tank cases are summarized in Table 4.4-1. Cases A through E vary according to whether 1) a fast flow channel through the grout and basemat exists, 2) the cementitious materials degrade at 501 years in a single time step, 3) the liner fails early, and 4) the grout volume is used to calculate the chemical transition time. These four factors define the physical and chemical transition times for each waste tank type. The transition times are provided in Table 4.2-32 for each waste tank and case and are discussed in Section 4.4.3. The property transitions in the waste tank system control the timing and magnitude of contaminant releases, and therefore the tables will aid the interpretation of the dose results. Additional process change timelines for the different tank types associated with the Base Case through E are provided in Section 4.4.3 (Tables 4.4-2 through Table 4.4-9).

No Closure Cap Sensitivity Case Discussion

The no closure cap analysis evaluates the sensitivity of the 100-meter groundwater pathway dose to the engineered closure cap. The deterministic case, the Base Case, is simulated using PORFLOW, but the closure-cap material zone is set equal to background infiltration for the No Cap Case. Using the HELP model, background infiltration was estimated to be 16.45 in/yr. [WSRC-STI-2007-00184 Figure 29 and Table 31] This is analogous to modeling a soils only closure cap with no barrier, drainage, or erosion control layers. The impact of removing the engineered closure cap is determined by comparing the timing and magnitude of the dose peaks of the sensitivity case with the Base Case. For a comparison of radionuclide fluxes below the waste tanks for these two cases (from HTF PA Rev. 0), see the no cap barrier analysis in SRR-CWDA-2012-00080.

Synergistic Sensitivity Case Discussion

In order to address uncertainty related to three key modeling parameters, a synergistic sensitivity case was developed using the PORFLOW deterministic model. The three parameters analyzed further are gas transport impacts on reducing grout, liner failure times, and solubility controlling phases. The synergistic case evaluates the combined results of pessimistic assumptions regarding these three key modeling parameters.

The starting point for the case development is Case C. As described in Section 4.4.2.3, Case C models a fast flow path that bypasses the reducing grout fill and thus the reducing grout is not assumed to affect the chemistry of the infiltrating water. This assumption causes the solubility phase to change from reducing to oxidized in tens to hundreds of years following closure (for waste tanks with initially failed liners) or failure of the waste tank liner as seen in Tables 4.4-2 through 4.4-9. This assumption addresses the uncertainty related to the duration of the assumed reducing conditions by eliminating the influence of the reducing grout fill.

There were two additional modifications to the Case C model to address the other two parameters. In Case C, the waste tank liners are assumed to fail early with Type I tank liners failing at 1,142 years, Type II tank liners at 2,506 years, Type III and IIIA tank liners at 2.077 years and Type IV liners at 75 years (except for Tanks 12, 14, 15, and 16 which are assumed failed at time of closure). To address the synergistic impact of earlier liner failure, the failure time for Type I, II, III, and IIIA tanks was modeled at 500 years while the liner failure time for Type IV tanks was modeled at 75 years.

The second modification to Case C was made to address alternative solubility controlling phases. Table 5.6-45 presents the values modeled for this case.

Table 5.6-45: Synergistic Sensitivity Case Solubility Controlling Phases

	Reduced Region II Solubility (mol/L)		Oxidized Region II Solubility (mol/L)		Oxidized Region III Solubility (mol/L)
	Non-submerged	Submerged	Non-submerged	Submerged	All tanks
Pu	1.7E-09 (Pu(OH) ₄)	1.7E-09 (Pu(OH) ₄)	3.0E-7 (Pu(OH) ₄)	4.5E-10 (PuO ₂ (OH) ₂)	5.7E-5 (Pu(OH) ₄)
Tc	3.3E-8 (TcO ₂ .H ₂ O)	1.1E-31 (Tc ₂ S ₇)	No solubility control - Modeled as instantaneous release	No solubility control - Modeled as instantaneous release	No solubility control - Modeled as instantaneous release
U	3.5E-05 (UO ₂)	3.5E-05 (UO ₂)	1.8E-5 (Schoepite)	2.5E-7 (Becquerelite)	3.4E-5 (Becquerelite)
Np	5.1E-9 (NpO)	1.6E-9 (Np(OH) ₄)	6.8E-7 (NpO ₂ (OH))	2.5E-5 (NpO ₂ (OH))	1.3E-4 (Np(OH) ₄)

5.6.7.1.1 Alternative Scenario MOP 100-Meter Groundwater Pathway Dose

The 100-meter radionuclide concentrations for Cases B through E (documented in Appendices I thru L) were used to calculate the total dose associated with the individual MOP peak 100-meter groundwater pathways identified in Section 5.4 (a discussion of how peak concentrations are determined by sector is provided in Section 5.2). Figures 5.6-40 through 5.6-47 provide the 10,000-year groundwater pathway doses for Cases B through E.

Figure 5.6-40: Case B MOP Groundwater Pathway Dose

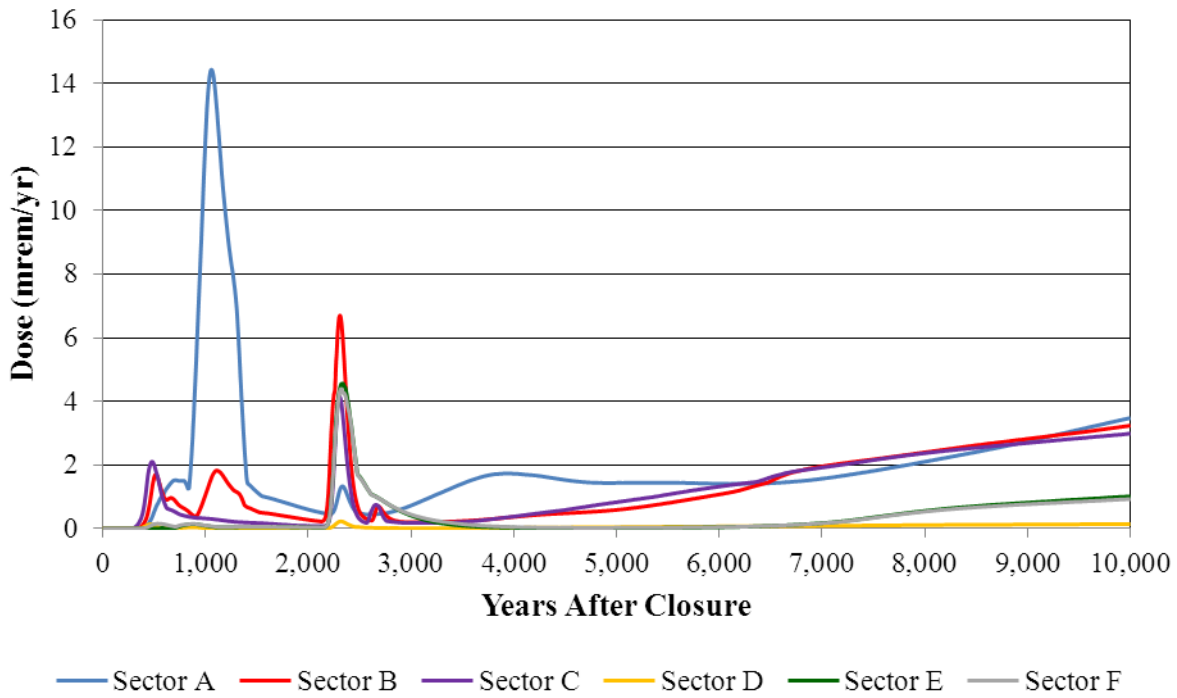


Figure 5.6-41: Case B Individual Radionuclide Contributors to MOP Groundwater Pathway Dose

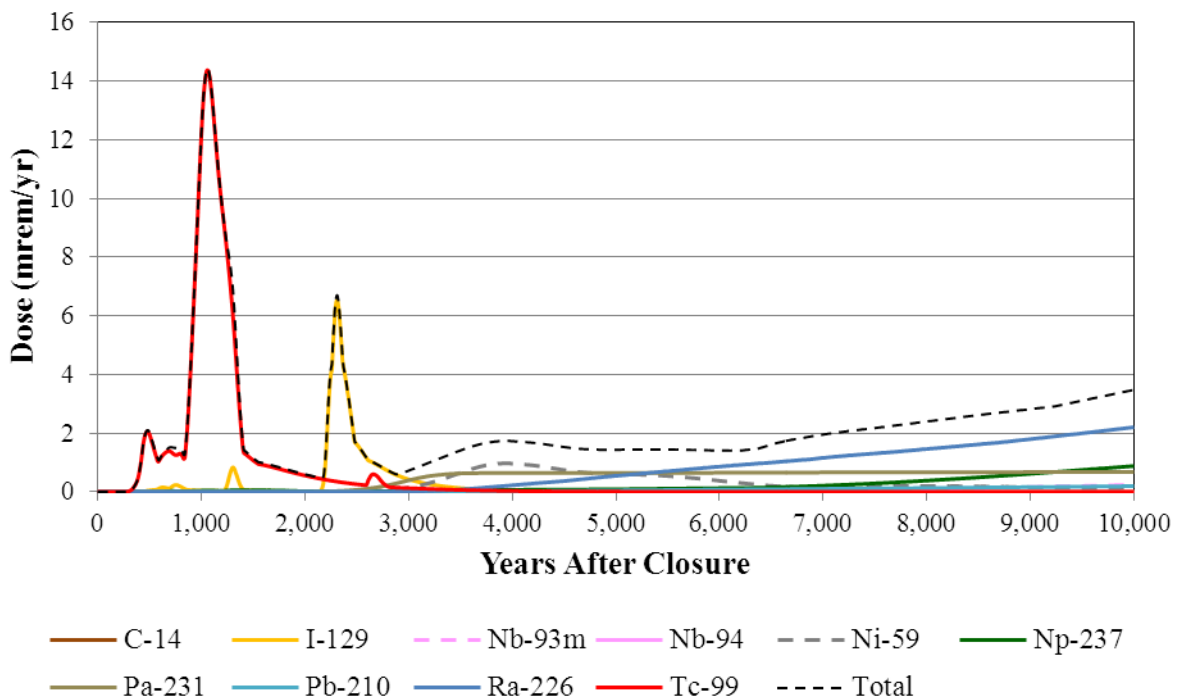


Figure 5.6-42: Case C MOP Groundwater Pathway Dose

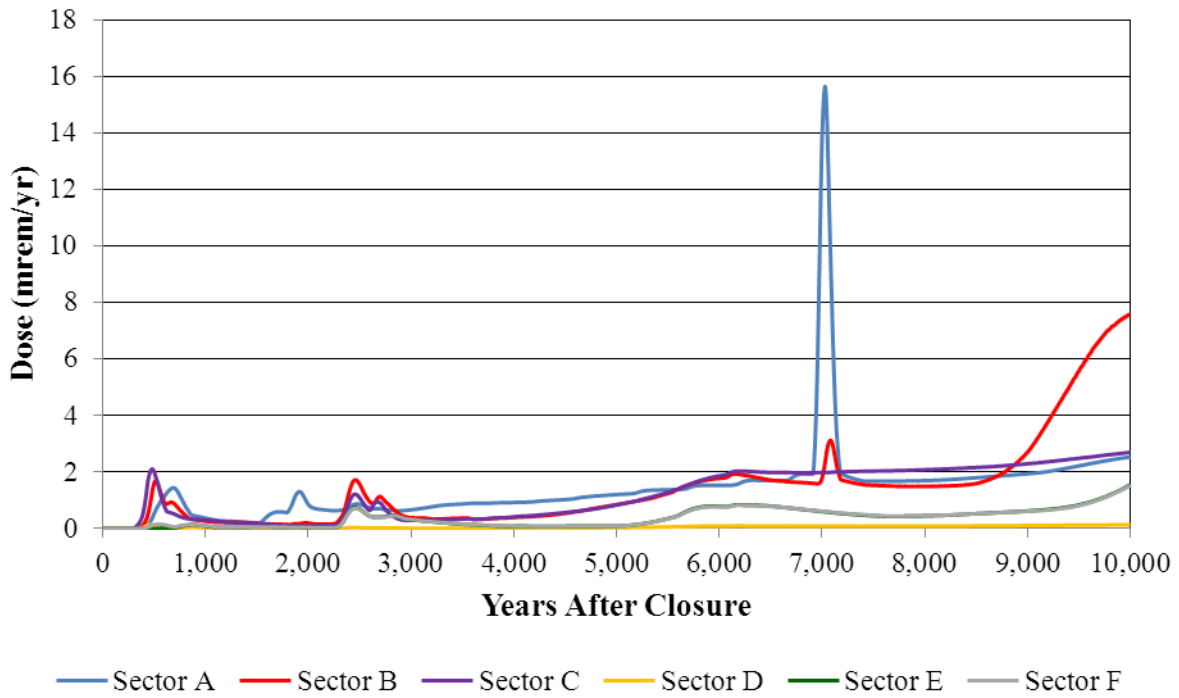


Figure 5.6-43: Case C Individual Radionuclide Contributors to MOP Groundwater Pathway Dose

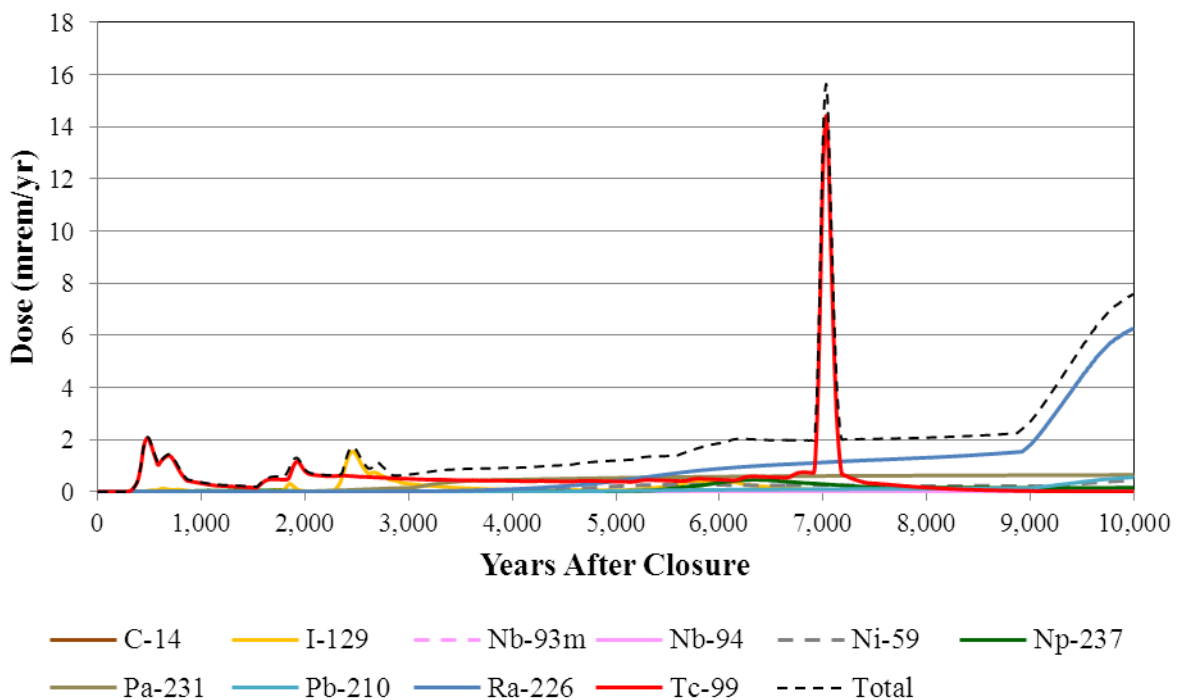


Figure 5.6-44: Case D MOP Groundwater Pathway Dose

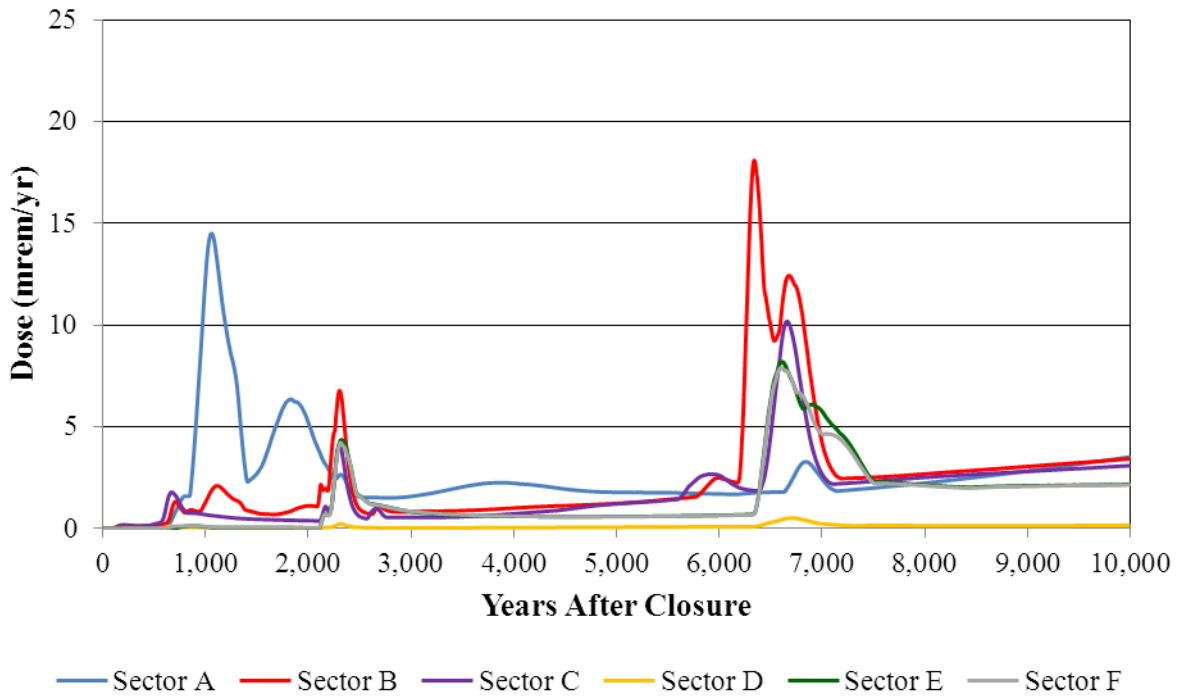


Figure 5.6-45: Case D Individual Radionuclide Contributors to MOP Groundwater Pathway Dose

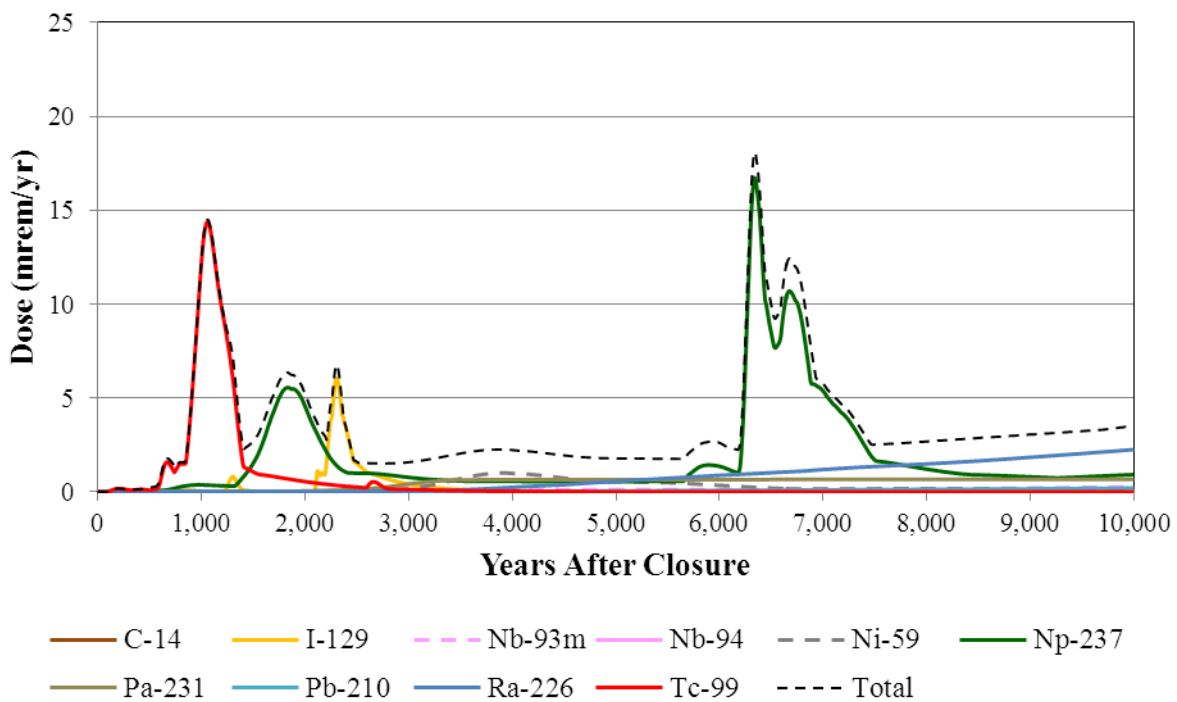


Figure 5.6-46: Case E MOP Groundwater Pathway Dose

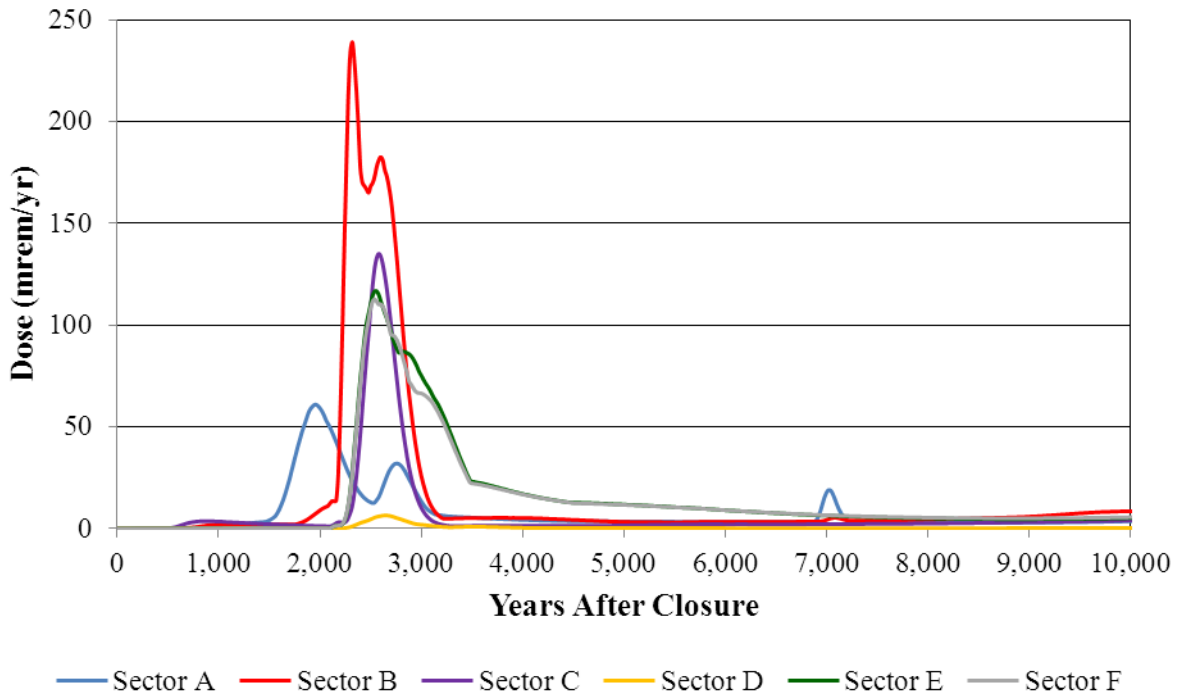
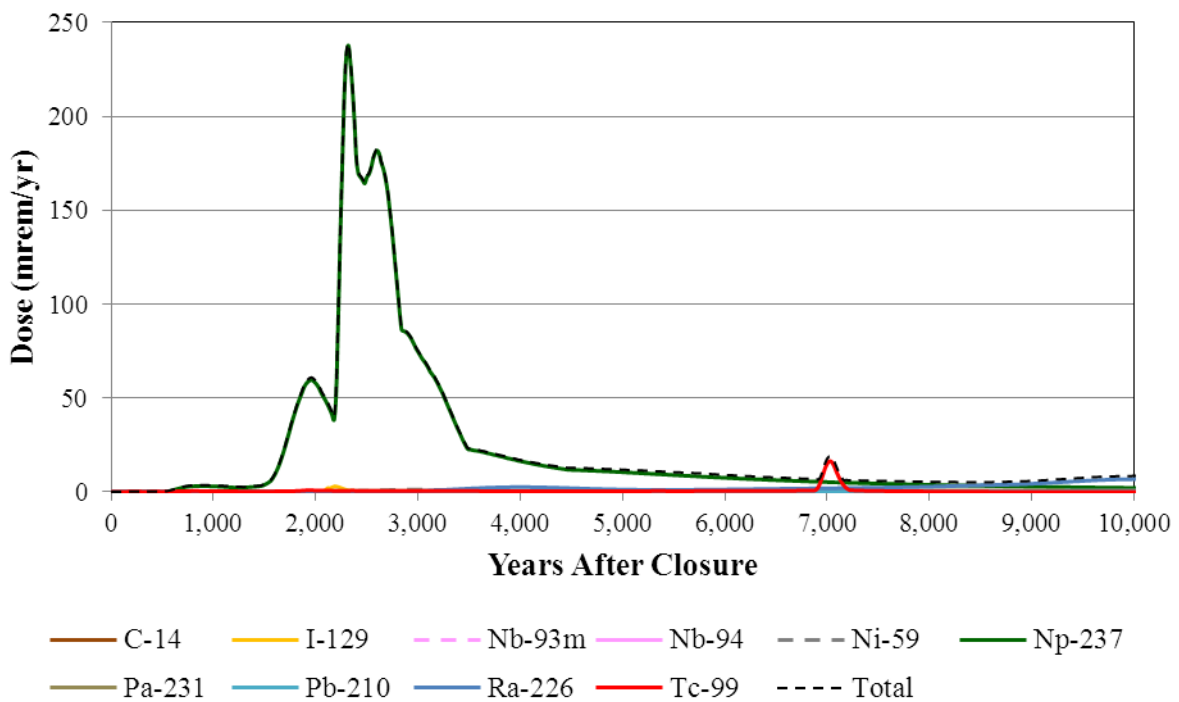


Figure 5.6-47: Case E Individual Radionuclide Contributors to MOP Groundwater Pathway Dose



5.6.7.1.2 No Closure Cap MOP 100-Meter Groundwater Pathway Dose

The 100-meter radionuclide concentrations for the No Cap Case (documented in Appendix H) are used to calculate the total dose associated with the individual MOP peak 100-meter groundwater pathways identified in Section 5.4 (a discussion of how peak concentrations are determined by sector is provided in Section 5.2). Figures 5.6-48 and 5.6-49 display the No Cap Case peak 100-meter groundwater-pathway dose time histories by sector for 10,000 years and 20,000 years respectively. Figure 5.6-50 displays the individual radionuclide contributions for the No Cap Case. The total dose is also plotted with the individual radionuclides to see their relative contribution.

Figure 5.6-48: No Closure Cap Case MOP Groundwater Pathway Dose – 10,000 Year

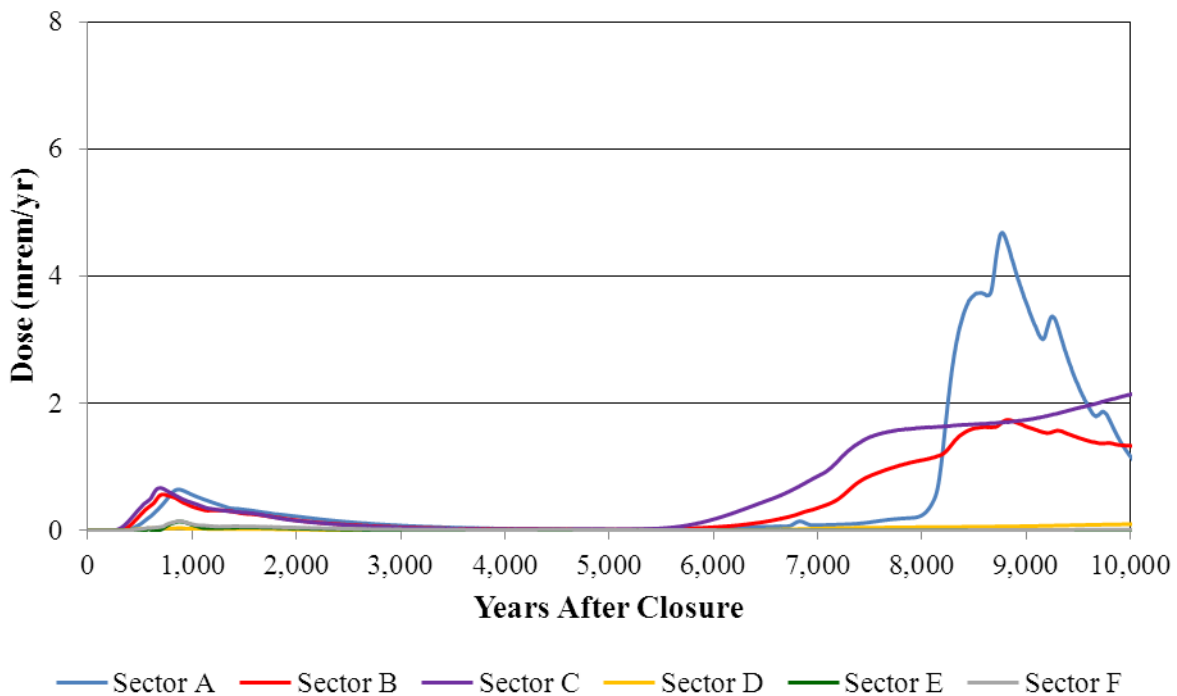


Figure 5.6-49: No Closure Cap Case MOP Groundwater Pathway Dose – 20,000 Year

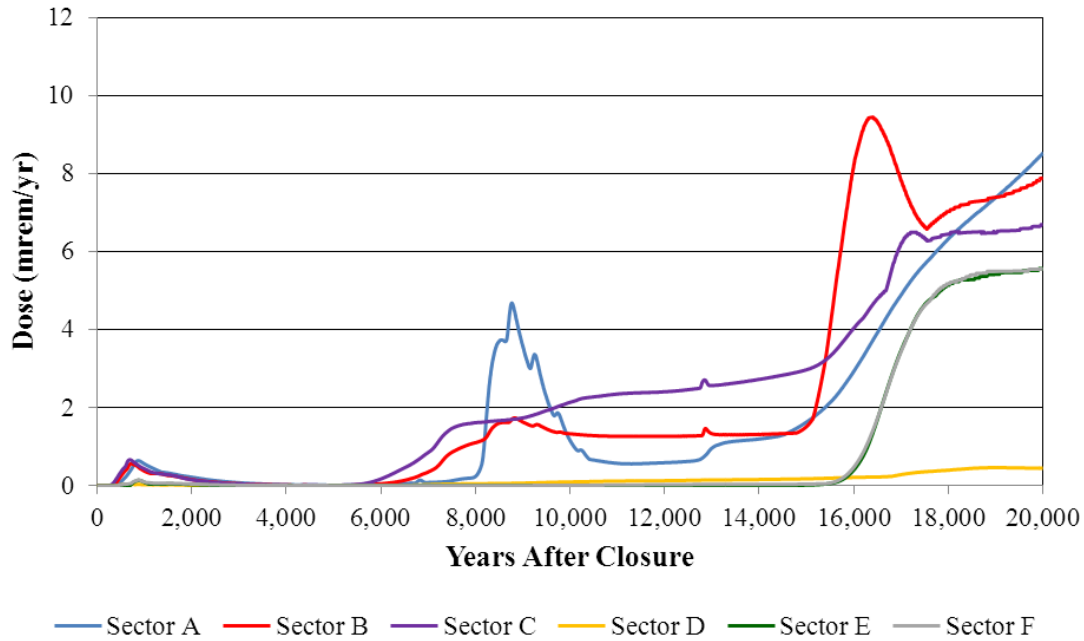
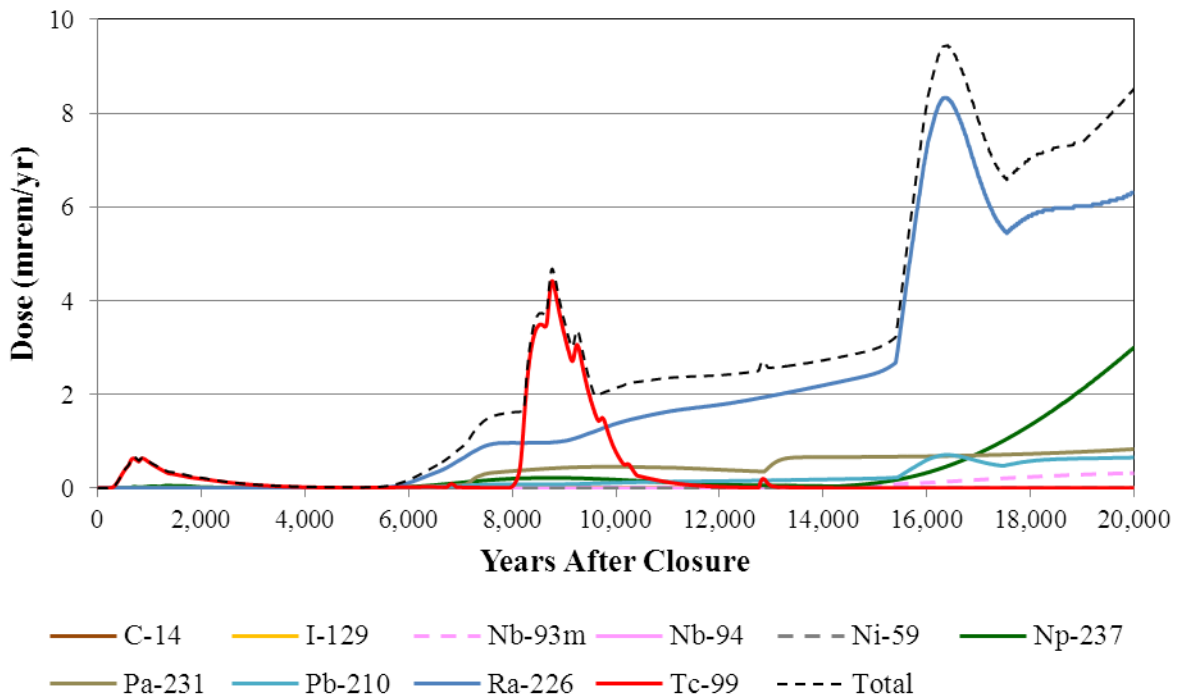


Figure 5.6-50: No Closure Cap Case Individual Radionuclide Contributors to MOP Dose – 20,000 Years



5.6.7.1.3 Synergistic Sensitivity Case 100-Meter Dose Results

Figures 5.6-51 and 5.6-52 display the peak, MOP dose time histories by sector for the synergistic case for 10,000 years and 20,000 years, respectively. Figure 5.6-53 displays the individual radionuclide contributions to the total for 20,000 years.

Figure 5.6-51: Synergistic Case MOP Groundwater Pathway Dose by Sector - 10,000 Years

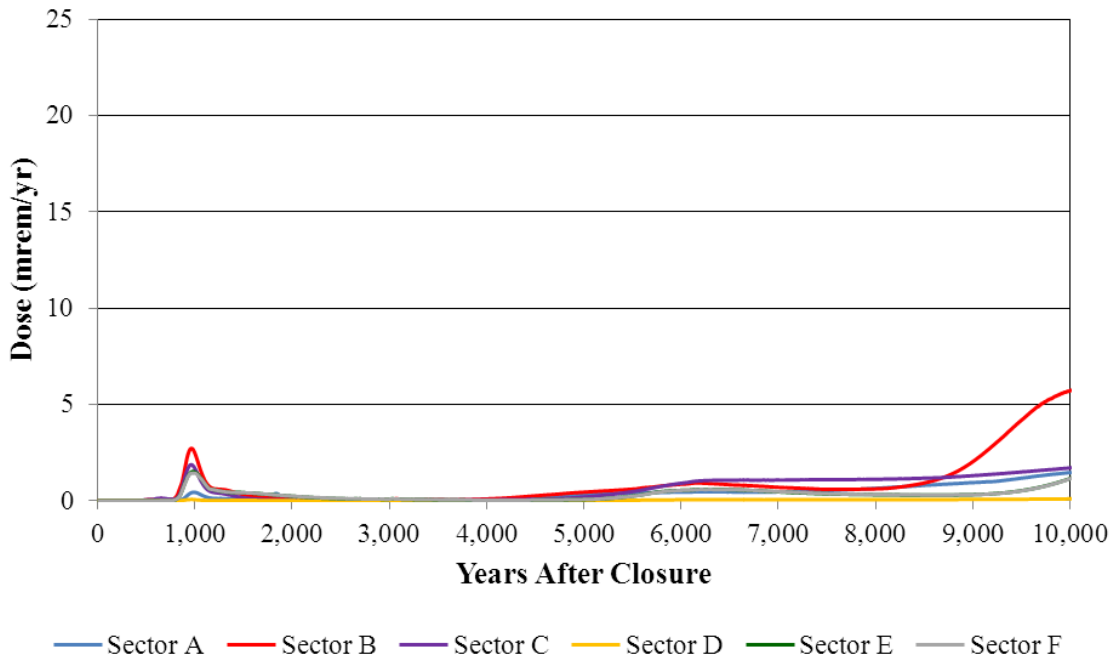


Figure 5.6-52: Synergistic Case MOP Groundwater Pathway Dose by Sector - 20,000 Years

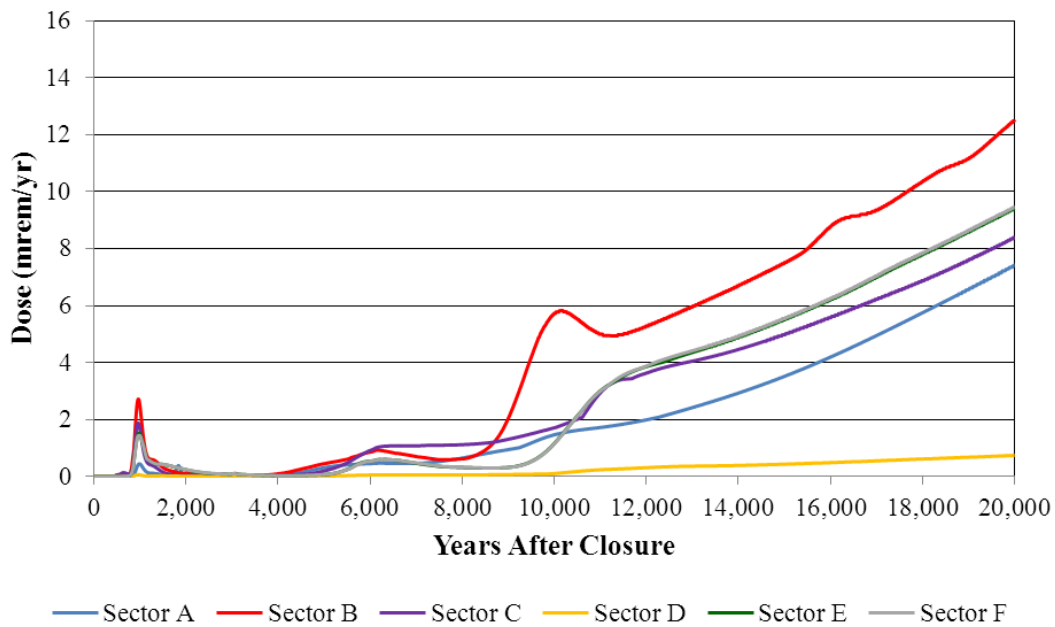
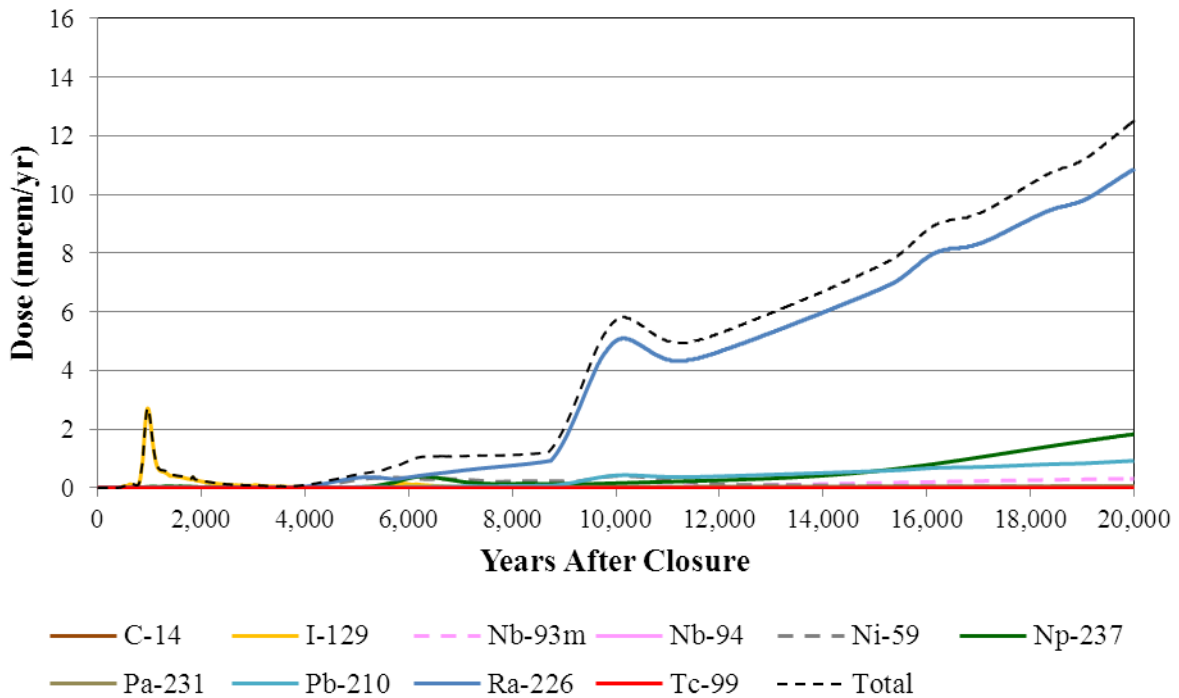


Figure 5.6-53: Synergistic Case Individual Radionuclide Contributors to MOP Dose – 20,000 Years



5.6.7.1.4 Alternative Scenario MOP 100-Meter Groundwater Pathway 100,000 Year Dose

The 100-meter radionuclide concentrations for Cases B through E were evaluated for a period of 100,000 years. Figures 5.6-54 through 5.6-63 provide the 100,000-year groundwater pathway doses and the individual radionuclide contributors to the total dose for Cases B through E.

Figure 5.6-54: Base Case MOP Groundwater Pathway Dose

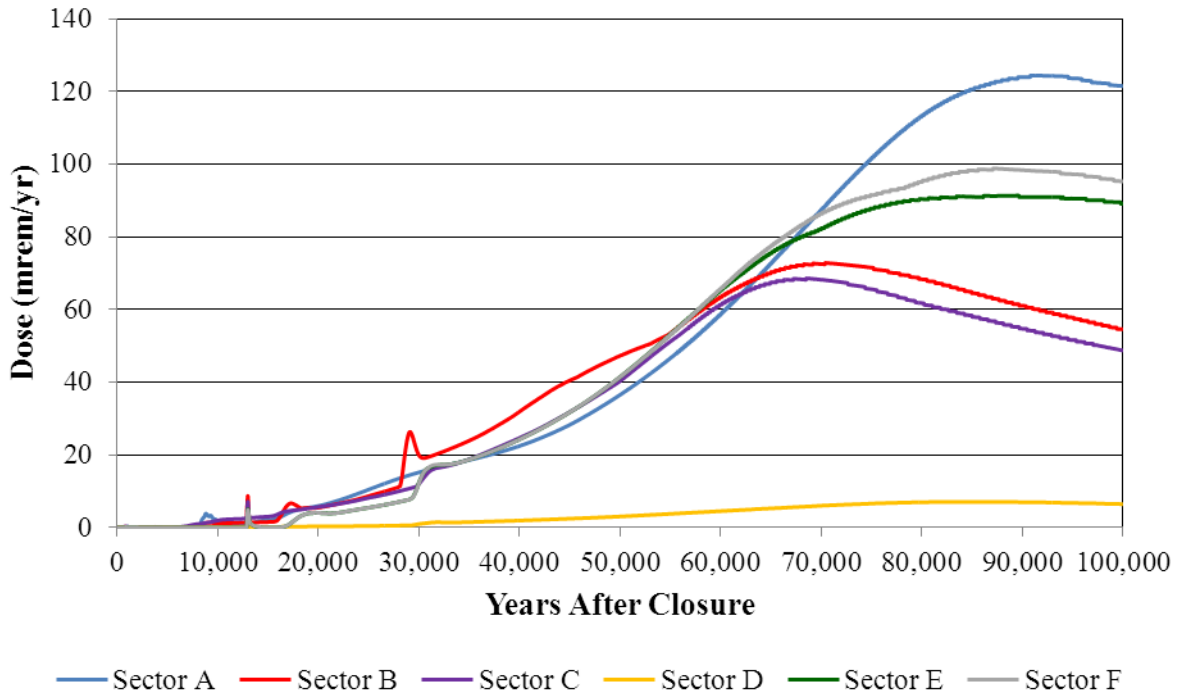


Figure 5.6-55: Base Case Individual Radionuclide Contributors to MOP Groundwater Pathway Dose

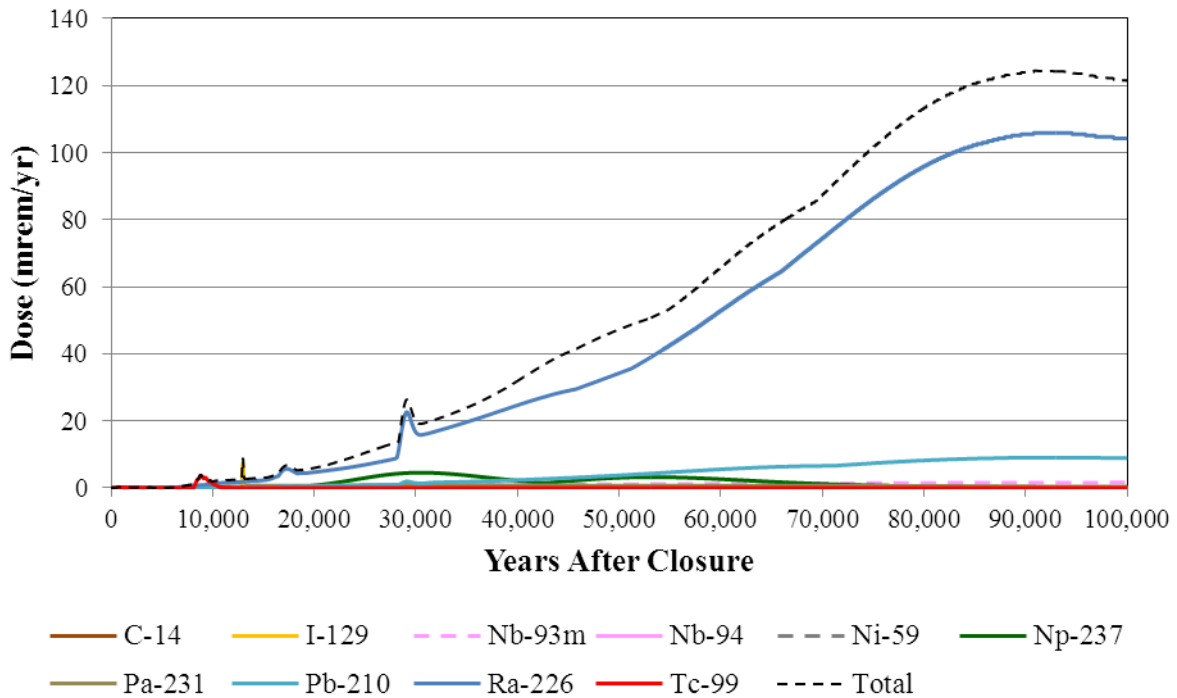


Figure 5.6-56: Case B MOP Groundwater Pathway Dose

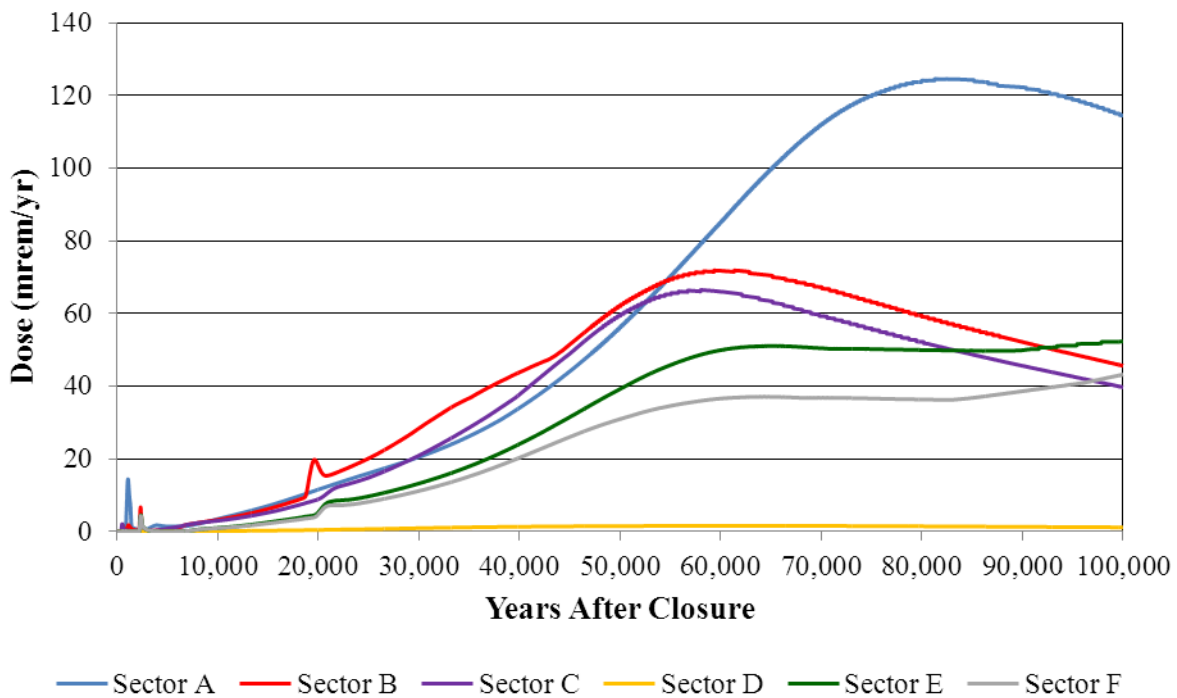


Figure 5.6-57: Case B Individual Radionuclide Contributors to MOP Groundwater Pathway Dose

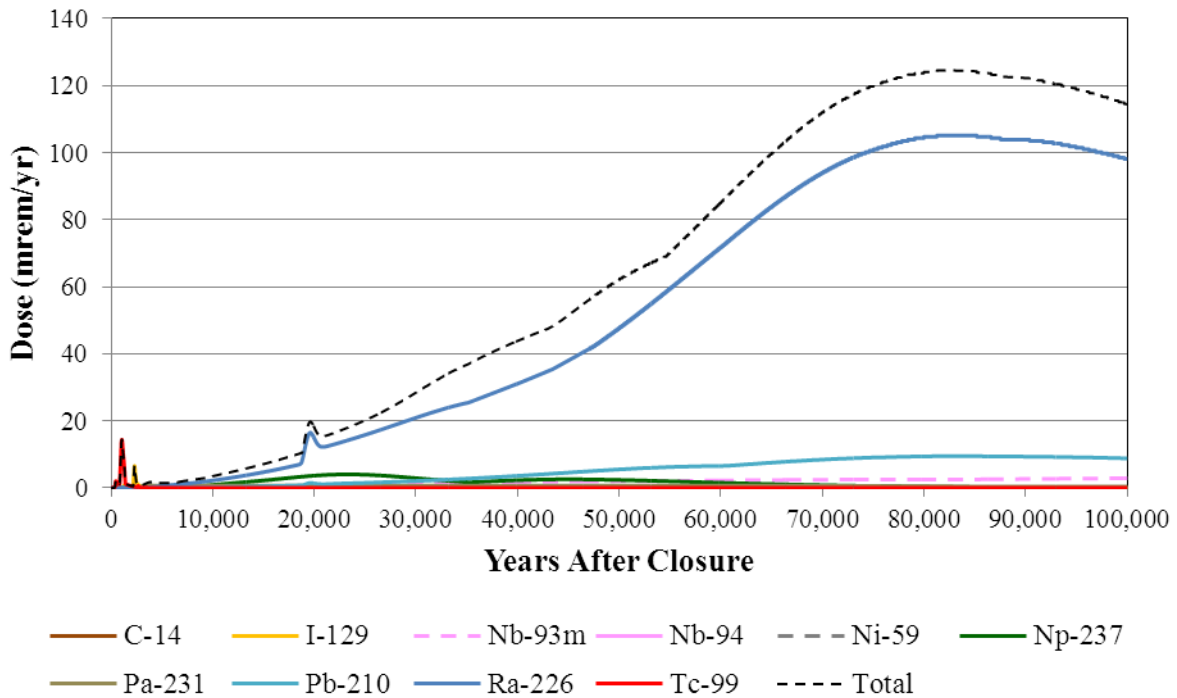


Figure 5.6-58: Case C MOP Groundwater Pathway Dose

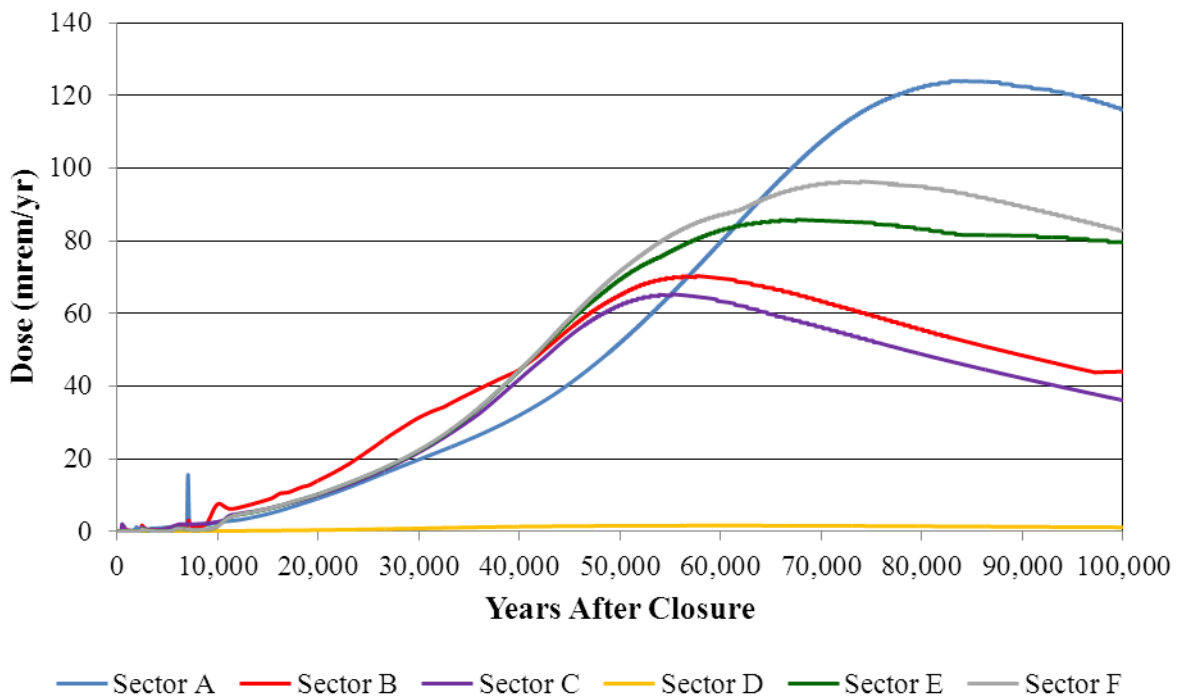


Figure 5.6-59: Case C Individual Radionuclide Contributors to MOP Groundwater Pathway Dose

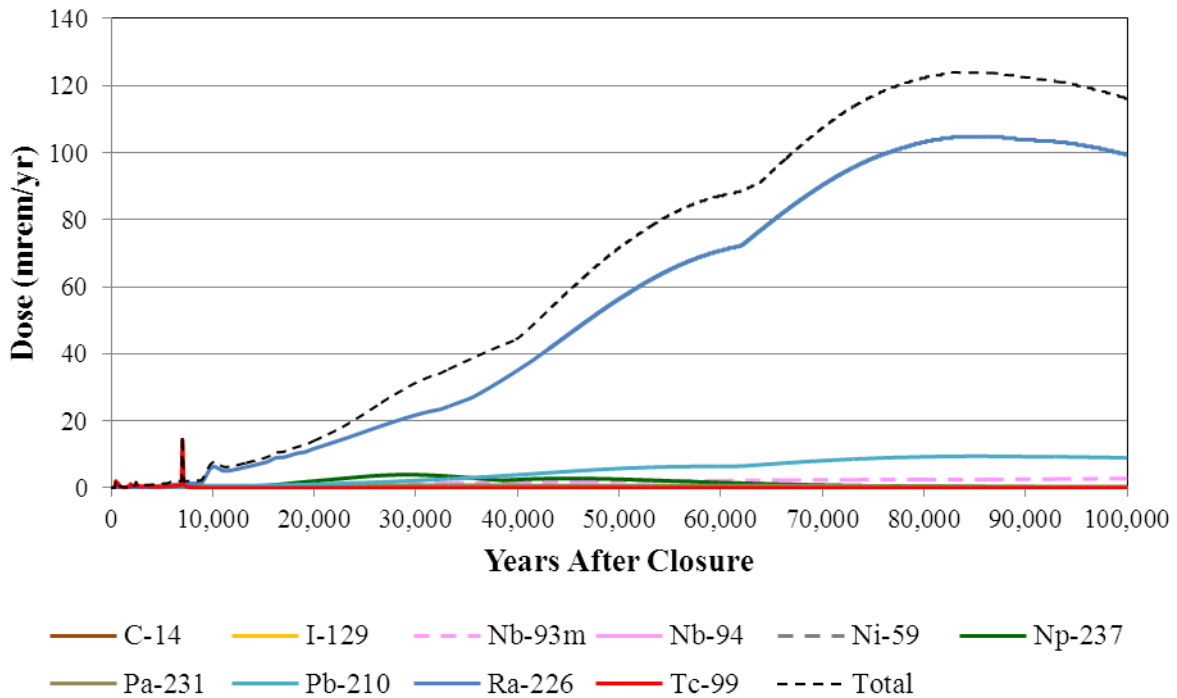


Figure 5.6-60: Case D MOP Groundwater Pathway Dose

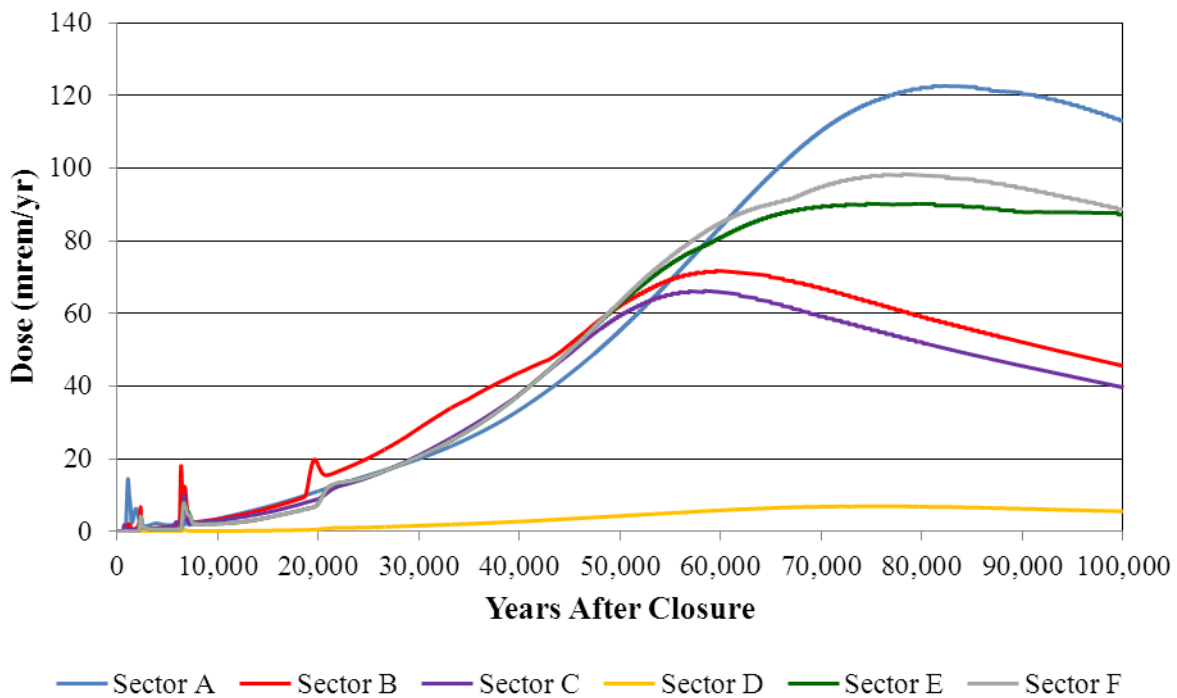


Figure 5.6-61: Case D Individual Radionuclide Contributors to MOP Groundwater Pathway Dose

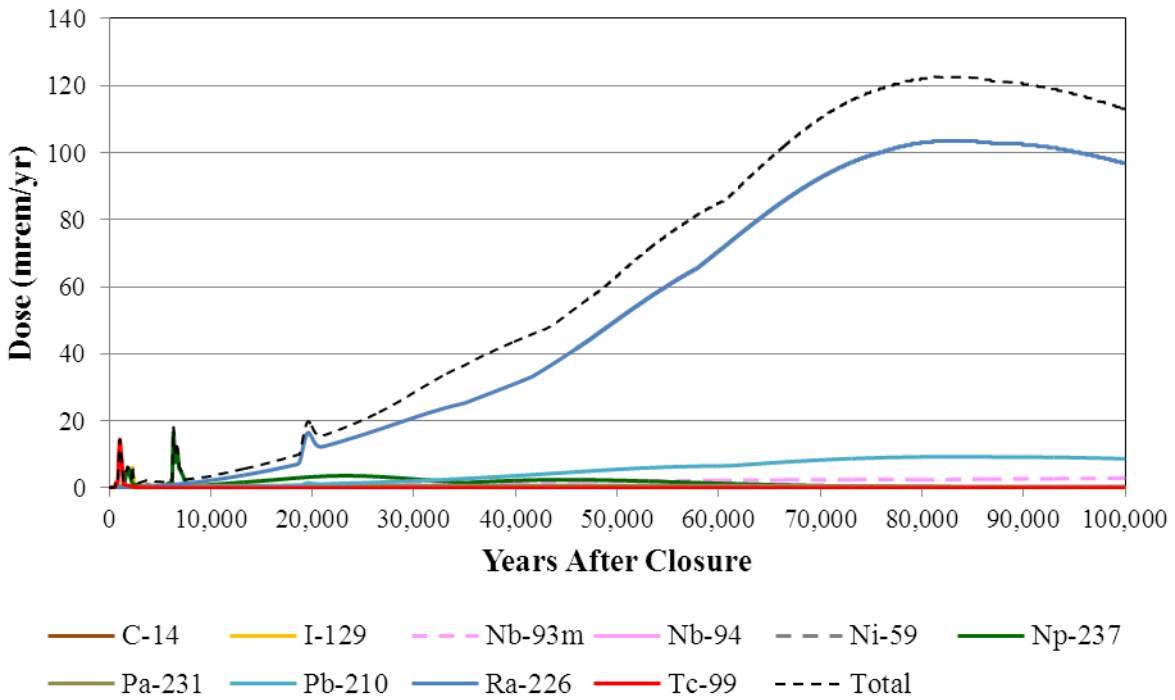


Figure 5.6-62: Case E MOP Groundwater Pathway Dose

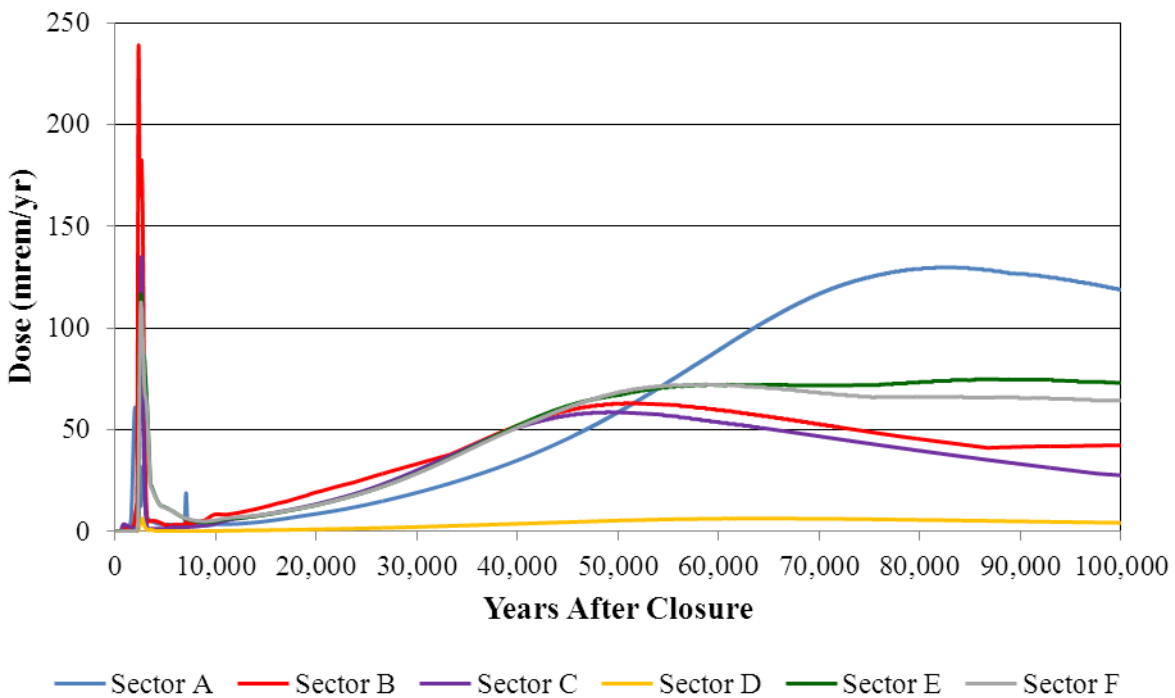
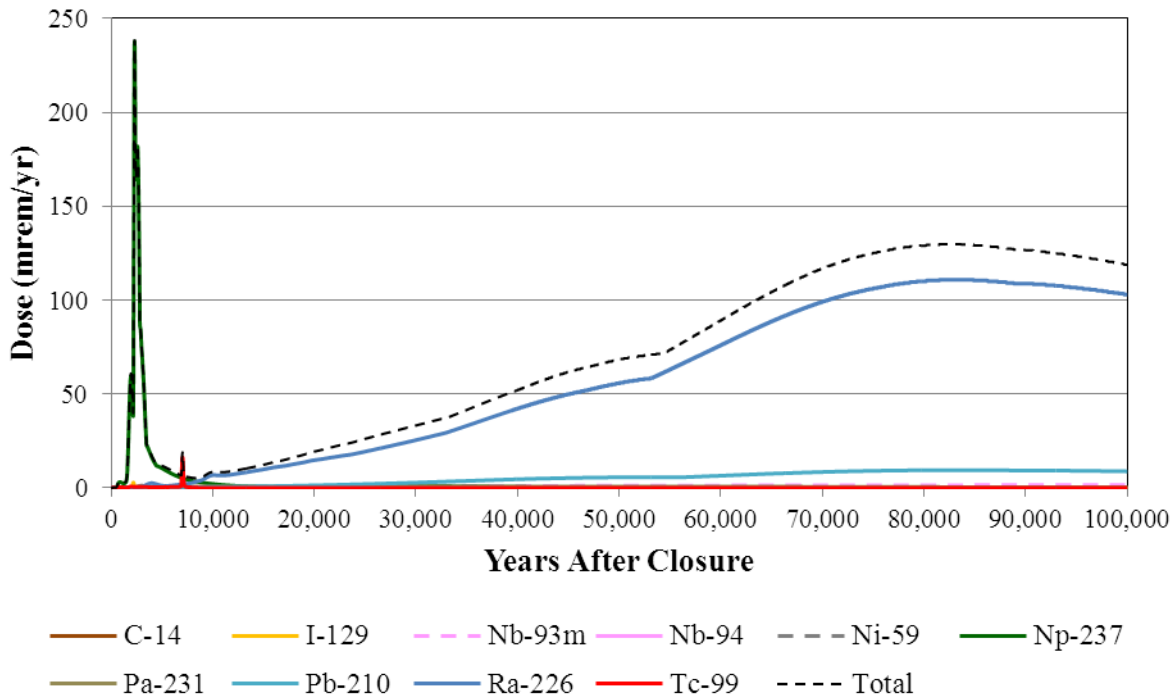


Figure 5.6-63: Case E Individual Radionuclide Contributors to MOP Groundwater Pathway Dose



5.6.7.2 Grout Transition Time Analysis using the PORFLOW Deterministic Model

To study the impact of grout transition-time variability, a sensitivity study was performed using the PORFLOW Deterministic Model. To simulate the possible effect that varying the waste-tank grout transition time might have on dose results, the waste-tank grout transition times were modified so both faster and slower grout transition times were used. The PORFLOW Deterministic Model was run for the Base Case and for Case C except that the grout transition time was varied. In addition to the expected grout transition time, a grout transition time of 0.5 and a grout transition time of twice what is expected were studied. The impact of grout transition time variability on dose for the Base Case and for Case C is displayed in Figures 5.6-64 through 5.6-69.

Figure 5.6-64: Base Case Grout Transition Time Study

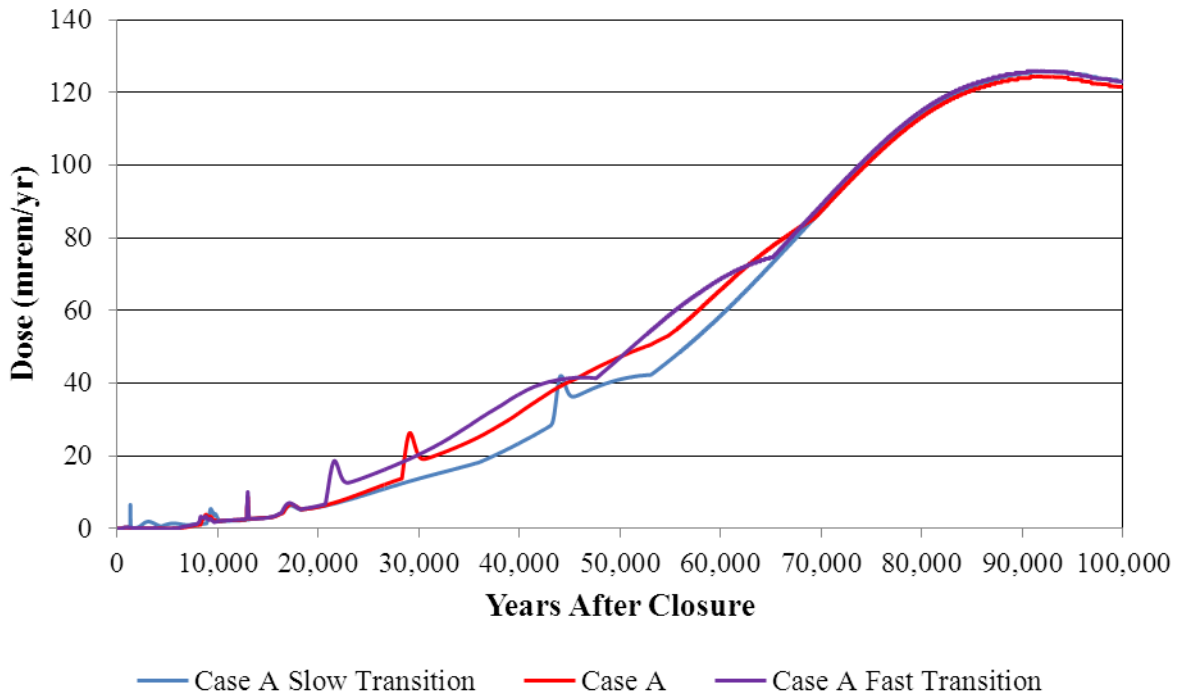


Figure 5.6-65: Case C Grout Transition Time Study

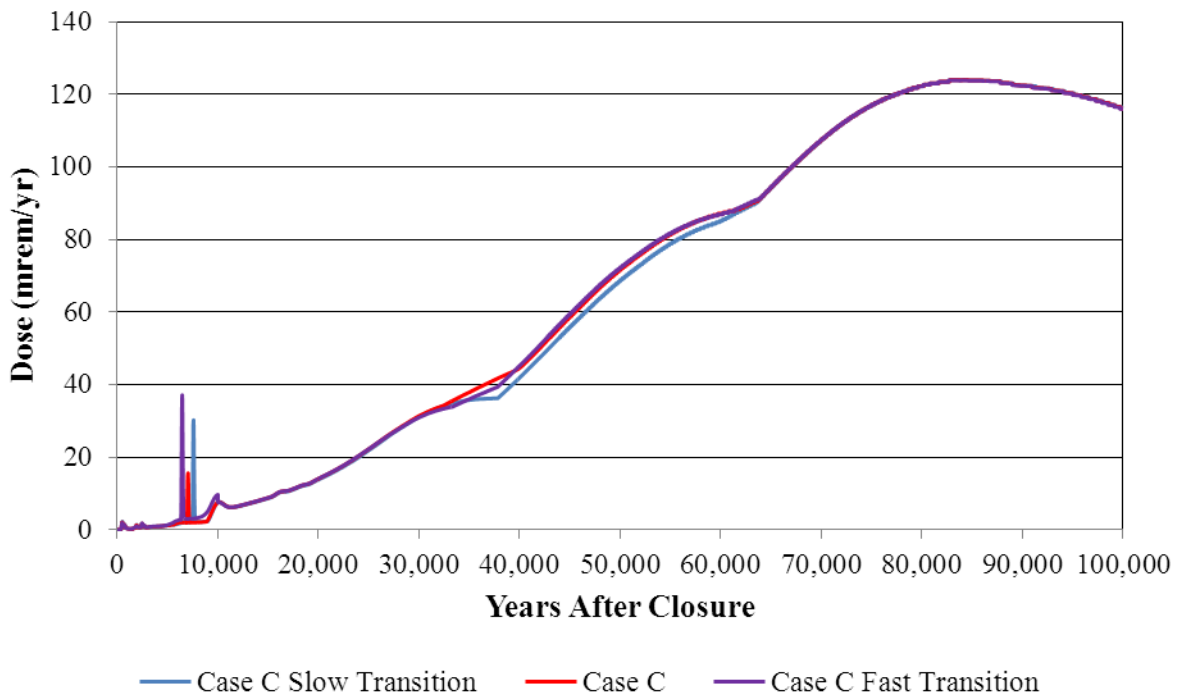


Figure 5.6-66: Individual Radionuclide Contributors to MOP Dose for Base Case Fast Grout Transition Time

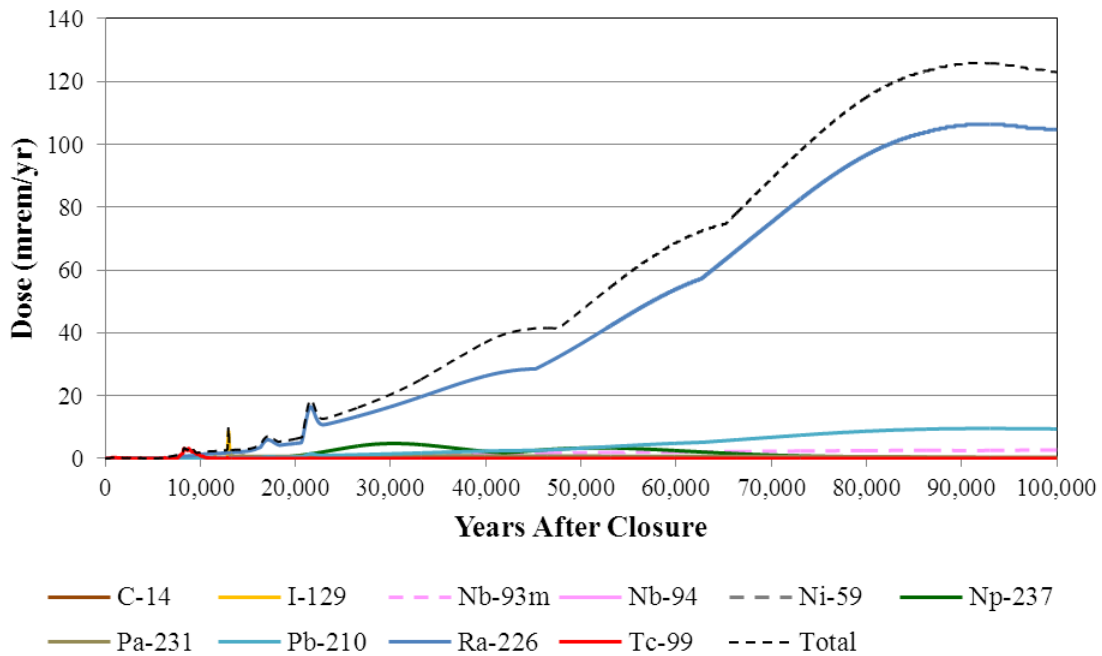


Figure 5.6-67: Individual Radionuclide Contributors to MOP Dose for Base Case Slow Grout Transition Time

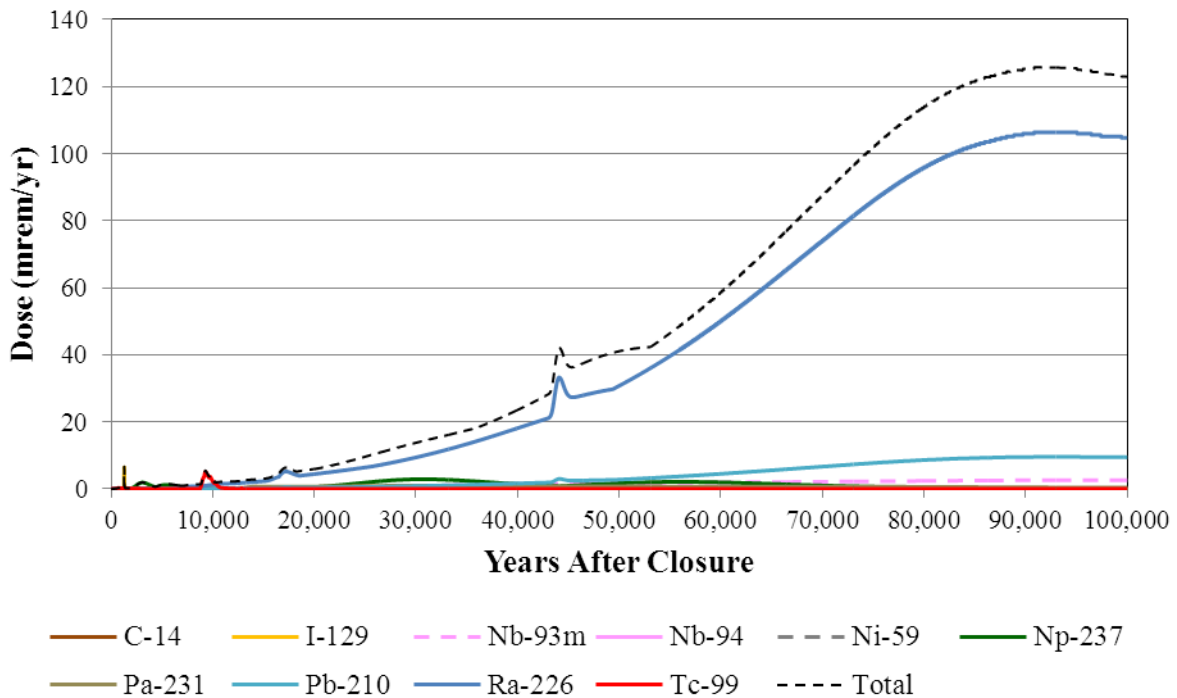


Figure 5.6-68: Individual Radionuclide Contributors to MOP Dose for Case C Fast Grout Transition Time

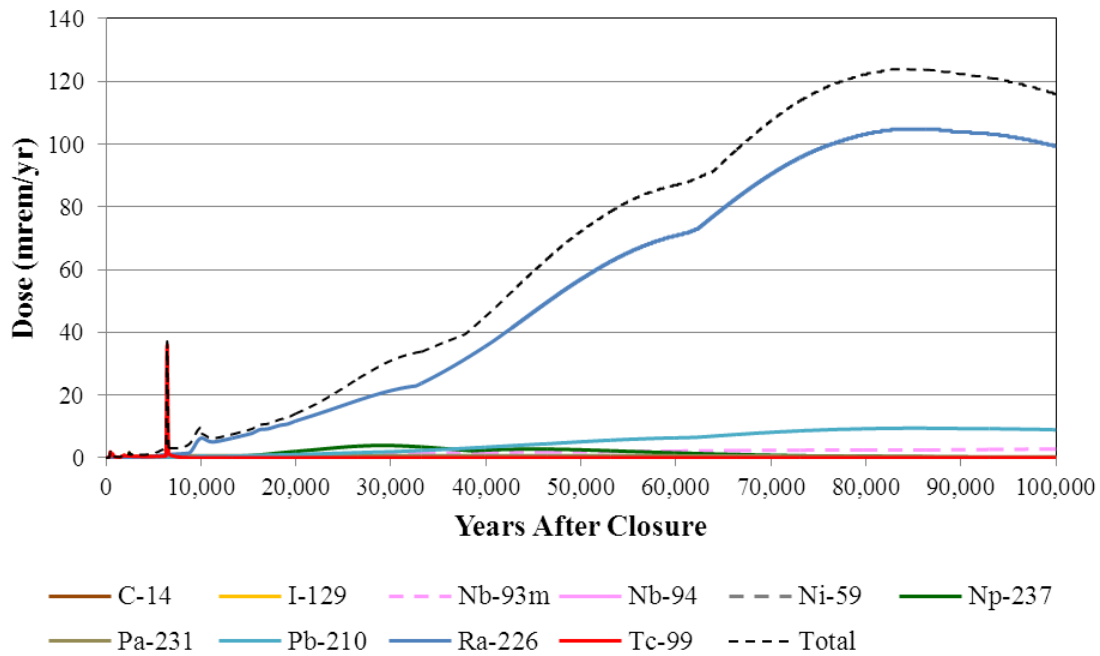
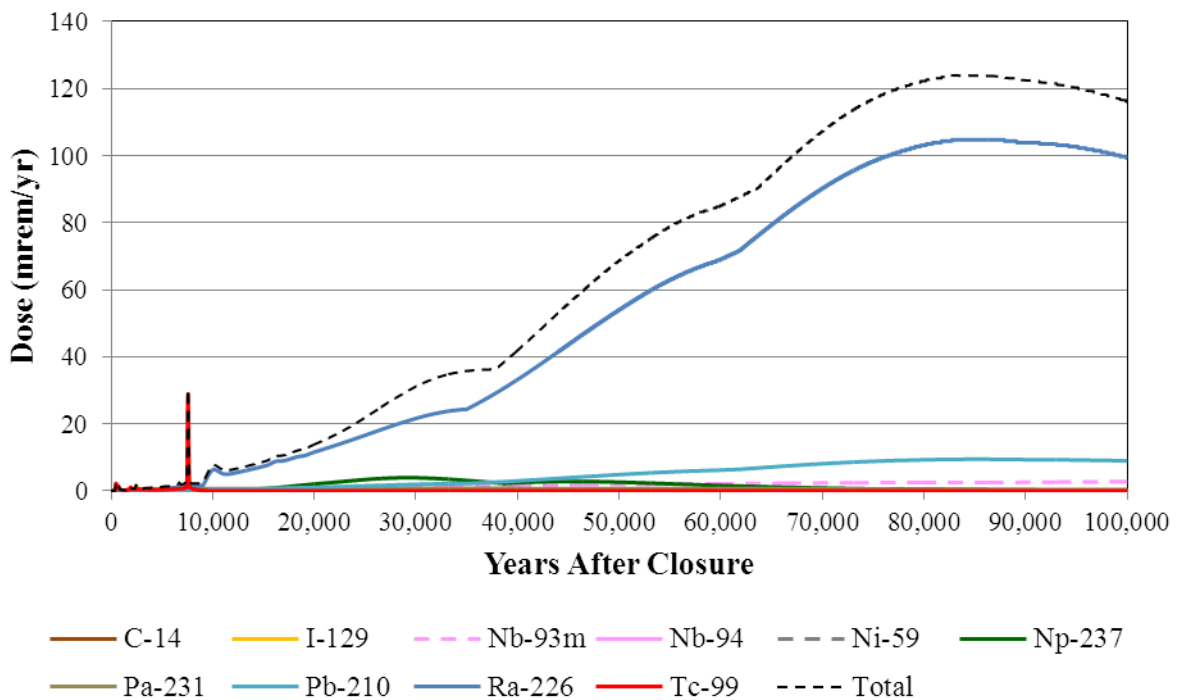


Figure 5.6-69: Individual Radionuclide Contributors to MOP Dose for Case C Slow Grout Transition Time



5.6.7.3 Solubility Value Analysis using the PORFLOW Deterministic Model

To study the impact of solubility variability on the dose associated with key radionuclides, a sensitivity study was performed using the PORFLOW Deterministic Model. The radionuclides studied (i.e., Pu-239, Np-237, Tc-99, U-234) were those radionuclides that have historically exhibited both impact on dose and sensitivity to solubility variability. This non-mechanistic study artificially imposed the selected solubility values on the radionuclides of interest and held the selected solubility values constant regardless of changing waste tank conditions. The solubility values used were derived from SRNL-STI-2012-00404 and were chosen to provide a range of solubility values, including pessimistic values. The solubility values are reproduced in Table 5.6-46. The PORFLOW Deterministic Model was run using the Base Case assumptions, except that the selected solubility values were varied. The impact of solubility variability is displayed in Figure 5.6-70. Figures 5.6-71 through 5.6-73 provide the individual radionuclide contributors to the total dose for each of the solubility studies. It should be noted that significant impacts are displayed only in the most bounding study (Study 1 - Pessimistic Solubility Values - No Fe co-precipitation), and even then the doses of interest occur beyond 10,000 years.

Table 5.6-46: Values for Solubility Study

Radionuclide	Study 1 - Pessimistic Solubility Values - No Fe Co-precipitation	Study 2 - Typical Solubility Values - No Fe Co-precipitation	Study 3 - Pessimistic Solubility Values - Fe Co-precipitation Assumed
Pu-239	1.1E-07	1.6E-11	1.6E-10
Tc-99	Instantaneous release	1.1E-08	1.3E-12
Np-237	1.0E-04	3.4E-05	3.0E-13
U-234	3.4E-04	4.3E-06	1.8E-10

Values derived from SRNL-STI-2012-00404

Figure 5.6-70: Comparison of Solubility Studies with the Base Case

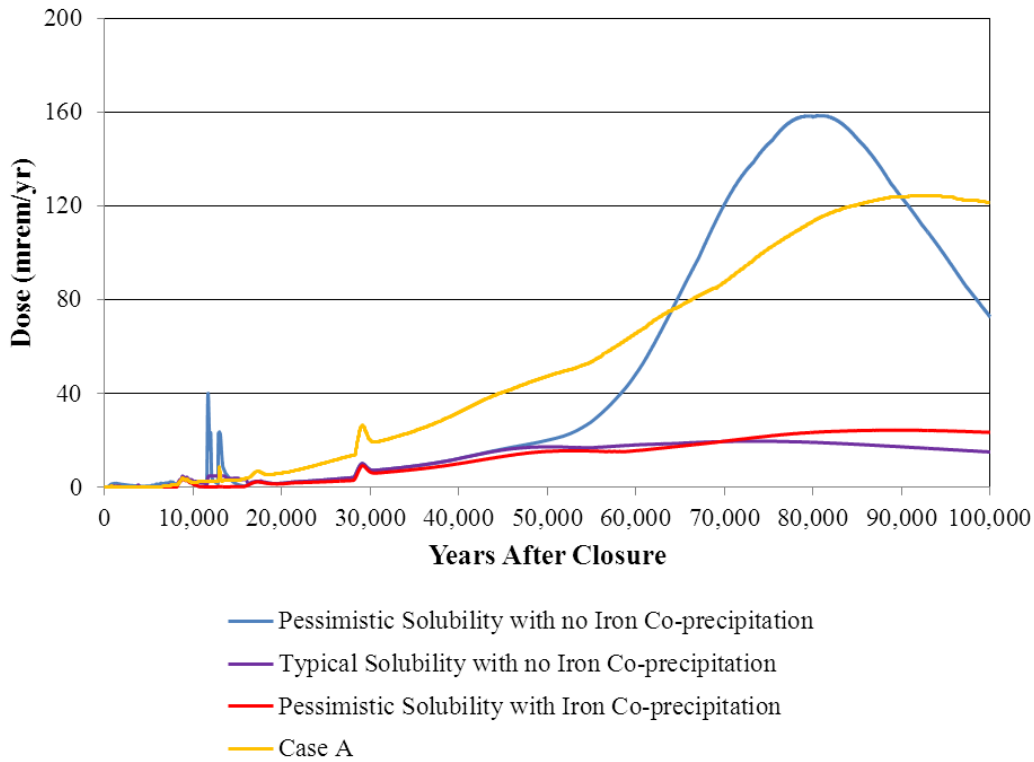


Figure 5.6-71: Individual Radionuclide Contributors to MOP Dose for the Pessimistic Solubility with no Iron Co-precipitation

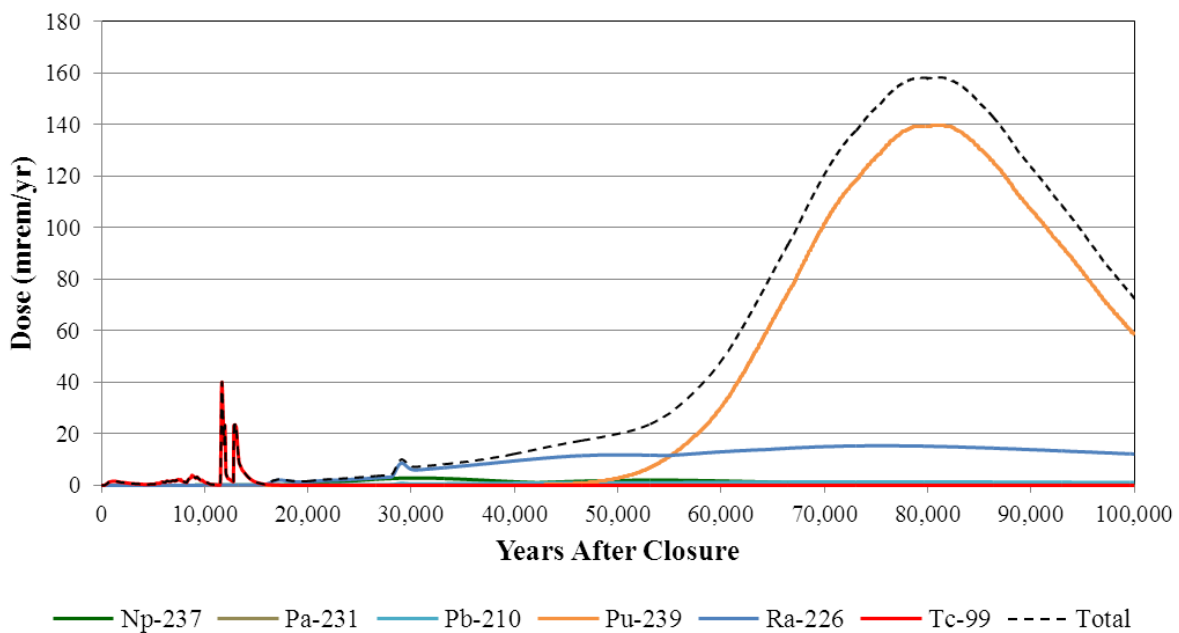


Figure 5.6-72: Individual Radionuclide Contributors to MOP Dose for the Typical Solubility with no Iron Co-precipitation

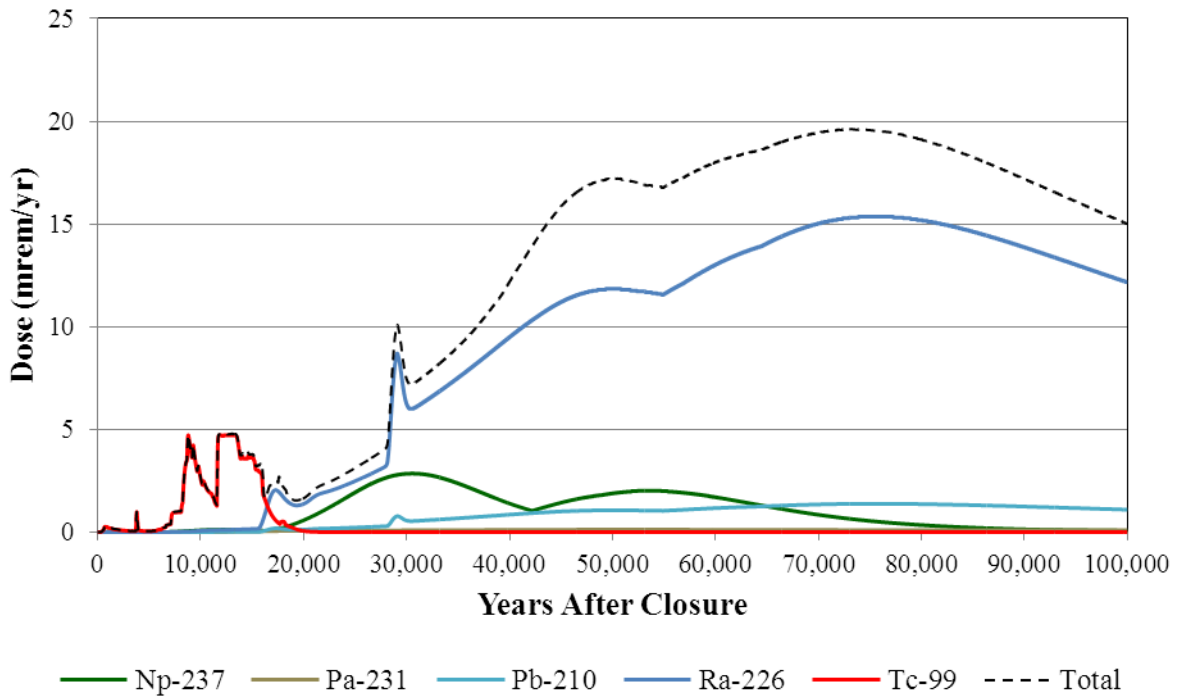
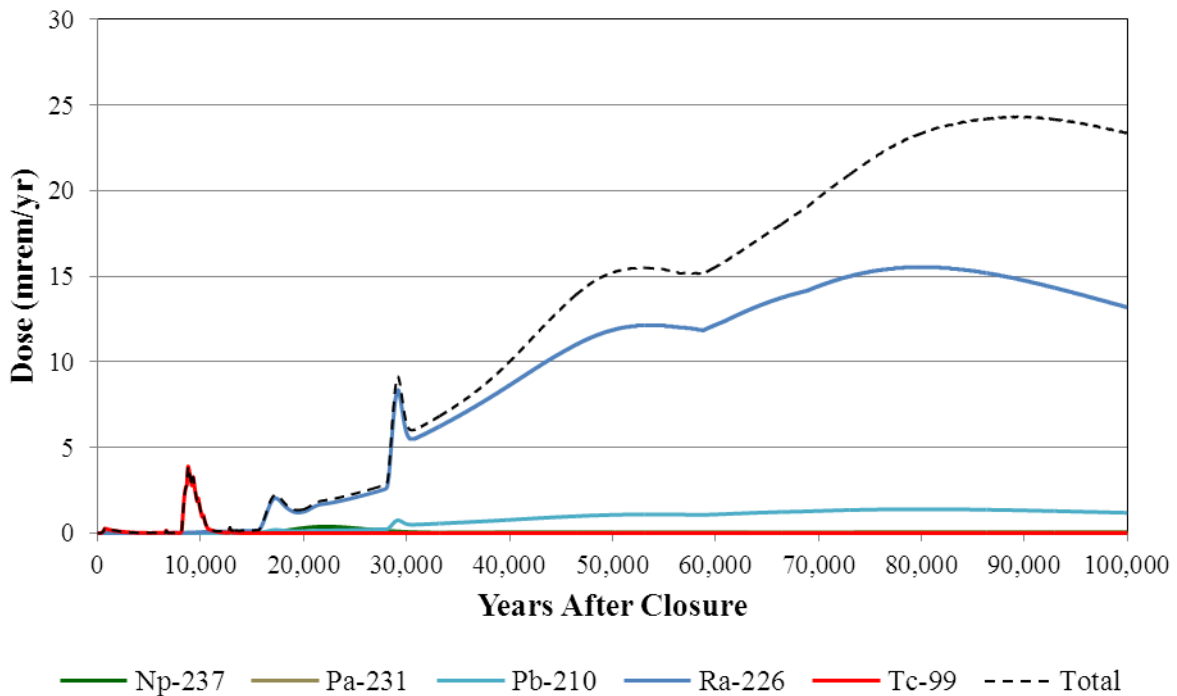


Figure 5.6-73: Individual Radionuclide Contributors to MOP Dose for the Pessimistic Solubility with Iron Co-precipitation



5.6.7.4 Calcareous Zone Analysis using the PORFLOW Deterministic Model

To study the impact of calcareous zone presence, a sensitivity study was performed using the PORFLOW Deterministic Model. To simulate the possible effect the presence of calcareous zones might have on dose results, the PORFLOW soil properties were modified so that the effective porosity of the soil was 12.5 %, versus the 25 % used in the Base Case. The lower soil effective porosity reflects the water flow in the calcareous zone where the water would flow through a spatially limited mobile zone of connected fractures and voids. In addition to decreasing the effective porosity which reflects the decrease in the mobile zone (the participating volume through which water is flowing), the effective bulk density term, used to determine the retardation, was decreased from 1.04 to 0.52 g/cm³. The decrease in the effective bulk density has the effect of neglecting the solid mass in the immobile zone as a site for sorption. The impact of calcareous zone study is displayed in Figures 5.6-74 and 5.6-75.

Figure 5.6-74: Comparison of the Calcareous Zone Sensitivity MOP Dose to the Base Case MOP Dose

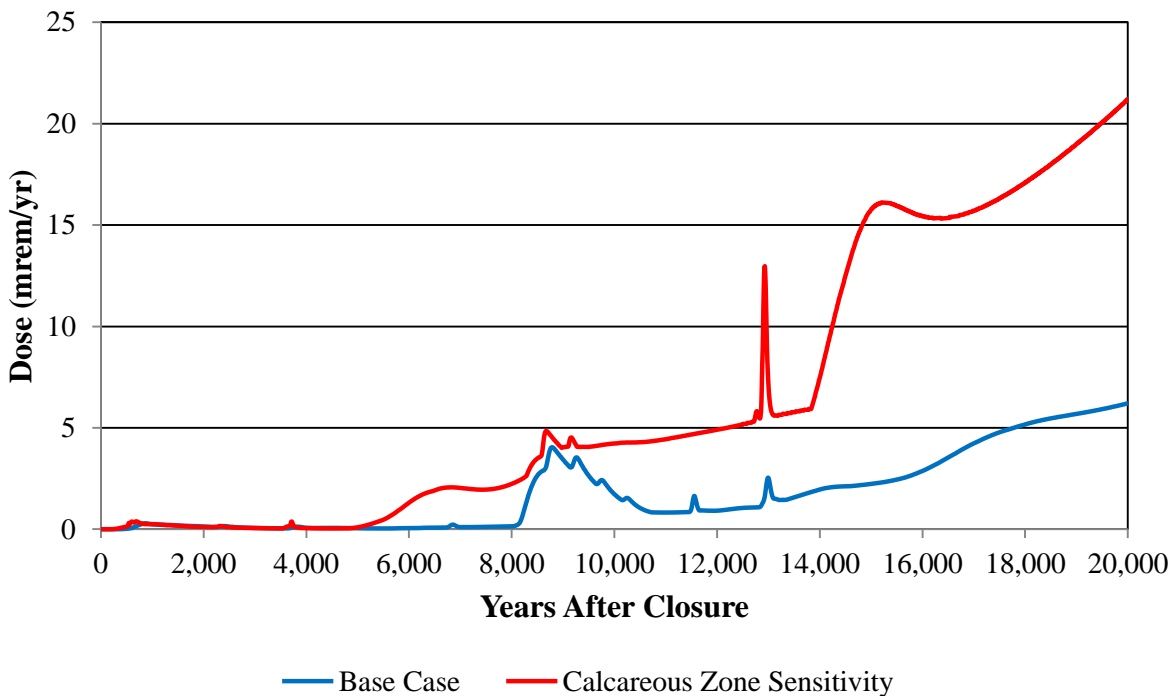
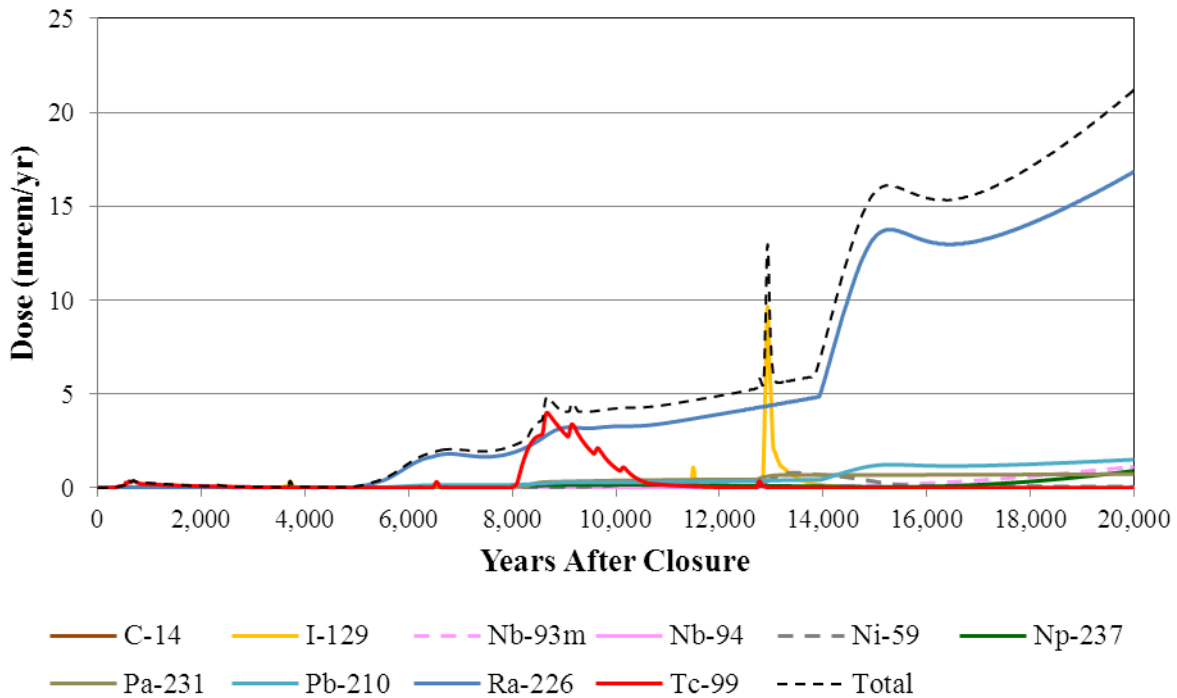


Figure 5.6-75: Individual Radionuclide Contributors to MOP Dose for the Calcareous Zone Sensitivity Case



5.6.7.5 K_d Variability Zone Analysis using the PORFLOW Deterministic Model

To study the impact of K_d variability, a sensitivity study was performed using the PORFLOW Deterministic Model. To simulate the possible effect that K_d variability might have on dose results, the PORFLOW far field soil properties were modified so that the soil had different K_d values than were used in the Base Case. Soil K_d values one half and one quarter of the expected K_d were studied and compared to the Base Case. The impact of K_d variability is displayed in Figures 5.6-76 through 5.6-79.

Figure 5.6-76: Soil K_d Variability MOP Groundwater Pathway Dose

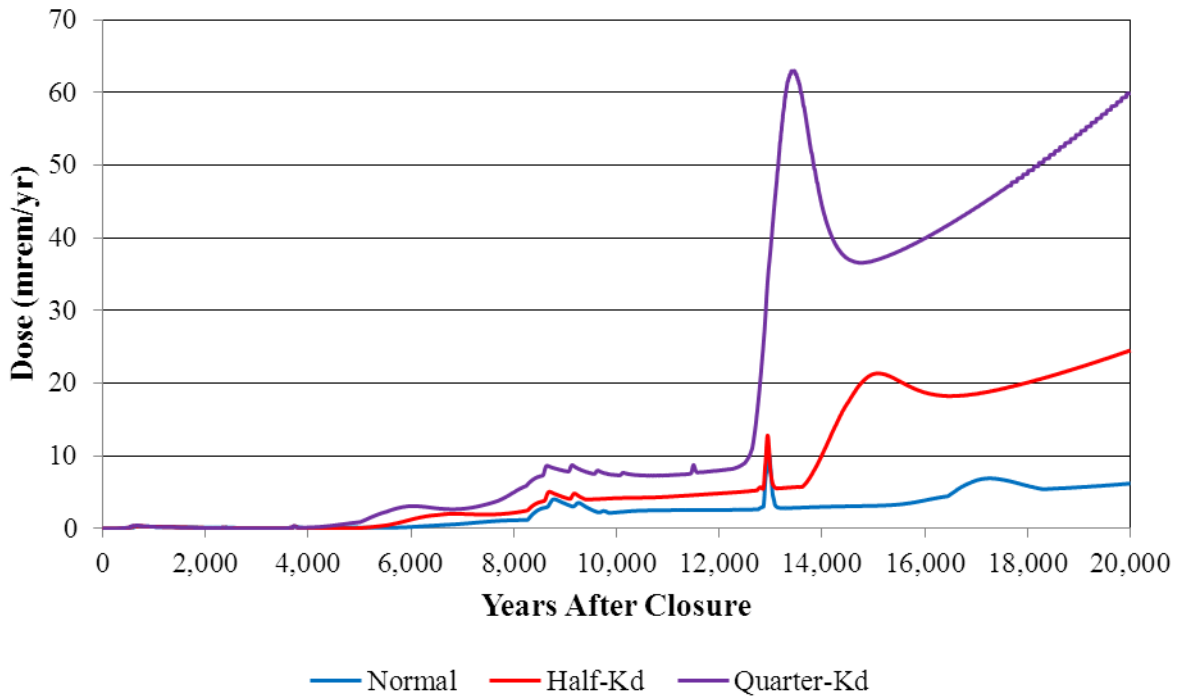


Figure 5.6-77: Individual Radionuclide Contributors to MOP Dose, Normal K_d (Base Case)

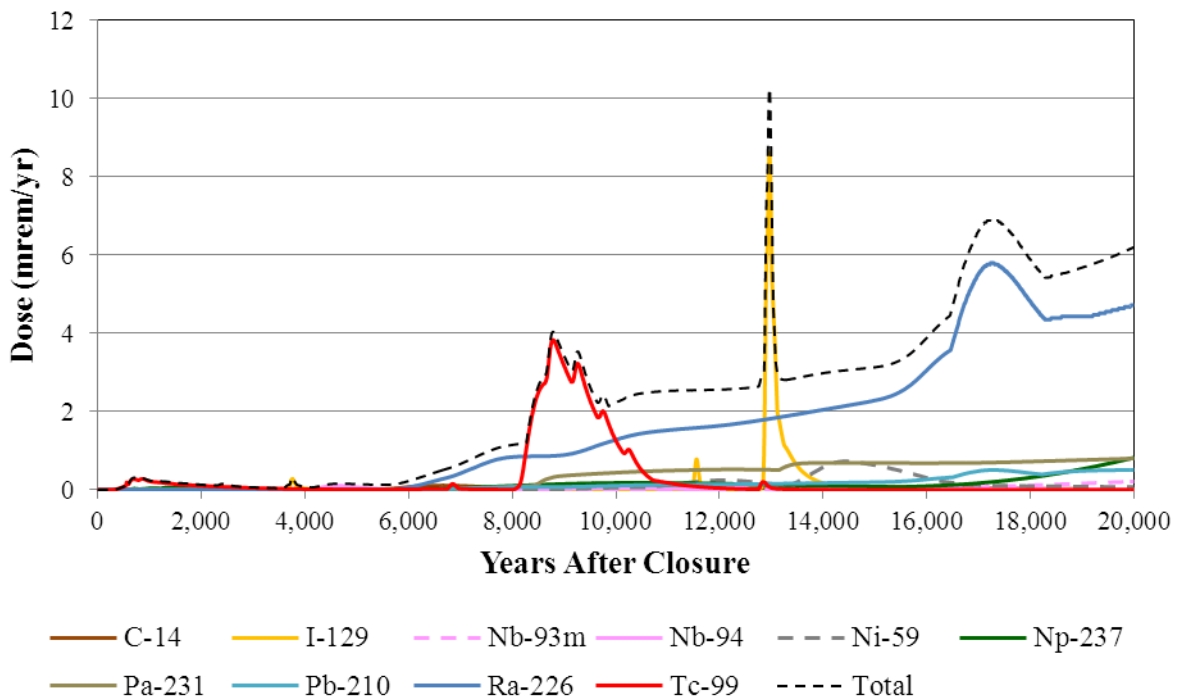


Figure 5.6-78: Individual Radionuclide Contributors to MOP Dose for Half the Soil K_d

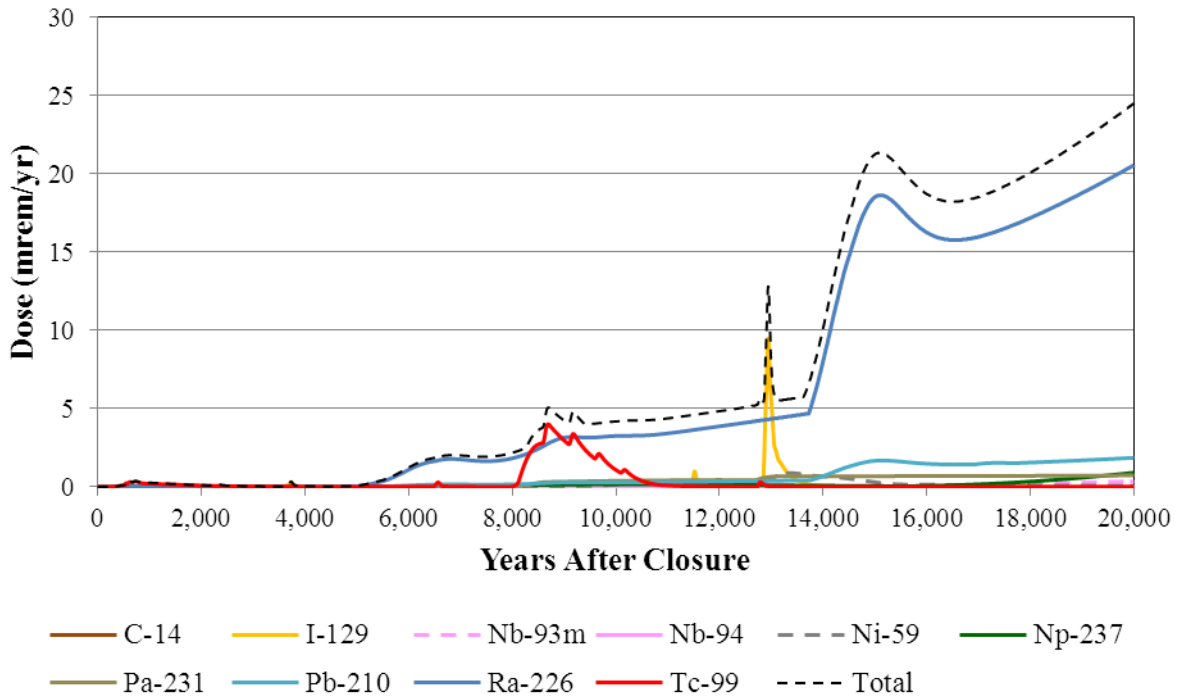
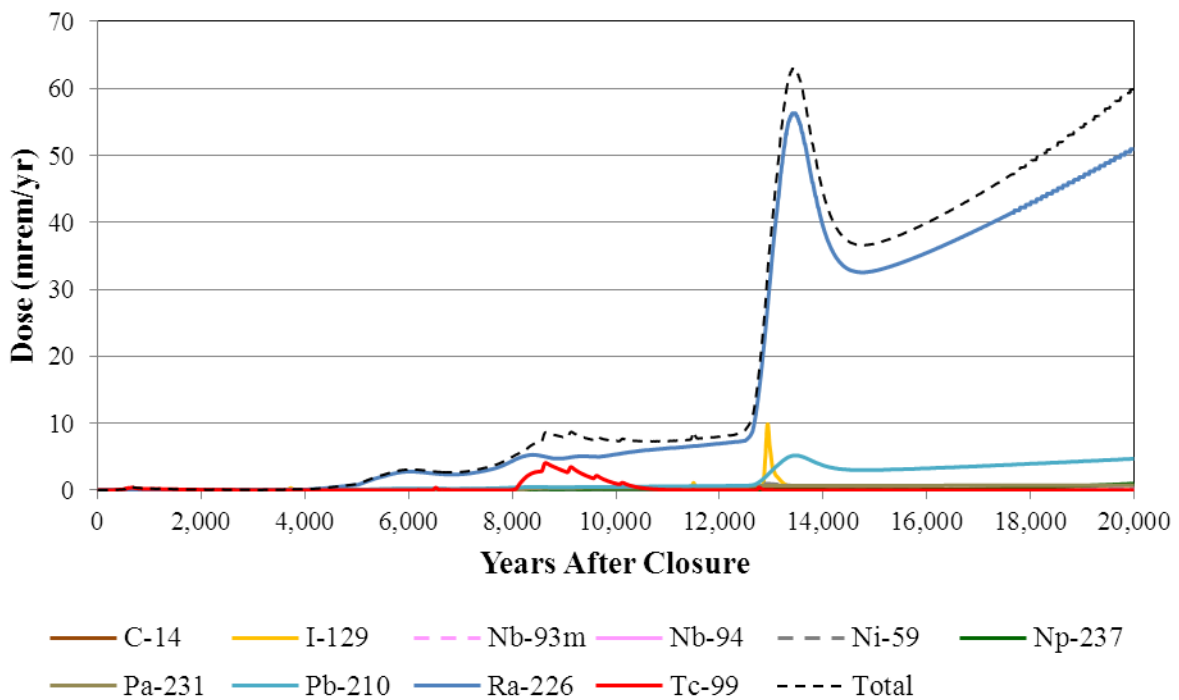


Figure 5.6-79: Individual Radionuclide Contributors to MOP Dose for Quarter the Soil K_d



5.6.7.6 Liner Failure Times Analysis using the PORFLOW Deterministic Model

To study the impact of liner failure-time variability, a sensitivity study was performed using the PORFLOW Deterministic Model. To capture the impact of the time of liner failure on dose, 12 different flow fields reflecting different liner failure times were utilized. The PORFLOW Deterministic Model was run using the Base Case assumptions except that different flow fields were simulated reflecting four different liner failure times (immediate, early, moderate, late), as described in Section 5.6.3.2. Table 5.6-47 presents the liner failure times utilized in this study. Assuming different liner failure times and different associated waste tank case resulted in changes to the waste tank flow fields (e.g., flow runs 1 through 4, 25 through 28, and 49 through 52 from Section 5.6.3.2), and these different waste tank flow fields were imposed upon each waste tank type for the purposes of this study. Tank 11 represents Type I tanks, Tank 13 represents Type II tanks, Tank 22 represents Type IV tanks, and Tank 39 represents Type III and IIIA tanks. The impact of liner failure time variability is displayed in Figures 5.6-80 through 5.6-91.

Table 5.6-47: Liner Failure Times

Label	Failure Time (Year) for No Fast Flow Path (Base Case)				Failure Time (Year) for Partial Flow Path (Cases B and C) and Full Fast Flow Path (Cases D and E)			
	Type I Liner	Type II Liner	Type III/IIIA Liner	Type IV Liner	Type I Liner	Type II Liner	Type III/IIIA Liner	Type IV Liner
Immediate	0	0	0	0	0	0	0	0
Early	2,100	2,506	3,100	500	100	100	100	75
Moderate	11,397	12,687	12,751	3,638	1,142	2,506	2,077	1,000
Late	15,000	14,500	14,500	8,000	11,000	12,000	12,000	3,638

Figure 5.6-80: No Fast Flow Path Type I Tank MOP Dose (Base Case)

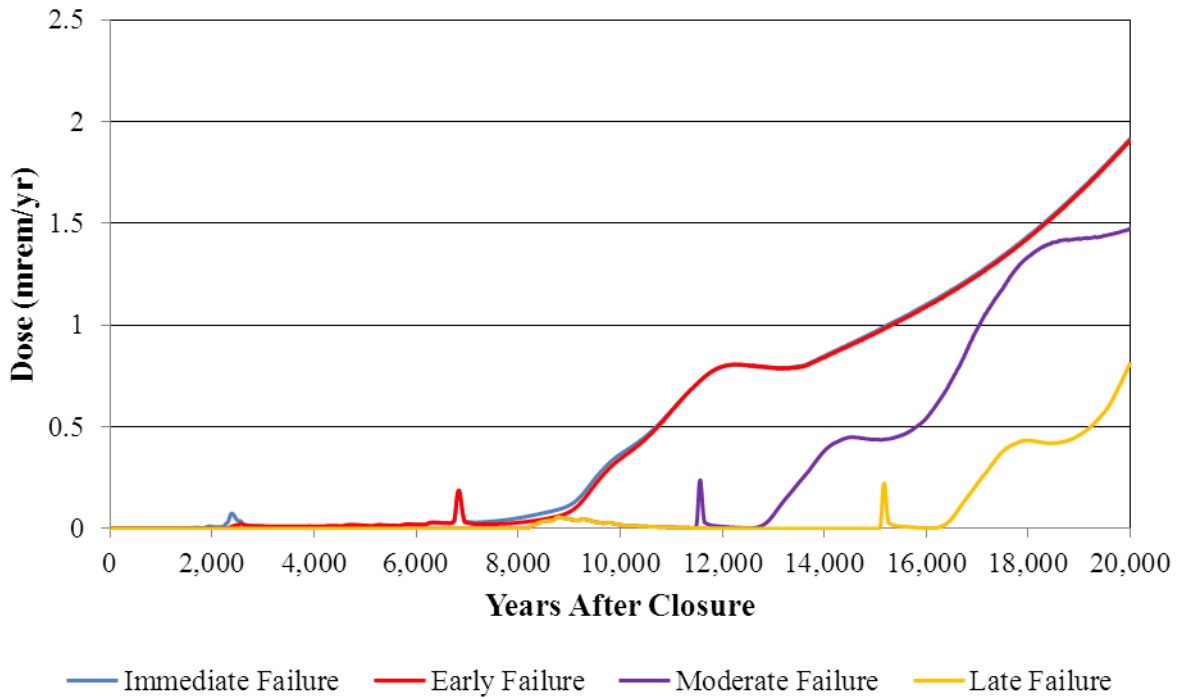


Figure 5.6-81: No Fast Flow Path Type II Tank MOP Dose (Base Case)

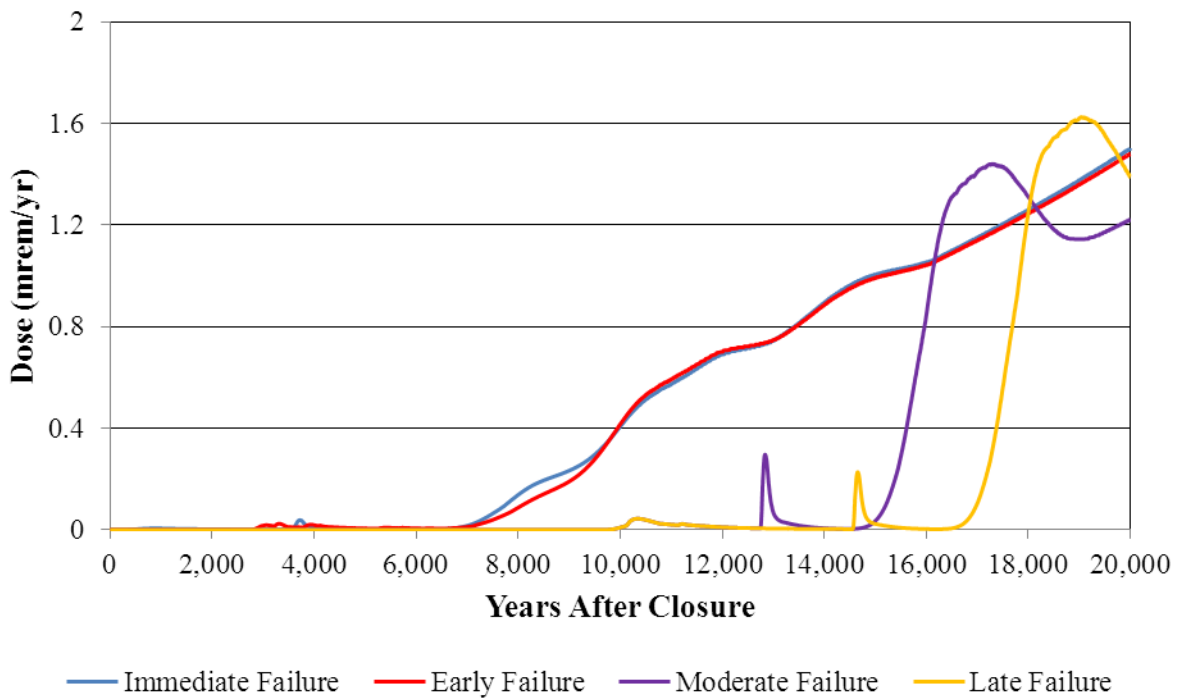


Figure 5.6-82: No Fast Flow Path Type IV Tank MOP Dose (Base Case)

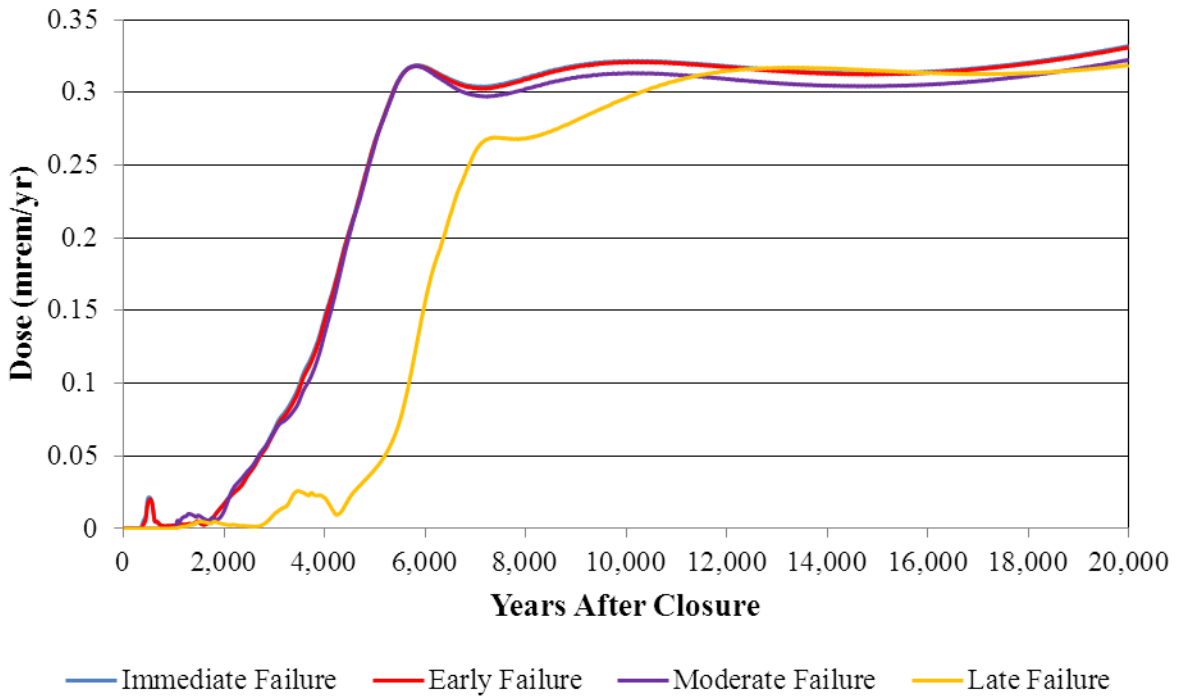


Figure 5.6-83: No Fast Flow Path Type III and IIIA Tank MOP Dose (Base Case)

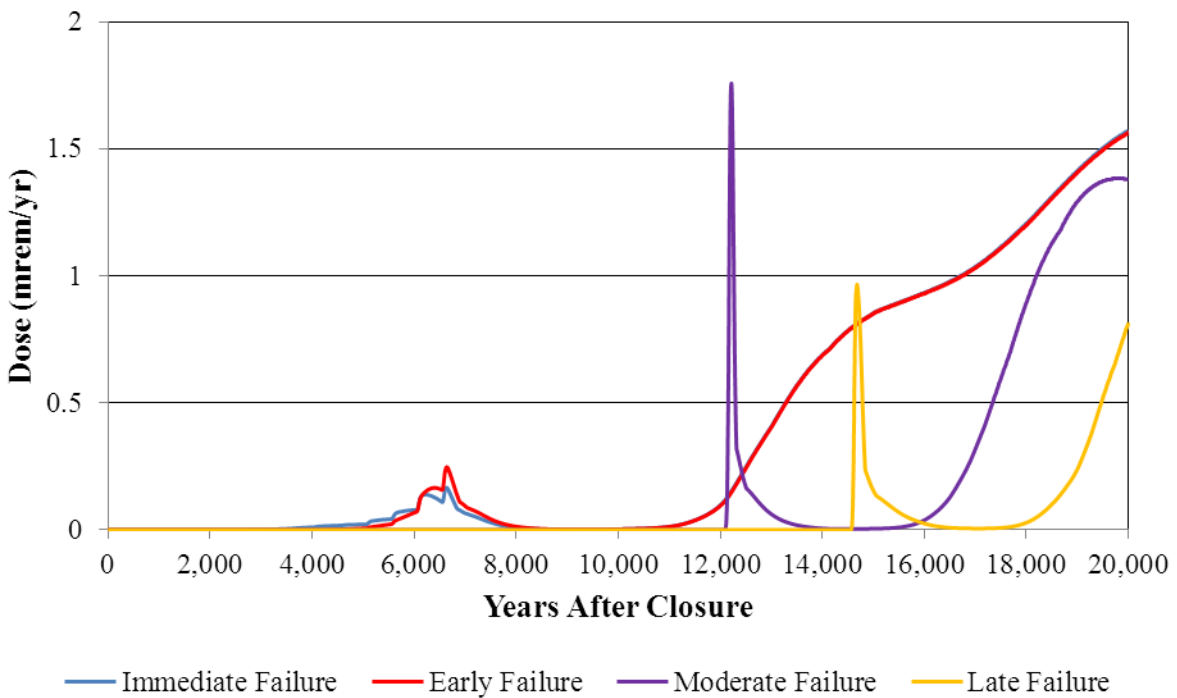


Figure 5.6-84: Partial Fast Flow Path Type I Tank MOP Dose (Cases B and C)

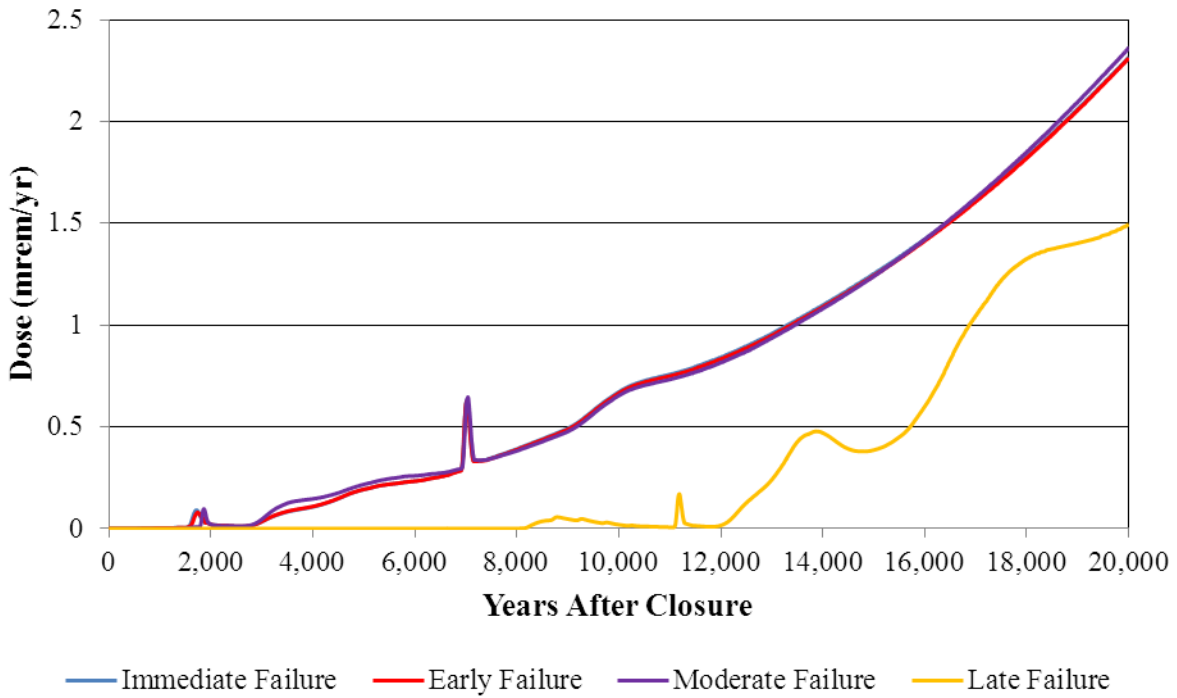


Figure 5.6-85: Partial Fast Flow Path Type II Tank MOP Dose (Cases B and C)

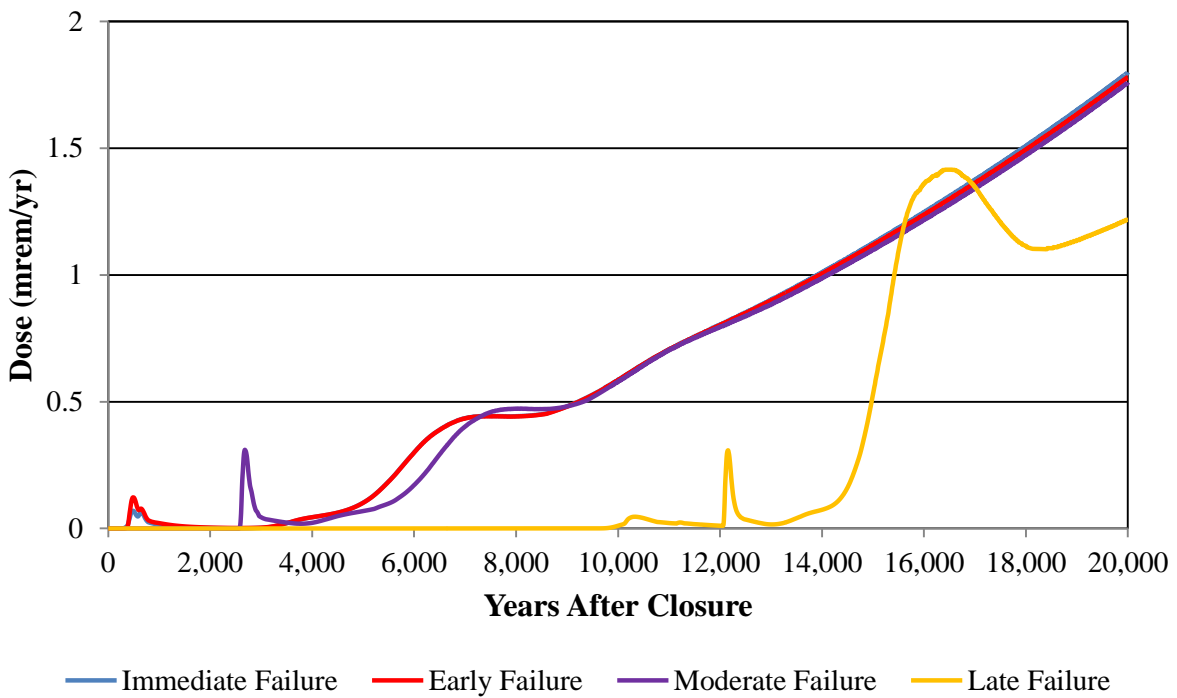


Figure 5.6-86: Partial Fast Flow Path Type IV Tank MOP Dose (Cases B and C)

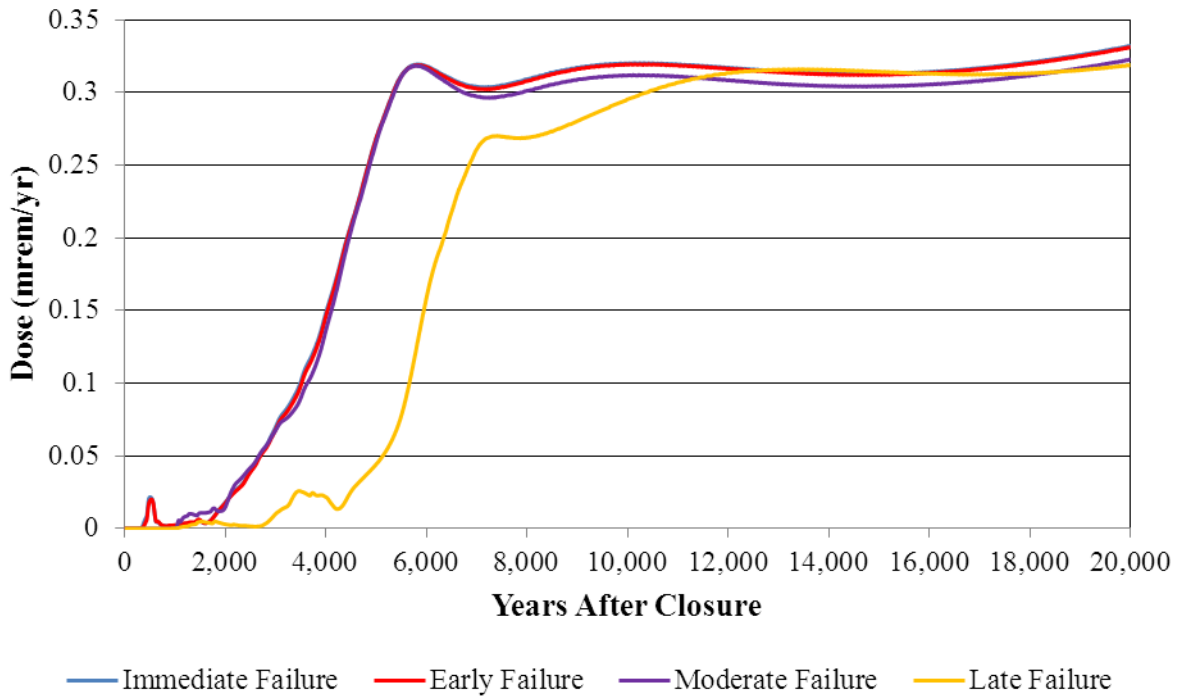


Figure 5.6-87: Partial Fast Flow Path Type III and IIIA Tanks MOP Dose (Cases B and C)

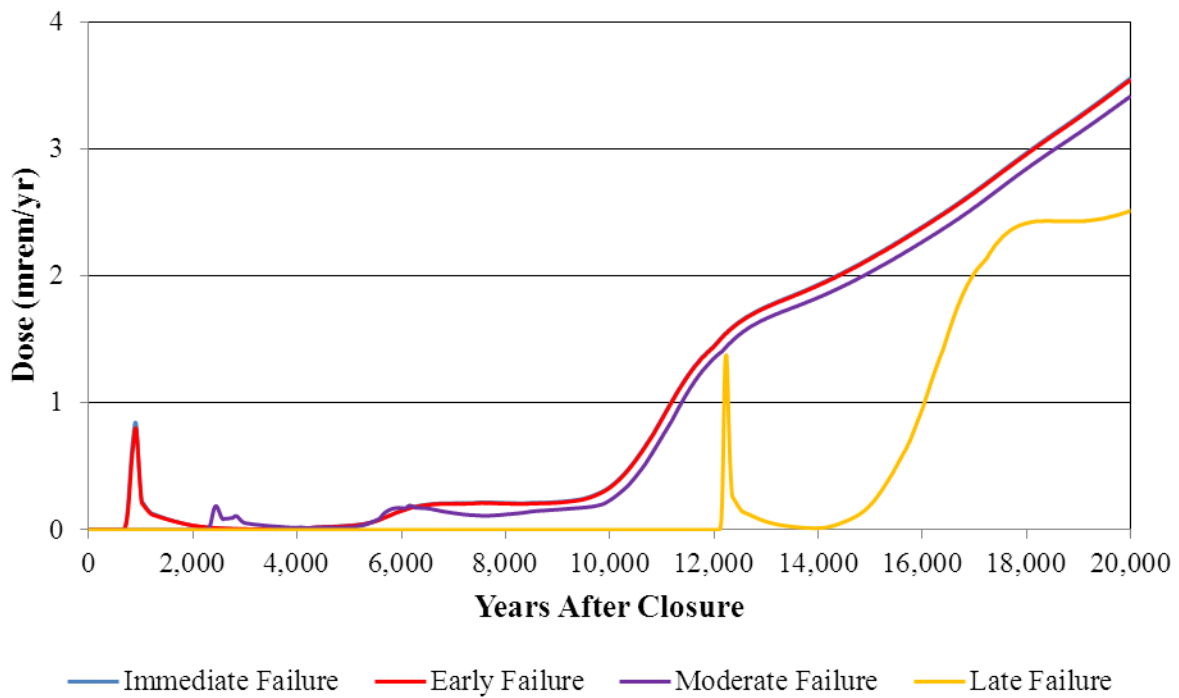


Figure 5.6-88: Full Fast Flow Path Type I Tank MOP Dose (Cases D and E)

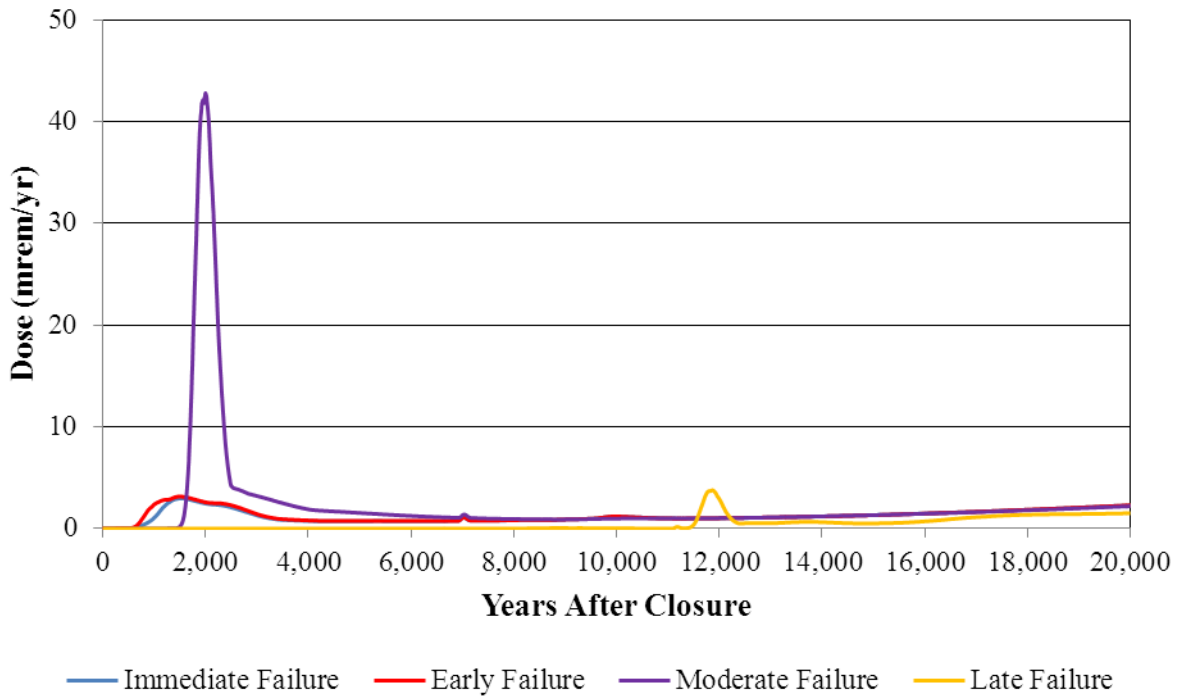


Figure 5.6-89: Full Fast Flow Path Type II Tank MOP Dose (Cases D and E)

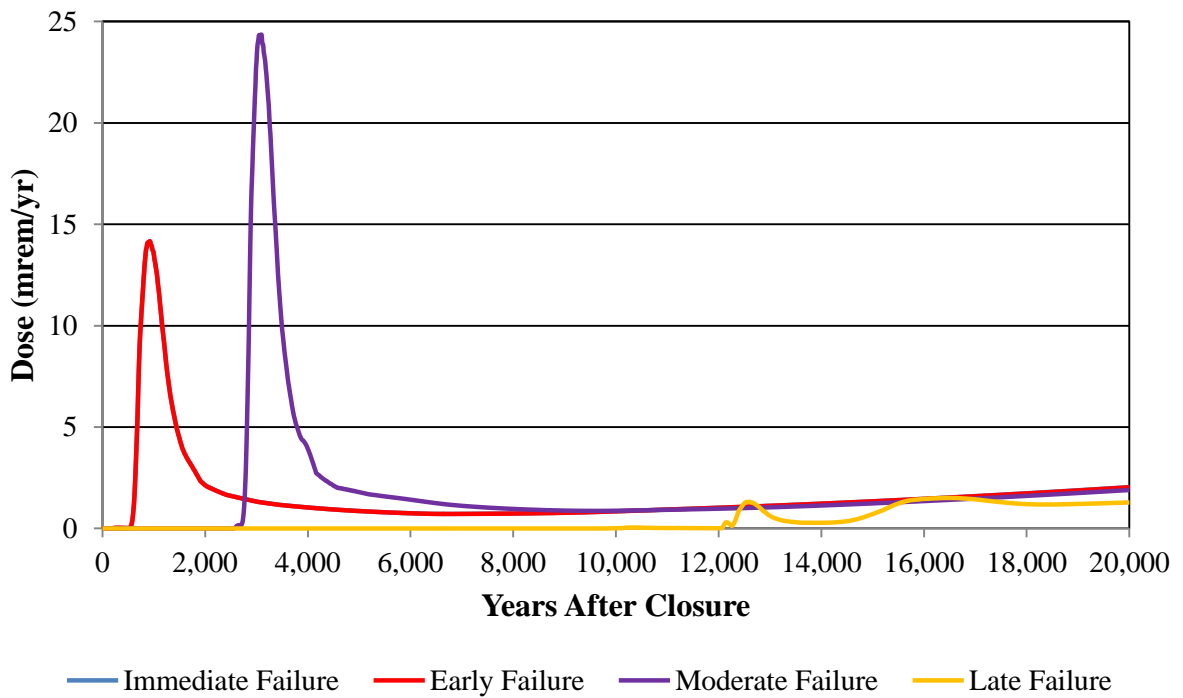


Figure 5.6-90: Full Fast Flow Path Type IV Tanks MOP Dose (Cases D and E)

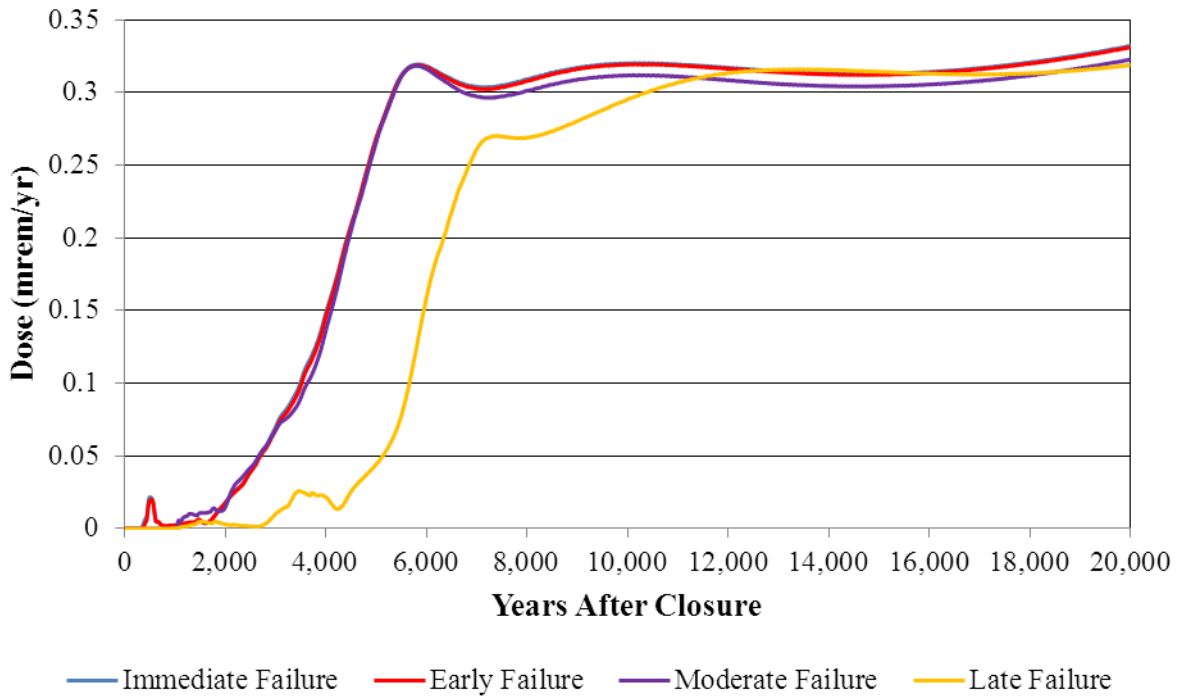
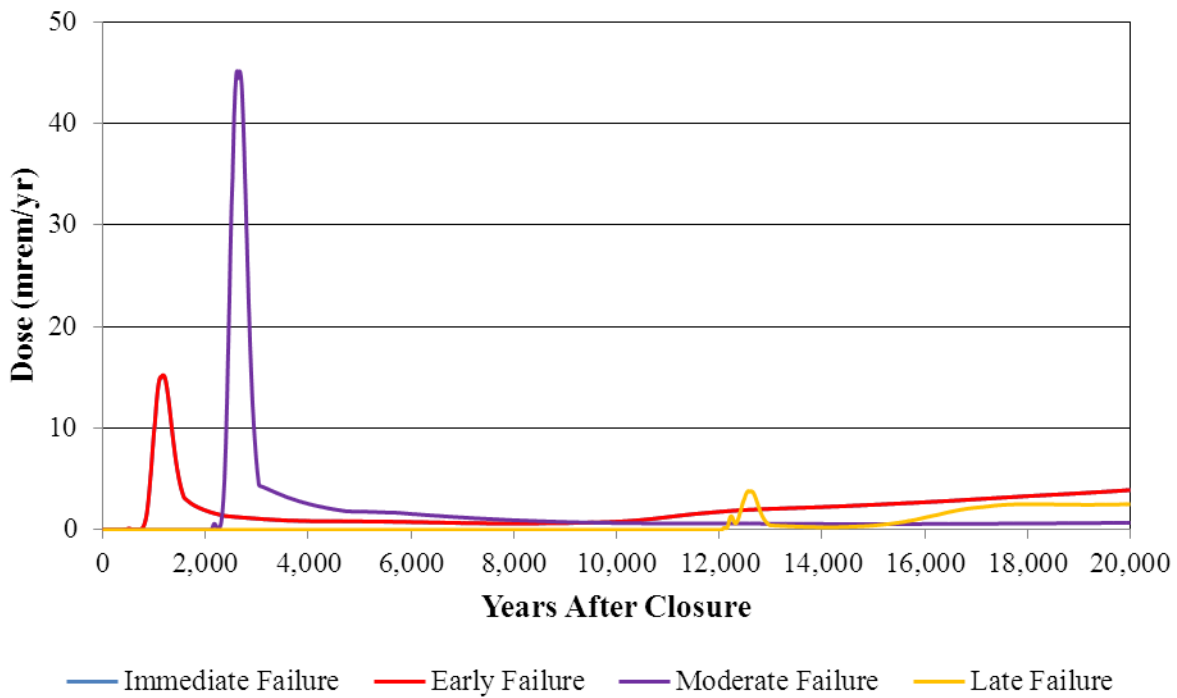


Figure 5.6-91: Full Fast Flow Path Type III and IIIA Tank MOP Dose (Cases D and E)



5.6.7.7 Cementitious Degradation Analysis using the PORFLOW Deterministic Model

To study the impact of cementitious degradation timing variability, a sensitivity study was performed using the PORFLOW Deterministic Model. To capture the impact of cementitious degradation timing on flow, three different flow fields reflecting different concrete and grout degradation rates were utilized. The PORFLOW Deterministic Model was run using the Base Case assumptions except that “normal,” “fast,” and “slow” degradation rates were simulated using a scaling factor as described in Section 5.6.3.2. The scaling factor imposed faster and slower cementitious degradation rates, which resulted in changes to the tank flow fields (e.g., flow runs 3, 7, and 11 from Section 5.6.3.2). Each waste tank type is represented in the cementitious degradation study with Tank 11 representing Type I tanks, Tank 13 representing Type II tanks, Tank 22 representing Type IV tanks, and Tank 39 representing Type III and IIIA tanks. The impact of cementitious degradation timing variability on each waste tank type is displayed in Figures 5.6-92 through 5.6-95.

Figure 5.6-92: Cementitious Degradation Timing Type I Tank MOP Dose

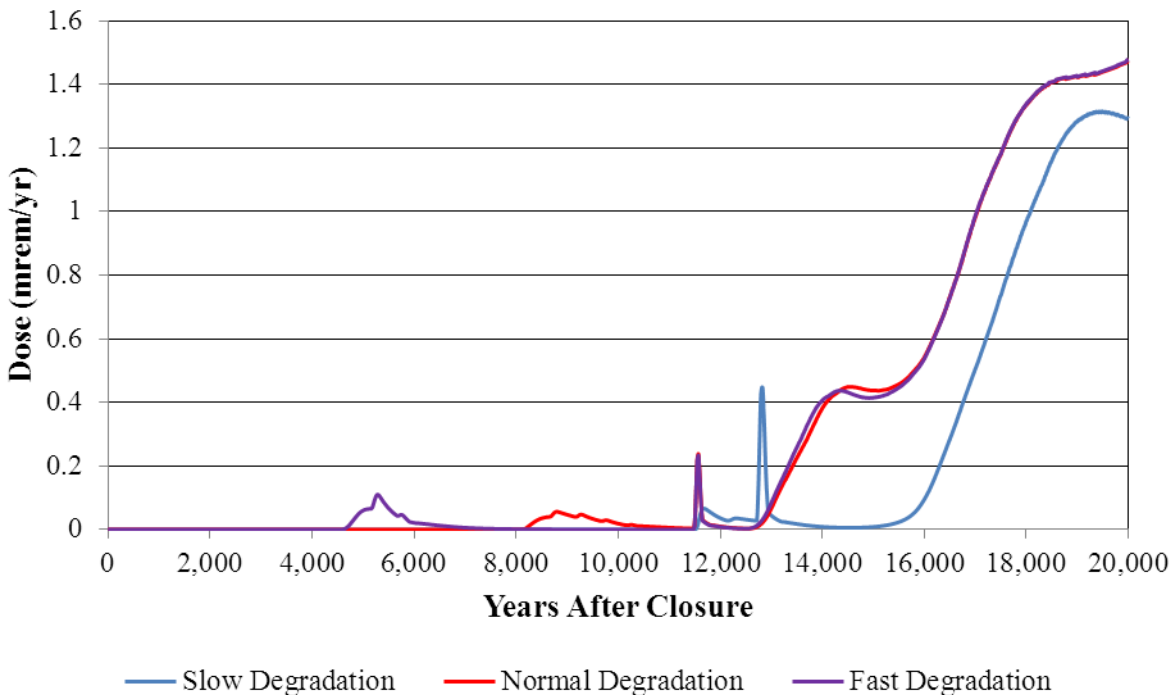


Figure 5.6-93: Cementitious Degradation Timing Type II Tank MOP Dose

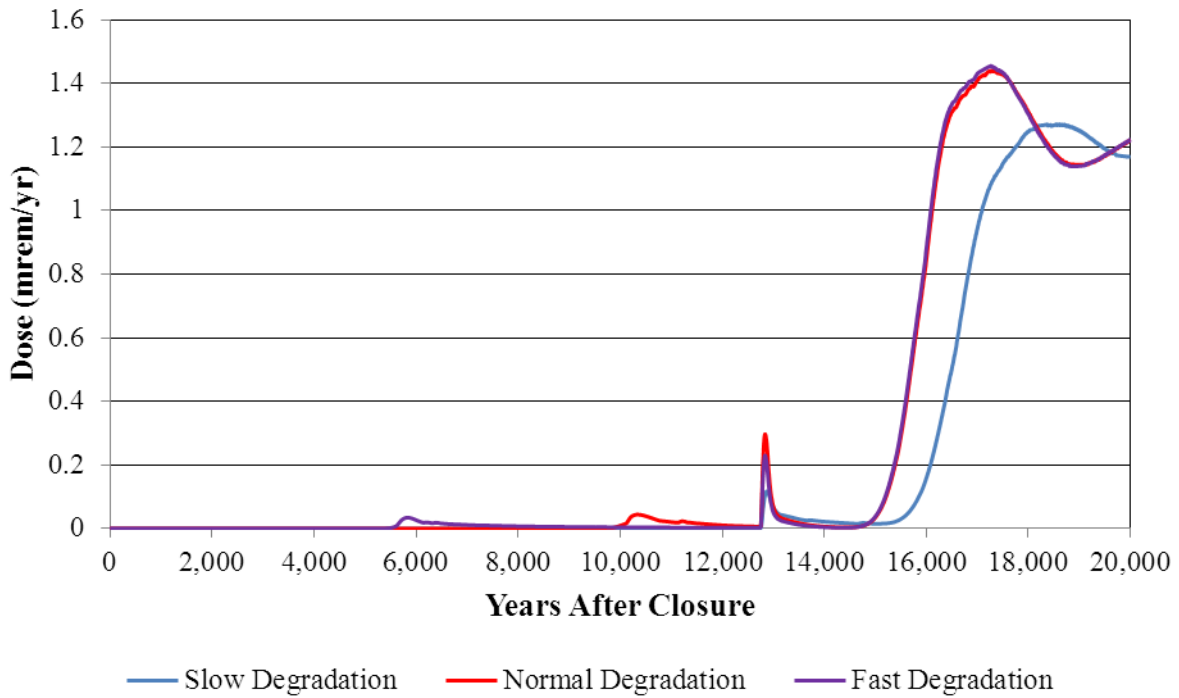


Figure 5.6-94: Cementitious Degradation Timing Type IV Tank MOP Dose

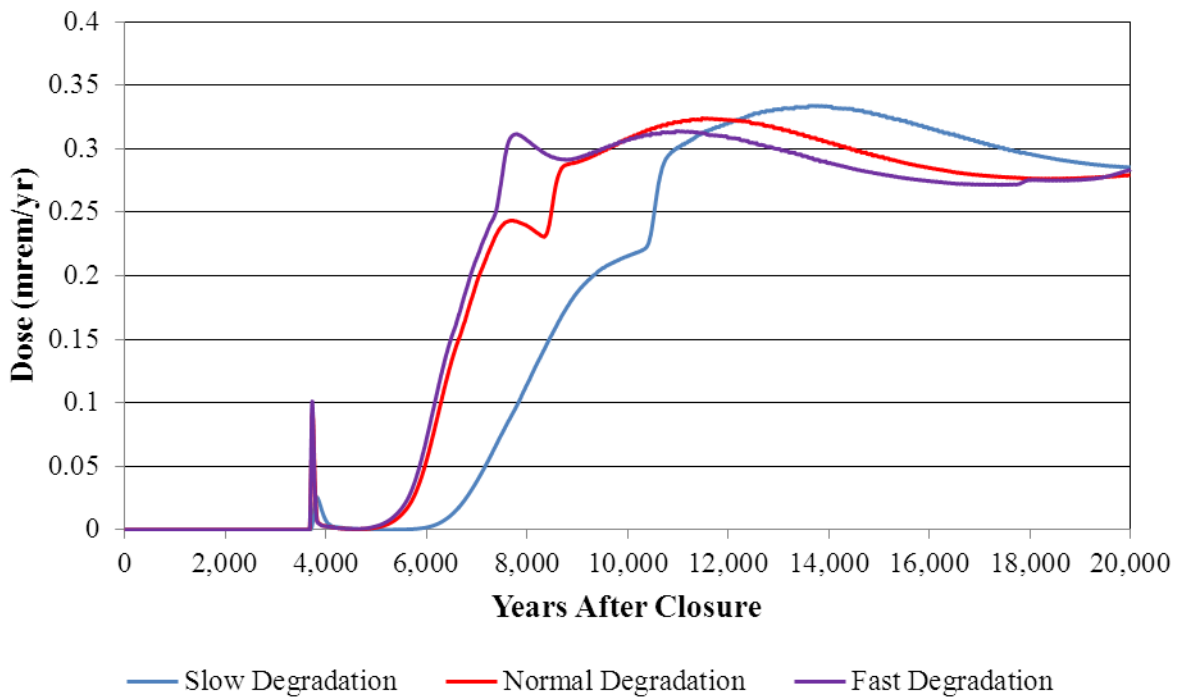
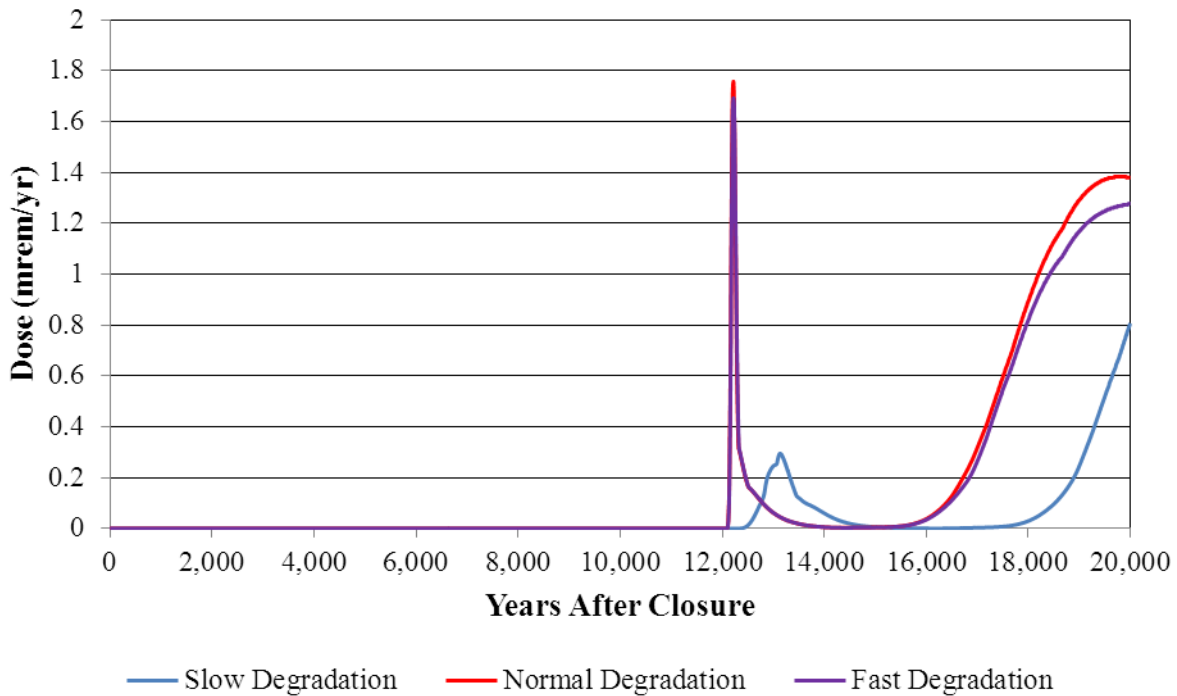


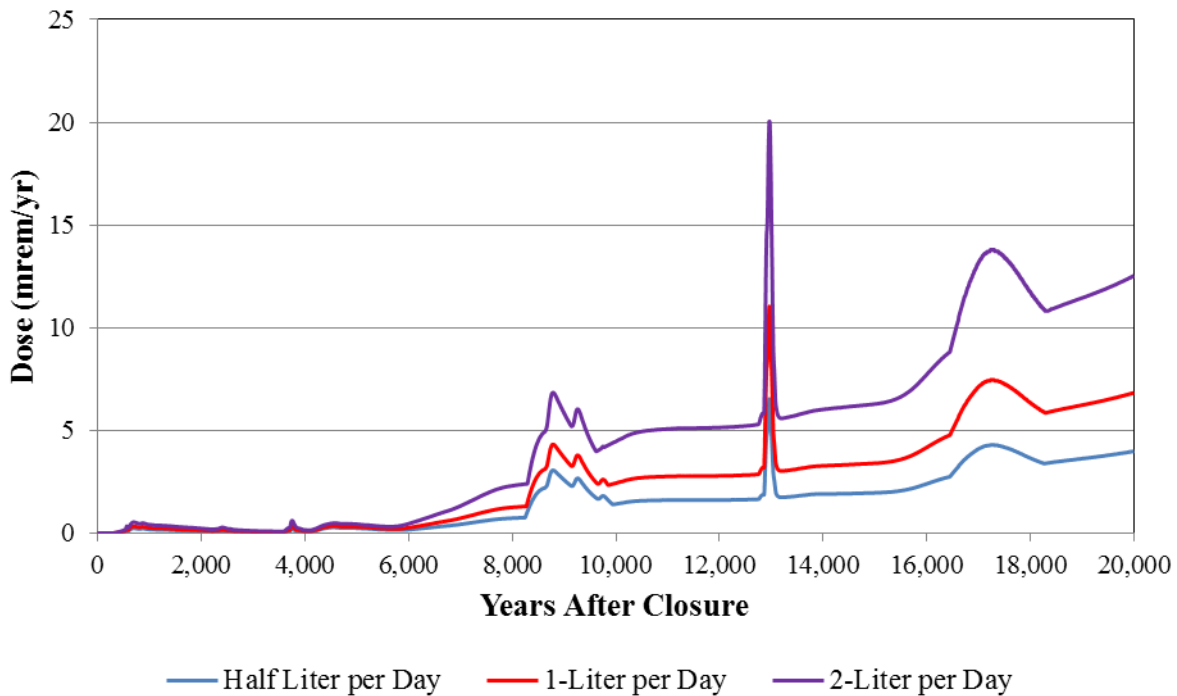
Figure 5.6-95: Cementitious Degradation Timing Type III and IIIA Tanks MOP Dose



5.6.7.8 Water Ingestion Analysis using the PORFLOW Deterministic Model

To study the impact of Water Ingestion variability, a sensitivity study was performed using the PORFLOW Deterministic Model. The PORFLOW Deterministic Model was run using the Case-A assumptions except that the drinking water consumption rate was varied. In addition to the expected drinking water consumption rate (1 L/d), drinking water consumption rates of 0.5 L/d and 2 L/d were studied. The impact of water variability is displayed in Figure 5.6-96.

Figure 5.6-96: Water Ingestion Rate Variability on MOP Groundwater Pathway Dose



5.6.8 Sensitivity Analysis Using the HTF Probabilistic Model

This section presents the sensitivity of the closure system to alternative conditions using the GoldSim probabilistic model.

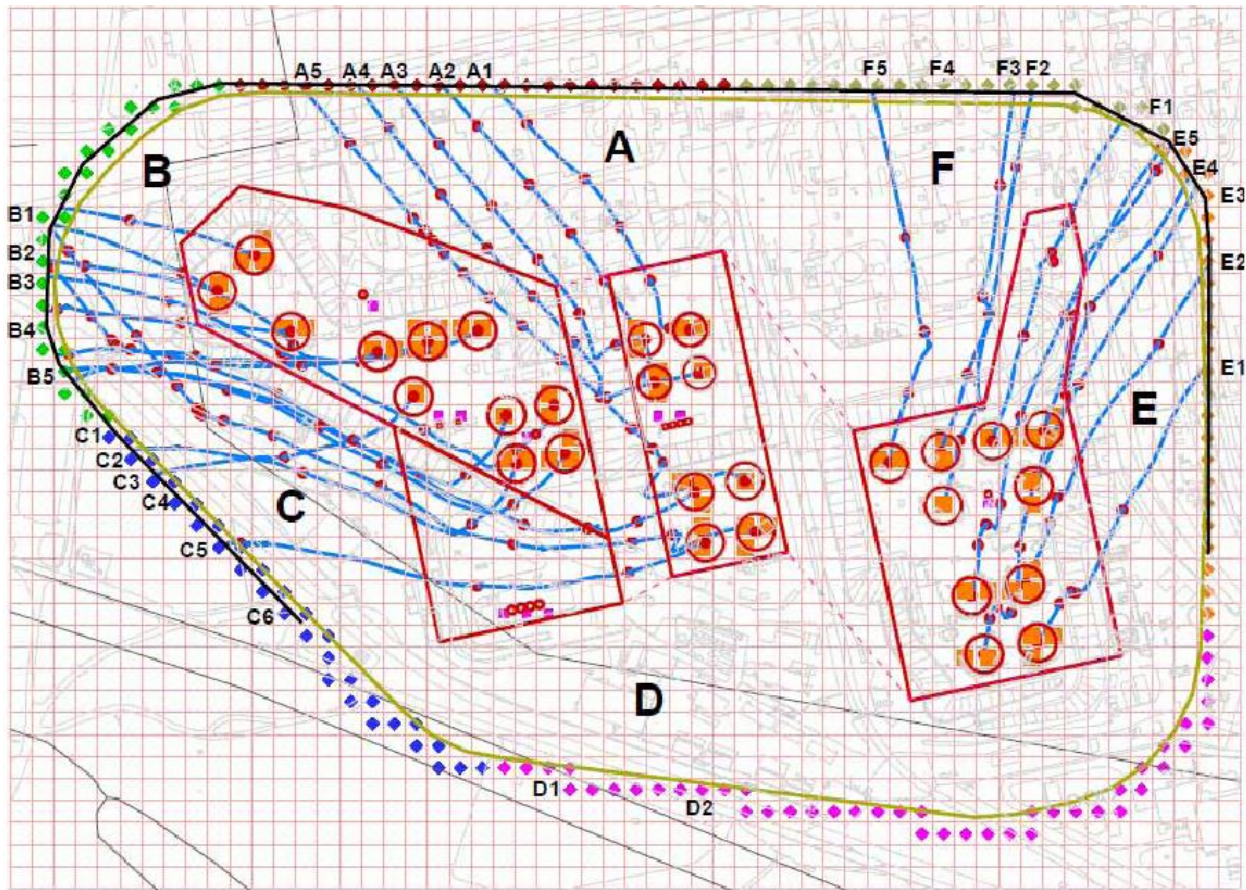
5.6.8.1 Influences of Flow Field Changes

This sensitivity analysis information is designed to evaluate the potential effects of changes in the water table divide on the analysis results. The GoldSim radionuclide transport model is an abstraction of the HTF GoldSim Model. The GoldSim saturated zone sub-model is constructed from spatial and velocity data associated with specific stream traces generated from the HTF GoldSim Model. For this reason, the HTF GoldSim Model is not amenable to changing the groundwater flow patterns without the development of a GoldSim model from which 1) groundwater flow velocities, 2) path lengths along the stream traces, and 3) the lengths of perpendiculars from the analysis wells to the stream traces can be abstracted. Modifying the PORFLOW generated flow field would yield less than satisfactory results since arguably there are no criteria to establish the appropriateness of the new flow field over the existing one. Still, from a risk-based perspective, it is necessary to be able to provide an estimate of an upper bound for the total dose to a MOP, assuming that the groundwater divide traversing the HTF could shift.

Since neither the HTF PORFLOW or GoldSim models are readily amenable to a standalone analysis pertaining to major changes in the flow field (such as would be seen if the location of the groundwater divide changes within the HTF), it was decided to take a simple conservative approach using the HTF GoldSim Model by summing up the maximum dose

concentrations from the individual sectors (Sectors A through F) as shown in Figure 5.6-97. Note that for the HTF GoldSim Model, because none of the stream traces presented in Figure 5.6-97 cross the 100-meter boundary in Sector D, Sector D was not analyzed for dose and therefore, there is no contribution from that sector in this analysis. Despite there being no contribution from Sector D, for simplicity the text will refer to the summation as the summation of results from Sectors A through F. Also, note that the total dose values presented in Section 5.5 (for specific time steps) represent the maximum of total dose values taken from Sectors A through F. The Base Case will be used for this analysis.

Figure 5.6-97: PORFLOW Stream Traces with Hypothetical 100-Meter Boundary and Associated GoldSim Well Locations



The grid used in the Figure 5.6-97 background is coarser than the grid used in the HTF PORFLOW Model, but the figure accurately reflects the locations of the wells and positions of the stream traces associated with the grid refinement. Insight to the sensitivity of the system to changes in the groundwater divide can be obtained by assuming all waste tank releases converge. It is recognized that conceptually, the superposition of localized peak dose values from all sectors is physically inconsistent. Although summing the peak concentrations is unrealistic, it does provide a conservative assumption, which is applicable in a bounding calculation. Additionally, an important insight pertaining to the sensitivity of the system to flow rates can be derived by systematically varying the flow rates. To evaluate the influence of potential changes in stream trace Darcy velocities, a set of three additional GoldSim simulations were performed where the Darcy velocity for each waste tank and ancillary equipment release were set to the maximum, minimum, and mean Darcy velocity values. This was done to prove that increasing (or decreasing) the Darcy velocity can have both attenuating and conservative effects. On the attenuating side, there is more water available for dilution. On the conservative side, the radionuclides will migrate faster increasing the influence of the more highly sorbing radionuclides over the time-period of interest and offsetting the attenuating effect of radionuclide decay. The fact that stream trace lengths are not changed is a necessary simplification, but in general, since some of the pathway lengths could increase and some could decrease it is assumed that this would be an offsetting assumption.

As shown in Figure 5.6-98, summing the locally maximized dose values for all sectors will, as expected, have a limited effect on the dose increases. Since the Base Case result is based on the largest of those locally maximized dose values, the magnitude of the summation of doses is limited to five times the Base Case value, which means that all sectors have the same maximum total doses. As can be seen in Figure 5.6-98 and Table 5.6-48, superposition of the Base Case doses for each sector generates an early-time (840 years) peak of approximately 1.7 mrem/yr, or approximately three times the Case-A equivalent of 0.5 mrem/yr. The early-time peak is formed by the release of Tc-99 from the primary sand layer in the Type II tanks. The 10,000-year peak dose based on the summed doses is 5.7 mrem/yr, or 1.5 times the Base Case dose at that time of 3.8 mrem/yr. The 10,000-year peak dose is controlled by the release of Tc-99 from the annular spaces of the lined, Type I tanks. The 20,000-year peak dose based on the summed doses is 30.7 mrem/yr, approximately 2.5 times the Base Case dose at that time of 12.3 mrem/yr. The 20,000-year peak dose is controlled by the release of Ra-226 from several tank types. Note that the spike at 13,000 years is controlled by the release of I-129 from the western Type IIIA tanks.

Figure 5.6-98: Comparison of Base Case Results with Sum of Max Dose, All Sectors, Base Case

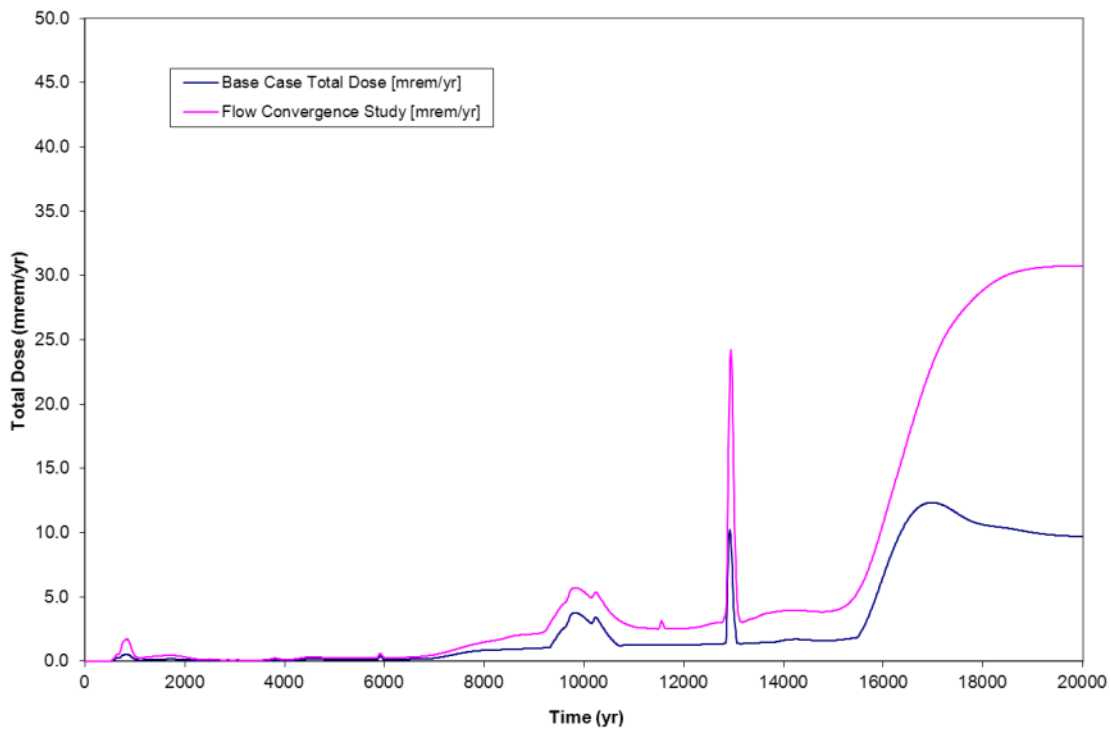


Table 5.6-48: Peak Dose Results for Various Periods of Time

Run ID	Early Peak Dose (mrem/yr)	Time of Early Peak Dose (yr)	10,000-Year Peak Dose (mrem/yr)	Time of 10,000-Year Peak Dose (yr)	20,000-Year Peak Dose (mrem/yr)	Time of 20,000-Year Peak Dose (yr)
Base Case	0.5	840	3.8	9,800	12	17,000
Sum of All Sectors	1.7	840	5.7	9,800	31	19,700
Sum of All Sectors (min Darcy velocity)	3.3	940	5.6	9,800	40	13,000
Sum of All Sectors (max Darcy velocity)	1.0	750	4.0	9,700	37	17,500
Sum of All Sectors (mean Darcy velocity)	1.9	800	4.4	9,800	37	19,200

To evaluate the sensitivity of concentrations (and associated doses) at the 100-meter boundary to changes in flow-field velocities, three additional GoldSim simulations were performed. The first of the simulations assumed that the Darcy velocities for all sources (waste tanks and ancillary equipment) were the same value, the maximum value for all of the waste tank releases from Table 5.6-49. Therefore, the saturated zone Darcy velocity for each source was set to 14.39 ft/yr. The second of the simulations assumed that the Darcy

velocities for all sources (waste tanks and ancillary equipment) were the same value, the minimum value for all of the waste tank releases from Table 5.6-49. Therefore, the saturated zone Darcy velocity for each source was set to 3.62 ft/yr. The third of the simulations assumed that the Darcy velocities for all sources (waste tanks and ancillary equipment) were the mean value for all of the waste tank releases from Table 5.6-49. Therefore, the saturated zone Darcy velocity for each source was set to 7.37 ft/yr. As can be seen by examining Table 5.6-48, the largest increase in the Base Case summed dose for the early peak occurs under the minimum flow conditions. For the minimum flow case, the summed dose increases to 3.3 mrem/year or approximately a factor of 6.6 times the Base Case early-peak dose, putting an approximate upper bound on the peak dose of 6.6 times the modeled peak dose. As can also be seen by examining Table 5.6-48, the largest increase in the Base Case summed dose for the 10,000-year maximum dose occurs under the minimum flow conditions. For the minimum flow case, the summed dose increases to 5.6 mrem/yr or approximately a factor of 1.5 times the Base Case 10,000 year maximum dose, putting an approximate upper bound on the peak dose of 1.5 times the modeled peak dose. Also shown in Table 5.6-48, the largest increase in the Base Case summed dose for the 10,000-year maximum dose occurs under the minimum flow conditions. For the minimum flow case, the summed dose increases to 40.2 mrem/yr or approximately a factor of 3.3 times the Base Case 10,000 year maximum dose, putting an approximate upper bound on the peak dose of 3.3 times the modeled peak dose. This analysis indicates that the change in the flow regime is unlikely to have a critical influence on the implication of dose results.

In addition, by comparing the summed doses for the bounding scenarios to the summed doses for the Base Case, it is also possible to see generalized influences of the flow changes on specific features of the model. As can be seen by comparing Figure 5.6-98 to Figure 5.6-99, if the Darcy velocities for all waste tanks and ancillary equipment releases are increased to the waste tank specific maximum, the early-time peak radionuclide summed dose decreases, from the Base Case summed dose of approximately 1.7 mrem/yr to 1.0 mrem/yr. This change reflects the influence of increased flow on non-sorbing and slightly sorbing species, such as Tc-99. The increase in Darcy velocity will increase the volume of water mixing with the solute as the plume spreads. The 10,000-year peak dose based on the summed doses is 4.0 mrem/yr, or 70 % of the Base Case summed dose at that time of 5.7 mrem/yr. The 10,000-year peak dose controlled by the release of Tc-99 from the annuli of the lined Type I tanks has been reduced by the increased dilution. The 20,000-year the peak dose based on the summed doses is 36.7 mrem/yr, approximately a 20 % increase over the Case-A summed dose of 30.7 mrem/yr. The increased peak dose is controlled by the more rapid breakthrough of Ra-226 released from different tanks. The influence of the increased velocity is easily seen in the breakthrough of Ra-226 released from lined Type I tanks prior to 14,000 years. Note that the I-129 spike at 13,000 years is only slightly lowered indicating that the Base Case spike is controlled by releases from Tanks 35, 36, and 37 which have relatively high velocities (Table 5.6-49) and short transport distances to the 100-meter boundary. The short transport distances decrease the degree of attenuation due to dispersion.

Table 5.6-49: Average Saturated Zone Darcy Velocities for Waste Tanks

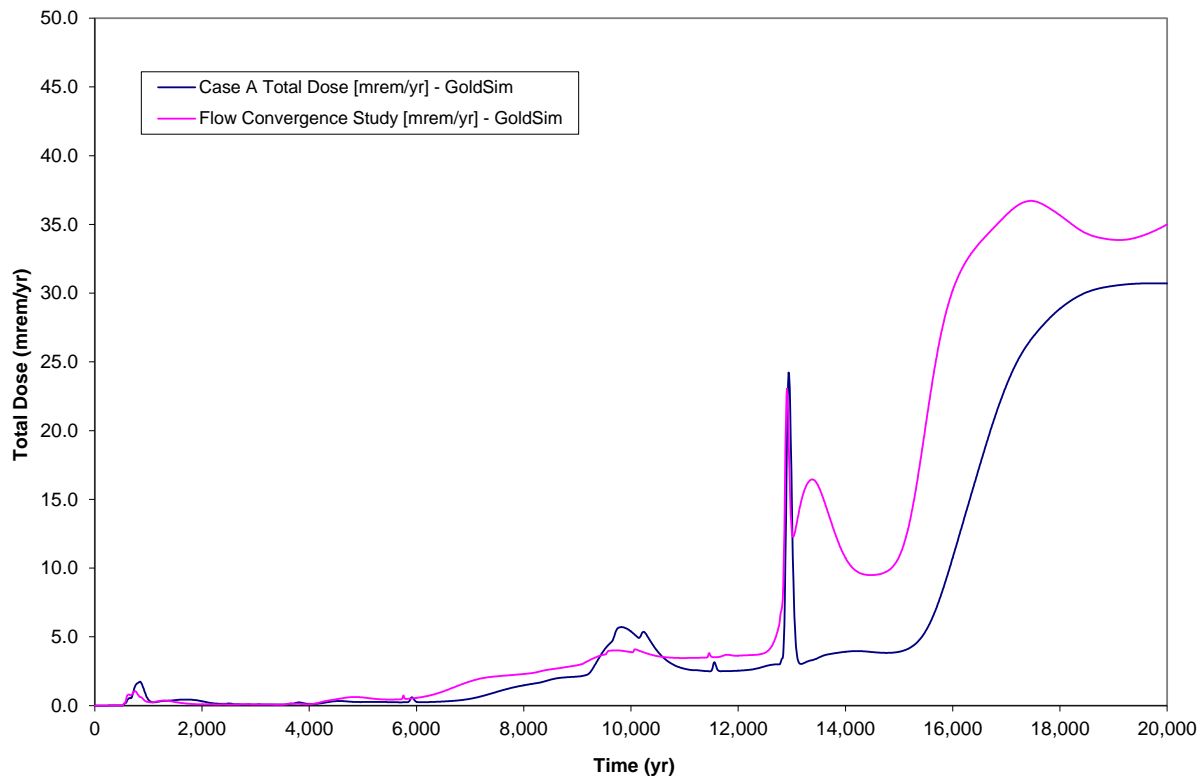
Tank	Mean Darcy Velocity (ft/yr)
Tank 9	4.01
Tank 10	3.62 ^a
Tank 11	4.1
Tank 12	3.93
Tank 13	12.15
Tank 14	4.26
Tank 15	10.62
Tank 16	14.39 ^b
Tank 21	10.52
Tank 22	9.24
Tank 23	8.65
Tank 24	8.87
Tank 29	6.25
Tank 30	6.1
Tank 31	6.5
Tank 32	5.88
Tank 35	8.12
Tank 36	9.1
Tank 37	8.73
Tank 38	6.28
Tank 39	7.1
Tank 40	8.37
Tank 41	8.66
Tank 42	6.26
Tank 43	6.82
Tank 48	5.61
Tank 49	10.68
Tank 50	4.74
Tank 51	4.26
Mean Value	7.37

[SRR-CWDA-2010-00093, Rev. 2]

a Minimum Darcy Velocity

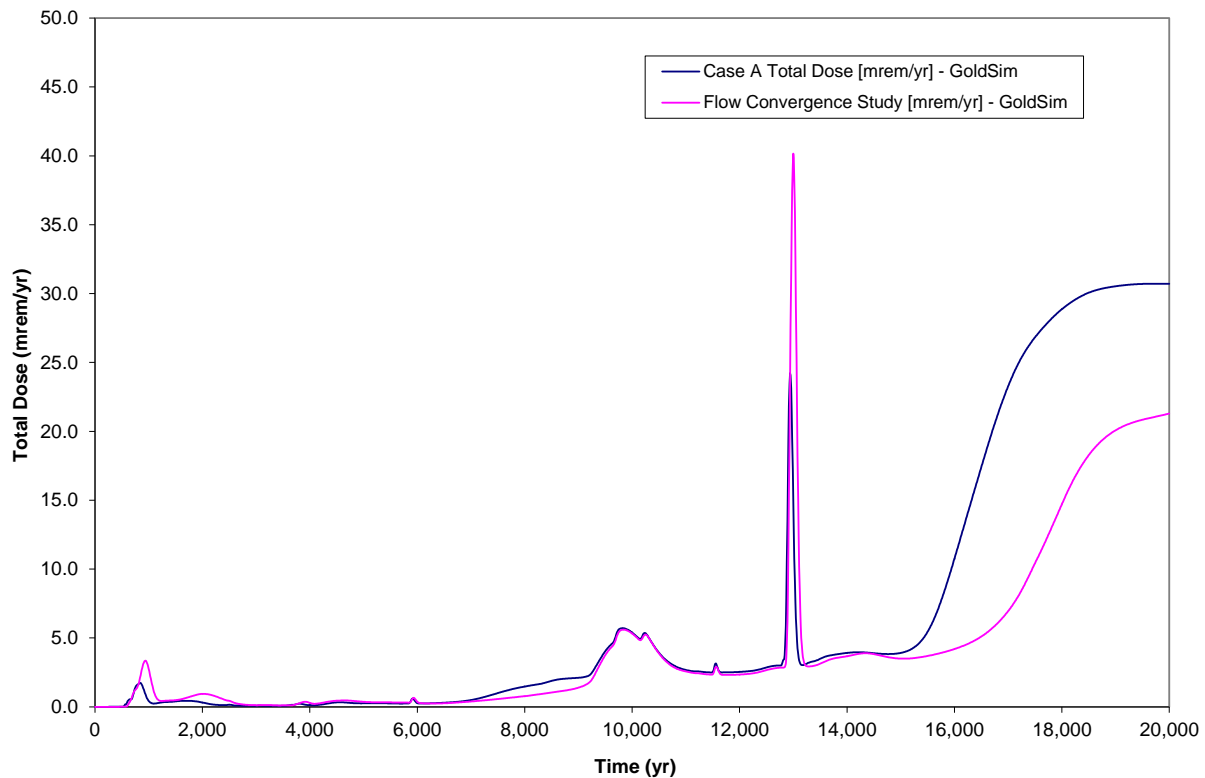
b Maximum Darcy Velocity

Figure 5.6-99: Comparison of Base Case Results with Sum of Max Dose, All Sectors, Max Velocity Analysis



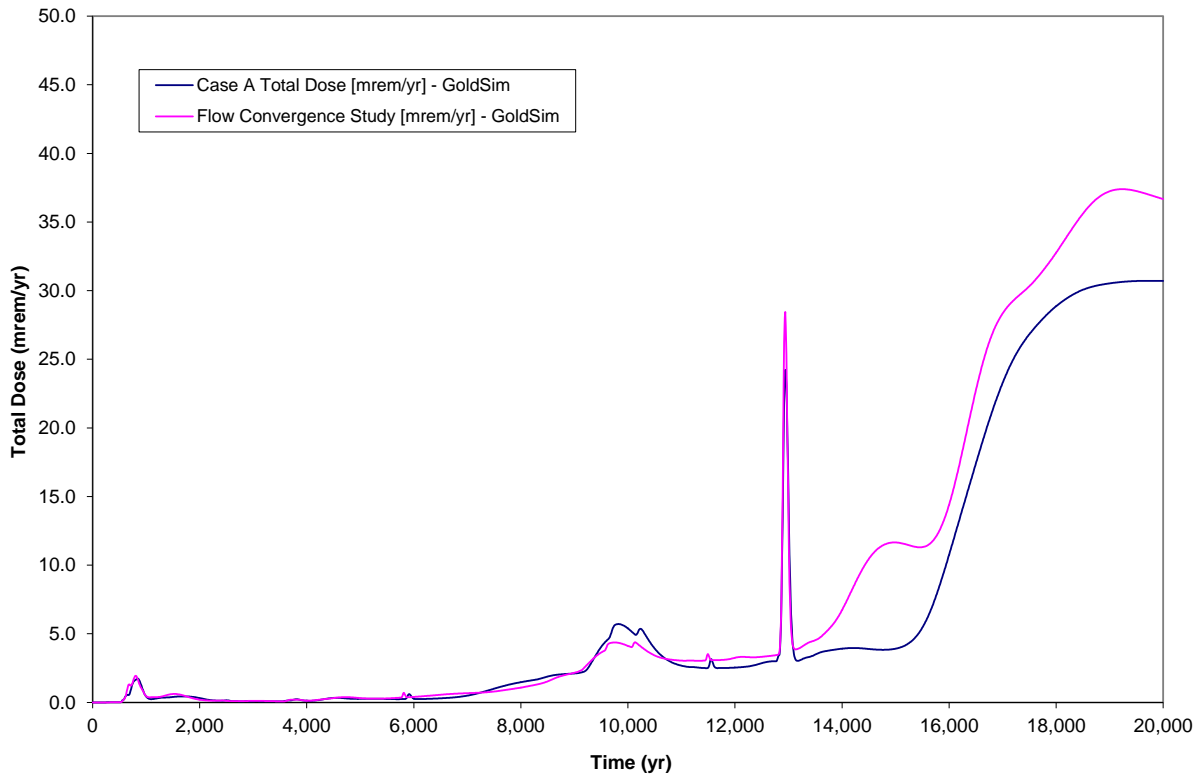
The second of the simulations assumed that the Darcy velocities for all sources (waste tanks and ancillary equipment) were the same value, the minimum value for all of the waste tank releases from Table 5.6-49. Therefore, the saturated zone Darcy velocity for each source was set to 3.62 ft/yr. As can be seen by comparing Figure 5.6-99 to Figure 5.6-100, if the Darcy velocities for all waste tanks and ancillary equipment releases are decreased to the waste tank specific minimum, the early-time peak radionuclide dose increases from approximately 1.7 mrem/yr to 3.3 mrem/yr, almost doubling. The 10,000-year peak dose based on the summed doses is 5.6 mrem/yr, showing only a slight change from the Case-A summed dose of 5.7 mrem/yr. The small change in the 10,000-year peak dose, controlled by the release of Tc-99 from the annuli of the lined Type I tanks, is reflected in the low Darcy velocities seen in the vicinity of the Tank I tanks, Tanks 9 through 11 (see Table 5.6-49). The 20,000-year peak dose based on the summed doses is 40.2 mrem/yr, approximately a 33 % increase over the Case-A summed dose of 30.7 mrem/yr. The increase in peak dose is caused by a dramatic increase in the I-129 breakthrough curve peak from the Type IIIA releases which controls the peak dose after 10,000 years in the minimum velocity run (as opposed to the Ra-226 breakthrough peak which controls the peak dose in the Base Case results). This is as expected because of the large decrease in the Darcy velocities within the vicinity of Tanks 35, 36, and 37 and the associated decrease in dilution.

Figure 5.6-100: Comparison of Base Case Results with Sum of Max Dose, All Sectors, Min Velocity Analysis



The third of the simulations assumed that the Darcy velocities for all sources (waste tanks and ancillary equipment) were the mean value for all of the waste tank releases from Table 5.6-49. Therefore, the saturated zone Darcy velocity for each source was set to 7.37 ft/yr. As can be seen by comparing Figure 5.6-99 to Figure 5.6-101, if the Darcy velocities for all waste tanks and ancillary equipment releases are set to the mean of the waste tank specific values, the early-time peak radionuclide dose slightly increases (12 %) from approximately 1.7 mrem/yr to 1.9 mrem/yr. The 10,000-year peak dose based on the summed doses is 4.4 mrem/yr, showing a decrease of 23 % from the Case-A summed dose of 5.7 mrem/yr. The change in the 10,000-year peak dose is mainly controlled by the increase in the Darcy velocities and associated dilution on the Tc-99 in the vicinity of the lined Type I tanks (see Table 5.6-49). The 20,000-year the peak dose based on the summed doses is 37.4 mrem/yr, an approximately 22 % increase over the Base Case summed dose of 30.7 mrem/yr. The increase in peak dose reflects the combined effects on Ra-226 100-meter boundary breakthrough peaks for different waste tanks.

Figure 5.6-101: Comparison of Base Case Results with Sum of Max Doses, All Sectors, Mean Velocity Analysis

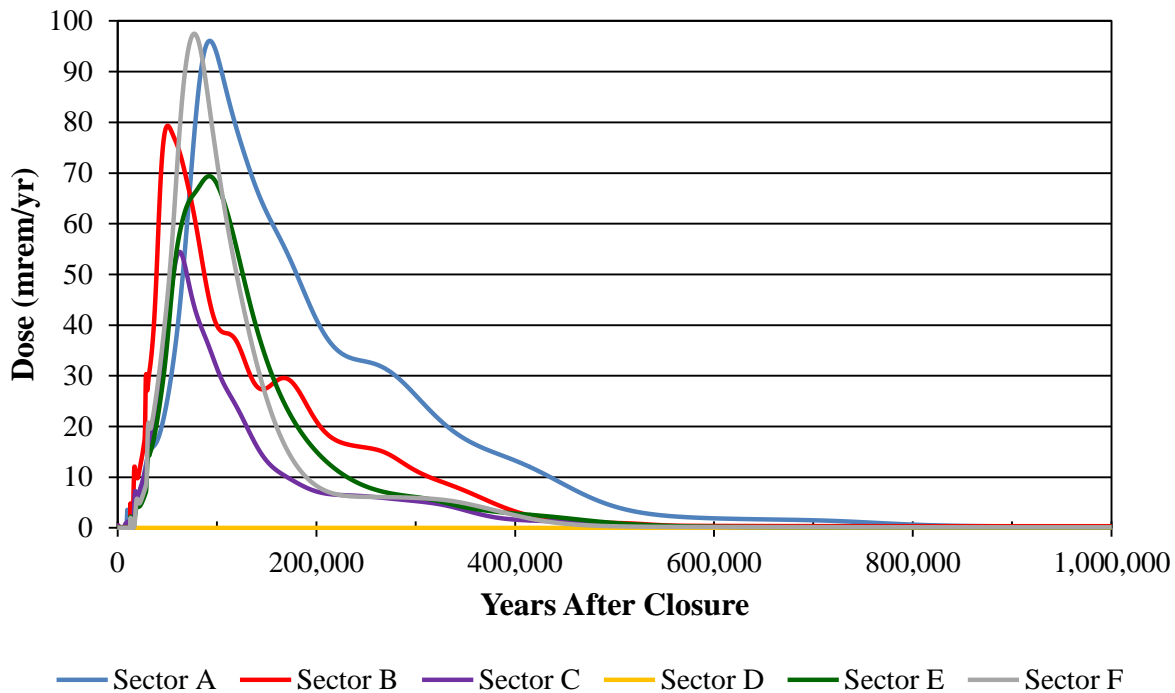


The analysis indicates that although a change in the water table divide could change the flow directions and velocities associated with releases from individual waste tanks (and ancillary equipment), it is unlikely that it would lead to a peak dose that would exceed the performance objective. Additionally, the analysis showed the sensitivity of the system to the saturated zone Darcy velocities, which are likely to change if the water table divide location changes.

5.6.9 Sensitivity Analysis Using the HTF Probabilistic Model in Deterministic Mode

This section presents a run using the GoldSim model in deterministic mode. This single run was performed to provide confidence that the discussion of the 100-meter peak doses (see Section 5.5) included the peak doses over all time for Base Case. The GoldSim model was setup to run deterministically for 1-million years, using relatively course time steps. Although there are differences in transport modeling between GoldSim and PORFLOW, this figure (Figure 5.6-102) shows that dose for each sector peaks around 100,000 years and there are no secondary dose peaks occurring at later times. Figure 5.5-3 shows these primary peaks occurring within 100,000 years, for all sectors, when modeled in PORFLOW; thus, the dose analysis in Section 5.5 includes consideration of the peak dose over all time.

Figure 5.6-102: 100-Meter Sector MOP Peak Groundwater Pathway Dose Results within 1,000,000 Years Using the GoldSim Model in Deterministic Mode



5.7 RCRA/CERCLA Risk Analysis

The RCRA/CERCLA risk assessment for the HTF closure follows the ACP protocols for human health and ecological risk assessments. [ERD-AG-003_F.17, ERD-AG-003_P.1.4, ERD-AG-003_P.1.5, ERD-AG-003_P.5.2, and ERD-AG-003_P.10.1] Based on available characterization data and estimated volume of residual material expected to remain in each of the waste tanks and ancillary equipment, the chemical and radiological inventory used for PA modeling has been calculated for HTF as discussed in Section 3.3. As discussed in Section 4.8, the placement of a low-permeability closure cap with at least 10 feet of clean backfill soil will ensure that the surface soils (0 to 1 foot) and the subsurface soils (1 to 4 feet) will not be contaminated and that there is no pathway for human health or ecological risk. The potential receptors of contamination include:

- The industrial worker excavating deep soil containing PTSM
- The resident who will be exposed to groundwater (ingestion, inhalation, and dermal contact)

Modeling was conducted to determine the peak concentrations of the non-radiological and radiological contaminants in the groundwater over 1,000 years.

5.7.1 Principal Threat Source Material

The PTSMs are the materials that include or contain hazardous substances, pollutants, or contaminants that act as a reservoir for migration of contamination to groundwater, surface

water, or air, or that act as a source for direct exposure. The EPA defines PTSM as the source materials considered highly toxic or mobile that generally cannot be reliably contained or would present a significant risk to human health or the environment should exposure occur. [OSWER 9380.3-06FS]

The HTF waste tanks and ancillary equipment will contain a heel of highly contaminated material that would present a significant risk should exposure occur, so they are, by definition, PTSM. The waste tanks and the heels remaining in the waste tanks will be stabilized and then covered as part of waste tank closure. This approach is consistent with ACP remediation of reactor seepage basins, which contain highly contaminated soils determined to be PTSM. No additional evaluation will be made to determine that the source material is PTSM.

5.7.2 Contaminant Migration Constituents of Concern

The CMCOG were identified through a system that is consistent with both ACP protocols and the PA. The CMCOG were identified by modeling the release of contaminants and their travel through the vadose zone. The basis of the CMCOG evaluation is the same model used for the PA to meet 10 CFR 61 requirements. The concentrations of contaminants that are modeled to reach the water table are compared to the MCL or RSLs/PRGs, in cases where the constituent does not have an MCL. Any constituents that are predicted to exceed these standards (i.e., fraction greater than 1.0) in the groundwater directly beneath HTF (1 meter from boundary) would be identified as CMCOG as shown in Tables 5.7-1 and 5.7-2. No CMCOG were identified using the described protocols.

Table 5.7-1: Groundwater Radionuclide Concentrations at 1 Meter from HTF

Radionuclide	MCL** (pCi/L)	Residential Tap Water PRG* (pCi/L)	Peak Concentration (pCi/L) 1 to 1,000 Years	Fraction of MCL or PRG at 1m
Ac-227	N/A	2.37E-01	1.8E-07	7.7E-07
Al-26	N/A	2.75E+00	5.3E-08	1.9E-08
Am-241	N/A	4.58E-01	1.0E-04	2.3E-04
Am-242m	N/A	6.74E-01	2.6E-09	3.9E-09
Am-243	N/A	4.62E-01	7.1E-06	1.5E-05
C-14	2.0E+03	MCL used	3.0E-03	1.5E-06
Cf-249	N/A	3.75E-01	4.7E-17	1.2E-16
Cf-251	N/A	3.61E-01	5.5E-18	1.5E-17
Cl-36	7.0E+02	MCL used	3.7E-02	5.2E-05
Cm-243	N/A	5.03E-01	2.2E-14	4.3E-14
Cm-244	N/A	5.70E-01	1.3E-12	2.2E-12
Cm-245	N/A	4.58E-01	2.4E-08	5.3E-08
Cm-247	N/A	4.79E-01	6.1E-17	1.3E-16
Cm-248	N/A	5.00E-03	6.3E-17	1.3E-14
Co-60	1.0E+02	MCL used	1.7E-11	1.7E-13
Cs-135	9.0E+02	MCL used	3.2E-02	3.6E-05

Table 5.7-1: Groundwater Radionuclide Concentrations at 1 Meter from HTF (Continued)

Radionuclide	MCL** (pCi/L)	Residential Tap Water PRG* (pCi/L)	Peak Concentration (pCi/L) 1 to 1,000 Years	Fraction of MCL or PRG at 1m
Eu-152	6.0E+01	MCL used	3.5E-13	5.8E-15
Eu-154	2.0E+02	MCL used	2.0E-13	1.0E-15
H-3	2.0E+04	MCL used	1.1E+02	5.6E-03
I-129	1.0E+00	MCL used	5.1E-03	5.1E-03
K-40	N/A	1.93E+00	4.8E-03	2.5E-03
Nb-93m	1.0E+03	MCL used	6.4E+01	6.4E-02
Nb-94	N/A	6.13E+00	2.5E-02	4.0E-03
Ni-59	3.0E+02	MCL used	4.6E+00	1.5E-02
Ni-63	5.0E+01	MCL used	3.7E+00	7.3E-02
Np-237	N/A	7.71E-01	5.6E-01	7.2E-01
Pa-231	N/A	2.75E-01	7.1E-05	2.6E-04
Pb-210	N/A	5.41E-02	3.1E-06	5.7E-05
Pd-107	N/A	1.90E+02	7.0E-01	3.7E-03
Pt-193	3.0E+03	MCL used	1.1E-04	3.6E-08
Pu-238	N/A	3.64E-01	1.3E-05	3.6E-05
Pu-239	N/A	3.53E-01	4.9E-04	1.4E-03
Pu-240	N/A	3.53E-01	2.7E-04	7.6E-04
Pu-241	N/A	2.71E+01	4.5E-08	1.6E-09
Pu-242	N/A	3.72E-01	8.5E-07	2.3E-06
Pu-244	N/A	3.48E-01	3.9E-09	1.1E-08
Ra-226+Ra-228	5.0E+00	MCL used	2.8E-04	5.7E-05
Se-79	N/A	6.53E+00	1.2E-05	1.9E-06
Sm-151	1.0E+03	MCL used	1.4E-05	1.4E-08
Sn-126	N/A	1.86E+00	4.1E-07	2.2E-07
Sr-90	8.0E+00	MCL used	6.8E-02	8.5E-03
Tc-99	9.0E+02	MCL used	3.2E+02	3.6E-01
Th-229	N/A	2.13E-01	1.9E-06	8.9E-06
Th-230	N/A	5.23E-01	2.2E-07	4.1E-07
Th-232	N/A	4.71E-01	7.1E-08	1.5E-07
U-232	N/A	1.63E-01	3.6E-11	2.2E-10
U-233	N/A	6.63E-01	3.0E-04	4.6E-04
U-234	N/A	6.74E-01	3.6E-04	5.3E-04
U-235	N/A	6.84E-01	8.2E-07	1.2E-06
U-236	N/A	7.11E-01	6.4E-06	9.0E-06
U-238	N/A	7.44E-01	7.2E-06	9.7E-06
Zr-93	2.0E+03	MCL used	1.1E-05	5.5E-09

* Residential tap water PRGs are provided in tables at EPA-PRGs_11-13-2007 based on a target cancer risk of 1.0E-06

** MCL values for beta and photon emitters are calculated in EPA 815-R-02-001 based on a beta-gamma 4 mrem/yr dose

N/A Not Available

Table 5.7-2: Groundwater Chemical Concentrations at 1 Meter from HTF

Chemical	MCL** (µg/L)	Tap Water RSLs* (µg/L)	Peak Concentration (µg/L) 1 to 1,000 Yrs	Fraction of MCL or PRG at 1m
Ag	1.0E+02	MCL used***	6.1E-03	6.1E-05
Al	2.0E+02	MCL used	1.7E-06	8.6E-09
As	1.0E+01	MCL used	2.0E-06	2.0E-07
B	N/A	3.1E+03	8.4E+01	2.7E-02
Ba	2.0E+03	MCL used	9.7E-03	4.8E-06
Cd	5.0E+00	MCL used	1.1E-02	2.3E-03
Cl	2.5E+05	MCL used	7.8E-01	3.1E-06
Co	N/A	4.7E+00	4.7E-05	9.9E-06
Cr	1.0E+02	MCL used	1.8E-07	1.8E-09
Cu	1.3E+03	MCL used	3.9E-04	3.0E-07
F	4.0E+03	MCL used	2.3E-01	5.7E-05
Fe	3.0E+02	MCL used***	2.9E-03	9.5E-06
Hg	2.0E+00	MCL used	2.9E-06	1.4E-06
I	N/A	1.6E+02	1.3E-02	7.9E-05
Mn	5.0E+01	MCL used***	1.8E-01	3.6E-03
Mo	N/A	7.8E+01	5.2E-07	6.7E-09
N	1.0E+04	MCL used	1.6E+01	1.6E-03
Ni	N/A	7.3E+02	1.4E-01	1.9E-04
Pb	1.5E+01	MCL used	6.5E-09	4.3E-10
PO ₄	N/A	7.6E+05	2.1E+01	2.8E-05
Sb	6.0E+00	MCL used	1.1E-09	1.8E-10
Se	5.0E+01	MCL used	7.6E-10	1.5E-11
SO ₄	2.5E+05	MCL used	1.1E+02	4.3E-04
Sr	N/A	9.3E+03	7.6E-03	8.2E-07
U	3.0E+01	MCL used	2.1E-05	7.0E-07
Zn	5.0E+03	MCL used***	3.8E-03	7.6E-07

* EPA_RSLs_April2012

** EPA 816-F-09-0004

*** EPA 816-F-10-079

N/A Not Available

5.7.3 Evaluation of Results

The CMCOCs are often addressed by the placement of a low permeability cap as is planned for the HTF closure (described in Section 3.2.4). Sections 2.4.2 and 2.4.3 describe the *SRS Long Range Comprehensive Plan* (PIT-MISC-0041) as founded on the following:

- The entire site will be owned and controlled by the federal government in perpetuity
- The property will be used only for industrial purposes
- Site boundaries will remain unchanged
- Residential use will not be allowed

Therefore, a scenario in which an inadvertent intruder establishes a residence on the HTF and obtains drinking water from the water table below is very unlikely. A more probable location for the MEI would be at either the UTR seepage line located approximately 2 miles northwest of the HTF or the Fourmile Branch seepage line, approximately 1 mile south of the HTF. As discussed previously, all isotopes, including total beta-gamma emitters, meet the MCLs or PRGs at the 1-meter boundary in 1,000 years and therefore would be below the MCLs or PRGs at either seepage line in 1,000 years.

5.8 ALARA Analysis

The SRS has an ALARA program and processes established in company level policies and procedures that are well documented. [E7-1, Procedure DE-DP-384, SRNS-J6000-2011-00030] The goal of the ALARA process is the attainment of the lowest practical dose level after taking into account social, technical, economic, and public policy considerations. Depending on the situation, the ALARA analysis can range from simple qualitative statements evaluating different operation and disposal options for LLW to rigorous quantitative analyses that consider individual and collective doses to the MOP. The rigor of the ALARA analysis should be commensurate with the magnitude of the calculated dose and the decisions to be made regarding the disposal facility. Based on the magnitude of the dose results of the HTF PA, a qualitative assessment of ALARA alternative disposal analysis is justified. Additionally, an in-depth ALARA cost-benefit analysis is not appropriate at this time, because the cost of new technology and personnel exposures will not be available until after final waste tank cleaning and sampling operations. A more in-depth ALARA analysis will be completed as part of the DOE O 435.1, Chg. 1 Tier 2 closure authorization documentation for specific waste tank, closure actions.

The ALARA process is applied to HTF in several ways, 1) making conservative assumptions when modeling tank farm waste inventory, releases, and dose to receptors, 2) by evaluating waste tank cleaning and stabilization alternatives, and 3) by implementing cleaning processes prior to waste tank closure that remove residual material.

The following excerpts are from the two governing regulations that define performance objectives.

DOE M 435.1-1, Chapter IV, P.(2)(f) states:

Performance assessments shall include a demonstration that projected releases of radionuclides to the environment shall be maintained as low as reasonable achievable (ALARA).

DOE G 435.1-1 provides additional guidance on meeting this requirement. The Guide states in part:

that the goal of the ALARA process is not the attainment of a particular dose level (or, in this case, level of release), but rather the attainment of the lowest practical dose level after taking into account social, technical, economic, and public policy considerations. The PA should include assessments that focus on alternatives for LLW disposal. ALARA is meant to provide a documented answer to the question: "Have I done all that I can reasonably do to reduce radiation doses or releases to the environment?"

Section 61.41 of 10 CFR 61, Protection of the General Population from Releases of Radioactivity, states:

Reasonable effort should be made to maintain releases of radioactivity in effluents to the general environment as low as is reasonable achievable.

The DOE's approach to radiation protection is based on meeting the performance objectives identified in DOE M 435.1-1 and 10 CFR 61. These documents specify maximum doses for various pathways based upon the ALARA principle.

The HTF PA modeling effort provides evidence of the SRS efforts to reduce radioactive releases to the general environment to levels ALARA. Considerable conservatisms are applied during the modeling effort and are summarized in Section 7.2. One of the appreciable conservatisms is the evaluation point for dose. In the HTF PA modeling, radionuclide dose to receptors is evaluated at a 1-meter and 100-meter buffer zones surrounding HTF and at the seepline. However, based on SRS land use plans, no MOP will have unrestricted access to the HTF, because current SRS boundaries will remain unchanged, and the land will remain under the ownership of the federal government, consistent with the site's designation as a NRMP. By demonstrating protection to the 1-meter and the 100-meter boundary, the PA is also demonstrating public protection at the site boundary (approximately 5 miles away). In fact, the dose due to radionuclides at the site boundary would only be greatly diminished in comparison to the 1-meter and 100-meter boundary dose, because as radionuclides travel a greater distance through the air and subsurface, the more dispersion and dilution occurs. Therefore, the PA demonstrates protection of the public at the site boundary to a much greater degree than at the 1-meter or 100-meter boundary.

Social, technical, economic and public policy aspects were considered in the alternative disposal analysis included in the EIS for waste tank closure. [Section 3.2.3, DOE-EIS-0303] In May 2002, DOE issued the EIS on waste tank cleaning and stabilization alternatives. DOE studied five alternatives:

1. Empty, clean, and fill waste tank with grout
2. Empty, clean, and fill waste tank with sand
3. Empty, clean, and fill waste tank with saltstone
4. Clean and remove waste tanks
5. No action

The EIS concluded the “empty, clean, and fill with grout” was the preferred option with the best approach to minimize human health and safety risks associated with operational closure of waste tanks. [DOE-EIS-0303]

In addition, the NDAA Section 3116, and DOE M 435.1-1 require that highly radioactive radionuclides be removed to the maximum extent practical. [NDAA_3116] This basic ALARA principle is accomplished through the cleaning of the waste tanks prior to closure. Section 3.3.2 delineates the estimations of waste tank inventory after waste tank cleaning.

In summary, the analysis of alternative disposal techniques; the application of cleaning the waste tanks to the maximum extent practical; the stabilization of the remaining inventory with grout; and meeting the performance objectives of DOE M 435.1-1 and 10 CFR 61 are all evidence of the application of ALARA in limiting the release of radionuclides into the environment. Furthermore, an additional ALARA analysis will be performed following closure of HTF to support the CERCLA closure, including the final design considerations for the closure cap to evaluate further opportunities to reduce environmental releases. Therefore, the principle of ALARA is satisfied.

6.0 INADVERTENT INTRUDER ANALYSIS

This section of the PA presents the analyses of the doses to a hypothetical individual who inadvertently intrudes into the HTF closed systems after the period of institutional control has ended.

The purpose of this section is to present the inadvertent intruder results for the analyses described in Section 4 of this PA.

- Section 6.1 presents peak 1-meter groundwater concentrations for the radionuclides and chemicals discussed in the Source Term Screening Section of the PA (Section 4.2.1).
- Section 6.2 and 6.3 present the individual biotic pathway formulas used to calculate the dose to the acute and chronic intruder.
- Section 6.4 presents acute and chronic dose analyses.
- Section 6.5 presents inadvertent intruder UA/SA.
- Much of the pertinent background information for the analysis is described in the preceding sections.
- Section 1 presents the regulatory limits associated with inadvertent intrusion.
- Section 2 presents design assumptions related to inadvertent intrusion (Sections 2.6.3 and 2.6.4)
- Section 3 provides technical detail on key barriers to inadvertent intrusion. Pertinent sections include Sections 3.2.1.7, 3.2.2.7.2, 3.2.3.1, and 3.2.4.1.
- Section 4 presents the inadvertent intrusion analysis approach for the acute and chronic intruder. Pertinent sections include 4.2.3, 4.2.3.2, 4.2.3.3, 4.6.2, and 4.7.3. Pertinent figures include 4.2-33 and 4.2-34. Pertinent tables include 4.4-11 and 4.6-2.
- Section 5 presents the airborne dose to an inadvertent intruder along with a description of the UA/SA pertinent to the inadvertent intruder analyses. Pertinent sections include 5.3 and 5.6.

6.1 Groundwater Concentrations at 1 Meter

The purpose of this section is to present the 1-meter groundwater concentrations for the radionuclides and chemicals discussed in Section 4.2.1. Maximum groundwater concentrations are given for the modeling mesh locations that adjoin a perimeter boundary enveloping the analyzed source terms (Figure 5.2-1). Results are presented for the three distinct aquifers modeled (the UTRA-UZ, the UTRA-LZ, and the Gordon Aquifer). The 1-meter concentrations are calculated using the same approach as the 100-meter concentrations (described in Section 5.2), wherein the peak concentration values are used.

The groundwater concentrations at 1 meter are calculated using the HTF PORFLOW Model for the Base Case modeling scenario discussed in Section 4.4. A summary of the key parameters used in the baseline HTF PORFLOW Model (Base Case) are provided in Table 5.2-1. The PORFLOW 1-meter concentrations are provided for six sectors as shown on Figure 5.2-5, with

results provided for the aquifers. Dividing the results into sectors allows variability in peak concentration for different areas of the HTF to be more easily seen. The six sectors are searched for each radionuclide and chemical to find the maximum groundwater concentrations at 1 meter from HTF for each computational mesh and at each time-step.

Tables 6.1-1 through 6.1-3 show the peak 1-meter radionuclides concentrations for the three aquifers in a 10,000-year period. These radionuclide concentrations reflect the peak concentrations for each radionuclide in the highest sector. These values are conservatively high for the radionuclides present in multiple decay chains because the totals are simply the sum of the individual peaks within that sector for a given radionuclide, without regard to timing or location within the sector (as explained in Section 5.2.1). Tables 6.1-4 through 6.1-6 show the peak 1-meter chemical concentrations for the three aquifers in a 10,000-year period. These chemical concentrations also reflect the peak concentrations for the highest sector.

As shown in these tables, the peak concentrations occur in the UTRA-UZ and the UTRA-LZ. The peak concentrations in these two aquifers are generally similar because the TCCZ, which separates the two UTRA zones, is not expected to be a significant barrier to plume migration laterally and downward. In comparison to the UTRA-UZ and UTRA-LZ, the Gordon Aquifer 1-meter peak concentrations are typically much lower. The Gordon Confining Unit, which separates the UTRA-UZ and UTRA-LZ from the underlying Gordon Aquifer, is sufficiently continuous in H Area to function as a significant flow barrier and classified as a confining unit.

The 1-meter radionuclide and chemical concentration curves (for 20,000 years) associated with the six sectors and three aquifers for the Base Case, as described in Section 4.4.2, are captured in Appendix G.

Table 6.1-1: Radiological 1-Meter Concentrations for UTRA-UZ

Rad	(MCL) (pCi/L)*	Sector A Concentrations		Sector B Concentrations		Sector C Concentrations		Sector D Concentrations		Sector E Concentrations		Sector F Concentrations	
		(pCi/L)	Year Peak Occurs										
Ac-227	N/A	1.8E-07	638	1.7E-08	1,000	1.3E-07	1,000	1.7E-07	1,000	1.0E-09	1,000	6.3E-08	716
Al-26	N/A	2.3E-08	1,000	<1E-30	1,000	1.4E-29	1,000	5.3E-08	1,000	<1E-30	1,000	4.4E-17	1,000
Am-241	Total α	1.0E-04	1,000	<1E-30	1,000	5.2E-26	1,000	6.5E-05	1,000	<1E-30	1,000	3.9E-13	1,000
Am-242m	Total α	2.6E-09	1,000	<1E-30	1,000	1.3E-30	1,000	1.6E-09	1,000	<1E-30	1,000	9.7E-18	1,000
Am-243	Total α	7.1E-06	1,000	<1E-30	1,000	3.5E-27	1,000	4.4E-06	1,000	<1E-30	1,000	2.7E-14	1,000
C-14	2,000	3.0E-03	744	4.3E-10	1,000	1.5E-05	1,000	1.1E-03	726	4.6E-08	1,000	1.8E-04	1,000
Cf-249	Total α	4.7E-17	1,000	<1E-30	1,000	<1E-30	1,000	2.9E-17	1,000	<1E-30	1,000	1.8E-25	1,000
Cf-251	Total α	5.5E-18	1,000	<1E-30	1,000	<1E-30	1,000	3.4E-18	1,000	<1E-30	1,000	2.1E-26	1,000
Cl-36	700	3.7E-02	548	1.5E-02	924	1.5E-02	926	1.4E-02	572	7.8E-03	1,000	8.6E-03	1,000
Cm-243	Total α	9.0E-16	644	<1E-30	1,000	<1E-30	1,000	2.2E-14	124	<1E-30	1,000	1.0E-25	810
Cm-244	Total α	2.2E-16	104	<1E-30	676	<1E-30	982	1.3E-12	78	<1E-30	544	4.2E-27	208
Cm-245	Total α	2.4E-08	1,000	<1E-30	1,000	1.2E-29	1,000	1.5E-08	1,000	<1E-30	1,000	9.1E-17	1,000
Cm-247	Total α	6.1E-17	1,000	<1E-30	1,000	<1E-30	1,000	3.8E-17	1,000	<1E-30	1,000	2.3E-25	1,000
Cm-248	Total α	6.3E-17	1,000	<1E-30	1,000	<1E-30	1,000	3.9E-17	1,000	<1E-30	1,000	2.4E-25	1,000
Co-60	100	1.7E-13	30	<1E-30	192	<1E-30	152	1.7E-11	22	<1E-30	150	1.2E-20	60
Cs-135	900	3.2E-02	752	1.4E-08	1,000	1.3E-03	1,000	1.7E-02	978	5.2E-07	1,000	1.2E-02	1,000
Cs-137	200	4.6E-03	596	3.0E-13	1,000	9.7E-08	884	2.4E-03	590	2.8E-11	914	7.8E-06	690
Eu-152	200	6.1E-17	78	<1E-30	506	<1E-30	394	3.5E-13	58	<1E-30	406	3.5E-28	156
Eu-154	60	4.1E-17	50	<1E-30	322	<1E-30	212	2.0E-13	38	<1E-30	260	3.9E-29	100

Table 6.1-1: Radiological 1-Meter Concentrations for UTRA-UZ (Continued)

Rad	(MCL) (pCi/L)*	Sector A Concentrations		Sector B Concentrations		Sector C Concentrations		Sector D Concentrations		Sector E Concentrations		Sector F Concentrations	
		(pCi/L)	Year Peak Occurs										
H-3	20,000	1.1E+02	56	4.6E-01	80	3.3E+00	62	1.1E+02	46	3.4E-02	62	3.2E+00	72
I-129	1	5.1E-03	534	4.0E-03	662	4.0E-03	662	3.5E-03	532	2.5E-03	704	2.9E-03	690
K-40	N/A	4.8E-03	638	2.6E-05	1,000	1.0E-03	1,000	2.3E-03	760	7.0E-07	968	1.5E-03	794
Nb-93m	1,000	6.4E+01	530	2.3E+01	828	3.6E+01	814	5.1E+01	538	1.4E+01	836	2.7E+01	830
Nb-94	N/A	2.0E-02	534	1.8E-02	572	1.9E-02	572	2.5E-02	534	1.4E-02	586	1.7E-02	580
Ni-59	300	4.6E+00	686	4.7E-04	1,000	7.0E-01	1,000	2.5E+00	834	4.6E-04	1,000	1.7E+00	902
Ni-63	50	3.7E+00	632	3.1E-05	1,000	5.1E-02	990	1.5E+00	612	3.3E-05	998	2.5E-01	842
Np-237	Total α	5.6E-01	596	7.0E-02	1,000	2.7E-01	988	3.4E-01	962	5.5E-03	1,000	2.0E-01	686
Pa-231	Total α	7.1E-05	600	9.7E-06	1,000	4.5E-05	1,000	6.0E-05	1,000	7.0E-07	1,000	2.6E-05	690
Pb-210	N/A	3.1E-06	1,000	2.8E-21	1,000	6.0E-11	1,000	1.3E-06	1,000	6.7E-16	1,000	1.3E-08	1,000
Pd-107	N/A	7.0E-01	686	7.2E-05	1,000	1.1E-01	1,000	3.8E-01	836	6.9E-05	1,000	2.5E-01	902
Pt-193	3,000	1.1E-04	606	5.8E-11	1,000	1.6E-07	904	4.9E-05	594	9.4E-11	918	1.7E-06	788
Pu-238	Total α	1.3E-05	892	<1E-30	1,000	1.4E-24	1,000	8.2E-06	888	<1E-30	1,000	3.5E-13	1,000
Pu-239	Total α	4.9E-04	1,000	<1E-30	1,000	6.5E-23	1,000	3.0E-04	1,000	<1E-30	1,000	1.5E-11	1,000
Pu-240	Total α	2.7E-04	1,000	<1E-30	1,000	3.5E-23	1,000	1.7E-04	1,000	<1E-30	1,000	8.3E-12	1,000
Pu-241	300	4.5E-08	1,000	<1E-30	1,000	3.9E-29	1,000	2.8E-08	1,000	<1E-30	1,000	1.9E-16	1,000
Pu-242	Total α	8.5E-07	1,000	<1E-30	1,000	1.1E-25	1,000	5.3E-07	1,000	<1E-30	1,000	2.7E-14	1,000
Pu-244	Total α	3.9E-09	1,000	<1E-30	1,000	5.2E-28	1,000	2.4E-09	1,000	<1E-30	1,000	1.2E-16	1,000
Ra-226	Total α /Ra	2.7E-04	1,000	4.0E-19	1,000	8.6E-09	1,000	1.1E-04	1,000	1.0E-13	1,000	1.3E-06	1,000
Ra-228	Total Ra	1.3E-05	1,000	<1E-30	1,000	3.7E-17	1,000	1.2E-05	1,000	9.1E-27	1,000	1.0E-11	1,000

Table 6.1-1: Radiological 1-Meter Concentrations for UTRA-UZ (Continued)

Rad	(MCL) (pCi/L)*	Sector A Concentrations		Sector B Concentrations		Sector C Concentrations		Sector D Concentrations		Sector E Concentrations		Sector F Concentrations	
		(pCi/L)	Year Peak Occurs										
Se-79	N/A	5.4E-06	1,000	<1E-30	1,000	5.8E-26	1,000	1.2E-05	1,000	<1E-30	1,000	3.0E-14	1,000
Sm-151	1,000	1.4E-05	896	<1E-30	1,000	6.0E-27	1,000	8.7E-06	900	<1E-30	1,000	4.7E-14	1,000
Sn-126	N/A	4.1E-07	1,000	<1E-30	1,000	<1E-30	1,000	3.9E-07	1,000	<1E-30	1,000	1.4E-16	1,000
Sr-90	8	6.8E-02	576	2.5E-08	982	3.9E-05	762	3.2E-02	568	2.1E-08	786	4.9E-04	708
Tc-99	900	3.1E+02	540	2.0E+02	740	2.0E+02	742	3.2E+02	564	1.3E+02	840	1.4E+02	826
Th-229	Total α	1.3E-06	1,000	4.8E-10	1,000	9.4E-09	1,000	1.9E-06	1,000	5.7E-12	1,000	9.2E-09	1,000
Th-230	Total α	1.6E-07	1,000	<1E-30	1,000	1.2E-22	1,000	2.2E-07	1,000	<1E-30	1,000	4.9E-14	1,000
Th-232	Total α	6.7E-08	1,000	<1E-30	1,000	1.1E-27	1,000	7.1E-08	1,000	<1E-30	1,000	5.7E-16	1,000
U-232	Total U**	2.7E-11	800	<1E-30	1,000	5.9E-26	1,000	3.6E-11	796	<1E-30	1,000	1.1E-17	1,000
U-233	Total U**	1.9E-04	1,000	2.3E-07	1,000	2.5E-06	1,000	3.0E-04	1,000	7.3E-09	1,000	1.0E-06	1,000
U-234	Total U**	2.5E-04	1,000	<1E-30	1,000	1.0E-18	1,000	3.6E-04	1,000	2.6E-30	1,000	1.7E-10	1,000
U-235	Total U**	5.0E-07	1,000	<1E-30	1,000	2.0E-21	1,000	8.2E-07	1,000	<1E-30	1,000	3.4E-13	1,000
U-236	Total U**	3.9E-06	1,000	<1E-30	1,000	1.6E-20	1,000	6.4E-06	1,000	<1E-30	1,000	2.6E-12	1,000
U-238	Total U**	4.4E-06	1,000	<1E-30	1,000	1.8E-20	1,000	7.2E-06	1,000	<1E-30	1,000	3.0E-12	1,000
Zr-93	2,000	1.0E-05	1,000	<1E-30	1,000	1.6E-25	1,000	1.1E-05	1,000	<1E-30	1,000	8.8E-14	1,000
Total Alpha	15	5.6E-01	NA	7.0E-02	NA	2.7E-01	NA	3.4E-01	NA	5.5E-03	NA	2.0E-01	NA
Total Ra	5	2.8E-04	NA	4.0E-19	NA	8.6E-09	NA	1.2E-04	NA	1.0E-13	NA	1.3E-06	NA
Sum of beta-gamma MCL fractions		5.2E-01	NA	2.5E-01	NA	2.7E-01	NA	4.6E-01	NA	1.6E-01	NA	2.0E-01	NA

* MCL values for beta and photon emitters are calculated in EPA 815-R-02-001 based on a beta-gamma dose of 4 mrem/yr.

** Total uranium is evaluated in Table 6.1-3.

N/A Not Applicable

Table 6.1-2: Radiological 1-Meter Concentrations for UTRA-LZ

Rad	(MCL) (pCi/L) *	Sector A Concentrations		Sector B Concentrations		Sector C Concentrations		Sector D Concentrations		Sector E Concentrations		Sector F Concentrations	
		(pCi/L)	Year Peak Occurs										
Ac-227	N/A	3.2E-08	1,000	2.8E-08	1,000	8.0E-08	1,000	8.4E-08	1,000	2.2E-13	1,000	3.4E-09	1,000
Al-26	N/A	<1E-30	1,000	<1E-30	1,000	<1E-30	1,000	1.3E-29	1,000	<1E-30	1,000	<1E-30	1,000
Am-241	Total α	<1E-30	1,000	<1E-30	1,000	<1E-30	1,000	3.5E-25	1,000	<1E-30	1,000	<1E-30	1,000
Am-242m	Total α	<1E-30	1,000	<1E-30	1,000	<1E-30	1,000	8.0E-30	1,000	<1E-30	1,000	<1E-30	1,000
Am-243	Total α	<1E-30	1,000	<1E-30	1,000	<1E-30	1,000	2.5E-26	1,000	<1E-30	1,000	<1E-30	1,000
C-14	2,000	2.3E-09	1,000	1.3E-10	1,000	5.7E-06	1,000	1.0E-04	1,000	3.9E-14	1,000	4.7E-08	1,000
Cf-249	Total α	<1E-30	1,000										
Cf-251	Total α	<1E-30	1,000										
Cl-36	700	1.5E-02	796	8.4E-03	934	1.0E-02	662	1.1E-02	648	1.7E-04	1,000	4.4E-03	1,000
Cm-243	Total α	<1E-30	1,000	<1E-30	1,000	<1E-30	1,000	<1E-30	656	<1E-30	1,000	<1E-30	1,000
Cm-244	Total α	<1E-30	442	<1E-30	1,000	<1E-30	742	<1E-30	412	<1E-30	726	<1E-30	546
Cm-245	Total α	<1E-30	1,000	<1E-30	1,000	<1E-30	1,000	8.7E-29	1,000	<1E-30	1,000	<1E-30	1,000
Cm-247	Total α	<1E-30	1,000										
Cm-248	Total α	<1E-30	1,000										
Co-60	100	<1E-30	124	<1E-30	306	<1E-30	196	2.0E-26	110	<1E-30	204	<1E-30	156
Cs-135	900	1.9E-07	1,000	7.8E-09	1,000	1.1E-04	1,000	5.8E-03	1,000	4.3E-13	1,000	5.6E-06	1,000
Cs-137	200	7.6E-12	942	1.7E-13	612	3.6E-09	932	2.0E-06	794	1.4E-17	1,000	1.2E-10	1,000
Eu-152	200	<1E-30	330	<1E-30	866	<1E-30	558	<1E-30	308	<1E-30	540	<1E-30	408
Eu-154	60	<1E-30	210	<1E-30	554	<1E-30	356	<1E-30	196	<1E-30	346	<1E-30	260

Table 6.1-2: Radiological 1-Meter Concentrations for UTRA-LZ (Continued)

Rad	(MCL) (pCi/L)*	Sector A Concentrations		Sector B Concentrations		Sector C Concentrations		Sector D Concentrations		Sector E Concentrations		Sector F Concentrations	
		(pCi/L)	Year Peak Occurs										
H-3	20,000	8.3E+01	62	4.6E+00	88	2.0E+01	72	2.6E+01	66	2.4E-04	84	2.3E+00	82
I-129	1	3.2E-03	632	2.0E-03	738	2.0E-03	588	2.1E-03	580	6.7E-04	810	2.2E-03	758
K-40	N/A	2.4E-05	1,000	2.2E-05	1,000	1.1E-03	1,000	1.4E-03	1,000	3.1E-10	1,000	1.3E-05	938
Nb-93m	1,000	1.2E+01	570	9.3E+00	848	1.7E+01	826	2.4E+01	542	7.2E-01	882	6.9E+00	854
Nb-94	N/A	1.5E-02	568	9.4E-03	604	1.1E-02	544	1.3E-02	542	3.6E-03	630	1.2E-02	606
Ni-59	300	1.2E-03	1,000	3.3E-04	1,000	2.5E-01	1,000	9.3E-01	906	9.1E-09	1,000	1.0E-02	1,000
Ni-63	50	7.9E-05	1,000	2.0E-05	1,000	1.7E-02	1,000	1.6E-01	820	6.1E-10	1,000	6.5E-04	1,000
Np-237	Total α	1.1E-01	1,000	9.1E-02	1,000	1.8E-01	924	1.9E-01	880	7.2E-07	1,000	1.2E-02	1,000
Pa-231	Total α	1.5E-05	1,000	1.2E-05	1,000	2.8E-05	1,000	3.0E-05	1,000	9.6E-11	1,000	1.5E-06	1,000
Pb-210	N/A	2.1E-16	1,000	6.8E-22	1,000	3.4E-14	1,000	7.5E-10	1,000	2.3E-25	1,000	1.4E-17	1,000
Pd-107	N/A	1.8E-04	1,000	4.9E-05	1,000	3.7E-02	1,000	1.4E-01	904	1.4E-09	1,000	1.6E-03	1,000
Pt-193	3,000	1.6E-10	1,000	3.6E-11	1,000	3.5E-08	1,000	1.2E-06	772	1.2E-15	1,000	1.4E-09	952
Pu-238	Total α	<1E-30	1,000	<1E-30	1,000	<1E-30	1,000	1.3E-23	1,000	<1E-30	1,000	<1E-30	1,000
Pu-239	Total α	<1E-30	1,000	<1E-30	1,000	<1E-30	1,000	7.0E-22	1,000	<1E-30	1,000	<1E-30	1,000
Pu-240	Total α	<1E-30	1,000	<1E-30	1,000	<1E-30	1,000	3.8E-22	1,000	<1E-30	1,000	<1E-30	1,000
Pu-241	300	<1E-30	1,000	<1E-30	1,000	<1E-30	1,000	1.9E-28	1,000	<1E-30	1,000	<1E-30	1,000
Pu-242	Total α	<1E-30	1,000	<1E-30	1,000	<1E-30	1,000	1.2E-24	1,000	<1E-30	1,000	<1E-30	1,000
Pu-244	Total α	<1E-30	1,000	<1E-30	1,000	<1E-30	1,000	5.6E-27	1,000	<1E-30	1,000	<1E-30	1,000
Ra-226	Total α /Ra	3.0E-14	1,000	9.9E-20	1,000	5.6E-12	1,000	1.0E-07	1,000	4.4E-23	1,000	2.8E-15	1,000
Ra-228	Total Ra	1.1E-25	1,000	<1E-30	1,000	7.6E-27	1,000	1.1E-17	1,000	<1E-30	1,000	9.3E-30	1,000

Table 6.1-2: Radiological 1-Meter Concentrations for UTRA-LZ (Continued)

Rad	(MCL) (pCi/L)*	Sector A Concentrations		Sector B Concentrations		Sector C Concentrations		Sector D Concentrations		Sector E Concentrations		Sector F Concentrations	
		(pCi/L)	Year Peak Occurs										
Se-79	N/A	<1E-30	1,000	<1E-30	1,000	<1E-30	1,000	6.7E-26	1,000	<1E-30	1,000	<1E-30	1,000
Sm-151	1,000	<1E-30	1,000	<1E-30	1,000	<1E-30	1,000	3.6E-26	1,000	<1E-30	1,000	<1E-30	1,000
Sn-126	N/A	<1E-30	1,000	<1E-30	1,000	<1E-30	1,000	1.4E-30	1,000	<1E-30	1,000	<1E-30	1,000
Sr-90	8	3.6E-08	924	1.8E-08	1,000	5.8E-06	844	4.3E-04	686	3.1E-13	954	2.4E-07	820
Tc-99	900	2.7E+02	752	2.1E+02	724	2.4E+02	690	2.5E+02	634	3.5E+01	988	1.1E+02	902
Th-229	Total α	6.8E-10	1,000	5.9E-10	1,000	6.6E-09	1,000	1.3E-08	1,000	5.4E-15	1,000	7.3E-11	1,000
Th-230	Total α	1.6E-30	1,000	<1E-30	1,000	<1E-30	1,000	4.5E-22	1,000	<1E-30	1,000	<1E-30	1,000
Th-232	Total α	<1E-30	1,000	<1E-30	1,000	<1E-30	1,000	2.6E-27	1,000	<1E-30	1,000	<1E-30	1,000
U-232	Total U**	<1E-30	1,000	<1E-30	1,000	<1E-30	1,000	1.3E-25	1,000	<1E-30	1,000	<1E-30	1,000
U-233	Total U**	3.8E-07	1,000	3.4E-07	1,000	1.8E-06	1,000	2.4E-06	1,000	2.8E-12	1,000	4.1E-08	1,000
U-234	Total U**	1.1E-26	1,000	<1E-30	1,000	<1E-30	1,000	2.1E-18	1,000	<1E-30	1,000	<1E-30	1,000
U-235	Total U**	2.3E-29	1,000	<1E-30	1,000	<1E-30	1,000	5.5E-21	1,000	<1E-30	1,000	<1E-30	1,000
U-236	Total U**	1.8E-28	1,000	<1E-30	1,000	<1E-30	1,000	4.3E-20	1,000	<1E-30	1,000	<1E-30	1,000
U-238	Total U**	2.0E-28	1,000	<1E-30	1,000	<1E-30	1,000	4.9E-20	1,000	<1E-30	1,000	<1E-30	1,000
Zr-93	2,000	<1E-30	1,000	<1E-30	1,000	<1E-30	1,000	4.0E-25	1,000	<1E-30	1,000	<1E-30	1,000
Total Alpha	15	1.1E-01	NA	9.1E-02	NA	1.8E-01	NA	1.9E-01	NA	7.2E-07	NA	1.2E-02	NA
Total Ra	5	3.0E-14	NA	9.9E-20	NA	5.6E-12	NA	1.0E-07	NA	4.4E-23	NA	2.8E-15	NA
Sum of beta-gamma MCL fractions		3.2E-01	NA	2.5E-01	NA	2.9E-01	NA	3.1E-01	NA	4.0E-02	NA	1.4E-01	NA

* MCL values for beta and photon emitters are calculated in EPA 815-R-02-001 based on a beta-gamma dose of 4 mrem/yr.

** Total uranium is evaluated in Table 6.1-3.

N/A Not Applicable

Table 6.1-3: Radiological 1-Meter Concentrations for Gordon Aquifer

Rad	(MCL) (pCi/L)*	Sector A Concentrations		Sector B Concentrations		Sector C Concentrations		Sector D Concentrations		Sector E Concentrations		Sector F Concentrations	
		(pCi/L)	Year Peak Occurs										
Ac-227	N/A	3.7E-14	1,000	2.2E-13	1,000	2.0E-13	1,000	7.9E-14	1,000	5.8E-24	1,000	3.4E-18	1,000
Al-26	N/A	<1E-30	1,000										
Am-241	Total α	<1E-30	1,000										
Am-242m	Total α	<1E-30	1,000										
Am-243	Total α	<1E-30	1,000										
C-14	2,000	1.2E-19	1,000	2.8E-17	1,000	1.2E-16	1,000	1.7E-16	1,000	<1E-30	1,000	3.8E-22	1,000
Cf-249	Total α	<1E-30	1,000										
Cf-251	Total α	<1E-30	1,000										
Cl-36	700	4.3E-07	1,000	6.3E-07	1,000	2.9E-07	1,000	5.8E-08	1,000	7.5E-14	1,000	2.1E-10	1,000
Cm-243	Total α	<1E-30	1,000	<1E-30	1,000	<1E-30	1,000	<1E-30	942	<1E-30	1,000	<1E-30	1,000
Cm-244	Total α	<1E-30	620	<1E-30	1,000	<1E-30	920	<1E-30	590	<1E-30	904	<1E-30	726
Cm-245	Total α	<1E-30	1,000										
Cm-247	Total α	<1E-30	1,000										
Cm-248	Total α	<1E-30	1,000										
Co-60	100	<1E-30	174	<1E-30	328	<1E-30	236	<1E-30	158	<1E-30	252	<1E-30	206
Cs-135	900	4.9E-16	1,000	1.4E-13	1,000	5.5E-13	1,000	8.4E-13	1,000	4.5E-28	1,000	3.1E-18	1,000
Cs-137	200	9.2E-21	1,000	2.7E-18	1,000	1.2E-17	986	2.0E-17	960	<1E-30	1,000	5.8E-23	1,000
Eu-152	200	<1E-30	464	<1E-30	990	<1E-30	690	<1E-30	444	<1E-30	676	<1E-30	544
Eu-154	60	<1E-30	296	<1E-30	636	<1E-30	440	<1E-30	284	<1E-30	432	<1E-30	346

Table 6.1-3: Radiological 1-Meter Concentrations for Gordon Aquifer (Continued)

Rad	(MCL) (pCi/L)*	Sector A Concentrations		Sector B Concentrations		Sector C Concentrations		Sector D Concentrations		Sector E Concentrations		Sector F Concentrations	
		(pCi/L)	Year Peak Occurs										
H-3	20,000	8.4E-04	114	1.8E-03	104	1.3E-03	100	4.0E-04	96	2.8E-12	122	6.7E-07	124
I-129	1	9.3E-07	870	1.2E-06	848	3.6E-07	804	1.0E-07	1,000	2.6E-10	1,000	1.4E-07	1,000
K-40	N/A	2.4E-12	1,000	5.0E-11	1,000	4.6E-11	1,000	3.4E-11	1,000	6.8E-23	1,000	3.1E-15	1,000
Nb-93m	1,000	1.4E-03	972	2.2E-03	952	1.2E-03	942	2.7E-04	962	8.7E-08	950	6.4E-05	938
Nb-94	N/A	7.1E-06	638	8.8E-06	632	2.8E-06	612	7.1E-07	708	2.2E-09	696	1.1E-06	684
Ni-59	300	2.4E-11	1,000	2.8E-09	1,000	2.9E-09	1,000	3.1E-09	1,000	1.8E-22	1,000	1.8E-13	1,000
Ni-63	50	1.4E-12	1,000	1.7E-10	1,000	1.7E-10	1,000	1.9E-10	1,000	1.1E-23	1,000	1.0E-14	1,000
Np-237	Total α	1.6E-07	1,000	8.7E-07	1,000	7.7E-07	1,000	2.8E-07	1,000	2.9E-17	1,000	9.8E-12	1,000
Pa-231	Total α	2.0E-11	1,000	1.1E-10	1,000	9.9E-11	1,000	3.6E-11	1,000	3.6E-21	1,000	1.4E-15	1,000
Pb-210	N/A	2.3E-29	1,000	1.7E-26	1,000	2.1E-24	1,000	2.6E-23	1,000	<1E-30	1,000	<1E-30	1,000
Pd-107	N/A	3.6E-12	1,000	4.3E-10	1,000	4.4E-10	1,000	4.7E-10	1,000	2.7E-23	1,000	2.7E-14	1,000
Pt-193	3,000	2.6E-18	1,000	3.0E-16	1,000	3.2E-16	1,000	3.6E-16	1,000	2.2E-29	1,000	1.8E-20	1,000
Pu-238	Total α	<1E-30	1,000										
Pu-239	Total α	<1E-30	1,000										
Pu-240	Total α	<1E-30	1,000										
Pu-241	300	<1E-30	1,000										
Pu-242	Total α	<1E-30	1,000										
Pu-244	Total α	<1E-30	1,000										
Ra-226	Total α /Ra	3.3E-27	1,000	2.3E-24	1,000	3.7E-22	1,000	4.4E-21	1,000	<1E-30	1,000	<1E-30	1,000
Ra-228	Total Ra	<1E-30	1,000										

Table 6.1-3: Radiological 1-Meter Concentrations for Gordon Aquifer (Continued)

Rad	(MCL) (pCi/L)*	Sector A Concentrations		Sector B Concentrations		Sector C Concentrations		Sector D Concentrations		Sector E Concentrations		Sector F Concentrations	
		(pCi/L)	Year Peak Occurs										
Se-79	N/A	<1E-30	1,000										
Sm-151	1,000	<1E-30	1,000	<1E-30	1,000	<1E-30	1,000	<1E-30	1,000	<1E-30	1,000	<1E-30	1,000
Sn-126	N/A	<1E-30	1,000										
Sr-90	8	3.9E-15	1,000	9.1E-14	930	8.6E-14	920	8.8E-14	850	1.0E-25	1,000	6.5E-18	940
Tc-99	900	2.7E-01	1,000	3.2E-01	1,000	1.3E-01	1,000	2.7E-02	1,000	1.9E-06	1,000	1.6E-03	1,000
Th-229	Total α	4.5E-16	1,000	3.9E-15	1,000	3.5E-15	1,000	1.7E-15	1,000	5.0E-26	1,000	1.2E-19	1,000
Th-230	Total α	<1E-30	1,000										
Th-232	Total α	<1E-30	1,000										
U-232	Total U**	<1E-30	1,000										
U-233	Total U**	3.6E-13	1,000	2.4E-12	1,000	2.2E-12	1,000	9.5E-13	1,000	5.0E-23	1,000	5.0E-17	1,000
U-234	Total U**	<1E-30	1,000										
U-235	Total U**	<1E-30	1,000										
U-236	Total U**	<1E-30	1,000										
U-238	Total U**	<1E-30	1,000										
Zr-93	2,000	<1E-30	1,000										
Total Alpha	15	1.6E-07	NA	8.7E-07	NA	7.7E-07	NA	2.8E-07	NA	2.9E-17	NA	9.8E-12	NA
Total Ra	5	3.3E-27	NA	2.3E-24	NA	3.7E-22	NA	4.4E-21	NA	<1E-30	NA	<1E-30	NA
Sum of beta-gamma MCL fractions		3.0E-04	NA	3.6E-04	NA	1.4E-04	NA	3.0E-05	NA	2.4E-09	NA	2.0E-06	NA

* MCL values for beta and photon emitters are calculated in EPA 815-R-02-001 based on a beta-gamma dose of 4 mrem/yr.

** Total uranium is evaluated in Table 6.1-3.

N/A Not Applicable

Table 6.1-4: Chemical 1-Meter Concentrations for UTRA-UZ

Constituent	(MCL) (µg/L)	Sector A		Sector B		Sector C		Sector D		Sector E		Sector F	
		(µg/L)	Year Peak Occurs										
Ag	100	6.1E-03	760	3.7E-09	1,000	3.9E-04	1,000	3.7E-03	928	9.9E-08	1,000	2.7E-03	998
Al	200	7.4E-07	1,000	<1E-30	1,000	4.5E-28	1,000	1.7E-06	1,000	<1E-30	1,000	1.4E-15	1,000
As	10	2.0E-06	1,000	<1E-30	1,000	6.4E-16	1,000	1.9E-06	1,000	1.4E-24	1,000	1.0E-10	1,000
B	NA	7.1E+01	86	2.1E+00	572	3.0E+00	170	3.7E+01	150	1.6E+00	586	3.1E+00	180
Ba	2,000	9.7E-03	866	2.0E-12	1,000	3.0E-05	1,000	3.5E-03	856	4.4E-09	1,000	9.8E-04	1,000
Cd	5	1.1E-02	886	4.9E-12	1,000	1.1E-04	1,000	6.6E-03	1,000	5.1E-09	1,000	2.7E-03	1,000
Cl	250,000	7.8E-01	548	3.2E-01	926	3.2E-01	926	3.0E-01	572	1.7E-01	1,000	1.8E-01	1,000
Co	NA	4.7E-05	1,000	2.6E-22	1,000	1.2E-10	1,000	2.9E-05	1,000	5.0E-17	1,000	7.7E-08	1,000
Cr	100	3.2E-08	1,000	<1E-30	1,000	4.0E-26	1,000	1.8E-07	1,000	<1E-30	1,000	1.8E-16	1,000
Cu	1,300	3.9E-04	1,000	8.0E-24	1,000	2.0E-10	1,000	3.7E-04	1,000	1.5E-17	1,000	2.8E-07	1,000
F	4,000	1.9E-01	534	1.7E-01	572	1.7E-01	572	2.3E-01	534	1.3E-01	586	1.5E-01	580
Fe	300	2.7E-03	1,000	<1E-30	1,000	5.7E-16	1,000	2.9E-03	1,000	2.3E-26	1,000	9.2E-09	1,000
Hg	2	1.6E-06	1,000	<1E-30	1,000	1.5E-25	1,000	2.9E-06	1,000	<1E-30	1,000	2.1E-14	1,000
I	NA	1.3E-02	534	1.0E-02	662	1.0E-02	662	8.6E-03	532	6.3E-03	704	7.0E-03	690
Mn	50	1.8E-01	860	2.8E-11	1,000	2.9E-04	1,000	6.5E-02	850	8.3E-08	1,000	9.7E-03	1,000
Mo	NA	2.2E-07	1,000	<1E-30	1,000	2.4E-27	1,000	5.2E-07	1,000	<1E-30	1,000	1.2E-15	1,000
N	10,000	1.3E+01	532	1.2E+01	572	1.2E+01	572	1.6E+01	534	9.4E+00	586	1.1E+01	580
Ni	N/A	1.4E-01	684	1.4E-05	1,000	2.1E-02	1,000	7.5E-02	836	1.4E-05	1,000	5.0E-02	902
Pb	15	6.5E-09	1,000	<1E-30	1,000	<1E-30	1,000	6.2E-09	1,000	<1E-30	1,000	2.2E-18	1,000
PO ₄	NA	1.7E+01	86	3.1E-01	572	1.1E+00	166	1.2E+01	152	2.4E-01	586	1.6E+00	176
Sb	6	4.7E-10	1,000	<1E-30	1,000	<1E-30	1,000	1.1E-09	1,000	<1E-30	1,000	6.6E-20	1,000
Se	50	3.3E-10	1,000	<1E-30	1,000	3.5E-30	1,000	7.6E-10	1,000	<1E-30	1,000	1.8E-18	1,000
SO ₄	250,000	8.8E+01	86	1.4E+00	172	5.1E+00	168	5.8E+01	154	7.4E-01	586	7.5E+00	176
Sr	NA	7.6E-03	640	4.7E-05	1,000	2.3E-03	1,000	4.2E-03	736	1.2E-06	982	2.7E-03	782
U	30	1.3E-05	1,000	<1E-30	1,000	5.1E-20	1,000	2.1E-05	1,000	<1E-30	1,000	8.7E-12	1,000
Zn	5,000	3.8E-03	894	1.6E-12	1,000	3.7E-05	1,000	2.2E-03	1,000	1.7E-09	1,000	9.0E-04	1,000

N/A Not Applicable

Table 6.1-5: Chemical 1-Meter Concentrations for UTRA-LZ

Constituent	(MCL) (µg/L)	Sector A		Sector B		Sector C		Sector D		Sector E		Sector F	
		(µg/L)	Year Peak Occurs										
Ag	100	5.6E-08	1,000	2.3E-09	1,000	2.4E-05	1,000	1.3E-03	1,000	8.1E-14	1,000	1.9E-06	1,000
Al	200	<1E-30	1,000	<1E-30	1,000	<1E-30	1,000	4.3E-28	1,000	<1E-30	1,000	<1E-30	1,000
As	10	7.5E-23	1,000	<1E-30	1,000	9.4E-23	1,000	3.3E-15	1,000	<1E-30	1,000	3.3E-29	1,000
B	NA	8.4E+01	100	2.3E+01	214	2.8E+01	196	2.9E+01	180	4.1E-01	630	4.3E+00	202
Ba	2,000	8.1E-10	1,000	1.9E-12	1,000	6.1E-07	1,000	4.1E-04	1,000	1.2E-16	1,000	5.0E-09	1,000
Cd	5	2.8E-09	1,000	2.4E-12	1,000	1.9E-06	1,000	1.2E-03	1,000	1.4E-16	1,000	3.4E-08	1,000
Cl	250,000	3.1E-01	798	1.8E-01	932	2.1E-01	662	2.3E-01	648	3.7E-03	1,000	9.4E-02	1,000
Co	NA	1.2E-16	1,000	1.8E-23	1,000	5.5E-15	1,000	9.4E-10	1,000	8.1E-28	1,000	2.4E-19	1,000
Cr	100	<1E-30	1,000	<1E-30	1,000	<1E-30	1,000	4.8E-28	1,000	<1E-30	1,000	<1E-30	1,000
Cu	1,300	1.1E-16	1,000	2.2E-25	1,000	2.0E-15	1,000	1.5E-09	1,000	5.3E-29	1,000	3.0E-20	1,000
F	4,000	1.4E-01	568	8.7E-02	604	1.0E-01	544	1.2E-01	542	3.3E-02	630	1.1E-01	606
Fe	300	1.5E-23	1,000	<1E-30	1,000	8.4E-26	1,000	2.2E-15	1,000	<1E-30	1,000	<1E-30	1,000
Hg	2	<1E-30	1,000	<1E-30	1,000	<1E-30	1,000	2.5E-25	1,000	<1E-30	1,000	<1E-30	1,000
I	NA	7.9E-03	632	4.9E-03	738	5.0E-03	588	5.2E-03	580	1.6E-03	810	5.3E-03	758
Mn	50	7.9E-09	1,000	3.6E-11	1,000	6.4E-06	1,000	4.0E-03	1,000	2.3E-15	1,000	4.3E-08	1,000
Mo	NA	<1E-30	1,000	<1E-30	1,000	<1E-30	1,000	2.8E-27	1,000	<1E-30	1,000	<1E-30	1,000
N	10,000	9.9E+00	568	6.2E+00	604	7.3E+00	544	8.4E+00	542	2.4E+00	630	7.6E+00	606
Ni	N/A	3.5E-05	1,000	9.9E-06	1,000	7.5E-03	1,000	2.8E-02	908	2.7E-10	1,000	3.2E-04	1,000
Pb	15	<1E-30	1,000										
PO ₄	NA	2.1E+01	102	9.6E+00	214	1.2E+01	196	1.2E+01	188	6.0E-02	630	2.3E+00	198
Sb	6	<1E-30	1,000										
Se	50	<1E-30	1,000	<1E-30	1,000	<1E-30	1,000	4.0E-30	1,000	<1E-30	1,000	<1E-30	1,000
SO ₄	250,000	1.1E+02	102	4.6E+01	214	5.6E+01	196	5.5E+01	192	1.9E-01	630	1.1E+01	198
Sr	NA	5.2E-05	1,000	3.5E-05	1,000	1.8E-03	1,000	2.3E-03	1,000	5.1E-10	1,000	2.3E-05	912
U	30	5.9E-28	1,000	<1E-30	1,000	<1E-30	1,000	1.4E-19	1,000	<1E-30	1,000	<1E-30	1,000
Zn	5,000	9.2E-10	1,000	7.9E-13	1,000	6.5E-07	1,000	4.1E-04	1,000	4.6E-17	1,000	1.1E-08	1,000

N/A Not Applicable

Table 6.1-6: Chemical 1-Meter Concentrations for Gordon Aquifer

Constituent	(MCL) (µg/L)	Sector A		Sector B		Sector C		Sector D		Sector E		Sector F	
		(µg/L)	Year Peak Occurs										
Ag	100	4.0E-16	1,000	1.1E-13	1,000	4.3E-13	1,000	6.6E-13	1,000	2.3E-28	1,000	3.3E-18	1,000
Al	200	<1E-30	1,000										
As	10	<1E-30	1,000										
B	NA	7.4E-02	348	8.2E-02	344	3.1E-02	316	6.3E-03	306	2.5E-07	696	1.2E-04	686
Ba	2,000	5.3E-20	1,000	1.6E-17	1,000	4.3E-16	1,000	1.2E-15	1,000	<1E-30	1,000	7.0E-23	1,000
Cd	5	7.8E-19	1,000	4.0E-16	1,000	1.6E-14	1,000	4.4E-14	1,000	<1E-30	1,000	5.9E-21	1,000
Cl	250,000	9.1E-06	1,000	1.3E-05	1,000	6.3E-06	1,000	1.2E-06	1,000	1.6E-12	1,000	4.4E-09	1,000
Co	NA	5.1E-30	1,000	1.1E-26	1,000	5.8E-24	1,000	4.2E-23	1,000	<1E-30	1,000	<1E-30	1,000
Cr	100	<1E-30	1,000										
Cu	1,300	<1E-30	1,000	6.2E-28	1,000	2.9E-24	1,000	4.3E-23	1,000	<1E-30	1,000	<1E-30	1,000
F	4,000	6.6E-05	638	8.2E-05	632	2.6E-05	612	6.6E-06	708	2.0E-08	696	1.0E-05	686
Fe	300	<1E-30	1,000										
Hg	2	<1E-30	1,000										
I	NA	2.3E-06	866	2.8E-06	848	8.9E-07	806	2.5E-07	1,000	6.4E-10	1,000	3.4E-07	1,000
Mn	50	2.6E-19	1,000	6.0E-17	1,000	1.1E-15	1,000	3.0E-15	1,000	<1E-30	1,000	1.3E-22	1,000
Mo	NA	<1E-30	1,000										
N	10,000	4.7E-03	638	5.8E-03	632	1.9E-03	612	4.7E-04	708	1.4E-06	696	7.1E-04	686
Ni	N/A	7.1E-13	1,000	8.6E-11	1,000	8.7E-11	1,000	9.5E-11	1,000	5.4E-24	1,000	5.4E-15	1,000
Pb	15	<1E-30	1,000										
PO ₄	NA	3.2E-02	344	3.5E-02	340	1.2E-02	316	2.5E-03	304	3.6E-08	696	3.9E-05	402
Sb	6	<1E-30	1,000										
Se	50	<1E-30	1,000										
SO ₄	250,000	1.5E-01	344	1.7E-01	338	6.0E-02	314	1.2E-02	304	1.1E-07	696	1.8E-04	400
Sr	NA	8.1E-12	1,000	2.0E-10	1,000	1.7E-10	1,000	1.2E-10	1,000	2.3E-22	1,000	1.4E-14	1,000
U	30	<1E-30	1,000										
Zn	5,000	2.6E-19	1,000	1.3E-16	1,000	5.4E-15	1,000	1.5E-14	1,000	<1E-30	1,000	2.0E-21	1,000

N/A Not Applicable

6.2 Acute Exposure Scenarios

The acute intruder exposure pathways are discussed in detail in Section 4.2.3.2. The acute exposure scenario is graphically represented in Figure 4.2-33. Provided below are the individual elements of the acute intruder biotic pathways that were identified for analysis and inclusion in the acute intruder scenario dose. The GoldSim computer code was used to calculate doses utilizing the dose formulas provided in this section. Unless otherwise noted, formulas were based on those used in LADTAP (WSRC-STI-2006-00123) or in the PA for INL tank farm (DOE-ID-10966). While these documents were used as guides for the other formulas, ultimately the bases for all the formulas can be traced to Regulatory Guide 1.109. Unit conversions are not explicitly stated in the equations, but are coded into GoldSim.

6.2.1 Acute Intruder Ingestion Dose Pathway - Ingestion of Re-Suspended Drill Cuttings

The drill cuttings ingestion exposure route assumes that a transfer line is penetrated during the installation of a drinking water well. The contamination inside the transfer line is mixed with the volume of the drill cuttings and brought to the surface. The radionuclide concentration in the drill cuttings is calculated using the following formula.

$$C_{SD} = \frac{C_{Xfer} \times d_w \times c_w}{\frac{d_w^2}{4} \times \pi \times l_w}$$

where:

- C_{SD} = concentration in soil due to drill cuttings (pCi/m³)
- C_{Xfer} = transfer line surface radionuclide concentration (pCi/ft²)
- d_w = well diameter (ft), Table 4.6-8
- c_w = transfer line circumference (ft), Table 4.6-8
- l_w = well depth (ft), Table 4.6-8

The receptor in turn is exposed by ingesting the drill cuttings during drilling activities. Only the exposure from the drill cuttings is included in this calculation (i.e., this does not include any other ingestion sources). The dose is calculated using the following formula.

$$D = \frac{C_{SD} \times F_{DC} \times U_D \times DCF}{\rho_{SS}}$$

where:

- D = dose from consumption of contaminated drill cuttings during drilling activities (rem)
- C_{SD} = concentration in soil due to drill cuttings, as defined above (pCi/m³)
- F_{DC} = fraction of time exposed to drill cuttings (unitless), Table 4.6-9

- U_D = human consumption rate of dirt (kg/yr), Table 4.6-9
 DCF = ingestion DCF (rem/ μ Ci), Table 4.7-1
 ρ_{SS} = density of sandy soil (g/cm³), Table 4.6-8

6.2.2 Acute Intruder Inhalation Dose Pathway - Inhalation of Drill Cuttings

The drill cuttings inhalation route assumes that a transfer line is penetrated during the installation of a drinking water well. The contamination inside the transfer line is mixed with the volume of the drill cuttings and brought to the surface. The receptor in turn is exposed by breathing dust from the drill cuttings during drilling activities. Only the exposure from the drill cuttings is included in this calculation (i.e., this does not include any other direct exposure sources). This formula was derived following the approach of the previous pathway calculations. The dose is calculated using the following formula.

$$D = \frac{C_{SD} \times F_{DC} \times DCF \times U_A \times L_{SiA}}{\rho_{SS}}$$

where:

- D = dose from inhalation of contaminated drill cuttings during drilling activities (rem)
 C_{SD} = concentration in soil due to drill cuttings, as defined in Section 6.2.1 (pCi/m³)
 F_{DC} = fraction of time exposed to drill cuttings (unitless), Table 4.6-9
 DCF = inhalation DCF (rem/ μ Ci), Table 4.7-1
 U_A = air intake (m³/yr), Table 4.6-9
 L_{SiA} = soil loading in air (kg/m³), Table 4.6-8
 ρ_{SS} = density of sandy soil (g/cm³), Table 4.6-8

6.2.3 Acute Intruder Direct Exposure Dose Pathways - Direct Exposure to Drill Cuttings

The drill cuttings direct exposure route assumes that a transfer line is penetrated during the installation of a drinking water well. The contamination inside the transfer line is mixed with the volume of the drill cuttings and brought to the surface. The receptor in turn is directly exposed to the drill cuttings during well drilling operations. Only the exposure from the drill cuttings is included in this calculation (i.e., this does not include any other direct exposure sources). This formula was derived following the approach of the previous pathway calculations. The dose is calculated using the following formula.

$$D = C_{SD} \times F_{DC} \times DCF$$

where:

D	=	dose from direct exposure to contaminated drill cuttings during drilling activities (rem)
C_{SD}	=	concentration in soil due to drill cuttings, as defined in Section 6.2.1 (pCi/m ³)
F_{DC}	=	fraction of time exposed to drill cuttings (unitless), Table 4.6-9
DCF	=	external DCF, 15 cm (rem/yr per $\mu\text{Ci}/\text{m}^3$), Table 4.7-1

6.3 Chronic Exposure Scenarios

The exposure pathways for the HTF Chronic Intruder Agricultural (Post-Drilling) Scenario are discussed in detail in Section 4.2.3.2. The chronic intruder scenario is graphically represented in Figure 4.2-34. Provided below are the individual elements of the chronic intruder biotic pathways that were identified for analysis and inclusion in the chronic intruder scenario dose. The GoldSim computer code was used to calculate doses utilizing the dose formulas provided below and utilizing the PORFLOW or GoldSim calculated 1-meter and seepage concentrations as inputs. Unless otherwise noted, formulas were based on those used in LADTAP (WSRC-STI-2006-00123) or in the PA for the INL tank farm facility. [DOE-ID-10966] While these documents were used as guides for the other formulas, ultimately the bases for all the formulas can be traced to Regulatory Guide 1.109.

The chronic intruder exposure pathways detailed below are used in calculating the dose to the chronic intruder receptor with the 1-meter well water as a primary water source defined as the concentration in the first modeled mesh location outside the facility boundary. The stream is the secondary water source for the pathways involving swimming, fishing/boating, and fish ingestion. The stream concentrations used in these dose calculations for the secondary water source pathways are the peak aquifer concentrations (as discussed in Section 5.2.3), and conservatively assume no stream dilution. Unit conversions are not explicitly stated in the equations, but are coded into GoldSim. All transfer times are assumed negligible due to the half-lives of the radionuclides and the long-term analysis of the PA.

6.3.1 Chronic Intruder Ingestion Dose Pathways

6.3.1.1 Ingestion of Water

The drinking water exposure route assumes the well used by the receptor is located 1-meter from the facility as a drinking water source. The incidental ingestion of water from showering and during recreational activities is assumed negligible when compared to ingestion of drinking water. The dose from consumption of drinking water is calculated using the following formula.

$$D = C_{GW} \times U_w \times DCF$$

where:

- D = dose from consumption of contaminated groundwater for 1 year (rem/yr)
 C_{GW} = radionuclide concentration in groundwater from the 1-meter well (pCi/L)
 U_W = human consumption rate of water (L/yr), Table 4.6-9
 DCF = ingestion DCF (rem/ μ Ci), Table 4.7-1

6.3.1.2 Ingestion of Beef and Milk

The beef and dairy exposure route assumes cattle drink contaminated stock water and eat fodder irrigated with contaminated water. The stock water and irrigation water is from the 1-meter well. The fodder is contaminated from direct deposition of contaminated irrigation water on plants and from deposition of contaminated irrigation water on soil followed by root uptake by plants. The buildup of radionuclide concentration in the soil from successive years of irrigation is accounted for. The radionuclide concentration in fodder from deposition and root uptake is calculated using the following formulas. Due to the relatively small volume of drill cuttings, their inventory is used for the vegetable ingestion pathway, as the impact will be more influential for the vegetable pathway than the beef and milk pathways.

$$C_f = C_{GW} \times I \times (LEAF + SOIL \times T_{SIV}) \times F_I$$

$$LEAF = \frac{r \times (1 - e^{-\lambda_e t_V})}{Y_V \times \lambda_e}$$

$$\lambda_e = \lambda_i + \lambda_w$$

$$SOIL = \frac{1 - e^{-\lambda_B t_b}}{\rho_S \times \lambda_B}$$

$$\lambda_L = \frac{P_R + I_R \times F_I - E_R}{S_D \times (S_M + \rho_{SS} \times K_d)}$$

$$\lambda_B = \lambda_i + \lambda_L$$

where:

- C_f = radionuclide concentration in fodder (pCi/kg)
 C_{GW} = radionuclide concentration in groundwater from the 1-meter well (pCi/L)
 I = irrigation rate (L/m²-d), Table 4.6-8
 $LEAF$ = radionuclide deposition and retention rate on the vegetation's leaves (m²d/kg)
 $SOIL$ = radionuclide deposition and buildup rate in the soil (m²d/kg)
 T_{SIV} = soil to vegetation ratio (unitless), Table 4.6-1

F_I	=	fraction of the time vegetation is irrigated (unitless), Table 4.6-8
r	=	fraction of material deposited on leaves that is retained (unitless), Table 4.6-8
λ_e	=	weathering and radiological decay constant (1/d)
t_V	=	time vegetation is exposed to irrigation (d), Table 4.6-7
Y_V	=	vegetation production yield (kg/m ²), Table 4.6-7
λ_i	=	radiological decay constant (1/d) [ln2/half-life of radionuclide i]
λ_w	=	weathering decay constant (1/d), Table 4.6-8
λ_B	=	soil buildup rate (1/d)
t_b	=	buildup time of radionuclides in soil (d), Table 4.6-7
ρ_S	=	areal surface density of soil (kg/m ²), Table 4.6-8
λ_L	=	soil retention rate (1/d)
P_R	=	precipitation rate (in/yr), Table 4.6-8
I_R	=	irrigation rate (in/yr), Table 4.6-8
E_R	=	evapotranspiration rate (in/yr), Table 4.6-8
S_D	=	depth of garden (cm), Table 4.6-8
S_M	=	soil moisture content (unitless), Table 4.6-8
ρ_{SS}	=	density of sandy soil (g/cm ³), Table 4.2-39
K_d	=	distribution coefficient (mL/g), Table 4.2-25

Following the cattle consumption of the contaminated water and fodder, the receptor consumes the contaminated beef and milk from the cattle. Beef and milk are treated separately. The dose is calculated using the following formulas.

Beef:

$$D = T_B \times (FF_B \times C_f \times Q_{FB} + C_{GW} \times Q_{WB}) \times DCF \times U_B \times F_B$$

Milk:

$$D = T_M \times (FF_M \times C_f \times Q_{FM} + C_{GW} \times Q_{WM}) \times DCF \times U_M \times F_M$$

where:

D	=	dose from consumption of contaminated beef or milk for 1 year (rem/yr)
T_B	=	beef transfer coefficient (d/kg), Table 4.6-3
T_M	=	milk transfer coefficient (d/L), Table 4.6-2
FF_i	=	beef or milk cattle intake fraction from irrigated field/pasture (unitless), Table 4.6-9
C_f	=	radionuclide concentration in fodder, as defined above (pCi/kg)

Q_{Fi}	=	consumption rate of fodder by beef or milk cattle (kg/d), Table 4.6-9
C_{GW}	=	radionuclide concentration in groundwater from the 1-meter well (pCi/L)
Q_{Wi}	=	consumption rate of water by beef or milk cattle (L/d), Table 4.6-9
DCF	=	ingestion DCF (rem/ μ Ci), Table 4.7-1
U_B	=	human consumption rate of beef (kg/yr), Table 4.6-9
U_M	=	human consumption rate of milk (L/yr), Table 4.6-9
F_B	=	fraction of beef produced locally (unitless), Table 4.6-7
F_M	=	fraction of milk produced locally (unitless), Table 4.6-7

6.3.1.3 Ingestion of Vegetables

The dose to humans from ingestion of contaminated leafy vegetables and produce is calculated assuming three contamination routes, 1) direct deposition of contaminated irrigation water on plants, 2) deposition of contaminated irrigation water on soil followed by root uptake by plants, and 3) deposition of contaminated drill cuttings in the garden followed by root uptake by plants. The irrigation water is from the 1-meter well. The contaminated drill cuttings are assumed to be from a transfer line that is penetrated during the installation of a drinking water well. The contamination inside the transfer line is mixed with the volume of the drill cuttings and brought to the surface. The drill cuttings are then mixed in the volume of the garden. The radionuclide concentration in the garden soil from the deposition of drill cuttings is calculated using the following formula.

$$C_{SD} = \frac{C_{Xfer} \times d_w \times c_w}{A_g \times S_D \times \rho_{SS}}$$

where:

C_{SD}	=	concentration in soil due to drill cuttings (pCi/m ³)
C_{Xfer}	=	transfer line surface radionuclide concentration (pCi/ft ²)
d_w	=	well diameter (ft), Table 4.6-8
c_w	=	transfer line circumference (ft), Table 4.6-8
A_g	=	area of garden (m ²), Table 4.6-8
S_D	=	depth of garden (cm), Table 4.6-8
ρ_{SS}	=	density of sandy soil (g/cm ³), Table 4.6-8

The receptor in turn consumes the contaminated vegetables. The consumption of leafy vegetables and produce are treated separately. The dose is calculated using the following formulas.

$$D_{IV} = D_{GW} + D_{DC}$$

$$D_{GW} = C_{GW} \times I \times (LEAF + SOIL \times T_{SV}) \times DCF \times (U_{LV} \times k + U_{OV}) \times F_V \times F_I$$

$$D_{DC} = C_{SD} \times T_{SV} \times DCF \times (U_{LV} \times k + U_{OV}) \times F_V$$

where:

D_{IV}	=	dose from consumption of contaminated vegetables for 1 year (rem/yr)
D_{GW}	=	dose from consumption of contaminated vegetables associated with using contaminated well water for 1 year (rem/yr)
D_{DC}	=	dose from consumption of contaminated vegetables associated with drill cuttings in the garden soil for 1 year (rem/yr)
C_{GW}	=	radionuclide concentration in groundwater from the 1-meter well (pCi/L)
I	=	irrigation rate (L/m ² -d), Table 4.6-8
$LEAF$	=	radionuclide deposition and retention rate on the vegetable's leaves, as defined in Section 6.3.1.2 (m ² d/kg)
$SOIL$	=	radionuclide deposition and buildup rate in the soil, as defined in Section 6.3.1.2 (m ² d/kg)
T_{StV}	=	soil to vegetable ratio (unitless), Table 4.6-1
DCF	=	ingestion DCF (rem/μCi), Table 4.7-1
U_{LV}	=	human consumption rate of leafy vegetables (kg/yr), Table 4.6-9
U_{OV}	=	human consumption rate of other vegetables (produce) (kg/yr), Table 4.6-9
k	=	fraction of material deposited on leaves that is retained after washing (unitless), Table 4.6-8
F_V	=	fraction of leafy vegetables and produce produced locally (unitless), Table 4.6-7
F_I	=	fraction of time vegetables are irrigated (unitless), Table 4.6-8
C_{SD}	=	concentration in soil due to drill cuttings (pCi/m ³), as defined above

6.3.1.4 Ingestion of Fish

The fish exposure route assumes fish are caught from a stream contaminated from the aquifer, and the receptor in turn consumes the contaminated fish. The dose is calculated using the following formula.

$$D = C_{SW} \times U_F \times T_F \times DCF$$

where:

D	=	dose from consumption of contaminated fish for 1 year (rem/yr)
C_{SW}	=	radionuclide concentration in water from the stream (undiluted aquifer) (pCi/L)

- U_F = human consumption rate of finfish (kg/yr), Table 4.6-9
 T_F = fish bioaccumulation factor (L/kg), Table 4.6-4
 DCF = ingestion DCF (rem/ μ Ci) Table 4.7-1

6.3.1.5 Ingestion of Soil

The soil ingestion exposure route assumes soil is contaminated from two contamination routes, 1) the soil is irrigated with groundwater from the 1-meter well and 2) deposition of contaminated drill cuttings in the garden soil. The contaminated drill cuttings are assumed to be from a transfer line that is penetrated during the installation of a drinking water well. The contamination inside the transfer line is mixed with the volume of the drill cuttings and brought to the surface. The drill cuttings are then mixed in the volume of the garden. The formulas were derived following the approach of the previous pathway calculations. A soil buildup factor was applied to the irrigation contamination route to account for the buildup of radionuclide concentration in the soil from successive years of irrigation. The radionuclide concentration in the soil from irrigation is calculated using the following formulas.

$$C_{SI} = C_{GW} \times I \times F_I \times SOIL$$

where:

- C_{SI} = radionuclide concentration in soil irrigated with water from the 1-meter well (pCi/m³)
 C_{GW} = radionuclide concentration in groundwater from the 1-meter well (pCi/L)
 I = irrigation rate (L/m²-d), Table 4.6-8
 F_I = fraction of the time soil is irrigated (unitless), Table 4.6-8
 $SOIL$ = radionuclide deposition and buildup rate in soil, as defined in Section 6.3.1.2 (m²d/kg)

The receptor consumes the contaminated soil. The dose from the ingestion of soil contaminated from both contamination routes is calculated using the following formula.

$$D = (C_{SD} + C_{SI}) \times DCF \times U_D$$

where:

- D = dose from consumption of contaminated soil for 1 year (rem/yr)
 C_{SD} = radionuclide concentration in soil contaminated with drill cuttings, as defined in Section 6.3.1.3 (pCi/kg)
 C_{SI} = radionuclide concentration in soil irrigated with water from the 1-meter well, as defined above (pCi/kg)
 DCF = ingestion DCF (rem/ μ Ci), Table 4.7-1
 U_D = human consumption rate of dirt (kg/yr), Table 4.6-9

6.3.1.6 Ingestion of Poultry and Eggs

The poultry and egg exposure route assumes poultry drink contaminated stock water and consume fodder irrigated with contaminated water. The stock water and irrigation water is from the 1-meter well. The fodder is contaminated from direct deposition of contaminated irrigation water on plants and from deposition of contaminated irrigation water in soil followed by root uptake by plants. Following the poultry consumption of the contaminated water and fodder, the receptor consumes the contaminated poultry and eggs. Poultry and eggs are treated separately. The concentration in fodder and the dose is calculated using the following formulas.

$$C_f = C_{GW} \times I \times (LEAF + SOIL \times T_{SIV}) \times F_I$$

Poultry:

$$D = T_P \times (FF_P \times C_f \times Q_{FP} + C_{GW} \times Q_{WP}) \times DCF \times U_P \times F_P$$

Eggs:

$$D = T_E \times (FF_P \times C_f \times Q_{FP} + C_{GW} \times Q_{WP}) \times DCF \times U_E \times F_E$$

where:

D	=	dose from consumption of contaminated poultry or eggs for 1 year (rem/yr)
C_f	=	radionuclide concentration in fodder (pCi/kg)
C_{GW}	=	radionuclide concentration in groundwater from the 1-meter well (pCi/L)
I	=	irrigation rate (L/m ² -d), Table 4.6-8
$LEAF$	=	radionuclide deposition and retention rate on the vegetation's leaves, as defined in Section 6.3.1.2 (m ² d/kg)
$SOIL$	=	radionuclide deposition and buildup rate in the soil, as defined in Section 6.3.1.2 (m ² d/kg)
T_{SIV}	=	soil to vegetation ratio (unitless), Table 4.6-1
F_I	=	fraction of the time vegetation is irrigated (unitless), Table 4.6-8
T_P	=	poultry transfer coefficient (d/kg), Table 4.6-5
T_E	=	egg transfer coefficient (d/kg), Table 4.6-6
FF_P	=	poultry or egg intake fraction from irrigated field/pasture (unitless), Table 4.6-9
Q_{FP}	=	consumption rate of fodder by poultry (kg/d), Table 4.6-9
Q_{WP}	=	consumption rate of water by poultry (L/d), Table 4.6-9
DCF	=	ingestion dose conversion factor (rem/μCi), Table 4.7-1

U_P	=	human consumption rate of poultry (kg/yr), Table 4.6-9
U_E	=	human consumption rate of eggs (kg/yr), Table 4.6-9
F_P	=	fraction of poultry produced locally (unitless), Table 4.6-7
F_E	=	fraction of eggs produced locally (unitless), Table 4.6-7

6.3.2 Chronic Intruder Direct Exposure Dose Pathways

6.3.2.1 Direct Exposure from Irrigated Soil

The irrigated soil direct exposure route assumes soil is contaminated from two contamination routes, 1) the soil is irrigated with groundwater from the 1-meter well and 2) deposition of contaminated drill cuttings in the garden soil. The receptor in turn is exposed during time spent caring for a garden. The contaminated drill cuttings are assumed to be from a transfer line that is penetrated during the installation of a drinking water well. The contamination inside the transfer line is mixed with the volume of the drill cuttings and brought to the surface. The drill cuttings are then mixed in the volume of the garden. The dose is calculated using the following formula.

$$D = (C_{SD} + C_{SI}) \times F_G \times DCF \times \rho_{SS}$$

where:

D	=	dose from direct exposure to contaminated soil for 1 year (rem/yr)
C_{SD}	=	radionuclide concentration in soil contaminated with drill cuttings, as defined in Section 6.3.1.3 (pCi/kg)
C_{SI}	=	radionuclide concentration in soil irrigated with water from the 1-meter well, as defined in Section 6.3.1.5 (pCi/kg)
F_G	=	fraction of time spent in garden (unitless), Table 4.6-9
DCF	=	external DCF, 15 centimeter (rem/yr per $\mu\text{Ci}/\text{m}^3$), Table 4.7-1
ρ_{SS}	=	density of sandy soil (g/cm^3), Table 4.6-8

6.3.2.2 Direct Exposure from Swimming

The swimming direct exposure route assumes the receptor receives dose from swimming in a stream contaminated from the aquifer. The dose is calculated using the following formula.

$$D = GF_S \times t_S \times C_{SW} \times DCF$$

where:

D	=	dose from direct exposure to contaminated stream water for 1 year (rem/yr)
GF_S	=	swimming geometry factor (unitless), Table 4.6-9
t_S	=	time per year spent swimming (hr/yr), Table 4.6-9

C_{SW} = radionuclide concentration in water from the stream (undiluted aquifer) (pCi/L)

DCF = external DCF, water immersion (rem/yr per $\mu\text{Ci}/\text{m}^3$), Table 4.7-1

6.3.2.3 *Direct Exposure from Fishing/Boating*

The fishing/boating direct exposure route assumes the receptor receives dose from fishing or boating in a stream contaminated from the aquifer. The dose is calculated using the following formula.

$$D = GF_B \times t_B \times C_{SW} \times DCF$$

where:

D = dose from direct exposure to contaminated stream water for 1 year (rem/yr)

GF_B = boating geometry factor (unitless), Table 4.6-9

t_B = time per year spent boating (hr/yr), Table 4.6-9

C_{SW} = radionuclide concentration in water from the stream (undiluted aquifer) (pCi/L)

DCF = external DCF, water immersion (rem/yr per $\mu\text{Ci}/\text{m}^3$), Table 4.7-1

6.3.3 Chronic Intruder Inhalation Dose Pathways

6.3.3.1 *Inhalation during Irrigation*

The irrigation inhalation exposure route assumes soil is irrigated with groundwater from the 1-meter well and the receptor in turn is exposed by breathing, while the garden is irrigated, but only during the time spent caring for a garden. This formula was derived following the approach of the previous pathway calculations. To account for the quantity of contaminants released into the air and available for inhalation, an Airborne Release Fraction (ARF) is included in the pathway formula. The ARF is conservatively assumed to be 1E-04 taken from DOE-HDBK-3010-94 and is used for all subsequent MOP water inhalation pathway calculations. The dose is calculated using the following formula.

$$D = \frac{C_{GW} \times DCF \times U_A \times F_G \times C_{WA} \times ARF}{\rho_w}$$

where:

D = dose from inhalation of contaminated groundwater in the air from irrigation for 1 year (rem/yr)

C_{GW} = radionuclide concentration in groundwater from the 1-meter well (pCi/L)

DCF = inhalation DCF (rem/ μCi), Table 4.7-1

U_A = air intake (m^3/yr), Table 4.6-9

- F_G = fraction of time spent in garden (unitless), Table 4.6-9
 C_{WA} = water contained in air at ambient conditions (g/m^3), Table 4.6-8
 ARF = airborne release fraction (unitless), Table 4.6-8
 ρ_w = water density (g/mL), Table 4.6-8

6.3.3.2 Inhalation while Showering

The showering inhalation exposure route assumes receptor is exposed by breathing humid air within the shower. The source of water for the shower is the 1-meter well. This pathway formula was derived following the approach of the previous pathway calculations. The dose is calculated using the following formula.

$$D = \frac{C_{GW} \times DCF \times U_A \times t_S \times C_{WS} \times ARF}{\rho_w}$$

where:

- D = dose from inhalation of contaminated groundwater while showering for 1 year (rem/yr)
 C_{GW} = radionuclide concentration in groundwater from the 1-meter well (pCi/L)
 DCF = inhalation DCF (rem/ μCi), Table 4.7-1
 U_A = air intake (m^3/yr), Table 4.6-9
 t_S = fraction of time spent in shower (unitless), Table 4.6-9
 C_{WS} = water contained in air at shower conditions (g/m^3), Table 4.6-8
 ARF = airborne release fraction (unitless), Table 4.6-8
 ρ_w = water density (g/ml), Table 4.6-8

6.3.3.3 Inhalation of Dust from Irrigated Soil

The irrigated soil inhalation exposure route assumes soil is contaminated from two contamination routes, 1) the soil is irrigated with groundwater from the 1-meter well and 2) deposition of contaminated drill cuttings in the garden soil. The receptor in turn is exposed by breathing dust during time spent caring for a garden. The contaminated drill cuttings are assumed to be from a transfer line that is penetrated during the installation of a drinking water well. The contamination inside the transfer line is mixed with the volume of the drill cuttings and brought to the surface. The drill cuttings are then mixed in the volume of the garden. This formula was derived following the approach of the previous pathway calculations. The dose is calculated using the following formula.

$$D = U_A \times L_{SiA} \times (C_{SD} + C_{SI}) \times DCF \times F_G$$

where:

- D = dose from inhalation of contaminated dust for 1 year (rem/yr)
 U_A = air intake (m³/yr), Table 4.6-9
 L_{SiA} = soil loading in air while working in a garden (kg/m³), Table 4.6-8
 C_{SD} = radionuclide concentration in soil contaminated with drill cuttings, as defined in Section 6.3.1.3 (pCi/kg)
 C_{SI} = radionuclide concentration in soil irrigated with water from the 1-meter well, as defined in Section 6.3.1.5 (pCi/kg)
 DCF = inhalation DCF (rem/μCi), Table 4.7-1
 F_G = fraction of time spent in garden (unitless), Table 4.6-9

6.3.3.4 Inhalation while Swimming

The swimming inhalation exposure route assumes a stream contaminated from the aquifer and the receptor inhales saturated air. This formula was derived following the approach of the previous pathway calculations. The dose is calculated using the following formula.

$$D = \frac{U_A \times GF_S \times t_S \times C_{SW} \times DCF \times C_{WA} \times ARF}{\rho_W}$$

where:

- D = dose from inhalation of contaminated stream water while swimming during 1 year (rem/yr)
 U_A = air intake (m³/yr), Table 4.6-9
 GF_S = swimming geometry factor (unitless), Table 4.6-9
 t_S = time per year spent swimming (hr/yr), Table 4.6-9
 C_{SW} = radionuclide concentration in water from the stream (undiluted aquifer) (pCi/L)
 DCF = inhalation DCF (rem/μCi), Table 4.7-1
 C_{WA} = water contained in air at ambient conditions (g/m³), Table 4.6-8
 ARF = airborne release fraction (unitless), Table 4.6-8
 ρ_W = water density (g/mL), Table 4.6-8

6.4 Inadvertent Intruder Analysis Results

The intruder doses are calculated using the pathway equations identified in Section 6.2 for the Acute Intruder Scenario and in Section 6.3 for the Chronic Intruder Agricultural (Post-Drilling) Scenario. For the Acute Intruder, doses are calculated assuming the Acute Intruder drills into a 3-inch diameter transfer line at any time after the 100-year period of institutional control following HTF closure. For the Chronic Intruder, annual doses are calculated assuming

contamination 1) from drill cuttings, 2) from the use of water obtained from a well representative of each of the six sectors (identified as Sectors 1A, 1B, 1C, 1D, 1E, and 1F in Figure 5.2-5), and 3) from the seepline for recreational activities. Refer to Table 4.4-19 for a listing of the contaminant source used in each biotic pathway.

The peak dose to the acute intruder in the 10,000-year performance period is 0.73 millirem at year 100. The peak is due almost exclusively from direct exposure to drill cuttings (Table 6.4-1). Unlike the chronic intruder, the Acute Intruder scenario does not include a groundwater contribution and therefore, does not vary by HTF Sector. Figure 6.4-1 presents the expected dose to the acute intruder during 10,000 years. Figure 6.4-2 illustrates the concentrations in the soil, as a function of time after HTF closure, for the radionuclides that contribute to the acute intruder dose shown in Table 6.4-1.

Figure 6.4-1: Acute Intruder Dose Results within 10,000 Years - Drilling into a 3-Inch Transfer Line

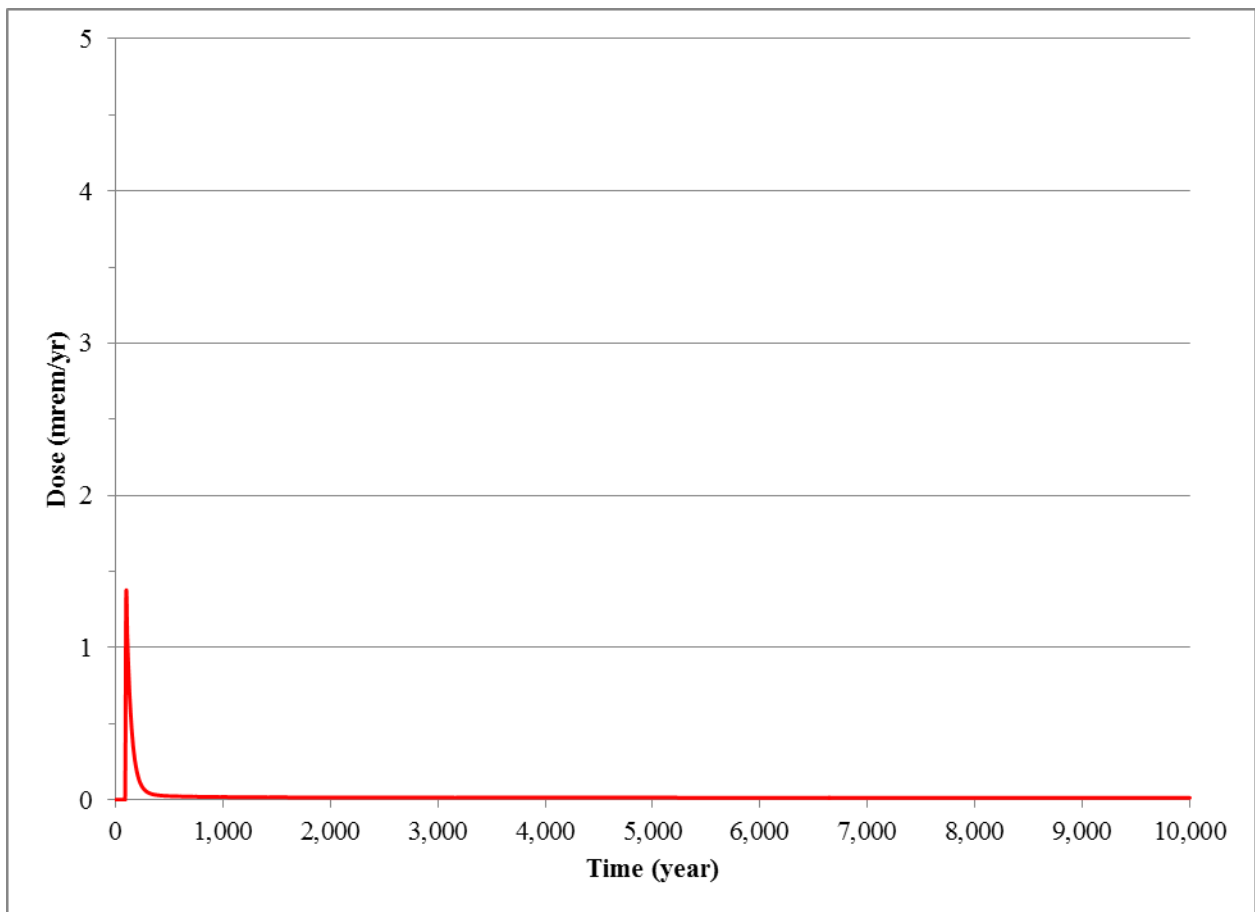


Figure 6.4-2: Concentration of Contributing Radionuclides in the Soil from Drill Cuttings

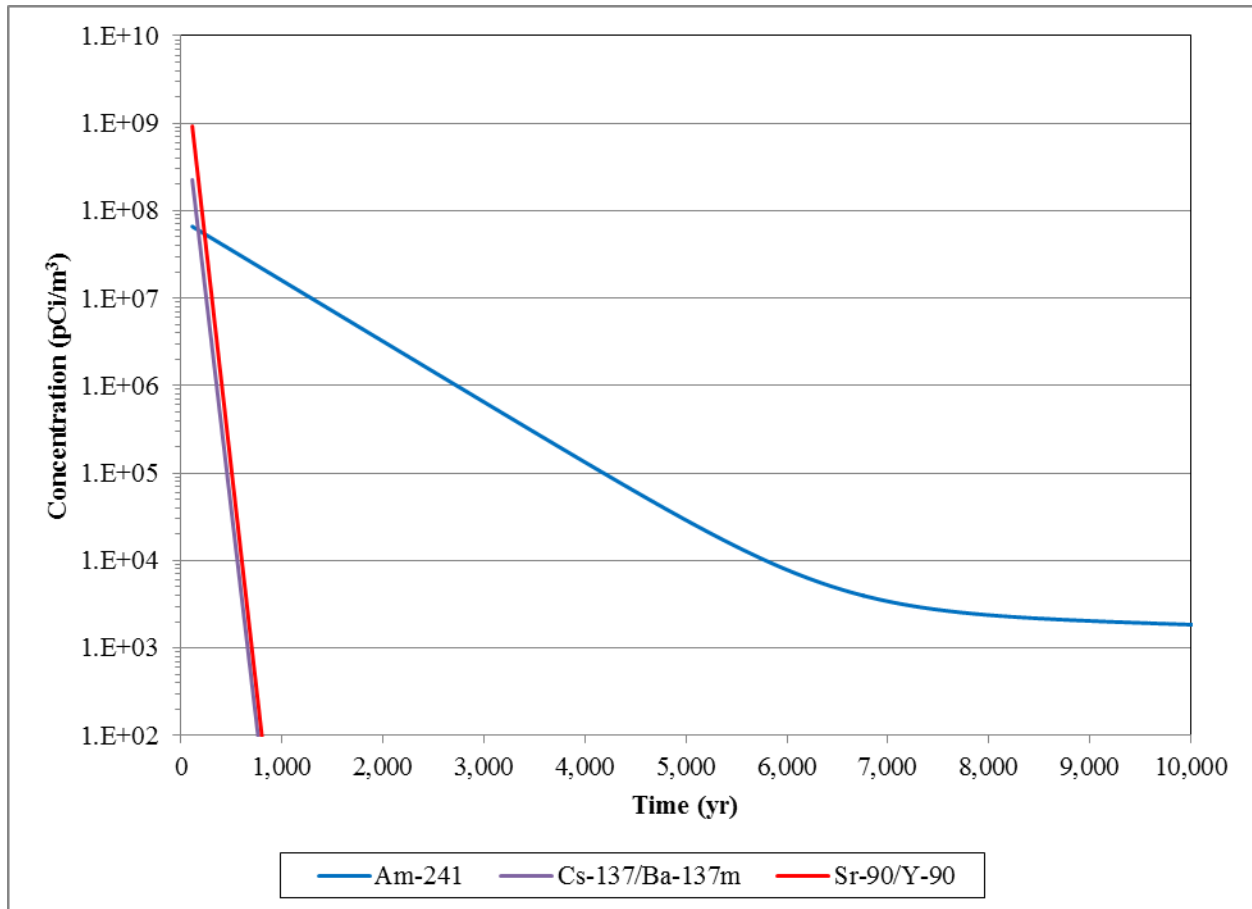


Table 6.4-1: Acute Intruder Dose Contributors

Acute Intruder Pathway Contributors	Peak Contribution (mrem)	Principal Radionuclide Pathway Dose (%)
Drill Cuttings Direct Exposure	1.3 (95 %)	Cs-137/Ba-137m (96 %) Sr-90/Y-90 (3 %)
Drill Cuttings Ingestion	0.022 (1.6 %)	Pu-238 (51 %) Sr-90/Y-90 (31 %)
Drill Cuttings Inhalation	0.044 (3.3 %)	Pu-238 (76 %) Am-241 (18 %)
Total	1.3 (100 %)	

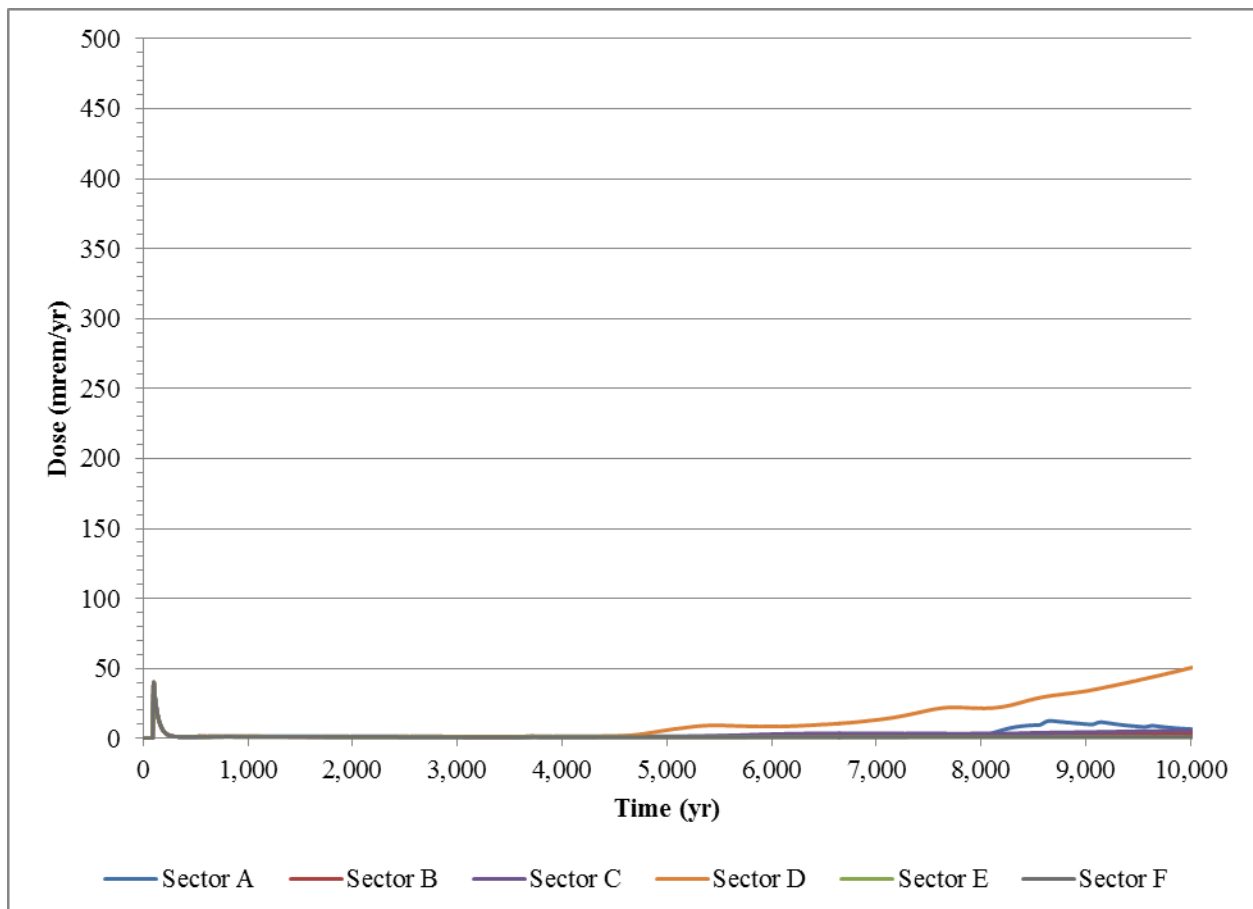
The initial inventories in the transfer lines, along with DCFs for the drill cuttings pathways and the radionuclide half-lives may be used to explain these results. Together, Sr-90/Y-90 and Cs-137/Ba-137m make up more than 80 % of the initial 3-inch transfer line, curie inventory. The DCF for Cs-137/Ba-137m ($4.4E+00 \text{ (cm}^3\text{/rem)} / (\mu\text{Ci/yr})$) is more than two orders of magnitude greater than the DCF for Sr-90/Y-90 ($3.9E-02 \text{ (cm}^3\text{/rem)} / (\mu\text{Ci/yr})$), resulting in a greater contribution to dose from Cs-137/Ba-137m. The half-lives for Cs-137 and Sr-90 are both about

30 years, indicating that these radionuclides would decay quickly and could only provide a significant dose contribution in an early intruder scenario.

The total expected dose to the chronic intruder is calculated for each of the six sectors using 1) soil concentrations contaminated with drill cuttings spread across the garden 2) water concentrations from a well located on the 1-meter perimeter of HTF that is shown in Figure 5.2-1, and 3) stream concentrations (e.g., seepline) (Section 6.3 and Table 4.4-20). The contributions to the peak dose are calculated using the highest concentration for each radionuclide in the sector (a discussion of how peak concentrations are determined by sector is provided in Section 6.1).

Figure 6.4-3 presents the annual dose to the chronic intruder for each of the six 1-meter sectors for a 10,000-year period after HTF facility closure. As shown in Figure 6.4-3, the dose to the chronic intruder is an initial peak following the end of institutional controls, the earliest an intruder could possibly access the site to drill inadvertently into a transfer line. For all sectors, the 100-year peak is the contribution from contaminated drill cuttings distributed across a garden. The dose gradually increases at the end of the 10,000 year time period. The releases contaminate groundwater that migrates into the 1-meter water well, and to the seepline. The contaminated water is then used according to the various biotic pathways to reach the receptor.

Figure 6.4-3: Annual Dose to Chronic Intruder - 10,000 Years after HTF Facility Closure



Note: Early peak is associated with all sectors.

Table 6.4-2 presents the significant biotic pathways contributing to peak dose within 10,000 years as well as the principal radionuclides. The peak dose for the chronic intruder scenario in a 10,000-year period is 50 mrem/yr, at year 10,000 in Sector D. The peak is primarily (74 %) from ingestion of water taken from a well in the area with soils contaminated with drill cuttings.

Table 6.4-2: Chronic Intruder Peak Dose Contributors - 10,000 Years after HTF Facility Closure

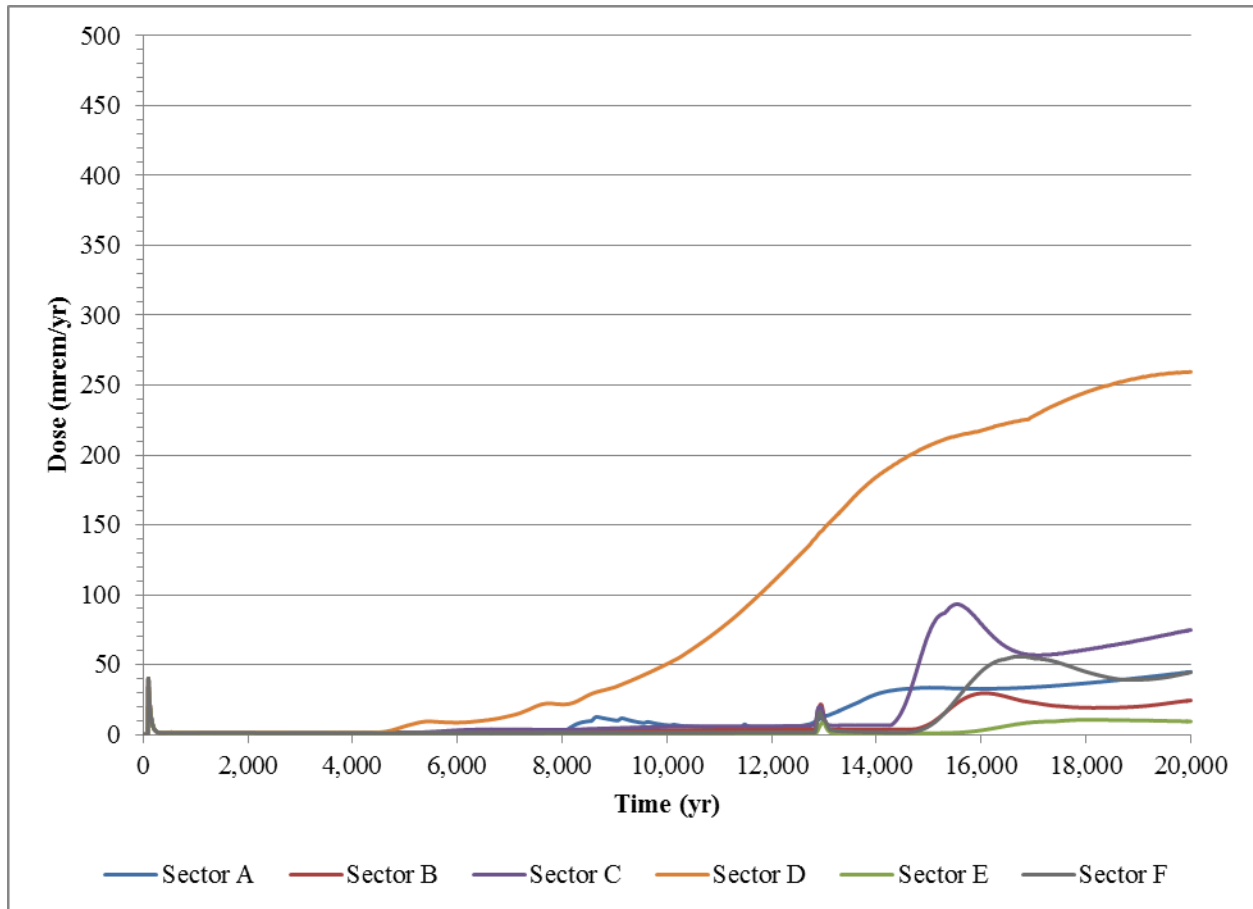
Chronic Intruder Pathway Contributors	Contribution to Peak (mrem/yr)	Principal Radionuclide Pathway Dose (%)
Water Ingestion	38 (74%)	Ra-226 (31 %) U-234 (29 %) U-233 (11 %)
Vegetable Ingestion	12 (23 %)	Ra-226 (28 %) U-234 (28 %) U-233 (11 %)
All others	1.1 (2.3 %)	N/A
TOTAL	50	

Note that the vegetable ingestion pathway is calculated as the sum of the vegetable uptake from contaminated 1-meter well water and the vegetable uptake from contaminated drill cuttings in the soil. Thus, the contaminated drill cuttings drive the early doses (as with the acute intruder scenario, discussed above).

Several conservatisms are incorporated into the Chronic Intruder analysis that should be acknowledged when evaluating the peak dose. The Chronic Intruder scenario assumes that the intruder drills into a transfer line immediately (e.g., 100 years) following the end of the 100-year institutional control period. When evaluating the early peak, it should be noted that almost the entire dose comes from the short-lived isotope, Sr-90/Y-90, even a relatively small delay in intruder drilling would result in a significant reduction in the peak dose (as evident in Figure 6.4-3). The likelihood of drilling through the closure cap, erosion barrier (described in Section 3.2.4) soon after the 100-year period of institutional control and active closure cap maintenance is very remote. No credit is taken for the uncertainty associated with drilling through the steel transfer line or, for some transfer line segments, the concrete encasement containing the transfer lines. Finally, the cross-sectional area of all of the transfer line segments is 74,000 ft² compared to the total HTF footprint of approximately 1,745,800 ft², so the opportunity for an intruder to drill into a transfer line exists for only about 4 % of the total area of HTF. [SRR-CWDA-2010-00023, Rev. 3, SRNL-STI-2010-00135] These assumptions suggest that the dose estimates for the Chronic and Acute Intruder are very conservative.

Figure 6.4-4 presents the calculated dose to the Chronic Intruder out to 20,000 years after closure.

Figure 6.4-4: Annual Dose to Chronic Intruder - 20,000 Years after HTF Facility Closure



Note: Early peak is associated with all sectors.

6.5 Inadvertent Intruder Uncertainty/Sensitivity Analyses

The purpose of this section is to consider the effects on the Inadvertent Human Intruder of uncertainties in the conceptual models used, and to evaluate sensitivities in the parameters used in the mathematical models. The intruder analyses consider both the acute intruder and the chronic intruder. Within the HTF GoldSim Model, the intruder is identified as the IHI.

The acute intruder receives an exposure solely from drill cuttings via direct external exposure, ingestion, and inhalation, as described in Section 6.2. The drill cuttings are based on the assumed inventory within a 3-inch diameter transfer line, uniformly distributed within HTF as described in Section 4.4.2.6.

The chronic intruder receives exposure from the various pathways described in Section 6.3. As discussed in Section 6.3, the chronic intruder receives the IHI dose after drilling a well through a 3-inch diameter line at the 1-m boundary of the HTF PA. In addition to well water, the intruder is assumed exposed to drill cuttings mixed into a garden.

Section 6.5.1 presents several deterministic sensitivity analyses evaluating the impact of varying the location, and respective inventory, of the potential intruder, drilling site. Specifically,

Section 6.5.1.1 evaluates the sensitivity of the peak intruder dose relative to using drill cuttings from drilling into a 4-inch transfer line. Section 6.5.1.2 evaluates the sensitivity of the peak intruder dose relative to using drill cuttings from drilling into a waste tank instead of a transfer line. Section 6.5.1.3 evaluates the sensitivity of the peak intruder dose to drawing water from wells drilled within the 1-meter boundary. By evaluating these end member cases in Sections 6.5.1.1, 6.5.1.2, and 6.5.1.3, a range of uncertainty in dose can be established.

Section 6.5.2 presents a probabilistic analysis of the chronic intruder dose within 10,000 years. This probabilistic analysis examines uncertainty and provides a summary of parameters that are significant to peak doses.

6.5.1 Intruder Single Parameter Deterministic Sensitivity Analysis

The purpose of this section is to present the dose sensitivity with respect to varying the location of the drilling intrusion. The drill cutting inventories were modified to show the impact this parameter had on both the chronic and acute IHI scenario results.

6.5.1.1 Impact of Drilling into a 4-inch Transfer Line vs. a 3-inch Transfer Line

To investigate the effect of an intruder drilling into 4-inch diameter transfer line versus a 3-inch diameter transfer line, the transfer line inventory for a 4-inch diameter line was substituted for the 3-inch diameter transfer-line inventory used in the Base Case modeling that is presented in Section 6.4. This scenario is not considered likely; as discussed in Section 4.2.3.2, only 0.24 % of the HTF transfer lines are 4-inch diameter lines. All other parameters from the chronic intruder scenario were held constant.

As presented in Figures 6.5-1 and 6.5-2, the inventory change (from the 3-inch diameter transfer-line inventory to the 4-inch diameter transfer-line inventory) has an impact on the magnitude of the peak dose that occurs at the time of the intrusion (100 years after system closure) for both the acute IHI and the chronic IHI doses. This point in time is assumed the earliest time after closure that drilling could affect a transfer line.

The acute IHI dose at 100 years from drilling through a 4-inch diameter transfer line is 2.6 mrem, which is approximately 2 times higher than the 100-year dose associated with drilling into a 3-inch diameter transfer line. Similarly, the chronic IHI dose at 100 years from drilling through a 4-inch diameter transfer line is 74 mrem/yr, which is approximately 2 times higher than the 100-year dose associated with drilling into a 3-inch diameter transfer line. Because of the rapid decay of the contributing radionuclides to dose attributed to the drill cuttings (as discussed in Section 6.4), the shape and the magnitude of the dose curves presented in Figures 6.5-1 and 6.5-2 are very similar to the Base Case presented in Section 6.4.

Figure 6.5-1: Acute Intruder Dose Impact from Drilling into a 4-inch Transfer Line vs. a 3-inch Transfer Line

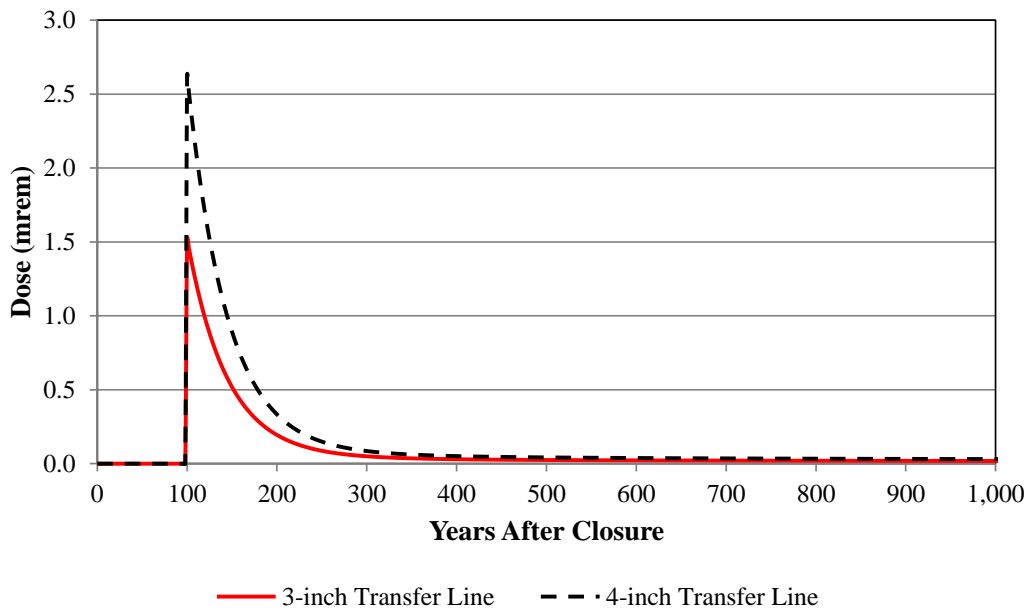
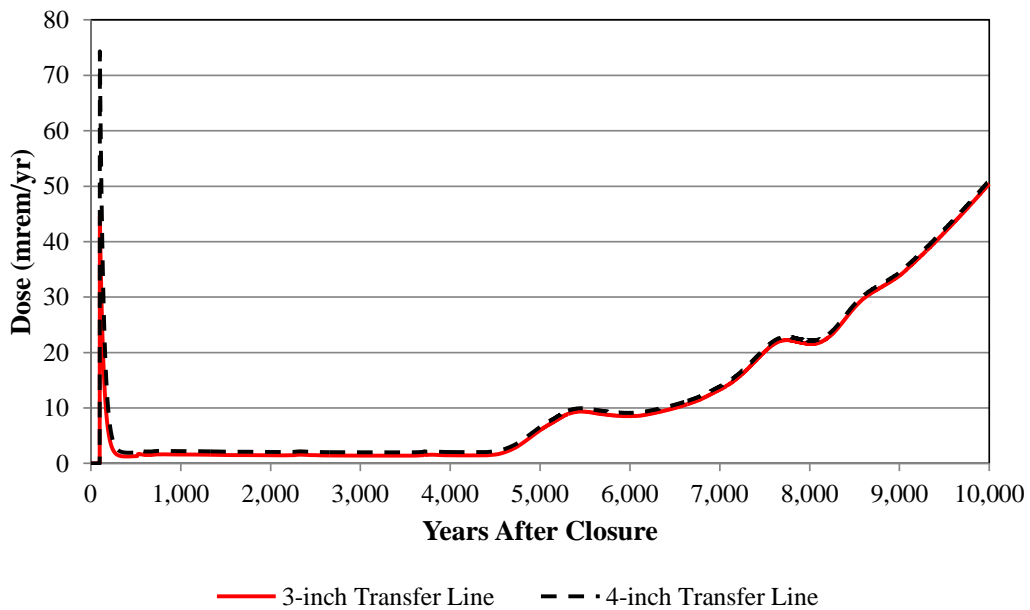


Figure 6.5-2: Chronic Intruder Dose Impact from Drilling into a 4-inch Transfer Line vs. a 3-inch Transfer Line



6.5.1.2 Impact of Drilling into a Waste Tank vs. a 3-inch Transfer Line

To investigate the effect of an intruder drilling into a waste tank, which is not considered a credible scenario (see Section 4.2.3.2), a conservative Tank 13 drill cutting inventory was substituted for the transfer line drilling inventory. Waste tank engineered barriers (e.g., closure cap erosion barrier, waste tank top concrete, and waste tank liner roof, etc.) are expected to prevent drilling directly into the waste tank inventory; therefore, this scenario was not considered to occur until at least 500 years after HTF closure. With the exception of the waste tank walls, all of the steel objects in the system will be encased by several feet of grout in the horizontal direction. All pumps, pipes, etc. that extend into the waste tank are suspended from the risers. The waste tanks are currently subject to a corrosion protection program that prevents corrosion of the walls by maintaining a high pH. [WSRC-TR-2002-00327] After placement of grout, the pH will remain high due to the properties of the grout. [WSRC-TR-97-0102] This will minimize the degradation effects on the carbon steel liner components and ensure the waste tank presents a credible drilling barrier, especially in the first 500 years. All other parameters from the IHI scenario were held constant during the sensitivity run.

As presented in Figures 6.5-3 and 6.5-4, the timing of the intrusion (100 years after HTF closure for the transfer line versus 500 years for the waste tank) for both the acute IHI and chronic IHI doses has an impact on the magnitude of the peak dose that occurs. The acute IHI dose at 500 years from drilling through Tank 13 is 14 mrem, which is approximately 9 times higher than the 100-year dose associated with drilling into a 3-inch diameter transfer line. Alternatively, the chronic IHI dose at 500 years from drilling through Tank 13 is 100 mrem/yr, or approximately 2 times higher than the 100-year dose associated with drilling into a 3-inch diameter transfer line. As with the 4-inch diameter transfer line comparison (in Section 6.5.1.1), the contributing radionuclides rapidly decay, reducing the effect of the dose attributed to the drill cuttings (as discussed in Section 6.4). However, unlike the transfer line comparison, the shape of the curve and the peaks at later years presented in Figures 6.5-3 and 6.5-4 are higher than the Base Case presented in Section 6.4 due to contributions from longer-lived radionuclides associated with the Tank 13 drill cutting inventory.

Figure 6.5-3: Acute Intruder Dose Impact from Drilling into Tank 13 vs. a 3-inch Transfer Line

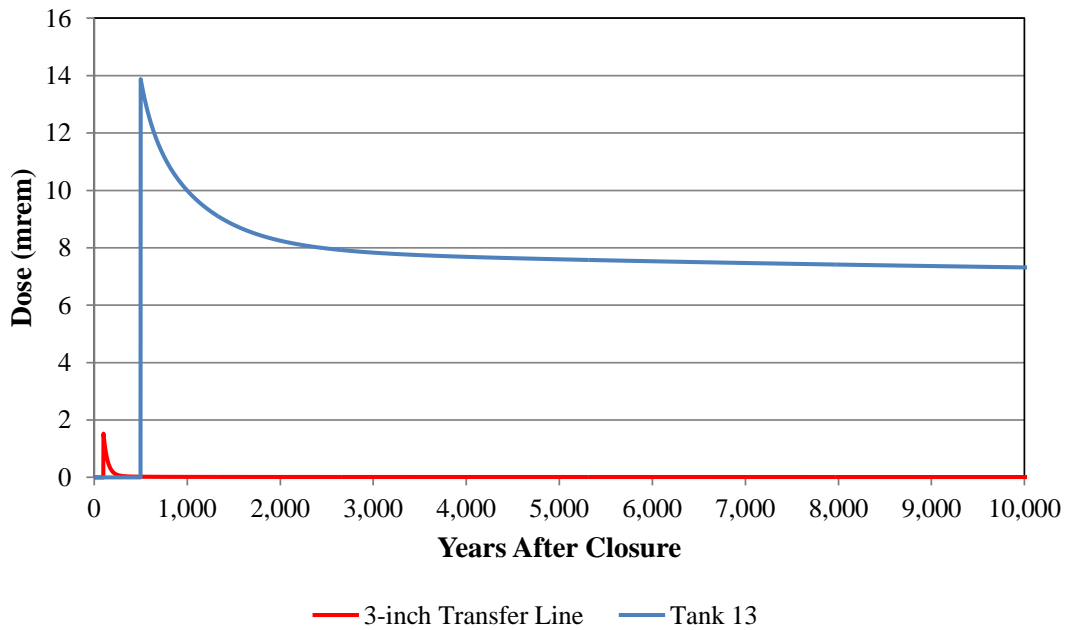
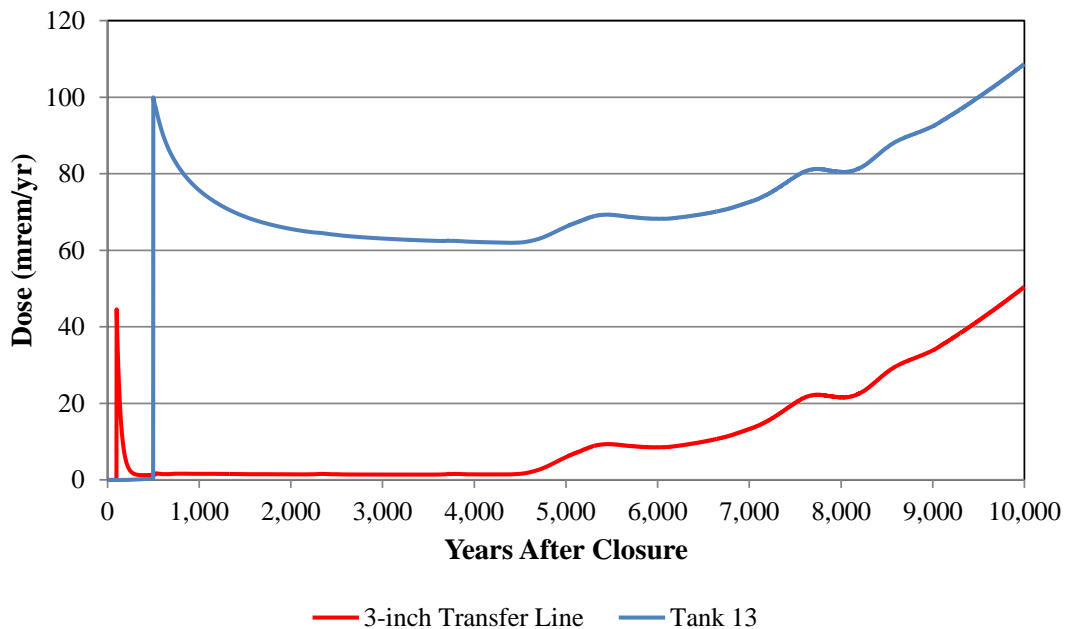


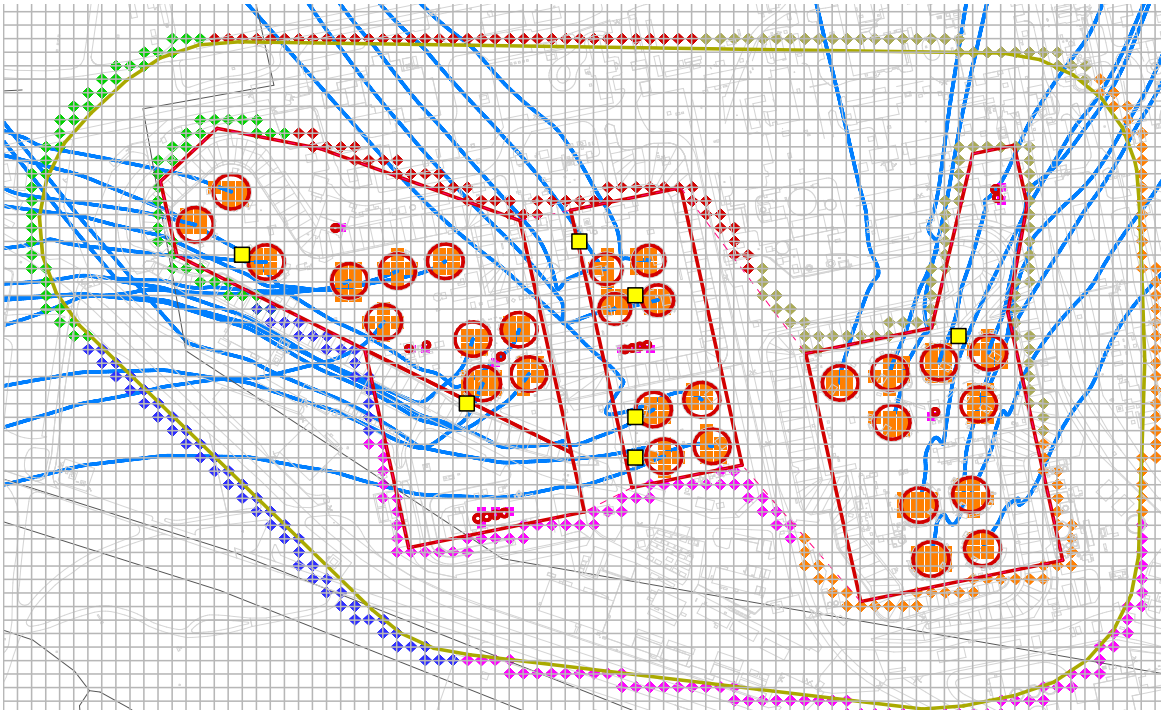
Figure 6.5-4: Chronic Intruder Dose Impact from Drilling into Tank 13 vs. a 3-inch Transfer Line



6.5.1.3 Impact of Drilling within 1-Meter Boundary Line

To investigate the effect of a chronic intruder drilling into locations between the waste tanks and the 1-meter boundary of the facility (see the red line in Figure 6.5-5), seven locations were selected for evaluation (see the yellow squares in Figure 6.5-5).

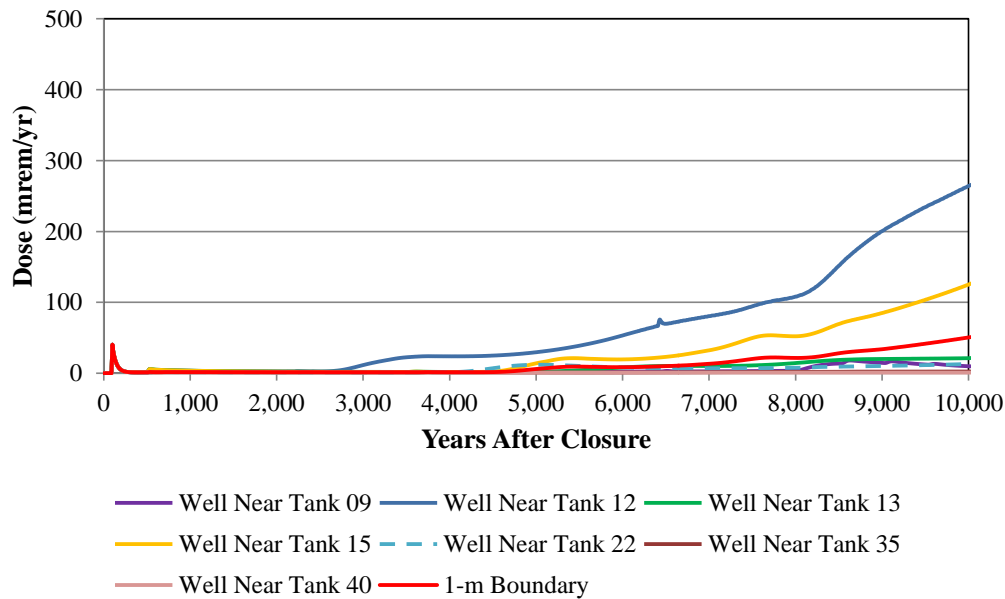
Figure 6.5-5: Hypothetical Drilling Locations within the 1-Meter Facility Boundary



Note The yellow squares indicate hypothetical drilling locations. The yellow square furthest to the left is near Tank 35, the next one is near Tank 22. The well locations near the middle of the tank farm are near Tanks 9, 12, 13, and 15 (from top to bottom). The yellow square furthest to the right is near Tank 40.

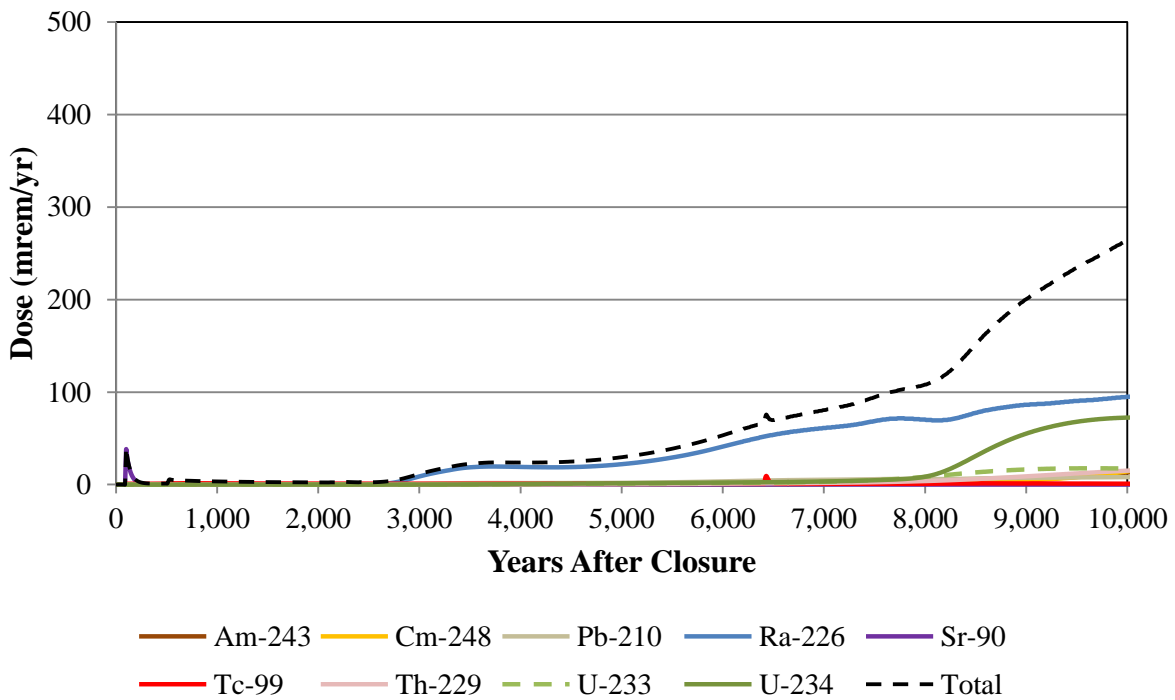
As presented in Figure 6.5-6, the drilling location does have an impact on the magnitude and the timing of the peak dose to the chronic intruder within a 10,000-year period, especially when drilling near tanks that are modeled with initially failed liners (i.e., Tank 12, shown in blue, and Tank 15, shown in yellow). The early dose at 100 years after closure (associated with an intrusion event) was 45 mrem/yr for all seven locations and is the same as in the Base Case presented in Section 6.4, associated with the maximum value at the 1-meter boundary, regardless of sector (shown in red in Figure 6.5-6). These early doses are the same because this early peak is driven by drill cuttings, which is not dependent upon water concentrations. The higher doses at later times from the wells near Tanks 12 (approximately 264 mrem/yr) and Tank 15 (approximately 125 mrem/yr) are generally higher due to the closer proximity to the contaminant sources, but are still below the 500 mrem/yr performance objective. For Tank 12, this dose is dominated by contributions from Ra-226, followed by U-234 and U-233 (see Figure 6.5-7). This is consistent with dose contributors from Tank 15 and the results from the 1-meter boundary.

Figure 6.5-6: Chronic Intruder Dose Results - Drilling into Select Locations within 1-Meter Facility Boundary



Note Early peak (at year 100) is associated with all wells, including the 1-meter boundary.

Figure 6.5-7: Chronic Intruder Dose Contributors for a Well Drilled within the 1-Meter Boundary, Near Tank 12



Note Figure only shows radionuclides with dose contributions of at least 5 mrem/yr within 10,000 years. Am-243, Cm-248, Pb-210, and Th-229 overlap at 10,000 years (with dose contributions of 8 to 15 mrem/yr).

6.5.2 Intruder Probabilistic Uncertainty Analysis

PORFLOW was used to develop the flow data for both the deterministic and probabilistic models at both the HTF 100-meter boundary and the 1-meter boundary. Due to complexities between the three-dimensional flow modeling in PORFLOW and the one-dimensional approach used in GoldSim, the GoldSim model overestimates the contaminant concentrations near the sources (i.e., waste tanks and ancillary equipment). This overestimation is attributed to a lack of sufficient horizontal spreading in the contaminant plume within GoldSim. [SRR-CWDA-2010-00093, Rev. 2] At the 100-meter boundary, the distance from the contaminant sources is large enough to allow sufficient mixing of contaminants within groundwater, which provides for the very similar results seen in the benchmarking analysis provided in Section 5.6. Near the contaminant sources, however, the plume remains overly concentrated along the centerline of the plume (see the solid blue lines in Figure 6.5-5).

Regardless of this known overestimation of concentration, the IHI model is based on releases from the HTF waste tanks and ancillary equipment, using the same parameters as in the MOP analysis. Thus, the uncertainty analysis conducted for the MOP related to waste tank release parameters is also applicable to the IHI model, tempered with the understanding that the dose values provided will be overly conservative.

Unlike the deterministic approach, which assumes a maximum concentration along the 1-meter boundary, the HTF GoldSim Model assumes that the chronic intruder uses water from a well directly adjacent to Tank 12. This location was selected based on the results from the analysis described in Section 6.5.1.3, above, which demonstrated that a well near Tank 12 showed the highest potential dose to an IHI. This location is within the 1-m boundary, near the plume centerline, and because Tank 12 is modeled as having an initially failed steel liner, the dose contribution is considered conservative relative to the IHI doses reported in Section 6.4.

The probabilistic HTF GoldSim Model was run for 1,000 realizations with the well adjacent to Tank 12 set as the site of the IHI well. The peak of the mean (at any time within the 10,000-year period of performance) of the IHI dose for the Base Case is 762 mrem/yr (see Figure 6.5-8). This dose compares to a median peak dose of 495 mrem/yr and illustrates that the mean is greater than the median indicating that a few realizations sampled at the tail of the parameter distributions can cause the mean to be high.

To provide insight into the degree of conservatism applied within the GoldSim model, relative to dose results for a well drilled adjacent to Tank 12, a deterministic GoldSim model was run. This model used the same parameter values and settings as the PORFLOW deterministic model (per Section 6.5.1.3). As shown in Figure 6.5-9, the deterministic GoldSim model (black, dashed curve) shows a peak dose of 735 mrem/yr within 10,000 years for a well adjacent to Tank 12. This is about 3 times higher than the deterministic PORFLOW result (264 mrem/yr). As described in Section 7.1.4 of the *H-Area Tank Farm Stochastic Fate and Transport Model* report, this increase is a function of the difference in the breakthrough times between PORFLOW and GoldSim associated with horizontal flow in the PORFLOW model that lengthens the path of contaminant flow. [SRR-CWDA-2010-00093, Rev. 2]

Figure 6.5-8: Probabilistic IHI Dose Results from a Well near Tank 12, within 1-Meter Boundary

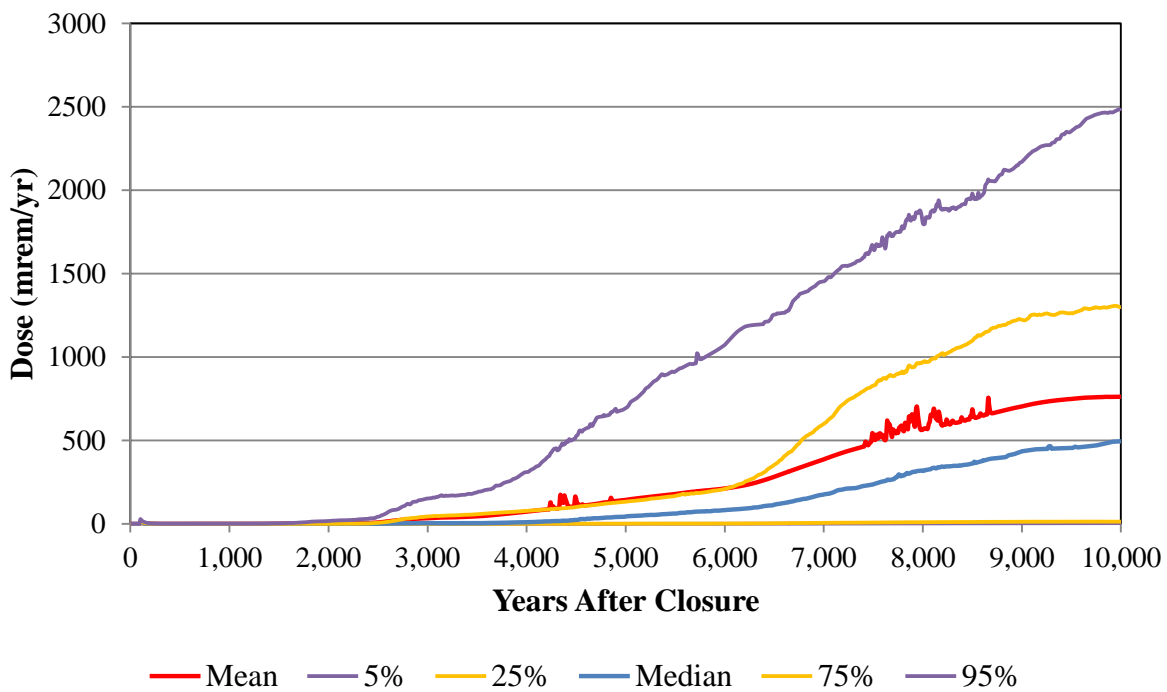
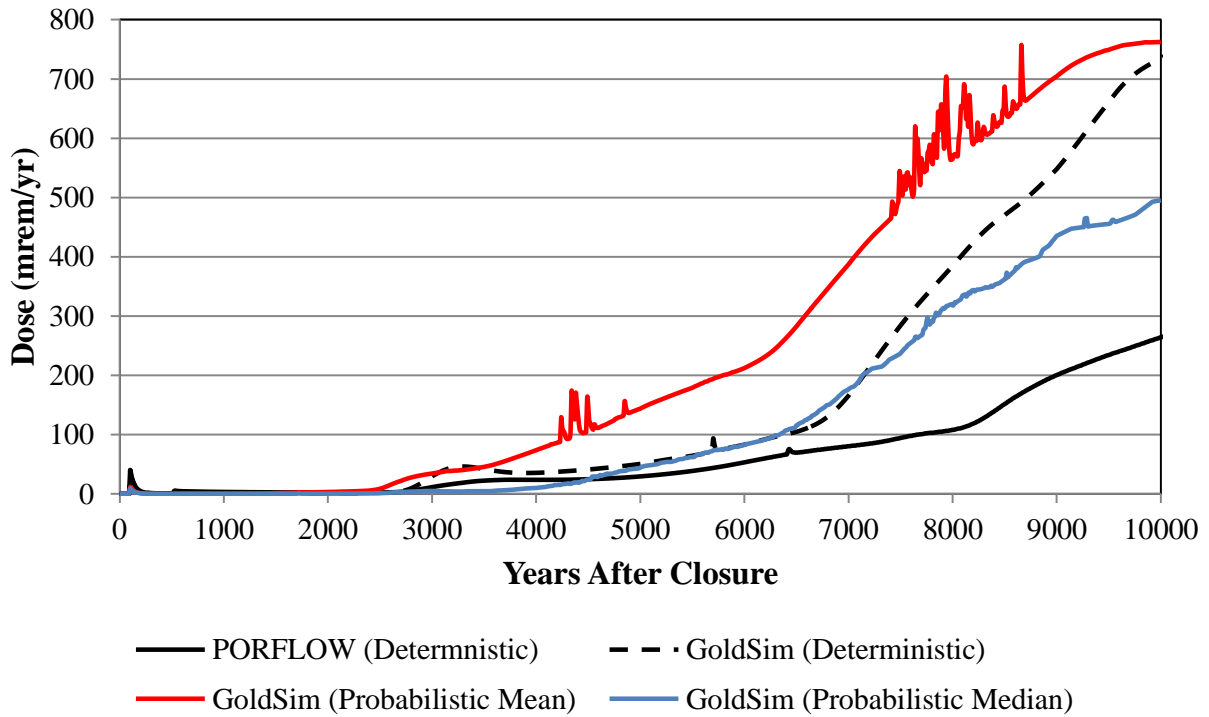


Figure 6.5-9: Comparison of Probabilistic Doses to Deterministic Doses from a Well near Tank 12, within 1-Meter Boundary



Regardless of this conservatism, results from the probabilistic model provide insights into parameter sensitivities within the system. An investigation of the uncertainty parameters revealed that many of the same parameters that influence the MOP dose also significantly influence the IHI dose. For example, the well completion stratum (the parameter that selects which aquifer water is drawn from for MOP and IHI use) and parameters related to release and doses of Tc-99 (e.g. Tc-99 inventory multiplier) are important to intruder dose.

7.0 INTERPRETATION OF RESULTS

Summary for Section 7.0

Section 7.1 summarizes the interpretation of results presented in Sections 5 and 6.

Section 7.2 summarizes the conservatisms used in modeling.

7.1 Performance Assessment Results

This section provides an interpretation of the results presented in Sections 5 and 6. Section 7.1.1 summarizes the behavior of each component within the integrated system. Section 7.1.2 summarizes the results of the 100-meter groundwater pathway dose and the dose at the stream. The airborne dose and the all-pathways dose results are summarized in Sections 7.1.3 and 7.1.4, respectively. The dose to the inadvertent acute and chronic intruder are discussed and summarized in Section 7.1.5. The radon flux is presented in Section 7.1.6. Section 7.2 describes the conservatisms used in modeling, and is organized according to system component.

7.1.1 Integrated System Behavior

Provided below is a short description of the impact that various segments of the ICM have on dose results (the segments are discussed in Section 4.4.3). Chemical and physical transition times discussed in this section are drawn from Tables 4.4-2 through 4.4-9. For the purpose of the following discussion, the Case-A groundwater total dose from Sector A, which is the sector that produces the peak dose within both 10,000 and 100,000 years, will be used to illuminate segment behaviors. The Case-A groundwater total dose is provided in Figure 7.1-1 along with contributions from individual radionuclides. This figure will be used in conjunction with Figure 7.1-2, which identifies the source of releases and certain modeled transition times, and Figure 7.1-3, which plots trends in parameter behavior for segments of the integrated system in order to highlight the system behavior.

Figure 7.1-1: Individual Radionuclide Contributors to Sector-A 100-Meter Peak Groundwater Pathway Dose, 10,000 Years, Base Case

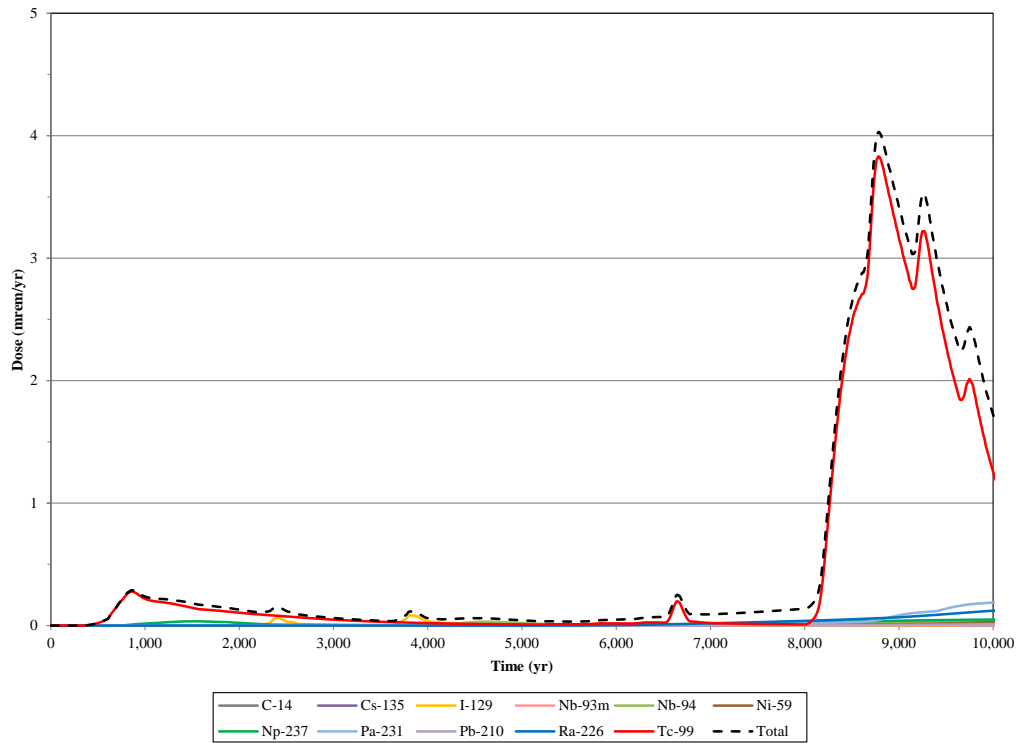


Figure 7.1-2: Individual Source Contributors to Sector-A 100-Meter Peak Groundwater Pathway Dose, 20,000 Years, Base Case

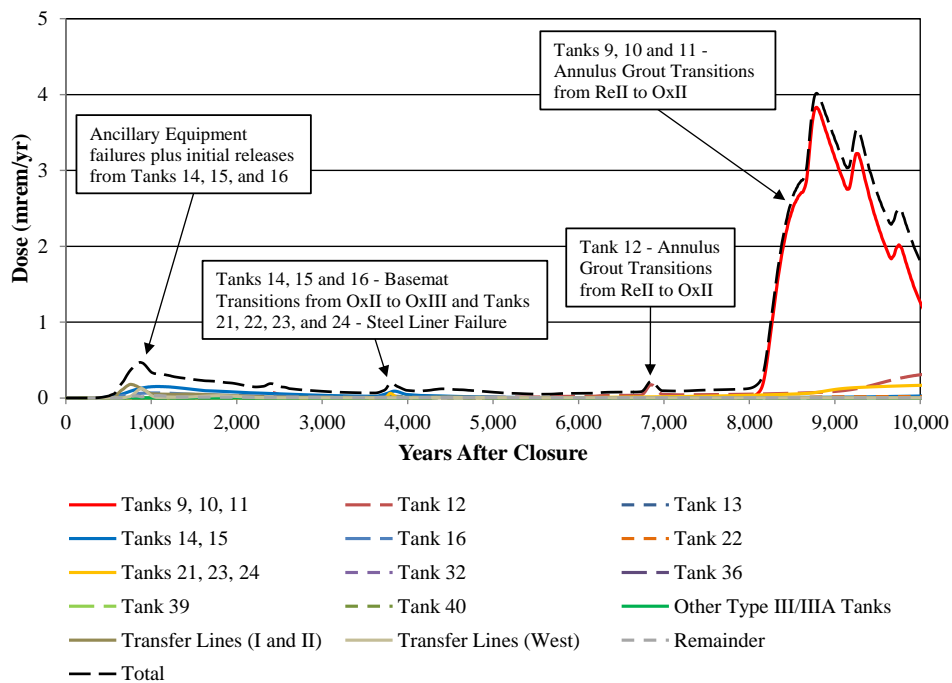
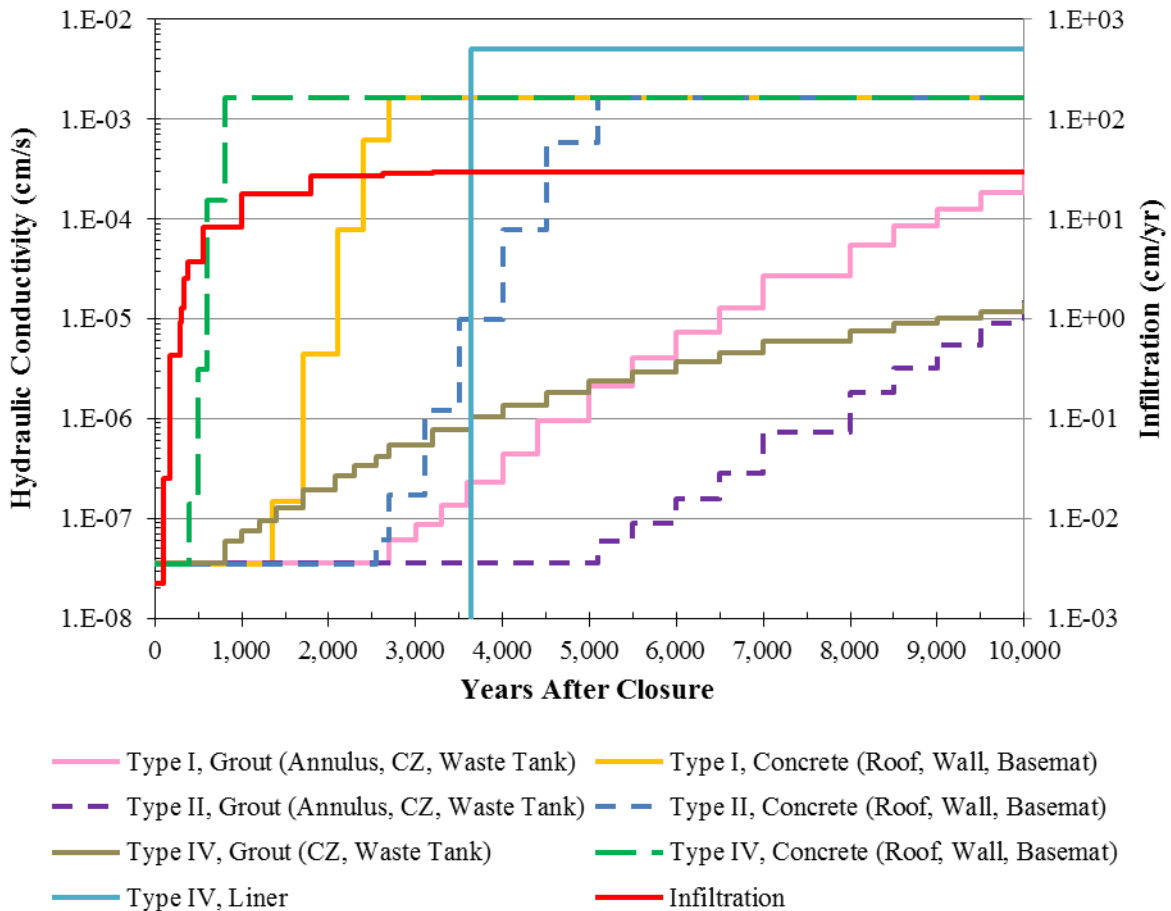


Figure 7.1-3: Model Input Timeline for Various HTF Model Segments



7.1.1.1 Closure Cap

Emplacement of a closure cap above HTF is intended to provide multiple protective features (e.g., erosion control, deterrent to inadvertent intruders), but its key role in the integrated system is to limit the amount of infiltrating water reaching the waste tanks and ancillary equipment. As illustrated in Figure 7.1-3, for the Base Case, infiltration through the closure cap reaches steady state, and nearly background infiltration levels, around 2,600 years (e.g., less than a 2 % increase in infiltration rate after 2,600 years). The closure cap's ability to effectively reduce the amount of infiltrating water to the waste tanks and ancillary equipment is essentially limited to the first 2,600 years after site closure.

The closure-cap barrier analysis (Section 5.6.6) demonstrates that increased infiltration from simulating removal of the closure cap can cause the peak flux in 10,000 years to occur earlier for some radionuclides. The closure cap is moderately effective as a barrier for those mobile radionuclides not greatly influenced by sorption onto oxidized cementitious material (e.g., Tc-99, Ra-226, and I-129). The overall impact of the closure cap on dose is greater for the slow-moving radionuclides, Pu-239 and Np-237. However, because these radionuclides take time to move through the system, the impact is only relevant later (> 5,000 years).

Plutonium and neptunium move slowly through the system due to high K_d values in cementitious materials.

7.1.1.2 Waste Tank Top

The timing of waste tank roof concrete degradation affects the flow rate into the waste tank. Early concrete degradation, as modeled in some alternate cases, allows the steady state flow values to be reached earlier, but does not appear to have as pronounced an impact on flow as other segments (e.g., liner failure, fast flow paths).

7.1.1.3 Waste Tank Liner Top

The entire liner is modeled as failing simultaneously therefore, isolated failure of the waste-tank roof liner is not discernible.

7.1.1.4 Waste Tank Grout

The waste tank grout is important for two reasons, the integrity of the grout prevents flow to the CZ, but it also acts as a sink to inventory. The upward diffusion of contaminants from the CZ builds up in the grout, resulting in further travel times to exit the waste tank. The reducing environment that exists early in the waste tank grout typically corresponds with less soluble waste forms, thereby slowing the movement of these contaminants (primarily Tc-99) out. However, upon transition to more oxidizing conditions (e.g., from Reducing Region II to Oxidizing Region II), the grout is no longer as effective in sorbing certain radionuclides, such as Tc-99, and a large release of Tc-99 ensues.

Additionally, the timing of grout degradation affects the flow rate to the CZ. Early grout degradation is modeled in alternate Cases B and D, enabling the steady state flow values to be reached earlier. Grout degradation can have different impacts depending upon whether the waste tank liner has failed. The grout degradation does not have an immediate impact on flow as other segments (e.g., liner failure). Because grout degradation occurs very slowly (see Figure 7.1-3, waste tank grout hydraulic conductivity) it can have a significant effect on dose in instances where the flow through the grout affects chemical transition times, especially for oxidation potential of sensitive radionuclides, like Tc-99.

7.1.1.5 Contamination Zone

The CZ modeling segment has a significant impact on dampening releases for solubility-controlled radionuclides, especially Tc-99. The modeled solubility limits control the release rate of contaminants from the CZ, and higher solubility limits lead to increased release rates. These radionuclides, most notably Tc-99, undergo precipitation when concentrations exceed the solubility limit in the CZ. The effect of solubility limits is radionuclide and chemical state dependent.

7.1.1.6 Tank Liner Sides and Floor

The waste tank liner sides and floor are very important to the integrated system because independent of all other waste tank components the liner most effectively limits mass transport from the waste tanks. In fact, for most waste tank types, releases to the natural environment do not occur unless the liner has failed, with the exception of Type II tanks which can have releases from the sand pads and annulus.

The effect of increased flow resulting from liner failure (see Figure 7.1-3) is earlier hydraulic degradation of material zones in the waste tanks, and earlier chemical transitions, which control the solubility and thus the release rates of certain radionuclides (e.g., Tc-99, Pu-239). However, in general, as discussed in Section 5.6, liner failure has little impact on the magnitude of the dose peak within 10,000 years, but instead controls the timing of the peak.

7.1.1.7 Basemat

Results from the alternate cases (Cases B, D, C, and E) provide some insight into the function of the basemat on overall dose (Section 5.6.7). Peak results do not differ significantly between Case B and D where the only difference is the existence of a fast flow path through the basemat in Case D. This suggests that unimpeded flow through a fast flow path, through the basemat (and the grout) does not, by itself significantly affect peak dose.

7.1.1.8 Waste Tank Annulus Grout and Sand Pads

Because liner integrity is so effective at preventing mass releases prior to liner failure, this makes the impact of the waste tank annulus grout and sand pads more relevant to the integrated system. Peak dose within 10,000 years is greatly controlled by releases from Type II tanks because they have inventory in the sand pads and annulus, which is not contained by the liners. In these waste tanks, inventory in the sand pads diffuse into the annulus adding to the inventory already in the annulus.

7.1.1.9 Vadose Zone beneath Waste Tank

The vadose zone beneath the waste tanks has a very similar radionuclide-specific effect to that of the basemat. The vadose zone depth can have a considerable affect if the vadose layer is thick or if the radionuclide in question has a high K_d in soil. Plutonium travel time in soil is slowed considerably due to plutonium's affinity to sorb to certain soils. Increasing the rate at which plutonium sorbs to soils, or increasing the thickness through which it must travel, will lead to significant decreases in the quantity and timing of plutonium reaching the 100-meter well.

7.1.2 Groundwater Pathway Results

7.1.2.1 100-Meter Water from Well Groundwater Pathway Doses

The 100-meter groundwater pathway dose is the most significant contributor to the all-pathways dose, and therefore to understand the controlling parameters for this main dose contributor better, several analyses were conducted. The different analyses are presented in this section.

7.1.2.1.1 Deterministic Analysis

Several deterministic analyses were conducted for the HTF PA. The dose results for the Base Case, presented in Section 5.5, are used as a comparison against performance objectives. However, in order to evaluate the impact on radionuclide transport under worst-case scenario conditions, such as complete hydraulic degradation of the waste tank grout at early time, and the inclusion of fast flow paths through the grout and basemat, several alternative waste cases were also evaluated and results presented in Section 5.6.7.

First, the Base Case results are presented, and then the results for the alternative cases, Cases B through E and the No Cap Case, are summarized.

Section 5.5 presented the Base Case groundwater pathway dose results. These results indicate that within 10,000 years, the peak 100-meter groundwater pathway dose is from Sector A (4.0 mrem/yr) (Table 5.5-1), with the next highest peak doses originating in Sectors B (1.5 mrem/yr) and C (2.2 mrem/yr). The majority of contaminants migrating from Type I and II tanks follow a path to the 100-meter boundary at Sector A. Sectors B and C receive the majority of contaminant concentrations from plumes emanating from Type II and IV tanks.

The maximum doses within 10,000 years for the Base Case are recorded in Sectors A, B, and C because; 1) certain Type I and II tanks (e.g., Tanks 12, 14, 15, and 16) initially have degraded liners at closure, thus releases from these waste tanks start immediately, 2) inventory in the annulus and sand pads in the associated tanks release prior to liner failure (this timing is a function of the annulus grout transition from Reducing Region II to Oxidizing Region II), and 3) Type IV tanks have liners that fail within 10,000 years. As indicated in Table 5.5-3 presented in Section 5.5, Type III and IIIA tanks do not contribute to the peak dose within the 10,000-year period because the steel liner has yet to fail. This is also true for the Type I and II tanks that have initially intact liners at facility closure.

It is important to recognize that the peak doses are associated with specific locations and times. Because there are over 40 unique and independent inventory sources modeled in the HTF model, there is significant temporal and spatial complexity inherent in the modeling system. Removal of any one inventory source may reduce the doses (including the peak dose where applicable) associated with that source, but the overall HTF PA peak dose will not necessarily be reduced by a corresponding amount. The overall HTF PA peak dose will merely move to a different location and time. The peak groundwater pathway doses vary over time and location (e.g., the six HTF sectors), and while not fully independent (due to plume overlap), there is variability across the five sectors.

In addition to Case-A deterministic analysis, various deterministic sensitivity analyses were performed. Section 5.6.7 presents dose results for the alternate cases, Cases B through E, as well as the impact to dose from removing the closure cap. Section 4.4.2 describes the different cases, Cases B through E, in detail. Section 5.6.7.3 describes the conditions of the no closure cap analysis. The complete hydraulic degradation of the waste tank grout (and annulus grout) at 501 years, and the inclusion of fast flow paths through the grout, as in Case B and D, has the most impact on peak dose within 10,000 years. These conditions result in a much earlier peak dose by almost 7,000 years (e.g., at year 2,650 instead of year 9,520) and the peak dose to increase from 1.0 mrem/yr in the Base Case to 2.6 mrem/yr in Cases B and D. The complete hydraulic degradation of the waste tank grout (and annulus grout) at 501 years, and the inclusion of fast flow paths through the grout, as in Cases B and D, has a significant impact on peak dose within 10,000 years. These conditions result in an earlier peak dose and a peak dose magnitude increase (from 4.0 mrem/yr in the Base Case to over 14 mrem/yr in Cases B though D). As indicated in Section 5.6.7, the No Cap Case peak dose (approximately 5.0 mrem/yr) is

not significantly greater than the Base Case peak. Section 5.6.7 also presents dose results for various sensitivity studies of significant parameters (e.g., grout transition time, key solubility values, liner failure time). These sensitivity studies show that there are multiple barriers to release and variability surrounding these single barriers does not appear to be so great as to have an unacceptable impact on peak dose within 10,000 years. In addition, the sensitivity studies show that dose impact of an individual parameter can be highly dependent on other parameters with the impact of the sensitivity varying in different manners depending on the parameters involved, with the sensitivity often varying non-linear and/or counter-intuitively in some cases.

7.1.2.1.2 Probabilistic Analysis

Section 5.6.4 presents the results for the UA, which propagates uncertainty in model input parameters and evaluates the impact uncertainty has on endpoints (such as peak dose). The different waste tank cases were captured in an all-cases modeling run in order to sample a range of parameter uncertainty distributions and the model simulation was run out 10,000 years (5,000 realizations) and 100,000 years (1,000 realizations). Individual modeling runs were performed for two individual cases (Cases A and D) with each model simulation run out 10,000 years (3,000 realizations).

Table 7.1-1 indicates the range of uncertainty in peak dose for the cases evaluated. The probabilistic UA for the 100-meter groundwater pathway doses within 10,000 years indicated a peak of the mean equal to 15 mrem/yr at 10,000 years for the All-Cases UA and 13 mrem/yr for the Case-A UA.

Table 7.1-1: Summary Statistics from Uncertainty Analyses

Cases Evaluated	Within 10,000 Years			Regardless of Time in 10,000 Years
	Peak of the Mean (mrem/yr)	Peak of the Median (50th percentile) (mrem/yr)	Peak of the 95th Percentile (mrem/yr)	Mean of the Peaks (mrem/yr) (From Table 5.6-22)
All Cases	15	5.6	58	220
Case A	13	2.3	24	85
Case D	35	12	112	210

Data extracted from Tables 5.6-32 and 5.6-33
Case A = Base Case

The last column of Table 7.1-1 indicates the mean value of all 1,000 peaks from the probabilistic model regardless of the time the peak occurred. These values are higher than the deterministically derived peak 100-meter groundwater pathway dose because most of the individual stochastic distributions are reasonably conservative. End member sampling of these conservative values (which typically have distributions weighted to the side of conservatism) drive the individual realization peak higher, which skews the mean toward higher percentiles. Similarly, the mean value of the peaks will always be higher than the peak of the mean time history curves. The statistical time history of MOP doses

for “All Cases” are displayed in Figure 7.1-4 (0 to 10,000 Years) and Figure 7.1-5 (0 to 100,000 Years).

Single realization analysis of the top five peak realizations for the All Cases, Base Case, and Case D UA models (Section 5.6.4) identified certain parameters as being important controllers on peak dose. The single realization analysis identified the parameters that control the release and dose of Tc-99 as having the most impact on the peak dose.

Figure 7.1-4: Statistical Time History of MOP Doses for All Cases (0 to 10,000 Years)

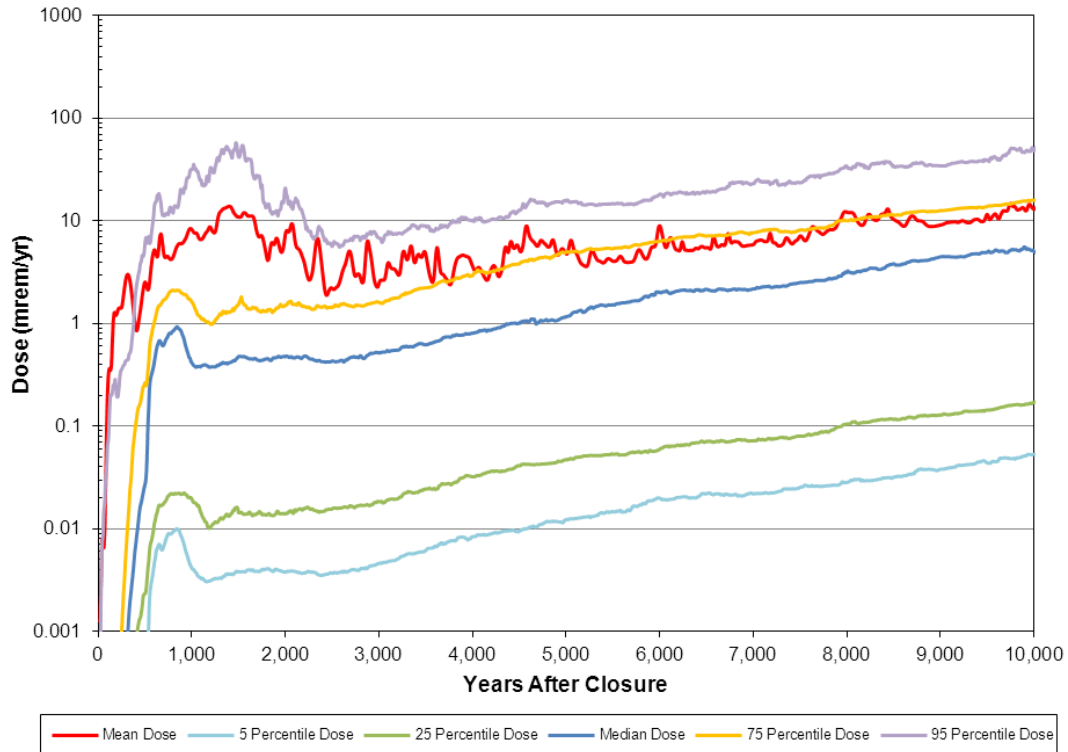
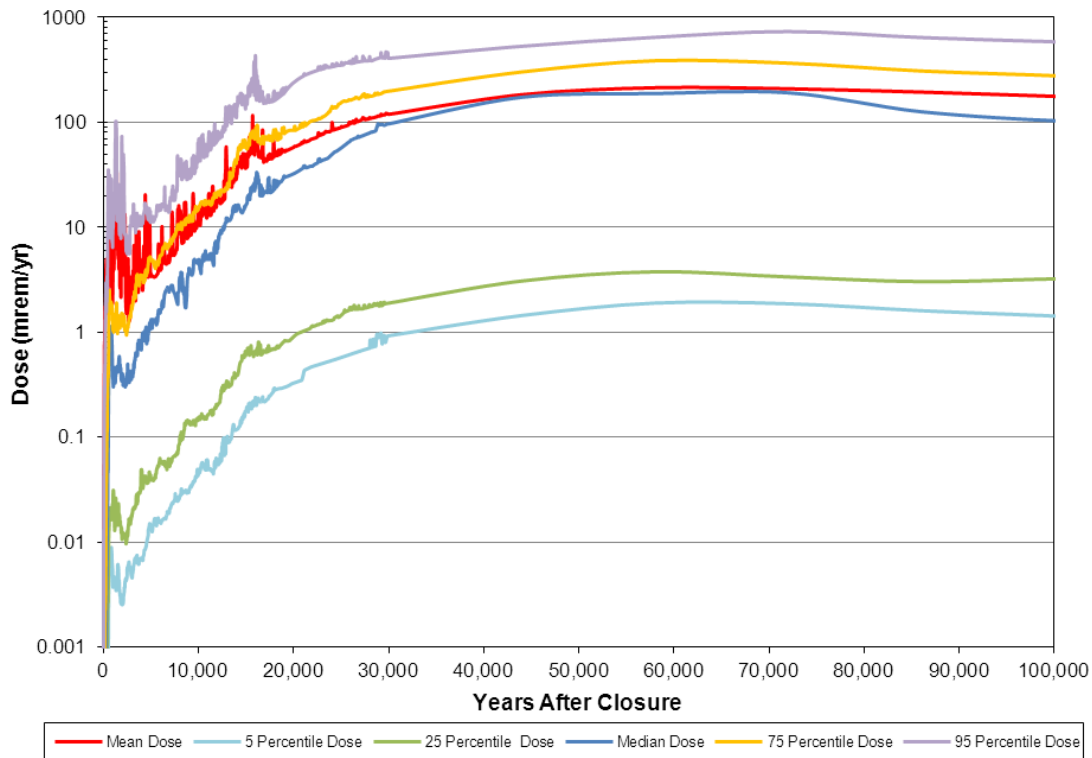


Figure 7.1-5: Statistical Time History of MOP Doses for All Cases (0 to 100,000 Years)



7.1.2.1.3 Sensitivity Analysis

Two GoldSim probabilistic models were simulated for the sensitivity analyses, a model for the Base Case, and one model for the fast flow Case D. The results are presented in Section 5.6.5. The SA determined that peak dose is most sensitive to parameters relating to Tc-99 and to inventory variability. Because the maximum dose within 10,000 years is primarily from contributions from Tc-99, it is expected that dose is sensitive to parameters relating to Tc-99. In addition, the sensitivity analysis determined that the results are sensitive to water well completion stratum, which is expected because the Gordon Aquifer contaminant concentration is significantly lower than the UTRA-UZ and UTRA-LZ, and the impact of drilling into the Gordon Aquifer can dominate other parameters and lead to lower doses. It should be noted that the Base Case deterministic results used the well of highest concentration for peak dose calculations, and did not take into account that a large percentage of wells would expect to be drilled into the Gordon Aquifer.

7.1.2.1.4 Barrier Analysis

Ten deterministic models were simulated to evaluate systematically, the ability of different barriers to limit waste migration. The different barriers evaluated include the closure cap, grout, CZ, steel liner, and the natural barrier. The barriers with the most impact on releases from the source waste tanks are the steel liners, which primarily

influence the timing of the peak, the CZ, which greatly controls the magnitude of the peak, and the grout, which can affect the magnitude and timing of the peak. The closure cap and the natural barrier have less of an impact on radionuclide fluxes. The importance of the barrier on radionuclide transport is element-specific for the CZ, the grout and the natural barrier, whereas the liner and closure cap are inclined to have a similar affect for all radionuclides. Although an independent barrier analysis of the annulus grout was not done, it is apparent from the interpretation of the time histories presented in Section 5.6.6 that the timing of annulus grout transition (Type II tanks) greatly influences the timing of Tc-99 peaks. The annulus transition triggers a large decrease in Tc-99 sorption onto the annulus grout (from a K_d of 5,000 mL/g to 0.8 mL/g). This transition combined with a significant inventory in the annulus (some initially in the sand pads) produces significant releases prior to liner failure.

7.1.2.1.5 Summary Insights from Different Analyses

The results of the different deterministic alternative cases are as expected, in that worst-case conditions result in earlier and greater peak doses within 10,000 years. Despite the pessimistic assumptions used in these cases, the magnitude of the peaks remain low (< 12 mrem/yr), lending confidence in the overall ability of the HTF closure conditions to limit radionuclide migration. Similarly, the barrier analysis deterministic cases provided insight into the sensitivity of the model to liner failure and the importance of chemical transition times on peak flux (especially the impact of the annulus and CZ transitions on Tc-99 releases). The uncertainty analyses illustrated that the Base Case deterministic model results generally lay within the mean and median time history curves displayed in Figures 7.1-4 and 7.1-5, and as expected, the Base Case model is most sensitive to parameters controlling Tc-99. The SA identified Tc-99 as a significant radionuclide, and indicated given certain conditions rapid transport of this radionuclide can significantly influence dose to the MOP.

7.1.2.2 Water at the Stream Groundwater Pathway Doses

The peak, groundwater pathway dose at the stream, within 10,000 years is approximately 0.04 mrem/yr and is associated with UTR (Section 5.5.2.1). The Fourmile Branch dose is higher than the UTR, within 20,000 years (Figure 5.5-15) because releases from the Type II tanks with initially failed liners, and the Type IV tanks (which are expected to have liner failure earlier than other waste tank types) will primarily go to Fourmile Branch.

7.1.3 Airborne Dose

The dose from airborne radionuclides at the 100-meter boundary based on Type I and II tank cases is negligible (< 0.001 mrem/yr). The very small dose is from C-14 in the form of carbon dioxide. Even these results were very conservative because the flux rates were based on simplified models as described in Section 4.5.

7.1.4 All-Pathways Dose

The peak all-pathways annual dose for the MOP at 100 meters is calculated using the highest 100-meter, groundwater pathway dose results during a 10,000-year period in combination with the air pathway results. As calculated in Section 5.3, the air pathway dose is negligible;

therefore, the all-pathway dose is the same as the groundwater pathway dose. The detailed discussion of the groundwater pathway dose in Section 7.1.2 therefore applies to the all-pathways dose. The peak all-pathways annual dose regardless of sector is shown in Figure 7.1-6 (within 10,000 years) and Figure 7.1-7 (within 100,000 years)

Figure 7.1-6: Peak All-Pathways MOP Dose within 10,000 Years

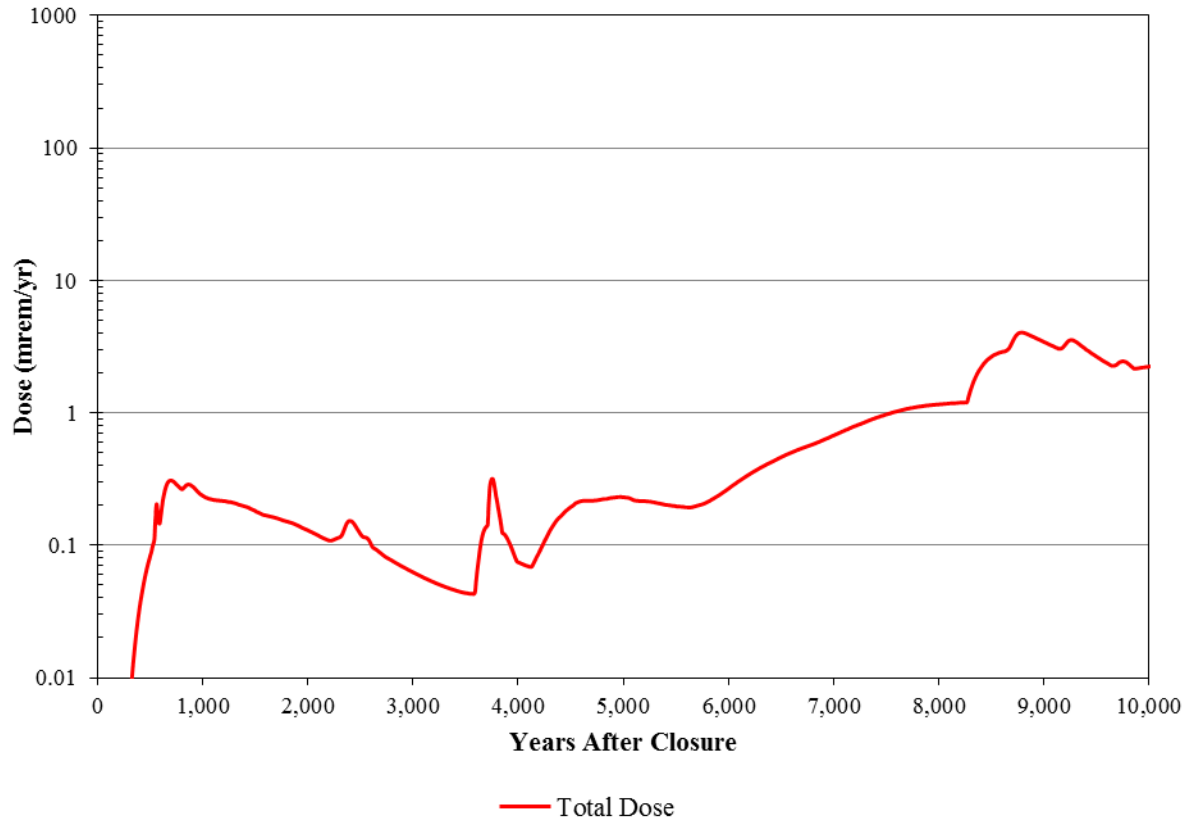
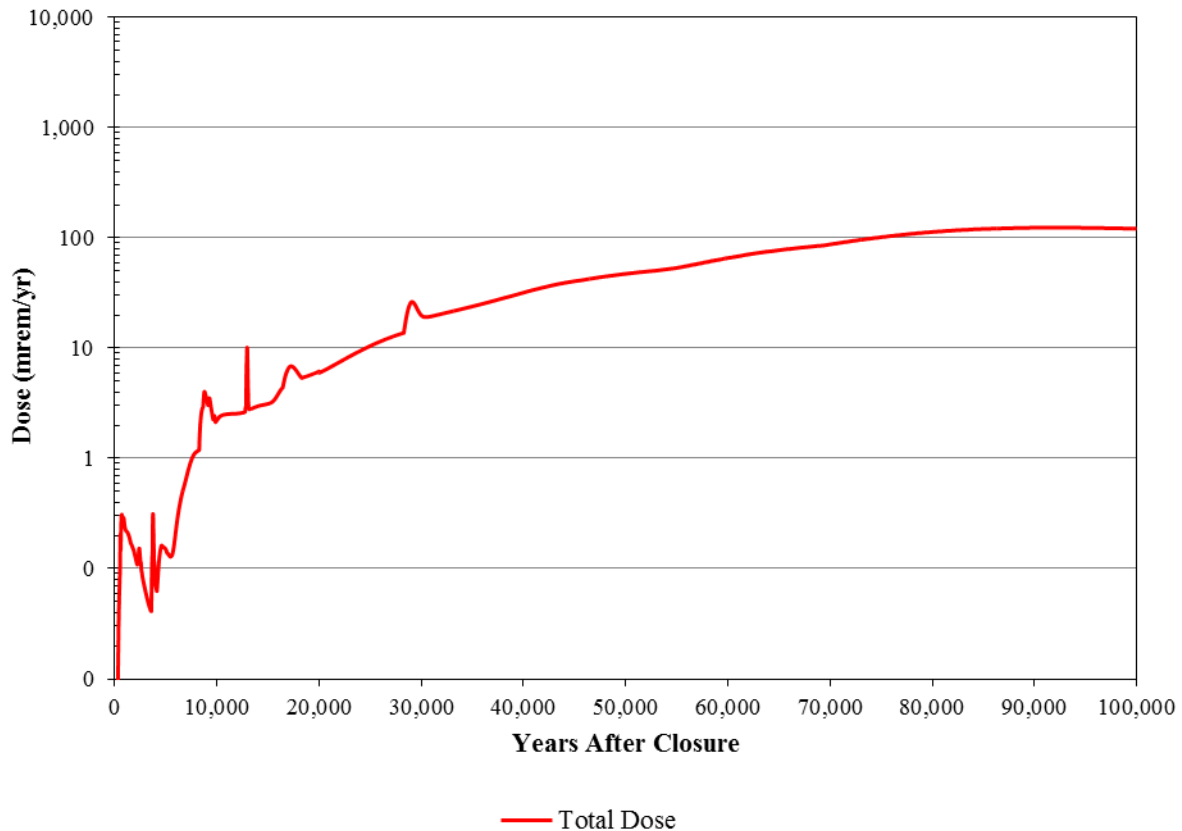


Figure 7.1-7: Peak All-Pathways MOP Dose within 100,000 Years



7.1.5 Inadvertent Intruder Dose

The key findings from the various inadvertent intruder analyses, presented in Sections 6.4 and 6.5, are provided below.

7.1.5.1 Intruder Deterministic Analysis

Results for the deterministic intruder analyses are presented in Section 6.4. The peak dose for the acute intruder in a 10,000-year period was 1.3 millirem at year 100, which was primarily (83 %) due to exposure to drill cuttings. The peak acute dose to the IHI is shown in Figure 7.1-8 (within 10,000 years). The acute intruder scenario did not include a groundwater contribution and therefore did not vary by HTF sector.

The peak dose for the chronic intruder scenario in a 10,000-year period was 50 mrem/yr. The peak is almost entirely from ingestion of vegetables that grew in soils contaminated with drill cuttings. The principal radionuclide contributor to this vegetable dose was from the short-lived isotope Sr-90/Y-90 (with a half-life of about 30 years). Because the peak dose is primarily due to drill cuttings and not groundwater contamination, the peak dose to the chronic intruder during a 10,000-year period does not vary by HTF sector. The peak annual chronic dose to the IHI (regardless of sector) is shown in Figure 7.1-9 (within 10,000 years) and Figure 7.1-10 (within 20,000 years)

Figure 7.1-8: Peak Acute Dose to the IHI within 10,000 Years

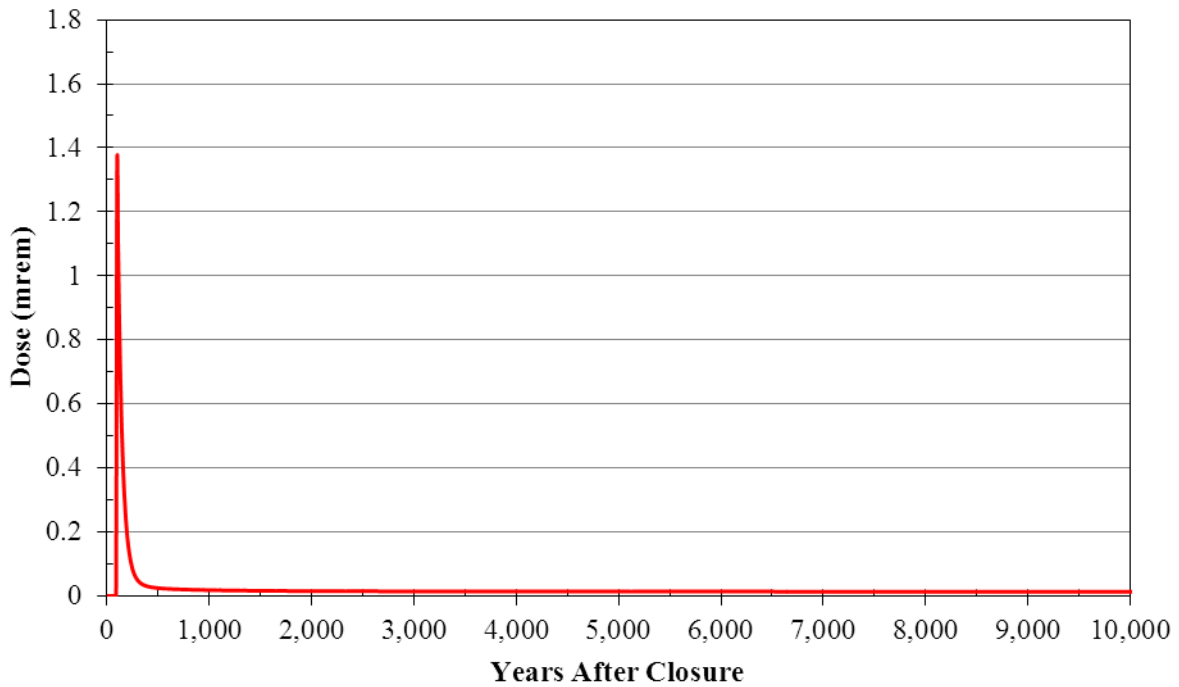


Figure 7.1-9: Peak Dose to the IHI within 10,000 Years

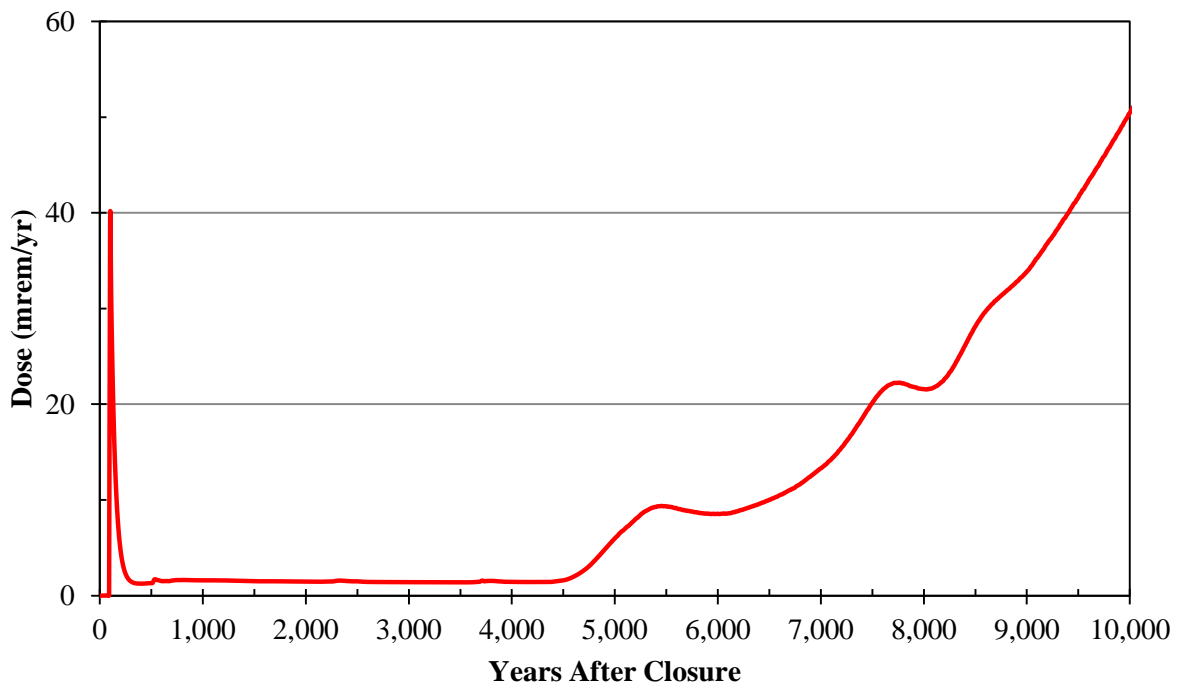
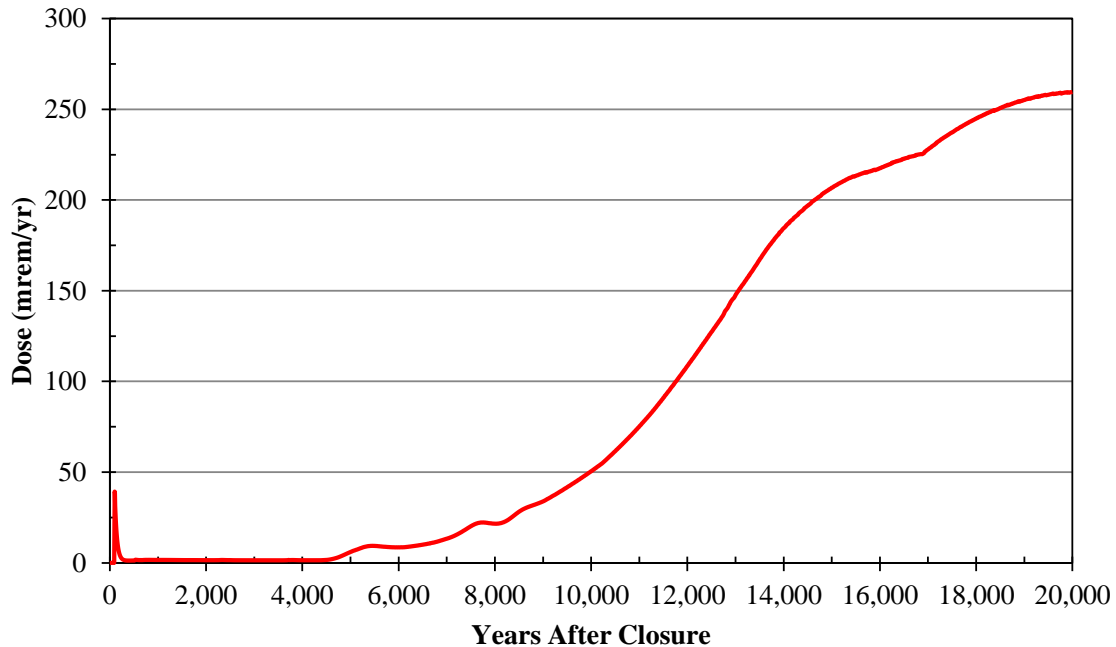


Figure 7.1-10: Peak Dose to the IHI within 20,000 Years



7.1.5.2 Intruder Probabilistic/Sensitivity Analysis

The probabilistic HTF GoldSim Model was used to evaluate sensitivity of various endpoints to uncertainty in input parameters. The probabilistic HTF GoldSim Model was run for 1,000 realizations with the well adjacent to Tank 12 set as the site of the IHI well. An investigation of the uncertainty parameters revealed that many of the same parameters that influence the MOP dose also significantly influence the IHI dose. For example, the well completion stratum (the parameter that selects which aquifer water is drawn from for MOP and IHI use) and parameters related to release and doses of Tc-99 (e.g. Tc-99 inventory multiplier) are important to intruder dose

Because the acute intruder receives a dose solely from exposure to drill cuttings, an equivalent probabilistic analysis was not conducted; however, a deterministic analysis was conducted to evaluate the impact on the acute intruder peak dose to drilling into a waste tank, which has a much greater inventory. This sensitivity analysis (Section 6.5.1.2) concluded that drilling into Tank 13 (which has a high initial inventory) increases the acute intruder dose 9 times (to 14 millirem).

Similarly a deterministic analysis was conducted to evaluate the impact of drilling into a 4-inch transfer line compared to a 3-inch transfer line on the chronic intruder peak dose within 10,000 years (Section 6.5.1.1) and to drilling within the 1-meter boundary (Section 6.5.1.3). The 4-inch transfer line analysis indicated that the peak dose increased to 74 mrem/yr (approximately double the peak dose associated with a 3-inch transfer line at 100 years). Section 6.5.1.3 indicated that drilling 1 meter from a number of waste tanks within the 1-meter boundary had no impact on the Base Case peak deterministic dose (all peak doses were less than or equal to the Base Case peak dose of 45 mrem/yr).

7.1.5.3 Summary Insights from Different Intruder Analyses

The various intruder analyses indicate that both the acute and chronic intruder peak doses are sensitive to the initial inventory of the drill cuttings and the parameters related to release and doses of Tc-99.

7.1.6 Radon Flux

These simplified models described in Section 4.5 also resulted in a peak (instantaneous) radon flux at the ground surface of $1.23\text{E-}14$ pCi/m²/s as presented in Table 5.3-9.

7.1.7 Summary of Performance Assessment Results

A summary of the PA results is captured in Table 7.1-2.

Table 7.1-2: Summary of the Performance Assessment Results

Protection of the MOP		Notes
MOP Conclusion		Modeling emphasis was placed on minimizing uncertainty associated with doses within the initial 10,000 years after HTF closure. Based on risk-informed decision-making principles, less emphasis was placed on reducing modeling conservatism associated with doses determined to be well past 10,000 years, even if projected doses could exceed 25 mrem/yr.
Deterministic (Base Case)	0.3 mrem/yr Within 1,000 years	Deterministic modeling of Base Case results in a peak dose almost two orders of magnitude below 25 mrem/yr for 1,000 years and almost an order of magnitude below 25 mrem/yr even out to 10,000 years after HTF closure. The Base Case doses beyond 10,000 years peak at approximately year 91,000 with a dose equivalent to approximately 20 % of the 620 mrem/yr dose received by the average United States resident.
	4.0 mrem/yr Within 10,000 years	
	120 mrem/yr Peak dose within 100,000 years	
Deterministic (Alternative or Sensitivity Cases)	12, 2.1 mrem/yr Case B, C (within 1,000 years)	Deterministic modeling of alternative waste tank configurations shows that the dose results remain below 25 mrem/yr for 1,000 years after HTF closure even assuming alternative waste tank failure scenarios. The alternative waste tank cases include a configuration that assumes a fast flow path exists through the entire closed system. The fast flow configuration (Case D, described in Section 4.4.2.4) sensitivity analysis results were presented in Section 5.6.7.4 to assess the impact of input variability on the groundwater pathways. The Case E results are high due to Case E simultaneously and non-mechanistically simulating multiple "failed" barriers (e.g., a fast flow path exists though the entire closed system and the waste tank grout imparts no reducing capacity upon the waste tank waste). The Case E results are less than the 620 mrem/yr dose received by the average United States resident.
	14, 16 mrem/yr Case B, C (within 10,000 years)	
	12 mrem/yr Case D (within 1,000 years)	
	18 mrem/yr Case D (within 10,000 years)	
	3.7 mrem/yr Case E (within 1,000 years)	
	240 mrem/yr Case E (within 10,000 years)	
	0.7 mrem/yr No Closure Cap (within 1,000 years)	Deterministic modeling of the Base Case waste tank scenario shows that dose results remain below 25 mrem/yr for 1,000 years after HTF closure when assuming no closure cap is placed over the HTF.
	4.7 mrem/yr No Closure Cap (within 10,000 years)	
	2.7 mrem/yr Synergistic Case (within 1,000 years)	
	5.7 mrem/yr Synergistic Case (within 10,000 years)	
13 mrem/yr Synergistic Case (within 20,000 years)	This non-mechanistic synergistic sensitivity analysis (Case F) is presented to address uncertainty related to three Base Case key modeling parameters. The three parameters analyzed further are gas transport impacts on reducing grout, liner failure times, and solubility controlling phases. The synergistic case evaluates the combined results of altering these three key modeling parameters. The resulting peak doses are relatively low despite the synergistic case reflecting multiple modified assumptions, thus further providing reasonable assurance that dose results will remain below 25 mrem/yr for 1,000 years after HTF closure for the reasonably expected scenarios.	

Base Case = Case A

Table 7.1-2: Summary of the Performance Assessment Results (Continued)

Protection of the MOP		Notes
MOP Conclusion		Modeling emphasis was placed on minimizing uncertainty associated with doses within the initial 10,000 years after HTF closure. Based on risk-informed decision-making principles, less emphasis was placed on reducing modeling conservatism associated with doses determined to be well past 10,000 years, even if projected doses could exceed 25 mrem/yr.
Deterministic (Base Case)	0.3 mrem/yr Within 1,000 years	Deterministic modeling of Case A results in a peak dose almost two orders of magnitude below 25 mrem/yr for 1,000 years and almost an order of magnitude below 25 mrem/yr even out to 10,000 years after HTF closure. The Case A doses beyond 10,000 years peak at approximately year 91,000, with a dose equivalent to approximately 20 percent of the 620 mrem/yr dose received by the average United States resident.
	4.0 mrem/yr Within 10,000 years	
	120 mrem/yr Peak dose within 100,000 years	
Deterministic (Alternative or Sensitivity Cases)	12, 2.1 mrem/yr Case B, C (within 1,000 years)	Deterministic modeling of alternative waste tank configurations shows that the dose results remain below 25 mrem/yr for 1,000 years after HTF closure even assuming alternative waste tank failure scenarios. The alternative waste tank cases include a configuration that assumes a fast flow path exists through the entire closed system. The fast flow case (Case D, described in Section 4.4.2.4) sensitivity analysis results were presented in Section 5.6.7.4 to assess the impact of input variability on the groundwater pathways. The Case E results are high due to Case E simultaneously and non-mechanistically simulating multiple “failed” barriers (e.g., a fast flow path exists though the entire closed system and the waste tank grout imparts no reducing capacity upon the tank waste). The Case E results are less than the 620 mrem/yr dose received by the average United States resident.
	14, 16 mrem/yr Case B, C (within 10,000 years)	
	12 mrem/yr Case D (within 1,000 years)	
	18 mrem/yr Case D (within 10,000 years)	
	3.7 mrem/yr Case E (within 1,000 years)	
	240 mrem/yr Case E (within 10,000 years)	
	0.7 mrem/yr No Closure Cap (within 1,000 years)	Deterministic modeling of the Base Case waste tank scenario shows that dose results remain below 25 mrem/yr for 1,000 years after HTF closure when assuming no closure cap is placed over the HTF.
	4.7 mrem/yr No Closure Cap (within 10,000 years)	
	2.7 mrem/yr Synergistic Case (within 1,000 years)	
	5.7 mrem/yr Synergistic Case (within 10,000 years)	
13 mrem/yr Synergistic Case (within 20,000 years)	This non-mechanistic synergistic sensitivity analysis (Case F) is presented to address uncertainty related to three Base Case key modeling parameters. The three parameters analyzed further are gas transport impacts on reducing grout, liner failure times, and solubility controlling phases. The synergistic case evaluates the combined results of altering these three key modeling parameters. The resulting peak doses are relatively low despite the synergistic case reflecting multiple modified assumptions, thus further providing reasonable assurance that dose results will remain below 25 mrem/yr for 1,000 years after HTF closure for the reasonably expected scenarios.	

Base Case = Case A

Table 7.1-2: Summary of the Performance Assessment Results (Continued)

Protection of the Inadvertent Human Intruder			Notes
IHI Conclusion			Modeling emphasis was placed on minimizing uncertainty associated with doses within the initial 10,000 years after HTF closure. Based on risk-informed decision-making principles, less emphasis was placed on reducing modeling conservatisms associated with doses determined to be well past 10,000 years, even if projected doses could exceed 500 mrem/yr.
Deterministic (Base Case)	1.3 mrem	Acute IHI Dose (within 1,000 and 10,000 years)	Deterministic modeling of the Base Case IHI dose results in a peak acute dose more than two orders of magnitude below 500 millirem for 1,000 years after HTF closure.
	40 mrem/yr	Chronic IHI Dose (within 1,000 years)	
	50 mrem/yr	Chronic IHI Dose (within 10,000 years)	
	260 mrem/yr	Chronic IHI Dose (within 20,000 years)	
Probabilistic peak of mean (Base Case)	760 mrem/yr	Within 10,000 years	The peak of the mean dose of 760 mrem/yr is higher than the median peak dose of 500 mrem/yr, and illustrates that the mean is greater than the median indicating that a few realizations sampled at the tail of the parameter distributions can cause the mean dose to be high. As explained in Section 6.5.2, the GoldSim model IHI results were conservative (i.e., about three times higher than the deterministic PORFLOW results) due to differences in the models. These dose results are comparable to the 620 mrem/yr dose received by the average United States resident.

Base Case = Case A

7.2 Conservatisms Included in the HTF PA

Many assumptions were made during model development that introduces conservatism into the magnitude and timing of radionuclides releases from the HTF. This section reviews those conservatisms by HTF component.

7.2.1 General

This section focuses on those conservatisms that are not specifically associated with a physical component of the model (e.g., closure cap, grout), but can be categorized as conservatisms included in the general modeling approach.

The initial conceptual design used in the HTF PA model is an aphysical simplification of the actual infrastructure of HTF ancillary equipment design. This approach is required for analytical modeling. Certain equipment features and design elements have been omitted in the conceptual model that, if included, would decrease the modeled release rates of contaminants (Section 3.2.2).

One of the appreciable conservatisms is the evaluation point for dose. In the HTF PA modeling, radionuclide dose to receptors is evaluated at a 1 meter, 100-meter buffer zone surrounding HTF, and at the seepline. However, based on SRS land use plans, no MOP will have unrestricted access to the HTF, because current SRS boundaries will remain unchanged, and the land will remain under the ownership of the federal government, consistent with the site's designation as a NERP. By demonstrating protection to the 1-meter and the 100-meter boundaries, the PA is also demonstrating public protection at the site boundary (approximately 5 miles away). In fact, the dose due to radionuclides at the site boundary would only be greatly diminished in comparison to the 1-meter and 100-meter boundary dose, because as radionuclides travel a greater distance through the air and subsurface, the more dispersion and dilution occurs (Section 5.8).

Several conservatisms were included in the groundwater concentrations used in the computation of the dose to the MOP and intruder.

- The peak concentration values from PORFLOW for the 100-meter results are recorded for the depths of the three aquifers of concern (i.e., UTRA-UZ, UTRA-LZ, and Gordon Aquifer), and are based on the peak regardless of aquifer for each radionuclide. Using the sectors to determine the highest groundwater concentrations causes the calculated peak doses to be higher than they actually are, since the peak concentrations are determined for each radionuclide independent of the location within the sector (Section 5.2.1).
- The stream concentrations used in dose calculations for secondary water source pathways are the peak aquifer concentrations (as discussed in Section 5.2.3), and conservatively assume no stream dilution. The stream is the secondary water source for the pathways involving swimming, fishing/boating, and fish ingestion (Section 5.4.1).
- The use of sectors in determining groundwater concentrations added conservatism to the peak dose results, because the peak concentrations are determined for each radionuclide independent of the location within the sector or the aquifer (Section 5.2.1).

Several conservatisms were included in the dose calculations specific to the Inadvertent Intruder Scenarios. These are included below.

- Well drilling through a transfer line is considered a low probability event, especially while the line maintains some structural integrity. Nevertheless, as a bounding case for the purposes of the PA, it has been assumed that a well driller could drill through an intact transfer line immediately after the end of institutional control (Section 4.2.3.3).

7.2.2 Closure Cap

The following are some of the measures, which were taken to ensure conservative HELP model infiltration results.

- The precipitation data utilized included maximum daily precipitation up to 6.7 inches (e.g., significant pulses of water).

- The maximum slope length of the closure cap (e.g., 585 feet) was utilized to determine both runoff and lateral drainage for the entire closure cap.
- The erosion barrier assumption is that it is in-filled with a sandy soil. The use of a less permeable infill would reduce infiltration.
- A saturated hydraulic conductivity was assigned to the intact portions of the HDPE geomembrane even though water transport through HDPE is a vapor diffusion process.
- A conservative GCL degradation model is used in the HELP model. It is assumed that every HDPE geomembrane hole generated over time is penetrated by a pine root that subsequently penetrates the GCL. However, the results of the probability based root penetration model demonstrated that this is not the case and that most of the HDPE geomembrane holes were not penetrated by roots over the period of interest. This conservatism leads to a much more rapid closure-cap degradation model, in approximately 2,600 years after closure (Section 3.2.4.1.2).

7.2.3 Waste Tanks

When developing the waste-tank model geometries for the different tank types, the waste tank dimensions default to the minimum. For example, if wall thickness or basemat thickness varied, the minimum dimension was used for the entire wall or basemat (Section 4.4.1). This conservatism has large implications when applying degradation rates.

7.2.4 Contaminant Zone and Contaminant Release Model

The CZ controls the timing and magnitude of releases for the majority of the residual inventory in HTF (some inventory is modeled to exist in the Type II tank annulus and sand pads, see Section 4.4.4.2). The contaminant release model applies solubility controls to specific elements in the CZ, these controls act to limit the amount a solid can dissolve and exist in the aqueous phase. Only radionuclides in the aqueous phase are available for advective transport out of the CZ. In addition, other than the solubility control, the waste release model does not credit any additional potential contaminant retardation mechanisms, such as retardation associated with iron oxides/hydroxides from the corroded waste tank liner; therefore further maximizing contaminant release from this zone.

A fundamental part of establishing solubility-controlled stabilized contaminant release rates is selection of a solubility-controlling phase for each radionuclide. For some of the radionuclides of interest there are studies that can guide selection, for others there are no studies. For this reason, selection of solubility controlling phases when developing the contaminant release model was generally very conservative, meaning that where multiple phases were possible, the phase with the highest solubility is selected. The process attempted to balance scientific knowledge with the need to be cautious and biased toward higher solubility. For example, while it is likely that radionuclides such as plutonium and neptunium will be co-precipitated with iron in the CZ, the solubility values used for plutonium and neptunium in the base case do not assume co-precipitation (Section 4.2.1). Additionally, some contaminants were simulated as having no identified solubility controls, with their releases modeled as instantaneous, for example I-129 (see Tables 4.2-10 and 4.2-11). No solubility controls essentially maximize releases for that radionuclide.

The deterministic model (PORFLOW) does not implement solubility controls for multiple isotopes of the same element. Each isotope of an element is treated independently so that they are not collectively added to reach an elemental solubility limit. Therefore, the amount of an element such as uranium in solution is based on the single isotope, when in fact it should be based on the total amount of uranium in the inventory. Because the waste release within the CZ is solubility controlled, this treatment of solubility by PORFLOW allows for greater release from the CZ than would be expected. This approach can cause the peak dose to be modeled conservatively by treating U-233 and U-234 independently and allowing them to contribute to the 10,000-year peak dose, when in fact they would have the tendency to slow each other's release (Section 5.6.2.1.2).

7.2.5 Inventory

As discussed in Section 3.3.2, the process used to estimate the waste tanks' residual material at operational closure created estimates that were both bounding and reasonable. For those contributors projected to have insignificant impact on dose, the estimates were developed with considerable conservatism. The inventory for many radionuclides was increased to ensure the values used were reasonably conservative. The methodology used to develop the inventory estimates added conservatism. The residual volume used was conservative, particularly for most annulus residuals. Further conservatism was added by using the maximum inventory within a tank grouping.

The reasonable estimates developed for those contributors expected to affect dose also provide some level of conservatism over what is expected to remain at operational closure of the waste tanks. Many of the inventory estimates affecting dose are based on sample analysis and the WCS, with WCS generated values being generally conservative. Each reactor spent fuel assembly that was reprocessed is assumed to have received the maximum burn-up possible therefore; the amounts of actual fission products contained in an assembly were in fact, less than those entered into WCS (Section 3.4.1.2). [LWO-PIT-2007-00025]

7.2.6 Grout

The permeability of degraded grout has not been measured, as this gradual process will occur over thousands of years (Section 3.2.3.2). For modeling purposes in this PA, degradation of the grout is conservatively modeled by significantly increasing the hydraulic conductivity in the Base Case. For example, the hydraulic conductivity for Type I tank grout increases by four orders of magnitude in less than 10,000 years.

7.2.7 Steel Liner

As indicated in Section 5.6.6 (Barrier Analysis), the waste tank steel liners are important barriers to radionuclide migration. The following are modeling assumptions that maximize the releases out of the waste tanks following liner failure.

- All waste tanks of the same type were assumed to fail simultaneously, which can have a significant impact on peak dose timing for some radionuclides, as discussed in Section 7.2.5.
- For certain Type I and II tanks (e.g., 12, 14, 15, and 16) the steel liner is assumed to be absent, or otherwise not a hindrance to advection and diffusion (Section 4.2).

- After failure, advection and diffusion is assumed not hindered by the liner. Retardation due to the presence of corrosion products is not included in the model (Section 4.2.2.2.6).
- When estimating the time of liner failure for the submerged and non-submerged waste tank types, the failure distributions used in the stochastic model are those distributions estimated based on steel corrosion rates under varying conditions. The conditions are represented using very conservative diffusion coefficients, and reflect faster diffusion rates than are typically reported (Section 4.2.2.2.6).

7.2.8 Stainless Steel Transfer Lines and Ancillary Equipment

The transfer lines and ancillary equipment are a source for contaminants at the HTF. In the HTF PA, the stainless steel transfer lines and ancillary equipment are modeled separately from the waste tanks. The timing of radionuclide releases from these sources is dependent on rates of general corrosion and pitting penetration of the steel, which dictate when these features “fail.” The HTF PA is very conservative in its estimate of transfer line and ancillary equipment lifetime. A 0.04 mil/yr bounding rate was used for general corrosion of steel transfer lines in WSRC-STI-2007-00460. Pitting of the stainless steel transfer lines starts faster than general corrosion, however, by 500 years, after exposure to soil with groundwater, the pitting rate decreases significantly and the pitting depth is less than the depth of general corrosion (Section 4.2.2.2.6).

Based on these conservative corrosion rates, failure of various diameter stainless steel pipes was estimated to occur between 2,900 to 4,725 years. [WSRC-STI-2007-00460] The 25 % failure time for a 1-inch diameter transfer line with a minimum 120-millimeter wall thickness exposed to soils with significant amounts of groundwater was estimated at 6,000 years. This estimate represents the most conservative failure time for the HTF transfer lines under site conditions. Given this long lifetime estimate, it is extremely conservative to apply a failure time of 510 years to all steel transfer lines and ancillary equipment, which is the assumption used in HTF modeling. This modeling assumption was done to maximize the dose contributions of the ancillary inventory (Section 4.2.2.2.6).

The following include further conservatisms regarding the modeling of the ancillary equipment and transfer lines.

- All ancillary equipment is assumed to fail simultaneously.
- Once the stainless steel containment for ancillary equipment fails, the source term associated with the ancillary equipment was assumed available for release directly into the soil surrounding the ancillary equipment. It is assumed that no hold up or containment of the source term is provided by any of the cementitious materials surrounding the vessels, pits, and waste lines, such as the secondary containment structures (Section 4.4.2.6).
- No solubility control is assumed for ancillary equipment inventory. The ancillary equipment inventory is immediately released to the soil after failure with no holdup in the CZ or in any cementitious material.

7.2.9 Volatile Radionuclide and Radon Analyses

The following conservatisms were used in the airborne radionuclide and radon analysis that conservatively bound the flux of radionuclides from the CZ to the surface.

- Boundary conditions were used that force all of the gaseous radionuclides to move upward from the stabilized CZ to the land surface. In reality, some of the gaseous radionuclides diffuse sideways and downward in the air-filled pores surrounding the stabilized CZ; hence ignoring this has the effect of increasing the flux at the land surface.
- The removal of radionuclides by pore water moving vertically downward through the model domain was ignored. This mechanism would likely remove some dissolved radionuclides. Its omission had the effect of increasing the estimate of instantaneous radionuclide flux at the land surface in simulations conducted as a part of this investigation.
- The HDPE geomembrane, the GCL, and the primary steel liner of the waste tanks were excluded in the modeling. Inclusion of these materials in the model would significantly reduce the gaseous flux at the land surface due to their material properties (e.g., low air-filled porosity).
- Cover materials above the erosion barrier (e.g., top soil and upper backfill layers) were excluded. The diffusion pathway is shortened, which could increase the flux at the land surface with the exclusion of these materials.
- Use of the Type I and II tanks and minimum closure cap thickness in the modeling provided the shortest pathway from the CZ to the surface.
- The entire estimated HTF residual inventory was concentrated into a 1-foot stabilized contaminant layer in one waste tank to determine the maximum dose and flux.

8.0 PERFORMANCE EVALUATION

Summary for Section 8.0

Section 8.1 describes how the PA will be used.

Section 8.2 describes future work to be done to support maintenance of the PA.

8.1 Use of Performance Assessment Results

This PA for SRS was prepared to support the eventual operational closure of the HTF underground radioactive waste tanks and ancillary equipment. This PA provides the technical basis and results for use in subsequent documents to demonstrate compliance with pertinent requirements for the operational closure and eventual final facility closure of the HTF found in DOE O 435.1, Chg. 1, NDAA Section 3116, Construction Permit #17,424-IW, and FFA. [NDAA_3116, SCDHEC R. 61.67, SCDHEC R 61.82, DHEC_01-25-1993, WSRC-OS-94-42] The key requirements from these documents necessitate development and calculation of the following for the HTF.

- Potential radiological doses to a hypothetical MOP
- Potential radiological doses to a hypothetical inadvertent intruder
- Radiological dose to a human receptor via the air pathway
- Radon flux
- Water concentrations

All of these calculations were performed to provide results over a minimum of 10,000 years. The water concentrations were calculated for both radioactive and non-radioactive contaminants at multiple locations outside the HTF.

The regulatory process includes a Basis for Section 3116 Determination for Closure of HTF document, which will be used to demonstrate compliance with the NDAA Section 3116. The Basis for Section 3116 Determination for Closure of HTF document will be reviewed and approved by DOE, in consultation with the NRC. Approval of the Basis for Section 3116 Determination for Closure of HTF document by the Secretary of Energy is then required to document that the residual waste can be classified as non-high-level radioactive waste for the purposes of on-site disposition. The Secretary of Energy determination under NDAA Section 3116 incorporates by reference 10 CFR 61, Subpart C performance objectives. This HTF PA provides the technical basis that will be used to demonstrate compliance with 10 CFR 61.41 and 61.42 performance objectives that will be presented in the Basis for Section 3116 Determination for Closure of HTF document. [10 CFR 61] This HTF PA is also prepared to address the remaining DOE M 435.1-1 performance objectives and to support implementation of applicable DOE O 435.1, Chg. 1 requirements including a Tier 1 closure plan, waste tank-specific special analyses, and Tier 2 closure plans.

Reasonable assurance that operational closure of the HTF Facility will not adversely impact compliance with the SCDHEC requirements will be evaluated using two primary documents that

are supported by this HTF PA. The first is to be an HTF IWW GCP, which will establish the general protocols, requirements, and processes for closure of HTF facility. The second document(s) is the waste tank-specific closure modules that authorize the grouting of a specific waste tank, group of waste tanks, and/or ancillary equipment. Both the HTF IWW GCP and the HTF waste tank-specific closure modules will be reviewed and approved by the DOE and SCDHEC. The HTF PA will also support the final closure of the HTF consistent with CERCLA.

8.2 Further Work

As required by DOE M 435.1-1, maintenance of the HTF PA will include future updates to incorporate new information, update model codes, analysis of actual residual inventories, etc., as appropriate. Because PA results are in part, based on data that is uncertain, due to utilization of projected conditions thousands of years into the future, a maintenance program (SRR-CWDA-2012-00020) has been put in place to continue to reduce uncertainty in the inputs and assumptions, providing greater confidence in the results of the analyses, and in the long-term plans for public and environmental protection. The purpose of the PA maintenance program is to confirm the continued adequacy of a PA and to increase confidence in the results of the PA.

As part of the maintenance program, the HTF PA will be reviewed as opportunities for model improvement are identified or as additional studies are conducted. Opportunities for model improvement could include such tasks as use of improved modeling software or correction of previously identified model irregularities (e.g., SRR-CWDA-2012-00070 identified six HTF PA irregularities having either “no impact” or a “negligible impact” that were left unmodified). As additional data become available the PA may need to be revised, and additional modeling may be required. Based on information, results, and interpretations presented in Sections 5, 6, and 7, the various areas of future work may be included in the maintenance program to facilitate discussion for improving the PA in future revisions.

Future work is also planned in the area of input refinement and confirmation. For example, further work will be conducted to refine and confirm the existing radionuclide inventories that will be present in HTF at site closure. This work includes additional sampling and analyses of existing waste and refinement of potential waste estimates for un-sampled areas, such as the piping and other ancillary equipment. Sampling of the waste tanks after cleaning and before grouting will be necessary for inventory evaluation to ensure that the groundwater protection performance objectives are met. Future waste tank sampling will also take into account the waste release assumptions regarding iron co-precipitation, and sampling plans will address the need to investigate not just total radionuclide inventories, but chemical compositions as well. As part of input refinement and confirmation, future materials testing will be performed (e.g., validation of grout properties, site-specific soil K_d testing). This future work will consider uncertainty in material properties due to biases in testing methods including laboratory versus field experiments, as well as techniques used to measure properties (e.g., centrifuge versus flexible wall perimeter, column based testing, and influence of cementitious material on vadose zone geochemistry). The future materials testing will concentrate on those contaminants that have been identified as having the most impact on dose results (e.g., radium, technetium, neptunium).

An engineered closure cap will be installed over the HTF following the closure of the waste tanks and ancillary equipment. The design information provided in the PA is for planning purposes, and is based on the current HTF conceptual closure cap design presented in SRNL-ESB-2008-00023. The closure cap design will be finalized closer to the time of HTF closure, to take advantage of possible advances in materials and closure cap technology that could be used to improve the design.

9.0 PREPARERS

BAGWELL, LAURA - SAVANNAH RIVER NATIONAL LABORATORY

M.S. Geology – Texas A&M University

B.S. Geology – University of South Carolina

Experience: Ms. Bagwell is a Principal Engineer with SRNL. Her 19-year SRS career includes regulatory compliance for waste management facilities; soil and groundwater characterization for closure projects; geotechnical support for new missions; and vadose zone monitoring. As a member of SRNL's Environmental Sciences Directorate, she provides geologic expertise for environmental characterization and remediation projects at SRS and across the DOE complex.

Contribution: Ms. Bagwell reviewed historical literature and interpreted subsurface geology near H-Area Tank Farm.

BURNS, HEATHER - SAVANNAH RIVER NATIONAL LABORATORY

B.S. Chemical Engineering - Vanderbilt University

Experience: Ms. Burns is a Principal Engineer/Project Manager at SRNL with over 25 years of experience related to various waste treatments of radioactive, hazardous, and mixed solid and liquid wastes at SRS. She has been involved with both the stabilization/solidification and the thermal destruction of these wastes. She also developed the maintenance program for performance assessments in an effort to improve waste management practices at SRS. As part of this program, she took the lead as principal investigator on improving the monitoring program at the burial grounds by leading the effort to design, install, and operate the first vadose-zone monitoring program in the DOE Complex.

Contribution: Ms. Burns provided the project management and oversight for the SRNL support of the modeling efforts for the H-Tank Farm Performance Assessment.

DEAN, BEN – SAVANNAH RIVER REMEDIATION LLC / CLOSURE & WASTE DISPOSAL AUTHORITY

B.S. Chemical Engineering - Clemson University

Experience: With over 13 years of experience, seven at SRS, Mr. Dean has primarily worked with characterization of waste within the tank farms. He was involved with the characterization efforts for the F-Area Tank Farm and Saltstone Disposal Facility Performance Assessments. In addition, he has been involved with the current tank closure sampling process and result evaluation. Prior to joining WSRC, Mr. Dean spent six years in the chemical industry (chlor-alkali and fiberglass) with experience in operations, process engineering, and statistics.

Contributions: Mr. Dean assisted in development of the residual characterization estimates (waste tanks, transfer lines, ancillary equipment, and intruder scenario). In addition, he supported pathway-dose calculation development.

DIXON, KENNETH - SAVANNAH RIVER NATIONAL LABORATORY

M.E. Civil Engineering - University of South Carolina

M.S. Agricultural Engineering - University of Georgia

B.S. Agricultural Engineering - University of Georgia

Experience: Mr. Dixon is a Principal Engineer at SRNL with over 17 years of experience related to groundwater hydrology, soil and groundwater characterization and remediation, and computational simulation. He has been the principal investigator on a number of vadose zone modeling studies at SRS aimed at assessing the impacts of contaminant migration from waste sites and decommissioned building slabs. Recently his efforts have been focused on PA support including measuring the physical and hydraulic properties of various cementitious waste forms and contaminant transport modeling in support of the air and radon pathway analyses.

Contribution: Mr. Dixon is the principal investigator on the air and radon pathway PORFLOW analysis.

DENHAM, MILES - SAVANNAH RIVER NATIONAL LABORATORY

Ph.D. Geology - Texas A&M University

M.S. Geology - State University of New York at Stony Brook

B.S. Geology/Chemistry - Knox College

Experience: Dr. Denham is a Fellow Scientist at the SRNL with 18 years of experience in environmental geochemistry, mineralogy, and geochemical modeling. He has been principal investigator on a wide range of projects encompassing fields such as metal and radionuclide transport, metal and radionuclide remediation, and occurrence of natural radionuclides in soil and groundwater. He is currently the technical lead on a major initiative, funded through DOE EM-32, focusing on developing characterization, remediation, and long-term monitoring approaches that facilitate use of attenuation-based remedies for sites contaminated with metals and radionuclides.

Contribution: Dr. Denham contributed geochemical modeling of waste release to support overall modeling of groundwater pathways.

FARFAN, EDUARDO - SAVANNAH RIVER NATIONAL LABORATORY

Ph.D. Nuclear and Radiological Engineering - University of Florida

M.S. Nuclear and Radiological Engineering - University of Florida

B.S. Nuclear Engineering - University of Florida

Experience: Dr. Farfan is a Principal Engineer at SRNL. His experience includes five years teaching in Nuclear Engineering and Health Physics Departments. His research involves internal dosimetry risk assessment, probabilistic risk assessment, radon assessment, and computational modeling. A number of his research projects have involved collaborative efforts with the Centers for Disease Control and Prevention. Additionally, Dr. Farfan holds adjunct professor appointments at Clemson University and Idaho State University and is an online professor at Excelsior College. As a member of SRNL Environmental Analysis Section's Environmental

Dosimetry Group, he provides expertise for various SRS dose and risk assessment projects involving airborne and liquid radionuclide releases.

Contribution: Dr. Farfan performs dose/risk assessments using the computer models: AXAIRQ, AXAOTHER, CAP88, IMBA, LADTAP, LUDEP, LUDUC, MAXDOSE, POPDOSE, and VENTSAR.

FLACH, GREGORY - SAVANNAH RIVER NATIONAL LABORATORY

Ph.D. Mechanical Engineering - North Carolina State University

M.S. Mechanical Engineering - North Carolina State University

B.S. Mechanical Engineering - University of Kentucky

Experience: Dr. Flach is a Fellow Engineer at SRNL with over 20 years of experience related to groundwater hydrology, computational simulation, and numerical code development. He has been the principal investigator on a number of groundwater modeling studies at SRS involving regional and local scale hydrology, contaminant migration from waste sites, and evaluation of environmental cleanup alternatives. Over the last decade, his efforts have focused on PA and CA related projects and research involving dual-domain formulations of contaminant transport.

Contribution: Dr. Flach is one of the principal modeling investigators focusing on the PORFLOW modeling of groundwater pathways.

FOUNTAIN, DORI – SAVANNAH RIVER REMEDIATION LLC / CLOSURE & WASTE DISPOSAL AUTHORITY

B.S. Business Administration - Southern Wesleyan University

Experience: Ms. Fountain has over 22 years of experience at SRS. Her assignments include (but are not limited to) program administration and special assignments within Project, Engineering, & Construction. She has served as a consultant on special team initiatives for Bechtel Corporation (Bechtel Group) at SRS and at other DOE sites. In her assignment with the Closure & Waste Disposal Authority, she is responsible for providing project technical support and configuration control management for waste facility closure and technology innovation activities. She supports the development and editorial processes for regulatory documents and oversees production and issue process under the guidelines of the DOE and other government and state codes, regulations, and requirements (including the NRC, SCDHEC, the EPA, and public oversight committees).

Contribution: Lead Technical Specialist for the application of the HTF PA document format/layout, editorial processes, production activities, and graphic/figure development (e.g., sketches, flow sheets, tables, etc.).

GARCIA-DIAZ, BRENDA - SAVANNAH RIVER NATIONAL LABORATORY

Ph.D. Chemical Engineering - University of South Carolina

M.S. Environmental Engineering - University of Puerto Rico - Mayaguez

B.S. Chemical Engineering - University of Puerto Rico - Mayaguez

Experience: Dr. Garcia-Diaz is a Senior Engineer at SRNL with over nine years of experience related to computational simulation and electrochemistry. She has participated in a number of corrosion studies at SRS to characterize waste tank material degradation, to improve corrosion inhibitor limits and to understand corrosion mechanisms in complex solutions. Dr. Garcia-Diaz has worked to combine fundamental modeling with corrosion rate analysis to predict failure times for corrosion prone materials.

Contribution: Dr. Garcia-Diaz was one of the principal corrosion investigators focusing on the degradation modeling of the waste tanks steel liners.

HOMMEL, STEVE – SAVANNAH RIVER REMEDIATION LLC / CLOSURE & WASTE DISPOSAL AUTHORITY

M.S. Information Systems - University of Phoenix

B.S. Earth Science - University of Nevada, Las Vegas

Experience: Mr. Hommel has nearly 10 years of experience working on PA models for HLW projects. Prior to coming to SRS, he used GoldSim to develop validation models for the Total System PA of the DOE's Yucca Mountain Project. In addition to modeling work, his expertise includes statistical and data analyses, software development, and technical checking.

Contributions: Mr. Hommel conducted quality assurance and data verification for the development of the PA and inputs to PORFLOW and GoldSim computer simulations. He performed calculations and data analyses in the development of dose results. Mr. Hommel also prepared and reviewed various PA sections.

JONES, WILLIAM - SAVANNAH RIVER NATIONAL LABORATORY

M.S. Geology - East Carolina University

B.A. Anthropology - East Carolina University

Experience: Mr. Jones is a Principal Scientist at SRNL, with over 20 years of experience related to geology, groundwater hydrology, geochemistry, and geotechnical engineering. He has been involved in closure cap installation, design, and performance evaluation and principal investigator for a variety of groundwater geochemistry and environmental clean-up projects.

Contributions: Mr. Jones' focus has been design and long-term performance evaluation of the closure cap.

JORDAN, JEFFREY - SAVANNAH RIVER NATIONAL LABORATORY

M.S. Mechanical Engineering - Georgia Institute of Technology

B.S. Physics - Furman University

B.A. History - Furman University

Experience: Mr. Jordan is a Senior Engineer at SRNL. He has an M.S. in Mechanical Engineering with a concentration in computational simulation. He has several years of experience with computational modeling of engineered systems. He has been working with groundwater modeling and contaminant transport for the past 2 years.

Contributions: Mr. Jordan focused on developing and evaluating the PORFLOW modeling of groundwater pathways.

KAPLAN, DANIEL - SAVANNAH RIVER NATIONAL LABORATORY

Ph.D. Environmental Geochemistry - The University of Georgia

M.S. Soil Science - University of New Hampshire

B.S. Plant and Soil Science - University of New Hampshire

Experience: Dr. Kaplan is a Senior Fellow Scientist at SRNL with over 20 years of experience related to environmental geochemistry, environmental remediation, surface chemistry, redox chemistry, environmental actinide chemistry, and mineralogy. He has been a principal investigator on a number of multi-year laboratory investigations into geochemical properties of interest to the PA. He has contributed to four PAs at the Hanford Site, six private utilities' EIS', and the Yucca Mountain PA.

Contributions: Dr. Kaplan's primary contribution has been in working with a team of researchers responsible for generating geochemical input parameters and the conceptual model used in the PA.

KNEPP, ANTHONY – INDEPENDENT CONTRACTOR

M.S. Environmental Engineering - Clemson University

Experience: Mr. Knepp has over 30 years of experience as an environmental engineer and former manager who has worked on various nuclear waste planning, design, and cleanup projects for the DOE. He directed the Single Shell Tank Performance Assessment for the Richland Office of DOE, evaluated the environmental cleanup program at Los Alamos for the National Academy of Sciences, and provided technical direction to soil and groundwater cleanup of radioactive waste for the Department of Energy. Mr. Knepp managed the investigation of the impact of leaking radioactive waste from single shell tanks at the Hanford Site.

Contributions: Mr. Knepp provided an independent technical review of the PA.

LANGTON, CHRISTINE - SAVANNAH RIVER NATIONAL LABORATORY

Ph.D. Materials Science and Engineering - Pennsylvania State University

M.S. Geochemistry - Pennsylvania State University

B.S. Geochemistry - Pennsylvania State University

Experience: Dr. Langton is a Senior Fellow Research Scientist at SRNL with over 25 years of experience related to development of cementitious formulations for radioactive salt waste processing, grout formulations for waste tank closures and reactor basin closures, and concrete mix designs for radioactive waste disposal vaults. She has also conducted research on characterization of moisture movement through concrete and pastes under low pressures, leaching of contaminants from waste forms, and characterization of the mineralogy and microstructure associated with chemical and physical degradation of concrete.

Contributions: Dr. Langton's contributions have been the development of closure grout formulations, cementitious material property characterization, and evaluation of the effects and extent of chemical degradation of the cementitious barriers after HTF closure.

LAYTON, MARK – SAVANNAH RIVER REMEDIATION LLC / CLOSURE & WASTE DISPOSAL AUTHORITY

B.S. Nuclear Engineering - University of Cincinnati

Experience: Mr. Layton has over 20 years of experience at SRS in various regulatory compliance organizations. The majority of this time was spent working on HLW regulatory compliance assignments and supporting various Safety Basis activities. Mr. Layton also provided safety basis support for numerous other facilities at SRS and across the DOE complex, including Sandia, Pantex, and Oak Ridge.

Contributions: Mr. Layton was PA development team lead. In addition, he assisted in the preparation and review of various PA sections and provided support to the PA modeling.

LESTER, BARRY – SAVANNAH RIVER REMEDIATION LLC / CLOSURE & WASTE DISPOSAL AUTHORITY

M.S. Geology - Pennsylvania State University

B.S. Earth Science - Pennsylvania State University

Experience: Mr. Lester has over 30 years of experience working in the field of hydrogeology and the development and application of numerical and analytical groundwater flow and contaminant transport codes. He is presently working in support of the H-Area Tank Farm performance assessment modeling efforts. Prior to coming to the Savannah River Site, Mr. Lester worked for the Office of Civilian Radioactive Waste Management division where he helped develop the Yucca Mountain Total Systems Performance Analysis Model. He has also worked for the Office of Environmental Management developing numerical groundwater flow and radionuclide transport models for the Nevada Test Site.

Contributions: Mr. Lester is the primary developer of the GoldSim radionuclide transport model used in the stochastic transport simulations.

MILLINGS, MARGARET - SAVANNAH RIVER NATIONAL LABORATORY

M.S. Geology - University of Georgia

B.S. Geology - The University of the South

Experience: Ms. Millings is a Senior Scientist with the Savannah River National Laboratory with nine years of experience related to groundwater and surface water hydrology, coastal plain geology and geochemistry. At SRNL, she has been involved in various subsurface characterization and monitoring programs and assisted in several environmental remediation projects at the SRS.

Contributions: Ms. Millings was principal investigator providing material property interpretations for the vadose zone to be used in the PORFLOW modeling; in addition, provided assistance in the review of the Tan Clay Confining Zone and water table conditions near H-Area Tank Farm.

O'BRYANT, RANA – SAVANNAH RIVER REMEDIATION LLC / CLOSURE & WASTE DISPOSAL AUTHORITY

M.S. Project Management - The George Washington University

M.B.A. Business Administration - Nova Southeastern University

B.S. Chemical Engineering - University of Tennessee

Experience: Ms. O'Bryant has over 23 years of experience at SRS that started in M Area as a process engineer, maintenance coordinator, and operator-in-charge of an "A" Physical/Chemical wastewater facility. She also spent over five years as a project team lead for environmental restoration activities. For the past 11 years, Ms. O'Bryant's primary responsibility was the characterization of LLW within the tank farms.

Contributions: Ms. O'Bryant provided development of sections related to inventory.

PHIFER, MARK - SAVANNAH RIVER NATIONAL LABORATORY

M.S. Civil Engineering (Environmental and Geotechnical) - University of Tennessee

B.S. Civil Engineering - Tennessee Tech

South Carolina Registered Professional Engineer (No. 12310)

Experience: Mr. Phifer is a Senior Fellow Engineer with the SRNL. He has 25 years of environmental and geotechnical experience at SRS. The first 10 years included environmental regulatory compliance, civil/environmental design, project engineering (closure of a mixed waste landfill and basins (80 acres)), and management (environmental remediation technology). The subsequent 15 years have been at the SRNL developing, deploying, and evaluating waste site closure, groundwater remediation, and radioactive waste disposal technologies. These technologies include horizontal and vertical barrier systems, diffusion barriers, closure caps (including their degradation), waste subsidence, low-level radioactive waste disposal facilities, cementitious barriers and waste forms, permeable reactive barriers, GeoSiphon/GeoFlow groundwater treatment systems, sulfate reduction remediation, reductive dechlorination, and vadose zone and aquifer characterization and testing. For the last seven years, Mr. Phifer has in addition worked on PA and CA related activities.

Contributions: Mr. Phifer was one of the principal investigators focusing on the closure cap configuration and degradation and infiltration estimates.

ROSENBERGER, KENT – SAVANNAH RIVER REMEDIATION LLC / CLOSURE & WASTE DISPOSAL AUTHORITY

B.S. Nuclear Engineering - Pennsylvania State University

Experience: Mr. Rosenberger has over 20 years of experience at SRS primarily in the area of radiological controls. He has spent the last six years supporting tank closure and Saltstone regulatory documents including 3116 waste determination and PA document development. He previously has held positions in radiological engineering project and operations support and facility operational radiological control management. Mr. Rosenberger has considerable experience with the SRS HLW processes and facilities, in addition to experience with reactor, chemical separations, plutonium processing, and storage, and laboratory facilities.

Contributions: Mr. Rosenberger provided management oversight and review.

SAFLEY, LESLIE - PORTAGE, INC./CLOSURE & WASTE DISPOSAL AUTHORITY

M.B.A. Business Administration - Oklahoma State University

M.S. Geology - Oregon State University

B.S. Geology - Oregon State University

Experience: Mr. Safley has over ten years of experience performing data analysis and regulatory document development on DOE waste management and disposal contracts. At SRS, he performs geological analysis and engineering support in the development and interpretation of modeling results. Prior to SRS, he worked on the DOE's Yucca Mountain Project performing data qualification and analysis, quality assurance audits and self-assessments, and database administration.

Contributions: Mr. Safley primarily worked with development of air-pathway analysis sections and preparation of supporting document on off-site well drilling activities. In addition, he assisted in the review of various other PA sections.

SHEPPARD, RICHARD – SAVANNAH RIVER REMEDIATION LLC / CLOSURE & WASTE DISPOSAL AUTHORITY

M.S. Nuclear Science - University of Michigan

B.S. Mathematics - Michigan Technological University

Experience: Mr. Sheppard has over 33 years of experience within the nuclear industry. During his period of commercial nuclear industry experience, his emphasis was on accident analyses and dose assessments for various commercial nuclear power plants and regulatory and licensing activities associated with construction and operation. During his period at SRS, Mr. Sheppard coordinated hazard and safety analyses for design projects at various SRS nuclear facilities. He has spent the past four years supporting the waste determination and PA efforts associated with Saltstone and the closure of waste Tanks 18 and 19.

Contributions: Mr. Sheppard assisted in the preparation and review of various PA sections including the Uncertainty and Sensitivity Analyses.

TAUXE, JOHN - NEPTUNE AND COMPANY, INC.

Ph.D. Civil Engineering - University of Texas at Austin

M.S. Civil Engineering - University of Texas at Austin

B.A. Earth Science - Wesleyan University

Experience: Dr. Tauxe has been working in the earth and environmental sciences and engineering since 1981, and has developed expertise in quantitative hydrology and hydrogeology, and in computer programming, concentrating in the modeling of contaminant fate and transport in the environment. His relevant professional experience centers on modeling in support of radiological performance assessment in a probabilistic context at several sites in the DOE complex since 1994.

Contributions: Dr. Tauxe supervised uncertainty and sensitivity analysis work within Neptune and Company and provided interpretation of these analyses.

WATKINS, DAVID - SAVANNAH RIVER REMEDIATION LLC / CLOSURE & WASTE DISPOSAL AUTHORITY

B.S. Geology - College of Charleston

Experience: Mr. Watkins has over 28 years of experience in environmental monitoring, regulatory compliance, geologic characterizations, and project management. His assignments over the last 20 years at SRS have included preparing and reviewing Regulatory Compliance documents including RFI/RI/BRAs, RFI Work Plans, Records of Decision, Statement of Basis/Proposed Plans, Corrective Measure Studies/Feasibility Studies, and RCRA Part B Permit Renewal Applications. Mr. Watkins has performed hydrogeologic characterizations, data compilation, and groundwater monitoring for various Operable Units at the SRS and prepared associated maps and reports. Mr. Watkins also has experience in preparing and reviewing construction authorization environmental reports for commercial nuclear power plants.

Contributions: Mr. Watkins provided development of sections related to hydrogeology, waste tank design, source term release, radionuclide transport, and RCRA/CERCLA compliance. In addition, he assisted in the preparation and review of various other PA sections.

WIERSMA, BRUCE - SAVANNAH RIVER NATIONAL LABORATORY

Ph.D. Chemical Engineering - Iowa State University

M.S. Chemical Engineering - Iowa State University

B.S. Chemical Engineering - Purdue University

Experience: Dr. Wiersma is an Advisory Engineer at SRNL with over 20 years of experience related to materials, corrosion, and structural integrity issues. His primary responsibilities have been associated with the structural integrity of the high-level radioactive waste tanks. In his role, he has been responsible for planning experimental corrosion performance of material programs, establishing criteria to evaluate the programs and assessing the applicability or feasibility of the results or methods recommended to the field. Bruce serves as a member on several expert panels related to waste tanks and has published many technical articles on aluminum corrosion, and on corrosion of stainless steel and carbon steel in radioactive wastes.

Contributions: Dr. Wiersma was one of the principal investigators for the life estimation of the waste tank steel liners for H-Tank Farm modeling.

**ZIMMERY, JEFFREY - TETRA TECH NUS, INC. / CLOSURE & WASTE DISPOSAL
AUTHORITY**

B.S. Health Physics - Francis Marion University, Florence, SC

Experience: Mr. Zimmerly has over 10 years of experience in nuclear environmental engineering, health physics, and regulatory compliance. His experience includes preparing and reviewing of Environmental Impact Statements for DOE, including the SRS HLW Tank Closure EIS and the SEIS for Salt Disposition at SRS. Mr. Zimmerly has experience in preparing and reviewing License Renewal environmental reports for existing commercial nuclear power plants and the environmental reports for Early Site Permits/Combined Operating License Applications for new commercial nuclear power generation.

Contributions: Mr. Zimmerly provided development sections related to the description of exposure pathways and equations. In addition, he assisted in the review of various other PA sections.

10.0 REFERENCES

10 CFR 20, *Standards for Protection Against Radiation*, U.S. Nuclear Regulatory Commission, Washington DC, January 5, 2010.

10 CFR 50, Appendix I, *Numerical Guides for Design Objectives and Limiting Conditions for Operation to Meet the Criterion "as Low as is Reasonably Achievable" for Radioactive Material*, U.S. Nuclear Regulatory Commission, Washington DC, January 4, 2011.

10 CFR 61, *Licensing Requirements for Land Disposal of Radioactive Waste*, U.S. Nuclear Regulatory Commission, Washington DC, January 5, 2010.

10 CFR 830, *Nuclear Safety Management*, U.S. Nuclear Regulatory Commission, Washington DC, January 15, 2010.

1Q Manual, Procedure 20-1, *Quality Assurance Manual, Software Quality Assurance*, Savannah River Site, Aiken, SC, Rev. 11, December 17, 2008.

1Q Manual, Procedure 2-1, *Quality Assurance Manual, Quality Assurance Program*, Savannah River Site, Aiken, SC, Rev. 10, December 17, 2008.

40 CFR 61-Subpart H, Title 40, *Protection of Environment*, Part 61, *National Emission Standards for Hazardous Air Pollutants*, Subpart H, *National Emission Standards for Emissions of Radionuclides other than Radon from Department of Energy Facilities*, U.S. Nuclear Regulatory Commission, Washington DC, April 19, 2012.

AA98142C-031, *ASME Code Calculations for High Level Waste Evaporator*, Savannah River Site, Aiken, SC, Rev. 1, June 17, 1993.

AA98142C-040, *Evaporator Outline and Assembly*, Savannah River Site, Aiken, SC, Rev. G, January 9, 1996.

ACRi-1994, (Copyright), *PORFLOW Validation*, Version 2.5, Analytic & Computational Research, Inc., Bel Air, CA, March 31, 1994.

ACRi-2008, (Copyright), *PORFLOW User's Manual*, Version 6.0, Analytic and Computational Research, Inc., Bel Air, CA, July 21, 2008.

ANL-EAD-4, Yu, C., et al., *User's Manual for RESRAD Version 6*, Argonne National Laboratory, Chicago, IL, July 2001.

ANL-EAIS-8, Yu, C., et al., *Data Collection Handbook to Support Modeling the Impacts of Radioactive Material in Soil*, Argonne National Laboratory, Chicago, IL, April 1993.

ASME NQA-1, (Copyright), *Quality Assurance Requirements for Nuclear Facility Applications*, The American Society of Mechanical Engineers, New York, NY, March 14, 2008.

ASTM D 6092 – 97, (Copyright), *Standard Practice for Specifying Standard Sizes of Stone for Erosion Control*, ASTM International, West Conshohocken, PA, June 01, 2008.

ASTM D 6103 – 04, (Copyright), *Standard Test Method for Flow Consistency of Controlled Low Strength Material (CLSM)*, ASTM International, West Conshohocken, PA, March 11, 2004.

B-SQP-C-00002, *Software Quality Assurance Plan for GoldSim for the Savannah River Site's Liquid Waste Program*, Savannah River Site, Aiken, SC, Rev. 0, April 23, 2012.

B-SQP-C-00003, *Software Quality Assurance Plan for ReadFlowFields.dll for the Savannah River Site's Liquid Waste Program*, Savannah River Site, Aiken, SC, Rev. 0, July 12, 2012.

CAP-88, Beres, D.A., *The Clean Air Act Assessment Package - 1988 (CAP-88) A Dose and Risk Assessment Methodology for Radionuclide Emissions to Air Volume 1 User's Manual*, U.S. Environmental Protection Agency, Washington DC, October 1990.

CBU-PIT-2005-00120, Caldwell, T.B., *Ancillary Equipment Residual Radioactivity Estimate to Support Tank Closure Activities for F-Tank Farm*, Savannah River Site, Aiken, SC, Rev. 0, June 16, 2005.

CBU-PIT-2005-00228, Hamm, B.A., *High-Level Waste Tank Farm Closure, Radionuclide Screening Process (First-Level), Development and Application*, Savannah River Site, Aiken, SC, Rev. 0, November 7, 2006.

C-CH-H-8096, *Replacement High Level Waste Evaporator Jacketed Yard Piping Support Details*, Savannah River Site, Aiken, SC, Rev. 0, September 30, 1993.

C-CM-H-7026, *Waste Transfer System 241—96H Valve Box Plan and Sections Structural*, Savannah River Site, Aiken, SC, Rev. 0, April 27, 2005.

CDC-2006, *Risk Based Screening of Radionuclide Releases from the Savannah River Site*, Center for Disease Control, Atlanta, GA, August 2006.

C-ESR-G-00003, Waltz, R.S., *SRS High Level Waste Tank Leaksite Information*, Savannah River Site, Aiken, SC, Rev. 5, January 4, 2011.

D116001, *200 Area Building 241-F&H Bottom Cooling Coils for Waste Storage Tank*, Savannah River Site, Aiken, SC, Rev. 10, July 21, 1955.

D116048, *200 Area Building 241-F&H Vertical Cooling Coils for Waste Storage Tank*, Savannah River Site, Aiken, SC, Rev. 37, September 8, 1955.

D116850, *Pump Tank 12' 0" Diameter X 8' 6"*, Savannah River Site, Aiken, SC, Rev. 24, December 4, 1985.

D129961, *Buildings 241 F/H E.P. No. 241H-352.78, E.P. No. 241F-352.78*, Savannah River Site, Aiken, SC, Rev. 7, August 6, 1952.

D139006, *Tank Detail, Sheet 1*, Savannah River Site, Aiken, SC, Rev. 9, January 6, 1971.

D189542, *Bldg 241 H DWPF Sludge Precipitate Transfer Valve Box Detail Process Sh. 1*, Savannah River Site, Aiken, SC, Rev. 49, May 4, 2000.

D199324, *Bldg. 241 H Tank 40 Waste Transfer Facilities Valve Box Det. Y340 Process Sh. 1*, Savannah River Site, Aiken, SC, Rev. 26, August 22, 1986.

DHEC_01-25-1993, *Bureau of Water, Permit to Construct, F and H-Area High-Level Radioactive Waste Tank Farms, Construction Permit #17,424-IW*, South Carolina Department of Health and Environmental Control, Columbia, SC, January 25, 1993.

DHEC_03-03-1993, *F and H Area High Level Radioactive Waste Tank Farms Construction Permit No.: 17, 424-IW, Partial Permit to Operate*, as amended, South Carolina Department of Health and Environmental Control, Columbia, SC, March 3, 1993.

DHEC_09-12-1988, Crapse, B., *Project: Tank 50 As-Builts Construction Permit No. 14520 County: Aiken*, South Carolina Department of Health and Environmental Control, Columbia, SC, September 12, 1988.

DOE Format Guide, DRAFT - *Format and Content Guide for U.S. Department of Energy Low-Level Waste Disposal Facility Performance Assessments and Composite Analyses*, U.S. Department of Energy, Washington DC, May 11, 2007.

DOE G 435.1-1, *Implementation Guide for use with DOE M 435.1-1*, U.S. Department of Energy, Washington DC, July 9, 1999.

DOE M 435.1-1, *Radioactive Waste Management Manual*, U.S. Department of Energy, Washington DC, Chg. 1, January 9, 2007.

DOE O 414.1D, *Quality Assurance*, U.S. Department of Energy, Washington DC, April 25, 2005.

DOE O 435.1, Chg. 1, *Radioactive Waste Management*, U.S. Department of Energy, Washington DC, August 28, 2001.

DOE P 450.4A, *Integrated Safety Management Policy*, Savannah River Site, Aiken, SC, Rev. 0, October 15, 1996.

DOE_02-09-2006, *Compliance with DOE M 435.1-1 Waste Incidental to Reprocessing (WIR) requirements and Implementation of Section 3116(a) of the National Defense Authorization Act for Fiscal Year 2005 (NDAA)*, Department of Energy, Washington DC, February 9, 2006.

DOE_02-23-2011, Wallo, A., *Use of International Commission of Radiological Protection Publication 60, Radiation Protection (1991a) and 72 Age-dependent Doses to the Members of the Public from Intake of Radionuclides Part 5, Compilation of Ingestion and Inhalation Coefficients for the Savannah River Site Performance Assessments*, U.S. Department of Energy, Washington DC, February 23, 2011.

DOE-EIS-0303 ROD, *Savannah River Site High-Level Waste Tank Closure Final Environmental Impact Statement Record of Decision*, U.S. Department of Energy, Washington DC, August 19.

DOE-EIS-0303, *Savannah River Site High-Level Waste Tank Closure Final Environmental Impact Statement*, Savannah River Site, Aiken, SC, May 2002.

DOE-HDBK-3010-94, *Airborne Release Fractions/Rates and Respirable Fractions for Nonreactor Nuclear Facilities, Volume 1 - Analysis of Experimental Data*, U.S. Department of Energy, Washington DC, December 1994.

DOE-ID-10966, *Performance Assessment for the Tank Farm Facility at the Idaho National Engineering and Environmental Laboratory, Final*, Idaho National Laboratory, Idaho Falls, ID, Rev. 1, April 2003.

DP-1358, Poe, W.L., *Leakage from Waste Tank 16, Amount, Fate, and Impact*, Savannah River Site, Aiken, SC, November 1974.

DP-1448, Stone, J.A., *Evaluation of Concrete as a Matrix for Solidification of Savannah River Plant Waste*, Savannah River Site, Aiken, SC, Rev. 0, June 30, 1977.

DP-478, Daniel, A.N., *Underground Storage of Low Level Radioactive Wastes at the Savannah River Plant, Engineering Considerations*, Savannah River Site, Aiken, SC, Rev. 2, June 1960.

E7 Manual, Procedure 2.31, *Conduct of Engineering and Technical Support Procedure Manual, Engineering Calculations*, Savannah River Site, Aiken, SC, Rev. 10, September 27, 2007.

E7 Manual, Procedure 2.60, *Conduct of Engineering and Technical Support Procedure Manual, Technical Reviews*, Savannah River Site, Aiken, SC, Rev. 14, April 24, 2012.

E7-1, Procedure DE-DP-384, *PD & CS Design Services Conduct of Engineering and Technical Support, ALARA Design Considerations and Reviews*, Savannah River Site, Aiken, SC, Rev. 1, November 20, 2008.

EPA 815-R-02-001, *Radionuclides in Drinking Water: A Small Entity Compliance Guide*, U.S. Environmental Protection Agency, Washington DC, February 2002.

EPA 816-F-09-0004, *National Primary Drinking Water Regulations*, U.S. Environmental Protection Agency, Washington DC, May 2009.

EPA 816-F-10-079, *Secondary Drinking Water Regulations: Guidance for Nuisance Chemicals*, U.S. Environmental Protection Agency, Washington DC, January 7, 2011.

EPA_RSLs_April2012, *Regional Screening Level (RSL) Summary Table April 2012*, U.S. Environmental Protection Agency, April 2012.

EPA-402-R-93-081, *Federal Guidance Report No. 12, External Exposure to Radionuclides in Air, Water, and Soil*, U.S. Environmental Protection Agency, Washington DC, September 1993.

EPA-520-1-88-020, *Federal Guidance Report No. 11, Limiting Values of Radionuclide Intake and Air Concentration and Dose Conversion Factors for Inhalation, Submersion, and Ingestion*, U.S. Environmental Protection Agency, Washington DC, September 1998.

EPA-600-2-87-049, Schroeder, P.R., et al., *Verification of the Lateral Drainage Component of the HELP Model Using Physical Models*, U.S. Environmental Protection Agency, Cincinnati, OH, July 1987.

EPA-600-2-87-050, Schroeder, P.R. and Peyton, R.L., *Verification of the Hydrologic Evaluation of Landfill Performance (HELP) Model Using Field Data*, U.S. Environmental Protection Agency, Cincinnati, OH, July 1987.

EPA-600-P-95-002Fa-c, *U.S. EPA Exposure Factors Handbook (Final Report)*, U.S. Environmental Protection Agency, Washington DC, August 1997.

EPA-600-R-94-168a, Schroeder, P.R., et al., *The Hydrologic Evaluation of Landfill Performance (HELP) Model: User's Guide for Version 3*, U.S. Environmental Protection Agency, Cincinnati, OH, September 1994.

EPA-600-R-94-168b, Schroeder, P.R., et al., *The Hydrologic Evaluation of Landfill Performance (HELP) Model: Engineering Documentation for Version 3*, U.S. Environmental Protection Agency, Cincinnati, OH, September 1994.

EPA-822-R-00-001, *Estimated Per Capita Water Ingestion and Body Weight in the United States - An Update, Based on Data Collected by the United States Department of Agriculture's 1994 - 1996 and 1998 Continuing Survey of Food Intakes by Individuals*, U.S. Environmental Protection Agency, Washington DC, October 2004.

EPA-PRGs_11-13-2007, *Radionuclide Toxicity and Preliminary Remediation Goals for Superfund*, U.S. Environmental Protection Agency, November 13, 2007.

ERD-AG-003_F.17, *Environmental Restoration Division, Conceptual Site Model Development*, Savannah River Site, Aiken, SC, Rev. 0, September 21, 2000.

ERD-AG-003_P.1.4, *Environmental Restoration Division, Development of Exposure Groups*, Savannah River Site, Aiken, SC, Rev. 1, January 22, 1998.

ERD-AG-003_P.1.5, *Environmental Restoration Division, Exposure Pathways*, Savannah River Site, Aiken, SC, Rev. 0, August 10, 1997.

ERD-AG-003_P.5.2, *Environmental Restoration Division, Contaminant Migration Constituents of Concern*, Savannah River Site, Aiken, SC, Rev. 2, September 27, 2000.

ERD-AG-003_P.10.1, *Soil and Groundwater Closure Projects, Evaluation of Source Materials at SRS Waste Units*, Savannah River Site, Aiken, SC, Rev 1, September 11, 2006.

G-SQP-A-00012, Hang, T., *PORFLOW Software Quality Assurance Plan*, Savannah River Site, Aiken, SC, Rev 0, June 2007. HNF-SD-WM-TI-707, Rittmann, P.D., *Exposure Scenarios and Unit Dose Factors for Hanford Tank Waste Performance Assessments*, Hanford Site, Richland, WA, Rev. 3, July 2003.

GTG-2010d, (Copyright), *User's Guide GoldSim Probabilistic Simulation Environment Volume 1 of 2*, GoldSim Technology Group, Issaquah, WA, Ver. 10.5, December 2010.

GTG-2010e, (Copyright), *User's Guide GoldSim Contaminant Transport Module*, GoldSim Technology Group, Issaquah, WA, Ver. 6.0, December 2010.

HNF-SD-WM-TI-707, *Exposure Scenarios and Unit Dose Factors for Hanford Tank Waste Performance Assessments*, Fluor Federal Services, Richland, WA, Rev. 3, July 2003.

IAEA-364, (Copyright), *Handbook of Parameter Values for the Prediction of Radionuclide Transfer in Template Environments, Produced in Collaboration with the International Union of Radioecologists*, International Atomic Energy Agency, Technical Reports Series 364, Rev. 10-23-56, International Atomic Energy Agency, Vienna, June 1994.

IAEA-472, (Copyright), *Handbook of Parameter Values for the Prediction of Radionuclide Transfer in Terrestrial and Freshwater Environments, Technical Reports Series No. 472*, International Atomic Energy Agency, Vienna, January 2010.

ICRP-72 (Copyright), *Radiation Protection: ICRP Publication 72 - Age-Dependent Doses to Members of the Public from Intake of Radionuclides: Part 5 Compilation of Ingestion and Inhalation Dose Coefficients*, International Commission on Radiological Protection, Didcot, Oxfordshire, September 1995.

ISSN 0017-9078, (Copyright), Hamby, D.M., *Site-Specific Parameter Values for the Nuclear Regulatory Commission's Food Pathway Dose Model*, Health Physics Radiation Protection Journal, Vol. 62, No. 2, Charleston, SC, Rev 0, February 1992.

ISSN 0167-9473 Vol. 38, No. 4, (Copyright), Friedman, J.H., *Stochastic Gradient Boosting*, Savannah River Site, Aiken, SC, Rev. 0, March 26, 1999.

ISSN 0885-6125 Vol. 24, No. 2, (Copyright), Breiman, L., *Machine Learning, Bagging Predictors*, University of California, Berkeley, CA, August 1, 1996.

ISSN 0885-6125 Vol. 40, No. 2, (Copyright), Dietterich, T.G., *An Experimental Comparison of Three Methods for Constructing Ensembles of Decision Trees: Bagging, Boosting, and Randomization*, Oregon State University, Corvallis, OR, January 1, 2000.

ISSN 1019-0643, (Copyright), Bradbury, M.H., and Sarott, F., *Sorption Databases for the Cementitious Near-Field of a L/ILW Repository for Performance Assessment*, Paul Scherrer Institute, Labor für Entsorgung, Villigen PSI, Switzerland, Rev. 0, March 1995.

K-CLC-F-00034, McHood, M.D., *APSF Soft Zone Settlement Analysis*, Savannah River Site, Aiken, SC, Rev. 0, June 1, 1998.

K-CLC-F-00073, Li, W.T., *Static Settlement of F-Area Waste Storage Tanks 18 and 19*, Savannah River Site, Aiken, SC, Rev. 2, June 20, 2006.

K-ESR-G-00013, Lewis, M.R., *SRS Soft Zone Initiative – Historical Perspective*, Savannah River Site, Aiken, SC, Rev. 0, January 2008.

LWO-PIT-2007-00025, Hill, P.J., *Response to the NRC's Request for Additional Information Comment #15*, Savannah River Site, Aiken, SC, Rev. 0, March 6, 2007.

ML071550458, Camper, L.W., *Enhanced Consultation Process for Waste Determination Activities Conducted under the Ronald W. Reagan National Defense Authorization Act for Fiscal Year 2005*, U.S. Nuclear Regulatory Commission, Washington DC, June 15, 2007.

ML083190829, Simpkins, A.A., et al., *Description of Methodology for Biosphere Dose Model BDOSE*, U.S. Nuclear Regulatory Commission, Washington DC, Rev. 1, November 30, 2008.

ML100970781, Lowman, D., *Savannah River Site H-Area Tank Farm Input Packages/References*, U.S. Nuclear Regulatory Commission, Washington DC, April 13, 2010.

M-ML-G-0005, *Structural Integrity Database (F/H Areas)*, Savannah River Site, Aiken, SC, Rev. 45, August 21, 2003.

MP 1-01, Policy 4.2, *Management Policies, Quality Assurance*, Savannah River Site, Aiken, SC, Rev 5, December 22, 2009.

NCRP-123 Vol. 1, (Copyright), *Screening Models for Releases of Radionuclides to Atmosphere, Surface Water, and Ground*, Vol. 1, National Council on Radiation Protection and Measurements, Bethesda, MD, January 22, 1996.

NCRP-123 Vol. 2, (Copyright), *Screening Models for Releases of Radionuclides to Atmosphere, Surface Water and Ground-Work Sheets*, Vol. 2, National Council on Radiation Protection and Measurements, Bethesda, MD, January 22, 1996.

NCRP-160, (Copyright), *Ionizing Radiation Exposure of the Population of the United States (2009)*, National Council on Radiation Protection and Measurements, Bethesda, MD, March 2009.

NDAA_3116, *Public Law 108-375, Ronald W. Reagan National Defense Authorization Act for Fiscal Year 2005, Section 3116, Defense Site Acceleration Completion*, Accessed January 4, 2011.

NRMP-2005, *Natural Resources Management Plan for the Savannah River Site*, Savannah River Site, Aiken SC, May 2005.

NUREG_CR-4370, *Update of Part 61 Impacts Analysis Methodology*, U.S. Nuclear Regulatory Commission, Washington DC, Vol. 1, January 31, 1986.

NUREG_CR-5512, Kennedy, W.E., Jr., et al., *Residual Radioactive Contamination From Decommissioning, Technical Basis for Translating Contamination Levels to Annual Total Effective Dose Equivalent, Final Report*, Vol. 1, U.S. Nuclear Regulatory Commission, Washington DC, October 1992.

NUREG_CR-6377, *Effects of Radionuclide Concentrations by Cement/Ground-Water Interactions in Support of Performance Assessment of Low-Level Radioactive Waste Disposal Facilities*, U.S. Nuclear Regulatory Commission, Washington DC, May 1, 1998.

NUREG-0782, *Draft Environmental Impact Statement on 10 CFR Part 61 "Licensing Requirements for Land Disposal of Radioactive Waste,"* U.S. Nuclear Regulatory Commission, Washington DC, September 1981.

NUREG-0945, *Final Environmental Impact Statement on 10 CFR 61 "Licensing Requirements for Land Disposal of Radioactive Waste," Summary and Main Report, Vol. 1,* U.S. Nuclear Regulatory Commission, Washington DC, March 1982.

NUREG-1573, *A Performance Assessment Methodology for Low-Level Radioactive Waste Disposal Facilities*, U.S. Nuclear Regulatory Commission, Washington DC, October 2000.

NUREG-1623, Johnson, T.L., *Design of Erosion Protection for Long-Term Stabilization*, U.S. Nuclear Regulatory Commission, Washington DC, September 2002.

NUREG-1854, *NRC Staff Guidance for Activities Related to U.S. Department of Energy Waste Determinations, Draft Final Report for Interim Use*, U.S. Nuclear Regulatory Commission, Washington DC, August 2007.

NUREG-1923, *Safety Evaluation Report for an Early Site Permit (ESP) at the Vogtle Electric Generating Plant (VEGP) ESP Site*, U.S. Nuclear Regulatory Commission, Washington DC, July 2009.

ORNL-5786, Baes, C.F., III, et al., *A Review and Analysis of Parameters for Assessing Transport of Environmentally Released Radionuclides through Agriculture*, Oak Ridge National Laboratory, Oak Ridge, TN, September 1984.

OSWER 9380.3-06FS, *A Guide to Principal Threat and Low Level Threat Wastes*, U.S. Environmental Protection Agency, Washington DC, November 1991.

PIT-MISC-0041, *Discussion Draft, SRS Long Range Comprehensive Plan*, Savannah River Site, Aiken, SC, Rev. 0, December 2000.

PIT-MISC-0089, *Savannah River Site End State Vision*, Savannah River Site, Aiken, SC, Rev. 0, July 26, 2005.

PIT-MISC-0104, *Soil Survey of Savannah River Plant Area, Parts of Aiken, Barnwell, and Allendale Counties, South Carolina*, Soil Conservation Service, U.S. Department of Agriculture, Washington DC, June 1990.

PIT-MISC-0112, Aadland, R., et al., *Hydrogeologic Framework of West-Central South Carolina*, Report 5, South Carolina Department of Natural Resources, Columbia, SC, 1995.

PNNL-13421, Staven, L.H., et al., *A Compendium of Transfer Factors for Agricultural and Animal Products*, Pacific Northwest Laboratory, Richland, WA, June 2003.

PORTAGE-08-022, *H-Area Tank Farm Model Development for Tanks in the Water Table PORFLOW Version 6.20.0*, Savannah River Site, Aiken, SC, Rev. 0, November 2008.

P-PJ-H-7973, *New Hill In-Tank Precipitation Waste Transfer System Tk-50 Valve Box Details Process*, Savannah River Site, Aiken, SC, Rev. 1, July 2, 2002.

P-PM-H-7723, *Waste Removal and Extended Sludge Processing Facility Tank 21 Valve Box Details Sht. 1 Process*, Savannah River Site, Aiken, SC, Rev. 3, April 2, 1998.

P-PM-H-7726, *Waste Removal & Extended Sludge Processing Facility, Tank 21 & 22 Valve Box Assembly Process*, Savannah River Site, Aiken, SC, Rev. 2, January 22, 1998.

PV179667, *Bldg 241H 200H Area Waste Storage Facility Finished Pump Tank Assembly Process EP Y520-1-1 & 521-1-1*, Savannah River Site, Aiken, SC, Rev. 7, June 1, 1981.

Q-SQA-A-00005, Phifer, M.A., *Software Quality Assurance Plan for the Hydrologic Evaluation of Landfill Performance (HELP) Model*, Savannah River Site, Aiken, SC, Rev. 0, October 2006.

Q-SQP-A-00002, Farfán, E.B., *Software Quality Assurance Plan for Environmental Dosimetry*, Savannah River Site, Aiken, SC, Rev. 2, May 2007.

Q-SQP-G-00003, Flach, G.P., *Software Quality Assurance Plan for Aquifer Model Refinement Tool (MESH3D)*, Savannah River Site, Aiken, SC, Rev. 0, February 26, 2007.

Regulatory Guide 1.109, *Calculation of Annual Doses to Man From Routine Releases of Reactor Effluents for the Purpose of Evaluating Compliance with 10 CFR 50*, Appendix I, U.S. Nuclear Regulatory Commission, Washington DC, Rev. 1, October 1977.

S5-2-11980, *Sludge Washing Facilities Waste Storage Tank 16 Transfer Tie-In Valve Box Details*, Savannah River Site, Aiken, SC, Rev. 0, March 3, 1983.

S5-2-1341, *Final Waste Evaporator Additional Waste Storage Facilities Diversion Box No. 3 Plan and Details*, Savannah River Site, Aiken, SC, Rev. 17, February 20, 1997.

S5-2-4262, *Waste Evaporator Diversion Box No. 5 Concrete Plan and Details*, Savannah River Site, Aiken, SC, Rev. 6, May 6, 1998.

SCDHEC R.61-58, *State Primary Drinking Water Regulation*, Bureau of Water, South Carolina Department of Health and Environmental Control, Columbia, SC, August 28, 2009.

SCDHEC R.61-67, *Standards for Wastewater Facility Construction*, South Carolina Department of Health and Environmental Control, Columbia, SC, May 24, 2002.

SCDHEC R.61-68, *Water Classification & Standards*, South Carolina Department of Health and Environmental Control, Columbia, SC, April 25, 2008.

SCDHEC R.61-82, *Proper Closeout of Wastewater Treatment Facilities*, South Carolina Department of Health and Environmental Control, Columbia, SC, April 11, 1980.

SE5-2-2004260, *Evaporator Building Equipment Arrangement Lower Plan Process*, Savannah River Site, Aiken, SC, Rev. 5, March 24, 2003.

SE5-2-2004313, *Replacement HLW Evaporator, Section "C-C", Concrete*, Savannah River Site, Aiken, SC, Rev. 2, March 28, 1994.

Spec-3019, Christy, W.O., *Specification for Building Materials & Plumbing, Supplement No. 4*, Savannah River Site, Aiken, SC, May 5, 1960.

SRNL-ESB-2007-00035, Millings, M., et al., *Addendum to Integrated Hydrogeological Modeling Report of the General Separations Area (GSA)*, Savannah River Site, Aiken, SC, October 24, 2007.

SRNL-ESB-2008-00023, Phifer, M.A., et al., *H-Area Tank Farm Closure Cap and Infiltration*, Savannah River Site, Aiken, SC, Rev. 0, May 21, 2008.

SRNL-L3200-2012-00023, Flach, G.P., and Hang, T., *SRNL Design Checking for H-Tank Farm PA Rev. 1 PORFLOW Modeling*, Savannah River Site, Aiken, SC, Rev. 0, August 14, 2012.

SRNL-PSE-2006-00097, Bibler, N.E., *Calculation of Radiation Heat Loads and Dose Rates in SRS Tanks 18 and 19 Residual Wastes*, Savannah River Site, Aiken, SC, April 27, 2005.

SRNL-STI-2009-00150, McDowell-Boyer, L., et al., *Distribution Coefficients (K_{ds}), K_d Distributions, and Cellulose Degradation Product Correction Factors for the Composite Analysis*, Savannah River Site, Aiken, SC, Rev. 1, April 2009.

SRNL-STI-2009-00178, Hinton, T., et al., *Systems Model of Carbon Dynamics in Four Mile Branch on the Savannah River Site*, Savannah River Site, Aiken, SC, Rev. 1, March 25, 2009.

SRNL-STI-2009-00473, Kaplan, D.I., *Geochemical Data Package for Performance Assessment Calculations Related to the Savannah River Site*, Savannah River Site, Aiken, SC, March 15, 2010.

SRNL-STI-2010-00018, Farfán, E.B., *Air Pathway Dose Modeling for the H-Area Tank Farm*, Savannah River Site, Aiken, SC, January 22, 2010.

SRNL-STI-2010-00035, Langton, C. A., *Chemical Degradation Assessment for the H-Area Tank Farm Concrete Tanks and Fill Grouts*, Savannah River Site, Aiken, SC, Rev. 0, January 29, 2010.

SRNL-STI-2010-00047, Garcia-Diaz, B.L., *Life Estimation of High Level Waste Tank Steel for H-Tank Farm Closure Performance Assessment*, Savannah River Site Aiken, SC, March 2010.

SRNL-STI-2010-00135, Dixon, K., *Air and Radon Pathway Modeling for the H-Area Tank Farm*, Savannah River Site, Aiken, SC, Rev. 0, June 2010.

SRNL-STI-2010-00148, Jones, W.E., et al., *Hydrogeologic Data Summary in Support of the H-Area Tank Farm Performance Assessment*, Savannah River Site, Aiken, SC, Rev. 0, February 2010.

SRNL-STI-2010-00439, Oji, L.N., et al., *Characterization of Additional Tank 19F Floor Samples*, Savannah River Site, Aiken, SC, Rev. 0, August 31, 2010.

SRNL-STI-2010-00447, Jannik, G.T., et al., *Land and Water Use Characteristics and Human Health Input Parameters for Use in Environmental Dosimetry and Risk Assessments at the Savannah River Site*, Savannah River Site, Aiken, SC, Rev. 0, August 6, 2010.

SRNL-STI-2010-00493, Seaman, J.C., and Kaplan, D.I., *Chloride, Chromate, Silver, Thallium, and Uranium Sorption to SRS Soils, Sediments, and Cementitious Materials*, Savannah River Site, Aiken, SC, Rev. 0, September 29, 2010.

SRNL-STI-2010-00667, Almond, P.M., and Kaplan, D.I., *Distribution Coefficients (K_d) Generated from a Core Sample Collected from the Saltstone Disposal Facility*, Savannah River Site, Aiken, SC, Rev. 0, April 29, 2011.

SRNL-STI-2011-00011, Kaplan, D.L., *Estimated Neptunium Sediment Sorption Values as a Function of pH and Measured Barium and Radium K_d Values*, Savannah River Site, Aiken, SC, Rev. 0, January 23, 2011.

SRNL-STI-2011-00498, Dien, L., et al., *Mobilization and Characterization of Colloids Generated From Cement Leachates Moving Through a SRS Sandy Sediment*, Savannah River Site, Aiken, SC, Rev. 0, September 20, 2011.

SRNL-STI-2011-00551, Langton, C.A., et al., *Tanks 18 and 19-F Structural Flowable Grout fill Material Evaluation and Recommendations*, Savannah River Site, Aiken, SC, Rev. 0, September 2011.

SRNL-STI-2011-00672, Almond, P.M., et al., *Variability of K_d Values in Cementitious Materials and Sediments*, Savannah River Site, Aiken, SC, Rev. 0, February 2012.

SRNL-STI-2012-00404, Denham, M., and Millings, M., *Evolution of Chemical Conditions and Estimated Solubility Controls on Radionuclides in the Residual Waste Layer During Post-Closure Aging of High-Level Waste Tank*, Savannah River Site, Aiken, SC, Rev. 0, August TBD, 2012.

SRNL-STI-2012-00465, Jordan, J.M., et al., *PORFLOW Modeling Supporting the H-Tank Farm Performance Assessment*, Savannah River Site, Aiken, SC, August 2012.

SRNL-TR-2010-00096, Denham, M., *Vapor - Aqueous Solution Partition Coefficients for Radionuclides Pertinent to High Level Waste Tank Closure*, Savannah River Site, Aiken, SC, July 2010.

SRNL-TR-2010-00213, Whiteside, T., *Software Testing and Verification of PORFLOW Versions 6.30.1 and 6.30.2*, Savannah River Site, Aiken, SC, Rev. 0, July 2010.

SRNL-TR-2012-00160, Bagwell, L., *A Review of Subsurface Soft Zones at Savannah River Site with Emphasis on H Area Tank Farm*, Savannah River Site, Aiken, SC, Rev. 0, July 2012.

SRNS-J6000-2011-00030, *Savannah River Site 2012 ALARA Goals*, Savannah River Site, Aiken, SC, December 2011.

SRNS-STI-2008-00286, Kaplan, D.I., et al., *Range and Distribution of Technetium K_d Values in the SRS Subsurface Environment*, Savannah River Site, Aiken, SC, Rev. 1, October 28, 2008.

SRNS-STI-2009-00190, Mamatey, A.R., *Savannah River Site Environmental Report for 2008*, Savannah River Site, Aiken, SC, October 6, 2009.

SRNS-STI-2011-00059, *Savannah River Environmental Report for 2010*, Savannah River Site, Aiken, SC, August 2011.

SRNS-TR-2009-00076, *Savannah River Site Groundwater Protection Program*, Savannah River Site, Aiken, SC, Rev. 1, February 2009.

SRR-CWDA-2009-00017, *Performance Assessment for the Saltstone Disposal Facility at the Savannah River Site*, Savannah River Site, Aiken, SC, Rev. 0, October 29, 2009.

SRR-CWDA-2010-00019, *H-Area Tank Farm Grout and Concrete Degradation Modeling Information*, Savannah River Site, Aiken, SC, Rev. 0, March 15, 2010.

SRR-CWDA-2010-00023, (Superseded) *H-Area Tank Farm Closure Inventory for use in Performance Assessment Modeling*, Savannah River Site, Aiken, SC, Rev. 1, November 2010.

SRR-CWDA-2010-00023, *H-Tank Farm Waste Tank Closure Inventory for use in Performance Assessment Modeling*, Savannah River Site, Aiken, SC, Rev. 3, May 10, 2012.

SRR-CWDA-2010-00033, *Comment Response Matrix for Nuclear Regulatory Commission (NRC) Requests for Additional Information (RAIs) on the Saltstone Disposal Facility Performance Assessment (SRR-CWDA-2009-00017, Revision 0, dated October 29, 2009)*, Savannah River Site, Aiken, SC, Rev. 1, July 23, 2010.

SRR-CWDA-2010-00054, *Evaluation of Well Drilling Records in the Vicinity of SRS from CY2005 Through CY2009*, Savannah River Site, Aiken, SC, Rev. 0, July 12, 2010.

SRR-CWDA-2010-00080, *Software Quality Assurance Plan (SQAP) for the H-Area Tank Farm (HTF) Performance Assessment (PA) Probabilistic Model*, Savannah River Site, Aiken, SC, Rev. 0, August 2010.

SRR-CWDA-2010-00093, (Superseded), *H-Area Tank Farm Stochastic Fate and Transport Model*, Savannah River Site, Aiken, SC, Rev. 1, November 2010.

SRR-CWDA-2010-00093, *H-Area Tank Farm Stochastic Fate and Transport Model*, Savannah River Site, Aiken, SC, Rev. 2, August 2012.

SRR-CWDA-2010-00105, (Copyright), *GWB Essentials Guide*, The Geochemist's Workbench Release 8.0, Department of Geology, University of Illinois, Urbana, IL, August 3, 2010.

SRR-CWDA-2010-00154, *Software Quality Assurance Plan (SQAP) for The Geochemist's Workbench*, Savannah River Site, Aiken, SC, Rev. 0, November 2010.

SRR-CWDA-2011-00054, *Comment Response Matrix for United States Nuclear Regulatory Commission Staff Comments on the Draft Basis for Section 3116 Determination and Associated Performance Assessment for the F-Tank Farm at the Savannah River Site*, Savannah River Site, Aiken, SC, Rev. 1, October 25, 2011.

SRR-CWDA-2012-00020, *Savannah River Site Liquid Waste Facilities Performance Assessment Maintenance Program FY2012 Implementation Plan*, Savannah River Site, Aiken, SC, Rev. 0, March 2012.

SRR-CWDA-2012-00044, *Evaluation of Features, Events, and Processes in the H-Area Tank Farm Performance Assessment*, Savannah River Site, Aiken, SC, Rev. 1, October 30, 2012.

SRR-CWDA-2012-00051, *Critical Assumptions in the F-Tank Farm Operational Closure Documentation Regarding Waste Tank Internal Configurations*, Savannah River Site, Aiken, SC, Rev. 0, March 28, 2012.

SRR-CWDA-2012-00070, *Performance Assessment for the H-Area Tank Farm at the Savannah River Site: Quality Assurance Report*, Savannah River Site, Aiken, SC, Rev. 0, August 2012.

SRR-CWDA-2012-00080, *Barrier Analysis Report from the Performance Assessment for the H-Area Tank Farm at the Savannah River Site*, Savannah River Site, Aiken, SC, Rev. 0, August 28, 2012.

SRR-CWDA-2012-00093, *Savannah River Site F-Tank Farm NRC Onsite Observation Visit; June 12, 2012*, Savannah River Site, Aiken, SC, June 12, 2012.

SRR-LWDL-2012-00001, *2010 U.S. Census Bureau Data for Eight Counties within 50-Mile Radius of SRS*, Aiken County QuickFacts, U.S. Census Bureau, Washington DC, January 2012.

SRR-RP-2009-00764, French, J.W., *Savannah River Remediation LLC (SRR) Quality Assurance Management Plan*, Savannah River Site, Aiken, SC, Rev. 0, July 1, 2009.

SRR-STI-2012-00346, *Annual Radioactive Waste Tank Inspection Program - 2011*, Savannah River Site, Aiken, SC, June 2012.

SRS-REG-2007-00002, *Performance Assessment for the F-Tank Farm at the Savannah River Site*, Savannah River Site, Aiken, SC, Rev. 1, March 31, 2010.

SRT-EST-2003-00134, Jannik, G.T., *Cesium-137 Bioconcentration Factor for Freshwater Fish in the SRS Environment*, Savannah River Site, Aiken, SC, Rev. 0, July 15, 2003.

T-CLC-E-00018, Carey, S.A., *Low-Activity Waste (LAW) Vault Structural Degradation Prediction*, Savannah River Site, Rev 1, June 2006.

T-CLC-F-00373, Macaraeg, E., *Tanks 18 and 19 Closure Structural Calculation*, Savannah River Site, Aiken, SC, May 2006.

T-CLC-F-00421, Carey, S.A., *Structural Assessment of F-Area Tank Farm After Final Closure*, Savannah River Site, Aiken SC, Rev. 0, December 18, 2007.

Title 48_Chapter 1_SC Laws, *South Carolina Pollution Control Act, Environmental Protection and Conservation*, South Carolina Legislative Council, Columbia, SC, Current through the 2008 Session.

USGS OFR 2010-1059, (Copyright), Dart, R.L., et al., *Earthquakes in South Carolina and Vicinity 1698-2009*, Open-File Report 2010-1059, 1 Sheet, U.S. Geological Survey, Denver, CO, September 7, 2010.

W145225, *200 Area Waste Storage Tanks - 241 F & H, Design of Concrete Tank Concrete*, Savannah River Site, Aiken, SC, Rev. 4, July 7, 1954.

W145293, *200 Area Waste Storage Tanks 241 F & H, Bottom Slab - Plan, Sections & Details Concrete*, Savannah River Site, Aiken, SC, Rev. 16, September 4, 1951.

W145367, *200 Area Waste Storage Tanks - 241 F & H Steel Pan Plate Details Steel*, Savannah River Site, Aiken, SC, Rev. 1, July 7, 1954.

W145379, *200 Area Type I Tanks 1 - 8 and 9 - 12 Waste Storage Tanks 241 F & H 75'-0" Dia. Steel Tank Details , Steel*, Savannah River Site, Aiken, SC, Rev. 4, April 2004.

W145573, *200 Area Type I Tanks 1 - 8 and 9 - 12 Waste Storage Tanks 241-H General Arrangement & Construction Details, Concrete and Steel*, Rev. 29, April 5, 2004.

W146377, *200 Area Bldg 241H Waste Storage Tanks Excavation - Plan & Sections Civil*, Savannah River Site, Aiken, SC, Rev. 9, August 19, 1954.

W147544, *200 Area Building 241-H Diversion Box General Arrangement & Const Details Concrete & Steel*, Savannah River Site, Aiken, SC, Rev. 128, August 16, 1972.

W148228, *Area 200 Building 241H Waste Line Encasement Plan & Sections Concrete*, Savannah River Site, Aiken, SC, Rev. 48, October 18, 1955.

W148413, *Savannah River Plant, 200 Area Bldg, 241H, Waste Line Encasement Details Concrete*, Savannah River Site, Aiken, SC, Rev. 48, March 16, 1954.

W149426, *200 Area Building 241H Encasement of Catch Tank Plan & Sections Concrete*, Savannah River Site, Aiken, SC, Rev. 4, October 19, 1959.

W158080, *200 Area Bldg 241H Diversion Box Plan & Sections Concrete*, Savannah River Site, Aiken, SC, Rev. 9, November 4, 1997.

W158908, *Savannah River Plant, 200 Area Bldg, 241H, Waterproofing for Tanks in "H" Area Concrete*, Savannah River Site, Aiken, SC, Rev. 21, May 21, 1954.

W162672, *200 Area-Type II Tanks 13-16, Waste Storage Tanks 241-H, 85'-0" DIA. Steel Tank Details Steel*, Savannah River Site, Aiken, SC, Rev. 30, April 6, 2004.

W162675, *200 Area Bldg. 241-H 85'-0" Dia Waste Storage Tank Base Slab - Plan, Section & Details Concrete*, Savannah River Site, Aiken, SC, Rev. 7, June 20, 1955.

W162676, *200 Area - Bldg. 241-H, 85'-0" Dia. Waste Storage Tank Concrete Wall & Column Details Concrete*, Savannah River Site, Aiken, SC, Rev. 14, October 20, 1955.

W162688, *200 Area, Waste Storage Tanks - 241 H, Pan for 85' -0" Diam - Plate Details Steel*, Savannah River Site, Aiken, SC, Rev. 14, August 2, 1955.

W163018, *200 Area - Bldg. 241H, 85'-0" Dia. Waste Storage Tanks General Arrangement & Construction Details Concrete & Steel*, Savannah River Site, Aiken, SC, Rev. 28, November 7, 1955.

W163048, *200 Area - Bldg 241-H, 85'-0" Diam. Waste Storage Tanks, Excavation -Plan & Sections Concrete*, Savannah River Site, Aiken, SC, Rev. 11, May 26, 1955.

W163278, *200 Area - Bldg 241-H, Feed Wells at 85' ϕ Tank Plans, Section & Detail Concrete & Steel*, Savannah River Site, Aiken, SC, Rev. 3, August 22, 1956.

W163386, *200 Area 241-H Bldg Pumping Pit Equipment Arrg't Sections*, Savannah River Site, Aiken, SC, Rev. 37, November 4, 1997.

W163510, *Pumping Pit & Diversion Box 241-H Stainless Steel Lining Plans - Sections - Details Steel & Concrete*, Savannah River Site, Aiken, SC, Rev. 18, May 27, 1977.

W163527, *200 Area - Bldg. 241-H Pumping Pit Equipment Arrg't. - Plan*, Savannah River Site, Aiken, SC, Rev. 77, February 12, 1986.

W163593, *200 Area Building 241-H Vertical Cooling Coils for 85'-0" Dia. Waste Storage Tank*, Savannah River Site, Aiken, SC, Rev. 4, January 3, 1956.

W163613, *Area #200 Bldg #241H Pumping Pit & Diversion Box Plans - Sections - Details - Cover SCH Concrete Covers*, Savannah River Site, Aiken, SC, Rev. 50, April 19, 1999.

W163658, *200 Area Building 241H Bottom Cooling Coils for 85'-0" Dia. Waste Storage Tank*, Savannah River Site, Aiken, SC, Rev. 2, March 29, 1955.

W2010385, *Overheads Cell Piping Arrangement Sect. & Details, Sheet 1 Process*, Savannah River Site, Aiken, SC, Rev. 6, April 2, 2003.

W2017867, *Figure 4-25 Waste Transfer System H-Area HLW Tank Farm*, Savannah River Site, Aiken, SC, Rev. A, August 20, 1991.

W230826, *Bldg. 241-H Additional Waste Facilities Excavation Plan & Sections Civil*, Savannah River Site, Aiken, SC, Rev. 0, March 13, 1959.

W230907, *Bldg. 241-H Additional Waste Storage Tanks 85' - 0" Dia. Steel Tank Plan & Details Steel*, Savannah River Site, Aiken, SC, Rev. 6, February 8, 1960.

W230945, *Bldg. 241-H Additional Waste Storage Tanks Bottom Slab Plan & Details Concrete*, Savannah River Site, Aiken, SC, Rev. 6, February 8, 1960.

W230976, *Bldg. 241-H Type IV Tanks 21-24 Additional Waste Storage Tanks Wall Details - Sheet No. 1 Concrete & Instruments*, Savannah River Site, Aiken, SC, Rev. 7, April 15, 2004.

W231023, *Bldg. 241-H Additional Waste Storage Tanks Dome Plan & Details Concrete*, Savannah River Site, Aiken, SC, Rev. 2, January 9, 1963.

W231132, *Bldg's 241H, 242H & 242-1H Central Farm Evaporator Plot Plan Tanks 21, 22, 23 & 24 Electrical*, Savannah River Site, Aiken, SC, Rev. 82, October 8, 1998.

W231206, *Bldg. 241-H Additional Waste Storage Tanks, Riser & Plug Details Concrete & Instruments Process*, Savannah River Site, Aiken, SC, Rev. 27, January 30, 1995.

W231210, *Bldg. 241-H Tank Nos. 21, 22, 23 & 24 Equip & Piping Arrgt - Details Process & Concrete*, Savannah River Site, Aiken, SC, Rev. 20, March 22, 1978.

W231220, *Bldg. 241-H, Additional Waste Facilities Grading Plan Civil*, Savannah River Site, Aiken, SC, Rev. 35, September 16, 1975.

W231221, *200-H Area Soil Mechanics, Civil Soil Boring Log Profiles Sheet No. - 1*, Savannah River Site, Aiken, SC, Rev. 4, April 18, 1963.

W231244, *Bldg. 241-H Additional Waste Storage Tanks Miscellaneous Details Concrete*, Savannah River Site, Aiken, SC, Rev. 12, March 4, 1970.

W231299, *Bldg. 242-H Central Farm Evaporator Plans & Details Concrete & Plumbing*, Savannah River Site, Aiken, SC, Rev. 42, April 16, 2002.

W234134, *Bldg. 241-H Tank Nos. 21, 22, 23 & 24 Piping Arrangement - Sect - Sh. 2 Process & Concrete*, Savannah River Site, Aiken, SC, Rev. 3, January 28, 1963.

W236439, *Bldg. 241-8H, Additional High Level Waste Storage Facilities Excavation Plan - Civil*, Savannah River Site, Aiken, SC, Rev. 34, February 13, 1967.

W236495, *200 Area Bldg. 241-H, High Level Waste Storage Facilities, Base Slab Plan - Sections & Details Concrete*, Savannah River Site, Aiken, SC, Rev. 8, June 12, 1967.

W236499, *200 Area Bldg. 241-H, High Level Waste Storage Facilities, Wall and Column Sections & Details Concrete*, Savannah River Site, Aiken, SC, Rev. 6, October 29, 1968.

W236508, *Salt Removal Type III Tanks Phase I, H Area Tank 29 Additional H. L. Storage Tanks Equipment & Piping Arrangement*, Savannah River Site, Aiken, SC, Rev. 147, November 22, 2005.

W236519, *200 Area Bldg. 241-H Type III Tanks 29-32 High Level Waste Storage Facilities Primary Liner Plans & Details Steel*, Savannah River Site, Aiken, SC, Rev. 55, April 14, 2004.

W236562, *200 Area Bldg. 241-H High Level Waste Storage Facilities General Arrangements & Const Detls Concrete*, Savannah River Site, Aiken, SC, Rev. 29, July 3, 1991.

W236577, *Bldg 241-H High Level Waste Storage Facilities Top Slab Reinf. Layout Concrete*, Savannah River Site, Aiken, SC, Rev. 7, August 1, 1968.

W236630, *200 Area Bldg 241-H High Level Waste Storage Facilities Diversion Box Plans & Details Concrete & Steel*, Savannah River Site, Aiken, SC, Rev. 32, January 29, 1997.

W236993, *200 Area Bldg. 241-H, High Level Waste Storage Tanks Cooling Slots, Plan & Details Steel*, Savannah River Site, Aiken, SC, Rev. 7, May 17, 1968.

- W238746, *Bldg. 241-H Waste Transfer Facilities Plot Plan - Sh. 2 Civil*, Savannah River Site, Aiken, SC, Rev. 16, September 16, 1994.
- W238758, *Bldg. 241-H & 242-3H Waste Conc. Trans. Pump Pit Plans - Sections - Details Concrete*, Savannah River Site, Aiken, SC, Rev. 28, April 29, 1976.
- W238862, *Bldg. 241-H Waste Conc. Trans. Pump Pit Pump Pit Liner Steel*, Savannah River Site, Aiken, SC, Rev. 4, May 1, 1970.
- W448840, *Bldg. 241-12H, Tanks 36 & 37 Additional Waste Storage Tanks Cooling Slots, Plans & Details Steel*, Savannah River Site, Aiken, SC, Rev. 23, August 26, 1975.
- W448842, *Bldg. 241-12H Tanks 35, 36 & 37 Additional Waste Storage Tanks Secondary Liner Plans & Details Steel*, Savannah River Site, Aiken, SC, Rev. 47, July 8, 1976.
- W448844, *Bldg. 241-12H Tanks 35, 36 & 37 Additional Waste Storage Tanks Wall & Column Sections & Details Concrete*, Savannah River Site, Aiken, SC, Rev. 18, December 12, 1975.
- W448847, *Bldg 241-12H, Tanks 35, 36, & 37 Additional Waste Storage Tanks Base Slab Reinforcing Concrete*, Savannah River Site, Aiken, SC, Rev. 49, August 26, 1977.
- W448849, *Bldg. 241-12H Tanks 35, 36, & 37 Additional Waste Storage Tanks General Arrangement Concrete & Steel*, Savannah River Site, Aiken, SC, Rev. 28, July 24, 1996.
- W449644, *Bldg 242 Evaporator Assembly*, Savannah River Site, Aiken, SC, Rev. 24, September 8, 1995.
- W449710, *Bldg. 241-12H Additional Fac. High Level Waste Stg. Cooling Coil Elev. Tank #36 Process*, Savannah River Site, Aiken, SC, Rev. 10, March 18, 1975.
- W449795, *Bldg. 241-12H Tanks 35, 36 & 37 Additional Waste Storage Tanks Top Slab Plan - Tank #35 Concrete*, Savannah River Site, Aiken, SC, Rev. 39, July 24, 1996.
- W449796, *Bldg. 241-12H Tanks 35,36 & 37 Additional Waste Storage Tanks Top Slab Plan - Tank #36 Concrete*, Savannah River Site, Aiken, SC, Rev. 45, July 24, 1996.
- W449797, *Bldg. 241-12H Tanks 35, 36 & 37 Additional Waste Storage Tanks Top Slab Plan - Tank #37 Concrete*, Savannah River Site, Aiken, SC, Rev. 45, July 24, 1996.
- W449815, *Bldg 241-12H - Add. Stg. Tk. #35 Exterior Thermocouples Arrgt & Details Sh. 1 Instruments*, Savannah River Site, Aiken, SC, Rev. 11, November 1, 2000.
- W449824, *Bldg. 241-12H, Tank 35 Additional Waste Storage Tanks Cooling Slots - Plans & Details Steel*, Savannah River Site, Aiken, SC, Rev. 22, August 27, 1986.
- W449843, *Building 241-12H Addnl. High Lvl. Waste Stg. Tanks Excavation Plan Civil*, Savannah River Site, Aiken, SC, Rev. 27, March 11, 1975.
- W449931, *Bldg 241-12H Tks. 35, 36, 37 Additional H.L. Stg. Fac. Underground Thermocouples Instruments*, Savannah River Site, Aiken, SC, Rev. 3, May 9, 1975.
- W700242, *Bldg 241-12H Addl High Level Waste Stg Tanks Grading Plan - Phase 2 Civil*, Savannah River Site, Aiken, SC, Rev. 25, April 28, 1978.
-

W700286, *Bldg. 241-12H Additional Fac. High Level Waste Stg. Cooling Coil Elev. Tank #37 Process*, Savannah River Site, Aiken, SC, Rev. 10, March 18, 1975.

W700505, *Bldg. 241-12H, Tanks 37, Addnl High Lvl. Waste Stg. Tanks Plot Plan Phase 2 Civil*, Savannah River Site, Aiken, SC, Rev. 40, April 23, 1996.

W700547, *Building 241-H, Additional Waste Storage Tanks Plans Diversion Box No. 6 Concrete & Steel*, Savannah River Site, Aiken, SC, Rev. 51, June 28, 2006.

W700715, *Bldg. 241-15H, Stg. Tk #38 Exterior Thermocouples Arrgt. & Details Sh. 1 Instruments*, Savannah River Site, Aiken, SC, Rev. 35, June 26, 1981.

W700834, *Bldg.241-15H Addl. High Level Waste STG Tanks Excavation Plan Civil*, Savannah River Site, Aiken, SC, Rev. 79, September 27, 1978.

W700855, *Bldg 241-15H Tanks 38 thru 43, Additional Waste Storage Tanks, Base Slab Reinforcing Concrete*, Savannah River Site, Aiken, SC, Rev. 41, July 24, 2000.

W700856, *Bldg. 241-15H Tanks 38 thru 43 Additional Waste Storage Tanks General Arrangements Concrete & Steel*, Savannah River Site, Aiken, SC, Rev. 19, December 29, 1977.

W701036, *Bldg 241-15H Addl. High Level Waste Stg. Tanks Storm Water Drainage & Grading Plan Civil*, Savannah River Site, Aiken, SC, Rev. 144, July 22, 1996.

W701130, *Bldg. 241-H Waste Storage Fac. FY'76 Cooling Coil Elev. T38-T43 Process*, Savannah River Site, Aiken, SC, Rev. 26, January 19, 1979.

W701336, *Bldg 241-15H Tanks 38, 39, 40, 41, 42 & 43 Additional Waste Storage Tanks Leak Detection System Concrete*, Savannah River Site, Aiken, SC, Rev. 6, April 21, 1997.

W702019, *Bldg. 241-15H Add. Storage Facilities Underground Thermocouples Instrumentation*, Savannah River Site, Aiken, SC, Rev. 26, April 21, 1997.

W702194, *Bldg. 242-16H FY 76 Evaporator House-Upper Plan Equipment Arrangement Process*, Savannah River Site, Aiken, SC, Rev. 56, August 30, 1996.

W702199, *Bldg 242-16H FY'76 Evaporator House Cross-Section Equipment Arrg't. Process*, Savannah River Site, Aiken, SC, Rev. 57, May 25, 1978.

W702678, *Bldg 242-16H Evap. House FY'76 Sst Lining Sheet No. 1 Equipment Arrangement Process*, Savannah River Site, Aiken, SC, Rev. 31, January 29, 1979.

W702679, *Bldg 242-16H Evap. House FY'76 Sst Lining Sheet No. 2 Equipment Arrangement Process*, Savannah River Site, Aiken, SC, Rev. 22, November 18, 1977.

W702700, *241-15H, Tanks 38, 39, 40, 41, 42 & 43, Additional Waste Storage Tanks Cooling Slots Plan & Details TK 41, Steel*, Savannah River Site, Aiken, SC, Rev. 7, September 21, 1977.

W702909, *Bld'g 242-18H CTS Pump Pit Replacement Piping Arr'g't Plan Process*, Savannah River Site, Aiken, SC, Rev. 42, July 9, 1980.

W702913, *Building 242-18H CTS Pump Pit Replacement Plan, Sections, and Details Concrete Sheet #1*, Savannah River Site, Aiken, SC, Rev. 21, August 1, 1978.

W702914, *Building 242-18H CTS Pump Pit Replacement Plans, Sections, and Details Concrete Sheet 2*, Savannah River Site, Aiken, SC, Rev. 15, January 30, 1980.

W702915, *Building 242-18H CTS Pump Pit Replacement Stainless Steel Liner Details Concrete*, Savannah River Site, Aiken, SC, Rev. 32, April 11, 1980.

W702976, *Bldg. 241F-H Waste Management Improvements Modified Leak Detection Box Process and Instruments*, Savannah River Site, Aiken, SC, Rev. 52, December 21, 1998.

W703006, *Bld'g. 242 Demister Addition to Westinghouse Evaporators Process*, Savannah River Site, Aiken, SC, Rev. 0, March 21, 1977.

W703874, *Bldg. 241-H Diversion Box #7 Plans, Sections & Details Sh#1 Concrete*, Savannah River Site, Aiken, SC, Rev. 96, January 12, 1993.

W704339, *Bldg. 241-15H, Tanks 38, 39, 40, 41, 42 & 43, Additional Waste Storage Tanks Wall & Column Sections & Details Concrete*, Savannah River Site, Aiken, SC, Rev. 14, June 8, 1978.

W704340, *Bldg. 241-54F Tanks 44, 45, 46, 47 Additional Waste Storage Tanks Wall & Column Sections & Details Concrete*, Savannah River Site, Aiken, SC, Rev. 2, March 1, 1978.

W704700, *Building 241-51H Add'l High Level Waste Stg. Tks. Grading & Storm Drainage Plan Civil*, Savannah River Site, Aiken, SC, Rev. 75, December 2, 1994.

W706301, *Bldg.241-51H, Addl High Level Waste Stg Tanks Excavation Plan Civil Sheet 2*, Savannah River Site, Aiken, SC, Rev. 17, April 14, 1978.

W706690, *Additional Waste Storage Tanks, Top Slab Plan & Risers Tank 48*, Rev. 48, December 5, 2005.

W707031, *Bldg. 241-H, Add. Stg. Tnks. 48 & 49 Exterior Thermocouples Arrgt. & Details Sh. 1 Instruments*, Savannah River Site, Aiken, SC, Rev. 28, May 16, 1978.

W707111, *Bldg. 241-15H, Bld'g, 241-51H Tks 48, 39, 50 & 51, Additional Waste Storage Tanks Secondary Liner Plan & Details, Steel*, Savannah River Site, Aiken, SC, Rev. 5, November 6, 1978.

W707114, *Bldg. 241-15H Bld'g 241-51H, Tks 48, 39, 50 & 51 Additional Waste Storage Tanks General Arrangements Concrete & Steel*, Savannah River Site, Aiken, SC, Rev. 9, July 31, 1979.

W707138, *Bld'g 241-51H Tks 48, 49, 50 & 51 Additional Waste Storage Tanks, Base Slab Reinforcing Concrete*, Savannah River Site, Aiken, SC, Rev. 11, February 9, 1979.

W707253, *Bld'g 241-51H Tks 48, 49, 50 & 51 Additional Waste Storage Tanks Leak Detection System Concrete & Process*, Savannah River Site, Aiken, SC, Rev. 11, January 9, 1980.

W707288, *Bldg. 241-15H, Tanks 48, 49, 50 & 51, Additional Waste Storage Tanks Cooling Slots Plan & Details, Concrete*, Savannah River Site, Aiken, SC, Rev. 2, November 5, 1979.

W708852, *Bldg. 241-H, Waste Storage Fac. FY'78 Cooling Coil Elev. T48-T51, Process*, Savannah River Site, Aiken, SC, Rev. 8, January 19, 1979.

W714352, *Bldg 241H Replace Waste Headers HPP5&6 Ppg Arrgt U.G. Plan Sh:4 Process*, Savannah River Site, Aiken, SC, Rev. 97, November 10, 1981.

W714951, *Bldg. 241-H Replace Waste Headers Pump Pit 5&6 Sects. & Dets. Sheet-2 Concrete*, Savannah River Site, Aiken, SC, Rev. 46, January 22, 1981.

W714953, *Bldg. 241-H Replace Waste Headers Pump Pit 5&6 Liner Plan & Det's Sh#1 Steel*, Savannah River Site, Aiken, SC, Rev. 3, July 21, 1980.

W715343, *Bldg 241F&H Waste Storage Facilities Leak Detection Box Assy Process*, Savannah River Site, Aiken, SC, Rev. 10, September 12, 1980.

W715395, *200 Area - Bldg. 241-H, Tanks 9-10 Waste Removal Facilities Layout - Grading - Sewers Civil*, Savannah River Site, Aiken, SC, Rev. 19, September 15, 1994.

W740180, *Bldg 241H Tank Y342 Waste Transfer Facilities Valve Box Assembly Y342-15-1 Process*, Savannah River Site, Aiken, SC, Rev. 28, November 13, 2007.

W752789, *DWPF Pump Pits Tank Assembly - Equipment Requirements Dwg. Process Mechanical*, Savannah River Site, Aiken, SC, Rev. 3, January 7, 1994.

W778702, *241H Area New Waste Transfer Facility, Site Layout & Fencing Plan Civil*, Savannah River Site, Aiken, SC, Rev. 9, February 10, 1995.

W778815, *241H Area New Waste Transfer Facility, Pump Pits & Diversion Box Conc. Outline & Reinforcing Plan & Sections Sheet 1 Concrete Structural*, Savannah River Site, Aiken, SC, Rev. 2, December 21, 1990.

W778818, *241H Area New Waste Transfer Facility, Pump Pits & Diversion Box Conc. Outline & Reinforcing North Elevation & Sections Concrete Structural*, Savannah River Site, Aiken, SC, Rev. 1, February 7, 1986.

W778850, *241H Area New Waste Transfer Facility, Pump Pit Liner Plate HPP7 HPP8 HPP9 & HPP10 Floor Plans Steel Structural*, Savannah River Site, Aiken, SC, Rev. 2, December 20, 1990.

W800445, *Bldg 241H Y351-15-1 Waste Removal Facilities Valve Box Assembly Process*, Savannah River Site, Aiken, SC, Rev. 25, May 9, 2006.

W802781, *Bldg 241H Y340-15-1 Waste Removal Facility Valve Box Assembly Process*, Savannah River Site, Aiken, SC, Rev. 14, January 29, 1988.

W807558, *Bldg. 241H Tank 51 Waste Transfer Facilities Valve Box Assembly Process*, Savannah River Site, Aiken, SC, Rev. 9, April 21, 1997.

W835332, *Bldg. 242-25H Evaporator Building Equipment Arrangement Upper Plan Process*, Savannah River Site, Aiken, SC, Rev. 4, November 12, 1998.

W835333, *Bldg. 242-25H Evaporator Building Equipment Arrangement Section "A-A" Process*, Savannah River Site, Aiken, SC, Rev. 3, March 17, 2003.

W835335, *Bldg. 242-25H Evaporator Building Equipment Arrangement Section "B-B" Process*, Savannah River Site, Aiken, SC, Rev. 4, March 17, 2003.

W838269, *Bldg. 242 25H Evaporator Building Equipment Arrangement Section "C-C" Process*, Savannah River Site, Aiken, SC, Rev. 2, February 9, 2000.

WSRC-IM-2004-00008, *DSA Support Document - Site Characteristics and Program Descriptions*, Savannah River Site, Aiken SC, Rev. 1, June 2007.

WSRC-MS-2003-00617, Stevenson, D.A., et al., *2001-2002 Upper Three Runs Sequence of Earthquakes at the SRS, South Carolina*, Savannah River Site, Aiken, SC, September 19, 2003.

WSRC-MS-92-513, Cook, J.R., et al., *Selection and Cultivation of Final Vegetative Cover for Closed Waste Sites at the Savannah River Site, SC*, Savannah River Site, Aiken, SC, February 28, 1993.

WSRC-MS-95-0524, Hiergesell, R.A., *Regional Water Table Map of the Savannah River Site IQ-95*, Savannah River Site, Aiken, SC, 1995.

WSRC-OS-94-42, *Federal Facility Agreement for the Savannah River Site*, Savannah River Site, Aiken, SC, August 16, 1991.

WSRC-RP-2005-01675, Langton, C.A., *HLW Tank Intruder Deterrent Grout*, Savannah River Site, Aiken, SC, Rev. 0, April 26, 2005.

WSRC-RP-91-17, Hamby, D.M., *Land and Water Use Characteristics in the Vicinity of the Savannah River Site*, Savannah River Site, Aiken, SC, March 1, 1991.

WSRC-RP-92-1360, Garrett, T.C., *Radiological Performance Assessment for the Z-Area Saltstone Disposal Facility*, Savannah River Site, Aiken, SC, December 18, 1992.

WSRC-RP-94-54, Thayer, P., et al., *Petrographic Analysis of Mixed Carbonate-Clastic Hydrostratigraphic Units in the General Separations Area*, Savannah River Site, Aiken, SC, December 17, 1994.

WSRC-STI-2006-00123, Jannik, G.T. and Dixon, K.L., *LADTAP-PA: A Spreadsheet for Estimating Dose Resulting from E-Area Groundwater Contamination at the Savannah River Site*, Savannah River Site, Aiken, SC, Rev. 0, August 2006.

WSRC-STI-2006-00196, *Dispersion of Savannah River Site Sediments as a Function of pH: Implications for Colloid-Facilitated Contaminant Transport*, Savannah River Site, Aiken SC, Rev. 0, September 30, 2006.

WSRC-STI-2006-00198, Phifer, M.A., et al., *Hydraulic Property Data Package for the E-Area and Z-Area Soils, Cementitious Materials, and Waste Zones*, Savannah River Site, Aiken SC, Rev. 0, September 2006.

WSRC-STI-2007-00004, Lee, P.L., et al., *Baseline Parameter Update for Human Health Input and Transfer Factors for Radiological Performance Assessments at the Savannah River Site*, Savannah River Site, Aiken, SC, Rev. 4, June 13, 2008.

WSRC-STI-2007-00061, Subramanian, K.H., *Life Estimation of High Level Waste Tank Steel for F-Tank Farm Closure Performance Assessment*, Savannah River Site, Aiken, SC, Rev. 2, June 2008.

WSRC-STI-2007-00184, Phifer, M.A., *FTF Closure Cap Concept and Infiltration Estimates*, Savannah River Site, Aiken, SC, Rev. 2, October 15, 2007.

WSRC-STI-2007-00369, Dixon, K., et al., *Hydraulic and Physical Properties of Tank Grouts and Base Mat Surrogate Concrete for FTF Closure*, Savannah River Site, Aiken, SC, Rev. 0, October 2007.

WSRC-STI-2007-00460, Subramanian, K.H., *Life Estimation of Transfer Lines for Tank Farm Closure Performance Assessment*, Savannah River Site, Aiken, SC, Rev. 0, October 2007.

WSRC-STI-2007-00544, Denham, M.E., *Conceptual Model of Waste Release from the Contaminated Zone of Closed Radioactive Waste Tanks*, Savannah River Site, Aiken, SC, Rev. 2, November 16, 2010.

WSRC-STI-2007-00613, Kabela, E.D., et al., *Summary of Data Processing for the 2002-2006 SRS Meteorological Database*, Savannah River Site, Aiken, SC, December 13, 2007.

WSRC-STI-2007-00640, Kaplan, D.I., et al., *Partitioning of Dissolved Radionuclides to Concrete Under Scenarios Appropriate for Tank Closure Performance Assessments*, Savannah River Site, Aiken, SC, December 21, 2007.

WSRC-STI-2007-00641, Langton, C.A., et al., *Grout Formulations and Properties for the Tank Farm Closure*, Savannah River Site, Aiken, SC, Rev. 0, November 12, 2007.

WSRC-STI-2008-00057, *Savannah River Site Environmental Report for 2007*, Savannah River Site, Aiken, SC, December 2007.

WSRC-TR-2000-00310, Cumbest, R.J., et al., *Comparison of Cenozoic Faulting at the Savannah River Site to Fault Characteristics of the Atlantic Coast Fault Province: Implications for Fault Capability*, Savannah River Site, Aiken, SC, September 28, 2009.

WSRC-TR-2002-00327, Cole, C.M., et al., *CSTF Corrosion Control Program*, Savannah River Site, Aiken, SC, Rev. 4, December 17, 2007.

WSRC-TR-2003-00250, Hiergesell, R.A., et al., *An Updated Regional Water Table of the Savannah River Site and Related Coverages*, Savannah River Site, Aiken, SC, Rev. 0, December 2003.

WSRC-TR-2003-00436, Phifer, M. and Nelson, E., *Saltstone Disposal Facility Closure Cap Configuration and Degradation Base Case: Institutional Control to Pine Forest Scenario*, Savannah River Site, Aiken, SC, Rev. 0, September 22, 2003.

WSRC-TR-2004-00106, Flach, G.P., *Groundwater Flow Model of the General Separations Area Using PORFLOW*, Savannah River Site, Aiken, SC, Rev. 0, July 14, 2004.

WSRC-TR-2005-00201, Wike, L.D., et al., *SRS Ecology: Environmental Information Document*, Savannah River Site, Aiken, SC, Rev. 0, March 2006.

WSRC-TR-2007-00118, Kabela, E.D., et al., *Savannah River Site Annual Meteorology Report for 2006*, Savannah River Site, Aiken, SC, Rev. 0, April 20, 2007.

WSRC-TR-2007-00283, Millings, M.R., et al., *Hydrogeologic Data Summary in Support of the F-Area Tank Farm (FTF) Performance Assessment (PA)*, Savannah River Site, Aiken, SC, Rev. 0, July 2007.

WSRC-TR-90-0284, Stephenson, D.E., *Review of Seismicity and Ground Motion Studies Related to the Development of Seismic Design Criteria at SRS*, Savannah River Site, Aiken, SC, 1990.

WSRC-TR-95-0046, Denham, M.E., *SRS Geology & Hydrogeology Environmental Information Document*, Savannah River Site, Aiken, SC, Rev. 0, August 31, 1999.

WSRC-TR-96-0231, Friday, G.P., et al., *Radiological Bioconcentration Factors for Aquatic, Terrestrial, and Wetland Ecosystems at the Savannah River Site*, Savannah River Site, Aiken, SC, December 31, 1996.

WSRC-TR-96-0399, Vol. 1, Flach, G.P., et al., *Integrated Hydrogeological Modeling of the General Separations Area*, Vol. 1, Savannah River Site, Aiken, SC, Rev. 0, August 1, 1997.

WSRC-TR-96-0399, Vol. 2, Flach, G.P., et al., *Integrated Hydrogeological Modeling of the General Separations Area*, Vol. 2, Savannah River Site, Aiken, SC, Rev. 1, April 1, 1999.

WSRC-TR-97-0102, Caldwell, T.B., *Tank Closure Grout*, Savannah River Site, Aiken, SC, Rev. 0, April 18, 1997.

WSRC-TR-98-00045, Hiergesell, R.A., *The Regional Water Table of the Savannah River Site and Related Coverages*, Savannah River Site, Aiken, SC, September 1998.

WSRC-TR-98-00271, Langton, C.A., et al., *Laboratory and Field Testing of High Performance-Zero Bleed CLSM Mixes for Future Tank Closure Applications*, Savannah River Site, Aiken, SC, March 30, 1998.

WSRC-TR-99-00282, Hamm, L.L., and Aleman, S.E., *FACT (Version 2.0), Subsurface Flow and Contaminant Transport, Documentation and User's Guide*, Savannah River Site, Aiken, SC, 2000.

WSRC-TR-99-00369, Chen, K.F., *Flood Hazard Recurrence Frequencies for C-, F-, E-, S-, H-, Y-, and Z-Areas*, Savannah River Site, Aiken, SC, September 30, 1999.

WSRC-TR-99-4083, Aadland, R.K., et al., *Significance of Soft Zone Sediments at the Savannah River Site*, Savannah River Site, Aiken, SC, Rev. 0, September 1999.

11.0 GLOSSARY

Absorption	Particles entrance of one phase into a different bulk phase by penetrating a surface.
Accuracy	Closeness of the result of a measurement to the true value of the quantity.
Actinide	Group of elements of atomic number 89 through 103. Laboratory analysis of actinides by alpha spectrometry generally refers to the elements plutonium, americium, uranium, and curium but may also include neptunium and thorium.
Acute Intruder	Acute intruder is a person or persons who perform a well installation and unknowingly is exposed to contaminated drill cuttings brought to the surface at the time of drilling via direct external exposure, ingestion, and inhalation.
Adsorption	The enrichment or agglomeration of particles on a surface or interface.
Air Content	Amount of air incorporated into the grout as the result of mixing and placement.
Air Pathway	Exposure pathway to radioactive material dispersed in the air in the form of dusts, fumes, particulates, mists, vapors, or gases.
ALARA	As Low As Reasonably Achievable - making every reasonable effort to maintain exposures to radiation as far below the dose limits as is practical consistent with the purpose for which the licensed activity is undertaken, taking into account the state of technology, the economics of improvements in relation to state of technology, the economics of improvements in relation to benefits to the public health and safety, and other societal and socioeconomic considerations.
Amorphous	Latin meaning without form. Non-crystalline structure.
Ancillary Equipment	Ancillary equipment associated with the waste tanks, including such equipment as transfer line piping, pump tanks, or evaporators, which are used to distribute or control the transfer of waste, from one storage point to another storage point.
Annulus	The annulus also referred to as the secondary containment of a waste tank. The secondary containment surrounds the waste tank shell (primary liner) of Types I, II, III, and IIIA tanks, providing a location for collection of any leakage from the waste tank shell (primary liner).
Aquifer	Saturated, permeable geologic unit that can transmit significant quantities of water under ordinary hydraulic gradients.
Argillaceous	Containing, made of, or resembling clay; clayey.
Atomic Energy Commission	Federal agency created in 1946 to manage the development, use, and control of nuclear energy for military and civilian application. It was abolished by the Energy Reorganization Act of 1974 and succeeded by the Energy Research and Development Administration. Functions of the Energy Research and Development Administration eventually were taken over by the U.S. Department of Energy and the U.S. Nuclear Regulatory Commission.

Background Radiation	Naturally occurring radiation, fallout, and cosmic radiation. Generally, the lowest level of radiation obtainable within the scope of an analytical measurement, i.e., a blank sample.
Base Case	Waste tank Case A, modeling scenario in which the closure cap is assumed in place and no fast flow path exists from outside the waste tank system, through the waste tank, and exiting the system. It was assumed that the concrete that makes up the walls, the waste tank grout, and basemat concrete degrades over time (with these changes simulated by increasing hydraulic conductivity).
Basemat	Concrete pad upon which the waste tank is constructed. The pad has close tolerances for leveling of waste tank and the concrete is quality controlled to ensure the structural integrity to waste tank foundation. The basemat is also referred to as floor slab or foundation.
Bioaccumulation Factor	Calculations that define parameters used to calculate contaminant concentrations via a variety of environmental mechanisms.
Biotic Pathway	Amounts and rates of radionuclides transferred by living components (e.g., animals, plants, or bacterial life) of an ecosystem.
Blackwater Stream	Waterways that contain high concentrations of naturally occurring tannic acid that gives the water a tea color.
Bleed Water	Water that separates from the grout as the result of solids settling.
Calcareous Zone	Located within the Santee Formation and the lowermost part of the overlying Dry Branch Formation, zones consist of silty and clayey fine sands, fine-grained clays, and calcareous shell fragments deposited in nearshore and inner shelf environments. Soft zones within the calcareous zones in the vicinity of the General Separations Area, which includes the HTF, are not cavernous voids, but are small, isolated, poorly connected, three-dimensional features filled with loose, fine-grained, water-saturated sediment.
Carbonation	The reaction of carbon dioxide gas with the hydrated phases of the Portland cement in the grout blocking the pores in the grout.
Cementitious	Like or relevant to or having the properties of cement.
Central Savannah River Area	Eighteen-county area in Georgia and South Carolina surrounding Augusta, Georgia. The Savannah River Site is included in the Central Savannah River Area. Counties are Richmond, Columbia, McDuffie, Burke, Emanuel, Glascock, Jenkins, Jefferson, Lincoln, Screven, Taliaferro, Warren, and Wilkes in Georgia and Aiken, Edgefield, Allendale, Barnwell, and McCormick in South Carolina.
CERCLA	Comprehensive Environmental Response, Compensation, and Liability Act, commonly known as Superfund, enacted by Congress on December 11, 1980. This law provides to clean up uncontrolled or abandoned hazardous-waste sites as well as accidents, spills, and other emergency releases of pollutants and contaminants into the environment. Through the Act, U.S. Environmental Protection Agency was given power to seek out those parties responsible for any release and assure their cooperation in the cleanup.

Chronic Intruder	A person or persons that lives on site, consumes food crops grown and animals reared on site, and performs recreational activities on the closure site which is contaminated by both drill cuttings and irrigation well water. Exposure is by external contact, ingestion, and inhalation.
Citizens Advisory Board	The Savannah River Site Citizens Advisory Board is composed of 25 individuals from South Carolina and Georgia. The board members are chosen to reflect the cultural diversity of the population affected by Savannah River Site. The Board provides advice and recommendations to the U.S. Department of Energy on environmental remediation, waste management, and related issues. All meetings are open to the public and public participation is encouraged. Public comment periods are offered at various times throughout the meetings.
Clean Water Act	The Clean Water Act is the cornerstone of surface water quality protection in the United States (the Act does not deal directly with groundwater nor with water quantity issues). The law employs a variety of regulatory and non-regulatory tools to sharply reduce direct pollutant discharges into waterways, finance municipal wastewater treatment facilities, and manage polluted runoff.
Industrial Wastewater General Closure Plan	Plan that presents the environmental regulatory standards and guidelines pertinent to the closure of the waste tanks and describes that process for evaluating and selecting the closure design (i.e., residual inventory and form.)
Colloidal	A substance microscopically dispersed evenly throughout another substance. A colloidal system consists of two separate phases: a <i>dispersed phase</i> (or <i>internal phase</i>) and a <i>continuous phase</i> (or <i>dispersion medium</i>) in which the colloid is dispersed. A colloidal system may be solid, liquid, or gas.
Compressive Strength	Force per unit area required to break an unconfined grout or concrete sample.
Concentration	Amount (e.g., in grams or moles) per volume of a substance.
Conductivity Probes	The conductivity probe is a simple electrical device that works on the principle that liquids conduct electricity more readily than air. If a liquid comes in contact with the probe it will complete an electrical circuit and send a signal for indication or alarm purposes of a waste leak in ancillary equipment.
Cone Penetration Test	The cone penetration test is an in-situ testing method used to determine the geotechnical engineering properties of soils and delineating soil stratigraphy. The cone penetration test is one of the most used and accepted in-situ test methods for soil investigation. The test method consists of pushing an instrumented cone; tip first, into the ground at a controlled rate.
Confining Unit	Geologic unit that inhibits the flow of water.
Consumption Rates	Physical human health exposure parameters used for evaluating pathway-specific dose.

Cooling Coils	Cooling coils are installed in the waste tanks to remove the decay heat that is generated by the waste in the waste tanks. Arrangements and designs of cooling coils differ, depending on the type of waste tank. Type I and II tanks, in addition to having vertical cooling coils, also have cooling coils across the bottom of the tank to provide a means for cooling the bottom of the waste tank.
Co-Precipitation	Co-precipitation as defined here is the incorporation of an element into the crystal structure of a solid phase that is predominantly made of other elements or the trapping of an element within the bulk mass of a phase made up of other elements, but not necessarily within the crystal lattice.
Core Pipe	Internal pipe of transfer line that comes into contact with the waste materials. The core pipe is usually located within a jacket pipe.
Cretaceous	The geological time period between 140 and 65 million years ago.
Curie	A unit of radioactivity; the quantity of nuclear material that has 3.7E+10 disintegrations per second.
Darcy Velocity	Formula for measuring velocity and flow of groundwater.
Depassivation	Deterioration of steel that has been covered with a passivating product (e.g., concrete) as a result of the introduction of too much chloride.
Desorption	The opposite process to <u>adsorption</u> meaning the removal of aggregated particles from a surface.
Deterministic	When fixed parameters are used in calculations versus a distribution of values (probabilistic).
Diffusion	Movement of contaminants from an area of higher concentration to an area of lower concentration.
Diffusion Coefficient	The rate of diffusion of particles, depending on the particle size, viscosity and temperature.
Dip Tubes	Dip Tubes are used to provide an estimate of the rate of leakage into the annulus and to serve as a backup for the conductivity probes. Dip tubes operate by relying on the hydrostatic pressure (height) of the liquid column to cause a backpressure on the dip tube.
Dispersivity	Equal to the dispersion coefficient divided by the velocity.
Distribution Coefficient	The quantity of a solute sorbed by a solid, per unit weight of solid, divided by the quantity of the solute dissolved in the water per unit volume of water.
Diversion Box	Diversion box is a shielded reinforced concrete structure containing transfer line nozzles to which jumpers are connected in order to direct waste transfers to the desired location.
Dolomitic	A magnesia-rich sedimentary rock resembling limestone.
Dose Conversion Factor	A factor used to convert radionuclide concentrations in environmental media to doses. Factors are used for inhalation, ingestion, immersion, and external exposure.
Dose Limits	The permissible upper bounds of radiation doses.
Effective Diffusion Coefficient	The diffusion coefficient of a species through a saturated porous medium taken over the pore area of the medium through which diffusion occurs under steady-state conditions.

Erosion Barrier	The layer within a multi-part closure cap made of rock (riprap) and filler materials designed to prevent riprap movement during a Probable Maximum Precipitation event and therefore forms a barrier to further erosion and gully formation (i.e., provide closure cap physical stability). It will be used to maintain a minimum 10 feet of clean material above the waste tanks and significant ancillary equipment to act as an intruder deterrent. It will also act to preclude burrowing animals from access to underlying closure cap layers. It also provides minimal water storage for the promotion of evapotranspiration.
Escarpment	A steep slope or long cliff caused by erosion or faulting separating two level areas of differing heights.
Ettringite	Ettringite is hexacalcium aluminate trisulfate hydrate. Ettringite is found in hydrated Portland cement system as a result of the reaction of calcium aluminate with calcium sulfate, both present in Portland cement.
Evaporator	Steam-heated, water-cooled system installed in the tank farms to concentrate underground waste tank contents, in order to reduce the liquid waste volume.
Evapotranspiration	Evapotranspiration is a term used to describe the sum of evaporation and plant transpiration from the earth's land surface to atmosphere. Evaporation accounts for the movement of water to the air from sources such as the soil, canopy interception, and water bodies.
Exposure	Being exposed to ionizing radiation or to radioactive material.
Exposure Pathway	The means by which humans are exposed to contaminants. The key exposure pathways are air and water, with most exposures via drinking water, crops, other foods, inhalation, and direct radiation.
External Dose	That portion of the dose equivalent received from radiation sources outside the body.
Federal Facility Agreement	Agreement between U.S. Environmental Protection Agency, U.S. Department Of Energy, and South Carolina Department of Health and Environmental Control that directs the comprehensive remediation of the Savannah River Site. It contains requirements for 1) site investigation and remediation of releases and potential releases of hazardous substances, and 2) interim status corrective action for releases of hazardous wastes or hazardous constituents.
Flow	Ability of the grout to spread evenly without vibration (self-level).
Flux	The time rate of change or concentration. For example, curies per year leaving the contamination zone
Fly Ash	Fly ash is a mineral admixture used in grout to enhance finishing characteristics, make the mix more economical, and to improve pumping. It is finer in consistency than cement, and its particles are round. These fine particles make the mix finish easier, and pump easier.
Gaussian plume equation	An equation that represents dispersion of a material from a release point.
General Separations Area	Centralized area of Savannah River Site including the heavily industrialized E, F, H, S, and Z Areas.

The Geochemist's Workbench	The Geochemist's Workbench is a set of software tools for manipulating chemical reactions, calculating stability diagrams and the equilibrium states of natural waters, tracing reaction processes, modeling reactive transport, and plotting the results of these calculations. The package is designed for solving problems in aqueous geochemistry, including those encountered in environmental protection and remediation, the petroleum industry, and economic geology.
Geosynthetic Clay Liner	A woven fabric-like material primarily used for the lining of landfills. It is a kind of geomembrane and geosynthetic, which incorporates a bentonite or other clay, which has a very low hydraulic conductivity.
GoldSim	A simulation software program designed to dynamically model the release and transport of radioactive constituents. The fundamental output consists of predicted mass fluxes at specified locations within a system, and predicted concentrations within environmental media (e.g., groundwater, soil, air).
Goethite	Red, yellow, or brown mineral; an oxide of iron that is a common constituent of rust found in soil and other low temperature environments.
Gradient Boosting Model	Modeling approach that utilizes binary recursive partitioning algorithms that deconstruct a response into the relative influence from a given set of explanatory variables (stochastic model input parameters).
Grahams Law	Grahams Law states that the rate of diffusion of a gas is inversely proportional to the square root of its molecular weight.
Groundwater Flow	The rate of groundwater movement through the subsurface.
Grout	A cement mixture, sufficiently fluid, which can be pumped into equipment cavities creating a watertight bond, and increasing the strength of the existing structural foundation. Capable of slowing the vertical movement or migration of water.
Hematite	A widely distributed mineral, which is an important iron ore, occurring in crystalline, massive, or granular form, and reddish-brown when powdered.
Herpetofauna	Term used that refers to reptiles and amphibians, collectively.
High Density Polyethylene Geomembrane	A geomembrane with a thickness of 0.06 in (60 mil) that forms a composite hydraulic barrier in the closure cap to promote lateral drainage through the overlying lateral drainage layer and minimize infiltration to the waste tanks and ancillary equipment.
Homogenous	Similar or uniform structure or composition throughout.
Hydraulic Conductivity	Velocity of water flow through saturated materials (e.g., concrete, grout, soil)
Hydrostratigraphy	A geologic framework based on hydrologic properties (as opposed to lithofacies); where the discrete rock bodies have considerable lateral extent.
Igneous Rock	An aggregate of interlocking silicate minerals formed by cooling and solidification of magma or lava. Igneous rocks are formed by volcanic processes.
Indurated	Hard or thickened.
Institutional Control	A 100-year period in which U.S. Department Of Energy retains ownership and control of H-Area Tank Farm such that facility maintenance and controls will be performed to prevent inadvertent intrusion and protect public health and the environment.

Interfluvial	The region of higher land between two rivers that are in the same drainage system.
Internal Dose	That portion of the dose equivalent received from radioactive material taken into the body.
Jurassic	The geological period between 210 and 140 million years ago.
Kelco-Crete	A special viscosity modifying admixture. Kelco-Crete is included in the mix design to enhance physical stability of grout (minimizing segregation) and achieve a robust mix.
Lacustrine Sediments	A type of non-lithified deposit that comes from lakes, which previously occupied the area. Generally, these include fine-grained soils that have settled through the water column and accumulate on the lake bottom.
Latin Hypercube Sampling	A form of sampling that can be applied to multiple variables. The method is commonly used to reduce the number of runs necessary for a Monte Carlo simulation to achieve a reasonably accurate random distribution.
Leachate	Leachate is the liquid that drains or 'leaches' from a closure system. It can contain both dissolved and suspended material.
Leaching	Leaching occurs when infiltrating water seeps into the closure system and transports contaminants out of the system.
Leak Detection Boxes	Leak detection boxes provide for the collection and detection of leakage from the transfer lines.
Line Encasement (Sealed Concrete Trench)	Enclosed core pipes in a covered reinforced concrete encasement below ground. Any core pipe leakage into the encasement and in-leakage of groundwater into the encasement will gravity drain to catch tank.
Liquification	The process by which saturated, unconsolidated <u>sediments</u> are transformed into a substance that acts like a liquid.
Lithified Terrigenous Sediment	Sediments derived from the erosion of rocks on land.
Lithology	The description of rocks, especially in hand specimen and in outcrop, on the basis of such characteristics as color, mineralogic composition, and grain size.
Macroinvertebrate	Any nonvertebrate organism that is large enough to be seen without the aid of a microscope.
Maximally Exposed Individual	A hypothetical individual who, because of proximity, activities, or living habits, could potentially receive the maximum possible dose of radiation or of a hazardous chemical from a given event or process.
Maximum Contaminant Level	The highest level of a contaminant that is allowed in drinking water, below which there is no known or expected risk to health.
Mean Sea Level	The reference point used as a standard for determining terrestrial and atmospheric elevation or ocean depths and is calculated as the average of hourly tide levels measured by mechanical tide gauges over extended periods of time.
Member of the Public	A representative individual who is assumed to be located at the boundary of the DOE controlled area until the assumed active institutional control period ends (i.e., 100 years after closure), at which point the receptor is assumed to move to the point of maximum exposure at or outside of the 100-meter buffer zone.

Mesozoic	An area of geologic time, from the end of the Paleozoic to the beginning of the Cenozoic, or from about 225 million years to about 65 million years ago.
Metamorphosed Sedimentary Rock	Rock that is formed by the consolidation of sediment particles or of the remains of plants and animals.
Miocene-Age	Middle of Tertiary Period, dating back 13-25 million years.
Molality	Relating to a solution that contains X moles of solute per liter of solution, where X is a number.
Monte Carlo Method	An analytical method in which a large number of realizations are simulated using randomly sampled values for each uncertain parameter distribution. All the realizations are then assembled into probability distributions of possible outcomes. This method propagates different types of uncertainty into model results, and enables easy identification of the parameters most impacting results.
National Pollutant Discharge Elimination System	As authorized by the Clean Water Act, the National Pollutant Discharge Elimination System permit program controls water pollution by regulating point sources that discharge pollutants into waters of the United States. Point sources are discrete conveyances such as pipes or man-made ditches.
NDAA Section 3116	<i>Ronald W. Reagan National Defense Authorization Act (NDAA) for Fiscal Year 2005</i> was passed by Congress on October 9, 2004 and signed by the President on October 28, 2004. Section 3116 specifies that the term “high-level radioactive waste” does not include radioactive waste that results from reprocessing spent nuclear fuel if the Secretary of Energy determines, in consultation with the U. S. Nuclear Regulatory Commission, that the waste meets certain criteria.
Occupational Dose	The dose received by an individual in the course of employment in which the individual’s assigned duties involves exposure to radiation or to radioactive material. Occupational dose does not include doses received from background radiation or from any medical administration the individual has received.
Operable Unit	Operable unit is a discrete action that comprises an incremental step toward comprehensively addressing site Comprehensive Environmental Response, Compensation, and Liability Act problems. This discrete portion of a remedial response manages migration, or eliminates or mitigates a release, threat of release, or pathway of exposure. The remediation of a site is divided into a number of operable units, depending on the complexity of the problems associated with the site. Operable units will not impede implementation of subsequent actions, including final action at the site. H-Area Tank Farm is a part of the General Separations Area Eastern Groundwater Operable Unit.
Operational Period	Period of time during which waste tanks are in operation, waste is removed from the waste tanks and ancillary equipment, the systems are grouted, and a closure cap is installed.
Outcrop	Also referred to as seepage, it is the location where groundwater from aquifers discharges to the surface.

Oxalic Acid	Oxalic acid is a relatively strong organic acid, being about 10,000 times stronger than acetic acid.
Oxidation Potential	The measure of a material to oxidize or lose electrons.
Oxidized	Combined with or having undergone a chemical reaction with oxygen.
Paleozoic	The geological period between 600 to 230 million years ago.
PAR Pond	A lake constructed at Savannah River Site in 1958 to provide cooling water for P-Reactor and R-Reactor.
Peak Ground Acceleration	A measure of earthquake acceleration on the ground expressed in g, the acceleration due to Earth's gravity, equivalent to g-force. Damage to structures can be correlated to the ground motion measured by seismic instruments.
Perennial Stream	A perennial stream has flowing water year-round during a typical year. The water table is located above the stream bed for most of the year. Groundwater is the primary source of water for stream flow. Run-off from rainfall is a supplemental source of water for stream flow.
Performance Category	Performance category classification is a graded approach used to establish design and evaluation requirements for structures, systems and components. Performance categories range from 0 to 4 in order of increasingly stringent mitigation and performance requirements and with decreasing values of annual probability of exceedance of acceptable behavior limits. Performance categories are developed with regards to acts of nature (e.g., earthquake, hurricane, tornado flood, rain, or snow precipitation, volcanic eruption, lightning strike, or extreme cold or heat) which may threaten workers, the public, or the environment by potential damage to structures, systems and components.
Permeability	Capability of a material to let pass other molecules or particles.
Phosphatic	Pertaining to, or containing, phosphorus, phosphoric acid, or phosphates; as in phosphatic sediments.
Pitting	Localized corrosion of a metal surface, confined to a point or small area that takes the form of cavities.
Plume	A body of contaminated groundwater emanating from a specific source.
Pore	One of many small openings in a solid substance of any kind that contribute to the substance's porosity (the measure of the void spaces in a material).
PORFLOW	A Comprehensive Fluid Dynamics simulation software program developed to accurately solve problems involving transient or steady state fluid flow, heat, salinity and mass transport in multi-phase, variably saturated, porous or fractured media with dynamic phase change. The porous/fractured media may be anisotropic and heterogeneous, arbitrary sources (e.g., wells) may be present and, chemical reactions or radioactive decay may take place. It accommodates alternate fluid and property relations and complex and arbitrary boundary conditions.
Porosity	Grout porosity is defined as the percentage of total volume of cured grout that is not occupied by the starting cementitious materials and the products that result from reaction of these cementitious materials with water. More generally, porosity is the measure of the void spaces in a material calculated as the fraction of the volume of voids over the total volume.
Potable Water	Potable water is water safe for human consumption.

Precambrian	An informal term to include all geologic time from the beginning of the Earth to the beginning of the Cambrian period 570 million years ago.
Preliminary Remediation Goal	Health-based chemical or radionuclide concentration in an environmental media associated with a particular exposure scenario. They may be developed based on exposure scenarios evaluated prior to or as a result of a baseline risk assessment.
Principal Threat Source Material	The materials that include or contain hazardous substances, pollutants or contaminants that act as a reservoir for migration of contamination to groundwater, surface water or air, or that act as a source for direct exposure.
Probabilistic	A model that assigns a likelihood to events or data within a population, as expressed by a ranked numerical value or an estimate of best case, worst case or most likely.
Probable Maximum Precipitation	Theoretically, the greatest depth of precipitation for a given duration that is physically possible over a given size storm area at a particular geographical location at a certain time of the year.
Progeny	Decay products or descendants of specific radionuclides.
Public Dose	The dose received by a member of the public from exposure to radiation. Public dose does not include occupational dose or doses received from background radiation or from any medical administration the individual has received.
Pump Pit	Pump pits are shielded reinforced concrete structures located below grade at the low points of transfer lines, contain pump tanks and are usually lined with stainless steel.
Pump Tank	Most pump pits house a pump tank with the pump pits providing secondary containment for pump tanks. The pump tanks have a nominal capacity of approximately 7,200 gallons each. The pump tanks installed in H-Area Tank Farm are all of the same basic size.
RCRA	The Resource Conservation and Recovery Act is the public law that creates the framework for the proper management of hazardous and nonhazardous solid waste.
Redox	Redox (shorthand for oxidation/reduction reaction) describes all chemical reactions in which atoms have their oxidation number (oxidation state) changed.
Remedial Investigation Process	The mechanism for collecting data to characterize site conditions, determine the nature of the waste, or assess risk to human health and the environment as overseen by the U.S. Environmental Protection Agency.
Residual Radioactivity	Radioactivity in structures, materials, soils, groundwater, and other media at a site remaining after closure.
Riemann or Lebesgue Measures	Statistical method of integration.
Riser	The risers through the waste tank tops provide for access to the tank and annulus interiors. Risers are used primarily to provide for the installation of equipment such as pumps and cooling equipment, instrumentation such as level probes and leak detection, and ventilation, and to provide access to the waste tank interior for sampling, depth measurement, and inspection.
Saltstone	A process in which low-activity salt solution is mixed with dry chemicals (cement, slag, and fly ash) to form a homogeneous grout mixture.

Sand Layer	All Type II waste tanks have a 1-inch thick primary sand layer between the primary and secondary liners and a 1-inch thick secondary sand layer between the secondary liner and basemat. These sand layers are also commonly referred to as “Sand Pads”.
Saturated Zone	The saturated zone encompasses the area below ground in which all interconnected openings within the geologic medium are completely filled with water.
Sector	A logical division or grouping.
Seepage	Also referred to as outcrop or far field, it is the location where groundwater from the upper aquifers is discharged to the surface.
Segregation	Separation of sand from binder as the result of impact, and separation of water from grout as the result of gravity settling of the solids from the grout slurry.
Set Time	Time after mixing at which the grout responds as a solid.
Shotcrete	Shotcrete is a substance applied via pressure hoses. Shotcrete is usually concrete conveyed through a hose and pneumatically projected at high velocity onto a surface. Shotcrete undergoes placement and compaction at the same time due to the force with which it is projected from the nozzle. Shotcrete was used in the construction of Type IV tanks.
Shrinkage	Percent length change of grout samples cured at 73°F as a function of curing time in saturated and drying environments.
Silica Fume	Silica fume, also known as microsilica, is a byproduct of the reduction of high-purity quartz with coke in electric arc furnaces in the production of silicon and ferrosilicon alloys. Silica fume is used as an addition in Portland cement concretes to improve properties. It has been found that silica fume improves compressive strength, bond strength, and abrasion resistance. Addition of silica fume also reduces the permeability of concrete to chloride ions, which protects concrete’s reinforcing steel from corrosion.
Slag	Slag was introduced into the design mixes, which in addition to its hydraulic activity, also provides chemical reducing power to the mix. Slag has been shown to possess chemically reducing properties that are favorable for technetium reduction and for plutonium and selenium.
Slug Test	A slug test is a particular type of aquifer test where water is quickly added or removed from a groundwater well, and the change in hydraulic head is monitored through time, to determine the near-well aquifer characteristics. It is a method used by hydrogeologists to determine the transmissivity and storativity of the material the well is completed in.
Solubility	The ability of a substance to dissolve in a solvent. Solubility may also refer to the measure of this ability for a particular substance in a particular solvent, equal to the quantity of substance dissolving in a fixed quantity of solvent to form a saturated solution under specified temperature and pressure. The extent of the solubility of a substance in a specific solvent is measured as the saturation concentration, where adding more solute does not increase the concentration of the solution. The extent of solubility ranges widely, from infinitely soluble, such as ethanol in water, to poorly soluble, such as silver chloride in water. The term <i>insoluble</i> is often applied to poorly or very poorly soluble compounds.

Source Term	The amount and type of radioactive material released into the environment.
Spalling	Destruction of a surface by frost, heat, corrosion, or mechanical causes.
Stabilized Contaminant	Grouted waste remaining in the waste tanks or ancillary equipment after system closure.
Stochastic	A probabilistic distribution of parameters.
Stoichiometry	Calculation of the quantitative relationships between the amounts of reactants and products formed during a chemical reaction.
Stream Trace	Generated by PORFLOW, line represents the direction of movement of groundwater plume as it flows from each of the waste tanks to hypothetical 100-meter well locations. Because the flow is also vertical through the UTR and Gordon aquifers, the actual travel distance to reach 100 meters from the HTF boundary is greater than 100 meters.
Supernate	Liquid salt solution found above the sludge layer after settling of solids in waste tanks has occurred as a result of a liquid waste transfer to one of the waste processing facilities or receipt tanks.
TERRA Code	A three dimensional finite element code for the simulation of the earth's mantle.
Thermodynamic	The science of heat and temperature and of the laws governing the conversion of heat into mechanical, electrical, or chemical energy.
Tortuosity	The property of a curve being tortuous (twisted; having many turns). Commonly used to describe diffusion in porous media.
Total Effective Dose Equivalent	The sum of the deep-dose equivalent for external exposures and the committed effective dose equivalent for internal exposures.
TNX	One of the first facilities put into operation at the Savannah River Site. This facility provided a wide range of technical support and development for Separations. TNX was a code designation and had no logical derivation.
Tracer	An amount of material introduced into a system model in order to follow the behavior of some component of that system.
Triassic	The geological time-period between 248 and 213 million years ago.
Vadose Zone	The area directly beneath the conceptual closure cap and overlying the water table, including both undisturbed soil and backfill, which contains the majority of the potential contamination sources.